

Contemporary Cardiology
Series Editor: Peter P. Toth

Elena Aikawa
Joshua D. Hutcheson *Editors*

Cardiovascular Calcification and Bone Mineralization

 Humana Press

Contemporary Cardiology

Series Editor

Peter P. Toth

Ciccarone Center for the Prevention of Cardiovascular Disease

Johns Hopkins University School of Medicine

Baltimore, MD, USA

For more than a decade, cardiologists have relied on the Contemporary Cardiology series to provide them with forefront medical references on all aspects of cardiology. Each title is carefully crafted by world-renown cardiologists who comprehensively cover the most important topics in this rapidly advancing field. With more than 75 titles in print covering everything from diabetes and cardiovascular disease to the management of acute coronary syndromes, the Contemporary Cardiology series has become the leading reference source for the practice of cardiac care.

More information about this series at <http://www.springer.com/series/7677>

Elena Aikawa • Joshua D. Hutcheson
Editors

Cardiovascular Calcification and Bone Mineralization

 Humana Press

Editors

Elena Aikawa
Department of Medicine
Brigham and Women's Hospital
Harvard Medical School
Boston, MA
USA

Joshua D. Hutcheson
Department of Biomedical Engineering
Florida International University
Miami, FL
USA

ISSN 2196-8969

Contemporary Cardiology

ISBN 978-3-030-46724-1

<https://doi.org/10.1007/978-3-030-46725-8>

ISSN 2196-8977 (electronic)

ISBN 978-3-030-46725-8 (eBook)

© Springer Nature Switzerland AG 2020

This work is subject to copyright. All rights are reserved by the Publisher, whether the whole or part of the material is concerned, specifically the rights of translation, reprinting, reuse of illustrations, recitation, broadcasting, reproduction on microfilms or in any other physical way, and transmission or information storage and retrieval, electronic adaptation, computer software, or by similar or dissimilar methodology now known or hereafter developed.

The use of general descriptive names, registered names, trademarks, service marks, etc. in this publication does not imply, even in the absence of a specific statement, that such names are exempt from the relevant protective laws and regulations and therefore free for general use.

The publisher, the authors and the editors are safe to assume that the advice and information in this book are believed to be true and accurate at the date of publication. Neither the publisher nor the authors or the editors give a warranty, expressed or implied, with respect to the material contained herein or for any errors or omissions that may have been made. The publisher remains neutral with regard to jurisdictional claims in published maps and institutional affiliations.

This Humana imprint is published by the registered company Springer Nature Switzerland AG
The registered company address is: Gewerbestrasse 11, 6330 Cham, Switzerland

Foreword

Cardiovascular calcification is the most common type of ectopic calcification. It is a frequent complication of vascular disease such as atherosclerosis and constitutes an important vascular aspect of systemic disorders including diabetes, renal failure, premature aging, and inflammatory disease. Furthermore, calcific aortic valve disease, considered a distinct type of cardiovascular calcification, is the most prevalent form of heart valve disease in the developed world and is projected to steadily increase during the next few decades. The calcific changes augment morbidity and mortality in cardiovascular disease and create significant obstacles during vascular interventions and surgeries such as coronary artery bypass grafting and heart valve replacement. Overall, the number of patients with complications of cardiovascular calcification and the cost in terms of human suffering and healthcare costs are rising.

Historically, the interest in cardiovascular calcification was triggered by a number of observations by early pathologists, who reported the resemblance of the calcification to *bona fide* bone as well as associations between calcification and vascular disease. As early as 1863 Rudolph L.C. Virchow, “the father of modern pathology,” noted that “we have really to do with an ossification” and “the plates, which pervade the inner wall of the vessel, are real plates of bone.”

The descriptions of the cardiovascular calcification involved elements of bone, cartilage, and even bone marrow-like tissues and fat. In light of these observations together with the more recent findings of bone-regulatory factors, our perception of calcification as something irreversible and unregulated changed. The prospects of prevention and treatment became tangible as we realized that the trajectory of cardiovascular calcification could indeed be modified. This realization coincided with the emergence of new approaches in cell and molecular biology and improved clinical imaging for quantification of calcification and percutaneous vascular and valvular interventions. The discovery of osteochondrogenic differentiation in vascular cells could also be seen as a precursor to the subsequent rise of the stem cell field, all of which contributed to the establishment of cardiovascular calcification as a highly translational, evolving, and dynamic research field.

The integration of the different aspects of calcification led to a greater understanding of how mineralization impairs the physiology of the cardiovascular

system. We know that calcified regions can influence the stability of atherosclerotic lesions depending on the size, shape, and location of the mineral. We have examined how vascular cells derived from the endothelium, vascular media, or adventitia turn normally compliant vessels into bone and cartilage and how extensive mineralization alters the elasticity of the arteries. As a consequence, blood pressure regulation and organ perfusion will suffer. We are also familiar with the deleterious effects of calcific build-up on the aortic valve that results in aortic stenosis, impaired coronary blood flow, and ultimately heart failure.

We later discovered how essential signaling in bone growth is re-purposed to promote cardiovascular calcification. Enhanced levels of phosphate, glucose, and lipids resulting from kidney disease, diabetes, and atherosclerosis have powerful effects on mineral precipitation and the reactivation of developmental factors. Bone-promoting factors such as the bone morphogenetic proteins, Wnt signaling, and alkaline phosphatase are activated in the vessels, but can also be counteracted by an array of calcification inhibitors. The formation of osteoclasts, central in bone resorption, is activated in the calcified vessels through osteoprotegerin and its ligands. This has allowed for an understanding of the role of bone-remodeling in shaping vascular calcification, a process that could be exploited for therapeutic aims. The emergence of new tools such as single cell sequencing and “omics” approaches will enable us to further characterize the individual calcifying cells and their signaling patterns, and thereby enhance our understanding of their unique features. We should also be able to better examine cell responses elicited by the surrounding matrix and how modifications of matrix components such as elastin would alter the course of calcification.

The similarities between arteries and bone also extend to extracellular vesicles. These bone-related mediators of mineral precipitation have similarly been shown to drive smooth muscle cell mineralization in the vascular wall. Moreover, we have gained insight into the interactions between biomechanical factors, oxidative stress, and inflammation that are able to create “perfect storms” that can further cardiovascular calcification. This is especially notable in the aortic valves where the two sides of the valves experience striking differences in flow conditions and calcific changes. Simultaneously, biomineralization of prosthetic valves is continuing to gain in importance given the growing number of valve replacement and the effects of calcification on the integrity and longevity of the prosthetic valves.

In order to address the differences between the cardiovascular calcification and normal bone mineralization, new bridges had to be created between vascular, valvular, and bone biology. Paradoxes were found in these comparisons between bones and arteries, allowing us to obtain information that will eventually assist in the targeting of anti-calcific treatments to the vessels while sparing the bones. This is a critical point since cardiovascular calcification frequently coexists with bone disorders, which are characterized by deficiencies in mineralized bone such as osteoporosis.

The last few decades have radically changed our view of cardiovascular calcification, and this newfound awareness is finding its way into day-to-day patient care. The underlying basic science of cardiovascular calcification is moving swiftly to

suggest new treatment strategies. The clinical sciences are continuously enhancing the imaging modalities used to detect and monitor calcification over time. There is a clear expectation that our expanding knowledge will ultimately be translated to new and better strategies for prevention and treatment of clinical calcific disease. It will be greatly supported by the effort to summarize the present understanding of cardiovascular calcification in this comprehensive scientific work. This volume is written and edited by experts in different areas of cardiovascular calcification, several of which have made ground-breaking discoveries and created new perspectives on calcification. Their combined efforts are certain to prove useful to trainees and experts at all levels who wish to broaden their knowledge base in cardiovascular calcification.

Kristina I. Boström, MD, PhD
Division of Cardiology,
David Geffen School of Medicine, UCLA
Los Angeles, CA, USA

Preface

Calcification—the formation of calcium-based minerals—is an integral part of human physiology and disease. Calcium mineral in bones provides the structural support required for upright posture and locomotion, and interacts with other tissues to maintain whole body homeostasis. Bone is remarkably dynamic with active turnover governed by precise cellular and molecular mechanisms that adapt the skeleton in response to cues such as mechanical loading, fracture, and inflammation. The underlying mechanisms remain poorly understood and constitute active areas of research that seek to develop therapeutics and engineered tissues to promote mineralization, treat bone disorders, and restore normal skeletal function.

Humans have long recognized, however, the harmful effects of excessive mineralization. In Greek mythology, the sheer sight of the monster Medusa turned onlookers to stone. Christianity, Judaism, and Islam all describe the fate of Lot's wife, who turned to salt after looking back on the condemned city of Sodom. As bones provide mechanical rigidity and structure for the body, the function of all other organs relies on varying degrees of compliance. Pathological mineral formation in soft tissues—known as ectopic calcification—compromises organs' biomechanical integrity and function. This is perhaps most apparent and widely studied in the context of cardiovascular disease. Calcification of arteries and the aortic valve increases the resistance to blood flow from the heart. The resultant increase in cardiac work can lead to heart failure. The presence of small calcium mineral deposits—known as microcalcification—in atherosclerotic plaques causes mechanical stress. Elevated mechanical stress can result in plaque rupture, the most common cause of acute heart attacks and strokes. The recognition that many of the mechanisms that lead to cardiovascular calcification mirror the active processes that regulate bone remodeling has led to hope that therapeutics could prevent or reverse this pathology in at-risk individuals. To date, however, treatment strategies do not exist, and ongoing research continues to fill critical knowledge gaps in cardiovascular calcification.

Likely due to the appreciation that aortic valve and arterial calcification are the best predictors of and direct contributors to general morbidity and mortality, cardiovascular calcification is the most commonly reported form of ectopic calcification. Mineralization, however, has been noted in a myriad of tissues and pathologies,

including degenerative brain diseases, cancers, the placenta, and traumatic injuries, and ongoing studies seek to understand the associated mechanisms and significance of calcification in these contexts. Calcification studies, including those on cardiovascular and bone mineral, often exist within field-specific silos. Even within a given field, such as cardiovascular calcification, communication barriers often occur between scientists who focus on specific topics such as calcific aortic valve disease, atherosclerotic calcification, diabetes or chronic kidney disease-mediated calcification, and peripheral artery disease. The disease context frequently takes precedence over calcification when researchers seek the most appropriate audience at conferences or through journal publications. The unique goal of this book is to break these silos and aggregate knowledge and research techniques from across various fields of calcification into a single source. This will provide a resource to researchers, clinicians, and other medical professionals and promote interdisciplinary dialogue, potentially leading to solutions to problems within fields through cross-disciplinary knowledge transfer.

Reflecting both the expertise of the editors and the large associated clinical significance, discussions on cardiovascular calcification comprise a majority of the text. The associated chapters, written by renowned experts from across cardiovascular research and medicine, discuss the current mechanistic hypotheses in various vascular beds and disease contexts. The contributions conclude with chapters that provide a translational view that describe how mechanistic insight from basic research has begun to transform cardiovascular diagnostics and clinical decision-making, including potential forthcoming therapeutic approaches. Between the cardiovascular-focused sections, experts in bone mineralization and non-cardiovascular forms of ectopic calcification provide insight into current paradigms from across the spectrum of calcification. Being the most mature of these fields, bone research has informed many of the mechanistic pathways and methodologies utilized in other calcification studies. The section on bone mineralization may continue to serve as a useful reference for investigators in ectopic calcification, but as these fields continue to mature, bone researchers may begin to learn from approaches developed to address pathological mineral formation.

The mechanisms, experimental methods, and clinical insight presented in the following chapters provide a starting point for future conversations and collaborations to advance all areas of calcification research. Initiating interdisciplinary conversations can often be a daunting task, and much credit goes to the authors who contributed chapters to this book for their enthusiasm to participate in this effort. The contributions were written with a goal of appealing to all interested readers. The authors elegantly delivered on this goal without sacrificing depth. Where possible, the chapters are cross-referenced within the text such that the interested readers can take their own starting point and allow the material to suggest the next relevant chapter—a choose your own adventure approach! We (not completely objectively), however, suggest starting with *The History of Cardiovascular Calcification*, which provides some historical context to frame the subsequent chapters.

In addition to thanking the authors for the outstanding and timely contributions, we would also like to acknowledge the efforts of Sheik Mohideen, who served as the project coordinator for this book. Sheik ensured that everything stayed organized and on schedule and made this an overall enjoyable process. We would also like to thank Garth Haller, Gregory Sutorius, Michelle Tam, Jeffrey Taub and Priyanka Srinivasan for editorial support and helping to deliver this from a vague idea to a realizable goal and finally to a finished product. Our collaborators, mentees, and mentors provided invaluable support, opinions, and contributions that helped bring this book to fruition. Last, but certainly not least, we would like to thank our families for their support, love, and patience during this exciting process.

Boston, MA, USA
Miami, FL, USA

Elena Aikawa, MD, PhD, FAHA
Joshua D. Hutcheson, PhD

Contents

Part I Cardiovascular Calcification

1	The History of Cardiovascular Calcification	3
	Joshua D. Hutcheson and Elena Aikawa	
2	Basic Pathology of Arterial and Valvular Calcification in Humans	13
	Atsushi Sakamoto, Yu Sato, Alope V. Finn, and Renu Virmani	
3	Developmental Pathways and Aortic Valve Calcification	47
	M. Victoria Gomez-Stallons, Keira Hassel, and Katherine E. Yutzey	
4	Differential Mechanisms of Arterial and Valvular Calcification	73
	Maximillian A. Rogers and Elena Aikawa	
5	Calcifying Extracellular Vesicles: Biology, Characterization, and Mineral Formation	97
	Hooi Hooi Ng, Jessica E. Molina, and Joshua D. Hutcheson	
6	Role of Biomechanical Stress and Mechanosensitive miRNAs in Calcific Aortic Valve Disease	117
	Nicolas Villa-Roel, Kitae Ryu, and Hanjoong Jo	
7	The Role of Chronic Kidney Disease in Ectopic Calcification	137
	Joanne Laycock, Malgorzata Furmanik, Mengxi Sun, Leon J. Schurgers, Rukshana Shroff, and Catherine M. Shanahan	
8	The Role of Calcification in Peripheral Artery Disease.	167
	Tanner I. Kim and Raul J. Guzman	
9	Bioprosthetic Heart Valve Calcification: Clinicopathologic Correlations, Mechanisms, and Prevention	183
	Frederick J. Schoen and Robert J. Levy	

Part II Ectopic Calcification

- 10 Electron Microscopy for the Characterization of Soft Tissue Mineralization** 219
Elena Tsolaki and Sergio Bertazzo
- 11 Cardiovascular Calcification in Hutchinson-Gilford Progeria and Correlation with Age-Related Degenerative Calcification** 235
Richard N. Mitchell
- 12 Calcinosis in Scleroderma** 247
Sonia Nasreen Ahmad, Elena Gostjeva, Jianfei Ma, and Richard Stratton
- 13 Placental Calcification: Long-standing Questions and New Biomedical Research Directions** 263
Ana Correia-Branco, Sampada Kallol, Nimish Adhikari, Carlo Donato Caiaffa, Nirmala Jayaraman, Olga Kashpur, and Mary C. Wallingford
- 14 Heterotopic Ossification Following Traumatic Blast Injury** 297
Thomas E. Robinson, Sophie C. Cox, and Liam M. Grover

Part III Bone Mineralization

- 15 The Paradoxical Relationship Between Skeletal and Cardiovascular Mineralization** 319
Sidney Iriana, Yin Tintut, and Linda L. Demer
- 16 Cellular Contributors to Bone Homeostasis** 333
Martina Rauner, Katharina Jähn, Haniyeh Hemmatian, Juliane Colditz, and Claudia Goetsch
- 17 Bone Biology, Modeling, Remodeling, and Mineralization** 373
Matthew R. Allen and Sharon M. Moe
- 18 Osteoclasts in Cardiovascular Calcification** 391
Samantha K. Atkins, Farwah Iqbal, Johana Barrientos, Cecilia Giachelli, and Elena Aikawa

Part IV Imaging, Treatment, and Target Discovery

- 19 Imaging Cardiovascular Calcification Activity with ¹⁸F-Fluoride PET** 423
Evangelos Tzolos and Marc R. Dweck
- 20 The Role of Elastin Degradation in Vascular Calcification: Possibilities to Repair Elastin and Reverse Calcification** 441
Fatema-Tuj Zohora, Nasim Nosoudi, Saketh Ram Karamched, and Naren Vyavahare

21 Clinical Trials and Calcification-Based Treatment Decisions 481
Jane A. Leopold

22 Surgical Versus Transcatheter Aortic Valve Replacement 509
Farhang Yazdchi and Prem Shekar

**23 Target Discovery in Calcification Through Omics
and Systems Approaches 525**
Mark C. Blaser, Arda Halu, Louis A. Soddic, Masanori Aikawa,
and Elena Aikawa

Index 553

Contributors

Nimish Adhikari, BS Department of Computer Science, School of Arts and Sciences, Tufts University, Medford, MA, USA

Sonia Nasreen Ahmad, MD Centre for Rheumatology and Connective Tissue Diseases, Royal Free Hospital, UCL, London, UK

Division of Medicine & Department of Internal Medicine, Holy Family and Red Crescent Medical College and Hospital, Dakha, Bangladesh

Elena Aikawa, MD, PhD, FAHA Center for Interdisciplinary Cardiovascular Sciences, Center for Excellence in Vascular Biology, Division of Cardiovascular Medicine, Department of Medicine, Brigham and Women's Hospital, Harvard Medical School, Boston, MA, USA

Masanori Aikawa, MD, PhD Center for Interdisciplinary Cardiovascular Sciences, Division of Cardiovascular Medicine, Department of Medicine, Brigham and Women's Hospital, Harvard Medical School, Boston, MA, USA

Channing Division of Network Medicine, Department of Medicine, Brigham and Women's Hospital, Harvard Medical School, Boston, MA, USA

Center for Excellence in Vascular Biology, Division of Cardiovascular Medicine, Department of Medicine, Brigham and Women's Hospital, Harvard Medical School, Boston, MA, USA

Matthew R. Allen, PhD Department of Anatomy, Cell Biology and Physiology, Indiana University School of Medicine and Roudebush Veterans Affairs Medical Center, Indianapolis, IN, USA

Samantha K. Atkins, MS, PhD Center for Interdisciplinary Cardiovascular Sciences, Division of Cardiovascular Medicine, Department of Medicine, Brigham and Women's Hospital, Harvard Medical School, Boston, MA, USA

Johana Barrientos, BS in Biology Center for Interdisciplinary Cardiovascular Sciences, Division of Cardiovascular Medicine, Department of Medicine, Brigham and Women's Hospital, Harvard Medical School, Boston, MA, USA

Sergio Bertazzo, PhD Department of Medical Physics & Biomedical Engineering, University College London, London, UK

Mark C. Blaser, PhD Center for Interdisciplinary Cardiovascular Sciences, Division of Cardiovascular Medicine, Department of Medicine, Brigham and Women's Hospital, Harvard Medical School, Boston, MA, USA

Carlo Donato Caiaffa, PhD National Institute of Science and Technology for Regenerative Medicine, Institute of Biophysics Carlos Chagas Filho, Federal University of Rio de Janeiro, Rio de Janeiro, RJ, Brazil

Juliane Colditz, PhD Department of Medicine III, Medical Faculty of the Technische Universität Dresden, Dresden, Germany

Ana Correia-Branco, MSc, PhD Mother Infant Research Institute, Tufts Medical Center, Boston, MA, USA

Sophie C. Cox, PhD, BEng School of Chemical Engineering, University of Birmingham, Edgbaston, Birmingham, UK

Linda L. Demer, MD, PhD Department of Medicine, University of California, Los Angeles, Los Angeles, CA, USA

Department of Physiology, University of California, Los Angeles, Los Angeles, CA, USA

Department of Bioengineering, University of California, Los Angeles, Los Angeles, CA, USA

Marc R. Dweck, PhD British Heart Foundation Centre for Cardiovascular Sciences, University of Edinburgh, Edinburgh, UK

Aloke V. Finn, MD CVPPath Institute, Inc., Gaithersburg, MD, USA

Malgorzata Furmanik, BSc, MSc, PhD Department of Biochemistry, Cardiovascular Research Institute Maastricht, Maastricht University, Maastricht, The Netherlands

Cecilia Giachelli, PhD Department of Bioengineering, University of Washington, Seattle, WA, USA

Claudia Goettsch, PhD Department of Cardiology, Medical Faculty, RWTH Aachen University, Aachen, Germany

M. Victoria Gomez-Stallons, PhD Division of Molecular Cardiovascular Biology, The Heart Institute, Cincinnati Children's Medical Center, Cincinnati, OH, USA

Elena Gostjeva, BSc, PhD Department of Biological Engineering, Massachusetts Institute of Technology Cambridge, Cambridge, MA, USA

Liam M. Grover, PhD, BMedSc(Hons) School of Chemical Engineering, University of Birmingham, Edgbaston, Birmingham, UK

Raul J. Guzman, MD Division of Vascular Surgery, Yale University School of Medicine, New Haven, CT, USA

Arda Halu, PhD Center for Interdisciplinary Cardiovascular Sciences, Division of Cardiovascular Medicine, Department of Medicine, Brigham and Women's Hospital, Harvard Medical School, Boston, MA, USA

Channing Division of Network Medicine, Department of Medicine, Brigham and Women's Hospital, Harvard Medical School, Boston, MA, USA

Keira Hassel, BS Division of Molecular Cardiovascular Biology, The Heart Institute, Cincinnati Children's Medical Center, Cincinnati, OH, USA

Haniyeh Hemmatian, PhD Department of Osteology and Biomechanics, University Medical Center Hamburg-Eppendorf, Hamburg, Germany

Joshua D. Hutcheson, PhD Department of Biomedical Engineering, Florida International University, Miami, FL, USA

Farwah Iqbal, PhD Center for Excellence in Vascular Biology, Division of Cardiovascular Medicine, Department of Medicine, Brigham and Women's Hospital, Harvard Medical School, Boston, MA, USA

Sidney Iriana, BS, MS Chicago Medical School, Rosalind Franklin University of Medicine and Science, Chicago, IL, USA

Katharina Jähn, PhD Department of Osteology and Biomechanics, University Medical Center Hamburg-Eppendorf, Hamburg, Germany

Nirmala Jayaraman, BA Mother Infant Research Institute, Tufts Medical Center, Boston, MA, USA

Hanjoong Jo, PhD Wallace H. Coulter Department of Biomedical Engineering, Georgia Institute of Technology and Emory University, Atlanta, GA, USA

Division of Cardiology, Department of Medicine, Emory University, Atlanta, GA, USA

Sampada Kallol, PhD Institute of Biochemistry and Molecular Medicine, University of Bern, Bern, Switzerland

Saketh Ram Karamched, PhD Bioengineering, Clemson University, Clemson, SC, USA

Olga Kashpur, PhD Mother Infant Research Institute, Tufts Medical Center, Boston, MA, USA

Tanner I. Kim, MD Division of Vascular Surgery, Yale University School of Medicine, New Haven, CT, USA

Joanne Laycock, BSc(Hons), PhD BHF Centre of Research Excellence, School of Cardiovascular Medicine and Sciences, King's College London, London, UK

Jane A. Leopold, MD Division of Cardiovascular Medicine, Brigham and Women's Hospital, Harvard Medical School, Boston, MA, USA

Robert J. Levy, MD The Division of Cardiology, Department of Pediatrics, The Children's Hospital of Philadelphia, Philadelphia, PA, USA

The Perelman School of Medicine at the University of Pennsylvania, Philadelphia, PA, USA

Jianfei Ma, MBBCh Centre for Rheumatology and Connective Tissue Diseases, Royal Free Hospital Campus, University College London Medical School, London, UK

Richard N. Mitchell, MD, PhD Harvard Medical School and Brigham and Women's Hospital, Boston, MA, USA

Sharon M. Moe, MD Division of Nephrology, Department of Medicine, Indiana University School of Medicine and Roudebush Veterans Affairs Medical Center, Indianapolis, IN, USA

Jessica E. Molina, BS Biomedical Engineering, Florida International University, Miami, FL, USA

Hooi Hooi Ng, PhD Biomedical Engineering and Human & Molecular Genetics, Florida International University, Miami, FL, USA

Nasim Nosoudi, PhD College of Information Technology and Engineering, Marshall University, Huntington, WV, USA

Martina Rauner, PhD Department of Medicine III, Medical Faculty of the Technische Universität Dresden, Dresden, Germany

Thomas E. Robinson, MEng School of Chemical Engineering, University of Birmingham, Edgbaston, Birmingham, UK

Maximillian A. Rogers, PhD Department of Medicine, Brigham and Women's Hospital, Harvard Medical School, Boston, MA, USA

Kitae Ryu, PhD Wallace H. Coulter Department of Biomedical Engineering, Georgia Institute of Technology and Emory University, Atlanta, GA, USA

Louis A. Saddic, MD, PhD Center for Interdisciplinary Cardiovascular Sciences, Division of Cardiovascular Medicine, Department of Medicine, Brigham and Women's Hospital, Harvard Medical School, Boston, MA, USA

Department of Anesthesiology, Perioperative and Pain Medicine, Brigham and Women's Hospital, Harvard Medical School, Boston, MA, USA

Atsushi Sakamoto, MD, PhD CVPPath Institute, Inc., Gaithersburg, MD, USA

Yu Sato, MD CVPPath Institute, Inc., Gaithersburg, MD, USA

Frederick J. Schoen, MD, PhD Department of Pathology, Brigham and Women's Hospital, Harvard Medical School, Boston, MA, USA

Leon J. Schurgers, PhD Department of Biochemistry, Cardiovascular Research Institute Maastricht, Maastricht University, Maastricht, The Netherlands

Catherine M. Shanahan, BSc(Hons), PhD BHF Centre of Research Excellence, School of Cardiovascular Medicine and Sciences, King's College London, London, UK

Prem Shekar, MD Division of Cardiac Surgery, Brigham and Women's Hospital, Harvard Medical School, Boston, MA, USA

Rukshana Shroff, MD, FRCPC, PhD Great Ormond Street Hospital for Children, London, UK

Richard Stratton, MA, MD, FRCP, PhD Centre for Rheumatology and Connective Tissue Diseases, Royal Free Hospital Campus, University College London Medical School, London, UK

Mengxi Sun, PhD BHF Centre of Research Excellence, School of Cardiovascular Medicine and Sciences, King's College London, London, UK

Yin Tintut, PhD Department of Medicine, University of California, Los Angeles, Los Angeles, CA, USA

Department of Physiology, University of California, Los Angeles, Los Angeles, CA, USA

Department of Orthopaedic Surgery, University of California, Los Angeles, Los Angeles, CA, USA

Elena Tsolaki, MS Department of Medical Physics & Biomedical Engineering, University College London, London, UK

Evangelos Tzolos, MD British Heart Foundation Centre for Cardiovascular Sciences, University of Edinburgh, Edinburgh, UK

Nicolas Villa-Roel, BS Wallace H. Coulter Department of Biomedical Engineering, Georgia Institute of Technology and Emory University, Atlanta, GA, USA

Renu Virmani, MD CVPPath Institute, Inc., Gaithersburg, MD, USA

Naren Vyavahare, PhD Bioengineering, Clemson University, Clemson, SC, USA

Mary C. Wallingford, PhD Mother Infant Research Institute, Tufts Medical Center, Boston, MA, USA

Farhang Yazdchi, MD, MS Division of Cardiac Surgery, Brigham and Women's Hospital, Harvard Medical School, Boston, MA, USA

Katherine E. Yutzey, PhD Division of Molecular Cardiovascular Biology, The Heart Institute, Cincinnati Children's Medical Center, Cincinnati, OH, USA

Fatema-Tuj Zohora, MS Bioengineering, Clemson University, Clemson, SC, USA

Part I
Cardiovascular Calcification

Chapter 1

The History of Cardiovascular Calcification



Joshua D. Hutcheson and Elena Aikawa

Introduction to the History of Cardiovascular Calcification

Despite the critical role of calcium-based mineral in human locomotion, food ingestion, and determination of morbidity, our understanding of mineralization mechanisms continues to evolve. Recognition of the structural integrity and biomechanical strength of bones goes back to Neanderthal populations, which used bones to develop tools and weapons [1]. The recognition of bone as an active tissue that continuously remodels has developed over the past century [2], and research into the mechanisms that regulate bone turnover remain ongoing. More recently, calcification has gained recognition as an indicator of pathological remodeling in soft tissues, and many of the associated mechanisms appear to mirror active bone mineral deposition. Much like bone, ectopic calcification in soft tissues remains an active area of research with many efforts focused on therapeutics that can stop or reverse the pathological mineralization without affecting bone mineral. Our purpose in this chapter is to briefly review the history of calcific mineral research and the history of calcification in human health and disease, which we hope will serve as an introduction to the other chapters in this section. A full history of the tremendous amount of work that has gone into the study of cardiovascular calcification could fill an entire textbook. The subsequent chapters include literature reviews and historical records to orient the reader on the subject matter discussed in each. This

J. D. Hutcheson

Department of Biomedical Engineering, Florida International University, Miami, FL, USA

E. Aikawa (✉)

Center for Interdisciplinary Cardiovascular Sciences, Center for Excellence in Vascular Biology, Division of Cardiovascular Medicine, Department of Medicine, Brigham and Women's Hospital, Harvard Medical School, Boston, MA, USA

e-mail: eaikawa@bwh.harvard.edu

© Springer Nature Switzerland AG 2020

E. Aikawa, J. D. Hutcheson (eds.), *Cardiovascular Calcification and Bone Mineralization*, Contemporary Cardiology,

https://doi.org/10.1007/978-3-030-46725-8_1

chapter provides a short, high-level overview to demonstrate the evolution in our understanding of the formation, regulation, and implication of calcific mineral in cardiovascular disease.

Pathological Mineralization: Marker and Maker of Cardiovascular Morbidity

Due to the ability to identify mineral with high contrast using computed tomography, vascular calcification has become a reliable marker to determine the presence of atherosclerotic plaques [3, 4]. The presence of mineral in mummified human remains has shown that atherosclerotic plaque development is not a unique consequence of modern life [5, 6]. While our relatively sedentary modern lifestyle and abundance of high-energy food sources can exacerbate arterial remodeling, whole body computed tomography scans of mummies from four geographical populations showed a positive correlation between the degree of calcification and estimated age at the time of death [5]. One quarter of the mummies exhibited calcification in at least one vascular bed, and 9% had calcification in three or more beds. The prevalence of vascular calcification across geographic distinct populations, even in Inuit mummies who likely led an active lifestyle with a heart-healthy marine-based diet [6], suggests a basic human predisposition for atherosclerosis regardless of diet and lifestyle.

Given the clear association between calcification and atherosclerosis, coronary artery calcium scores have emerged as the most reliable tool to stratify individual risk of future cardiovascular morbidity and mortality [7, 8]. Higher calcium mineral in the coronary arteries associates with elevated risk of major acute cardiovascular events, and individuals with a coronary artery calcium score of zero have exceedingly low cardiovascular event risk. In a complete reversal from recent dogma in aggressive use of lipid-lowering statin therapeutics, the American Heart Association now suggests that doctors may consider foregoing lipid-lowering statin treatment of patients with moderately high “bad” cholesterol levels but no detectable vascular mineral [9]. Atherosclerosis leads to narrowing of the arterial wall as noted by Leonardo da Vinci in the early 1500s [10]. The resultant reduced blood flow can result in tissue necrosis. The advent of catheter-based interventions and bypass procedures allows clinicians to intervene—although not always without complications—inpatients who present with conditions such as stable angina. Acute events, however, caused by the sudden rupture of atherosclerotic plaques and subsequent artery-occluding thrombosis remain a major unmet problem in cardiovascular medicine.

The association between calcification and acute cardiovascular event risk has challenged previous notions that the presence of mineral provides mechanical stability in atherosclerosis [11, 12]. Computational analyses have shown that microcalcifications embedded in the fibrous cap of atherosclerotic plaques can exacerbate

mechanical stress and potentiate plaque rupture—the leading cause of thrombotic events that result in heart attacks [13–15]. These computational predictions that associate mineral morphology with plaque instability support clinical observations that the presence of “spotty” calcification in coronary arteries associates with elevated risk compared to dense calcification [16–18]. Though computed tomography does not provide the spatial resolution necessary to image small plaque-destabilizing microcalcifications (~5–15 μm), the “spotty” calcification (>30 μm), features may indicate ongoing calcification remodeling and a higher likelihood of the presence of microcalcifications. Positron emission tomography (PET) can detect ^{18}F -sodium fluoride tracer, which binds hydroxyapatite mineral [19]. The high mineral surface area in regions of microcalcifications amplifies the PET signal [20], offering a potential diagnostic technique to identify vulnerable plaque [21].

Atherosclerotic calcification occurs in plaques that form in the intima of the arteries, but mineral can also form in the medial layer independent of the presence of plaques. Widespread medial calcification is also known as Monckeberg’s arteriosclerosis. First described by J. G. Monckeberg in 1903 [22], calcification of the elastin-rich medial layer of large- and medium-sized arteries reduces elasticity important in blood flow and increases system resistance. The resultant increase in cardiac work required to move blood through the body can lead to heart failure [23]. Unlike atherosclerotic calcification, Monckeberg’s arteriosclerosis associates with worse outcomes as the mineralization progresses and becomes larger. The clinical outcomes associated with medial calcification, such as Monckeberg’s arteriosclerosis, are similar to those for calcific aortic valve disease. Thin, membranous aortic valve leaflets respond to changes in cardiac pressure to ensure unidirectional blood flow from the heart to the rest of the body. When mineral deposition hinders the motion of these leaflets, the heart must generate higher pressure during systolic contraction to eject blood, ultimately resulting in ventricular remodeling and heart failure if the valve is not replaced [24]. The resultant aortic stenosis was first reported by Lazare Riviere in 1663 [25, 26], and in 1904, Monckeberg—of the medial calcification fame discussed above—noted the importance of calcific mineral in aortic valve leaflet degeneration in the aged and patients with rheumatic fever [27]. In the developing world, rheumatic fever remains a major contributor to calcific aortic valve disease and aortic stenosis. Both Monckeberg’s arteriosclerosis and calcific aortic valve disease are prevalent in diabetics and individuals with chronic kidney disease [28], which may be due to an imbalance of factors that inhibit and promote mineralization in these individuals. Calcific aortic valve disease can also result from aging and inflammatory-driven remodeling similar to those that mediate plaque formation during atherosclerosis [29]. Inflammation-derived calcification in arteries and valves was first comprehensively investigated using *in vivo* and *ex vivo* molecular imaging in mouse models [29, 30], and more recently this phenomenon has been confirmed in humans [31, 32]. Mineralization caused by mineral imbalance and inflammatory cues share similarities, but many of the factors controlling mineral deposition appear distinct [33, 34].

The Tangled History of Physiological and Pathological Calcification

Regardless of the drivers of the mineralization in cardiovascular tissues, calcification of arterial beds and aortic valve leaflets contributes significantly to morbidity and mortality, which begs the question: how does the mineral arise? Current mechanistic understanding of cellular phenotypes and mineral formation in cardiovascular calcification is discussed more thoroughly in subsequent chapters, but it is now clear that mineralization often begins through active and controlled cellular processes. Cardiovascular mineralization was once thought to solely arise from cell death by necrosis or apoptosis. However, in response to pathological cues, resident cells within valve and vascular tissues can adopt phenotypic markers that mirror those observed in bone [35–37]. The associated mechanisms remain active areas of research, but early electron microscopy studies observed that the mineral formation resembles calcification of cartilage in the epiphyseal plate during bone development. First reported by H. Clarke Anderson in the late 1960s [38], cartilage cells release specialized extracellular vesicles named as matrix vesicles, which sequester calcium and phosphate ions to form a nucleation core [39–41]. In 1976, Kook M. Kim, who performed early seminal research also using electron microscopy in aortic valve calcium mineral morphology and composition [42], noted the presence of matrix vesicles in association with calcification in human aortic valve leaflets and aortae [43]. In 1983, Anderson and colleagues extended their earlier work on vesicle-driven mineral formation to pathological vascular calcification, noting that “matrix vesicle-like structures are involved in the calcification of atherosclerotic lesions, as well as in arterial medial calcification” derived from vascular smooth muscle cells [44]. Subsequent studies have shown that the vesicles in vascular calcification can also derive from other cells involved in arterial wall remodeling [45] and arise from intracellular trafficking mechanisms that appear different than those reported in bone [46, 47].

Also in a somewhat distorted mirror image of bone, cardiovascular calcification is influenced by mechanical forces. Leonardo Da Vinci recognized the importance of vascular geometry and altered blood flow patterns in cardiovascular function (i.e., blood does not follow laminar, unidirectional flow patterns) [10]. Atherosclerotic plaques do not form in random locations throughout the vasculature. Studies in the mid-1970s led by Margot Roach and others showed that plaques develop in regions of altered shear stress [48]. Lipid deposition, arterial remodeling, and subsequent calcification tend to localize to regions of disturbed, oscillatory blood flow or eddies. Similarly, aortic valve calcification begins on the aortic aspect of the leaflets, in regions exposed to high blood oscillations during the cardiac cycle [49, 50]. Leonardo Da Vinci was the first to describe the disturbed flow and its application to the cardiovascular system. Perhaps the greatest achievement in his anatomical work was the discovery of the way aortic valve works. For his entire life, Leonardo was fascinated by eddies of water and wind currents. He

employed his knowledge to determine that blood flow through the part of the aorta known as sinus of Valsalva produces eddies that contribute to valve closure. The sinuses of Valsalva are named after the Italian anatomist Antonio Valsalva, who published his study in the early 1700s. These structures could more correctly be called the sinuses of Leonardo, if Leonardo Da Vinci had published his discoveries two centuries before Valsalva [51]. The oscillatory shear stress induced in these regions of disturbed flow can alter endothelial cell phenotypes, which direct underlying remodeling within the tissue and may result in ectopic calcification. Analogous to bone, this behavior is reminiscent of osteocytes that sense oscillatory shear as interstitial fluid moves within bone during cyclic loading. As first reported in the mid-1990s [52], the resultant mechanotransduction and paracrine signaling increase mineralization by osteoblasts within the bone. The compressive deformation of bone tissue may also induce remodeling independent of fluid shear (though the two are difficult to decouple). In contradistinction, tensile mechanical loading and deformation can induce remodeling and calcification in valve [53] and vascular tissues [54].

The similar, though not always overlapping, features of physiological bone mineralization and cardiovascular calcification belie the common clinical observation that increased cardiovascular mineral coexists with osteoporotic bone loss in patients. Termed the “calcification paradox” by Linda Demer and others in the late 1990s [55], studies have shown that bone and vascular cells respond in an opposite manner to stimuli such as pro-inflammatory oxidized LDL [55] and retinoids [56]. The basis of the divergent responses, however, remains poorly understood. Further studies are needed to better comprehend the similarities and differences between physiological and pathological mineral formation in order to develop therapeutics that modulate these processes independently.

Concluding Remarks

Despite the fact that calcification has contributed to morbidity and mortality as far back as ancient civilizations and has been widely studied for centuries, therapeutic approaches to prevent or treat ectopic calcification remain elusive. As discussed in subsequent chapters, our understanding of the molecular and material mechanisms of pathological mineral formation continues to evolve. The overarching goal of the following text is to aggregate calcification knowledge from across a variety of fields/tissues/diseases. Filling lingering knowledge gaps in mineralization will require multidisciplinary expertise in molecular biology, biochemistry, medicine, engineering, and materials science among others. Breaking research silos will be an important part of overcoming remaining challenges. The history of cardiovascular calcification and other types of ectopic calcification is still being written.

References

1. Rougier H, Crevecoeur I, Beauval C, Posth C, Flas D, Wissing C, Furtwangler A, Germonpre M, Gomez-Olivencia A, Semal P, van der Plicht J, Bocherens H, Krause J. Neandertal cannibalism and Neandertal bones used as tools in Northern Europe. *Sci Rep.* 2016;6:29005. PMC4933918.
2. Urist MR. Bone: formation by autoinduction. *Science.* 1965;150:893–9.
3. Hecht HS. Coronary artery calcium scanning: past, present, and future. *JACC Cardiovasc Imaging.* 2015;8:579–96.
4. Mori H, Torii S, Kutyna M, Sakamoto A, Finn AV, Virmani R. Coronary artery calcification and its progression: what does it really mean? *JACC Cardiovasc Imaging.* 2018;11:127–42.
5. Thompson RC, Allam AH, Lombardi GP, Wann LS, Sutherland ML, Sutherland JD, Soliman MA, Frohlich B, Mininberg DT, Monge JM, Vallodolid CM, Cox SL, Abd el-Maksoud G, Badr I, Miyamoto MI, el-Halim Nur el-Din A, Narula J, Finch CE, Thomas GS. Atherosclerosis across 4000 years of human history: the Horus study of four ancient populations. *Lancet.* 2013;381:1211–22.
6. Wann LS, Narula J, Blankstein R, Thompson RC, Frohlich B, Finch CE, Thomas GS. Atherosclerosis in 16th-century Greenlandic Inuit Mummies. *JAMA Netw Open.* 2019;2:e1918270. PMC6991216.
7. Martin SS, Blaha MJ, Blankstein R, Agatston A, Rivera JJ, Virani SS, Ouyang P, Jones SR, Blumenthal RS, Budoff MJ, Nasir K. Dyslipidemia, coronary artery calcium, and incident atherosclerotic cardiovascular disease: implications for statin therapy from the multi-ethnic study of atherosclerosis. *Circulation.* 2014;129:77–86. PMC3919521.
8. Vliegenthart R, Oudkerk M, Hofman A, Oei HH, van Dijck W, van Rooij FJ, Witteman JC. Coronary calcification improves cardiovascular risk prediction in the elderly. *Circulation.* 2005;112:572–7.
9. Grundy SM, Stone NJ, Bailey AL, Beam C, Birtcher KK, Blumenthal RS, Braun LT, de Ferranti S, Faiella-Tommasino J, Forman DE, Goldberg R, Heidenreich PA, Hlatky MA, Jones DW, Lloyd-Jones D, Lopez-Pajares N, Ndumele CE, Orringer CE, Peralta CA, Saseen JJ, Smith SC Jr, Sperling L, Virani SS, Yeboah J. 2018 AHA/ACC/AACVPR/AAPA/ABC/ACPM/ADA/AGS/APhA/ASPC/NLA/PCNA guideline on the management of blood cholesterol: executive summary: a report of the American College of Cardiology/American Heart Association task force on clinical practice guidelines. *J Am Coll Cardiol.* 2019;73:3168–209.
10. Boon B. Leonardo da Vinci on atherosclerosis and the function of the sinuses of Valsalva. *Neth Heart J.* 2009;17:496–9. PMC2804084.
11. Hutcheson JD, Maldonado N, Aikawa E. Small entities with large impact: microcalcifications and atherosclerotic plaque vulnerability. *Curr Opin Lipidol.* 2014;25:327–32. Pmc4166045.
12. Lin TC, Tintut Y, Lyman A, Mack W, Demer LL, Hsiai TK. Mechanical response of a calcified plaque model to fluid shear force. *Ann Biomed Eng.* 2006;34:1535–41.
13. Kelly-Arnold A, Maldonado N, Laudier D, Aikawa E, Cardoso L, Weinbaum S. Revised microcalcification hypothesis for fibrous cap rupture in human coronary arteries. *Proc Natl Acad Sci U S A.* 2013;110:10741–6. PMC3696743.
14. Maldonado N, Kelly-Arnold A, Cardoso L, Weinbaum S. The explosive growth of small voids in vulnerable cap rupture: cavitation and interfacial debonding. *J Biomech.* 2013;46:396–401. PMC4019735.
15. Maldonado N, Kelly-Arnold A, Vengrenyuk Y, Laudier D, Fallon JT, Virmani R, Cardoso L, Weinbaum S. A mechanistic analysis of the role of microcalcifications in atherosclerotic plaque stability: potential implications for plaque rupture. *Am J Physiol Heart Circ Physiol.* 2012;303:H619–28. PMC3468470.
16. Criqui MH, Denenberg JO, Ix JH, McClelland RL, Wassel CL, Rifkin DE, Carr JJ, Budoff MJ, Allison MA. Calcium density of coronary artery plaque and risk of incident cardiovascular events. *JAMA.* 2014;311:271–8. PMC4091626.

17. Ehara S, Kobayashi Y, Yoshiyama M, Shimada K, Shimada Y, Fukuda D, Nakamura Y, Yamashita H, Yamagishi H, Takeuchi K, Naruko T, Haze K, Becker AE, Yoshikawa J, Ueda M. Spotty calcification typifies the culprit plaque in patients with acute myocardial infarction: an intravascular ultrasound study. *Circulation*. 2004;110:3424–9.
18. Thilo C, Gebregziabher M, Mayer FB, Zwerner PL, Costello P, Schoepf UJ. Correlation of regional distribution and morphological pattern of calcification at CT coronary artery calcium scoring with non-calcified plaque formation and stenosis. *Eur Radiol*. 2010;20:855–61.
19. Dweck MR, Chow MW, Joshi NV, Williams MC, Jones C, Fletcher AM, Richardson H, White A, McKillop G, van Beek EJ, Boon NA, Rudd JH, Newby DE. Coronary arterial 18F-sodium fluoride uptake: a novel marker of plaque biology. *J Am Coll Cardiol*. 2012;59:1539–48.
20. Creager MD, Hohl T, Hutcheson JD, Moss AJ, Schlotter F, Blaser MC, Park MA, Lee LH, Singh SA, Alcaide-Corral CJ, Tavares AAS, Newby DE, Kijewski MF, Aikawa M, Di Carli M, Dweck MR, Aikawa E. (18)F-fluoride signal amplification identifies microcalcifications associated with atherosclerotic plaque instability in positron emission tomography/computed tomography images. *Circ Cardiovasc Imaging*. 2019;12:e007835. PMC6338081.
21. Joshi NV, Vesey AT, Williams MC, Shah AS, Calvert PA, Craighead FH, Yeoh SE, Wallace W, Salter D, Fletcher AM, van Beek EJ, Flapan AD, Uren NG, Behan MW, Cruden NL, Mills NL, Fox KA, Rudd JH, Dweck MR, Newby DE. 18F-fluoride positron emission tomography for identification of ruptured and high-risk coronary atherosclerotic plaques: a prospective clinical trial. *Lancet*. 2014;383:705–13.
22. Mönckeberg JG. Ueber die reine Mediaverkalkung der Extremitätenarterien und ihr Verhalten zur Arteriosklerose. *Virchows Arch Pathol Anat*. 1903;171:141–67.
23. Shroff R, Long DA, Shanahan C. Mechanistic insights into vascular calcification in CKD. *J Am Soc Nephrol*. 2013;24:179–89.
24. Strange G, Stewart S, Celermajer D, Prior D, Scalia GM, Marwick T, Ilton M, Joseph M, Codde J, Playford D, National Echocardiography Database of Australia contributing sites. Poor long-term survival in patients with moderate aortic stenosis. *J Am Coll Cardiol*. 2019;74(15):1851–63.
25. Leopold JA. Cellular mechanisms of aortic valve calcification. *Circ Cardiovasc Interv*. 2012;5:605–14. PMC3427002.
26. Vaslef SN, Roberts WC. Early descriptions of aortic valve stenosis. *Am Heart J*. 1993;125:1465–74.
27. Mönckeberg JG. Der normale histologische Bau und die Sklerose der Aortenklappen. *Virchows Arch Pathol Anat Physiol*. 1904;176:472–514.
28. Zhu D, Mackenzie NC, Farquharson C, Macrae VE. Mechanisms and clinical consequences of vascular calcification. *Front Endocrinol (Lausanne)*. 2012;3:95. PMC3412412.
29. Aikawa E, Nahrendorf M, Figueiredo JL, Swirski FK, Shtatland T, Kohler RH, Jaffer FA, Aikawa M, Weissleder R. Osteogenesis associates with inflammation in early-stage atherosclerosis evaluated by molecular imaging in vivo. *Circulation*. 2007;116:2841–50.
30. Aikawa E, Nahrendorf M, Sosnovik D, Lok VM, Jaffer FA, Aikawa M, Weissleder R. Multimodality molecular imaging identifies proteolytic and osteogenic activities in early aortic valve disease. *Circulation*. 2007;115:377–86.
31. Abdelbaky A, Corsini E, Figueroa AL, Subramanian S, Fontanez S, Emami H, Hoffmann U, Narula J, Tawakol A. Early aortic valve inflammation precedes calcification: a longitudinal FDG-PET/CT study. *Atherosclerosis*. 2015;238:165–72.
32. Dweck MR, Jones C, Joshi NV, Fletcher AM, Richardson H, White A, Marsden M, Pessotto R, Clark JC, Wallace WA, Salter DM, McKillop G, van Beek EJ, Boon NA, Rudd JH, Newby DE. Assessment of valvular calcification and inflammation by positron emission tomography in patients with aortic stenosis. *Circulation*. 2012;125:76–86.
33. Amann K. Media calcification and intima calcification are distinct entities in chronic kidney disease. *Clin J Am Soc Nephrol*. 2008;3:1599–605.
34. Hutcheson JD, Blaser MC, Aikawa E. Giving calcification its due: recognition of a diverse disease: a first attempt to standardize the field. *Circ Res*. 2017;120:270–3. Pmc5260841.

35. Mohler ER 3rd, Gannon F, Reynolds C, Zimmerman R, Keane MG, Kaplan FS. Bone formation and inflammation in cardiac valves. *Circulation*. 2001;103:1522–8.
36. Osman L, Yacoub MH, Latif N, Amrani M, Chester AH. Role of human valve interstitial cells in valve calcification and their response to atorvastatin. *Circulation*. 2006;114:1547–52.
37. Steitz SA, Speer MY, Curinga G, Yang HY, Haynes P, Aebersold R, Schinke T, Karsenty G, Giachelli CM. Smooth muscle cell phenotypic transition associated with calcification: upregulation of Cbfa1 and downregulation of smooth muscle lineage markers. *Circ Res*. 2001;89:1147–54.
38. Anderson HC. Vesicles associated with calcification in the matrix of epiphyseal cartilage. *J Cell Biol*. 1969;41:59–72. PMC2107736.
39. Anderson HC. Molecular biology of matrix vesicles. *Clin Orthop Relat Res*. 1995;314:266–80.
40. Wuthier RE, Lipscomb GF. Matrix vesicles: structure, composition, formation and function in calcification. *Front Biosci (Landmark Ed)*. 2011;16:2812–902.
41. Wuthier RE, Wu LN, Sauer GR, Genge BR, Yoshimori T, Ishikawa Y. Mechanism of matrix vesicle calcification: characterization of ion channels and the nucleational core of growth plate vesicles. *Bone Miner*. 1992;17:290–5.
42. Kim KM, Huang SN. Ultrastructural study of calcification of human aortic valve. *Lab Investig*. 1971;25:357–66.
43. Kim KM. Calcification of matrix vesicles in human aortic valve and aortic media. *Fed Proc*. 1976;35:156–62.
44. Tanimura A, McGregor DH, Anderson HC. Matrix vesicles in atherosclerotic calcification. *Proc Soc Exp Biol Med*. 1983;172:173–7.
45. New SE, Goetsch C, Aikawa M, Marchini JF, Shibasaki M, Yabusaki K, Libby P, Shanahan CM, Croce K, Aikawa E. Macrophage-derived matrix vesicles: an alternative novel mechanism for microcalcification in atherosclerotic plaques. *Circ Res*. 2013;113:72–7. Pmc3703850.
46. Goetsch C, Hutcheson JD, Aikawa M, Iwata H, Pham T, Nykjaer A, Kjolby M, Rogers M, Michel T, Shibasaki M, Hagita S, Kramann R, Rader DJ, Libby P, Singh SA, Aikawa E. Sortilin mediates vascular calcification via its recruitment into extracellular vesicles. *J Clin Invest*. 2016;126:1323–36. Pmc4811143.
47. Kapustin AN, Chatrou ML, Drozdov I, Zheng Y, Davidson SM, Soong D, Furmanik M, Sanchis P, De Rosales RT, Alvarez-Hernandez D, Shroff R, Yin X, Muller K, Skepper JN, Mayr M, Reutelingsperger CP, Chester A, Bertazzo S, Schurgers LJ, Shanahan CM. Vascular smooth muscle cell calcification is mediated by regulated exosome secretion. *Circ Res*. 2015;116:1312–23.
48. Cornhill JF, Roach MR. A quantitative study of the localization of atherosclerotic lesions in the rabbit aorta. *Atherosclerosis*. 1976;23:489–501.
49. Fernandez Esmerats J, Villa-Roel N, Kumar S, Gu L, Salim MT, Ohh M, Taylor WR, Nerem RM, Yoganathan AP, Jo H. Disturbed flow increases UBE2C (ubiquitin E2 ligase C) via loss of miR-483-3p, inducing aortic valve calcification by the pVHL (von Hippel-Lindau protein) and HIF-1alpha (hypoxia-inducible factor-1alpha) pathway in endothelial cells. *Arterioscler Thromb Vasc Biol*. 2019;39:467–81. PMC6393167.
50. Schlotter F, Halu A, Goto S, Blaser MC, Body SC, Lee LH, Higashi H, DeLaughter DM, Hutcheson JD, Vyas P, Pham T, Rogers MA, Sharma A, Seidman CE, Loscalzo J, Seidman JG, Aikawa M, Singh SA, Aikawa E. Spatiotemporal multi-omics mapping generates a molecular atlas of the aortic valve and reveals networks driving disease. *Circulation*. 2018;138:377–93. PMC6160370.
51. Isaacson W. Leonardo da Vinci. New York, NY: Simon & Schuster; 2017.
52. Turner CH, Forwood MR, Otter MW. Mechanotransduction in bone: do bone cells act as sensors of fluid flow? *FASEB J*. 1994;8:875–8.
53. Balachandran K, Suscosky P, Jo H, Yoganathan AP. Elevated cyclic stretch induces aortic valve calcification in a bone morphogenic protein-dependent manner. *Am J Pathol*. 2010;177:49–57. PMC2893650.

54. Carew TE, Patel DJ. Effect of tensile and shear stress on intimal permeability of the left coronary artery in dogs. *Atherosclerosis*. 1973;18:179–89.
55. Parhami F, Morrow AD, Balucan J, Leitinger N, Watson AD, Tintut Y, Berliner JA, Demer LL. Lipid oxidation products have opposite effects on calcifying vascular cell and bone cell differentiation. A possible explanation for the paradox of arterial calcification in osteoporotic patients. *Arterioscler Thromb Vasc Biol*. 1997;17:680–7.
56. Rogers MA, Chen J, Nallamshetty S, Pham T, Goto S, Muehlschlegel JD, Libby P, Aikawa M, Aikawa E, Plutzky J. Retinoids repress human cardiovascular cell calcification with evidence for distinct selective retinoid modulator effects. *Arterioscler Thromb Vasc Biol*. 2020;40:656–69. PMC7047603.

Chapter 2

Basic Pathology of Arterial and Valvular Calcification in Humans



Atsushi Sakamoto, Yu Sato, Alope V. Finn, and Renu Virmani

Introduction

The presence of vascular calcium is synonymous with the development of atherosclerosis and has long been used as a surrogate marker for the presence of vascular disease. Population-based imaging studies suggested that coronary artery calcification associates with the extent of atherosclerotic plaque burden and is an established predictor of future cardiac events [1]. However, at the pathological level, the relationship between coronary artery calcification and plaque instability is complex and is not fully understood. Moreover, peripheral arteries such as the lower extremity have distinct characteristics, since both intimal and medial calcifications are commonly observed, whereas coronary artery calcification is predominantly intimal. Carotid artery disease is limited to the unique anatomic location at the bulb of the carotid bifurcation where blood flow disturbance contributes to the acceleration of the atherosclerotic process.

Valvular calcification including degenerative aortic valve and mitral annular calcification is commonly observed in the elderly population due to population aging especially in the developed nations. Pathologic and clinical studies have suggested a link between risk factors of atherosclerosis and valvular calcification, while the mechanisms of vascular and valvular calcification are not necessarily overlapping. Some of the congenital and acquired valvular heart diseases are often associated with valvular calcification; examples of the latter include bicuspid/unicuspid aortic valve, mitral valve prolapse, and rheumatic heart disease.

In this chapter, we will focus on calcification regarding human coronary and peripheral artery disease as well as aortic and mitral valvular calcification from a pathologic perspective.

A. Sakamoto · Y. Sato · A. V. Finn · R. Virmani (✉)
CVPath Institute, Inc., Gaithersburg, MD, USA
e-mail: rvirmani@cvpath.org

Classification of Vascular Calcification

Arterial wall calcification is categorized into three distinct types: (1) inflammatory (atherosclerotic, mostly intimal), (2) metabolic (chronic kidney disease [CKD] and diabetes mellitus [DM], which include intimal and medial), and (3) genetic causes, e.g., pseudoxanthoma elasticum, generalized arterial calcification of infancy, arterial calcifications attributable to deficiency in CD73, and others (Table 2.1) [2]. Atherosclerotic intimal calcification and medial calcification are thought to occur through different mechanisms (e.g., intimal calcification is related to lipid deposition or inflammation, while medial calcification is associated with specific location and is considered mostly a metabolic process although some overlap exists with intimal). A combination of risk factors such as hyperlipidemia, DM, and CKD all are associated with calcification of both the intimal and medial wall of particular blood vessels. Medial calcification is believed to originate from the conversion of smooth muscle cells (SMC) to osteochondrogenic-like cells due to upregulation of specific

Table 2.1 Proposed categorization of common disease-associated pathological calcification

	Category I	Category II	Category III
Mediators	Inflammatory	Metabolic	Genetic
Commonly associated diseases	Atherosclerosis	Chronic kidney disease; diabetes mellitus	Genetic disorders, e.g., PXE, GACI, ACDC, Marfan syndrome
Arterial site	Intima	Media	Usually media
Regulatory manner	Gain of activators; loss of inhibitors	Loss of inhibitors; gain of activators	Loss of inhibitors; gain of activators
Molecular aspects	Osteogenesis and/or chondrogenesis; matrix vesicle release	Nucleation in vesicles or elastin; osteogenesis	Defects in various genes, e.g., <i>ENPP1</i> , <i>ABCC6</i> , <i>NT5E</i> , <i>SLC20A2</i> , <i>MGP</i> , <i>OPG</i> , <i>Ank</i>
Circulating factors	Lipids; cytokines; fetuin	Phosphate; uremic toxins; glucose; soluble RAGE; fetuin	Various, e.g., ATP, pyrophosphate, adenosine, inorganic phosphate
Example local factors	Oxidized lipids; cytokines; matrix metalloproteinases	Elastin; proteases; AGEs; RAGE; transglutaminase; MGP	Elastin; fibrillin; pyrophosphate
Functional effect	Vascular stiffness; plaque vulnerability	Vascular stiffness	Vascular stiffness
Possible analogous ossification	Endochondral ossification	Intramembranous ossification	Variable

Permission from Demer and Tintut [2]

PXE pseudoxanthoma elasticum, *GACI* generalized arterial calcification of infancy, *ACDC* arterial calcifications due to deficiency in CD73, *miRs* micro RNAs, *ENPP1* ectonucleotidase pyrophosphate phosphodiesterase, *ABCC6* ATP-binding cassette subfamily C member 6, *NT5E* 5'-nucleotidase, ecto (CD73), *SLC20A2* solute carrier family 20 (phosphate transporter), member 2, *AGEs* advanced glycation end products, *RAGE* receptor for AGEs, *MGP* matrix gamma-carboxyglutamic acid protein, *OPG* osteoprotegerin, *Ank* ankylosis protein

osteogenic biomarkers [3]. Additionally, metabolic mediators may be involved along with genetic predisposition, which can lead to medial as well as intimal calcification in the arterial wall. Thus, although we classified calcification into three broad categories, it must be recognized that a considerable overlap of mechanisms likely exists. More detailed mechanisms of vascular calcification are provided in Chap. 6.

Pathology of Coronary Artery Calcification

Natural History of Atherosclerosis Progression

The natural history of atherosclerosis includes a dynamic process from early lesion development to advanced stage of lesion progression complicated by acute luminal thrombosis (Fig. 2.1). Histologically, non-atherosclerotic intimal lesions (i.e., adaptive intimal thickening [AIT] or diffuse intimal thickening [AHA type I]) already exist from birth [4] and are often observed in atherosclerosis-prone regions. Although AIT is considered as a response to blood flow and is not considered an atherosclerotic process, it is likely an important transitional lesion especially in high-risk regions where more advanced atherosclerotic lesions (i.e., pathologic intimal thickening [PIT]) are observed [5].

Fatty streak (FS) or intimal xanthomas (AHA type II) are characterized by infiltration of foamy macrophages and, to a lesser extent, lipid-laden SMC in the intima. Regression of FS has been observed over time, although the reason why macrophages migrate back into the lumen and diminish in certain locations is unclear [6]. Focal areas of accumulation of SMCs with proteoglycan-rich extracellular matrix (ECM) are found at the areas of intimal thickening without inflammation. It remains unclear whether the intimal proliferation is an adaptive vascular reaction against blood flow or a precursor of an advanced atherosclerosis [6, 7].

PIT (AHA type III) is recognized as the earliest lesions of the progressive atherosclerosis. “Lipid pool” is an essential intimal characteristic of PIT which is composed by ECM proteoglycans and collagen type III derived from SMC as well as extracellular lipids, most of which are located deep within the plaque, close to the media [7]. Lipid pool is different from necrotic core (NC), a characteristic feature of fibroatheroma (FA) that contains acellular debris and lacks ECM; these lesions may be focal or diffuse. There is a lack of SMCs but remnants of SMC are observed within the lipid pool in PIT lesions. Negatively charged sulfate proteoglycans (e.g., versican, biglycan, and decorin) are observed in these locations and are proposed as contributors of lipoprotein retention at sites of lipid pools, which is the earliest initial atherogenic process [8–10], although the precise mechanism remains unclear.

FAs are characterized by the presence of an acellular NC, which must be distinguished from lipid pool PIT lesions since they imply further progression of atherosclerosis (AHA Type IV) [11]. FAs are the most distinguishable advanced plaque that consists of a well-defined lipid-rich NC encapsulated by surrounding

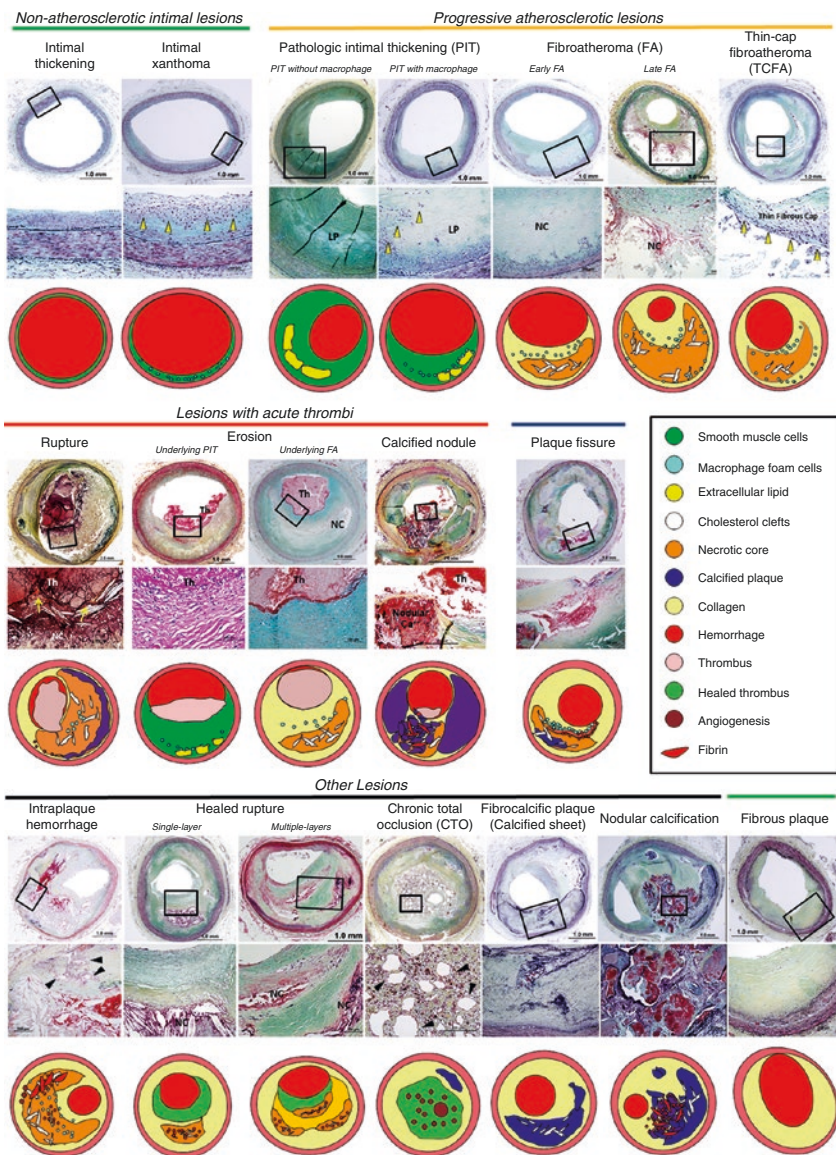


Fig. 2.1 Spectrum of human atherosclerosis progression. The two nonprogressive lesions are adaptive intimal thickening (AHA type I) and intimal xanthomas (foam cell collections know as fatty streaks, AHA type II). Pathological intimal thickening (PIT, AHA type III, transitional lesions) marks the first of the progressive plaques since they are the assumed precursor to more advanced fibroatheroma (FA), which are classified into early and late FA. Thin-cap fibroatheroma (TCFA) is a precursor lesion of plaque rupture. Lesions with acute thrombosis are rupture, erosions (occur on a substrate of PIT or FA), and calcified nodules, and luminal discontinuity with or without thrombus is plaque fissure. Other lesions seen in the coronary arteries are intraplaque hemorrhage, healed plaque ruptures (single-layer or multiple-layers), chronic total occlusion, fibrocalcific plaque (usually with calcified sheets), nodular calcification and fibrous plaques. (Modified with permission from Virmani et al. [7] and Yahagi et al. [11]) Abbreviations: Ca²⁺, calcification; FC, fibrous cap; LP, lipid pool; NC, necrotic core; Th thrombus

fibrous tissue [7, 12], and we have proposed dividing it into early and late stages. The early stage of FA shows infiltration of macrophages into the lipid pool accompanied by focal regions of loss of ECM with greater presence of free cholesterol but focal distribution of proteoglycans and other matrix proteins, like type III collagen, while NC of late FA demonstrates larger amount of free cholesterol and discrete accumulation of cellular debris. The ECM in the NC of late FA is mostly depleted, presumably due to protein degradation by matrix metalloproteinases released from macrophages and SMCs. Moreover, large numbers of apoptotic macrophages are often observed within the NC, leading to abundance of apoptotic bodies within the NC. Intraplaque hemorrhage, apparently derived from leaky vasa vasorum, which has a poor endothelial cell-cell integrity near the NC, can lead to a substantial rapid luminal narrowing, secondary to intraplaque hemorrhage.

As the plaque progresses, the NC develops an overlying layer of thick fibrous tissue, i.e., fibrous cap, which is composed mostly of types I and III collagen, proteoglycans, and interspersed SMCs with overlying endothelial cell layer. When the fibrous cap is thin, the lesion is known as a thin fibrous cap fibroatheroma (TCFA) or often described as “vulnerable plaque,” which may ultimately rupture resulting in a luminal thrombus that may or may not occlude the lumen. It is the fibrous cap thickness that determines whether the plaque is called a thin cap. The cutoff that is used to define a plaque as vulnerable was determined by measuring plaques with ruptures. The mean thickness of the cap nearest the site of rupture was $23 \pm 19 \mu\text{m}$ and 95% of the caps measured $<65 \mu\text{m}$ [13]; accordingly, the cap of TCFA was defined as less than $65 \mu\text{m}$. Not only is the cap $<65 \mu\text{m}$ but is composed mostly of type I collagen with infiltration by macrophages and T lymphocytes [14–16]. SMCs are rarely observed or may be absent due to apoptosis as shown by Libby et al. [17].

Plaque rupture (PR) is the most frequent cause of acute coronary syndrome (ACS) and accounts for 65% of all cases of luminal thrombosis [7]. Compared with TCFA, the NC is larger and there are a greater number of inflammatory cells in the fibrous cap of ruptured plaque. In general, the rupture of the fibrous cap occurs at the thinnest region where the cap is the weakest. It has been reported that the cap usually ruptures in the shoulder regions; nevertheless, a prior autopsy study demonstrated that an equal number of ruptures occurred at the middle portion of the fibrous cap, especially if death occurred during exercise [18]. Different processes may be responsible for the final event of rupture, where macrophage density is the highest, and increased protease activity as well as high shear and tensile stresses [19] could contribute to weakening of the fibrous cap at the rupture site [20]. Moreover, macrophage- or SMC-derived microcalcifications within a thin fibrous cap have been proposed to play an important role in the initiation of rupture [21]. At the sites of rupture, cellular and noncellular elements of circulating blood may contact directly with highly thrombogenic components of the NC (e.g., tissue factor), which could result in luminal thrombus formation. A platelet-rich white thrombus is observed at the culprit rupture site, while the thrombus containing fibrin and trapped erythrocytes is located at the sites of propagation at proximal and distal regions of rupture

site. Thrombus organization then follows and is characterized by accumulation of inflammatory cells, endothelial cells, and SMCs admixed with ECM such as proteoglycans and type III collagen.

Plaque erosion (PE) is the second most prevalent cause of ACS (25–30%). PE is defined as an acute thrombus in direct contact with the intima in an area devoid of endothelium. Fibrous cap disruption is absent in PE [22]. The underlying lesion of PE is usually less advanced than in ruptured plaques and normally exhibits characteristics of early lesions (i.e., PIT or FA) usually without an extensive NC, hemorrhage, or calcification. Numerous SMCs and increased levels of proteoglycans such as versican, hyaluronan, as well as type III collagen are observed near the thrombus attachment site of erosion. In contrast, the rupture sites show more advanced lesions of necrotic core with a thin disrupted cap, and stable lesions are rich in type I collagen and calcium with or without a necrotic core [23]. Fewer macrophages and T lymphocytes are observed in erosion unlike ruptured plaques that are rich in inflammatory cells [22, 23]. Our early studies on sudden coronary death showed PE occurred in greater proportion in women, at a younger age, with less underlying luminal narrowing, less plaque burden, greater emboli, and less calcification than ruptured plaques [22].

Healed plaque ruptures (HPR) can be detected in severely narrowed arteries showing breaks in the type I collagen-rich fibrous cap with an overlying plaque rich in SMCs surrounded by proteoglycans and/or a type III or type I collagen-rich matrix, which is dependent on the phase of healing [24]. Proteoglycans and type III collagen are the dominant matrices in early-healed lesions with eventual replacement by type I collagen over time. Repeat PR is considered to be one of the causes of rapid plaque progression with luminal narrowing [24, 25]. Percent cross-sectional luminal narrowing increases as the number of healed ruptures increases at the same site, contributing to the progression of percent stenosis [24].

Fibrocalcific plaques are the lesion with a thick fibrous cap and an extensive deposition of calcification [24, 26], typically observed in patients with a history of stable angina and severe luminal narrowing. Coronary calcification is highly correlated with plaque burden; however, the amount of coronary calcification and plaque instability are not correlated in a linear manner, because the greater the calcification, the more stable the plaque, with lack of thrombus [27]. Usually severely narrowed fibrocalcific plaques have minimal or absence of NC. Fibrocalcific plaques may represent the final end stage of ruptured plaques, or HPR or FA may also represent “burnt-out” lesion with dominance of calcification.

Calcified nodule is the least frequent (<5%) cause of ACS [7] and occurs in arteries that are highly calcified and tortuous. Pathologically, we believe that highly calcified fibroatheromas may break and form fragmented calcified nodules that protrude into the lumen with disruption of the cap and loss of endothelium that lead to luminal thrombus which is platelet-rich “white” thrombus. The eruptive calcified nodule is usually eccentric, protruding into the lumen. Fibrin is frequently found between the spicules of calcium, with or without osteoclasts and inflammatory cells. Calcified nodule is generally more prevalent in older men and women and in patients

with tortuous coronary arteries, DM, or CKD. The location of this lesion is most frequent at the sites of maximal tortuosity such as mid-right coronary artery or left anterior descending artery or near bifurcation of left main artery. Pathologically, “calcified nodule” and “nodular calcification” should be distinguished, with former lesion demonstrating a luminal thrombus with disrupted fibrous cap and latter lesions lacking thrombus but showing presence of an intact fibrous cap. Nodular calcification likely shares a similar etiology as calcified nodule, but the fibrous cap remains intact. Both lesions, i.e., calcified nodules and nodular calcification, are more common and are seen in highly calcified tortuous arteries. These lesions may show medial disruption with nodules of calcium protruding into the adventitia. Intraplaque fibrin is also detected in nodular calcification, likely resulting from disruption of capillaries.

Atherosclerotic Intimal Calcification and Its Progression

Intimal calcification is strongly associated with atherosclerotic plaque progression. Calcification is classified depending on the size and type of plaque [27, 28] (Fig. 2.2a, b). In pathologic studies, microcalcification is defined as calcium particles varying in size from $\geq 0.5 \mu\text{m}$ to less than $15 \mu\text{m}$ in diameter. Punctate calcification occurs as calcium deposits are $\geq 15 \mu\text{m}$ but less than 1mm and are thought to be the result of calcification of macrophage-derived apoptotic bodies and are commonly seen in superficial and deeper areas of the NC. Fragmented calcification occurs when deposits become $\geq 1 \text{mm}$ and the mechanisms are poorly understood. Sheet calcification is observed when greater than 1 quadrant of the vessel circumference is calcified and may be seen in stable and unstable plaques. Nodular calcification, as mentioned above, is identified when nodular calcium deposits are confined within the plaque or may protrude into the lumen, but the fibrous cap is intact. However, when the nodules of calcium protrude through the plaque into the lumen and there is loss of endothelium with overlying thrombus, such a lesion is called “calcified nodule.” These definitions are applicable not only to coronary arteries but also to peripheral arteries and also to intimal and medial calcification.

In general, early lesions (i.e., AIT and FS) show lack of calcification. PIT is the earliest lesions which exhibit calcification and occurs in lipid pools arising as microcalcification recognized by von Kossa and/or Alizarin red [28] (Fig. 2.3a). Early microcalcification may originate from apoptotic body from SMC, which are detectable by light microscopy when the size is generally $\geq 0.5 \mu\text{m}$ [29–31]. High-resolution microscopy has also demonstrated that initial microcalcification occurs within extracellular vesicles of $100\text{--}300 \text{nm}$ in diameter [32–34]. (More information on extracellular vesicles is provided in Chap. 5.) Microcalcifications are located around the advanced calcification, which is often observed in the intima within the lipid pool and is close to the internal elastic lamina. We have reported a 57% incidence of calcifications of ≥ 0.5 but $< 15 \mu\text{m}$ in PIT, whereas in early FA the incidence

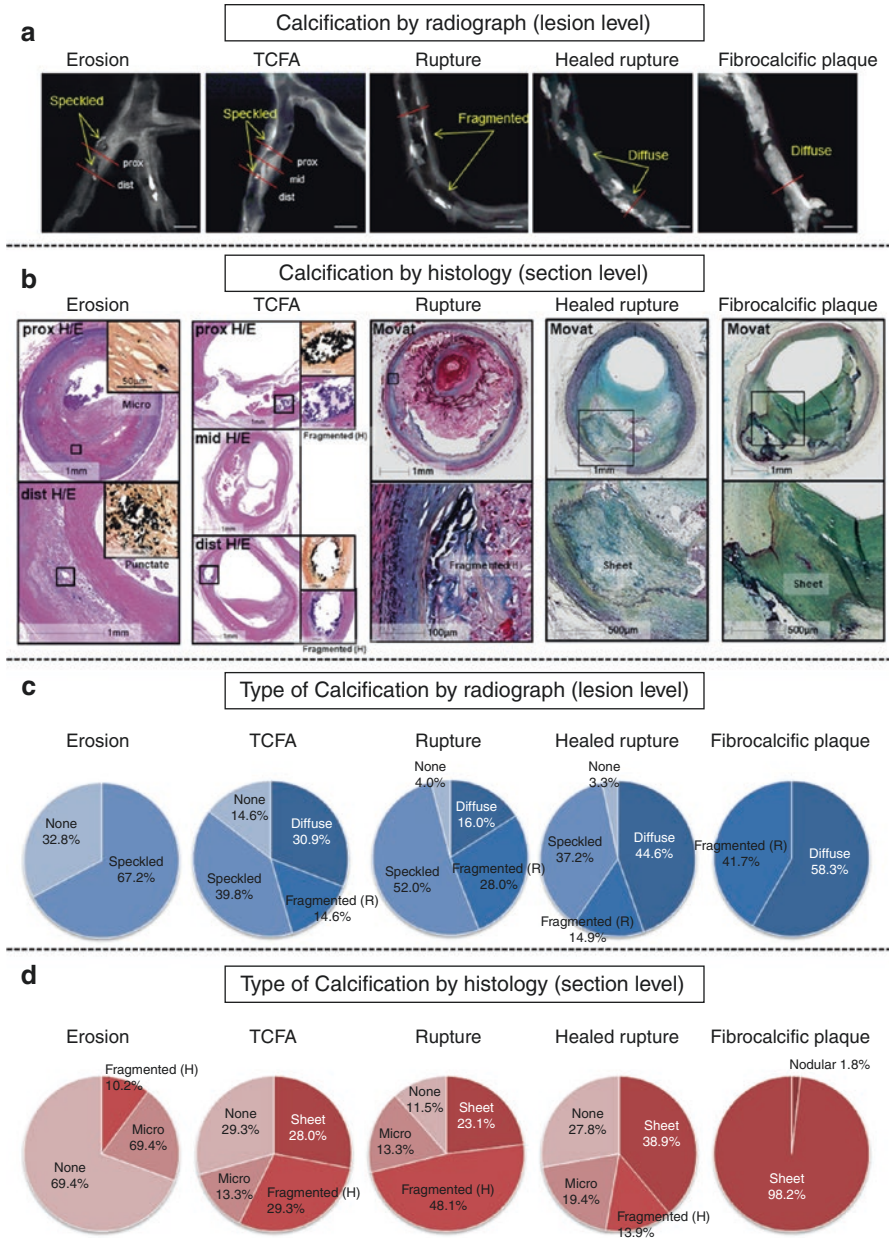


Fig. 2.2 Types of calcification by radiography and histology. **(a)** The typical patterns of calcification by radiography for each plaque type. **(b)** Corresponding histology with low- and high-power images of sections taken from the areas shown in radiographs as red line. Scale bar (white line) in radiograph indicates magnification. Microcalcification by histology is invisible by radiograph in proximal section from a case of coronary erosion. Speckled calcification by radiograph corresponds to punctate or fragmented calcification by histology. TCFA lesions show three sites of sectioning and two spots (proximal and distal) of speckled calcium with the middle section showing TCFA without calcification. Plaque rupture site shows fragmented

of early and punctate calcification is 100% [35]. Further, areas of calcifications detected within the lipid pool coexist with osteogenic proteins (e.g., osteoprotegerin [OPG], osteopontin [OPN], and matrix Gla protein [MGP]) (Fig. 2.3a, b).

The FAs are often accompanied by focal calcification, also known as microcalcification (Fig. 2.3b). Microcalcification may also occur from macrophage- or SMC-derived extracellular vesicles or from apoptotic bodies, released by macrophages and SMCs [36]. Macrophage apoptosis may result in a different morphological appearance of calcification (i.e., large punctate, blocky appearance) compared to fine microcalcification originated from SMC apoptosis [35]. CD68 antigen associated with macrophage-related microcalcifications is co-located in early NC (Fig. 2.3b). Microcalcifications often fuse into larger masses and involve both the NC and the surrounding collagen-rich ECM to form speckled and fragments of calcification. This specific pattern of calcification also begins from the deeper region of the NC close to the internal elastic lamina (Fig. 2.3c) and extends from the outer rim of the NC (Fig. 2.3d, f) into the surrounding collagenous matrix. Center of NC either becomes fully calcified or may remain noncalcified even in late stage of the disease. Nonetheless, further progression of plaque calcification results in calcified sheets or nodules (Fig. 2.3g-i); however the mechanisms are poorly understood.

Although coronary artery calcification highly correlates with total coronary plaque volume, the pathologic data suggest that highly calcified lesions are not associated with plaque instability. Indeed, previous studies of sudden coronary death victims showed that the majority of acute PRs occur in areas of either no or micro- or fragmented speckled calcification and severe calcified segments were associated with HPRs or fibrocalcific plaques [37] (Fig. 2.2a-d and 2.3e). TCFA, a precursor lesion of PR, also showed that the type of calcification is similar to PR [37]. Overall our data suggest that the calcification patterns seen in unstable (PR, TCFA, and PE) coronary plaques are usually micro- or fragmented or no calcification and only approximately 25% of cases show presence of sheet calcium (i.e., calcification involving ≥ 1 quadrant). The total percent calcified area in PRs is $<5\%$ with a total area of $0.58 \pm 0.99 \text{ mm}^2$, whereas the calcified area in stable plaque is $\sim 1 \text{ mm}^2$ suggesting that mildly to moderately calcified segments are the most likely to rupture [37, 38]. Microcalcification within a thin fibrous cap (typically $10 \mu\text{m}$ in diameter) facilitates PR through local increase in stress that leads to interfacial debonding due to mismatch in material properties between microcalcification and surrounding tissue [21, 30]. Huang et al. reported there was no significant correlation between percent area of calcification and stress. In fact, large amounts of calcification, by virtue of bearing mechanical load, actually decrease stresses, whereas removing a large amount of calcium may increase instability of the plaque [39].



calcification by radiograph, which corresponds to fragmented calcification by histology. Healed rupture and fibrocalcific plaques sites both show diffuse calcification by radiograph which corresponds to sheet calcification by histology. **c** and **d** show type of calcification by radiography (lesion level) and histology (section level) in different types of plaques. (Reproduced with permission from Mori et al. [27]). Abbreviations: Dist distal; fragmented (H), fragmented by histology; H/E, hematoxylin-eosin stain; Mid, middle; Prox, proximal; TCFA, thin-cap fibroatheroma

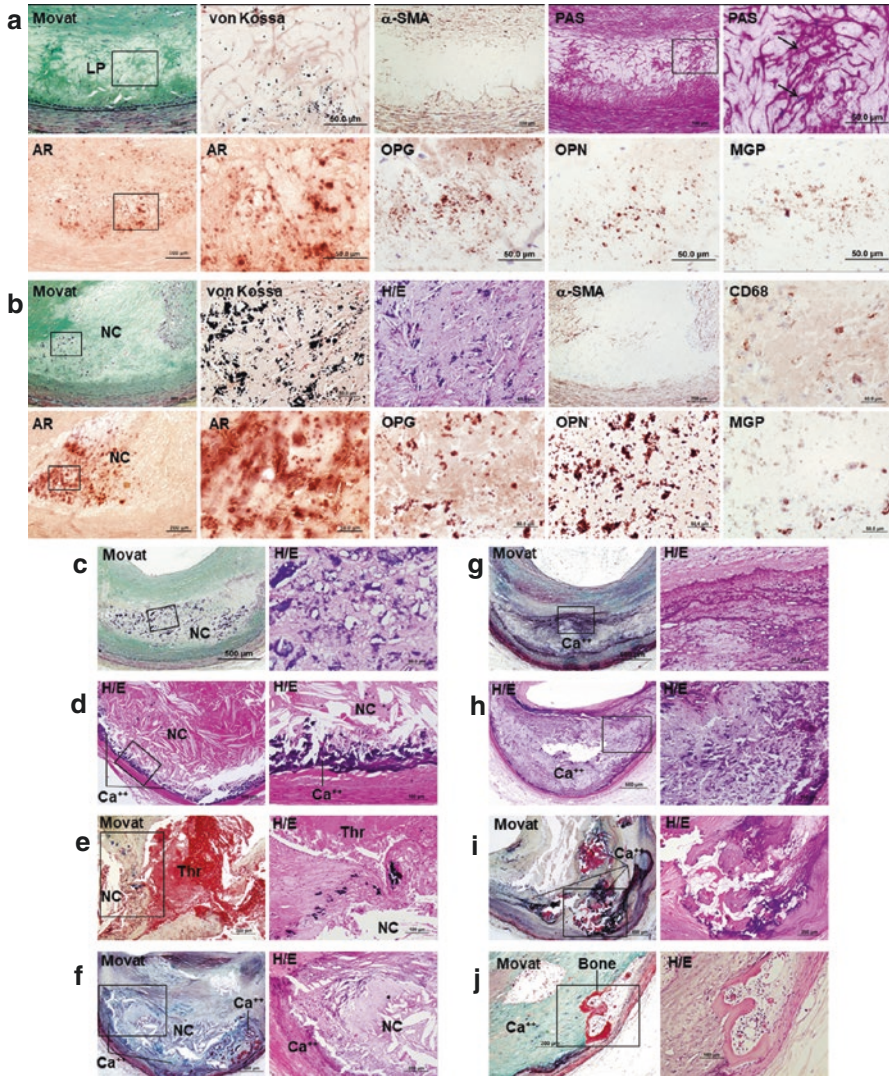


Fig. 2.3 Histologic progression of coronary calcification. Non-decalcified arterial segments (**a, b**) and decalcified segments (**c–j**) were serially sectioned for microscopic assessment. (**a**) Pathologic intimal thickening (PIT) characterized by lipid pool (LP) that lacks smooth muscle cells (SMCs; negative for α -smooth muscle actin [α -SMA]) and the presence of apoptotic SMCs, which can be identified by prominent basement membrane stained positive with periodic acid–Schiff (PAS), and the arrows point to in the high-power image (top right corner). Early microcalcification ($\geq 0.5 \mu\text{m}$, typically $< 15 \mu\text{m}$ in diameter) and calcification are detected by von Kossa and Alizarin red (AR) staining within the LP (corresponding with a boxed area in the Movat image) where bone-related proteins such as osteoprotegerin (OPG), osteopontin (OPN), and matrix Gla protein (MGP) are detected. (**b**) Early fibroatheroma not only lacks SMCs but also is infiltrated by macrophages, which eventually undergo apoptosis and calcification, which is observed as punctate ($\geq 15 \mu\text{m}$) areas of calcification. The microcalcification in early necrotic core (NC) shows variable amounts of staining for macrophage CD68 antigen; however, von Kossa and AR staining clearly show rela-

Pathologically, diffuse areas of calcification are described as sheet calcification which are frequently observed in HPRs and fibrocalcific plaques. Sheet calcification can be easily detected by radiography, CT as well as intravascular imaging (Fig. 2.4).

Immunohistochemical studies and gene expression analysis have demonstrated that bone morphogenetic protein (BMP), OPN, bone sialoprotein, and the osteoblast specific transcription factor for bone formation are highly expressed in the calcified arteries. Heavily calcified lesions usually show absence of inflammatory cells. It is still actively debated whether all calcification is active or passive, more and more evidence is in favor of an active process [40, 41] although few of us still adhere to the degenerative mechanism without biological regulation and consists of precipitation of calcium phosphate crystals due to pH changes in the environment [2, 42, 43].

In areas of arterial calcification, bone formation can be detected in approximately 10% of cases (Fig. 2.3j), particularly in heavily calcified segments, suggesting osteogenesis is induced at sites of heavy arterial calcification. While the incidence of bone formation in coronary arteries is rare, peripheral artery bone formation in patients who underwent lower limb amputation is common with the reported incidence is 19% to 83% [44, 45].

Pathology of Peripheral Artery Calcification

Morphologically the arterial system is categorized into three types, i.e., large vessels (aorta and its main branches), medium-sized arteries (the main visceral arteries), and small arteries. The conducting arteries are elastic arteries including the aorta and iliac and carotid arteries. The tunica media is the largest layer of the wall and is comprised of multilayered elastic lamellae that are separated by SMCs with interspersed proteoglycans and collagen. The coronary and lower extremity arteries such as femoral, popliteal, and tibial arteries are classified into muscular arteries.

tively larger punctate areas of calcification resulting from macrophage cell death within the NC as compared with microcalcification of dying SMCs. These calcified macrophages show colocalization of bone-related proteins. Substantial amount of macrophage calcification can be observed in early NC (c), but the degree of calcification in NC typically increases toward the medial wall where fragmented calcifications can be seen (d). Microcalcification resulting from macrophage or SMC deaths can also be detected within a thin fibrous cap and may be associated with plaque rupture (e). Calcification generally progress into the surrounding area of the NC (f), which leads to the development of sheets of calcification where both collagen matrix (g) and NC itself are calcified (h). Nodular calcification may occur within the plaque in the absence of luminal thrombus and is characterized by breaks in calcified plates with fragments of calcium separated by fibrin (i). Ossification may occur at the edge of an area of calcification especially in nodular calcification (j). (Modified and reproduced with permission from Otsuka et al. [28]). Abbreviations: AR, alizarin red; Ca⁺⁺, calcification; H/E, hematoxylin and eosin; LP, lipid pool; MGP matrix Gla protein; NC necrotic core; OPG osteoprotegerin; OPN osteopontin; PAS periodic acid–Schiff; SMA smooth muscle cell actin; Thr thrombus

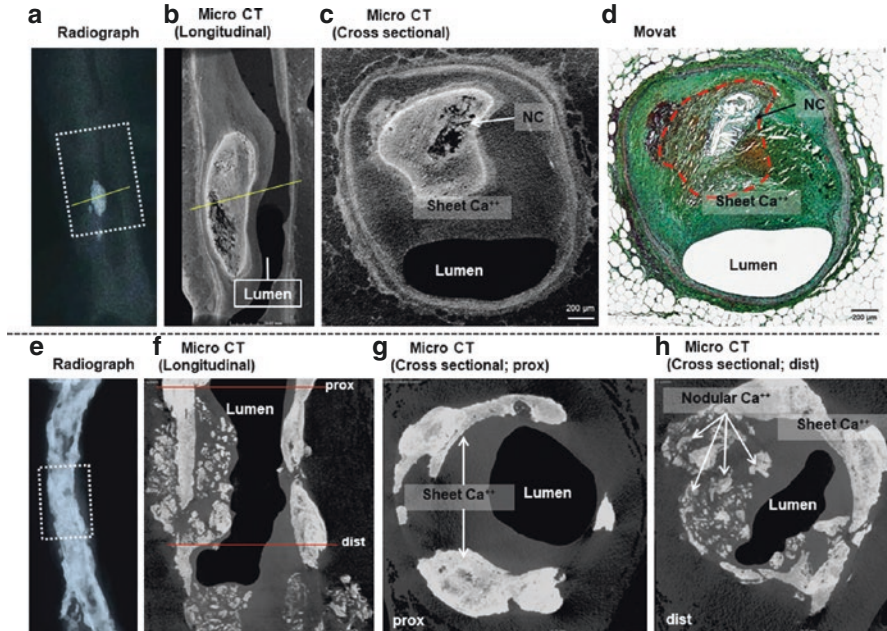


Fig. 2.4 Calcification detected by micro CT. (**a, b**) Radiograph and micro CT lesions from a distal left anterior descending artery in longitudinal view. A fragment of calcium shown by radiography (**a**) can be seen by micro CT (**b**) that has been stained using potassium iodine. The calcified area shows as bright image, while the NC within the site of calcification appears as black void space. (**c**) Micro CT cross section. Following decalcification, histological Movat sections (**d**) show a fibroatheroma with calcification. Yellow lines in **a** and **b** indicate the location of cross-section in **c** and **d**. Red dotted line in Movat staining represents border of sheet calcification. (**e–h**) Images of distal right coronary artery obtained from a 55-year-old male who died suddenly during hemodialysis. Radiography (**e**) and micro CT images (**f–h**) were obtained with contrast medium (10% MD-76 contrast, Mallinckrodt Inc., Missouri). The image in **e** shows extensive diffuse calcification, and the boxed area shows matched micro CT (**f**). Sheet and nodular calcification are observed. Red lines in **f** indicate the location of cross section in **g** and **h**. (Modified and reproduced with permission from Mori et al. [27]). Abbreviations: dist, distal; Ca⁺⁺, calcification; CT, computed tomography; NC, necrotic core; prox, proximal

The media of these arteries is characterized by distinct internal and external elastic membrane, and in between the two layers of elastic lamellae, there is a relatively thick layer of SMCs with interspersed proteoglycans and collagen. The small arteries are the intraparenchymal arteries and arterioles.

Medial Calcification or Mönkeberg's Sclerosis

Medial calcification, which is also called Mönkeberg's sclerosis, is a feature of peripheral artery disease (PAD) making it different from coronary artery disease, although intimal calcifications is common in both locations (Fig. 2.5 and 2.6; also

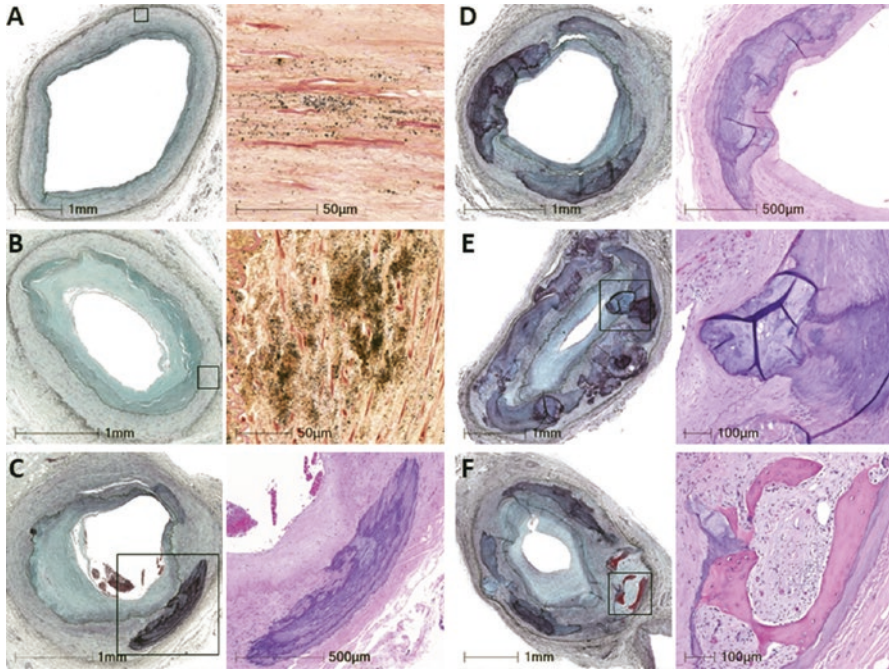


Fig. 2.5 Representative histological images of medial calcium progression in human lower extremity peripheral arteries. (a) Medial microcalcification (black dots) of the media by von Kossa stain of non-decalcified section in an artery showing adaptive intimal thickening. (b) Medial punctate calcification of the media by von Kossa stain. Varying degrees (micro to punctate) of calcification are seen circumferentially involving the media. (c) Medial fragment of calcification is seen in Movat and H&E stains of a decalcified section. (d) Medial sheet calcification involving nearly three quarters of the circumference. (e) Combination of medial nodular and sheet calcification covering the circumference of the medial wall. (f) Bone formation in the presence of near circumferential medial sheet calcification with presence with lacunae containing osteoblasts and bone marrow. (Reproduced with permission from Torii et al. [55])

described in Chap. 9). In Mönckeberg's sclerosis, the media of small- and medium-sized muscular and large muscular arteries become calcified with or without associated intimal atherosclerosis; while the etiology is unknown, it is considered as non-inflammatory processes. In the early stage, the elastic lamina is affected with hydroxyapatite crystal deposition followed by adjacent medial wall involvement by the calcific deposits. In general, intimal and adventitial layers are spared in cases of isolated medial calcification. Coronary artery disease is the leading cause of death in women in the United States; however, it is uncommon in women <50 years of age and is difficult to diagnose clinically. Mammography is recommended in women over the age of 40 years. Multiple observational studies have shown an association between presence of Mönckeberg's medial calcification in breast artery and coronary artery calcification, allowing mammography as a cardiovascular risk stratification tool [46].

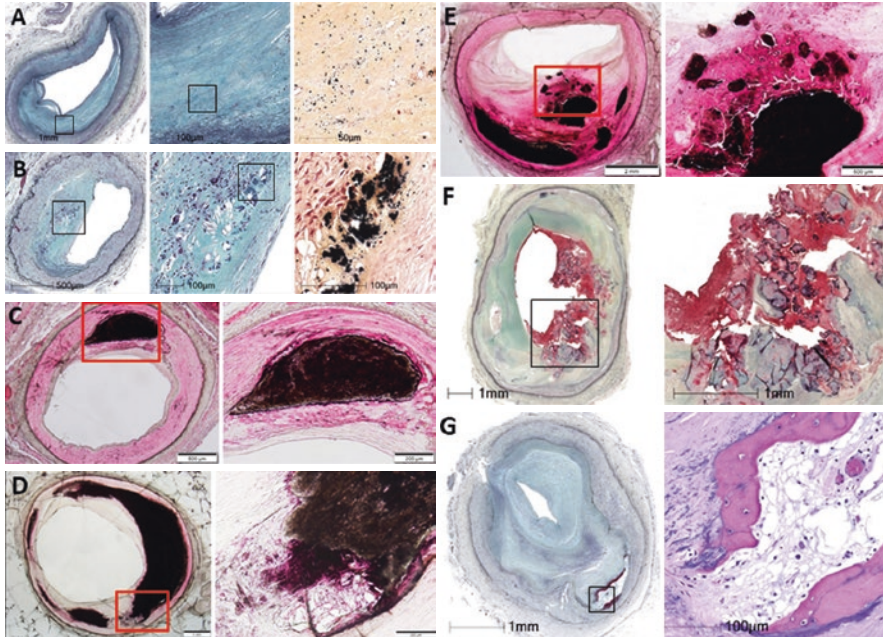


Fig. 2.6 Representative histological images of intimal calcium progression in human lower extremity peripheral arteries. **(a)** Intimal microcalcification is observed in areas of lipid pools (boxed area) where there is SMC loss from apoptosis; von Kossa stain from a corresponding non-decalcified section showing microcalcification (black dots). The calcifications cannot be seen on Movat pentachrome-stained section, because of small size. **(b)** Intimal punctate calcification in the area adjacent to the lipid pool shown in Movat- and von Kossa-stained sections (non-decalcified section). **(c)** Intimal fragment calcification with microcalcification in media (red box) (non-decalcified section). **(d)** Intimal sheet calcification (arrow) that involves more than 50% of the circumference with adjoining two areas of fragments of medial calcifications (arrowheads) (non-decalcified section). **(e)** Intimal nodular calcification (non-decalcified section). **(f)** Calcified nodule with luminal fibrin thrombus; note absence of endothelium lining and collagen over the surface of the nodules (Movat stain, decalcified section). **(g)** Intimal bone formation. (Reproduced with permission from Torii et al. [55])

Older age, larger body mass index, end-stage CKD, autonomic neuropathies, osteoporosis, dyslipidemia, and DM are reported as risk factors for medial calcification [47–49]. Lower serum levels of bone-related proteins such as OPN and MGP (that belongs to the vitamin K-dependent proteins), along with high levels of alkaline phosphatase, bone sialoprotein, and collagen type II, are related to medial calcification in PAD patients; however, the precise underlying etiology is still unclear [48].

Lower Extremity Calcification

Arteries in different locations show different features and speed of atherosclerotic progression. According to a previous autopsy study, which assessed total 1074 elderly individuals (age 60 to 90) who died from various causes, progression of

atherosclerosis in each artery was assessed. The degree of atherosclerosis increased with age and was maximum in coronary, aorta, and common iliac, followed by femoral, and the least in the carotid and intracerebral arteries [50]. Another pathologic study of 100 autopsy cases (age 20 to 82; 70 men and 30 women) compared atherosclerotic plaques in carotid, coronary, and femoral arteries; the coronary and the carotid plaques were larger and richer in lipid and foam cells than in the femoral arteries, and the latter were more fibrous in nature and developed more slowly [51]. Another study compared femoral and carotid endarterectomy specimens showed a higher prevalence of FA in carotid samples (75%), while femoral plaques were most frequently fibrocalcific (93%), with a higher prevalence of osteoid metaplasia most frequent in femoral (63%) than carotid arteries (20%) [52].

The most advanced stage of PAD is critical limb ischemia (CLI) which is strongly associated with worse cardiovascular outcomes [53]. A pathologic study that evaluated lower limb amputations showed that 76% of segments had medial calcification involving 55% of the circumference. Severe medial calcification (>75% of the circumference) was observed in 37% of the vessels. The highest degree of atherosclerotic narrowing was observed in the anterior and posterior tibial arteries (73% and 72%, respectively), followed by peroneal (68%), popliteal (67%), femoral (64%), and dorsalis pedis (59%) arteries. At the same time, medial calcification was the most prominent in anterior and posterior tibial arteries (58% and 59%), followed by peroneal (55%), dorsalis pedis (54%), popliteal (51%), and femoral (44%) arteries. Coexistent medial calcification and atherosclerotic disease was observed in 77% of arterial segments. However, there was no correlation between medial calcification and degree of atherosclerosis [44]. According to a recent pathologic study involving 239 lower extremity arteries collected from 75 CLI patients who underwent amputation, the atherosclerosis process was more frequent in femoral and popliteal arteries (FEM-POP) than in infrapopliteal arteries (INFRA-POP; anterior and posterior tibial, peroneal and dorsalis pedis) (67.6% vs 38.5%, respectively). Narula et al. reported that only 69% of arteries showed >70% luminal stenosis. Presence of chronic total occlusion (CTO) was more frequent in INFRA-POP than FEM-POP arteries without significant atherosclerosis, while acute thrombi were more frequently seen in FEM-POP than INFRA-POP, suggesting more frequent atherothromboembolic etiology for INFRA-POP in patients with CLI [54]. Moreover, in a more recent study of 12 low extremities from 8 elderly asymptomatic cadavers with abundant atherosclerotic risk factors, the arteries were intact from femoral to dorsalis pedis, and whole length of which was sectioned at 3–4 mm intervals [55]. Atherosclerotic lesions were observed in 93% of above-knee arteries, while in below-knee arteries atherosclerotic lesions were significantly less frequent (57%). Above-knee arteries showed higher prevalence of calcified nodule than below-knee lesions. Acute thrombi were detected in eight above-knee arteries, whereas none were observed in below-knee arteries. However, CTO was seen in ten below-knee vessels; the pathogenesis of CTO was embolic in origin in half of the cases. These results suggest atherothromboembolic etiology is frequent in below-knee lesions. Intimal (75.3%) and medial (86.2%) calcifications were commonly detected. Severity of intimal calcification correlated with percent stenosis, whereas medial calcification did not show any correlation with present stenosis, and severity of medial calcification above- and below-knee arteries was similar (Fig. 2.7).

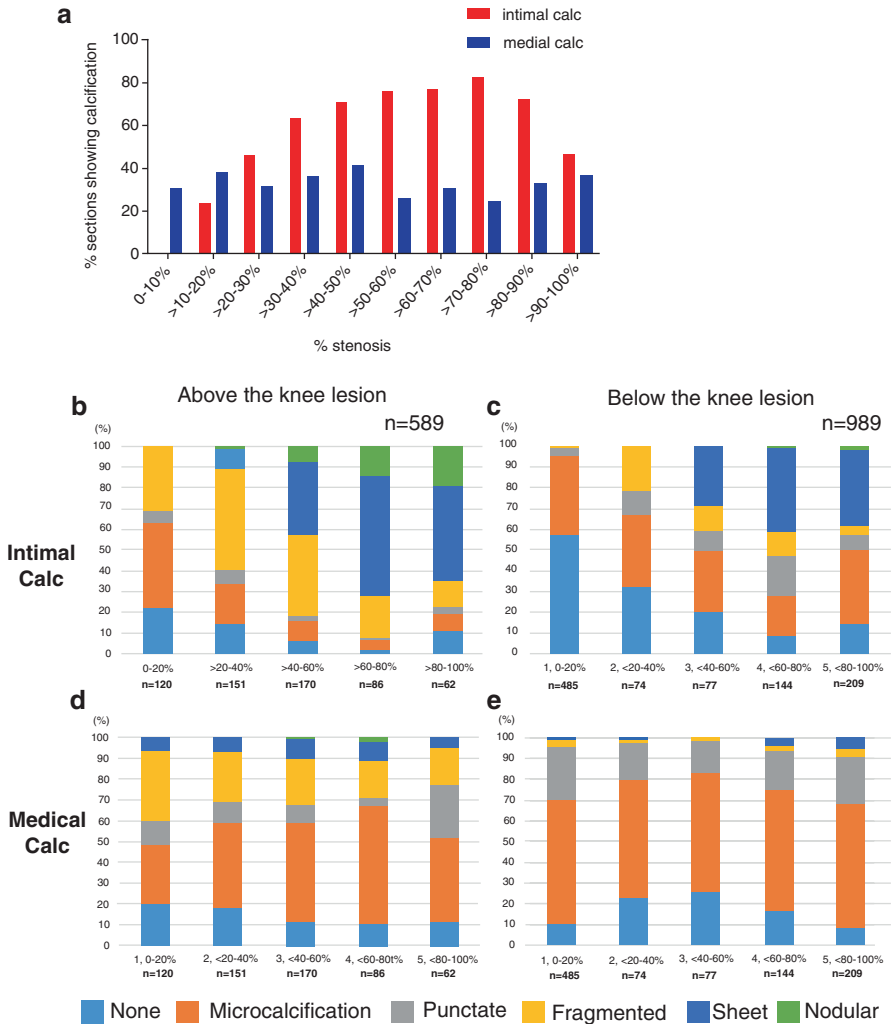


Fig. 2.7 The relationship between percent stenosis and intimal/medial calcification at incremental cross-sectional area narrowing in peripheral artery. **(a)** Relationship between the % sections showing calcification and % stenosis in peripheral artery. Note a good correlation between % stenosis and atherosclerotic intimal calcification, whereas no correlation was observed between % stenosis and medial calcification. **(b-e)** Prevalence of various types of intimal **(b, c)** and medial **(d, e)** calcification morphologies at 20% incremental cross-sectional area narrowing at AK **(b, d)** and BK **(c, e)** lesions. Severe intimal calcification (sheet and nodular calcification) was more frequent in AK than BK lesions, beginning as early as 10–20% cross-sectional area narrowing. In contrast, severe medial calcification was not as frequent in AK and BK; however, fragment calcification was more frequent in AK lesions compared with BK lesions. (Reproduced with permission from Torii et al. [55]). Abbreviations: AK, above the knee; BK, below the knee; dist, distal; Ca⁺⁺, calcification; CT, computed tomography; NC, necrotic core; prox, proximal

Carotid Artery Calcification

Atherosclerotic lesions in the carotid vasculature share common features of advanced atherosclerosis in coronaries, and the classifications applied for coronary artery disease are also applicable to the carotid artery disease (Fig. 2.1). Many similarities exist between the carotid and coronary artery; however, there are several unique features of carotid plaque morphology related to the high flow rates and the shear forces caused by the bifurcation of the common carotid artery into the internal and external carotids. Glagov et al. were the first to show in human carotid arteries that regions with moderate to high shear stress where flow remains unidirectional are spared of intimal thickening [56]. They divided the region of the common carotid and the bifurcation into five different locations (i.e., the common carotid, proximal internal carotid, the midpoint of carotid sinus, distal internal carotid, and external carotid). They showed maximum intimal thickening at the proximal internal carotid and midpoint of carotid sinus, i.e., regions with low wall shear stress with maximum disturbed flow [56]. Plaques tend to occur where flow velocity and shear stress are reduced and flow departs from a laminar, whereas unidirectional flow patterns are protective. Also, the flow characteristics tend to increase the residence time of circulating particles in susceptible regions, while particles are cleared rapidly from regions of high wall shear stress and laminar unidirectional flow. Thus, the unique geometry and flow patterns in the carotid bifurcation contribute to both the degree and type of atherosclerotic plaque [57].

It should be noted that sites of plaque rupture usually result in an ulcerated plaque in the carotid artery, because of high flow rates which are associated with embolic phenomenon, with not only the embolizing thrombus but also the presence of underlying plaque. Thrombus is uncommonly observed at sites of rupture. Erosions have been described in the carotid arteries but are a rare cause of thrombosis. However, advance calcification of the carotid bifurcation especially in DM and end-stage CKD is associated with calcified nodules with thrombosis (Fig. 2.8). Mauriello et al. studied a total of 194 plaques from patients presenting with stroke, transient ischemic attack (TIA), and asymptomatic individuals and showed acute thrombus was most frequent in stroke (88%) and TIA (27%) but was least in asymptomatic individuals (12%) undergoing endarterectomy [58]. They also showed that the most frequent cause of thrombosis was plaque rupture (92%) and calcified nodule (8%) and erosion was rare (<1%) [59]. In another study of 229 cases of carotid atherosclerotic specimens, calcification was a common finding in carotid plaques, being present in 77.3% of cases, and was significantly associated with intraplaque hemorrhage and a large NC. Two types of calcification were identified: hydroxyapatite and calcium oxalate; the presence of hydroxyapatite was more frequent in unstable lesions, while calcium oxalate salt was mainly detected in stable plaques [60]. DM is an important risk factor for ischemic stroke, and a greater calcified area was observed in patients with DM than those without DM [61].

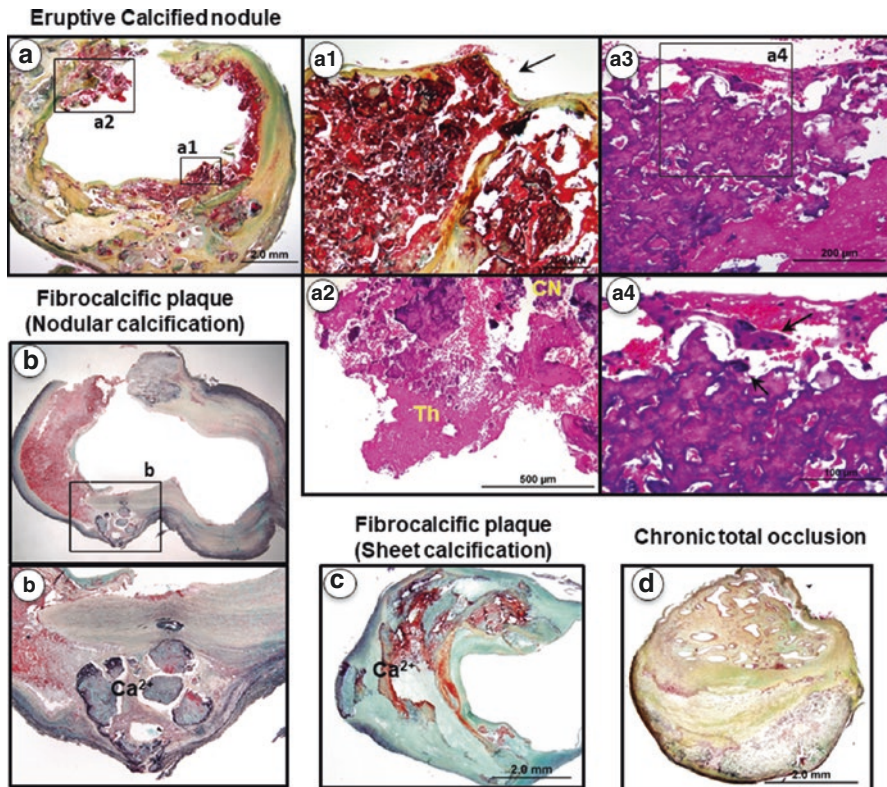


Fig. 2.8 Carotid plaque: Calcified nodule and lesion stabilization/healing. (a) Calcified nodule, considered a less frequent cause of carotid thrombosis relative to plaque rupture. In panel (a1), a high-power image demonstrates a thin fibrous cap (black arrow) over the region of nodular calcification. In panel (a2), the calcific nodules at the luminal surface with a superimposed luminal thrombus (Th). Panels (a3) and (a4) show high-power images of the luminal surface from an area of nodular calcification with platelet/fibrin thrombus and multinucleated osteoclasts (arrows). (b, c) Carotid nodular calcification within the deep neointima (absence of thrombosis) and sheet of calcification, respectively. (d) Chronic total occlusion showing healed recanalized thrombus consisting of SMC in a collagenous matrix with neoangiogenesis; note a paucity of inflammatory cells. (Modified and reproduced with permission obtained from Kolodgie FD, et al. *Semin Vasc Surg.* 2017;30:31–43 and Yazdani SK, *Curr Treat Options Cardiovasc Med.* 2010;12:297–314. Modified Movat pentachrome staining except for “a2-a4” hematoxylin and eosin). Abbreviations: Ca^{2+} , calcification; CN, calcified nodule; Th thrombus

Pathology of Aortic Valve Calcification

Structure of Aortic Valve

The normal aortic valve is composed of three semicircular cusps (i.e., left coronary cusp [LCC], right coronary cusp [RCC], and non-coronary cusp [NCC]), which are asymmetric and are attached to the aorta at three commissures. The cusps are thin

and translucent with a thickness of less than 1 mm. The histologic structure of the aortic valve cusps consists of a fibroelastic layer on the ventricular surface (ventricularis), a proteoglycan-rich layer (spongiosa) in the mid-portion of the cusp, and dense collagen on the aortic surface (fibrosa). The valve thickness increased with age, least in individuals <20 years (0.67 ± 0.21 mm), followed by 20–59 years (0.87 ± 0.27 mm), and is greatest in individuals >60 years (1.42 ± 0.51 mm). It is reported that the site of closure of the valve becomes thicker with advanced age [62].

Aortic Valve Calcification (Tricuspid)

The prevalence of calcific aortic stenosis has been estimated to be 0.4% in the general population and 1.7% in the population aged over 65 years in developed countries [63]. Calcific aortic valve stenosis is a progressive disease with pathologic findings ranging from minimal fibrocalcific changes in early disease to end-stage lesions characterized by fibrotic thickening and nodular calcification (Fig. 2.9a–e). Early valve calcification appears as tiny stippled microcalcification or small nodular concretions at the site of zona fibrosa on the aortic surface of the cusp, most of the time accompanied by early atherosclerotic changes [64] (Fig. 2.9a, b). The attachment of the aortic root and the area located near the line of valve closure are the most affected regions for early calcific deposition. At these locations, there is a high mechanical stress which likely contributes to calcification (see Chap. 6). Site-specific predisposition to calcification, in particular the predilection for calcific lesions to form on the aortic rather than the ventricular surface of the valve, may be related to increased mRNA levels of osteogenic markers associated with bone formation [65]. Hemodynamic shear stresses caused by differences in disturbed flow on the aortic and ventricular surfaces may be responsible for the differential effects that lead to calcification predominantly involving valvular endothelial cells (VECs) producing pathological paracrine factors, like bone morphogenetic protein 4 (BMP4), pleiotrophin, and hyaluronan and proteoglycan link protein 1. In contrast, ventricular-side VECs, which experience high magnitude and unidirectional shear stress, produce paracrine factors like osteoprotegerin (OPG) and C-type natriuretic peptide (CNP), which may inhibit calcification, while these factors are decreased on the aortic surface allowing calcification [66, 67].

During the progression of calcification, microcalcifications gradually merged into larger complex nodules. The calcification begins in the interstitial cells within the base of the fibrosa and then extends toward the middle portion of the cusp with sparing of the free margin and may eventually protrude into the aortic surface. A pathologic study including 247 surgically excised aortic valves (mean age 64.1 ± 13.4 years) showing morphologic features of aortic stenosis found that almost 70% of calcified aortic valves were tricuspid and 30% were congenitally abnormal, with 27% of those being bicuspid, 2.4% unicuspid, and 1 (0.4%) valve quadricuspid. Ulcerations of the calcific nodules on the aortic surface were present in 42% of valves which had severe calcification [68]. Prior to the calcification, the

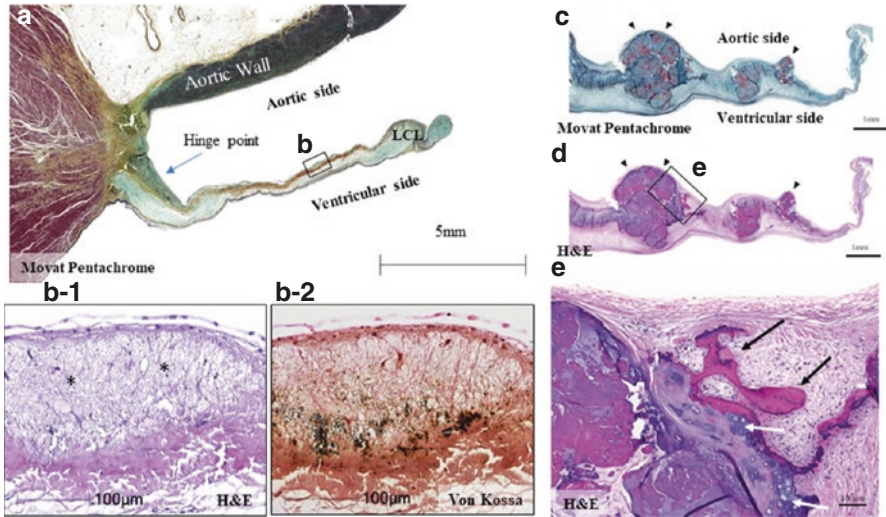


Fig. 2.9 Representative histology images of aortic valve calcification. **(a, b)** Early AV calcification resembles atherosclerotic changes. Aortic valve leaflet from a 47-year-old man who died of accidental head trauma. **(a)** Low-power image of LCL (Movat pentachrome stain). **(b1 and b2)** High-power images from **a** (black box) at the site of closure of the valve showing lipid insudation (*) (**B1**; H&E) with calcification as black dots (**B2**; von Kossa stain). **(c–e)** Bone formation within advanced AS. Degenerative aortic valve leaflet from a 70-year-old woman who underwent surgical valve replacement for severe aortic valve stenosis. Low-power images of Movat pentachrome (**c**) and H&E stain (**d**) show nodular calcification on the aortic surface (black arrow head). Top and bottom surface indicate aortic and ventricular side, respectively. **(E)** High-power image of H&E stain from the boxed area in **d**. Ossification (black arrow) and cartilaginous metaplasia (white arrow) are found at the edge of nodular calcification. (Modified and reproduced with permission from Sakamoto et al. *Eur Heart J.* 2019;40:1374–1377). Abbreviations: AS, aortic valve stenosis; AV, aortic valve; H&E, hematoxylin and eosin; LCL, left coronary valve leaflet

valve leaflets showed mild fibrous thickening without left ventricular outflow obstruction. With progression of disease, the cusps become increasingly fibrotic and calcified, eventually forming irregular calcific nodules on the aortic aspect of the cusp, resulting in valve obstruction (Fig. 2.9c–e). Of note, calcification is usually more pronounced in the non-coronary cusp rather than the right and the left coronary cusps. Roberts et al. suggested that this may be related to larger surface area of the non-coronary cusp, while others hypothesized that it could be due to greater stress during diastole on the non-coronary cusp as compared to the right and left cusps [69].

Risk factors predictive of aortic valve calcification are similar to those of coronary atherosclerosis. These include age, male gender, smoking, elevated cholesterol level, lipoprotein (a), hypertension, DM, metabolic syndrome, and CKD with or without dialysis. In a Multi-Ethnic Study of Atherosclerosis (MESA), patients with aortic valve calcification were identified and followed up for 2.4 ± 0.9 years by CT [70]. Risk factors for incident aortic valve calcification included age, male gender,

body mass index, current smoking, and the use of lipid lowering and antihypertensive medications. Among those with valve calcification at baseline, the median rate of valve calcification progression was 2 Agatston units/year (interquartile range – 21 to 37). Baseline Agatston score was a strong, independent predictor of disease progression, especially among patients with high calcium scores at baseline [70]. More detailed mechanisms of aortic valve calcification are provided in Chap. 4.

Congenital Aortic Valve Disease and Calcification (Bicuspid and Unicuspid)

Bicuspid aortic valve is a common congenital cardiac anomaly present in 1–2% of the general population (a male to female ratio of 1.4–4:1) [71], whereas the incidence of unicuspid aortic valve is 0.02% [72], and the quadricuspid valve is the rarest (0.008%) [73]. Bicuspid aortic valves commonly show signs of calcification by the time individuals reach age 30 [74] and ultimately leads to aortic stenosis [75]. Bicuspid and unicuspid valves are more likely to show higher grade of calcification than tricuspid valves [68, 76]. Indeed, a large series of data regarding surgically removed tricuspid, bicuspid, and unicuspid aortic valves reported that pathologic features (e.g., degree of cusp calcification, ossification, cartilaginous metaplasia, and ulceration) were progressively more severe in valves exhibiting fewer cusps (unicuspid and bicuspid) [76] (Fig. 2.10). The increased severity of changes in congenital aortic valves may result from abnormal blood flow and stress distribution across the abnormal valve causing accelerated calcification and earlier failures.

The term “raphe” defines the conjoined area of two underdeveloped leaflets turning into a malformed commissure between two leaflets. The common feature of a raphe is a ridge that is rich in elastic fibers [77]. The commissure of a valve is the space between the two parallel attachments of two adjacent cusps to the aortic wall generally not adhering to each other. An obliteration of the two (or three) or one commissure is present in bicuspid and unicuspid aortic valves, respectively.

Unicuspid aortic valves are categorized as one of the two morphologic types: (1) a dome-shaped acommisural valve containing three aborted commissures (or raphe) or (2) a unicommisural valve with slit-like opening that reaches the aortic wall with a single intact commissure. Unicommisural, unicuspid aortic valves account for 60% of aortic stenosis cases in patients <15 years of age [78]. Leaflet dysplasia is common and the severity of leaflet calcification is variable; however, dysplasia of unicuspid valve has been reported to be more severe compared to bicuspid valve and is dependent on the patient age [76].

The bicuspid aortic valve has two leaflets, which have been previously described as type 0, type 1, and type 2 [79]. Sievers et al. showed the frequency of the types of bicuspid aortic valve from their surgical experience from 304 cases prior to the removal of the diseased bicuspid aortic valve (Fig. 2.11). Type 0 has a frequency of 7% that is associated with an absence of raphe with the commissures located

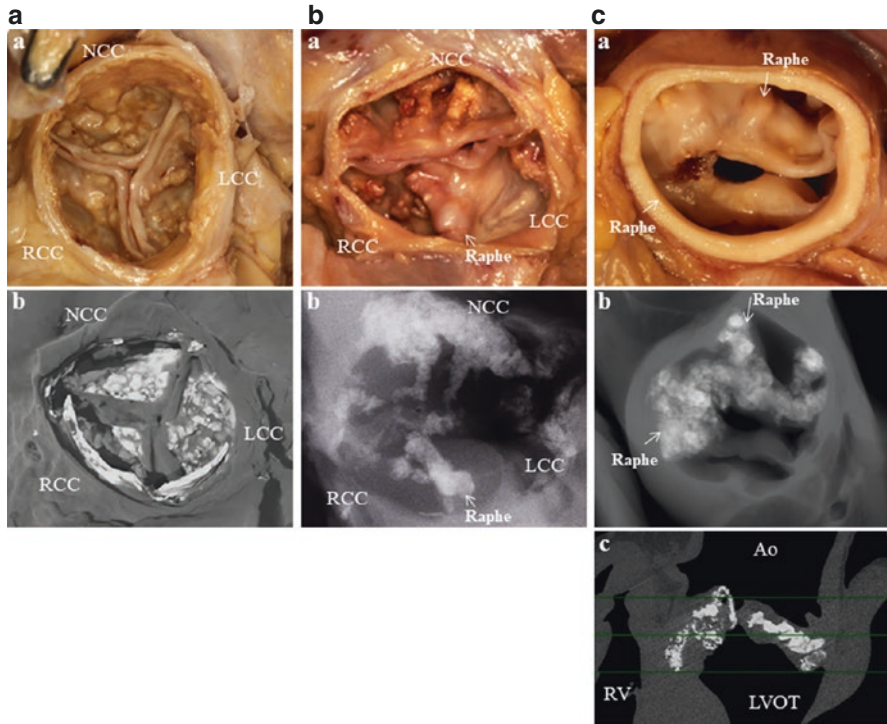


Fig. 2.10 Images of calcified stenotic aortic valve (aortic view): tricuspid, bicuspid and unicuspid. (a) Stenotic tricuspid aortic valve (gross [a] and micro CT [b] images). (b) Stenotic congenital bicuspid aortic valve (gross [a] and X-ray [b] images). RCC and LCC are forming a conjoint leaflet. (c) Stenotic congenital unicuspid aortic valve, a unicommisural valve with slit-like opening that reaches the aortic wall with a single intact commissure (gross [a] and micro CT [b]; transverse, and [c] sagittal views). Abbreviations: CT, computed tomography; NCC, non-coronary cusp; LCC, left coronary cusp; RCC right coronary cusp

anterior-posterior or lateral (right-left) and later is more common of the two. Type 1, the most common form of a bicuspid valve (88%), has three developmental cusps and two commissures instead of three. The most frequent configuration is the two cusps are unequal in size, with the larger being the conjoint cusp. Conjoint LCC and RCC are the most dominant (71%), followed by conjoint NCC and RCC (15%), and the least is LCC and NCC (3%) [79]. The size of the conjoint cusp is typically less than two times the size of the non-conjoint cusp and contains a median raphe. In this report, abnormal aortic valves with two raphe are also classified as type 2 bicuspid valve (5%); however, many others have classified these as unicuspid or unicommisural valve [80–82].

In congenital bicuspid valves, calcification begins in the raphe and appears as a linear opacity on radiographic examination and extends into the free margin of the cusp and largely sparing the true commissures but may spread to the line of closure. Bicuspid valve-oriented severe aortic stenosis is characterized by calcification

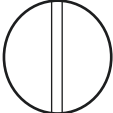


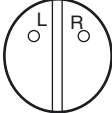
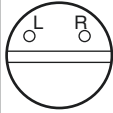
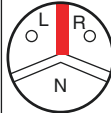
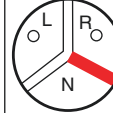
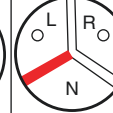
<p>Main category: number of raphes</p>	<p>Type 0 : No Raphe</p>  <p>7%</p>		<p>Type 1 : 1 Raphe</p>  <p>88%</p>		<p>Type 2 : 2 Raphes</p>  <p>5%</p>	
	<p>Subcategory: spatial position of cusps in Type 0 and raphes in Types 1 and 2</p>	 <p>Lat 4%</p>	 <p>ap 2%</p>	 <p>L-R 71%</p>	 <p>R-N 15%</p>	 <p>N-L 3%</p>

Fig. 2.11 Schematic presentation of the classification system of bicuspid aortic valve. Red lines in schematic drawings represent a raphe. Three different main categories according to the number of raphes are: type 0, no raphe (7%); type 1 with one raphe, the most common type of configurations (88%); and type 2 with two raphes (5%). The three types are subcategorized as ap, lat, L-R, R-N, N-L, and L-R/R-N. (Modified and reproduced with permission from Sievers and Schmidtke [79]). Abbreviation: ap, anterior-posterior; lat, lateral; L, left coronary sinus; R, right coronary sinus; N, non-coronary sinus

spreading to the tissue of the conjoint and non-conjoint cusps, and calcific nodules may ulcerate on the aortic surface (Fig. 2.10). On the other hand, calcification in rheumatic aortic stenosis is variably present and starts in the fused commissures and extends into the body of the cusp. In congenital bicuspid valve stenosis, histological appearance of calcification has been reported to occur diffusely within the cusp spongiosa [83].

Pathology of Mitral Valve Calcification

Structure of Mitral Valve

The mitral valve, both functionally and morphologically, consists of five individual structures, i.e., (1) annulus, (2) anterior and posterior leaflets, (3) chordae tendineae, (4) papillary muscles, and (5) the left ventricle, which are required for the proper mitral valve function [84]. The mitral annulus is a fibrous ring that is attached to the mitral valve leaflets at the point of where the atrial and ventricular walls meet. During the systolic phase, the mitral annulus folds at the intercommissural axis as well as anteroposteriorly. This folding results in the leaflet coaptation and avoids leaflet distortion along the lines of annular attachment mitigating the mechanical force exerted on the mitral valve leaflets [85]. Fibrous trigones are located in the region of the anterior mitral leaflet and are placed right and left, with right being

larger spanning the aortic annulus. The atrioventricular conduction bundle goes through the right fibrous trigone. The coronary sinus is located close to the posterior mitral annulus and is usually superior to the left circumflex artery (Fig. 2.12a).

The normal mitral valve leaflet consists of an anterior (or aortic) and the posterior (or the mural) leaflet. Posterior leaflet usually consists of three scallops (92%) (i.e., anterior [P1], middle [P2], and posterior [P3] scallops), whereas, in 8% of cases, there may be only two or even five scallops [86]. The anterior leaflet is semi-circular occupying one third of the circumference, whereas the posterior leaflet is long and narrow forming two thirds of the circumference (Fig. 2.12b). Gross examination shows the mitral valve leaflets as thin, pliable, delicate, and translucent. Just as the aortic valve, the mitral valve too has three layers, i.e., the atrialis (a fibroelastic layer on the atrial aspect of the leaflet), the spongiosa (has loose fibro-myxomatous tissue rich in glycosaminoglycans), and the fibrosa (has a dense collagenous layer that extends toward the ventricular surface) (Fig. 2.12d). The chordae tendineae are inserted on (1) the leaflet free edge, (2) the ventricular surface beyond the free edge (i.e., the rough zone), and (3) the basal ventricular surface, which are present only on the posterior leaflet. The chordae of the mitral valve vary in numbers, length, and thickness, with the chordae from each of the leaflet inserting into the anterolateral and the posteromedial papillary muscles (Fig. 2.12c).

The papillary muscles arise normally between the apex and the middle one third of the left ventricle. The chordae tendineae arise from the tip of the papillary muscle heads, which tether the mitral valve leaflets to the papillary muscle. The papillary muscles are an extension of the underlying left ventricular wall. Any change in the shape and size of the left ventricle will result in valve dysfunction.

Pathology of Mitral Annulus Calcification

The mitral valve leaflets are translucent, gelatinous, and transmit light at birth and, however, gradually turn opaque by the age of 20 years. The leaflets become opaque due to fibrosis and lipid infiltration. The closure lines on both the anterior and posterior leaflets are situated away from the free edge of the leaflets. Mitral annulus calcification (MAC) is observed mostly beyond the age of 70 years. Several studies suggested that MAC is associated with known atherosclerotic risk factors such as hypertension, dyslipidemia, DM, CKD, and smoking [87]. Prior autopsy reports revealed 10% of individuals aged >50 years had MAC; nevertheless, the incidence is increasing as the population lives longer in Western World, i.e., 37% in 80–89 years and 45% in 90–99 years [88, 89]. A large-scale population-based echocardiography study (the Cardiovascular Health Study) showed occurrence of MAC in 42% of individuals >65 years [90]. There is a clear association between MAC and aortic stenosis, e.g., 27% of the elderly population (>65 years) have both disorders. Increased mitral valve mechanical stress, such as presence of hypertension, aortic stenosis, hypertrophic cardiomyopathy, and mitral valve prolapse, may lead to MAC formation. In fact, the pressure gradient of mitral valve in patients

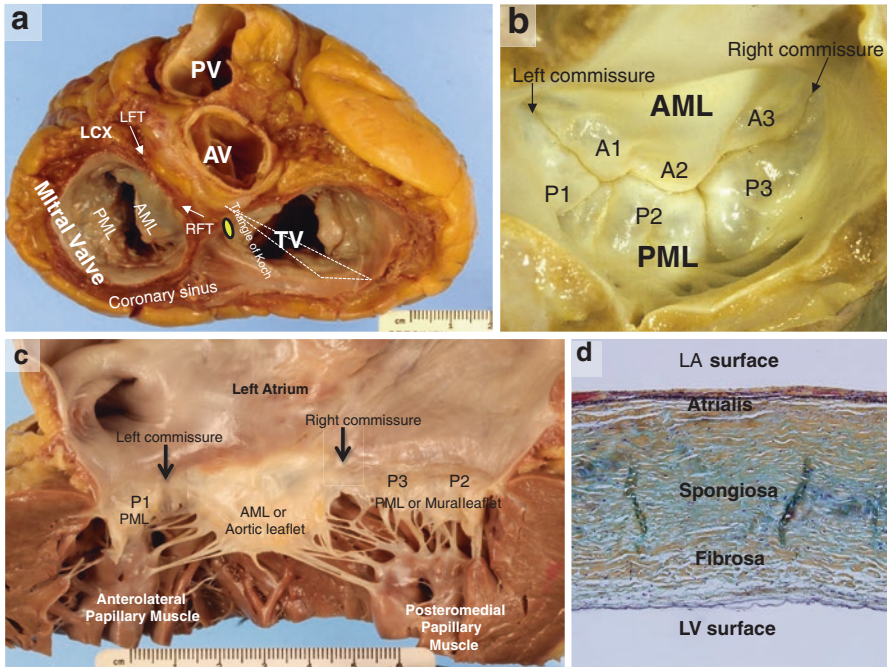


Fig. 2.12 Normal mitral valve and surrounding structures. (a) Superior view of the base of the heart shows the spatial relations of the four cardiac valves (aortic, mitral, pulmonary, and tricuspid). The left heart valves are close together and by inter-atrial septum and the base of the ventricular septum. Atrioventricular node is located within the triangle of Koch near its apex and lies close to the junction of the septal and anterior tricuspid leaflets. Note that the coronary sinus hugs the posterior mitral annulus with an intervening posterior left atrial wall. The left circumflex artery lies adjacent to the left trigone and passes inferior to the continuation of the coronary sinus. The aortic valve is separated from the anterior mitral leaflet by fibrous tissue and on the right and left are located the fibrous trigones. (b, c) Gross atrial view of the mitral valve showing anterior and posterior leaflets (b). The anterior leaflet is larger and the chordae arise from the ventricular surface at 45-degree angle. The anterior leaflet is separated from the posterior leaflet by the commissures (black arrow) with fan-shaped branching commissural chordae (c). The posterior leaflet has three, often poorly defined, scallops, each with chordal attachments (b). (d) A histological section of a mitral valve leaflet (Movat pentachrome stain) demonstrates the atrialis which is rich in elastic fibers and collagen, glycosaminoglycans rich spongiosa in the mid-portion (green), and dense collagenous tissue (yellow) which is observed on the ventricular surface of the leaflet. Abbreviations: AML, anterior mitral leaflet; AV, aortic valve; LA, left atrium; LCX, left circumflex artery; LFT, left fibrous trigone; LV, left ventricle; PML, posterior mitral leaflet; PV, pulmonary valve; RFT, right fibrous trigone; TV, tricuspid valve

with severe MAC increases progressively at a rate of 0.8 ± 2.4 mmHg/year [91]. In another report, among 100 unselected elderly patients with MAC (62 to 100 years), mitral stenosis (MS) was observed in 6% of patients, and 58% of these patients had some degree of MS and/or mitral regurgitation [92]. Moreover, in large-scale prospective study, 12–26% in all MS cases were classified as degenerative MS (mean age: 64 ± 14 years) [93].

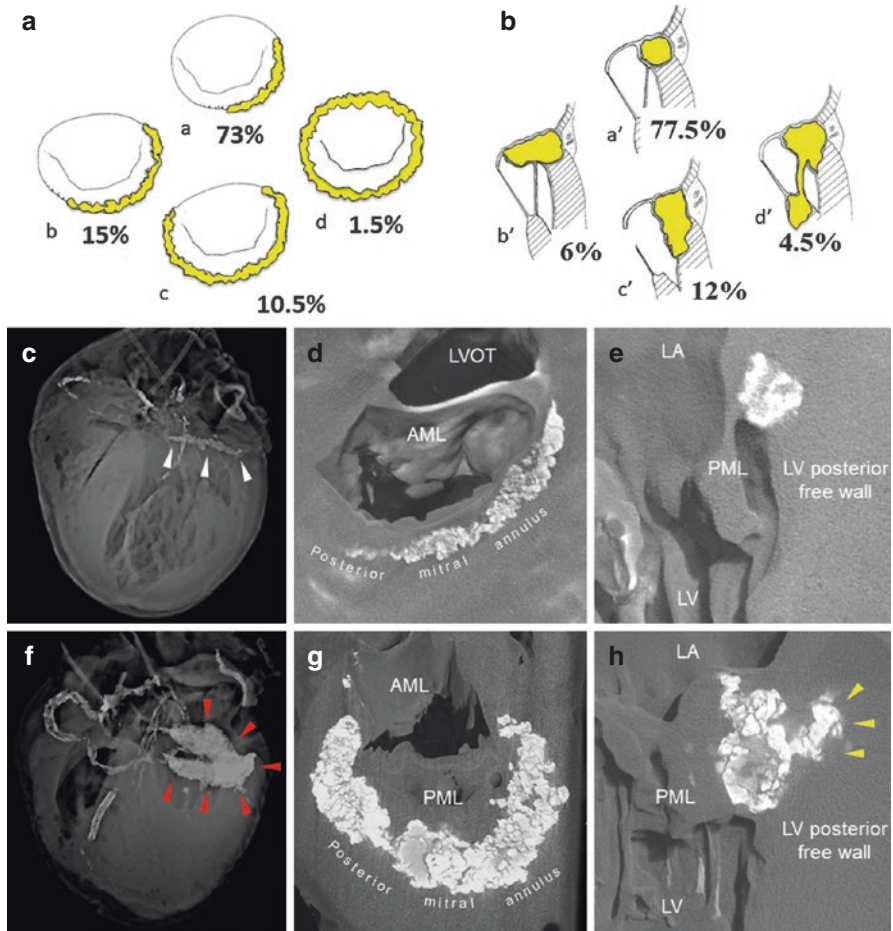


Fig. 2.13 Mitral annular calcification. The classification of mitral annular calcification includes circumferentially (**a**) and vertically (**b**). Calcification involves at least one third of the whole posterior annulus in 88% of patients (73% have equal or less than 1/4 of the annulus; 15% have greater than 1/4), the whole posterior annulus in 10.5%, and circumferential in 1.5% (**a**). Vertical calcification is limited to the annulus only 77% and extends into the leaflet tissue in 6%, the myocardium in 12% of patients, and the papillary muscles in 4.5% (**b**). Reproduced with permission from Carpentier et al. [97]. (**c–e**) A heart from a 87-year-old white female with history of coronary artery disease, diabetes mellitus, and hyperlipidemia. MAC (white arrow heads) was detected by postmortem radiograph (**c**) and micro CT images (**d, e**). Transverse micro CT image showed MAC involving approximately two third of the whole posterior annulus (**d**). Calcification was limited in the annulus itself in vertical image (**e**). (**f–h**) A heart from a 42-year-old white male with history of end-stage renal disease on dialysis with severe mitral valve stenosis secondary to annular calcification. A postmortem radiograph (**f**) and CT images (**g, h**) of the heart shows marked mitral annular calcification (red arrowheads) that involves the whole posterior mitral annulus and the attachment of the anterior leaflet (**g**). Vertically, the calcification was involved the annulus itself and extends to the leaflet tissue and the ventricular myocardium (yellow arrowheads) (**h**). Abbreviation: AML, anterior mitral leaflet; CT, computed tomography; LA, left atrium; LV, left ventricle; LVOT, left ventricular outflow tract; MAC, mitral annular calcification; PML, posterior mitral leaflet

MAC has been associated with higher prevalence of atrioventricular block, bundle branch block, and intraventricular conduction delays [94, 95] and may be caused by direct extension of calcific deposits to the region of the atrioventricular node and the bundle of His [96].

Pathologically, the severity of calcification varies from mild, with focal small calcific deposits, to severe with large calcific nodules involving the entire annulus projecting into the left ventricular cavity or as spurs which project into the left ventricular posterolateral basal wall. A study of surgically excised mitral valves showed extensive calcification of annulus and severe valve insufficiency, annular circumferential calcification involved at least one third to two thirds of the posterior annulus in 88% of patients, while the complete posterior annulus is involved in 10.5%, and rarest, a D-shaped circumferential involvement, occurs in 1.5% cases. The calcification was limited to the annulus in 77% of cases and extended into the leaflet tissue in 6%, while involvement of the ventricular myocardium occurred in 12%, and rarely it extended into the papillary muscles (4.5%) [97] (Fig. 2.13).

Conclusion

Vascular calcification has been classified into three types with the most prevalent being atherosclerotic intimal calcification, followed by medial calcification, and least frequent is genetic calcification. Several overlapping factors are associated with all three types of calcification. Coronary artery calcification is considered as part and parcel of advanced coronary atherosclerosis and has been correlated with plaque burden. It is commonly used as a risk predictor for future cardiovascular events; however, the extent of coronary calcium does not correlate with percent stenosis. Pathologically, the presence of small, fragmented, or spotty calcification is a better predictor for rupture-prone unstable plaque, while advanced calcification (diffuse, fibrocalcific plaque or sheets of calcium) is a better predictor for stable plaque. The mechanism of coronary calcification has been likened to bone formation but remains controversial.

Unlike coronary artery calcification, Mönckeberg's medial calcification is commonly observed in the peripheral arteries and is accelerated in patients with DM and CKD. Risk factors related to atherosclerosis probably enhance calcification of both intima and media. Indeed, multiple observational studies have shown an association between Mönckeberg's medial calcification in breast artery and coronary artery calcification, allowing mammography as a cardiovascular risk stratification tool.

Carotid arteries have a unique geometry, which influences the flow patterns in the region of bifurcation contributing to both the degree and type of atherosclerotic plaque. In symptomatic or asymptomatic individuals undergoing endarterectomy, the common calcified lesions are sheet calcium and less frequently nodular calcification.

Calcific tricuspid aortic valve stenosis is associated with significant morbidity and mortality and is usually observed in individuals >70 years. There are pathologic and mechanistic similarities between arterial atherosclerosis and aortic valve calcification. Congenital bicuspid valves are observed in 1–2% of population and tend to calcify earlier than tricuspid valves. Raphe is observed in 88% of bicuspid valve, and the most common configuration is conjoint right and left coronary cusps.

Mitral valve apparatus is more complex consisting of anterior and posterior leaflets, chordae tendineae, papillary muscles, left ventricle, and atrial walls. Mitral annulus is prone to calcification and usually seen in elderly females; however 30% of aging population have mitral and aortic valve calcification. The pathogenesis of mitral annulus calcification is not well understood. MAC is also associated with higher risk of cardiovascular events such as valvular stenosis and insufficiency, arrhythmias, and increased mortality. MAC usually starts in the posterior leaflet and most frequently involves one third to two thirds of posterior mitral annulus and rarely could be circumferential.

Greater understanding of vascular and valvular calcification is needed not only for better risk stratification of patients and for improvement of patient outcomes but also with the goal to prevent cardiovascular calcification.

References

1. Wilson PW, D'Agostino RB, Levy D, et al. Prediction of coronary heart disease using risk factor categories. *Circulation*. 1998;97(18):1837–47. PMID: 9603539.
2. Demer LL, Tintut Y. Inflammatory, metabolic, and genetic mechanisms of vascular calcification. *Arterioscler Thromb Vasc Biol*. 2014;34(4):715–23. PMID: 24665125.
3. Qiao JH, Mertens RB, Fishbein MC, et al. Cartilaginous metaplasia in calcified diabetic peripheral vascular disease: morphologic evidence of enchondral ossification. *Hum Pathol*. 2003;34(4):402–7. PMID: 12733123.
4. Ikari Y, McManus BM, Kenyon J, et al. Neonatal intima formation in the human coronary artery. *Arterioscler Thromb Vasc Biol*. 1999;19(9):2036–40. PMID: 10479643.
5. Stary HC, Chandler AB, Glagov S, et al. A definition of initial, fatty streak, and intermediate lesions of atherosclerosis. A report from the committee on vascular lesions of the council on arteriosclerosis, American Heart Association. *Circulation*. 1994;89(5):2462–78. PMID: 8181179.
6. Velican C. A dissecting view on the role of the fatty streak in the pathogenesis of human atherosclerosis: culprit or bystander? *Med Interne*. 1981;19(4):321–37. PMID: 7038828.
7. Virmani R, Kolodgie FD, Burke AP, et al. Lessons from sudden coronary death: a comprehensive morphological classification scheme for atherosclerotic lesions. *Arterioscler Thromb Vasc Biol*. 2000;20(5):1262–75. PMID: 10807742.
8. Nakagawa K, Nakashima Y. Pathologic intimal thickening in human atherosclerosis is formed by extracellular accumulation of plasma-derived lipids and dispersion of intimal smooth muscle cells. *Atherosclerosis*. 2018;274:235–42. PMID: 29622338.
9. Nakashima Y, Fujii H, Sumiyoshi S, et al. Early human atherosclerosis: accumulation of lipid and proteoglycans in intimal thickenings followed by macrophage infiltration. *Arterioscler Thromb Vasc Biol*. 2007;27(5):1159–65. PMID: 17303781.

10. Nakashima Y, Wight TN, Sueishi K. Early atherosclerosis in humans: role of diffuse intimal thickening and extracellular matrix proteoglycans. *Cardiovasc Res.* 2008;79(1):14–23. PMID: 18430750.
11. Yahagi K, Kolodgie FD, Otsuka F, et al. Pathophysiology of native coronary, vein graft, and in-stent atherosclerosis. *Nat Rev Cardiol.* 2016;13(2):79–98. PMID: 26503410.
12. Stary HC, Chandler AB, Dinsmore RE, et al. A definition of advanced types of atherosclerotic lesions and a histological classification of atherosclerosis. A report from the committee on vascular lesions of the council on arteriosclerosis, American Heart Association. *Arterioscler Thromb Vasc Biol.* 1995;15(9):1512–31. PMID: 7670967.
13. Burke AP, Farb A, Malcom GT, et al. Coronary risk factors and plaque morphology in men with coronary disease who died suddenly. *N Engl J Med.* 1997;336(18):1276–82. PMID: 9113930.
14. Tearney GJ, Regar E, Akasaka T, et al. Consensus standards for acquisition, measurement, and reporting of intravascular optical coherence tomography studies: a report from the International Working Group for Intravascular Optical Coherence Tomography Standardization and Validation. *J Am Coll Cardiol.* 2012;59(12):1058–72. PMID: 22421299.
15. Kolodgie FD, Burke AP, Farb A, et al. The thin-cap fibroatheroma: a type of vulnerable plaque: the major precursor lesion to acute coronary syndromes. *Curr Opin Cardiol.* 2001;16(5):285–92. PMID: 11584167.
16. Falk E, Nakano M, Bentzon JF, et al. Update on acute coronary syndromes: the pathologists' view. *Eur Heart J.* 2013;34(10):719–28. PMID: 23242196.
17. Geng YJ, Libby P. Evidence for apoptosis in advanced human atheroma. Colocalization with interleukin-1 beta-converting enzyme. *Am J Pathol.* 1995;147(2):251–66. PMID: 7639325.
18. Burke AP, Farb A, Malcom GT, et al. Plaque rupture and sudden death related to exertion in men with coronary artery disease. *JAMA.* 1999;281(10):921–6. PMID: 10078489.
19. Gijssen FJ, Wentzel JJ, Thury A, et al. Strain distribution over plaques in human coronary arteries relates to shear stress. *Am J Physiol Heart Circ Physiol.* 2008;295(4):H1608–14. PMID: 18621851.
20. Sukhova GK, Schonbeck U, Rabkin E, et al. Evidence for increased collagenolysis by interstitial collagenases-1 and -3 in vulnerable human atheromatous plaques. *Circulation.* 1999;99(19):2503–9. PMID: 10330380.
21. Vengrenyuk Y, Carlier S, Xanthos S, et al. A hypothesis for vulnerable plaque rupture due to stress-induced debonding around cellular microcalcifications in thin fibrous caps. *Proc Natl Acad Sci U S A.* 2006;103(40):14678–83. PMID: 17003118.
22. Farb A, Burke AP, Tang AL, et al. Coronary plaque erosion without rupture into a lipid core. A frequent cause of coronary thrombosis in sudden coronary death. *Circulation.* 1996;93(7):1354–63. PMID: 8641024.
23. Kolodgie FD, Burke AP, Farb A, et al. Differential accumulation of proteoglycans and hyaluronan in culprit lesions: insights into plaque erosion. *Arterioscler Thromb Vasc Biol.* 2002;22(10):1642–8. PMID: 12377743.
24. Mann J, Davies MJ. Mechanisms of progression in native coronary artery disease: role of healed plaque disruption. *Heart.* 1999;82(3):265–8. PMID: 10455072.
25. Burke AP, Kolodgie FD, Farb A, et al. Healed plaque ruptures and sudden coronary death: evidence that subclinical rupture has a role in plaque progression. *Circulation.* 2001;103(7):934–40. PMID: 11181466.
26. Kragel AH, Reddy SG, Wittes JT, et al. Morphometric analysis of the composition of atherosclerotic plaques in the four major epicardial coronary arteries in acute myocardial infarction and in sudden coronary death. *Circulation.* 1989;80(6):1747–56. PMID: 2598434.
27. Mori H, Torii S, Kutyna M, et al. Coronary artery calcification and its progression: what does it really mean? *JACC Cardiovasc Imaging.* 2018;11(1):127–42. PMID: 29301708.
28. Otsuka F, Sakakura K, Yahagi K, et al. Has our understanding of calcification in human coronary atherosclerosis progressed? *Arterioscler Thromb Vasc Biol.* 2014;34(4):724–36. PMID: 24558104.

29. Kockx MM, De Meyer GR, Muhring J, et al. Apoptosis and related proteins in different stages of human atherosclerotic plaques. *Circulation*. 1998;97(23):2307–15. PMID: 9639374.
30. Kelly-Arnold A, Maldonado N, Laudier D, et al. Revised microcalcification hypothesis for fibrous cap rupture in human coronary arteries. *Proc Natl Acad Sci U S A*. 2013;110(26):10741–6. PMID: 23733926.
31. Kapustin AN, Shanahan CM. Calcium regulation of vascular smooth muscle cell-derived matrix vesicles. *Trends Cardiovasc Med*. 2012;22(5):133–7. PMID: 22902179.
32. Tanimura A, McGregor DH, Anderson HC. Calcification in atherosclerosis. I *Human Stud J Exp Pathol*. 1986;2(4):261–73. PMID: 2946818.
33. Bertazzo S, Gentleman E, Cloyd KL, et al. Nano-analytical electron microscopy reveals fundamental insights into human cardiovascular tissue calcification. *Nat Mater*. 2013;12(6):576–83. PMID: 23603848.
34. Hutcheson JD, Goettsch C, Bertazzo S, et al. Genesis and growth of extracellular-vesicle-derived microcalcification in atherosclerotic plaques. *Nat Mater*. 2016;15(3):335–43. PMID: 26752654.
35. Otsuka F, Kramer MC, Woudstra P, et al. Natural progression of atherosclerosis from pathologic intimal thickening to late fibroatheroma in human coronary arteries: a pathology study. *Atherosclerosis*. 2015;241(2):772–82. PMID: 26058741.
36. New SE, Goettsch C, Aikawa M, et al. Macrophage-derived matrix vesicles: an alternative novel mechanism for microcalcification in atherosclerotic plaques. *Circ Res*. 2013;113(1):72–7. PMID: 23616621.
37. Burke AP, Weber DK, Kolodgie FD, et al. Pathophysiology of calcium deposition in coronary arteries. *Herz*. 2001;26(4):239–44. PMID: 11479935.
38. Narula J, Nakano M, Virmani R, et al. Histopathologic characteristics of atherosclerotic coronary disease and implications of the findings for the invasive and noninvasive detection of vulnerable plaques. *J Am Coll Cardiol*. 2013;61(10):1041–51. PMID: 23473409.
39. Huang H, Virmani R, Younis H, et al. The impact of calcification on the biomechanical stability of atherosclerotic plaques. *Circulation*. 2001;103(8):1051–6. PMID: 11222465.
40. Rajamannan NM, Evans FJ, Aikawa E, et al. Calcific aortic valve disease: not simply a degenerative process: a review and agenda for research from the National Heart and Lung and Blood Institute Aortic Stenosis Working Group. Executive summary: calcific aortic valve disease-2011 update. *Circulation*. 2011;124(16):1783–91. PMID: 22007101.
41. Yutzy KE, Demer LL, Body SC, et al. Calcific aortic valve disease: a consensus summary from the Alliance of Investigators on Calcific Aortic Valve Disease. *Arterioscler Thromb Vasc Biol*. 2014;34(11):2387–93. PMID: 25189570.
42. Sage AP, Tintut Y, Demer LL. Regulatory mechanisms in vascular calcification. *Nat Rev Cardiol*. 2010;7(9):528–36. PMID: 20664518.
43. Panh L, Lairez O, Ruidavets JB, et al. Coronary artery calcification: from crystal to plaque rupture. *Arch Cardiovasc Dis*. 2017;110(10):550–61. PMID: 28735837.
44. Soor GS, Vukin I, Leong SW, et al. Peripheral vascular disease: who gets it and why? A histomorphological analysis of 261 arterial segments from 58 cases. *Pathology*. 2008;40(4):385–91. PMID: 18446629.
45. Torii S, Mustapha JA, Narula J, et al. Histopathologic characterization of peripheral arteries in subjects with abundant risk factors: correlating imaging with pathology. *JACC Cardiovasc Imaging*. 2018;6. PMID: 30553660.
46. Bui QM, Daniels LB. A review of the role of breast arterial calcification for cardiovascular risk stratification in women. *Circulation*. 2019;139(8):1094–101. PMID: 30779650.
47. Lachman AS, Spray TL, Kerwin DM, et al. Medial calcinosis of Monckeberg. A review of the problem and a description of a patient with involvement of peripheral, visceral and coronary arteries. *Am J Med*. 1977;63(4):615–22. PMID: 910809.
48. Amos RS, Wright V. Monckeberg's arteriosclerosis and metabolic bone disease. *Lancet*. 1980;2(8188):248–9. PMID: 6105406.

49. Kamenskiy A, Poulson W, Sim S, et al. Prevalence of calcification in human femoropopliteal arteries and its association with demographics, risk factors, and arterial stiffness. *Arterioscler Thromb Vasc Biol.* 2018;38(4):e48–57. PMID: 29371245.
50. Sawabe M, Arai T, Kasahara I, et al. Sustained progression and loss of the gender-related difference in atherosclerosis in the very old: a pathological study of 1074 consecutive autopsy cases. *Atherosclerosis.* 2006;186(2):374–9. PMID: 16129442.
51. Dalager S, Paaske WP, Kristensen IB, et al. Artery-related differences in atherosclerosis expression: implications for atherogenesis and dynamics in intima-media thickness. *Stroke.* 2007;38(10):2698–705. PMID: 17761918.
52. Herisson F, Heymann MF, Chetiveaux M, et al. Carotid and femoral atherosclerotic plaques show different morphology. *Atherosclerosis.* 2011;216(2):348–54. PMID: 21367420.
53. Diehm N, Silvestro A, Baumgartner I, et al. Chronic critical limb ischemia: European experiences. *J Cardiovasc Surg.* 2009;50(5):647–53. PMID: 19741580.
54. Narula N, Dannenberg AJ, Olin JW, et al. Pathology of peripheral artery disease in patients with critical limb ischemia. *J Am Coll Cardiol.* 2018;72(18):2152–63. PMID: 30166084.
55. Torii S, Mustapha JA, Narula J, et al. Histopathologic characterization of peripheral arteries in subjects with abundant risk factors: correlating imaging with pathology. *JACC Cardiovasc Imaging.* 2019;12(8 Pt 1):1501–13. PMID: 30553660.
56. Zarins CK, Giddens DP, Bharadvaj BK, et al. Carotid bifurcation atherosclerosis. Quantitative correlation of plaque localization with flow velocity profiles and wall shear stress. *Circ Res.* 1983;53(4):502–14. PMID: 6627609.
57. Nakazawa G, Yazdani SK, Finn AV, et al. Pathological findings at bifurcation lesions: the impact of flow distribution on atherosclerosis and arterial healing after stent implantation. *J Am Coll Cardiol.* 2010;55(16):1679–87. PMID: 20394871.
58. Mauriello A, Sangiorgi G, Virmani R, et al. Evidence of a topographical link between unstable carotid plaques and luminal stenosis: can we better stratify asymptomatic patients with significant plaque burden? *Int J Cardiol.* 2012;155(2):309–11. PMID: 22192293.
59. Mauriello A, Sangiorgi GM, Virmani R, et al. A pathobiologic link between risk factors profile and morphological markers of carotid instability. *Atherosclerosis.* 2010;208(2):572–80. PMID: 19683236.
60. Bischetti S, Scimeca M, Bonanno E, et al. Carotid plaque instability is not related to quantity but to elemental composition of calcification. *Nutr Metab Cardiovasc Dis.* 2017;27(9):768–74. PMID: 28739184.
61. Yahagi K, Kolodgie FD, Lutter C, et al. Pathology of human coronary and carotid artery atherosclerosis and vascular calcification in diabetes mellitus. *Arterioscler Thromb Vasc Biol.* 2017;37(2):191–204. PMID: 27908890.
62. Sahasakul Y, Edwards WD, Naessens JM, et al. Age-related changes in aortic and mitral valve thickness: implications for two-dimensional echocardiography based on an autopsy study of 200 normal human hearts. *Am J Cardiol.* 1988;62(7):424–30. PMID: 3414519.
63. Nkomo VT, Gardin JM, Skelton TN, et al. Burden of valvular heart diseases: a population-based study. *Lancet.* 2006;368(9540):1005–11. PMID: 16980116.
64. Gomez-Stallons MV, Tretter JT, Hassel K, et al. Calcification and extracellular matrix dysregulation in human postmortem and surgical aortic valves. *Heart.* 2019;105(21):1616–21. PMID: 31171628.
65. Rajamannan NM, Subramaniam M, Rickard D, et al. Human aortic valve calcification is associated with an osteoblast phenotype. *Circulation.* 2003;107(17):2181–4. PMID: 12719282.
66. Yip CY, Simmons CA. The aortic valve microenvironment and its role in calcific aortic valve disease. *Cardiovasc Pathol.* 2011;20(3):177–82. PMID: 21256052.
67. Simmons CA, Grant GR, Manduchi E, et al. Spatial heterogeneity of endothelial phenotypes correlates with side-specific vulnerability to calcification in normal porcine aortic valves. *Circ Res.* 2005;96(7):792–9. PMID: 15761200.
68. Butany J, Collins MJ, Demellawy DE, et al. Morphological and clinical findings in 247 surgically excised native aortic valves. *Can J Cardiol.* 2005;21(9):747–55. PMID: 16082434.

69. Roberts WC, Ko JM. Weights of individual cusps in operatively-excised stenotic three-cuspid aortic valves. *Am J Cardiol.* 2004;94(5):681–4. PMID: 15342312.
70. Owens DS, Katz R, Takasu J, et al. Incidence and progression of aortic valve calcium in the Multi-ethnic Study of Atherosclerosis (MESA). *Am J Cardiol.* 2010;105(5):701–8. PMID: 20185020.
71. Fedak PW, Verma S, David TE, et al. Clinical and pathophysiological implications of a bicuspid aortic valve. *Circulation.* 2002;106(8):900–4. PMID: 12186790.
72. Novaro GM, Mishra M, Griffin BP. Incidence and echocardiographic features of congenital unicuspid aortic valve in an adult population. *J Heart Valve Dis.* 2003;12(6):674–8. PMID: 14658804.
73. Yotsumoto G, Iguro Y, Kinjo T, et al. Congenital quadricuspid aortic valve: report of nine surgical cases. *Ann Thorac Cardiovasc Surg.* 2003;9(2):134–7. PMID: 12732093.
74. Yener N, Oktar GL, Erer D, et al. Bicuspid aortic valve. *Ann Thorac Cardiovasc Surg.* 2002;8(5):264–7. PMID: 12472407.
75. Robicsek F, Thubrikar MJ, Cook JW, et al. The congenitally bicuspid aortic valve: how does it function? Why does it fail? *Ann Thorac Surg.* 2004;77(1):177–85. PMID: 14726058.
76. Collins MJ, Butany J, Borger MA, et al. Implications of a congenitally abnormal valve: a study of 1025 consecutively excised aortic valves. *J Clin Pathol.* 2008;61(4):530–6. PMID: 17965218.
77. Roberts WC. The congenitally bicuspid aortic valve. A study of 85 autopsy cases. *Am J Cardiol.* 1970;26(1):72–83. PMID: 5427836.
78. Roberts WC. Morphologic aspects of cardiac valve dysfunction. *Am Heart J.* 1992;123(6):1610–32. PMID: 1595543.
79. Sievers HH, Schmidtke C. A classification system for the bicuspid aortic valve from 304 surgical specimens. *J Thorac Cardiovasc Surg.* 2007;133(5):1226–33. PMID: 17467434.
80. Falcone MW, Roberts WC, Morrow AG, et al. Congenital aortic stenosis resulting from a unicommissural valve. Clinical and anatomic features in twenty-one adult patients. *Circulation.* 1971;44(2):272–80. PMID: 5562562.
81. Edwards JE. Pathology of left ventricular outflow tract obstruction. *Circulation.* 1965;31:586–99. PMID: 14275999.
82. McKay R, Smith A, Leung MP, et al. Morphology of the ventriculoaortic junction in critical aortic stenosis. Implications for hemodynamic function and clinical management. *J Thorac Cardiovasc Surg.* 1992;104(2):434–42. PMID: 1495307.
83. Isner JM, Chokshi SK, DeFranco A, et al. Contrasting histoarchitecture of calcified leaflets from stenotic bicuspid versus stenotic tricuspid aortic valves. *J Am Coll Cardiol.* 1990;15(5):1104–8. PMID: 2312966.
84. Ho SY. Anatomy of the mitral valve. *Heart.* 2002;88 Suppl 4:iv5–10. PMID: 12369589.
85. Silbiger JJ. Anatomy, mechanics, and pathophysiology of the mitral annulus. *Am Heart J.* 2012;164(2):163–76. PMID: 22877801.
86. Lam JH, Ranganathan N, Wigle ED, et al. Morphology of the human mitral valve. I. Chordae tendinae: a new classification. *Circulation.* 1970;41(3):449–58. PMID: 5415982.
87. Adler Y, Fink N, Spector D, et al. Mitral annulus calcification – a window to diffuse atherosclerosis of the vascular system. *Atherosclerosis.* 2001;155(1):1–8. PMID: 11223420.
88. Roberts WC, Shirani J. Comparison of cardiac findings at necropsy in octogenarians, nonagenarians, and centenarians. *Am J Cardiol.* 1998;82(5):627–31. PMID: 9732892.
89. Abramowitz Y, Jilaihawi H, Chakravarty T, et al. Mitral annulus calcification. *J Am Coll Cardiol.* 2015;66(17):1934–41. PMID: 26493666.
90. Barasch E, Gottdiener JS, Larsen EK, et al. Clinical significance of calcification of the fibrous skeleton of the heart and aortosclerosis in community dwelling elderly. The Cardiovascular Health Study (CHS). *Am Heart J.* 2006;151(1):39–47. PMID: 16368289.
91. Tyagi G, Dang P, Pasca I, et al. Progression of degenerative mitral stenosis: insights from a cohort of 254 patients. *J Heart Valve Dis.* 2014;23(6):707–12. PMID: 25790617.

92. Aronow WS, Kronzon I. Correlation of prevalence and severity of mitral regurgitation and mitral stenosis determined by Doppler echocardiography with physical signs of mitral regurgitation and mitral stenosis in 100 patients aged 62 to 100 years with mitral annular calcium. *Am J Cardiol.* 1987;60(14):1189–90. PMID: 3687754.
93. Iung B, Baron G, Butchart EG, et al. A prospective survey of patients with valvular heart disease in Europe: The Euro Heart Survey on Valvular Heart Disease. *Eur Heart J.* 2003;24(13):1231–43. PMID: 12831818.
94. Nestico PF, Depace NL, Morganroth J, et al. Mitral annular calcification: clinical, pathophysiology, and echocardiographic review. *Am Heart J.* 1984;107(5 Pt 1):989–96. PMID: 6372421.
95. Fulkerson PK, Beaver BM, Auseon JC, et al. Calcification of the mitral annulus: etiology, clinical associations, complications and therapy. *Am J Med.* 1979;66(6):967–77. PMID: 156499.
96. Takamoto T, Popp RL. Conduction disturbances related to the site and severity of mitral annular calcification: a 2-dimensional echocardiographic and electrocardiographic correlative study. *Am J Cardiol.* 1983;51(10):1644–9. PMID: 6858870.
97. Carpentier AF, Pellerin M, Fuzellier JF, et al. Extensive calcification of the mitral valve anulus: pathology and surgical management. *J Thorac Cardiovasc Surg.* 1996;111(4):718–29; discussion 729–30. PMID: 8614132.

Chapter 3

Developmental Pathways and Aortic Valve Calcification



M. Victoria Gomez-Stallons, Keira Hassel, and Katherine E. Yutzey

Introduction

Calcific aortic valve disease (CAVD) is a progressive disease, initially presenting with aortic valve (AV) sclerosis, often leading to AV stenosis and insufficiency later in life [1, 2]. Early features of AV sclerosis, characterized by valve thickening, are present in more than 25% of the elderly population [3]. Valve stenosis is related to obstruction of blood outflow, and insufficiency is failure of valve leaflet closure leading to backward blood flow. AV stenosis is typically defined by restriction of the valve leaflet opening during systole, associated with a mean pressure gradient of at least 10 mm Hg in humans [3]. End-stage stenosis, often resulting from extensive valve leaflet calcification, is the most common type of valve disease leading to angina, syncope, and heart failure [2]. With CAVD progression, ventricular function can be affected, and, by the time symptoms are detected, valve disease often is severe. Without treatment, life expectancy for 90% of patients with severe AV stenosis is less than 10 years [2].

Currently, the most common clinical therapy for CAVD is AV replacement (AVR). However, there are significant complications associated with AVR, including the need for anticoagulation medication, and a second surgery usually is required after 5–10 years, due to limited durability of artificial valves [4, 5]. Because of the advanced age of many affected individuals, approximately 50% of patients referred for AVR are contraindicated for surgery [6–8]. Transcatheter aortic valve implantation (TAVI), a less invasive procedure that does not require open-heart surgery, is increasingly available for high-risk patients, especially for the elderly [9]. A disadvantage of this approach is that the long-term durability and potential need for

M. V. Gomez-Stallons · K. Hassel · K. E. Yutzey (✉)
Division of Molecular Cardiovascular Biology, The Heart Institute, Cincinnati Children's
Medical Center, Cincinnati, OH, USA
e-mail: Maria.Stallons@uc.edu; hasselkr@mail.uc.edu; Katherine.Yutzey@cchmc.org

subsequent replacement for TAVI have not yet been established. Thus, more long-term studies are needed, and this procedure is not widely used in younger patients. If proven to be effective, TAVI may become available to more patients, thus reducing the need for AVR open-heart surgery. To date, there are no pharmacologic-based treatments that can prevent the progression or inhibit the development of CAVD, highlighting the necessity for new therapeutic approaches. Interestingly, over half of surgically replaced AVs are associated with congenital malformations, including bicuspid aortic valve (BAV), establishing a relationship between valve development and disease mechanisms [10].

The pathogenesis of CAVD includes activation of signaling pathways and transcription factors involved in both heart valve and bone development [11–14]. These include transforming growth factor β (TGF β), bone morphogenetic protein (BMP), Wnt, and Notch signaling, as well as transcription factors Sox9 and Runx2 that play critical developmental roles during valve progenitor specification, proliferation, differentiation, and stratification. Similar to heart valves, bone is a complex connective tissue composed of specialized cell types that produce a collagen-rich extracellular matrix (ECM). Importantly, developmental pathways of cartilage, tendon, and bone are also active in developing valves [reviewed in [14–17]], highlighting parallels between valves and the skeleton. Most recently, these developmental pathways have also been found to be active in CAVD [13, 18–20], although their roles remain poorly understood. In this chapter, we discuss the molecular mechanisms of valve and bone development as they relate to CAVD pathogenesis.

Overview of Aortic Valves (AVs)

Aortic Valve Structure

In a normal heart, the mature AVs are made up of highly structured ECM layers and valve interstitial cells (VIC) that are surrounded by a layer of valve endothelial cells (VEC). The AV ECM is stratified into three distinct layers, fibrosa, spongiosa, and ventricularis, each providing different biomechanical properties and structural support (Fig. 3.1). The fibrosa layer located on the aortic side of the valve is primarily composed of fibrillar type I and III collagens that are oriented along the valve border providing stiffness and tensile strength [21, 22]. On the opposite side, the ventricularis layer of the AV is made up of elastic fibers, primarily radially oriented to promote leaflet motion [23, 24]. AV leaflet movement is made possible by collagen and elastic-rich layers that allow for extension and recoil of the leaflets during each heartbeat. The spongiosa, a proteoglycan-rich layer, is found between the collagen and elastic layers, enabling valve compression and preserving valve integrity. The aortic annulus, mainly comprised of fibrous collagen, is where leaflets attach to the aortic root of the heart and functions to distribute mechanical forces. Importantly, proper expression and organization of ECM components is essential for valve development, maintenance, and function.

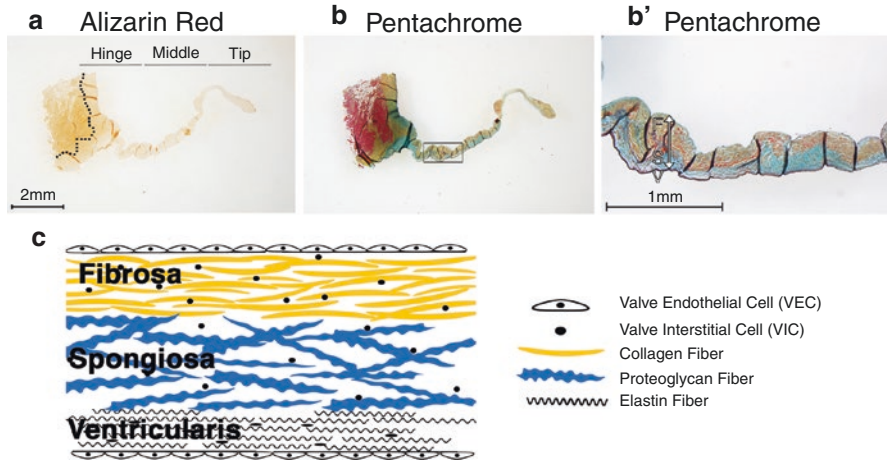


Fig. 3.1 Extracellular matrix (ECM) composition of a healthy aortic valve includes stratified layers of collagen, proteoglycans, and elastin. (a) Healthy human adult aortic valve leaflets do not exhibit calcification as indicated by lack of Alizarin Red staining. (b, b') Aortic valve leaflet ECM stratification is apparent by Movat's pentachrome stain with the fibrosa on the aortic side of the valve composed of collagen (yellow), the spongiosa composed of proteoglycans (blue), and the ventricularis comprised of elastin (black) on the ventricular side of the valve. (c) Schematic representation of valve interstitial cells (VICs) embedded within the ECM layers and surrounded by valve endothelial cells (VECs)

Valve Cell Diversity

The ECM composition of mature valves is dependent on synthesis by VICs. During valve remodeling, VICs express genes involved in collagen, proteoglycan, and elastin production associated with stratification of AV ECM layers [25, 26]. In mammals, valve stratification occurs postnatally, when VICs are highly synthetic and cell proliferation rates are low [26, 27]. In contrast, normal adult VICs remain quiescent with minimal proliferation and maintain baseline gene expression of ECM components necessary to support valve homeostasis [25].

In the adult AV, VICs comprise a heterogeneous and highly plastic population of resident cells [28]. VICs can transition through a number of different phenotypes in response to environmental changes and cytokines, during developmental valve remodeling, homeostasis, and disease. Based on *in vitro* and embryonic studies, the majority of resident VICs in a normal valve are quiescent (qVIC) and are derived from embryonic mesenchymal cells of the endocardial cushions [28]. A population of proliferating VICs (pVIC) has also been identified, as resident to the valves involved in valve repair. In addition, activated VICs (aVIC) are characterized by alpha smooth muscle actin (α SMA) expression, with increased proliferation, migration, and ECM remodeling activity. Lastly, osteoblast-like VICs (obVIC) have been identified in heart valve leaflets and are involved in calcification, chondrogenesis, and osteogenesis of the heart valves. obVICs can secrete alkaline phosphatase, osteocalcin, osteopontin, and

bone sialoprotein, all factors involved in normal bone mineralization. Diverse VIC populations also were identified by single cell gene expression analysis of remodeling mouse valves at postnatal day (P)7 and P30 [29]. During valve remodeling at P7, two distinct populations of collagen and glycosaminoglycan expressing VICs are present during active ECM stratification. In contrast, P30 VICs were clustered into four populations with leaflet specificity and unique expression of complement factors, ECM proteins, and osteogenic factors. In addition to ECM-producing VICs, multiple populations of hematopoietic-derived cells, including macrophages and dendritic cells, are present in remodeling and adult valves [30–32]. Melanocytes also were identified based on expression of key regulators *Dct* and *Mitf*. It is likely that the diverse populations of VICs and their transition states are essential for normal development, homeostasis, and function of the AV, but it is unknown whether, and if so how, they contribute to calcific aortic valve disease.

The outer layer of valve leaflets is comprised of VECs that play critical roles in establishing valve structure during development, as well as maintaining valve leaflet integrity and function during adult stages [17]. In contrast to vascular endothelial cells, VECs are aligned perpendicular to blood flow, following the direction of collagen fibers [33], and their function is highly influenced by hemodynamic forces [34]. Interestingly, disruption of the continuous outer layer of VECs is a key feature of early valve disease [34, 35]; however their pathological role remains unclear. Single cell gene expression analysis has uncovered localized subsets of endothelial cells present at P7 and P30 in murine heart valves [29]. Strikingly, these endothelial cell populations include three spatially different subsets characterized by differential expression of Prox1, a lymphatic marker, on the fibrosa side, Endomucin on the fibrosa and ventricularis sides, and Hapln1 expressed exclusively in the coaptation region. These differentially localized endothelial cell populations also are present in adult mouse, human, and pig AVs. The specific functions of these populations have not yet been established, but they may mediate the effects of differential hemodynamic or biomechanical stimuli on heart valve organization, homeostasis, or disease.

Development of the Aortic Valves

Overview

During embryonic development, the heart is the first organ to form and starts to beat by 18 days after conception in humans. The heart initially starts as a primitive tube composed of an endocardial endothelial cell layer surrounded by a layer of myocardial cells [36]. The first step in valve development includes the formation of endocardial cushions in the outflow tract (OFT) and atrioventricular canal (Fig. 3.2). Myocardium-derived signals induce an endothelial-to-mesenchymal transition (EndMT) of neighboring endothelial cells generating mesenchymal cells that populate the endocardial cushions [37, 38]. Subsequently, the mesenchymal progenitor cells give rise to VICs that contribute to mature valve structures [27, 39]. Cell

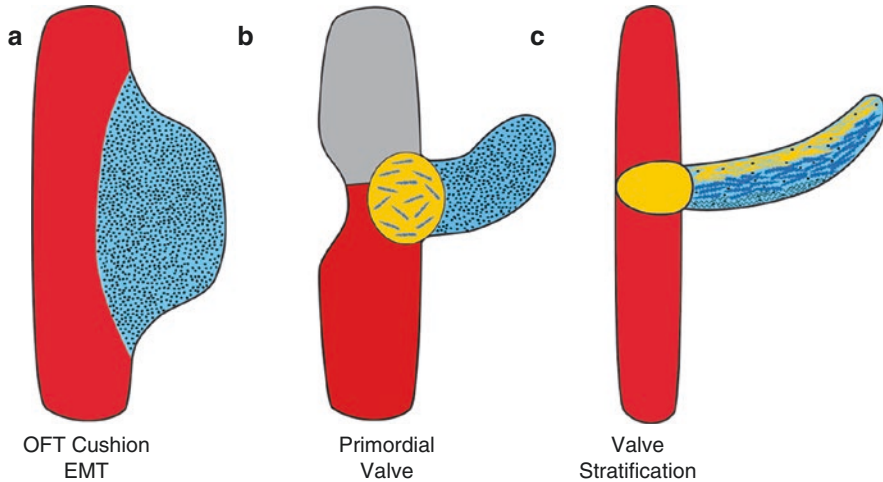


Fig. 3.2 Valve development progresses through outflow tract (OFT) cushion development, the valve primordia, and mature valve stratification. **(a)** Aortic valve progenitor cells arise by an endothelial-to-mesenchymal transition (EndMT) creating mesenchymal cells in the OFT endocardial cushions. **(b)** Primitive valve leaflets are apparent as the undifferentiated valve primordia in the developing fetus. **(c)** After birth the valve leaflet ECM is stratified into three layers, the fibrosa, spongiosa, and ventricularis, which are composed of collagen, proteoglycans, and elastin, respectively. Note that images are not at the same scale

lineage studies in mice demonstrate that most cells populating the valves after birth are of endothelial origin [27, 39]. In addition, neural crest cells (NCC) have been shown to be critical in the formation and remodeling of semilunar valves but are absent from atrioventricular valves [40–43]. In the early stages of development, mesenchymal cells remain highly proliferative surrounded by an immature ECM [44]. Although valves are not fully developed by this time, endocardial cushions of the OFT and atrioventricular canal are capable of functioning as valves to promote unidirectional blood flow in the early embryo [45]. Valve leaflets form after septation of the OFT cushions and fusion of the atrioventricular canal cushions [46]. Formation of the valve leaflets is characterized by thinning and elongation of the valve primordia, as well as remodeling of the valve ECM, giving rise to mature, highly organized layers consisting of elastin, proteoglycan, and collagen [14, 26]. As the ECM matures, proliferation of valve cells decreases, and VICs are relatively quiescent in the adult [25].

Embryonic Origins of Aortic Valves

Cells of different origins populate the AVs. The valve leaflets are surrounded by a layer of VECs that is continuous with the endocardial endothelial layer [47]. In the OFT where aortic and pulmonic semilunar valves are formed, subpopulations of

endocardial and mesenchymal cells are derived from the second heart field [48]. Using the endothelial-specific *Tie2-Cre ROSA26R* reporter mice, studies have shown that some of the mesenchymal cells of the OFT cushions are derived from endothelial progenitors through EndMT [27, 39]. Initially, the mature AVs were thought to be mainly populated by endothelial-derived cells. However, more recent studies revealed a significant contribution of neural crest-derived cells to the developing endocardial cushions of the OFT and mature valve leaflets, as indicated by *Wnt1-Cre* murine lineage trace studies [49–52]. Both endothelial and neural-crest derived cells populate AVs during development and in adult mice. However, it remains unclear whether cell origin is indicative of a specific subpopulation of the aortic VICs contributing to specific features of development and disease.

Transcription Factors Involved in Aortic Valve Development

During valve leaflet morphogenesis, the elongation and thinning of endocardial cushions occur with remodeling and stratification of the ECM, while VICs remain quiescent in mature valves [25, 26]. The highly proliferative mesenchymal cells of the endocardial cushions undergo decreased proliferation during leaflet elongation, which coincides with expression of ECM proteins, including elastin and fibrillar collagen. The transcription factor nuclear factor of activated T cells 1 (Nfatc1) is a key regulator of endocardial cushions and valve leaflet remodeling. Nfatc1 is highly expressed in endothelial cells of the endocardial cushions where it promotes cell proliferation and prevents vascular endothelial growth factor (VEGF)-mediated EndMT [53, 54]. Loss of Nfatc1 leads to heart valve remodeling defects and embryonic death in mice [55, 56]. During leaflet elongation, RANKL-mediated regulation of Nfatc1 stimulates expression of *cathepsin K* and promotes ECM remodeling [53].

Multiple transcription factors and signaling pathways important for development of skeletal and connective tissue lineages also are expressed in developing heart valves (Fig. 3.3). The transcription factor Sox9, essential for cartilage development, is expressed in endocardial cushions and remodeling valves [57], in which it is required for proper expression of proteoglycans in the spongiosa layer [58]. Scleraxis, a basic helix-loop-helix (bHLH) transcription factor required for tendon and ligament development, also is locally expressed in developing valves, and loss of scleraxis results in valve remodeling defects and myxomatous phenotypes in adult animals [57, 59]. Moreover, BMP2 treatment in avian valve progenitor cultures leads to *Sox9* expression and activation of its target gene *Aggrecan*, while treatment with FGF4 results in *scleraxis* and *tenascin* activation [57]. In addition, important regulators of bone differentiation and calcification such as Runx2 and osteocalcin are not expressed during normal valve development but are characteristic of a calcified AV phenotype [11, 14]. The bHLH transcription factor Twist1 is expressed in endocardial cushions mesenchyme and promotes cell migration and proliferation; however Twist1 expression decreases in later stages of valve remodeling [18, 60]. Activation of Twist1 leads to induction of downstream targets involved in cell proliferation and migration,

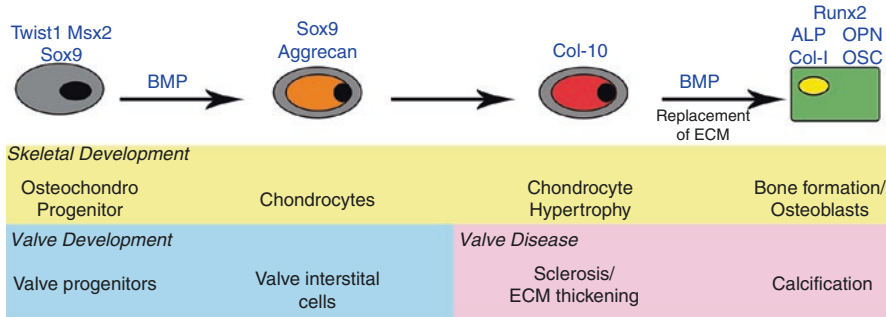


Fig. 3.3 Regulatory events of skeletal development are conserved with heart valve development and calcific disease. Developing heart valve cells and osteochondro-progenitors have similar gene expression profiles and regulatory pathways related to cartilage differentiation. Osteogenic gene expression and regulatory pathways are active in bone formation and CAVD. As an example of conserved regulatory mechanisms, BMP signaling is shown as a regulator of skeletal development, valve formation, and CAVD

including *Tbx20* and *Collagen2A1* [18, 61]. Activation of Sox9 and *Tbx20* is essential for endocardial cushions cell proliferation and expansion of the valve progenitor cell population. In developing endocardial cushions, transcription factors Msx1 and Msx2 are expressed in endocardial and mesenchymal cells during EndMT, while their loss leads to decreased endocardial cushion formation [62]. Interestingly, Twist1, Sox9, and Msx1/2 are activated in pediatric and adult AV disease [18, 19], suggesting their reactivation may be involved in disease pathology.

Signaling Pathways Involved in Aortic Valve Development

A number of signaling pathways play essential roles during AV development, including endocardial cushion formation and EndMT. BMP2 signaling is required for the initial steps of EndMT, in which BMP2 secreted by the myocardium induces the endocardium to initiate endocardial cushion formation in the OFT and atrioventricular canal [38]. Likewise, canonical Wnt/ β -catenin and TGF β signaling pathways are necessary for EndMT, as well as proliferation of mesenchymal endocardial cushion cells [37, 63, 64]. Together with the BMP pathway, Notch signaling is also required for EndMT, and in the endocardium, Notch represses endothelial cell adhesion gene expression [65]. Notch signaling also is involved in valve leaflet morphogenesis, and mutations in human *NOTCH1* are associated with congenital BAV and increased incidence of CAVD [66]. During valve development, the mesenchymal cells of the endocardial cushions are highly proliferative and express Twist1, Msx1/2, and *Tbx20* transcription factors [14]. These factors function to promote valve mesenchymal cell proliferation and expression of ECM genes [18, 60]. At later stages of valve remodeling, Wnt/ β -catenin signaling stimulates gene expression of ECM collagen-related fibrosa layer

markers in cultured VICs [67], and loss of β -catenin in VICs leads to production of cartilage-like nodules in adult AVs of mice [68]. Together these studies support a role for reactivation of developmental factors and mechanisms during AV disease.

Skeletal Development

Overview of Endochondral Bone Formation

The skeleton is predominantly made up of cartilage and bone. Each of these tissues is populated by specialized cell types: chondrocytes in cartilage and osteoblasts and osteoclasts in bone (Fig. 3.3). More detailed information on osteoclast function in bone and cardiovascular tissues is provided in Chap. 20. Interestingly, chondrocytes and osteoblasts have a mesenchymal origin and share a common progenitor (“osteochondro” progenitor cells) [69]. During development, bones are formed from three embryonic lineages: neural crest, paraxial mesoderm, and lateral plate mesoderm. Planar bones of the skull form by intramembranous ossification, in which migrating neural crest cells and paraxial mesoderm-derived cells condense into sheet-like structures, differentiate into osteoblast bone-forming cells and produce mineralized tissue. However, most bones in the body form by endochondral bone formation [70, 71]. During this process, chondrocytes produce a cartilage template that is remodeled by osteoclast reabsorbing cells and converted into bone by osteoblasts [72]. Here, we will focus on endochondral bone formation. During the last two decades, extensive progress has been made in understanding the molecular mechanisms controlling the development of cartilage and bone [73, 74].

During endochondral bone formation, the replacement of cartilage with mineralized bone initiates with differentiation of proliferating chondrocytes to a non-proliferative, hypertrophic state. This hypertrophic cartilage is then invaded by osteoblast progenitors, osteoclasts, blood vessel endothelial cells, and hematopoietic cells from the perichondrium, a layer of connective tissue that surrounds cartilage of the developing bone. The hypertrophic cartilage is broken down, incoming pre-osteoblasts differentiate into bone-forming osteoblasts, and hematopoietic and endothelial cells establish bone marrow at the primary ossification center [75]. Osteoblast progenitors in the perichondrium differentiate into osteocytes that deposit bone around the cartilage template. As development continues, the primary ossification center expands, and secondary ossification centers begin to form at one or both ends of the developing bone. This leads to the formation of epiphyseal growth plate cartilage resulting in longitudinal bone growth [71, 76]. These growth plates consist of chondrocytes organized into structural and functional zones, each with a unique expression pattern [77]. Small and quiescent cells are found in the reserve zone near the secondary ossification center, while proliferating chondrocytes are located in the bordering proliferative zone. These proliferating chondrocytes undergo clonal expansion and line up in the direction of longitudinal growth. Proliferating chondrocytes eventually reach the hypertrophic zone, where they stop proliferating. While some hypertrophic chondrocytes may undergo apoptosis, recent

studies suggest that some hypertrophic chondrocytes have the ability to become osteoblasts [78]. Over time, the growth plates get thinner, and the cartilage template is replaced by bone.

Characteristics of Cartilage and Bone Tissue

Cartilage and bone have distinct characteristics; interestingly, both share similarities with the AV tissues. Cartilage formation includes mesenchymal condensation, differentiation into proliferative chondrocytes, and maturation into hypertrophic chondrocytes. The main components of mature cartilaginous tissue are chondroitin sulfate proteoglycans, providing structural cushioning and flexibility to the skeleton [79, 80], while inhibiting angiogenesis, resulting in avascular mature cartilage [79]. Remarkably, these are also main features of the spongiosa layer in the mature AV [81], drawing structural parallels between heart valves and cartilage. In addition, the cartilage ECM prevents tissue mineralization, which is also a suggested role for the proteoglycan-rich layer of the AV [82]. A critical transcription factor in cartilage formation is Sox9, which is required for proliferation and differentiation of chondrocyte progenitors [83, 84]. Interestingly, high levels of Sox9 are found in developing and mature AVs.

The bone cell lineage is made up of a group of cells including mesenchymal “osteochondro” progenitors, pre-osteoblasts, osteoblasts, osteocytes, and osteoclasts (Fig. 3.3). Similar to valve progenitor cells and diseased AVs, mesenchymal transcription factors Twist1, Msx2, and Sox9 are expressed in osteochondro progenitor cells [74]. Like healthy differentiated VICs, pre-osteoblasts express high levels of type I collagen, as well as periostin, osteonectin, and osteopontin [67, 85], which have also been found to be increased in AV disease. Differentiated osteoblasts are the principal bone-making cells that produce a rich type I collagen matrix, in addition to calcification-specific proteins, such as osteocalcin and alkaline phosphatase [86]. Prior to bone mineralization, osteoblasts express the transcription factor Runx2, as well as ECM proteins osteocalcin and bone sialoprotein [13, 86]. During mature bone formation, Runx2 regulates gene expression of the transcription factor Osterix/Sp7 in osteoblasts and osteocytes [87]. Osteocyte expression of Runx2 and Sp7 is required for deposition of calcium phosphate and hydroxyapatite leading to bone mineralization [86]. Balancing activities of bone-forming osteoblasts and bone-reabsorbing osteoclasts maintain normal bone homeostasis.

Transcriptional Regulation of Skeletal Development

During cartilage development, proliferating chondrocytes are characterized by expression of cartilage marker genes *Col2a1* and *aggrecan*. A hallmark of the chondrocyte hypertrophic state is expression of *Col10a1*, instead of *Col2a1*. During collagen differentiation and maturation, the transcription factor Sox9 regulates expression of *Col2a1* and *aggrecan*, as well as *Col10a1* [88–93]. Thus, Sox9, as the

master regulator of chondrogenesis, controls proliferation and differentiation of non-hypertrophic chondrocytes [88, 94]. Mutations in human *TWIST1* result in skeletal dysplasia Saethre-Chotzen syndrome, characterized by early fusion of cranial sutures of the skull due to premature bone differentiation [95]. In the skeleton, *Twist1* is expressed early in osteochondro progenitor cells, and its expression inhibits terminal differentiation of both cartilage and bone [96]. To inhibit cartilage differentiation, *Twist1* can bind to *Sox9* preventing activation of cartilage-specific gene expression [97]. In pre-osteoblasts, *Twist1* can bind to *Runx2* blocking its transcriptional activation of bone differentiation genes including *osteocalcin* [96], thus preventing bone differentiation. The transcription factor *Msx2*, also involved in early stages of skeleton development, is expressed in mesenchymal osteochondro progenitors and is downregulated during osteoblast differentiation [74]. Overexpression of *Msx2* in osteoblasts prevents bone differentiation and mineralization, whereas loss of *Msx2* accelerates terminal bone stages [98]. Like *Twist1*, *Msx2* is expressed in mesenchymal progenitors and inhibits osteogenic differentiation. Thus, *Twist1* and *Msx2* are critical to preserve the mesenchymal progenitor stage during skeletal development.

Similar to *Twist1* and *Msx2*, *Sox9* is essential for specification of osteochondro progenitor cells, but it is not expressed in differentiated osteoblasts [99]. During early stages of chondrocyte development, *Sox9* induces cell proliferation, and its expression is required for chondrocyte differentiation [99]. As a transcription factor, *Sox9* promotes growth of cartilage progenitors and induces cartilage differentiation while preventing bone differentiation [80, 86]. *Sox9* can bind to *Runx2* inhibiting its transcriptional activity, resulting in hypertrophic cartilage growth and inhibition of osteogenic differentiation [100]. Thus, inhibition of *Sox9* expression in osteoblasts is necessary for bone differentiation and mineralization, while *Runx2* has been identified as critical for promoting bone formation and mineralization [74, 101]. Murine gain- and loss-of-function studies revealed that *Runx2* is necessary and sufficient to drive osteoblast differentiation [101]. Loss of *Runx2* expression in mice results in the lack of mineralized bone, while *Runx2* haploinsufficiency leads to reduced bone formation both in mice and humans [86]. Even after birth, introduction of a dominant negative form of *Runx2* results in decreased bone mineralization, highlighting the importance of *Runx2* in both bone mineralization and homeostasis throughout life [102]. Healthy heart valves from developmental or adult stages lack *Runx2* expression, as well as calcification. However, expression of *Runx2* has been detected in human and mouse CAVD [19, 103].

Nfatc1 is a critical mediator of RANKL-induced osteoclast differentiation [86, 104]. As a transcription factor, *Nfatc1* plays an important role in osteoclast activation via induction of genes involved in osteoclast adhesion, migration, and degradation of bone matrix [105, 106]. In bone, RANKL activity is antagonized by the receptor decoy osteoprotegerin (OPG) that promotes bone calcification [107, 108]. During osteoblast differentiation, *Nfatc1* stimulates cell proliferation and promotes osteoblast differentiation by cooperating with *Osterix/Sp7* to induce *Colla1* gene expression [109, 110]. The RANKL and OPG-mediated regulation of *Nfatc1*

transcriptional activity is essential for proper balance between bone calcification and resorption [104]. A similar balance of OPG and RANKL signaling in CAVD has been suggested [111]; however its role in adult valve homeostasis and disease remains unknown.

Signaling Pathways Involved in Bone Development

Various signaling cascades are involved during the different stages of endochondral bone formation including TGF β , BMP, Wnt, and Notch [71]. Together these networks interact to regulate transcription factor activation, as well as gene expression, in chondrocyte and osteoblast cell lineages. Similar molecular interactions occur in heart valve development and pathogenesis [14].

BMPs were originally identified as osteogenic factors with the ability to promote ectopic bone formation when implanted into competent tissues [112, 113]. During cartilage formation, skeletal element condensation is highly dependent on active BMP signaling and is inhibited by the BMP ligand antagonist, gremlin [114]. At the transcriptional level, BMP plays critical roles in osteochondrogenic gene induction, including *Sox9* gene expression [115]. Mice with loss of the BMP/TGF β signaling intermediate *Smad4*, using *Col2a1-Cre* expressed in osteochondrogenic progenitors, exhibit dwarfism as a result of growth plate disorganization [116]. Likewise mice with *Col2a1-Cre*-mediated loss of the BMP signaling intermediate *Smad1/5* develop severe chondrodysplasia [117], demonstrating that BMP signaling through *Smad1/5* is required for endochondral bone formation. The Wnt signaling cascade also has essential functions during bone formation. At the transcriptional level, Wnt/ β -catenin induces activation of *Runx2* leading to osteoblast differentiation while preventing *Sox9* expression thereby inhibiting chondrogenesis [80]. Even in the presence of *Runx2*, Wnt/ β -catenin signaling is required for complete activation of the osteogenic program. In mice, loss of β -Catenin expression in early mesenchymal osteochondro progenitors results in loss of osteoblast differentiation [86]. Both BMP and Wnt pathways act together to induce bone calcification; however neither pathway alone is sufficient to drive an osteogenic response [118].

Notch signaling plays a critical role in endochondral bone formation. In early osteochondro progenitors, Notch signaling is necessary for cell proliferation, while increased levels prevent terminal differentiation of chondrocytes and endochondral ossification [119]. Notch inhibits chondrogenesis via *Sox9* transcriptional suppression [120]. Furthermore, activation of Notch signaling can inhibit Wnt/ β -catenin and *Runx2* transcriptional activity preventing osteoblast differentiation [121–123]. Similarly, loss of Notch1/2 function leads to increased osteoblast differentiation and bone mass in mice [124]. In addition to the Notch pathway, TGF β signaling plays an important role in maintenance of bone mass via regulation of bone formation and resorption. Human TGF β 1 gain-of-function mutations result in Camurati-Engelmann disease (CED) characterized by diaphyseal thickening and fluctuating

bone volumes [125], while similar phenotypes are seen in mice with this mutation [126]. On the other hand, loss of TGF β 1 in cartilage promotes chondrocyte hypertrophy resulting in cartilage degeneration [127].

Similarities Between Valve and Skeletal Development

Many studies have identified pathways active in development of heart valves, as well as skeletal development, including both cartilage and bone (Fig. 3.3). Not surprisingly, similarities also exist between the structural makeup of the heart valves and skeleton, highlighting common ECM components that play critical roles in both development and disease of these tissues. Understanding these similarities will be essential to reveal the pathological role of developmental pathways in the initiation and progression of AV disease.

Reactivation of Developmental Pathways in CAVD

Overview

Studies of human CAVD provide evidence that a number of valve and bone developmental pathways are active in diseased valves [128]. Early studies identified an association between the Notch signaling pathway and CAVD, as mutations in human *NOTCH1* were linked to both BAV and CAVD [66]. Notably, studies in mice and cultured VICs demonstrated the protective role of Notch signaling against valve calcification [129, 130]. On the other hand, activation of Wnt/ β -catenin and BMP signaling pathways has been associated with progression of CAVD. Studies of human diseased AV samples revealed Wnt/ β -catenin activation, supporting a role for Wnt/ β -catenin during CAVD via osteogenic gene induction [131, 132]. However, the underlying Wnt/ β -catenin-related mechanism driving CAVD pathogenesis remains unknown. In addition, pSmad1/5/8 activation, indicative of active BMP signaling, has been observed in human and mouse CAVD [133]. Importantly, pSmad1/5/8 activation is observed exclusively in adult calcified AVs and is not detected in pediatric diseased valves that do not calcify [19], suggesting a critical role for BMP-pSmad1/5/8 signaling in the pathogenesis of adult CAVD (Fig. 3.3). The intersection of Notch and BMP signaling is essential for AV development and has been shown to play a role during AV calcification in vitro [129, 134].

Early stage and pediatric AV disease is primarily associated with ECM dysregulation similar to early cartilage development, while late stage adult CAVD is associated with leaflet thickening and development of calcific nodules reminiscent of late stage bone formation [19, 135]. Thus, early stages may be linked to dysregulation of developmental pathways involved in normal valve ECM formation and cartilage formation, while late stage calcific disease includes induction of osteogenic pathways involved primarily in bone formation.

Cell Origins of Calcifying Aortic VICs During CAVD

The development of AV stenosis has been linked to inflammation, disrupted lipid metabolism, dystrophic calcification, and bone formation [136]. Based on these findings, there has been an interest in identifying cell types and pathogenic mechanisms that contribute to the progression of CAVD. Advanced CAVD is characterized by the presence of calcium deposits normally found on the fibrosa side of AVs [11, 137, 138]. Studies suggest there may be a number of different sources for calcifying cells of the AVs during disease, including osteogenic trans-differentiation of VICs, circulating osteo-progenitor cells, infiltrating immune cells, and cells derived from EndMT events [139]. Chondrocyte-like cells localized to the annular and hinge regions of the AVs may also contribute to calcification through their production of the valve ECM components, including collagens and proteoglycans [135, 140]. Histological studies of postmortem adult human AV leaflets prior to clinical CAVD diagnosis (no clinical AV stenosis) revealed increased collagen and proteoglycan ECM, as well as elastin fragmentation, even prior to AV thickening or calcification [135]. Similarly, pigs subjected to a high-fat diet exhibited increased ECM production and valve leaflet thickening, hypothesized to be early indicators of AV sclerosis, prior to calcification, in a large animal model [141]. Together, these studies support an early pathological role for increased ECM production by VICs in the development of CAVD.

Moreover, a recent study using transcriptomics and proteomics of human stenotic AVs [142] showed increased expression of myofibrogenesis and oxidative stress genes during the fibrotic stage, while the calcific stage was characterized by increased expression of calcification factors. Both fibrotic and calcific stages were associated with significant inflammation, confirming an early pathological role for inflammation in CAVD progression. Furthermore, this study identified VICs derived from the fibrosa layer of the AVs as the main drivers of calcification in CAVD, with profibrotic and procalcific characteristics, in contrast to ventricularis-derived VICs with low calcification potential. However, it remains unknown whether these different cell types and origins have specific roles and functions during AV disease.

CAVD: A Bone-Like Process of Calcification

Because of its association with aging, CAVD was believed to be a passive, degenerative disease. However, recent studies have demonstrated that CAVD is an active, cellular-driven process [5]. A hallmark in the progression of CAVD is AV stenosis caused by extensive calcific deposits (Fig. 3.4). In adult healthy valves, resident VICs remain quiescent with fibroblast-like characteristics. In human CAVD, markers of endochondral bone formation have been observed in VICs associated with areas of calcification, supporting activation of an osteoblast-like cell phenotype during disease progression [19]. Likewise, there is increasing evidence that AV

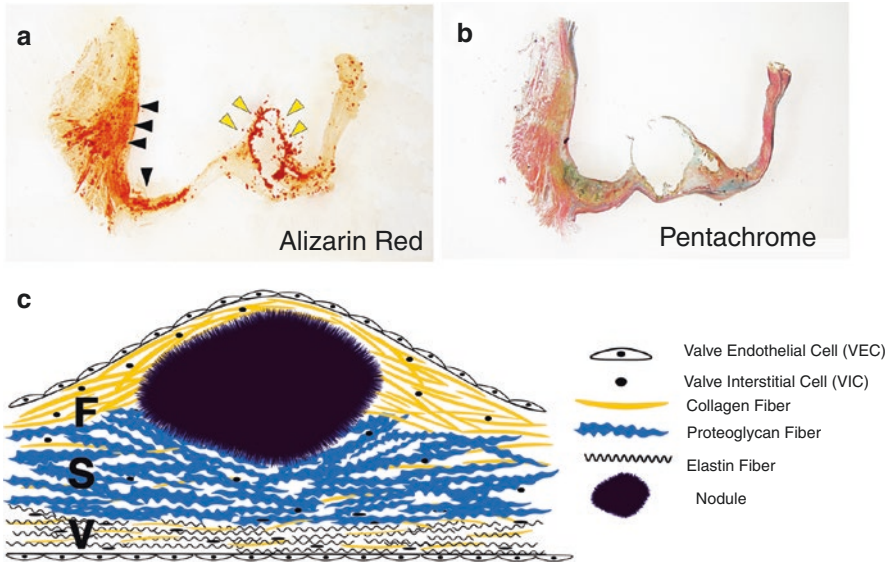


Fig. 3.4 Diseased aortic valves display calcification and disorganization of ECM components. **(a)** Aortic valve calcification is apparent in postmortem human leaflets with calcification indicated by positive Alizarin Red staining (red). Calcific nodules are prevalent on the aortic side of the leaflet middle region (yellow arrowheads), and intrinsic calcification is observed within the valve tissue at the hinge (black arrowheads). **(b)** ECM dysregulation is apparent in Movat's pentachrome-stained calcified aortic valve. **(c)** Schematic representation of nodular calcification originating in the collagen-rich fibrosa, which disrupts the organization of ECM layers, as well as the gross valve anatomy, if large nodules are present

calcification during CAVD occurs via an endochondral bone formation-like process [137]. In developing bone, osteogenic genes, Runx2 and osteocalcin (OCN), are critical regulators of bone mineralization [143], and these genes also are expressed in CAVD (Fig. 3.3). Together these data demonstrate that osteogenic genes are active in CAVD.

Some of the pathological events associated with CAVD are believed to initiate at the endothelial barrier. VECs comprise the outer layer of the AVs, making them the first line of response to hemodynamic forces and systemic circulating factors [144]. VEC dysfunction leads to infiltration of cells and cytokines that are able to promote activation of native quiescent VICs. Consequently, activated myofibroblast-like VICs are responsible for the initial steps of CAVD, including AV sclerosis and stiffness [145]. Thus, there is increasing evidence that the progression from AV sclerosis to stenosis involves a bone-like process of calcification via osteo-progenitor cells arising from different origins, including activated VICs. However, it is important to highlight that there are many additional risks factors associated with disease, including atherosclerosis, late-stage kidney disease, diabetes, and aging, that likely stimulate activation of additional pathogenic pathways in CAVD [146]. However, the relationship between pathogenic and developmental pathways in the initiation and progression of CAVD remains poorly understood.

One of the key features of AV stenosis is the presence of calcific nodules. Likewise, molecular pathways involved in bone mineralization, such as the BMP and Wnt/ β -catenin signaling cascades, in addition to factors involved in endochondral bone formation, such as proteoglycans, alkaline phosphatase, Runx2, osteopontin, and bone sialoprotein, have been implicated in human CAVD [13]. Osteogenic gene induction is a key feature observed in end-stage CAVD of distinct etiologies, suggesting a common mechanism involved during AV calcification. Interestingly, osteogenic gene induction can be initiated as a result of inflammation, via cytokine production [147] and oxidative stress, leading to activation of transcription factor Runx2 and the Wnt signaling pathway, key players in the process of mineralization [148].

Developmental Transcription Factors in CAVD

The pathogenesis of CAVD remains poorly understood, but various studies suggest that valve disease discovered later in life may be related to defects in valve development [66, 149]. Importantly, congenitally malformed valves such as BAV have a higher probability of calcifying, and CAVD occurs at a younger age in individuals with BAV. In addition, transcriptional networks of heart valve development have been identified in diseased AVs. The chondrogenic factor Sox9 has been shown to have a protective role in CAVD and is regulated by nuclear localization [150]. Heterozygous loss of Sox9 expression in *Col2a1*-expressing lineages leads to AV calcification in mice [58], while ectopic expression of Sox9 prevents AV calcification and osteogenic gene induction [82]. There is increased Sox9 expression in diseased calcified AVs, as well as pediatric valves that do not calcify [19]; thus its pathological role in CAVD is not well understood. Similar to Sox9, increased Msx2 expression has been found in human diseased AVs [19], and its expression is sufficient to promote vascular calcification via activation of the Wnt pathway [151]; however, the role of Msx2 in CAVD remains unknown. Nfatc1 has also been shown to be expressed in calcified AVs [152], and the RANKL antagonist OPG can inhibit AV calcification in hypercholesterolemic mice [153]. In addition, Runx2 and its downstream targets *Osteocalcin* and *Alkaline Phosphatase (ALP)* also are increased in human CAVD samples [137]. Of note, osteogenic gene induction occurs in calcified AVs with different comorbidities, suggesting its activation may be a final step in CAVD.

Intersecting Signaling Pathways in CAVD

Recent studies revealed the active regulation of osteogenic processes in aortic mineralization [154–157], indicating a parallel between vascular aortic calcification and bone formation. However, the mechanism driving the process of

calcification in AVs remains less known. Previous studies have demonstrated that VICs, either cultured in vitro with osteogenic media or genetically manipulated for Notch1 inhibition, exhibit calcification and osteogenic gene induction, including *Runx2* and *ALP*, as well as increased BMP signaling [67, 129, 158]. Similar to atherosclerotic lesions, BMP2 and BMP4 are expressed in human calcified AVs [137]. In addition, preferential expression of pSmad1/5/8, indicative of BMP signaling, was observed on the fibrosa side of calcified AVs [133]. Specifically, pSmad1/5/8 activation is exclusively expressed in calcified adult diseased valves, in contrast to pediatric diseased valves that do not calcify [19]. Likewise, *Notch1*^{+/-} and high-fat fed *ApoE*^{-/-} mice with AV disease exhibit increased pSmad1/5/8 activation [129, 130, 159]. In addition, loss of the BMP pathway inhibitors, Smad6 and MGP, leads to valve calcification in mice [160, 161]. Conversely, conditional loss of the BMP receptor ALK3 in VICs prevents development of CAVD lesions in the *Klotho* mouse model of premature aging [140]. Altogether these data support an important role for BMP signaling in the development of CAVD.

Analysis of calcified AVs provided initial evidence for a role of Wnt/ β -catenin signaling in CAVD. β -catenin expression is significantly increased in calcified AVs when compared to healthy normal valves [162]. Moreover, expression of the chondrogenic factor Sox9, as well as osteogenic factors Runx2, bone sialoprotein, and osteocalcin, was also upregulated. Supporting a role for Wnt signaling, increased expression of receptor LRP5 and ligand Wnt3 has been identified in calcified AVs when compared to controls [68]. Together these data support a role for Wnt/ β -catenin during osteochondrogenic gene induction and development of AV calcification. BMP signaling has been shown to participate in activation of noncanonical signaling independent of Smads, via JNK, p38 and MAPK cascades. Studies revealed that non-Smad signals were associated with Wnt/ β -catenin activation, leading to ALP expression and matrix calcification [163, 164]. These data support a model where BMP and Wnt- β -catenin signaling pathways intersect to activate downstream expression of factors involved in AV calcification; however this interaction has not yet been elucidated in vivo.

Mutations in human *NOTCH1* are associated with BAV and CAVD [66]. Studies in mice and cultured VICs demonstrated that Notch signaling protects against mineralization [66, 129]. In addition, adult mice with heterozygous loss of *Notch1* or *RBPJ*, a Notch effector, fed a high-fat diet present with AV calcification [130]. Similarly, endothelial-specific deletion of the Notch ligand Jag1 leads to AV calcification associated with abnormal ECM remodeling [165]. The transcription factor Hey2, a downstream effector of the Notch pathway, can directly inhibit Runx2-mediated transcriptional activation of osteogenic genes [66]. Interestingly, murine loss of Hey2 results in AV stenosis and activation of osteogenic genes. Together these data support a protective role for Notch signaling in the development of CAVD.

The pathogenesis of CAVD is associated with an increase in myofibroblasts, characterized by increased α SMA expression. Past studies have shown that TGF β 1 mediates differentiation of VICs into α SMA-expressing myofibroblasts, resulting in increased tension and realignment of ECM fibers [166]. Explanted human AVs from

patients with end-stage CAVD exhibit increased TGF β 1 expression, suggesting a positive role for TGF β 1 in the development of CAVD. In contrast, TGF β 1 treatment of in vitro cultured porcine VICs inhibited calcific nodule formation and murine TGF β 1 loss-of-function results in CAVD in vivo [150]. Together these findings support a critical role for TGF β 1 in CAVD pathogenesis, potentially related to specific levels of TGF β 1.

Conclusions

Currently, the only clinical therapy available for CAVD is AV replacement (surgery or TAVI). Unfortunately, these procedures are associated with significant complications, and little is known about the long-term effectiveness of TAVI. Thus, there remains an unmet clinical need for the development of pharmaceutical therapies that can prevent or inhibit the development or progression of disease. The increasing knowledge of the critical drivers of valve disease, including developmental and osteogenic mechanisms, together with new data from state-of-the-art technologies such as transcriptomics, proteomics, single cell analysis, and network medicine [167], represents important progress toward the identification of new therapeutic targets and treatment strategies for CAVD.

References

1. Otto CM, Kuusisto J, Reichenbach DD, Gown AM, O'Brien KD. Characterization of the early lesion of 'degenerative' valvular aortic stenosis. Histological and immunohistochemical studies. *Circulation*. 1994;90(2):844–53.
2. Carabello BA, Paulus WJ. Aortic stenosis. *Lancet*. 2009;373(9667):956–66.
3. Nishimura RA, Otto CM, Bonow RO, Carabello BA, Erwin JP 3rd, Guyton RA, et al. 2014 AHA/ACC guideline for the management of patients with valvular heart disease. *J Am Coll Cardiol*. 2014;63(22):e57–185.
4. Lindman BR, Bonow RO, Otto CM. Current management of calcific aortic stenosis. *Circ Res*. 2013;113(2):223–37.
5. Rajamannan NM, Evans FJ, Aikawa E, Grande-Allen KJ, Demer LL, Heistad DD, et al. Calcific aortic valve disease: not simply a degenerative process: a review and agenda for research from the National Heart and Lung and Blood Institute Aortic Stenosis Working Group. Executive summary: calcific aortic valve disease-2011 update. *Circulation*. 2011;124(16):1783–91.
6. Bouma BJ, van Den Brink RB, van Der Meulen JH, Verheul HA, Cheriex EC, Hamer HP, et al. To operate or not on elderly patients with aortic stenosis: the decision and its consequences. *Heart*. 1999;82(2):143–8.
7. Iung B, Baron G, Butchart EG, Delahaye F, Gohlke-Barwolf C, Levang OW, et al. A prospective survey of patients with valvular heart disease in Europe: The Euro Heart Survey on Valvular Heart Disease. *Eur Heart J*. 2003;24(13):1231–43.
8. Varadarajan P, Kapoor N, Bansal RC, Pai RG. Clinical profile and natural history of 453 nonsurgically managed patients with severe aortic stenosis. *Ann Thorac Surg*. 2006;82(6):2111–5.

9. Desai CS, Roselli EE, Svensson LG, Bonow RO. Transcatheter aortic valve replacement: current status and future directions. *Semin Thorac Cardiovasc Surg.* 2013;25(3):193–6.
10. Roberts WC, Ko JM. Frequency by decades of unicuspid, bicuspid and tricuspid aortic valves in adults having isolated aortic valve replacement for aortic stenosis, with or without associated aortic regurgitation. *Circulation.* 2005;111:920–5.
11. Rajamannan NM, Subramaniam M, Rickard DJ, Stock SR, Donovan J, Springett M, et al. Human aortic valve calcification is associated with an osteoblast phenotype. *Circulation.* 2003;107:2181–4.
12. O'Brien KD. Pathogenesis of calcific aortic valve disease: a disease process comes of age (and a good deal more). *Arterioscler Thromb Vasc Biol.* 2006;2006:1721–8.
13. Bostrom K, Rajamannan NM, Towler DA. The regulation of valvular and vascular sclerosis by osteogenic morphogens. *Circ Res.* 2011;109:564–77.
14. Combs MD, Yutzey KE. Heart valve development: regulatory networks in development and disease. *Circ Res.* 2009;105:408–21.
15. Karsenty G, Kronenberg HM, Settembre C. Genetic control of bone formation. *Annu Rev Cell Dev Biol.* 2009;25:629–48.
16. Hinton RB, Yutzey KE. Heart valve structure and function in development and disease. *Annu Rev Physiol.* 2011;73:29–46.
17. Lincoln J, Lange AW, Yutzey KE. Hearts and bones: shared regulatory mechanisms in heart valve, cartilage, tendon, and bone development. *Dev Biol.* 2006;294(2):292–302.
18. Chakraborty S, Wrigg EE, Hinton RB, Merrill WH, Spicer DB, Yutzey KE. Twist1 promotes heart valve cell proliferation and extracellular matrix gene expression during development in vivo and is expressed in human diseased aortic valves. *Dev Biol.* 2010;347:167–79.
19. Wrigg EE, Hinton RB, Yutzey KE. Differential expression of cartilage and bone-related proteins in pediatric and adult diseased aortic valves. *J Mol Cell Cardiol.* 2011;50:561–9.
20. Miller JD, Weiss RM, Heistad DD. Calcific aortic valve stenosis: methods, models, and mechanisms. *Circ Res.* 2011;108:1392–412.
21. Broom ND. The observation of collagen and elastin structures in wet whole mounts of pulmonary and aortic leaflets. *J Thorac Cardiovasc Surg.* 1978;75(1):121–30.
22. Kershaw JD, Misfeld M, Sievers HH, Yacoub MH, Chester AH. Specific regional and directional contractile responses of aortic cusp tissue. *J Heart Valve Dis.* 2004;13(5):798–803.
23. Schoen FJ. Aortic valve structure-function correlations: role of elastic fibers no longer a stretch of the imagination. *J Heart Valve Dis.* 1997;6(1):1–6.
24. Vesely I. The role of elastin in aortic valve mechanics. *J Biomech.* 1998;31(2):115–23.
25. Aikawa E, Whittaker P, Farber M, Mendelson K, Padera RF, Aikawa M, et al. Human semilunar cardiac valve remodeling by activated cells from fetus to adult: implications for postnatal adaptation, pathology, and tissue engineering. *Circulation.* 2006;113(10):1344–52.
26. Hinton RB Jr, Lincoln J, Deutsch GH, Osinska H, Manning PB, Benson DW, et al. Extracellular matrix remodeling and organization in developing and diseased aortic valves. *Circ Res.* 2006;98(11):1431–8.
27. Lincoln J, Alfieri CM, Yutzey KE. Development of heart valve leaflets and supporting apparatus in chicken and mouse embryos. *Dev Dyn.* 2004;230(2):239–50.
28. Liu AC, Joag VR, Gotlieb AI. The emerging role of valve interstitial cell phenotypes in regulating heart valve pathobiology. *Am J Pathol.* 2007;171(5):1407–18.
29. Hulin A, Hortells L, Gomez-Stallons MV, O'Donnell A, Chetal K, Adam M, et al. Maturation of heart valve cell populations during postnatal remodeling. *Development.* 2019;146(12).
30. Hulin A, Anstine LJ, Kim AJ, Potter SJ, DeFalco T, Lincoln J, et al. Macrophage transitions in heart valve development and myxomatous valve disease. *Arterioscler Thromb Vasc Biol.* 2018;38(3):636–44.
31. Anstine LJ, Horne TE, Horwitz EM, Lincoln J. Contribution of extra-cardiac cells in murine heart valves is age-dependent. *J Am Heart Assoc.* 2017;6(10):e007097.
32. Visconti RP, Ebihara Y, LaRue AC, Fleming PA, McQuinn TC, Masuya M, et al. An in vivo analysis of hematopoietic stem cell potential: hematopoietic origin of cardiac valve interstitial cells. *Circ Res.* 2006;98(5):690–6.

33. Deck JD. Endothelial cell orientation on aortic valve leaflets. *Cardiovasc Res.* 1986;20(10):760–7.
34. Butcher JT, Nerem RM. Valvular endothelial cells regulate the phenotype of interstitial cells in co-culture: effects of steady shear stress. *Tissue Eng.* 2006;12(4):905–15.
35. Stein PD, Wang CH, Riddle JM, Sabbah HN, Magilligan DJ Jr, Hawkins ET. Scanning electron microscopy of operatively excised severely regurgitant floppy mitral valves. *Am J Cardiol.* 1989;64(5):392–4.
36. Bruneau BG. The developmental genetics of congenital heart disease. *Nature.* 2008;451(7181):943–8.
37. Person AD, Klewer SE, Runyan RB. Cell biology of cardiac cushion development. *Int Rev Cytol.* 2005;243:287–335.
38. Ma L, Lu MF, Schwartz RJ, Martin JF. *Bmp2* is essential for cardiac cushion epithelial-mesenchymal transition and myocardial patterning. *Development.* 2005;132(24):5601–11.
39. de Lange FJ, Moorman AF, Anderson RH, Manner J, Soufan AT, de Gier-de Vries C, et al. Lineage and morphogenetic analysis of the cardiac valves. *Circ Res.* 2004;95(6):645–54.
40. Nomura-Kitabayashi A, Phoon CK, Kishigami S, Rosenthal J, Yamauchi Y, Abe K, et al. Outflow tract cushions perform a critical valve-like function in the early embryonic heart requiring BMPRIA-mediated signaling in cardiac neural crest. *Am J Physiol Heart Circ Physiol.* 2009;297(5):H1617–28.
41. Jain R, Engleka KA, Rentschler SL, Manderfield LJ, Li L, Yuan L, et al. Cardiac neural crest orchestrates remodeling and functional maturation of mouse semilunar valves. *J Clin Invest.* 2011;121(1):422–30.
42. Kirby ML, Gale TF, Stewart DE. Neural crest cells contribute to normal aorticopulmonary septation. *Science.* 1983;220(4601):1059–61.
43. Kirby ML, Turnage KL 3rd, Hays BM. Characterization of conotruncal malformations following ablation of “cardiac” neural crest. *Anat Rec.* 1985;213(1):87–93.
44. Schroeder JA, Jackson LF, Lee DC, Camenisch TD. Form and function of developing heart valves: coordination by extracellular matrix and growth factor signaling. *J Mol Med (Berl).* 2003;81(7):392–403.
45. Yalcin HC, Shekhar A, McQuinn TC, Butcher JT. Hemodynamic patterning of the avian atrioventricular valve. *Dev Dyn.* 2011;240(1):23–35.
46. Butcher JT, McQuinn TC, Sedmera D, Turner D, Markwald RR. Transitions in early embryonic atrioventricular valvular function correspond with changes in cushion biomechanics that are predictable by tissue composition. *Circ Res.* 2007;100(10):1503–11.
47. Armstrong EJ, Bischoff J. Heart valve development: endothelial cell signaling and differentiation. *Circ Res.* 2004;95(5):459–70.
48. Verzi MP, McCulley DJ, De Val S, Dodou E, Black BL. The right ventricle, outflow tract, and ventricular septum comprise a restricted expression domain within the secondary/anterior heart field. *Dev Biol.* 2005;287(1):134–45.
49. Snarr BS, Kern CB, Wessels A. Origin and fate of cardiac mesenchyme. *Dev Dyn.* 2008;237(10):2804–19.
50. Jiang X, Rowitch DH, Soriano P, McMahon AP, Sucov HM. Fate of the mammalian cardiac neural crest. *Development.* 2000;127(8):1607–16.
51. Nakamura T, Colbert MC, Robbins J. Neural crest cells retain multipotential characteristics in the developing valves and label the cardiac conduction system. *Circ Res.* 2006;98(12):1547–54.
52. Hutson MR, Kirby ML. Model systems for the study of heart development and disease. *Cardiac neural crest and conotruncal malformations. Semin Cell Dev Biol.* 2007;18(1):101–10.
53. Combs MD, Yutzey KE. VEGF and RANKL regulation of NFATc1 in heart valve development. *Circ Res.* 2009;105(6):565–74.
54. Wu B, Wang Y, Lui W, Langworthy M, Tompkins KL, Hatzopoulos AK, et al. *Nfatc1* coordinates valve endocardial cell lineage development required for heart valve formation. *Circ Res.* 2011;109(2):183–92.

55. de la Pompa JL, Timmerman LA, Takimoto H, Yoshida H, Elia AJ, Samper E, et al. Role of the NF-ATc transcription factor in morphogenesis of cardiac valves and septum. *Nature*. 1998;392(6672):182–6.
56. Ranger AM, Grusby MJ, Hodge MR, Gravalles EM, de la Brousse FC, Hoey T, et al. The transcription factor NF-ATc is essential for cardiac valve formation. *Nature*. 1998;392(6672):186–90.
57. Lincoln J, Alfieri CM, Yutzey KE. BMP and FGF regulatory pathways control cell lineage diversification of heart valve precursor cells. *Dev Biol*. 2006;292:290–302.
58. Lincoln J, Kist R, Scherer G, Yutzey KE. Sox9 is required for precursor cell expansion and extracellular matrix organization during mouse heart valve development. *Dev Biol*. 2007;305(1):120–32.
59. Levay AK, Peacock JD, Lu Y, Koch M, Hinton RB Jr, Kadler KE, et al. Scleraxis is required for cell lineage differentiation and extracellular matrix remodeling during murine heart valve formation in vivo. *Circ Res*. 2008;103(9):948–56.
60. Shelton EL, Yutzey KE. Twist1 function in endocardial cushion cell proliferation, migration, and differentiation during heart valve development. *Dev Biol*. 2008;317(1):282–95.
61. Lee MP, Yutzey KE. Twist1 directly regulates genes that promote cell proliferation and migration in developing heart valves. *PLoS One*. 2011;6(12):e29758.
62. Chen YH, Ishii M, Sucov HM, Maxson RE Jr. Msx1 and Msx2 are required for endothelial-mesenchymal transformation of the atrioventricular cushions and patterning of the atrioventricular myocardium. *BMC Dev Biol*. 2008;8:75.
63. Hurlstone AF, Haramis AP, Wienholds E, Begthel H, Korving J, Van Eeden F, et al. The Wnt/beta-catenin pathway regulates cardiac valve formation. *Nature*. 2003;425(6958):633–7.
64. Liebner S, Cattellino A, Gallini R, Rudini N, Iurlaro M, Piccolo S, et al. Beta-catenin is required for endothelial-mesenchymal transformation during heart cushion development in the mouse. *J Cell Biol*. 2004;166(3):359–67.
65. Timmerman LA, Grego-Bessa J, Raya A, Bertran E, Perez-Pomares JM, Diez J, et al. Notch promotes epithelial-mesenchymal transition during cardiac development and oncogenic transformation. *Genes Dev*. 2004;18(1):99–115.
66. Garg V, Muth AN, Ransom JF, Schluterman MK, Barnes R, King IN, et al. Mutations in NOTCH1 cause aortic valve disease. *Nature*. 2005;437(7056):270–4.
67. Alfieri CM, Cheek J, Chakraborty S, Yutzey KE. Wnt signaling in heart valve development and osteogenic gene induction. *Dev Biol*. 2010;338(2):127–35.
68. Fang M, Alfieri CM, Hulin A, Conway SJ, Yutzey KE. Loss of beta-catenin promotes chondrogenic differentiation of aortic valve interstitial cells. *Arterioscler Thromb Vasc Biol*. 2014;34(12):2601–8.
69. Ducy P, Zhang R, Geoffroy V, Ridall AL, Karsenty G. Osf2/Cbfa1: a transcriptional activator of osteoblast differentiation. *Cell*. 1997;89(5):747–54.
70. Karsenty G. The complexities of skeletal biology. *Nature*. 2003;423(6937):316–8.
71. Kronenberg HM. Developmental regulation of the growth plate. *Nature*. 2003;423(6937):332–6.
72. Long F, Ornitz DM. Development of the endochondral skeleton. *Cold Spring Harb Perspect Biol*. 2013;5(1):a008334.
73. Berendsen AD, Olsen BR. Bone development. *Bone*. 2015;80:14–8.
74. Karsenty G. Transcriptional control of skeletogenesis. *Annu Rev Genomics Hum Genet*. 2008;9:183–96.
75. Maes C, Kobayashi T, Selig MK, Torrekens S, Roth SI, Mackem S, et al. Osteoblast precursors, but not mature osteoblasts, move into developing and fractured bones along with invading blood vessels. *Dev Cell*. 2010;19(2):329–44.
76. Karsenty G, Wagner EF. Reaching a genetic and molecular understanding of skeletal development. *Dev Cell*. 2002;2(4):389–406.
77. Mundlos S. Expression patterns of matrix genes during human skeletal development. *Prog Histochem Cytochem*. 1994;28(3):1–47.

78. Yang L, Tsang KY, Tang HC, Chan D, Cheah KS. Hypertrophic chondrocytes can become osteoblasts and osteocytes in endochondral bone formation. *Proc Natl Acad Sci U S A*. 2014;111(33):12097–102.
79. Goldring MB, Tsuchimochi K, Ijiri K. The control of chondrogenesis. *J Cell Biochem*. 2006;97:33–44.
80. Lefebvre V, Bhattaram P. Vertebrate skeletogenesis. *Curr Top Dev Biol*. 2010;90:291–317.
81. Yoshioka M, Yuasa S, Matsumura K, Kimura K, Shiomi T, Kimura N, et al. Chondromodulin-I maintains cardiac valvular function by preventing angiogenesis. *Nat Med*. 2006;12:1151–9.
82. Peacock JD, Levay AK, Gillaspie DB, Tao G, Lincoln J. Reduced Sox9 function promotes heart valve calcification phenotypes in vivo. *Circ Res*. 2010;106:712–9.
83. Bi W, Huang W, Whitworth DJ, Deng JM, Zhang Z, Behringer RR, et al. Haploinsufficiency of Sox9 results in defective cartilage primordia and premature skeletal mineralization. *Proc Natl Acad Sci U S A*. 2001;98(12):6698–703.
84. Huang W, Chung UI, Kronenberg HM, de Crombrughe B. The chondrogenic transcription factor Sox9 is a target of signaling by the parathyroid hormone-related peptide in the growth plate of endochondral bones. *Proc Natl Acad Sci U S A*. 2001;98(1):160–5.
85. Chakraborty S, Cheek J, Sakthivel B, Aronow BJ, Yutzey KE. Shared gene expression profiles in developing heart valves and osteoblasts. *Physiol Genomics*. 2008;35:75–85.
86. Long F. Building strong bones: molecular regulation of the osteoblast lineage. *Nat Rev Mol Cell Biol*. 2012;13:27–38.
87. Nakashima K, Zhou X, Kunkel G, Zhang Z, Deng JM, Behringer RR, et al. The novel zinc finger-containing transcription factor osterix is required for osteoblast differentiation and bone formation. *Cell*. 2002;108:17–29.
88. Bell DM, Leung KK, Wheatley SC, Ng LJ, Zhou S, Ling KW, et al. SOX9 directly regulates the type-II collagen gene. *Nat Genet*. 1997;16(2):174–8.
89. Bridgewater LC, Lefebvre V, de Crombrughe B. Chondrocyte-specific enhancer elements in the Col1a2 gene resemble the Col2a1 tissue-specific enhancer. *J Biol Chem*. 1998;273(24):14998–5006.
90. Lefebvre V, Huang W, Harley VR, Goodfellow PN, de Crombrughe B. SOX9 is a potent activator of the chondrocyte-specific enhancer of the pro alpha1(II) collagen gene. *Mol Cell Biol*. 1997;17(4):2336–46.
91. Ng LJ, Wheatley S, Muscat GE, Conway-Campbell J, Bowles J, Wright E, et al. SOX9 binds DNA, activates transcription, and coexpresses with type II collagen during chondrogenesis in the mouse. *Dev Biol*. 1997;183(1):108–21.
92. Sekiya I, Tsuji K, Koopman P, Watanabe H, Yamada Y, Shinomiya K, et al. SOX9 enhances aggrecan gene promoter/enhancer activity and is up-regulated by retinoic acid in a cartilage-derived cell line, TC6. *J Biol Chem*. 2000;275(15):10738–44.
93. Xie WF, Zhang X, Sakano S, Lefebvre V, Sandell LJ. Trans-activation of the mouse cartilage-derived retinoic acid-sensitive protein gene by Sox9. *J Bone Miner Res*. 1999;14(5):757–63.
94. Bi W, Deng JM, Zhang Z, Behringer RR, de Crombrughe B. Sox9 is required for cartilage formation. *Nat Genet*. 1999;22(1):85–9.
95. Yousfi M, Lasmoles F, Lomri A, Delannoy P, Marie PJ. Increased bone formation and decreased osteocalcin expression induced by reduced twist dosage in Saethre-Chotzen syndrome. *J Clin Invest*. 2001;107:1153–61.
96. Bialek P, Kern B, Yang X, Schrock M, Sosoc D, Hong N, et al. A twist code determines the onset of osteoblast differentiation. *Dev Cell*. 2004;6:423–35.
97. Gu S, Boyer TG, Naski M. Basic helix-loop-helix transcription factor Twist1 inhibits transactivator function of master chondrogenic regulator Sox9. *J Biol Chem*. 2012;287:21082–92.
98. Dodig M, Tadic T, Kronenberg MS, Dacic S, Liu YH, Maxson RE, et al. Ectopic Msx2 overexpression inhibits and Msx2 antisense stimulates calvarial osteoblast differentiation. *Dev Biol*. 1999;209:298–307.

99. Akiyama H, Chaboissier M-C, Martin JF, Schedl A, de Crombrugge B. The transcription factor Sox9 has essential roles in successive steps of the chondrocyte differentiation pathway and is required for expression of Sox5 and Sox6. *Genes Dev.* 2002;16:2813–28.
100. Dy P, Wang W, Bhattaram P, Wang Q, Wang L, Ballock RT, et al. Sox9 directs hypertrophic maturation and blocks osteoblast differentiation of growth plate chondrocytes. *Dev Cell.* 2012;22:597–609.
101. Ducey P, Zhang R, Geoffroy V, Ridall AL, Karsenty G. Osf/Cbfa1: a transcriptional activator of osteoblast differentiation. *Cell.* 1997;89:747–54.
102. Ducey P, Starbuck M, Priemel M, Shen J, Pinero G, Geoffroy V, et al. A Cbfa1-dependent genetic pathway controls bone formation beyond embryonic development. *Genes Dev.* 1999;13:1025–36.
103. Cheek JD, Wrigg EE, Alfieri CM, James JF, Yutzey KE. Differential activation of valvulogenic, chondrogenic, and osteogenic pathways in mouse models of myxomatous and calcific aortic valve disease. *J Mol Cell Cardiol.* 2012;52:689–700.
104. Boyle WJ, Simonet WS, Lacey DL. Osteoclast differentiation and activation. *Nature.* 2003;423:337–42.
105. Takayanagi H, Kim S, Koga T, Nishina H, Isshiki M, Yoshida H, et al. Induction and activation of the transcription factor NFATc1 (NFAT2) integrate RANKL signaling and terminal differentiation of osteoclasts. *Dev Cell.* 2002;8:889–901.
106. Ishida N, Hayashi K, Hoshijima M, Ogawa T, Koga S, Miyatake Y, et al. Large scale gene expression analysis of osteoclastogenesis in vitro and elucidation of NFAT2 as a key regulator. *J Biol Chem.* 2002;277:41147–56.
107. Simonet WS, Lacey DL, Dunstan CR, Kelley M, Chang MS, Luthy R, et al. Osteoprotegerin: a novel secreted protein involved in the regulation of bone density. *Cell.* 1997;89:309–19.
108. Yasuda H, Shima N, Nakagawa N, Mochizuki SA, Yanagawa K, Fujise N, et al. Identity of osteoclastogenesis inhibitor factor (OCIF) and osteoprotegerin (OPG): a mechanism by which OPG/OCIF inhibits osteoclastogenesis in vitro. *Endocrinology.* 1998;139:1329–37.
109. Koga T, Matsui Y, Asagiri M, Kodama T, de Crombrugge B, Nakashima K, et al. NFAT and Osterix cooperatively regulate bone formation. *Nat Med.* 2005;11:880–5.
110. Winslow MM, Pan M, Starbuck M, Gallo EM, Deng L, Karsenty G, et al. Calcineurin/NFAT signaling in osteoblasts regulates bone mass. *Dev Cell.* 2006;10:771–82.
111. Kaden JJ, Bickelhaupt S, Grobholz R, Haase KK, Sarikoc A, Kilic R, et al. Receptor activator of nuclear factor κ B ligand and osteoprotegerin regulate aortic valve calcification. *J Mol Cell Cardiol.* 2004;36:57–66.
112. Urist MR. Bone: formation by autoinduction. *Science.* 1965;150(3698):893–9.
113. Ripamonti U, Van Den Heever B, Sampath TK, Tucker MM, Rueger DC, Reddi AH. Complete regeneration of bone in the baboon by recombinant human osteogenic protein-1 (hOP-1, bone morphogenetic protein-7). *Growth Factors.* 1996;13(3–4):273–89.
114. Barna M, Niswander L. Visualization of cartilage formation: insight into cellular properties of skeletal progenitors and chondrodysplasia syndromes. *Dev Cell.* 2007;12(6):931–41.
115. Chimal-Monroy J, Rodriguez-Leon J, Montero JA, Ganan Y, Macias D, Merino R, et al. Analysis of the molecular cascade responsible for mesodermal limb chondrogenesis: Sox genes and BMP signaling. *Dev Biol.* 2003;257(2):292–301.
116. Zhang J, Tan X, Li W, Wang Y, Wang J, Cheng X, et al. Smad4 is required for the normal organization of the cartilage growth plate. *Dev Biol.* 2005;284(2):311–22.
117. Retting KN, Song B, Yoon BS, Lyons KM. BMP canonical Smad signaling through Smad1 and Smad5 is required for endochondral bone formation. *Development.* 2009;136(7):1093–104.
118. Rawadi G, Vayssiere B, Dunn F, Baron R, Roman-Roman S. BMP-2 controls alkaline phosphatase expression and osteoblast mineralization by a Wnt autocrine loop. *J Bone Min Res.* 2003;18:1842–53.
119. Mead TJ, Yutzey KE. Notch pathway regulation of chondrocyte differentiation and proliferation during appendicular and axial skeleton development. *Proc Natl Acad Sci U S A.* 2009;106:14420–5.

120. Crowe R, Zikherman J, Niswander L. Delta-1 negatively regulates the transition from prehypertrophic to hypertrophic chondrocytes during cartilage formation. *Development*. 1999;126(5):987–98.
121. Sciaudone M, Gazzero E, Priest L, Delanty AM, Canalis E. Notch1 impairs osteoblastic cell differentiation. *Endocrinology*. 2003;144:5631–9.
122. Zamurovic N, Cappellen D, Rohner D, Susa M. Coordinated activation of Notch, Wnt, and transforming growth factor-beta signaling pathways in bone morphogenetic 2-induced osteogenesis. *J Biol Chem*. 2004;279:37704–15.
123. Deregowski V, Gazzero E, Priest L, Rydzziel S, Canalis E. Notch 1 overexpression inhibits osteoblastogenesis by suppressing Wnt/b-catenin but not bone morphogenetic protein signaling. *J Biol Chem*. 2006;281:6203–10.
124. Hilton MJ, Tu X, Wu X, Bai S, Zhao H, Kobayashi T, et al. Notch signaling maintains bone marrow mesenchyme progenitors by suppressing osteoblast differentiation. *Nat Med*. 2008;14:306–14.
125. Blaney Davidson EN, van der Kraan PM, van den Berg WB. TGF-beta and osteoarthritis. *Osteoarthr Cartil*. 2007;15(6):597–604.
126. Tang Y, Wu X, Lei W, Pang L, Wan C, Shi Z, et al. TGF-beta1-induced migration of bone mesenchymal stem cells couples bone resorption with formation. *Nat Med*. 2009;15(7):757–65.
127. Crane JL, Cao X. Bone marrow mesenchymal stem cells and TGF-beta signaling in bone remodeling. *J Clin Invest*. 2014;124(2):466–72.
128. Wirrig EE, Yutzey KE. Conserved transcriptional regulatory mechanisms in aortic valve development and disease. *Arterioscler Thromb Vasc Biol*. 2014;34(4):737–41.
129. Nigam V, Srivastava D. Notch1 represses osteogenic pathways in aortic valve cells. *J Mol Cell Cardiol*. 2009;47:828–34.
130. Nus M, MacGrogan D, Martinez-Poveda B, Benito Y, Casanova JC, Fernandez-Aviles F, et al. Diet-induced aortic valve disease in mice haploinsufficient for the Notch pathway effector RBPJK/CSL. *Arterioscler Thromb Vasc Biol*. 2011;31:1580–8.
131. Caira FC, Stock SR, Gleason TG, McGee EC, Huang J, Bonow RO, et al. Human degenerative valve disease is associated with up-regulation of low-density lipoprotein-related protein 5 receptor-mediated bone formation. *J Am Coll Cardiol*. 2006;47:1707–12.
132. Rajamannan NM, Subramaniam M, Caira F, Stock SR, Spelsberg TC. Atorvastatin inhibits hypercholesterolemia-induced calcification in the aortic valves via the Lrp5 receptor pathway. *Circulation*. 2005;112(9 Suppl):I229–34.
133. Ankeny RF, Thourani VH, Weiss D, Vega JD, Taylor WR, Nerem RM, et al. Preferential activation of SMAD1/5/8 on the fibrosa endothelium in calcified human aortic valves – association with low BMP antagonists and SMAD6. *PLoS One*. 2011;6:e20969.
134. Luna-Zurita L, Prados B, Grego-Bessa J, Luxan G, del Monte G, Benguria A, et al. Integration of a Notch-dependent mesenchymal gene program and Bmp2-driven cell invasiveness regulates murine cardiac valve formation. *J Clin Invest*. 2010;120(10):3493–507.
135. Gomez-Stallons MV, Tretter JT, Hassel K, Gonzalez-Ramos O, Amofa D, Ollberding NJ, et al. Calcification and extracellular matrix dysregulation in human postmortem and surgical aortic valves. *Heart*. 2019;105(21):1616–1621.
136. Mohler ER 3rd. Mechanisms of aortic valve calcification. *Am J Cardiol*. 2004;94(11):1396–402, A6.
137. Mohler ER, Gannon F, Reynolds C, Zimmerman R, Keane MG, Kaplan FS. Bone formation and inflammation in cardiac valves. *Circulation*. 2001;103:1522–8.
138. Srivatsa SS, Harrity PJ, Maercklein PB, Kleppe L, Veinot J, Edwards WD, et al. Increased cellular expression of matrix proteins that regulate mineralization is associated with calcification of native human and porcine xenograft bioprosthetic heart valves. *J Clin Invest*. 1997;99(5):996–1009.
139. Mohler ER 3rd, Kaplan FS, Pignolo RJ. Boning-up on aortic valve calcification. *J Am Coll Cardiol*. 2012;60(19):1954–5.
140. Gomez-Stallons MV, Wirrig-Schwendeman EE, Hassel KR, Conway SJ, Yutzey KE. Bone morphogenetic protein signaling is required for aortic valve calcification. *Arterioscler Thromb Vasc Biol*. 2016;36(7):1398–405.

141. Sider KL, Zhu C, Kwong AV, Mirzaei Z, de Lange CF, Simmons CA. Evaluation of a porcine model of early aortic valve sclerosis. *Cardiovasc Pathol.* 2014;23(5):289–97.
142. Schlotter F, Halu A, Goto S, Blaser MC, Body SC, Lee LH, et al. Spatiotemporal multi-omics mapping generates a molecular atlas of the aortic valve and reveals networks driving disease. *Circulation.* 2018;138(4):377–93.
143. Nishimura R, Hata K, Matsubara T, Wakabayashi M, Yoneda T. Regulation of bone and cartilage development by network between BMP signalling and transcription factors. *J Biochem.* 2012;151(3):247–54.
144. Gould ST, Srigunapalan S, Simmons CA, Anseth KS. Hemodynamic and cellular response feedback in calcific aortic valve disease. *Circ Res.* 2013;113(2):186–97.
145. Poggianti E, Venneri L, Chubuchny V, Jambrik Z, Baroncini LA, Picano E. Aortic valve sclerosis is associated with systemic endothelial dysfunction. *J Am Coll Cardiol.* 2003;41(1):136–41.
146. Yutzey KE, Demer LL, Body SC, Huggins GS, Towler DA, Giachelli CM, et al. Calcific aortic valve disease: a consensus summary from the Alliance of Investigators on Calcific Aortic Valve Disease. *Arterioscler Thromb Vasc Biol.* 2014;34(11):2387–93.
147. Galeone A, Paparella D, Colucci S, Grano M, Brunetti G. The role of TNF-alpha and TNF superfamily members in the pathogenesis of calcific aortic valvular disease. *ScientificWorldJournal.* 2013;2013:875363.
148. Byon CH, Javed A, Dai Q, Kappes JC, Clemens TL, Darley-Usmar VM, et al. Oxidative stress induces vascular calcification through modulation of the osteogenic transcription factor Runx2 by AKT signaling. *J Biol Chem.* 2008;283(22):15319–27.
149. Cripe L, Andelfinger G, Martin LJ, Shoener K, Benson DW. Bicuspid aortic valve is heritable. *J Am Coll Cardiol.* 2004;44(1):138–43.
150. Huk DJ, Austin BF, Horne TE, Hinton RB, Ray WC, Heistad DD, et al. Valve endothelial cell-derived Tgfbeta1 signaling promotes nuclear localization of Sox9 in interstitial cells associated with attenuated calcification. *Arterioscler Thromb Vasc Biol.* 2016;36(2):328–38.
151. Shao JS, Cheng SL, Pingsterhaus JM, Charlton-Kachigian N, Loewy AP, Towler DA. Msx2 promotes cardiovascular calcification by activating paracrine Wnt signals. *J Clin Invest.* 2005;115(5):1210–20.
152. Alexopoulos A, Bravou V, Peroukides S, Kaklamanis L, Varakis J, Alexopoulos D, et al. Bone regulatory factors NFATc1 and Osterix in human calcific aortic valves. *Int J Cardiol.* 2010;139(2):142–9.
153. Weiss RM, Lund DD, Chu Y, Brooks RM, Zimmerman KA, El Accaoui R, et al. Osteoprotegerin inhibits aortic valve calcification and preserves valve function in hypercholesterolemic mice. *PLoS One.* 2013;8(6):e65201.
154. Tanimura A, McGregor DH, Anderson HC. Matrix vesicles in atherosclerotic calcification. *Proc Soc Exp Biol Med.* 1983;172(2):173–7.
155. Tanimura A, McGregor DH, Anderson HC. Calcification in atherosclerosis. *I Human Stud J Exp Pathol.* 1986;2(4):261–73.
156. Urist MR, Strates BS. Bone formation in implants of partially and wholly demineralized bone matrix. Including observations on acetone-fixed intra and extracellular proteins. *Clin Orthop Relat Res.* 1970;71:271–8.
157. Wozney JM, Rosen V, Celeste AJ, Mitsock LM, Whitters MJ, Kriz RW, et al. Novel regulators of bone formation: molecular clones and activities. *Science.* 1988;242(4885):1528–34.
158. Ferdous Z, Jo H, Nerem RM. Differences in valvular and vascular cell responses to strain in osteogenic media. *Biomaterials.* 2011;32(11):2885–93.
159. Yao Y, Bennett BJ, Wang X, Rosenfeld ME, Giachelli C, Lusis AJ, et al. Inhibition of bone morphogenetic proteins protects against atherosclerosis and vascular calcification. *Circ Res.* 2010;107:485–94.
160. Galvin KM, Donovan MJ, Lynch CA, Meyer RI, Paul RJ, Lorenz JN, et al. A role for *smad6* in development and homeostasis of the cardiovascular system. *Nat Genet.* 2000;24:171–4.

161. Luo G, Ducy P, McKee MD, Pinero GJ, Loyer E, Behringer RR, et al. Spontaneous calcification of arteries and cartilage in mice lacking matrix GLA protein. *Nature*. 1997;386:78–81.
162. Caira FC, Stock SR, Gleason TG, McGee EC, Huang J, Bonow RO, et al. Human degenerative valve disease is associated with up-regulation of low-density lipoprotein receptor-related protein 5 receptor-mediated bone formation. *J Am Coll Cardiol*. 2006;47(8):1707–12.
163. Rawadi G, Vayssiere B, Dunn F, Baron R, Roman-Roman S. BMP-2 controls alkaline phosphatase expression and osteoblast mineralization by a Wnt autocrine loop. *J Bone Miner Res*. 2003;18(10):1842–53.
164. Baron R, Rawadi G. Wnt signaling and the regulation of bone mass. *Curr Osteoporos Rep*. 2007;5(2):73–80.
165. Hofmann JJ, Briot A, Enciso J, Zovein AC, Ren S, Zhang ZW, et al. Endothelial deletion of murine Jag1 leads to valve calcification and congenital heart defects associated with Alagille syndrome. *Development*. 2012;139(23):4449–60.
166. Walker GA, Masters KS, Shah DN, Anseth KS, Leinwand LA. Valvular myofibroblast activation by transforming growth factor-beta: implications for pathological extracellular matrix remodeling in heart valve disease. *Circ Res*. 2004;95(3):253–60.
167. Atkins SK, Aikawa E. Valve under the microscope: shining a light on emerging technologies elucidating disease mechanisms. *Heart*. 2019;105(21):1610–1.

Chapter 4

Differential Mechanisms of Arterial and Valvular Calcification



Maximillian A. Rogers and Elena Aikawa

Cardiovascular calcification is a form of ectopic calcification (calcification in soft tissues that do not normally calcify) in which minerals deposit in cardiovascular organs. Ectopic calcification can be seen in multiple tissue types, notably in the medial smooth muscle layer and the intimal atherosclerotic plaque layer of the arteries, as well in the cardiac valves (see Chap. 2 for histopathological presentations of vascular and valvular calcification). In the heart, some of the most serious calcification detriments occur in the aortic valve and coronary arteries, as such the aortic valve will be the focus of the present vascular and valvular calcification mechanistic comparison. In arteries, calcification increases stiffness that contributes to hypertension [1] and heart failure [2], in addition to increasing plaque rupture risk [3]. In heart valves, calcification narrows the valve opening, impairing blood flow, referred to as calcific aortic valve disease (CAVD) or aortic stenosis. Aortic stenosis leads to heart failure with high mortality rate [4]. Aortic valve disease is the third most common cardiovascular disease in the United States, following hypertension and coronary artery disease [5].

The prevalence of cardiovascular calcification varies among studies with typically increasing prevalence in aged populations [6]; however, calcification increases the risk of cardiovascular events independently of age [7]. In adults the presence of

M. A. Rogers (✉)

Department of Medicine, Brigham and Women's Hospital, Harvard Medical School,
Boston, MA, USA

e-mail: mrogers@research.bwh.harvard.edu

E. Aikawa

Center for Interdisciplinary Cardiovascular Sciences, Center for Excellence in Vascular
Biology, Division of Cardiovascular Medicine, Department of Medicine, Brigham and
Women's Hospital, Harvard Medical School, Boston, MA, USA

© Springer Nature Switzerland AG 2020

E. Aikawa, J. D. Hutcheson (eds.), *Cardiovascular Calcification and Bone Mineralization*, Contemporary Cardiology,
https://doi.org/10.1007/978-3-030-46725-8_4

vascular calcification varies widely with more observed in adults with kidney disease and lower levels seen in premenopausal women and in the aorta compared to the coronary artery [7–10]. Increased valvular calcification is also associated with kidney disease patients on dialysis [11]. Vascular calcification and aortic stenosis occur in some pediatric populations, including idiopathic infantile arterial calcification [12], Hutchinson-Gilford progeria syndrome [13], and congenital valve disease [14]. Despite the severity and wide prevalence of cardiovascular calcification, there are currently no US Food and Drug Administration-approved drug therapies for this life-threatening condition.

Vascular and valvular calcification can co-occur, as is frequently the case in kidney disease patients; however, in the general population, aortic root rather than valve calcification has been shown to associate with coronary artery calcification [15]. Similar mechanisms may drive some aspects of vascular and valvular calcification, but these diseases are distinct pathologies. Understanding the mechanistic differences that independently drive these critical cardiovascular pathologies, including with the use multi-omics and big data analysis, could lead to therapies for these unmet medical needs [16]. Here the major mechanisms associated with cardiovascular calcification are outlined by highlighting some differences between vascular and valvular pathologies.

Arterial and Valvular Tissue Microenvironments and Cells

Calcification Morphology and Tissue Microenvironment

In arteries and heart valves, calcification morphology appears as spherical particles, fibers, and compact material when visualized by density-dependent color scanning electron microscopy [17] (Fig. 4.1). The origin of these forms of calcification is

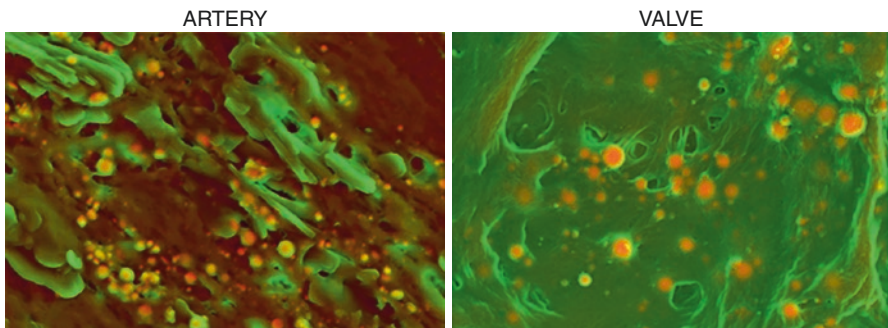


Fig. 4.1 Density-dependent scanning electron microscopy of calcification in human carotid artery and human aortic valve. Calcification (red) and tissue matrix (green) shown for calcified human artery isolated during carotid endarterectomy and aortic valve isolated during valve replacement surgery. (Previously unpublished images courtesy of Elena Aikawa (Brigham and Women’s Hospital, Harvard Medical School))

currently under debate, as several mechanisms have been suggested in both arteries and valves. Extracellular vesicles have been demonstrated to contribute to the formation of vascular calcification [18, 19] as well as being involved in valvular calcification [20, 21]. Apoptosis has been suggested to be involved in the formation of calcified nodules from vascular [22] and valvular cells [23]. Accumulated cell debris along with extracellular matrix produces nodules that can serve as scaffolds for hydroxyapatite formation. Inhibiting apoptosis suppresses transforming growth factor beta 1-induced calcification without effecting nodule formation [24]. Inhibiting actin polymerization suppresses nodule formation but not calcification in sheep valve cells [24], which suggests that calcification and nodule formation are not always codependent on each other.

Perhaps the most obvious difference between arterial and valvular calcification is in the tissue microenvironments and cell types within (Fig. 4.2). Arteries contain three layers: endothelium, medial smooth muscle cells, and connective tissue [25]. In addition to an endothelial layer, the aortic valve contains three layers, fibrosa, spongiosa, and ventricularis [26], which differ in their mechanical properties due to differences in extracellular matrix components allowing movement of the valve. Vascular calcification occurs in the medial smooth muscle cell layer particularly in metabolic disease patients like those with diabetes mellitus [27] and chronic kidney disease [28] and in the collagen-rich intima plaque layer fibrous vapor in close proximity to necrotic core in patients with atherosclerosis [29]. Calcification in the aortic valve preferentially occurs in the fibrosa layer, which faces the aorta and is comprised of collagen [26].

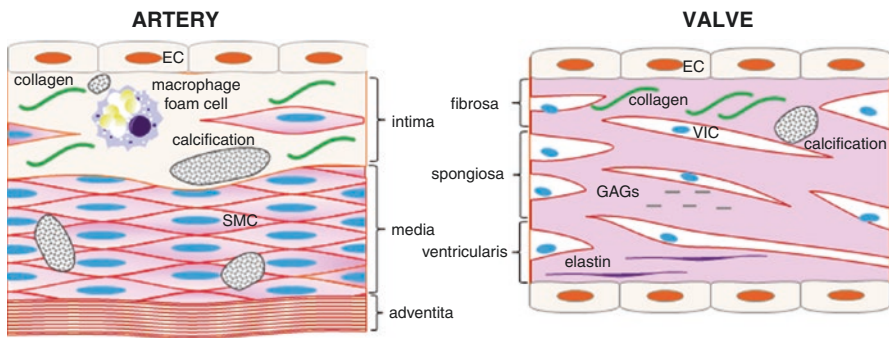


Fig. 4.2 Differences in arterial and valvular calcification microenvironments. Arteries contain multiple layers including endothelium, intima (plaque seen in atherosclerosis patients), media, and adventitia (connective tissue). Aortic valve layers differ for arteries and include endothelium, fibrosa (collagen rich), spongiosa (glycosaminoglycans/GAGs rich), and ventricularis (elastin rich). The luminal surface of arteries, called the endothelium, contains a layer of endothelial cells (EC). The aortic valve is encased in a layer of endothelial cells. The major cell type of arteries is smooth muscle cells (SMC), and the major cell type of valves is valvular interstitial cells (VIC). In the artery calcification can occur in the media layer, often seen in diabetics and patients with chronic kidney disease, or in the intima layer often seen in atherosclerosis patients. In the valve calcification is found on the aortic side in the collagen-rich fibrosa layer. Images were generated using Motifolio illustration tool kit (Motifolio Inc., Ellicott City, MD)

Smooth Muscle Cells and Valvular Interstitial Cells

The predominant cell type in the artery wall is smooth muscle cells (SMC), which are typically present only in low numbers in healthy human aortic valves [30]. The predominant cell type in the valve is valvular interstitial cells (VIC). VIC are fibroblastic cells that produce extracellular matrix proteins and matrix remodeling proteins [31]. During fetal development VIC are thought to be activated myofibroblasts as they express the SMC marker α -smooth muscle actin that is lost after birth [32]. VIC phenotypic state as fibroblastic cells or activated myofibroblasts is potentially a key mechanism in the calcification potential of these cells. In vitro culturing of VIC in DMEM media leads to a more activated myofibroblast-like phenotype, but switching to a fibroblast media reduces expression of cytoskeletal proteins and bone marker proteins [30]. This raises two questions: are calcifying arterial cells similar or different from calcifying valvular cells, and are these two cell types distinct from bone osteoblasts? Supporting cell-type differences between calcifying SMC and VIC, human SMC generate increased calcium content, runt-related transcription factor 2 (RUNX2), tissue non-specific alkaline phosphatase (TNAP protein, *ALPL* gene) activity, and collagen type 1 and glycosaminoglycan compared to VIC in collagen gels cultured in osteogenic media with cyclic strain [33]. Calcifying cardiovascular cells are also likely different from bone osteoblasts. Transcriptomics comparing calcifying SMC with osteoblasts suggest these cells maintain distinct transcriptional programs, but with some commonalities between them in extracellular matrix and biomineralization genes [34]. Supporting some shared mechanisms, inhibiting TNAP or RUNX2, suppresses cardiovascular [35, 36] and bone mineralization [37, 38]. Deletion of ecto-nucleotide pyrophosphatase/phosphodiesterase 1, an enzyme involved in the production of the calcification inhibitor pyrophosphate, reduces the inhibitory effects of extracellular nucleotides on both SMC and osteoblast mineralization, but with mechanistic differences between the two cell types [39]. Supporting some mineralization differences, molecular mechanisms have been demonstrated to inhibit SMC and VIC calcification without negatively impacting bone osteoblast mineralization. Inhibiting sortilin in SMC that loads TNAP onto calcifying extracellular vesicles [40], as well as inhibiting dynamin-related protein 1 that mediates mitochondrial fission regulating calcium buffering and cellular metabolism [41] in SMC and VIC, suppresses cardiovascular cell calcification without negatively impacting bone osteoblast mineralization. A direct multi-omics comparison between calcifying SMC, VIC, and osteoblasts remains to be performed. Incorporating induced pluripotent stem cell (iPSC) technology with a multi-omics comparison by converting iPSC from the same donor to calcifying VIC [42], SMC [43] and osteoblasts [44] may assist in this endeavor by reducing comparison issues due to donor-to-donor variability. Added insight into the transcriptional and translational programs that account for differences in calcifying vascular, valvular, and bone cells could identify key drivers of these likely distinct cardiovascular pathologies.

Progenitor Cells

TNAP is a key enzyme in osteogenic differentiation, which promotes cardiovascular cell calcification potential [40]. TNAP is also a marker of pluripotent stem cells, cell differentiation, and is involved in mineralization and development processes, particularly skeletal development [45]. TNAP is involved in mineralization by hydrolyzing the calcification inhibitor pyrophosphate and providing free phosphate for the generation of hydroxyapatite crystals. TNAP protein is increased in calcified areas of human valve [46] and arteries of patients with diabetes [47] and chronic kidney disease [48]. In vitro, cardiovascular cells calcify via TNAP-dependent and TNAP-independent mechanisms [49]. While calcification can occur in the absence of TNAP activity, the involvement of TNAP in some forms of cardiovascular calcification raises an interesting connection to stem cells, as TNAP is a marker of pluripotency [45]. Another protein involved in pluripotency is lamin A. Cells with higher levels of lamin A have decreased efficiency in undergoing reprogramming to induced pluripotent stem cells [50]. Lamin A mutations produce an alternative spliced product of lamin A called progerin (also produced in normal aged cells) that binds to lamin A/C and induces nuclear aberrations [8]. The unprocessed form of lamin A called prelamin A induces calcification of vascular smooth muscle cells in a TNAP-dependent manner [51]. Mutation of the lamin A gene is the cause of Hutchinson-Gilford progeria syndrome in which accelerated calcification occurs in the arteries and heart valves [13]. Together these data raise the possibility that osteogenic differentiation of cells involves a molecular mechanism in which cardiovascular cells become calcifying cardiovascular cells by dedifferentiating to a more stem cell-like state. Circulating and resident populations of stem cells have been attributed to the cardiovascular calcification process. Unique to vasculature calcification is the involvement of cells from the outermost layer of the vessel wall called the adventitia. Mesenchymal stem cell-like cells (Gli1-positive cells) in the arterial adventitia are SMC precursors, and these cells migrate into the media and intima layers of artery in atherosclerotic chronic kidney disease mice where they serve as a major source of calcifying cells [52]. The valve has a different set of multipotent mesenchymal progenitor cells that contribute to calcification [53]. Additionally, circulating endothelial progenitor cells with osteoblastic properties are elevated in patients with aortic stenosis and in the endothelial and deeper cell layers calcified aortic valve [54]. Whether progenitor cells utilize different mechanisms in the arteries than in the valve is unknown but possible given the different origins of these cells.

Endothelial Cells

Like arteries, aortic valves are covered by a continuous monolayer of endothelial cells. Endothelial cells have been shown to be involved in vascular and valvular calcification and potentially could exhibit differential responses to calcific disease

regulating factors. A transcriptional and histological comparison of porcine vascular endothelial cells and aortic valvular endothelial cells exposed to laminar shear stress found over 400 differentially expressed genes between these cell types [55]. Valve endothelial cells were found to be inflammatory and expressed genes associated more with chondrogenesis, whereas vascular endothelial cells expressed more genes associated with osteogenesis. In agreement with a role of endothelial cells in calcification, overexpression of TNAP in the endothelium increases vascular calcification in atherosclerotic mice [35]. Endothelial cells may undergo a differentiation process referred to as endothelial-to-mesenchymal-transition (EndMT), in which these cells lose endothelial properties (including markers like endothelial cadherin) and gain characteristics of mesenchymal cells or myofibroblasts (including markers like α -smooth muscle actin, vimentin, and collagen type 1). These EndMT cells have increased motility and can migrate in tissues. EndMT generates a type of progenitor-like cell that can renew the valvular VIC population and maintain tissue homeostasis [56]. EndMT transformation is induced via transforming growth factor β [57]. Aortic valve endothelial cells undergo EndMT in the presence of high chondroitin sulfate, an extracellular matrix component, suggesting that matrix alterations can promote the formation of cells involved in fibrosis [58]. Porcine valves exposed to stretch in osteogenic media containing transforming growth factor β develop calcific nodule formation on the aortic surface in a bone morphogenic protein(BMP)-2–4 dependent manner [59], further supporting a role of EndMT in valve calcification. In arterial endothelial cells, pro-inflammatory cytokines (tumor necrosis factor α and interleukin-1 β) induce EndMT in a BMP pathway in which BMP-9 induces osteogenic differentiation and calcification [60]. Inflammation clearly plays a role in EndMT, and mechanical stress can induce inflammation. The mechanical stress received in constantly opening and closing valves is different from that in arteries. While studies in valve and vascular tissues support a role of EndMT in cardiovascular calcification, future studies should compare localized inflammation levels in valve and vascular tissues from the same patients. Comparing the levels of inflammation in specific locations could help demonstrate a role of EndMT molecular mechanisms in explaining why calcification occurs in just one cardiovascular tissue type or both in the same patient.

T Lymphocytes

T lymphocytes have been shown to be involved in both bicuspid and tricuspid aortic valves. However, a direct assessment of differences and the relative contribution of T cells to valvular disease using aged-matched bicuspid, tricuspid, and non-disease valve tissues are lacking. Bicuspid aortic valves that occur due to developmental defects often lead to aortic stenosis and do so at a much younger rate age than individuals with a normally developed tricuspid aortic valve [61]. Evidence suggests that T lymphocytes may promote this process. Clonal expansions of infiltrating T lymphocytes are observed in aortic valves with the strongest association seen in

older patient tricuspid aortic valves with severe calcification as well as younger patient bicuspid valves with calcified aortic stenosis [62]. Activated CD8+ T cells and CD4+ T cells in the memory-effector subset are increased in both calcified tricuspid and bicuspid valves, and CD4+ T cells are increased in patients with concurrent atherosclerotic disease [62]. These cells indicate an adaptive immune response in bicuspid and tricuspid valve calcification that includes CD8+ T cell activation, clonal expansion, and differentiation to a memory-effector phenotype; however, what is driving this immune response is not entirely clear, including whether it is driven by different mechanisms in bicuspid and tricuspid CAVD. Identifying the molecular mechanisms of T cells in valve calcification could lead to potential immunotherapies for this disease. One tantalizing link to activated T cells may be through a transcription factor found largely in immune cells but also found in calcified valve along with being implicated in vascular calcification: nuclear factor of activated T cells (NFAT) cytoplasmic, calcineurin-dependent 1 (NFATc1). NFATc1 is a factor involved in osteoclastogenesis and interferon gamma released by activated T cells suppresses osteoclast mineral resorption in valve [63]. Additionally, human SMC calcification induced by oxidized low-density lipoprotein increases NFATc1, and inhibition of NFATc1 blocks calcification in SMC [64]. Oxidized lipids, including those within the calcification risk factor lipoprotein(a) (Lp(a)), associate with valvular [65] and vascular [66, 67] calcification. This raises the possibility that oxidized lipids are driving T cell activation, clonal expansion, and osteogenic differentiation in cardiovascular tissues. Interestingly, atherosclerotic mice expressing E06 antibody that targets oxidized phospholipids have reduced vascular and valvular calcification [68], but whether this action occurs partly via T cell modulation has not been examined.

Macrophages/Monocytes

Macrophages play dual mechanistic roles in cardiovascular calcification by both promoting ectopic calcification and being involved in the mineral resorption process. Macrophages release the osteogenic protein BMP-2. In atherogenic mice with macrophages lacking the transient receptor potential cation channel subfamily C member 3 gene that regulates BMP2 expression, there is reduced BMP-2 and RUNX2 in calcified areas, in addition to reduced calcified plaque [69]. Calcified aortic valves have enhanced macrophage infiltration, with increases seen in both pro-inflammatory and anti-inflammatory cytokines [70]. Treating VIC with conditioned media from unstimulated and inflammatory stimuli (lipopolysaccharide) increases BMP, TNAP, and calcification [70]. At first glance this shared effect from both unstimulated and stimulated macrophages may seem somewhat unexpected; however, a related finding occurs with the mineral resorption action of macrophages with both “classically activated” and “alternatively activated” macrophages having decreased osteoclastogenesis potential [71]. In human atherosclerotic plaques, macrophages with the osteoclast differentiation and bone resorption marker carbonic

anhydrase type II surround calcium deposits [72]. These macrophages express relatively low cathepsin K, a major enzyme required in osteoclast mineral resorption activity, and high mannose receptor, a marker of “alternatively activated” also referred to as anti-inflammatory macrophages. In vitro, osteoclastogenesis is suppressed when monocyte cells are treated with interleukin 4 that drives an “alternatively activated” macrophage program [72]. In contrast, in calcified valve “classically activated” also called inflammatory macrophages are observed near calcification. Stimulating monocytes with the pro-inflammatory cytokine, interferon gamma suppresses osteoclastogenesis [62]. Whether this is truly a vascular and valve mechanistic difference or both classical and alternative activation of macrophages inhibits osteoclastogenesis in both tissues remains to be demonstrated. Support for a role of pro-inflammatory macrophages in addition to anti-inflammatory macrophages in vascular calcification exists, as classically activated macrophages secreted extracellular vesicles that contribute to vascular calcification [73].

Dendritic Cells, B Cells, and MAST Cells

Vascular dendritic cells are found in the early foci of arterial intima and atherosclerotic lesions [74]. In addition to calcification in the extracellular matrix, calcium-containing microdeposits are observed in the cytoplasm of vascular dendritic cells, suggesting these cells may play a role in calcium accumulation and deposition [75]. In the aortic valve, dendritic cells are localized beneath the endothelium of the aortic side [76], an area prone to calcification. Dendritic cells can produce pro-inflammatory cytokines [77] and as such may be involved in inflammation mediated calcification pathways. Additionally, dendritic cells are antigen-presenting cells, so it is also possible that these cells play a role in T cell activation, but the mechanistic roles of dendritic cells in cardiovascular calcification are unknown. Like dendritic cells, B cells can induce T cell activation. In mice, mature B cell depletion by CD20-specific monoclonal antibody reduces T cell-derived interferon-gamma secretion and atherosclerosis [78]. Osteoprotegerin inhibits in vitro and in vivo calcification and is involved in antibody responses and B cell maturation [79]. B cells are not normally found in heart valves but accumulate in the aortic side of human stenotic aortic valves [80, 81], and the amount of B cells in valves associate with valve calcification [81]. More work is needed to understand the role of B cells and the interaction of these cells with other immune cells including T cells, dendritic cells, and macrophages in cardiovascular calcification.

Several lines of evidence point toward a role of activated mast cells in cardiovascular calcification, involving multiple molecular mechanisms, such as matrix remodeling and inflammatory signaling. Mast cells localize with macrophages and neovessels primarily in calcified regions of aortic leaflets [82]. Increased mast cells correlated with the severity of aortic stenosis [82]. Mechanistically, mast cells produce cathepsin G, an angiotensin II-forming enzyme that degrades elastic fibers and induces transforming growth factor-beta1 and valve remodeling [83]. In the artery

activated mast cells accumulate 200-fold more at atheromatous erosion or rupture sites than in unaffected coronary intima [84]. In calcified carotid atherosclerotic plaque mast cells associate with macrophages in areas of early calcification [85]. Whether mast cells play independent mechanistic roles or codependent with other immune cells and if these actions are similar or different in the arteries and heart valve requires further study.

Arterial and Valvular Calcification Molecular Mechanisms

Beyond the mechanisms described in the previous section on the vascular and valve tissue and cell differences, additional molecular mechanisms have been proposed in the development of cardiovascular calcification. Cardiovascular calcification mechanisms have been extensively reviewed [16, 86–90], as such only a few key additional molecular mechanisms will be discussed in further detail here.

Mineral Metabolism

Serum magnesium inversely correlates with coronary artery calcification in chronic kidney disease patients, particularly those with high serum phosphate levels [91]. Magnesium prevents rat SMC calcification [92] and inhibits hydroxyapatite formation independent of apoptosis and TNAP regulation in bovine SMC [93]. In patients with calcific aortic valve disease, serum magnesium also inversely associates with valve calcification prevalence, whereas serum phosphate is positively associated with valve calcification prevalence [94]. Elevated phosphate is a risk factor for cardiovascular events in both chronic kidney disease patients [95] and the general population [96]. Phosphate regulation is a major driver of vascular calcification in dialysis patients, with medial calcification occurring independent of evidence for atherosclerosis and inflammation [48]. PiT-1 is the major phosphate transporter in SMC, and PiT-1 knockdown inhibits calcification, whereas PiT-1 overexpression increases SMC calcification [97]. PiT-1 is increased in calcified human aortic valves, and knockout of PiT-1 restores AKT levels in human VIC treated with inorganic phosphate [98]. Supporting a mechanistic role of AKT in the calcification process, overexpression of AKT inhibits apoptosis and calcification in inorganic phosphate-treated VIC [98]. AKT activation induces vascular calcification via RUNX2 in diabetic mice and mouse SMC [99], but a separate study using human and bovine SMC and rat aortic rings showed AKT activation suppresses calcification [100]. Supporting a role of BMP in PiT-1-mediated calcification, oxidized low-density lipoprotein increases BMP-2 in a PiT-1-dependent manner in human aortic VIC [101]. It is unclear if there are distinct differences in the full mechanistic pathways involving PiT-1 in vascular versus valvular calcification, but in both cases, PiT-1 promotes calcific pathology.

There are contradictory reports on the role of iron in cardiovascular calcification. In uremic rats, iron administration reduces *Runx2* and *Pit-1* expression and vascular calcification [102]. In human SMC, iron increases calcification via IL-24 and BMP-2 induction [103], whereas iron citrate suppresses BMP-2 and calcification in rat SMC [104]. The role of calcium levels in cardiovascular calcification is also somewhat complex. Elevated calcium associates with both increased vascular and valvular calcification in hemodialysis patients. In hemodialysis patients with parathyroid hormone levels greater than or equal to 300 pg/mL, lowering dialysate calcium levels (1.25 mmol/L from 1.75 mmol/L) slows the progression of coronary artery calcification [105]. Higher serum calcium levels associate with valve calcification in patients on hemodialysis [106]. The mechanistic roles of elevated calcium outside of hemodialysis patients are unclear. In male calcific aortic valve disease patients, lower serum calcium levels are inversely associated with valve calcification [107], although this inverse association was not seen in a separate aortic valve calcification study [108]. In mice with experimentally induced chronic kidney disease that develops vascular and valvular calcification, phosphate but not calcium serum levels are increased [109, 110]. Whether mineral metabolism mechanisms differ in vascular and valvular calcification requires further study, but it clearly plays a role in the formation of cardiovascular pathology.

Endogenous Calcification Inhibitors

Several endogenously produced calcification inhibitors have been demonstrated to play mechanistic roles in cardiovascular calcification [111]. Pyrophosphate directly inhibits the nucleation of calcium phosphate crystals. Pyrophosphate inhibits calcification in animal models of both vascular [112] and valvular [113] calcification. MGP can bind calcium and calcium matrices, although the exact mechanisms through which MGP inhibits calcification are still not entirely clear. MGP deficiency in mice leads to arterial calcification [114]. The MGP polymorphism rs1800801 is associated with vascular calcification in humans [115], and an activator of MGP vitamin K may suppress valvular calcification in humans [116]. Like MGP, fetuin-A is a calcium binder and calcification inhibitor. Mice lacking fetuin-A develop ectopic calcification [117]. Fetuin-A is inversely associated with coronary artery calcification in cardiovascular disease patients [118]. The role of fetuin-A in valvular calcification is complex, with studies both showing an association and others no association [119].

The calcification inhibitor osteoprotegerin (OPG) is involved in osteoclastogenesis via acting as a decoy receptor for receptor activator of NF- κ B ligand, and OPG deficiency increases vascular calcification in atherogenic mice in part by upregulation of osteochondrogenic genes [120]. In agreement with a role in calcification inhibition, exogenous OPG administration attenuates aortic valve calcification in hypercholesterolemic mice [121]. In observational studies in humans, however, serum OPG shows a positive association with cardiovascular disease [122], whether

this is due to OPG responding to or mediating disease is unclear. Osteopontin (OPN) is another calcification inhibitor with a potential link to mineral resorption. OPN not only inhibits mineral deposition by blocking hydroxyapatite crystal growth but also induces monocytic cell expression of carbonic anhydrase II promoting acidification of the extracellular milieu and possibly mineral clearance [123]. OPN is likely an inducible calcification inhibitor, given loss of OPN alone does not induce calcification, but when combined with loss of MGP [124] or high phosphate [125], loss of OPN increases vascular calcification. Complicating OPN mechanistic interpretation, increased levels of OPN are observed in patients with end-stage renal disease, ectopic calcification, and aortic valve calcification [126]. Whether this is part of a protective response is possible but unclear.

Klotho is a well-known inhibitor of ectopic calcification that works via reducing phosphate levels in addition to other mechanisms including downregulating collagen type 1 and runx2 as demonstrated in porcine VIC [127]. Mice lacking klotho have valvular and vascular calcification [128], and chronic kidney disease patients have reduced klotho [129]. Taken together these studies show largely similar vascular and valvular responses to endogenous calcification inhibitors, whether additional inhibitors specific to calcification in one tissue type but not the other exists is unknown.

Inflammation, Lipids, and Oxidative Stress

Inflammation promotes vascular and valvular calcification in in vitro and in vivo models [103, 130, 131], and increased inflammatory cells are found in both calcified human arteries and valves [62, 85]. Despite having increased calcification, the number of inflammatory cells in calcified valves is unchanged in patients with type 2 diabetes mellitus compared to nondiabetics [132]. This raises a couple of possibilities: in type 2 diabetes mellitus, early increased inflammation may promote calcification, but inflammation is subsequently reduced by the time aortic valves are surgically removed. Alternatively, while inflammation plays a major role in the calcification process, additional non-inflammation-mediated molecular mechanisms may co-occur to further promote valvular calcification in type 2 diabetics. In contrast to valve, both calcification and inflammatory cells (macrophages, T cells) are increased in coronary lesions of type 2 diabetics compared to nondiabetics [133]. This raises the possibility of inflammation being involved in both vascular and valvular calcification but differing in arteries compared to valves by playing a larger mechanistic role in further promoting vascular calcification in type 2 diabetics. Oxidized lipids promote inflammation and vascular and valvular calcification [134]. In valves, lipoproteins including Lp(a), a lipoprotein that is genetically associated to CAVD and potentially promotes calcification via inflammation, are frequently observed in the acellular space of the extracellular matrix [135]. Reduced lipid uptake by cells and lipid retention in the extracellular matrix in the valve helps explain why statins, which function by increasing cellular lipid clearance, do not work as a calcific aortic

valve disease therapy. In the arteries, lipoproteins are frequently taken up by cells leading to increased foam cell formation in the intima layer. Lipid clearance by cells can be initially beneficial but also contributes to calcification by promoting foam cell apoptosis and calcifying vesicle release [136]. There is some evidence of foam cells in valves in humans [137] and rabbits [138] with atherosclerosis, but the extent to which this is related to atherosclerosis rather than CAVD is unclear as foam cell pathology is not commonly reported in calcified valves. Therefore, yet to be fully explored, calcification mechanistic differences likely involve lipid uptake in arteries compared to valve. Lipid is metabolized via enzymatic and nonenzymatic pathways, and altered lipid metabolism contributes to vascular disease [139]. Supporting the involvement of lipid metabolism in vascular calcification, the cholesterol metabolite 25-hydroxycholesterol stimulates mineralization in bovine vascular cells [140]. Lipids and inflammation can also stimulate oxidative stress. Oxidative stress stimulates opposite responses in vascular cells where it promotes calcification compared to bone cells where it inhibits calcification [141]. Helping to mechanistically explain this phenomenon, oxidative stress increases mitochondrial fission, and as vascular cells undergo osteogenic differentiation mitochondria fragment, whereas in bone cells they elongate by mitochondrial dynamics mechanisms [41]. This change in mitochondrial dynamics occurring via altered DRP1 activity controls osteogenic differentiation. Inhibition of mitochondrial fission inhibits both SMC and VIC calcification, but not osteoblasts mineralization [41]. Additionally, oxidative stress induces a key regulator of osteogenesis, RUNX2 in calcifying SMC [142]. Supporting some mechanistic similarities, both vascular and valvular cells express similar antioxidant and anti-inflammatory genes in response to shear stress [55]. Whether specifically localized increases of oxidative stress occur in arteries compared the valve or vice versa in cases in which only one of the two tissues calcify in the same individual remains to be assessed. Taken together, these studies support that inflammation, lipids, and oxidative stress are related mechanistic pathways that promote calcific disease. Further examination of these mechanisms in the context of assessing differences between vascular and valve calcification is needed to help identify targetable key drivers of these distinct pathologies.

Genetic Drivers of Calcification

Several genes have been associated with cardiovascular calcification through genome-wide association studies [143–153], reviewed further in [16]. Genes associated with vascular calcification include *ABCA4*, *ADAMTS9*, *ATP2B1*, *CDKN2A/B*, *CHIT1*, *COL4A1/2*, *GLIS1*, *MRAS*, *OPCML*, *PHACTR1*, *SORT1*, *TBC1D4*, *TCF7L2*, *TNFRSF8*, and *WWOX*. Genes associated with valvular calcification include *IL6*, *LPA*, *NAVI*, *ALPL* (TNAP protein), *PALMD*, *CACNA1C*, *RUNX2*, and *TEX41*. Of these genes *ALPL*, *IL6*, *LPA*, *TNAP*, and *RUNX2* are linked to both vascular and valvular disease. Whether any of the genome-wide association studies identified genes confer vascular or valvular specific mechanisms in driving calcification is currently unknown and should be an area of future research efforts.

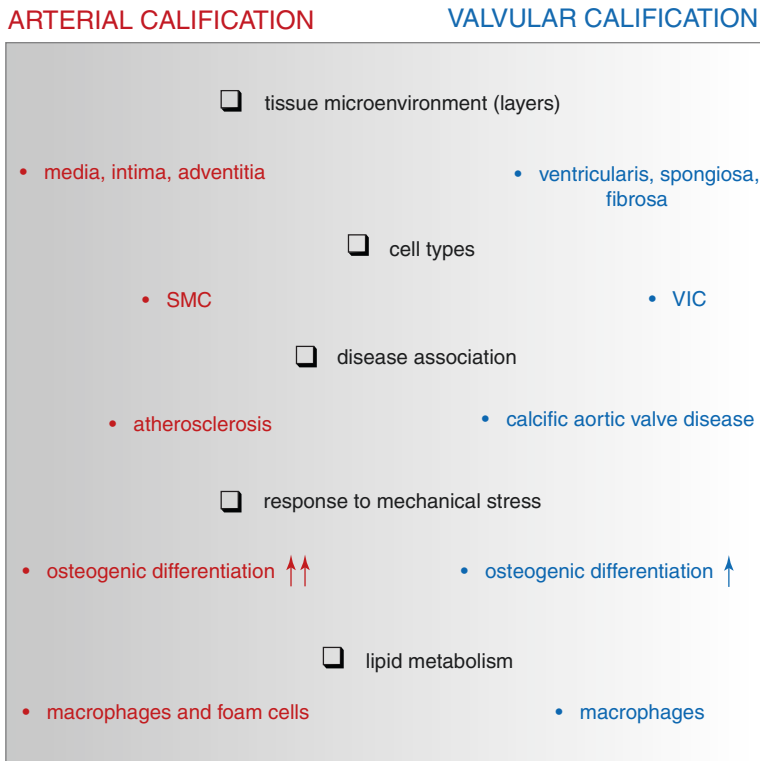


Fig. 4.3 Established differences between vascular and valvular calcification. Several differences are currently known to exist between vascular and valvular calcification, including tissue microenvironments, cell types involved, associated diseases, and the extent of response to mechanical stress in pro-calcific conditions

Conclusions

While in some cases like chronic kidney disease vascular and valvular calcification can co-occur, this is not always the case, particularly in the general population. Only 30–50% of patients with aortic valve stenosis have atherosclerosis [154], and it is unclear whether these diseases are regulated by the same or different mechanisms. Patients with calcified valves do not always have calcified arteries and vice versa. Several of the mechanisms that have been shown to induce vascular calcification also induce valvular calcification, supporting the existence of shared disease drivers. On the other hand, as outlined in this chapter, there are differences in vascular and valvular calcification that distinguish these diseases on a molecular mechanism level (Fig. 4.3). This suggests that despite some similarities, vascular and valvular calcifications are distinct entities in their pathogenesis. Further differences are likely to be discovered but require more direct comparisons between diseased vascular- and valvular-calcified tissues and disease models. There are limitations in reviewing the mechanistic differences in these two diseases. First, there is a limited amount of

mechanistic reports in which a direct comparison is made between both vascular and valves tissues and models. Second, majorities of molecular mechanisms that have been proposed are typically first established in one tissue type like bone or arteries and then assessed in valve. This creates the potential for literature bias in which shared mechanisms with positive results are more likely to be reported. Furthermore, calcification models vary widely with differences in species, calcification-inducing media components, and others contributing to diverse responses. Standardization of calcification research efforts may help to address some of these issues. Actively pursuing the identification of the molecular mechanisms that account for differences in vascular and valvular calcification may uncover key drivers of these distinct pathologies and lead to effective therapies for these critical unmet medical needs.

References

1. Jensky NE, Criqui MH, Wright MC, Wassel CL, Brody SA, Allison MA. Blood pressure and vascular calcification. *Hypertension*. 2010;55:990–7.
2. Leening MJ, Elias-Smale SE, Kavousi M, Felix JF, Deckers JW, Vliegenthart R, Qudkerk M, Hofman A, Steverberg EW, Stricker BH, Witteman JC. Coronary calcification and the risk of heart failure in the elderly: the Rotterdam study. *JACC Cardiovasc Imaging*. 2012;5:874–80.
3. Kelly-Arnold A, Maldonado N, Laudier D, Aikawa E, Cardoso L, Weinbaum S. Revised microcalcification hypothesis for fibrous cap rupture in human coronary arteries. *Proc Natl Acad Sci U S A*. 2013;110:10741–6.
4. Varadarajan P, Kapoor N, Bansal RC, Pai RG. Survival in elderly patients with severe aortic stenosis is dramatically improved by aortic valve replacement: results from a cohort of 277 patients aged > or =80 years. *Eur J Cardiothorac Surg*. 2006;30:722–7.
5. Rajamannan NM, Bonow RO, Rahimtoola SH. Calcific aortic stenosis: an update. *Nat Clin Pract Cardiovasc Med*. 2007;4:254–62.
6. Lindroos M, Kupari M, Heikkilä J, Tilvis R. Prevalence of aortic valve abnormalities in the elderly: an echocardiographic study of a random population sample. *J Am Coll Cardiol*. 1993;21:1220–5.
7. Iribarren C, Sidney S, Sternfeld B, Browner WS. Calcification of the aortic arch: risk factors and association with coronary heart disease, stroke, and peripheral vascular disease. *JAMA*. 2000;283:2810–5.
8. Lee TC, O'Malley PG, Feuerstein I, Taylor AJ. The prevalence and severity of coronary artery calcification on coronary artery computed tomography in black and white subjects. *J Am Coll Cardiol*. 2003;41:39–44.
9. Callaway MP, Richards P, Goddard P, Rees M. The incidence of coronary artery calcification on standard thoracic CT scans. *Br J Radiol*. 1997;70:572–4.
10. Russo D, Palmiero G, De Blasio AP, Balletta MM, Andreucci VE. Coronary artery calcification in patients with CRF not undergoing dialysis. *Am J Kidney Dis*. 2004;44:1024–30.
11. Raggi P, Boulay A, Chasan-Taber S, Amin N, Dillon M, Burke SK, Chertow GM. Cardiac calcification in adult hemodialysis patients: a link between end-stage renal disease and cardiovascular disease? *J Am Coll Cardiol*. 2002;39:695–701.
12. Rutsch F, Ruf N, Vaingankar S, Toliat MR, Suk A, Höhne W, Schauer G, Lehmann M, Roscioli T, Schnabel D, Eppel JT, Knisely A, Superti-Furga A, McGill J, Filippone M, Sinaiko AR, Vallance H, Hinrichs B, Smith W, Ferre M, Terkeltaub R, Nürnberg P. Mutations in ENPP1 are associated with 'idiopathic' infantile arterial calcification. *Nat Genet*. 2003;34:379–81.

13. Badame AJ. Progeria. *Arch Dermatol.* 1989;125:540–4.
14. Brown JW, Ruzmetov M, Vijay P, Rodefeld MD, Turrentine MW. Surgery for aortic stenosis in children: a 40-year experience. *Ann Thorac Surg.* 2003;76:1398–411.
15. Henein M, Hällgren P, Holmgren A, Sörensen K, Ibrahim P, Kofoed KF, Larsen LH, Hassager C. Aortic root, not valve, calcification correlates with coronary artery calcification in patients with severe aortic stenosis: a two-center study. *Atherosclerosis.* 2015;243:631–7.
16. Rogers MA, Aikawa E. Cardiovascular calcification : artificial intelligence and big data accelerate mechanistic discovery. *Nat Rev Cardiol.* 2019;16:261–74.
17. Bertazzo S, Gentleman E, Cloyd KL, Chester AH, Yacoub MH, Stevens MM. Nano-analytical electron microscopy reveals fundamental insights into human cardiovascular tissue calcification. *Nat Mater.* 2013;12:576–83.
18. Hutcheson JD, Goetsch C, Bertazzo S, Maldonado N, Ruiz JL, Goh W, Yabusaki K, Faits T, Bouten C, Franck G, Quillard T, Libby P, Aikawa M, Weinbaum S, Aikawa E. Genesis and growth of extracellular-vesicle-derived microcalcification in atherosclerotic plaques. *Nat Mater.* 2016;15:335–43.
19. Kapustin AN, Chatrou ML, Drozdov I, Zheng Y, Davidson SM, Soong D, Furmanik M, Sanchis P, De Rosales RT, Alvarez-Hernandez D, Shroff R, Yin X, Muller K, Skepper JN, Mayr M, Reutelingsperger CP, Chester A, Bertazzo S, Schurgers LJ, Shanahan CM. Vascular smooth muscle cell calcification is mediated by regulated exosome secretion. *Circ Res.* 2015;116:1312–23.
20. Kim KM. Calcification of matrix vesicles in human aortic valve and aortic media. *Fed Proc.* 1976;35:156–62.
21. Cui L, Rashdan NA, Zhu D, Milne EM, Ajuh P, Milne G, Helfrich MH, Lim K, Prasad S, Lerman DA, Vesey AT, Dweck MR, Jenkins WS, Newby DE, Farguharson C, Macrae VE. End stage renal disease-induced hypercalcemia may promote aortic valve calcification via Annexin VI enrichment of valve interstitial cell derived-matrix vesicles. *J Cell Physiol.* 2017;232:2985–95.
22. Proudfoot D, Skepper JN, Hegyi L, Bennett MR, Shanahan CM, Weissberg PL. Apoptosis regulates human vascular calcification in vitro: evidence for initiation of vascular calcification by apoptotic bodies. *Circ Res.* 2000;87:1055–62.
23. Hutcheson JD, Venkataraman R, Baudenbacher FJ, Merryman WD. Intracellular Ca(2+) accumulation is strain-dependent and correlates with apoptosis in aortic valve fibroblasts. *J Biomech.* 2012;45:888–94.
24. Jian B, Narula N, Li QY, Mohler ER 3rd, Levy RJ. Progression of aortic valve stenosis: TGF-beta1 is present in calcified aortic valve cusps and promotes aortic valve interstitial cell calcification via apoptosis. *Ann Thorac Surg.* 2003;75:457–65.
25. Wagenseil JE, Mecham RP. Vascular extracellular matrix and arterial mechanics. *Physiol Rev.* 2009;89:957–89.
26. Ankeny RF, Thourani VH, Weiss D, Vega JD, Taylor WR, Nerem RM, Jo H. Preferential activation of SMAD1/5/8 on the fibrosa endothelium in calcified human aortic valves—association with low BMP antagonists and SMAD6. *PLoS One.* 2011;6:e20969.
27. Everhart JE, Pettitt DJ, Knowler WC, Rose FA, Bennett PH. Medial arterial calcification and its association with mortality and complications of diabetes. *Diabetologia.* 1988;31:16–23.
28. Goodman WG, Goldin J, Kuizon BD, Yoon C, Gales B, Sider D, Wang Y, Chung J, Emerick A, Greaser L, Elashoff RM, Salusky IB. Coronary-artery calcification in young adults with end-stage renal disease who are undergoing dialysis. *N Engl J Med.* 2000;342:1478–83.
29. Fitzpatrick LA, Severson A, Edwards WD, Ingram RT. Diffuse calcification in human coronary arteries. Association of osteopontin with atherosclerosis. *J Clin Invest.* 1994;94:1597–604.
30. Latif N, Sarathchandra P, Chester AH, Yacoub MH. Expression of smooth muscle cell markers and co-activators in calcified aortic valves. *Eur Heart J.* 2015;36:1335–45.
31. Latif N, Quillon A, Sarathchandra P, McCormack A, Lozanoski A, Yacoub MH, Chester AH. Modulation of human valve interstitial cell phenotype and function using a fibroblast growth factor 2 formulation. *PLoS One.* 2015;10:e0127844.

32. Aikawa E, Whittaker P, Farber M, Mendelson K, Padera RF, Aikawa M, Schoen FJ. Human semilunar cardiac valve remodeling by activated cells from fetus to adult: implications for postnatal adaptation, pathology, and tissue engineering. *Circulation*. 2006;113:1344–52.
33. Ferdous Z, Jo H, Nerem RM. Differences in valvular and vascular cell responses to strain in osteogenic media. *Biomaterials*. 2011;32:2885–93.
34. Alves RD, Eijken M, van de Peppel J, van Leeuwen JP. Calcifying vascular smooth muscle cells and osteoblasts: independent cell types exhibiting extracellular matrix and biomineralization-related mimics. *BMC Genomics*. 2014;15:965.
35. Romanelli F, Corbo A, Salehi M, Yadav MC, Salman S, Petrosian D, Rashidbaigi OJ, Chait J, Kuruvilla J, Plummer M, Radichev I, Margulies KB, Gerdes AM, Pinkerton AB, Millán JL, Savinov AY, Savinova OV. Overexpression of tissue-nonspecific alkaline phosphatase (TNAP) in endothelial cells accelerates coronary artery disease in a mouse model of familial hypercholesterolemia. *PLoS One*. 2017;12:e0186426.
36. Sun Y, Byon CH, Yuan K, Chen J, Mao X, Heath JM, Javed A, Zhang K, Anderson PG, Chen Y. Smooth muscle cell-specific runx2 deficiency inhibits vascular calcification. *Circ Res*. 2012;111:543–52.
37. Liu J, Nam HK, Campbell C, Gasque KC, Millán JL, Hatch NE. Tissue-nonspecific alkaline phosphatase deficiency causes abnormal craniofacial bone development in the *Alpl*($-/-$) mouse model of infantile hypophosphatasia. *Bone*. 2014;67:81–94.
38. Zhang S, Zhousheng X, Luo J, He N, Mahlios J, Quarles LD. Dose-dependent effects of runx2 on bone development. *J Bone Miner Res*. 2009;24:1889–904.
39. Patel JJ, Zhu D, Opdebeeck B, D’Haese P, Millán JL, Bourne LE, Wheeler-Jones CPD, Arnett TR, MacRae VE, Orris IR. Inhibition of arterial medial calcification and bone mineralization by extracellular nucleotides: the same functional effect mediated by different cellular mechanisms. *J Cell Physiol*. 2018;233:3230–43.
40. Goetsch C, Hutcheson JC, Aikawa M, Iwata H, Pham T, Nykjaer A, Kjolby M, Rogers MA, Michel T, Shibasaki M, Hagita S, Kramann R, Rader DJ, Libby P, Singh SA, Aikawa E. Sortilin mediates vascular calcification via its recruitment into extracellular vesicles. *J Clin Invest*. 2016;126:1323–36.
41. Rogers MA, Maldonado N, Hutcheson JD, Goetsch C, Goto S, Yamada I, Faits T, Sesaki H, Aikawa M, Aikawa E. Dynamin-related protein 1 inhibition attenuates cardiovascular calcification in the presence of oxidative stress. *Cir Res*. 2017;121:220–33.
42. Nachlas ALY, Li S, Jha R, Singh M, Xu C, Davis ME. Human iPSC-derived mesenchymal stem cells encapsulated in PEGDA hydrogels mature into valve interstitial-like cells. *Acta Biomater*. 2018;71:235–46.
43. Trillhaase A, Haferkamp U, Rangnau A, Märten M, Schmidt B, Trilck M, Seibler P, Aherrahrou R, Erdmann J, Aherrahrou Z. Differentiation of human iPSCs into VSMCs and generation of VSMC-derived calcifying vascular cells. *Stem Cell Res*. 2018;31:62–70.
44. Panicker LM, Srikanth MP, Castro-Gomes T, Miller D, Andrews NW, Feldman RA. Gaucher disease iPSC-derived osteoblasts have developmental and lysosomal defects that impair bone matrix deposition. *Hum Mol Genet*. 2018;27:811–22.
45. Štefková K, JiřinaProcházková J, Pacherník J. Alkaline phosphatase in stem cells. *Stem Cell Int*. 2015;2015:628368.
46. Rajamannan NM, Subramaniam M, Rickard D, Stock SR, Donovan J, Springett M, Orszulak T, Fullerton DA, Takik AJ, Bonow RO, Spelsberg T. Human aortic valve calcification is associated with an osteoblast phenotype. *Circulation*. 2003;107:2181–4.
47. Shanahan CM, Cary NR, Salisbury JR, Proudfoot D, Weissberg PL, Edmonds ME. Medial localization of mineralization-regulating proteins in association with Mönckeberg’s sclerosis: evidence for smooth muscle cell-mediated vascular calcification. *Circulation*. 1999;100:2168–76.
48. Shroff RC, McNair R, Figg N, Skepper JN, Schurgers L, Gupta A, Hiorns M, Donald AE, Deanfield J, Rees L, Shanahan CM. Dialysis accelerates medial vascular calcification in part by triggering smooth muscle cell apoptosis. *Circulation*. 2008;118(17):1748–57.

49. Goto S, Rogers MA, Blaser MC, Higashi H, Lee LH, Schlotter F, Body SC, Aikawa M, Singh SA, Aikawa E. Standardization of human calcific aortic valve disease *in vitro* modeling reveals passage-dependent calcification. *Front Cardiovasc Med.* 2019;6:49.
50. Zuo B, Yang J, Wang F, Wang L, Yin Y, Dan J, Liu N, Liu L. Influences of lamin A levels on induction of pluripotent stem cells. *Biol Open.* 2012;1:1118–27.
51. Liu Y, Drozdov I, Shroff R, Beltran LE, Shanahan CM. Prelamin A accelerates vascular calcification via activation of the DNA damage response and senescence-associated secretory phenotype in vascular smooth muscle cells. *Circ Res.* 2013;112:e99–109.
52. Kramann R, Goettsch C, Wongboonsin J, Iwata H, Schneider RK, Kuppe C, Kaesler N, Chang-Panesso M, Machado FG, Gratwohl S, Madhurima K, Hutcheson JD, Jain S, Aikawa E, Humphreys BD. Adventitial MSC-like cells are progenitors of vascular smooth muscle cells and drive vascular calcification in chronic kidney disease. *Cell Stem Cell.* 2016;19:628–42.
53. Chen JH, Yip CYY, Sone ED, Simmons CA. Identification and characterization of aortic valve mesenchymal progenitor cells with robust osteogenic calcification potential. *Am J Pathol.* 2009;174:1109–19.
54. Gössl M, Khosla S, Zhang X, Higano N, Jordan KL, Loeffler D, Enriquez-Sarano M, Lennon RJ, McGregor U, Lerman LO, Lerman A. Role of circulating osteogenic progenitor cells in calcific aortic stenosis. *J Am Coll Cardiol.* 2012;60:1945–53.
55. Butcher JT, Tressel S, Johnson T, Turner D, Sorescu G, Jo H, Nerem RM. Transcriptional profiles of valvular and vascular endothelial cells reveal phenotypic differences: influence of shear stress. *Arterioscler Thromb Vasc Biol.* 2006;26:69–77.
56. Bischoff J, Aikawa E. Progenitor cells confer plasticity to cardiac valve endothelium. *J Cardiovasc Transl Res.* 2011;4:71–19.
57. Piera-Velazquez S, Li Z, Jimenez SA. Role of endothelial-mesenchymal transition (EndoMT) in the pathogenesis of fibrotic disorders. *Am J Pathol.* 2011;179:1074–80.
58. Dahal S, Huang P, Murray BT, Mahler GJ. Endothelial to mesenchymal transformation is induced by altered extracellular matrix in aortic valve endothelial cells. *J Biomed Mater Res A.* 2017;105:2729–41.
59. Balachandran K, Sucusky P, Jo H, Yoganathan AP. Elevated cyclic stretch induces aortic valve calcification in a bone morphogenic protein-dependent manner. *Am J Pathol.* 2010;177:49–57.
60. Sánchez-Duffhues G, García de Vinuesa A, van de Pol V, Geerts ME, de Vries MR, Janson SG, van Dam H, Lindeman JH, Goumans MJ, Ten Dijke P. Inflammation induces endothelial-to-mesenchymal transition and promotes vascular calcification through downregulation of BMPR2. *J Pathol.* 2019;247:333–46.
61. Beppu S, Suzuki S, Matsuda H, Ohmori F, Nagata S, Miyatake K. Rapidity of progression of aortic stenosis in patients with congenital bicuspid aortic valves. *Am J Cardiol.* 1993;71:322–7.
62. Winchester R, Wiesendanger M, O'Brien W, Zhang HZ, Maurer MS, Gillam LD, Schwartz A, Marboe C, Stewart AS. Circulating activated and effector memory T cells are associated with calcification and clonal expansions in bicuspid and tricuspid valves of calcific aortic stenosis. *J Immunol.* 2011;187:1006–14.
63. Nagy E, Lei Y, Martínez-Martínez E, Body SC, Schlotter F, Creager M, Assmann A, Khabbaz K, Libby P, Hansson GK, Aikawa E. Interferon- γ released by activated CD8+ T lymphocytes impairs the calcium resorption potential of osteoclasts in calcified human aortic valves. *Am J Pathol.* 2017;187:1413–25.
64. Goettsch C, Rauner M, Hamann C, Sinnigen K, Hempel U, Bornstein SR, Hofbauer LC. Nuclear factor of activated T cells mediates oxidised LDL-induced calcification of vascular smooth muscle cells. *Diabetologia.* 2011;54:2690–701.
65. Zheng KH, Tsimikas S, Pawade T, Kroon J, Jenkins WSA, Doris MK, White AC, Timmers NKLM, Hjortnaes J, Rogers MA, Aikawa E, Arsenault BJ, Witztum JL, Newby DE, Koschinsky ML, Fayad ZA, Stroes ESG, Boekholdt SM, Dweck MR. Lipoprotein(a) and oxidized phospholipids promote valve calcification in patients with aortic stenosis. *J Am Coll Cardiol.* 2019;73:2150–62.

66. An WS, Kim SE, Kim KH, Bae HR, Rha SH. Associations between oxidized LDL to LDL ratio, HDL and vascular calcification in the feet of hemodialysis patients. *J Korean Med Sci.* 2009;24:S115–20.
67. Qasim AN, Martin SS, Mehta NN, Wolfe ML, Park J, Schwartz S, Schutta M, Iqbal N, Reilly MP. Lipoprotein(a) is strongly associated with coronary artery calcification in type-2 diabetic women. *Int J Cardiol.* 2011;150:17–21.
68. Que X, Hung MY, Yeang C, Gonen A, Prohaska TA, Sun X, Diehl C, Määttä A, Gaddis DE, Bowden K, Pattison J, MacDonald JG, Ylä-Herttuala S, Mellon PL, Hedrick CC, Ley K, Miller YI, Glass CK, Peterson KL, Binder CJ, Tsimikas S, Witztum JL. Oxidized phospholipids are proinflammatory and proatherogenic in hypercholesterolemic mice. *Nature.* 2018;558:301–6.
69. Dube PR, Chikkamenahalli LL, Birnbaumer L, Vazquez G. Reduced calcification and osteogenic features in advanced atherosclerotic plaques of mice with macrophage-specific loss of TRPC3. *Atherosclerosis.* 2018;270:199–204.
70. Li G, Qiao W, Zhang W, Li F, Shi J, Dong N. The shift of macrophages toward M1 phenotype promotes aortic valvular calcification. *J Thorac Cardiovasc Surg.* 2017;153:1318–27.e1.
71. Rogers MA, Aikawa M, Aikawa E. Macrophage heterogeneity complicates reversal of calcification in cardiovascular tissues. *Circ Res.* 2017;121:5–7.
72. Chinetti-Gbaguidi G, Daoudi M, Rosa M, Vinod M, Louvet L, Copin C, Fanchon M, Vanhoutte J, Derudas B, Belloy L, Haulon S, Zawadzki C, Susen S, Massy ZA, Eeckhoutte J, Staels B. Human alternative macrophages populate calcified areas of atherosclerotic lesions and display impaired RANKL-induced osteoclastic bone resorption activity. *Circ Res.* 2017;121:19–30.
73. New SE, Goettsch C, Aikawa M, Marchini JF, Shibasaki M, Yabusaki K, Libby P, Shanahan CM, Croce K, Aikawa E. Macrophage-derived matrix vesicles: an alternative novel mechanism for microcalcification in atherosclerotic plaques. *Circ Res.* 2013;113(1):72–7.
74. Bobryshev YV, Lord RS. Detection of vascular dendritic cells and extracellular calcium-binding protein S-100 in foci of calcification in human arteries. *Acta Histochem Cytochem.* 1995;28:371–80.
75. Bobryshev YV, Lord RS. Detection of vascular dendritic cells accumulating calcified deposits in their cytoplasm. *Tissue Cell.* 1998;30:383–8.
76. Choi JH, Do Y, Cheong C, Koh H, Boscardin SB, Oh YS, Bozzacco L, Trumpfheller C, Park CG, Steinman RM. Identification of antigen-presenting dendritic cells in mouse aorta and cardiac valves. *J Exp Med.* 2009;206:497–505.
77. Koltsova EK, Ley K. How dendritic cells shape atherosclerosis. *Trends Immunol.* 2011;32:540–7.
78. Ait-Oufella H, Herbin O, Bouaziz JD, Binder CJ, Uyttenhove C, Laurans L, Taleb S, Van Vré E, Esposito B, Vilar J, Sirvent J, Van Snick J, Tedgui A, Tedder TF, Mallat Z. B cell depletion reduces the development of atherosclerosis in mice. *J Exp Med.* 2010;207(8):1579–87.
79. Yun TJ, Tallquist MD, Aicher A, Rafferty KL, Marshall AJ, Moon JJ, Ewings ME, Mohaupt M, Herring SW, Clark EA. Osteoprotegerin, a crucial regulator of bone metabolism, also regulates B cell development and function. *J Immunol.* 2001;166:1482–91.
80. Steiner I, Krbal L, Rozkoš T, Harrer J, Laco J. Calcific aortic valve stenosis: Immunohistochemical analysis of inflammatory infiltrate. *Pathol Res Pract.* 2012;208:231–4.
81. Natorska J, Marek G, Sadowski J, Undas A. Presence of B cells within aortic valves in patients with aortic stenosis: relation to severity of the disease. *J Cardiol.* 2016;67:80–5.
82. Wypasek E, Natorska J, Grudzień G, Filip G, Sadowski J, Undas A. Mast cells in human stenotic aortic valves are associated with the severity of stenosis. *Inflammation.* 2013;36:449–56.
83. Helske S, Syväranta S, Kupari M, Lappalainen J, Laine M, Lommi J, Turto H, Mäyränpää M, Werkkala K, Kovanen PT, Lindstedt KA. Possible role for mast cell-derived cathepsin G in the adverse remodelling of stenotic aortic valves. *Eur Heart J.* 2006;27:1495–504.
84. Kovanen PT, Kaartinen M, Paavonen T. Infiltrates of activated mast cells at the site of coronary atheromatous erosion or rupture in myocardial infarction. *Circulation.* 1995;92:1084–8.

85. Jeziorska M, McCollum C, Woolley DE. Calcification in atherosclerotic plaque of human carotid arteries: associations with mast cells and macrophages. *J Pathol.* 1998;185:10–7.
86. Wu M, Rementer C, Giachelli CM. Vascular calcification: an update on mechanisms and challenges in treatment. *Calcif Tissue Int.* 2013;93:365–73.
87. Sage AP, Tintut Y, Demer LL. Regulatory mechanisms in vascular calcification. *Nat Rev Cardiol.* 2010;7:528–36; 69. Leopold J. A. Cellular mechanisms of aortic valve calcification. *Circ Cardiovasc Interv.* 2012;5:605–14.
88. Proudfoot D, Shanahan CM. Molecular mechanisms mediating vascular calcification: role of matrix Gla protein. *Nephrology.* 2006;11:455–61.
89. Shao JS, Cai J, Towler DA. Molecular mechanisms of vascular calcification: lessons learned from the aorta. *Arterioscler Thromb Vasc Biol.* 2006;26:1423–30.
90. Pawade TA, Newby DE, Dweck MR. Calcification in aortic stenosis: the skeleton key. *J Am Coll Cardiol.* 2015;66:561–77.
91. Sakaguchi Y, Hamano T, Nakano C, Obi Y, Matsui I, Kusunoki Y, Mori D, Oka T, Hashimoto N, Takabatake Y, Takahashi A, Kaimori JY, Moriyama T, Yamamoto R, Horio M, Sugimoto K, Yamamoto K, Rakugi H, Isaka Y. Association between density of coronary artery calcification and serum magnesium levels among patients with chronic kidney disease. *PLoS One.* 2016;11:e0163673.
92. Bai Y, Zhang J, Xu J, Cui L, Zhang H, Zhang S, Feng X. Magnesium prevents β -glycerophosphate-induced calcification in rat aortic vascular smooth muscle cells. *Biomed Rep.* 2015;3:593–7.
93. Ter Braake AD, Tinnemans PT, Shanahan CM, Hoenderop JGJ, de Baaij JHF. Magnesium prevents vascular calcification in vitro by inhibition of hydroxyapatite crystal formation. *Sci Rep.* 2018;8:2069.
94. Hisamatsu T, Miura K, Fujiyoshi A, Kadota A, Miyagawa N, Satoh A, Zaid M, Yamamoto T, Horie M, Ueshima H, SESSA Research Group. Serum magnesium, phosphorus, and calcium levels and subclinical calcific aortic valve disease: a population-based study. *Atherosclerosis.* 2018;273:145–52.
95. Block GA, Hulbert-Shearon TE, Levin NW, Port FK. Association of serum phosphorus and calcium x phosphate product with mortality risk in chronic hemodialysis patients: a national study. *Am J Kidney Dis.* 1998;31:607–17.
96. Dingra R, Sullivan LM, Fox CS, Wang TJ, D'Agostino RB Sr, Gaziano JM, Vasan RS. Relations of serum phosphorus and calcium levels to the incidence of cardiovascular disease in the community. *Arch Intern Med.* 2007;167:879–85.
97. Li X, Yang HY, Giachelli CM. Role of the sodium-dependent phosphate cotransporter, Pit-1, in vascular smooth muscle cell calcification. *Circ Res.* 2006;98:905–12.
98. Hussein DE, Boulanger MC, Fournier D, Mahmut A, Bossé Y, Pibarot P, Mathieu P. High expression of the Pi-transporter SLC20A1/Pit1 in calcific aortic valve disease promotes mineralization through regulation of Akt. *PLoS One.* 2013;8:e53393.
99. Heath JM, Sun Y, Yuan K, Bradley WE, Litovsky S, Dell'Italia LJ, Chatham JC, Wu H, Chen Y. Activation of AKT by O-GlcNAcylation induces vascular calcification in diabetes. *Circ Res.* 2014;114:1094–102.
100. Ponnusamy A, Sinha S, Hyde GD, Borland SJ, Taylor RF, Pond E, Eyre HJ, Inkson CA, Gilmore A, Ashton N, Kalra PA, Canfield AE. FTI-277 inhibits smooth muscle cell calcification by up-regulating PI3K/Akt signaling and inhibiting apoptosis. *PLoS One.* 2018;13:e0196232.
101. Nadlonek NA, Lee JH, Weyant MJ, Meng X, Fullerton DA. Ox-LDL induces Pit-1 expression in human aortic valve interstitial cells. *J Surg Res.* 2013;184:6–9.
102. Seto T, Hamada C, Tomino Y. Suppressive effects of iron overloading on vascular calcification in uremic rats. *J Nephrol.* 2014;27:135–42.
103. Kawada S, Nagasawa Y, Kawabe M, Ohyama H, Kida A, Kato-Kogoe N, Nanami M, Hasuike Y, Kuragano T, Kishimoto H, Nakasho K, Nakanishi T. Iron-induced calcification in human aortic vascular smooth muscle cells through interleukin-24 (IL-24), with/without TNF-alpha. *Sci Rep.* 2018;8:658.

104. Ciceri P, Elli F, Braidotti P, Falleni M, Tosi D, Bulfamante G, Block GA, Cozzolino M. Iron citrate reduces high phosphate-induced vascular calcification by inhibiting apoptosis. *Atherosclerosis*. 2016;254:93–101.
105. Ok E, Asci G, Bayraktaroglu S, Toz H, Ozkahya M, Yilmaz M, Kircelli F, Ok ES, Ceylan N, Duman S, Cirit M, Monier-Faugere MC, Malluche HH. Reduction of dialysate calcium level reduces progression of coronary artery calcification and improves low bone turnover in patients on hemodialysis. *J Am Soc Nephrol*. 2016;27:2475–86.
106. Ikee R, Honda K, Ishioka K, Oka M, Maesato K, Moriya H, Hidaka S, Ohtake T, Kobayashi S. Differences in associated factors between aortic and mitral valve calcification in hemodialysis. *Hypertens Res*. 2010;33:622–6.
107. Ortlepp JR, Pillich M, Schmitz F, Mevissen V, Koos R, Weiss S, Stork L, Dronskowski R, Langebartels G, Autschbach R, Brandenburg V, Woodruff S, Kaden JJ, Hoffmann R. Lower serum calcium levels are associated with greater calcium hydroxyapatite deposition in native aortic valves of male patients with severe calcific aortic stenosis. *J Heart Valve Dis*. 2006;15:502–8.
108. Iwata S, Walker MD, Di Tullio MR, Hyodo E, Jin Z, Liu R, Sacco RL, Homma S, Silverberg SJ. Aortic valve calcification in mild primary hyperparathyroidism. *J Clin Endocrinol Metab*. 2012;97:132–7.
109. Aikawa E, Aikawa M, Libby P, Figueiredo JL, Rusanescu G, Iwamoto Y, Fukuda D, Kohler RH, Shi GP, Jaffer FA, Weissleder R. Arterial and aortic valve calcification abolished by elastolytic cathepsin S deficiency in chronic renal disease. *Circulation*. 2009;119:1785–94.
110. Figueiredo JL, Aikawa M, Zheng C, Aaron J, Lax L, Libby P, de Lima Filho JL, Gruener S, Fingerle J, Haap W, Hartmann G, Aikawa E. Selective cathepsin S inhibition attenuates atherosclerosis in apolipoprotein E-deficient mice with chronic renal disease. *Am J Pathol*. 2015;185:1156–66.
111. Bäck M, Aranyi T, Cancela ML, Carracedo M, Conceição N, Leftheriotis G, Macrae V, Martin L, Nitschke Y, Pasch A, Quaglino D, Rutsch F, Shanahan C, Sorribas V, Szeri F, Valdivielso P, Vanakker O, Kempf H. Endogenous calcification inhibitors in the prevention of vascular calcification: a consensus statement from the COST action EuroSoftCalcNet. *Front Cardiovasc Med*. 2019;18:196.
112. Lomashvili KA, Cobbs S, Hennigar RA, Hardcastle KI, O'Neill WC. Phosphate-induced vascular calcification: role of pyrophosphate and osteopontin. *J Am Soc Nephrol*. 2004;15:1392–401.
113. Rathan S, Yoganathan AP, O'Neill CW. The role of inorganic pyrophosphate in aortic valve calcification. *J Heart Valve Dis*. 2014;23:387–94.
114. Luo G, Ducy P, McKee MD, Pinero GJ, Loyer E, Behringer RR, et al. Spontaneous calcification of arteries and cartilage in mice lacking matrix GLA protein. *Nature*. 1997;386:78–81.
115. Sheng K, Zhang P, Lin W, Cheng J, Li J, Chen J. Association of Matrix Gla protein gene (rs1800801, rs1800802, rs4236) polymorphism with vascular calcification and atherosclerotic disease: a meta-analysis. *Sci Rep*. 2017;7:8713.
116. Brandenburg VM, Reinartz S, Kaesler N, Krüger T, Dirrrichs T, Kramann R, Peeters F, Floege J, Keszei A, Marx N, Schurgers LJ, Koos R. Slower progress of aortic valve calcification with vitamin K supplementation: results from a prospective interventional proof-of-concept study. *Circulation*. 2017;135:2081–3.
117. Schafer C, Heiss A, Schwarz A, Westenfeld R, Ketteler M, Floege J, Muller-Esterl W, Schinke T, Jahnke-Dechent W. The serum protein alpha 2-Heremans-Schmid glycoprotein/fetuin-A is a systemically acting inhibitor of ectopic calcification. *J Clin Invest*. 2003;112:357–66.
118. Ix JH, Katz R, de Boer IH, Kestenbaum BR, Peralta CA, Jenny NS, Budoff M, Allison MA, Criqui MH, Siscovick D, Shlipak MG. Fetuin-A is inversely associated with coronary artery calcification in community-living persons: the multi-ethnic study of atherosclerosis. *Clin Chem*. 2012;58:887–95.
119. Carracedo M, Bäck M. Fetuin a in aortic stenosis and valve calcification: not crystal clear. *Int J Cardiol*. 2018;265:77–8.

120. Callegari A, Coons ML, Ricks JL, Rosenfeld ME, Scatena M. Increased calcification in osteoprotegerin-deficient smooth muscle cells: dependence on receptor activator of NF- κ B ligand and interleukin 6. *J Vasc Res.* 2014;51:118–31.
121. Weiss RM, Lund DD, Chu Y, Brooks RM, Zimmerman KA, El Accaoui R, Davis MK, Hajj GP, Zimmerman MB, Heistad DD. Osteoprotegerin inhibits aortic valve calcification and preserves valve function in hypercholesterolemic mice. *PLoS One.* 2013;8:e65201.
122. Kiechl S, Werner P, Knoflach M, Furtner M, Willeit J, Schett G. The osteoprotegerin/RANK/RANKL system: a bone key to vascular disease. *Expert Rev Cardiovasc Ther.* 2006;4:801–11.
123. Steitz SA, Speer MY, McKee MD, Liaw L, Almeida M, Yang H, Giachelli CM. Osteopontin inhibits mineral deposition and promotes regression of ectopic calcification. *Am J Pathol.* 2002;161:2035–46.
124. Speer MY, McKee MD, Guldberg RE, Liaw L, Yang HY, Tung E, et al. Inactivation of the osteopontin gene enhances vascular calcification of matrix Gla protein-deficient mice: evidence for osteopontin as an inducible inhibitor of vascular calcification *in vivo*. *J Exp Med.* 2002;196:1047–55.
125. Paloian NJ, Leaf EM, Giachelli CM. Osteopontin protects against high phosphate-induced nephrocalcinosis and vascular calcification. *Kidney Int.* 2016;89:1027–36.
126. Yu PJ, Skolnick A, Ferrari G, Heretis K, Mignatti P, Pintucci G, Rosenzweig B, Diaz-Cartelle J, Kronzon I, Perk G, Pass HI, Galloway AC, Grossi EA, Grau JB. Correlation between plasma osteopontin levels and aortic valve calcification: potential insights into the pathogenesis of aortic valve calcification and stenosis. *J Thorac Cardiovasc Surg.* 2009;138:196–9.
127. Chen J, Lin Y, Sun Z. Deficiency in the anti-aging gene *Klotho* promotes aortic valve fibrosis through AMPK α -mediated activation of RUNX2. *Aging Cell.* 2016;15:853–60.
128. Kuro-o M, Matsumura Y, Aizawa H, Kawaguchi H, Suga T, Utsugi T, et al. Mutation of the mouse *klotho* gene leads to a syndrome resembling ageing. *Nature.* 1997;390:45–51.
129. Koh N, Fujimori T, Nishiguchi S, Tamori A, Shiomi S, Nakatani T, et al. Severely reduced production of *klotho* in human chronic renal failure kidney. *Biochem Biophys Res Commun.* 2001;280:1015–20.
130. Aikawa E, Nahrendorf M, Figueiredo JL, Swirski FK, Shtatland T, Kohler RH, Jaffer FA, Aikawa M, Weissleder R. Osteogenesis associates with inflammation in early-stage atherosclerosis evaluated by molecular imaging *in vivo*. *Circulation.* 2007;116:2841–50.
131. Zeng Q, Song R, Fullerton DA, Ao L, Zhai Y, Li S, Ballak DB, Cleveland JC Jr, Reece TB, McKinsey TA, Xu D, Dinarello CA, Meng X. Interleukin-37 suppresses the osteogenic responses of human aortic valve interstitial cells *in vitro* and alleviates valve lesions in mice. *Proc Natl Acad Sci U S A.* 2017;114:1631–6.
132. Mosch J, Gleissner CA, Body S, Aikawa E. Histopathological assessment of calcification and inflammation of calcific aortic valves from patients with and without diabetes mellitus. *Histol Histopathol.* 2017;32:293–306.
133. Yahagi K, Kolodgie FD, Lutter C, Mori H, Romero ME, Finn AV, Virmani R. Pathology of human coronary and carotid artery atherosclerosis and vascular calcification in diabetes mellitus. *Arterioscler Thromb Vasc Biol.* 2017;37:191–204.
134. Que X, Hung MY, Yeang C, Gonen A, Prohaska TA, Sun X, Diehl C, Määttä A, Gaddis DE, Bowden K, Pattison J, MacDonald JG, Ylä-Herttuala S, Mellon PL, Hedrick CC, Ley K, Miller YI, Glass CK, Peterson KL, Binder CJ, Tsimikas S, Witztum JL. Oxidized phospholipids are proinflammatory and proatherogenic in hypercholesterolaemic mice. *Nature.* 2018;558(7709):301–6.
135. Bouchareb R, Mahmut A, Nsaibia MJ, Boulanger MC, Dahou A, Lépine JL, Laflamme MH, Hadji F, Couture C, Trahan S, Pagé S, Bossé Y, Pibarot P, Scipione CA, Romagnuolo R, Koschinsky ML, Arsenaault BJ, Marette A, Mathieu P. Autotaxin derived from lipoprotein(a) and valve interstitial cells promotes inflammation and mineralization of the aortic valve. *Circulation.* 2015;132:677–90.
136. Chistiakov DA, Myasoedova VA, Melnichenko AA, Grechko AV, Orekhov AN. Calcifying Matrix Vesicles and Atherosclerosis. *Biomed Res Int.* 2017;2017:7463590.

137. Yamada T, Satoh S, Sueyoshi S, Mitsumata M, Matsumoto T, Ueno T, Uehara K, Mizutani T. Ubiquitin-positive foam cells are identified in the aortic and mitral valves with atherosclerotic involvement. *J Atheroscler Thromb*. 2009;16:472–9.
138. Simionescu N, Vasile E, Lupu F, Popescu G, Simionescu M. Prelesional events in atherogenesis. Accumulation of extracellular cholesterol-rich liposomes in the arterial intima and cardiac valves of the hyperlipidemic rabbit. *Am J Pathol*. 1986;123:109–25.
139. Yamauchi Y, Rogers MA. Sterol metabolism and transport in atherosclerosis and cancer. *Front Endocrinol*. 2018;9:509.
140. Watson KE, Bostrom K, Ravindranath R, Lam T, Norton B, Demer LL. TGF-beta 1 and 25-hydroxycholesterol stimulate osteoblast-like vascular cells to calcify. *J Clin Invest*. 1994;93:2106–13.
141. Mody N, Parhami F, Sarafian TA, Demer LL. Oxidative stress modulates osteoblastic differentiation of vascular and bone cells. *Free Radic Biol Med*. 2001;31(4):509–19.
142. Byon CH, Javed A, Dai Q, Kappes JC, Clemens TL, Darley-Usmar VM, McDonald JM, Chen Y. Oxidative stress induces vascular calcification through modulation of the osteogenic transcription factor Runx2 by AKT signaling. *J Biol Chem*. 2008;283:15319–27.
143. Thériault S, Dina C, Messika-Zeitoun D, Scouarnec SL, Capoulade R, Gaudreault N, Rigade S, Li Z, Simonet F, Lamontagne M, Clavel MA, Arsenault BJ, Boureau AS, Lecoite S, Baron E, Bonnaud S, Karakachoff M, Charpentier E, Fellah I, Roussel JC, Verhoye JP, Baufretton C, Probst V, Roussel R, the D.E.S.I.R. Study Group, Redon R, Dagenais F, Pibarot P, Mathieu P, Le Tourneau T, Bossé Y, Schott JJ. Genetic association analyses highlight IL6, ALPL, and NAV1 as three new susceptibility genes underlying calcific aortic valve stenosis. *bioRxiv*. 2019. <https://doi.org/10.1101/515494>.
144. O'Donnell CJ, Kavousi M, Smith AV, Kardia SL, Feitosa MF, Hwang SJ, Sun YV, Province MA, Aspelund T, Dehghan A, Hoffmann U, Bielak LF, Zhang Q, Eiriksdottir G, van Duijn CM, Fox CS, de Andrade M, Kraja AT, Sigurdsson S, Elias-Smale SE, Murabito JM, Launer LJ, van der Lugt A, Kathiresan S, CARDIOGRAM Consortium, Krestin GP, Herrington DM, Howard TD, Liu Y, Post W, Mitchell BD, O'Connell JR, Shen H, Shuldiner AR, Altshuler D, Elosua R, Salomaa V, Schwartz SM, Siscovick DS, Voight BF, Bis JC, Glazer NL, Psaty BM, Boerwinkle E, Heiss G, Blankenberg S, Zeller T, Wild PS, Schnabel RB, Schillert A, Ziegler A, Münzel TF, White CC, Rotter JJ, Nalls M, Oudkerk M, Johnson AD, Newman AB, Uitterlinden AG, Massaro JM, Cunningham J, Harris TB, Hofman A, Peyser PA, Borecki IB, Cupples LA, Gudnason V, Witteman JC. Genome-wide association study for coronary artery calcification with follow-up in myocardial infarction. *Circulation*. 2011;124:2855–64.
145. van Setten J, Isgum I, Smolonska J, Ripke S, de Jong PA, Oudkerk M, de Koning H, Lammers JW, Zanen P, Groen HJ, Boezen HM, Postma DS, Wijmenga C, Viergever MA, Mali WP, de Bakker PI. Genome-wide association study of coronary and aortic calcification implicates risk loci for coronary artery disease and myocardial infarction. *Atherosclerosis*. 2013;228:400–5.
146. Pechlivanis S, Scherag A, Mühleisen TW, Möhlenkamp S, Horsthemke B, Boes T, Bröcker-Preuss M, Mann K, Erbel R, Jöckel KH, Nöthen MM, Moebus S, Heinz Nixdorf Recall Study Group. Coronary artery calcification and its relationship to validated genetic variants for diabetes mellitus assessed in the Heinz Nixdorf recall cohort. *Arterioscler Thromb Vasc Biol*. 2010;30:1867–72.
147. Divers J, Palmer ND, Lu L, Register TC, Carr JJ, Hicks PJ, Hightower RC, Smith SC, Xu J, Cox AJ, Hruska KA, Bowden DW, Lewis CE, Heiss G, Province MA, Borecki IB, Kerr KF, Chen YD, Palmas W, Rotter JJ, Wassel CL, Bertoni AG, Herrington DM, Wagenknecht LE, Langefeld CD, Freedman BI. Admixture mapping of coronary artery calcified plaque in African Americans with type 2 diabetes mellitus. *Circ Cardiovasc Genet*. 2013;6:697–705.
148. Pelfus LM, Smith JA, Shimmin LC, Bielak LF, Morrison AC, Kardia SL, Peyser PA, Hixson JE. Genome-wide association study of gene by smoking interactions in coronary artery calcification. *PLoS One*. 2013;8:e74642.
149. Adams HH, Ikram MA, Vernooij MW, van Dijk AC, Hofman A, Uitterlinden AG, van Duijn CM, Koudstaal PJ, Franco OH, van der Lugt A, Bos D. Heritability and genome wide association analyses of intracranial carotid artery calcification: the Rotterdam study. *Stroke*. 2016;47:912–7.

150. Ferguson JF, Matthews GJ, Townsend RR, Raj DS, Kanetsky PA, Budoff M, Fischer MJ, Rosas SE, Kanthety R, Rahman M, Master SR, Qasim A, Li M, Mehta NN, Shen H, Mitchell BD, O'Connell JR, Shuldiner AR, Ho WK, Young R, Rasheed A, Danesh J, He J, Kusek JW, Ojo AO, Flack J, Go AS, Gadegbeku CA, Wright JT Jr, Saleheen D, Feldman HI, Rader DJ, Foulkes AS, Reilly MP, CRIC Study Principal Investigators. Candidate gene association study of coronary artery calcification in chronic kidney disease: findings from the CRIC study (Chronic Renal Insufficiency Cohort). *J Am Coll Cardiol.* 2013;62:789–98.
151. Thanassoulis G, Campbell CY, Owens DS, Smith JG, Smith AV, Peloso GM, Kerr KF, Pechlivanis S, Budoff MJ, Harris TB, Malhotra R, O'Brien KD, Kamstrup PR, Nordestgaard BG, Tybjaerg-Hansen A, Allison MA, Aspelund T, Criqui MH, Heckbert SR, Hwang SJ, Liu Y, Sjogren M, van der Pals J, Kälsch H, Mühleisen TW, Nöthen MM, Cupples LA, Caslake M, Di Angelantonio E, Danesh J, Rotter JJ, Sigurdsson S, Wong Q, Erbel R, Kathiresan S, Melander O, Gudnason V, O'Donnell CJ, Post WS, CHARGE Extracoronary Calcium Working Group. Genetic associations with valvular calcification and aortic stenosis. *N Engl J Med.* 2013;368:503–12.
152. Thériault S, Gaudreault N, Lamontagne M, Rosa M, Boulanger MC, Messika-Zeitoun D, Clavel MA, Capoulade R, Dagenais F, Pibarot P, Mathieu P, Bossé Y. A transcriptome-wide association study identifies PALMD as a susceptibility gene for calcific aortic valve stenosis. *Nat Commun.* 2018;9:988.
153. Guauque-Olarte S, Messika-Zeitoun D, Droit A, Lamontagne M, Tremblay-Marchand J, Lavoie-Charland E, Gaudreault N, Arsenault BJ, Dubé MP, Tardif JC, Body SC, Seidman JG, Boileau C, Mathieu P, Pibarot, Bossé Y. Calcium signaling pathway genes RUNX2 and CACNA1C are associated with calcific aortic valve disease. *Circ Cardiovasc Genet.* 2015;8:812–22.
154. Ottervanger JP, Thomas K, Sie TH, Haalebos MMP, Zijlstra F. Prevalence of coronary atherosclerosis in patients with aortic valve replacement. *Neth Heart J.* 2002;10:176–80.

Chapter 5

Calcifying Extracellular Vesicles: Biology, Characterization, and Mineral Formation



Hooi Hooi Ng, Jessica E. Molina, and Joshua D. Hutcheson

Extracellular Vesicles in Physiological and Pathological Calcification

Extracellular vesicles (EVs) are membrane-enclosed vesicles secreted from cells that contain cellular-derived content such as lipids, proteins, and cytokines [1]. EVs have received increased attention for their role as vehicles for intracellular communication as they have the ability to transfer content via membrane fusion to target cells, thereby modulating various physiological and pathological processes in both the target and parental cells. EVs incorporate into target cells through endocytosis, pinocytosis, or phagocytosis [2]. Mammalian cells release a broad range of EVs with diverse features. In the cardiovascular system, EVs have a myriad of physiological roles, including regulation of inflammation and coagulation, as well as activation of endothelial cells and platelets [3–5]. These EV-mediated processes are induced by stimulating the target cell surface receptors through bioactive ligands and proteins. The transfer of content to target cells is tightly regulated by the lipid composition in the EV membrane, and reports suggest that the phospholipid phosphatidylserine plays a major role to facilitate the membrane fusion process [6].

In physiological calcification, EVs known as matrix vesicles are enriched in membrane proteins that regulate extracellular matrix mineralization (see Chaps. 16 and 17 for thorough discussions on bone mineralization). Some of the membrane

H. H. Ng
Biomedical Engineering and Human & Molecular Genetics,
Florida International University, Miami, FL, USA

J. E. Molina
Biomedical Engineering, Florida International University, Miami, FL, USA

J. D. Hutcheson (✉)
Department of Biomedical Engineering, Florida International University, Miami, FL, USA
e-mail: jhutches@fiu.edu

proteins involved in these processes include the calcium-dependent phospholipid-binding annexin protein (annexins I, II, V and VI), as well as enzymes such as tissue non-specific alkaline phosphatase (TNAP) and ectonucleotide pyrophosphatase/phosphodiesterase-1 (ENPP1). These proteins and enzymes are essential to maintain the balance of pyrophosphate and inorganic phosphate for the formation of hydroxyapatite crystals and remodeling of the extracellular matrix [7]. The mineralization process is initiated by inhibition of pyrophosphate generated through the cleavage of nucleotide triphosphates by ENPP1 [8]. Inorganic phosphates that are derived from TNAP-mediated hydrolysis of pyrophosphate are loaded into EVs via transmembrane phosphate transporter proteins and react with calcium ions immobilized on the EV phospholipid bilayer. We have recently shown *in silico* that negatively charged phosphatidylserine is important in immobilizing positively charged calcium ions [9]. Phosphatidylserine-rich membrane of the EVs coupled with annexin proteins sequesters calcium and phosphate, driving the nucleation of immature minerals [10]. The phosphatidylserine-calcium-phosphate complex functions as an intravesicular niche to form mature apatite. As mineral matures and becomes increasingly crystalline, it can rupture the EV membrane and fuse with the underlying cartilaginous matrix [11], which leads to early mineralization events that are required for bone development and regeneration.

Calcifying EVs are reported to have a diameter in the range of 100–300 nm. In models of medial calcification, calcifying EVs released from vascular smooth muscle cells cultured in media with elevated calcium and phosphate have an average diameter of ~140 nm [12, 13]. Conversely, vascular smooth muscle cells cultured in a pro-calcific media that may recapitulate inflammation-driven intimal calcification (with β -glycerophosphate and L-ascorbic acid) release EVs that appear larger in size with a diameter of >150 nm. Minerals formed during early bone mineralization have similar chemical properties to the minerals deposited during pathological calcification, especially those found in medial and intimal layers of the coronary arteries [14]. This observation suggests that EVs released during pathological calcification may be underpinned by similar mechanisms that control bone mineralization. However, the cellular derivation of calcifying EVs in cardiovascular tissues appears different than those described in bone. One of the mechanisms by which calcifying EVs are formed intracellularly involves the protein sortilin [15]. Sortilin is elevated in calcifying arteries of both the human and murine atheroma and plays a vital role in mineral formation *in vitro*. The presence of serum sortilin in circulation also predicts the presence and abundance of abdominal aortic calcification [16]. In accordance with the risk prediction power of cardiovascular calcification (Chap. 23), the level of serum sortilin also predicts the rate of event-free mortality in 8-year follow-up studies.

Sortilin directly modulates calcification potential by regulating the intracellular trafficking of TNAP into the EVs, which serves to hydrolyze calcification inhibitors (e.g., pyrophosphate) into free phosphate for mineralization. Once released into the extracellular space, these TNAP-positive EVs begin the process of depositing



Fig. 5.1 Microcalcification formation within vulnerable fibrous caps of atherosclerotic plaques occurs in four stages. First, calcifying EVs accumulate in collagen-poor regions. Second, the EVs aggregate to form a larger structure. Third, the EVs merge as mineralization begins. Fourth, the mature mineral grows from this nucleation niche. (Figure adapted from Ref. [17])

mineral in the vascular wall. We have previously reported that the formation of microcalcification in human smooth muscle cells and a murine model of vascular calcification occurs in four stages (Fig. 5.1) [17]. First, microcalcification is initiated when calcifying EVs accumulate within collagen-poor regions of an atherosclerotic plaque. Second, interactions between these calcifying EVs lead to the formation of aggregates. Third, the nucleation of calcium phosphate within EVs leads to fusion of the EV membranes, forming microcalcifications. Finally, the microcalcification grows through interactions with additional EVs. When formed within a collagen-poor fibrous cap of an atherosclerotic plaque, these microcalcifications contribute to stress accumulation and the detrimental effects of plaque rupture. Indeed, clinical data and *in silico* studies suggest that plaque stability can be determined by calcification size and morphology of the fibrous cap collagen content in atherosclerosis [18]. Based on these studies, we can better understand how calcifying EVs are initiated and formed during calcification and the implications on cardiovascular morbidity. Future studies are needed to target these processes in order to intervene at an early stage of mineral formation and potentially prevent or reverse microcalcification.

It is clear that EVs are emerging as key players in the development of calcification. It is, however, worth noting that EVs are highly complex and heterogeneous in nature and may exert opposite functional effects in the vasculature. For example, endothelium-derived vesicles show both beneficial and harmful effects through reducing neointima formation [19] and inducing endothelial dysfunction [20], respectively. Therefore, additional efforts should be put in place to standardize the methodologies used to characterize the multifaceted aspect of EVs, so that data generated from these studies can be more comparable. We and others have comprehensively reviewed the roles of EVs in cardiovascular calcification [21–25] and will summarize a few key mediators that are commonly involved in the pathogenesis of vascular calcification in the following section.

Extracellular Vesicles in Vascular Calcification

It is well-established that vascular smooth muscle cell proliferation plays a vital role in the development of the atherosclerotic plaque [26]. More recently, vascular smooth muscle cell-derived EVs have been described as important mediators in vascular calcification in late stages of atherogenesis [17, 27]. Proteomic analysis reveals that intracellular contents of EVs released by vascular cells [28] show similar protein composition to those derived from chondrocytes and osteoblasts [29, 30]. Specifically, EVs derived from these cell types have comparable calcium binding proteins, surface receptors, cytoskeletal proteins, and extracellular matrix components. One of the calcium-dependent enzymes that cross-links with an extracellular matrix protein, transglutaminase 2 (TGM2), was found to be upregulated in EVs derived from the aorta of a rat model of medial calcification [31]. On the other hand, osteoprotegerin (OPG), a crucial regulator of bone homeostasis, was found in EVs derived from vascular smooth muscle cells, which also contained the calcium-binding protein annexin A6 [32]. In this study, Schoppet et al. reported that OPG has anti-calcification effects at physiological concentrations to inhibit the EV-driven mineral nucleation and accumulation of hydroxyapatite on the vascular wall. The initiation and rate of mineralization likely depend on the balance of factors within EVs that promote and inhibit mineral formation.

Pathological changes in calcium homeostasis trigger significant alterations in EV composition, including the formation of nucleating phosphatidylserine-annexin A6 and calcium-phosphate complexes, as well as a deficit in matrix gla protein, which would otherwise inhibit calcification [12, 28]. TNAP is one of the key enzymes that is involved in the pathogenesis of vascular calcification [15, 33]. However, the role of TNAP in vascular smooth muscle cells-derived EVs under pro-calcific conditions is controversial, as some studies reported increased in TNAP activity [34, 35], whereas others reported no changes in TNAP activity after short-term treatment [28]. These contradictory data suggest that the components within pro-calcific media used and duration of experiments may be a crucial point to consider when comparing EVs released under different calcifying conditions. Indeed, studies that reported increased TNAP activity used the combination of β -glycerophosphate and L-ascorbic acid to induce osteogenic differentiation, whereas studies that reported a reduction in TNAP used a high calcium-phosphate media. A recent study that tested the calcification potential of valve interstitial cells (VICs) under different calcifying conditions yielded similar results to that of the smooth muscle cells [36]. Goto et al. reported increased in TNAP activity in VICs cultured in media containing β -glycerophosphate and L-ascorbic acid, an effect that was also passage-dependent. TNAP-dependent calcification was not observed in these primary VICs cultured in high-phosphate media, and these observations are consistent with previous studies in vascular cells. In short, vascular smooth muscle cell- or VIC-derived EVs play a major role in pathological calcification when the balance between pro-calcific activators and anti-calcific regulators is lost. In addition to the role of vascular smooth muscle cells and VICs, macrophages may serve as an important contributor to EVs

that nucleate mineral. Particularly in the context of atherosclerosis, EVs are localized to areas of mineral deposition, and this process is highly driven by inflammatory cells and potentiates rupture of vulnerable plaques [37]. Macrophage-derived EVs also play an important role in promoting microcalcification [38]. New et al. found that the calcium-binding proteins S100A9 and annexin A5 are upregulated in calcifying macrophage-derived EVs, and these proteins interact with each other to form a S100A9-annexin A5-phosphatidylserine complex, which serves as a nucleation site for hydroxyapatite. The exact changes that lead to EV-mediated phenomena may depend on the extracellular cues that initiate calcification and the particular cell phenotypes that respond to these cues.

Methods to Analyze Extracellular Vesicle Properties

Recent interest in EV research has led to the advent of various characterization methods to identify EVs released from cells under physiological and pathological conditions. Despite the advances in methodologies to characterize EVs, uncertainty remains in regard to the most appropriate methods of data collection and interpretation due to the small size and complex nature of EVs. In this chapter, we will review the strengths and weaknesses associated with each of the commonly used methodological approaches for the identification of calcifying EVs. In particular, we detail the different methods used for structural analysis of EVs, which can be used in conjunction with conventional physical characterization methods. These fundamental analyses are important in the classification of EVs into subgroups, which can lead to further characterization using techniques such as mass spectroscopy. Through extensive characterization and understanding of the biological functions of these calcifying EVs, potential therapeutic strategies will soon become available by targeting the probable source of mineral formation.

Physical Analysis of Extracellular Vesicles

General Characterization of Extracellular Vesicles

Electromagnetic radiation and its interaction with biological constructs have proven to be an essential tool in research used to study molecular properties of macromolecular structures. Both absorption and scattering by characteristic determinants in molecules result in changes in the energy level or frequency of light. Specifically, analysis of scattered light through subsequent light polarization, angular allocation, and intensity can be used to identify physical properties of matter [39]. Light scattering techniques can be used to study particles in either dynamic or static states. Studying particles in their dynamic state, through a technique known as dynamic light scattering (DLS), offers a sensitive technique for particle detection. Particles in

a solution constantly move due to a random walk motion that becomes apparent at small length scales and through subsequent interaction with neighboring solvent particles. The random walk phenomenon, known as Brownian motion, is related to particle size. Time-dependent measurements in the intensity of scattered light from the particles can determine their hydrodynamic radius based upon Brownian motion relationships [40]. In DLS measurements, incident light exposure on a particular sample leads to light scattering from all particles within the sample. The summation of scattered light gathered from each particle is recorded as a net intensity value. As the particles move, this net intensity fluctuates at a rate dependent on the particle size [40]. Larger particles diffuse at a slower rate, resulting in less fluctuation in net intensity. An autocorrelation function, measuring net intensity at different time intervals, is then used to determine the translational diffusion coefficient (D) for the particles in solution. This diffusion coefficient is incorporated into the Stokes-Einstein relationship (Eq. 5.1) to determine the average hydrodynamic radius (R_h) of the particles within the solution, when both the viscosity (η) and absolute temperature (T) of the solution are known [40].

$$D = \frac{kT}{6\pi\eta R_h} \quad (5.1)$$

DLS also allows for determination of particle zeta potential, an indication of surface charge. A voltage applied across a sample will result in particle movement. Negatively and positively charged particles move with faster velocities toward positive and negative electrodes, respectively, with the velocity proportional to the magnitude of the particle charge. The particle velocity measured by changes in the DLS frequency can be used to calculate the electrophoretic mobility of the particle, which is then applied to Henry's equation for zeta potential measurements [41]. This size characterization technique has been used to study both time- and temperature-dependent calcification through the precipitation of primary calciprotein particles (CPPs) to an insoluble, crystalline structure [42, 43]. These studies looked at fetuin-A as a natural inhibitor of calcification and evaluated the endogenous capacity of the protein to limit the progression of calcification. While one group was working to create a more accessible light scattering technique for clinical use, both groups show similar results in their analysis of these CPPs. In relation to both intensity of the subsequent light and measured hydrodynamic radius of particles, a clear distinction was made as the CPPs transitioned from their soluble and smaller state to an insoluble precipitate structure [42, 43].

While DLS measurements provide an efficient and rapid means of analyzing average properties of monodisperse nanoparticles, it is limited in characterization of heterogeneous particles, such as EVs released by cells. DLS sensitivity can only distinguish particles that differ in size by a factor of 3, restricting its utility in differentiating different populations of EVs that have similar size characteristics [44]. Measuring the intensity of scattered light from all the particles within the solution can lead to bias measurements for large particles whose fluctuations in intensity are much lower than smaller particles. Moreover, the use of the Stokes-Einstein

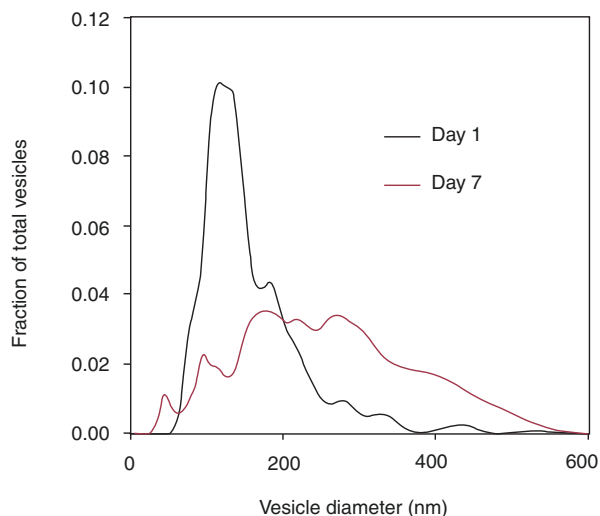
relationship to determine the hydrodynamic radius of particles within a sample assumes these particles are of a spherical shape [45].

In short, DLS measurements serve as a general data collection tool that provides average properties of EVs suspended in a media but cannot yield an accurate quantitative measure of EV heterogeneity within a sample. Nonetheless, DLS can be used as a preliminary tool to validate the presence and general characteristics of EVs.

Particle-by-Particle Analysis of Extracellular Vesicles

Nanoparticle tracking analysis (NTA) uses similar methodologies as DLS measurements to determine hydrodynamic size of particles based on Brownian motion [44]. NTA is preferred over DLS measurements, due to the fact that it is capable of distinguishing the hydrodynamic size properties of each particle in a solution by calculating the mean squared displacement of light scattered from individual particles, rather than average intensity fluctuations analyzed by DLS in a frame-by-frame analysis [44]. This technique not only allows for the determination of individual particle characteristics but also provides visualization of these particles in the solution. Since the volume of the imaging window is known, the number of particles visualized at any given time also provides a measure of EV concentration within a sample. In addition to providing concentration data, NTA has other obvious advantages over DLS measurements, with the most important being the removal of bias and increased sensitivity for polydisperse samples [44, 46]. NTA has been used to characterize calcifying EVs released from vascular smooth muscle cells cultured in pro-calcific media to evaluate the relationship between EV aggregation and mineral growth [12, 15, 17, 35, 38] (Fig. 5.2). This is particularly important, as information on aggregation of EVs will determine their fusion mineralization capacity of either forming microcalcification or macrocalcification.

Fig. 5.2 Nanoparticle tracking analyses show increase in diameter as EVs merge to build mineral over the course of 7 days in vitro. (Figure adapted from Ref. [17])



It is, however, worth noting that the accuracy of NTA in particle measurement remains challenging because of the nature of the technique by which particle displacement is calculated. Once a particle diffuses from the field of view, it can no longer be analyzed [46], and relatively low abundance EV populations may not be counted at a significantly high numbers to allow statistically meaningful analyses of properties. This may be a particular problem for analysis of calcifying EV samples, which may represent a small portion of the total EV population in a sample that consists of exosomes, microvesicles, and microparticles.

Flow cytometry (FCM) techniques have recently been developed for EV analyses, and several studies have shown the potential of this technique in analyzing different EV populations [47, 48]. Conventionally, FCM is used to quantitatively assess cells based on their chemical and physical properties [49], and this technique has recently taken its turn into the growing field of EV research. The use of FCM for EV analysis is feasible, as the necessary machinery is already utilized in most laboratories for cell sorting. However, this technique is limited by its sensitivity to collect scattered light from smaller particles, as the setup is only able to reach 200 nm in size [50]. Researchers have worked to normalize FCM measurements for EV detection through a high-sensitive approach which increased concentration detection as well as the detection limit [51], but is it enough for such a novel field of research knowing that EV size can reach a lower limit of around 30 nm? An alternative look at FCM moved from the use of light scattering to properties determined by fluorescence. This enhanced technology which was successfully used by Brussaard et al. in the detection of different viruses offered up to a 50x increase in concentration of detected EVs than conventional methods dependent solely on light scattering [52, 53].

More recently, tunable resistive pulse sensing (TRPS) emerged as a powerful technique to provide particle-by-particle characterization of size and charge properties. It uses the Coulter principle to provide a highly sensitive system for quantitative particle-by-particle characterization (Fig. 5.3). The Coulter principle, originally developed to determine size and concentration of cells in hematological analyses, measures the impedance of nonconductive particles as they disrupt an electric current within a conductive medium. TRPS incorporates a two-compartment setup,

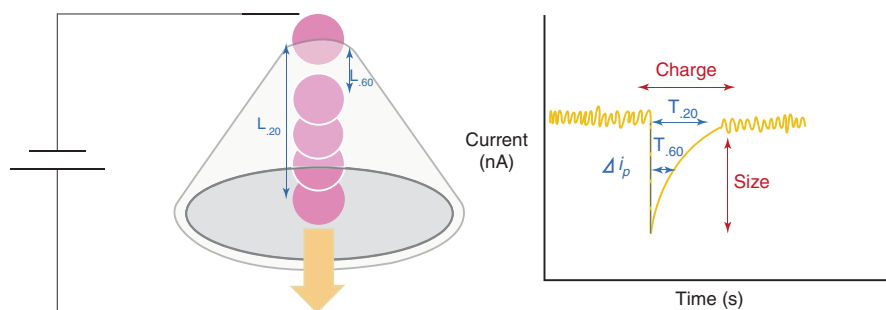


Fig. 5.3 Schematic diagram showing the tunable resistive pulse sensing (TRPS) technology that utilizes the Coulter principle to measure EV size and charge properties

divided by a nano-sized pore with electrodes on either side. A voltage is applied to the system with electrolyte solution in each compartment to induce a current through the pore. Particles diluted within electrolyte solution are placed in the upper fluid well compartment. Both applied pressure and electrophoretic mobility result in particle translocation through the pore, increasing the resistivity of the pore to current flow [54]. The current disruption is proportional to the size and charge properties of each particle.

Three different aspects of particle measurements using TRPS can be modified throughout sample reading to ensure maximum sensitivity and accuracy in particle detection. (i) Increasing the voltage applied to the system will increase the current, allowing higher resistivity for particles of smaller sizes. (ii) Increasing the pressure within the system will accelerate particle flow, allowing more accurate measurement of particles from a larger sample pool. (iii) Applying stretch to the nanopore can adapt the measurement to different particle sizes and help prevent blockages. Duration of the current disruption serves as an indicator of charge for each particle. Absolute calculation of zeta potential is also possible from the particle transit time using the Smoluchowski approximation (Eq. 2) [54, 55]. Particle translocation through the nanopore depends on electrophoretic mobility and convective mobility due to pressure applied to the system. The relative contribution of electrophoretic and convective mobility can be measured using calibration particles of a known size and charge prior to sample velocity measurements at a constant voltage (V) and pressure (P), providing the constant values, v_{xCal}^V and v_{xCal}^P . Determination of calibration particle translocation time can be compared to those time-dependent measurements obtained from the sample at different points within the pore. This will provide a particle's respective velocity relative to its intrinsic and pressure-driven movement. The summation of these velocity values ($v_{xSample}^i$) is averaged respective to each particle at that point. The zeta potential of both the calibration particles (ξ_{netCal}) and of the pore itself (ξ_m) are known constants and are taken into account during this approximation, as well.

$$\xi_{sample}^i = \frac{\sum_x (v_{xSample}^i - v_{xCal}^P P) / (v_{xCal}^V V)}{\sum_x} \xi_{netCal} + \xi_m$$

The limitations of TRPS include the short lifespan of the nanopore and difficulties related to choosing the correct nanopore for heterogeneous biological samples. Nanopore sizing is a critical determinant of the range of EVs that can be measured. Therefore, heterogeneous EV samples must be separated by size (e.g., through size chromatography column-based approaches) and measured using size-appropriate nanopores. Biological samples are also prone to aggregation, which can lead to blockage of the nanopore, preventing proper particle-by-particle analysis. The inclusion of nonionic detergents in the electrolyte solution may help prevent aggregation of particles in biological samples.

Adaptation of TRPS methods in newer resistive pulse sensing (RPS) technologies has increased sensitivity in particle analysis. A recently developed RPS

technology uses a multifunctional nanopipette that simultaneously measures changes in ionic current and potential through the similar translocation mechanism unique to TRPS analysis but utilizes a nanopipette system that may enhance controllability and reduce blockages [56].

In short, TRPS offers the most accurate quantification of small EVs based upon the Coulter principle, but the technique remains technically challenging and laborious compared to NTA. As TRPS and related techniques continue to develop, physical properties such as size, charge, and concentration of EVs may provide new information on characteristics of EVs released under various conditions (healthy vs diseased). This may contribute to therapeutic advances that can target these EVs to treat vascular calcification.

Structural Analysis of Extracellular Vesicles

The analyses discussed in the previous section have begun to elucidate size and charge characteristics of EVs, but they do not provide direct visualization of EV structure. The smallest EVs are around 30 nm in diameter, smaller than the resolution limits of a standard light microscope. The limitations in light microscopy lie in the consolidation of diffracted light from smaller particles that have a higher index of refraction at the visible light range, resulting in a blurred image [57]. The discovery that moving matter acts similarly to light, a phenomenon described as the wave-particle duality, led to the development of microscopy techniques using electron emission [58]. Due to electron mass being considerably larger than that of a photon, the corresponding wavelength is much lower (based on the matter-wave equation), resulting in lower level diffraction of smaller-sized samples, easy consolidation of light, and resolution below 0.05 nm. All electron microscopy techniques allow for the structural determination of EVs, but methods differ in both sample preparation and output image. Deciding which technique is best for EV analysis is dependent on the purpose of study [59].

Transmission electron microscopy (TEM) analyzes electrons that were able to pass through a specimen. Sample preparation for TEM involves fixation and dehydration of EVs, thus losing their natural conformation. After dehydration, the samples are sectioned into nanometer-sized films and placed on a carbon-coated grid for imaging, which provides the structural analysis of the EVs. TEM offers a higher-resolution image by capturing not only transmitted electrons for structural determination but also those scattered, thus increasing the contrast of the output image. On the other hand, scanning electron microscopy (SEM) offers topographic image of EVs by collecting electrons scattered from the surface. We have previously visualized calcifying EVs released from smooth muscle cells cultured under pro-calcific conditions that mimic those observed in calcified human plaques (Fig. 5.4) [17]. SEM, though similar in sample preparation with fixation and dehydration, does not necessitate the sectioning required for TEM. One limitation of SEM is the production of false ring-like images that can interfere with accurate structural and

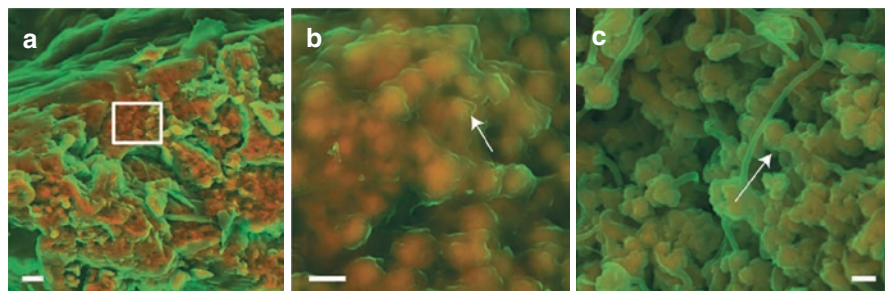


Fig. 5.4 Aggregation of EV and calcification within a calcified human carotid artery plaque. (a) Density-dependent color SEM shows calcifying EVs composing mineral (dense, orange features) in human atheroma. Bar = 2 μm . (b) Magnified image of a large calcification within human atheroma (a, white rectangle). Bar = 500 nm. (c) Calcifying EVs seeded into a three-dimensional collagen hydrogel recapitulate these structures. Bar = 500 nm. White arrows depict dense, orange features of calcium phosphate-rich calcifying EVs. (Figure adapted from Ref. [17])

concentration analyses. Both TEM and SEM require dehydration and fixation of EVs prior to analysis, which can deform the EVs and hinder final size verification. These limitations, while apparent, are known sources of error that should be accounted for during data analysis.

Cryo-electron microscopy (cryo-EM) provides a more realistic imaging technique for EVs, by utilizing a different fixation method that avoids dehydration and preserves the natural structure [60]. Through the cryo-immobilization technique, water is cooled to a glass-like state with liquid ethane, allowing for particles to remain hydrated [59]. TEM and cryo-TEM are often coupled with immunogold labeling, allowing for further quantification to identify specific surface proteins, verifying the presence of a particular subgroup of EVs [61]. In the context of vascular calcification, calcifying EVs that mediate mineralization contain TNAP, which can be targeted and labeled using this technique to confirm their presence [27].

Atomic force microscopy (AFM) is another common technique used to gain topographic information on EVs. While SEM and TEM techniques involve the direct interaction of an electron beam with the sample, AFM uses laser light to study the deflection of a cantilever coupled with a sharp tip interacting along the surface of particles [62]. Additionally, stiffness of the particles can be obtained through AFM measurements. As the cantilever moves closer to the surface of the particles, molecular forces (e.g., Van der Waals forces) increase the strength of the interaction between the EV surface and the tip. The displacement curve obtained during retraction of the cantilever can be used to determine the stiffness of the particle [63]. Rastering the cantilever across the EV surface results in a high-resolution 3D image, as well as the radius determination [62]. Sample preparation for AFM is straightforward and only involves immobilization of the sample along a mica surface [62, 64]. Though this can disrupt the natural state of the EV, embedding molecules that interact with EV surface proteins can mitigate deformation and allow for accurate size determination [62]. Moreover, similar to immunogold labeling for TEM, the mica

surface for AFM can be modified to include antibodies from which EVs can specifically bind. This enhances quantification of differential subgroups of EVs within a sample defined by unique surface proteins [62].

In short, these techniques provide a means for EV structural analyses. As discussed previously, during NTA and DLS analyses, EVs are assumed to be spherical. While less high-throughput, the methods discussed here do not require a priori assumptions about EV shape, and additional structural analyses using these microscopy techniques can help validate assumptions made in the indirect measurements of EV properties.

Biomolecular Analysis of Extracellular Vesicles

The ultimate goal of EV research is usually to determine biomolecular function. Beyond characterizing EV size and structure, methods are needed to analyze EV content. Of particular interest for calcifying EVs is the analysis of proteins and lipid moieties involved in mineralization. Insight into the molecular drivers of mineralization may ultimately lead to the discovery of relevant therapeutic targets.

Mass spectroscopy (MS) is one of the most common screening techniques used to identify the mass-to-charge ratio of ions within a sample, and the use of this technique, specifically high-throughput MS, has been used in protein analysis of EVs [65]. The use of MS in clinical settings has evolved greatly from drug testing, to newborn screening, to identification of blood-borne infections, to most recently providing a real-time look at cancerous tissue during surgery [66]. This screening technique can essentially be used to determine the presence of EVs and the specific lipidomic or proteomic profiles of these EVs, which will provide important clues on their biological functions. For example, MS is used as an unbiased tool to identify proteins that are enriched in calcifying EVs using common gene ontology database [35]. Functional annotation of these specific proteins can be applied to further classify these EVs into subgroups and identify their distinct roles in vascular calcification. Additionally, MS also allows for the determination of cellular derivation and mechanisms of calcifying EV formation from the vascular smooth muscle cells [13, 15]. Data obtained from mass spectroscopy can also be used as biomarkers in the future based on the specific subgroups of lipid or protein that are misregulated under pro-calcific conditions.

An increasing body of evidence from metabolomics analyses suggests that lipids play an important role in directing the physiological and pathophysiological functions of EVs. EVs derived from various sources are enriched in sphingomyelin, cholesterol, phosphatidylserine, and glycosphingolipids [67]. Analysis of these lipid species will help us to characterize the specific lipid composition in the EV bilayer and contribute significantly to our knowledge about the distinct lipid profiles that are essential in maintaining the structural and physical constituents of EVs released under pro-calcific conditions. In brief, EV lysis and lipid extraction methods are typically carried out in a single step through liquid-liquid phase extraction.

Analysis of the lipid species is achieved with lysis and extraction using a 4:1 tetrahydrofuran/water phase, followed by the separation of phospholipids and glyco-phospholipids by diethyl ether and water partitioning [68]. Additionally, EV lipids may be extracted by the Bligh and Dyer liquid-liquid phase extraction method, whereby most lipid species are dissolved in the organic layer of a chloroform/methanol/water (1:1:1 by volume) solution [69]. Lipid species from the organic phase are then separated and analyzed by gas chromatography (GC)-MS, liquid chromatography (LC)-MS, or direct infusion electrospray ionization into a high-resolution mass spectrometer. Due to the complexity and heterogeneity of EVs, accurate mass measurement is often ambiguous for the identification of specific lipid or metabolite species. To overcome the issue, additional analysis from MS experiments is often supplemented by obtaining the elution time (compared to known standards), fragmentation (tandem MS), ion mobility measurements, and relative isotope intensities [70, 71]. Analyses of these distinct lipid compositions present in the EVs will inform us about the stability of these vesicles in various extracellular environments. This may contribute to our knowledge about the specific lipids that confer the stability of EVs in vascular calcification, which is important for future clinical applications that involve liposomal drug delivery method. To ensure sufficient information is gathered regarding a particular subgroup of EVs, robust analyses of the particles such as quantification methods, biodistribution, circulating levels, and their pharmacokinetics must first be established.

In addition to lipid [72] and protein analysis, mass spectroscopy has the ability to identify possible genomic profile [73] of the EVs as well, which is typically determined by next-generation sequencing. Collectively, mass spectroscopy represents a powerful and reliable tool for biomolecular analysis of EVs, which would help to advance the field by identifying specific properties of calcifying EVs that participate in mineralization.

Analysis of Extracellular Vesicle Mineralization

Chapter 11 provides a thorough discussion on methods to visualize and analyze mineral properties. In this section, we briefly discuss methods to analyze and quantify EV-mediated mineralization. The properties discussed in the previous sections (size, charge, and biomolecular content) provide insight into the properties of EVs that may be important in directing calcification. However, analyses of these properties do not directly assess the mineralization potential of EVs. Assays for mineralization in cell cultures and tissue sections are well established and involve the utilization of colorimetric or fluorescent dyes that bind calcium or phosphate. Traditionally, alizarin red S staining of calcium and von Kossa staining of phosphate provide visualization of calcified regions in cultures and tissues and allow for quantification through light absorbance measurements of extracted dye. A method utilizing the color change that occurs when o-cresolphthalein complex 1 reacts with free calcium has also been used to quantify calcium extracted from mineralized tissue

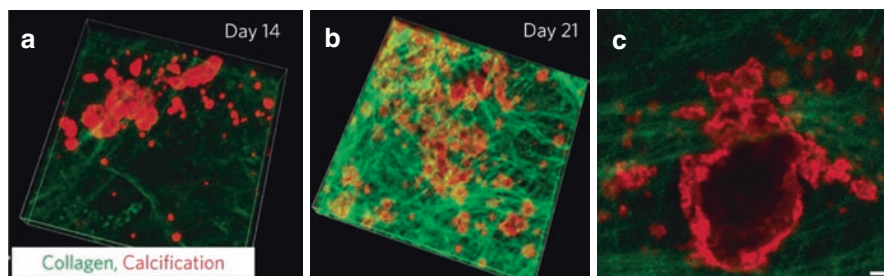


Fig. 5.5 Imaging of a near-infrared fluorescent calcium mineral probe (red fluorescence) shows increased mineralization from (a) day 14 to (b) day 21 in smooth muscle cells cultured in pro-calcific media. (c) High-resolution images show calcifications forming within a collagen (green fluorescence) network. Bar = 1 μm . (Figure adapted from Ref. [17])

and cultures using hydrochloric acid [17, 34, 38]. More recently, the development of fluorescent probes specific to calcium phosphate-based minerals has yielded higher-resolution, and more sensitive, assessment of mineral abundance and morphology (Fig. 5.5) [17, 35]. Longitudinal injection of fluorescent probes into mouse models has also provided a means to track changes in both bone and cardiovascular mineral formation over time [17, 74, 75]. Adaptation of these established assays to measure mineralization directly from EVs, however, is often not straightforward due to EVs' small size.

Similar to difficulties in measurement of the physical and biomolecular properties of EVs, limited starting material and small size present complications when trying to measure mineralization directly from EVs. Initial studies into EV mineralization relied solely on static characterization of associations between mineral and EVs within calcified tissues using electron microscopy (as discussed in section “[Structural Analysis of Extracellular Vesicles](#)”). Early seminal studies in the dynamic mechanisms of EV calcification used EVs isolated from mineralized tissue by protease digestion of the extracellular matrix [76, 77]. Nascent mineral scatters light at 340 nm. By suspending isolated EVs in a high calcium-phosphate solution and monitoring absorbance at 340 nm over time, the relative mineralization potential of EVs can be measured. EV samples with higher potential exhibit an increase in absorbance at 340 nm at earlier time points compared to those with lower mineralization potential. Similar studies have used fluorescent mineral dyes [35] or the colorimetric o-cresolphthalein complex 1 method [38] to measure mineral formation in suspended EVs, which allow for a lower amount of starting material and measurement of EV mineral from cell culture samples. These methods, however, are not conducive to visualize EV-directed mineralization.

Interactions with collagen fibers dictate mineral patterning by EVs in both physiological bone mineralization and pathological vascular calcification. Studies by Chen et al. used the known associations between calcifying EVs and collagen to measure EV-mediated mineral formation on collagen-coated coverslips using the o-cresolphthalein complex 1 method [34]. Building upon these studies, we seeded EVs from human coronary artery smooth muscle cells cultured in pro-calcific media

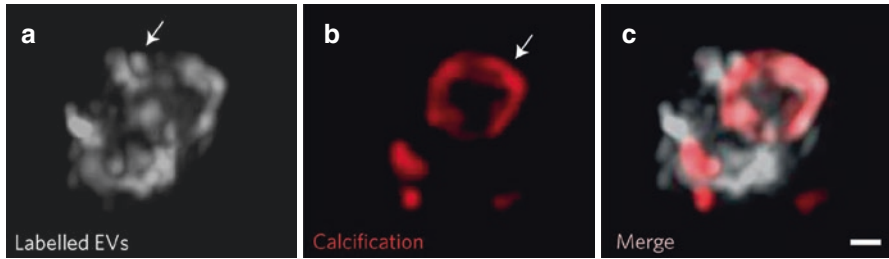


Fig. 5.6 (a) Structured illumination super-resolution microscopy shows fluorescently labeled EVs aggregating to build a (b, c) microcalcification. Bar = 500 nm. Arrows depict the near-infrared labeled EVs. (Figure adapted from Ref. [17])

on three-dimensional collagen hydrogels to visualize and quantify mineralization potential [17]. The mineral formed within the hydrogels recapitulates aspects of mineral observed in calcified atheroma, and fluorescent labeling of the EVs with CellTracker™ dyes enabled super-resolution optical imaging of calcifications formed from the merger of individual EVs (Fig. 5.6). The collagen fibers trap and dictate EV associations, serving as a scaffold for mineral morphology. The size and shape of microcalcifications within atherosclerotic plaques determine the accumulation of local stresses that can destabilize the plaque [18]. Subsequent plaque rupture results in artery occlusion and tissue infarction. Therefore, quantification of mineral formation and associated morphologies can provide insight into the pathological consequences of EV-mediated calcification and therapeutic strategies to reduce cardiovascular morbidity.

Future Perspectives

EVs are vectors that have important roles in the biological system which could modify the pathophysiological mechanisms during the progression of vascular calcification, by releasing either good or harmful mediators. The characterization of EVs released into cell culture media serves as an invaluable step to study the biological functions of these vesicles under pro-calcific conditions in a controlled environment and reproducible manner. This fundamental knowledge gained from in vitro study will provide us with meaningful information on the cellular activation of these EVs during disease progression and could be used as diagnostic or prognostic biomarkers in the future. In this chapter, we have outlined several common analyses used to characterize EVs. It is, however, worth mentioning that there remains the need to overcome some of the common technical challenges to quantify EVs. While extensive efforts have been made to accurately measure both the EV concentration and protein content [78], there is still an unmet need to standardize the EV isolation procedures across laboratories. Hence, a strong research effort is necessary to establish procedures for EV isolation in order to compare the downstream

analyses of different EV subgroups. This is especially important for allowing comparison of biological data to define EV dosage for clinical trial purposes. A combination of physical and biomolecular analysis of EVs may represent a major breakthrough in the field to define the concentration, size, and charge of EVs, as well as the protein and/or lipid content in these vesicles under pro-calcific conditions. This would give us valuable information on the dosage to use for clinical applications by titrating the concentration of EVs relative to the protein ratio. As outlined above, the opportunity to employ highly sensitive and accurate methodologies to characterize EVs continues to emerge in the field, and this will certainly help with advancement in the understanding of EV biology. Of note, a better understanding of EV biology together with standardized methods for EV isolation and quantification, functional characterization, as well as establishing potency assays will immensely enhance the future promise for EV-based diagnostic and therapeutic applications for the treatment of vascular calcification.

At present, the limitations of using EV-based diagnostics or therapeutics as a tool for clinical purposes include its applicability *in vivo*, particularly in the area of calcification. Despite the enormous promise of EVs as therapeutic vectors that can be delivered to different targeted locations within the body system, it requires laborious engineering expertise to optimize the interaction of these EVs with target cells [79]. Moreover, a majority of the current knowledge is derived from studies done *in vitro*, or with supraphysiological concentrations of EVs that are irrelevant to clinical scenarios observed in patients with vascular calcification. Hence, with the hope to better understand the roles of EVs *in vivo*, new methods are needed to delineate the mechanisms by which EVs are released temporally and spatially within the vascular wall, as well as from circulating cells. Furthermore, as detailed in section “[Biomolecular Analysis of Extracellular Vesicles](#)”, proteomic and lipidomic mapping using matrix-assisted laser desorption/ionization (MALDI) approaches in intact tissue may provide vital information on biomolecular changes in EVs during the progression of calcification. In summary, various methods to assess the characteristics of EVs released in vascular calcification represent a potential path toward future therapeutic avenues that reduce cardiovascular morbidity and mortality.

References

1. Colombo M, Raposo G, Thery C. Biogenesis, secretion, and intercellular interactions of exosomes and other extracellular vesicles. *Annu Rev Cell Dev Biol.* 2014;30:255–89.
2. Mulcahy LA, Pink RC, Carter DR. Routes and mechanisms of extracellular vesicle uptake. *Journal Extracell Vesicles.* 2014;3:24641.
3. Brill A, Dashevsky O, Rivo J, Gozal Y, Varon D. Platelet-derived microparticles induce angiogenesis and stimulate post-ischemic revascularization. *Cardiovasc Res.* 2005;67(1):30–8.
4. Jansen F, Yang X, Franklin BS, Hoelscher M, Schmitz T, Bedorf J, et al. High glucose condition increases NADPH oxidase activity in endothelial microparticles that promote vascular inflammation. *Cardiovasc Res.* 2013;98(1):94–106.

5. Owens AP 3rd, Mackman N. Microparticles in hemostasis and thrombosis. *Circ Res.* 2011;108(10):1284–97.
6. Chernomordik L, Kozlov MM, Zimmerberg J. Lipids in biological membrane fusion. *J Membr Biol.* 1995;146(1):1–14.
7. Anderson HC. Molecular biology of matrix vesicles. *Clin Orthop Relat Res.* 1995;314:266–80.
8. Huang MS, Sage AP, Lu J, Demer LL, Tintut Y. Phosphate and pyrophosphate mediate PKA-induced vascular cell calcification. *Biochem Biophys Res Commun.* 2008;374(3):553–8.
9. Pokhrel R, Gerstman BS, Hutcheson JD, Chapagain PP. In silico investigations of calcium phosphate mineralization in extracellular vesicles. *J Phys Chem B.* 2018;122(14):3782–9.
10. Wuthier RE, Wu LN, Sauer GR, Genge BR, Yoshimori T, Ishikawa Y. Mechanism of matrix vesicle calcification: characterization of ion channels and the nucleational core of growth plate vesicles. *Bone Miner.* 1992;17(2):290–5.
11. Skrtic D, Eanes ED. Membrane-mediated precipitation of calcium phosphate in model liposomes with matrix vesicle-like lipid composition. *Bone Miner.* 1992;16(2):109–19.
12. Kapustin AN, Chatrou ML, Drozdov I, Zheng Y, Davidson SM, Soong D, et al. Vascular smooth muscle cell calcification is mediated by regulated exosome secretion. *Circ Res.* 2015;116(8):1312–23.
13. Kapustin AN, Schoppet M, Schurgers LJ, Reynolds JL, McNair R, Heiss A, et al. Prothrombin loading of vascular smooth muscle cell-derived exosomes regulates coagulation and calcification. *Arterioscler Thromb Vasc Biol.* 2017;37(3):e22–32.
14. New SE, Aikawa E. Role of extracellular vesicles in de novo mineralization: an additional novel mechanism of cardiovascular calcification. *Arterioscler Thromb Vasc Biol.* 2013;33(8):1753–8.
15. Goetsch C, Hutcheson JD, Aikawa M, Iwata H, Pham T, Nykjaer A, et al. Sortilin mediates vascular calcification via its recruitment into extracellular vesicles. *J Clin Invest.* 2016;126(4):1323–36.
16. Goetsch C, Iwata H, Hutcheson JD, O'Donnell CJ, Chapurlat R, Cook NR, et al. Serum Sortilin associates with aortic calcification and cardiovascular risk in men. *Arterioscler Thromb Vasc Biol.* 2017;37(5):1005–11.
17. Hutcheson JD, Goetsch C, Bertazzo S, Maldonado N, Ruiz JL, Goh W, et al. Genesis and growth of extracellular-vesicle-derived microcalcification in atherosclerotic plaques. *Nat Mater.* 2016;15(3):335–43.
18. Kelly-Arnold A, Maldonado N, Laudier D, Aikawa E, Cardoso L, Weinbaum S. Revised microcalcification hypothesis for fibrous cap rupture in human coronary arteries. *Proc Natl Acad Sci U S A.* 2013;110(26):10741–6.
19. Jansen F, Stumpf T, Proebsting S, Franklin BS, Wenzel D, Pfeifer P, et al. Intercellular transfer of miR-126-3p by endothelial microparticles reduces vascular smooth muscle cell proliferation and limits neointima formation by inhibiting LRP6. *J Mol Cell Cardiol.* 2017;104:43–52.
20. Brodsky SV, Zhang F, Nasjletti A, Goligorsky MS. Endothelium-derived microparticles impair endothelial function in vitro. *Am J Physiol Heart Circ Physiol.* 2004;286(5):H1910–5.
21. Yang W, Zou B, Hou Y, Yan W, Chen T, Qu S. Extracellular vesicles in vascular calcification. *Clin Chim Acta.* 2019;499:118–22.
22. Bakhshian Nik A, Hutcheson JD, Aikawa E. Extracellular vesicles as mediators of cardiovascular calcification. *Front Cardiovasc Med.* 2017;4:78.
23. Blaser MC, Aikawa E. Roles and regulation of extracellular vesicles in cardiovascular mineral metabolism. *Front Cardiovasc Med.* 2018;5:187.
24. Zhang C, Zhang K, Huang F, Feng W, Chen J, Zhang H, et al. Exosomes, the message transporters in vascular calcification. *J Cell Mol Med.* 2018;22(9):4024–33.
25. Liberman M, Marti LC. Vascular calcification regulation by exosomes in the vascular wall. *Adv Exp Med Biol.* 2017;998:151–60.
26. Libby P, Ridker PM, Hansson GK. Inflammation in atherosclerosis: from pathophysiology to practice. *J Am Coll Cardiol.* 2009;54(23):2129–38.

27. Krohn JB, Hutcheson JD, Martinez-Martinez E, Aikawa E. Extracellular vesicles in cardiovascular calcification: expanding current paradigms. *J Physiol*. 2016;594(11):2895–903.
28. Kapustin AN, Davies JD, Reynolds JL, McNair R, Jones GT, Sidibe A, et al. Calcium regulates key components of vascular smooth muscle cell-derived matrix vesicles to enhance mineralization. *Circ Res*. 2011;109(1):e1–12.
29. Balcerzak M, Malinowska A, Thouverey C, Sekrecka A, Dadlez M, Buchet R, et al. Proteome analysis of matrix vesicles isolated from femurs of chicken embryo. *Proteomics*. 2008;8(1):192–205.
30. Xiao Z, Camalier CE, Nagashima K, Chan KC, Lucas DA, de la Cruz MJ, et al. Analysis of the extracellular matrix vesicle proteome in mineralizing osteoblasts. *J Cell Physiol*. 2007;210(2):325–35.
31. Chen NX, O'Neill K, Chen X, Kiattisunthorn K, Gattone VH, Moe SM. Transglutaminase 2 accelerates vascular calcification in chronic kidney disease. *Am J Nephrol*. 2013;37(3):191–8.
32. Schoppet M, Kavurma MM, Hofbauer LC, Shanahan CM. Crystallizing nanoparticles derived from vascular smooth muscle cells contain the calcification inhibitor osteoprotegerin. *Biochem Biophys Res Commun*. 2011;407(1):103–7.
33. Hutcheson JD, Blaser MC, Aikawa E. Giving calcification its due: recognition of a diverse disease: a first attempt to standardize the field. *Circ Res*. 2017;120(2):270–3.
34. Chen NX, O'Neill KD, Chen X, Moe SM. Annexin-mediated matrix vesicle calcification in vascular smooth muscle cells. *J Bone Miner Res*. 2008;23(11):1798–805.
35. Hutcheson JD, Goettsch C, Pham T, Iwashita M, Aikawa M, Singh SA, et al. Enrichment of calcifying extracellular vesicles using density-based ultracentrifugation protocol. *J Extracell Vesicles*. 2014;3:25129.
36. Goto S, Rogers MA, Blaser MC, Higashi H, Lee LH, Schlotter F, et al. Standardization of human calcific aortic valve disease in vitro modeling reveals passage-dependent calcification. *Front Cardiovasc Med*. 2019;6:49.
37. Hutcheson JD, Maldonado N, Aikawa E. Small entities with large impact: microcalcifications and atherosclerotic plaque vulnerability. *Curr Opin Lipidol*. 2014;25(5):327–32.
38. New SE, Goettsch C, Aikawa M, Marchini JF, Shibasaki M, Yabusaki K, et al. Macrophage-derived matrix vesicles: an alternative novel mechanism for microcalcification in atherosclerotic plaques. *Circ Res*. 2013;113(1):72–7.
39. Berne BJ, Pecora R. *Dynamic light scattering: with applications to chemistry, biology, and physics*. Mineola, New York: Dover Publications; 2000.
40. Hassan PA, Rana S, Verma G. Making sense of Brownian motion: colloid characterization by dynamic light scattering. *Langmuir*. 2015;31(1):3–12.
41. Bhattacharjee S. DLS and zeta potential – what they are and what they are not? *J Control Release*. 2016;235:337–51.
42. Pasch A, Farese S, Gräber S, Wald J, Richtering W, Floege J, et al. Nanoparticle-based test measures overall propensity for calcification in serum. *J Am Soc Nephrol*. 2012;23(10):1744–52.
43. Heiss A, Duchesne A, Denecke B, Grötzinger J, Yamamoto K, Renné T, et al. Structural basis of calcification inhibition by α 2-HS glycoprotein/Fetuin-A. *J Biol Chem*. 2003;278(15):13333–41.
44. Filipe V, Hawe A, Jiskoot W. Critical evaluation of Nanoparticle Tracking Analysis (NTA) by NanoSight for the measurement of nanoparticles and protein aggregates. *Pharm Res*. 2010;27(5):796–810.
45. Svedberg T, Rinde H. The determination of the distribution of size of particles in disperse systems I. *J Am Chem Soc*. 1923;45(4):943–54.
46. Malloy A, Carr B. Nanoparticle tracking analysis – the Halo™ System. *Particle & Particle Systems Characterization*. 2006;23(2):197–204.
47. de Rond L, Libregts S, Rikkert LG, Hau CM, van der Pol E, Nieuwland R, et al. Refractive index to evaluate staining specificity of extracellular vesicles by flow cytometry. *J Extracell Vesicles*. 2019;8(1):1643671.

48. Shen W, Guo K, Adkins GB, Jiang Q, Liu Y, Sedano S, et al. A single Extracellular Vesicle (EV) flow cytometry approach to reveal EV heterogeneity. *Angew Chem Int Ed Engl.* 2018;57(48):15675–80.
49. Shapiro HM. *Practical flow cytometry.* Hoboken, New Jersey: Wiley; 2005.
50. Chandler W, Yeung W, Tait J. A new microparticle size calibration standard for use in measuring smaller microparticles using a new flow cytometer. *J Thromb Haemost.* 2011;9(6):1216–24.
51. Robert S, Lacroix R, Poncelet P, Harhouri K, Bouriche T, Judicone C, et al. High-sensitivity flow cytometry provides access to standardized measurement of small-size microparticles—brief report. *Arteriosclerosis, Thrombosis, and Vascular Biology.* 2012;32(4):1054–8.
52. Brussaard CPD, Marie D, Bratbak G. Flow cytometric detection of viruses. *J Virol Methods.* 2000;85(1–2):175–82.
53. Arraud N, Gounou C, Linares R, Brisson AR. A simple flow cytometry method improves the detection of phosphatidylserine-exposing extracellular vesicles. *J Thromb Haemost.* 2015;13(2):237–47.
54. Blundell ELCJ, Vogel R, Platt M. Particle-by-particle charge analysis of DNA-modified nanoparticles using tunable resistive pulse sensing. *Langmuir.* 2016;32(4):1082–90.
55. Vogel R, Pal AK, Jambhrunkar S, Patel P, Thakur SS, Reátegui E, et al. High-resolution single particle zeta potential characterisation of biological nanoparticles using tunable resistive pulse sensing. *Sci Rep.* 2017;7:17479.
56. Panday N, Qian G, Wang X, Chang S, Pandey P, He J. Simultaneous ionic current and potential detection of nanoparticles by a multifunctional nanopipette. *ACS Nano.* 2016;10(12):11237–48.
57. Shaked NT, Zalevsky Z, Satterwhite LL. *Biomedical optical phase microscopy and nanoscopy.* Oxford, UK: Elsevier Science; 2012.
58. Goodhew PJ, Humphreys J. *Electron microscopy and analysis.* Boca Raton, Florida: CRC Press; 2000.
59. Chuo ST-Y, Chien JC-Y, Lai CP-K. Imaging extracellular vesicles: current and emerging methods. *J Biomed Sci.* 2018;25:91.
60. Choi H, Mun JY. Structural analysis of exosomes using different types of electron microscopy. *Appl Microscopy.* 2017;47(3):171–5.
61. Cizmar P, Yuana Y. *Detection and characterization of extracellular vesicles by transmission and cryo-transmission electron microscopy, Extracellular vesicles.* New York, NY: Springer; 2017. p. 221–32.
62. Szatanek R, Baj-Krzyworzeka M, Zimoch J, Lekka M, Siedlar M, Baran J. The methods of choice for Extracellular Vesicles (EVs) characterization. *Int J Mol Sci.* 2017;18(6):1153.
63. Sokolov I, Dokukin ME, Guz NV. Method for quantitative measurements of the elastic modulus of biological cells in AFM indentation experiments. *Methods.* 2013;60(2):202–13.
64. Binnig G, Quate CF, Gerber C. Atomic force microscope. *Phys Rev Lett.* 1986;56(9):930–3.
65. Choi D-S, Kim D-K, Kim Y-K, Gho YS. Proteomics of extracellular vesicles: exosomes and ectosomes. *Mass Spectrom Rev.* 2015;34(4):474–90.
66. Jannetto PJ, Fitzgerald RL. Effective use of mass spectrometry in the clinical laboratory. *Clin Chem.* 2016;62(1):92–8.
67. Record M, Carayon K, Poirot M, Silvente-Poirot S. Exosomes as new vesicular lipid transporters involved in cell-cell communication and various pathophysiologicals. *Biochim Biophys Acta.* 2014;1841(1):108–20.
68. Del Boccio P, Raimondo F, Pieragostino D, Morosi L, Cozzi G, Sacchetta P, et al. A hyphenated microLC-Q-TOF-MS platform for exosomal lipidomics investigations: application to RCC urinary exosomes. *Electrophoresis.* 2012;33(4):689–96.
69. Bligh EG, Dyer WJ. A rapid method of total lipid extraction and purification. *Can J Biochem Physiol.* 1959;37(8):911–7.
70. Kliman M, May JC, McLean JA. Lipid analysis and lipidomics by structurally selective ion mobility-mass spectrometry. *Biochim Biophys Acta.* 2011;1811(11):935–45.

71. Ecker J, Scherer M, Schmitz G, Liebisch G. A rapid GC-MS method for quantification of positional and geometric isomers of fatty acid methyl esters. *J Chromatogr B Analyt Technol Biomed Life Sci.* 2012;897:98–104.
72. Hu T, Zhang JL. Mass-spectrometry-based lipidomics. *J Sep Sci.* 2018;41(1):351–72.
73. Gupta N, Benhamida J, Bhargava V, Goodman D, Kain E, Kerman I, et al. Comparative proteogenomics: combining mass spectrometry and comparative genomics to analyze multiple genomes. *Genome Res.* 2008;18(7):1133–42.
74. Aikawa E, Aikawa M, Libby P, Figueiredo JL, Rusanescu G, Iwamoto Y, et al. Arterial and aortic valve calcification abolished by elastolytic cathepsin S deficiency in chronic renal disease. *Circulation.* 2009;119(13):1785–94.
75. Aikawa E, Nahrendorf M, Figueiredo JL, Swirski FK, Shtatland T, Kohler RH, et al. Osteogenesis associates with inflammation in early-stage atherosclerosis evaluated by molecular imaging in vivo. *Circulation.* 2007;116(24):2841–50.
76. Genge BR, Wu LN, Wuthier RE. Kinetic analysis of mineral formation during in vitro modeling of matrix vesicle mineralization: effect of annexin A5, phosphatidylserine, and type II collagen. *Anal Biochem.* 2007;367(2):159–66.
77. Genge BR, Wu LN, Wuthier RE. In vitro modeling of matrix vesicle nucleation: synergistic stimulation of mineral formation by annexin A5 and phosphatidylserine. *J Biol Chem.* 2007;282(36):26035–45.
78. Webber J, Clayton A. How pure are your vesicles? *J Extracell Vesicles.* 2013;2:19861.
79. Vader P, Mol EA, Pasterkamp G, Schiffelers RM. Extracellular vesicles for drug delivery. *Adv Drug Deliv Rev.* 2016;106(Pt A):148–56.

Chapter 6

Role of Biomechanical Stress and Mechanosensitive miRNAs in Calcific Aortic Valve Disease



Nicolas Villa-Roel, Kitae Ryu, and Hanjoong Jo

Abbreviations

ALP	Alkaline phosphatase
AV	Aortic valve
BAV	Bicuspid aortic valve
CAVD	Calcific aortic valve disease
D-Flow	Disturbed flow
ECM	Extracellular matrix
GPCR	G protein-coupled receptor
miRNA	microRNA
S-Flow	Stable flow
TAV	Tricuspid aortic valve
VEC	Valvular endothelial cell
VIC	Valvular interstitial cell

N. Villa-Roel · K. Ryu
Wallace H. Coulter Department of Biomedical Engineering,
Georgia Institute of Technology and Emory University, Atlanta, GA, USA
e-mail: nvr@gatech.edu; kitae.ryu@emory.edu

H. Jo (✉)
Wallace H. Coulter Department of Biomedical Engineering,
Georgia Institute of Technology and Emory University, Atlanta, GA, USA
Division of Cardiology, Department of Medicine, Emory University, Atlanta, GA, USA
e-mail: hjo@emory.edu

Introduction

Calcific aortic valve disease (CAVD) is a leading underlying cause of mortality among the aging population and represents a growing burden in developed countries [1]. Although it was originally thought to be a degenerative disease, aortic valve (AV) calcification is now known to be an active process predominantly led by endothelial dysfunction and osteogenic differentiation of valvular interstitial cells (VICs), leading to additional cardiovascular events [2].

CAVD is estimated to occur in 25–30% of adults aged 65 or older and is associated with a 50% increased risk of myocardial infarction [3–6]. CAVD ranges from thickening and hardening of the AV leaflets (sclerosis) to narrowing of the AV area due to impaired motion of calcified leaflets (stenosis) [2]. The only currently accepted therapeutic option for CAVD is valve replacement [7, 8]. This is in large part due to the lack of sufficient mechanistic insights into CAVD. Recent studies by numerous investigators have been addressing this critical gap. Here, we will review the role of biomechanical forces on AV biology and pathophysiology with specific focus on mechanosensitive microRNAs (miRNAs) and their therapeutic potentials.

Development of CAVD begins with subclinical inflammation in the AV endothelium, followed by thickening due to cellular infiltration and extracellular matrix (ECM) remodeling, exacerbated by cytokines released by various AV cells including valvular endothelial cells (VECs), VICs, and immune cells [4, 9–12]. These cytokines are hypothesized to also promote osteogenic differentiation of VICs, which is characterized by an upregulation of bone-related transcription factors, intermediates, and proteins, such as alkaline phosphatase (ALP), bone morphogenic proteins, osteocalcin, osteopontin, and RUNX2 [13–15].

It is important to note that calcification occurs preferentially on one side of the AV, namely, the fibrosa side. This layer of the AV faces the aorta and is exposed to complex and highly variable hemodynamic conditions [16]. Additionally, regions of the AV that experience relatively elevated axial stretch, such as near the aortic root, are more susceptible to calcification [17]. In this chapter we discuss the role of these biomechanical forces with a focus on mechanosensitive miRNAs and their target genes, which may be used as novel therapeutic approaches for treating and preventing CAVD.

Aortic Valve Structure and Biomechanical Forces

The AV regulates blood flow from the left ventricle to the aorta, supplying the systemic vasculature with oxygenated blood [2]. During systole, the AV is open, allowing blood to flow out of the contracted left ventricle at a peak velocity of approximately 1 m/s in physiological conditions [18]. In mild stenotic conditions, this peak velocity can increase to nearly 3 m/s, and, in severe stenosis, it can surpass 4 m/s. During diastole, the ventricle relaxes, and the AV closes due to the difference

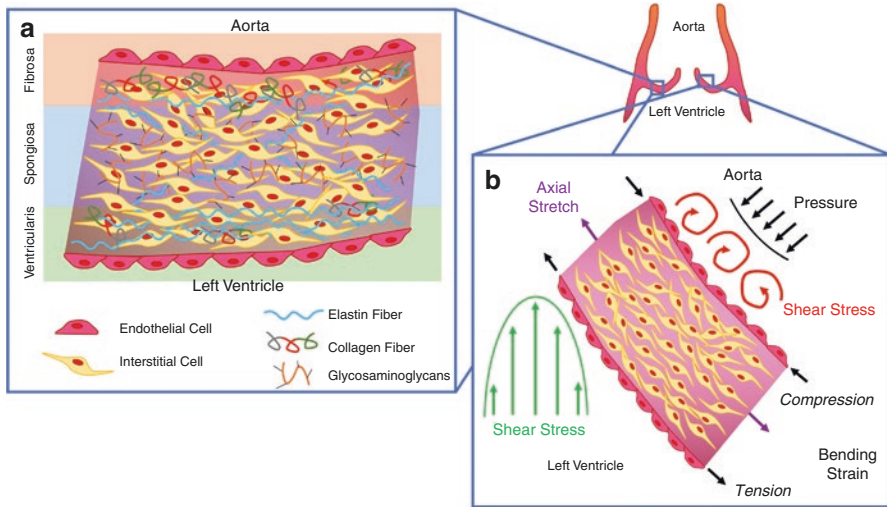


Fig. 6.1 Structure and biomechanical forces in the aortic valve. (a) The fibrosa side, which faces the aorta, is composed of valve endothelial cells (VECs) and valve interstitial cells (VICs). Its extracellular matrix (ECM) is composed primarily of collagen fibers with some sparse elastin fibers. The spongiosa contains most of the VICs as well as glycosaminoglycans and some elastin fibers. The ventricularis side, which faces the left ventricle, is mostly composed of elastin fibers and contains some VICs as well as VECs. (b) During systole, the aortic valve (AV) experiences bending strain: the ventricularis is stretched, whereas the fibrosa is compressed. Blood flow across the ventricularis during ejection applies pulsatile, unidirectional shear stress on the VECs. During diastole, pressure is applied on the AV as it relaxes. Axial stretch prevents regurgitation by creating a tight seal in the radial and circumferential directions. The fibrosa experiences complex, time-varying, non-stable flow conditions, resulting in low, oscillatory shear stress.

in pressures between the ventricle and the aorta. In physiological conditions, the transvalvular pressure ranges from 80 to 120 mmHg; however, in pathological conditions, it can reach up to 180 mmHg [19], leading to further AV dysfunction.

The AV leaflets, each less than 1 mm in thickness, are composed of three separate, complex layers, the fibrosa, spongiosa, and ventricularis (Fig. 6.1a). These layers dictate the mechanical function of the tissue and control its behavior:

1. *Fibrosa*: This layer faces the aorta and is comprised of a VEC monolayer, directly in contact with blood, and VICs below impregnated within ECM. This layer is mostly composed of type I and type III collagen aligned in a circumferential manner and a small amount of elastin fibers [20]. This composition allows the AV to withstand high mechanical loads.
2. *Spongiosa*: This layer is located in the middle of the AV leaflet. It contains most of the VICs and is comprised predominantly of glycosaminoglycans and proteoglycans [21]. Its main extracellular component, however, is hyaluronan, which can hold large amounts of water and serve as a shock absorber throughout the cardiac cycle [22].

3. *Ventricularis*: This layer faces the left ventricle and is comprised of VECs and VICs [5]. Its ECM contains some collagen, but its composition is mostly elastin fibers aligned radially [21, 23]. This composition allows the ventricularis to withstand compression during systole and ensure the AV opens and closes consistently [22].

The ever-present movement of the AV creates a dynamic mechanical environment whose understanding is critical for studying the pathobiological processes that regulate CAVD. The main forces exerted on the AV during the cardiac cycle are pressure, bending strain, axial stretch, and shear stress (Fig. 6.1b).

1. *Pressure*: During diastole, the ventricular pressure drops, whereas the aortic pressure remains stable, closing the AV. In physiological conditions, the transvalvular pressure (difference between diastolic aortic and ventricular pressures) ranges from 80 to 120 mmHg [24]. In hypertensive patients, this pressure can exceed 180 mmHg [19]. The SMART study found a correlation between systolic blood pressure and cardiovascular calcification [25], suggesting a potential link between blood pressure and associated biomechanical forces on AV pathobiology. Other studies have also found links between increased systemic pressure and CAVD [26–29]; however, its effects on the underlying molecular mechanisms of the disease remain unclear.
2. *Bending strain*: During systole, the concave fibrosa layer compresses, while the convex ventricularis layer extends under tension [30]. It is hypothesized that increased bending strain can induce more rapid and extensive calcification [31]. This was observed in patients with bicuspid aortic valves (BAV). Several groups have found that the BAVs experience higher bending strains and patients can develop symptomatic CAVD nearly 20 years prior to tricuspid aortic valve (TAV) patients [32–36]. BAV is the most common congenital heart defect, with a prevalence of around 2%. The altered biomechanical conditions associated with BAV are considered as an important cause of the accelerated and aggressive disease phenotype and have been used as an important CAVD model system to understand its mechanisms [37].
3. *Axial stretch*: A crucial step during the cardiac cycle is having the AV leaflets create a tight seal during diastole to prevent blood from regurgitating back into the left ventricle [30]. Axial stretch occurs in two directions: circumferential and radial. In humans, the AV leaflets deform more in the circumferential direction than the radial direction [38]. The region of maximum tension is located where the leaflet attaches to the aortic root (hinge region), which is also the region that tends to calcify first in CAVD [17]. A vicious cycle is generated when increased axial stretch leads to AV dysfunction, exacerbating the levels of stretch of the AV.
4. *Shear stress*: This force is exerted on the AV by blood flow parallel to the endothelial surface. The fibrosa experiences complex, time-varying, non-stable flow conditions (d-flow) including oscillatory shear stress, while the ventricularis is exposed to a pulsatile but relatively stable flow (s-flow) conditions including unidirectional shear stress [16, 39]. These different shear profiles correlate with the preferential calcification pattern of the fibrosa [40–42]. Interestingly, in the AV, the non-coronary cusp (lacking a coronary ostium) experiences lower magnitude

shear stress than the left and right coronary cusps and usually calcifies first [39]. Additional studies have also found that BAVs experience lower shear stress and more d-flow than TAVs, further implicating the role of shear stress in CAVD [43].

Mechanosensing in the Aortic Valve

Cells in the AV, such as VECs and VICs, sense various biomechanical forces through a variety of molecules and subcellular structures known as mechanosensors [44]. Most knowledge on mechanosensory mechanisms has been gained by studying vascular ECs. These include cell surface proteins (ion channels PIEZO1 and PIEZO2, glycocalyx, G protein-coupled receptors, G proteins, Notch1, and protein kinase receptors T kinase receptor and ST kinase receptor), subcellular structures (primary cilia and caveolae), cell-cell junction (PECAM-1, VE-cadherin, VEGFR2 mechanosensory complex), integrins, and intracellular actin cytoskeleton [45] (Fig. 6.2). Although these endothelial mechanosensors may serve similar functions in VECs

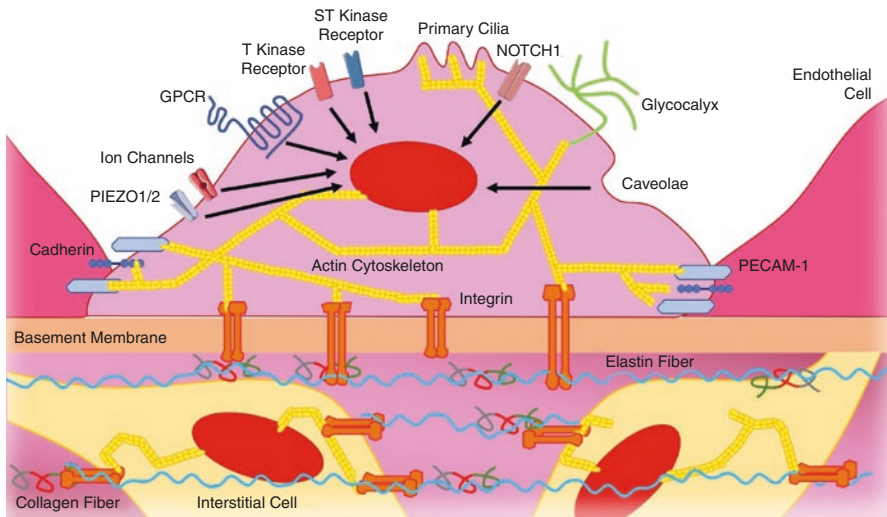


Fig. 6.2 Mechanosensors in the aortic valve. Integrins bind to the actin cytoskeleton and to extracellular matrix to sense the mechanical environment surrounding the cell and transmit the information to the cellular interior. G protein-coupled receptors bind to extracellular ligands and activate downstream signaling (black arrows). The glycocalyx is a glycoprotein network that traps ions and molecules in the blood, allowing interactions with cellular membrane channels and receptors. PECAM-1 forms a mechanosensory complex with VE-cadherin and VEGF receptor II at the cell junctions, where biomechanical forces are recognized and transmitted to the cellular interior. Primary cilia and caveolae are subcellular structures that have been identified as mechanosensors in the vascular endothelium. Their function as mechanosensors in the aortic valve (AV) has not been determined. Surface proteins, such as PIEZO1/2, NOTCH1, T kinase receptor, and ST kinase receptor, have also been identified as mechanosensors in vascular endothelial cells; however, their function in the AV is not fully understood

and VICs, they remain to be validated. Here, we highlight a few of the major mechanosensors in the endothelium.

Integrins are transmembrane adhesion receptors that have traditionally been found to bind ligands at the cell surface, within the ECM, and in the cytoplasm [46]. Integrins transduce signals from the outer environment to the cellular interior. Integrins have also been recognized as sensors of the mechanical environment that surrounds the cell, resulting in intracellular signal transduction pathway changes [47]. Furthermore, integrins receive intracellular signals that can regulate their ligand-binding affinity, enabling a tunable communication between the cell membrane and the rest of the cell [48]. Overall, integrins play a key role in cell adhesion, migration, proliferation, and cell survival, dictated by cues from the extracellular environment along with intracellular signaling.

Transmission of signals by integrins is dependent on their binding to the cytoskeleton [49]. Integrins co-localize with other cytoskeletal proteins near the cell surface, forming complexes known as focal adhesions [50, 51]. These complexes act as mediators between mechanical transduction among the integrins, external stimuli, and the cell [52]. Focal adhesions have the capability of sensing forces such as shear stress and tension [53–55]. Focal adhesions are also responsible for signaling changes in the cellular phenotype in response to mechanical and other cues. These can include signals for cell remodeling, proliferation, apoptosis, migration, and angiogenesis [56–59].

G protein-coupled receptors (GPCR) also bind to extracellular ligands to activate downstream signaling via G protein-activated signal transduction pathways [60]. GPCR are sensitive to changes in flow across the endothelium [61]. Although their role in AV biology is not clear, GPCR have been shown to become activated under certain mechanical stimuli, and their function has been well documented in the context of other diseases [62, 63].

ECs express proteoglycans and glycoproteins conjugated with long carbohydrate chains called glycosaminoglycans, on their cell surface [64, 65]. This glycoprotein network, called the glycocalyx, provides a physical barrier between the cells and the blood, where ions and other molecules found in the blood are trapped, allowing interactions between them and membrane channels and receptors [66, 67]. It has been shown that, under d-flow, the glycocalyx changes shape and its function is impaired [68, 69]. In the AV, the glycocalyx has been found to bind low-density lipoprotein and immunoglobulins more tightly in animals fed a high-cholesterol diet, particularly in the fibrosa [70, 71]. Higher affinity for these molecules can lead to increased infiltration and lesion formation, providing a link between mechanosensors and AV regions susceptible to calcification [69].

PECAM-1 has been extensively characterized as a mechanosensor located in vascular endothelial junctions [72, 73]. PECAM-1 forms a mechanosensory complex along with VE-cadherin and VEGF receptor II (VEGFR2) in the endothelial cell junction, where it recognizes shear stress and stretch and transmits the signal to intracellular biochemical responses such as intracellular calcium influx [74–76]. The mechanosensory response from this PECAM-1/VE-cadherin/VEGFR2

complex leads to activation of various signaling pathways, including PI3K, Akt, and eNOS [77–83]. Although it is known to play a role in adhesion and cell migration [84], its effect on AV biology and dysfunction has not been fully characterized.

In vascular ECs, primary cilia serve as mechanosensors [85]. These membrane-bound structures protrude into the vessel lumen and bend during blood flow, leading to calcium influx via mechanosensitive channels and intracellular signal transduction pathway [86–89]. Abnormal ciliary length has been associated with altered blood flow sensing [90]. Their function in the AV was reported in the context of AV development [91], but definitive evidence supporting their role as AV mechanosensors is lacking at present.

PIEZO1 is a mechanically activated ion channel, serving as a mechanosensor of shear stress in vascular ECs [92]. Activation of PIEZO1 has been linked to atherogenic processes such as inflammation, angiogenesis, vascular formation and remodeling, and ATP release leading to nitric oxide production and regulation of vascular tone [93–96]. In the AV, PIEZO1 regulates AV development and outflow tract formation [97, 98]; however, its role as a mechanosensor in the AV has not yet been elucidated.

miRNAs in the Aortic Valve

We recently reviewed the role of shear-sensitive genes and signaling pathways in flow-mediated AV biology and disease [99]; therefore, this chapter will focus on discussing the role of miRNAs.

The miRNAs are small (18–22), non-coding nucleotide sequences that bind to the 3' untranslated region of their target genes, leading to that gene's degradation or inhibition of translation [100]. The roles of protective and pathological miRNAs have been well documented in many cardiovascular diseases, including atherosclerosis, heart failure, diabetes, and hypertension [101–105].

To identify miRNAs involved in CAVD, human AV leaflets obtained from patients with various AV calcification and stenoses were compared to controls by using miRNA array studies. These studies revealed many miRNAs differentially expressed in calcified AVs compared to the non-diseased controls [106–110], the underlying mechanisms, and potential target genes of each miRNA in AV calcification [111–117]. Additional array studies identified miRNAs differentially expressed in BAV leaflets in comparison to the TAVs [118, 119].

Most of the miRNAs studied in the context of CAVD have been implicated in the regulation of osteogenic differentiation of VICs (Table 6.1 and Fig. 6.3). The majority of miRNAs that are differentially regulated in CAVD patients seem to be down-regulated and play anti-calcific roles; however, some miRNAs such as miR-29b, miR-34a, miR-92a, and miR-181b are increased in CAVD leaflets compared to controls and play pro-calcific roles. We will first discuss those miRNAs with undefined mechanosensitivity, followed by shear- and stretch-sensitive miRNAs.

miRNAs with Undefined Mechanosensitivity in the Aortic Valve

miR-29b is increased during osteoblast differentiation of human VICs [116], suggesting it as a pro-calcific miRNA. *miR-29b* modulates osteoblastic differentiation by downregulating *TGF-β3* and upregulating expression of *wnt*, *β-catenin*, *Runx2*, and *Smad3*. It is unknown at present if *miR-29b* is mechanosensitive.

miR-34a is a pro-calcific miRNA and is increased in CAVD leaflets and in VICs treated with osteogenic stimulus [117]. *miR-34a* directly targets *Notch1* and increases calcification signals by upregulating *Runx2*. While it was shown to be shear-sensitive in HUVECs [120], it remains to be validated if *miR-34a* is also shear-sensitive in AV ECs.

miR-92a is overexpressed in human calcified BAV leaflets compared to the TAV, suggesting its role as a potential biomarker of CAVD [118]. While *miR-92a* expression is well-known to be increased by d-flow conditions in vascular ECs, its flow-dependent expression in AV ECs and whether it induces pro-calcific responses in AV remain to be validated. In vascular ECs, *miR-92a* directly targets *KLF-2* and *KLF-4*, which are some of the most well-characterized mechanosensitive and anti-atherogenic genes [121–123].

miR-138 is decreased in calcified AVs and inhibits osteogenesis of VICs [124]. Expression of *miR-138* was reduced in leaflets from CAVD patients compared to

Table 6.1 miRNAs implicated in CAVD

Role	Mechano-sensitivity	miRNA	Validated targets	Cells/tissue	Function	Reference
Pro-calcific	Undefined	<i>miR-29b</i>	<i>TGF-β3</i>	Human VIC	Promotes calcification of VICs through activation of Wnt/β-catenin/Smad3	[116]
		<i>miR-34a</i>	<i>Notch1</i>	Human VIC human AV leaflets	Downregulation of <i>Notch1</i> and upregulation of <i>Runx2</i>	[117]
		<i>miR-92a</i>	<i>KLF-2</i> <i>KLF-4</i>	Human AV leaflets	Overexpressed in BAV compared to TAV	[118, 121–123]
Shear	Undefined	<i>miR-181b</i>	<i>TIMP3</i>	Human VEC porcine AV leaflets	Increases shear-sensitive MMP activity	[114]
		<i>miR-214</i>	<i>TGF-β1</i>	Human VEC porcine AV leaflets	Increased in d-flow compared to s-flow and in fibrosa of PAV. Decreases <i>TGF-β1</i> but may not affect calcification	[131]

Table 6.1 (continued)

Role	Mechano-sensitivity	miRNA	Validated targets	Cells/tissue	Function	Reference
Anti-calcific	Undefined	miR-138	FOXC1	Human VIC human AV leaflets	Decreased in calcified AVs. Inhibits calcification of VICs	[124]
		miR-204	Runx2	Human VIC human AV leaflets	Decreased in calcified AVs. Inhibits calcification of VICs	[125]
		miR-30b	Runx2 Smad1 Caspase-3	Human VIC	Inhibits ALP activity and calcification of VICs	[126]
		miR-449c-5p	Smad4	Human VIC human AV leaflets	Decreased in calcified AVs. Inhibits calcification of VICs	[115]
		miR-638	Sp7	Human VIC	Inhibits calcification of VICs	[127]
		miR-141	BMP-2	Human AV leaflets porcine VIC	Decreases expression in BAV compared to TAV. Inhibits calcification of VICs	[128]
		miR-195	Smad7 BMP-2 Runx2	Human VIC Human AV leaflets	Downregulated in BAV compared to TAV. Silencing increases VIC calcification	[129]
Shear		miR-486-5p	EfnA1Prnd	Human VEC porcine AV leaflets	Downregulated in d-flow compared to s-flow and in fibrosa of PAV Increases migration and reduces early apoptosis	[132]
		miR-483-3p	Ube2c Ash2L	Human VEC porcine AV leaflets	Downregulated in d-flow compared to s-flow and in fibrosa of PAV Upregulates pVHL, silencing the HIF1 α pathway	[133]
Stretch		miR-148-3p	IKBKKB	Human VIC	Decreases NF- κ B signaling and target gene expression	[112]
		miR-214	ATF4	Porcine AV leaflets	Protects against ATF4-mediated stretch-induced calcification	[135]

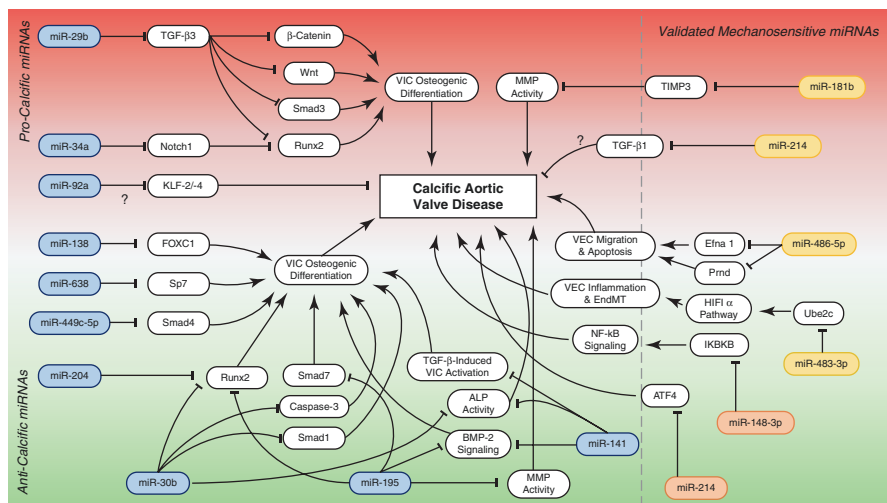


Fig. 6.3 miRNAs involved in CAVD. Various miRNA microarray studies have been conducted to identify miRNAs differentially expressed between calcified vs. non-calcified aortic valves (AVs), bicuspid vs. tricuspid AVs, fibrosa vs. ventricularis, and d-flow vs. s-flow. Although most identified miRNAs have undefined mechanosensitivity (blue), some have been validated as shear-sensitive (yellow) and stretch-sensitive (orange)

non-calcified AVs. Overexpression of miR-138 prevented osteogenic differentiation of VICs, while miR-138 inhibitor enhanced the osteogenic differentiation by targeting *FOXC1*.

miR-204 expression is downregulated in calcified human AVs and by BMP-2 treatment in VICs [125]. miR-204 inhibited osteoblastic differentiation of VICs by targeting *Runx2*.

miR-30b also regulates osteogenic differentiation of VICs [126]. Transfection of VICs with miR-30b reduced expression of *Runx2*, *Smad1*, and *Caspase-3* and inhibited ALP activity.

miR-449c-5p expression is reduced in CAVD leaflets compared with non-calcified AVs. miR-449c-5p targets *Smad4*, thereby preventing osteogenic differentiation of VICs [115].

miR-638 also plays a role in VIC osteogenic differentiation by directly targeting *Sp7* [127].

miR-141 regulates BMP-2-dependent AV calcification [128]. miR-141 expression was decreased in human BAV tissue compared to the TAV. Furthermore, in porcine VICs, overexpression of miR-141 attenuated TGF- β -induced activation, BMP-2 signaling, and ALP activity.

miR-195 is downregulated in BAV leaflets compared to the TAV and promotes AV calcification [129]. Treatment of VICs with miR-195 inhibitor (anti-miR-195) increased expression of *Smad7*, *BMP-2*, and *Runx2*, activity of MMP-2, and calcification. miR-195 was shown to directly target *Smad7*.

Shear-Dependent miRNAs in AV

Numerous miRNAs are regulated by shear stress in VECs in vitro and in vivo. We identified miRNAs that are regulated in a shear stress- and AV leaflet side-dependent manner (ventricularis vs. fibrosa side) using both human AV ECs and porcine AV (PAV) leaflets [130, 131].

To better understand shear-dependent and side-dependent miRNAs in human AVECs (HAVECs), we carried out miRNA microarrays using total RNA from human fibrosa-side ECs and ventricularis-side ECs exposed to d-flow or s-flow [130]. This study revealed that expression of 30 and 3 miRNAs is regulated in a shear- and side-dependent manner, respectively. Furthermore, studies using endothelial-enriched RNAs from healthy PAVs showed additional side-dependent miRNAs that are differentially expressed in the fibrosa and ventricularis sides [131]. Given the preferential development of AV calcification in the fibrosa side (exposed to pro-calcific biomechanical forces) compared to the ventricularis side (exposed to anti-calcific biomechanical forces), these side-dependent miRNAs may represent the effect of different mechanical force environments on miRNA expression patterns. This study identified 7 miRNAs (miR-100, miR-130a, miR-181a/b, miR-199a-3p, miR-199a-5p, and miR-214) significantly overexpressed in the fibrosa side compared to the ventricularis side. Some of these miRNAs were characterized for their roles in AV function.

miR-486-5p is one of the most shear-responsive miRNAs, and its expression is upregulated under s-flow in vitro and on the ventricularis of PAVs [132]. Overexpression of miR-486-5p in HAVECs was found to decrease expression of *Efnal* and *Prnd*, which are involved in cell migration and early apoptosis.

miR-181b is a pro-calcific miRNA that is upregulated in the fibrosa and in response to d-flow compared to s-flow [114]. We found that miR-181b directly targets tissue inhibitor of metalloproteinase-3 (TIMP3), which manages uncontrolled ECM degradation by inhibiting matrix metalloproteinases (MMPs). Silencing of miR-181b leads to decreased MMP activity in HAVECs.

miR-214 is overexpressed in the fibrosa of PAVs compared to the ventricularis and in response to d-flow compared to s-flow [131]. Expression of miR-214 under d-flow was attenuated using anti-miR-214. Silencing of miR-214 also resulted in increased TGF- β 1 protein expression; however, there was no effect on calcification.

miR-483-3p is a highly shear-sensitive miRNA expressed in HAVECs and inhibits AV calcification by regulating the hypoxia-inducible factor 1 α (HIF1 α) pathway [133]. miR-483-3p is upregulated in the ventricularis side compared to the fibrosa in PAV leaflets and in response to s-flow vs. d-flow in HAVECs. Overexpression of miR-483-3p in HAVECs leads to decreased inflammation and decreased endothelial-mesenchymal transition (EndMT). Mechanistically, miR-483-3p directly targets ubiquitin-conjugating enzyme 2c (Ube2c), which itself is upregulated in d-flow. UBE2C silences von Hippel-Lindau protein (pVHL), a known repressor of HIF1 α [134], and its downstream target genes. Furthermore, treatment of PAVs with

miR-483-3p mimic and HIF1 α inhibitor prevented calcification of PAV leaflets. Consistent with the *ex vivo* and *in vitro* results, immunohistochemical staining studies of human AV leaflets demonstrated that the fibrosa side overexpressed markers of calcification (Alizarin red and RUNX2), inflammation (VCAM1), EndMT (TWIST1), HIF1 α , and UBE2C compared to the ventricularis side, while pVHL expression was higher in the ventricularis side. These findings suggest a potential of miR-483-3p mimic and HIF1 α inhibitors as potential therapeutics for CAVD.

Stretch-Dependent miRNAs in AV

miR-148-3p expression is downregulated by stretching (14%) compared to a static condition in VICs [112] and may serve an anti-calcific function. The downregulation of miR-148-3p led to upregulation of *IKBKB*, NF- κ B signaling, and inflammatory responses in VICs compared to static conditions.

miR-214 is another stretch-dependent miRNA, decreasing by hyper-stretching (15%) relative to physiological stretch (10%) in PAV leaflets [135]. The study suggested that miR-214 may serve an anti-calcific role in the AV by directly targeting activating transcription factor 4 (ATF4), which is implicated in endoplasmic reticulum stress and linked to cardiovascular calcification.

Future Perspectives in Calcific Aortic Valve Disease Research and Treatment

Here, we summarized the AV structures, hemodynamics, and mechanosensors, as well as the recently discovered miRNAs that are implicated in CAVD pathophysiology. Our focus was on discussing the roles of these miRNAs in AV calcification and the roles of biomechanical forces on miRNA expression. Due to the predominant development of AV calcification in the fibrosa side (exposed to d-flow) and in the leaflet hinge regions (exposed to high stretch and strain), it is critical to define the molecular mechanisms such as the role of miRNAs by which these biomechanical forces regulate CAVD pathophysiology. Given the relative convenience and specificity of miRNA mimics (gain of function) and inhibitors such as anti-miRs and antagomiRs (loss of function) to manipulate their expression level and *in vivo* efficacies, targeting pro-calcific or anti-calcific miRNAs represents an exciting opportunity to develop novel therapeutics to prevent and reduce CAVD. Further, these miRNAs are easily detectable and quantified in blood samples, making them ideal as biomarkers to detect CAVD at an early stage. Despite these potential therapeutic candidates, there are several limitations to overcome. First, although numerous studies have emerged recently, there is still significant paucity in our molecular and cellular understanding of CAVD pathophysiology. Second, the role of mechanosensors and mechanotransduction pathways has been studied mostly in vascular ECs,

while this knowledge is relatively lacking in valvular cells. Therefore, the mechanobiological understanding of AV cells needs to be significantly expanded. Third, there continues to be a significant gap in understanding the role of numerous miRNAs in pathophysiological mechanisms of CAVD. While there are many miRNAs that have been better characterized in other cell types, tissues, and disease contexts, the role and mechanisms of each miRNA in AV cells are not necessarily the same and should be validated. Last, technical limitations in AV-targeted delivery of miRNA therapeutics, such as miRNA mimics, anti-miRs, or antagomiRs, should be addressed. Successful delivery of these miRNA therapeutics in an AV-limited manner would overcome concerns regarding their potential off-target effects in other tissues, improving their safety and efficacy as therapeutics.

In summary, the AV is a complex and dynamic structure which is subject to ever-present biomechanical forces. The field of AV mechanics and biomechanical stress-mediated signaling has advanced greatly over the past decade; however, there is still no viable therapeutic for CAVD aside from AV open heart surgery or transcatheter valve replacement. In the future, targeting the mechanosensitive factors, such as miRNAs, discussed here could provide better options for the management of CAVD.

Acknowledgments This work was supported by funding from NIH R01 grants HL095070, HL114772, HL113451 to HJ.

Sources of Funding NIH R01 grants HL095070, HL114772, HL113451, and HHSN268201000043C to HJ.

NV is supported by the Cell and Tissue Engineering NIH Biotechnology Training Grant (T32 GM-008433).

Disclosures None.

References

1. Benjamin EJ, et al. Heart disease and stroke Statistics-2019 update: a report from the American Heart Association. *Circulation*. 2019;139(10):e56–e528.
2. Rajamannan NM, et al. Calcific aortic valve disease: not simply a degenerative process: a review and agenda for research from the National Heart and Lung and Blood Institute Aortic Stenosis Working Group. Executive summary: calcific aortic valve disease-2011 update. *Circulation*. 2011;124(16):1783–91.
3. Hsu SY, et al. Aortic valve sclerosis is an echocardiographic indicator of significant coronary disease in patients undergoing diagnostic coronary angiography. *Int J Clin Pract*. 2005;59(1):72–7.
4. Otto CM, et al. Association of aortic-valve sclerosis with cardiovascular mortality and morbidity in the elderly. *N Engl J Med*. 1999;341(3):142–7.
5. Leopold JA. Cellular mechanisms of aortic valve calcification. *Circ Cardiovasc Interv*. 2012;5(4):605–14.
6. Mohler ER, et al. Development and progression of aortic valve stenosis: atherosclerosis risk factors—a causal relationship? A clinical morphologic study. *Clin Cardiol*. 1991;14(12):995–9.

7. Muneretto C, et al. A comparison of conventional surgery, transcatheter aortic valve replacement, and sutureless valves in “real-world” patients with aortic stenosis and intermediate- to high-risk profile. *J Thorac Cardiovasc Surg*. 2015;150(6):1570–7.. discussion 1577–9
8. Dasi LP, et al. On the mechanics of transcatheter aortic valve replacement. *Ann Biomed Eng*. 2017;45(2):310–31.
9. Czarny MJ, Resar JR. Diagnosis and management of valvular aortic stenosis. *Clin Med Insights Cardiol*. 2014;8(Suppl 1):15–24.
10. Otto CM, et al. Characterization of the early lesion of 'degenerative' valvular aortic stenosis. Histological and immunohistochemical studies. *Circulation*. 1994;90(2):844–53.
11. Wallby L, et al. T lymphocyte infiltration in non-rheumatic aortic stenosis: a comparative descriptive study between tricuspid and bicuspid aortic valves. *Heart*. 2002;88(4):348–51.
12. Olsson M, et al. Accumulation of T lymphocytes and expression of interleukin-2 receptors in nonrheumatic stenotic aortic valves. *J Am Coll Cardiol*. 1994;23(5):1162–70.
13. Kaden JJ, et al. Interleukin-1 beta promotes matrix metalloproteinase expression and cell proliferation in calcific aortic valve stenosis. *Atherosclerosis*. 2003;170(2):205–11.
14. Rajamannan NM, et al. Human aortic valve calcification is associated with an osteoblast phenotype. *Circulation*. 2003;107(17):2181–4.
15. Jian B, et al. Progression of aortic valve stenosis: TGF-beta1 is present in calcified aortic valve cusps and promotes aortic valve interstitial cell calcification via apoptosis. *Ann Thorac Surg*. 2003;75(2):457–65.. discussion 465–6
16. Richards J, et al. Side-specific endothelial-dependent regulation of aortic valve calcification: interplay of hemodynamics and nitric oxide signaling. *Am J Pathol*. 2013;182(5):1922–31.
17. Singh R, et al. Age-related changes in the aortic valve affect leaflet stress distributions: implications for aortic valve degeneration. *J Heart Valve Dis*. 2008;17(3):290–8.. discussion 299
18. Lancellotti P. Grading aortic stenosis severity when the flow modifies the gradient valve area correlation. *Cardiovasc Diagn Ther*. 2012;2(1):6–9.
19. Then KL, Rankin JA. Hypertension: a review for clinicians. *Nurs Clin North Am*. 2004;39(4):793–814.
20. Sacks MS, Schoen FJ, Mayer JE. Bioengineering challenges for heart valve tissue engineering. *Annu Rev Biomed Eng*. 2009;11:289–313.
21. Wiltz D, et al. Extracellular matrix organization, structure, and function. In: Aikawa E, editor. *Calcific Aortic Valve Disease*. Rijeka, Croatia: InTech; 2013, pp. 3–30.
22. Schoen FJ. Aortic valve structure-function correlations: role of elastic fibers no longer a stretch of the imagination. *J Heart Valve Dis*. 1997;6(1):1–6.
23. Chen JH, Simmons CA. Cell-matrix interactions in the pathobiology of calcific aortic valve disease: critical roles for matricellular, matricrine, and matrix mechanics cues. *Circ Res*. 2011;108(12):1510–24.
24. Parnell A, Swanevelder J. High transvalvular pressure gradients on intraoperative transesophageal echocardiography after aortic valve replacement: what does it mean? *HSR Proc Intensive Care Cardiovasc Anesth*. 2009;1(4):7–18.
25. Takx RA, et al. The interdependence between cardiovascular calcifications in different arterial beds and vascular risk factors in patients at high cardiovascular risk. *Atherosclerosis*. 2015;238(1):140–6.
26. Iwata S, et al. Higher ambulatory blood pressure is associated with aortic valve calcification in the elderly: a population-based study. *Hypertension*. 2013;61(1):55–60.
27. Bermejo J. The effects of hypertension on aortic valve stenosis. *Heart*. 2005;91(3):280–2.
28. Ivanovic B, Tadic M, Dincic D. The effects of arterial hypertension on aortic valve stenosis. *Vojnosanit Pregl*. 2010;67(7):588–92.
29. Kaden JJ, Haghi D. Hypertension in aortic valve stenosis--a Trojan horse. *Eur Heart J*. 2008;29(16):1934–5.
30. Chester AH, et al. The living aortic valve: from molecules to function. *Glob Cardiol Sci Pract*. 2014;2014(1):52–77.

31. Arjunon S, et al. Aortic valve: mechanical environment and mechanobiology. *Ann Biomed Eng.* 2013;41(7):1331–46.
32. Beppu S, et al. Rapidity of progression of aortic stenosis in patients with congenital bicuspid aortic valves. *Am J Cardiol.* 1993;71(4):322–7.
33. Stewart BF, et al. Clinical factors associated with calcific aortic valve disease. Cardiovascular health study. *J Am Coll Cardiol.* 1997;29(3):630–4.
34. Boon A, et al. Cardiac valve calcification: characteristics of patients with calcification of the mitral annulus or aortic valve. *Heart.* 1997;78(5):472–4.
35. Katayama S, et al. Bicuspid aortic valves undergo excessive strain during opening: a simulation study. *J Thorac Cardiovasc Surg.* 2013;145(6):1570–6.
36. Conti CA, et al. Biomechanical implications of the congenital bicuspid aortic valve: a finite element study of aortic root function from in vivo data. *J Thorac Cardiovasc Surg.* 2010;140(4):890–6, 896.e1–2.
37. Siu SC, Silversides CK. Bicuspid aortic valve disease. *J Am Coll Cardiol.* 2010;55(25):2789–800.
38. Martin C, Sun W. Biomechanical characterization of aortic valve tissue in humans and common animal models. *J Biomed Mater Res A.* 2012;100(6):1591–9.
39. Freeman RV, Otto CM. Spectrum of calcific aortic valve disease: pathogenesis, disease progression, and treatment strategies. *Circulation.* 2005;111(24):3316–26.
40. Ankeny RF, et al. Preferential activation of SMAD1/5/8 on the fibrosa endothelium in calcified human aortic valves--association with low BMP antagonists and SMAD6. *PLoS One.* 2011;6(6):e20969.
41. Agmon Y, et al. Aortic valve sclerosis and aortic atherosclerosis: different manifestations of the same disease? Insights from a population-based study. *J Am Coll Cardiol.* 2001;38(3):827–34.
42. Weston MW, LaBorde DV, Yoganathan AP. Estimation of the shear stress on the surface of an aortic valve leaflet. *Ann Biomed Eng.* 1999;27(4):572–9.
43. Barker AJ, et al. Bicuspid aortic valve is associated with altered wall shear stress in the ascending aorta. *Circ Cardiovasc Imaging.* 2012;5(4):457–66.
44. Tarbell JM, et al. Fluid mechanics, arterial disease, and gene expression. *Annu Rev Fluid Mech.* 2014;46:591–614.
45. Demos C, Tamargo I, Jo H. Biomechanical regulation of endothelial function in atherosclerosis. In: Ohayon J, Finet G, Pettigrew R, editors. *Biomechanics of coronary atherosclerotic plaque: from model to patient.* Cambridge, MA: Academic Press; 2020, pp. 3–50.
46. Yang B, Rizzo V. Shear stress activates eNOS at the endothelial apical surface through beta1 containing Integrins and Caveolae. *Cell Mol Bioeng.* 2013;6(3):346–54.
47. Zhao F, et al. Roles for GP IIb/IIIa and alphavbeta3 integrins in MDA-MB-231 cell invasion and shear flow-induced cancer cell mechanotransduction. *Cancer Lett.* 2014;344(1):62–73.
48. Takada Y, Ye X, Simon S. The integrins. *Genome Biol.* 2007;8(5):215.
49. Ziegler WH, et al. Integrin connections to the cytoskeleton through Talin and vinculin. *Biochem Soc Trans.* 2008;36(Pt 2):235–9.
50. Parsons JT, et al. Focal adhesion kinase: a regulator of focal adhesion dynamics and cell movement. *Oncogene.* 2000;19(49):5606–13.
51. Ciobanaru C, Faivre B, Le Clainche C. Integrating actin dynamics, mechanotransduction and integrin activation: the multiple functions of actin binding proteins in focal adhesions. *Eur J Cell Biol.* 2013;92(10–11):339–48.
52. Zebda N, Dubrovskiy O, Birukov KG. Focal adhesion kinase regulation of mechanotransduction and its impact on endothelial cell functions. *Microvasc Res.* 2012;83(1):71–81.
53. Lehoux S, et al. Differential regulation of vascular focal adhesion kinase by steady stretch and pulsatility. *Circulation.* 2005;111(5):643–9.
54. Li S, et al. The role of the dynamics of focal adhesion kinase in the mechanotaxis of endothelial cells. *Proc Natl Acad Sci U S A.* 2002;99(6):3546–51.

55. Hirakawa M, et al. Sequential activation of RhoA and FAK/paxillin leads to ATP release and actin reorganization in human endothelium. *J Physiol*. 2004;558(Pt 2):479–88.
56. Hsu HJ, et al. Stretch-induced stress fiber remodeling and the activations of JNK and ERK depend on mechanical strain rate, but not FAK. *PLoS One*. 2010;5(8):e12470.
57. Sokabe M, et al. Mechanotransduction and intracellular signaling mechanisms of stretch-induced remodeling in endothelial cells. *Heart Vessels*. 1997; Suppl 12:191–3.
58. Wu CC, et al. Directional shear flow and Rho activation prevent the endothelial cell apoptosis induced by micropatterned anisotropic geometry. *Proc Natl Acad Sci U S A*. 2007;104(4):1254–9.
59. Wang JG, et al. Uniaxial cyclic stretch induces focal adhesion kinase (FAK) tyrosine phosphorylation followed by mitogen-activated protein kinase (MAPK) activation. *Biochem Biophys Res Commun*. 2001;288(2):356–61.
60. Katritch V, Cherezov V, Stevens RC. Structure-function of the G protein-coupled receptor superfamily. *Annu Rev Pharmacol Toxicol*. 2013;53:531–56.
61. Chachisvilis M, Zhang YL, Frangos JA. G protein-coupled receptors sense fluid shear stress in endothelial cells. *Proc Natl Acad Sci U S A*. 2006;103(42):15463–8.
62. Cuerrier CM, et al. Effect of thrombin and bradykinin on endothelial cell mechanical properties monitored through membrane deformation. *J Mol Recognit*. 2009;22(5):389–96.
63. Christopoulos A. Advances in G protein-coupled receptor allostery: from function to structure. *Mol Pharmacol*. 2014;86(5):463–78.
64. Becker BF, Chappell D, Jacob M. Endothelial glycocalyx and coronary vascular permeability: the fringe benefit. *Basic Res Cardiol*. 2010;105(6):687–701.
65. Alphonsus CS, Rodseth RN. The endothelial glycocalyx: a review of the vascular barrier. *Anaesthesia*. 2014;69(7):777–84.
66. Afratis N, et al. Glycosaminoglycans: key players in cancer cell biology and treatment. *FEBS J*. 2012;279(7):1177–97.
67. Mehta D, Ravindran K, Kuebler WM. Novel regulators of endothelial barrier function. *Am J Physiol Lung Cell Mol Physiol*. 2014;307(12):L924–35.
68. Kolarova H, et al. Modulation of endothelial glycocalyx structure under inflammatory conditions. *Mediat Inflamm*. 2014;2014:694312.
69. Chien S. Molecular and mechanical bases of focal lipid accumulation in arterial wall. *Prog Biophys Mol Biol*. 2003;83(2):131–51.
70. Sarphie TG. Interactions of IgG and beta-VLDL with aortic valve endothelium from hypercholesterolemic rabbits. *Atherosclerosis*. 1987;68(3):199–212.
71. Sarphie TG. A cytochemical study of the surface properties of aortic and mitral valve endothelium from hypercholesterolemic rabbits. *Exp Mol Pathol*. 1986;44(3):281–96.
72. Kobayashi H, Boelte KC, Lin PC. Endothelial cell adhesion molecules and cancer progression. *Curr Med Chem*. 2007;14(4):377–86.
73. Szmítko PE, et al. New markers of inflammation and endothelial cell activation: Part I. *Circulation*. 2003;108(16):1917–23.
74. Tzima E, et al. A mechanosensory complex that mediates the endothelial cell response to fluid shear stress. *Nature*. 2005;437(7057):426–31.
75. Chiu YJ, McBeath E, Fujiwara K. Mechanotransduction in an extracted cell model: Fyn drives stretch- and flow-elicited PECAM-1 phosphorylation. *J Cell Biol*. 2008;182(4):753–63.
76. Collins C, et al. Localized tensional forces on PECAM-1 elicit a global mechanotransduction response via the integrin-RhoA pathway. *Curr Biol*. 2012;22(22):2087–94.
77. Coon BG, et al. Intramembrane binding of VE-cadherin to VEGFR2 and VEGFR3 assembles the endothelial mechanosensory complex. *J Cell Biol*. 2015;208(7):975–86.
78. Komarova YA, et al. Protein interactions at endothelial junctions and signaling mechanisms regulating endothelial permeability. *Circ Res*. 2017;120(1):179–206.
79. Russell-Puleri S, et al. Fluid shear stress induces upregulation of COX-2 and PGI2 release in endothelial cells via a pathway involving PECAM-1, PI3K, FAK, and p38. *Am J Physiol Heart Circ Physiol*. 2017;312(3):H485–h500.

80. Fleming I, et al. Role of PECAM-1 in the shear-stress-induced activation of Akt and the endothelial nitric oxide synthase (eNOS) in endothelial cells. *J Cell Sci.* 2005;118(Pt 18):4103–11.
81. Qin WD, et al. Low shear stress induced HMGB1 translocation and release via PECAM-1/PARP-1 pathway to induce inflammation response. *PLoS One.* 2015;10(3):e0120586.
82. Conway DE, et al. VE-cadherin phosphorylation regulates endothelial fluid shear stress responses through the polarity protein LGN. *Curr Biol.* 2017;27(14):2219–25.e5.
83. Pamukcu B, Lip GY, Shantsila E. The nuclear factor- κ B pathway in atherosclerosis: a potential therapeutic target for atherothrombotic vascular disease. *Thromb Res.* 2011;128(2):117–23.
84. Privratsky JR, Newman PJ. PECAM-1: regulator of endothelial junctional integrity. *Cell Tissue Res.* 2014;355(3):607–19.
85. Jin X, et al. Cilioplasm is a cellular compartment for calcium signaling in response to mechanical and chemical stimuli. *Cell Mol Life Sci.* 2014;71(11):2165–78.
86. Luu VZ, et al. Role of endothelial primary cilia as fluid mechanosensors on vascular health. *Atherosclerosis.* 2018;275:196–204.
87. Nauli SM, et al. Endothelial cilia are fluid shear sensors that regulate calcium signaling and nitric oxide production through polycystin-1. *Circulation.* 2008;117(9):1161–71.
88. Nauli SM, et al. Non-motile primary cilia as fluid shear stress mechanosensors. *Methods Enzymol.* 2013;525:1–20.
89. Pala R, et al. The roles of primary cilia in cardiovascular diseases. *Cell.* 2018;7(12).
90. Spasic M, Jacobs CR. Lengthening primary cilia enhances cellular mechanosensitivity. *Eur Cell Mater.* 2017;33:158–68.
91. Toomer KA, et al. A role for primary cilia in aortic valve development and disease. *Dev Dyn.* 2017;246(8):625–34.
92. Li J, et al. Piezo1 integration of vascular architecture with physiological force. *Nature.* 2014;515(7526):279–82.
93. Albarran-Juarez J, et al. Piezo1 and Gq/G11 promote endothelial inflammation depending on flow pattern and integrin activation. *J Exp Med.* 2018;215(10):2655–72.
94. Kang H, et al. Piezo1 mediates angiogenesis through activation of MT1-MMP signaling. *Am J Physiol Cell Physiol.* 2019;316(1):C92–c103.
95. Ranade SS, et al. Piezo1, a mechanically activated ion channel, is required for vascular development in mice. *Proc Natl Acad Sci U S A.* 2014;111(28):10347–52.
96. Wang S, et al. Endothelial cation channel PIEZO1 controls blood pressure by mediating flow-induced ATP release. *J Clin Invest.* 2016;126(12):4527–36.
97. Faucherre A, et al. Piezo1 is required for outflow tract and aortic valve development. *J Mol Cell Cardiol.* 2019;3(143):51–62.
98. Duchemin AL, Vignes H, Vermot J. Mechanically activated piezo channels modulate outflow tract valve development through the Yap1 and Klf2-Notch signaling axis. *Elife.* 2019;16(8):e44706.
99. Fernandez Esmerats J, Heath J, Jo H. Shear-sensitive genes in aortic valve endothelium. *Antioxid Redox Signal.* 2016;25(7):401–14.
100. Guo H, et al. Mammalian microRNAs predominantly act to decrease target mRNA levels. *Nature.* 2010;466(7308):835–40.
101. Nazari-Jahantigh M, et al. MicroRNA-specific regulatory mechanisms in atherosclerosis. *J Mol Cell Cardiol.* 2015;89(Pt A):35–41.
102. Kumar S, et al. Role of flow-sensitive microRNAs in endothelial dysfunction and atherosclerosis: mechanosensitive athero-miRs. *Arterioscler Thromb Vasc Biol.* 2014;34(10):2206–16.
103. Kalozeumi G, Yacoub M, Sanoudou D. MicroRNAs in heart failure: small molecules with major impact. *Glob Cardiol Sci Pract.* 2014;2014(2):79–102.
104. Moura J, Borsheim E, Carvalho E. The role of MicroRNAs in diabetic complications-special emphasis on wound healing. *Genes (Basel).* 2014;5(4):926–56.

105. Neves VJ, et al. Exercise training in hypertension: role of microRNAs. *World J Cardiol.* 2014;6(8):713–27.
106. Wang H, et al. MicroRNA expression signature in human calcific aortic valve disease. *Biomed Res Int.* 2017;2017:4820275.
107. Nigam V, et al. Altered microRNAs in bicuspid aortic valve: a comparison between stenotic and insufficient valves. *J Heart Valve Dis.* 2010;19(4):459–65.
108. Takahashi K, et al. Dysregulation of ossification-related miRNAs in circulating osteogenic progenitor cells obtained from patients with aortic stenosis. *Clin Sci (Lond).* 2016;130(13):1115–24.
109. Ni WJ, Ma DH, Leng XM. NcRNAs in CAVD: a review of recent studies. *J Cardiovasc Pharmacol.* 2018;
110. Fiedler J, et al. Identification of miR-143 as a major contributor for human stenotic aortic valve disease. *J Cardiovasc Transl Res.* 2019;12(5):447–58.
111. Ohukainen P, et al. MicroRNA-125b and chemokine CCL4 expression are associated with calcific aortic valve disease. *Ann Med.* 2015;47(5):423–9.
112. Patel V, et al. The stretch responsive microRNA miR-148a-3p is a novel repressor of IKBKB, NF-kappaB signaling, and inflammatory gene expression in human aortic valve cells. *FASEB J.* 2015;29(5):1859–68.
113. Song R, et al. Altered microRNA expression is responsible for the pro-osteogenic phenotype of interstitial cells in calcified human aortic valves. *J Am Heart Assoc.* 2017;6(4):1–17.
114. Heath JM, et al. Mechanosensitive microRNA-181b regulates aortic valve endothelial matrix degradation by targeting TIMP3. *Cardiovasc Eng Technol.* 2018;9(2):141–50.
115. Xu R, et al. MicroRNA-449c-5p inhibits osteogenic differentiation of human VICs through Smad4-mediated pathway. *Sci Rep.* 2017;7(1):8740.
116. Fang M, et al. Mir-29b promotes human aortic valve interstitial cell calcification via inhibiting TGF-beta3 through activation of wnt3/beta-catenin/Smad3 signaling. *J Cell Biochem.* 2018;119(7):5175–85.
117. Toshima T, et al. Therapeutic inhibition of microRNA-34a ameliorates aortic valve calcification via modulation of Notch1-Runx2 signaling. *Cardiovasc Res.* 2019;
118. Nader J, et al. miR-92a: a novel potential biomarker of rapid aortic valve calcification. *J Heart Valve Dis.* 2017;26(3):327–33.
119. Sabatino J, et al. MicroRNAs fingerprint of bicuspid aortic valve. *J Mol Cell Cardiol.* 2019;134:98–106.
120. Fan W, et al. Shear-sensitive microRNA-34a modulates flow-dependent regulation of endothelial inflammation. *J Cell Sci.* 2015;128(1):70–80.
121. Boon RA, Hergenreider E, Dimmeler S. Atheroprotective mechanisms of shear stress-regulated microRNAs. *Thromb Haemost.* 2012;108(4):616–20.
122. Bonauer A, et al. MicroRNA-92a controls angiogenesis and functional recovery of ischemic tissues in mice. *Science.* 2009;324(5935):1710–3.
123. Wu W, et al. Flow-dependent regulation of Kruppel-like factor 2 is mediated by MicroRNA-92a. *Circulation.* 2011;124(5):633–41.
124. Lu P, Yin B, Liu L. MicroRNA-138 suppresses osteoblastic differentiation of Valvular interstitial cells in degenerative calcific aortic valve disease. *Int Heart J.* 2019;60(1):136–44.
125. Wang Y, et al. MicroRNA-204 targets Runx2 to attenuate BMP-2-induced osteoblast differentiation of human aortic valve interstitial cells. *J Cardiovasc Pharmacol.* 2015;66(1):63–71.
126. Zhang M, et al. MicroRNA-30b is a multifunctional regulator of aortic valve interstitial cells. *J Thorac Cardiovasc Surg.* 2014;147(3):1073–1080.e2.
127. Jiao W, et al. MicroRNA-638 inhibits human aortic valve interstitial cell calcification by targeting Sp7. *J Cell Mol Med.* 2019;23(8):5292–302.
128. Yanagawa B, et al. miRNA-141 is a novel regulator of BMP-2-mediated calcification in aortic stenosis. *J Thorac Cardiovasc Surg.* 2012;144(1):256–62.
129. Du J, et al. Downregulated MicroRNA-195 in the bicuspid aortic valve promotes calcification of valve interstitial cells via targeting SMAD7. *Cell Physiol Biochem.* 2017;44(3):884–96.

130. Holliday CJ, et al. Discovery of shear- and side-specific mRNAs and miRNAs in human aortic valvular endothelial cells. *Am J Physiol Heart Circ Physiol.* 2011;301(3):H856–67.
131. Rathan S, et al. Identification of side- and shear-dependent microRNAs regulating porcine aortic valve pathogenesis. *Sci Rep.* 2016;6:25397.
132. Holliday-Ankeny CJ, et al. The function of shear-responsive and side-dependent microRNA-486-5p in aortic valve endothelium. *Cardiovas Pathol* 22, 2013(3).
133. Fernandez Esmerats J, et al. Disturbed flow increases UBE2C (ubiquitin E2 ligase C) via loss of miR-483-3p, inducing aortic valve calcification by the pVHL (von Hippel-Lindau protein) and HIF-1alpha (hypoxia-inducible factor-1alpha) pathway in endothelial cells. *Arterioscler Thromb Vasc Biol.* 2019;39(3):467–81.
134. Maxwell PH, Pugh CW, Ratcliffe PJ. The pVHL-hIF-1 system. A key mediator of oxygen homeostasis. *Adv Exp Med Biol.* 2001;502:365–76.
135. Salim MT, et al. miR-214 is stretch-sensitive in aortic valve and inhibits aortic valve calcification. *Ann Biomed Eng.* 2019;47(4):1106–15.

Chapter 7

The Role of Chronic Kidney Disease in Ectopic Calcification



Joanne Laycock, Malgorzata Furmanik, Mengxi Sun, Leon J. Schurgers, Rukshana Shroff, and Catherine M. Shanahan

What Is Chronic Kidney Disease?

Chronic kidney disease (CKD) is a progressive disorder, characterised by a gradual decline in functional nephrons and a reduction in glomerular filtration rate (GFR). CKD is defined by a GFR below 60 ml/min/1.73m² [1]. As the GFR deteriorates further, there is a graded increase in the risk of cardiovascular morbidity [2]. CKD culminates in end-stage kidney disease (ESKD); by this stage, patients require dialysis or renal transplantation.

Cardiovascular disease is the most common cause of death in CKD patients receiving dialysis. The rate of cardiovascular mortality in dialysis patients in their 20s is comparable to octogenarians [3]. The high risk of cardiovascular mortality in CKD patients is strongly correlated with vascular calcification. In ESKD there are a number of risk factors including disturbances in mineral metabolism, secondary hyperparathyroidism (SHPT) and a build-up of uraemic toxins that predispose patients to CKD bone mineral disorder (BMD) and to ectopic calcification [4].

J. Laycock · M. Sun · C. M. Shanahan (✉)
BHF Centre of Research Excellence, School of Cardiovascular Medicine and Sciences,
King's College London, London, UK
e-mail: joanne.laycock@york.ac.uk; cathy.shanahan@kcl.ac.uk

M. Furmanik · L. J. Schurgers
Department of Biochemistry, Cardiovascular Research Institute Maastricht, Maastricht
University, Maastricht, The Netherlands
e-mail: gosia.furmanik@maastrichtuniversity.nl; l.schurgers@maastrichtuniversity.nl

R. Shroff
Great Ormond Street Hospital for Children, London, UK
e-mail: rukshana.shroff@gosh.nhs.uk

The Risk Factors of CKD and Their Association with Ectopic Calcification

Dysregulated Mineral Metabolism: CKD Leads to Hyperphosphataemia, which is Exacerbated by Klotho Deficiency and Ineffective Fibroblast Growth Factor 23 (FGF23)

The kidney is a major regulator of serum phosphorous (P); it is important for both P excretion and regulating the resorption of P and calcium (Ca) to accommodate bone turnover. In CKD there is a decline in renal function, and P excretion by the kidney is impaired; therefore, raised serum P is associated with CKD.

The kidney relies on autocrine signalling from FGF23 to maintain P homeostasis [5–7]. When serum P levels are high, FGF23 is synthesised by bone osteocytes and osteoblasts to raise circulating levels of FGF23. FGF23 binds to the fibroblast growth factor receptor (FGFR) on the basolateral membrane of the kidney tubules, and this has two downstream effects to reduce serum P towards homeostatic levels [8]:

1. Increased P excretion. FGF23 blocks the synthesis and increases endocytosis of the Na/P cotransporter on the apical membrane of the kidney tubule [6]. The reduced number of P transporters decreases P reabsorption from the filtrate, therefore increasing P excretion.
2. Reduced vitamin D levels to reduce Ca and P resorption. FGF23 blocks the synthesis of 1α -hydroxylase (required for activation of vitamin D) and upregulates the synthesis of 24 hydroxylase (an enzyme that deactivates vitamin D). The combined effect is reduced levels of active vitamin D [6]. This prevents further increase of serum P as vitamin D promotes bone turnover and resorption of Ca and P.

In patients with CKD, the initial rise in serum P is compensated for by increased FGF23 production, and P homeostasis is maintained. As CKD progresses and the GFR declines further, the kidneys are unable to react to sufficiently lower P despite high serum FGF23 levels.

This is exacerbated by a klotho deficiency linked to CKD. Klotho is a protein required to confer the FGFR specific to FGF23, and in the absence of klotho, FGF23 is unable to bind to the FGFR and act on the kidney tubule to reduce serum P towards normal levels [9]. This P retention leads to persistent hyperphosphataemia and stimulates a further increase in FGF23 levels; however homeostatic mechanisms can no longer restore the P balance.

A chronic increase in serum P prevails [10] and increases parathyroid hormone (PTH) secretion. In a state of klotho deficiency, FGFRs in the parathyroid gland are unable to respond to high circulating levels of FGF23, and this negative feedback mechanism to prevent excessive PTH secretion is lost.

Dysregulated Mineral Metabolism: Vitamin D Deficiency in CKD and Reduced Ca Intake

Vitamin D is a term used to describe several related compounds, it is obtained as previtamin D and exists in the circulation in the inactive form of 25-hydroxy vitamin D. 25-hydroxy vitamin D is hydrolysed by the 1α -hydroxylase enzyme to the active form $1\alpha,25$ -dihydroxy vitamin D. The majority of 1α -hydroxylase is expressed in the kidney; therefore the kidney plays a key role in regulating the activation of vitamin D.

Patients with CKD are often deficient in vitamin D. The detrimental effects of vitamin D deficiency on bone mineral disorders such as rickets, led to the discovery of vitamin D in the early 1900s and are now widely known as reviewed by [11].

Vitamin D in its active form, $1\alpha,25$ -dihydroxy vitamin D (referred to as vitamin D here in) is important for Ca intake and homeostasis by three key mechanisms:

1. Increase Ca absorption from the small intestine. Vitamin D increases transcription of the Ca channel TRPV6 and calbindin in the small intestine to increase the efficiency of Ca absorption from 10% to 40% [12].
2. Increase resorption of Ca and P from bone. Vitamin D upregulates RANKL expression in osteoblasts and drives the maturation of pre-osteoclasts to osteoclasts which resorb Ca and P from bone and release it into the circulation [13].
3. Reduce PTH secretion. Vitamin D increases expression of the vitamin D receptor (VDR) and the calcium-sensing receptor (CaSR) in the parathyroid glands to increase their sensitivity to both Ca and vitamin D. The effect of vitamin D on the parathyroid gland is to downregulate PTH expression in order to prevent excessive Ca and P resorption and extensive bone turnover [14].

Vitamin D deficiency leads to an initial reduction in serum Ca. Low levels of circulating Ca stimulate the parathyroid gland to secrete PTH. The state of vitamin D deficiency affects two negative feedback mechanisms of PTH secretion. Vitamin D cannot downregulate PTH expression or upregulate the expression of the CaSR in the parathyroid gland to increase its sensitivity to circulating Ca.

Dysregulated Mineral Metabolism: CKD Is a State of SHPT Resulting in Hypercalcaemia and Hyperphosphataemia

PTH plays a key role in maintaining mineral homeostasis, it acts on multiple regulatory pathways, and PTH itself is regulated by multiple negative feedback mechanisms.

The parathyroid gland is well known to contain CaSRs, and PTH is the primary regulator of serum Ca; it is secreted when serum Ca levels are low [15]. For

example, the low serum Ca levels observed in early CKD stimulate PTH secretion; PTH has three mechanisms of action to increase serum Ca:

1. PTH increases Ca reabsorption from the kidney tubule.
2. PTH upregulates transcription of CYP27B1 in the kidney to increase 1α -hydroxylase activation of vitamin D and leads to increased serum vitamin D levels.
3. PTH increases resorption of Ca and P from bone. PTH increases bone turnover in a similar manner to vitamin D by upregulating the expression of RANKL in osteoblasts. RANKL drives the maturation of pre-osteoclasts to mature osteoclasts, which resorb Ca and P from the bone matrix and release it into the circulation.

Hyperphosphataemia also upregulates PTH secretion. PTH promotes P and Ca resorption from bone raising serum P levels further; however PTH also increases P excretion by the kidney; therefore its overall effect is to decrease serum P [16].

In a state of health, PTH increases serum Ca and reduces serum P levels to restore homeostasis; the stimuli to upregulate PTH secretion are removed, therefore acting as a negative feedback mechanism. Excessive PTH secretion is also prevented by FGF23 and vitamin D, which act as a negative feedback mechanism and bind to the FGFRs and vitamin D receptors (VDRs) in the parathyroid gland to downregulate PTH secretion.

CKD is a state of disrupted mineral metabolism; multiple mechanisms lead to high serum P and low serum Ca levels, both of which stimulate PTH secretion (Fig. 7.1). The kidney is unable to excrete P despite the high levels of PTH; serum Ca levels are restored by increased Ca and P resorption from bone; however this further increases the serum P levels. Chronic hyperphosphataemia continues to stimulate PTH secretion. In CKD both negative feedback mechanisms of PTH are lost due to vitamin D deficiency and klotho deficiency resulting in ineffective FGF23; therefore a chronic secretion of PTH persists. Excessive PTH secretion contributes to excessive bone turnover, reducing bone density and leading to CKD-BMD [17]. The excessive resorption of Ca and P from bone leads to chronic hypercalcaemia and chronic hyperphosphataemia, which is a direct stimulus for vascular calcification and other forms of ectopic calcification [18].

Dysregulated Mineral Metabolism: The Risk of Ectopic Calcification and Cardiovascular Disease

Disrupted mineral metabolism leads to a multitude of risk factors for ectopic calcification in CKD. High levels of serum P even within the normal range have been associated with increased risk of cardiovascular events and death [19]. Patients in the early stages of CKD may develop hyperphosphataemia, and its prevalence was over 50% in a study of over 25 thousand haemodialysis patients in ESKD [20]. In

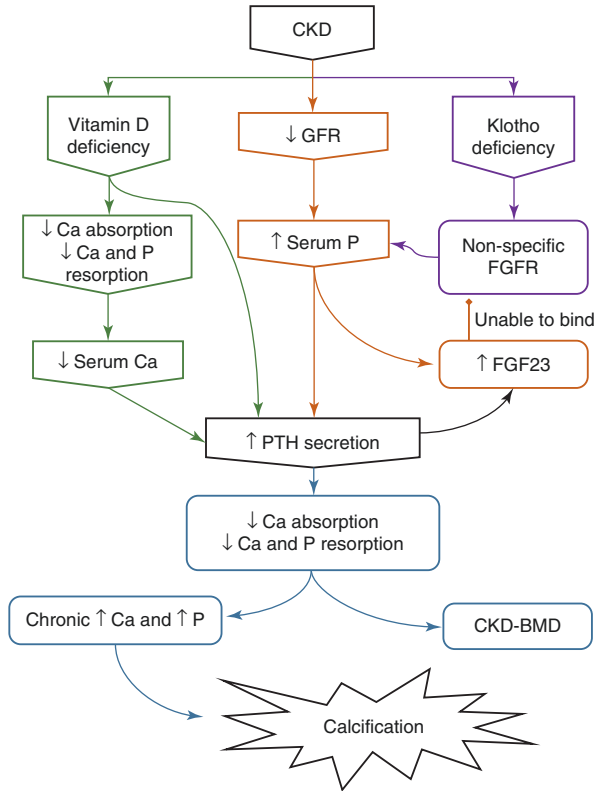


Fig. 7.1 Overview of dysregulated mineral metabolism in CKD. Multiple factors in CKD contribute to dysregulated mineral metabolism. The orange boxes indicate the decline in GFR and impaired P excretion that leads to raised serum P and triggers the PTH and FGF23 negative feedback loops to reduce serum P. As shown in the purple boxes, CKD is a state of klotho deficiency, and the FGFR requires klotho to confer it specific to FGF23; therefore serum P and PTH continue to increase despite increased FGF23 levels. The green boxes show that CKD is also a state of vitamin D deficiency, leading to reduced Ca absorption from the small intestine and reduced Ca and P resorption from bone; there is an initial decrease in serum Ca which also stimulates PTH secretion. As indicated in the blue boxes, high levels of PTH drive Ca reabsorption in the kidney and increase both Ca and P resorption from bone leading to CKD-BMD, a chronic increase in serum Ca and P and increased risk of ectopic calcification

both children and adults on dialysis, hyperphosphataemia was associated with the progression of vascular calcification [21].

The direct effect of SHPT observed in CKD on calcification is not known; however high PTH levels have been linked to an increased prevalence and severity of abdominal aortic calcification in patients with primary hyperparathyroidism [22].

The effect of vitamin D status on calcification in the CKD population has been studied, and both low and high levels of vitamin D have been associated with an increased risk of vascular calcification in children with CKD [23]. This suggests that vitamin D deficiency observed in CKD requires careful management.

The Alternative CKD Risk Factors for Calcification: The Uraemic Milieu

Disrupted mineral metabolism is not the only risk factor for vascular calcification in CKD, and uraemic serum has been shown to induce calcification independently of P concentration [24]. The systemic dysregulation in CKD can enable additional uraemic toxins to accumulate, which in healthy conditions would be excreted by the kidneys [25]. Patients in ESKD receive dialysis either in the form of haemodialysis or peritoneal dialysis to filter some of these uraemic toxins; however this can also be associated with problems. Some proteins may be excessively filtered immediately post-dialysis, and large fluctuations are observed [26].

The high turnover of bone in patients with CKD-BMD leads to elevated levels of alkaline phosphatase (ALP) [27]. ALP is an osteoblast marker mainly expressed by the liver and bone. High ALP levels are correlated with increased risk of cardiovascular disease, calcification and mortality [27]. Several large observational studies have found that ESKD patients had elevated serum ALP levels and that this was an independent risk factor of mortality [28, 29].

Experimental models suggest that impaired NaCl excretion in CKD increases the risk of hypertension. This has a detrimental positive feedback effect as sustained hypertension is a strong independent risk factor of ESKD [30]. Furthermore, systolic hypertension has been associated with faster progression of aortic valve calcification, and 5-year coronary artery calcification was accelerated even in pre-hypertensive patients [31, 32].

To compensate for impaired excretion and increased serum levels of P and NaCl, patients with CKD are advised to limit their intake of certain foods. Dietary restriction of P protects against conditions such as hyperphosphataemia, hypertension, proteinuria and other heart and bone problems [33]. However, vitamin K consumption is also reduced, a study of 172 CKD patients found that over 50% consumed less than the recommended adequate intake for vitamin K, and CKD patients are known to suffer from subclinical vitamin K deficiency [34, 35]. To confound this further, the uraemic environment is known to reduce vitamin K activity and increase the risk of ectopic calcification. It was demonstrated in rats that uraemia leads to a functional vitamin K deficiency; this was accompanied by increased renal and aortic Ca content [36]. Furthermore, loss of vitamin K activity is associated with calcification in CKD patients; haemodialysis patients prescribed warfarin (a vitamin K antagonist) had increased prevalence of vascular calcification [37].

Inflammation is another risk factor that has received much attention in the context of CKD, cardiovascular disease and its role in promoting vascular calcification [38]. The inflammatory markers C-reactive protein (CRP) IL-6, IL-1, and TNF α have been found to be elevated in CKD patients and associated with increased coronary artery calcification and mortality [39–44].

What Is Ectopic Calcification?

The dysregulated mineral metabolism and the uraemic milieu observed in CKD predispose patients to ectopic calcification. Ectopic calcification is the inappropriate biomineralisation of soft tissue that usually involves the deposition of calcium phosphate salts, including hydroxyapatite (HA). HA is formed from the crystallisation of Ca ions and inorganic P (Pi) ions; it has a mineral composition similar to that found in bone [45]. At physiological pH of 7.4, Pi exists predominantly as H_2PO_4^- and HPO_4^{2-} in a 1:4 ratio and is neutralised by Ca^{2+} ions to produce HA $\text{Ca}_{10}(\text{PO}_4)_6(\text{OH})_2$ [46].

Vascular Calcification: CKD Is Associated with Arteriosclerosis

Vascular calcification is the deposition of HA crystals in the extracellular matrix (ECM) of the vessel wall. Once considered a passive degenerative process that occurs in ageing, vascular calcification has now been recognised as a highly regulated, cell-mediated process similar to bone ossification [4].

There are two distinct types of vascular calcification (see Chap. 2 for histopathological characterization of different vascular calcification types). In atherosclerosis, calcification occurs in lipid-rich plaques at damaged patches of the tunica intima. Atherosclerosis is associated with traditional cardiovascular risk factors including age, obesity, dyslipidaemia and smoking [4].

Arteriosclerosis (also known as Monckeberg's sclerosis) is associated with CKD and diabetes, it is characterised by calcification of the vascular smooth muscle cells (VSMCs) in the tunica media. Sheet like calcification forms in the tunica media layer resulting in a concentric thickening of the vessel wall and increased vascular stiffness that leads to systolic hypertension and left ventricular hypertrophy [47].

Although distinct diseases, atherosclerosis and arteriosclerosis can coexist in various combinations particularly in older diabetics and adults with CKD. These patients have been exposed to traditional cardiovascular risk factors for atherosclerosis and disease-specific risk factors for arteriosclerosis [48].

Coronary autopsy samples from renal patients had comparable tunica intima calcification to non-renal patients (atherosclerosis) but a higher proportion of tunica media calcification (arteriosclerosis) [49]. In young dialysis patients and those without comorbidity, calcification is exclusively in the tunica media [50]. From here onwards, vascular calcification in CKD will refer to arteriosclerosis.

Mechanisms of Vascular Calcification and the Impact of CKD

Vascular calcification is a highly regulated process that occurs in the matrix surrounding VSMCs. The molecular structure of Ca and P biominerals in an ectopic calcified human plaque in part resembles that of bone. Common features include the localisation of glycosaminoglycans and collagen with mineralisation, suggesting that similar mechanisms regulate physiological and pathological calcification [51].

Both processes require a microenvironment that enables extracellular crystal growth; this is formed by the accumulation of extracellular vesicles (EVs) in the ECM, where mineral nucleation and calcification can then occur [52]. To initiate ectopic vascular calcification, several molecular processes must occur simultaneously; this includes osteochondrogenic differentiation, downregulation of mineralisation inhibitors and the release of pro-calcific EVs [53] (Fig. 7.2).

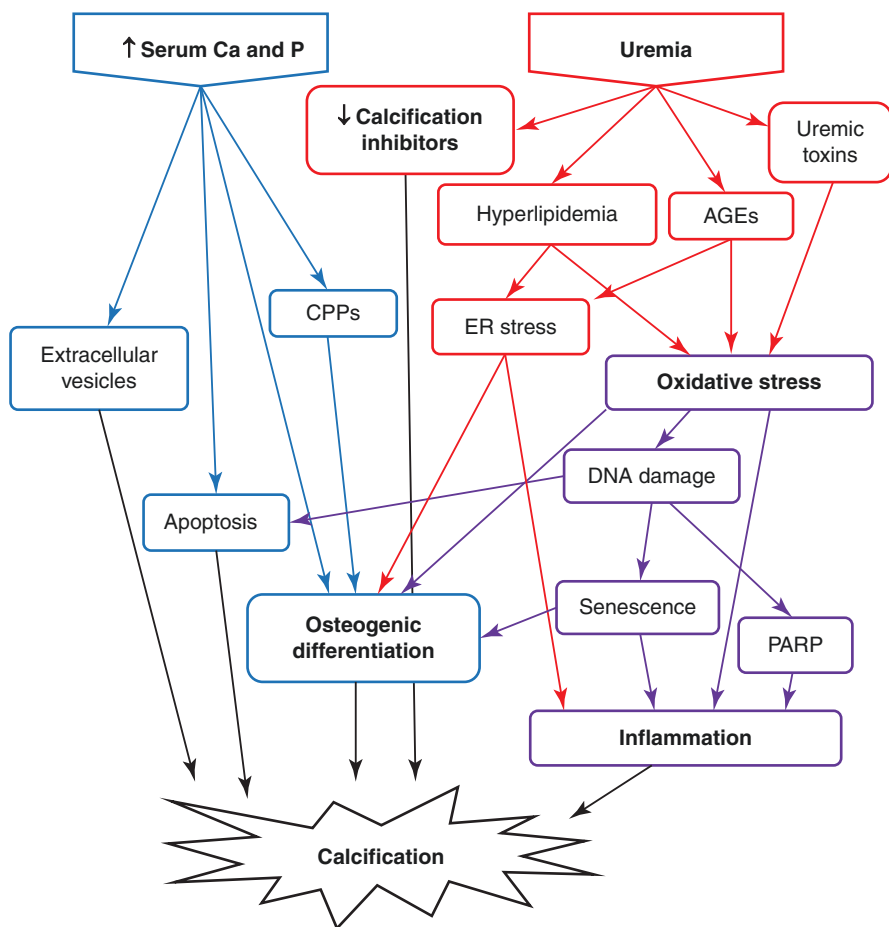


Fig. 7.2 Mechanisms of calcification in CKD. In CKD a multitude of mechanisms are affected that contribute to drive calcification. As shown in the blue boxes, high serum Ca and P drive apoptosis, osteogenic differentiation and the accumulation of both extracellular vesicles and CPPs. The red boxes indicate that the uraemic environment is characterised by a loss of calcification inhibitors as well as the accumulation of uraemic toxins, AGEs and hyperlipidaemia. The purple boxes show that this environment drives oxidative stress leading to DNA damage; the cellular responses to DNA damage include apoptosis, senescence and activation of the DDR pathway with increased PARP. This leads to an increased inflammatory response which directly promotes calcification as well as increasing osteogenic differentiation. Furthermore, the uraemic environment drives ER stress, contributing further to inflammation and osteogenic differentiation

Dysregulated mineral metabolism in CKD plays a key role in driving calcification; however, high levels of Ca and P alone do not result in the passive deposition of HA crystals in the vasculature [4]. A combination of risk factors found in the uraemic milieu is required to enable this pathological calcification to develop [21].

Apoptosis of Vascular Smooth Muscle Cells

Apoptosis of VSMCs play a key role in promoting calcification. Apoptotic bodies in the ECM provide a nidus for the accumulation of HA crystals and the initiation of calcification they are in part accountable for the increased ectopic calcification observed in CKD [4]. Apoptosis was shown to drive calcification in a VSMC model of calcification. VSMCs undergo apoptosis prior to calcification, and inhibition of apoptosis reduces calcification by 40% [54]. Indirect evidence linking apoptosis to calcification was also found in vivo, histological analysis of vessels from CKD dialysis patients found areas of apoptosis adjacent to calcified areas [50]. Ex vivo culture of these vessels in high Ca and P media mimicking the dysregulated mineral metabolism observed in CKD has been shown to drive apoptotic cell death and reduce VSMC density by 30% [55].

Extracellular Vesicle Release

EVs are small extracellular membranous particles, which, contrary to apoptotic bodies, are released by living cells. The release of mineralisation competent EVs of 100–300 nm in diameter into the ECM provides a nucleation site for HA crystals to form and is important in both physiological and ectopic calcification [56, 57]. Healthy VSMCs release EVs into the ECM; however they do not support mineralisation as they do not contain HA and are loaded with mineralisation inhibitors; matrix gla protein (MGP), prothrombin, osteopontin and fetuin-A that prevent mineral nucleation and crystal growth [56, 58].

High Ca and P conditions not only increase the rate of apoptosis in human VSMCs but also increase EV release [59]. Initially, this may be a defence mechanism to extrude excess HA; however accumulation of EVs can drive calcification. VSMCs persistently exposed to the high Ca and P levels observed in CKD release EVs that contain preformed calcium phosphate $\text{Ca}(\text{H}_2\text{PO}_4)_2$, were depleted of MGP and enabled HA crystal growth [59]. Raised extracellular Ca as observed in CKD was required for release of calcific EVs from VSMCs; these EVs shared properties with chondrocyte matrix vesicles [56]. This includes expression of Ca-binding annexins and exposed phosphatidylserine on the surface of EVs providing a site for HA nucleation, therefore supporting the early stages of ectopic calcification. Detailed information on the role of EVs in calcification is provided in Chap. 5.

Perturbation in the Level of Physiological Calcification Inhibitors

The expression of calcification inhibitors MGP, pyrophosphate, fetuin-A and osteopontin in healthy arteries plays a key role in preventing calcification.

MGP is endogenously expressed in both VSMCs and chondrocytes with local expression of MGP in the vessel wall required for inhibition of vascular calcification. This was shown in an experiment on MGP knockout mice which develop spontaneous vascular calcification. Re-expression of MGP in VSMCs prevented calcification, but high circulating levels of MGP did not [60]. MGP is expressed in its inactive form as dephosphorylated-uncarboxylated MGP (dp-ucMGP) and requires serine phosphorylation and γ -glutamate carboxylation to form active p-cMGP [61]. ucMGP has five glutamic acid residues which require vitamin K for their γ -carboxylation to form five γ -carboxyglutamate (GLA) residues and produce carboxylated MGP (cMGP).

As shown in Fig. 7.3, CKD patients are often deficient in vitamin K; the prevalence and severity of vitamin K deficiency is higher in CKD than the general population for two reasons. The first, dietary restrictions in CKD that limit P intake also reduce vitamin K consumption. The second, during γ -glutamate carboxylation, vitamin K is oxidised and must be recycled by reduction for subsequent carboxylase activity; CKD patients are often prescribed warfarin (a vitamin K antagonist), which blocks the reductase pathway and prevents vitamin K recycling [62]. In addition, uraemia was shown to reduce vitamin K γ -carboxylase activity in a rat model leading to accumulation of ucMGP and calcification that was reversed by vitamin K treatment [36].

In CKD, the local expression of ucMGP in VSMCs is increased [60], however, in a state of vitamin K deficiency which often occurs in CKD, γ -glutamate carboxylation is limited, and therefore ucMGP cannot be activated and accumulates at sites where calcification has been able to proceed (Fig. 7.3) [63]. This functional vitamin K deficiency affects several mineralisation inhibitors discussed below [37].

Fetuin-A is synthesised in the liver and bone, and in healthy individuals, it is present in high levels in the circulation and plays a key role in bone remodelling [64]. Fetuin-A is taken up by VSMCs where it reduces apoptosis and is concentrated in EVs to reduce HA crystal formation [65]. The protective effect of fetuin-A against calcification was demonstrated in deficient mice which showed an increased susceptibility to widespread calcification [66]. The key role of fetuin-A is to act as a circulating calcification inhibitor by binding Ca ions and HA with high affinity to remove excess mineral from the circulation. Binding of fetuin-A and HA forms fetuin-mineral complexes, also known as calcium phosphate-containing particles (CPPs) [66]. CPPs remove Ca and P from the serum. At low concentrations, CPPs decrease inflammatory cytokine secretion, therefore protecting against ectopic calcification [66]. CPPs are quickly cleared from the blood and are not detected in serum of healthy individuals [67]. Elevated Ca and P levels in CKD provide the perfect environment for CPPs to form, and they are present at high levels [68]. As fetuin-A forms CPPs with Ca and P, a decline in GFR is correlated with decreased serum fetuin-A [69]. In CKD, clearance of CPPs from the blood is reduced, and high concentrations of CPPs remain in the circulation. High concentrations of CPPs

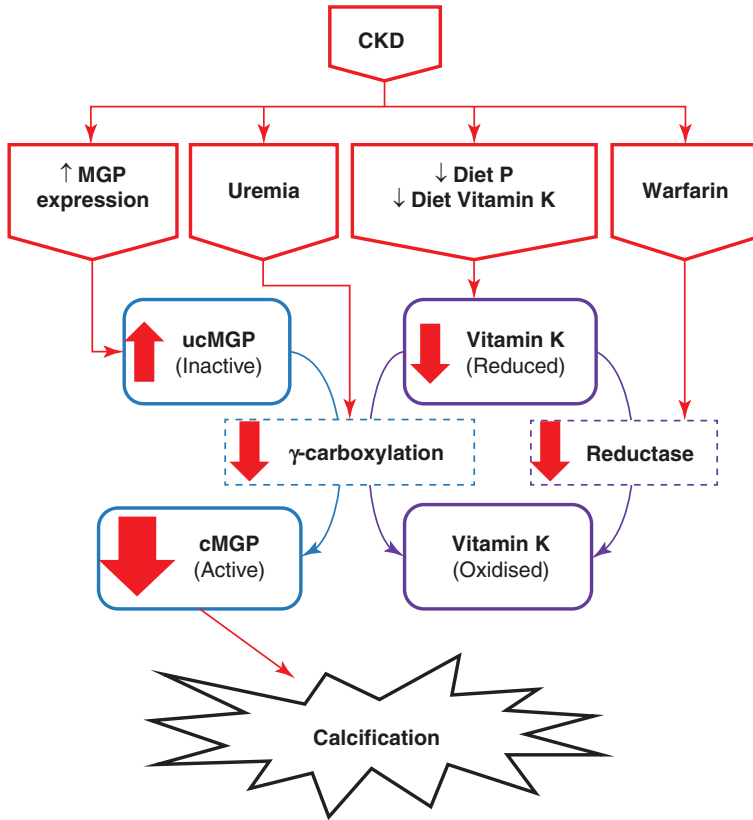


Fig. 7.3 The effect of CKD on the activation of MGP. MGP is expressed in its inactive, uncarboxylated form (ucMGP); as shown in blue, it is γ -carboxylated to active carboxylated MGP (cMGP) which inhibits calcification. The purple boxes show that vitamin K is required for γ -carboxylation; during this process vitamin K is oxidised and must be recycled by reduction for subsequent carboxylase activity. The red boxes and arrows indicate the effect of CKD on the activation of MGP. CKD increases the expression of ucMGP; however it remains and accumulates as inactive ucMGP for several reasons. The uraemic environment reduces γ -carboxylase activity. A reduced P diet advised in CKD also reduces intake of vitamin K which is required for γ carboxylation of ucMGP. Warfarin is often prescribed in CKD and impedes reductase activity and prevents the recycling of vitamin K. These factors lead to reduced levels of active cMGP and calcification ensues

stimulate inflammatory cytokines and cause apoptosis in macrophages in a dose-dependent manner; these conditions could exacerbate ectopic calcification [68, 70]. CPPs have been shown to correlate with calcification in rats with renal failure [71]. Additionally, levels of CPPs correlate with coronary artery calcification [72] and predict all-cause mortality in predialysis CKD patients [73].

Pyrophosphate is a potent endogenous inhibitor of calcification; the main source of pyrophosphate in VSMCs is the hydrolysis of adenosine triphosphate (ATP) generating AMP and pyrophosphate [46]. Pyrophosphate can also be released into extracellular fluid to inhibit mineralisation; physiological levels of 3–5 μM pyrophosphate completely inhibited VSMC calcification in rat aortas both in vitro and in vivo [74]. Pyrophosphate can be dephosphorylated and inactivated by alkaline

phosphatase (ALP), and the high levels of ALP observed in CKD catalyse the breakdown of pyrophosphate [75]. Plasma levels of pyrophosphate were found to be lower in patients on haemodialysis ($2.26 \pm 0.19 \mu\text{M}$) as compared to healthy patients ($3.26 \pm 0.17 \mu\text{M}$), and pyrophosphate was reduced by a further 32% immediately post-dialysis [26]. ALP activity and pyrophosphate hydrolysis were upregulated in aortic rings from uraemic rats as well as in aortic rings from normal rats incubated with uraemic rat plasma, suggesting that circulating factors present in uraemic plasma lead to pyrophosphate deficiency [76].

Osteopontin is another calcification inhibitor important for bone remodelling that is normally expressed in mineralised tissues such as bone and teeth [77]. Osteopontin was shown to accumulate in calcified vessels and reduces the extent of calcification *in vivo*, as MGP/osteopontin double-deficient mice had more extensive calcification than MGP single-deficient mice [78]. Post-translational phosphorylation is required for osteopontin to have an inhibitory effect on calcification [79]. As with pyrophosphate, the upregulated ALP activity observed in CKD leads to dephosphorylation and inactivation of osteopontin, reducing its effect on inhibiting calcification.

Osteoprotegerin (OPG) is a protein whose deficiency in mice has seemingly contradictory effects because it causes both osteoporosis and soft tissue calcification. OPG-deficient mice exhibit a decrease in bone density and mass and at the same time medial calcification of the aorta and renal arteries [80]. OPG is a secreted factor that decreases osteoclast activity by inhibiting receptor activator of nuclear factor kappa B ligand (RANKL) activation of its receptor RANK. This signalling is essential for the maturation of osteoclast progenitors [81], thus the increased bone resorption and osteoporosis in its absence. OPG is endogenously expressed in the media of the aorta [80], but the mechanisms by which it inhibits vascular calcification are yet unknown. However, increased levels of serum OPG were shown to correlate with vascular calcification and associate with negative cardiovascular outcomes in CKD patients [82–84]. Circulating levels of OPG are increased in pre-dialysis, dialysis and post-transplant CKD patients, suggesting that OPG is upregulated in vascular injury in kidney disease [85].

Bone morphogenetic protein 7 (BMP-7), a member of the TGF β superfamily, is an example of an inhibitor of vascular calcification. BMP-7 deficient mice, however, do not have a vascular or soft tissue calcification phenotype. Mice lacking BMP-7 show skeletal abnormalities, delayed ossification of bones as well as kidney and eye defects [86]. Polymorphisms in the BMP-7 gene have been linked to inverse relationships between bone mineralisation and vascular calcification in the coronary and carotid arteries and abdominal aorta in diabetes patients [87]. BMP-7 has also been shown to play a role in VSMC differentiation and maintaining their differentiated phenotype *in vitro* [88]. Moreover, intraperitoneal injection of BMP-7 prevented vascular calcification in a mouse model of CKD [89]. Interestingly, BMP-7 has been shown to be decreased in the kidneys of CKD patients leading to aggravation of fibrosis. Exogenous administration or transgenic overexpression of BMP-7 has been shown to have beneficial anti-fibrogenic effects in rodent models of CKD suggesting that there is therapeutic potential for BMP-7 treatment in CKD patients [90].

Several other factors (SMAD6, fibrillin-1 and carbonic anhydrase II) have been linked to preventing soft tissue mineralisation [91–93]. However, their effects have not been studied in the context of vascular calcification in CKD.

Osteo/Chondrogenic Differentiation

VSMCs, osteocytes, chondrocytes and adipocytes, are all derived from mesenchymal stem cells. The terminal differentiation of these stem cells is dependent on the paracrine and autocrine factors in the microenvironment [94]. VSMCs have great phenotypic plasticity and can dedifferentiate into mesenchymal-like cells; this is important during cell stress and in vascular repair. VSMCs may either proliferate and aid in repair or in pathological conditions, reach senescence or undergo an osteo/chondrocyte phenotypic change [95].

The high levels of P observed in CKD drive cellular stress and osteo/chondrocytic differentiation; the type III sodium-dependent P transporters, PiT-1 and PiT-2, play a key role in modulating this in VSMCs. It has been demonstrated in mouse models that PiT-1 promotes vascular calcification by both P uptake-dependent and P uptake-independent functions and PiT-1 played a key role despite the required P concentration to induce cellular stress being well above the maximal P intake [96]. On the other hand, PiT-2 protects against P-induced vascular calcification; PiT-2 deficient VSMCs were found to have lower levels of OPG and increased calcification [97].

Osteo/chondrocytic differentiation of contractile VSMCs involves the downregulation of VSMC markers; α -SMC actin, SM22 α and myocardin along with upregulation of osteo/chondrocytic genes; including osterix, ALP, osteopontin, type 1 collagen and osteocalcin [53]. Expression of these genes are regulated by osteogenic transcription factors Runx2 and Sox9, which are also upregulated in calcified vessels and in VSMCs that spontaneously calcify [98]. A cell lineage study in mice lacking the calcification inhibitor MGP found that 97% of calcifying cells in the tunica media were derived from VSMCs, which had early upregulation of Runx2 and downregulation of myocardin [99]. Notably the osteo/chondrocytic differentiation preceded calcification. Similarly, in human arteries with arteriosclerosis, evidence of osteo/chondrocytic differentiation was observed; this included upregulation of ALP along with other osteogenic markers such as bone gla protein (BGP), bone sialoprotein (BSP) and collagen II [100]. As discussed above, ALP is a hydroxylase enzyme that dephosphorylates calcification inhibitors, pyrophosphate and osteopontin, deeming them inactive and promoting calcification [46, 79]. In vitro co-expression of ALP and collagen I was sufficient to induce mineralisation in high P medium [101]. The tunica media has a collagen-rich matrix; therefore this suggests that the dysregulated mineral metabolism and increased ALP activity observed in CKD would be enough to enable ECM mineralisation in the vasculature.

Ageing-Related DNA Damage and Senescence

As discussed above, Klotho is a cofactor of FGF23, and lower levels of Klotho observed in CKD contribute to disrupted mineral metabolism and aggravate vascular calcification [102, 103]. Importantly, mice deficient in Klotho, FGF23 and Memo, another regulator of FGF23 signalling, exhibit symptoms resembling accelerated ageing, including a short lifespan, infertility, skin atrophy, osteoporosis and calcification of the aorta and other arteries, accompanied by intimal thickening [6, 104, 105]. In addition, ectopic calcification of various organs is observed [104]. In humans, a homozygous Klotho mutation causes tumoural calcinosis, which manifests itself with carotid and dural artery calcifications and ectopic calcifications of soft tissues [102]. Decreased Klotho levels have been observed in calcified arteries showing its important role in inhibiting vascular calcification [106]. Additionally, elevated P is associated with increased cardiovascular calcification and mortality in ageing populations [107]. These studies show a link between ageing and increased calcification, and increased P is the common denominator. Increased P has been shown to contribute to ageing-related processes [108]; it is therefore no surprise that excess P in CKD has been found to promote premature ageing [109, 110].

Ageing is a series of time-related, degenerative processes beginning in adulthood that eventually end life [111]. It is now accepted that ageing is caused in part by the accumulation of genetic damage throughout life [111, 112]. The DNA damage response (DDR) signalling network is essential in the maintenance of genomic stability, via the initiation and coordination of DNA repair mechanisms with appropriate cell cycle arrest checkpoints. This evolutionarily conserved signalling cascade has two distinct but coordinated functions: it prevents or arrests the duplication and partitioning of damaged DNA into daughter cells to impede the propagation of corrupted genetic information, and it coordinates cellular efforts to repair DNA damage and maintain genome integrity [113–115].

DNA damage has been shown to accumulate during ageing both in humans and rodents [116–119]. Aside from increased occurrence of DNA lesion development, elevated levels of DNA damage are also a consequence of a decline in efficiency of DNA repair pathways [112]. Collectively, spontaneous mutations and DNA damage gradually impair the function of genes involved in stress responses and DNA repair. DNA repair becomes less efficient and more error-prone leading to cascading accumulation of DNA damage and mutations, which further exacerbate age-related physiological decline.

The most prominent examples of how accumulated DNA damage and defective DNA repair pathways affect the organism are segmental progeroid syndromes, diseases in which multiple phenotypes generally associated with normal ageing appear prematurely. It now appears that most, if not all, human premature ageing diseases are caused by heritable mutations in genes affecting genome maintenance either directly or indirectly: Hutchinson-Gilford progeria [116], Werner syndrome [117], ataxia telangiectasia [120], Nijmegen breakage syndrome [118], trichothiodystrophy [119], Bloom syndrome [121] and Cockayne syndrome [122].

Unsuccessful or insufficient DNA damage repair can have two consequences for the cell: apoptosis or cellular senescence. Senescent cells cease dividing, are resistant to apoptosis and undergo distinctive phenotypic alterations [111, 123], such as expression of p16^{INK4a} [124], increased senescence-associated β -galactosidase activity [125] and secretion of a bioactive senescence-associated secretory phenotype (SASP) consisting of inflammatory cytokines, chemokines, growth factors and proteases [126, 127]. Unlike apoptotic cells, which are rapidly removed, senescent cells remain viable and continue to contribute to tissue stress responses long after the onset of senescence [128].

Vascular ageing lies at the heart of vascular calcification, and recent evidence points to the role of DNA damage in vascular ageing pathologies. Many cancer treatments, which are known to induce DNA damage, carry a risk of late effects including cardiovascular diseases [129]. The segmental progeroid syndromes, Hutchinson-Gilford progeria syndrome (HGPS) [130] and Werner syndrome [131] exhibit age-related phenotypes in the vasculature. HGPS is caused by a mutation in the lamin A/C (*LMNA*) gene that leads to the accumulation of a truncated form of prelamin A, referred to as progerin [132], which leads to the accumulation of DNA damage and senescence [133]. As a result, HGPS patients show premature atherosclerosis/arteriosclerosis, characterised by VSMC degeneration and calcification [134]. The same mechanism involving prelamin A and senescence has been shown to promote calcification in vessels of children on dialysis [133], as uraemic conditions promote DNA damage via oxidative stress [135]. Senescent VSMCs from children and adults on dialysis have been shown to have all the hallmarks of aged cells, with DNA damage accumulation and the SASP, which promotes calcification [109, 110, 133]. Moreover, elevated levels of SASP factors such as BMP2 and IL6 have been detected in the serum of both children and adults on dialysis correlating with calcification [109]. The link between CKD and DNA damage-induced senescence is further illustrated by studies showing that uraemic toxins; indoxyl sulphate and p-cresyl sulphate induce VSMC senescence (increased p16^{INK4a} and prelamin A expression) and calcification, in vitro and in a rat model of CKD [136, 137].

DNA damage and senescence also drive osteogenic differentiation of VSMCs, and inhibition of DNA damage signalling can block calcification [133, 138]. Intriguingly, poly ADP ribose polymerases (PARP), components of the DDR, have been shown to promote calcification, as poly ADP ribose (PAR), their product, whose synthesis is increased with DNA damage, has the ability to concentrate Ca and P forming the direct nidus for mineralisation [139]. PARP inhibitors can block VSMC calcification in a rat model of CKD [140] which further supports the conclusion that vascular calcification in CKD is linked to premature ageing [141, 142]. What remains unclear is how the presence of uraemic toxins and increased P leads to DNA damage. The most likely culprit is oxidative stress, as it is induced both by uraemic toxins and high P, it has also been shown to induce DNA damage in the vasculature [108, 143, 144]. Oxidative stress is discussed further in the following section.

Inflammation

The hallmarks of inflammation in the vessel wall include increased expression of TNF α , IL1 β , IL6, IL8, monocyte chemoattractant protein 1 (MCP1), OPG and intracellular adhesion molecule-1 (ICAM-1) by VSMCs [109, 133] and recruitment of leukocytes [136]. Although the acute release of pro-inflammatory cytokines is beneficial, sustained release is detrimental and leads to vessel remodelling. TNF α can induce mineralisation of calcifying VSMCs in vitro [145, 146]. Pro-inflammatory cytokines also increase the synthesis of CRP from the liver [147]. CRP may also be a direct vascular toxin, as CRP and complement activation have been detected in atherosclerotic lesions [148].

Numerous factors have been identified in CKD that promote vascular calcification by triggering inflammatory responses; this includes senescence and CPPs (as discussed above), as well as advanced glycation end products (AGEs), lipids, oxidative stress, ER stress bacterium and HA itself.

AGEs are formed via a non-enzymatic glycosylation reaction between glucose and proteins; they usually form as a result of hyperglycaemia; however, they are also increased in nondiabetic patients with uraemia [149]. AGEs have many detrimental effects, including accelerating atherosclerosis. AGEs trigger an inflammatory response by interacting with their receptors, which are expressed by a wide range of tissues. This interaction leads to oxidative stress and increased secretion of cytokines and inflammatory factors, such as ICAM-1, TNF α , IL-6 and others, the exact response depending on the cell type and receptors involved. Therefore, unsurprisingly, AGEs have been shown to induce vascular calcification [150].

Patients with CKD are at risk of metabolic syndrome and dyslipidaemia. Hyperlipidaemia is a major cardiovascular risk factor [136, 151, 152]; it can induce oxidative stress and lends itself to loading of cholesterol (in the form of LDL) into VSMCs. Cholesterol promotes both VSMC osteogenic differentiation and VSMC differentiation into macrophage-like cells; therefore it directly contributes to vascular calcification and amplifies the inflammatory responses in the vasculature [153–156].

Oxidative stress is another inducer of inflammation in VSMCs; as mentioned above, oxidative stress can be triggered by AGEs and hyperlipidaemia as well as by uraemia itself; therefore it is a common occurrence in CKD [157, 158] [157]. Oxidative stress is caused by an imbalance between enzymes producing and scavenging reactive oxygen species (ROS) leading to accumulation of ROS. Oxidative stress has been shown to induce TNF α and activate NF κ B signalling, which leads to the production of further inflammatory factors such as MCP-1, IL-1 β and TGF β [157]. Oxidative stress-induced inflammation ultimately leads to osteogenic differentiation and calcification of VSMCs.

The common occurrence of oxidative stress along with the perturbations in Ca homeostasis that are observed in CKD can activate ER stress. ER stress is a cellular stress response that leads to activation of the unfolded protein response, a set of signalling pathways starting with three ER-resident ER stress transducers, IRE1,

PERK and ATF6, which sense ER stress [159]. Activation of the unfolded protein response leads to increased transcription of genes that help resolve ER stress, such as chaperones Grp78, Grp94 and proteins involved in ER biogenesis. It can also lead to apoptosis if the ER stress is persistent and unresolved [160]. ER stress has been shown to mediate vascular calcification [161] by promoting apoptosis and osteogenic differentiation of VSMCs [162, 163]. Importantly, ER stress has been shown to mediate calcification induced by uraemia-related factors in vitro such as lipids [164–167], AGEs, hyperphosphataemia and TNF α [145, 168] and in a rat model of CKD induced by 5/6 nephrectomy [145]. ER stress is also implicated in metabolic syndrome [169].

Finally, recent evidence suggests that sterile inflammation might not be the whole story. *Porphyromonas gingivalis*, a bacterium behind periodontal disease, has been implicated in many diseases of ageing, including CKD [170]. Although the exact mechanism of this is unclear, *P. gingivalis* can enter the bloodstream and increase the inflammation load in the body, thus contributing to disease processes that are worsened by inflammation. Recent studies suggest that this pathogen can promote VSMC calcification in vitro [171–173].

After calcification has occurred, the resulting HA has been shown to further increase inflammation by inducing IL1 β and TNF α secretion in macrophages [174–176]. HA also induces apoptosis and promotes osteogenic differentiation further contributing to a pro-calcific environment in the vessel wall and exacerbating calcification [177–180].

Treatment Strategies

Treatments to Reduce the Risk Factors of Calcification

A specific therapy to prevent vascular calcification has not yet been found, and current treatment strategies focus on regulating the Ca and P balance and reducing secondary hyperparathyroidism (Fig. 7.4). Patients with CKD are often advised to take a low P diet; they may be treated with P-binders or vitamin B3 derivatives that modulate intestinal PiT-2 to reduce P absorption [181]. Current therapies to treat SHPT and reduce the risks of CKD-BMD also include vitamin D receptor activators (VDRAs), calcimimetics and parathyroidectomy [182].

P-binders are routinely prescribed to patients with ESKD. There are many different types of P-binders; they bind P in the gastrointestinal tract and reduce P absorption. Ca-based P-binders such as calcium acetate and calcium carbonate are effective in lowering phosphataemia; however, they are associated with raised serum Ca and increased risk of cardiovascular calcification [183, 184]. Meta-analysis showed that non-Ca-based P-binders such as sevelamer showed a significant decrease in hypercalcaemia compared to Ca-based P-binders; however, they were less effective at lowering P and PTH levels, they had increased risk of gastrointestinal adverse events and there was no difference in all-cause mortality [185].

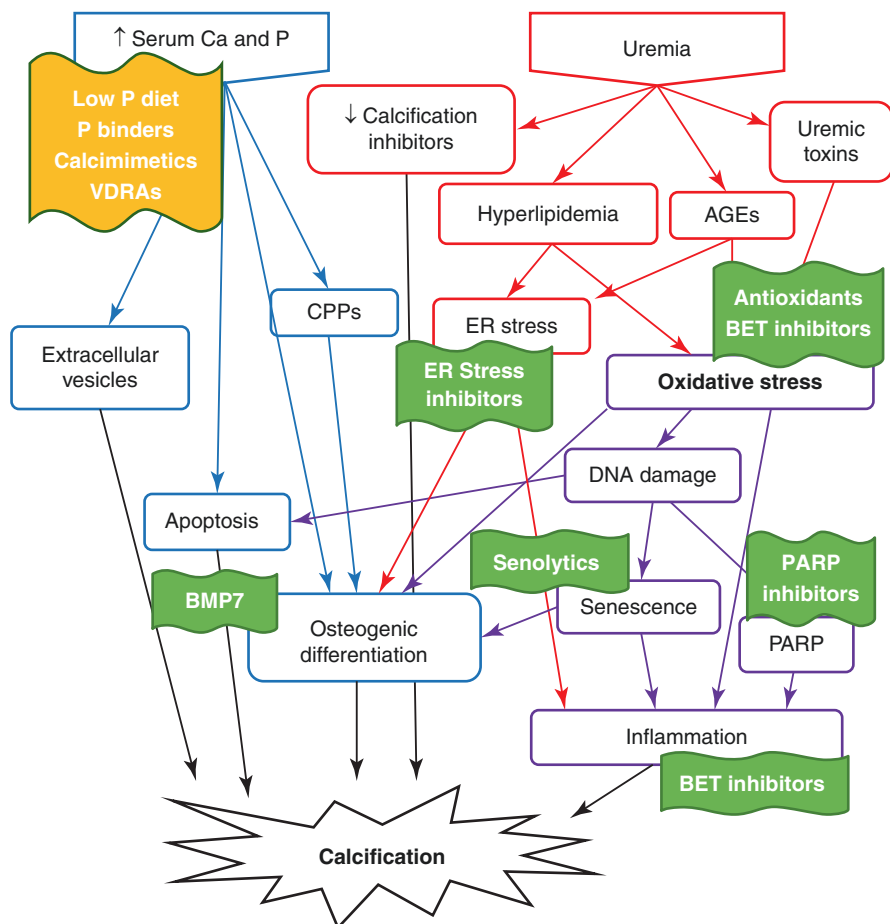


Fig. 7.4 Treatment strategies for calcification in CKD. Treatments shown in the yellow shape are in clinical use and all potential treatments are shown in green shapes. CKD patients are often advised to have a low P diet along with P binders, calcimimetics or VDRA to prevent secondary hyperparathyroidism and prevent elevated Ca and P levels which are key risk factors for calcification. The individual mechanisms of calcification can also be directly targeted, for example by antioxidants, ER stress inhibitors, BET inhibitors, PARP inhibitors, senolytics or BMP-7

New non-Ca-based P-binders with improved safety and tolerability are required. Several studies both in rats and CKD patients have shown that bicalomer is as effective as sevelamer at correcting hyperphosphataemia but has fewer gastrointestinal side effects [186–189]. P-binders are not routinely used in the early stages of CKD where FGF-23 is increased to compensate for dysregulated mineral metabolism and prevent hyperphosphataemia; however, a rise in FGF-23 is associated with progression of CKD-BMD and calcification [184]. A randomised control trial to investigate the effectiveness of P-binders in patients with moderate to advanced CKD and normal phosphataemia found that all three P-binders reduced serum P and slowed

down progression of secondary hyperparathyroidism; however, they also increased vascular calcification highlighting the potential time-dependency of any treatment strategy [190].

In patients with ESRD, hyperphosphataemia is also managed by dialysis treatment, which helps to remove uraemic toxins including excess P. P-clearance can be improved by extending dialysis treatment times, increasing frequency of treatment or improving dialysis technique such as with haemodiafiltration [191]. Preserving residual renal function (RRF) has been shown to reduce cardiovascular events and improve long-term survival in CKD patients. Peritoneal dialysis is associated with a slower decrease in RRF than haemodialysis; in fact loss of RRF is 24–80% higher in haemodialysis than in peritoneal dialysis; therefore peritoneal dialysis is thought to provide better P control [192, 193].

Cinacalcet is a type II calcimimetic; it is an allosteric activator of the Ca receptor and increases sensitivity to extracellular Ca; therefore it decreases secretion of PTH. Multiple studies have shown that in CKD patients on dialysis, cinacalcet reduces circulating levels of PTH, Ca, P and HA and prevented the progression of vascular and cardiac valve calcification [194, 195]. VSMCs also express the CaR, and studies in vitro suggest the drug may also directly impact on cell phenotype.

Vitamin D deficiency in CKD exacerbates the disrupted mineral metabolism; many patients particularly children are prescribed VDRA to prevent secondary hyperparathyroidism and CKD-BMD [14]. The direct effect of VDRA on vascular calcification is controversial in the literature, and in children on dialysis both high and low levels of vitamin D were associated with increased carotid intima thickness and vascular calcification [23]. This suggests that vitamin D has a bimodal effect on calcification and there is a narrow physiological range where VDRA are beneficial to vascular calcification in CKD patients.

Treatments to Directly Target Calcification

There is an extensive and growing understanding of the mechanisms involved in the development of vascular calcification; this opens the door to new therapies that directly target mechanisms of calcification such as inflammation and senescence (Fig. 7.4).

Bromodomain and extra-terminal (BET) proteins play a key role in epigenetics; they bind acetylated lysines on chromatin to regulate gene transcription. A clinical study in CKD patients treated with the BET inhibitor apabetalone found that a single dose countered the activation of multiple risk factors associated with calcification in CKD, including inflammation, oxidative stress and endothelial dysfunction [196]. CKD patients treated with apabetalone also had reduced expression of the calcification risk factor ALP, were less likely to experience cardiovascular events and had an improved GFR. BET proteins are a potential novel therapeutic for CKD that would target multiple systems that are disrupted and contribute to ectopic calcification in CKD [197].

The association of senescence with age-related diseases suggests it may be beneficial to specifically target senescent cells therapeutically. These strategies consist of senolysis, immune-mediated senescent cell clearance and SASP neutralisation. Senolytics are drugs that can specifically eliminate senescent cells. Senolytics have been shown to eliminate senescent cells *in vivo* and have beneficial effects in models of ageing and age-related disease [198, 199]; however, whether they inhibit vascular calcification has not yet been examined. In addition, drugs that target the DDR may also be effective in treating calcification, in particular PARP inhibitors [139].

Summary

There are a multitude of risk factors for ectopic calcification in CKD that arise from the uraemic environment and build-up of uraemic toxins; a progressively disrupted mineral metabolism develops, which is further complicated by dietary restrictions and prescribed medication. Vascular calcification is well studied in the CKD cohort as these patients are at risk via a multitude of detrimental mechanisms. This growing body of knowledge continues to improve the understanding and management of the condition and paves the way for the development of new treatment strategies.

References

1. Levey AS, Eckardt K-U, Tsukamoto Y, Levin A, Coresh J, Rossert J, et al. Definition and classification of chronic kidney disease: a position statement from Kidney Disease: Improving Global Outcomes (KDIGO). *Kidney Int.* 2005;67(6):2089–100.
2. Go AS, Chertow GM, Fan D, McCulloch CE, Hsu C-Y. Chronic kidney disease and the risks of death, cardiovascular events, and hospitalization. *N Engl J Med.* 2004;351(13):1296–305.
3. Foley RN, Parfrey PS, Sarnak MJ. Epidemiology of cardiovascular disease in chronic renal disease. *J Am Soc Nephrol.* 1998;9(12 Suppl):S16–23.
4. Shroff R, Long DA, Shanahan C. Mechanistic insights into vascular calcification in CKD. *J Am Soc Nephrol.* 2013;24(2):179–89.
5. Kuro-o M. Overview of the FGF23-Klotho axis. *Pediatr Nephrol.* 2010;25(4):583–90.
6. Shimada T, Kakitani M, Yamazaki Y, Hasegawa H, Takeuchi Y, Fujita T, et al. Targeted ablation of Fgf23 demonstrates an essential physiological role of FGF23 in phosphate and vitamin D metabolism. *J Clin Invest.* 2004;113(4):561–8.
7. Shimada T, Hasegawa H, Yamazaki Y, Muto T, Hino R, Takeuchi Y, et al. FGF-23 is a potent regulator of vitamin D metabolism and phosphate homeostasis. *J Bone Miner Res.* 2004;19(3):429–35.
8. Mazzaferro S, Pasquali M, Pirro G, Rotondi S, Tartaglione L. The bone and the kidney. *Arch Biochem Biophys.* 2010;503(1):95–102.
9. Hu MC, Kuro-o M, Moe OW. Secreted klotho and chronic kidney disease. *Adv Exp Med Biol.* 2012;728:126–57.
10. John GB, Cheng CY, Kuro-o M. Role of Klotho in aging, phosphate metabolism, and CKD. *Am J Kidney Dis.* 2011;58(1):127–34.
11. DeLuca HF. The vitamin D story: a collaborative effort of basic science and clinical medicine. *FASEB J.* 1988;2(3):224–36.

12. Holick MF. Vitamin D deficiency. *N Engl J Med.* 2007;357(3):266–81.
13. Turner AG, Hanrath MA, Morris HA, Atkins GJ, Anderson PH. The local production of 1,25(OH)D promotes osteoblast and osteocyte maturation. *J Steroid Biochem Mol Biol.* 2013;
14. Brown AJ, Dusso AS, Slatopolsky E. Vitamin D analogues for secondary hyperparathyroidism. *Nephrol Dial Transplant.* 2002;17 Suppl 10:10–9.
15. Souberbielle J-CP, Roth H, Fouque DP. Parathyroid hormone measurement in CKD. *Kidney Int.* 2009;77(2):93–100.
16. Koeppen BM, Stanton BA. *Berne and levy physiology*: Elsevier; 2010.
17. Moe SM, Chen NX, Seifert MF, Sindors RM, Duan D, Chen X, et al. A rat model of chronic kidney disease-mineral bone disorder. *Kidney Int.* 2009;75(2):176–84.
18. Hruska KA, Mathew S, Lund R, Qiu P, Pratt R. Hyperphosphatemia of chronic kidney disease. *Kidney Int.* 2008;74(2):148–57.
19. Tonelli M, Sacks F, Pfeffer M, Gao Z, Curhan G. Relation between serum phosphate level and cardiovascular event rate in people with coronary disease. *Circulation.* 2005;112(17):2627–33.
20. Tentori F, Blayney MJ, Albert JM, Gillespie BW, Kerr PG, Bommer J, et al. Mortality risk for dialysis patients with different levels of serum calcium, phosphorus, and PTH: the Dialysis Outcomes and Practice Patterns Study (DOPPS). *Am J Kidney Dis.* 2008;52(3):519–30.
21. Shroff R. Phosphate is a vascular toxin. *Pediatr Nephrol.* 2012;28(4):583–93.
22. Pepe J, Diacinti D, Fratini E, Nofroni I, D'Angelo A, Pilotto R, et al. High prevalence of abdominal aortic calcification in patients with primary hyperparathyroidism as evaluated by Kauppila score. *Eur J Endocrinol.* 2016;175(2):95–100.
23. Shroff R, Egerton M, Bridel M, Shah V, Donald AE, Cole TJ, et al. A bimodal association of vitamin D levels and vascular disease in children on dialysis. *J Am Soc Nephrol.* 2008;19(6):1239–46.
24. Chen NX, O'Neill KD, Duan D, Moe SM. Phosphorus and uremic serum up-regulate osteopontin expression in vascular smooth muscle cells. *Kidney Int.* 2002;62(5):1724–31.
25. Liabeuf S, Cheddani L, Massy ZA. Uremic toxins and clinical outcomes: the impact of kidney transplantation. *Toxins.* 2018;10(6).
26. Lomashvili KA, Khawandi W, O'Neill WC. Reduced plasma pyrophosphate levels in hemodialysis patients. *J Am Soc Nephrol.* 2005;16(8):2495–500.
27. Kovesdy CP, Ureche V, Lu JL, Kalantar-Zadeh K. Outcome predictability of serum alkaline phosphatase in men with pre-dialysis CKD. *Nephrol Dial Transplant.* 2010;25(9):3003–11.
28. Regidor DL, Kovesdy CP, Mehrotra R, Rambod M, Jing J, McAllister CJ, et al. Serum alkaline phosphatase predicts mortality among maintenance hemodialysis patients. *J Am Soc Nephrol.* 2008;19(11):2193–203.
29. Caravaca-Fontan F, Azevedo L, Bayo MA, Gonzales-Candia B, Luna E, Caravaca F. High levels of both serum gamma-glutamyl transferase and alkaline phosphatase are independent predictors of mortality in patients with stage 4-5 chronic kidney disease. *Nefrologia.* 2017;37(3):267–75.
30. Klag MJ, Whelton PK, Randall BL, Neaton JD, Brancati FL, Ford CE, et al. Blood pressure and end-stage renal disease in men. *N Engl J Med.* 1996;334(1):13–8.
31. Tastet L, Capoulade R, Clavel MA, Larose E, Shen M, Dahou A, et al. Systolic hypertension and progression of aortic valve calcification in patients with aortic stenosis: results from the PROGRESSA study. *Eur Heart J Cardiovasc Imaging.* 2017;18(1):70–8.
32. Lehmann N, Erbel R, Mahabadi AA, Kalsch H, Mohlenkamp S, Moebus S, et al. Accelerated progression of coronary artery calcification in hypertension but also prehypertension. *J Hypertens.* 2016;34(11):2233–42.
33. Rysz J, Franczyk B, Ciałkowska-Rysz A, Gluba-Brzózka A. The effect of diet on the survival of patients with chronic kidney disease. *Nutrients.* 2017;9(5):495.
34. Holden RM, Morton AR, Garland JS, Pavlov A, Day AG, Booth SL. Vitamins K and D status in stages 3–5 chronic kidney disease. *Clin J Am Soc Nephrol.* 2010;5(4):590–7.
35. Cozzolino M, Mangano M, Galassi A, Ciceri P, Messa P, Nigwekar S. Vitamin K in chronic kidney disease. *Nutrients.* 2019;11(1):168.

36. Kaesler N, Magdeleyns E, Herfs M, Schettgen T, Brandenburg V, Fliser D, et al. Impaired vitamin K recycling in uremia is rescued by vitamin K supplementation. *Kidney Int.* 2014;86(2):286–93.
37. Fusaro M, Tripepi G, Noale M, Plebani M, Zaninotto M, Piccoli A, et al. Prevalence of vertebral fractures, vascular calcifications, and mortality in warfarin treated hemodialysis patients. *Curr Vasc Pharmacol.* 2015;13(2):248–58.
38. Moe SM, Chen NX. Inflammation and vascular calcification. *Blood Purif.* 2005;23(1):64–71.
39. Kimmel PL, Phillips TM, Simmens SJ, Peterson RA, Weihs KL, Alleyne S, et al. Immunologic function and survival in hemodialysis patients. *Kidney Int.* 1998;54(1):236–44.
40. Barreto DV, Barreto FC, Liabeuf S, Temmar M, Lemke HD, Tribouilloy C, et al. Plasma interleukin-6 is independently associated with mortality in both hemodialysis and pre-dialysis patients with chronic kidney disease. *Kidney Int.* 2010;77(6):550–6.
41. Miyamoto T, Carrero JJ, Stenvinkel P. Inflammation as a risk factor and target for therapy in chronic kidney disease. *Curr Opin Nephrol Hypertens.* 2011;20(6):662–8.
42. Oh J, Wunsch R, Turzer M, Bahner M, Raggi P, Querfeld U, et al. Advanced coronary and carotid arteriopathy in young adults with childhood-onset chronic renal failure. *Circulation.* 2002;106(1):100–5.
43. Hwang IC, Park HE, Kim HL, Kim HM, Park JB, Yoon YE, et al. Systemic inflammation is associated with coronary artery calcification and all-cause mortality in chronic kidney disease. *Circ J.* 2016;80(7):1644.
44. Stompor T, Pasowicz M, Sulłowicz W, Dembinska-Kiec A, Janda K, Wojcik K, et al. An association between coronary artery calcification score, lipid profile, and selected markers of chronic inflammation in ESRD patients treated with peritoneal dialysis. *Am J Kidney Dis.* 2003;41(1):203–11.
45. Schlieper G, Aretz A, Verberckmoes SC, Kruger T, Behets GJ, Ghadimi R, et al. Ultrastructural analysis of vascular calcifications in uremia. *J Am Soc Nephrol.* 2010;21(4):689–96.
46. Villa-Bellosta R, Egido J. Phosphate, pyrophosphate, and vascular calcification: a question of balance. *Eur Heart J.* 2017;38(23):1801–4.
47. Blacher J, London GM, Safar ME, Mourad JJ. Influence of age and end-stage renal disease on the stiffness of carotid wall material in hypertension. *J Hypertens.* 1999;17(2):237–44.
48. McIntyre CW. Calcium balance during hemodialysis. *Semin Dial.* 2008;21(1):38–42.
49. Gross ML, Meyer HP, Ziebart H, Rieger P, Wenzel U, Amann K, et al. Calcification of coronary intima and media: immunohistochemistry, backscatter imaging, and x-ray analysis in renal and nonrenal patients. *Clin J Am Soc Nephrol.* 2007;2(1):121–34.
50. Shroff RC, McNair R, Figg N, Skepper JN, Schurgers L, Gupta A, et al. Dialysis accelerates medial vascular calcification in part by triggering smooth muscle cell apoptosis. *Circulation.* 2008;118(17):1748–57.
51. Duer MJ, Friscic T, Proudfoot D, Reid DG, Schoppet M, Shanahan CM, et al. Mineral surface in calcified plaque is like that of bone: further evidence for regulated mineralization. *Arterioscler Thromb Vasc Biol.* 2008;28(11):2030–4.
52. Hutcheson JD, Goettsch C, Bertazzo S, Maldonado N, Ruiz JL, Goh W, et al. Genesis and growth of extracellular-vesicle-derived microcalcification in atherosclerotic plaques. *Nat Mater.* 2016;15(3):335–43.
53. Shanahan CM, Crouthamel MH, Kapustin A, Giachelli CM. Arterial calcification in chronic kidney disease: key roles for calcium and phosphate. *Circ Res.* 2011;109(6):697–711.
54. Proudfoot D, Skepper JN, Hegyi L, Bennett MR, Shanahan CM, Weissberg PL. Apoptosis regulates human vascular calcification in vitro: evidence for initiation of vascular calcification by apoptotic bodies. *Circ Res.* 2000;87(11):1055–62.
55. Shroff RC, McNair R, Skepper JN, Figg N, Schurgers LJ, Deanfield J, et al. Chronic mineral dysregulation promotes vascular smooth muscle cell adaptation and extracellular matrix calcification. *J Am Soc Nephrol.* 2010;21(1):103–12.

56. Kapustin AN, Davies JD, Reynolds JL, McNair R, Jones GT, Sidibe A, et al. Calcium regulates key components of vascular smooth muscle cell-derived matrix vesicles to enhance mineralization. *Circ Res.* 2011;109(1):e1–e12.
57. Anderson HC. Matrix vesicles and calcification. *Curr Rheumatol Rep.* 2003;5(3):222–6.
58. Kapustin AN, Schoppet M, Schurgers LJ, Reynolds JL, McNair R, Heiss A, et al. Prothrombin loading of vascular smooth muscle cell-derived exosomes regulates coagulation and calcification. *Arterioscler Thromb Vasc Biol.* 2017;37(3):e22–32.
59. Reynolds JL, Joannides AJ, Skepper JN, McNair R, Schurgers LJ, Proudfoot D, et al. Human vascular smooth muscle cells undergo vesicle-mediated calcification in response to changes in extracellular calcium and phosphate concentrations: a potential mechanism for accelerated vascular calcification in ESRD. *J Am Soc Nephrol.* 2004;15:2857–67.
60. Krueger T, Westenfeld R, Ketteler M, Schurgers LJ, Floege J. Vitamin K deficiency in CKD patients: a modifiable risk factor for vascular calcification? *Kidney Int.* 2009;76(1):18–22.
61. Epstein M. Matrix Gla-Protein (MGP) not only inhibits calcification in large arteries but also may be renoprotective: connecting the dots. *EBioMedicine.* 2016;4:16–7.
62. Wuyts J, Dhondt A. The role of vitamin K in vascular calcification of patients with chronic kidney disease. *Acta Clin Belg.* 2016;71(6):462–7.
63. Cranenburg EC, Vermeer C, Koos R, Boumans ML, Hackeng TM, Bouwman FG, et al. The circulating inactive form of matrix Gla Protein (ucMGP) as a biomarker for cardiovascular calcification. *J Vasc Res.* 2008;45(5):427–36.
64. Brylka L, Jahnen-Dechent W. The role of fetuin-A in physiological and pathological mineralization. *Calcif Tissue Int.* 2013;93(4):355–64.
65. Reynolds JL, Skepper JN, McNair R, Kasama T, Gupta K, Weissberg PL, et al. Multifunctional roles for serum protein fetuin-a in inhibition of human vascular smooth muscle cell calcification. *J Am Soc Nephrol.* 2005;16(10):2920–30.
66. Paloian NJ, Giachelli CM. A current understanding of vascular calcification in CKD. *Am J Physiol Renal Physiol.* 2014;307(8):F891–900.
67. Smith ER, Cai MM, McMahon LP, Pedagogos E, Toussaint ND, Brumby C, et al. Serum fetuin-A concentration and fetuin-A-containing calciprotein particles in patients with chronic inflammatory disease and renal failure. *Nephrology.* 2013;18(3):215–21.
68. Smith ER, Ford ML, Tomlinson LA, Rajkumar C, McMahon LP, Holt SG. Phosphorylated fetuin-A-containing calciprotein particles are associated with aortic stiffness and a procalcific milieu in patients with pre-dialysis CKD. *Nephrol Dialy Transpl.* 2012;27(5):1957–66.
69. Zhan JL, Liang JB, Wang ZB. Relations of fetuin-A with estimated glomerular filtration rate and carotid artery calcification in patients with chronic kidney disease. *Nan Fang Yi Ke Da Xue Xue Bao.* 2013;33(11):1689–91.
70. Viegas CSB, Santos L, Macedo AL, Matos AA, Silva AP, Neves PL, et al. Chronic kidney disease circulating calciprotein particles and extracellular vesicles promote vascular calcification: a role for GRP (Gla-Rich Protein). *Arterioscler Thromb Vasc Biol.* 2018;38(3):575–87.
71. Matsui I, Hamano T, Mikami S, Fujii N, Takabatake Y, Nagasawa Y, et al. Fully phosphorylated fetuin-A forms a mineral complex in the serum of rats with adenine-induced renal failure. *Kidney Int.* 2009;75(9):915–28.
72. Hamano T, Matsui I, Mikami S, Tomida K, Fujii N, Imai E, et al. Fetuin-mineral complex reflects extraosseous calcification stress in CKD. *J Am Soc Nephrol.* 2010;21(11):1998–2007.
73. Smith ER, Ford ML, Tomlinson LA, Bodenham E, McMahon LP, Farese S, et al. Serum calcification propensity predicts all-cause mortality in predialysis CKD. *J Am Soc Nephrol.* 2014;25(2):339–48.
74. Villa-Bellosta R, Sorribas V. Calcium phosphate deposition with normal phosphate concentration. -Role of pyrophosphate. *Circ J.* 2011;75(11):2705–10.
75. Schoppet M, Shanahan CM. Role for alkaline phosphatase as an inducer of vascular calcification in renal failure? *Kidney Int.* 2008;73(9):989–91.

76. Lomashvili KA, Garg P, Narisawa S, Millan JL, O'Neill WC. Upregulation of alkaline phosphatase and pyrophosphate hydrolysis: potential mechanism for uremic vascular calcification. *Kidney Int.* 2008;73(9):1024–30.
77. Nemcsik J, Kiss I, Tisler A. Arterial stiffness, vascular calcification and bone metabolism in chronic kidney disease. *World J Nephrol.* 2012;1(1):25–34.
78. Speer MY, McKee MD, Guldberg RE, Liaw L, Yang HY, Tung E, et al. Inactivation of the osteopontin gene enhances vascular calcification of matrix Gla protein-deficient mice: evidence for osteopontin as an inducible inhibitor of vascular calcification in vivo. *J Exp Med.* 2002;196(8):1047–55.
79. Jono S, Peinado C, Giachelli CM. Phosphorylation of osteopontin is required for inhibition of vascular smooth muscle cell calcification. *J Biol Chem.* 2000;275(26):20197–203.
80. Bucay N, Sarosi I, Dunstan CR, Morony S, Tarpley J, Capparelli C, et al. Osteoprotegerin-deficient mice develop early onset osteoporosis and arterial calcification. *Genes Dev.* 1998;12(9):1260–8.
81. Katagiri T, Takahashi N. Regulatory mechanisms of osteoblast and osteoclast differentiation. *Oral Dis.* 2002;8(3):147–59.
82. Nitta K, Akiba T, Uchida K, Kawashima A, Yumura W, Kabaya T, et al. The progression of vascular calcification and serum osteoprotegerin levels in patients on long-term hemodialysis. *Am J Kidney Dis.* 2003;42(2):303–9.
83. Mesquita M, Demulder A, Damry N, Melot C, Wittersheim E, Willems D, et al. Plasma osteoprotegerin is an independent risk factor for mortality and an early biomarker of coronary vascular calcification in chronic kidney disease. *Clin Chem Lab Med.* 2009;47(3):339–46.
84. Chae SY, Chung W, Kim YH, Oh YK, Lee J, Choi KH, et al. The correlation of serum osteoprotegerin with non-traditional cardiovascular risk factors and arterial stiffness in patients with pre-dialysis chronic kidney disease: results from the KNOW-CKD study. *J Korean Med Sci.* 2018;33(53):14.
85. Montanez-Barragan A, Gomez-Barrera I, Sanchez-Nino MD, Ucerro AC, Gonzalez-Espinoza L, Ortiz A. Osteoprotegerin and kidney disease. *J Nephrol.* 2014;27(6):607–17.
86. Jena N, Martín-Seisdedos C, McCue P, Croce CM. BMP7 null mutation in mice: developmental defects in skeleton, kidney, and eye. *Exp Cell Res.* 1997;230(1):28–37.
87. Freedman BI, Bowden DW, Ziegler JT, Langefeld CD, Lehtinen AB, Rudock ME, et al. Bone morphogenetic protein 7 (BMP7) gene polymorphisms are associated with inverse relationships between vascular calcification and BMD: the diabetes heart study. *J Bone Miner Res.* 2009;24(10):1719–27.
88. Dorai H, Vukicevic S, Sampath TK. Bone morphogenetic protein-7 (osteogenic protein-1) inhibits smooth muscle cell proliferation and stimulates the expression of markers that are characteristic of SMC phenotype in vitro. *J Cell Physiol.* 2000;184(1):37–45.
89. Mathew S, Davies M, Lund R, Saab G, Hruska KA. Function and effect of bone morphogenetic protein-7 in kidney bone and the bone-vascular links in chronic kidney disease. *Eur J Clin Invest.* 2006;36:43–50.
90. Mitu G, Hirschberg R. Bone morphogenetic protein-7 (BMP7) in chronic kidney disease. *Front Biosci Landmrk.* 2008;13:4726–39.
91. Galvin KM, Donovan MJ, Lynch CA, Meyer RI, Paul RJ, Lorenz JN, et al. A role for Smad6 in development and homeostasis of the cardiovascular system. *Nat Genet.* 2000;24(2):171–4.
92. Ramirez F, Gayraud B, Pereira L. Marfan syndrome: new clues to genotype-phenotype correlations. *Ann Med.* 1999;31(3):202–7.
93. Shah GN, Bonapace G, Hu PY, Strisciuglio P, Sly WS. Carbonic anhydrase II deficiency syndrome (osteopetrosis with renal tubular acidosis and brain calcification): novel mutations in CA2 identified by direct sequencing expand the opportunity for genotype-phenotype correlation. *Hum Mutat.* 2004;24(3):272.
94. Oreffo RO, Cooper C, Mason C, Clements M. Mesenchymal stem cells: lineage, plasticity, and skeletal therapeutic potential. *Stem Cell Rev.* 2005;1(2):169–78.

95. Opitz F, Schenke-Layland K, Cohnert TU, Stock UA. Phenotypical plasticity of vascular smooth muscle cells-effect of in vitro and in vivo shear stress for tissue engineering of blood vessels. *Tissue Eng.* 2007;13(10):2505–14.
96. Chavkin NW, Chia JJ, Crouthamel MH, Giachelli CM. Phosphate uptake-independent signaling functions of the type III sodium-dependent phosphate transporter, PiT-1, in vascular smooth muscle cells. *Exp Cell Res.* 2015;333(1):39–48.
97. Yamada S, Leaf EM, Chia JJ, Cox TC, Speer MY, Giachelli CM. PiT-2, a type III sodium-dependent phosphate transporter, protects against vascular calcification in mice with chronic kidney disease fed a high-phosphate diet. *Kidney Int.* 2018;94(4):716–27.
98. Tyson KL, Reynolds JL, McNair R, Zhang Q, Weissberg PL, Shanahan CM. Osteo/chondrocytic transcription factors and their target genes exhibit distinct patterns of expression in human arterial calcification. *Arterioscler Thromb Vasc Biol.* 2003;23(3):489–94.
99. Speer MY, Yang HY, Brabb T, Leaf E, Look A, Lin WL, et al. Smooth muscle cells give rise to osteochondrogenic precursors and chondrocytes in calcifying arteries. *Circ Res.* 2009;104(6):733–41.
100. Shanahan CM, Cary NR, Salisbury JR, Proudfoot D, Weissberg PL, Edmonds ME. Medial localization of mineralization-regulating proteins in association with Monckeberg's sclerosis: evidence for smooth muscle cell-mediated vascular calcification. *Circulation.* 1999;100(21):2168–76.
101. Murshed M, Harmey D, Millan JL, McKee MD, Karsenty G. Unique coexpression in osteoblasts of broadly expressed genes accounts for the spatial restriction of ECM mineralization to bone. *Genes Dev.* 2005;19(9):1093–104.
102. Ichikawa S, Imel EA, Kreiter ML, Yu X, Mackenzie DS, Sorenson AH, et al. A homozygous missense mutation in human KLOTHO causes severe tumoral calcinosis. *J Clin Investig.* 2007;117(9):2684–91.
103. Hu MC, Shi MJ, Zhang JN, Quinones H, Griffith C, Kuro-O M, et al. Klotho deficiency causes vascular calcification in chronic kidney disease. *J Am Soc Nephrol.* 2011;22(1):124–36.
104. Kuro-o M, Matsumura Y, Aizawa H, Kawaguchi H, Suga T, Utsugi T, et al. Mutation of the mouse klotho gene leads to a syndrome resembling ageing. *Nature.* 1997;390(6655):45–51.
105. Haenzi B, Bonny O, Masson R, Lienhard S, Dey JH, Kuro-o M, et al. Loss of Memo, a novel FGFR regulator, results in reduced lifespan. *FASEB J.* 2014;28(1):327–36.
106. Lim K, Lu TS, Molostvov G, Lee C, Lam FT, Zehnder D, et al. Vascular klotho deficiency potentiates the development of human artery calcification and mediates resistance to fibroblast growth factor 23. *Circulation.* 2012;125(18):2243–55.
107. Larsson TE, Olauson H, Hagstrom E, Ingelsson E, Arnlov J, Lind L, et al. Conjoint effects of serum calcium and phosphate on risk of total, cardiovascular, and noncardiovascular mortality in the community. *Arterioscler Thromb Vasc Biol.* 2010;30(2):333–9.
108. Kuro-o M. A potential link between phosphate and aging--lessons from Klotho-deficient mice. *Mech Ageing Dev.* 2010;131(4):270–5.
109. Sanchis P, Ho CY, Liu Y, Beltran LE, Ahmad S, Jacob AP, et al. Arterial "inflammaging" drives vascular calcification in children on dialysis. *Kidney Int.* 2019;95(4):958–72.
110. Stenvinkel P, Luttropp K, McGuinness D, Witasp A, Qureshi AR, Wernerson A, et al. CDKN2A/p16INK4(a) expression is associated with vascular progeria in chronic kidney disease. *Aging.* 2017;9(2):494–507.
111. Lopez-Otin C, Blasco MA, Partridge L, Serrano M, Kroemer G. The hallmarks of aging. *Cell.* 2013;153(6):1194–217.
112. Moskalev AA, Shaposhnikov MV, Plyusnina EN, Zhavoronkov A, Budovsky A, Yanai H, et al. The role of DNA damage and repair in aging through the prism of Koch-like criteria. *Ageing Res Rev.* 2013;12(2):661–84.
113. d'Adda di Fagagna F. Living on a break: cellular senescence as a DNA-damage response. *Nat Rev Cancer.* 2008;8(7):512–22.
114. Jackson SP, Bartek J. The DNA-damage response in human biology and disease. *Nature.* 2009;461(7267):1071–8.

115. Harper JW, Elledge SJ. The DNA damage response: ten years after. *Mol Cell*. 2007;28(5):739–45.
116. Atamna H, Cheung I, Ames BN. A method for detecting abasic sites in living cells: age-dependent changes in base excision repair. *Proc Natl Acad Sci U S A*. 2000;97(2):686–91.
117. Mecocci P, Fano G, Fulle S, MacGarvey U, Shinobu L, Polidori MC, et al. Age-dependent increases in oxidative damage to DNA, lipids, and proteins in human skeletal muscle. *Free Radic Biol Med*. 1999;26(3–4):303–8.
118. Morgan WF, Corcoran J, Hartmann A, Kaplan MI, Limoli CL, Ponnaiya B. DNA double-strand breaks, chromosomal rearrangements, and genomic instability. *Mutat Res*. 1998;404(1–2):125–8.
119. Mandavilli BS, Rao KS. Neurons in the cerebral cortex are most susceptible to DNA-damage in aging rat brain. *Biochem Mol Biol Int*. 1996;40(3):507–14.
120. Ali AAE, Timinszky G, Arribas-Bosacoma R, Kozlowski M, Hassa PO, Hassler M, et al. The zinc-finger domains of PARP1 cooperate to recognize DNA strand breaks. *Nat Struct Mol Biol*. 2012;19(7):685–92.
121. Preston CR, Flores C, Engels WR. Age-dependent usage of double-strand-break repair pathways. *Curr Biol*. 2006;16(20):2009–15.
122. Chun HH, Gatti RA. Ataxia-telangiectasia, an evolving phenotype. *DNA Repair (Amst)*. 2004;3(8–9):1187–96.
123. Campisi J, d’Adda di Fagagna F. Cellular senescence: when bad things happen to good cells. *Nat Rev Mol Cell Biol*. 2007;8(9):729–40.
124. Alcorta DA, Xiong Y, Phelps D, Hannon G, Beach D, Barrett JC. Involvement of the cyclin-dependent kinase inhibitor p16 (INK4a) in replicative senescence of normal human fibroblasts. *Proc Natl Acad Sci U S A*. 1996;93(24):13742–7.
125. Dimri GP, Lee X, Basile G, Acosta M, Scott G, Roskelley C, et al. A biomarker that identifies senescent human cells in culture and in aging skin in vivo. *Proc Natl Acad Sci U S A*. 1995;92(20):9363–7.
126. Coppe JP, Patil CK, Rodier F, Sun Y, Munoz DP, Goldstein J, et al. Senescence-associated secretory phenotypes reveal cell-nonautonomous functions of oncogenic RAS and the p53 tumor suppressor. *PLoS Biol*. 2008;6(12):2853–68.
127. Acosta JC, O’Loughlen A, Banito A, Guijarro MV, Augert A, Raguz S, et al. Chemokine signaling via the CXCR2 receptor reinforces senescence. *Cell*. 2008;133(6):1006–18.
128. Baker DJ, Wijshake T, Tchkonja T, LeBrasseur NK, Childs BG, van de Sluis B, et al. Clearance of p16Ink4a-positive senescent cells delays ageing-associated disorders. *Nature*. 2011;479(7372):232–6.
129. Aleman BM, Moser EC, Nuver J, Suter TM, Maraldo MV, Specht L, et al. Cardiovascular disease after cancer therapy. *EJC Suppl*. 2014;12(1):18–28.
130. Hennekam RC. Hutchinson-Gilford progeria syndrome: review of the phenotype. *Am J Med Genet A*. 2006;140(23):2603–24.
131. Goto M. Hierarchical deterioration of body systems in Werner’s syndrome: implications for normal ageing. *Mech Ageing Dev*. 1997;98(3):239–54.
132. Gruenbaum Y, Margalit A, Goldman RD, Shumaker DK, Wilson KL. The nuclear lamina comes of age. *Nat Rev Mol Cell Biol*. 2005;6(1):21–31.
133. Liu Y, Drozdov I, Shroff R, Beltran LE, Shanahan CM. Prelamin a accelerates vascular calcification via activation of the DNA damage response and senescence-associated secretory phenotype in vascular smooth muscle cells. *Circ Res*. 2013;112(10):e99–e109.
134. Salamat M, Dhar PK, Neagu DL, Lyon JB. Aortic calcification in a patient with Hutchinson-Gilford progeria syndrome. *Pediatr Cardiol*. 2010;31(6):925–6.
135. Vaziri ND. Oxidative stress in uremia: nature, mechanisms, and potential consequences. *Semin Nephrol*. 2004;24(5):469–73.
136. Libby P. Inflammation in atherosclerosis. *Nature*. 2002;420(6917):868–74.

137. Opdebeeck B, Maudsley S, Azmi A, De Mare A, De Leger W, Meijers B, et al. Indoxyl sulfate and p-cresyl sulfate promote vascular calcification and associate with glucose intolerance. *J Am Soc Nephrol.* 2019;30(5):751–66.
138. Kapustin AN, Chatrou ML, Drozdov I, Zheng Y, Davidson SM, Soong D, et al. Vascular smooth muscle cell calcification is mediated by regulated exosome secretion. *Circ Res.* 2015;116(8):1312–23.
139. Müller KH, Hayward R, Rajan R, Whitehead M, Cobb AM, Ahmad S, et al. Poly(ADP-ribose) links the DNA damage response and biomineralization. *Cell Rep.* 2019;27(11):3124–38.e13.
140. Quinn PM, Buck TM, Mulder AA, Ohonin C, Alves CH, Vos RM, et al. Human iPSC-derived retinas recapitulate the fetal CRB1 CRB2 complex formation and demonstrate that photoreceptors and muller glia are targets of AAV5. *Stem Cell Rep.* 2019;12(5):906–19.
141. Kooman JP, Dekker MJ, Usvyat LA, Kotanko P, van der Sande FM, Schalkwijk CG, et al. Inflammation and premature aging in advanced chronic kidney disease. *Am J Physiol Renal Physiol.* 2017;313(4):F938–F50.
142. Shanahan CM. Mechanisms of vascular calcification in CKD - evidence for premature ageing? *Nat Rev Nephrol.* 2013;9(11):661–70.
143. Andreassi MG. DNA damage, vascular senescence and atherosclerosis. *J Mol Med (Berl).* 2008;86(9):1033–43.
144. Muteliefu G, Shimizu H, Enomoto A, Nishijima F, Takahashi M, Niwa T. Indoxyl sulfate promotes vascular smooth muscle cell senescence with upregulation of p53, p21, and prelamin A through oxidative stress. *Am J Physiol Cell Physiol.* 2012;303(2):C126–34.
145. Masuda M, Miyazaki-Anzai S, Levi M, Ting TC, Miyazaki M. PERK-eIF2alpha-ATF4-CHOP signaling contributes to TNFalpha-induced vascular calcification. *J Am Heart Assoc.* 2013;2(5):e000238.
146. Tintut Y, Patel J, Parhami F, Demer LL. Tumor necrosis factor-alpha promotes in vitro calcification of vascular cells via the cAMP pathway. *Circulation.* 2000;102(21):2636–42.
147. Moutachakir M, Hanchi AL, Baraou A, Boukhira A, Chellak S. Immunoanalytical characteristics of C-reactive protein and high sensitivity C-reactive protein. *Ann Biol Clin.* 2017;75(2):225–9.
148. Torzewski J, Torzewski M, Bowyer DE, Frohlich M, Koenig W, Waltenberger J, et al. C-reactive protein frequently colocalizes with the terminal complement complex in the intima of early atherosclerotic lesions of human coronary arteries. *Arterioscler Thromb Vasc Biol.* 1998;18(9):1386–92.
149. Bohlender JM, Franke S, Stein G, Wolf G. Advanced glycation end products and the kidney. *Am J Physiol Renal Physiol.* 2005;289(4):F645–F59.
150. Wang Z, Jiang Y, Liu N, Ren L, Zhu Y, An Y, et al. Advanced glycation end-product Nepsilon-carboxymethyl-lysine accelerates progression of atherosclerotic calcification in diabetes. *Atherosclerosis.* 2012;221(2):387–96.
151. Chen J, Muntner P, Hamm LL, Jones DW, Batuman V, Fonseca V, et al. The metabolic syndrome and chronic kidney disease in US adults. *Ann Intern Med.* 2004;140(3):167–74.
152. Kurella M, Lo JC, Chertow GM. Metabolic syndrome and the risk for chronic kidney disease among nondiabetic adults. *J Am Soc Nephrol.* 2005;16(7):2134–40.
153. Proudfoot D, Davies JD, Skepper JN, Weissberg PL, Shanahan CM. Acetylated low-density lipoprotein stimulates human vascular smooth muscle cell calcification by promoting osteoblastic differentiation and inhibiting phagocytosis. *Circulation.* 2002;106(24):3044–50.
154. Taylor J, Butcher M, Zeadin M, Politano A, Shaughnessy SG. Oxidized low-density lipoprotein promotes osteoblast differentiation in primary cultures of vascular smooth muscle cells by up-regulating osterix expression in an Msx2-dependent manner. *J Cell Biochem.* 2011;112:581–8.
155. Shankman LS, Gomez D, Cherepanova OA, Salmon M, Alencar GF, Haskins RM, et al. KLF4-dependent phenotypic modulation of smooth muscle cells has a key role in atherosclerotic plaque pathogenesis. *Nat Med.* 2015;21(6):628–37.

156. Rong JX, Shapiro M, Trogan E, Fisher EA. Transdifferentiation of mouse aortic smooth muscle cells to a macrophage-like state after cholesterol loading. *Proc Natl Acad Sci U S A*. 2003;100(23):13531–6.
157. Byon CH, Heath JM, Chen Y. Redox signaling in cardiovascular pathophysiology: a focus on hydrogen peroxide and vascular smooth muscle cells. *Redox Biol*. 2016;9:244–53.
158. Mizobuchi M, Towler D, Slatopolsky E. Vascular calcification: the killer of patients with chronic kidney disease. *J Am Soc Nephrol*. 2009;20(7):1453–64.
159. Walter P, Ron D. The unfolded protein response: from stress pathway to homeostatic regulation. *Science*. 2011;334(6059):1081–6.
160. Tabas I, Ron D. Integrating the mechanisms of apoptosis induced by endoplasmic reticulum stress. *Nat Cell Biol*. 2011;13(3):184–90.
161. Furmanik M, Shanahan CM. Endoplasmic reticulum stress in arterial smooth muscle cells: a novel regulator of vascular disease. *Curr Cardiol Rev*. 2017;13(2):94–105.
162. Duan XH, Chang JR, Zhang J, Zhang BH, Li YL, Teng X, et al. Activating transcription factor 4 is involved in endoplasmic reticulum stress-mediated apoptosis contributing to vascular calcification. *Apoptosis*. 2013;18(9):1132–44.
163. Liberman M, Johnson RC, Handy DE, Loscalzo J, Leopold JA. Bone morphogenetic protein-2 activates NADPH oxidase to increase endoplasmic reticulum stress and human coronary artery smooth muscle cell calcification. *Bioch Bioph Res Co*. 2011;413:436–41.
164. Shiozaki Y, Okamura K, Kohno S, Keenan AL, Williams K, Zhao XY, et al. The CDK9-cyclin T1 complex mediates saturated fatty acid-induced vascular calcification by inducing expression of the transcription factor CHOP. *J Biol Chem*. 2018;293(44):17008–20.
165. Masuda M, Ting TC, Levi M, Saunders SJ, Miyazaki-Anzai S, Miyazaki M. Activating transcription factor 4 regulates stearate-induced vascular calcification. *J Lipid Res*. 2012;53(8):1543–52.
166. Masuda M, Miyazaki-Anzai S, Keenan AL, Okamura K, Kendrick J, Chonchol M, et al. Saturated phosphatidic acids mediate saturated fatty acid-induced vascular calcification and lipotoxicity. *J Clin Invest*. 2015;125(12):4544–58.
167. Miyazaki-Anzai S, Masuda M, Demos-Davies KM, Keenan AL, Saunders SJ, Masuda R, et al. Endoplasmic reticulum stress effector CCAAT/enhancer-binding protein homologous protein (CHOP) regulates chronic kidney disease-induced vascular calcification. *J Am Heart Assoc*. 2014;3(3):e000949.
168. Panda DK, Bai XY, Sabbagh Y, Zhang Y, Zaun HC, Karellis A, et al. Defective interplay between mTORC1 activity and endoplasmic reticulum stress-unfolded protein response in uremic vascular calcification. *Am J Physiol Renal Physiol*. 2018;314(6):F1046–F61.
169. Hotamisligil GS. Endoplasmic reticulum stress and the inflammatory basis of metabolic disease. *Cell*. 2010;140(6):900–17.
170. Chopra A, Sivaraman K. An update on possible pathogenic mechanisms of periodontal pathogens on renal dysfunction. *Crit Rev Microbiol*. 2019:1–25.
171. Chen TC, Lin CT, Chien SJ, Chang SF, Chen CN. Regulation of calcification in human aortic smooth muscle cells infected with high-glucose-treated *Porphyromonas gingivalis*. *J Cell Physiol*. 2018;233(6):4759–69.
172. Liu GR, Deng J, Zhang Q, Song WB, Chen SL, Lou XX, et al. *Porphyromonas gingivalis* lipopolysaccharide stimulation of vascular smooth muscle cells activates proliferation and calcification. *J Periodontol*. 2016;87(7):828–36.
173. Yang WW, Guo B, Jia WY, Jia Y. *Porphyromonas gingivalis*-derived outer membrane vesicles promote calcification of vascular smooth muscle cells through ERK1/2-RUNX2. *Febs Open Bio*. 2016;6(12):1310–9.
174. Pazar B, Ea HK, Narayan S, Kolly L, Bagnoud N, Chobaz V, et al. Basic calcium phosphate crystals induce monocyte/macrophage IL-1 β secretion through the NLRP3 inflammasome in vitro. *J Immunol*. 2011;186(4):2495–502.
175. Nadra I, Mason JC, Philippidis P, Florey O, Smythe CD, McCarthy GM, et al. Proinflammatory activation of macrophages by basic calcium phosphate crystals via protein kinase C and

- MAP kinase pathways: a vicious cycle of inflammation and arterial calcification? *Circ Res.* 2005;96(12):1248–56.
176. Nadra I, Boccaccini AR, Philippidis P, Whelan LC, McCarthy GM, Haskard DO, et al. Effect of particle size on hydroxyapatite crystal-induced tumor necrosis factor alpha secretion by macrophages. *Atherosclerosis.* 2008;196(1):98–105.
177. Ewence AE, Bootman M, Roderick HL, Skepper JN, McCarthy G, Epple M, et al. Calcium phosphate crystals induce cell death in human vascular smooth muscle cells: a potential mechanism in atherosclerotic plaque destabilization. *Circ Res.* 2008;103:e28–34.
178. Motskin M, Wright DM, Muller K, Kyle N, Gard TG, Porter AE, et al. Hydroxyapatite nano and microparticles: correlation of particle properties with cytotoxicity and biostability. *Biomaterials.* 2009;30(19):3307–17.
179. Sage AP, Jinxiu L, Tintut Y, Demer LL. Hyperphosphatemia-induced nanocrystals upregulate the expression of bone morphogenetic protein-2 and osteopontin genes in mouse smooth muscle cells in vitro. *Kidney Int.* 2011;79(4):414–22.
180. Lei Y, Sinha A, Nosoudi N, Grover A, Vyavahare N. Hydroxyapatite and calcified elastin induce osteoblast-like differentiation in rat aortic smooth muscle cells. *Exp Cell Res.* 2014;323(1):198–208.
181. Isakova T, Ix JH, Sprague SM, Raphael KL, Fried L, Gassman JJ, et al. Rationale and approaches to phosphate and fibroblast growth factor 23 reduction in CKD. *J Am Soc Nephrol.* 2015;26(10):2328–39.
182. Cozzolino M, Olivi L, Voli E, Ciceri P, Brancaccio D. [Prevention and treatment of secondary hyperparathyroidism in non-dialyzed patients with stage 3–5 chronic kidney disease]. *Giornale italiano di nefrologia.* 2009;26 Suppl 49:S30–5.
183. Locatelli F, Del Vecchio L, Violo L, Pontoriero G. Phosphate binders for the treatment of hyperphosphatemia in chronic kidney disease patients on dialysis: a comparison of safety profiles. *Expert Opin Drug Saf.* 2014;13(5):551–61.
184. Cernaro V, Santoro D, Lucisano S, Nicocia G, Lacquaniti A, Buemi M. The future of phosphate binders: a perspective on novel therapeutics. *Expert Opin Investig Drugs.* 2014;23(11):1459–63.
185. Navaneethan SD, Palmer SC, Craig JC, Elder GJ, Strippoli GF. Benefits and harms of phosphate binders in CKD: a systematic review of randomized controlled trials. *Am J Kidney Dis.* 2009;54(4):619–37.
186. Hatakeyama S, Murasawa H, Narita T, Oikawa M, Fujita N, Iwamura H, et al. Switching hemodialysis patients from sevelamer hydrochloride to bicalomer: a single-center, non-randomized analysis of efficacy and effects on gastrointestinal symptoms and metabolic acidosis. *BMC Nephrol.* 2013;14:222.
187. Ito K, Takeshima A, Shishido K, Wakasa M, Kumata C, Matsuzaka K, et al. Treatment of hyperphosphatemia with bicalomer in Japanese patients on long-term hemodialysis with gastrointestinal symptoms. *Ther Apher Dial.* 2014;18 Suppl 2:19–23.
188. Taniguchi K, Kakuta H. Bicalomer, a novel phosphate binder with a small swelling index, improves hyperphosphatemia in chronic kidney disease rat. *Eur J Pharmacol.* 2015;766:129–34.
189. Akizawa T, Tsukada J, Kameoka C, Kuroishi K, Yamaguchi Y. Long-term safety and efficacy of bicalomer in hyperphosphatemic patients with chronic kidney disease not on dialysis. *Ther Apher Dial.* 2017;21(2):173–9.
190. Block GA, Wheeler DC, Persky MS, Kestenbaum B, Ketteler M, Spiegel DM, et al. Effects of phosphate binders in moderate CKD. *J Am Soc Nephrol.* 2012;23(8):1407–15.
191. Kuhlmann MK. Phosphate elimination in modalities of hemodialysis and peritoneal dialysis. *Blood Purif.* 2010;29(2):137–44.
192. Marron B, Remon C, Perez-Fontan M, Quiros P, Ortiz A. Benefits of preserving residual renal function in peritoneal dialysis. *Kidney Int Suppl.* 2008;108:S42–51.
193. Floege J. Phosphate binders in chronic kidney disease: a systematic review of recent data. *J Nephrol.* 2016;29(3):329–40.

194. Bover J, Urena P, Ruiz-Garcia C, daSilva I, Lescano P, del Carpio J, et al. Clinical and practical use of calcimimetics in dialysis patients with secondary hyperparathyroidism. *Clin J Am Soc Nephrol*. 2016;11(1):161–74.
195. Raggi P, Chertow GM, Torres PU, Csiky B, Naso A, Nossuli K, et al. The ADVANCE study: a randomized study to evaluate the effects of cinacalcet plus low-dose vitamin D on vascular calcification in patients on hemodialysis. *Nephrol Dial Transplant*. 2011;26(4):1327–39.
196. Wasiaik S, Tsujikawa LM, Halliday C, Stotz SC, Gilham D, Jahagirdar R, et al. Benefit of Apabetalone on plasma proteins in renal disease. *Kidney Int Rep*. 2018;3(3):711–21.
197. Kulikowski E, Halliday C, Johansson J, Sweeney M, Lebioda K, Wong N, et al. Apabetalone mediated epigenetic modulation is associated with favorable kidney function and alkaline phosphatase profile in patients with chronic kidney disease. *Kidney Blood Press Res*. 2018;43(2):449–57.
198. Yosef R, Pilpel N, Tokarsky-Amiel R, Biran A, Ovadya Y, Cohen S, et al. Directed elimination of senescent cells by inhibition of BCL-W and BCL-XL. *Nat Commun*. 2016;7:11190.
199. Childs BG, Baker DJ, Wijshake T, Conover CA, Campisi J, van Deursen JM. Senescent intimal foam cells are deleterious at all stages of atherosclerosis. *Science*. 2016;354(6311):472–7.

Chapter 8

The Role of Calcification in Peripheral Artery Disease



Tanner I. Kim and Raul J. Guzman

Population Studies and Risk Factors

Although the exact prevalence of peripheral artery calcification is unknown, the finding of a calcified vascular bed by imaging is common (Figs. 8.1, 8.2, and 8.3). In a cohort of asymptomatic patients over 70 years old who received whole-body computed tomography (CT), the presence of any calcified bed was detected in nearly all subjects [4]. A separate study using CT found the presence of calcified arterial beds in at least one-third of Americans over the age of 45 [5, 6].

Fig. 8.1 Medial artery calcification on an x-ray with calcified dorsalis pedis and posterior tibial arteries



T. I. Kim · R. J. Guzman (✉)
Division of Vascular Surgery, Yale University School of Medicine, New Haven, CT, USA
e-mail: Tanner.kim@yale.edu; raul.guzman@yale.edu

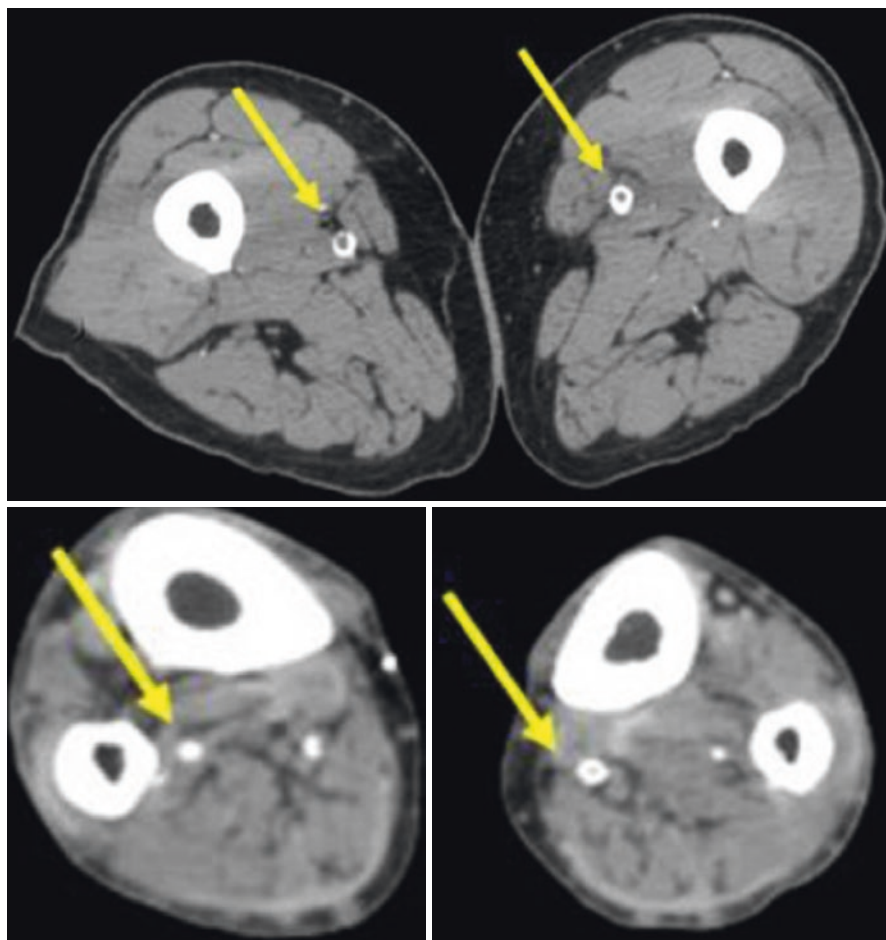


Fig. 8.2 Computed tomography scans of the lower extremity with arrows pointing to calcified arteries

Two factors strongly linked with peripheral artery calcification are end-stage renal disease (ESRD) and diabetes [7–9]. The relationship between ESRD and calcification is thought to be mediated primarily through imbalances in the homeostasis of calcium and phosphorus (for a mechanistic discussion on the role of renal disease in ectopic calcification, see Chap. 7) [1]. Arterial calcification can be observed in subjects as young as 20 years of age with ESRD [10]. Diabetes promotes peripheral artery calcification through hyperglycemia, inflammation, and advanced glycation end-products among other described mechanisms [7, 11]. Peripheral artery and coronary calcification are common findings among patients with diabetes and are related to its chronicity [12]. A study using x-ray found evidence of peripheral calcification in 53.5% of 367 subjects with diabetes [13]. The presence of peripheral artery calcification in the tarsal arteries has been shown to have a positive predictive value of over 93% for a diabetic patient with peripheral vascular disease [14]. A separate

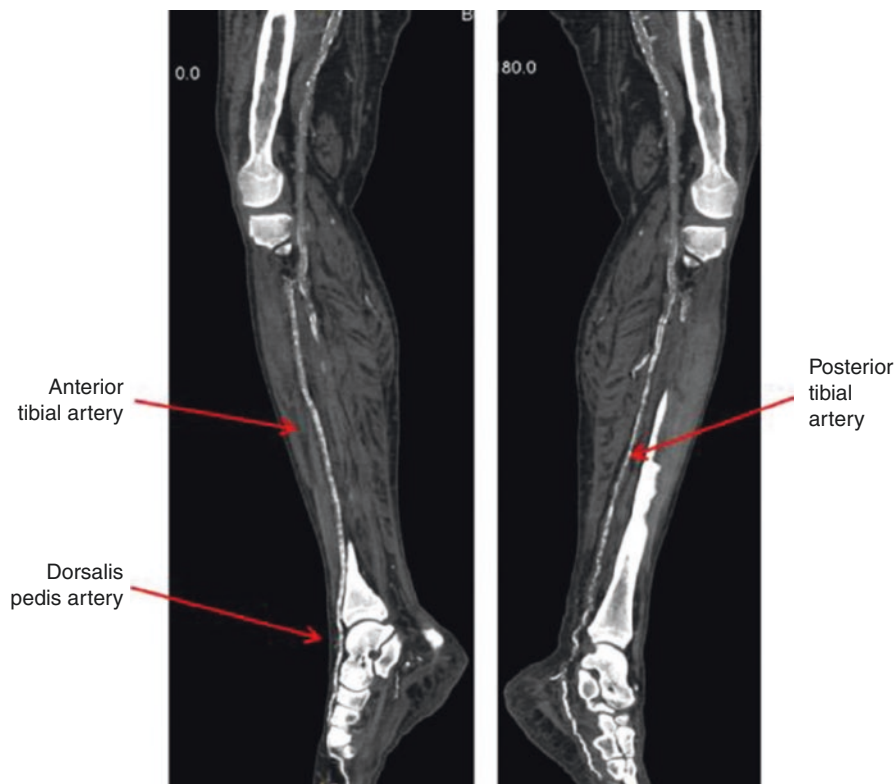


Fig. 8.3 Computed tomography scans with calcified tibial arteries

study of 289 subjects with diabetes used both ultrasound and x-ray to assess superficial femoral artery calcification [15]. Ultrasound was more sensitive to the presence of calcification, and detected medial artery calcification in 65.8% of patients compared to 12.2% with x-ray. The severity of medial artery calcification was also found to be associated with both diabetic microvascular and macrovascular complications.

A prospective study by Deas et al. evaluated tibial artery calcification by CT in 222 patients without ESRD. Its presence was associated with an abnormal ankle-brachial index (ABI), symptomatic PAD, age, male sex, diabetes, and tobacco use [16]. After adjustment for the presence of PAD, the factors age, sex, and tobacco use remained significant. Other studies have demonstrated similar findings, with risk factors similar to that of atherosclerosis including age, hypertension, male sex, diabetes, kidney disease, elevated c-reactive protein (CRP), and hyperlipidemia [9, 12, 17]. Peripheral artery calcification is also correlated with coronary artery calcification, which shares many of the same risk factors and is itself associated with increased rates of mortality [10, 12, 18–21].

However, risk factors for the progression of peripheral vascular calcification are not well established. Singh et al. evaluated 58 subjects with type 2 diabetes and preserved renal function with lower extremity CT over a period of 1 year. The strongest predictor of worsening calcification was the severity of baseline calcification. Although few

studies have tracked the changes in peripheral artery calcification over time, this may suggest that the presence of calcification accelerates the progression of further calcification. Other risk factors including age, ethnicity, estimated glomerular filtration rate (eGFR), and peripheral neuropathy were also predictive of worsening calcification [22].

Histology

Once considered a single pathologic entity, arterial calcification is now understood to occur as at least four distinct processes, in part related to its location in the arterial wall (intimal or medial), cardiac valves, or a diffuse form known as calciphylaxis. Of the four major types of calcification, medial artery calcification, historically referred to as Monckeberg's sclerosis, is the most commonly observed in PAD (Fig. 8.4). Although medial artery calcification is associated with metabolic

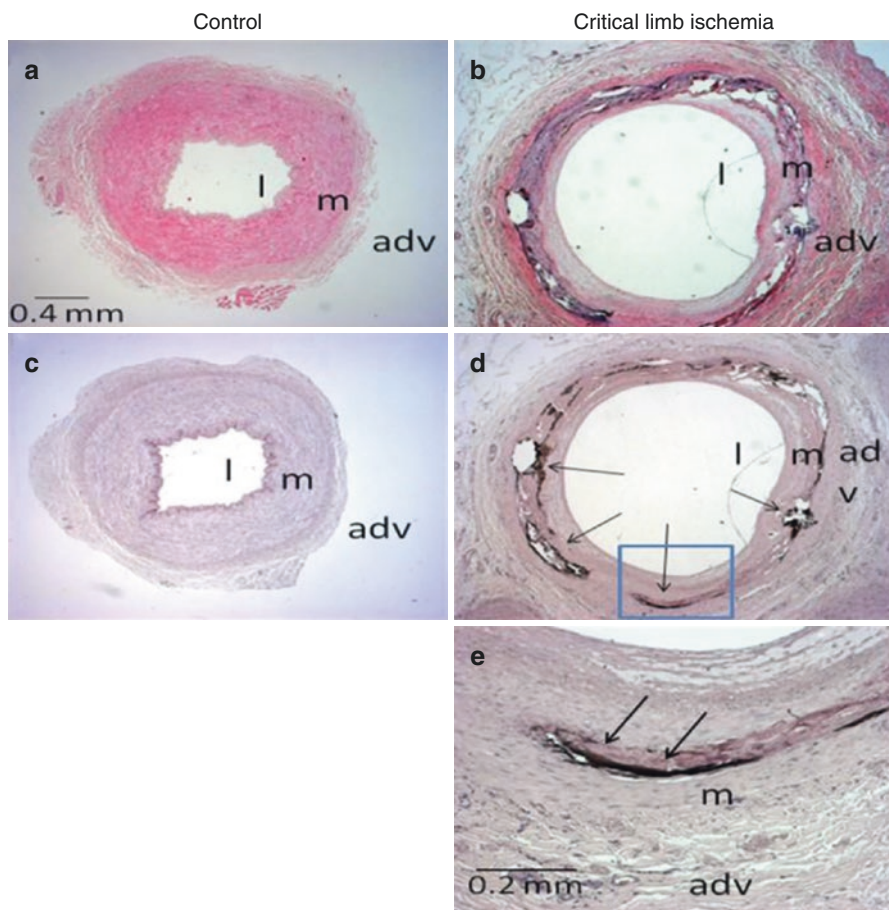


Fig. 8.4 Histology of a normal vessel and a vessel with critical limb ischemia. Arrows point to calcification. I intima, M media, Adv adventitia

abnormalities including hypercalcemia and hyperphosphatemia, it may also occur in the absence of these factors, differentiating it from calciphylaxis [23]. Results from autopsies in subjects with PAD demonstrated that medial calcification was found in 72% of lower extremity arteries, while intimal atherosclerosis was present in less than 25% [24–27]. This is in contrast to the intimal disease predominantly observed in the coronary and carotid arteries, although medial artery calcification may develop in conjunction with atherosclerosis or independent of it [27, 28]. A study using 431 femoropopliteal arteries from tissue donors of various ages found the presence of medial calcification in 46% of specimens and in over 60% of specimens from those greater than 60 years old [29]. Calcium deposits were also seen in the arteries of those as young as 18 years old. Calcified arteries were observed to have more discontinuous elastic fibers and were associated with increased longitudinal and circumferential stiffness even after adjustment for age.

Calcification and PAD Severity

Peripheral artery calcification can be visualized with imaging modalities such as x-ray and CT, and its presence in patients with PAD has been associated with poor outcomes. Initial studies using x-ray demonstrated that it was predictive of amputation and mortality, especially among those with diabetes [30–33]. CT is a more sensitive form of imaging and provides the added ability to quantify the amount of calcification [34]. Several studies have shown that increasing calcification scores correlate with severity of PAD symptoms [2, 9, 35]. A study of 116 patients with symptomatic PAD used CT to quantify the amount of peripheral artery calcification. Higher levels correlated with increasing Rutherford ischemia categories ($R = 0.6$), and this was maintained after adjusting for traditional cardiovascular risk factors [2]. The increasing calcium burden also correlates with worse functional outcomes. A cross-sectional study of 162 patients with diabetes used CT to assess tibial artery calcification and found that higher levels were independently associated with diabetic foot ulcers [36]. Further studies are needed to characterize the relationship between peripheral artery calcification and its effects on pedal perfusion.

Outcomes of Patients with Peripheral Calcification and PAD

In patients with PAD, the presence of peripheral artery calcification is associated with worse limb-related outcomes as was first noted in a 20-year longitudinal study of over 4550 Pima Indians [30] (Table 8.1). Medial artery calcification detected by x-ray was associated with increased age, diabetes, and male sex. Over the study period, diabetic subjects with medial artery calcification had a 5.5-fold higher rate of amputations compared to those without medial calcification. A separate study used CT to evaluate lower extremity calcification in 82 patients with symptomatic PAD with a mean follow-up of 21 months [35]. Patients were classified into quartiles based on levels of calcification and correlated with Rutherford ischemia

Table 8.1 Longitudinal studies on the outcomes of patients with peripheral arterial calcification

Study	Type of imaging (region of body analyzed)	Follow-up	Outcome measures (amputation or mortality)
Everhart et al [30]	Foot x-ray (pedal arteries)	20 years	Increased risk of amputation (HR: 5.5)
Niskanen et al [31]	Thigh x-ray (femoral arteries)	10 years	Increased risk of cardiovascular mortality (OR: 4.2)
Lehto et al [32]	Lower extremity x-ray (femoral artery)	7 years	Increased risk of all-cause mortality (OR: 1.6)
Mayfield et al [33]	Foot x-ray (pedal arteries)	6 to 8 years	Increased risk of amputation (HR: 3.3) and all-cause mortality (HR: 1.6)
London et al [8]	Pelvic and thigh x-ray (iliac and femoral arteries)	89 months	Increased risk of all-cause mortality (RR: 15.7)
Guzman et al [3]	Lower extremity CT (tibial arteries)	13.8 months	Increased risk of amputation (HR: 11.27)
Allison et al [38]	Whole-body CT (coronary, carotid, thoracic aorta, abdominal aorta, iliac arteries)	7.8 years	Increased risk of all-cause mortality (HR: 1.67 for iliac artery calcification)
Huang et al [35]	Lower extremity CT (common iliac to tibial arteries)	21 months	Increased risk of amputation (HR: 2.88) and all-cause mortality (HR: 5.16)
Chowdhury et al [39]	Lower extremity CT (infrarenal aorta to tibial arteries)	46 months	Increased risk of all-cause mortality (highest mortality observed among highest quartile of calcium scores)

CT computed tomography, HR hazard ratio, OR odds ratio, RR relative risk

classifications. Those in the highest quartile had a 2.88-fold higher risk of amputation compared to those in the lowest quartile. In a larger cohort, non-contrast CT was used to evaluate tibial artery calcification in 229 patients with PAD and it found that higher levels of tibial artery calcification were associated with PAD severity [3]. Furthermore, high levels of tibial artery calcification were also a risk factor for amputation and were shown to be a better predictor of amputation than ankle-brachial index (ABI) and cardiovascular risk factors combined.

Peripheral calcification also has been identified as a risk factor for cardiovascular disease and all-cause mortality, and its presence is associated with coronary artery disease and coronary calcification [12, 37]. Interestingly, the association between calcification and mortality is not equivalent across vascular beds [38]. Allison et al. examined 4544 patients with whole-body CT scan and quantified calcification in the thoracic aorta, abdominal aorta, coronary, carotid, and iliac arteries. Carotid and thoracic calcification were associated with the highest rates of all-cause mortality. However, after adjustment for cardiovascular risk factors, iliac artery calcification had the highest hazard ratio of 1.79 for all-cause mortality. In patients with symptomatic PAD, Huang et al. demonstrated that patients with high levels of peripheral calcification had a 5.16-fold higher risk for all-cause mortality compared to those with little to none [35]. Chowdhury et al. similarly used lower extremity CT to

grade calcification in 220 patients with symptomatic PAD [39]. The highest quartile of calcification was associated with diabetes, ischemic heart disease, chronic kidney disease, and all-cause mortality over a median follow-up period of 46 months.

The Effect of Calcification on Treatment Options for PAD

Endovascular interventions are among the most commonly performed procedures for lower extremity revascularization in the setting of PAD [40]. However, peripheral artery calcification significantly reduces the efficacy of these interventions. Heavily calcified lesions are often difficult to cross with wires and catheters, and its presence is associated with increased rates of technical failure [41]. Angioplasty is often ineffective in the setting of heavily calcified lesions and has been associated with higher rates of bailout stenting in the femoropopliteal region [42]. A review of 525 endovascular interventions for superficial femoral artery disease demonstrated that the presence of calcification was predictive of reduced primary patency and increased rates of restenosis [43]. Kang et al. reviewed 124 patients with critical limb ischemia who had undergone infrapopliteal angioplasty. Extensive calcification by computed tomography angiography (CTA) was associated with lower technical success and amputation [44]. Calcification involving greater than 50% of the anterior wall of the common femoral artery has also been shown to be a risk factor for failure of percutaneous closure devices [45].

Newer technologies including drug-coated balloons and stents have also been hindered by the presence of calcification. A series of 91 patients who underwent drug-coated balloon angioplasty of femoropopliteal lesions demonstrated that severe calcification on angiography was associated with late lumen loss at 6 months [46]. After drug-coated balloon angioplasty, higher circumferential calcium involvement was associated with higher rates of flow-limiting dissections [47]. Also, patients with more circumferential calcification had higher rates of late lumen loss and lower primary patency. Calcification has also been associated with higher rates of in-stent restenosis after drug-coated stent placement [48].

Technologies including scoring balloons and atherectomy have been used to address the difficulties of treating calcified lesions with endovascular procedures, although outcomes have only shown modest improvement [49–51]. Other strategies including vessel preparation with atherectomy followed by drug-coated balloon angioplasty also have not resulted in improved outcomes [52–54]. Intravascular ultrasound after angioplasty of calcified lesions has shown increased rates of dissection and decreased patency, [55] and interestingly, arterial calcification decreases the uptake of paclitaxel, limiting its effectiveness [47, 56]. Intravascular lithotripsy has been recently introduced as a means of addressing heavily calcified peripheral arteries; however long-term data are lacking [57, 58].

Medial artery calcification increases neointimal hyperplasia after angioplasty and also contributes to poor long-term patency [59]. In preclinical studies, Marshall et al. found increased rates of neointimal hyperplasia in arteries with medial

calcification following angioplasty compared with controls. The bone morphogenic protein (BMP-2) was increased in calcified arteries suggesting an active role in neointimal hyperplasia. Positron emission tomography (PET) has been used to help predict restenosis after balloon angioplasty of the lower extremities, and findings of persistent femoral artery inflammation and micro-calcification have been associated with higher rates of restenosis [60].

In contrast to the poor outcomes observed with endovascular interventions, the presence of calcification has not been shown to decrease mid-term efficacy of lower extremity bypass. A study of 101 infrapopliteal bypasses in patients with calcified arteries requiring balloon control showed no significant difference in outcomes compared to those who did not require balloon control. At 24-months, primary and secondary patency rates for bypasses to so called “unclampable” arteries were 60% and 65% respectively, and these were not significantly different from the noncalcified group [61]. A similar study of 441 distal bypasses included 69 “unclampable” outflow vessels and found no difference in primary patency and limb salvage up to 5-years [62]. However, such data from retrospective chart reviews were obtained before standardized methods to quantify calcification were developed, and as such, the extent of peripheral artery calcification and differences between the groups could not be confirmed.

Calcification and Arterial Stiffness

Peripheral artery calcification has also been associated with arterial stiffness [29, 63, 64]. Medial calcification is associated with destruction of the elastic elements of the media [65]. Biopsies of femoropopliteal arteries with medial calcification have shown the presence of discontinuous elastic fibers and an association with decreased longitudinal and circumferential compliance [29, 66]. Arterial stiffness can be clinically assessed with blood pressure cuff, ultrasound, or applanation tonometry, and its presence in PAD is associated with adverse cardiovascular events and all-cause mortality [1, 64, 67–70]. Zettervall et al. used preoperative pulse pressure to evaluate outcomes in patients undergoing endovascular tibial interventions for critical limb ischemia [71]. An elevated pulse pressure greater than 80 mm Hg was associated with increased rates of periprocedural complications and increased long-term mortality at 5 years. However, the mechanisms that relate lower extremity arterial stiffness to worse outcomes are not well understood. It is believed that increased arterial stiffness that results from medial calcification decreases compliance and reduces the efficacy of endovascular interventions [71]. Increased arterial stiffness is also likely to be associated with decreased pedal perfusion and is also related to peripheral neuropathy [32, 36]. Kizu et al. used ultrasound and transcutaneous oxygen tension (TcPO₂) to evaluate distal perfusion in 68 patients with diabetes. TcPO₂ was inversely correlated with femoral artery stiffness as measured by ultrasound, and associated with increased rates of insulin resistance [72]. Another study using pulse wave velocity compared distal perfusion in diabetic patients and demonstrated

that higher pulse wave volume recordings were associated with lower flow rates and higher resistive indices in the popliteal artery [73].

Higher levels of arterial stiffness have also been correlated with shorter walking distance in patients with PAD [74]. Interestingly, endovascular treatment may help decreased arterial stiffness. Jacomella et al. compared the effect of balloon angioplasty on arterial stiffness in patients with claudication. At 3-months post angioplasty, the aortic augmentation index, a measure of arterial stiffness, was significantly improved compared to the control group who received conservative treatment [75]. This was thought to be due to improved walking capabilities in those treated with angioplasty, but mechanistic studies related to this effect are not available.

Treatment for Calcification in PAD

There are currently no accepted treatments for peripheral artery calcification, though multiple therapies are currently under investigation in preclinical and clinical studies. Both intimal and medial artery calcification are active processes that involve the osteogenic differentiation of vascular smooth muscle cells (VSMC) and the expression of osteochondrogenic markers such as Runx2 [1, 76]. However, the associated pathologies and drivers of intimal and medial calcification remain markedly different. While intimal calcification involves hyperlipidemia and inflammation, medial artery calcification involves metabolic derangements associated with diabetes and renal failure. Medial artery calcification is also associated with metaplastic bone formation which is not seen in intimal calcification [77]. There still remains much to be understood on a cellular level regarding differences between both forms of calcification, and as such the majority of therapeutic studies target the direct mechanisms of mineral formation. For example, vitamin K has been introduced as a possible treatment for calcification as Matrix Gla protein (MGP), a known inhibitor of calcification, is activated by vitamin K-dependent carboxylation of glutamic acid residues and is secreted by vascular smooth muscle cells [78]. A study of 4807 patients found lower levels of abdominal aortic calcification in those with high levels of vitamin K [79]. Several clinical trials are currently in progress testing the hypothesis that vitamin K can slow calcification, predominantly in patients with chronic kidney disease or ESRD [78]. Sodium thiosulfate has also been introduced as a possible treatment for vascular calcification and has been tested in small studies of patients with ESRD, although significant side effects including anorexia and metabolic acidosis occurred [80, 81].

Other ongoing studies include the novel drug SNF472 (Sanifit) which is an intravenous form of myo-inositol hexaphosphate (IP6) and is currently in a phase 2b clinical trial [78]. Preclinical studies have shown that it inhibits formation and growth of calcium phosphate microcrystals in soft tissue without influencing serum calcium or phosphate levels. Metformin use has also been associated with lower calcium scores in tibial arteries in a cross-sectional cohort study of patients with diabetes [82]. Magnesium prevents formation of hydroxyapatite crystals *in vitro*,

and it can reverse vascular calcification in rat models [83]. The effect of MAGnesium supplementation on vascular CALcification in Chronic Kidney Disease (MAGiCAL-CKD) is an ongoing randomized clinical trial of 250 patients treated with either slow-release magnesium hydroxide or placebo for 12-months to investigate whether magnesium can slow the progression of coronary artery calcium [84]. In preclinical studies, chelation therapy with ethylene-diamine tetraacetic acid (EDTA)-loaded albumin nanoparticles reversed medial artery calcification in mice [85]. At 4 weeks after treatment cessation, there was no evidence of recurrent calcium accumulation. The majority of potential treatments for vascular calcification are still in the early stages of development, with no targeted treatments for the medial form.

Conclusion

Medial artery calcification is the predominant form of calcification in the extremities. It is common in patients with PAD, and especially among patients with diabetes and chronic kidney disease. Its presence is associated with limb loss, cardiovascular events, and mortality. It is associated with increased arterial stiffness and complicates efforts at endovascular intervention for patients with symptomatic peripheral artery occlusive disease. As we improve our understanding of the mechanisms controlling peripheral artery calcification, we hope to improve outcomes for patients with PAD and particularly those facing amputation.

References

1. Ho CY, Shanahan CM. Medial arterial calcification: an overlooked player in peripheral arterial disease. *Arterioscler Thromb Vasc Biol.* 2016;36(8):1475–82.
2. Zettervall SL, Marshall AP, Fleiser P, Guzman RJ. Association of arterial calcification with chronic limb ischemia in patients with peripheral artery disease. *J Vasc Surg.* 2018;67(2):507–13.
3. Guzman RJ, Brinkley DM, Schumacher PM, Donahue RMJ, Beavers H, Qin X. Tibial artery calcification as a marker of amputation risk in patients with peripheral arterial disease. *J Am Coll Cardiol.* 2008;51(20):1967–74.
4. Allison MA, Criqui MH, Wright CM. Patterns and risk factors for systemic calcified atherosclerosis. *Arterioscler Thromb Vasc Biol.* 2004;24(2):331–6.
5. Jain T, Peshock R, McGuire DK, Willett D, Yu Z, Vega GL, et al. African Americans and Caucasians have a similar prevalence of coronary calcium in the Dallas Heart Study. *J Am Coll Cardiol.* 2004;44(5):1011–7.
6. Bild DE, Detrano R, Peterson D, Guerci A, Liu K, Shahar E, et al. Ethnic differences in coronary calcification: the Multi-Ethnic Study of Atherosclerosis (MESA). *Circulation.* 2005;111(10):1313–20.
7. Stabley JN, Towler DA. Arterial calcification in diabetes mellitus. *Arterioscler Thromb Vasc Biol.* 2017;37(2):205–17.
8. London GM, Guérin AP, Marchais SJ, Métivier F, Pannier B, Adda H. Arterial media calcification in end-stage renal disease: impact on all-cause and cardiovascular mortality. *Nephrol Dial Transplant.* 2003;18(9):1731–40.

9. Ohtake T, Oka M, Ikee R, Mochida Y, Ishioka K, Moriya H, et al. Impact of lower limbs' arterial calcification on the prevalence and severity of PAD in patients on hemodialysis. *J Vasc Surg*. 2011;53(3):676–83.
10. Goodman WG, Goldin J, Kuizon BD, Yoon C, Gales B, Sider D, et al. Coronary-artery calcification in young adults with end-stage renal disease who are undergoing dialysis. *N Engl J Med*. 2000;342(20):1478–83.
11. Demer LL, Tintut Y. Inflammatory, metabolic, and genetic mechanisms of vascular calcification. *Arterioscler Thromb Vasc Biol*. 2014;34(4):715–23.
12. Costacou T, Huskey ND, Edmundowicz D, Stolk R, Orchard TJ. Lower-extremity arterial calcification as a correlate of coronary artery calcification. *Metabolism*. 2006;55(12):1689–96.
13. Cardenas V, Seo K, Sheth S, Meyr AJ. Prevalence of lower-extremity arterial calcification in patients with diabetes mellitus complicated by foot disease at an urban US tertiary-care center. *J Am Podiatr Med Assoc*. 2018;108(4):267–71.
14. Smith CD, Bilmen JG, Iqbal S, Robey S, Pereira M. Medial artery calcification as an indicator of diabetic peripheral vascular disease. *Foot Ankle Int*. 2008;29(2):185–90.
15. Liu KH, Chu WCW, Kong APS, Choi Ko GT, Ma RCW, Chan JWS, et al. US assessment of medial arterial calcification: a sensitive marker of diabetes-related microvascular and macrovascular complications. *Radiology*. 2012;265(1):294–302.
16. Deas DS, Marshall AP, Bian A, Shintani A, Guzman RJ. Association of cardiovascular and biochemical risk factors with tibial artery calcification. *Vasc Med Lond Engl*. 2015;20(4):326–31.
17. An WS, Son YK, Kim S-E, Kim K-H, Yoon SK, Bae H-R, et al. Vascular calcification score on plain radiographs of the feet as a predictor of peripheral arterial disease in patients with chronic kidney disease. *Int Urol Nephrol*. 2010;42(3):773–80.
18. Kugathasan P, Johansen MB, Jensen MB, Aagaard J, Nielsen RE, Jensen SE. Coronary artery calcification and mortality risk in patients with severe mental illness. *Circ Cardiovasc Imaging*. 2019;12(3):e008236.
19. Poornima IG, Mackey RH, Allison MA, Manson JE, Carr JJ, LaMonte MJ, et al. Coronary Artery Calcification (CAC) and post-trial cardiovascular events and mortality within the Women's Health Initiative (WHI) estrogen-alone trial. *J Am Heart Assoc*. 2017;6(11).
20. Allison MA, Wright CM. Age and gender are the strongest clinical correlates of prevalent coronary calcification (R1). *Int J Cardiol*. 2005;98(2):325–30.
21. Schurgin S, Rich S, Mazzone T. Increased prevalence of significant coronary artery calcification in patients with diabetes. *Diabetes Care*. 2001;24(2):335–8.
22. Singh DK, Winocour P, Summerhayes B, Kaniyur S, Viljoen A, Sivakumar G, et al. Prevalence and progression of peripheral vascular calcification in type 2 diabetes subjects with preserved kidney function. *Diabetes Res Clin Pract*. 2012;97(1):158–65.
23. Vattikuti R, Towler DA. Osteogenic regulation of vascular calcification: an early perspective. *Am J Physiol-Endocrinol Metab*. 2004;286(5):E686–96.
24. O'Neill WC, Han KH, Schneider TM, Hennigar RA. Prevalence of nonatheromatous lesions in peripheral arterial disease. *Arterioscler Thromb Vasc Biol*. 2015;35(2):439–47.
25. Gongora-Rivera F, Labreuche J, Jaramillo A, Steg PG, Hauw J-J, Amarencu P. Autopsy prevalence of coronary atherosclerosis in patients with fatal stroke. *Stroke*. 2007;38(4):1203–10.
26. Stary HC, Chandler AB, Dinsmore RE, Fuster V, Glagov S, Insull W, et al. A definition of advanced types of atherosclerotic lesions and a histological classification of atherosclerosis. A report from the Committee on Vascular Lesions of the Council on Arteriosclerosis, American Heart Association. *Circulation*. 1995;92(5):1355–74.
27. Soor GS, Vukin I, Leong SW, Oreopoulos G, Butany J. Peripheral vascular disease: who gets it and why? A histomorphological analysis of 261 arterial segments from 58 cases. *Pathology (Phila)*. 2008;40(4):385–91.
28. Shao J-S, Cai J, Towler DA. Molecular mechanisms of vascular calcification: lessons learned from the aorta. *Arterioscler Thromb Vasc Biol*. 2006;26(7):1423–30.

29. Kamenskiy A, Poulson W, Sim S, Reilly A, Luo J, MacTaggart J. Prevalence of calcification in human femoropopliteal arteries and its association with demographics, risk factors, and arterial stiffness. *Arterioscler Thromb Vasc Biol.* 2018;38(4):e48–57.
30. Everhart JE, Pettitt DJ, Knowler WC, Rose FA, Bennett PH. Medial arterial calcification and its association with mortality and complications of diabetes. *Diabetologia.* 1988;31(1):16–23.
31. Niskanen L, Siitonen O, Suhonen M, Uusitupa MI. Medial artery calcification predicts cardiovascular mortality in patients with NIDDM. *Diabetes Care.* 1994;17(11):1252–6.
32. Lehto S, Niskanen L, Suhonen M, Rönnemaa T, Laakso M. Medial artery calcification. A neglected harbinger of cardiovascular complications in non-insulin-dependent diabetes mellitus. *Arterioscler Thromb Vasc Biol.* 1996;16(8):978–83.
33. Mayfield JA, Caps MT, Boyko EJ, Ahroni JH, Smith DG. Relationship of medial arterial calcinosis to autonomic neuropathy and adverse outcomes in a diabetic veteran population. *J Diabetes Complicat.* 2002;16(2):165–71.
34. Agatston AS, Janowitz WR, Hildner FJ, Zusmer NR, Viamonte M, Detrano R. Quantification of coronary artery calcium using ultrafast computed tomography. *J Am Coll Cardiol.* 1990;15(4):827–32.
35. Huang C-L, Wu I-H, Wu Y-W, Hwang J-J, Wang S-S, Chen W-J, et al. Association of lower extremity arterial calcification with amputation and mortality in patients with symptomatic peripheral artery disease. *PLoS One.* 2014;9(2):e90201.
36. Guzman RJ, Bian A, Shintani A, Stein CM. Association of foot ulcer with tibial artery calcification is independent of peripheral occlusive disease in type 2 diabetes. *Diabetes Res Clin Pract.* 2013;99(3):281–6.
37. Shin HS, Jung Park M, Nyeo Jeon K, Min Cho J, Soo Bae K, Seob Choi D, et al. Lower extremity arterial calcification as a predictor of coronary atherosclerosis in patients with peripheral arterial disease. *Iran J Radiol [Internet].* 2016 [cited 2019 Aug 4];13(2). Available from: <https://www.ncbi.nlm.nih.gov/pmc/articles/PMC5037928/>
38. Allison MA, Hsi S, Wassel CL, Morgan C, Ix JH, Wright CM, et al. Calcified atherosclerosis in different vascular beds and the risk of mortality. *Arterioscler Thromb Vasc Biol.* 2012;32(1):140–6.
39. Chowdhury MM, Makris GC, Tarkin JM, Joshi FR, Hayes PD, Rudd James HF, et al. Lower limb arterial calcification (LLAC) scores in patients with symptomatic peripheral arterial disease are associated with increased cardiac mortality and morbidity. *PLoS ONE [Internet].* 2017 [cited 2019 Aug 2];12(9). Available from: <https://www.ncbi.nlm.nih.gov/pmc/articles/PMC5590737/>
40. Jones WS, Mi X, Qualls LG, Vemulapalli S, Peterson ED, Patel MR, et al. Trends in settings for peripheral vascular intervention and the effect of changes in the outpatient prospective payment system. *J Am Coll Cardiol.* 2015;65(9):920–7.
41. Itoga NK, Kim T, Sailer AM, Fleischmann D, Mell MW. Lower extremity computed tomography angiography can help predict technical success of endovascular revascularization in the superficial femoral and popliteal artery. *J Vasc Surg.* 2017;66(3):835–843.e1.
42. Laird JR, Katzen BT, Scheinert D, Lammer J, Carpenter J, Buchbinder M, et al. Nitinol stent implantation versus balloon angioplasty for lesions in the superficial femoral artery and proximal popliteal artery twelve-month results from the RESILIENT randomized trial. *Circ Cardiovasc Interv.* 2010;3(3):267–76.
43. Bakken AM, Palchik E, Hart JP, Rhodes JM, Saad WE, Davies MG. Impact of diabetes mellitus on outcomes of superficial femoral artery endoluminal interventions. *J Vasc Surg.* 2007;46(5):946–58; discussion 958.
44. Kang IS, Lee W, Choi BW, Choi D, Hong M-K, Jang Y, et al. Semiquantitative assessment of tibial artery calcification by computed tomography angiography and its ability to predict infrapopliteal angioplasty outcomes. *J Vasc Surg.* 2016;64(5):1335–43.
45. Manunga JM, Gloviczki P, Oderich GS, Kalra M, Duncan AA, Fleming MD, et al. Femoral artery calcification as a determinant of success for percutaneous access for endovascular abdominal aortic aneurysm repair. *J Vasc Surg.* 2013;58(5):1208–12.

46. Tepe G, Beschoner U, Ruether C, Fischer I, Pfaffinger P, Noory E, et al. Drug-eluting balloon therapy for femoropopliteal occlusive disease: predictors of outcome with a special emphasis on calcium. *J Endovasc Ther.* 2015;22(5):727–33.
47. Fanelli F, Cannavale A, Gazzetti M, Lucatelli P, Wlderker A, Cirelli C, et al. Calcium burden assessment and impact on drug-eluting balloons in peripheral arterial disease. *Cardiovasc Intervent Radiol.* 2014;37(4):898–907.
48. Ichihashi S, Shibata T, Fujimura N, Nagatomi S, Yamamoto H, Kyuragi R, et al. Vessel calcification as a risk factor for in-stent restenosis in complex femoropopliteal lesions after Zilver PTX paclitaxel-coated stent placement. *J Endovasc Ther.* 2019;1:1526602819860124.
49. Rocha-Singh KJ, Zeller T, Jaff MR. Peripheral arterial calcification: prevalence, mechanism, detection, and clinical implications. *Catheter Cardiovasc Interv.* 2014;83(6):E212–20.
50. Amighi J, Schillinger M, Dick P, Schlager O, Sabeti S, Mlekusch W, et al. De novo superficial femoropopliteal artery lesions: peripheral cutting balloon angioplasty and restenosis rates—randomized controlled trial. *Radiology.* 2008;247(1):267–72.
51. Shammam NW, Lam R, Mustapha J, Ellichman J, Aggarwala G, Rivera E, et al. Comparison of orbital atherectomy plus balloon angioplasty vs. balloon angioplasty alone in patients with critical limb ischemia: results of the CALCIUM 360 randomized pilot trial. *J Endovasc Ther.* 2012;19(4):480–8.
52. Zeller T, Langhoff R, Rocha-Singh KJ, Jaff MR, Blessing E, Amann-Vesti B, et al. Directional atherectomy followed by a paclitaxel-coated balloon to inhibit restenosis and maintain vessel patency: twelve-month results of the DEFINITIVE AR Study. *Circ Cardiovasc Interv.* 2017;10(9).
53. Cioppa A, Stabile E, Popusoi G, Salemme L, Cota L, Pucciarelli A, et al. Combined treatment of heavy calcified femoro-popliteal lesions using directional atherectomy and a paclitaxel coated balloon: one-year single centre clinical results. *Cardiovasc Revascularization Med Mol Interv.* 2012;13(4):219–23.
54. Foley TR, Cotter RP, Kokkinidis DG, Nguyen DD, Waldo SW, Armstrong EJ. Mid-term outcomes of orbital atherectomy combined with drug-coated balloon angioplasty for treatment of femoropopliteal disease. *Catheter Cardiovasc Interv.* 2017;89(6):1078–85.
55. Fitzgerald PJ, Ports TA, Yock PG. Contribution of localized calcium deposits to dissection after angioplasty. An observational study using intravascular ultrasound. *Circulation.* 1992;86(1):64–70.
56. Tzafiriri AR, Garcia-Polite F, Zani B, Stanley J, Muraj B, Knutson J, et al. Calcified plaque modification alters local drug delivery in the treatment of peripheral atherosclerosis. *J Control Release.* 2017;264:203–10.
57. Brodmann M, Holden A, Zeller T. Safety and feasibility of intravascular lithotripsy for treatment of below-the-knee arterial stenoses. *J Endovasc Ther.* 2018;25(4):499–503.
58. Brodmann M, Schwindt A, Argyriou A, Gammon R. Safety and feasibility of intravascular lithotripsy for treatment of common femoral artery stenoses. *J Endovasc Ther.* 2019;26(3):283–7.
59. Marshall AP, Luo W, Wang X, Lin T, Cai Y, Guzman RJ. Medial artery calcification increases neointimal hyperplasia after balloon injury. *Sci Rep [Internet].* 2019 [cited 2019 Aug 9];9. Available from: <https://www.ncbi.nlm.nih.gov/pmc/articles/PMC6547750/>
60. Chowdhury MM, Tarkin JM, Albaghdadi MS, Evans NR, Le EPV, Berrett TB, et al. Vascular positron emission tomography and restenosis in symptomatic peripheral arterial disease: a prospective clinical study. *JACC Cardiovasc Imaging.* 2020;13(4):1008–17.
61. Misare BD, Pomposelli FB, Gibbons GW, Campbell DR, Freeman DV, LoGerfo FW. Infrapopliteal bypasses to severely calcified, unclampable outflow arteries: two-year results. *J Vasc Surg.* 1996;24(1):6–16.
62. Ballotta E, Renon L, Toffano M, Piccoli A, Da Giau G. Patency and limb salvage rates after distal revascularization to unclampable calcified outflow arteries. *J Vasc Surg.* 2004;39(3):539–46.
63. Guérin AP, London GM, Marchais SJ, Metivier F. Arterial stiffening and vascular calcifications in end-stage renal disease. *Nephrol Dial Transplant.* 2000;15(7):1014–21.

64. Odink AE, Mattace-Raso FUS, van der Lugt A, Hofman A, Hunink MGM, Breteler MMB, et al. The association of arterial stiffness and arterial calcification: the Rotterdam Study. *J Hum Hypertens.* 2008;22(3):205–7.
65. Atkinson J. Age-related medial elastocalcinosis in arteries: mechanisms, animal models, and physiological consequences. *J Appl Physiol* (Bethesda, MD 1985). 2008;105(5):1643–51.
66. Desyatova A, MacTaggart J, Kamenskiy A. Constitutive modeling of human femoropopliteal artery biaxial stiffening due to aging and diabetes. *Acta Biomater.* 2017;64:50–8.
67. Blacher J, Guerin AP, Pannier B, Marchais SJ, London GM. Arterial calcifications, arterial stiffness, and cardiovascular risk in end-stage renal disease. *Hypertension.* 2001;38(4):938–42.
68. Oikonomou E, Siasos G, Georgiopoulos G, Vavuranakis E, Vogiatzi G, Maniatis K, et al. Arterial stiffness and vascular calcification predicts adverse cardiovascular events in subjects with coronary artery disease after percutaneous coronary intervention. *J Am Coll Cardiol.* 2018;71(11 Supplement):A109.
69. Ramirez JL, Spaulding KA, Zahner GJ, Khetani SA, Schaller MS, Gasper WJ, et al. Radial artery tonometry is associated with major adverse cardiac events in patients with peripheral artery disease. *J Surg Res.* 2019;235:250–7.
70. Kals J, Lieberg J, Kampus P, Zagura M, Eha J, Zilmer M. Prognostic impact of arterial stiffness in patients with symptomatic peripheral arterial disease. *Eur J Vasc Endovasc Surg.* 2014;48(3):308–15.
71. Zettervall SL, Buck DB, Darling JD, Lee V, Schermerhorn ML, Guzman RJ. Increased pre-operative pulse pressure predicts procedural complications and mortality in patients undergoing tibial interventions for critical limb ischemia. *J Vasc Surg.* 2016;63(3):673–7.
72. Kizu A, Koyama H, Tanaka S, Maeno T, Komatsu M, Fukumoto S, et al. Arterial wall stiffness is associated with peripheral circulation in patients with type 2 diabetes. *Atherosclerosis.* 2003;170(1):87–91.
73. Suzuki E, Kashiwagi A, Nishio Y, Egawa K, Shimizu S, Maegawa H, et al. Increased arterial wall stiffness limits flow volume in the lower extremities in type 2 diabetic patients. *Diabetes Care.* 2001;24(12):2107–14.
74. Brewer LC, Chai H-S, Bailey KR, Kullo IJ. Measures of arterial stiffness and wave reflection are associated with walking distance in patients with peripheral arterial disease. *Atherosclerosis.* 2007;191(2):384–90.
75. Jacomella V, Shenoy A, Mosimann K, Kohler MK, Amann-Vesti B, Husmann M. The impact of endovascular lower-limb revascularisation on the aortic augmentation index in patients with peripheral arterial disease. *Eur J Vasc Endovasc Surg.* 2013;45(5):497–501.
76. Durham AL, Speer MY, Scatena M, Giachelli CM, Shanahan CM. Role of smooth muscle cells in vascular calcification: implications in atherosclerosis and arterial stiffness. *Cardiovasc Res.* 2018;114(4):590–600.
77. Amann K. Media calcification and intima calcification are distinct entities in chronic kidney disease. *Clin J Am Soc Nephrol CJASN.* 2008;3(6):1599–605.
78. Schantl AE, Ivarsson ME, Leroux J-C. Investigational pharmacological treatments for vascular calcification. *Adv Ther.* 2019;2(1):1800094.
79. Shea MK, Holden RM. Vitamin K status and vascular calcification: evidence from observational and clinical studies. *Adv Nutr.* 2012;3(2):158–65.
80. Sage AP, Tintut Y, Demer LL. Regulatory mechanisms in vascular calcification. *Nat Rev Cardiol.* 2010;7(9):528–36.
81. Adirekkiat S, Sumethkul V, Ingsathit A, Domrongkitchaiporn S, Phakdeekitcharoen B, Kantachuvesiri S, et al. Sodium thiosulfate delays the progression of coronary artery calcification in haemodialysis patients. *Nephrol Dial Transplant.* 2010;25(6):1923–9.
82. Mary A, Hartemann A, Liabeuf S, Aubert CE, Kemel S, Salem JE, et al. Association between metformin use and below-the-knee arterial calcification score in type 2 diabetic patients. *Cardiovasc Diabetol.* 2017;16(1):24.

83. Diaz-Tocados JM, Peralta-Ramirez A, Rodríguez-Ortiz ME, Raya AI, Lopez I, Pineda C, et al. Dietary magnesium supplementation prevents and reverses vascular and soft tissue calcifications in uremic rats. *Kidney Int.* 2017;92(5):1084–99.
84. Bressendorff I, Hansen D, Schou M, Kragelund C, Brandt L. The effect of magnesium supplementation on vascular calcification in chronic kidney disease—a randomised clinical trial (MAGiCAL-CKD): essential study design and rationale. *BMJ Open.* 2017;7(6):e016795.
85. Karamched SR, Nosoudi N, Moreland HE, Chowdhury A, Vyavahare NR. Site-specific chelation therapy with EDTA-loaded albumin nanoparticles reverses arterial calcification in a rat model of chronic kidney disease. *Sci Rep.* 2019;9(1):1–11.

Chapter 9

Bioprosthetic Heart Valve Calcification: Clinicopathologic Correlations, Mechanisms, and Prevention



Frederick J. Schoen and Robert J. Levy

Valvular heart disease is an important clinical problem. Since there is yet no effective medical therapy for most heart valve disease, hemodynamic adjustment by replacement of the defective valve by a substitute (or otherwise surgically removing or resolving the structural defect) is the only effective treatment. Tissue heart valves are composed of animal tissue (i.e., a xenograft), an unrelated human's tissue (i.e., an allograft), or a patient's own tissue (i.e., an autograft), as a valve replacement. Most widely used for this purpose is a *bioprosthetic valve* or *bioprosthesis*, a particular type of fabricated tissue valve that combines a chemically treated (and thus nonliving) biologic tissue with a synthetic supporting frame [1]. Although contemporary bioprostheses mimic the structure and function of the natural aortic valve, they suffer a high rate of progressive and age-dependent structural valve deterioration resulting in device failure. Two distinct processes (largely but perhaps not entirely independent)—intrinsic calcification (synonym mineralization) and non-calcific tissue degradation—account for structural valve deterioration. These degradation mechanisms are largely a result of the complex changes to tissues used in bioprostheses induced by valve fabrication prior to implantation and the progressive interactions with the physiologic environment that occur following implantation. This chapter summarizes (1) general concepts of healthy heart valve functional structure (2) heart valve disease, (3) contemporary valve replacement technologies

F. J. Schoen (✉)

Department of Pathology, Brigham and Women's Hospital, Harvard Medical School,
Boston, MA, USA

e-mail: fschoen@bwh.harvard.edu

R. J. Levy

The Division of Cardiology, Department of Pediatrics, The Children's Hospital of
Philadelphia, Philadelphia, PA, USA

The Perelman School of Medicine at the University of Pennsylvania, Philadelphia, PA, USA

© Springer Nature Switzerland AG 2020

E. Aikawa, J. D. Hutcheson (eds.), *Cardiovascular Calcification and Bone
Mineralization*, Contemporary Cardiology,

https://doi.org/10.1007/978-3-030-46725-8_9

and the functional structure of bioprosthetic tissue, (4) clinicopathologic correlations in bioprosthetic heart valve failure, (5) calcific and other mechanisms in bioprosthetic valve failure, and (6) mechanism-based strategies for mitigation of experimental and clinical bioprosthetic valve calcification.

Native Heart Valve Functional Structure

An understanding of the principles of native heart valve function and dysfunction is essential to understanding bioprosthetic heart valve pathology.

Healthy native heart valves maintain unidirectional blood flow via an extraordinarily dynamic, mechanically adapted and durable structure that withstands high-repetitive mechanical stress and strain of opening and closing, approximately 40 million cycles per year, over many years (i.e., 3 billion cycles over 75 years!). All four cardiac valves have a highly responsive internal micro-architecture that accommodates substantial changes in size and shape of the valve cusps and leaflets that occur during the cardiac cycle. Moreover, effective and durable valve functional motion depends on complex cell-cell and cell-extracellular matrix (ECM) interactions and structural changes that occur over both short- and long-time frames (illustrated in Fig. 9.1 for the aortic valve) [2–4].

Heart valves have a layered architectural pattern, typified by the functional anatomy of the aortic valve (AV): (1) a dense collagenous layer (the *fibrosa*), close to the outflow surface, which provides strength, (2) a central core of loose connective tissue rich in amorphous ECM (predominately glycosaminoglycans [GAGs]) which facilitates relative internal motions and rearrangements of cells and extracellular matrix (the *spongiosa*), and (3) a layer, closest to the inflow surface rich in elastin that enables recoil after cuspal stretching during diastole (the *ventricularis*). Thus, the essential functional components of the heart valves comprise the ECM components enumerated above and cells that synthesize and maintain the ECM, including deep valvular interstitial cells (VIC) and valvular endothelial cells (VECs) that line the blood-contacting valve surfaces.

The quantity, quality, and spatial distribution of the valvular ECM enable both the cyclical functional mechanics over the second-to-second periodicity of the cardiac cycle and the long-term (lifetime) durability of a valve. Macroscopic mechanical stimuli, both shear and solid stresses, that occur dynamically during normal valvular function as cyclical blood flow moves and flows over the leaflets, are translated into microscopic forces that impact biological phenomena at the tissue and cellular levels. Thus, although the mechanisms are not yet entirely clear, VICs and VECs sense the local tissue mechanical environment and, through their interactions with the ECM, transduce forces into molecular changes that mediate valvular homeostasis and pathobiology. Through such mechanisms, healthy heart valves can not only adapt in large measure to altered stress states but also to repair injury via remodeling mediated by the synthesis, repair, and remodeling of the several ECM components [5, 6].

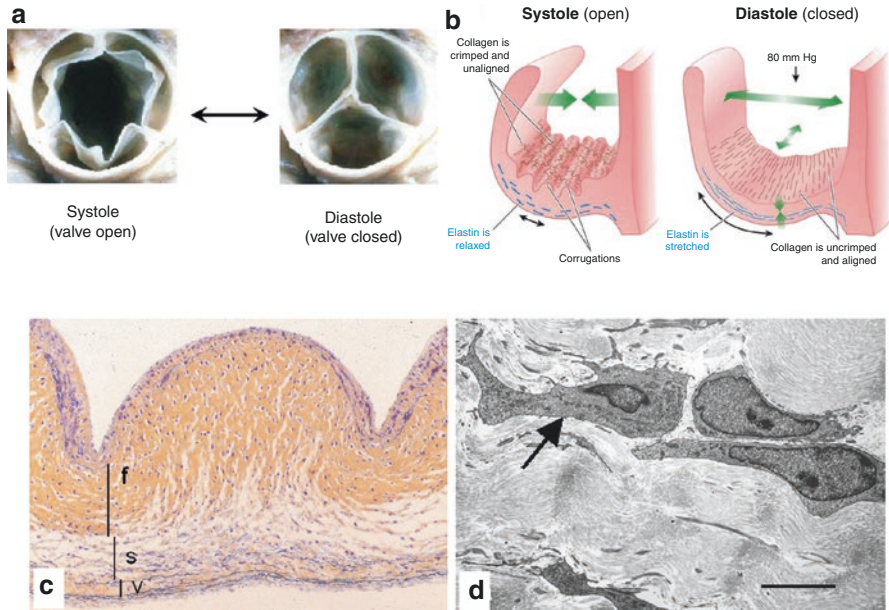


Fig. 9.1 Aortic valve functional structure at macroscopic and microscopic levels. **(a)** Outflow aspect of aortic valve in open (*left*) and closed (*right*) positions, corresponding to systole and diastole, respectively. **(b)** Schematic representation of architecture and configuration of an individual aortic valve cusp in cross section showing collagen and elastin changes in systole and diastole. **(c)** Tissue architecture, shown as low-magnification photomicrograph of cuspal cross section in the nondistended state (corresponding to systole), emphasizing the three major layers: ventricularis (*v*), spongiosa (*s*), and fibrosa (*f*). The outflow surface is at the top. Original magnification: 100×. Movat pentachrome stain (collagen, yellow, predominant in fibrosa; elastin, black, prominent in ventricularis). Nuclei of valvular interstitial cells (VICs) are visible as purple dots. **(d)** Transmission electron photomicrograph of relaxed fresh porcine aortic valve (characteristic of the systolic configuration), demonstrating the fibroblast morphology of VICs (arrow), the dense, surrounding closely apposed collagen with wavy crimp, and the potential for VIC-collagen and VIC-VIC interactions. Scale bar: 5 μm. **((a)** Reproduced with permission from Schoen and Edwards [111]. **(b-d)** Reproduced with permission from Schoen [3])

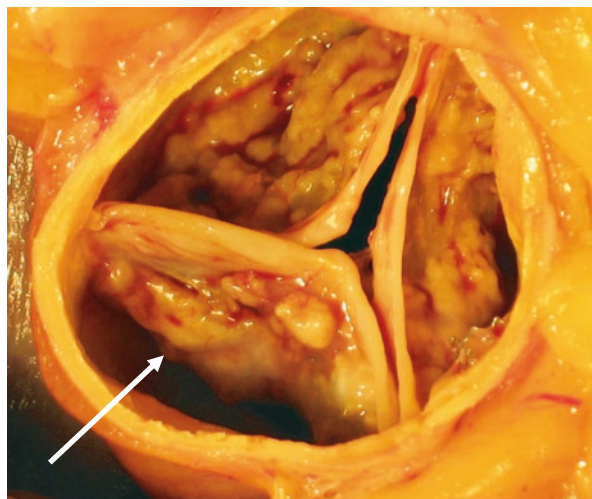
However, when environmental change becomes excessive and prolonged, or injury to key components occurs, clinically significant valve pathology may result [7].

Thus, VIC health is prerequisite to healthy valve function and durability. Indeed, as the most abundant cell type in the heart valves, and distributed throughout all its layers, VICs are generally considered the most influential cell in normal aortic valve function and pathology of both native and bioprosthetic valves. VICs synthesize ECM and express matrix-degrading enzymes (including matrix metalloproteinases [MMPs] and tissue inhibitors to metalloproteinases [TIMPs]) that effect remodeling of collagen and other matrix components. Thus, through matrix remodeling and ongoing repair of functional damage to collagen and the other ECM components, VICs enable extended valve performance.

Valvular Heart Disease

Disease of the heart valves is the second most frequent form of heart disease (behind atherosclerotic coronary artery and ischemic heart disease) and results in significant mortality and morbidity. Aortic stenosis (AS), illustrated in Fig. 9.2, is the most common and deleterious functional abnormality and the most serious manifestation of the more general process of calcific aortic valve disease (CAVD). AS is characterized by the formation of calcific masses initially within the aortic valve cusps that inhibit valve opening and ultimately protrude through the out-flow surfaces into the sinuses of Valsalva (i.e., the spaces behind the aortic valve cusps into which they open) [8]. The calcific process begins in the valvular fibrosa layer, at the margins of attachment (the points of maximal cusp flexion and thereby mechanical stress). Both the incidence and severity of CAVD increase with age, with only 5% of individuals younger than 45 years but more than 20% of subjects older than 75 years having AV calcification [9, 10]. AS to some degree is present in more than 10% of individuals >70 years of age; in over 2% it is severe. AV calcification in older patients most often occurs in trileaflet valves; the pathologic result is termed aortic sclerosis [11]. Overall, 25,000 persons per year in the United States die from valvular heart disease, of which 17,000 have AS, a number which is expected to triple by 2050 as the aging population dramatically increases [12]. Owing to the secondary deterioration in cardiac function that results from AS, approximately half of individuals with critical AS succumb to the disease within 2–3 years following the onset of symptoms (thus, the natural history of AS is comparable to that of some of the most frequently encountered cancers!).

Fig. 9.2 Calcific valvular degeneration manifest as aortic stenosis of a previously normal valve having three cusps (viewed from aortic aspect). Nodular masses of calcium are heaped-up within the sinuses of Valsalva (*arrow*). (Reproduced with permission from Schoen and Edwards [111])



Bicuspid aortic valve (BAV), a common congenital cardiac abnormality affecting approximately 2% of the population and usually exhibiting normal function during early life, is a strong risk factor for premature valve calcification and AS. Indeed, by age 60 years, 85% of individuals who have a BAV develop stenosis, and approximately half of adults undergoing valve replacement for AS have a BAV. Moreover, calcific stenosis of a BAV is generally accelerated, appearing approximately a decade earlier than in an anatomically normal aortic valve (with three cusps). It is generally thought that the major factor accelerating AS in BAV is the elevated stresses within the anatomically abnormal valve.

The pathogenesis of CAVD (and hence AS) is largely uncertain. Key controversies relate to the extent to which its mechanisms are shared with those of atherosclerosis, the extent to which degenerative and inflammatory processes play relative roles, and the extent to which the initiation and progression of calcification are actively regulated (see Chap. 4 for a discussion on similarities and differences between arterial and valvular calcification) [13]. The pathogenesis of bioprosthetic valve calcification (discussed in detail below) may share some features with native valve CAVD, including that cell injury is likely an important early event that induces tissue vulnerability to the mineralization process. In CAVD, the increased mechanical stress on and/or ischemia of resident VICs induced by aging-related valvular remodeling, inflammation, and other mechanical and biochemical processes could play an important role in early cell injury (apoptosis or necrosis) or osteogenic differentiation of VICs (see Chap. 6 for more on mechanical stresses in native CAVD). In bioprosthetic valves, calcification is nucleated within residual cells that have been devitalized by glutaraldehyde pretreatment. Irrespective of mechanism of cell injury, damaged cells are both incapable of excluding excess calcium ions and have membranes that provide a rich source of phosphorus containing substrate for calcium-phosphorus crystal precipitation. Passive calcification of dead or damaged cells is called *dystrophic* calcification.

Physiologic mineralization of skeletal tissue and that occurring pathologically in calcific diseases (including CAVD and bioprosthetic valve calcification) also shares essential features [14]. Firstly, the mineral deposited initially in both normal and pathological calcification is almost always a poorly crystalline form of hydroxyapatite, $\text{Ca}_{10}(\text{P04})_6(\text{OH})_2$, often substituted in carbonate. Once nucleated, mineral crystals proliferate in normal serum concentrations of calcium and phosphate and can serve as nuclei or templates for the precipitation of new crystals. A second feature common to virtually all forms of calcification (including that which occurs in atherosclerotic plaque, valvular degeneration, bioprosthetic heart valves, and other cardiovascular calcification) is crystal nucleation and early progression in association with cell membranes, usually in the form of extracellular membrane-bound vesicles or aging or devitalized cells [15]. Mineral initiation in developing bones and other skeletal and dental structures also involve extracellular “matrix vesicles.” ECM components, especially collagen and elastin, may also play a role in physiologic and pathologic calcification. Moreover, there is an interesting reciprocal relationship between osteoporosis and cardiovascular calcification; indeed, recent clinical and experimental studies in atherosclerosis and osteoporosis have demonstrated that oxidative stress and oxidized lipids decrease bone formation in the skeletal system, while they increase bone formation in the cardiovascular system in atherosclerosis [16].

Heart Valve Replacement

Surgical aortic valve replacement utilizing an open chest approach and incorporating cardiopulmonary bypass is the traditional treatment for severe symptomatic aortic stenosis (AS); this treatment markedly improves symptoms and quality of life and prolongs survival. Valve replacement has low operative mortality (3% for aortic valve replacement [AVR]). Moreover, long-term outcomes are generally favorable; survival is 50–70% at 10–15 years following valve replacement [17]. Nevertheless, one or more valve-related problems necessitate reoperation or cause death in approximately 60–70% of patients with substitute valves within 10–15 years post-operatively [18, 19]. The overall *rates* of valve-related complications are similar for mechanical prostheses and bioprostheses. However, the frequency and nature of valve-related complications are markedly dependent on the prosthesis type, model, size, site of implantation, and patient characteristics (e.g., ventricular function, arrhythmias). Since the valve materials and design/hemodynamics do not resemble those of natural heart valves, mechanical valves tend to induce platelet deposition and blood coagulation, and patients receiving them must be treated with lifelong anticoagulation to reduce the risk of thrombosis and thromboembolic events. In contrast, the most frequent cause of bioprosthetic valve dysfunction is structural valve degeneration (SVD), often resulting from calcification [20, 21].

Surgical Valve Replacement

Surgical valve replacement uses either mechanical or tissue valve substitutes (Fig. 9.3). All substitute heart valves have three generic components — a mobile rigid “occluder” or flexible leaflet (either synthetic or biologic), a superstructure to contain and guide the motion of the moving part(s), and a fabric-covered sewing cuff (used to sew or otherwise anchor the valve to the tissues). Widely used mechanical prosthetic heart valves employ rigid occluders and a cage-like superstructure



Fig. 9.3 Mechanical and bioprosthetic heart valves. (a) St. Jude Medical bileaflet tilting disk heart valve. (b) Hancock porcine aortic valve bioprosthesis. (c) Carpentier-Edwards bovine pericardial valve. (Reproduced by permission from Schoen and Butany [21])

(today, both virtually always composed of pyrolytic carbon, a material with high strength, excellent fatigue and wear resistance, and exceptional biocompatibility, including relative thromboresistance).

In contrast, tissue valves have a trileaflet configuration with a central orifice and thus superficially bear strong resemblance to natural valves. Bioprostheses are tissue valves that have been chemically treated in glutaraldehyde, preserving the tissue, decreasing its immunological reactivity, and rendering the cells of the tissue nonviable. Immunosuppression is not employed with bioprosthetic valves, as is required for whole organ transplants (e.g., kidney, liver, or heart). However, owing to chemical treatment, bioprosthetic valves no longer contain cells capable of remodeling or responding to injury as does normal tissue. Fabricated tissue valve cusps are usually mounted on a fabric-covered metal or plastic stent with three posts (called struts) to simulate the geometry of a native aortic valve. As with mechanical valves, the base ring is covered by a fabric sewing cuff to facilitate surgical implantation and healing. Also used occasionally are tissue valves derived from human cadaveric aortic or pulmonary valves with or without the associated vascular conduit (called allografts or homografts); allograft valves are generally not glutaraldehyde preserved, and recipients do not usually receive immunosuppressive medication. Tissue valves generally have good hemodynamic profiles, a low incidence of thromboembolic complications without chronic anticoagulation, and a low reinfection rate following valve replacement for endocarditis. Since thrombotic complications are less frequent in patients with tissue valves than those with mechanical valves, chronic anticoagulation therapy is generally unnecessary in patients having tissue replacement valves. Avoiding the need for chronic anticoagulation is a key attraction of bioprosthetic (and other tissue) heart valves [22].

Nearly 100,000 valve substitutes are implanted surgically each year in the United States and almost 300,000 worldwide; today, approximately 20% replacements use mechanical valves, and 80% use tissue valves (composed of animal or human tissue) [23, 24]. The ratio of bioprostheses implanted relative to mechanical valves has been increasing over the past several decades, owing to their favorable hemodynamic profile, low thrombogenicity, and improvements in tissue treatments intended to decrease calcification and otherwise enhance durability. Moreover, owing to a substantial evidence base demonstrating superiority of recent technical innovations in enhancing outcomes, and manufacturing and other considerations, pericardial bioprosthetic valves are used almost exclusively.

Transcatheter Aortic Valve Implantation (TAVI) and Other Bioprostheses Interventions

Owing to advanced age, frailty, and often multiple comorbidities, which raise periprocedural risk, a substantial fraction of patients with AS, estimated at least 30–40%, is deemed unsuitable for surgical aortic valve replacement [25]. Previously, there

was no effective surgical intervention suitable for these patients. In classical open surgical AVR, the chest is opened through a large sternal incision, and the native valve is removed and replaced by a prosthesis. In contrast, in transcatheter aortic valve implantation (TAVI), the device is passed into the femoral artery retrograde up the aorta to the aortic valve and deployed, thereby opening the valve. The diseased valve is not removed; rather, the valve cusps are pushed aside by a stent-mounted valve that holds open the valve orifice. The transcatheter aortic valves with the largest clinical experience are composed of either a balloon expandable stainless-steel stent that houses a bovine pericardial valve or a self-expandable nitinol stent that houses a porcine pericardial trileaflet valve (Fig. 9.4). As a less invasive alternative to conventional AVR, TAVI extends the opportunity for effective mechanical correction to a potentially large population of otherwise untreatable individuals [26, 27] and has rapidly become the new standard of care for many patients with AS who would otherwise be deemed inoperable.

Clinical experience with TAVI is growing rapidly. Randomized and observational clinical trials comparing TAVI to classical open surgical AVR suggest that survival following TAVI in high-risk patients is equivalent to or better than that following surgical AVR to at least 2 years [28, 29], and studies are beginning to show benefit in some low- and intermediate-risk patients [30].

Another important approved interventional procedure that uses a bioprosthetic valve is pulmonary valve replacement for pulmonary regurgitation post-tetralogy of Fallot or other congenital heart disease repair. For example, the catheter-deployed Melody valve manufactured by Medtronic is fabricated from a glutaraldehyde fixed bovine jugular vein bioprosthesis [31]. Mitral and pulmonary valve interventional bioprosthetic devices are also being developed [32]. With the rise of transcatheter procedures worldwide, the use of bioprosthetic valves is estimated to

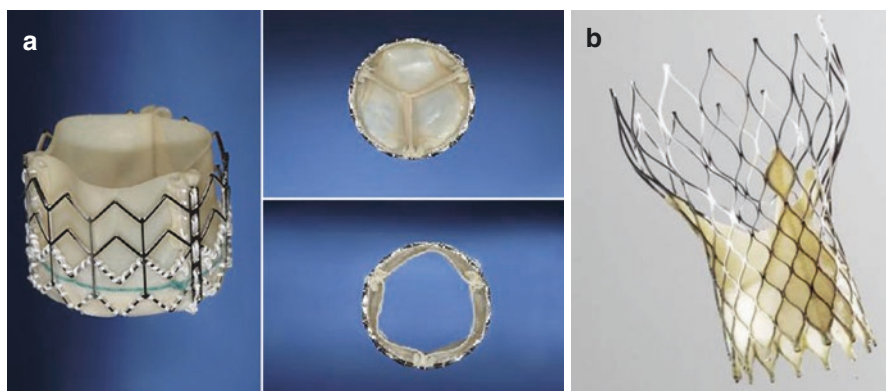


Fig. 9.4 Transcatheter aortic valves. (a) The Sapien (R) valve consists of three equine pericardial leaflets fixed to a balloon expandable steel stent. It is hand crimped over a delivery balloon prior to deployment via balloon expansion. (b) The CoreValve (R) is constructed of porcine pericardium attached to a self-expanding nickel-titanium alloy (nitinol) stent. (Reproduced by permission from Schoen and Butany [21])

increase dramatically. Nevertheless, the durability of valves implanted via a transcatheter implantation route or other interventional techniques is largely uncertain as is whether and to what extent calcification will limit clinical success [33, 34]. What is clear is that the fabrication technology for leaflet fixation of interventional bioprosthetic valves is similar to the fabrication technology used to create surgically implanted bioprosthetic devices, and transcatheter valve crimping may induce additional structural damage that could accelerate tissue degradation, including calcification, following implantation [35].

Structural Considerations in Bioprosthetic Heart Valves

As stated earlier, a “bioprosthesis” is a tissue valve fabricated from animal-derived tissue (i.e., a xenograft or heterograft)— today most frequently chemically preserved bovine (cow) pericardium (Fig. 9.5). The structure and composition of valve-derived and pericardial biomaterials are somewhat different. A porcine aortic valve is a complete heart valve, altered by chemical treatment (and the protein cross-linking and mechanical changes that result) and the constraints of mounting and anatomic structure on a prosthetic stent. Normal porcine valves (like human valves) have absent-to-sparse blood vessels. In contrast, bovine pericardium used in valves is derived from the parietal pericardium as a sheet of collagenous material, does not

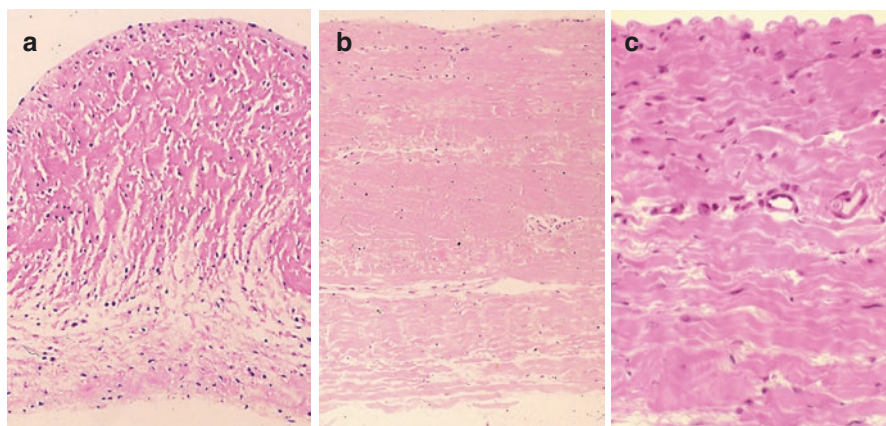


Fig. 9.5 Cross-sectional microscopic structures of porcine aortic valve and bovine pericardium used in bioprosthetic valves. **(a)** Porcine aortic valve cusp in the nondistended state (corresponding to systole), showing layered architecture with diffusely distributed interstitial cells (similar to Fig. 9.1c). Outflow surface at top. Thickness approximately 300 μm . **(b)** Bovine parietal pericardium, showing dense-laminated fibrous tissue with diffusely distributed cells. Outflow cuspal surface at top, tissue aspect originally toward the heart in the animal from which the tissue was derived. Thickness approximately 500 μm . **(c)** Higher-power photomicrograph of bovine pericardium showing wavy collagen bundles, interstitial fibroblasts, and scattered blood vessels. All stained with hematoxylin and eosin. (Reproduced by permission from Schoen [112])

have the underlying functional architecture of a valve cusp, and is not as compact as that of porcine valve fibrosa. Additionally, the cells of porcine aortic valve are VICs, while the interstitial cells of pericardium are fibroblasts. Pericardial tissue is composed almost entirely of type I collagen, whereas porcine valve contains a mixture of type I and type III collagens. Pericardium has (a) a smooth serosal layer, originally toward the heart and covered in the animal by mesothelial cells, which are generally lost in valve processing; (b) a fibrosa (almost the entire thickness), which contains collagen, sparse elastic fibers, and occasional nerves, blood vessels, and lymphatics; and (c) rough pericardial connective tissue, with loosely arranged collagen and elastic fibers, on the side that was originally facing away from the heart. Thus, the surface of valve pericardium that previously faced the pericardial space is smooth, while the other is the rough external surface from which blood vessels and fat were dissected away during valve fabrication. Pericardial valves are typically manufactured with the rough side tissue facing toward the inflow, to keep this surface well washed and thereby minimize the possibility of thrombosis. Moreover, in contrast to porcine aortic valve cusps whose natural attachments to the supporting aortic wall are preserved, thereby facilitating stress transfer from the cusps to the aortic wall, pericardial bioprosthetic valve cusps are pieces of tissue that are artificially trimmed and attached to a stent. Thus, cuspal stresses in pericardial valves are concentrated at the attachment points of tissue to the frame.

Bioprosthetic Valve Structural Degeneration

Structural valve degeneration (SVD) is defined as “Dysfunction or deterioration involving the operated valve (exclusive of infection and thrombosis), as determined by reoperation, autopsy or clinical investigation” [36]. Bioprosthetic valve SVD is manifested as thickening, stiffening, tearing, or disruption of the bioprosthetic valve leaflets with eventual associated valve hemodynamic dysfunction, manifested as stenosis or regurgitation.

Cuspal calcification is the major pathologic mechanism of structural degeneration (Fig. 9.6) [37]. In our study, porcine aortic valve failure was caused by calcification in approximately 85% [38]. The incidence of failure increases with longer postoperative intervals. Structural degeneration is unusual in bioprostheses implanted less than 5 years, and the incidence rises rapidly thereafter (Fig. 9.7); nevertheless, the level of calcification accumulated in explanted bioprostheses varies widely (Fig. 9.8). Clinical data indicate that the meantime to valve failure owing to structural dysfunction manifested as primary tissue failure of both porcine aortic valve and pericardial bioprosthetic mitral or aortic valve replacements is approximately 15–20 years following implantation [39–41], consistent for bioprostheses fabricated from both porcine aortic valve and bovine pericardium.

The mineral that forms in bioprosthetic valves is a poorly crystalline calcium phosphate, chemically related to hydroxyapatite in musculoskeletal mineralization. Moreover, crystal formation is largely associated with cell membranes. In the bone,

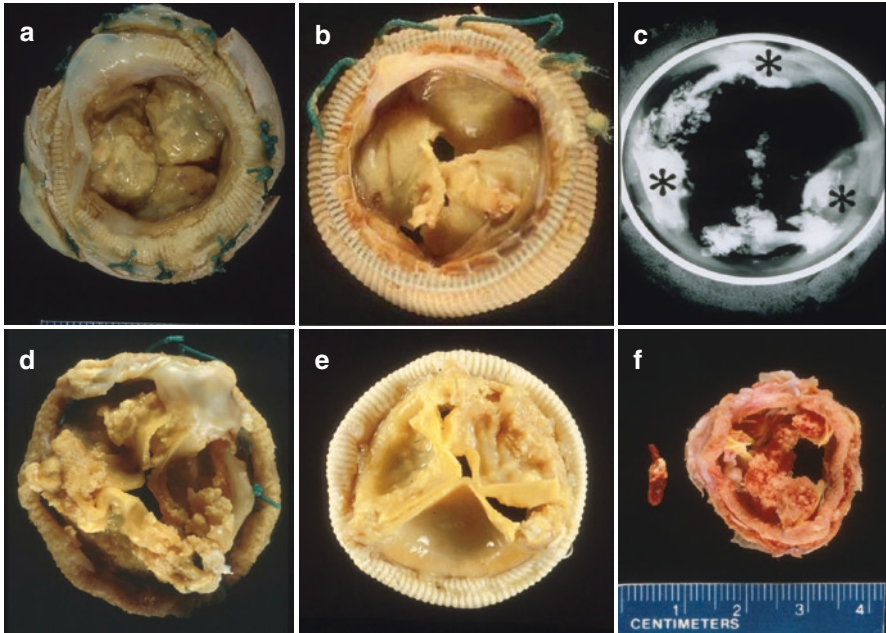


Fig. 9.6 Structural dysfunction of bioprosthetic valves. (a) Calcific stenosis of porcine valve bioprosthesis. (b) Calcification with secondary tear in porcine aortic valve bioprosthesis. (c) Radiograph of porcine aortic valve bioprosthesis with massive calcification (commissures denoted by asterisks). (d) Calcific stenosis of bovine pericardial valve. (e) Calcification with secondary tear (arrow) leading to severe regurgitation of bovine pericardial valve. (f) Massive calcification of a porcine aortic valve bioprosthesis with secondary calcific embolus removed at surgery from the left anterior descending coronary artery. ((a and f) Reproduced by permission from Schoen [112]. (c) Reproduced by permission from Schoen and Butany [21]. (d and e) Reproduced by permission from Schoen [113])

the membranous elements at which calcification is nucleated are known as matrix vesicles. In pathological calcification (of which bioprosthetic tissue mineralization is representative), a similar role is played by membranes and their fragments derived from degenerate, aging, injured, or dead cells. In both physiological and pathological calcification, deposits also occur in extracellular matrix elements.

The kinetics of calcification and the rate of failure are strongly influenced by the age of the recipient at valve implantation across the entire age spectrum for both porcine valves and pericardial valves (Fig. 9.9). Younger patients calcify more rapidly, leading to a higher failure rate. For example, the freedom from structural valve degeneration at 20 years for patients was 37% for those <60 years, 53% for those 60–70 years, and 92% for those over 70 years. The rate of bioprosthetic mitral valve failure is greater than that of the aortic, for example, meantime to failure for patients <60 years with aortic pericardial valves was 18 years but only 12 years for those in the same age group with mitral pericardial valves. Moreover, children, adolescents, and young adults often have an especially accelerated failure rate. Accelerated

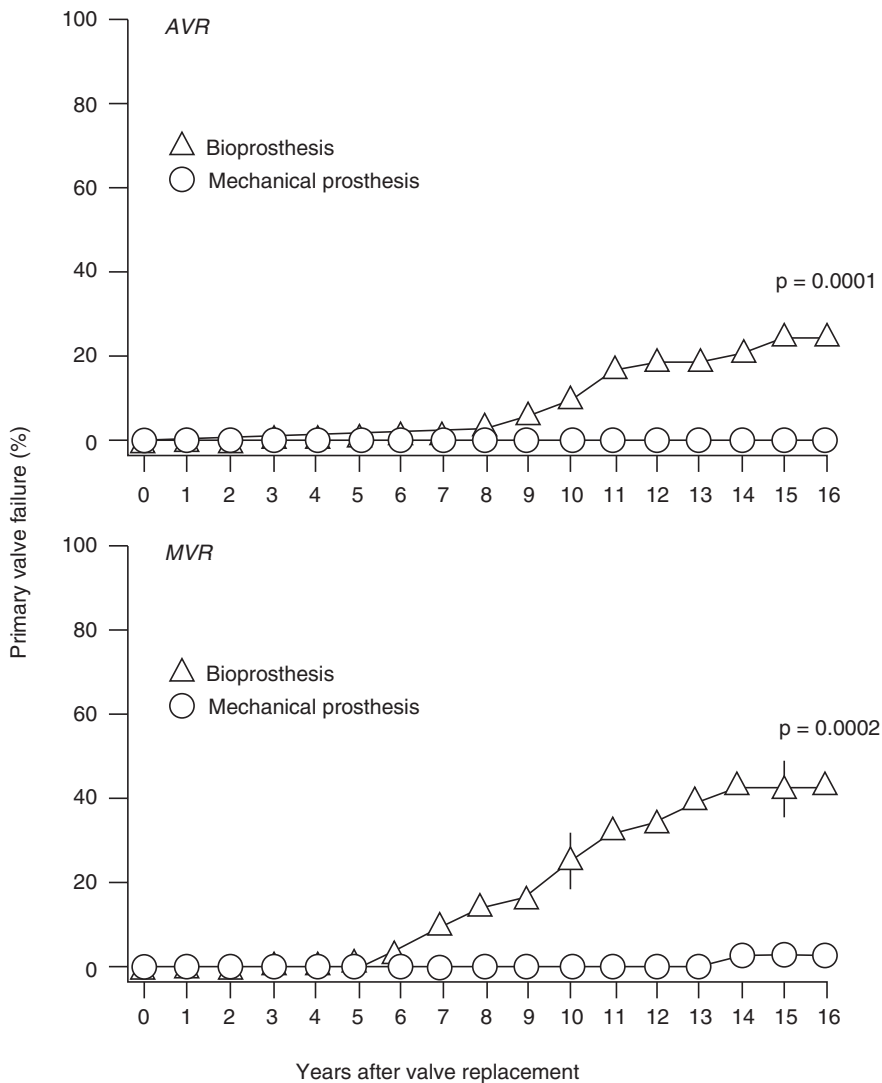
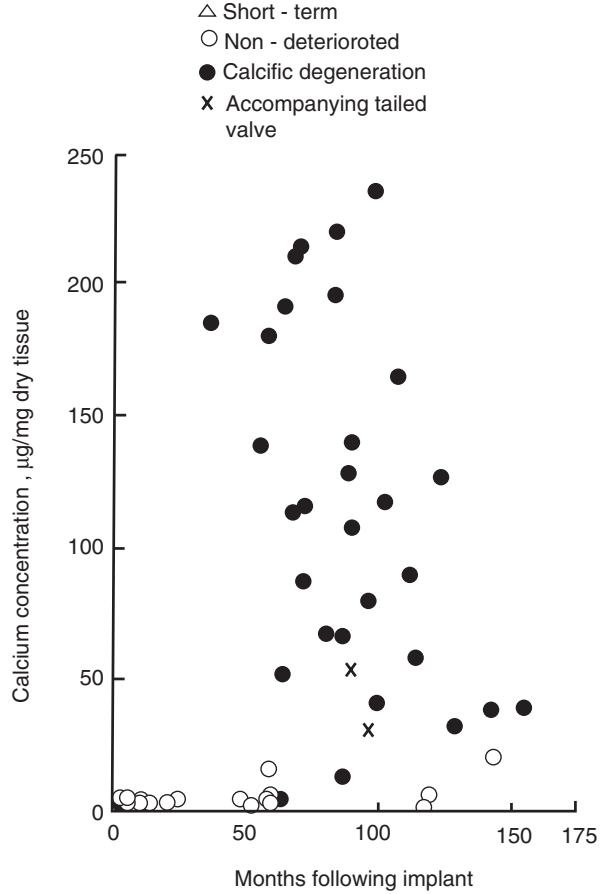


Fig. 9.7 Frequency of primary valve failure for mechanical and tissue valves following mitral valve replacement (MVR) and aortic valve replacement (AVR). For bioprosthetic valves, cuspal mineralization is the major responsible pathologic mechanism with regurgitation through tears, the most frequent failure mode. For mechanical valves, the most common complication is not primary valve failure, but thromboembolism. (Reproduced by permission from Hammermeister et al. [19])

Fig. 9.8 Calcium concentration of removed porcine bioprosthetic valves, measured by atomic absorption spectroscopy, plotted against duration of function. Valves included very short-term implants, deteriorated valves removed at autopsy or cardiac transplantation, valves suffering structural deterioration, and those removed in tandem with a failed valve. (From Schoen et al. [54])



failure occurs by 5 years in many of those <35 years old [42], although the specific rate of failure may be dependent on the specific valve type. Thus, bioprosthetic valves have a low rate of failure in the elderly; since such patients have an especially high risk of anticoagulant-related hemorrhage and thus would prefer to avoid this therapy, bioprosthetic valves are particularly attractive in this patient population. As mentioned above, the durability of transcatheter valves and the role of calcification in their potential failure is yet unknown. However, some data suggest a rate of at least moderate SVD of approximately 13% at 5 years [43].

Calcification following implantation of bioprosthetic valves occurs in a tissue is made vulnerable by the chemical treatment and physical changes that are induced during valve fabrication and their consequences following implantation [44]. Indeed, unimplanted bioprosthetic valves show several structural differences

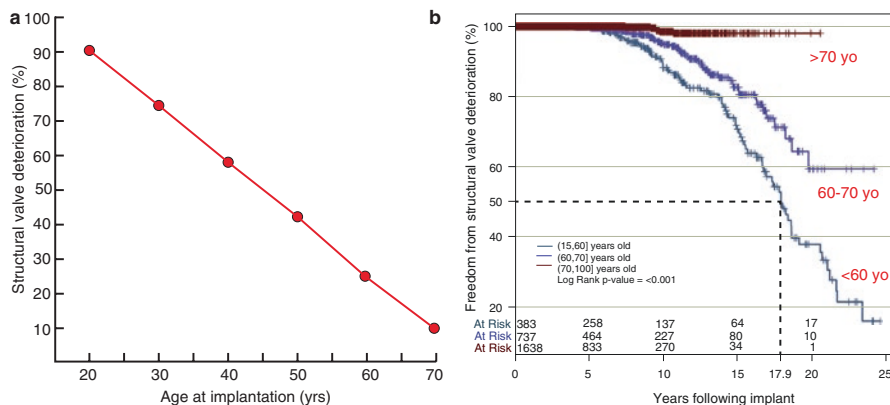


Fig. 9.9 Age dependence of structural bioprosthetic valve calcification. **(a)** Summary data for studies of structural valve deterioration of biological valves at 15–20 years based on the patient’s age at implantation. Young age is a key risk factor for early bioprosthetic valve failure (Rahimtoola [17]). **(b)** Freedom from explantation from structural valve deterioration stratified by age groups for clinical bovine pericardial valves in the aortic position. The mean durability in patients less than 60 years old is 17.9 years following implantation. (Modified by permission from Bourguignon et al. [40])

from healthy native tissue comprising aortic valve or pericardium. These changes include flattening of the cuspal corrugations (aortic valve), loss of pre-existing surface endothelium or mesothelium (aortic valve or pericardial bioprostheses, respectively), autolytic disruption of porcine or bovine interstitial cells, collagen bundle loosening, and loss of GAGs. Chemical preservation induces a fixed geometric configuration of the leaflets so that their motion during the cardiac cycle often causes non-physiologic movement and focal buckling. Moreover, and very importantly, the interstitial cells (of porcine aortic valve or bovine pericardium) lose their viability during glutaraldehyde treatment; thus, physiologic cuspal remodeling is not possible.

Following implantation, pathologic changes occur in all types of bioprostheses. The cuspal surfaces become variably covered by fibrin, platelets, monocytes/macrophages, and occasionally multinucleated giant cells. Proteins with other constituents of plasma and often erythrocytes penetrate into the cusps (called fluid insudation and cuspal hematoma, respectively). Accumulations of the blood can stiffen the cusps and possibly provide cellular nucleation sites for mineralization. Valve function *in vivo* also gradually results in generalized architectural homogenization with connective tissue disruption, loss of staining of interstitial cell nuclei, and lipid accumulation. Although mineralization, collagen degeneration, and possibly GAG depletion contribute to valve failure, to what extent other nonspecific pathologic processes contribute to late failure modes is uncertain. The valve sewing cuff and basal regions of the cusps also become variably covered by a fibrous sheath of host origin (pannus), which, when excessive, can lead to orifice obstruction or focal cusp immobilization or other mechanical changes that can contribute to calcification.

Calcific and Noncalcific Mechanisms of Bioprosthetic Valve Structural Deterioration

Experimental Models for Investigation of Bioprosthetic Valve Calcification

Animal models have facilitated the investigation of the pathophysiology of bioprosthetic tissue calcification and have served as a preclinical screen for the development of new or modified materials and design configurations. Informative animal models have included (1) orthotopic valve replacements (in the tricuspid, pulmonary, mitral, or aortic positions) or conduit-mounted valves in sheep or calves [45] and (2) isolated tissue (i.e., not in a valve) samples implanted subcutaneously in rodents or intramuscularly in rabbits [46–49]. In both circulatory and non-circulatory models, bioprosthetic tissue calcifies progressively with a morphology similar to that observed in clinical specimens but with markedly accelerated kinetics. In vitro models of biomaterials calcification have been investigated but have yielded only limited useful information in studying mechanisms or preventive strategies [50–52]. Compared with the several years normally required for calcification of clinical bioprosthetic valves, valve replacements in sheep or calves calcify extensively in 3 to 6 months. However, large animal models are expensive and technically complex, and such animals grow rapidly, have differences in anatomy from that of humans, and are without the pathologic substrate into which human implants are placed, often yielding varying results among subjects treated similarly. Such studies have limited value in elucidating mechanisms of calcification and other biomaterials-tissue interactions. Nevertheless, these models are required for regulatory approval for clinical studies of a new or significantly altered design or tissue treatment, and they often raise important issues that other studies have not revealed [53].

The limitations of large animal models stimulated the development of subdermal (synonym, *subcutaneous*, i.e., under the skin) implant models. Subdermal bioprosthetic implants in rats, rabbits, and mice provide the following useful features: (1) a markedly accelerated rate of calcification in a morphology comparable to that seen in circulatory explants; (2) low cost that permits many specimens to be studied with a given set of experimental conditions, thereby allowing quantitative characterization and statistical comparisons; and (3) quick retrieval of specimens from the experimental animals, which facilitates the careful manipulation and rapid processing required for detailed analyses. Specific factors that may play a role in calcification can be isolated, and hypothetical mechanisms can be studied in detail and relatively expeditiously. The model also emulates the clinical outcomes of accelerated calcification in younger individuals, and thus rapidly growing 3-week-old weanling rats have been used predominantly as the experimental model, with the calcification process followed over time (Fig. 9.10a). In the subcutaneous model, calcification occurs progressively to a degree similar to that encountered in clinical specimens in 3 weeks (approximately 120 mg/mg calcium) [54] in tissue implanted subcutaneously in rats; maximal levels (200–250 mg/mg calcium) occur in approximately 8 weeks (Fig. 9.10a) [37, 46–49]. The degree and kinetics of calcification are similar for calf and cow pericardium and for porcine aortic valve. Mitral valve implants in sheep (both porcine aortic and bovine pericardial valves)

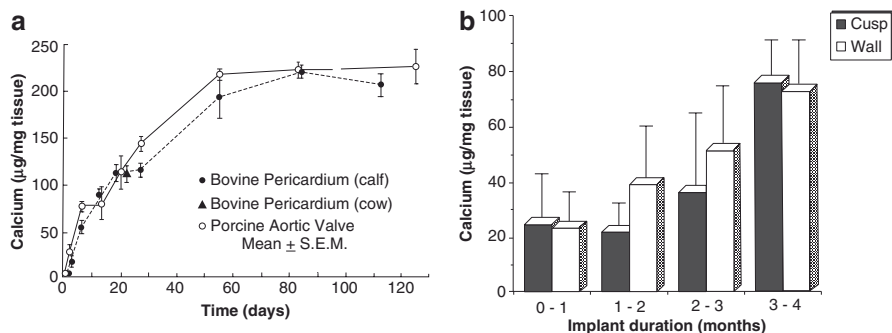


Fig. 9.10 Progression of experimental calcification in glutaraldehyde-pretreated bioprosthetic tissues in several animal models. In both models shown, calcification kinetics are accelerated greatly over that observed for clinical implants. **(a)** Calcification of tissue from bovine pericardial bioprosthetic tissue [calf and adult cow] and porcine aortic valve, implanted subcutaneously in rats, as determined by calcium and phosphorus assay. **(b)** Calcification of cusps and adjacent aortic wall in porcine aortic bioprosthetic valves implanted as orthotopic mitral valve replacements in juvenile sheep. **((a)** Reproduced by permission from Schoen et al. [49]. **(b)** Reproduced by permission from Schoen et al. [45])

accumulate similar levels of mineral in 3–5 months (Fig. 9.10b) [45]. The aortic wall portions that are incorporated into bioprostheses fabricated from porcine aortic valves also calcify to a similar degree, but generally without clinical consequence.

The subcutaneous model has been widely used to screen potential strategies for calcification inhibition (*anticalcification*). Data from these models provide a data set to which studies on inhibitory approaches can be compared. Promising approaches can be investigated further in a large animal valve implant model. However, strategies that appeared efficacious in subcutaneous implants have not always proven favorable when used on valves implanted into the circulation.

Pathophysiology of Bioprosthetic Heart Valve Calcification

Data from valve explants from patients and subdermal and circulatory experiments in animal models using bioprosthetic heart valve tissue have elucidated the mechanisms, earliest events, and determinants of bioprosthetic valve calcification. Fundamentally, calcification of bioprosthetic tissue appears to depend on exposure of a susceptible substrate to calcium-containing extracellular fluid; other local implant-related, mechanical, and circulating substances may play a regulatory role (Fig. 9.11). Three factors are most important in regulating bioprosthetic tissue mineralization: (1) host biological factors (local environment of function and recipient's metabolic state); (2) implant biomaterial factors (the structure and chemistry of the substrate biomaterial); and (3) biomechanical factors (degree and locations of stresses and deformations). Residual phosphorus in cell-related membranes localizes the Ca-P mineral nucleation sites. Consistent with a dystrophic mechanism, the initial calcification sites in bioprosthetic tissue are predominantly nonviable cells and cell membrane fragments, although ECM elements can also calcify [55] (Fig. 9.12). Features of this mechanism are illustrated in Fig. 9.13 and discussed in detail below.

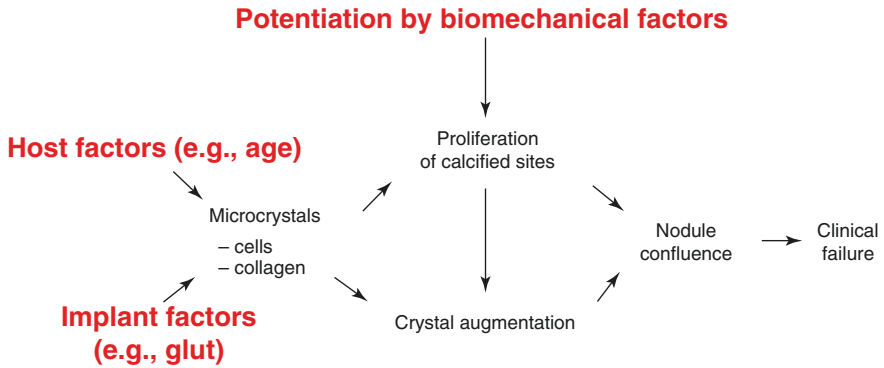


Fig. 9.11 Schematic model for sequence of events in the calcification of clinical bioprosthetic heart valves supported by experimental data, emphasizing the key roles of host, implant structural and biomechanical factors. (Reproduced from Schoen et al. [48])

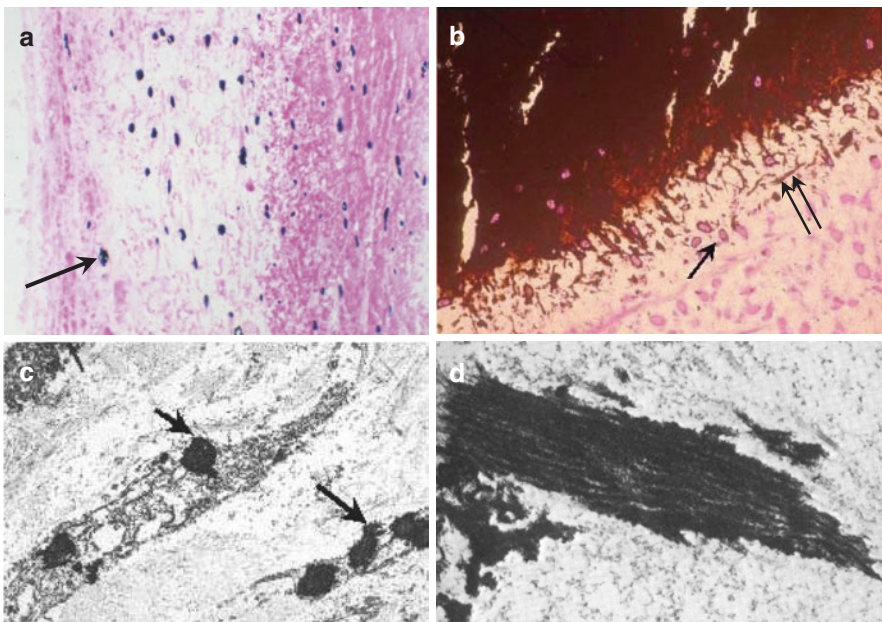


Fig. 9.12 Initiation of bioprosthetic valve calcification in structural tissue elements of bioprosthetic tissue. (a) Initial discrete calcific deposits (delineated by arrow) associated with residual cells in glutaraldehyde-pretreated porcine aortic valve tissue implanted subcutaneously in rat. (b) Edge of enlarging deposit in porcine bioprosthesis implanted in growing sheep for 5 months, demonstrating predominant site of growing edge of calcification in cells of the residual porcine valve matrix (arrows). (b) Photomicrograph of the edge of expanding calcific deposit in experimental porcine aortic valve bioprosthesis implanted in a sheep, demonstrating both round and streak-like calcific densities, representing calcification initiated in cells (single arrow) and collagen (double arrow), respectively. Originally approximately 300 \times . (c) Transmission electron microscopic photomicrograph of cell membrane-associated calcific deposits (arrows). Bar = 1 μ m. (d) Transmission electron microscopic photomicrograph of calcification in collagen. Bar = 1 μ m. (a and b) von Kossa stain: calcium phosphates black or dark brown. ((b) Reproduced by permission from Schoen et al. [114]. (c) Reproduced by permission from Schoen et al. [49]. (d) Reproduced by permission from Schoen et al. [48])

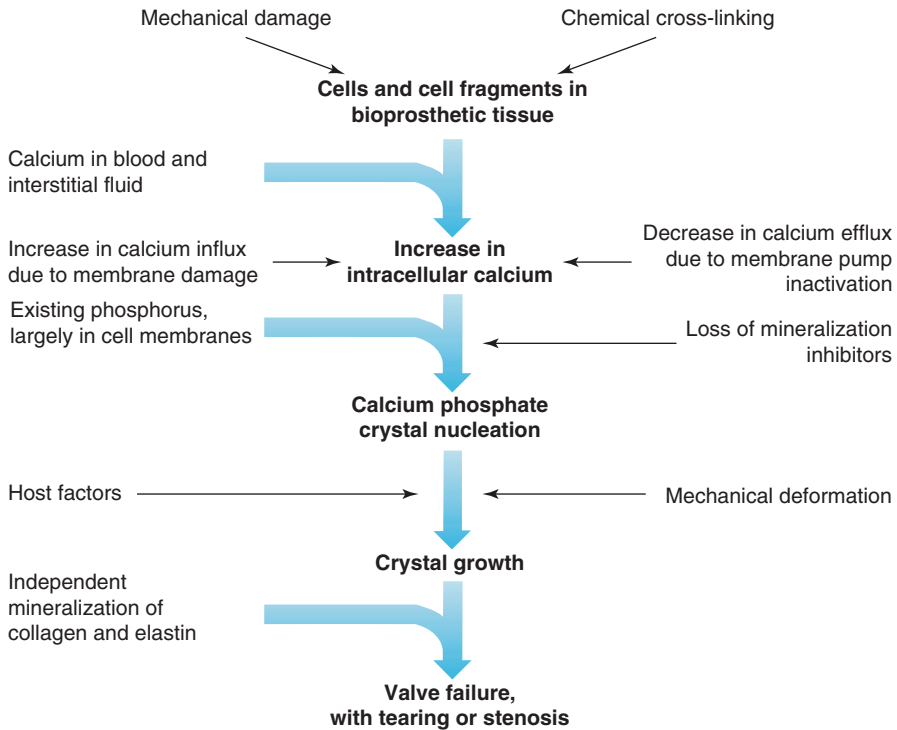


Fig. 9.13 Extended hypothetical model for the calcification of bioprosthetic tissue. This model considers host factors, implant factors, and mechanical damage and relates initial sites of mineral nucleation to increased intracellular calcium in association with residual cells and cell fragments in bioprosthetic tissue. The ultimate macroscopic result of calcification is valve failure, with tearing or stenosis. The key contributory role of existing phosphorus in cell membranes in determining the initial sites of crystal nucleation is emphasized, and a possible role for the independent mineralization of collagen and/or elastin is noted. Mechanical deformation probably accelerates both nucleation and growth of calcific crystals, although the precise mechanisms are unclear. (Modified by permission from Schoen [115] and Schoen [3])

Physiologically, extracellular calcium concentration in tissues is approximately 1 mg/ml (10^{-3} M); in contrast, the intracellular concentration of calcium (in the cytoplasm) is 1000–10,000 times lower (approximately 10^{-7} M). This steep calcium gradient is maintained in healthy cells with intact membranes by mechanisms that pump calcium to the exterior using calcium ATPases and other avenues for extrusion. In cells which have been rendered nonviable by glutaraldehyde fixation (or are otherwise injured during valve function), the normal cellular handling of calcium ions is disabled. Cell membranes and other intercellular structures are high in phosphorus (as phosphesters, especially phosphatidylserine, which can bind calcium); such sites serve as nucleators. Glutaraldehyde pretreatment also stabilizes these phosphorous stores. Other susceptible sites can include collagen and elastic fibers

of the extracellular matrix (discussed below), denatured proteins, phosphoproteins, fatty acids, blood platelets, and, in the case of infection, bacteria.

Calcification of the extracellular matrix structural proteins collagen and elastin has been observed in clinical and experimental implants of bioprosthetic and homograft valvular and vascular tissue and has been studied using a rat subdermal model. Collagen-containing implants are widely used in various surgical applications, such as tendon prostheses and surgical absorptive sponges, but their usefulness is often compromised owing to calcium phosphate deposits and resultant stiffening. Cross-linking by either glutaraldehyde or formaldehyde promotes the calcification of collagen sponge implants made of purified collagen [56]. Although elastin is not stabilized by glutaraldehyde cross-linking, elastin calcification can also occur [57].

Role of Host Biological Factors

The most important host metabolic factors relate to young age, with more rapid calcification taking place in younger patients or experimental animals and pathologic alterations of mineral concentrations in the circulating blood. Although the relationship with age is well-established clinically and incontrovertible, the mechanisms accounting for this “physiologic” effect of age are uncertain. Factors that can change blood chemistry such as comorbidities (e.g., chronic kidney impairment, hypercalcemia, or diabetes) may aggravate the mineral deposition process. Moreover, it is possible that the mechanisms responsible for bioprosthetic valve calcification may be at least partially regulated through naturally occurring inhibitors to crystal nucleation and growth or mineralization cofactors.

Role of Substrate Factors

In both circulatory and subcutaneous models, the morphology, kinetics, and chemistry of calcification in porcine aortic valve and bovine pericardial tissue are largely identical. In addition, structural deterioration of bioprosthetic heart valves derives from the chemical, mechanical, and morphological changes that occur during fabrication of bioprosthetic valves. Glutaraldehyde (1,5-pentanedialdehyde; $\text{CHO}[\text{CH}_2]_3\text{CHO}$) is the most frequently used chemical preservative for bioprosthetic tissue. Forming complex, degradation-resistant, Schiff base- and pyridinium-derived cross-links between protein molecules of many types, glutaraldehyde efficiently cross-links collagen, the most abundant structural valve protein. The role of glutaraldehyde (GA) in promoting calcification is well-established and strong [58, 59]. Two key processes, both directly related to the chemical effects of GA, are believed to dominate: (1) reaction between the residual phosphorus and associated phosphoesters in the tissue with calcium in the surrounding fluid to yield calcium-phosphate mineral and (2) chemical reactions related to the presence of active residual-free aldehyde functional groups induced by GA fixation [60].

Thus, in addition to cellular devitalization and stabilizing phosphorus in the tissue, glutaraldehyde treatment produces functional group residuals (i.e., aldehydes, various carbonyls, Schiff bases, etc.) by which not only cells but potentially matrix glycosaminoglycans and structural proteins, such as collagen and elastin, may also bind calcium. Tissue levels of reactive functional group residuals can be directly correlated to bioprosthetic tissue calcification [61–63]. Indeed, tissue levels of calcification correlate with aldehyde content [58]. The close association between aldehyde content and the calcification of bovine pericardial tissue suggests that processing of bioprosthetic valves to reduce the content or reactivity of reactive residual aldehydes may offer a significant advantage in terms of reducing the potential for long-term bioprosthetic valve calcification [64–68]. Collagen and elastic fiber calcification may occur through reactive aldehyde-related mechanisms. Thus, stabilizing those components in the biological tissue might improve calcification resistance [69].

Role of Biomechanical Factors

Although experimental and clinical calcification of bioprosthetic tissues can occur in situations where mechanical stress and strain are minimal or absent, and dynamic stress does not seem prerequisite for calcification to occur, mechanical activity can stimulate calcification. Bioprosthetic tissue mineralization is enhanced at the sites of intense mechanical deformations generated by repetitive motion, such as the points of flexion in heart valves. Moreover, in the subcutaneous model, calcification is enhanced in areas of tissue folds, bends, and areas of shear [48]. Furthermore, long-term cyclic wear on materials has been demonstrated to cause permanent geometric deformations that are due to ECM degradation in tissue-based valves, specifically unraveling the collagen triple helix. Recently, it has been suggested that pre-implantation crimping of the pericardium in transcatheter aortic valves can lead to material damage that promotes calcification [70]. Also, long-term bioprosthetic valve function is accompanied by collagen degradation in the most highly stressed regions [71, 72], and highly stressed regions typically manifest the earliest and most substantial calcification. Nevertheless, although these data suggest that local tissue disruption mediates the mechanical effect, the precise mechanisms by which mechanical factors influence calcification are uncertain.

Role of Immunologic Factors

Although a potential role for inflammatory and immune processes has been postulated by some investigators [73, 74], no direct evidence of a role of immunologic mechanisms in calcification or structural degeneration has been demonstrated. Indeed, many lines of evidence suggest that neither nonspecific inflammation nor specific immunologic responses appear to potentiate calcification of glutaraldehyde-fixed bioprosthetic tissue in a clinical or experimental setting. Specific evidence

against a contributory role of effector immunologic processes is as follows: (1) calcification in either circulatory or subcutaneous locations is not usually associated with inflammation, (2) the extent and morphology of experimental mineralization are not altered by enclosure of valve cusps in filter chambers that prevent host cell contact with tissue but allow free diffusion of extracellular fluid [48] or implantation of valve tissue in congenitally athymic (“nude”) mice, who have essentially no T-cell function [75], and (3) clinical data show that second bioprosthetic valve replacements fail no sooner than initial replacements. Moreover, clinical and experimental data detecting antibodies to valve tissue probably reflect a secondary response to valve damage and resultant exposure of new antigenic determinants due to failure, rather than its cause. Interestingly, the aortic valves of human heart transplant patients who have died as a result of massive cellular myocardial rejection show very little inflammation in the valves [76]. This may reflect the typical paucity of blood vessels in the valve cusps, the inability of circulating inflammatory cells to adhere to moving cups in a high shear stress environment, or a lack of contact with significantly antigenic substances.

Thus, the key determinants of bioprosthetic valve mineralization drivers are (1) biochemical environment, (2) implant structure and chemistry, and (3) mechanical factors. Calcification is accelerated by young recipient age, likely a result of age-related biochemical differences in systemic calcium and phosphorus metabolism. Moreover, evidence does not support a causal immunologic or inflammatory basis for bioprosthetic valve calcification or failure. Therefore, the primary approaches to inhibiting valve calcification have targeted the processes involved in the nucleation of calcific deposits and thus have sought to remove or alter the cell-based phospholipids of the substrate. However, since progressive collagen damage cannot be repaired in a devitalized valve, degradation of the valvular collagenous skeleton would likely become the limiting factor in durability of valves protected from calcification. The role of degradation of GAGs in limiting bioprosthetic valve durability is less well characterized, but evidence suggests that improved GAG preservation also may be beneficial [77].

Noncalcific Mechanisms of Bioprosthetic Valve Structural Deterioration

Although bioprostheses mimic some features typical of aortic valve structure, the cusps and configurations of a contemporary bioprosthesis following chemical pretreatment and manipulation during manufacture differ in many respects from those of a native valve. Chemical fixation of porcine aortic valve or bovine pericardial tissue with glutaraldehyde destroys the viability of the resident cells of the tissues, either VICs (of porcine aortic valves) or fibroblasts (of bovine pericardial valves). Thus, since nonviable cells are incapable of remodeling collagen, ongoing repair of the bioprosthetic valve ECM by the cells of the transplanted tissue is impossible, and any damage to the ECM is cumulative. Moreover, devitalized VECs of porcine

AV bioprostheses are largely denuded by handling, thereby increasing the permeability of the tissue to fluid. Finally, fixation locks the collagenous network mechanically into a configuration that inhibits the smooth internal cuspal structural rearrangements of the ECM accompanying normal valvular function, thereby inducing some abnormal motions (e.g., buckling) of the cuspal tissue during opening and closing of a fixed bioprosthesis and causing internal structural damage [78].

Thus, noncalcific damage to the valvular structural matrix accrues through a combination of factors which include abnormal valve motion, owing to stent mounting and fixation-induced mechanical changes in the tissue, inhibition of the structural rearrangements which occur during normal valve function, loss of cell-mediated remodeling and replenishment of the valvular extracellular matrix, and damage both due to chemical and possibly molecular determinants. Chemical pretreatment obviates the dynamic structural rearrangements that optimize natural valve function, often causing buckling. This causes increased flexural stresses that can induce damage to cuspal collagen fibers, particularly in regions subjected to compressive stresses. Tears are frequently localized to the commissures and cuspal bases, areas in which stresses are concentrated.

Calcific and noncalcific damage could be synergistic. Collagen disruption could expose or produce new calcium nucleation sites, create internal spaces which facilitate calcific crystal growth, or promote fluid insudation. Conversely, mechanical damage could result from calcification-induced structural disruption or stress concentrations within the cusp. Clearly, maintenance of tissue structural integrity is critical to extending durability of tissue heart valves, through prevention of both calcific and noncalcific mechanisms of deterioration.

Prevention of Bioprosthetic Valve Calcification

Since calcification of bioprosthetic valves is an important limitation to their clinical success, there have been widespread efforts toward mitigation or total prevention. Three generic strategies have been investigated for preventing calcification of biomaterial implants: (1) systemic therapy with anticalcification agents; (2) local therapy with implantable drug delivery devices; and (3) biomaterial modifications, such as removal of a calcifiable component, addition of an exogenous agent, or chemical alteration [79].

A rational approach to preventing bioprosthetic calcification must integrate safety and efficacy considerations with the scientific basis for inhibition of known mechanisms of calcium phosphate crystal formation in these tissues. Furthermore, analogous to the regulatory approval conditions and before implementation of any new or modified drug or device, a potential antimineralization treatment must be

demonstrated to be safe and effective. The treatment should not impede valve performance such as hemodynamics or durability. Investigations of an anticalcification strategy must demonstrate not only the effectiveness of the therapy but also the absence of adverse effects [80]. In this setting, adverse effects could include systemic or local toxicity, a tendency toward thrombosis or infection, induction of immunological or other inflammatory effects, or accelerated structural degradation, with either immediate loss of mechanical properties or progress but premature deterioration and failure. Indeed, there are several examples whereby an antimineralization treatment contributed to an unacceptable degradation of the tissue [81–83].

From an efficacy standpoint, experimental studies have demonstrated that adequate doses of systemic agents used to treat clinical metabolic bone disease, including calcium chelators (e.g., bisphosphonates such as ethane hydroxybisphosphonate [EHBP]), can dramatically lower the calcification potential of bioprosthetic tissue implanted subcutaneously in rats [84]. However, systemic therapy is unlikely to be safe, because such chemicals generally also interfere with physiologic calcification (i.e., bone growth), causing growth retardation. To avoid this difficulty, investigators have considered controlled drug release, studied as co-implants of a drug delivery system adjacent to the prosthesis, in which the effective drug concentration would be confined to the site where it is needed (i.e., the implant). In this approach, systemic side effects would likely be prevented [85]. A localized anticalcification effect would be particularly attractive in young people. Although studies incorporating EHBP in nondegradable polymers, such as ethylene-vinyl acetate (EVA), polydimethylsiloxane (silicone), silastic, and polyurethanes, showed effectiveness of this strategy in animal models, this approach would be challenging to implement clinically, and thus has not been further pursued.

Several approaches to prevent calcification and thereby enhance durability of tissue valves have been studied experimentally, and several have been approved for use in contemporary clinical valves. The most practical strategy for preventing calcification of clinical bioprosthetic heart valves involves biomaterial modifications, by either removal or modification of a calcifiable component, addition of an exogenous agent, or chemical alteration of the substrate (Fig. 9.14). The agents most widely studied, for efficacy, mechanisms, lack of adverse effects, and potential clinical utility, are summarized briefly below. Combination therapies using multiple agents may provide a synergy of beneficial effects. Some of the approaches that have been investigated in preclinical and clinical studies are described below; several have achieved been approved by the US FDA and regulatory bodies abroad and have proven successful in clinical bioprosthetic valves. Clinical studies have suggested that antimineralization therapy of bioprosthetic heart valves reduces the incidence of SVD (Fig. 9.15) [86].

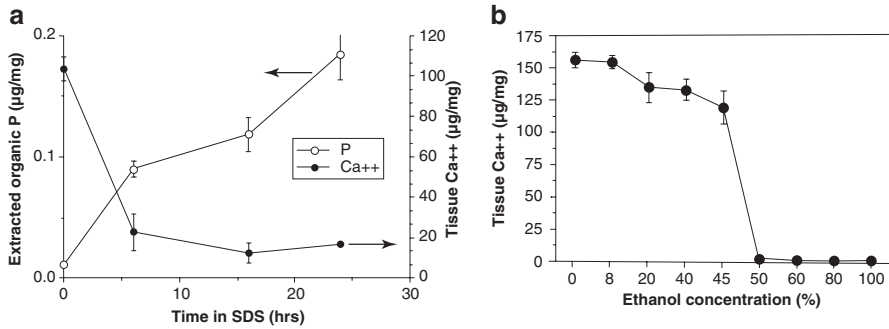


Fig. 9.14 Experimental demonstration of mechanism-based anticalcification therapies. **(a)** Effects of preincubation in 1% sodium dodecyl sulfate (SDS) on calcification in a rat subcutaneous model of glutaraldehyde cross-linked porcine aortic valve, after 21 days implantation. Lipid extraction progressively diminishes tissue vulnerability to calcification. These results provide support for the mechanistic inferences and principle that phosphoester (especially phospholipid) extraction is an important (but perhaps not the only potential) target for inhibition of bioprosthetic tissue calcification. **(b)** Decreased calcification of ethanol-treated (24 hours) glutaraldehyde cross-linked porcine aortic valve in a rat subcutaneous model of glutaraldehyde cross-linked porcine aortic valve, after 21 days implantation. There is a sharp dose-response relationship. ((a) Reproduced by permission from Schoen et al. [114]. (b) Reproduced by permission from Vyavahare et al. [116])

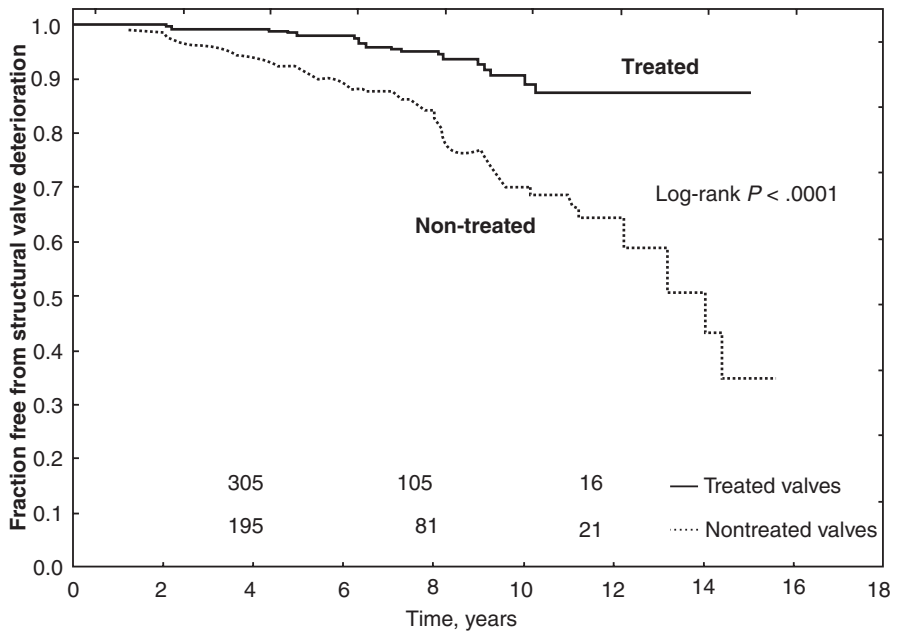


Fig. 9.15 Clinical data showing enhanced freedom from structural valve deterioration in patients receiving a valve treated with an anticalcification agent compared with those who have received a nontreated valve numbers of patients at risk are shown at 4, 8, and 12 years. (Reproduced by permission from Flameng et al. [86])

Inhibitors of Hydroxyapatite Formation

Trivalent Metal Ions

Pretreatment of bioprosthetic tissue with iron and aluminum (e.g., FeCl_3 and AlCl_3) inhibited calcification of subdermal implants with glutaraldehyde-pretreated porcine aortic valve cusps or pericardium [87]. Such compounds are hypothesized to act through complexation of the cation (Fe or Al) with phosphate, thereby preventing calcium phosphate formation. Both ferric ion and the trivalent aluminum ion inhibit alkaline phosphatase, an important enzyme in bone formation. This may be related to their mechanism for preventing the initiation of calcification. This treatment has been used in clinical valves.

Calcium Diffusion Inhibitor

2-alpha-amino-oleic acid (AOATM, Biomedical Designs, Inc., Atlanta, GA) bonds covalently to bioprosthetic tissue through an amino linkage to residual aldehyde functions and inhibits calcium flux through bioprosthetic cusps [88, 89]. AOATM is effective in mitigating cusp, but not aortic wall, calcification in rat subdermal and valve implants of porcine aortic valves in the sheep mitral valve positions. This compound has been used clinically, and the results of long-term explants indicate the occurrence of calcification in AOA pretreated bioprostheses [90].

Removal/Modification of Calcifiable Material

Surfactants

Incubation of bioprosthetic tissue with sodium dodecyl sulfate (SDS) and other detergents extracts the majority of acidic phospholipids [91]; this is associated with reduced mineralization, probably resulting from suppression of the initial cell-membrane-oriented calcification. This approach has also been used clinically with reports of calcification leading to device explantation, despite SDS pretreatment [92].

Alcohol Treatments

Ethanol preincubation of glutaraldehyde-cross-linked porcine aortic valve bioprostheses prevents calcification of the valve cusps in both rat subdermal implants and sheep mitral valve replacements (Fig. 9.13) [93]. Eighty percent ethanol

pretreatment (1) extracts almost all phospholipids and cholesterol from glutaraldehyde-cross-linked cusps; (2) causes a permanent alteration in collagen conformation; (3) affects cuspal interactions with water and lipids; and (4) enhances cuspal resistance to collagenase. Ethanol-pretreated bioprostheses have also been used clinically, and since there have been published reports of calcified ethanol-pretreated explants, the long-term effectiveness of this approach is unclear [94].

Glutaraldehyde Neutralization

As glutaraldehyde cross-linking itself aggravates tissue calcification, several approaches have been suggested to neutralize residual aldehyde residues in the tissue after glutaraldehyde cross-linking. Several amino acids, amines, and natural compounds such as taurine have been used to bind to unreacted glutaraldehyde residues. These treatments have shown promise in preventing tissue calcification in rodent subcutaneous models and sheep heart valve replacement models. Interestingly, there is some evidence that both (1) extended post-fixation storage of tissues in glutaraldehyde and, (2) paradoxically, fixation of bioprosthetic tissue in extraordinarily high concentrations of glutaraldehyde (5–10× those normally used) [95] appear to inhibit calcification after the anticalcification treatment has shown a partial return of calcification for the tissues. Other approaches to detoxification of glutaraldehyde have been considered [96, 97]. Moreover, combinations of multiple treatments such as removing phospholipids, glutaraldehyde neutralization, followed by storage in glutaraldehyde-free solutions have shown promise in animal studies to prevent calcification [98–100].

Decellularization

Since the initial mineralization sites are devitalized connective cells of bioprosthetic tissue, these cells may be removed from the tissue, with the intent of making the bioprosthetic matrix less prone to calcification [101]. Decellularized tissues have been used as scaffolds for tissue-engineered heart valves that might be populated with host cells and would grow with patients and hopefully will not calcify. In vivo animal studies have seen some success for patency of a functional valve [102]. However, clinical experiments have shown valve failure due to inflammation and calcification [103]. It is clear from these studies that extracellular matrix in the tissue (collagen and elastin) can degrade and create sites for calcification. Physical stabilization of collagen and elastin by pentagalloyl glucose has been shown to reduce valvular calcification [104].

Modification of Glutaraldehyde Fixation and Other Tissue Fixatives

Several studies have investigated modifications of glutaraldehyde residues and alternatives to conventional glutaraldehyde pretreatment. Bioprosthetic tissue can be neutralized (“detoxified”) by treatment with lysine or diamine; this inhibits calcification of subdermal implants [105, 106].

Removing phospholipids or neutralizing aldehyde residues by end-capping with amines, reduction with borohydride, or using high-temperature fixation strategies has been now clinically used for preventing tissue calcification. Efficacy has not been established for this strategy.

Non-glutaraldehyde cross-linking of bioprosthetic tissue with epoxides, carbodiimides, acyl azides, and other compounds reduces their calcification in rat subdermal implant studies, for example, with triglycidylamine (TGA), an epoxy cross-linker [107]. Additionally, alternative cross-linking chemistries and photooxidative preservative in large animal implants in sheep [108] or epoxies) with tissue still embedded with devitalized cells result in marked calcification [109]. This further supports the notion that glutaraldehyde products themselves, in conjunction with devitalized cells, may serve as high-affinity sites for calcification. One product where the bioprosthetic valve is stored in so-called dry conditions after glycerol treatment is now clinically available (Inspiris Resilia™ by Edwards Lifesciences, Irvine, California) [110]. We are not aware of long-term results that pertain to calcification.

It is concluded that calcification, although mechanistically investigated for decades, remains a major impediment to the extended safety and effectiveness of bioprosthetic heart valves. With the rapid development of interventional approaches for bioprosthetic valve implantation, and their approval for potential use in low-risk populations, addressing calcification as a major cause of structural degeneration continues to be a high priority.

Acknowledgments RJL efforts have been supported by NIH grant R01 HL143008, the Kibel Fund for Aortic Valve Research, and both Erin’s Fund and the William J Rashkind Endowment of the Children’s Hospital of Philadelphia.

Dr.Schoen serves or has served a consultant to the following companies which develop and/or market replacement heart valves or related products: CroiValve, Edwards Lifesciences, WL Gore, LivaNova/Sorin Biomedical, Medtronic, Sadra/Boston Scientific, St. Jude Medical, Symetis Valve, Tissx, and Xeltis.

References

1. Carpentier A. Lasker Clinical Research Award. The surprising rise of nonthrombogenic valvular surgery. *Nat Med.* 2007;13:1165–8.
2. Schoen FJ. Evolving concepts of heart valve dynamics. The continuum of development, functional structure, pathology and tissue engineering. *Circulation.* 2008;118:1864–80.

3. Schoen FJ. Mechanisms of function and disease in natural and replacement heart valves. *Annu Rev Pathol.* 2012;7:161–83.
4. Ayoub S, Ferrari G, Gorman RC, Gorman JH, Schoen FJ, Sacks MS. Heart valve biomechanics and underlying mechanobiology. *Compr Physiol.* 2016;6:1743–80.
5. Rabkin-Aikawa E, Farber M, Aikawa M, Schoen FJ. Dynamic and reversible changes of interstitial cell phenotype during development and remodeling of cardiac valves. *J Heart Valve Dis.* 2004;13:841–7.
6. Aikawa E, Whittaker P, Farber M, Mendelson K, Padera RF, Aikawa M, Schoen FJ. Human semilunar cardiac valve remodeling by activated cells from fetus to adult: implications for postnatal adaptation, pathology and tissue engineering. *Circulation.* 2006;113:1344–52.
7. Rabkin E, Aikawa M, Stone JR, Fukumoto Y, Libby P, Schoen FJ. Activated interstitial myofibroblasts express catabolic enzymes and mediate matrix remodeling in myxomatous heart valves. *Circulation.* 2001;104:2525–32.
8. Schoen FJ, Mitchell RN. The heart. In: Kumar V, Fausto N, Aster JC, Abbas A, editors. *Robbins/Cotran pathologic basis of disease.* 8th ed. Philadelphia: W.B. Saunders; 2010. p. 529–87.
9. Susheel KK, Velagapudi P, Rebecca HT, Dawn A, Martin LB. Valvular heart disease in patients ≥ 80 years of age. *J Am Coll Cardiol.* 2018;71:2058–72.
10. Benjamin EJ, et al. Heart disease and stroke statistics – 2019 update: ahajournals. *Circulation.* 2019;139:e56–e528.
11. Freeman RV, Otto CM. Spectrum of calcific aortic valve disease: pathogenesis, disease progression, and treatment strategies. *Circulation.* 2005;111:3316–26.
12. Thaden JJ, Nkomo VT, Enriquez-Sarano M. The global burden of aortic stenosis. *Prog Cardiovasc Dis.* 2014;56:565–71.
13. Aikawa E, Schoen FJ. Calcific and degenerative heart valve disease. In: Willis MS, Homeister JW, Stone JR, editors. *Cellular and molecular basis of cardiovascular disease.* Academic Press, London; 2014. p. 161–80.
14. Schoen FJ, Harasaki H, Kim KM, Anderson HC, Levy RJ. Biomaterial-associated calcification: pathology, mechanisms and strategies for prevention. *J Biomed Mater Res.* 1988;22(A1):11–36.
15. Hasegawa T. Ultrastructure and biological function of matrix vesicles in bone mineralization. *Histochem Cell Biol.* 2018;149:289–304.
16. Cho KI, Sakuma I, Sohn IS, Jo SH, Koh KK. Inflammatory and metabolic mechanisms underlying the calcific aortic valve disease. *Atherosclerosis.* 2018;277:60–5.
17. Rahimtoola SH. Choice of prosthetic heart valve in adults. *J Am Coll Cardiol.* 2010;55:2413–26.
18. Bloomfield P, Wheatley DJ, Prescott RJ, Miller HC. Twelve-year comparison of a Bjork-Shiley mechanical heart valve with porcine bioprosthesis. *N Engl J Med.* 1991;324:573–9.
19. Hammermeister KE, Sethi GK, Henderson WG, Grover FL, Oprian C, Rahimtoola SH. Outcomes 15 years after valve replacement with a mechanical versus a bioprosthetic valve: final report of the veterans affairs randomized trial. *J Am Coll Cardiol.* 2000;36:1152–8.
20. Schoen FJ, Levy RJ. Calcification of tissue heart valve substitutes: progress toward understanding and prevention. *Ann Thorac Surg.* 2005;79:1072–80.
21. Schoen FJ, Butany J. Cardiac valve replacement and related interventions. In: Buja LM, Butany J, editors. *Cardiovascular pathology.* 4th ed. Academic Press, London; 2016. p. 529–76.
22. Goldstone AB, Chiu P, Baiocchi M, Lingala B, Patrick WL, Fischbein MP, Woo YJ. Mechanical or biologic prostheses for aortic-valve and mitral-valve replacement. *N Engl J Med.* 2017;377:1847–57.
23. Brown JM, O'Brien SM, Wu C, Sikora JH, Griffith BP, Gammie JS. Isolated aortic valve replacement in North America comprising 108,687 patients in 10 years: changes in risks, valve types, and outcomes in the Society of Thoracic Surgeons National Database. *J Thorac Cardiovasc Surg.* 2009;137:80–90.
24. Mohr FW. Current perspectives on treatment of valvular heart disease. *Nat Rev Cardiol.* 2014;11:637–8.
25. Lung B, Cachier A, Baron G, Messika-Zeitoun D, Delahaye F, Tornos P, Gohlke-Bärwolf C, Boersma E, Ravaud P, Vahanian A. Decision-making in elderly patients with severe aortic stenosis: why are so many denied surgery? *Eur Heart J.* 2005;26:2714–20.

26. Durko AP, Osnabrugge RL, Kappetein AP. Long-term outlook for transcatheter aortic valve replacement. *Trends Cardiovasc Med*. 2018;28:174–83.
27. Howard C, Jullian L, Joshi M, Noshirwani A, Bashir M, Harky A. TAVI and the future of aortic valve replacement. *J Card Surg*. 2019;34:1577–90.
28. Tice JA, Sellke FW, Schaff HV. Transcatheter aortic valve replacement in patients with severe aortic stenosis who are at high risk for surgical complications: summary assessment of the California Technology Assessment Forum. *J Thorac Cardiovasc Surg*. 2014;148:482–91.
29. Reardon MJ, Adams DH, Kleiman NS, Yakubov SJ, Coselli JS, Deeb GM, Gleason TG, Lee JS, Hermiller JB Jr, Chetcuti S, Heiser J, Merhi W, Zorn GL 3rd, Tadros P, Robinson N, Petrossian G, Hughes GC, Harrison JK, Maini B, Mumtaz M, Conte JV, Resar JR, Aharonian V, Pfeffer T, Oh JK, Qiao H, Popma JJ. 2-year outcomes in patients undergoing surgical or self-expanding transcatheter aortic valve replacement. *J Am Coll Cardiol*. 2015;14(66):113–21.
30. Popma JJ, Deeb GM, Yakubov SJ, Mumtaz M, Gada H, O’Hair D, Bajwa T, Heiser JC, Merhi W, Kleiman NS, Askew J, Sorajja P, Rovin J, Chetcuti SJ, Adams DH, Teirstein PS, Zorn GL 3rd, Forrest JK, Tchétché D, Resar J, Walton A, Piazza N, Ramlawi B, Robinson N, Petrossian G, Gleason TG, Oh JK, Boulware MJ, Qiao H, Mugglin AS, Reardon MJ, Evolut Low Risk Trial Investigators. Transcatheter aortic-valve replacement with a self-expanding valve in low-risk patients. *Engl J Med*. 2019;380:1706–15.
31. McElhinney DB, Hellenbrand WE, Zahn EM, Jones TK, Cheatham JP, Lock JE, Vincent JA. Short- and medium-term outcomes after transcatheter pulmonary valve placement in the expanded multicenter US melody valve trial. *Circulation*. 2010;122:507–16.
32. Urena M, Himbert D, Brochet E, Carrasco JL, Jung B, Nataf P, Vahanian A. Transseptal transcatheter mitral valve replacement using balloon-expandable transcatheter heart valves: a step-by-step approach. *JACC Cardiovasc Interv*. 2017;10:1905–19.
33. Costa G, Criscione E, Todaro D, Tamburino C, Barbanti M. Long-term transcatheter aortic valve durability. *Interv Cardiol*. 2019;14:62–9.
34. Sawaya F, Jørgensen TH, Søndergaard L, Ole De Backer O. Transcatheter bioprosthetic aortic valve dysfunction: what we know so far. *Front Cardiovasc Med*. 6:145. <https://doi.org/10.3389/fcvm.2019.00145>.
35. Alavi SH, Groves EM, Kheradvar A. The effects of transcatheter valve crimping on pericardial leaflets. *Ann Thorac Surg*. 2014;97:1260–6.
36. Akins CW, Miller DC, Turina MI, Kouchoukos NT, Blackstone EH, Grunkemeier GL, Takkenberg JJ, David TE, Butchart EG, Adams DH, Shahian DM, Hagl S, Mayer JE, Lytle BW, Councils of the American Association for Thoracic Surgery; Society of Thoracic Surgeons; European Association for Cardio-Thoracic Surgery; Ad Hoc Liaison Committee for Standardizing Definitions of Prosthetic Heart Valve Morbidity. Guidelines for reporting mortality and morbidity after cardiac valve interventions. *J Thorac Cardiovasc Surg*. 2008;135:732–9.
37. Schoen FJ, Levy RJ. Pathophysiology of bioprosthetic heart valve calcification. In: Bodnar E, Yacoub MH, editors. *Biological and bioprosthetic valves*. New York: Yorke; 1986. p. 418–29.
38. Schoen FJ, Hobson CE. Anatomic analysis of removed prosthetic heart valves: causes of failure of 33 mechanical valves and 58 bioprostheses, 1980 to 1983. *Hum Pathol*. 1985;16:549–59.
39. Bourguignon T, Bouquiaux-Stablo AL, Loardi C, Mirza A, Candolfi P, Marchand M, Aupart MR. Very late outcomes for mitral valve replacement with the Carpentier-Edwards pericardial bioprosthesis: 25-year follow-up of 450 implantations. *J Thorac Cardiovasc Surg*. 2014;148:2004–11.
40. Bourguignon T, Bouquiaux-Stablo AL, Candolfi P, Mirza A, Loardi C, May MA, El-Khoury R, Marchand M, Aupart M. Very long-term outcomes of the Carpentier-Edwards Perimount valve in aortic position. *Ann Thorac Surg*. 2015;99:831–7.
41. Wang M, Furnary AP, Li HF, Grunkemeier GL. Bioprosthetic aortic valve durability: a meta-regression of published studies. *Ann Thorac Surg*. 2017;104:1080–7.
42. Saleeb SF, Gauvreau K, Mayer JE, Newburger JW. Aortic valve replacement with bovine pericardial tissue valve in children and young adults. *Circulation*. 2019;139:983–5.

43. Didier R, Eltchaninoff H, Donzeau-Gouge P, Chevreur K, Fajadet J, Leprince P, Leguerrier A, Lièvre M, et al. Five-year clinical outcome and valve durability after transcatheter aortic valve replacement in high-risk patients. *Circulation*. 2018;138:2597–607.
44. Ferrans VJ, Spray TL, Billingham ME, Roberts WC. Structural changes in glutaraldehyde-treated porcine heterografts used as substitute cardiac valves. Transmission and scanning electron microscopic observations in 12 patients. *Am J Cardiol*. 1978;41:1159–84.
45. Schoen FJ, Hirsch D, Bianco RW, Levy RJ. Onset and progression of calcification in porcine aortic bioprosthetic valves implanted as orthotopic mitral valve replacements in juvenile sheep. *J Thorac Cardiovasc Surg*. 1994;108:880–7.
46. Levy RJ, Ferrans VJ, Dearden LC, Nashef A, Goodman AP, Carpentier A. Calcification of cardiac valve bioprostheses. Biochemical, histologic, and ultrastructural observations in a subcutaneous implantation model system. *J Thorac Cardiovasc Surg*. 1982;83:602–9.
47. Levy RL, Schoen FJ, Levy JT, Nelson AC, Howard SL, Oshry LJ. Biologic determinants of dystrophic calcification and osteocalcin deposition in glutaraldehyde preserved porcine aortic valve leaflets implanted subcutaneously in rats. *Am J Pathol*. 1983;113:143–55.
48. Schoen FJ, Levy RJ, Nelson AC, Bernhard WF, Nashef A, Hawley M. Onset and progression of experimental bioprosthetic heart valve calcification. *Lab Invest*. 1985;52:523–32.
49. Schoen FJ, Tsao JW, Levy RJ. Calcification of bovine pericardium used in cardiac valve bioprostheses: implications for the mechanisms of bioprosthetic tissue mineralization. *Am J Pathol*. 1986;123:134–45.
50. Bernacca GM, Fisher AC, Wilkinson R, Mackay TG, Wheatley DJ. Calcification and stress distribution in bovine pericardial heart valves. *J Biomed Mater Res*. 1992;26:959–66.
51. Schoen FJ, Golomb G, Levy RJ. Calcification of bioprosthetic heart valves: a perspective on models. *J Heart Valve Dis*. 1992;1:110–4.
52. Mako WJ, Vesely I. In vivo and in vitro models of calcification in porcine aortic valve cusps. *J Heart Valve Dis*. 1997;6:316–23.
53. Zhang BL, Richard W, Bianco RW, Schoen FJ. Preclinical Assessment of cardiac valve substitutes: current status and considerations for engineered tissue heart valves. *Front Cardiovasc Med*. 2019. <https://doi.org/10.3389/fcvm.2019.00072>.
54. Schoen FJ, Kujovich J, Webb CL, Levy RJ. Chemically determined mineral content of explanted porcine aortic valve bioprostheses: correlation with radiographic assessment of calcification and clinical data. *Circulation*. 1987;76:1061–6.
55. Schoen F, Levy RJ. Tissue heart valves: current challenges and future research perspectives. *J Biomed Mater Res*. 1999;47:439–65.
56. Levy RJ, Schoen FJ, Sherman FS, Nichols J, Hawley MA, Lund SA. Calcification of subcutaneously implanted Type I collagen sponges: effects of glutaraldehyde and formaldehyde pretreatments. *Am J Pathol*. 1986;122:71–82.
57. Bailey MT, Pillarisetti S, Xiao H, Vyavahare NR. Role of elastin in pathologic calcification of xenograft heart valves. *J Biomed Mater Res A*. 2003;66:93–102.
58. Golomb G, Schoen FJ, Smith MS, Linden J, Dixon M, Levy RJ. The role of glutaraldehyde induced crosslinks in calcification of bovine pericardium used in cardiac valve bioprostheses. *Am J Pathol*. 1987;127:122–30.
59. Grabenwoger M, Sider J, Fitzal F, Zelenka C, Windberger U, Grimm M, Moritz A, Böck P, Wolner E. Impact of glutaraldehyde on calcification of pericardial bioprosthetic heart valve material. *Ann Thorac Surg*. 1996;62:772–7.
60. Simionescu DT. Prevention of calcification in bioprosthetic heart valves: challenges and perspectives. *Expert Opin Biol Ther*. 2004; 4:1971–85.
61. Zilla P, Fullard L, Trescony P, Meinhart J, Bezuidenhout D, Gortlitz M, Human P, von Oppell U. Glutaraldehyde detoxification of aortic wall tissue: a promising perspective for emerging bioprosthetic valve concepts. *J Heart Valve Dis*. 1997;6:510–20.
62. Cunanan CM, Cabiling CM, Dinh TT, Shen SH, Tran-Hata P, Rutledge JH 3rd, Fishbein MC. Tissue characterization and calcification potential of commercial bioprosthetic heart valves. *Ann Thorac Surg*. 2001;71:S417–21.

63. Tod TJ, Dove JS. The association of bound aldehyde content with bioprosthetic tissue calcification. *J Mater Sci Mater Med*. 2016;27(1):8. <https://doi.org/10.1007/s10856-015-5623-z>.
64. Webb CL, Benedict JJ, Schoen FJ, Linden JA, Levy RJ. Inhibition of bioprosthetic heart valve calcification with aminobisphosphonate covalently bound to residual aldehyde groups. *Ann Thorac Surg*. 1988;46:309–16.
65. Shang H, Claessens SM, Tian B, Wright GA. Aldehyde reduction in a novel pericardial tissue reduces calcification using rabbit intramuscular model. *J Mater Sci Mater Med*. 2017;28(1):16. <https://doi.org/10.1007/s10856-016-5829-8>.
66. Christian AJ, Alferiev IS, Connolly JM, Ischiropoulos H, Levy RJ. The effects of the covalent attachment of 3-(4-hydroxy-3,5-di-tert-butylphenyl)propyl amine to glutaraldehyde pretreated bovine pericardium on structural degeneration, oxidative modification and calcification of rat subdermal implants. *J Biomed Mater Res*. 2015;103:2441–8.
67. Christian AJ, Lin H, Alferiev IS, Connolly JM, Ferrari G, Hazen SL, Ischiropoulos H, Levy RJ. The susceptibility of bioprosthetic heart valve leaflets to oxidation. *Biomaterials*. 2014;35:2097–102.
68. Lee S, Levy RJ, Christian AJ, Hazen SL, Frick NE, Lai EK, Grau JB, Bavaria JE, Ferrari G. Calcification and oxidative modifications are associated with progressive bioprosthetic heart valve dysfunction. *J Am Heart Assoc*. 2017;6(5). pii: e005648. <https://doi.org/10.1161/JAHA.117.005648>.
69. Tripi DR, Vyavahare NR. Neomycin and pentagalloyl glucose enhanced cross-linking for elastin and glycosaminoglycans preservation in bioprosthetic heart valves. *J Biomater Appl*. 2014;28:757–66.
70. Zareian R, Tseng JC, Fraser R, Meganck J, Kilduff M, Sarraf M, Dvir D, Kheradvar A. Effect of stent crimping on calcification of transcatheter aortic valves. *Interact Cardiovasc Thorac Surg*. 2019;29:64–73.
71. Sacks MS, Schoen FJ. Collagen fiber disruption occurs independent of calcification in clinically explanted bioprosthetic heart valves. *J Biomed Mater Res*. 2002;62:359–71.
72. Sun W, Sacks M, Fulchiero G, Lovekamp J, Vyavahare N, Scott M. Response of heterograft heart valve biomaterials to moderate cyclic loading. *J Biomed Mater Res A*. 2004;69:658–69.
73. Human P, Zilla P. The possible role of immune responses in bioprosthetic heart valve failure. *J Heart Valve Dis*. 2001;10:460–6.
74. Human P, Zilla P. Inflammatory and immune processes: the neglected villain of bioprosthetic degeneration? *J Long-Term Eff Med Implants*. 2001;11:199–220.
75. Levy RJ, Schoen FJ, Howard S. Mechanism of calcification of porcine aortic valve cusps: role of T-lymphocytes. *Am J Cardiol*. 1983;52:629–31.
76. Mitchell RN, Jonas RA, Schoen FJ. Pathology of explanted cryopreserved allograft heart valves: comparison with aortic valves from orthotopic heart transplants. *J Thorac Cardiovasc Surg*. 1998;115:118–27.
77. Shah SR, Vyavahare NR. The effect of glycosaminoglycan stabilization on tissue buckling in bioprosthetic heart valves. *Biomaterials*. 2008;29:1645–53.
78. Vesely I, Boughner D, Song T. Tissue buckling as a mechanism of bioprosthetic valve failure. *Ann Thorac Surg*. 1988;46:302–8.
79. Schoen FJ, Levy RJ, Hilbert SL, Bianco RW. Antimineralization treatments for bioprosthetic heart valves. *J Thorac Cardiovasc Surg*. 1992;104:1285–8.
80. Vyavahare NR, Chen W, Joshi R, Lee CH, Hirsch D, Levy J, Schoen FJ, Levy RJ. Current progress in anticalcification for bioprosthetic and polymeric heart valves. *Cardiovasc Pathol*. 1997;6:219–29.
81. Jones M, Eidbo EE, Hilbert SL, Ferrans VJ, Clark RE. Anticalcification treatments of bioprosthetic heart valves: in vivo studies in sheep. *J Card Surg*. 1989;4:69–73.
82. Gott JPI, Pan-Chih, Dorsey LM, Jay JL, Jett GK, Schoen FJ, Girardot JM, Guyton RA. Calcification of porcine valves: a successful new method of antimineralization. *Ann Thorac Surg*. 1992; 53:207-15.

83. Schoen FJ. Pathologic findings in explanted clinical bioprosthetic valves fabricated from photooxidized bovine pericardium. *J Heart Valve Dis.* 1998;7:174–9.
84. Levy RJ, Schoen FJ, Lund SA, Smith MS. Prevention of leaflet calcification of bioprosthetic heart valves with diphosphonate injection therapy. Experimental studies of optimal dosages and therapeutic durations. *J Thorac Cardiovasc Surg.* 1987;94:551–7.
85. Levy RJ, Wolfrum J, Schoen FJ, Hawley MA, Lund SA, Langer R. Inhibition of calcification of bioprosthetic heart valves by local controlled-released diphosphonate. *Science.* 1985;228:190–2.
86. Flameng W, Rega F, Vercauteren M, Herijgers P, Meuris B. Antimineralization treatment and patient-prosthesis mismatch are major determinants of the onset and incidence of structural valve degeneration in bioprosthetic heart valves. *J Thorac Cardiovasc Surg.* 2014;147:1219–24.
87. Webb CL, Schoen FJ, Flowers WE, Alfrey AC, Horton C, Levy RJ. Inhibition of mineralization of glutaraldehyde pretreated bovine pericardium by AlCl₃: mechanisms and comparisons with FeCl₃, LaCl₃, and Ga(NO₃)₃ in rat subdermal model studies. *Am J Pathol.* 1991;138:971–81.
88. Chen W, Kim JD, Schoen FJ, Levy RJ. Characterization of dose-dependent anti-calcification effect of 2-amino oleic acid on glutaraldehyde cross-linked bioprosthetic heart valve cusps and aortic wall. *J Biomed Mater Res.* 1994;28:1485–95.
89. Chen W, Schoen FJ, Myers DJ, Levy RJ. Synergistic inhibition of calcification of porcine aortic root with preincubation in FeCl₃ and alpha-amino oleic acid in a rat subdermal model. *J Biomed Mater Res.* 1997;38:43–8.
90. Butany J, Zhou T, Leong SW, Cunningham KS, Thangaroopan M, Jegatheeswaran A, Feindel C, David TE. Inflammation and infection in nine surgically explanted Medtronic Freestyle stentless aortic valves. *Cardiovasc Pathol.* 2007;16:258–67.
91. Hirsch D, Drader J, Thomas T, Schoen FJ, Levy JT, Levy RJ. Inhibition of the calcification of glutaraldehyde pretreated porcine aortic valve cusps with sodium dodecyl sulfate: preincubation and controlled release studies. *J Biomed Mater Res.* 1993;27:1477–84.
92. Butany J, Leong SW, Cunningham KS, D’Cruz G, Carmichael K, Yau TM. A 10-year comparison of explanted Hancock-II and Carpentier-Edwards supraannular bioprostheses. *Cardiovasc Pathol.* 2007;16:4–13.
93. Vyavahare N, Hirsch D, Lerner E, Baskin JZ, Schoen FJ. Prevention of bioprosthetic heart valve calcification by ethanol preincubation. Efficacy and mechanism. *Circulation.* 1997;95:479–88.
94. Wiedemann D, Bonaros N, Laufer G, Kocher A. Aortic bioprosthetic valve deterioration 8 months after implantation. *Ann Thorac Surg.* 2010;89:277–9.
95. Zilla P, Weissenstein C, Bracher M, Zhang Y, Koen W, Human P, von Oppell U. High glutaraldehyde concentrations reduce rather than increase the calcification of aortic wall tissue. *J Heart Valve Dis.* 1997;6:502–9.
96. Grabenwöger M, Grimm M, Eybl E, Leukauf C, Müller MM, Plenck H Jr, Böck P. Decreased tissue reaction to bioprosthetic heart valve material after L-glutamic acid treatment. A morphological study. *J Biomed Mater Res.* 1992;26:1231–40.
97. Weissenstein C, Human P, Bezuidenhout D, Zilla P. Glutaraldehyde detoxification in addition to enhanced amine cross-linking dramatically reduces bioprosthetic tissue calcification in the rat model. *J Heart Valve Dis.* 2000;9:230–40.
98. Meuris B, De Praetere H, Strasly M, Trabucco P, Lai JC, Verbrugge P, Herijgers P. A novel tissue treatment to reduce mineralization of bovine pericardial heart valves. *J Thorac Cardiovasc Surg.* 2018;156:197–206.
99. Zilla P, Weissenstein C, Bracher M, Human P. The anticalcific effect of glutaraldehyde detoxification on bioprosthetic aortic wall tissue in the sheep model. *J Card Surg.* 2001;16:467–72.
100. Connolly JM, Bakay MA, Alferiev IS, Gorman RC, Gorman JH 3rd, Kruth HS, Ashworth PE, Kutty JK, Schoen FJ, Bianco RW, Levy RJ. Triglycidyl amine crosslinking combined with ethanol inhibits bioprosthetic heart valve calcification. *Ann Thorac Surg.* 2011;92:858–65.

101. Naso F, Gandaglia A. Different approaches to heart valve decellularization: a comprehensive overview of the past 30 years. *Xenotransplantation*. 2018;25. <https://doi.org/10.1111/xen.12354>.
102. Dohmen PM, Lembcke A, Holinski S, Pruss A, Konertz W. Ten years of clinical results with a tissue-engineered pulmonary valve. *Ann Thorac Surg*. 2011;92:1308–14.
103. Simon P, Kasimir MT, Seebacher G, Weigel G, Ullrich R, Salzer-Muhar U, Rieder E, Wolner E. Early failure of the tissue engineered porcine heart valve SYNERGRAFT in pediatric patients. *Eur J Cardiothorac Surg*. 2003;23:1002–6.
104. Deborde C, Simionescu DT, Wright C, Liao J, Sierad LN, Simionescu A. Stabilized collagen and elastin-based scaffolds for mitral valve tissue engineering. *Tissue Eng Part A*. 2016;22:1241–51.
105. Zilla P, Bezuidenhout D, Torrianni M, Hendriks M, Human P. Diamine-extended glutaraldehyde- and carbodiimide crosslinks act synergistically in mitigating bioprosthetic aortic wall calcification. *J Heart Valve Dis*. 2005;14:538–2245.
106. Trantina-Yates AE, Human P, Zilla P. Detoxification on top of enhanced, diamine-extended glutaraldehyde fixation significantly reduces bioprosthetic root calcification in the sheep model. *J Heart Valve Dis*. 2003;12:93–100.
107. Connolly JM, Alferiev I, Clark-Gruel JN, Eidelman N, Sacks M, Palmatory E, Kronsteiner A, Defelice S, Xu J, Ohri R, Narula N, Vyavahare N, Levy RJ. Triglycidylamine crosslinking of porcine aortic valve cusps or bovine pericardium results in improved biocompatibility, biomechanics, and calcification resistance: chemical and biological mechanisms. *Am J Pathol*. 2005;166:1–13.
108. Moore MA, Phillips RE Jr, McIlroy BK, Walley VM, Hendry PJ. Evaluation of porcine valves prepared by dye-mediated photooxidation. *Ann Thorac Surg*. 1998;66 Suppl:S245S–248.
109. Tam H, Zhang W, Infante D, Parchment N, Sacks M, Vyavahare N. Fixation of bovine pericardium-based tissue biomaterial with irreversible chemistry improves biochemical and biomechanical properties. *J Cardiovasc Transl Res*. 2017;10:194–205.
110. Bartus K, Litwinowicz R, Bilewska A, Stapor M, Bochenek M, Rozanski J, Sadowski J, Filip G, Kapelak B, Kusmierczyk M. Intermediate-term outcomes after aortic valve replacement with a novel RESILIA™ tissue bioprosthesis. *J Thorac Dis*. 2019;11:3039–46.
111. Schoen FJ, Edwards WD. Valvular heart disease: general principles and stenosis. In: Silver MD, Gotlieb AI, Schoen FJ, editors. *Cardiovascular pathology*. 3rd ed. Churchill Livingstone, New York; 2001. p. 402–42.
112. Schoen FJ. Pathology of heart valve substitution with mechanical and tissue prostheses. In: Silver MD, Gotlieb AI, Schoen FJ, editors. *Cardiovascular pathology*. 3rd ed. Churchill Livingstone, New York; 2001. p. 629–77.
113. Schoen FJ, et al. Causes of failure and pathologic findings in surgically removed Ionescu-Shiley standard bovine pericardial heart valve bioprostheses: emphasis on progressive structural deterioration. *Circulation*. 1987;76:618–27.
114. Schoen FJ, Levy RJ, Piehler HR. Pathological considerations in replacement cardiac valves. *Cardiovasc Pathol*. 1992;1:29–52.
115. Schoen FJ. *Interventional and surgical cardiovascular pathology: clinical correlations and basic principles*. Philadelphia: WB Saunders; 1989.
116. Vyavahare N, Hirsch D, Lerner E, Baskin JZ, Schoen FJ, Bianco R, Kruth HS, Zand R, Levy RJ. Calcification of glutaraldehyde-pretreated porcine aortic valve cusps is inhibited by ethanol in a dose-dependent manner. Prevention of bioprosthetic heart valve calcification by ethanol preincubation: efficacy and mechanisms. *Circulation*. 1997;95:479–88.

Part II
Ectopic Calcification

Chapter 10

Electron Microscopy for the Characterization of Soft Tissue Mineralization



Elena Tsolaki and Sergio Bertazzo

Electron Microscopy

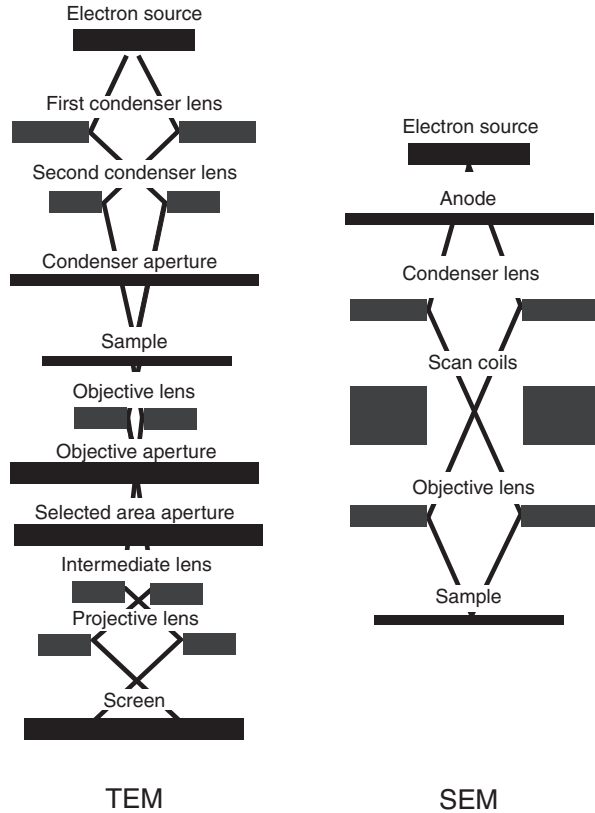
Electron microscopes, unlike optical microscopes, which use light, employ interactions between an electron beam and a sample for image formation. The electrons are produced by an electron gun, a filament cathode (usually made of tungsten), which when heated causes electrons to escape its surface. These electrons are then accelerated by an electric field towards the anode and focused through electromagnetic lenses (Fig. 10.1) [1]. Once the primary electron beam interacts with the atoms in the sample, a range of charged particles originating from the primary beam, secondary charged particles and photons [2] are generated, which are collected to form an image, a chemical spectrum or an electron diffraction pattern [3].

The two most common types of electron microscopes (Fig. 10.1) are scanning and transmission electron microscopes [2], with the primary difference between the two being that the scanning electron microscope (SEM) relies on the secondary products of the interactions [1] to produce an image of the surface of the sample. The transmission electron microscope (TEM), on the other hand, uses the ability of the electron beam to penetrate through the sample [1] providing a similar image of what would be seen in an optical microscope, albeit with much higher resolution.

The clearest advantage of electron microscopes over light microscopes is their high resolution. State-of-the-art SEMs have a resolution of around 0.4 nm [4]. Conventional SEMs usually have a resolution limit of about 1 nm [5], which is at least a hundred times higher resolution than that obtained by conventional optical microscopes [6]. TEMs, on the other hand, can achieve a resolution of angstroms [7].

E. Tsolaki · S. Bertazzo (✉)
Department of Medical Physics & Biomedical Engineering, University College London,
London, UK
e-mail: elena.tsolaki.15@ucl.ac.uk; s.bertazzo@ucl.ac.uk

Fig. 10.1 Schematic diagrams of electron beam path in a transmission electron microscope and a scanning electron microscope



Electron microscopes have been used countless times in the study of cells and biological structures and tissues and have provided valuable information on minerals formed in biological systems. A large part of the knowledge on bone and bone mineral ultrastructure comes from electron microscopy studies [8]. Moreover, several researchers have shown the importance of using electron microscopy in the study of pathological calcification [9, 10]. SEM aided the identification and provided detailed structural information on the minerals observed, amongst others, in cardiovascular, kidney, ocular, and breast tissue. It also allowed for comparison between different structures. Despite the fact that in physiological and pathological calcification [9, 10] minerals are formed from calcium phosphates, SEM visualisation of calcium phosphate minerals has indicated major structural differences. For cardiovascular calcification, it has allowed for the identification of three distinct structures, which have provided valuable information on the progression of the mineralising process and associated diseases. The first mineralising structure formed in the cardiovascular tissue is calcium phosphate particles, whereas at later stages of the disease, compact calcification and calcific fibres are also observed [9]. This information led to the conclusion that there is more than one mechanism of formation of cardiovascular calcification and also that, as the disease progresses, different

mineralization mechanisms come into play. Finally, these studies have shown that even though calcium phosphate is present in cardiovascular minerals, the structures of all three types of calcification found are different from bone [9].

This chapter will give an overview of how SEM and TEM are applied to provide information on the morphology, composition and crystallinity of the minerals present in pathological calcification in general. The basic principles of SEM and TEM will be discussed, and details will be given on sample preparation methods for biological tissues where pathological calcification is to be studied. Furthermore, insights on the imaging techniques for different types of analyses will be provided.

Scanning Electron Microscopy and Pathological Minerals

Imaging

In SEM imaging, secondary and backscattered electrons are detected. Secondary electrons are the electrons resulting from interactions of the primary beam with the sample surface and hence carry topographic information [2]. Secondary electron images are the most common and well-recognised SEM images (Fig. 10.2a, b). Two detectors are employed for secondary electron images. The in-lens detector is built in the path of the primary electron beam of modern SEMs. It detects electrons emitted from a very small volume on the surface of the sample at large angles [11], which carry specific topographic information of the imaged area, resulting in high-resolution images (Fig. 10.2a). The resolution of the in-lens images increases at low voltages, as shorter penetration depths are achieved [12]. Most widely used, however, is the secondary electron (SE) detector, which can be found on all SEMs. This detector collects secondary electrons emitted from the interaction point at a wider range of small angles, therefore from a larger volume and depth. As a result, the final images are of lower resolution compared to the in-lens detector, with some information on the sample surface being lost (Fig. 10.2b).

Backscattered electrons result from collisions between the primary beam and the nucleus of the atoms found in the sample, which cause primary electrons to be reflected back. The backscattered electron (BSE) detector is not widely used for the imaging of biological samples, due to its lower resolution. The backscattered signal is invaluable, however, when information on atomic density is required. Larger atoms result in a higher number of backscattered electrons and subsequently to a higher signal in comparison to smaller atoms [1]. The difference in atomic densities between different materials produces a high contrast image. BSE images are therefore useful in the study of biological minerals, as inorganic material can easily be identified in the organic matrix during imaging. In the case of cardiovascular calcification, the elemental composition of the mineral is calcium phosphate. As calcium is a larger atom than carbon (the main element of organic material), it appears as white (Fig. 10.2c) in a dark background. BSE imaging can therefore be used as a tool for an easy initial assessment of the presence of minerals in organic tissues.

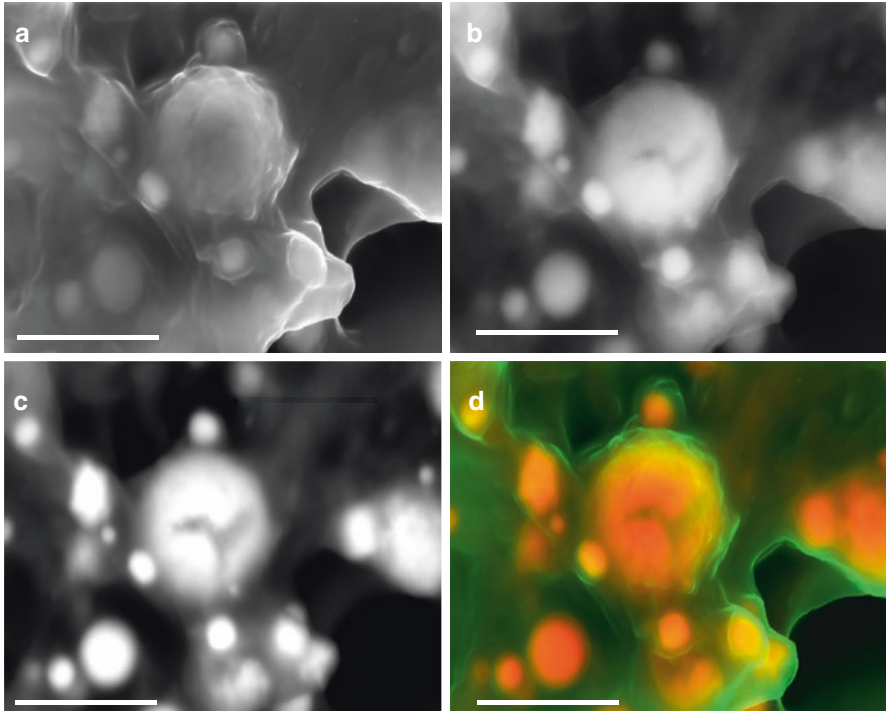


Fig. 10.2 Electron micrographs of calcific particles in organic material. (a) In-lens electron micrograph of the sample, where topographical information can be observed in high resolution. (b) SE micrograph of the sample, where considerable amount of topographical information is lost. (c) BSE micrograph of the sample, where topographical information is lost. It is possible to distinguish between organic (black) and inorganic (white) material. (d) DDC-SEM micrograph of the sample, where topographical and chemical information can be obtained with the in-lens electron micrograph being assigned the green channel and the BSE micrograph being assigned the red channel. Therefore, dense (inorganic) material appears as orange and less dense (organic) material as green. Scale bars = 1 μm

Density-Dependent Color Scanning Electron Microscopy (DDC-SEM)

In pathological mineral research, both topography and atomic density information are usually of interest. As a biological system, pathological mineralization requires the understanding of mineral components and the biological features associated with them to achieve a deeper understanding of the complex mineralization processes. A single image carrying all this information can be achieved through the use of density-dependent color (DDC) SEM.

The DDC-SEM method requires micrographs obtained by the different detectors [9] to be manipulated into one final image. Adobe Photoshop, Image J or any image

manipulation software can be used to overlay the electron micrographs and to assign different color channels to each one of them. Due to differences between the contrast of the in-lens, SE and BSE micrographs, each individual color on the final image carries specific information (Fig. 10.2d). Dual color images can be produced through the use of the SE (or in-lens) and BSE micrographs, and in cases where all three detectors are available, multicolor images can be produced. The most common images are dual color images [9, 10, 13, 14] where the green channel is assigned to the SE (or in-lens) image and the red channel to the BSE image. Thus, DDC-SEM images of minerals in soft tissue are produced where the mineral appears as red-orange (information originating from the BSE micrograph) and the less dense material, the organic matrix, appears as green (information which originates from the in-lens or SE detector) (Fig. 10.2d).

Chemical Analysis: Energy-Dispersive X-Ray Spectroscopy (EDS)

Scanning electron microscopes coupled with an energy-dispersive x-ray spectroscopy (EDS) detector are also commonly used [1]. The detector is used to gain chemical data on the material of study through the detection of x-rays originating from the sample surface. They are a secondary product of the interaction between the primary beam and the atoms of the sample and are usually referred to as characteristic x-rays, as their energy is associated with the energy difference in the electron levels of atoms, a property specific to each chemical element. A chemical spectrum or an elemental map of the sample surface can therefore be produced, the accuracy of which increases with appropriate beam voltage and working distance used.

The detector is most widely used in the study of archaeological and hard materials, as is also useful in the identification of unknown materials in samples. For that reason, it is also a valuable tool in the study of biological minerals. During imaging, a specific point in the tissue is chosen for analysis (Fig. 10.3a), and a spectrum (Fig. 10.3b) or an elemental map (Fig. 10.3c) can be produced. This can aid the fast identification of inorganic material in soft tissues, eliminating misinterpretation of any sample preparation artefacts.

SEM Sample Preparation of Biological Material

The first challenge of imaging biological material using electron microscopes is the un-physiological conditions required. Biological tissues are full of water, and microscopes operate under vacuum; therefore several preparation steps must be followed for successful imaging. Firstly, samples must be dehydrated and dried carefully for their ultrastructure to be preserved. Furthermore, to achieve good image

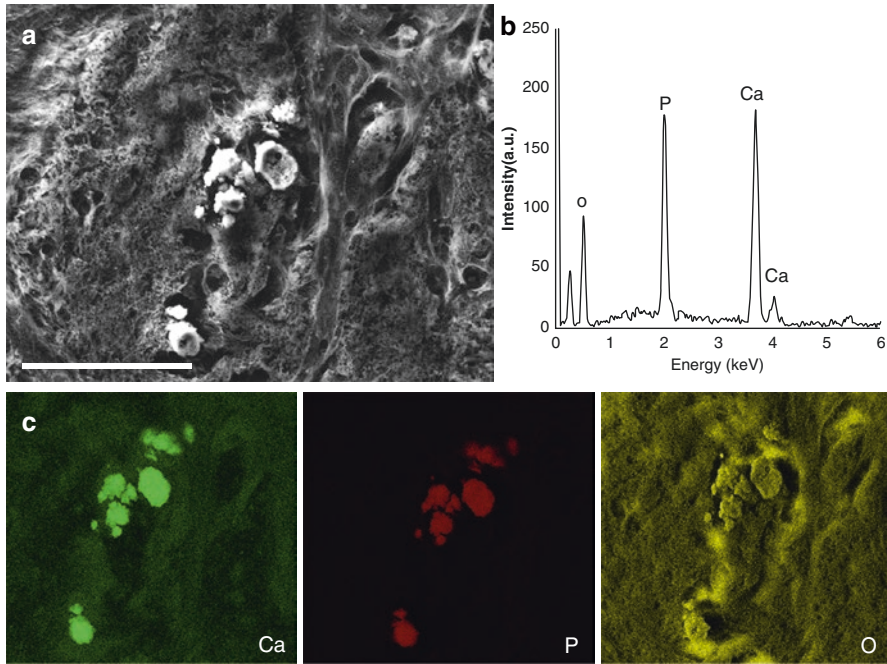


Fig. 10.3 Chemical analysis of a pathological mineral in soft tissue. (a) SE micrograph of the area of interest. Scale bar = 50 μm . (b) Chemical spectrum obtained from the area. (c) Maps of the distribution of calcium (Ca), phosphorus (P) and oxygen (O) in the area of interest

quality, coating and painting of the biological sample are required in order to build a conductive layer.

Following fixation, dehydration is the subsequent step of sample preparation. Tissue samples can be dehydrated through a series of increased ethanol-graded solutions. Other dehydration agents, such as acetone, can alternatively be used. The amount of time required for dehydration must be adjusted depending on the size of the sample of interest; larger samples require longer time intervals. If possible, it is recommended that the samples should be cut down to a few millimetres for better infiltration of the dehydrating agent.

The dehydration step is needed in cases where critical point [15] and hexamethyldisilazane (HMDS) [16] drying are used, as these require the presence of a dehydrating agent. It may, however, be omitted when the sample is simply air-dried. Critical point and HMDS drying are widely used methods for biological tissues because they avoid sample shrinkage, preserving its ultrastructure (Fig. 10.4a). Critical point drying is based on the substitution of the dehydration agent by carbon dioxide at critical state. Once carbon dioxide has fully infiltrated, it is then brought to its gas phase. As a result, the sample dries without the presence of capillary forces. For HMDS drying, the sample is immersed in HMDS after dehydration and then left to air-dry. Immersion in HMDS and subsequent evaporation is a process

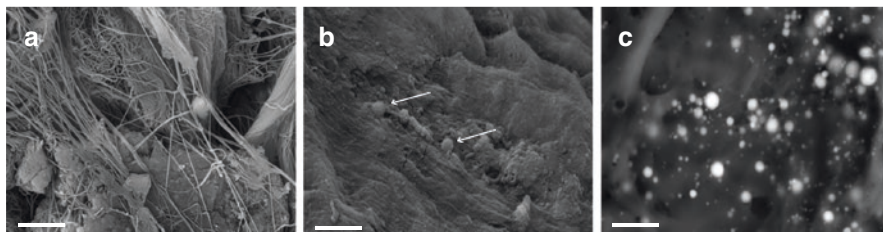


Fig. 10.4 Electron micrographs of biological tissues prepared with HMDS, compared to conventional air-drying. (a) BSE micrograph of collagen fibres of cardiovascular tissue preserved with HMDS drying. (b) BSE micrograph of a HMDS-prepared sample with potential calcified particles indicated by arrows. Some differences in color, indicating different densities, can be seen. It is, however, not certain whether these are mineralised. (c) BSE micrograph of air-dried samples where the organic material has collapsed on itself, allowing for clear identification of mineral particles. Scale bars = 1 μm

that preserves the ultrastructure of most organic samples. HMDS has low surface tension, which helps prevent capillary forces. HMDS also helps with the cross-linking of proteins [17].

These methods can be unsuitable for the study of pathological mineralization, especially where the minerals are of interest, as it is challenging to identify these minerals when they are covered by organic material. As the ultrastructure of the tissue is preserved, the electron beam will interact with a large amount of organic material prior to reaching the inorganic material beneath it, resulting in poor contrast differences between the two (Fig. 10.4b). HMDS and critical point dried samples might therefore produce misleading DDC-SEM micrographs.

For imaging of pathological minerals, simply air-drying the samples is preferred. Allowing the sample to air-dry creates capillary forces in the tissue, causing the organic matrix to collapse in on itself. These forces do not, however, apply to the mineral, which does not collapse at all. This difference in behaviour between the organic and inorganic material can be used for easier identification of pathological minerals in tissues. The electron micrographs of the air-dried samples provide very little topographic information on the organic matrix but allow for high contrast with the inorganic material (Fig. 10.4c).

Air-drying sample preparation protocol

1. Tissue samples must be cut down to small pieces of 2 to 5 millimetres and put in 4% formaldehyde for at least 24 hours at 4 °C.
2. Following step 1, the samples should be washed three times with distilled water, for 5 minutes each time.
3. The samples must then be dehydrated using ethanol at concentrations of 20%, 30%, 40%, 50%, 60%, 70%, 80%, and 90% for 10 minute intervals followed by three 10 minute interval 100% ethanol changes.
4. Samples must then be left to air-dry.

Note Formalin-fixed and paraffin-embedded histological slides can also be SEM imaged. The paraffin can be removed by immersing the slides in pure xylene for two 10 minute intervals. Simple air-drying can then be employed.

Coating and Silver Painting

A challenge of using an electron beam in the imaging of biological samples is the build-up of electrons on their surface. As insulators, biological tissues do not allow electrons to escape their surface, leading to sample damage and resulting in poor-quality, distorted images. To eliminate this phenomenon, the sample must be attached to an aluminum stub and a conductive coating must then be applied. The coating can be, amongst others, carbon, gold or platinum, and should usually have thickness between 5 and 15 nm, depending on sample roughness. To allow for chemical analysis of the samples, coating composition must be carefully considered, in order to avoid the overlapping of energy peaks. Such information can be obtained by identifying the energy values of the characteristic x-rays emitted by each element and is commonly available in electron microscopy facilities, as well as in handbooks. In the case of cardiovascular calcification, for instance, phosphorus has an energy x-ray peak close to platinum; thus, a platinum coating would be unsuitable.

In addition to the coating, it is also important to maintain good conductivity between the surface of the sample and the aluminum stub, such that any charge build-up may be eliminated. This can be done by applying a silver paint layer around the sample, which should extend to the bottom of the glass slide or aluminum stub. Application of the silver paint prior to coating ensures that both the sample and the silver paint are completely dry.

SEM sample preparation protocol

1. Tissue pieces or histological slides are secured on SEM aluminum stubs using conductive carbon adhesive tape.
2. The mounted samples are silver painted thoroughly and the paint is left to dry.
3. Carbon coating of 10 nm thickness is then applied.

Transmission Electron Microscopy and Pathological Minerals

Imaging

Like SEMs, transmission electron microscopes use a number of lenses and apertures to produce a uniform electron beam. The transmitted beam is captured by a camera system, with darker areas corresponding to denser regions in the sample while areas with higher transmission signal appearing brighter (Fig. 10.5a).

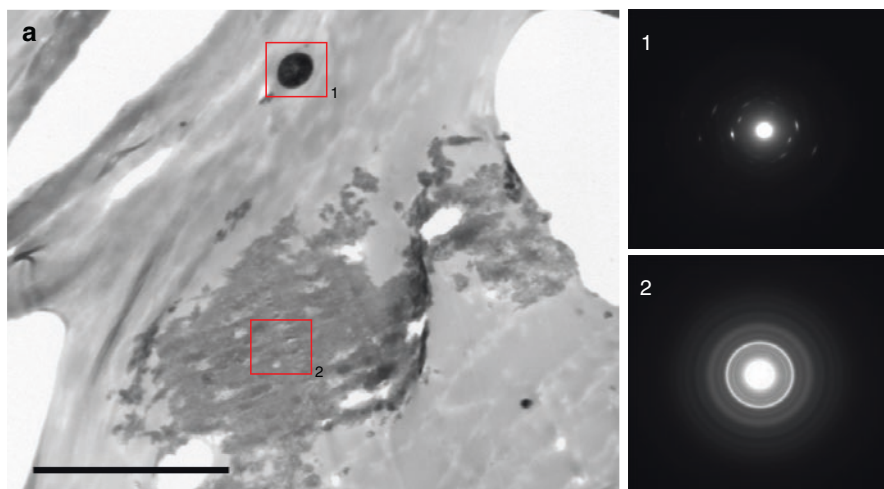


Fig. 10.5 TEM micrograph showing minerals (darker areas marked with rectangles) observed in cardiovascular soft tissue (light grey area) along with their electron diffraction patterns. (a) TEM micrograph of a cardiovascular sample, where calcified particles marked by **1** are denser and diffract as a single crystal, based on their electron diffraction pattern. Larger calcification marked by **2** appears less dense and has an amorphous structure. Scale bar = 2 μm

TEMs are based on the transmission of the beam through the sample, and therefore a sample thickness of 100 nm or lower is required [18]. Focused ion beam cutting and resin embedding followed by ultramicrotome cutting may be used for cutting the sample to the adequate thickness.

TEM microscopes can also be used for more precise EDS analysis. This is possible because of the higher voltages and thinner samples used, resulting in more accurate data on chemical composition at much higher resolution. TEMs also allow for capturing diffraction patterns (selected area electron diffraction (SAED) (Fig. 10.5), which provide information on the crystallinity and phase of the materials present.

In brief, the diffraction pattern appears as spots (Fig. 10.5a_1) in highly crystalline or at least partly crystalline samples, whereas for polycrystalline and amorphous materials, sharp or broader rings form, respectively (Fig. 10.5a_2) [19]. Further analysis of the distances and angles between the spots or rings in the SAED pattern provides information on lattice distances and chemical phases of the material.

TEM microscopy is frequently used in biology to study the ultrastructure of biological samples, owing to its high resolution. It has allowed for visualisation of cell organelles and also for protein localisation through immunogold labelling [20]. Immunogold labelling is a technique that allows for the staining of proteins similar to immunofluorescence, but with the proteins being tagged with gold nanoparticles rather than fluorescence markers. The use of gold nanoparticles enables TEM

imaging of the samples, ultimately allowing for high-resolution images to be obtained with the exact location of proteins within cells and tissues visualised [21].

TEM imaging has also proven to be particularly useful in the understanding of the formation mechanisms of biological minerals, as TEM imaging enables the localisation of minerals in relation to cells, cell organelles and extracellular matrix. As previously mentioned, EDS and SAED tools can provide information on the chemical composition, phase and crystallinity of the minerals present. This information is also valuable in the identification of the mineralization processes taking place as differences in the phase and crystallinity can hint that different mechanisms are responsible for the presence of minerals. SAED has been employed in the study of pathological minerals and has indeed given insights on the origins of the minerals present [9, 10]. In the case of cardiovascular calcification, SAED confirmed that the three different minerals identified by SEM [9] are of different chemical phases and crystallinity, further supporting the proposition that a combination of distinct mineralization mechanisms is taking place.

TEM Sample Preparation of Biological Material

Other than dehydration, a number of other steps are required for TEM images of good quality to be acquired from biological samples. TEM imaging relies on density differences in the sample; thus, contrast agents must be employed to add density variations in biological tissues, which are mainly made of carbon.

Contrast agents that stain specific parts of the sample must be used, such as osmium tetroxide [22], lead citrate [23] and uranyl acetate [24]. Osmium tetroxide attaches to lipids, resulting in cell membrane staining (Fig. 10.6a). It may be used

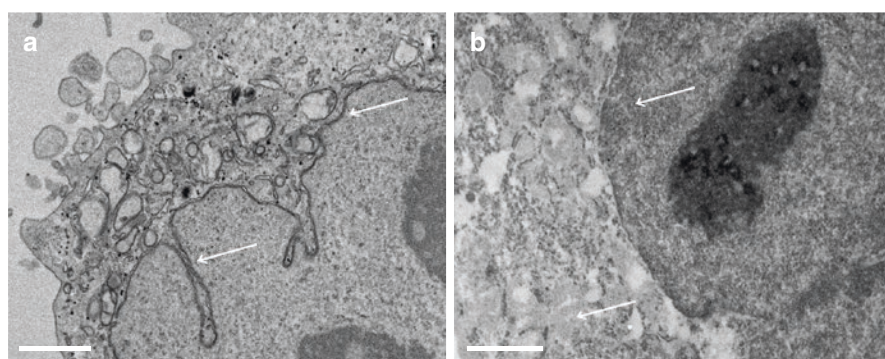


Fig. 10.6 TEM micrographs of resin-embedded samples with added contrast agents. **(a)** Cross section of epoxy resin-embedded Hela cell with osmium tetroxide staining; the double membrane of the nucleus is visible (arrows). **(b)** Cross section of epoxy resin-embedded Hela cell with uranyl acetate staining; although the nucleus is still visible, the double membrane and membranes of intracellular organelles are not seen (arrows). Scale bars = 1 μm

prior to sample dehydration as a contrast agent and also used as a fixative, because it stabilises proteins when attached to them.

En bloc osmium tetroxide staining

1. The sample must be immersed either in a solution of 1% osmium tetroxide in a 0.2 M cacodylate buffer or 1% aqueous osmium tetroxide, for up to 1.5 hours at room temperature.
2. The sample should then be washed using distilled water, three times for 5 minutes each prior to dehydration (see section “[SEM Sample Preparation of Biological Material](#)”) and resin embedding.

In addition to osmium tetroxide, uranyl acetate can also be used. The latter stains proteins due to its ability to react with phosphate and amino groups (Fig. 10.6b), but this stain is not useful if only membranes are to be visualised (Fig. 10.6b). Uranyl acetate can be applied after osmium tetroxide staining (*en bloc*) and, most widely, after resin embedding and sectioning.

En bloc uranyl acetate staining

1. Immerse the sample in 2% uranyl acetate aqueous solution for 2 hours at room temperature.
2. Following the previous step, the sample should be washed using distilled water, for three times of 5 minutes each.

Post-resin embedding uranyl acetate staining

1. Ultra-thin sections of the sample must be obtained through ultramicrotomy.
2. The sections must then be placed on TEM carbon grids and left to dry.
3. Once dried, grids must be placed on a drop of aqueous uranyl acetate at a concentration between 2% and 5%, for a few minutes.
4. The grids must then be washed with distilled water and left to air-dry for a few minutes prior to imaging.

Lead citrate may be employed to enhance a previous staining with either osmium tetroxide or uranyl acetate for its ability to react with both. This chemical is, however, difficult to handle, due to its very fast precipitation when in contact with air or water.

Other than contrast, TEM imaging requires samples of a thickness less than 100 nm. For such thickness to be achieved, samples may be resin-embedded and sectioned either using a ultramicrotome or a focused ion beam (FIB) [25]. For biological samples, resin embedding followed by ultramicrotome sectioning is preferred. Resin embedding is faster than FIB, and the contrasting steps allow for visualisation of cell organelles and other biological structures when TEM imaged. These sections can also be SEM imaged in cases where TEM analysis is not necessary. Both osmium tetroxide (Fig. 10.7a)- and uranyl acetate (Fig. 10.7b)-stained samples produce strong contrast, which can be visualised using the BSE detector of the SEM, with denser materials appearing as white and less dense materials as black

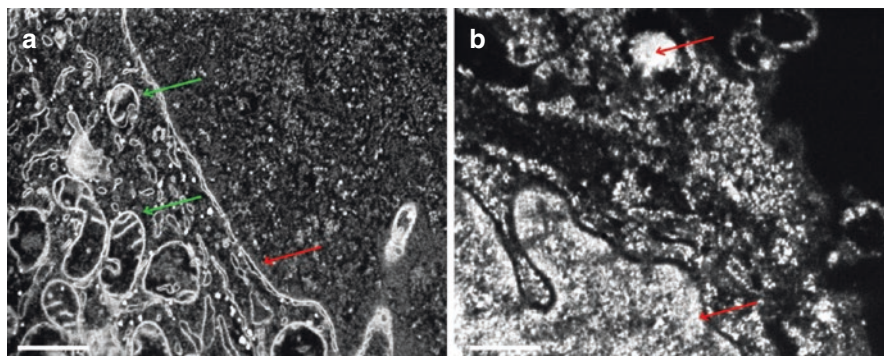


Fig. 10.7 SEM micrographs of resin-embedded sections stained with osmium tetroxide or uranyl acetate. **(a)** Osmium-stained and resin-embedded HeLa cell, sectioned and imaged on FIB-SEM; the double membrane of the nucleus is visible (red arrow), as well as membranes of intracellular organelles (green arrows). Scale bar = 500 nm. **(b)** Uranyl acetate-stained and resin-embedded HeLa cell, sectioned and imaged on FIB-SEM, with stained parts appearing as white (arrows). Scale bar = 300 nm

(Fig. 10.7a, b). Finally, resin-embedded blocks may be FIB sectioned in cases where more targeted sectioning is needed. Employing a FIB equipped with a BSE detector in these cases also allows for simultaneous sectioning and imaging of the areas of interest, instead of the longer process of ultramicrotome cutting followed by TEM imaging.

When imaging mineralised tissues, FIB sectioning presents a few advantages over ultramicrotomy. Ultramicrotome sectioning is suitable for samples containing mineral measurable in nanometres, but in cases where the sample contains more substantial amounts of mineral, completely or partly demineralising the tissue prior to processing is recommended. In the study of pathological minerals, however, such solutions are not ideal as the mineral is of main interest. FIB sectioning can be a more suitable alternative because biological minerals are denser than the organic matrix around them, and therefore both are easy to distinguish on TEM, even without contrast agents. For the study of pathological calcification, FIB also allows mineral structures to be sectioned with minimal damage (Fig. 10.8a). In cases where ultramicrotomy is used, the minerals are usually fractured (Fig. 10.8b) or pushed out of their original location, ultimately causing damage to the surrounding material. Finally, FIB enables more targeted sectioning because it allows for large samples being imaged by either the electron or ion beam prior to sectioning. Thus, the region to be sectioned can be chosen with higher spatial accuracy.

The most commonly used resins for biological sample infiltration and sectioning are epoxy, low acryl and white resins. Epoxy resin is mostly used in cases where only the visualisation of samples is required, whereas low acryl and white resins are more suitable for immunogold labelling, as they are hydrophilic resins that preserve the antigenicity of samples.

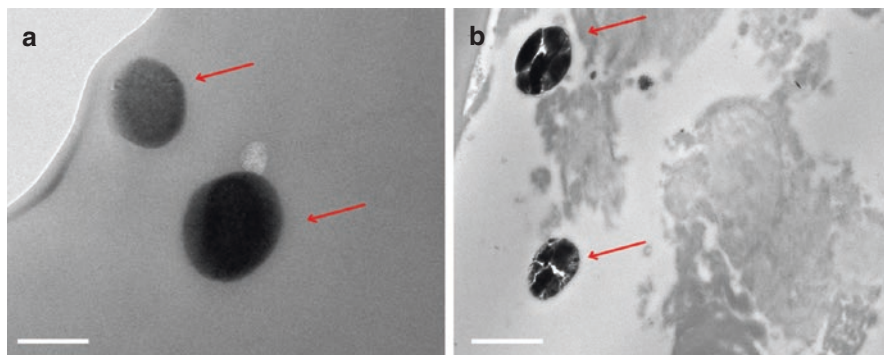


Fig. 10.8 TEM microscopy of cardiovascular tissue containing minerals. **(a)** FIB-sectioned sample where the minerals (arrows) are intact. Scale bar = 200 nm. **(b)** Resin-embedded sample sectioned by ultramicrotome. The mineral in the sample is visibly damaged (arrows) and cracks can be seen. Scale bar = 1 μ m

Resin embedding protocol

1. Epoxy resin embedding protocol: Biological tissues should be fixed for at least 24 hours in 4% formaldehyde at 4 °C prior to any other processing. Samples should be cut in small pieces of about 2 millimetres for better infiltration.
2. The sample should then be washed using distilled water for three times of 5 minutes each.
3. Contrasting may be performed using either osmium tetroxide or uranyl acetate.
4. The sample should be dehydrated using increased concentrations of the dehydrating agent (20%, 30%, 40%, 50%, 60%, 70%, 80%, 90%) for 10 minute changes, followed by three changes of pure dehydrating agent, for 10 minutes each.
5. Following dehydration, the sample should be immersed in resin solutions (with the dehydrating agent as solvent) of 25%, 33% and 50% for 3 hour intervals and left overnight in 66% resin.
6. On the second day, it should be immersed in pure resin three times, for 2/3 hour intervals followed by an overnight infiltration.
7. Finally, the resin should be changed again, and the sample should be placed in the oven for 24–48 hours at 60 °C for the resin to polymerise.
8. Once the resin infiltration and curing are completed, thin sections may be cut using an ultramicrotome.
9. The sections can then be retrieved using metal grids, which should be left to dry prior to TEM imaging.

The time intervals suggested can differ across resin types. However, in most cases, sample size should determine infiltration times. Thus, it is recommended that whenever the sample is a tissue, it should be cut into small pieces to allow easier infiltration at a shorter time span. Additionally, different resins might require different polymerisation times and temperatures. Epoxy or white resins, for instance,

require that the sample should stay in the oven for 24–48 hours at 60 °C, while low acryl resin requires much lower temperatures of –35 °C and an ultraviolet source for polymerisation to take place.

Focused ion beam cutting protocol

1. The sample must be secured on an aluminum stub, coated and silver painted carefully. Poor sample preparation might allow for sample movement or a charging effect, which might result in inaccurate FIB cutting.
2. The area of interest may be identified through the imaging of the whole sample using the electron or ion beam.
3. A platinum layer must then be deposited on top of the area of interest (Fig. 10.9a) to enhance the milling process and provide protection.
4. Following the previous step, very low currents (93 pA–2.8 nA) must be used for gallium milling. The material in front and behind the sample must be milled first, followed by the area on the right-hand side and the area immediately

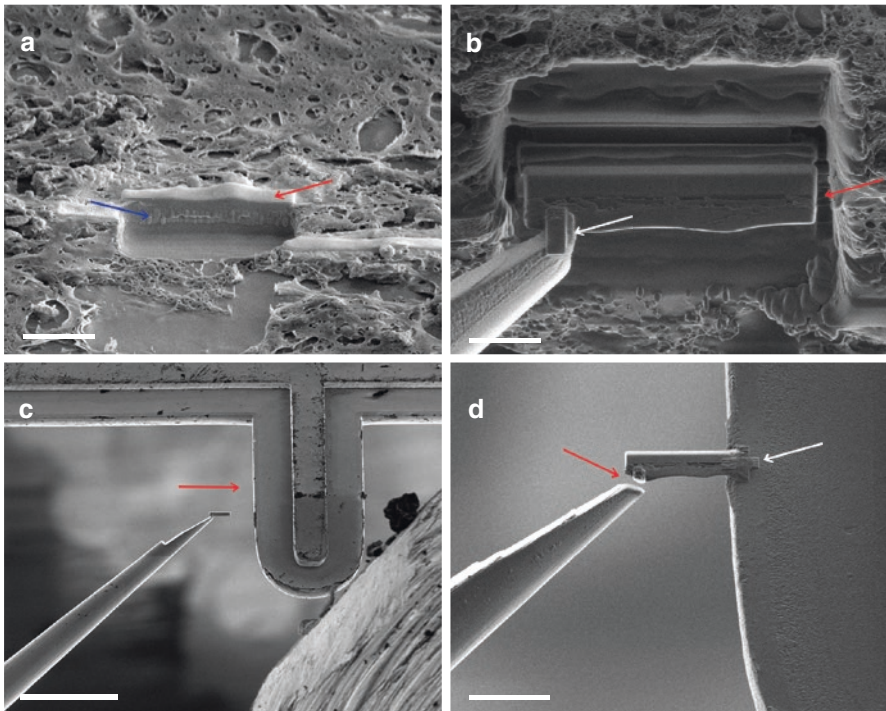


Fig. 10.9 FIB micro machining sequence. (a) A platinum layer must be deposited for protection of the target area (red arrow) before the gallium ion beam is used for milling (blue arrow). (b) The section is attached to the probe through platinum deposition (white arrow) and milled to be released from the sample (red arrows). Scale bar = 300 nm. (c) The section is transferred to the carbon grid (arrow) by the needle. Scale bar = 100 μm . (d) The section is then attached to the grid through platinum deposition (white arrow). Once the section is secured onto the grid (white arrow), its attachment to the probe is cut (red arrow). Scale bars = 10 μm

below the area of interest (the lamella), to allow for easier detaching from the rest of the sample (Fig. 10.9a).

5. The lamella is therefore shaped and thinned down to 100 nm.
6. When the lamella is ready (Fig. 10.9b), the sample must be attached to a needle probe (Fig. 10.9b) through the deposition of platinum.
7. The needle is then required to transfer the sample to the grid (Fig. 10.9c).
8. The lamella is then attached to the grid through platinum deposition (Fig. 10.9d) and is released from the probe through gallium milling (Fig. 10.9d).
9. Finally, the lamella should be cleaned and thinned down to about 50 nm.
10. The sample can then be transferred to the TEM for imaging.

Summary

Electron microscopy has been applied to biological research for several years, providing fundamental information on biological structures and processes. Its application to hard tissue research has also been proven useful, as it allows for good visualisation and characterization of minerals. Only rarely are such methods applied in the study of pathological minerals, however, as most studies focus on the organic component of diseases rather than the minerals, mainly due to challenges in handling and specific expertise required.

This chapter provides basic insights into sample preparation methods for successful visualisation, imaging and characterization of pathological minerals using electron microscopy. Such knowledge will hopefully lead to more mineral-driven research in the pathological mineralization field and ultimately allow for medicine, biology and material science to be combined in order to achieve a better understanding of calcific diseases.

References

1. Amelinckx S, Wiley I, Synergy, Wiley Online L. Electron microscopy: principles and fundamentals /edited by S. Amelinckx [and others]. Weinheim: VCH; 1997.
2. Janssens K. Electron microscopy. In: Modern methods for analysing archaeological and historical glass, Volume I, vol. 1. United Kingdom: Wiley; 2013. p. 129–54.
3. Thomas JM, Ducati C. Transmission electron microscopy. In: Characterization of solid materials and heterogeneous catalysts: from structure to surface reactivity, Volume 1&2, vol. 2. Weinheim: Wiley-VCH; 2012. p. 655–701.
4. Vladár AE, Postek MT, Ming B. On the sub-nanometer resolution of scanning electron and helium ion microscopes. *Microscopy Today*. 2018;17(2):6–13.
5. Bogner A, Jouneau PH, Thollet G, Basset D, Gauthier C. A history of scanning electron microscopy developments: towards “wet-STEM” imaging. *Micron*. 2007;38(4):390–401.
6. Heintzmann R, Ficz G. Breaking the resolution limit in light microscopy. *Brief Funct Genomic Proteomic*. 2006;5(4):289–301.

7. Ke X, Bittencourt C, Van Tendeloo G. Possibilities and limitations of advanced transmission electron microscopy for carbon-based nanomaterials. *Beilstein J Nanotechnol.* 2015;6:1541–57.
8. Shah FA, Ruscsák K, Palmquist A. 50 years of scanning electron microscopy of bone—a comprehensive overview of the important discoveries made and insights gained into bone material properties in health, disease, and taphonomy. *Bone Research.* 2019;7(1):15.
9. Bertazzo S, Gentleman E, Cloyd KL, Chester AH, Yacoub MH, Stevens MM. Nano-analytical electron microscopy reveals fundamental insights into human cardiovascular tissue calcification. *Nat Mater.* 2013;12(6):576–83.
10. Tan ACS, Pilgrim MG, Fearn S, Bertazzo S, Tsolaki E, Morrell AP, et al. Calcified nodules in retinal drusen are associated with disease progression in age-related macular degeneration. *Sci Trans Med.* 2018;10(466).
11. Polkowska A, Warmuzek M, Kalarus J, Polkowski W, Sobczak N. A comparison of various imaging modes in scanning electron microscopy during evaluation of selected Si/refractory sessile drop couples after wettability tests at ultra-high temperature. *Prace Instytutu Odlewnictwa (transactions of Foundry Research Institute).* 2017;57(4):337–55.
12. Joy DC, Joy CS. Low voltage scanning electron microscopy. *Micron.* 1996;27(3–4):247–63.
13. Hutcheson JD, Goettsch C, Bertazzo S, Maldonado N, Ruiz JL, Goh W, et al. Genesis and growth of extracellular-vesicle-derived microcalcification in atherosclerotic plaques. *Nat Mater.* 2016;15:335.
14. Bazin D, Jouanneau C, Bertazzo S, Sandt C, Dessombz A, Réfrégiers M, et al. Combining field effect scanning electron microscopy, deep UV fluorescence, Raman, classical and synchrotron radiation Fourier transform Infra-Red Spectroscopy in the study of crystal-containing kidney biopsies. *C R Chim.* 2016;19(11–12):1439–50.
15. Bray D. Critical point drying of biological specimens for scanning electron microscopy. In: Williams JR, Clifford AA, editors. *Supercritical fluid methods and protocols.* Totowa: Humana Press; 2000. p. 235–43.
16. Braet F, De Zanger R, Wisse E. Drying cells for SEM, AFM and TEM by hexamethyldisilazane: a study on hepatic endothelial cells. *J Microsc.* 2003;186(1):84–7.
17. Braet F, de Zanger R, Wisse E. Drying cells for SEM, AFM and TEM by hexamethyldisilazane: a study on hepatic endothelial cells. *J Microsc-Oxf.* 1997;186:84–7.
18. Ayache J, Beauvier L, Boumendil J, Ehret G, Laub D. *Sample preparation handbook for transmission electron microscopy.* New York: Springer; 2010.
19. Andrews KW, Dyson DJ, Keown SR. *Interpretation of electron diffraction patterns.* Boston: Springer; 1967.
20. Hayat MA. *Immunogold-silver staining: principles, methods and applications.* USA: CRC Press Inc; 1995.
21. Jones JC. Pre- and post-embedding immunogold labeling of tissue sections. *Methods Mol Biol.* 2016;1474:291–307.
22. Thiery G, Bernier J, Bergeron M. A simple technique for staining of cell membranes with imidazole and osmium tetroxide. *J Histochem Cytochem.* 1995;43(10):1079–84.
23. Venable JH, Coggeshall R. A simplified lead citrate stain for use in electron microscopy. *J Cell Biol.* 1965;25(2):407–8.
24. Glauert AM, Lewis PR. *Biological specimen preparation for transmission electron microscopy.* Princeton University Press; 1998.
25. Kizilyaprak C, Daraspe J, Humbel BM. Focused ion beam scanning electron microscopy in biology. *J Microsc.* 2014;254(3):109–14.

Chapter 11

Cardiovascular Calcification in Hutchinson-Gilford Progeria and Correlation with Age-Related Degenerative Calcification



Richard N. Mitchell

Abbreviations

EC	Endothelial cells
eNOS	Endothelial nitric oxide synthase
eNTPD1	Ectonucleoside triphosphate diphosphohydrolase-1
FACE-1	Farnesylated protein converting enzyme-1
HGPS	Hutchinson-Gilford progeria syndrome
KLF2	Krüppel-like factor 2
PPi	Inorganic pyrophosphate
ROS	Reactive oxygen species
TNAP	Tissue non-specific alkaline phosphatase
VSMC	Vascular smooth muscle cells
ZMPSTE24	Zinc metalloproteinase STE24

Hutchinson-Gilford Progeria Syndrome (HGPS)

The gross manifestations of Hutchinson-Gilford progeria syndrome (HGPS) were recognized as early as 1754 in an Englishman man who died at age 17. The entity was initially described clinically in 1886 by Jonathan Hutchinson [1], with a subsequent case reported in 1897 by Hastings Gilford [2]; in 1904, Gilford christened the disease “progeria” (literally “before old age”) [3]. HGPS is categorized as a premature aging (*progeroid*) syndrome; it occurs in roughly one in 20 million live births; there are approximately 400–500 cases described in the worldwide literature.

R. N. Mitchell (✉)

Harvard Medical School and Brigham and Women’s Hospital, Boston, MA, USA
e-mail: rmitchell@partners.org

© Springer Nature Switzerland AG 2020

E. Aikawa, J. D. Hutcheson (eds.), *Cardiovascular Calcification and Bone Mineralization*, Contemporary Cardiology,
https://doi.org/10.1007/978-3-030-46725-8_11

235

Affected individuals are initially healthy and asymptomatic, but at 18–24 months diverge from normal growth curves (“failure to thrive”), eventually exhibiting a characteristic phenotype comprising scleroderma-like skin, alopecia, osteopenia, skeletal dysplasias (including micrognathia and a “bird-beak” nose), joint contractures, and decreased subcutaneous tissue (lipodystrophy) [4]. In addition to cardiac conduction defects, individuals with HGPS most importantly develop markedly accelerated cardiovascular disease with vascular stiffening, valvular and vascular calcification, and severe atherosclerosis; patients characteristically die of myocardial infarction or stroke at 14–15 years of age. Because many of the features of HGPS phenocopy the changes associated with normal human senescence, it has been proposed as a model for physiologic aging (see final section). The implicit assumption is that therapy which can ameliorate the premature aging of progeria can potentially mitigate more typical physiologic senescence.

Mechanisms Underlying Non-HGPS Progeroid Syndromes

HGPS is actually just one of the more well-known of several progeroid (“resembling normal aging”) syndromes, each with somewhat distinct mechanisms and different manifestations [5].

Virtually all of the premature aging diseases are monogenic—attributable to mutations in a single gene. Several are associated with primary defects in DNA repair, often (although not uniformly) accompanied by heightened mutation rates and cancer incidence. Progeroid DNA repair disorders include (1) mutations in various RecQ helicases responsible for unwinding DNA during replication and repair (e.g., Werner syndrome, Bloom syndrome, and Rothmund-Thompson syndrome) and (2) mutations in a number of the proteins involved in nucleotide excision DNA repair (e.g., Cockayne syndrome and xeroderma pigmentosum). Mutations in the gene for the extracellular matrix protein fibrillin have also been linked to the Marfan-progeroid-lipodystrophy syndrome with individuals exhibiting a progeroid appearance at birth [6]. Interestingly, although all of these entities are associated with variably shortened lifespans, many patients with DNA repair defects can live into adulthood, and morbidity and mortality are not always attributable to cardiovascular causes.

Another pathway implicated in accelerated aging involves *klotho*, a transmembrane β -glucuronidase that acts as a co-receptor for the binding of various fibroblast growth factors; it is also an endogenous regulator of mitochondrial function and antioxidant production (reviewed in [7]). *Klotho* levels decrease with aging; in murine models, *klotho* deficiency leads to premature senescence while promoting vascular calcification. Of note, no genetic *klotho* deficiency disorders have been described in humans, although *klotho* polymorphisms have been linked to heterogeneities in aging phenotype onset and severity [8]. In cell cultures and in mouse models, reduced levels of *Klotho* upregulate *Runx2*, a central transcription factor control node for osteogenic differentiation; concurrently, *klotho* deficiency leads to

increased levels of tissue non-specific alkaline phosphatase (TNAP) which catabolizes inorganic pyrophosphate, an endogenous inhibitor of calcification. In general, oxidative stress and reactive oxygen species (ROS) feature broadly in any disorder that involves vascular and valvular calcification. Thus, the expression levels of several bone morphogenic proteins, as well as Runx2, are all upregulated by various ROS (reviewed in [7]).

Mechanisms Underlying HGPS Syndrome

This section will focus specifically on HGPS, one of the dozen so-called laminopathies caused by abnormal abundance or aberrant post-translational processing of lamin A [9].

Lamins are intermediate filaments associated with the inner nuclear membrane of the nuclear envelope; they provide nuclear structural integrity with additional roles in regulating nuclear shape, chromatin architecture, signal transduction, and gene transcription [10]. Divided into homologous A- and B-type proteins, both lamins are expressed in most differentiated mammalian cells; they are subject to alternative splicing and also undergo significant post-translational modification [11].

In particular, lamin A and lamin C are alternatively spliced A-type lamins encoded by the *LMNA* gene; HGPS is specifically a disorder of abnormal lamin A processing. Mature lamin A is generated by progressive modification from a prelamin A precursor (Fig. 11.1) [12]. After farnesylation, the C-terminal serine-isoleucine-methionine tripeptide is removed and replaced with a carboxymethyl residue. The farnesylation and carboxymethyl adduct leads to a more hydrophobic protein that intercalates into the lipid of the inner nuclear membrane. The carboxymethyl and farnesyl modifications form the substrate for zinc metalloproteinase STE24 (ZMPSTE24, also known as *farnesylated protein converting enzyme-1*, or FACE-1) to cleave the terminal 15 amino acids and release the mature lamin A molecule; this protein can then interact with a variety of nuclear membrane proteins to organize nuclear architecture and regulate gene activity. Importantly, if the farnesyl group is not ultimately removed, persistent membrane integration will lead to a distorted and dysfunctional nuclear architecture (see below).

HGPS typically occurs as a consequence of a de novo synonymous c.1824C>T mutation in the 11th exon of *LMNA* (Fig. 11.1). Although the C>T transition (GGC>GGT) codes for glycine in both cases (G608G), it also generates a new splice site in exon 11, ultimately leading to the deletion of 150 nucleotides that code for 50 amino acids, including the ZMPSTE24 cleavage site. Thus, the mutant farnesylated protein—called *progerin*—cannot be catabolized by FACE-1 and remains permanently attached to the nuclear membrane. As would be expected, mutations that affect the activity of ZMPSTE24 can also lead to persistent prelamin A association with the nuclear membrane and also cause a syndrome analogous to HGPS [13].

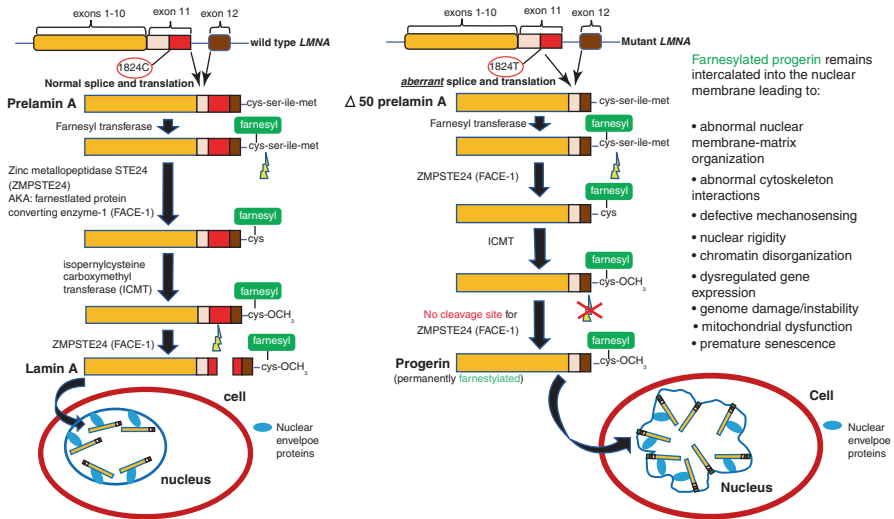


Fig. 11.1 Normal (left side) and classical mutant HGPS (right side) prelamin A processing and effects on cellular physiology. Wild type prelamin A is initially farnesylated at a cysteine residue near the C-terminus, followed by removal of the terminal serine-isoleucine-methionine tripeptide and then carboxymethylation; the farnesylation and carboxymethylation allow the precursor molecule to integrate into the inner nuclear membrane. This protein is then cleaved by zinc metalloproteinase STE24 (ZMPSTE24) to form the mature lamin A protein, which is no longer intercalated into the nuclear membrane, but does interact with a variety of nuclear envelope proteins to maintain normal nuclear shape and chromatin architecture. In the case of the HGPS prelamin A, a de novo synonymous mutation replaces the cytosine with a thymidine at position 1824 in the 11th exon; although this theoretically results in a conserved codon for glycine at position 608, the C>T transition generates an alternative splice site that removes 150 nucleotides from exon 11, resulting in the deletion of 50 amino acids including the cleavage site for ZMPSTE24. Subsequent farnesylation and carboxymethylation produces the progerin protein that remains associated with the inner nuclear membrane and leads to nuclear distortion with alterations in chromatin architecture, intracellular signaling, and mechanotransduction, ultimately leading to genomic instability and premature senescence. Note that low levels of progerin are synthesized ‘normally’ in aged cells and can be induced by oxidative stress and telomere shortening

The persistent nuclear membrane association of progerin leads to a host of intracellular defects, histologically reflected by distorted and irregular nuclear profiles (Fig. 11.1; reviewed in [14, 15]). Nuclear rigidity and distortion presumably lead to grossly abnormal chromatin architecture, with subsequent defective chromatin remodeling and ineffective access of transcriptional machinery to persistently condensed genomic DNA. DNA damage will result from mechanical strand breakage, and telomere shortening and genomic instability are predictable consequences. The distorted chromatin organization will, in turn, be reflected in aberrant gene transcription and intracellular signaling. It is likely that the nuclear membrane distortion will also lead to defective mechanosensing through altered nuclear-cytoskeletal interactions, which are expected to be especially important for normal vascular function [16, 17]. The dysregulated chromatin architecture will likely also lead to

dysfunctional mitoses and possible replication-associated catastrophe. Finally, the requirement for augmented DNA repair will engender excess mitochondrial demands with an additional component of oxidative stress.

Interestingly, although a number of murine models of progeria have been developed, they do not entirely recapitulate the disease phenotype in humans with complete fidelity (reviewed in [18]; (Table 11.1). Some of this is undoubtedly due to differences in cross-species protein interactions (human progerin may associate differently with nuclear membrane proteins than the mouse homologue), as well as the relative role of lamins A and C in murine nuclear architecture. Nevertheless, there are enough overlaps in the clinical course to assert that the basic theory regarding aberrant nuclear structure-function is likely correct. Moreover, the mouse models

Table 11.1 Murine models of HGPS

Model	Protein expression	Vascular changes ^a	Cardiac arrhythmia	Premature aging ^b
<i>LMNA</i> ^{HG/+} Heterozygous knock-in of mutant human <i>LMNA</i> coding for progerin	Combined human progerin and normal murine lamin A/C expression	No	Not reported	Yes 4–8 month lifespan
<i>LMNA</i> ^{HG/HG} Homozygous knock-in of mutant human <i>LMNA</i> coding for progerin	Exclusive human progerin expression	Not reported	Not reported	Yes 3–4 week lifespan
<i>BAC G608G transgene</i> Bacterial artificial chromosome containing human <i>LMNA</i> with c.1824C>T transition	Combined human progerin and normal murine lamin A/C expression	Yes	No	No
<i>LMNA</i> ^{G609G/+} Heterozygous knock-in of mutant murine <i>LMNA</i>	Combined murine progerin and normal murine lamin A/C expression	Yes	Not reported	Yes ~32-week lifespan
<i>LMNA</i> ^{G609G/G609G} Homozygous knock-in of mutant murine <i>LMNA</i>	Murine progerin and lamin C, with residual lamin A expression	Yes	Yes	Yes ~ 15-week lifespan
<i>ApoE</i> ^{-/-} <i>LMNA</i> ^{G609G/G609G} Homozygous knock-in of mutant murine <i>LMNA</i> in a mouse with congenital apoE deficiency ^c	Murine progerin and lamin C, with residual lamin A expression with absent apolipoprotein E	Yes, including atherosclerosis	Yes	Yes ~18-week lifespan
<i>Zmpste24</i> ^{-/-} Homozygous knock-out of ZMPSTE24	Murine prelamin A and lamin C	Yes	Yes	Yes 5–7 month lifespan

Adapted from [18]

^aIncludes calcification and VSMC loss; atherosclerosis is NOT seen unless noted

^bIncludes failure to thrive, stunting, alopecia, osteoporosis, loss of subcutaneous fat; normal wild-type life-span >2 years

^cHamczyk et al. [35]

can be exploited to study disease pathogenesis, as well as the efficacy of various therapeutic interventions.

Given the specific molecular processes underlying the biochemical changes in HGPS, a number of therapeutic interventions have been investigated. In particular, farnesyl transferase inhibitors (e.g., lonafarnib) have proved effective in single-arm clinical trials [19]. There is also augmented benefit to HGPS patients from the addition of statins (blocking upstream HMG-CoA reductase) and bisphosphonates (blocking farnesyl diphosphate synthase) introducing two additional inhibitors to the prelamin farnesylation pathway [20].

Mechanisms for Vascular Pathology in HGPS

Both endothelium and smooth muscle cells are impacted by progerin effects on nuclear transcription.

Endothelial pathology in HGPS Although less well investigated, endothelial cells (EC) with lamin A mutations exhibited accelerated senescence *in vitro* and a proinflammatory/atherogenic program of EC activation with sustained expression of leukocyte adhesion molecules (vascular cell adhesion molecule-1 and E-selectin), proinflammatory cytokines (interleukin-8 and monocyte chemoattractant protein-1), and prothrombotic genes (plasminogen activator inhibitor-1), with reduced expression of endothelial nitric oxide synthase (eNOS) and downregulation of Krüppel-like factor 2 (KLF2; a zinc finger transcription factor important in maintaining normal endothelial function at sites of laminar flow) [21–23]. Moreover, conditioned media from HGPS EC induced similar dysfunction in normal endothelium [23] suggesting that soluble mediators and/or extracellular vesicles may be involved [24, 25].

Vascular smooth muscle cell pathology in HGPS Vascular smooth muscle cell (VSMC) attrition, with increased proteoglycan matrix expression, occurs in murine progeria models as well as in HGPS patients [26, 27]. This VSMC loss may be attributable to error-prone DNA repair mechanisms including non-homologous end joining of double-stranded DNA breaks, leading to increased cell death through caspase-independent mechanisms (e.g., mitotic catastrophe) [28]. Loss of VSMC and increased matrix synthesis will ultimately engender stiffer, less compliant vessels; loss of normal endothelial function (e.g., with diminished eNOS production) will also lead to increased vascular tone; systemically, this can promote the hypertensive changes seen in progeria.

Cardiovascular calcification in HGPS An increased propensity to calcification underlies many of the vascular and valvular pathologies associated with HGPS (reviewed in [12]); these likely involve an increased production by VSMC of factors that drive osteogenic differentiation, as well as the loss of extracellular inorganic pyrophosphate (PPi), a major inhibitor of calcification [29] (Fig. 11.2).

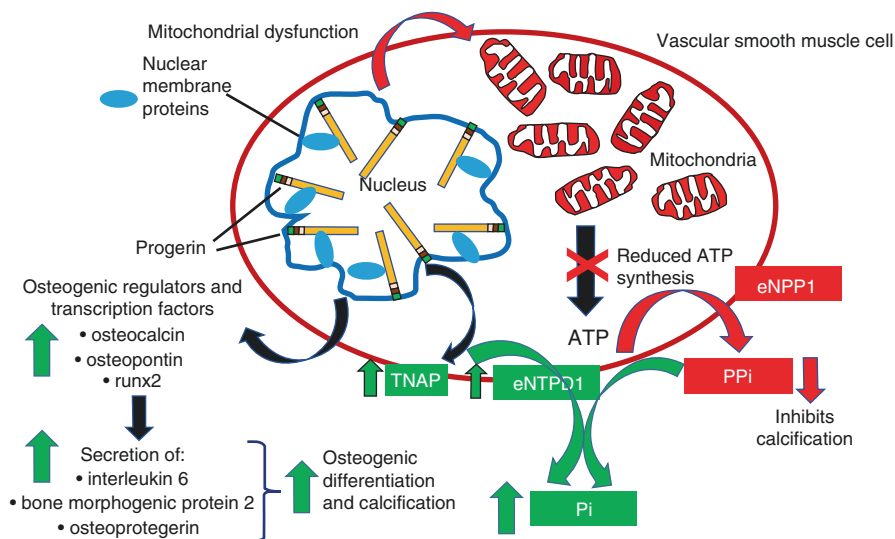


Fig. 11.2 Mechanisms of calcification in wild type and HGPS vascular smooth muscle cells. Nuclear distortion and instability lead to oxidative stress and mitochondrial dysfunction, which will result in reduced ATP production and ultimately diminished inorganic pyrophosphate (PPi) synthesis. Since extracellular PPi is a major inhibitor of calcification, mechanisms that reduce its synthesis or increase its degradation lead to greater matrix calcification. Thus, increased production by HGPS cells of tissue non-specific alkaline phosphatase (TNAP) and ectonucleoside triphosphate diphosphohydrolase-1 (eNTPD1) reduces the functional levels of PPi. At the same time, HGPS vascular smooth muscle cells are also synthesizing osteogenic transcription factors, such as runx2, as well as a host of osteogenic regulatory proteins that are associated with a senescent secretory VSMC phenotype. The net result is markedly increased propensity for matrix calcification. eNPP1: ectonucleotide pyrophosphatase/phosphodiesterase 1, an enzyme that breaks down extracellular ATP to generate PPi

PPi synthesis is reduced when mitochondrial dysfunction results in diminished ATP synthesis (the main source of PPi); this occurs in progeroid syndromes presumably through increased oxidative stress and defective mitochondrial turnover. In addition, knock-in mice carrying the mutant *Lmna*^{G609G/+} construct exhibited concurrent upregulation of enzymes that catabolize ATP (ectonucleoside triphosphate diphosphohydrolase-1; eNTPD-1) or PPi, including tissue non-specific alkaline phosphatase (TNAP) [30]; exogenous PPi reduced vascular calcification in this model.

On the flip side of the equation (reviewed in [12]), DNA damage (associated with cellular senescence) and oxidative stress conspire to reduce ZMPSTE24 expression in VSMC, resulting in increased prelamin A levels. In turn, accumulating prelamin A drives endogenous damage repair mechanisms and a senescent VSMC secretory phenotype [31]. As a result, VSMC produce increasing levels of osteogenic regulators such as osteocalcin and osteopontin, and the transcription factor Runx2, in addition to mediators that promote calcification, including interleukin 6, bone morphogenic protein 2, and osteoprotegerin (Fig. 11.2).

Although valvular calcification (most commonly in the aortic valve) has been reported in HGPS patients [32], nothing is known about the underlying mechanisms and whether the pathways involved might actually mirror typical valvular senescent calcification. Presumably, the same pathways described for VSMC also impact the propensity for calcification in valvular interstitial cells, but this has not been formally evaluated. Although there is an understandable paucity of human HGPS valvular specimens to analyze, the various murine models provide excellent opportunities to explore altered calcification in other sites. Indeed, to date, valvular degenerative pathologies have *not* even been reported in any of the mouse progeria systems.

Atherosclerosis in HGPS Severe atherosclerotic disease is a common feature in HGPS; indeed, as noted previously, the most common cause of death in affected patients is myocardial infarction or cerebrovascular accident. This predilection for early and severe atherosclerosis is not attributable to changes in circulating cholesterol levels or general inflammatory state of affected individuals [33], although EC dysfunction will likely lead to greater inflammatory cell recruitment at sites of vascular injury [22, 23]. Given that atherosclerosis also characteristically occurs at sites of low or turbulent shear stress (i.e., at branch points or sites of vascular curvature), and that EC KLF2 is down regulated in progeria, it also seems likely that defective mechanosensing in the vasculature will be a contributory factor [34]. The atherosclerotic plaques in HGPS closely resemble more typical age-related atherosclerosis although there increased adventitial fibrosis has been described; it is noteworthy that progerin is expressed in a significant fraction of all the cells (EC, intima, media, and adventitia) in these plaques [26].

Interestingly, most progeroid murine models exhibit vascular stiffening—likely as a consequence of VSMC loss and increased extracellular matrix synthesis—but atherosclerosis is not a feature in animals with progerin-only mutations (Table 11.1). This is likely due to the fact that mice are relatively resistant to atherosclerosis development, attributable to species differences in cholesterol and lipid metabolism. Nevertheless, expression of murine progerin on a background of congenital apolipoprotein E deficiency (ApoE^{-/-}) led to the development of accelerated atherosclerosis, as well as atherosclerosis-related mortality [35]. VSMC-specific progerin expression alone yielded a severe atherosclerotic phenotype (and a shortened lifespan) on the ApoE-deficient background, whereas progerin expression in the macrophage cell lineage alone did not.

Relation of HGPS to “Normal” Aging

Physiologic aging is fundamentally the consequence of genomic instability, telomere loss, epigenetic changes, and abnormal protein turnover [36]. The tissues in HGPS patients exhibit many of these molecular, biochemical, and cellular signatures. Consequently, the causal intracellular accumulation of progerin in HGPS patients is

promoted as an important window on the mechanisms that underlie physiologic senescence (reviewed in [18, 37]). Furthering the case that aging and progerin are mechanistically linked, oxidative stress and telomere shortening—associated with “normal” aging—also result in prelamin A synthesis [38] and progerin [39] expression in normal “aged” cells. Thus, there is at least a theoretical connection linking the aberrant nuclear membrane architecture associated with progerin to age-related pathologies such as cardiac fibrosis and diastolic dysfunction, vascular stiffening and hypertension, and atherosclerosis, stroke, and myocardial infarction. Presumably, the accelerated nature of the “physiologic” aging in HGPS results from the higher constitutive levels of progerin in virtually all cells leading to severe ongoing dysfunction, versus the relatively sparse progerin-positive cells in normal age-related lesions. In this regard, it is noteworthy that progerin levels do increase with age, but only marginally so; progerin is detectable in <0.01% of fibroblasts in primary cultures from young donor skin biopsies, but only in the range of 0.3–0.8% of fibroblasts from aged donors [40]. Nevertheless, by the time cells reach replicative senescence, the fraction of progerin-positive cells reached almost 90%. In the final analysis, HGPS probably does represent a true model of accelerated aging [18, 37]; it remains to be seen whether the interventions developed to slow the progress of progeria will also prove effective in the more physiologic setting of “normal” human senescence.

Conclusion

The fundamental pathogenesis underlying HGPS is well understood; moreover, the resulting biochemical abnormalities (e.g., persistent lamin farnesylation) are at least partially amenable to pharmacologic intervention. Thus, to the extent that the secondary manifestations of HGPS (lipodystrophy, alopecia, osteopenia, skeletal dysplasias, joint contractures, etc.) *truly* reflect accelerated “aging,” this incredibly rare entity has the potential to shine a very bright light on pathways that propel physiologic senescence. In particular, the endothelial and smooth muscle cell dysfunction in HGPS are almost certainly the proximate causes of the premature vascular (and valvular) calcification that occurs, as well as the accelerated atherosclerosis that represents the major cause of mortality in affected patients. Consequently, if accumulating progerin is indeed the driver for cardiovascular degenerative pathology (which is still an uncertain proposition), then the pharmacologic interventions developed to treat HGPS patients stand to provide major benefits for the entire (aging) population.

Acknowledgments The author wishes to recognize with appreciation the outstanding and innovative research and the comprehensive HGPS reviews developed by Dr. Vicente Andrés and colleagues at Centro Nacional de Investigaciones Cardiovasculares Carlos III in Madrid, Spain. In addition, Dr. Leslie B. Gordon (Hasbro Children’s Hospital and the Alpert Medical School of Brown University in Providence, RI, and Medical Director of the Progeria Research Foundation) has been a tireless and eloquent international leader and advocate in the pursuit of the understanding and treatment of HGPS; without Dr. Gordon and her colleagues at the PRF, we would know only a fraction of what is understood about the disease.

References

1. Hutchinson J. A case of congenital absence of hair with atrophic condition of the skin and its appendages. *Lancet*. 1886;1:923.
2. Gilford H. On a condition of mixed premature and immature development. *Med Chir Trans*. 1897;80:17–45.
3. Gilford H. Progeria: a form of senilism. *Practitioner*. 1904;73:188–217.
4. Meredith MA, Gordon LB, Clauss S, Sachdev V, Smith AC, Perry MB, et al. Phenotype and course of Hutchinson-Gilford progeria syndrome. *N Engl J Med*. 2008;358:592–604.
5. Navarro CL, Cau P, Lévy N. Molecular bases of progeroid syndromes. *Hum Mol Genet*. 2006;15 Spec No 2:R151–61.
6. Takenouchi T, Hida M, Sakamoto Y, Torii C, Kosaki R, Takahashi T, et al. Severe congenital lipodystrophy and a progeroid appearance: mutation in the penultimate exon of FBN1 causing a recognizable phenotype. *Am J Med Genet A*. 2013;161A:3057–62.
7. Pescatore LA, Gamarra LF, Liberman M. Multifaceted mechanisms of vascular calcification in aging. *Arterioscler Thromb Vasc Biol*. 2019;39:1307–16.
8. Arking DE, Krebsova A, Macek M Sr, Macek M Jr, Arking A, Mian IS, et al. Association of human aging with a functional variant of klotho. *Proc Natl Acad Sci U S A*. 2002;99:856–61.
9. Worman HJ. Nuclear lamins and laminopathies. *J Pathol*. 2012;226:316–25.
10. Gruenbaum Y, Foisner R. Lamins: nuclear intermediate filament proteins with fundamental functions in nuclear mechanics and genome regulation. *Annu Rev Biochem*. 2015;84:131–64.
11. Dittmer TA, Misteli T. The lamin protein family. *Genome Biol*. 2011;12:222–36.
12. Dorado B, Andrés V. A-type lamins and cardiovascular disease in premature aging syndromes. *Curr Opin Cell Biol*. 2017;46:17–25.
13. Barrowman J, Wiley PA, Hudon-Miller SE, Hrycyna CA, Michaelis S. Human ZMPSTE24 disease mutations: residual proteolytic activity correlates with disease severity. *Hum Mol Genet*. 2012;21:4084–93.
14. Vidak S, Foisner R. Molecular insights into the premature aging disease progeria. *Histochem Cell Biol*. 2016;145:401–17.
15. Gonzalo S, Kreienkamp R, Askjaer P. Hutchinson-Gilford progeria syndrome: a premature aging disease caused by LMNA gene mutations. *Ageing Res Rev*. 2017;33:18–29.
16. Ji JY. Endothelial nuclear lamina in mechanotransduction under shear stress. *Adv Exp Med Biol*. 2018;1097:83–104.
17. Qi YX, Han Y, Jiang Z. Mechanobiology and vascular remodeling: from membrane to nucleus. *Adv Exp Med Biol*. 2018;1097:69–82.
18. Hameczyk MR, del Campo L, Andrés V. Aging in the cardiovascular system: lessons from Hutchinson-Gilford progeria syndrome. *Annu Rev Physiol*. 2018;80:27–48.
19. Gordon LB, Massaro J, D'Agostino RB Sr, Campbell SE, Brazier J, Brown WT, et al. Impact of farnesylation inhibitors on survival in Hutchinson-Gilford progeria syndrome. *Circulation*. 2014;130:27–34.
20. Gordon LB, Kleinman ME, Massaro J, D'Agostino RB Sr, Shappell H, Gerhard-Herman M, et al. Clinical trial of the protein farnesylation inhibitors lonafarnib, pravastatin, and zoledronic acid in children with Hutchinson-Gilford progeria syndrome. *Circulation*. 2016;134:114–25.
21. Pantsulaia I, Ciszewski WM, Niewiarowska J. Senescent endothelial cells: potential modulators of immunosenescence and ageing. *Ageing Res Rev*. 2016;29:13–25.
22. Bonello-Palot N, Simoncini S, Robert S, Bourgeois P, Sabatier F, Levy N, et al. Prelamin A accumulation in endothelial cells induces premature senescence and functional impairment. *Atherosclerosis*. 2014;237:45–52.
23. Yap B, Garcia-Cardeña G, Gimbrone MA Jr. Endothelial dysfunction and the pathobiology of accelerated atherosclerosis in Hutchinson-Gilford progeria syndrome. *FASEB 22 (meeting abstract supplement)*. 2008; 471.11.

24. Hutcheson JD, Goetsch C, Bertazzo S, Maldonado N, Ruiz JL, Goh W, et al. Genesis and growth of extracellular vesicle-derived microcalcification in atherosclerotic plaques. *Nat Mater*. 2016;15:335–43.
25. Hutcheson JD, Aikawa E. Extracellular vesicles in cardiovascular homeostasis and disease. *Curr Opin Cardiol*. 2018;33:290–7.
26. Olive M, Harten I, Mitchell R, Beers JK, Djabali K, Cao K, et al. Cardiovascular pathology in Hutchinson-Gilford progeria: correlation with the vascular pathology of aging. *Arterioscler Thromb Vasc Biol*. 2010;30:2301–9.
27. Varga R, Eriksson M, Erdos MR, Olive M, Harten I, Kolodgie F, et al. Progressive vascular smooth muscle cell defects in a mouse model of Hutchinson-Gilford progeria syndrome. *Proc Natl Acad Sci U S A*. 2006;103:3250–5.
28. Zhang H, Xiong ZM, Cao K. Mechanisms controlling the smooth muscle cell death in progeria via down-regulation of poly (ADP-ribose) polymerase 1. *Proc Natl Acad Sci U S A*. 2014;111:E2261–70.
29. Villa-Bellosta R, Wang X, Millán JL, Dubyak GR, O'Neill WC. Extracellular pyrophosphate metabolism and calcification in vascular smooth muscle. *Am J Physiol Heart Circ Physiol*. 2011;301:H61–8.
30. Villa-Bellosta R, Rivera-Torres J, Osorio FG, Acín-Pérez R, Enriquez JA, López-Otín C, et al. Defective extracellular pyrophosphate metabolism promotes vascular calcification in a mouse model of Hutchinson-Gilford progeria syndrome that is ameliorated on pyrophosphate treatment. *Circulation*. 2014;127:2442–51.
31. Liu Y, Drozdov I, Shroff R, Beltran LE, Shanahan CM. Prelamin A accelerates vascular calcification via activation of the DNA damage response and senescence-associated secretory phenotype in vascular smooth muscle cells. *Circ Res*. 2013;112:e99–109.
32. Nair K, Ramachandran P, Krishnamoorthy KM, Dora S, Achuthan TJ. Hutchinson-Gilford progeria syndrome with severe calcific aortic valve stenosis and calcific mitral valve. *J Heart Valve Dis*. 2004;13:866–9.
33. Gordon LB, Harten IA, Patti ME, Lichtenstein AH. Reduced adiponectin and HDL cholesterol without elevated C-reactive protein: clues to the biology of premature atherosclerosis in Hutchinson-Gilford progeria syndrome. *J Pediatr*. 2005;146:336–41.
34. Song M, San H, Anderson SA, Cannon RO 3rd, Orlic D. Shear stress-induced mechanotransduction protein deregulation and vasculopathy in a mouse model of progeria. *Stem Cell Res Ther*. 2014;5:41–52.
35. Hameczyk MR, Villa-Bellosta R, Gonzalo P, Andrés-Manzano MJ, Nogales P, Bentzon JF, et al. Vascular smooth muscle-specific progerin expression accelerates atherosclerosis and death in a mouse model of Hutchinson-Gilford progeria syndrome. *Circulation*. 2018;138:266–82.
36. López-Otín C, Blasco MA, Partridge L, Serrano M, Kroemer G. Hallmarks of aging. *Cell*. 2013;153:1194–217.
37. Ashapkin VV, Kutueva LI, Kurchashova SY, Kireev II. Are there common mechanisms between Hutchinson-Gilford progeria syndrome and natural aging? *Front Genet*. 2019;10:455.
38. Ragnauth CD, Warren DT, Liu Y, McNair R, Tajsic T, Figg N, et al. Prelamin A acts to accelerate smooth muscle cell senescence and is a novel biomarker of human vascular aging. *Circulation*. 2010;121:2200–10.
39. Cao K, Blair CD, Faddah DA, Kieckhafer JE, Olive M, Erdos MR, et al. Progerin and telomere dysfunction collaborate to trigger senescence in normal human fibroblasts. *J Clin Invest*. 2011;121:2833–44.
40. McClintock D, Ratner D, Lokuge M, Owens DM, Gordon LB, Collins FS, et al. The mutant form of lamin A that causes Hutchinson-Gilford progeria is a biomarker of cellular aging in human skin. *PLoS One*. 2007;2:e1269.

Chapter 12

Calcinosis in Scleroderma



Sonia Nasreen Ahmad, Elena Gostjeva, Jianfei Ma, and Richard Stratton

Introduction

Calcinosis cutis is characterized by the deposition of calcium into the skin and subcutaneous tissues [1]. It has remained as one of the most elusive presentations of systemic sclerosis. A lack of information regarding its molecular pathology is one of the reasons that a definitive treatment for it has not yet been found. Calcinosis is found in various autoimmune connective tissue diseases, namely, systemic sclerosis, dermatomyositis, mixed connective tissue diseases, and sometimes systemic lupus erythematosus [2]. The calcinosis that occurs in systemic sclerosis is of a dystrophic nature, i.e., the calcification that occurs in the diseased tissues is in the presence of an abnormal calcium-phosphorus metabolism [3]. Repetitive trauma has clinically been found to be associated with calcinosis, most commonly in the hands and feet [4] and other pressure areas like elbows, knees, and ischial tuberosities. Around 40% of patients with limited cutaneous systemic sclerosis (lcSSc) have calcinosis [5], linked to a variety of complications like ulceration, recurrent infections, impaired mobility, and disfigurement.

S. N. Ahmad
Centre for Rheumatology and Connective Tissue Diseases,
Royal Free Hospital, UCL, London, UK

Division of Medicine & Department of Internal Medicine,
Holy Family and Red Crescent Medical College and Hospital, Dakha, Bangladesh

E. Gostjeva
Department of Biological Engineering, Massachusetts Institute
of Technology Cambridge, Cambridge, MA, USA

J. Ma · R. Stratton (✉)
Centre for Rheumatology and Connective Tissue Diseases,
Royal Free Hospital Campus, University College London Medical School, London, UK
e-mail: r.stratton@ucl.ac.uk

Crystal Composition

Calcium hydroxyapatite has been identified as the major component of soft tissue calcinosis in scleroderma patients [6]. A study by Hsu, Emge, and Schlesinger analyzed the spontaneously draining material from calcinosis sites by using X-ray diffraction. Their findings were similar to previous findings showing that hydroxyapatite was the only inorganic material; however, in most of the samples in the study, hydroxyapatite was found to be the minor component, and more than 50% was organic material [6]. Thus, the composition of the calcinosis in SSc resembles that of the bone and not of enamel, which is closer to the composition of calcinosis in dermatomyositis where the mineral-to-protein ratio is higher and the stiffness of the deposits is also elevated resembling enamel rather than the bone [6, 7]. Another study carried out by Lydon et al. looked into the structure and composition of calcinosis by using various analytical techniques, namely, micro-computed tomography, powder X-ray diffraction, electron microscopy, and infrared analyses. They found that hydroxyapatite with a carbonated component is made up of calcinotic deposits [8]. Vibrational spectroscopy, which uses both infrared and Raman spectroscopy, has been used for the accurate determination of molecular structures in analyzing calcinosis. The technique is highly selective and analyzes molecular properties on the basis of vibrations at molecular levels [9, 10]. In a study by Baldet et al. [11], X-ray diffraction, infrared spectroscopy, and differential thermal analysis revealed that the calcinosis in a lcSSc case consisted of type-B carbonate apatite.

Pathophysiology of Calcinosis

The basic underlying mechanism of calcinosis is still a mystery. Clinical observations have evolved several hypotheses. Pressure points such as over the elbows, forearms, knees, and ischial tuberosities are frequently affected by calcinosis in addition to hands and feet [4]. As these pressure points are susceptible to trauma or mechanical stress, it can be concluded that these may be precipitating factors for calcinosis. Chronic inflammation and vascular hypoxia are also presumed to contribute to the tissue damage, also potentially contributing to the evolution into dystrophic calcification [1].

The role of inflammation has been established to some extent in the pathophysiology of calcinosis found in juvenile dermatomyositis, where the lesions may be extensive [12]. Here it has been found that IL-6, IL-1B, and tumor necrosis factor are present in the subcutaneous fluid-phase calcinosis (“milk of calcium”) of juvenile dermatomyositis patients. Also, a case-control study in Australia involving 90 patients found that mannose-binding lectin (a receptor of the lectin pathway of complement) levels were significantly elevated in SSc patients with calcinosis vs. SSc patients without calcinosis as well as in patients with digital ulcers and pitting scars [13].

It has been noted in several studies that vascular hypoxia contributes to calcinosis. Firstly, the relation between digital ulceration and calcinosis has been observed in several studies [14] [15]. Secondly, a link between acro-osteolysis and calcinosis has been put forward (this is associated with severe digital ischemia) [16]. Thirdly, one study has found an association between the severity of microvascular disease, measured by nailfold capillaroscopy and calcinosis [17]. Fourth, it has been observed that there is an increase in the expression of advanced glycation/lipoperoxidation end products (AGEs), (a marker of oxidative stress which can occur due to ischemic reperfusion injury) in patients with calcinosis [18].

Recently studies have looked into the factors regulating tissue mineralization. Circulating inorganic pyrophosphate (PPi) was first identified as a key endogenous inhibitor of bone mineralization in the 1960s [19]. PPi acts as an inhibitor of mineralization by binding tightly to the surface of growing hydroxyapatite crystals, thus preventing them from serving as a nidus for mineralization and thus not allowing crystal growth [19–21]. Ectopic calcification is usually associated with a deficiency of one or more of these inhibitors. Although the association of plasma PPi levels and vascular calcification in advanced kidney disease patients has been studied [22–24], no such study has been carried out in autoimmune rheumatic diseases like SSc.

Circulatory levels of PPi are regulated by enzymes with nucleoside triphosphate pyrophosphohydrolase (NTPPPH) activity such as plasma ectonucleotide pyrophosphatase phosphodiesterase 1 (ENPP1) [25]. ENPP1 is an ectoenzyme and needs ATP to be present in the extracellular environment. One of the important ATP release pathways for PPi formation involves the ATP-binding cassette (ABC) subfamily C member 6 (ABCC6), an efflux transporter predominantly found in hepatocytes [26, 27]. ABCC6-mediated hepatic ATP release accounts for about 60–70% of all PPi found in circulation [27]. Accumulation of PPi is prevented by its degradation by tissue-nonspecific alkaline phosphatase (TNAP) [28]. The endonucleotidase CD73 forms an additional step of regulation of PPi plasma levels by converting adenosine monophosphate into inorganic phosphate and adenosine which serves as a TNAP inhibitor [29]. Deficiencies in ABCC6, ENPP1, and CD73 proteins lead to reduced plasma PPi levels, thus promoting hydroxyapatite mineralization in the peripheral tissues. More studies are required to look into these regulators of bone mineralization in SSc patients with and without calcinosis.

Advancements have been made in the genetic study of SSc patients [29]. Genetic susceptibility markers have been found in the human leukocyte antigen (HLA) region and in non-HLA genes. In Korean SSc patients, subcutaneous calcinosis was found to be associated with the *HLA-DRB1*04* allele [30]. Polymorphisms in the MMP3 gene were associated with calcinosis in patients with SSc, suggesting the role of matrix metalloproteinase in the extracellular matrix protein deposition in SSc [31].

Carboxylated matrix G1a (MGP), a vitamin K-dependent factor in the soft tissues and circulation, is another inhibitor of calciphyllaxis. These levels are reduced in uremic patients with calciphyllaxis, and thus, inhibitory effects on the promoters of calciphyllaxis, such as bone morphogenetic proteins 2 and 4 (BMP2 and BMP4)

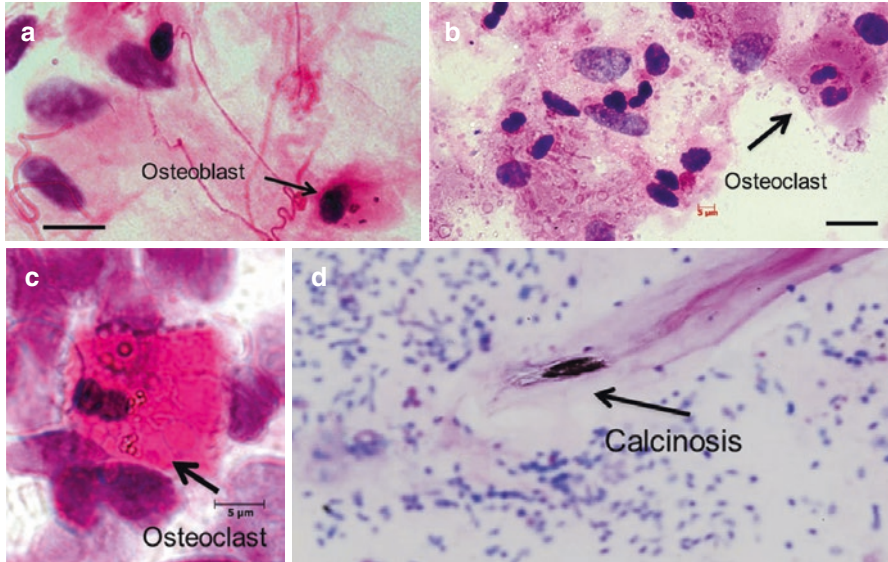


Fig. 12.1 Abnormal osteogenic cells within the scleroderma microenvironment. Shown by scleroderma skin tissue cells spread, Feulgen DNA staining of the nuclei, showing presence of bone regulatory cells (arrowed in “a,” “b,” and “c”) in microcalcified nodules in biopsies obtained from the involved forearm skin of systemic sclerosis (E. Gostjeva MIT). Various elements relevant to dysregulated bone metabolism were seen including calcinotic lesions (arrowed in “d”). Scale bars = 5 µm

are lowered. In a similar way, carboxylated MGP in susceptible SSc patients may be affected by lowered vitamin K levels too [32].

In our own analyses, a novel histologic method has been used to examine consecutive 1-mm-thick sections of SSc skin as tissue spread, for the presence of calcinotic lesions and for cell types relevant to the calcinosis (Fig. 12.1). These analyses show frequent osteoclast-like cells as well as potential osteoblasts in the region of the calcinotic microdeposits. Dysregulation of tissue-resident stem cells as osteoblast precursors and recruitment of monocytes as osteoclast precursors may be involved in setting up an osteogenic microenvironment.

Clinical Presentation

SSc calcinosis may be a complete incidental finding or more usually present with considerable pain, recurrent ulceration, or repeated infections. Lesions can vary in size from being inconspicuous to large tumoral deposits. A study of 52 patients with calcinosis in Florence by Bartoli et al. grouped calcinosis into visible and palpable and then according to their shapes and consistency as found on palpation or imaging [33]. Visible and palpable were classified as mousse (soft, cream-like) and stone



Fig. 12.2 Clinical appearance of calcinotic lesions in scleroderma (a) small ulcerating calcinosis lesions of pressure points over the distal interphalangeal joints in patient with severe flexure contractures. (b) Ulcerating calcinosis lesion over the posterior thigh in diffuse cutaneous disease. (c) Subcutaneous calcinosis seen over the dorsum of the fifth metacarpal bone

(single or multiple solid deposits) according to their macroscopic features; nonvisible but palpable were stone, net (diffuse, thin network), and plate (large, uniform, flat). In the same study, they found that mousse calcinosis was associated with pulmonary arterial hypertension and the stone variety with pulmonary involvement. Typical clinical features are shown in Fig. 12.2.

A case-control study [34] which included 167 hand radiographs of SSc patients matched with 168 hand radiographs of patients without SSc demonstrated that individuals with terminal tuft calcinosis had more digital ulcerations. A retrospective study of 101 SSc patients by Johnstone et al. [16] showed similar results, indicating that patients with moderate or severe acroosteolysis were more likely to have severe calcinosis. Another recent study of 68 hand radiographs with calcinosis showed that the thumb was more affected than other digits and followed by the index finger [35].

Scleroderma Disease Subset Associations with Calcinosis

Scleroderma can be subdivided into clinical subsets based on the pattern of skin involvement, namely, limited cutaneous systemic sclerosis (lcSSc), defined by skin involvement limited to the extremities and face; diffuse cutaneous subset (dcSSc),

Table 12.1 Systemic sclerosis disease subsets

SSc subsets	Defining clinical features	Pattern of internal organ involvement	Hallmark autoantibody profile
Diffuse cutaneous systemic sclerosis (dcSSc)	Skin fibrosis spreading proximal to the elbows and involving the trunk	Tendency to pulmonary fibrosis and scleroderma renal crisis. Esophageal and gut involvement similar in prevalence to lcSSc	Antinuclear factor present in high titer >90% of cases. ATA and ARA classical disease-specific antibodies
Limited cutaneous systemic sclerosis (lcSSc)	Skin fibrosis limited to extremities and face	Pulmonary fibrosis and renal crisis less common than in dcSSc. Peripheral vascular complications and PHT are major complications. PHT main cause of mortality in this subgroup	Antinuclear factor present in high titer >90% of cases. ACA classical disease-specific antibody
Systemic sclerosis sine scleroderma (ssSSc)	Absence of skin involvement but with typical organ fibrosis or scleroderma vascular disease, plus SSc-associated autoantibody	Vascular disease prominent. Pattern of organ involvement resembles lcSSc Nailfold capillaroscopy Or autoantibody profile used to confirm diagnosis	Antinuclear factor profile similar to limited disease

Classification is based on the pattern of cutaneous involvement and has prognostic significance on terms of organ involvement. Typical clinical and serologic features are shown. (ATA anti-topoisomerase, ARA anti-RNA polymerase, ACA anti-centromere antibody)

defined by skin involvement spreading proximal to the elbows or involving the trunk; and systemic sclerosis sine scleroderma, defined as typical organ or vascular involvement with a disease-specific autoantibody but without significant skin fibrosis (ssSSc) (Table 12.1).

Calcinosis is more frequently found in the limited disease subset rather than the diffuse type [36]. A large international multicenter cohort study was carried out which included 7056 patients with SSc; of the 22% of patients with calcinosis, 25% had lcSSc, 17% had dcSSc, and 28% were scleroderma sine sclerosis [37]. It is also found in patients who have long-standing disease with a mean of 7–10 years [33, 38, 39].

A retrospective multicenter international cohort study [39] of 5280 patients found 1290 (24.4%) patients to have calcinosis. These patients were found to be older and have long-standing disease. They were more likely to have digital ulceration, telangiectasia, acroosteolysis, cardiac disease, pulmonary hypertension, gastrointestinal involvement, and arthritis but less likely to have myositis. Osteoporosis was also found to be much more common in patients with calcinosis. The presence of anti-centromere antibody, anti-PM/Scl antibody, and anti-cardiolipin antibodies were found to be independently associated with calcinosis. This was similarly reflected in two other studies; one study showed a significant association (P value <0.0001) of calcinosis with positive anti-centromere antibody [40]. The second study, a Canadian study, found a significant association between calcinosis and the presence of anti-PM/Scl antibody [41].

Diagnostic Approach

Calcinotic deposits are mostly found clinically as subcutaneous nodules of various shapes and sizes. They are typically found at areas of repeated trauma, mostly the hands and the feet, but are also found in the elbows, knees, arms and legs, trunk, and face (in order of frequency) [2, 4, 42]. However, calcinosis may also be an incidental finding, with patients undergoing simple radiographs for other reasons, seen, for example, on X-ray or CT imaging in the subcutaneous tissues of the chest, abdomen, or neck, where they may be less apparent clinically. Figure 12.3 shows the radiologic appearance of calcinosis, showing lesions over the fingers, wrists, and nasal bridge and deep lesions over the anterior chest wall.

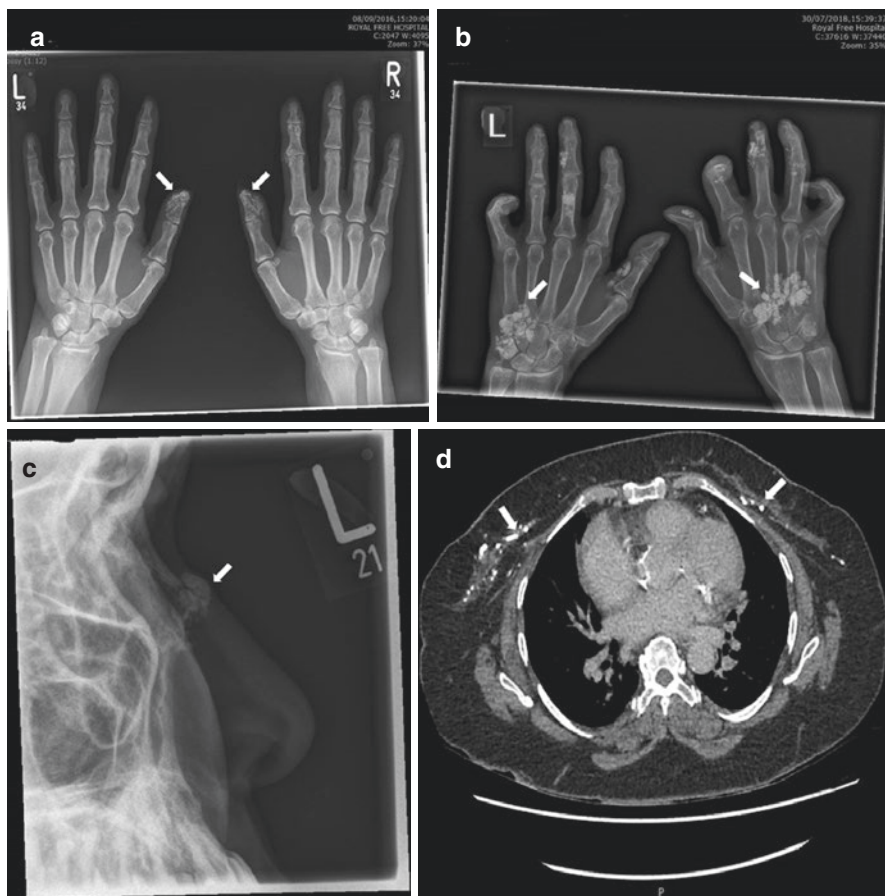


Fig. 12.3 Radiologic appearance of calcinotic lesions in systemic sclerosis. **(a)** Typical calcinosis affecting the distal finger pulps in limited cutaneous SSc with severe Raynaud's. **(b)** More extensive lesions affecting the carpus as well as phalanges and associated with flexor contractures. **(c)** Atypical sites may also be involved as in this lesion affecting the bridge of the nose. **(d)** CT of thorax showing subcutaneous calcinosis of anterior chest wall. Arrows indicate areas of calcinosis

Plain X-rays are extremely sensitive in detecting calcinosis and are recommended as the initial imaging evaluation in patients with scleroderma [42, 43]. In a retrospective study, various morphological patterns of calcinosis were noted, namely, nodular, sheet-like, reticular, amorphous, and linear radiographs [42]. With the use of X-rays, a scoring system was developed to assess the burden affecting the hands in patients in the same study. This was done based on the area of coverage, density, number, and anatomic location of the calcinosis lesions. Ultrasound [44] and computed tomography [45], however, have been found to be more useful in identifying the location of these deposits in soft tissues, although Cuomo et al. showed that ultrasound was not more sensitive than conventional radiographs in detecting calcinosis in SSc patients [46]. Dual-energy CT (DECT) is an advanced imaging modality that has been used to identify monosodium urate crystals in patients with gout [47]. DECT imaging has also been found to be useful in evaluating SSc calcinosis [48]; it is able to detect calcium deposited in the crystals by analyzing the content. DECT identified that calcinosis was most commonly found in the subcutaneous fat pads of the fingertips and along the tendon sheaths and muscle groups [48]. Multidetector computed tomography (MDCT) is another diagnostic imaging which has a greater contrast resolution [45]. It can provide three-dimensional images which may be better in assessing the extent of calcinotic lesion. However, both DECT and MDCT are in their experimental stages in this aspect, and many more studies are required before it can be said which mode of imaging, specialized CTs, or ultrasound is more useful in assessing calcinosis than plain radiography.

Treatment Modalities

Until now no effective management has been brought forward for the management of calcinosis; this may be due to the fact that the exact underlying mechanism has still not been identified. However, several medical therapies have studied in this regard with modest outcomes [36].

Therapies for Inflammation

First-line therapies are usually aimed at improving the underlying inflammation that is usually present. In this regard, colchicine and minocycline have been found to improve symptoms of calcinosis (inflammation and ulceration), possibly acting through their anti-inflammatory effect rather than reducing the size of the calcinosis [49]. These agents have been evaluated in case studies and small series, and there are report of both success and failure in patients using colchicine [49]. In one study there was improvement of symptoms of calcinosis within 2 months of start of treatment in a child with systemic sclerosis as well as in a child

with dermatomyositis [50]. However, in a separate retrospective study of patients with calcinosis associated with autoimmune connective tissue disease, only one of eight achieved complete resolution and two partial resolutions [4]. Adverse effects of the gastrointestinal system may limit its use in SSc patients in whom there is gastrointestinal involvement. Furthermore, minocycline, which is an antibiotic with anti-inflammatory properties, has been evaluated. In an open-labeled study, nine women with lcSSc were treated with minocycline; improvement in inflammation and ulceration was noted in eight patients within 2 months [51]. A retrospective study of six patients with calcinosis cutis associated with autoimmune connective tissue disease showed one patient to achieve a partial response, two patients failed to respond, and the response of the other three unknown [4]. The main side effect with minocycline is the blue-black discoloration of calcium deposits; in addition to that, hypersensitivity reactions and a lupus-like syndrome are also documented. Unlike colchicine, this drug is contraindicated in children.

Calcium Channel Blockers

Diltiazem is the most commonly used drug for the empirical treatment of calcinosis [49]. It alters the formation and crystallization of the calcium nidus by reduction of the intracellular calcium influx in the affected tissues and local macrophages. Various case reports have shown diltiazem to produce positive results for 1–12 years in patients taking doses from 240 to 480 mg/day [52–54]. In a retrospective study of 78 patients from the Mayo Clinic of patients with calcinosis in the setting of autoimmune connective tissue disease, diltiazem was found to be effective in 9 out of 17 patients as a first-line treatment [4]. On the other hand, only 3 out of 23 patients with radiographic calcinosis experienced regression of lesion with diltiazem [17]. The use of other calcium channel blockers in this regard have been less reported [49].

Bisphosphonates

Bisphosphonates, which are structural analogs of PPI, may play a role in the treatment of calcinosis by reducing the bone resorption. They can reverse the calcification process by inhibiting macrophage proinflammatory cytokine production [49]. Reports of the first-generation bisphosphonate, etidronate, have shown contradictory results [55, 56]. However, a more recent case report describes the clinical and radiologic resolution of calcinosis in one patient with lcSSc after 6 months of treatment with risedronate for glucocorticoid-induced osteoporosis [57]. Pamidronate intravenous infusion has been reported to be effective for calcinosis in several case reports mostly in dermatomyositis patients [49]. A mouse study published in 2015

looked into the potential efficacy of bisphosphonates to prevent ectopic calcification by feeding ABCC6^{-/-} mice a diet containing etidronate or alendronate. High doses of etidronate, but not alendronate which was used at a more standard dose, significantly reduced mineralization at 12 weeks [58]. More studies are needed to look into this further. One possible explanation for these results is that the anti-mineralization effect results not from the biological anti-osteoclastic activity of the bisphosphonate, for which alendronate is more potent, but rather from the delivery of a large number of PPI-analog molecules as in the high-dose etidronate group. It is possible that etidronate, in sufficient doses, might be beneficial in selected patients.

Warfarin

Patients with calcinosis have been found to have abnormally high levels of vitamin K, which is known to be involved in the calcium-binding process [49]. The view on warfarin for the treatment of calcinosis is conflicting, even though there are several studies which show that warfarin may be effective for small calcified deposits [59]. A double-blind placebo-controlled study [60] of seven patients with SSc or dermatomyositis and multiple subcutaneous calcifications showed a decrease in extraskeletal uptake on whole-body bone scintigraphy with injection of technetium 99 m diphosphonate in two of three patients who received warfarin for 18 months. However, another study [61] of six patients with long-standing and extensive calcinosis treated with low-dose warfarin for around 14.6 months showed clinical and radiological worsening in five patients, one of who was an SSc patient. The Mayo Clinic study showed that 4 of 19 ACTD patients with calcinosis who received warfarin for conditions other than calcinosis had no improvement in calcinosis compared with that group that did not receive warfarin [4].

Intravenous Immunoglobulin

Intravenous immunoglobulin therapy appears to have significant immunomodulatory effects when used in rheumatic diseases and confers benefit against certain aspects of SSc. Since calcinosis is believed to have an underlying autoimmune-inflammatory etiology, this mode of therapy has been assessed, with mixed results. There are conflicting data on dermatomyositis-associated calcinosis, with positive [62, 63] and negative [64] results. In a case report of a patient with lcSSc and calcinosis of the left index finger, there was a reduction in the size of the calcinotic deposit and resolution of the symptoms after 5 months of treatment with intravenous immunoglobulin [65]. The authors assume that this effect was based on the anti-inflammatory properties, probably related to the suppression of activated macrophages.

Biologic Agents

These agents may be considered to be promising, given the fact that inflammation is thought to play a major role in the pathogenesis of calcinosis. In a case report, a patient with SSc-myositis overlap and refractory calcinosis was treated with infliximab and showed a reduction in size of calcification and no new deposits at 41 months in serial pelvic-computed tomography imaging [66]. Rituximab, a chimeric anti-CD20 antibody, may be another potential therapy. An lcSSc patient with extensive calcinotic lesions experienced reduction in size of these on physical examination, and her pain significantly improved after 1 year of treatment with two courses of rituximab 18 months apart [36]. Another case reported a lady with lcSSc using the same regimen of rituximab to treat her interstitial lung disease and arthritis showed a complete resolution of the calcinosis in her hands 7 months after her first infusion [67].

Nonmedical Therapies

There have been a few case reports which have shown positive results with carbon dioxide laser tissue vaporization, a bloodless technique that allows excellent visualization and vaporization of calcium deposits [68, 69]. Extracorporeal shockwave lithotripsy has been analyzed in a prospective study of nine patients (three with SSc) with progressive calcinosis. After three sessions at 3-week intervals, there was a reduction in the median area of calcinosis and pain [70].

Although there is a certain risk as well as recurrence, surgical excision of calcium remains the mainstay of treatment for localized or large calcinotic lesions. These should be carried out by a skillful surgeon who has expertise in the area as there is the question of poor perfusion particularly in areas of the hand.

In the Mayo Clinic study, all 11 patients who underwent surgical excision alone responded (8 with complete response), as well as 16 out of 17 patient who received medical and surgical therapy (14 with complete response). In contrast, only 7 of the 19 patients treated with medical therapy alone had any response (one with complete response) [4]. Less invasive surgical procedures, like curettage, have been attempted to decrease complications [71]. A retrospective study of nine patients with SSc who underwent a debulking procedure using a high-speed micro-burr to soften calcinosis affecting the digits showed a high degree of patient's satisfaction and lower disability scores [72]. Unfortunately, no patients reported complete resolution of calcinosis, and seven patients had recurrence.

Conclusion

Calcinosis is a debilitation problem affecting nearly one quarter of patients with SSc. The appropriate management is not yet identified as the underlying exact pathogenesis is still largely unknown. However, with possibilities of inflammation

and vascular hypoxia playing a major role in calcinosis formation, certain studies show some promise. Despite this, surgery remains the mainstay of treatment for calcinosis, and a combination of medical and surgery yields better results. However, more randomized controlled trials are needed to look into the promising role biologics play in the near future, and more research is required to look into the underlying pathogenesis.

References

1. Chander S, Gordon P. Soft tissue and subcutaneous calcification in connective tissue diseases. *Curr Opin Rheumatol* [Internet]. 2012 [cited 2017 Nov 14];24:158–164. Available from: <https://insights.ovid.com/pubmed/?pmid=22227955>.
2. Gutierrez Jr A, Wetter DA. Calcinosis cutis in autoimmune connective tissue diseases. *Dermatol Ther* [Internet]. 2012 Mar 1 [cited 2017 Nov 3];25(2):195–206. Available from: <http://doi.wiley.com/10.1111/j.1529-8019.2012.01492.x>.
3. Reiter N, El-Shabrawi L, Leinweber B, Berghold A, Aberer E. Calcinosis cutis part I. Diagnostic pathway. *Am Acad Dermatology*. 2011;65(1):1–12.
4. Balin SJ, Wetter DA, Andersen LK, Davis MDP. Calcinosis cutis occurring in association with autoimmune connective tissue disease: the Mayo Clinic experience with 78 patients, 1996–2009. *Arch Dermatol*. 2012;148(4):455–62.
5. Steen VD, Ziegler GL, Rodnan GP, Medsger TA. Clinical and laboratory associations of anticentromere antibody in patients with progressive systemic sclerosis. *Arthritis Rheum* [Internet]. 1984 Feb [cited 2017 Nov 12];27(2):125–31. Available from: <http://www.ncbi.nlm.nih.gov/pubmed/6607734>.
6. Hsu V, Emge T, Schlesinger N. X-ray diffraction analysis of spontaneously draining calcinosis in scleroderma patients. *Scand J Rheumatol* [Internet]. Taylor & Francis; 2017 Mar 4 [cited 2017 Nov 18];46(2):118–21. Available from: <https://www.tandfonline.com/doi/full/10.1080/03009742.2016.1219766>.
7. Eidelman N, Boyde A, Bushby AJ, Howell PG, Sun J, Newbury DE, et al. Microstructure and mineral composition of dystrophic calcification associated with the idiopathic inflammatory myopathies. *Arthritis Res Ther* [Internet]. BioMed Central; 2009 Oct 26 [cited 2017 Nov 18];11(5):R159. Available from: <http://arthritis-research.biomedcentral.com/articles/10.1186/ar2841>.
8. Lydon C, Lowe T, Withers P, Herrick A, Brien PO, Winpenny R. Analysis and dissolution of SSC- related calcinosis. *Rheumatology* [Internet]. 2014;53(Suppl_1):149. Available from: <https://doi.org/10.1093/rheumatology/keu117.008>.
9. Colthup NB, Daly LH, Wiberley SE. Introduction to IR and Raman spectroscopy [Internet]. vol. 3rd Editio, Academic Press Inc. New York. 1990. Available from: <https://doi.org/10.1016/B978-0-12-182552-2.50004-8>.
10. Edwards HGM. Introduction to modern vibrational spectroscopy: by max diem. *Spectrochim Acta Part A Mol Spectrosc* [Internet]. 1993;50(14):2397–8. Available from: [https://doi.org/10.1016/0584-8539\(94\)80073-1](https://doi.org/10.1016/0584-8539(94)80073-1).
11. Baldet P, Pernot F, Blotman F, Bonnel F, Simon L. CRST syndrome. Ultrastructural and physico-chemical studies of calcifications (author's transl). *Ann Pathol* [Internet]. 1981 [cited 2017 Nov 18];1(4):259–69. Available from: <http://www.ncbi.nlm.nih.gov/pubmed/7317130>.
12. Mukamel M, Horev G, Mimouni M. New insight into calcinosis of juvenile dermatomyositis: A study of composition and treatment. *J Pediatr* [Internet]. 2001 [cited 2017 Nov 14];138(5):763–6. Available from: [http://www.jpeds.com/article/S0022-3476\(01\)76748-0/pdf](http://www.jpeds.com/article/S0022-3476(01)76748-0/pdf)

13. Osthoff M, Ngian GS, Dean MM, et al. Potential role of the lectin pathway of complement in the pathogenesis and disease manifestation of systemic sclerosis: a case inverted question mark control and cohort study. *Arthritis Res Ther.* 2014;16:480.
14. Avouac J, Mogavero G, Guerini H, Drape JL, Mathieu A, Kahan A, et al. Predictive factors of hand radiographic lesions in systemic sclerosis: a prospective study. *Ann Rheum Dis.* 2011;70:630–3.
15. Mouthon L, Mestre-Stanislas C, Berezne A, Rannou F, Tuilpain P, Revel M, et al. Impact of digital ulcers on disability and health related quality of life in systemic sclerosis. *Ann Rheum Dis.* 2010;69:214–7.
16. Johnstone EM, Hutchinson CE, Vail A et al. Acro-osteolysis in systemic sclerosis is associated with digital ischemia and severe calcinosis. *Rheumatology* [Internet]. 2012;51(12):2234–38. Available from: <https://doi.org/10.1016/B978-0-12-182552-2.50004-8>.
17. Vayssairat M, Hidouche D, Abdoucheli-Baudot N, Gaitz JP. Clinical significance of subcutaneous calcinosis in patients with systemic sclerosis. Does diltiazem induce its regression? *Ann Rheum Dis* [Internet]. 1998 [cited 2017 Nov 14];57:252–4. Available from: <http://ard.bmj.com/content/annrheumdis/57/4/252.full.pdf>
18. Davies CA, Jeziorska M, Freemont AJ, Herrick AL. Expression of osteonectin and matrix Gla protein in scleroderma patients with and without calcinosis. *Rheumatology* [Internet]. 2006 [cited 2017 Nov 3];45(11):1349–55. Available from: <https://doi.org/10.1093/rheumatology/kei277>.
19. Orriss IR, Arnett TRRR. Pyrophosphate: a key inhibitor of mineralisation. *Curr Opin Pharmacol.* 2016;28:57–68.
20. Russell RG, Casey PA FH. Simulation of phosphate excretion by the renal arterial infusion of 3'5'-AMP (cyclic AMP) – a possible mechanism of action of parathyroid hormone. *Calcif Tissue Res.* 1968;Suppl:54–54a.
21. O'Neil WC, Lomashvili KA, Maluche HH, et al. Treatment with pyrophosphate inhibits uremic vascular calcification. *Kidney Int.* 2011;79:512–7.
22. Villa-Belosta ROW. Pyrophosphate deficiency in vascular calcification. *Kidney Int.* 2018;93:1293–7.
23. O'Neil WC, Sigrist MKMC. Plasma pyrophosphate and vascular calcification in chronic kidney disease. *Nephro Dial Transpl.* 2010;25:187–91.
24. Lomashvili KA, Khawandi WOW. Reduced plasma pyrophosphate levels in haemodialysis patients. *J Am Soc Nephrol.* 2005;16:2495–500.
25. Jin HSHC, Huang Y, et al. Increased activity of TNAP compensates for reduced adenosine production and promotes ectopic calcification in the genetic disease ACDC. *Sci Signal.* 2016;9(ra):121.
26. Jansen RS, Duijst S, Mahakena S, et al. ABCC6- mediated ATP secretion by the liver is the main source of the mineralisation inhibitor inorganic pyrophosphate in the systemic circulation – brief report. *Arter Thromb Vasc Biol.* 2014;34:1985–9.
27. Jansen RS, Kucukosmanoglu A, de Haas M, et al. ABCC6 prevents ectopic mineralisation seen in pseudoxanthoma elasticum by inducing cellular nucleotide release. *Proc Natl Acad Sci USA.* 2013;110:20206–11.
28. Hessle L, Johnson KA, Anderson HC, et al. Tissue nonspecific alkaline phosphatase and plasma cell membrane glycoprotein-1 are central antagonistic regulators of bone mineralisation. *Proc Natl Acad Sci USA.* 2002;99:9445–9.
29. Bossini-Castillo L, Lopez-Isac E, Mayes MDMJ. Genetics of systemic sclerosis. *Semin Immunopathol.* 2015;37:443–51.
30. Joung CI, Jun JB, Chung WT, et al. Association between the HLA-DRB1 gene and clinical features of systemic sclerosis in Korea. *Scand J Rheumatol.* 2006;35(39–43):1040–8711.
31. Rech TF, Moraes SB, Bredemeier M, et al. Matrix metalloproteinase gene polymorphisms and susceptibility to systemic sclerosis. *Genet Mol Res.* 2016;15 <https://doi.org/10.4238/gmr15049077>.

32. Wallin R, Wajih N, Greenwood GTSD. Arterial calcification: a review of mechanisms, animal models, and the prospects for therapy. *Med Res Rev.* 2001;21:274–301.
33. Bartoli F, Fiori G, Braschi F, et al. Calcinosis in systemic sclerosis: subsets, distribution and complications. *Rheumatology.* 2016;55:1610–4.
34. Koutaissof S, Vanthuyne M, Smith V, et al. Hand radiological damage in systemic sclerosis: a comparison with a control group and clinical and functional correlations. *Semin Arthritis Rheum.* 2011;40:455–60.
35. Gauhar R, Wilkinson J, Harris J, Manning JHAL. Calcinosis preferentially affects the thumb compared to other fingers in patients with systemic sclerosis. *Scand J Rheumatol.* 2016;45:317–20.
36. Daoussis D, Antonopoulos I, Liossis SN, et al. Treatment of systemic sclerosis associated calcinosis: a case report of rituximab induced regression of CREST related calcinosis and review of the literature. *Semin Arthritis Rheum.* 2012;41:822–9.
37. Valenzuela A, Cuomo G, Sutton E et al. Frequency of calcinosis in a multicenter international cohort of patients with systemic sclerosis: a Scleroderma Clinical Trials Consortium Study (Abstract) in Proceedings of 13th International Workshop on Scleroderma Research, Boston, MA, USA, 2013.
38. Pai SHV. Are there risk factors for scleroderma-related calcinosis? *Mod Rheumatol.* 2018;28:518–22.
39. Valenzuela A, Baron M, Herrick AL, Proudman S, Stevens W, Rodriguez-Reyna TS, et al. Calcinosis is associated with digital ulcers and osteoporosis in patients with systemic sclerosis: a Scleroderma Clinical Trials Consortium study. *Semin Arthritis Rheum* [Internet]. 2016 [cited 2017 Nov 3];46(3):344–9. Available from: <https://doi.org/10.1016/j.semarthrit.2016.05.008>.
40. Steen VD, Ziegler GL, Rodnan GP, Medsger TA. Clinical and laboratory associations of anticentromere antibody in patients with progressive systemic sclerosis. *Arthritis Rheum* [Internet]. John Wiley & Sons, Inc.; 1984 Feb 1 [cited 2017 Nov 18];27(2):125–31. Available from: <http://doi.wiley.com/10.1002/art.1780270202>
41. D'Aoust J, Hudson M, Tatibouet S, et al. Clinical and serological correlates of anti-PM/Scl antibodies in systemic sclerosis: a multicenter study of 763 patients. *Arthritis Rheumatol.* 2014;66:1608–15.
42. Shahi V, Wetter DA, Howe BM, et al. Plain radiography is effective for the detection of calcinosis cutis occurring in association with autoimmune connective tissue disease. *Br J Dermatol.* 2014;170:1073–9.
43. Chung L, Valenzuela A, Firorentino D, et al. Validation of a novel radiographic scoring system for calcinosis affecting the hands of patients with systemic sclerosis. *Arthritis Care Res.* 2015;67:425–30.
44. Elhai M, Guerini H, Bazeli R, et al. Ultrasonographic hand features in systemic sclerosis and correlates with clinical, biologic, and radiographic findings. *Arthritis Care Res.* 2012;64:1244–9.
45. Freire V, Becce F, Feydy A, et al. MDCT imaging of calcinosis in systemic sclerosis. *Clin Radiol.* 2013;68:302–9.
46. Cuomo G, Zappia M, Abignano G, Iudici M, Rotondo AVG. Ultrasonographic features of the hand and wrist in systemic sclerosis. *Rheumatology.* 2009;48:1414–7.
47. Choi HK, Al-Arfaj AMEA. Dual energy computed tomography in tophaceous gout. *Ann Rheum Dis.* 2009;68:1609–12.
48. Hsu V, Bramwit MSN. Use of dual-energy computed for the evaluation of calcinosis in patients with systemic sclerosis. *Clin Rheumatol.* 2015;34:1557–61.
49. Dima A, Balanescu PBC. Pharmacological treatment in calcinosis cutis associated with connective tissue diseases. *Rom J Intern Med.* 2014;52:55–67.
50. Fuchs D, Fruchter L, Fishel B, Holtzman M, Yaron M. Colchicine suppression of local inflammation due to calcinosis in dermatomyositis and progressive systemic sclerosis. *Clin Rheumatol* [Internet]. 1986 Dec [cited 2017 Nov 13];5(4):527–30. Available from: <http://www.ncbi.nlm.nih.gov/pubmed/3816102>.

51. Robertson LP, Marshall RWHP. Treatment of cutaneous calcinosis in limited systemic sclerosis with minocycline. *Ann Rheum Dis.* 2003;62:267.
52. Palmieri GM, Sebes JI, Aelion JA, et al. Treatment of calcinosis with diltiazem. *Arthritis Rheumatol.* 1995;38:1646–54.
53. Dolan AL, Kassimos D, Gibson TKG. Diltiazem induces remission of calcinosis in scleroderma. *Br J Rheumatol.* 1995;34:576–8.
54. Farah MJ, Plamieri GMSJ, et al. The effect of diltiazem on calcinosis in a patient with CREST syndrome. *Arthritis Rheumatol.* 1990;33:1287–93.
55. Metzger AL, Singer FR, Bluestone RPC. Failure of disodium etidronate in calcinosis due to dermatomyositis and scleroderma. *N Engl J Med.* 1974;291:1294–6.
56. Rabens SFBJ. Disodium etidronate therapy for dystrophic cutaneous calcification. *Arch Dermatol.* 1975;111:357–61.
57. Fujii N, Hamano T, Isaka Y, et al. Risedronate: a possible treatment for extraosseous calcification. *Clin Calcium.* 2015;15:75–8.
58. Li Q, Sundberg JP, Levine MA, Terry SF, et al. The effects of bisphosphonates on ectopic soft tissue mineralization caused by mutation in the ABCC6 gene. *Cell Cycle.* 2015;14:1082–9.
59. Reiter N, El-Shabrawi L, Leinweber B, et al. Calcinosis cutis: part II. Treatment options. *J Am Acad Dermatol.* 2011;65:15–22.
60. Berger RG, Featherstone GL, Raasch RH, et al. Treatment of calcinosis universalis with low dose warfarin. *Am J Med.* 1987;83:72–6.
61. Lassoued K, Saiag P, Anglade MC, et al. Failure of warfarin in treatment of calcinosis universalis. *Am J Med.* 1988;84:795–6.
62. Penate Y, Guillermo N, Melwani P, et al. Calcinosis cutis associated with amyotrophic dermatomyositis: response to intravenous immunoglobulin. *J Am Acad Dermatol.* 2009;60:1076–7.
63. Toumy M, Janani S, Rachidi W, et al. Calcinosis universalis complicating juvenile dermatomyositis: improvement after intravenous immunoglobulin therapy. *Joint Bone Spine.* 2013;80:108–9.
64. Kalajian AH, Perryman JHCJ. Intravenous immunoglobulin therapy for calcinosis cutis: unreliable in our hands. *Arch Dermatol.* 2009;145:334.
65. Schanz S, Ulmer A, Fierlbeck G. Response of dystrophic calcification to intravenous immunoglobulin. *Arch Dermatol* [Internet]. American Medical Association; 2008 May 1 [cited 2017 Nov 12];144(5):585. Available from: <http://archderm.jamanetwork.com/article.aspx?doi=10.1001/archderm.144.5.585>.
66. Tosounidou S, MacDonald HSD. Successful treatment of calcinosis with infliximab in a patient with systemic sclerosis/myositis overlap syndrome. *Rheumatology.* 2014;53:960–1.
67. de Paula DR, Klem FB, Lorenzetti PG, et al. Rituximab induced regression of CREST related calcinosis. *Clin Rheumatol.* 2013;32:281–3.
68. Bottomley WW, Goodfield MJS-DR. Digital calcification in systemic sclerosis: effective treatment with good tissue preservation using the carbon dioxide laser. *Br J Dermatol.* 1996;135:302–4.
69. Chamberlain AJ, Walker NPJ. Successful palliation and significant remission of cutaneous calcinosis in CREST syndrome with carbon dioxide laser. *Dermatol Surg* [Internet]. 2003 Sep [cited 2017 Nov 13];29(9):968–70. Available from: <http://www.ncbi.nlm.nih.gov/pubmed/12930342>.
70. Sultan Bichat N, Menard J, Perceau G, et al. Treatment of calcinosis cutis by extracorporeal shock wave lithotripsy. *J Am Acad Dermatol.* 2012;66:424–9.
71. Saddic N, Miller JJ, Miller OF 3rd, Clarke JT. Surgical debridement of painful fingertip calcinosis cutis in CREST syndrome. *Arch Dermatol.* 2009;145:212–3.
72. Lapner MAGT. High speed burr debulking of digital calcinosis cutis in scleroderma patients. *J Hand Surg.* 2014;39:503–10.

Chapter 13

Placental Calcification: Long-standing Questions and New Biomedical Research Directions



Ana Correia-Branco, Sampada Kallol, Nimish Adhikari,
Carlo Donato Caiaffa, Nirmala Jayaraman, Olga Kashpur,
and Mary C. Wallingford

Introduction to the Placenta

The placenta is an essential organ that supports healthy pregnancy and fetal development. As an organ that mediates communication between two circulatory systems, it is a highly vascularized tissue that is paramount to supporting maternal cardiovascular health and fetal development during pregnancy. The placenta is an autonomous and temporary organ that forms *de novo* at the start of pregnancy. It is developed upon implantation of the blastocyst to the maternal endometrium, which initiates placentation. During placentation trophoblasts differentiate into several subtypes that mediate nutrient transport and gas exchange between mother and fetus. Cytotrophoblasts are the mononucleated cells that differentiate to form a multinucleated syncytiotrophoblast layer. This layer is in direct contact with the maternal circulation and serves as part of the functional unit of the placenta. Thus, the nutrients originating from the mother are delivered to the fetus via the syncytiotrophoblast layer.

A. Correia-Branco · N. Jayaraman · O. Kashpur · M. C. Wallingford (✉)
Mother Infant Research Institute, Tufts Medical Center, Boston, MA, USA
e-mail: okashpur@tuftsmedicalcenter.org; mwallingford@tuftsmedicalcenter.org

S. Kallol
Institute of Biochemistry and Molecular Medicine, University of Bern, Bern, Switzerland

N. Adhikari
Department of Computer Science, School of Arts and Sciences, Tufts University,
Medford, MA, USA
e-mail: Nimish.Adhikari@tufts.edu

C. D. Caiaffa
National Institute of Science and Technology for Regenerative Medicine,
Institute of Biophysics Carlos Chagas Filho, Federal University of Rio de Janeiro,
Rio de Janeiro, RJ, Brazil

Placental disease is associated with adverse maternal and fetal clinical outcomes including preeclampsia (PE), fetal growth restriction, preterm birth, and maternal and fetal loss of life [1–5]. Placental calcification is frequently observed in pregnancy, but its impact on acute diseases remains unclear. The consequences of placental abnormalities referring to gestational hypertension and placental abruption due to infarction (and/or calcification) are associated with pregnancy pathologies such as PE [6], [7]. PE is a complex and pregnancy-specific disorder characterized by hypertension and proteinuria after 20 weeks' gestation, which is thought to be caused by placental dysfunction, though the molecular etiology remains unclear [8]. It affects from 3% to 5% of pregnancies worldwide and is one of the leading causes of maternal and fetal morbidity and mortality [7, 9]. PE is a heterogeneous condition exhibiting a broad range of features, and hence the diagnosis is challenging. The standard features of PE are new-onset hypertension (defined as a systolic blood pressure, 140 mm Hg or more, or a diastolic blood pressure \rightarrow 90 mm Hg or more) and proteinuria (300 mg or higher in a 24 h urine specimen) [10]. The acute conditions of PE will be resolved by delivering the placenta, which is the only known treatment for this disease [9]. It is reported that women who have developed PE in pregnancy are at increased risk of cardiovascular disease, coronary artery calcification, stroke, and chronic kidney disease later life [11–15]. Considering these findings, one can speculate that the placental health may be an early indicator of maternal cardiovascular and renal disorders. Despite this major public health burden [16], the cause of placental dysfunction in preeclampsia remains poorly understood. No curative treatments are available besides inducing early placental delivery, which results in preterm birth, and early diagnostic indicators have not yet been identified. It remains unknown whether fetoplacental angioarchitectures and vascular pathologies, including ectopic vascular calcification, play a role in the etiology of some preeclampsia cases.

Placental Calcification and Maternal and Fetal Outcomes

Placental calcification is characterized by the deposition of calcium-phosphate minerals in placental tissue [17, 18]. Placental calcification is regarded as a physiological aging process, as human placenta is known to calcify with advancing gestational age, and is correlated with fetal maturity [19]. A clear exception to this is the pathological association between calcification and viral infection which has been elegantly discussed in recent publications [20–22]. Overall, clinical research on the association between placental calcification and clinical outcomes is limited, the etiology of placental calcification remains undefined, and the clinical significance of placental calcification appears to be controversial [23, 24]. This gap in knowledge has been emphasized in recent reviews, which suggest that an early appearance of placental calcification and assessment of distinct tissue-specific microcalcification patterns may provide a valuable tool for identification of placental pathologies and high-risk cases of adverse pregnancy outcomes [23–25].

Calcification has also been reported in association with clinical pathologies. Placental calcification and sub-chorionic fibrin deposition, placental ischemia, infarction, fibrinoid necrosis, and stromal fibrosis were associated with low birth weight infants [26]. A study that examined 50 pregnancy-induced hypertension (PIH) placentas and 50 placentas from normotensive mothers verified an increase in placental calcification, number of syncytial knots, areas of fibrinoid necrosis, and hyalinization in PIH placentas [27]. Concurrently, pregnancy-induced hypertension has been correlated with placental pathologies, including syncytial knots, fibrinoid necrosis, vasculosyncytial membrane formation, sclerosis, chorangiosis, and placental calcification [28].

While some groups have suggested that placental calcification has no clinical and no pathological significance [29], several others have determined that identification of grade III placental calcification is an indicator of increased risk for adverse pregnancy outcomes [24, 25, 30, 31]. Indeed, the early identification of grade III placental calcification before 36 weeks' gestation (preterm placental calcification) has been associated with pregnancy-induced hypertension and fetal growth restriction [32] and often prompts cesarean delivery [24, 30]. Furthermore, the prevalence of preterm placental calcification has been reported to range widely from 3.8% [32] to 23.7% [33]. This discordance in study findings may relate in part to regional population differences, study design, or the grading system by which calcium deposits are typically assessed and documented. With respect to differences relating to race or ethnicity, a study that included 32,295 African-American and Caucasian women showed that African-American women had a lower prevalence of placental calcification [34].

Placental calcification results in an echogenic foci that can be observed noninvasively by ultrasonography examination [17, 18, 35]. The Grannum classification system can be used to grade placenta ultrasounds into one of four categories according to specific mineral findings at the basal and chorionic plates as well as the placenta itself (Fig. 13.1). This Grannum system was developed in 1979 [36] and has been used in most studies that evaluate the relationship between placental calcification and clinical outcomes. Under the Grannum classification, grade 0 placentas display homogenous texture and uniform echogenicity, with minimal mineral deposition and a smooth chorionic plate, whereas grade III placentas are marked by abundant basal calcifications and characterized by significant chorionic plate interruption by echogenic indentations or ring-like structures resembling cotyledons that reach up to the basal plate [23, 36]. The Grannum system for grading placental tissue does not account for the tissue-specific microcalcification patterns that have been documented in other studies [25, 37].

While varying widely in study design, cohort characteristics, and findings and being limited by a crude grading system, several strong associations between placental calcification and delivery outcomes have been made. An early study of 2000 pregnant women identified an association between grade III placental calcification and the risk of low birth weight, poor condition at birth, and perinatal death [38]. An alternate study supported an association between grade II placental calcification and lower birth weight and grade III with growth retardation, but neither correlated with poor perinatal

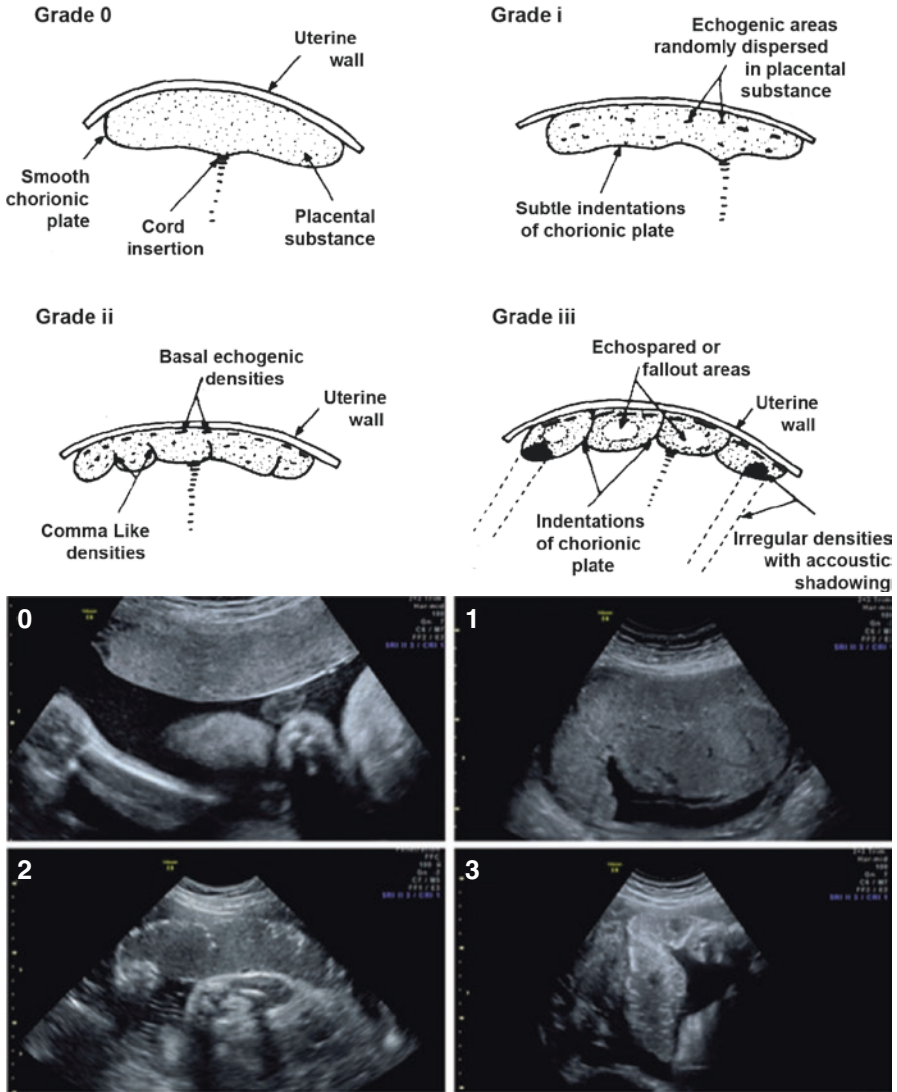


Fig. 13.1 The Grannum system of placental grading. The Grannum system for placental grading defines four grades. Grade 0 placentas lack echogenic foci, grade 1 placentas are characterized by randomly dispersed echogenic foci in the placenta, grade 2 placentas contain significant basal echogenic densities, and grade 3 are the most highly calcified placentas with chorionic plate indentations, acoustic shadowing, and echospared fallout regions (Images published with permission from Grannum et al. 1979 [36] and Mastroliola et al. 2016 [23])

outcome, maternal hypertension, fetal distress, or perinatal asphyxia [39]. In contrast, Miller et al. evaluated 246 placentas and found a grade III incidence of 39.4% and no association with altered fetal growth or birth weight [40]. Moreover, Vosmar et al. found no association between grade III and fetal growth restriction at term and a positive correlation between growth retardation and grade III detected prior to 36 weeks [41].

Poor fetal health has been associated with grade III placentas in several high-powered studies. Two studies by Chen et al. that included 776 and 889 low-risk pregnancies, respectively, found that the presence of preterm grade III placental calcification is a predictor of poor uteroplacental flow and adverse maternal and fetal outcomes including preterm birth low birth weight, low Apgar score, and neonatal death [30, 31]. A study of 15,122 pregnancies determined that the grade III preterm placental calcification is associated with increased risk factor of third-trimester stillbirth [42]. A study of 802 low-risk pregnancies observed an association of grade III placental calcification at 36 weeks' gestation with proteinuric pregnancy-induced hypertension and fetal growth restriction [32]. A study by Jamal et al. that enrolled 293 pregnancies demonstrated that preterm placental calcification is associated with abnormal placental and umbilical Doppler waveforms, low birth weight, and caesarean section deliveries and found that passive smoking was the only predictor of preterm placental calcification [43]. In contrast to these studies, a recent meta-analysis supports a positive association between grade III preterm placental calcification and labor induction, but not fetal distress, Apgar score, neonatal resuscitation, nor neonatal intensive care unit admission [24].

The conflicting conclusions drawn from these studies may relate to several aspects: poor ultrasound resolution in older scans; the limiting nature of Grannum grading, which does not distinguish cell type-specific calcification patterns; variance in clinical practices and protocols; population characteristics and sample size; low-risk and high-risk pregnancies; gestation day of the scan; and confounders such as cigarette smoking or alcohol consumption. In agreement with these conclusions, two studies have identified poor intraobserver agreement in grading placentae according to Grannum grades even among experienced observers despite standardized viewing conditions [44, 45]. Future studies with larger and more diverse cohorts are likely to shed new light on the biomedical significance of placental calcification.

Overall, these studies suggest that early detection of placental calcification is recognized to be associated with high-risk clinical outcomes in pregnancy. Highly calcified grade III placentas often promote early delivery and have been associated with a higher risk of adverse pregnancy outcome [24, 30]. Placental calcification usually increases with progressing gestational age and becomes apparent at 36 weeks' gestation, which is considered as preterm placental calcification [23]. Some of the studies showed that preterm placental calcification may be associated with maternal and fetal complications, such as intrauterine growth restriction (IUGR) [33, 39, 46–48], low birth weight [33, 38, 39, 46, 47, 49], low Apgar score [38], fetal distress [33], and pregnancy-induced hypertension [33, 47, 48, 50]. The exact mechanism for deposition of calcium in the placenta and its impact on fetal and maternal health remains unclear. In fact, placental dysfunction and the magnitude of these alterations may be keys to identify pregnancies at risk and to direct novel therapeutic

strategies to prevent it [51]. Moreover, exploration of cell type-specific calcification, their location, mineral structure, and nodule size and temporal analysis across gestation are required to determine mechanisms of calcification onset and progression and to distinguish which mineral profiles are pathologic in cases of placental dysfunction and high-risk pregnancies. This could potentiate the development of new biomedical tools for assessment, screening, and diagnosis of placental calcification to predict high-risk clinical outcomes in pregnancy.

Observed Mineral Deposition Patterns in Human Placenta

Mineral deposits in the placenta are composed of calcium and phosphate [17, 18]. In the placenta, mineral is arranged predominantly near the basement membrane, concordant to the site where both phosphate and calcium transporters reside and have been suggested to assist in the import of calcium and phosphate from the maternal circulation [52]. Accordingly, calcified lesions have been detected by the calcium stain Alizarin Red in terminal villi and surrounding basement membrane-containing nodules [53]. Alterations of placental phosphate or calcium transporters may underlie some placental calcification pathologies. In support of this, animal model studies have identified *Slc20a2* as the first genetic link to placental calcification. Wallingford et al. propose an evaluation of the association between type III phosphate transporter *Slc20a2* expression, placental calcification, and placental dysfunction in high-risk pregnancies, such as preeclampsia [53]. In accordance, reduced expression of *Slc20a2* has been observed in severe early preeclampsia [54]. Preeclampsia has also been associated with calcified tissue, fibrinoid necrosis of the vascular wall, lipid-loaded endothelial cells, diffuse trophoblastic hypertrophy, microinfarctions, fibrin deposits, vascular-syncytial, membrane surface reduction, and basement membrane thickening in a small cohort of 13 preeclamptic and 22 normotensive cases [55].

Placental calcification deposits on the basal plate have been associated with maternal floor infarction [56] as well as fetal growth restriction and mid-trimester loss [57]. A study by Zeng et al. (2017) identified a fine placental calcification that is typically located at the basement membrane of chorionic villi and can only be seen microscopically, termed the intravillous and intrafibrinous particulate microcalcification (IPMC) [37]. These particulates were predominantly located in the basement membranes of fibrotic chorionic villi and in perivillous fibrin. Compared to placentas without adverse outcomes, a higher incidence of IPMC was seen in intrauterine fetal demise cases [37].

Calcium and Phosphate Homeostasis in Pregnancy

An increased mobilization of minerals and altered mineral metabolism during pregnancy enables the unidirectional transport of these minerals across the maternal-fetal interface, the bulk of which occurs during the third trimester as skeletal

ossification progresses. In the nonpregnant state, the kidneys, intestines, and skeletal system play dominant roles in the maintenance of mineral homeostasis through interaction with several regulatory hormones including parathyroid hormone, fibroblast growth factor-23 (FGF23), calcitonin, vitamin D, and the sex steroids estradiol and testosterone. It remains largely unknown whether these factors or others regulate placental mineral transport and/or placental calcification. As discussed in other chapters, dyshomeostasis of these pathways leads to ectopic calcification and in many cases is associated with disease-associated ectopic vascular calcification. Animal models have been used to evaluate the impact of Fgf23 and PTH levels on placental function and fetal growth, concluding that the placenta may harbor unique regulatory mechanisms [58, 59]. The relationship between mineral homeostasis and ectopic placental calcification may come to light as our knowledge of placental mineral transport mechanisms advances and as placental calcification analyses, methods, and depth of study improve.

In pregnancy, the placenta meets the fetal need for mineral by actively transporting calcium, phosphorus, and magnesium from the maternal circulation to the fetus where they are accreted in the fetal skeleton before birth [60] (Fig. 13.2). Transport of minerals from the maternal circulation is supported by significant hormonal adaptations during pregnancy that mobilize minerals, such as decoupling of the bone resorption and bone formation rates that normally maintain homeostatic bone turnover [61]. The total net accumulation of calcium in a full-term fetus is about

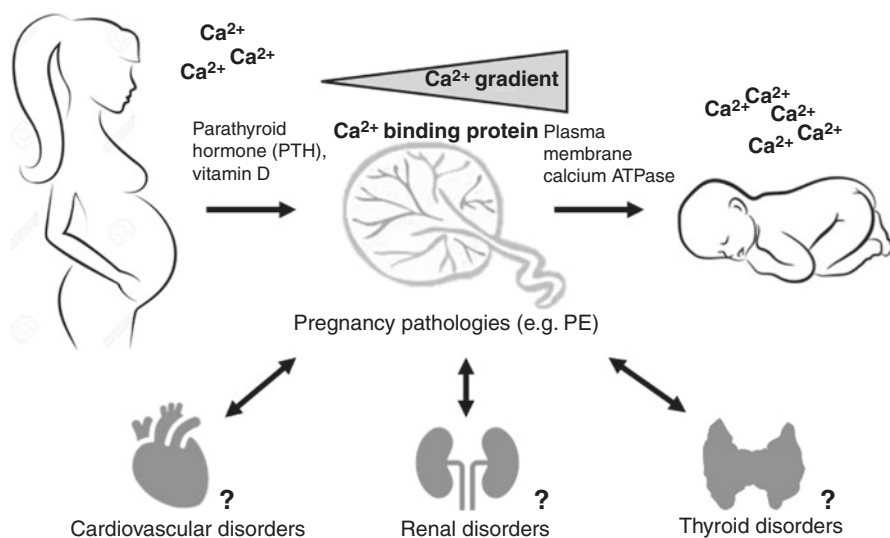


Fig. 13.2 Mineral homeostasis and transport and ectopic calcification in pregnancy and interaction of predisposing, coexisting, or resulting diseases. Transport of calcium from the maternal circulation to the fetal circulation occurs via carrier proteins located in the placenta. The calcium-phosphate homeostasis is regulated by the interaction of parathyroid hormones, vitamin D, calcium-binding protein, and plasma membrane calcium ATPases. The deposition of calcium in the placenta and its impact on pregnancy pathologies as well as its association with cardiovascular, renal, and thyroid disorders in maternal/fetal development are largely unknown

30 g [62–64], phosphorous is 20 g [65, 66] and magnesium is 0.8 g [62, 65, 66]. In late gestation, the placenta transports large amounts of calcium and phosphate to allow rapid fetal skeletal mineralization. The maternal-fetal transfer of calcium and phosphate uses an active transcellular transport mechanism that overcomes a concentration gradient across the placenta. This active transcellular transport mechanism occurs through the syncytiotrophoblast that cover the surface of villi and faces the intervillous space filled with maternal blood.

In the case of calcium, the transcellular transport of calcium across the placenta occurs in three steps. First, calcium is transported from the maternal circulation down an electrochemical gradient into the syncytiotrophoblasts through the epithelium calcium channel transient receptor potential vanilloid type 6, TRPV6, which is located on the maternal-facing microvillous (apical) membrane [67–69]. Second, after buffering with calcium-binding proteins such as calbindin-D9K in the trophoblast cytosol, it is delivered to the fetal-facing basal membrane. Finally, the calcium is effluxed across the basal membrane against the electrochemical gradient mediated by the plasma membrane calcium ATPase (PMCA) [70].

It has been reported that the fetal serum has higher concentration of phosphate than maternal serum as transport efflux is against a concentration gradient suggesting active transport of phosphate [71, 72]. It is also facilitated transport via transport proteins. Placental phosphate transport is regulated by parathyroid hormone, pH, and sodium availability [73–75]. In mammals, sodium-dependent phosphate symporters are categorized in three families: the type I, type II, and type III sodium-dependent phosphate transport families. Type I (SLC17) belong to the major facilitator family (MFS), and some family members transport anions in addition to phosphate. The type II sodium-dependent family (SLC34) members exclusively transport divalent $\text{HPO}_4(4)(2-)$, whereas the type III family members (SLC20) transport monovalent $\text{H}_2\text{PO}_4(4)(-)$ [76]. Recent studies have shown that phosphate from maternal circulation is transported by SLC20A1 and SLC20A2. Both SLC20A1 and SLC20A2 are expressed in human placenta [77], and altered expression of SLC20A1 and SLC20A2 is associated with placental dysfunction and pre-eclampsia (PE) [54]. Ohata et al. demonstrated that SLC34A2 is also expressed in the placenta, and its expression increases with the gestational age, whereas SLC34A1 and SLC34A3 gene expression was increased in late gestation, with very less expression compared to SLC34A2 [58]. Out of all of the sodium-dependent transporters, only Slc20a1, Slc20a2, and Slc34a2 result in subviability or embryonic lethality when ablated from the mouse genome.

Although serum phosphate and phosphate transporters both regulate ectopic calcification mechanisms, there are numerous other active and passive calcification pathways and candidate regulators, including PTH. In nonpregnant individuals, hormonal dysregulation leading to loss of mineral homeostasis can present significant consequences such as hypoparathyroidism, hyperphosphatemia (leading to ectopic calcifications), hypercalciuria (leading to nephrolithiasis and nephrocalcinosis), and low bone turnover. Vitamin D deficiency can lead to reduced calcium and phosphorus levels in serum (but not as low as in hypoparathyroidism) and rickets or osteomalacia [78]. The reduced activity of FGF23 results in hyperphosphatemia,

extraskeletal calcifications, and early mortality. Loss of calcitonin increases bone resorption, which is most apparent during lactation. The dysregulation of sex steroids increases bone resorption and may lead to osteoporosis. In pregnancy, creatinine clearance and glomerular filtration rate [79, 80] are increased during pregnancy. Other investigators have shown that PE and pregnancy-induced hypertension have been associated with hypocalciuria [81–85]. Further studies have found hypocalciuria to be associated with low 1,25-dihydroxyvitamin D levels [81–84], but independent of PTH, calcitonin, or ionized calcium levels [82–85]. The abnormalities in 1,25-dihydroxyvitamin D and urine calcium excretion are, therefore, probably secondary to a primary renal tubular defect occurring in PE and pregnancy-induced hypertension and are likely not the primary cause of the hypertension [83].

Indeed, it remains poorly understood how predisposing or coexisting conditions of the heart, kidney, or thyroid interact with mineral homeostasis, placental transport, and ectopic calcification mechanisms during pregnancy (Fig. 13.2). Maternal hypoparathyroidism in human pregnancy has been associated with the development of intrauterine fetal hyperparathyroidism [86–90], which is associated with spontaneous abortion, stillbirth, and neonatal death [91]. Moreover, placental dysfunction (specifically PE) may influence kidney damage and increase risk for chronic kidney disease, and indeed, prior PE is a risk factor for chronic kidney disease [14]. A direct assessment to delineate the association of placental calcification and PE and its impact on cardiovascular disease and renal and thyroid disorders is lacking from the literature. Furthermore, the direct link between serum calcium, phosphorous, and magnesium levels and transporter expression in the placenta and their role in the placental calcification remains to be elucidated. Overall, the molecular hallmarks of placental calcification are unclear. Further investigations are warranted to understand the underlying mechanism of placental calcification, its association with pregnancy pathologies such as PE and IUGR, and its impact on maternal and/or offspring health in later life.

Lessons from Animal Model Development Studies

The laboratory mouse (*Mus musculus*) is a tractable model that is amenable to genetic manipulation and as such is a useful model system for investigating mammalian placental development and function. The recently identified *Slc20a2* mouse is the first available model of ectopic placental calcification and currently remains the only available model [53]. However, the genetic link between *Slc20a2* and placental calcification argues that other models may have been overlooked and pro-calcific and anti-calcific gene knockout mice should be examined. Although placental mineralization phenotypes have not yet been reported for genetic models with the exception of *Slc20a2*, there is an immense body of developmental studies, which report on embryonic growth and development phenotypes and in some cases report expression or localization in mouse placenta. In the following paragraphs, we review the comparative anatomy of mouse and human placenta and summarize the

clinical and developmental studies for a subset of pro-calcific and anti-calcific factors that are good candidates for evaluation in placental pathologies.

In order to evaluate potential translation of mouse model findings to biology of the human placenta, there are a number of similarities and differences between human and mouse placentae that should be understood. Both human and mouse placentae are discoid in shape. Both have hemochorial maternal-fetal exchange interfaces, which are anatomically defined by direct interaction of the maternal circulation with trophoblasts, unique epithelial cells that develop from an extraembryonic structure termed the chorion. The fetal circulation in both human and mouse fetal blood interacts directly with placental endothelial cells that are also of extraembryonic origin arising from a transient embryonic structure termed the allantois. Finally, in both species, trophoblasts invade the maternal compartment of the placenta and remodel maternal spiral arteries, but to varying degrees. There are ~7000 placental orthologs expressed in both species. Of the genes known to cause placental phenotypes, 80% are common to both species [92]. Thus, the anatomical and genetic similarities coupled with the scope of available genetic tools together identify the mouse as a good candidate model organism to study placental calcification mechanisms.

There are however multiple differences between mouse and human placenta that should be accounted for when interpreting findings. These differences include cellular composition, structural differences in the maternal-fetal interface, and developmental rates. The cellular composition in mouse placenta includes trophoblast giant cells that border decidua, glycogen trophoblast cells, spongiotrophoblasts of the junctional zone, and multiple trophoblast cell types in the labyrinth – sinusoidal trophoblast giant cells, syncytiotrophoblast I, and syncytiotrophoblast II. Human placenta contains cytotrophoblasts that give rise to villous and extravillous trophoblasts during development, villous trophoblasts that fuse and form syncytiotrophoblast, and extravillous trophoblasts (EVT) that are defined by the expression of HLA-G and can be further subdivided into invading interstitial EVTs, endovascular EVTs that remodels spiral arteries, and endoglandular EVTs. Mouse placenta contains a labyrinthine interface with a trilaminar trophoblast layer, whereas the human placenta interface is a chorionic villi structure that contains one trophoblast monolayer termed the syncytiotrophoblast, which is replenished by an underlying noncontiguous cytotrophoblast layer. Outside of the maternal-fetal interface, other trophoblast subtypes termed extravillous and endovascular trophoblasts invade the decidua and uterine arteries. This invasion is much less extensive in mouse and is better modeled with the rat. Finally, the rate of development in relation to gestational length is in sharp contrast. Human gestation is 37–42 weeks, and the placenta is fully formed by 18–20 weeks [93], whereas mouse gestation is 18–21 days, and the placenta is fully formed by embryonic day (E) 12.5 [93].

Molecular Biology of Calcification in the Placenta

Numerous pro- and anti-calcific proteins that have been associated with calcification in both development and disease contexts are detected in a spatiotemporally specific manner as reported in the Human Placenta Atlas available from <http://www.proteinatlas.org> [94], the mouse placental transcriptome [95], and primary research articles (Table 13.1). Some of these candidate genes display altered expression in placental disease, and the deletion of most results in embryonic lethality, yet placental phenotypes remain unanalyzed for most knockout lines (Table 13.1). Among these, candidate pro-calcific placental proteins include members of multiple signaling pathways and, in effect, multiple types of proteins, including membrane proteins such as α Klotho and alkaline phosphatase, secreted factors such as Adm, BMPs, and MMPs, and transcription factors such as Runx2 and Sp7.

Table 13.1 Candidate regulatory calcification molecules in human and mouse placenta

Type	Gene	Alternate title (OMIM)	HPA RNA (pTEM)	FANTOM5 RNA (STM)	Mouse placenta expression	KO lethal stage
Pro	Adm	Adreno-medullin	192.2	756.6	TS11: ectoplacental cone; RNA-seq Hs, Mm [94–96]	Embryonic lethality, ~E13.5, abnormal placenta [97]
Anti	Ahsg	Fetuin A	0.2	0	RNA-seq Mm [95]	ND
Pro	Alpp	Plap; Palp	56	1666.7	RNA-seq Hs [94]	Embryonic lethality, ~E3.5 [98]
Anti	Ankh	Hank	14.5	15.4	RNA-seq Hs [94]	ND
Pro	Atf4	Cyclic Amp response element-binding protein 2; Creb2	423.6	404.6	RNA-seq Hs, Mm [94, 95]	Rmbryonic lethality prior to tooth bud stage, ~E12.5 [99]
Anti	Axl	Axl transforming gene	59.5	95	TS28: placenta, RNA-seq Hs, Mm [94, 95]	ND
Pro	Bglap	Bone Gla protein; osteocalcin	0.8	2.8	not determined	ND

(continued)

Table 13.1 (continued)

Type	Gene	Alternate title (OMIM)	HPA RNA (pTEM)	FANTOM5 RNA (STM)	Mouse placenta expression	KO lethal stage
Pro	Bmp2	Bone morphogenetic protein 2a; Bmp2a	19.7	2.7	TS17: chorioallantoic placenta, RNA-seq Hs [94, 95, 100, 101]	Embryonic lethality, complete penetrance, ~E8.0 [102]
Pro	Bmp4	Bone morphogenetic protein 2b; Bmp2b	77.9	13	TS17: chorioallantoic placenta, RNA-seq Hs, Mm [94, 95, 100]	Embryonic lethality, complete penetrance, ~E6.5 [103]
Anti	Bmp7	Osteogenic protein 1; Op1	44.8	50.4	RNA-seq Hs [94]	Prewaning lethality, complete penetrance, P1 [104]
Anti	Chrd	Chordin	4.2	3.4	TS15: ectoplacental cone, RNA-seq Hs, Mm [94, 95, 105]	Embryo turning, ~E8.5 [106]
Anti	Enpp1	Alkaline phosphodiesterase 1	76.8	63.7	RNA-seq Hs [94]	ND
Pro	Fgf23	Fibroblast growth factor 23	0.4	0	ND	ND
Anti	Gas6	Axl stimulatory factor; Axsf	91.7	58.8	RNA-seq Hs, Mm [94, 95]	ND
Anti	Grp	Gastrin-releasing polypeptide	0	0	ND	ND
Pro	K1	Alpha-Klotho	53.8	57	RNA-seq Hs [94]	ND
Anti	Mgp	Matrix gla protein; Mglap	350.3	319.2	RNA-seq Hs, Mm [94, 95, 105]	ND
Pro	Mmp13	Collagenase 3; Clg3	0	0	ND	ND

Table 13.1 (continued)

Type	Gene	Alternate title (OMIM)	HPA RNA (pTEM)	FANTOM5 RNA (STM)	Mouse placenta expression	KO lethal stage
Pro	Mmp9	Collagenase type V	3.5	12.7	TS11: ectoplacental cone, RNA-seq Hs [94, 107]	Not lethal
Anti	Msx2	Muscle segment homeobox, Drosophila, Homolog Of, 2; Msx2	57.7	76.3	RNA-seq Hs, Mm [94, 95]	ND
Anti	Nog	Mouse, Homolog Of; Nog	19.3	45.2	TS15: ectoplacental cone, RNA-seq Hs, Mm [94, 95]	Birth [108]
Pro	Pgf	Plgf	86.9	438.9	TS28: placenta, RNA-seq Hs [94, 109]	Not lethal, decreased placenta weight
Pro	Phospho1	Phosphoethanolamine/phosphocholine phosphatase 1	12.1	16.8	RNA-seq Hs, Mm [94, 95]	ND
Pro	Runx2	Core-binding factor, runt domain, alpha subunit 1; Cbfa1	2.7	4.2	RNA-seq Hs [94]	Birth [110]
Pro	Slc20a1	Pit1	49.5	343.7	RNA-seq Hs, Mm [94, 95]	Embryonic lethality during organogenesis, ~E12.5, pale placenta [111]
Pro	Slc20a2	Pit2	23.7	46.3	RNA-seq Hs, Mm [94, 95]	Prewaning lethality, incomplete penetrance, ectopic calcification [99]

(continued)

Table 13.1 (continued)

Type	Gene	Alternate title (OMIM)	HPA RNA (pTEM)	FANTOM5 RNA (STM)	Mouse placenta expression	KO lethal stage
Pro	Sox9	Testis-specific enhancer of Sox9	1.7	4.9	TS11: ectoplacental cone, RNA-seq Mm [95, 112]	Embryonic lethality, complete penetrance, ~E17.5 [113]
Pro	Sp7	Osterix; Osx	0	0	ND	Neonatal lethality, complete penetrance, P1 [114]
Pro	Spp1	Osteopontin; Opn	4918.4	1560.8	TS28: placenta, RNA-seq Hs [94, 115, 116]	Abnormal EPC
Pro	Tnap	Alkaline phosphatase, tissue-nonspecific	5.3	2.3	ND	Postnatal lethality, complete penetrance, P14 [117]
Pro	Tnf	Tumor necrosis factor, alpha; Tnfa	0.1	7.1	TS28: placenta [118, 119, 120]	ND
Pro	Tnfrsf-11b	Osteoprotegerin; Opg	6.9	10	TS28: placenta, RNA-seq Hs, Mm [94, 95, 120]	Postnatal lethality, incomplete penetrance, >P63 (6 months) [121]

HPA human placenta atlas, *pTEM* transcripts per million, *FANTOM5* functional annotation of mammalian genomes 5, *STM* standardized tags per million, *ND* not determined, *NA* not applicable, *TS* Theiler stage, *E* embryonic day, *EPC* ectoplacental cone

Pro-calcific Transmembrane Proteins

Alpha-Klotho (α Klotho) is a transmembrane protein that is involved in the maintenance of cellular calcium homeostasis and may play a role in regulating transfer of phosphate and calcium across the placenta [122]. It is detected in plasma as well as in syncytiotrophoblasts and endothelial cells of the maternal-fetal interface [123]. Low levels of α Klotho during pregnancy have been suggested to disrupt homeostatic balance resulting in calcified lesions along the umbilical cord and altered cord blood levels [122]. Even under normal conditions, α Klotho is found at higher concentrations in the blood of pregnant women compared to nonpregnant women [124].

Tissue-nonspecific alkaline phosphatase (Tnap), encoded by the *Alpl* gene, has been detected on both the maternal and fetal sides of the placenta and has been localized to both syncytiotrophoblasts and cytotrophoblasts [125–127]. Extensive *in vitro* and mouse model studies have demonstrated that Tnap has a positive association with vascular calcification, but this relationship has not yet been examined in the context of pregnancy [128, 129]. Importantly, placental alkaline phosphatase has been detected at higher concentrations in pregnant women with preeclampsia than in women with uncomplicated pregnancies [127], and human *in vitro* fertilization studies support that the placenta-specific alkaline phosphatase *Alpp* plays an essential role in embryo fertilization and implantation [130]. Both α Klotho and alkaline phosphatase are promising candidates for the regulation of maternal-fetal mineral transport and protection against calcification, but their roles in these processes remain incompletely understood.

Secreted Pro-calcific Factors

Secreted proteins such as growth factors (BMPs), signaling peptides (Adm and Bglap), and matrix metalloproteases (MMP9 and MMP13) have been studied for their role in both physiological and disease-associated calcification. Adrenomedullin (Adm) encodes both adrenomedullin and proadrenomedullin which are peptides produced by post-translational modifications that are released by the endothelium and have vasodilative effects on blood circulation [131, 132]. Adm is highly expressed in the placenta and in vascular endothelial cells. Adm and Endothelin-1 act in a negative feedback loop in rat follicles and corpora lutea in which Adm decreases Endothelin-1 levels and Endothelin-1 increases Adm levels [133]. During embryonic development, Adm is also expressed in trophoblast giant cells, decidua, yolk sac, ectoplacental cavity, and the embryo [96]. Adrenomedullin knockout mice are lethal at midgestation presenting hydrops fetalis and cardiovascular abnormalities, including hyperplastic ventricular trabeculae and underdeveloped arterial walls [134]. Adm ablation during embryo development induces trophoblast apoptosis at the maternal-fetal interface and reduced branching of the labyrinth vessels indicating a critical function of fetal Adm in the maternal adaptation to

pregnancy [135]. In accordance with the animal model phenotypes, Adm may also serve a role in the development of preeclampsia in pregnant women through regulation of the invasive potential of trophoblasts [136, 137], but its role in placental calcification is unexplored.

Bone gamma-carboxyglutamate protein (Bglap), also known as osteocalcin (OCN), is a small molecule secreted by osteoblasts. The gamma carboxyglutamate (Gla) domain is important for bone matrix mineralization being responsible for binding calcium and hydroxyapatite [138]. During skeletal development, Bglap expression is regulated by Bmp7 and is detected in cells of the osteoblast lineage during mesenchymal condensations [139]. Bglap is also induced by both TGF β and VEGFC stimulation in SG2 cells, suggesting that these pathways, which are also present in the placenta can regulate mesenchymal commitment to osteoblastic phenotypes [140]. Its effect on placental calcification is uninvestigated.

Bone morphogenetic proteins such as Bmp2 are members of the TGF β superfamily and can bind TGF β receptors to participate in many biological processes including mesoderm development, heart development, skeletal development, and axis formation. BMPs have been well characterized by their ability to induce ectopic bone formation when exogenously implanted in muscular tissue *in vivo* [141]. BMPs can also stimulate osteoblast differentiation from mesenchymal cells and induce osteocalcin and alkaline phosphatase expression [142]. The Bmp2 gene encodes a preproprotein containing two subunits that are linked by a disulfide bond after post-translational modification [143]. In mice, Bmp2 expression can be detected at the cartilaginous primordia during skeletal development of limbs and ribs, at cardiac valves, and at the ventricular-atrial cushioning during heart development [144]. Bmp2 expression is also correlated with embryo implantation in mice [145]. Both *in vivo* conditional knockout and *in vitro* studies support that Bmp2 is essential for endometrial decidualization and fertility in mice and humans [146]. In humans Bmp2 is detected in primary human extravillous trophoblasts during implantation and early placentation [147] and has been suggested to play a role in decidualization [148]. Similar to MMP findings, Bmp2 acts to promote trophoblast cell invasion during development potentially through production of the adhesion molecule N-Cadherin that may modulate epithelial-mesenchymal transition during spiral artery remodeling [146].

Bmp4 plays essential roles in mesoderm induction, bone and limb formation, heart development, tooth development, and fracture repair [149], although Bmp4 is a weaker inducer of osteogenic markers compared to Bmp2 [150]. Homozygous null mice for Bmp4 die with little or no mesoderm. Specifically knocking out Bmp4 at later stages has induced abnormalities during ventricle septation, atrioventricular cushioning [151], outflow tract septation [152], and craniofacial development [153]. In humans Bmp4 is found on the maternal side of human placenta, and its role in trophoblast cell development has been studied to consider its role in cell signaling during complications in pregnancy, but the role of Bmp4 in development of preeclampsia remains poorly understood [154–157]. *In vitro*, when self-renewal is blocked, Bmp4 has been shown to induce differentiation of human pluripotent cells into trophoblast [154].

Bmp7 is a secreted ligand belonging to the TGF β superfamily of proteins that can regulate gene expression by binding TGF β receptors. This signaling mechanism recruits and activates members of the Smad family of transcription factors. This protein induces ectopic bone formation and may promote fracture healing in human patients. Mechanisms for this were evaluated through an assay that measured the ability of BMPs to induce osteogenic transformation in a panel of cell lines. BMP7 was able to induce alkaline phosphatase (Alp), osteocalcin (Bglap), and matrix mineralization in mesenchymal stem cells; however, Bmp7 was a weaker inducer than Bmp2, Bmp6, and Bmp9 [150]. Bmp7-null embryos present postnatal lethality and do not survive more than 10 days; their phenotype is defined by severe ocular defects and kidney defects [158]. In humans Bmp7 localizes to the fetal side of the placenta, and its expression has been correlated with calcification [159].

The placental growth factor (Pgf) is homologous to the vascular endothelial growth factor gene and can regulate angiogenesis via selective binding to Vegfr1 [160–162]. Pgf can also upregulate the potent vasoconstrictor Endothelin-1 in a PAX5-dependent manner [163]. Pgf knockout mice develop a placental phenotype presenting with an enlarged junctional zone and reduced labyrinth. Double knockout mice for both Pgf and catechol-O-methyltransferase (Comt) results in an increase in the placental glycogen content and a reduction of maternal blood pressure, consistent with a role of Pgf in the development of preeclampsia [164]. However Pgf can also increase the levels of uteroplacental Mmp2 and Mmp9 potentially providing a route to amelioration of hypertension and intrauterine growth restriction in preeclampsia [165]. In human placenta, Pgf localizes to the syncytiotrophoblast layer [166], and this immunoreactivity is decreased in preeclamptic pregnancies [167]. Pgf has also been observed on the fetal side of the placenta in pregnancies complicated by fetal growth restriction [168].

The metalloproteinases Mmp9 and Mmp13 have both been detected in human placenta [167]. Mmp9 protein localizes to the placental bed, decidua, and villous trophoblast in human placenta [169]. Mmp13 localizes to maternal first trimester fibroblasts [170]. These molecules are secreted zinc metalloproteases that break down type I, III, IV and V collagens in the extracellular matrix [171]. Mmp9 extracellular matrix degradation activity improves extravillous trophoblast invasiveness [172]. Demethylation of the Mmp9 promoter by Tet2 (Ten-eleven translocation 2) is associated with trophoblast invasion, and downregulation of Tet2 has been suggested to contribute to preeclampsia-like phenotypes [173]. Mmp9 null mice exhibit impaired maternal-to-fetal connections, impaired embryonic development, and placental abnormalities, including an expanded layer of trophoblast giant cells and a reduction of the labyrinthine layer [174]. Clinically, pregnant women with preeclampsia have lower concentrations of Mmp9 which may relate to the decreased invasion and remodeling of the uterine spiral arteries that has been associated with preeclampsia [173].

Additional secreted factors that may play pro-calcific roles in the placenta include fibroblast growth factor 23 (Fgf23), secreted phosphoprotein 1 (Spp1), tumor necrosis factor alpha (TNF α), and TNF receptor superfamily member 11b

(Tnfrsf11b). Fibroblast growth factor 23 (FGF23) has been suggested to promote syncytiotrophoblast development alongside α Klotho [58]. Spp1, which is also called osteopontin (OPN), is upregulated during decidualization [175] and has been implicated in embryo implantation and early placentation [176]. Tumor necrosis factor alpha (TNF α), a cell signaling protein, promotes the development of matrix metalloproteinases, found in cytotrophoblasts of the maternal side of the placenta [177]. It has been suggested to enhance smooth muscle cell death and inflammation during spiral arteries remodeling based on histological examination of chorionic villi from human placenta [178, 179]. Finally, Tnfrsf11b, which encodes for osteoprotegerin, promotes calcification and is present in human placenta, but has yet to be studied for its potential role in placental calcification [180].

Pro-calcific Transcription Factors

Intracellular factors such as the transcription factors Atf4, Runx2, Sox9, and Sp7 also provide promising candidates for investigation of calcific signaling pathways in placenta. Activating transcription factor 4 (Atf4) has been studied extensively for its role in stress response during early development [181]. Atf4 expression has been detected in women with both early- and late-onset preeclampsia, with weaker signaling during early-onset stages during placental dysfunction [182]. Functionally, this may relate to increased levels of Pgf, as Atf4 has been shown to restrict placental growth factor expression in trophoblast cells under stress [183].

Runt-related transcription factor 2 (Runx2) is a transcription factor with a conserved Runt DNA-binding domain that contains 128 amino acids. Runx2 was identified as an inducer of the osteocalcin gene (Bglap) and has been extensively shown to have osteogenic effects both in bone development and in vascular disease [139, 184–186]. Runx2 has a primary role during osteoblast differentiation, cartilage hypertrophy, vascular invasion of the bone, and vascular calcification in atherosclerotic lesions [187]. Homozygous mice carrying a Runx2 mutation show complete absence of mature osteoblasts, Sp1, Bglap, and bone and are lethal just after birth due to breathing problems [188]. Runx2 expression has been detected in human placenta and has been shown to increase in response to GnRH treatment, also resulting in increased Mmp9 [189]. Runx2 has been suggested to promote formation of extravillous trophoblast cells during the first trimester of human pregnancy [189]. Runx2 has also been shown to promote osteogenesis in the placenta by impacting the conditions of both calcium and alkaline phosphatase regulation in amniotic epithelial cells [190].

SOX9 is a master transcriptional activator of chondrogenesis and is predominantly expressed in mesenchymal condensations during embryogenesis, both before and during the deposition of cartilage [191, 192]. SOX9 regulates chondrocyte differentiation during commitment of mesenchymal cells to a precursor of osteochondrogenic progenitors through both positive gene regulation and silencing the BMP inhibitors Noggin and Chordin [193]. Sox9 also encodes for sex determination

[192]. Although Sox9 is a master regulator of chondrocyte development and Sox9 positive cartilage has been detected in human placenta, the functional relationship between Sox9 and ectopic cartilaginous deposition in the placenta remains unknown.

Sp7, also called osterix, is a master regulator of osteoblast differentiation that contains a conserved three zinc-finger DNA-binding motif [194, 195]. During osteoblast differentiation, the osteogenic function of Sp7 can be independently regulated by Runx2 or Msx2, which are induced by Bmp2 [196]. Sp7 ablation in mice leads to bone formation failure due to complete absence of osteoblasts despite a lack of downregulation of Runx2 and chondrocyte marker genes [114]. Expression of Sp7 can be detected in a wide range of tissues including the heart, brain, placenta, and lung [194], but the role of Sp7 in placental calcification remains unexplored.

Anti-calcific Transmembrane Proteins

Ectonucleotide pyrophosphatase/phosphodiesterase 1, Enpp1, encodes for a membrane protein that has been shown to promote anti-calcific effects during development [197, 198]. Enpp1 inhibits joint mineralization [197]. Remarkably, inactivation of Enpp1 results in ectopic connective tissue calcification during fetal development which can be rescued in part by maternal oral consumption of pyrophosphate [198]. The placenta is likely a mediator of the Enpp1/PPi interaction during gestation, but placental effects remain unexamined in this model.

The membrane protein ANKH inorganic pyrophosphate transport regulator is also a pro-calcific molecule that has been detected in the placenta. Fetal development studies support that ANKH inhibits calcification in instances in which undermodeling for bone mineralization occurred [199]. ANKH is found on membranes of hypertrophic and chondrocytes of osteoblasts [200] and detected in placenta [201], but has not been evaluated for anti-calcific potential in the placenta.

AXL receptor tyrosine kinase, Axl, is a membrane protein that is stimulated by Gas6 and is localized to endothelial cells during fetal development and serves as a protective genetic factor during angiogenesis [202]. Altered genomic methylation of the Axl promoter has been associated with recurrent miscarriage, but the role for Axl in placenta and pregnancy is not well understood [203, 204].

Secreted Anti-calcific Factors

Mgp, Grp, Ahsg, Nog, Chrd, and Gas6 all encode for anti-calcific proteins that are secreted by the placenta [205–208]. Matrix Gla protein, Mgp, is a calcification inhibitor which is expressed by bone cells and vascular smooth muscle cells. Decreased expression and activity of Mgp is thought to play a role in vascular calcification mechanisms in the context of chronic kidney disease [209, 210]. Mgp has been detected in placental pericytes and may play a role in regulating calcification

in the placenta [209]. Gastrin-releasing peptide, Grp, is detected on the fetal side of the placenta [211] and has been shown to regulate angiogenesis, but the role of Grp in placental angiogenesis is not understood [212]. Alpha 2-HS glycoprotein (Ahsg) plays roles in both metabolism and vasculature development [213]. Ahsg also serves as a mineral chaperone and may have anti-calcific effects [214].

Noggin (Nog) is a secreted polypeptide that plays an important role in neural tube development and is known to directly inactivate pro-calcific members of the TGF β superfamily, such as Bmp4 [215]. The primary physiological role of Noggin is to directly antagonize BMPs during vertebrate dorsal-ventral patterning and skeletal development. Noggin null mice die at birth from multiple defects including bony fusion of the appendicular skeleton [216]. Noggin acts by sequestering its ligand and thus inhibiting BMP signaling by blocking the molecular epitopes that are essential for binding both type I and type II receptors [217]. Similar to Noggin, Chordin (Chrd) also sequesters ventralizing BMPs into latent complexes [218]. Functionally, reduced expression of Chordin associates with de-differentiated, pro-calcific smooth muscle cell states, and loss of Chordin enhances the osteogenic differentiation of human mesenchymal stem cells [219, 220].

Growth arrest-specific 6, Gas6, is a vitamin K-dependent coagulation protein. Gas6 plays a role in tissue scarring and inflammation during vascular development and has been localized to trophoblast cells [221]. Although Gas6 has an anti-inflammatory effect in patients with atherosclerosis [222], interaction of Gas6 with anti-inflammatory effects with placental calcification has not been established.

Anti-calcific Transcription Factors

Msx2 is a member of the homeobox gene family and encodes a transcriptional regulator. Msx2 negatively regulates the expression of Bglap (osteocalcin) during osteoblast differentiation through direct association with chromatin, and thus it works in balance with Runx2, Dxl5, and Dxl3, which promote transcriptional initiation of Bglap and osteoblast proliferation [223]. During development Msx2 is expressed as early as the blastocyst stage where it has been identified as a member of a core family of transcriptional activators that promote the differentiation of trophoblast and trophoblast lineages [224]. Msx2 has also been detected at later stages of pregnancy in human placental trophoblast lineages where it has been suggested to promote signaling for the WNT/ β -catenin pathway as syncytiotrophoblast and extravillous cytotrophoblast cells develop in vivo [225].

While the Slc20a2 null mouse currently remains the only in vivo genetic model of calcification, this large body of evidence suggests that placental calcification may be regulated and/or programmed through a paradigm of increasing activity of pro-calcific genes and decreasing activity of anti-calcific proteins across gestation. Together, these embryonic phenotypes and in vitro assays suggest that a systemic review should be done of placentas from pro- and anti-calcific animal models in order to test whether these signaling and mineralizing functions are maintained in the placenta. In addition to genetic manipulation and histological assessment, new

frontiers in computer vision provide promising routes to evaluate placental calcification mechanisms and pathophysiology through noninvasive in vivo body imaging approaches and computational image analysis.

Computer Vision: A New Frontier in Placental Calcification Research

True understanding of how ectopic calcification does impact placental function will be dependent upon nuanced analysis of in vivo body imaging data. While histology is still the gold standard for deducing tissue localization at the micron level, access to samples is limited, and histological sampling is often time-consuming, incomplete, and retrospective. In contrast, in vivo body imaging can permit an evaluation of both anatomy and physiology. In both clinical and basic science research fields, there are several imaging modalities that may be used and/or coupled to pursue this overarching question. For example, in the clinic, both magnetic resonance imaging (MRI) [226] and ultrasound imaging can be employed [30] during pregnancy. Basic science research using animal models is amenable to a wider range of imaging modalities including MRI, contrast-enhanced microCT, ultrasound biomicroscopy, deconvolution fluorescence microscopy, confocal microscopy, multiphoton microscopy, and optical transmission microscopy [227, 228]. In concert with technical advancements in imaging modalities, computational approaches to evaluating in vivo placenta imaging data are also advancing.

Computer vision image analysis techniques provide a particularly promising new frontier for the evaluation of placental physiology and structure-function relationships. A variety of computer vision techniques can be used to determine different properties of the placenta that are represented by features. Features are in practice simply numeric descriptors of certain properties of an image. Once determined, features can be used to test for correlation with clinical characteristics of the pregnancy as well as clinical maternal-fetal outcomes. A fundamental assumption of this approach is that image properties such as texture and contrast relate to various physical properties of the placenta. For example, deposition of calcium in the placenta can be simulated through texture analysis because calcification makes the placenta coarser.

Image type and image selection are important factors to consider in designing a computer vision analysis approach. MRI imaging is typically used to generate a three-dimensional view of the placenta, yet MRI imaging is costly and rarely applied in routine obstetric care, so the available data is limited. Alternatively, ultrasound (US) image evaluations are ubiquitous with much lower costs. While 3D US rendering is feasible, most ultrasound scans generate 2D cross-sections. Thus, 2D US images housed within clinical body imaging divisions can provide a wealth of largely untapped information. The choice of image type is mostly problem dependent and depends on what kind of data is needed and how much time can be allocated to this process. In addition to image type, image selection is of paramount importance while selecting an ultrasound image. The image must provide necessary details of the placenta without obstructing important areas.

Image features can be identified and quantified through texture analysis. Indeed, this approach has been used to support a positive relationship between placental maturity and sonographic texture [229]. Texture analysis can provide a numeric value to intuitive qualities like smoothness and roughness. Texture analysis has been employed to MRI image analysis to test for gestational age with positive results. Specifically, gray-level co-occurrence matrix (GLCM) texture features, also known as Haralick texture features, have been used to show an increase in placental heterogeneity throughout gestational age [19]. This knowledge permits identification of baseline textures in healthy placental MRI and has been used by Do et al. to demonstrate an association with gestational age. It remains to be seen how these baseline textures compare to cases of placental insufficiency and disease, as well as whether they aid in detection and diagnosis of maternal and fetal health conditions.

Image analysis is also increasingly combined with machine learning techniques that provide a prediction model for examining correlation with clinical characteristics and outcomes. A recent study by Sun et al. applied this approach to suspicious invasive placentation and identified correlates to adverse maternal clinical outcomes [226]. A multitude of machine learning and clustering methods, including Naïve Bayes, K Nearest Neighbor, k-means, and Multilayer Perceptron have been successfully used alongside texture analysis techniques for MRI and ultrasound images. For example, Romeo et al. used these machine learning methods to assess the presence of placenta accreta spectrum in patients with placenta previa with up to 98% accuracy [230]. Neural networks have also been used to evaluate *in vivo* placental imaging, namely, 3D ultrasounds. Looney et al. used neural networks to isolate the placenta from 3D ultrasounds and estimate placental volume, supporting that this method could be employed as a universal screening tool that provides an identifier for pregnancies at risk of developing problems [231]. As an alternate segmentation approach, wavelet decomposition using conditional random fields has been successfully used to develop segmentation methods for the fetus; these tools could potentially be applied to placenta segmentation using proper constraints and choice of the training set features [232].

Overall, machine learning approaches have shown immense promise in analyzing placental and fetal images. Image selection and number of data points required are crucial experimental design decisions. A model is only as good as the data we provide in it, and the data must be accurate enough for a correct prediction. In contrast, with too few data points, one runs the risk of overfitting to a dataset, and this is also an important consideration. Therefore, image analysis, in tandem with machine learning, is a powerful tool that may assist analysis of placental calcification both in basic and clinical research, but these approaches require us to exercise caution.

Conclusions

The placenta is an essential yet transient organ that supports healthy pregnancy and normal healthy fetal development. Placental vascular dysfunction is associated with preeclampsia, eclampsia, HELLP (hemolysis, elevated liver enzymes, low platelets) syndrome, fetal growth restriction, hemorrhage, preterm birth, and loss of life. Placental dysfunction can also negatively impact long-term maternal and offspring

health, as exposure to preeclampsia increases risk for cardiovascular disease, coronary artery calcification, and stroke later in life. The concept that adverse intrauterine factors such as preeclampsia can increase risk of diseases later in life was founded by epidemiologist David Barker and is now known as the Developmental Origins of Health and Disease (DOHaD) concept [233–236]. It remains largely unknown why calcium phosphate mineral deposits form in placental tissue in both normal and disease contexts and whether placental calcification and/or spatiotemporally specific calcification patterns will provide new insight into pathophysiology or serve as early diagnostic indicators of placental dysfunction. Herein we reviewed the association between placental calcification and clinical outcomes, histoanatomical features of mineral deposits in the placenta, mechanisms of calcium and phosphate homeostasis during pregnancy, and lessons learned about pro- and anti-calcific signaling molecules in placental tissue from both clinical and animal model studies. Many questions remain as to how mobilization, homeostasis, and maternal-fetal transport of calcium and phosphorus are regulated during pregnancy and how these processes may relate to ectopic placental calcification and both acute and long-term maternal and fetal health. Together, a large body of in vivo developmental phenotyping and mechanistic in vitro calcification studies warrant further investigation of these biology relationships and their biomedical significance. The rapidly advancing fields of noninvasive imaging and computational image analysis are also likely to provide structural and functional insight into the significance of placental calcification in the interpretation of placental diseases, while new molecular insights will likely come from assessment of placental development and pathophysiology in ectopic calcification animal models in which placental biology has been overlooked.

References

1. Tannetta D, Sargent I. Placental disease and the maternal syndrome of preeclampsia: missing links? *Curr Hypertens Rep.* 2013;15(6):590–9.
2. Ahmed A, Perkins J. Angiogenesis and intrauterine growth restriction. *Best Pract Res Clin Obstet Gynaecol.* 2000;14(6):981–98.
3. Hod T, Cerdeira AS, Ananth Karumanchi S. Molecular mechanisms of preeclampsia. *Cold Spring Harb Perspect Med.* 2015;5:a023473.
4. Roberts JM, Escudero C. The placenta in preeclampsia. *Pregnancy Hypertens.* 2012;2:72.
5. Semczuk M, Borczynska A, Bialas M, Rozwadowska N, Semczuk-Sikora A, Malcher A, et al. Expression of genes coding for proangiogenic factors and their receptors in human placenta complicated by preeclampsia and intrauterine growth restriction. *Reprod Biol.* 2013;13(2):133–8.
6. Scantlebury DC, Hayes SN, Garovic VD. Pre-eclampsia and maternal placental syndromes: an indicator or cause of long-term cardiovascular disease? *Heart.* 2012;98(15):1109–11.
7. Ray JG, Vermeulen MJ, Schull MJ, Redelmeier DA. Cardiovascular health after maternal placental syndromes (CHAMPS): population-based retrospective cohort study. *Lancet (London, England).* 2005;366(9499):1797–803.
8. Ying W, Catov JM, Ouyang P. Hypertensive disorders of pregnancy and future maternal cardiovascular risk. *J Am Heart Assoc.* 2018;7(17):1–9.
9. Young BC, Levine RJ, Karumanchi SA. Pathogenesis of preeclampsia. *Annu Rev Pathol.* 2010;5:173–92.
10. States U. Diagnosis and management of preeclampsia and eclampsia. *Int J Gynecol Obstet.* 2002;77(1):67–75.

11. Chesley LC, Annitto JE, Cosgrove RA. The remote prognosis of eclamptic women: sixth periodic report. *Am J Obstet Gynecol.* 1976;124(5):446–59.
12. Irgens HU, Roberts JM, Reisaeter L, Irgens LM, Lie RT. Long term mortality of mothers and fathers after pre-eclampsia: population based cohort study pre-eclampsia and cardiovascular disease later in life: who is at risk? *BMJ.* 2001;323(7323):1213–7.
13. Smith G, Pell J, Walsh D. Pregnancy complications and maternal risk of ischaemic heart disease: a retrospective cohort study of 129,290 births. *Lancet.* 2001;357:2002–6.
14. Facca TA, Kirsztajn GM, Sass N. Preeclampsia (marker of chronic kidney disease): from genesis to future risks. *J Bras Nefrol.* 2012;34(1):87–93. Available from: <http://www.ncbi.nlm.nih.gov/pubmed/22441189>.
15. White WM, Mielke MM, Araoz PA, Lahr BD, Bailey KR, Jayachandran M, et al. A history of preeclampsia is associated with a risk for coronary artery calcification 3 decades later. *Am J Obstet Gynecol.* 2016;214(4):519.e1–8.. Available from: <https://doi.org/10.1016/j.ajog.2016.02.003>
16. Cain MA, Salemi JL, Tanner JP, Kirby RS, Salihu HM, Louis JM. Pregnancy as a window to future health: maternal placental syndromes and short-term cardiovascular outcomes. *Am J Obstet Gynecol.* Mosby Inc. 2016;215:484.e1–484.e14.
17. Varma VA, Kim KM. Placental calcification: ultrastructural and X-ray microanalytic studies. *Scan Electron Microsc.* 1985;(Pt 4):1567–72 . Available from: <http://www.ncbi.nlm.nih.gov/pubmed/3006220>.
18. Poggi SH, Bostrom KI, Demer LL, Skinner HC, Koos BJ. Placental calcification: a metastatic process? *Placenta.* 2001;22:591–6.
19. Do QN, Lewis MA, Madhuranthakam AJ, Xi Y, Bailey AA, Lenkinski RE, et al. Texture analysis of magnetic resonance images of the human placenta throughout gestation: a feasibility study. *PLoS One.* 2019;1:14(1).
20. Pereira L. Congenital viral infection: traversing the uterine-Placental Interface. *Annu Rev Virol.* 2018;5(1):273–99.
21. Bailao L, Osborne NG, Rizzi MCS, Bonilla-musoles F, Duarte G, Bailao T. Ultrasound markers of fetal infection part 1. *Ultrasound Q.* 2005;21(4):295–308.
22. Gabrielli L, Bonasoni MP, Foschini MP, Silini EM, Spinillo A, Revello MG, et al. Histological analysis of term placentas from hyperimmune globulin-treated and untreated mothers with primary cytomegalovirus infection. *Fetal Diagn Ther.* 2019;45(2):111–7.
23. Mastrolia SA, Weintraub AY, Sciaky-Tamir Y, Tirosh D, Loverro G, Hershkovitz R. Placental calcifications: a clue for the identification of high-risk fetuses in the low-risk pregnant population? *J Matern Neonatal Med.* 2016;29(6):921–7.
24. Mirza FG, Ghulmiyyah LM, Tamim H, Makki M, Jeha D, Nassar A. To ignore or not to ignore placental calcifications on prenatal ultrasound: a systematic review and meta-analysis. *J Matern Neonatal Med.* 2018;31(6):797–804.
25. Wallingford MC, Benson C, Chavkin NW, Chin MT, Frasch MG. Placental vascular calcification and cardiovascular health: it is time to determine how much of maternal and offspring health is written in stone. *Front Physiol.* 2018;9(August):1–9.
26. Nigam J, Misra V, Singh P, Singh P, Chauhan S, Thakur B. Histopathological study of placentae in low birth weight babies in India. *Ann Med Health Sci Res.* 2014;4(8):79.
27. Salmani D, Purushothaman S, Somashekara SC, Gnanagurudasan E, Sumangaladevi K, Harikishan R, et al. Study of structural changes in placenta in pregnancy-induced hypertension. *J Nat Sci Biol Med.* 2014;5(2):352–5.
28. Nahar L, Nahar K, Hossain MI, Yasmin H, Annur BM. Placental changes in pregnancy induced hypertension and its impacts on fetal outcome. *Mymensingh Med J.* 2015;24(1):9–17. Available from: <http://www.ncbi.nlm.nih.gov/pubmed/25725662>.
29. Tindall V, Scott J. Placental calcification a study of 3,025 singleton and multiple pregnancies. *J Obs Gynaecol Br Commonw.* 1965;72:356–73.
30. Chen K, Chen L, Lee Y. Exploring the relationship between preterm placental calcification and adverse maternal and fetal outcome. *Ultrasound Obstet Gynecol.* 2011a;37(3):328–34.
31. Chen KH, Chen LR, Lee YH. The role of preterm placental calcification in high-risk pregnancy as a predictor of poor uteroplacental blood flow and adverse pregnancy outcome. *Ultrasound Med Biol.* 2012;38(6):1011–8.

32. McKenna D, Tharmaratnam S, Mahsud S, Dornan J. Ultrasonic evidence of placental calcification at 36 weeks' gestation: maternal and fetal outcomes. *Acta Obs Gynecol Scand*. 2005a;84:7–10.
33. Chitlange S, Hazari K, Joshi J, Al E. Ultrasonographically observed preterm grade III placenta and perinatal outcome. *Int J Gynaecol Obs*. 1990;31:325–8.
34. Chen Y, Huang L, Zhang H, Klebanoff M, Yang Z, Zhang J. Racial disparity in placental pathology in the collaborative perinatal project. *Int J Clin Exp Pathol*. 2015a;8(11):15042–54. Available from: <http://www.ncbi.nlm.nih.gov/pubmed/26823843>.
35. Al-Zuhair AG, Ibrahim ME, Mughal S. Calcium deposition on the maternal surface of the human placenta: a scanning electron microscopic study. *Arch Gynecol*. 1984;234:167.
36. Grannum P, Berkowitz R, Hobbins J. The ultrasonic changes in the maturing placenta and their relation to fetal pulmonic maturity. *Am J Obs Gynecol*. 1979;133:915–22.
37. Zeng J, Marcus A, Buhtoiarova T, Mittal K. Distribution and potential significance of intravillous and intrafibrinous particulate microcalcification. *Placenta*. 2017;50:94–8.
38. Proud J, Grant A. Third trimester placental grading by ultrasonography as a test of fetal well-being. *Br Med J (Clin Res Ed)*. 1987;294:1641–4.
39. Patterson R, Hayashi R, Cavazos D. Ultrasonographically observed early placental maturation and perinatal outcome. *Am J Obs Gynecol*. 1983;147:773–7.
40. Miller J, Brown H, Kissling G, Gabert H. The relationship of placental grade to fetal size and growth at term. *Am J Perinatol*. 1988;5:19–21.
41. Vosmar M, Jongsma H, van Dongen P. The value of ultrasonic placental grading: no correlation with intrauterine growth retardation or with maternal smoking. *J Perinat Med*. 1989;17:137–43.
42. Chen KH, Seow KM, Chen LR. The role of preterm placental calcification on assessing risks of stillbirth. *Placenta*. 2015b;36(9):1039–44.
43. Jamal A, Moshfeghi M, Moshfeghi S, Mohammadi N, Zarean E, Jahangiri N. Is preterm placental calcification related to adverse maternal and foetal outcome? *J Obstet Gynaecol (Lahore)*. 2017;37(5):605–9.
44. Sau A, Seed P, Langford K. Intraobserver and interobserver variation in the sonographic grading of placental maturity. *Ultrasound Obstet Gynecol*. 2004;23(4):374–7.
45. Moran M, Ryan J, Higgins M, Brennan PC, McAuliffe FM. Poor agreement between operators on grading of the placenta. *J Obstet Gynaecol (Lahore)*. 2011;31(1):24–8.
46. McKenna D, Tharmaratnam S, Mahsud S, Dornan J. Ultrasonic evidence of placental calcification at 36 weeks' gestation: maternal and fetal outcomes. *Acta Obstet Gynecol*. 2005b;84(1):7–10.
47. Baeza Valenzuela A, Garcia Mendez A. Premature aging of the placenta. *Ultrasonic diagnosis. Ginecol Obstet Mex*. 1995;63:287–92.
48. Hills D, Irwin G, Tuck S, Baim R. Distribution of placental grade in high-risk gravidas. *AJR*. 1984;143:1011–3.
49. Zhang LY, Yu YH, Hu ML. Association between ultrasonographic signs of placental premature aging and pregnancy outcome. *Di Yi Jun Yi Da Xue Xue Bao*. 2005;25(3):318–20.
50. Kazzi G, Gross T, Rosen M, Jaatoul-Kazzi N. The relationship of placental grade, fetal lung maturity, and neonatal outcome in normal and complicated pregnancies. *Am J Obs Gynecol*. 1984;148:54–8.
51. Heazell AEP, Worton SA, Higgins LE, Ingram E, Johnstone ED, Jones RL, et al. IFPA Gábor than award lecture: recognition of placental failure is key to saving babies' lives. *Placenta*. 2015;36(S1):S20–8.
52. Kasznica JM, Petcu EB. Placental calcium pump: clinical-based evidence. *Pediatr Pathol Mol Med*. 2003;22(3):223–7. Available from: <http://www.ncbi.nlm.nih.gov/pubmed/12746173>.
53. Wallingford MC, Gammill HS, Giachelli CM. Slc20a2 deficiency results in fetal growth restriction and placental calcification associated with thickened basement membranes and novel CD13 and laminin α 1 expressing cells. *Reprod Biol*. 2016;16(1):13–26. Available from: <https://doi.org/10.1016/j.repbio.2015.12.004>
54. Yang H, Kim TH, Lee GS, Hong EJ, Jeung EB. Comparing the expression patterns of placental magnesium/phosphorus-transporting channels between healthy and preeclamptic pregnancies. *Mol Reprod Dev*. 2014;81(9):851–60. Available from: <http://www.ncbi.nlm.nih.gov/pubmed/25155868>.

55. Istrate M, Mihiu C, Şuşman S, Melincovici CS, Măluţan AM, Buiga R, et al. Highlighting the R1 and R2 VEGF receptors in placentas resulting from normal development pregnancies and from pregnancies complicated by preeclampsia. *Rom J Morphol Embryol*. 2018;59(1):139–46. Available from: <http://www.ncbi.nlm.nih.gov/pubmed/29940621>.
56. Theophilou G, Sahashrabudhe N, Martindale EA, Heazell AEP. Correlation between abnormal placental appearance at routine 2nd trimester ultrasound scan and histological examination of the placenta after birth. *J Obstet Gynaecol (Lahore)*. 2012;32(8):760–3.
57. Pinar H, Carpenter M. Placenta and umbilical cord abnormalities seen with stillbirth. *Clin Obstet Gynecol*. 2010;53(3):656–72. Available from: <http://www.ncbi.nlm.nih.gov/pubmed/20661050>.
58. Ohata Y, Yamazaki M, Kawai M, Tsugawa N, Tachikawa K, Koinuma T, et al. Elevated fibroblast growth factor 23 exerts its effects on placenta and regulates vitamin D metabolism in pregnancy of Hyp mice. *J Bone Miner Res*. 2014;29(7):1627–38.
59. Ma Y, Samaraweera M, Cooke-Hubley S, Kirby BJ, Karaplis AC, Lanske B, et al. Neither absence nor excess of FGF23 disturbs murine fetal-placental phosphorus homeostasis or prenatal skeletal development and mineralization. *Endocrinology*. 2014;155(5):1596–605.
60. Salles JP. Bone metabolism during pregnancy. *Ann Endocrinol (Paris)*. 2016;77(2):163–8.
61. Ulrich U, Miller PB, Eyre DR, Chesnut CH 3rd, Schlebusch H, Soules MR. Bone remodeling and bone mineral density during pregnancy. *Arch Gynecol Obstet*. 2003;268(4):309–16.
62. Givens M, Macy IG. The chemical composition of human fetus. *Hum Milk Biochem Infant Formula Manuf Technol*. 1933;102:7–17.
63. Delvin EE, Salle BL, Glorieux FH. Vitamin D and calcium homeostasis in pregnancy: fetomaternal relationships. *Rickets*. 1991;21(8):91–105.
64. Sparks JW. Human intrauterine growth and nutrient accretion. *Semin Perinatol*. 1984;8(2):74–93.
65. Widdowson EM, Mccance RA. The metabolism of calcium, phosphorus, magnesium and strontium. *Pediatr Clin North Am*. 1965;12:595–614.
66. Ziegler EE, O'Donnell AM, Nelson SE, Fomon SJ. Body composition of the reference fetus. *Growth*. 1976;40(4):329–41.
67. Yang H, Kim TH, An BS, Choi KC, Lee HH, Kim JM, et al. Differential expression of calcium transport channels in placenta primary cells and tissues derived from preeclamptic placenta. *Mol Cell Endocrinol*. 2013;367(1–2):21–30.
68. Hache S, Takser L, LeBellef F, Weiler H, Leduc L, Forest JC, et al. Alteration of calcium homeostasis in primary preeclamptic syncytiotrophoblasts: effect on calcium exchange in placenta. *J Cell Mol Med*. 2011;15(3):654–67.
69. Bernucci L, Henriquez M, Diaz P, Riquelme G. Diverse calcium channel types are present in the human placental syncytiotrophoblast basal membrane. *Placenta*. 2006;27(11–12):1082–95.
70. Hayward CE, Renshall LJ, Sibley CP, Greenwood SL, Dilworth MR. Adaptations in maternal-fetal calcium transport in relation to placental size and fetal sex in mice. *Front Physiol*. 2017;8(December):1–10.
71. Schauburger C, Pitkin R. Maternal-perinatal calcium relationships. *Obstet Gynecol*. 1979;53:7406.
72. Brunette MG, Letendre S, Allard S. Phosphate transport through placenta brush border membrane BT – phosphate and mineral homeostasis. In: Massry SG, Olmer M, Ritz E, editors. *Phosphate and mineral homeostasis*. Boston: Springer; 1986. p. 543–8.
73. Brunette MG, Auger D, Lafond J. Effect of parathyroid hormone on PO₄ transport through the human placenta microvilli. *Pediatr Res*. 1989a;25(1):15–8. Available from: <http://www.ncbi.nlm.nih.gov/pubmed/2537487>.
74. Brunette MG, Leclerc M, Ramachandran C, Lafond J, Lajeunesse D. Influence of insulin on phosphate uptake by brush border membranes from human placenta. *Mol Cell Endocrinol*. 1989b;63(1):57–65. Available from: <http://www.ncbi.nlm.nih.gov/pubmed/2546843>.
75. Lajeunesse D, Brunette MG. Sodium gradient-dependent phosphate transport in placental brush border membrane vesicles. *Placenta*. 1988;9(2):117–28. Available from: <http://www.ncbi.nlm.nih.gov/pubmed/3399488>.
76. Virkki LV, Biber J, Murer H, Forster IC. Phosphate transporters: a tale of two solute carrier families. *Am J Physiol Renal Physiol*. 2007;293:F643–54.

77. Nishimura M, Aito SN. Tissue-specific mRNA expression profiles of human solute carrier transporter superfamilies. *Drug Metab Pharmacokinet.* 2008;23(1):22–44.
78. Kovacs CS, Kronenberg HM. Maternal-fetal calcium and bone metabolism during pregnancy, puerperium, and lactation *. *Endocr Rev.* 1997;18(6):832–72.
79. Gaboury CL, Woods LL. Renal reserve in pregnancy. *Semin Nephrol.* 1995;15(5):449–53.
80. Baylis C. Glomerular filtration and volume regulation in gravid animal models. *Baillieres Clin Obstet Gynaecol.* 1987;1(4):789–813.
81. Lalau JD, Jans I, el Esper N, Bouillon R, Fournier A. Calcium metabolism, plasma parathyroid hormone, and calcitriol in transient hypertension of pregnancy. *Am J Hypertens.* 1993;6(6 Pt 1):522–7.
82. Seely EW, Wood RJ, Brown EM, Graves SW. Lower serum ionized calcium and abnormal calcitropic hormone levels in preeclampsia. *J Clin Endocrinol Metab.* 1992;74(6):1436–40.
83. Frenkel Y, Barkai G, Mashlach S, Dolev E, Zimlichman R, Weiss M. Hypocalciuria of preeclampsia is independent of parathyroid hormone level. *Obstet Gynecol.* 1991;77(5):689–91.
84. August P, Marcaccio B, Gertner JM, Druzin ML, Resnick LM, Laragh JH. Abnormal 1,25-dihydroxyvitamin D metabolism in preeclampsia. *Am J Obstet Gynecol.* 1992;166(4):1295–9.
85. Pedersen EB, Johannesen P, Kristensen S, Rasmussen AB, Emmertsen K, Moller J, et al. Calcium, parathyroid hormone and calcitonin in normal pregnancy and preeclampsia. *Gynecol Obstet Investig.* 1984;18(3):156–64.
86. Bronsky D, Kiamko R, Moncada R, Rosenthal IM. Intra-uterine hyperthyroidism secondary to maternal hypothyroidism. *Pediatrics.* 1968;42(4):606–13.
87. Stuart C, Aceto TJ, Kuhn JP, Terplan K. Intrauterine hyperparathyroidism. Postmortem findings in two cases. *Am J Dis Child.* 1979;133(1):67–70.
88. Loughead JL, Mughal Z, Mimouni F, Tsang RC, Oestreich AE. Spectrum and natural history of congenital hyperparathyroidism secondary to maternal hypocalcemia. *Am J Perinatol.* 1990;7(4):350–5.
89. Sann L, David L, Thomas A, Frederich A, Chapuy MC, Francois R. Congenital hyperparathyroidism and vitamin D deficiency secondary to maternal hypoparathyroidism. *Acta Paediatr Scand.* 1976;65(3):381–5.
90. Aceto TJ, Batt RE, Bruck E, Schultz RB, Perz YR. Intrauterine hyperparathyroidism: a complication of untreated maternal hypoparathyroidism. *J Clin Endocrinol Metab.* 1966;26(5):487–92.
91. Eastell R, Edmonds CJ, de Chayal RC, McFadyen IR. Prolonged hypoparathyroidism presenting eventually as second trimester abortion. *Br Med J (Clin Res Ed).* 1985;291(6500):955–6.
92. Cox B, Kotlyar M, Evangelou AI, Ignatchenko V, Ignatchenko A, Whiteley K, et al. Comparative systems biology of human and mouse as a tool to guide the modeling of human placental pathology. *Mol Syst Biol.* 2009;5:279.
93. Boyd K, Muehlenbachs A, Rendi M, Garcia R, Gibson-Corley K. Female reproductive system. In: *Comparative anatomy and histology: a mouse, rat, and human atlas.* London: Elsevier/Academic Press; 2012. p. 253–84.
94. Uhlén M, Fagerberg L, Hallström BM, Lindskog C, Oksvold P, Mardinoglu A, et al. Tissue-based map of the human proteome. *Science (80).* 2015;347(6220):1260419.
95. Chu A, Casero D, Thamotharan S, Wadehra M, Cosi A, Devaskar SU. The placental transcriptome in late gestational hypoxia resulting in murine intrauterine growth restriction parallels increased risk of adult cardiometabolic disease. *Sci Rep.* 2019;9(1):1243.
96. Yotsumoto S, Shimada T, Cui CY, Nakashima H, Fujiwara H, Ko MSH. Expression of adrenomedullin, a hypotensive peptide, in the trophoblast giant cells at the embryo implantation site in mouse. *Dev Biol.* 1998;203(2):264–75.
97. Shindo T, Kurihara Y, Nishimatsu H, Moriyama N, Kakoki M, Wang Y, et al. Vascular abnormalities and elevated blood pressure in mice lacking adrenomedullin gene. *Circulation.* 2001;104(16):1964–71.
98. Dehghani H, Narisawa S, Millan JL, Hahnel AC. Effects of disruption of the embryonic alkaline phosphatase gene on preimplantation development of the mouse. *Dev Dyn.* 2000;217(4):440–8.
99. Koscielny G, Yaikhom G, Iyer V, Meehan TF, et al. The International Mouse Phenotyping Consortium Web Portal, a unified point of access for knockout mice and related phenotyping data. *Nucleic Acids Res.* 2014;42(Database issue):D802–9.

100. Goldman DC, Donley N, Christian JL. Genetic interaction between *Bmp2* and *Bmp4* reveals shared functions during multiple aspects of mouse organogenesis. *Mech Develop.* 2009;126(3):117–27.
101. Lyons KM, Pelton RW, Hogan BLM. Organogenesis and pattern formation in the mouse: RNA distribution patterns suggest a role for Bone Morphogenetic Protein-2A (BMP-2A). *Development.* 1990;109:833–44.
102. Zhang H, Bradley A. Mice deficient for BMP2 are nonviable and have defects in amnion/chorion and cardiac development. *Development.* 1996;122(10):2977–86.
103. Winnier G, Blessing M, Labosky PA, Hogan BL. Bone morphogenetic protein-4 is required for mesoderm formation and patterning in the mouse. *Genes Dev.* 1995;9(17):2105–16.
104. Zouvelou V, Passa O, Segkilia K, Tsalavos S, Valenzuela DM, Economides AN, et al. Generation and functional characterization of mice with a conditional BMP7 allele. *Int J Dev Biol.* 2009;53(4):597–603.
105. Stafford DA, Monica SD, Harland RM. Follistatin interacts with Noggin in the development of the axial skeleton. *Mech Dev.* 2014;131:78–85. <https://doi.org/10.1016/j.mod.2013.10.001>.
106. Bachiller D, Klingensmith J, Shneyder N, Tran U, Anderson R, Rossant J, et al. The role of chordin/*Bmp* signals in mammalian pharyngeal development and DiGeorge syndrome. *Development.* 2003;130(15):3567–78.
107. Harvey MB, Leco KJ, Arcellana-Panlilio MYA, Zhang X, Edwards DR, Schultz GA. Proteinase expression in early mouse embryos is regulated by leukaemia inhibitory factor and epidermal growth factor. *Development (Camb).* 1995;121:1005–14.
108. Tylzanowski P, Mebis L, Luyten FP. The Noggin null mouse phenotype is strain dependent and haploinsufficiency leads to skeletal defects. *Dev Dyn.* 2006;235(6):1599–607.
109. DiPalma T, Tucci M, Russo G, Maglione D, Lago CT, Romano A, et al. The placenta growth factor gene of the mouse. *Mamm Genome.* 1996;7(1):6–12. <https://doi.org/10.1007/s003359900003>.
110. Choi JY, Pratap J, Javed A, Zaidi SK, Xing L, Balint E, et al. Subnuclear targeting of Runx/*Cbfa*/*AML* factors is essential for tissue-specific differentiation during embryonic development. *Proc Natl Acad Sci USA.* 2001;98(15):8650–5.
111. Festing MH, Speer MY, Yang HY, Giachelli CM. Generation of mouse conditional and null alleles of the type III sodium-dependent phosphate cotransporter PiT-1. *Genesis.* 2009;47(12):858–63.
112. Ng LJ, Wheatley S, Muscat GE, Conway-Campbell J, Bowles J, Wright E, et al. SOX9 binds DNA, activates transcription, and coexpresses with type II collagen during chondrogenesis in the mouse. *Dev Biol.* 1997;183(1):108–21. <https://doi.org/10.1006/dbio.1996.8487>.
113. Palmer K, Fairfield H, Borgeia S, Curtain M, Hassan MG, Dionne L, et al. Discovery and characterization of spontaneous mouse models of craniofacial dysmorphology. *Dev Biol.* 2016;415(2):216–27.
114. Nakashima K, Zhou X, Kunkel G, Zhang Z, Deng JM, Behringer RR, et al. The novel zinc finger-containing transcription factor osterix is required for osteoblast differentiation and bone formation. *Cell.* 2002;108(1):17–29. Available from: <http://www.ncbi.nlm.nih.gov/pubmed/11792318>.
115. Botquin V, Hess H, Fuhrmann G, Anastassiadis C, Gross MK, Vriend G, et al. New POU dimer configuration mediates antagonistic control of an osteopontin preimplantation enhancer by Oct-4 and Sox-2. *Genes Dev.* 1998;12(13):2073–90. <https://doi.org/10.1101/gad.12.13.2073>.
116. Nomura S, Wills AJ, Edwards DR, Heath JK, Hogan BL. Developmental expression of *2ar* (osteopontin) and SPARC (Osteonectin) RNA as revealed by in situ hybridization. *J Cell Biol.* 1988;106(2):441–50. <https://doi.org/10.1083/jcb.106.2.441>.
117. Waymire KG, Mahuren JD, Jaje JM, Guilarte TR, Coburn SP, MacGregor GR. Mice lacking tissue non-specific alkaline phosphatase die from seizures due to defective metabolism of vitamin B-6. *Nat Genet.* 1995;11(1):45–51.
118. Freeman TC, Dixon AK, Campbell EA, Tait TM, Richardson PJ, Rice KM, Maslen GM, Metcalfe AD, Streuli CH, Bentley DR. Expression Mapping of Mouse Genes. MGI direct data submission to Mouse Genome Database (MGD). MGI. 1999:1349786, (URL: <http://www.informatics.jax.org>).

119. Roby KF, Laham N, Kröning H, Terranova PF, Hunt JS. Expression and localization of messenger RNA for tumor necrosis factor receptor (TNF-R) I and TNF-RII in pregnant mouse uterus and placenta. *Endocrine*. 1995;3(8):557–62. <https://doi.org/10.1007/BF02953019>.
120. Kohchi C, Noguchi K, Tanabe Y, Mizuno D, Soma G. Constitutive expression of TNF-alpha and -beta genes in mouse embryo: roles of cytokines as regulator and effector on development. *Int J Biochem*. 1994;26(1):111–9. [https://doi.org/10.1016/0020-711x\(94\)90203-8](https://doi.org/10.1016/0020-711x(94)90203-8).
121. Bucay N, Sarosi I, Dunstan CR, Morony S, Tarpley J, Capparelli C, et al. Osteoprotegerin-deficient mice develop early onset osteoporosis and arterial calcification. *Genes Dev*. 1998;12(9):1260–8.
122. Ohata Y, Arahori H, Namba N, Kitaoka T, Hirai H, Wada K, et al. Circulating levels of soluble α -klotho are markedly elevated in human umbilical cord blood. *J Clin Endocrinol Metab*. 2011;96(6):E943.
123. Godang K, Frøslie KF, Henriksen T, Isaksen GA, Voldner N, Lekva T, et al. Umbilical cord levels of sclerostin, placental weight, and birth weight are predictors of total bone mineral content in neonates. *Eur J Endocrinol*. 2013;168(3):371–8.
124. Loichinger MH, Townner D, Thompson KS, Ahn HJ, Bryant-Greenwood GD. Systemic and placental α -klotho: effects of preeclampsia in the last trimester of gestation. *Placenta*. 2016;41:53–61.
125. Bellazi L, Germond S, Dupont C, Brun-Heath I, Taillandier A, De Mazancourt P, et al. A sequence variation in the promoter of the placental alkaline phosphatase gene (ALPP) is associated with allele-specific expression in human term placenta. *Placenta*. 2010;31(9):764–9.
126. Chaparro A, Gaedecheus D, Ramírez V, Zuñiga E, Kusanovic JP, Inostroza C, et al. Placental biomarkers and angiogenic factors in oral fluids of patients with preeclampsia. *Prenat Diagn*. 2016;36(5):476–82.
127. Orozco AF, Jorgez CJ, Ramos-Perez WD, Popek EJ, Yu X, Kozinets CA, et al. Placental release of distinct DNA-associated micro-particles into maternal circulation: reflective of gestation time and preeclampsia. *Placenta*. 2009;30(10):891–7.
128. Cecati M, Giannubilo SR, Saccucci F, Sartini D, Ciavattini A, Emanuelli M, et al. Potential role of placental klotho in the pathogenesis of preeclampsia. *Cell Biochem Biophys*. 2016;74(1):49–57.
129. Savinov AY, Salehi M, Yadav MC, Radichev I, Millán JL, Savinova OV. Transgenic overexpression of tissue-nonspecific alkaline phosphatase (TNAP) in vascular endothelium results in generalized arterial calcification. *J Am Heart Assoc*. 2015;4(12):e002499.
130. Vatin M, Bouvier S, Bellazi L, Montagutelli X, Laissue P, Ziyat A, et al. Polymorphisms of human placental alkaline phosphatase are associated with in vitro fertilization success and recurrent pregnancy loss. *Am J Pathol*. 2014;184(2):362–8.
131. Boć-Zalewska A, Seremak-Mrozikiewicz A, Barlik M, Anna B, Mrozikiewicz PM, Grześkowiak E, et al. Adrenomedullin mRNA expression in placenta of preeclamptic women. *Ginekol Pol*. 2011;82(8):585–91. Available from: <http://www.ncbi.nlm.nih.gov/pubmed/21957602>.
132. Hung TH, Chen SF, Lo LM, Li MJ, Yeh YL, Hsieh TT. Myeloperoxidase in the plasma and placenta of normal pregnant women and women with pregnancies complicated by preeclampsia and intrauterine growth restriction. *Placenta*. 2012;33(4):294–303.
133. Li L, WS O, Tang F. Adrenomedullin in rat follicles and corpora lutea: expression, functions and interaction with endothelin-1. *Reprod Biol Endocrinol*. 2011;9:9.
134. Caron KM. Extreme hydrops fetalis and cardiovascular abnormalities in mice lacking a functional Adrenomedullin gene. *Proc Natl Acad Sci*. 2001;98(2):615–9. Available from: <http://www.pnas.org/cgi/doi/10.1073/pnas.021548898>.
135. Li M, Schwerbrock NMJ, Lenhart PM, Fritz-Six KL, Kadmiel M, Christine KS, et al. Fetal-derived adrenomedullin mediates the innate immune milieu of the placenta. *J Clin Invest*. 2013;123(6):2408–20.
136. Kraus DM, Feng L, Heine RP, Brown HL, Caron KM, Murtha AP, et al. Cigarette smoke-induced placental adrenomedullin expression and trophoblast cell invasion. *Reprod Sci*. 2014;21(1):63–71.
137. Beiswenger TR, Feng L, Brown HL, Heine RP, Murtha AP, Grotegut CA. The effect of cigarette smoke extract on trophoblast cell viability and migration: the role of adrenomedullin. *Reprod Sci*. 2012;19(5):526–33.

138. Pan LC, Price PA. The propeptide of rat bone γ -carboxyglutamic acid protein shares homology with other vitamin K-dependent protein precursors. *Proc Natl Acad Sci U S A*. 1985;82(18):6109–13.
139. Ducy P, Karsenty G. Two distinct osteoblast-specific cis-acting elements control expression of a mouse osteocalcin gene. *Mol Cell Biol*. 1995;15(4):1858–69.
140. Igarashi Y, Chosa N, Sawada S, Kondo H, Yaegashi T, Ishisaki A. VEGF-C and TGF- β reciprocally regulate mesenchymal stem cell commitment to differentiation into lymphatic endothelial or osteoblastic phenotypes. *Int J Mol Med*. 2016;37(4):1005–13.
141. Wozney JM, Rosen V, Celeste AJ, Mitsock LM, Whitters MJ, Kriz RW, et al. Novel regulators of bone formation: molecular clones and activities. *Science*. 1988;242(4885):1528–34. Available from: <http://www.ncbi.nlm.nih.gov/pubmed/3201241>.
142. Shirakabe K, Terasawa K, Miyama K, Shibuya H, Nishida E. Regulation of the activity of the transcription factor Runx2 by two homeobox proteins, Msx2 and Dlx5. *Genes Cells*. 2001;6(10):851–6. Available from: <http://www.ncbi.nlm.nih.gov/pubmed/11683913>.
143. Felin JE, Mayo JL, Loos TJ, Jensen JD, Sperry DK, Gaufin SL, et al. Nuclear variants of bone morphogenetic proteins. *BMC Cell Biol*. 2010;11:20. Available from: <http://www.ncbi.nlm.nih.gov/pubmed/20230640>.
144. Tan TY, Gonzaga-Jauregui C, Bhoj EJ, Strauss KA, Brigatti K, Puffenberger E, et al. Monoallelic BMP2 variants predicted to result in Haplo insufficiency cause craniofacial, skeletal, and cardiac features overlapping those of 20p12 deletions. *Am J Hum Genet*. 2017;101(6):985–94.
145. Mailman MD, Feolo M, Jin Y, Kimura M, Tryka K, Bagoutdinov R, et al. The NCBI dbGaP database of genotypes and phenotypes. *Nat Genet*. 2007;39(10):1181–6.
146. Zhao HJ, Klausen C, Li Y, Zhu H, Wang YL, Leung PCK. Bone morphogenetic protein 2 promotes human trophoblast cell invasion by upregulating N-cadherin via non-canonical SMAD2/3 signaling. *Cell Death Dis*. 2018a;1:9(2).
147. Zhao HJ, Chang HM, Zhu H, Klausen C, Li Y, Leung PCK. Bone morphogenetic protein 2 promotes human trophoblast cell invasion by inducing activin A production. *Endocrinology*. 2018b;159(7):2815–25.
148. Wang G, Zhang Z, Chen C, Zhang Y, Zhang C. Dysfunction of WNT4/WNT5A in deciduas: possible relevance to the pathogenesis of preeclampsia. *J Hypertens*. 2016;34(4):719–27.
149. Bakrania P, Efthymiou M, Klein JC, Salt A, Bunyan DJ, Wyatt A, et al. Mutations in BMP4 cause eye, brain, and digit developmental anomalies: overlap between the BMP4 and hedgehog signaling pathways. *Am J Hum Genet*. 2008;82(2):304–19.
150. Cheng H, Jiang W, Phillips FM, Haydon RC, Peng Y, Zhou L, et al. Osteogenic activity of the fourteen types of human bone morphogenetic proteins (BMPs). *J Bone Joint Surg Ser A*. 2003;85(8):1544–52.
151. Jiao K, Kulesa H, Tompkins K, Zhou Y, Batts L, Baldwin HS, et al. An essential role of Bmp4 in the atrioventricular septation of the mouse heart. *Genes Dev*. 2003;17(19):2362–7.
152. Liu W, Selever J, Wang D, Lu MF, Mosest KA, Schwartz RJ, et al. Bmp4 signaling is required for outflow-tract septation and branchial-arch artery remodeling. *Proc Natl Acad Sci U S A*. 2004;101(13):4489–94.
153. Liu W, Selever J, Murali D, Sun X, Brugger SM, Ma L, et al. Threshold-specific requirements for Bmp4 in mandibular development. *Dev Biol*. 2005;283(2):282–93.
154. Roberts RM, Ezashi T, Sheridan MA, Yang Y. Specification of trophoblast from embryonic stem cells exposed to BMP4. *Biol Reprod*. 2018;99:212–24.
155. Yabe S, Alexenko AP, Amita M, Yang Y, Schust DJ, Sadovsky Y, et al. Comparison of syncytiotrophoblast generated from human embryonic stem cells and from term placentas. *Proc Natl Acad Sci U S A*. 2016;113(19):E2598–607.
156. Jebbink JM, Boot RG, Keijser R, Moerland PD, Aten J, Veenboer GJM, et al. Increased glucocerebrosidase expression and activity in preeclamptic placenta. *Placenta*. 2015;36(2):160–9.
157. Home P, Kumar RP, Ganguly A, Saha B, Milano-Foster J, Bhattacharya B, et al. Genetic redundancy of GATA factors in the extraembryonic trophoblast lineage ensures the progression of preimplantation and postimplantation mammalian development. *Development*. 2017;144(5):876–88.
158. Dudley AT, Lyons KM, Robertson EJ. A requirement for bone morphogenetic protein-7 during development of the mammalian kidney and eye. *Genes Dev*. 1995;9(22):2795–807.

159. Shafiee A, Baldwin JG, Patel J, Holzapfel BM, Fisk NM, Khosrotehrani K, et al. Fetal bone marrow-derived mesenchymal stem/stromal cells enhance humanization and bone formation of BMP7 loaded scaffolds. *Biotechnol J*. 2017;12(2) <https://doi.org/10.1002/biot.201700414>.
160. Fischer C, Jonckx B, Mazzone M, Zaccogna S, Loges S, Pattarini L, et al. Anti-PIGF inhibits growth of VEGF(R)-inhibitor-resistant tumors without affecting healthy vessels. *Cell*. 2007;131(3):463–75.
161. Oliveira MS. Placental-derived stem cells: culture, differentiation and challenges. *World J Stem Cells*. 2015;7(4):769. Available from: <http://www.wjgnet.com/1948-0210/full/v7/i4/769.htm>.
162. Bais C, Wu X, Yao J, Yang S, Crawford Y, McCutcheon K, et al. PIGF blockade does not inhibit angiogenesis during primary tumor growth. *Cell*. 2010;141(1):166–77.
163. Li C, Gonsalves CS, Eiyomo Mwa Mpollo M-S, Malik P, Tahara SM, Kalra VK. MicroRNA 648 targets ET-1 mRNA and is cotranscriptionally regulated with MICAL3 by PAX5. *Mol Cell Biol*. 2015;35(3):514–28.
164. Parchem JG, Kanasaki K, Kanasaki M, Sugimoto H, Xie L, Hamano Y, et al. Loss of placental growth factor ameliorates maternal hypertension and preeclampsia in mice. *J Clin Invest*. 2018;128(11):5008–17.
165. Ren Z, Cui N, Zhu M, Khalil RA. Placental growth factor reverses decreased vascular and uteroplacental MMP-2 and MMP-9 and increased MMP-1 and MMP-7 and collagen types I and IV in hypertensive pregnancy. *Am J Physiol Heart Circ Physiol*. 2018;315(1):H33–47.
166. Kurtoglu E, Avci B, Kokcu A, Celik H, Dura MC, Malatyalioglu E, et al. Serum VEGF and PGF may be significant markers in prediction of severity of preeclampsia. *J Matern Neonatal Med*. 2016;29(12):1987–92.
167. Chen J, Khalil RA. Matrix metalloproteinases in normal pregnancy and preeclampsia. *Prog Mol Biol Transl Sci*. 2017;148:87–165. Available from: <http://www.ncbi.nlm.nih.gov/pubmed/28662830>.
168. Wu WB, Xu YY, Cheng WW, Yuan B, Zhao JR, Wang YL, et al. Decreased PGF may contribute to trophoblast dysfunction in fetal growth restriction. *Reproduction*. 2017;154(3):319–29.
169. Matjila M, Millar R, van der Spuy Z, Katz A. The differential expression of Kiss1, MMP9 and angiogenic regulators across the fetomaternal interface of healthy human pregnancies: implications for trophoblast invasion and vessel development. *PLoS One*. 2013;16:8(5).
170. Anacker J, Segerer SE, Hagemann C, Feix S, Kapp M, Bausch R, et al. Human decidua and invasive trophoblasts are rich sources of nearly all human matrix metalloproteinases. *Mol Hum Reprod*. 2011;17(10):637–52.
171. Yabluchanskiy A, Ma Y, Iyer RP, Hall ME, Lindsey ML. Matrix metalloproteinase-9: Many shades of function in cardiovascular disease. *Physiology*. 2013;28:391–403.
172. Apicella C, Ruano CSM, Méhats C, Miralles F, Vaiman D. The role of epigenetics in placental development and the etiology of preeclampsia. *Int J Mol Sci*. 2019;20(11):E2837. Available from: <http://www.ncbi.nlm.nih.gov/pubmed/31212604>.
173. Li X, Wu C, Shen Y, Wang K, Tang L, Zhou M, et al. Ten-eleven translocation 2 demethylates the MMP9 promoter, and its down-regulation in preeclampsia impairs trophoblast migration and invasion. *J Biol Chem*. 2018;293(26):10059–70.
174. Plaks V, Rinkenberger J, Dai J, Flannery M, Sund M, Kanasaki K, et al. Matrix metalloproteinase-9 deficiency phenocopies features of preeclampsia and intrauterine growth restriction. *Proc Natl Acad Sci U S A*. 2013;110(27):11109–14.
175. Gibson DA, Simitsidellis I, Kelepouri O, Critchley HOD, Saunders PTK. Dehydroepiandrosterone enhances decidualization in women of advanced reproductive age. *Fertil Steril*. 2018;109(4):728–734.e2.
176. Johnson GA, Burghardt RC, Bazer FW, Spencer TE. Osteopontin: roles in implantation and placental development. *Biol Reprod*. 2003;69(5):1458–71.
177. Basu J, Agamasu E, Bendek B, Salafia CM, Mishra A, Lopez JV, et al. Correlation between placental matrix metalloproteinase 9 and tumor necrosis factor- α protein expression throughout gestation in normal human pregnancy. *Reprod Sci*. 2018;25(4):621–7. Available from: <http://www.ncbi.nlm.nih.gov/pubmed/28820024>.
178. Basu J, Agamasu E, Bendek B, Salafia CM, Mishra A, Benfield N, et al. Placental tumor necrosis factor- α protein expression during normal human gestation. *J Matern Fetal Neonatal Med*. 2016;29(24):3934–8. Available from: <http://www.ncbi.nlm.nih.gov/pubmed/26988271>.

179. Weel IC, Baergen RN, Romão-Veiga M, Borges VT, Ribeiro VR, Witkin SS, et al. Association between placental lesions, cytokines and angiogenic factors in pregnant women with pre-eclampsia. *PLoS One*. 2016;11(6):e0157584.
180. Straface G, Biscetti F, Pitocco D, Bertoletti G, Misuraca M, Vincenzoni C, et al. Assessment of the genetic effects of polymorphisms in the osteoprotegerin gene, TNFRSF11B, on serum osteoprotegerin levels and carotid plaque vulnerability. *Stroke*. 2011;42(11):3022–8.
181. Puscheck EE, Awonuga AO, Yang Y, Jiang Z, Rappolee DA. Molecular biology of the stress response in the early embryo and its stem cells. *Adv Exp Med Bio*. 2015;843:77–128. Available from: <http://www.ncbi.nlm.nih.gov/pubmed/25956296>.
182. Fu J, Zhao L, Wang L, Zhu X. Expression of markers of endoplasmic reticulum stress-induced apoptosis in the placenta of women with early and late onset severe pre-eclampsia. *Taiwan J Obstet Gynecol*. 2015;54(1):19–23.
183. Mizuuchi M, Cindrova-Davies T, Olovsson M, Charnock-Jones DS, Burton GJ, Yung HW. Placental endoplasmic reticulum stress negatively regulates transcription of placental growth factor via ATF4 and ATF6 β : implications for the pathophysiology of human pregnancy complications. *J Pathol*. 2016;238(4):550–61.
184. Lin ME, Chen TM, Wallingford MC, Nguyen NB, Yamada S, Sawangmake C, et al. Runx2 deletion in smooth muscle cells inhibits vascular osteochondrogenesis and calcification but not atherosclerotic lesion formation. *Cardiovasc Res*. 2016;112(2):606.
185. Heo JS, Choi Y, Kim HS, Kim HO. Comparison of molecular profiles of human mesenchymal stem cells derived from bone marrow, umbilical cord blood, placenta and adipose tissue. *Int J Mol Med*. 2016;37(1):115–25.
186. Ulrich C, Rolauffs B, Abele H, Bonin M, Nieselt K, Hart ML, et al. Low osteogenic differentiation potential of placenta-derived mesenchymal stromal cells correlates with low expression of the transcription factors Runx2 and Twist2. *Stem Cells Dev*. 2013;22(21):2859–72.
187. Cohen GI, Aboufakher R, Bess RB, Frank J, Othman M, Doan D, et al. Relationship between carotid disease on ultrasound and coronary disease on CT angiography. *JACC Cardiovasc Imaging*. 2013;6(11):1160–7.
188. Komori T, Yagi H, Nomura S, Yamaguchi A, Sasaki K, Deguchi K, et al. Targeted disruption of Cbfa1 results in a complete lack of bone formation owing to maturational arrest of osteoblasts. *Cell*. 1997;89(5):755–64. Available from: <http://www.ncbi.nlm.nih.gov/pubmed/9182763>.
189. Peng B, Zhu H, Klausen C, Ma L, Wang YL, Leung PCK. GnRH regulates trophoblast invasion via RUNX2-mediated MMP2/9 expression. *Mol Hum Reprod*. 2015;22(2):119–29.
190. Wang Q, Wu W, Han X, Zheng A, Lei S, Wu J, et al. Osteogenic differentiation of amniotic epithelial cells: synergism of pulsed electromagnetic field and biochemical stimuli. *BMC Musculoskelet Disord*. 2014;15:251.
191. Wright E, Audette MC, Ye XY, Keating S, Hoffman B, Lye SJ, et al. Maternal vascular malperfusion and adverse perinatal outcomes in low-risk nulliparous women. *Obstet Gynecol*. 2017;130(5):1112–20.
192. Kent J, Wheatley SC, Andrews JE, Sinclair AH, Koopman P. A male-specific role for SOX9 in vertebrate sex determination. *Development*. 1996;122(9):2813.
193. Akiyama H. Control of chondrogenesis by the transcription factor Sox9. *Mod Rheumatol*. 2008;18(3):213–9. Available from: <http://www.ncbi.nlm.nih.gov/pubmed/18351289>
194. Milona MA, Gough JE, Edgar AJ. Expression of alternatively spliced isoforms of human Sp7 in osteoblast-like cells. *BMC Genomics*. 2003;7:4.
195. Gao Y, Jheon A, Nourkeyhani H, Kobayashi H, Ganss B. Molecular cloning, structure, expression, and chromosomal localization of the human Osterix (SP7) gene. *Gene*. 2004;341(1–2):101–10.
196. Matsubara T, Kida K, Yamaguchi A, Hata K, Ichida F, Meguro H, et al. BMP2 regulates Osterix through Msx2 and Runx2 during osteoblast differentiation. *J Biol Chem*. 2008;283(43):29119–25. Available from: <http://www.ncbi.nlm.nih.gov/pubmed/18703512>.
197. Jin Y, Cong Q, Gvozdenovic-Jeremic J, Hu J, Zhang Y, Terkeltaub R, et al. Enpp1 inhibits ectopic joint calcification and maintains articular chondrocytes by repressing hedgehog signaling. *Development*. 2018;145(18):dev164830.

198. Dedinszki D, Szeri F, Kozák E, Pomozi V, Tőkési N, Mezei TR, et al. Oral administration of pyrophosphate inhibits connective tissue calcification. *EMBO Mol Med*. 2017;9(11):1463–70.
199. Kornak U, Brancati F, Le Merrer M, Lichtenbelt K, Höhne W, Tinschert S, et al. Three novel mutations in the ANK membrane protein cause craniometaphyseal dysplasia with variable conductive hearing loss. *Am J Med Genet Part A*. 2010;152(4):870–4.
200. Orimo H. The mechanism of mineralization and the role of alkaline phosphatase in health and disease. *J Nippon Med Sch*. 2010;77(1):4–12. Available from: <http://www.ncbi.nlm.nih.gov/pubmed/20154452>.
201. Winn VD, Haimov-Kochman R, Paquet AC, Yang YJ, Madhusudhan MS, Gormley M, et al. Gene expression profiling of the human maternal-fetal interface reveals dramatic changes between midgestation and term. *Endocrinology*. 2007;148(3):1059–79.
202. Hu Y, Liu XP, Liu XX, Zheng YF, Liu WF, Luo ML, et al. Role of axl in preeclamptic EPCs functions. *J Huazhong Univ Sci Technol – Med Sci*. 2016;36(3):395–401.
203. Nielsen CH, Larsen A, Nielsen AL. DNA methylation alterations in response to prenatal exposure of maternal cigarette smoking: a persistent epigenetic impact on health from maternal lifestyle? *Arch Toxicol*. 2016;90:231–45.
204. Hanna CW, McFadden DE, Robinson WP. DNA methylation profiling of placental villi from karyotypically normal miscarriage and recurrent miscarriage. *Am J Pathol*. 2013;182(6):2276–84.
205. Sage AP, Tintut Y, Demer LL. Regulatory mechanisms in vascular calcification. *Nat Rev Cardiol*. 2010;7(9):528–36. Available from: <http://www.ncbi.nlm.nih.gov/pubmed/20664518>.
206. Demer LL, Tintut Y. Inflammatory, metabolic, and genetic mechanisms of vascular calcification. *Arterioscler Thromb Vasc Biol*. 2014;34(4):715–23. Available from: <http://www.ncbi.nlm.nih.gov/pubmed/24665125>.
207. Wu M, Rementer C, Giachelli CM. Vascular calcification: an update on mechanisms and challenges in treatment. *Calcif Tissue Int*. 2013;93(4):365–73.
208. Bäck M, Aranyi T, Cancela ML, Carracedo M, Conceição N, Leftheriotis G, et al. Endogenous calcification inhibitors in the prevention of vascular calcification: a consensus statement from the COST action EuroSoftCalcNet. *Front Cardiovasc Med*. 2019;18:5.
209. Proudfoot D, Skepper JN, Shanahan CM, Weissberg PL. Calcification of human vascular cells in vitro is correlated with high levels of matrix Gla protein and low levels of osteopontin expression. *Arterioscler Thromb Vasc Biol*. 1998;18(3):379–88.
210. Proudfoot D, Shanahan CM. Molecular mechanisms mediating vascular calcification: role of matrix Gla protein (review article). *Nephrology*. 2006;11:455–61.
211. Whitley JC, Giraud AS, Shulkes A. Expression of gastrin-releasing peptide (GRP) and GRP receptors in the pregnant human uterus at term. *J Clin Endocrinol Metab*. 1996;81(11):3944–50. Available from: <https://academic.oup.com/jcem/article-lookup/doi/10.1210/jcem.81.11.8923842>.
212. Martínez A, Zudaire E, Julián M, Moody TW, Cuttitta F. Gastrin-releasing peptide (GRP) induces angiogenesis and the specific GRP blocker 77427 inhibits tumor growth in vitro and in vivo. *Oncogene*. 2005;24(25):4106–13. Available from: <http://www.ncbi.nlm.nih.gov/pubmed/15750618>.
213. Hamamura K, Yanagida M, Ishikawa H, Banzai M, Yoshitake H, Nonaka D, et al. Quantitative measurement of a candidate serum biomarker peptide derived from α 2-HS-glycoprotein, and a preliminary trial of multidimensional peptide analysis in females with pregnancy-induced hypertension. *Ann Clin Biochem*. 2018;55(2):287–95.
214. Molvarec A, Kalabay L, Derzsy Z, Szarka A, Halmos A, Stenczer B, et al. Preeclampsia is associated with decreased serum α 2-HS glycoprotein (fetuin-A) concentration. *Hypertens Res*. 2009;32(8):665–9.
215. Tsurubuchi T, Allender EV, Siddiqui MR, Shim KW, Ichi S, Boshnjaku V, et al. A critical role of noggin in developing folate-nonresponsive NTD in Fkbp8 $-/-$ embryos. *Childs Nerv Syst*. 2014;30(8):1343–53.
216. Brunet LJ, McMahan JA, McMahan AP, Harland RM. Noggin, cartilage morphogenesis, and joint formation in the mammalian skeleton. *Science*. 1998;280(5368):1455–7. Available from: <http://www.ncbi.nlm.nih.gov/pubmed/9603738>.

217. Groppe J, Greenwald J, Wiater E, Rodriguez-Leon J, Economides AN, Kwiatkowski W, et al. Structural basis of BMP signalling inhibition by the cystine knot protein Noggin. *Nature*. 2002;420(6916):636–42.
218. Scott IC, Blitz IL, Pappano WN, Imamura Y, Clark TG, Steiglitiz BM, et al. Mammalian BMP-1/Tolloid-related metalloproteinases, including novel family member mammalian Tolloid-like 2, have differential enzymatic activities and distributions of expression relevant to patterning and skeletogenesis. *Dev Biol*. 1999;213(2):283–300.
219. Nakagawa Y, Ikeda K, Akakabe Y, Koide M, Uraoka M, Yutaka KT, et al. Paracrine osteogenic signals via bone morphogenetic protein-2 accelerate the atherosclerotic intimal calcification in vivo. *Arterioscler Thromb Vasc Biol*. 2010;30(10):1908–15.
220. Kwong FNK, Richardson SM, Evans CH. Chordin knockdown enhances the osteogenic differentiation of human mesenchymal stem cells. *Arthritis Res Ther*. 2008;10(3):R65. Available from: <http://www.ncbi.nlm.nih.gov/pubmed/18533030>.
221. Mulla MJ, Weel IC, Potter JA, Gysler SM, Salmon JE, Peraçoli MTS, et al. Antiphospholipid antibodies inhibit trophoblast toll-like receptor and inflammasome negative regulators. *Arthritis Rheumatol*. 2018;70(6):891–902.
222. Verdugo RA, Zeller T, Rotival M, Wild PS, Münzel T, Lackner KJ, et al. Graphical modeling of gene expression in monocytes suggests molecular mechanisms explaining increased atherosclerosis in smokers. *PLoS One*. 2013;8(1):e50888.
223. Hassan MQ, Javed A, Morasso MI, Karlin J, Montecino M, van Wijnen AJ, et al. Dlx3 transcriptional regulation of osteoblast differentiation: temporal recruitment of Msx2, Dlx3, and Dlx5 homeodomain proteins to chromatin of the osteocalcin gene. *Mol Cell Biol*. 2004;24(20):9248–61. Available from: <http://www.ncbi.nlm.nih.gov/pubmed/15456894>.
224. Bai Q, Assou S, Haouzi D, Ramirez JM, Monzo C, Becker F, et al. Dissecting the first transcriptional divergence during human embryonic development. *Stem Cell Rev Reports*. 2012;8(1):150–62.
225. Liang H, Zhang Q, Lu J, Yang G, Tian N, Wang X, et al. MSX2 induces trophoblast invasion in human placenta. *PLoS One*. 2016;11(4):e0153656.
226. Sun H, Qu H, Chen L, Wang W, Liao Y, Zoue L, et al. Identification of suspicious invasive placentation based on clinical MRI data using textural features and automated machine learning. *Eur Radiol*. 2019;29:6152.
227. Hsu CW, Wong L, Rasmussen TL, Kalaga S, McElwee ML, Keith LC, et al. Three-dimensional microCT imaging of mouse development from early post-implantation to early postnatal stages. *Dev Biol*. 2016;419(2):229–36.
228. Dickinson ME. Multimodal imaging of mouse development: tools for the postgenomic era. *Dev Dyn*. 2006;235(9):2386–400. Available from: <http://www.ncbi.nlm.nih.gov/pubmed/16871621>.
229. Chen CY, Su HW, Pai SH, Hsieh CW, Jong TL, Hsu CS, et al. Evaluation of placental maturity by the sonographic textures. *Arch Gynecol Obstet*. 2011b;284(1):13–8.
230. Romeo V, Ricciardi C, Cuocolo R, Stanzione A, Verde F, Sarno L, et al. Machine learning analysis of MRI-derived texture features to predict placenta accreta spectrum in patients with placenta previa. *Magn Reson Imaging*. 2019;64:71.
231. Looney P, Stevenson GN, Nicolaidis KH, Plasencia W, Molloholli M, Natsis S, et al. Fully automated, real-time 3D ultrasound segmentation to estimate first trimester placental volume using deep learning. *JCI Insight*. 2018;3:120178.
232. Gupta L, Sisodia RS, Pallavi V, Firion C, Ramachandran G. Segmentation of 2D fetal ultrasound images by exploiting context information using conditional random fields. In: *Proceedings of the annual international conference of the IEEE Engineering in Medicine and Biology Society, EMBS, Boston*. 2011. p. 7219–22.
233. Barker DJP, Osmond C. Infant mortality, childhood nutrition, and ischaemic heart disease in England and Wales. *Lancet*. 1986;1(8489):1077–81.
234. Barker DJP, Osmond C, Winter PD, Margetts B, Simmonds SJ. Weight in infancy and death from ischaemic heart disease. *Lancet*. 1989;2(8663):577–80.
235. Barker DJP, Godfrey KM, Gluckman PD, Harding JE, Owens JA, Robinson JS. Fetal nutrition and cardiovascular disease in adult life. *Lancet*. 1993;341(8850):938–41.
236. Barker DJP. The origins of the developmental origins theory. *J Intern Med*. 2007;261:412–7.

Chapter 14

Heterotopic Ossification Following Traumatic Blast Injury



Thomas E. Robinson, Sophie C. Cox, and Liam M. Grover

Abbreviations

AHO	Albright hereditary osteodystrophy
ALK	Activin receptor-like kinase
ALP	Alkaline phosphatase
ATP	Adenosine triphosphate
BMP	Bone morphogenetic protein
BNB	Blood-nerve barrier
cAMP	Cyclic adenosine monophosphate
CGRP	Calcitonin gene-related peptide
CNS	Central nervous system
COX	Cyclooxygenase
CT	Computed tomography
FDA	Food and Drug Administration
FOP	Fibrodysplasia ossificans progressiva
HIF	Hypoxia-inducible transcription factor
HO	Heterotopic ossification
IED	Improvised explosive device
IGF	Insulin-like growth factor
IL	Interleukin
IP	Interferon gamma-induced protein
MCP	Monocyte chemoattractant protein
MIP	Macrophage inflammatory protein
MMP	Matrix metalloprotein
MRSA	<i>Methicillin-resistant Staphylococcus aureus</i>

T. E. Robinson · S. C. Cox · L. M. Grover (✉)
School of Chemical Engineering, University of Birmingham, Edgbaston, Birmingham, UK
e-mail: TER281@student.bham.ac.uk; S.C.Cox@bham.ac.uk; L.M.Grover@bham.ac.uk

MSC	Mesenchymal stem cell
NSAID	Non-steroidal anti-inflammatory drug
POH	Progressive osseous heteroplasia
RAR	Retinoic acid receptor
SCI	Spinal cord injury
SP	Substance P
TBI	Traumatic brain injury
TGF	Transforming growth factor
TNF	Tumour necrosis factor
VEGF	Vascular endothelial growth factor

Blast Injury

Blast is the mechanism of injury that results following explosion. Blast injuries fall into four categories [1]:

1. Primary – the wave of blast overpressure passing through the body
2. Secondary – caused by debris hitting the body
3. Tertiary – caused by the body hitting an object
4. Quaternary – all other injuries, including crushing and burns

These types of injuries have likely existed since the first utilisation of explosives [2]. The original explosive, black powder, was invented in China in the ninth century for use in rockets, eventually guns and canon in the fourteenth century, and mining in the seventeenth century [3]. A mixture of naturally occurring compounds, black powder was only replaced with the advent of organic chemistry in the nineteenth century, and the production of the infamously unstable nitroglycerin. This was followed by compounds such as 2,4,6-trinitrotoluene (TNT), hexahydro-1,3,5-trinitro-1,3,5-triazine (RDX), and octahydro-1,3,5,7-tetranitro-1,3,5,7-tetrazocine (HMX), the explosives of choice today [4].

Accidental blast injuries, for example, from industrial incidents, are rare in civilian life though they do happen [5]. Explosions caused by deliberate action are far more notorious: terrorist explosive events have increased with the turn of the century, with a fourfold rise in occurrence and an eightfold increase in injury between 1999 and 2006 [6]. However, blast injuries are most common in warfare, particularly in recent conflicts. Blast accounted for only 9% of injuries in the American Civil War (1861–1865), and 35% in the Great War (1914–1918) [7]. Figures then rose in the later twentieth-century wars, until blast became the dominant injury mechanism in the recent conflicts in Iraq and Afghanistan. Between 70 and 80% of injuries to British and American soldiers in these conflicts were as a result of blast, the highest in any recent conflict [8–10]. The majority of these injuries were caused by improvised explosive devices (IEDs), which gave rise to over 70% of combat casualties in Iraq and 50% in Afghanistan, the most significant threat to the soldiers in these regions [11, 12]. In addition, 43–54% of wounds occurred in the extremities, the most commonly injured area in these conflicts [8, 9]. This is in contrast to thoracic injury, which made up only 5% of wounds in these conflicts, reduced from 13% in the Second World War.

Heterotopic Ossification

Aetiology and Epidemiology

Heterotopic ossification (HO) is the formation of bone where it ought not to exist. Etymologically, the term is derived from the Greek *hetero topos* (other place) and the Latin *ossification* (bone making). Different types of bone have been reported in HO, and indeed different types of bone may form depending on aetiology. Analysis of trauma-related HO revealed that it is composed of a heterogeneous mix of cortical and cancellous bone, in addition to fibrocartilage, with varying levels of mineralisation [13]. Like skeletal bone, the structure of which is discussed in detail in Chap. 17, HO contains arterioles, Haversian canals, and bone marrow and is subject to continuous remodelling, even after 3 years following presumed ‘maturation’ of the bone. These features of HO separate it from the mere calcification of tissues; HO is structured and organised at the cellular level, with a microstructure like orthotopic bone (Fig. 14.1). Macroscopically, however, HO is very different to skeletal bone. It grows polyaxially and appears floral in form, intimately associated with the soft tissue. It has also been reported to grow faster than skeletal bone, at 1.7 μm per day compared to the 1.0 μm per day of normal bone [14].

HO is not a new phenomenon; it was first described by Albucasis, the father of surgery, over a millennium ago [15]. Patin, the Doyen of the Faculty of Medicine in Paris, then described the condition in children in 1692 [16]. The disorder he described is now commonly called fibrodysplasia ossificans progressiva (FOP), a rare genetic form of HO. FOP is characterised by malformation of the hallux at birth, but is followed by gradual HO in the soft tissues, which can be exacerbated by even the smallest of traumatic events [17]. The cumulative effects of this ossification lead to gradual immobility and, ultimately, early death. Other genetic causes of HO include progressive osseous heteroplasia (POH), the intramembranous

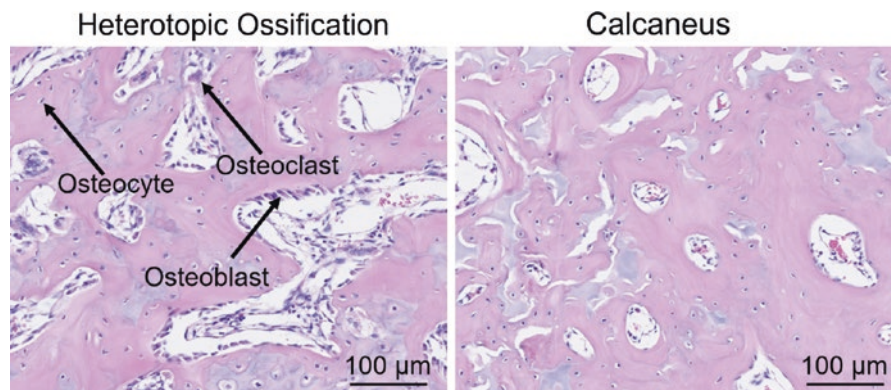


Fig. 14.1 Comparison of HO and skeletal bone (calcaneus) in a rodent, showing similar microstructure and osteocyte density but vastly increased numbers of osteoblasts and osteoclasts

ossification of dermal tissue, Albright hereditary osteodystrophy (AHO), and other similar conditions [18].

Thankfully, the genetic forms of HO are extremely rare; global incidence of FOP is one in two million [19]. However, the acquired form is far more common. HO can form following musculoskeletal trauma, including surgery, damage to the central nervous system (CNS), particularly traumatic brain injury (TBI) and spinal cord injury (SCI), and burns [20]. In addition, perhaps the most devastating cause of acquired HO is that following blast trauma. While it may be asymptomatic, HO can cause chronic pain, ulceration of the skin, particularly when the ectopic bone forms over a skin graft, ankylosis of the joints, arthrofibrosis, neurovascular entrapment, and issues with fitting and utilising prosthetic limbs [21].

The association between HO and combat is not new; one of the first descriptions of acquired HO was made following observations from the American Civil War and the Great War [22]. However, prevalence of HO in soldiers has recently increased due to two key reasons. The first, as discussed above is the rising use of IEDs making blast the predominant injury mechanism of injury, and the extremities the primary zone of wounding. The second is the increased survival rate, due to improved body armour, ubiquitous tourniquet use, improved air evacuation and care, haemostatic dressings, and other modern survival innovations [23–26]. Because of this, more people with multiple limb loss are surviving their injuries [27]. It is this combination of a higher survival rate but an increased incidence of severe extremity injury which has caused the recent upsurge in HO formation in wounded combatants [28].

The prevalence of HO in combat-related amputees has been consistently reported as around 63%. Risk factors include a blast mechanism, amputation through the zone of injury, presence and severity of TBI, an age less than 30, multiple extremity injuries, delayed wound healing, a high injury severity score, and bacterial colonisation [29–31]. In contrast, the rate of HO is only around 23% in civilian (non-blast-related) amputees, and the HO was mild in 94% of these cases [32]. This corroborates the finding that blast, and not just amputation, is a risk factor for HO. Non-blast cases may also be less likely to have TBI, and other risk factors for HO (Table 14.1).

Biology

Environment/Inflammation

With the exception of POH and AHO, which are formed by intramembranous ossification, HO, including FOP, is a process of endochondral bone formation. The formation of HO therefore requires three key things: osteoprogenitor cells, capable of differentiating into endochondral bone-forming cells, the signalling pathways that induce this differentiation, and a local environment which is conducive to bone formation [33]. The disease progression pathway of acquired HO begins with an inciting event, such as a blast injury, which causes an inflammatory response and the

Table 14.1 Clinical and biological risk factors for combat-related HO

Clinical	Biological
Blast mechanism of injury	Hypoxia
Extremity injuries (presence and number)	<i>Serum cytokines:</i>
High injury severity score	IL-3
Amputation (particularly through the zone of injury)	IL-6
Traumatic brain injury (presence and severity)	IL-10
Age (<30 years)	IL-12p70
Delayed wound healing	MCP1
Bacterial colonisation	<i>Wound effluent cytokines:</i>
	IL-3
	IL-13
	IP-10
	MIP-1 α

cell-signalling cascade that induces cells to differentiate and begin forming bone [34]. These cells may be local to the injury site, or recruited from circulation.

Inflammation is a common requisite to all types of HO. Macrophages, mast cells, and adaptive immune cells are known to play a role; the exact inflammatory mechanism that leads to HO remains unknown [35]. Inflammation precedes mineralisation, and as such anti-inflammatory therapies may be effective in preventing HO, but do not affect HO formation once mineralisation has begun. The inflammatory response following severe trauma is highly complex, with local and systemic components, acute and chronic factors, and an associated anti-inflammatory response [36]. Tissue analysis of combat-injured patients showed that formation of HO was associated with high levels of interleukins 3, 6, 10, and 12p70, monocyte chemoattractant protein 1 (MCP1/CCL2) in the serum, and interleukins 3 and 13, interferon gamma-induced protein 10 (IP-10/CXCL10), and macrophage inflammatory protein 1 alpha (MIP-1 α /CCL3) in the wound effluent, in addition to bacterial colonisation [37, 38]. A summary of both the clinical and biological risk factors for combat-related HO is given in Table 14.1.

Hypoxia is also a prerequisite condition for the formation of HO, as it is for normal bone, that stimulates hypoxia-inducible transcription factor 1 alpha (HIF1 α) [39]. HIF1 α has roles in cartilage proliferation and differentiation, as well as angiogenesis and osteogenesis, all of which are critical in osteochondral bone formation [40]. HIF1 α upregulates vascular endothelial growth factor (VEGF) and transcription factor SOX9, critical for angiogenesis and chondrogenesis, respectively. Both of these factors are upregulated in cells derived from patients with high-energy combat injuries who developed HO, along with a host of others including matrix metalloprotein 9 (MMP9) and insulin-like growth factor 2 (IGF2) [41]. It has also been suggested that the increased use of tourniquets, in addition to saving lives, may contribute to the increased incidence of HO by inducing hypoxia in the residual limb [42].

Cells

In addition to the necessary environment and the signals that induce osteochondral differentiation, there needs to be a population of cells both able and available to differentiate down this lineage. Perhaps the most promising candidate is the mesenchymal stem cell (MSC), a multipotent stromal cell which can differentiate into chondroblasts, osteoblasts, and brown adipocytes and form endochondral bone when implanted in vivo [43, 44]. MSCs were found in the debrided extremity muscle of combat-injured patients, and were found to have increased alkaline phosphatase (ALP) expression and mineralised matrix production compared to bone marrow-derived MSCs, and did not terminally differentiate [45, 46]. Additionally, MSCs were found to be fewer in number and less able to differentiate with increased age, correlating with the decrease in HO seen with age [47, 48]. When pretreated in hypoxic conditions, MSCs displayed an enhanced angiogenic capacity, increased VEGF production, and decreased apoptosis, showing that MSCs thrive in the hypoxic conditions seen in HO [49].

There are a number of other cell types that have the potential to produce HO. Skeletal muscle cells, myoblasts, have been shown to dedifferentiate and progress through an osteochondral route when exposed to transforming growth factor beta (TGF β), an inflammatory cytokine [50]. In response to bone morphogenetic protein 2 (BMP2), muscle cells were found to produce ALP and participate in HO formation, producing similar amounts of bone to MSCs [51, 52]. In addition to mature muscle cells, muscle stem cells, termed satellite cells, can also differentiate into adipocytes and osteocytes given the proper molecular cues, such as BMP2 [53]. There is also some evidence of these cells undergoing osteogenic differentiation even without BMP2 [54]. However, other studies suggest that satellite cells are terminally differentiated and that these results are due to co-contamination of other cell types [55]. A FOP model showed that smooth muscle cells don't contribute to HO, and the contribution of skeletal muscle progenitors was <5% [56].

A recently proposed source of cells is from the endoneurium. These cells have been shown to express osteogenic factors and to travel through the general circulation to the site of HO in a mouse model [57]. Either direct trauma, for example, from blast, or BMP2 can initiate the neuroinflammatory cascade. This involves the release of pain mediators, substance P (SP) and calcitonin gene-related peptide (CGRP), which recruit mast cells that in turn degranulate to release chemokines and recruit cells that open the blood-nerve barrier (BNB) [58]. This opening, which may be controlled by histamines secreted by mast cells or MMP9, allows the perineurial and endoneurial cells to cross the BNB [59]. SP has been found to be upregulated in both traumatic HO and FOP lesions, and preventing the SP signalling pathway at any point has been shown to inhibit injury-induced HO [60].

Additional potential contributors include epithelial cells, endothelial cells, and pericytes. Epithelial cells can transform into MSCs, which are known to occur during embryonic gastrulation and triggered by BMP and TGF β [61, 62].

Both of these factors were found to be overexpressed by the epithelial cells in the HO lesions of transgenic mice [63]. Endothelial cells are similarly able to transform into MSCs when exposed to TGF β [64]. Chondrocytes and osteoblasts in FOP lesions were found to express endothelial markers, suggesting a vascular endothelial origin, and brown adipose tissue may share this origin [65, 66]. A different study suggested that cells of endothelial origin contributed 40–50% of cells in a FOP model [56]. However, the role of these cell types may be less direct. Some studies suggest that epithelial cells do not differentiate into osteoblasts, but instead secrete factors that induce osteochondral differentiation in other cells [67]. Endothelial cells release paracrine factors that induce chondrocyte hypertrophy, which are not secreted by myoblasts, fibroblasts, or other hypertrophic chondrocytes [68]. Further, the angiogenic growth factor Ang1 enhances BMP2 signalling, osteoblast differentiation, and ectopic bone formation [69]. Endothelial cells are further important in their own right, as angiogenesis is a key requirement for HO formation. Pericytes, cells which line the outside of capillaries, have been shown to display osteogenic differentiation *in vitro* and *in vivo* [70]. However, these cells have a similar phenotype, gene expression, and differentiation potential to MSCs, making these cells and their potential role difficult to distinguish [71].

Endochondral HO lesions contain several tissue types, in addition to the soft tissue(s) it is formed in, including bone, cartilage, brown fat, and vasculature. The formation of HO thus requires all of the cell types found in these tissues, precisely located in both spatially and temporally. For example, the hypoxic conditions required for chondrogenesis and neovascularisation must precede and be separate from the normoxia required for osteogenesis. It is clear that several cell types have the potential to differentiate into HO forming cells, given the proper cues; however, elucidating which cells play a part in blast-related HO is far more complicated. There may be more than one source for the cells found in HO, and the different cell types that make up HO may have the same or differing precursor cells. It is also important to consider the cells that do not give rise to HO tissue, but have an indirect role by secreting paracrine factors. The cell types required for HO, and potential progenitor cells, are summarised in Table 14.2. Overall, it is clear that HO is a complex biological process, and it is likely that there are several pathways that can lead to it.

Table 14.2 Summary of cell types found in HO tissue and potential progenitor cells

Cell types found in HO	Potential progenitor cells
Osteoblasts	Mesenchymal stem cells
Osteoclasts	Myoblasts
Osteocytes	Satellite cells
Chondroblasts	Perineurial cells
Chondrocytes	Endoneurial cells
Brown adipocytes	Epithelial cells
Endothelial cells	Endothelial cells
	Pericytes

Diagnosis, Prevention, and Treatment

Diagnosis

The initial stages of HO diagnosis are rooted in clinical examination, which can provide some important information. Swelling, stiffness, warmth, and redness are all early signs of HO; however these symptoms are not specific to the condition, and may also indicate thrombophlebitis, cellulitis, myelitis, or a tumour [72]. Once HO is suspected, plain X-ray radiographs are the most common modality to image and monitor lesions. X-ray computed tomography (CT) is more expensive and time-consuming, but provides a more detailed 3D picture, which is a valuable perioperative tool. However, both X-ray modalities can only detect mineralised tissue and thus can only detect HO once mineralisation has begun [73]. Bone scintigraphy is a currently used technique for diagnosis, which can detect HO within 3 weeks of injury, several weeks earlier than radiographs. This technique can also be used to detect lesion maturity in order to correctly time excision surgery and to detect recurrence [74]. Elevation of serum ALP has been suggested as a marker of HO; however, ALP levels are dependent on hepatic and renal function, which may differ in blast-injured patients [75]. In HO caused by SCI, it was found that less than half of patients displayed elevated ALP levels [76]. It has also been proposed that the serum cytokines upregulated in HO may be used for early detection. However, these cytokines may differ by patient and wound type, and may be upregulated by the severe injury experienced by blast-injured patients, rather than specifically indicating HO [20].

New techniques are thus required in order to detect HO earlier, in order to begin a prophylactic regime as soon as possible. Given the issues with detecting serum markers of HO, focus is instead placed on imaging modalities. In Achilles tenotomy plus burn models, ultrasound, near-infrared, and Raman modalities were able to detect HO within a week of injury, which was only visible in microCT after several weeks [77–79]. Ultrasound was found to detect HO in 88.9% of afflicted SCI patients; however, at 62 days the mean interval was similar to confirmation of the condition by CT at a mean interval of 64 days [80]. Near-infrared imaging, though useful, requires the injection of a fluorescent tracer that may make it less attractive than Raman, which does not. In an ex vivo study of tissue from combat-wounded patients, Raman spectroscopy was able to differentiate between uninjured and injured muscle, unmineralised and mineralised HO lesions [81]. This technique can thus measure mineral maturity to aid surgical timing, but also may be used during the operation to identify lesion boundaries.

Current Preventions

Given the historical lack of mechanistic insight into HO formation, current preventions are based around non-specific anti-inflammatories. The exceptions to this are bisphosphonates, molecules with a P-C-P bridge that imitate the role of pyrophosphate in vivo but are not broken down by ALP. This is the only FDA-approved

medication to prevent or treat HO [31]. Bisphosphonates prevent the formation and aggregation of calcium phosphate crystals, and act as crystal poisons after adsorbing to the surfaces, in addition to interfering with biochemical processes when internalised by osteoclasts [82]. However, their efficacy in preventing HO is inconsistently reported. Etidronate, a first-generation bisphosphonate, was reported to lower the rate of HO following TBI and SCI [20]. However, etidronate was also shown to increase incidence of HO in burns patients [83]. A more consistent report, however, is that bisphosphonates only delay mineralisation, which recommences when treatment is stopped [84]. Another consideration is that bisphosphonates may delay fracture union, a common complication following blast injury [85]. However, this only appears to be following prolonged use of the drug, e.g. for osteoporosis, and rarely affects fracture healing when used for the first time following injury [86]. One interesting finding is that nitrogen-containing bisphosphonates hastened HO maturity, leading to prompter surgical excision [87]. However, due to the lack of clear evidence for efficacy, bisphosphonates are rarely administered for prevention of HO.

Commonly utilised prophylaxes for HO include non-steroidal anti-inflammatory drugs (NSAIDs) and radiotherapy. Both of these modalities are most commonly studied, and frequently administered clinically, for the prevention of HO in the hip. NSAIDs inhibit cyclooxygenase-2 (COX2), a key factor required for endochondral ossification, regulating the differentiation of MSCs and preventing angiogenesis [88]. Additionally, NSAIDs have been shown to suppress proliferation and induce apoptosis in osteoblasts and chondrocytes [89]. The efficacy of NSAIDs in preventing HO in the hip is generally taken to be good, though some studies dispute this [90, 91]. However the side effects of NSAIDs, including postoperative bleeding, hepatic and renal toxicity and failure, haematochezia, asthma, gastrointestinal bleeding, and other effects, often lead to discontinuation even in relatively healthy patients [91–94]. Blast-injured patients typically display severe systemic polytrauma, complex contaminated wounds, skeletal fractures, TBI, renal impairment, gastritis, and bleeding, which make the side effects of NSAIDs intolerable [95]. Primary prophylaxis against HO is therefore utilised rarely in combat-related amputees. However, there are attempts to curb these side effects. Local delivery of indomethacin, the most commonly prescribed NSAID for HO prophylaxis, was shown not to inhibit wound healing [96]. Local delivery allows a high concentration at the site, but a low systemic drug concentration, reducing side effects. The majority of NSAIDs utilised, including indomethacin, are non-selective, in that they inhibit both COX1 and COX2. Celecoxib is a selective COX2 inhibitor, which displayed equal efficacy to indomethacin but with fewer gastrointestinal side effects [97]. However, there are concerns about the effect of selective COX2 inhibitors on the cardiovascular system. Despite this, a small clinical trial of celecoxib in blast-injured patients showed a decrease in HO formation [21].

Radiotherapy is the other primary prophylaxis for HO, inhibiting proliferation and inducing terminal differentiation of MSCs [98]. In the hip, pre- and postoperative radiotherapy are equally as effective, though the total dose is usually higher when given in several fractions postoperatively compared to the single preoperative dose [99–101]. Preoperative radiotherapy is usually preferred as it reduces patient

burden following the procedure. However, radiotherapy in the elbow has been shown to have no effect on HO formation, but significantly increased non-union [102]. Additional side effects of radiotherapy include compromised soft tissue healing and detrimental effects on immunological functions [103]. There are also logistical limitations to the use of radiotherapy. Though timing guidelines are inconsistent, it is generally accepted that radiotherapy must be administered within 48–72 hours of injury. This may be unfeasible for blast-injured patients, particularly in combat where radiotherapy is not available in far-forward medical facilities [31]. Another concern of radiotherapy is carcinogenesis. There is thus far no evidence of carcinogenesis following radiotherapy in the hip [104]. However, given the discrepancy in the average age between combat-wounded patients and those who undergo procedures in the hip, and the potentially decades-long latency period following radiotherapy, this is a risk which must be considered in younger patients [105].

Comparisons between radiotherapy and administration of NSAIDs for HO prophylaxis in the hip reveal near-equal efficacy, with a slight leaning towards radiotherapy because of dose-dependent efficacy, fewer side effects, and greater patient compliance [106–108]. However, neither are suitable for the majority of blast-injured patients. In addition, neither modality showed prophylactic efficacy in a rodent blast model of HO [109, 110]. There is a clear need for new prophylaxes for HO with greater efficacy and fewer side effects which, combined with improved early diagnosis, can successfully be implemented in combat-injured patients.

Current Treatment

Thankfully, HO is often asymptomatic, even with large lesions, or only transiently symptomatic after prolonged activity or mechanical irritation, which may subside with maturation of the HO and the associated inflammation. The first line of treatment is always conservative and includes rest, physical therapy, stretching, dynamic splinting, injections, nerve ablations, pain medication, and prosthetic sock adjustment and padding [31, 73]. However, if symptoms persist, excision surgery is the only current treatment for HO; this is required for 41% of transfemoral and 15% of transtibial combat-related amputees [111]. Complete marginal excision of the ectopic bone lesions is recommended, and surgery should take place at least 180 days post-injury to allow the HO to mature, to reduce the risk of recurrence and re-excision [112]. In addition to HO excision, amputation revision, quadricepsplasty, contracture release, and excision of neuroma or skin graft are often required [95]. Excision surgery is technically demanding, with risk of haemorrhage, infection, wound complication, and neurovascular damage [112]. This surgery can be made more difficult by the HO changing the native anatomy and incarcerating important nerves and blood vessels [73]. Because of this preoperative planning is crucial, and CT is often utilised for both planning before and reference during surgery [95]. NSAIDs are routinely used as secondary prophylaxis to prevent recurrence; radiotherapy is only used in high-risk cases, because of concerns about impairment of wound healing [31].

Novel Therapies

Given the lack of safe and effective prophylaxes against HO for combat-injured patients, it is clear that new therapies are needed to prevent patients having to go through surgical excision. As the biological mechanisms behind HO are being elucidated, new druggable targets are emerging. Perhaps the most exciting potential new prophylaxis is through retinoic acid receptor γ (RAR γ) agonism. Retinoid signalling is a strong inhibitor of chondrogenesis, and thus endochondral bone formation. RAR γ agonists were shown to prevent chondrogenic differentiation *in vitro* and prevent HO in traumatic animal models [113]. The treatment was shown to inhibit BMP2 signalling and to stop cells from differentiating into chondroblasts even when subsequently exposed to BMP2 or implanted into otherwise osteogenic environments *in vivo*. However, a delay in fracture repair was seen, a clear contraindication for blast-injured patients, though the investigators suggest a window of opportunity for treatment after stabilisation but prior to healing [113].

Palovarotene, a RAR γ agonist, was examined further; while not the most potent of the molecules studied, palovarotene was already in clinical trials for emphysema [114, 115]. In a FOP model, palovarotene was shown to prevent HO and restore long bone growth, and in a complex combat blast injury model, it also significantly reduced HO but may delay wound healing especially in the presence of bacteria [116, 117]. However a further study, while confirming that palovarotene prevents chondrogenic differentiation and reduces HO, showed deleterious effects on the skeleton including overgrowth of synovial joints and long bone growth plate ablation [118]. Regardless, palovarotene was taken to clinical trial for FOP. A 28% reduction in HO was seen in phase two; 65% was the benchmark, though there was some dispute as the drug was only administered for flare-ups above a certain threshold [119]. Despite this, a phase three trial is ongoing, which is scheduled to end in 2020 [120].

Another potential strategy is inhibition of activin receptor-like kinase-2 (ALK2), a BMP receptor. Activated receptors phosphorylate the SMAD 1, 5, and 8 pathways that lead to bone formation; constitutive ALK2 activation is the genetic defect that leads to FOP. Thus, by inhibiting ALK2 with LDN-193189, a study has shown inhibition of HO formation in a FOP model [121]. The same ALK2 inhibitor also inhibited HO in an Achilles tenotomy plus burn model of HO [122]. Interestingly this study also showed that, by applying apyrase to the burn site, remote hydrolysis of ATP also inhibited HO, by decreasing extracellular ATP and increasing intracellular cyclic adenosine monophosphate (cAMP), an inhibitor of SMAD 1, 5, and 8 phosphorylation.

As discussed above HIF1 α plays a crucial role in osteochondral bone formation, by upregulating VEGF and SOX9, which are critical for angiogenesis and chondrogenesis, respectively. It has also been shown to increase the intensity and duration of BMP signalling and that inhibiting it restores normal BMP2 signalling and reduced HO formation in a FOP model [123]. In addition to a genetic model, treatment with PX-478 or rapamycin was shown to inhibit HIF1 α

and prevent HO in a trauma model [124]. Another HIF1 α inhibitor is the antibiotic echinomycin, which was shown to prevent HO in an Achilles tenotomy model [125]. Other antibiotics have also been shown to inhibit HO; vancomycin was shown to prevent HO in a complex blast with infection model [126]. Though presumed that this was due to antimicrobial action, vancomycin also inhibited HO even in the absence of MRSA infection. The authors postulate that this is due to upregulation of tissue necrosis factor alpha (TNF α), IL-6, and IL-10 and thus that vancomycin alters the immune response pathway to reduce HO.

Several other potential prophylaxes are also under investigation. Macrophages contribute to the inflammatory process and release factors, including BMP, which support differentiation and maturation of osteoblasts. By utilising clodronate to deplete macrophages, HO has been shown to be reduced in genetic and spinal cord injury plus cardiotoxin injection models [127, 128]. Cells transduced to produce Noggin, a BMP antagonist, decreased HO in Achilles tenotomy and demineralised bone matrix implantation models [129]. Pulsed electromagnetic fields, by increasing blood flow and preventing hypoxia, have been shown to reduce HO in hip and SCI patients [130, 131].

Outlook

Despite being described for over a millennium, HO is still a significant problem today. The increasing frequency of terrorist incidents and the growing prevalence of high-energy extremity injuries in combat mean that blast-related HO is likely to continue to be an issue in the future. Inconsistent efficacy and side effects that are intolerable in a blast-injured population mean that current prophylaxes for HO are unsuitable, leaving excision surgery as the only option for many. Promisingly, the biological processes behind blast-related HO are gradually being elucidated, revealing the critical biological pathways and new druggable targets. Many of these new therapies have shown great success in various animal models of HO. Nevertheless, the translation of new prophylaxes into the clinic is thus far lacking. This is, in part, due to the currently diminished combat leading to low numbers of new blast-related HO patients. However, there is still work to be done in order to illuminate the entire biological network behind blast-related HO. In addition, few studies utilise blast-injury models for HO, and it may be that new models are required in which to test potential therapeutics. A multidisciplinary approach is thus called for, in order to fully uncover the pathways behind the condition, design therapeutics to target these pathways, develop delivery systems and models to test these therapies, and finally to translate these therapies through trials and into the clinic. This work is ongoing, in the hope that when a major conflict next occurs, there will be a therapy waiting so that blast-injured patients do not have to suffer HO.

References

1. Jorolemon MR, Krywko DM. Blast injuries: StatPearls Publishing; Treasure Island, Florida, USA; 2019.
2. Clemedson C-J. Blast Injury. *Physiol Rev.* 1956;36:336–54.
3. Meyers S, Shanley ES. Industrial explosives – a brief history of their development and use. *J Hazard Mater.* 1990;23:183–201.
4. Chatterjee S, Deb U, Datta S, Walther C, Gupta DK. Common explosives (TNT, RDX, HMX) and their fate in the environment: emphasizing bioremediation. *Chemosphere.* 2017;184:438–51.
5. Kulla M, Maier J, Bieler D, Lefering R, Hentsch S, Lampl L, Helm M. Zivile Explosionstraumata – ein unterschätztes Problem? *Unfallchirurg.* 2016;119:843–53.
6. Wolf SJ, Bebarta VS, Bonnett CJ, Pons PT, Cantrill SV. Blast injuries. *Lancet.* 2009;374:405–15.
7. Hoencamp R, Vermetten E, Tan ECTH, Putter H, Leenen LPH, Hamming JF. Systematic review of the prevalence and characteristics of battle casualties from NATO coalition forces in Iraq and Afghanistan. *Injury.* 2014;45:1028–34.
8. Penn-Barwell JG, Roberts SAG, Midwinter MJ, Bishop JRB. Improved survival in UK combat casualties from Iraq and Afghanistan: 2003-2012. *J Trauma Acute Care Surg.* 2015;78:1014–20.
9. Owens BD, Kragh JF, Wenke JC, Macaitis J, Wade CE, Holcomb JB. Combat wounds in operation Iraqi freedom and operation enduring freedom. *J Trauma Inj Infect Crit Care.* 2008;64:295–9.
10. Schoenfeld AJ, Belmont PJ. Traumatic Combat Injuries. In: *Musculoskeletal.* New York: Inj. Mil. Springer New York; 2016. p. 11–23.
11. Wilson C. Improved explosive devices (IEDs) in Iraq and Afganistan: effects and counter-measures. *CRS Rep Congr.* 2007; 1–6.
12. Ramasamy A, Hill AM, Clasper JC. Improvised explosive devices: pathophysiology, injury profiles and current medical management. *J R Army Med Corps.* 2009;155:265–72.
13. Isaacson BM, Brown AA, Brunker LB, Higgins TF, Bloebaum RD. Clarifying the structure and bone mineral content of heterotopic ossification. *J Surg Res.* 2011;167:e163–70.
14. Isaacson BM, Potter BK, Bloebaum RD, Epperson RT, Kawaguchi BS, Swanson TM, Pasquina PF. Link between clinical predictors of heterotopic ossification and histological analysis in combat-injured service members. *J Bone Jt Surg.* 2016;98:647–57.
15. Al-Zahrāwī A Abū al-Qāsim Khalaf ibn, Spink M, Lewis G. *Albucasis on surgery and instruments.* A definitive edition of the Arabic text with English translation and commentary by M. S. Spink and G. L. Lewis. 1973.
16. Zaman SR. Heterotopic ossification of the elbows in a major petrol burn. *Case Rep.* 2012;2012:bcr0320126027.
17. Kaplan FS, Glaser DL, Pignolo RJ, Goldsby RE, Kitterman JA, Groppe J, Shore EM. Fibrodysplasia ossificans progressiva. *Best Pract Res Clin Rheumatol.* 2008;22:191–205.
18. Kaplan FS, Shore EM. Progressive osseous heteroplasia. *J Bone Miner Res.* 2000;15:2084–94.
19. Pignolo RJ, Shore EM, Kaplan FS. Fibrodysplasia ossificans progressiva: clinical and genetic aspects. *Orphanet J Rare Dis.* 2011;6:80.
20. Brady RD, Shultz SR, McDonald SJ, O'Brien TJ. Neurological heterotopic ossification: current understanding and future directions. *Bone.* 2018;109:35–42.
21. Hoyt BW, Pavey GJ, Potter BK, Forsberg JA. Heterotopic ossification and lessons learned from fifteen years at war: a review of therapy, novel research, and future directions for military and civilian orthopaedic trauma. *Bone.* 2018;109:3–11.
22. Dejerne A, Ceillier A. Para-osteo-arthropathies des paraplegiques par lesion medullaire; etude clinique et radiographique. *Ann Med.* 1918;5:497.
23. Eskridge SL, Macera CA, Galarneau MR, Holbrook TL, Woodruff SI, MacGregor AJ, Morton DJ, Shaffer RA. Injuries from combat explosions in Iraq: injury type, location, and severity. *Injury.* 2012;43:1678–82.

24. Kragh JF, Littrel ML, Jones JA, Walters TJ, Baer DG, Wade CE, Holcomb JB. Battle casualty survival with emergency tourniquet use to stop limb bleeding. *J Emerg Med.* 2011;41:590–7.
25. Mabry RL, Apodaca A, Penrod J, Orman JA, Gerhardt RT, Dorlac WC. Impact of critical care-trained flight paramedics on casualty survival during helicopter evacuation in the current war in Afghanistan. *J Trauma Acute Care Surg.* 2012;73:S32–7.
26. Bennett BL, Littlejohn L. Review of new topical hemostatic dressings for combat casualty care. *Mil Med.* 2014;179:497–514.
27. Dougherty PJ, McFarland LV, Smith DG, Esquenazi A, Blake DJ, Reiber GE. Multiple traumatic limb loss: a comparison of Vietnam veterans to OIF/OEF service members. *J Rehabil Res Dev.* 2010;47:333.
28. Daniels CM, Pavey GJ, Arthur J, Noller M, Forsberg JA, Potter BK. Has the proportion of combat-related amputations that develop heterotopic ossification increased? *J Orthop Trauma.* 2018;32:283–7.
29. Potter BK, Burns TC, Lacap AP, Granville RR, Gajewski DA. Heterotopic ossification following traumatic and combat-related amputations: prevalence, risk factors, and preliminary results of excision. *J Bone Jt Surg Ser A.* 2007;89:476–86.
30. Forsberg JA, Pepek JM, Wagner S, Wilson K, Flint J, Andersen RC, Tadaki D, Gage FA, Stojadinovic A, Elster EA. Heterotopic ossification in high-energy wartime extremity injuries: prevalence and risk factors. *J Bone Jt Surg.* 2009;91:1084–91.
31. Alfieri KA, Forsberg JA, Potter BK. Blast injuries and heterotopic ossification. *Bone Joint Res.* 2012;1:192–7.
32. Matsumoto ME, Khan M, Jayabalan P, Ziebarth J, Munin MC. Heterotopic ossification in civilians with lower limb amputations. *Arch Phys Med Rehabil.* 2014;95:1710–3.
33. Kaplan FS, Glaser DL, Hebela N, Shore EM. Heterotopic ossification. *J Am Acad Orthop Surg.* 2004;12:116–25.
34. Davies OG, Grover LM, Eisenstein N, Lewis MP, Liu Y. Identifying the cellular mechanisms leading to heterotopic ossification. *Calcif Tissue Int.* 2015;97:432–44.
35. Matsuo K, Chavez RD, Barruet E, Hsiao EC. Inflammation in fibrodysplasia ossificans progressiva and other forms of heterotopic ossification. *Curr Osteoporos Rep.* 2019. <https://doi.org/10.1007/s11914-019-00541-x>.
36. Vanzant EL, Lopez CM, Ozrazgat-Baslanti T, et al. Persistent inflammation, immunosuppression, and catabolism syndrome after severe blunt trauma. *J Trauma Acute Care Surg.* 2014;76:21–30.
37. Evans KN, Forsberg JA, Potter BK, Hawksworth JS, Brown TS, Andersen R, Dunne JR, Tadaki D, Elster EA. Inflammatory cytokine and chemokine expression is associated with heterotopic ossification in high-energy penetrating war injuries. *J Orthop Trauma.* 2012;26:e204–13.
38. Forsberg JA, Potter BK, Polfer EM, Safford SD, Elster EA. Do inflammatory markers portend heterotopic ossification and wound failure in combat wounds? *Clin Orthop Relat Res.* 2014;472:2845–54.
39. Merceron C, Ranganathan K, Wang E, et al. Hypoxia-inducible factor 2 α is a negative regulator of osteoblastogenesis and bone mass accrual. *Bone Res.* 2019;7:7.
40. Araldi E, Schipani E. Hypoxia, HIFs and bone development. *Bone.* 2010;47:190–6.
41. Davis TA, O'Brien FP, Anam K, Grijalva S, Potter BK, Elster EA. Heterotopic ossification in complex orthopaedic combat wounds: quantification and characterization of osteogenic precursor cell activity in traumatized muscle. *J Bone Jt Surg Ser A.* 2011;93:1122–31.
42. Isaacson B, Swanson T, Potter K, Pasquina P. Tourniquet use in combat-injured service members: a link with heterotopic ossification? *Orthop Res Rev.* 2014;6:27.
43. Downey J, Lauzier D, Kloen P, Klarskov K, Richter M, Hamdy R, Faucheux N, Scimè A, Balg F, Grenier G. Prospective heterotopic ossification progenitors in adult human skeletal muscle. *Bone.* 2015;71:164–70.
44. Scotti C, Tonnarelli B, Papadimitropoulos A, Scherberich A, Schaeren S, Schauerte A, Lopez-Rios J, Zeller R, Barbero A, Martin I. Recapitulation of endochondral bone formation

- using human adult mesenchymal stem cells as a paradigm for developmental engineering. *Proc Natl Acad Sci U S A*. 2010;107:7251–6.
45. Nesti LJ, Jackson WM, Shanti RM, Koehler SM, Aragon AB, Bailey JR, Sracic MK, Freedman BA, Giuliani JR, Tuan RS. Differentiation potential of multipotent progenitor cells derived from war-traumatized muscle tissue. *J Bone Jt Surg*. 2008;90:2390–8.
 46. Jackson WM, Aragon AB, Bulken-Hoover JD, Nesti LJ, Tuan RS. Putative heterotopic ossification progenitor cells derived from traumatized muscle. *J Orthop Res*. 2009;27:1645–51.
 47. Asumda FZ, Chase PB. Age-related changes in rat bone-marrow mesenchymal stem cell plasticity. *BMC cell biology*. 2011;12:44. <https://doi.org/10.1186/1471-2121-12-44>.
 48. Efimenko A, Dzhoyashvili N, Kalinina N, Kochegura T, Akchurin R, Tkachuk V, Parfyonova Y. Adipose-derived mesenchymal stromal cells from aged patients with coronary artery disease keep mesenchymal stromal cell properties but exhibit characteristics of aging and have impaired angiogenic potential. *Stem Cells Transl Med*. 2014;3:32–41.
 49. Liu L, Gao J, Yuan Y, Chang Q, Liao Y, Lu F. Hypoxia preconditioned human adipose derived mesenchymal stem cells enhance angiogenic potential via secretion of increased VEGF and bFGF. *Cell Biol Int*. 2013;37:551–60.
 50. Mu X, Li Y. Conditional TGF- β 1 treatment increases stem cell-like cell population in myoblasts. *J Cell Mol Med*. 2011;15:679–90.
 51. Bosch P, Musgrave DS, Lee JY, Cummins J, Shuler F, Ghivizzani SC, Evans C, Robbins PD, Huard J. Osteoprogenitor cells within skeletal muscle. *J Orthop Res*. 2000;18:933–44.
 52. Gao X, Usas A, Tang Y, et al. A comparison of bone regeneration with human mesenchymal stem cells and muscle-derived stem cells and the critical role of BMP. *Biomaterials*. 2014;35:6859–70.
 53. Asakura A, Rudnicki MA, Komaki M. Muscle satellite cells are multipotential stem cells that exhibit myogenic, osteogenic, and adipogenic differentiation. *Differentiation*. 2001;68:245–53.
 54. Hashimoto N, Kiyono T, Wada MR, Umeda R, Goto Y, Nonaka I, Shimizu S, Yasumoto S, Inagawa-Ogashiwa M. Osteogenic properties of human myogenic progenitor cells. *Mech Dev*. 2008;125:257–69.
 55. Starkey JD, Yamamoto M, Yamamoto S, Goldhamer DJ. Skeletal muscle satellite cells are committed to myogenesis and do not spontaneously adopt nonmyogenic fates. *J Histochem Cytochem*. 2011;59:33–46.
 56. Lounev VY, Ramachandran R, Wosczyzna MN, Yamamoto M, Maidment ADA, Shore EM, Glaser DL, Goldhamer DJ, Kaplan FS. Identification of progenitor cells that contribute to heterotopic skeletogenesis. *J Bone Joint Surg Am*. 2009;91:652–63.
 57. Lazard ZW, Olmsted-Davis EA, Salisbury EA, Gugala Z, Sonnet C, Davis EL, Beal E, Ubogu EE, Davis AR. Osteoblasts have a neural origin in heterotopic ossification. *Clin Orthop Relat Res*. 2015;473:2790–806.
 58. Davis EL, Davis AR, Gugala Z, Olmsted-Davis EA. Is heterotopic ossification getting nervous?: the role of the peripheral nervous system in heterotopic ossification. *Bone*. 2018;109:22–7.
 59. Gugala Z, Olmsted-Davis EA, Xiong Y, Davis EL, Davis AR. Trauma-induced heterotopic ossification regulates the blood-nerve barrier. *Front Neurol*. 2018;9:408.
 60. Kan L, Lounev VY, Pignolo RJ, et al. Substance P signaling mediates BMP-dependent heterotopic ossification. *J Cell Biochem*. 2011;112:2759–72.
 61. Hay ED. An overview of epithelio-mesenchymal transformation. *Acta Anat (Basel)*. 1995;154:8–20.
 62. Xu J, Lamouille S, Derynck R. TGF- β -induced epithelial to mesenchymal transition. *Cell Res*. 2009;19:156–72.
 63. Maroulakou IG, Shibata M-A, Anver M, et al. Heterotopic endochondrial ossification with mixed tumor formation in C3(1)/Tag transgenic mice is associated with elevated TGF-beta1 and BMP-2 expression. *Oncogene*. 1999;18:5435–47.

64. van Meeteren LA, ten Dijke P. Regulation of endothelial cell plasticity by TGF- β . *Cell Tissue Res.* 2012;347:177–86.
65. Medici D, Shore EM, Lounev VY, Kaplan FS, Kalluri R, Olsen BR. Conversion of vascular endothelial cells into multipotent stem-like cells. *Nat Med.* 2010;16:1400–6.
66. Tran K-V, Gealekman O, Frontini A, et al. The vascular endothelium of the adipose tissue gives rise to both white and brown fat cells. *Cell Metab.* 2012;15:222–9.
67. Rutherford RB, Racenis P, Fatherazi S, Izutsu K. Bone formation by BMP-7-transduced human gingival keratinocytes. *J Dent Res.* 2003;82:293–7.
68. Bittner K, Vischer P, Bartholmes P, Bruckner P. Role of the subchondral vascular system in endochondral ossification: endothelial cells specifically derepress late differentiation in resting chondrocytes in vitro. *Exp Cell Res.* 1998;238:491–7.
69. Jeong B-C, Kim H-J, Bae I-H, et al. COMP-Ang1, a chimeric form of Angiopoietin 1, enhances BMP2-induced osteoblast differentiation and bone formation. *Bone.* 2010;46:479–86.
70. Doherty MJ, Ashton BA, Walsh S, Beresford JN, Grant ME, Canfield AE. Vascular pericytes express osteogenic potential in vitro and in vivo. *J Bone Miner Res.* 1998;13:828–38.
71. Crisan M, Corselli M, Chen C-W, Péault B. Multilineage stem cells in the adult: a perivascular legacy? *Organogenesis.* 2011;7:101–4.
72. Vanden Bossche L, Vanderstraeten G. Heterotopic ossification: a review. *J Rehabil.* 2005;37:129–36.
73. Richards JT, Overmann A, Forsberg JA, Potter BK. Complications of combat blast injuries and wounds. *Curr Trauma Reports.* 2018;4:348–58.
74. Shehab D, Elgazzar AH, Collier BD. Heterotopic ossification. *J Nucl Med.* 2002;43:346–53.
75. Hsu J, Keenan M. Current review of heterotopic ossification. *Univ Pennsylvania Orthop J.* 2010;20:126–30.
76. Citak M, Grasmücke D, Suero EM, Cruciger O, Meindl R, Schildhauer TA, Aach M. The roles of serum alkaline and bone alkaline phosphatase levels in predicting heterotopic ossification following spinal cord injury. *Spinal Cord.* 2016;54:368–70.
77. Ranganathan K, Hong X, Cholok D, et al. High-frequency spectral ultrasound imaging (SUSI) visualizes early post-traumatic heterotopic ossification (HO) in a mouse model. *Bone.* 2018;109:49–55.
78. Perosky JE, Peterson JR, Eboda ON, Morris MD, Wang SC, Levi B, Kozloff KM. Early detection of heterotopic ossification using near-infrared optical imaging reveals dynamic turnover and progression of mineralization following Achilles tenotomy and burn injury. *J Orthop Res.* 2014;32:1416–23.
79. Peterson JR, Okagbare PI, De La Rosa S, et al. Early detection of burn induced heterotopic ossification using transcutaneous Raman spectroscopy. *Bone.* 2013;54:28–34.
80. Rosteius T, Suero EM, Grasmücke D, Aach M, Gisevius A, Ohlmeier M, Meindl R, Schildhauer TA, Citak M. The sensitivity of ultrasound screening examination in detecting heterotopic ossification following spinal cord injury. *Spinal Cord.* 2017;55:71–3.
81. Crane NJ, Polfer E, Elster EA, Potter BK, Forsberg JA. Raman spectroscopic analysis of combat-related heterotopic ossification development. *Bone.* 2013;57:335–42.
82. Russell RGG. Bisphosphonates: the first 40 years. *Bone.* 2011;49:2–19.
83. Shafer DM, Bay C, Caruso DM, Foster KN. The use of etidronate disodium in the prevention of heterotopic ossification in burn patients. *Burns.* 2008;34:355–60.
84. Haran MJ, Bhuta T, Lee BSB. Pharmacological interventions for treating acute heterotopic ossification. *Cochrane Database Syst Rev.* 2004; <https://doi.org/10.1002/14651858.cd003321.pub4>.
85. Yue B, Ng A, Tang H, Joseph S, Richardson M. Delayed healing of lower limb fractures with bisphosphonate therapy. *Ann R Coll Surg Engl.* 2015;97:333–8.
86. Kates SL, Ackert-Bicknell CL. How do bisphosphonates affect fracture healing? *Injury.* 2016;47:S65–8.
87. Sinha S, Biernaskie JA, Nickerson D, Gabriel VA. Nitrogen-containing bisphosphonates for burn-related heterotopic ossification. *Burn Open.* 2018;2:160–3.

88. Liu H, Zhao J-G, Li Y, Xia J, Zhao S. Non-steroidal anti-inflammatory drugs for preventing heterotopic bone formation after hip arthroplasty. *Cochrane Database Syst Rev.* 2017; <https://doi.org/10.1002/14651858.CD012861>.
89. Chang J-K, Li C-J, Liao H-J, Wang C-K, Wang G-J, Ho M-L. Anti-inflammatory drugs suppress proliferation and induce apoptosis through altering expressions of cell cycle regulators and pro-apoptotic factors in cultured human osteoblasts. *Toxicology.* 2009;258:148–56.
90. Kurz AZ, LeRoux E, Riediger M, Coughlin R, Simunovic N, Duong A, Laskovski JR, Ayeni OR. Heterotopic ossification in hip arthroscopy: an updated review. *Curr Rev Musculoskelet Med.* 2019;12:147–55.
91. Karunakar MA, Sen A, Bosse MJ, Sims SH, Goulet JA, Kellam JF. Indometacin as prophylaxis for heterotopic ossification after the operative treatment of fractures of the acetabulum. *J Bone Joint Surg Br.* 2006;88-B:1613–7.
92. Beckmann JT, Wylie JD, Kapron AL, Hanson JA, Maak TG, Aoki SK. The effect of NSAID prophylaxis and operative variables on heterotopic ossification after hip arthroscopy. *Am J Sports Med.* 2014;42:1359–64.
93. Kan S-L, Yang B, Ning G-Z, Chen L-X, Li Y-L, Gao S-J, Chen X-Y, Sun J-C, Feng S-Q. Nonsteroidal anti-inflammatory drugs as prophylaxis for heterotopic ossification after total hip arthroplasty: a systematic review and meta-analysis. *Medicine (Baltimore).* 2015;94:e828.
94. Bozimoski G. A review of nonsteroidal anti-inflammatory drugs. *AANA J.* 2015;83:425–33.
95. Potter BK, Forsberg JA, Davis TA, et al. Heterotopic ossification following combat-related trauma. *J Bone Jt Surg Ser A.* 2010;92:74–89.
96. Rivera JC, Hsu JR, Noel SP, Wenke JC, Rathbone CR. Locally delivered nonsteroidal anti-inflammatory drug: a potential option for heterotopic ossification prevention. *Clin Transl Sci.* 2015;8:591–3.
97. Macfarlane RJ, Han Ng B, Gamie Z, El Masry MA, Velonis S, Schizas C, Tsiridis E. Pharmacological treatment of heterotopic ossification following hip and acetabular surgery. *Expert Opin Pharmacother.* 2008;9:767–86.
98. Trott KR, Kamprad F. Radiobiological mechanisms of anti-inflammatory radiotherapy. *Radiother Oncol.* 1999;51:197–203.
99. Gregoritch SJ, Chadha M, Pelligrini VD, Rubin P, Kantorowitz DA. Randomized trial comparing preoperative versus postoperative irradiation for prevention of heterotopic ossification following prosthetic total hip replacement: preliminary results. *Int J Radiat Oncol Biol Phys.* 1994;30:55–62.
100. Seegenschmiedt MH, Keilholz L, Martus P, Goldmann A, Wölfel R, Henning F, Sauer R. Prevention of heterotopic ossification about the hip: final results of two randomized trials in 410 patients using either preoperative or postoperative radiation therapy. *Int J Radiat Oncol Biol Phys.* 1997;39:161–71.
101. Seegenschmiedt MH, Makoski HB, Micke O. Radiation prophylaxis for heterotopic ossification about the hip joint – a multicenter study. *Int J Radiat Oncol Biol Phys.* 2001;51:756–65.
102. Hamid N, Ashraf N, Bosse MJ, Connor PM, Kellam JF, Sims SH, Stull DE, Jeray KJ, Hymes RA, Lowe TJ. Radiation therapy for heterotopic ossification prophylaxis acutely after elbow trauma. *J Bone Jt Surg.* 2010;92:2032–8.
103. Juarez JK, Wenke JC, Rivera JC. Treatments and preventative measures for trauma-induced heterotopic ossification: a review. *Clin Transl Sci.* 2018;11:365.
104. Pakos EE, Papadopoulos D V, Gelalis ID, Tsantes AG, Gkiatas I, Kosmas D, Tsekeris PG, Xenakis TA. Is prophylaxis for heterotopic ossification with radiation therapy after THR associated with early loosening or carcinogenesis? *HIP Int.* 2019. 112070001984272.
105. Baird EO, Kang QK. Prophylaxis of heterotopic ossification – an updated review. *J Orthop Surg Res.* 2009;4:12.
106. Pakos EE, Ioannidis JPA. Radiotherapy vs. nonsteroidal anti-inflammatory drugs for the prevention of heterotopic ossification after major hip procedures: a meta-analysis of randomized trials. *Int J Radiat Oncol.* 2004;60:888–95.

107. Blokhuis TJ, Frölke JPM. Is radiation superior to indomethacin to prevent heterotopic ossification in acetabular fractures?: a systematic review. *Clin Orthop Relat Res.* 2009;467:526–30.
108. Burd TA, Hughes MS, Anglen JO. Heterotopic ossification prophylaxis with indomethacin increases the risk of long-bone nonunion. *J Bone Joint Surg Br.* 2003;85:700–5.
109. Robertson AD, Chiramonti AM, Nguyen TP, et al. Failure of indomethacin and radiation to prevent blast-induced heterotopic ossification in a Sprague-dawley rat model. *Clin Orthop Relat Res.* 2019;477:644–54.
110. Pellegrini VJD. Heterotopic ossification following extremity blast amputation: an animal model in the Sprague Dawley Rat. 2016.
111. Tintle SM, Shawen SB, Forsberg JA, Gajewski DA, Keeling JJ, Andersen RC, Potter BK. Reoperation after combat-related major lower extremity amputations. *J Orthop Trauma.* 2014;28:232–7.
112. Pavey GJ, Polfer EM, Nappo KE, Tintle SM, Forsberg JA, Potter BK. What risk factors predict recurrence of heterotopic ossification after excision in combat-related amputations? *Clin Orthop Relat Res.* 2015;473:2814–24.
113. Shimono K, Tung W-E, Macolino C, et al. Potent inhibition of heterotopic ossification by nuclear retinoic acid receptor- γ agonists. *Nat Med.* 2011;17:454–60.
114. Hind M, Stinchcombe S. Palovarotene, a novel retinoic acid receptor gamma agonist for the treatment of emphysema. *Curr Opin Investig Drugs.* 2009;10:1243–50.
115. Stolk J, Stockley RA, Stoel BC, et al. Randomised controlled trial for emphysema with a selective agonist of the γ -type retinoic acid receptor. *Eur Respir J.* 2012;40:306–12.
116. Chakkalakal SA, Uchibe K, Convente MR, Zhang D, Economides AN, Kaplan FS, Pacifici M, Iwamoto M, Shore EM. Palovarotene inhibits heterotopic ossification and maintains limb mobility and growth in mice with the human ACVR1 R206H fibrodysplasia ossificans progressiva (FOP) mutation. *J Bone Miner Res.* 2016;31:1666–75.
117. Pavey GJ, Qureshi AT, Tomasino AM, et al. Targeted stimulation of retinoic acid receptor- γ mitigates the formation of heterotopic ossification in an established blast-related traumatic injury model. *Bone.* 2016;90:159–67.
118. Lees-Shepard JB, Nicholas S-AE, Stoessel SJ, Devarakonda PM, Schneider MJ, Yamamoto M, Goldhamer DJ. Palovarotene reduces heterotopic ossification in juvenile FOP mice but exhibits pronounced skeletal toxicity. *elife.* 2018;7:e40814. <https://doi.org/10.7554/eLife.40814.001>.
119. Clementia Pharmaceuticals. An efficacy and safety study of palovarotene to treat preosseous flare-ups in FOP subjects. 2017. In: [ClinicalTrials.gov](https://clinicaltrials.gov). <https://clinicaltrials.gov/ct2/show/NCT02190747>. Accessed 24 Jun 2019.
120. Clementia Pharmaceuticals. An efficacy and safety study of palovarotene for the treatment of FOP. 2019. In: [ClinicalTrials.gov](https://clinicaltrials.gov). <https://clinicaltrials.gov/ct2/show/NCT03312634>. Accessed 24 Jun 2019.
121. Yu PB, Deng DY, Lai CS, et al. BMP type I receptor inhibition reduces heterotopic ossification. *Nat Med.* 2008;14:1363–9.
122. Peterson JR, De La Rosa S, Eboda O, et al. Treatment of heterotopic ossification through remote ATP hydrolysis. *Sci Transl Med.* 2014;6:255ra132.
123. Wang H, Lindborg C, Lounev V, et al. Cellular hypoxia promotes heterotopic ossification by amplifying BMP signaling. *J Bone Miner Res.* 2016;31:1652–65.
124. Agarwal S, Loder S, Brownley C, et al. Inhibition of Hif1 α prevents both trauma-induced and genetic heterotopic ossification. *Proc Natl Acad Sci U S A.* 2016;113:E338–47.
125. Zimmermann SM, Würzler-Hauri CC, Wanner GA, Simmen HP, Werner CML. Echinomycin in the prevention of heterotopic ossification – an experimental antibiotic agent shows promising results in a murine model. *Injury.* 2013;44:570–5.
126. Seavey JG, Wheatley BM, Pavey GJ, et al. Early local delivery of vancomycin suppresses ectopic bone formation in a rat model of Trauma-induced heterotopic ossification. *J Orthop Res.* 2017;35:2397–406.

127. Kan L, Liu Y, McGuire TL, Berger DMP, Awatramani RB, Dymecki SM, Kessler JA. Dysregulation of local stem/progenitor cells as a common cellular mechanism for heterotopic ossification. *Stem Cells*. 2009;27:150–6.
128. Genêt F, Kulina I, Vaquette C, et al. Neurological heterotopic ossification following spinal cord injury is triggered by macrophage-mediated inflammation in muscle. *J Pathol*. 2015;236:229–40.
129. Hannallah D, Peng H, Young B, Usas A, Gearhart B, Huard J, Surgery J. Retroviral delivery of noggin inhibits the formation of heterotopic ossification induced by BMP-4. *J Bone Jt Surg*. 2004;86:80–91.
130. Kocić M, Lazović M, Kojović Z, Mitković M, Milenković S, Cirić T. Methods of the physical medicine therapy in prevention of heterotopic ossification after total hip arthroplasty. *Vojnosanit Pregl*. 2006;63:807–11.
131. Durović A, Miljković D, Brdareski Z, Plavšić A, Jevtić M. Pulse low-intensity electromagnetic field as prophylaxis of heterotopic ossification in patients with traumatic spinal cord injury. *Vojnosanit Pregl*. 2009;66:22–8.

Part III
Bone Mineralization

Chapter 15

The Paradoxical Relationship Between Skeletal and Cardiovascular Mineralization



Sidney Iriana, Yin Tintut, and Linda L. Demer

Introduction

Calcific vasculopathy, also known as vascular calcification, is a widespread condition affecting almost all people over the age of 65 and involving most of the cardiovascular system, including the aorta, coronary arteries, carotid and other peripheral arteries, heart valves, and even arterioles. While calcification of these structures has been attributed to age, it is rapidly accelerated with metabolic disturbances such as atherosclerosis, chronic kidney disease, and diabetes, consistent with its regulated nature.

An important clue about the mechanism of vascular calcification is the close association between the severity of vascular calcification, especially aortic

S. Iriana
Chicago Medical School, Rosalind Franklin University of Medicine and Science,
Chicago, IL, USA
e-mail: sidney.iriانا@my.rfums.org

Y. Tintut
Department of Medicine, University of California, Los Angeles, Los Angeles, CA, USA
Department of Physiology, University of California, Los Angeles, Los Angeles, CA, USA
Department of Orthopaedic Surgery, University of California, Los Angeles,
Los Angeles, CA, USA
e-mail: ytintut@mednet.ucla.edu

L. L. Demer (✉)
Department of Medicine, University of California, Los Angeles, Los Angeles, CA, USA
Department of Physiology, University of California, Los Angeles, Los Angeles, CA, USA
Department of Bioengineering, University of California, Los Angeles,
Los Angeles, CA, USA
e-mail: ldemer@mednet.ucla.edu

calcification, and the severity of osteoporosis. This potential interdependency between skeletal and vascular systems has important implications for treatment of either condition, in that any agent that treats one of the conditions may aggravate the other.

Similarities Between Vascular and Skeletal Mineralization

Based on electron microprobe analysis, the mineral produced by vascular cells has the stoichiometry of hydroxyapatite, the same mineral as in skeletal bone [1]. In atherosclerosis, fully mature, ectopic bone tissue is found in 25–65% of calcified lesions [2, 3]. It is also often found in medial calcification [3] and even in saphenous vein bypass grafts (personal communication, J-H Qiao), indicating that it is not inherently limited to the arterial side of the vascular tree. This ectopic bone includes the cellular components considered specific to bone, such as osteoblasts, osteoclasts, chondroblasts, chondroclasts, and osteocytes [4] as well as hematopoietic marrow [5]. Osteoclast-like cells in calcific atherosclerosis are important because of their potential for reversal of calcific vasculopathy. They are found in a minority of calcified arteries [3, 6]. They express canonical markers of osteoclasts including receptor activator of nuclear factor- κ B, but their response to the receptor's ligand is impaired. Furthermore, their cathepsin K and resorptive activities are reduced, in part due to IL-18 released by vascular smooth muscle cells [7] and by IL-4 and loss of responsiveness to RANKL [8]. This failure of active resorption of hydroxyapatite by osteoclast-like cells may explain why calcified vascular lesions fail to regress despite interventions [9]. More information on osteoclastogenesis is provided in Chap. 18.

The mineralization process appears to follow nearly identical processes of gene expression cascades, extracellular vesicle release, and collagen-based crystal propagation [10]. The anatomical units of cortical bone have marked similarities to blood vessels. Cortical bone is made up of a parallel array of osteons, cylindrical units approximately 1 mm² in cross-sectional area, centered on blood vessels, where the endothelial cells are surrounded adluminally by a basement membrane, which is, in turn, surrounded by osteoblasts in a mineralizing matrix (Fig. 15.1). The osteoblasts that surround the vessel are the least advanced along the pathway to the mature osteocyte phenotype. Mineralization of their matrix increases with distance from the vessel. Both vascular smooth muscle cells and osteoblasts are mesenchymal in origin, and both produce collagen.

Location of Cardiovascular Calcification

Calcification may arise in vessels of all sizes in almost any tissue [11]. Other tissues, including the pineal gland, intestines, kidney, skeletal muscle, and myocardium, have been known to undergo mineralization; even the skeletal vasculature

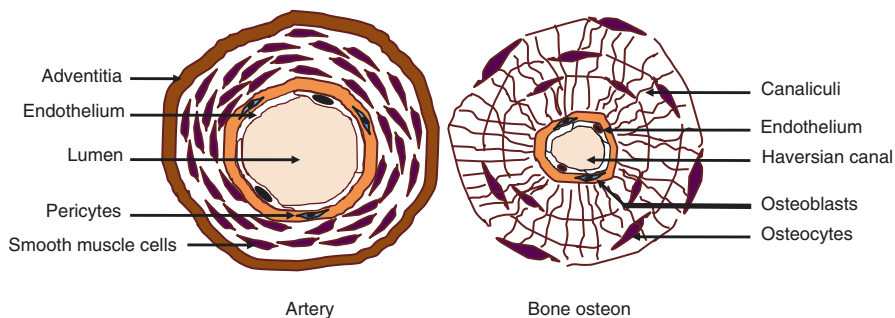


Fig. 15.1 Schematic showing similarities between the structure of arterial and bone tissues. (With permission from *Trends in Endocrinology and Metabolism*)

mineralizes [12]. The mineral deposits usually form in the intimal layer in patients with atherosclerosis, in the medial layer in patients with chronic kidney disease, and in both layers in patients with diabetes. In the aortic valve, the mineral deposits occur in the fibrosa layer; in the mitral valve, the deposits occur in the fibrous annular ring. Atherosclerotic (intimal) calcification is associated with hyperlipidemia, inflammation, and oxidative stress. In many cases, the earliest site of mineral deposition is along the internal elastic lamina. Medial calcification is associated with uremia, hyperphosphatemia, and hyperglycemia. In general, calcification reduces vasomotion and raises blood pressure, and these contribute to mortality [13]. About 13% of surgical specimens of calcific valvulopathy also contain ectopic bone tissue [14], known as osteoid metaplasia, and/or ectopic cartilage tissue, known as chondroid metaplasia [15].

Clinical Significance

The clinical consequences of calcific vasculopathy depend on the location. In the aorta, calcification increases stiffness, causing loss of the Windkessel effect, the recoil of the elastin-rich aorta during diastole. This impairs cardiac function, promotes systolic hypertension, and diminishes diastolic pressure, which is needed to perfuse the coronary arteries. In cardiac valves, leaflet calcification reduces excursion leading to a smaller orifice size, which increases resistance to flow, and may reduce ability of the valve to close fully. In the aortic valve, this causes symptoms of aortic stenosis such as hemodynamic instability, dyspnea, chest pain, and syncope. In coronary arteries, calcification serves as a marker for subclinical atherosclerosis, and it may directly contribute to plaque rupture, which leads to acute coronary syndrome or myocardial infarction [16]. Calcification in the aortic arch increases the work of the heart, and, by decreasing diastolic recoil, reduces diastolic perfusion of the coronaries, leading to myocardial ischemia. Peripheral artery calcification with symptomatic ischemia is a better predictor for lower extremity

amputation than traditional risk factors [17], and the extent of coronary artery calcification is an independent predictor of all-cause mortality [18–21]. Controversy remains as to whether calcification directly promotes cardiovascular events or if it may be protective, and this appears to depend on micro-architectural and macro-architectural features. For a given volume of mineral, a spotty pattern of calcium deposits has greater surface area than a contiguous pattern. Theoretical finite element analysis [16] predicts that rupture due to von Mises stress increases at the surfaces of a rigid inclusion in a distensible material and its amplitude is greater for larger deposits. Thus, the spotty pattern of multiple smaller deposits, which has greater mineral surface area per mineral volume, would theoretically be characterized by higher rupture risk for a given total amount of mineral, and this is confirmed in clinical studies [22].

Paradoxical Relation to Osteoporosis

Epidemiologic studies support an inverse relationship between vascular calcification and bone loss that is independent of age [23]. In a cohort of middle-aged women, bone mineral density (BMD) and aortic calcification were inversely associated in an age-independent manner [24]. In a cohort of postmenopausal Asian women, the degree of aortic calcification correlated with risk of vertebral fracture [25]. A study of 300 postmenopausal women showed severe abdominal aortic calcification only in the women with the most severe osteoporosis [26]. Other studies have also suggested an inverse association between coronary artery calcification and bone mineral density after adjusting for age, previous fracture history, physical activity, and other potential confounders [27]. In asymptomatic postmenopausal women with normal or low BMD, total coronary calcium scores are significantly higher in groups with osteoporosis compared with control groups [28]. In a study of over 2000 healthy postmenopausal women, the degree of aortic calcification was an independent predictor of hip fractures, diminished BMD, and accelerated bone loss [29]. Conversely, after normalizing for confounding factors, increased bone density was associated with reduced coronary artery calcification [30].

Notably, bone density is often measured by DEXA (dual energy x-ray analysis) at the lumbar spine. This technique measures the amount of x-ray attenuation from a beam passing from the front of the abdomen through the back of the lumbar spine. Since this beam pathway includes the abdominal aorta, changes in aortic calcification would be misinterpreted as changes in bone density in response to whatever intervention was tested. This apparent responsiveness to drugs may have caused investigators to choose the lumbar spine for testing treatments, given that the lumbar spine is rarely a site for fracture.

From a teleological perspective, a similar paradoxical relationship is seen for responses of soft tissue and skeletal bone to infectious processes and foreign body reactions. Evolutionarily, the immune system is focused on infection and foreign bodies. In soft tissues, the response of the immune system is to first send acute

cellular and antibody immune defenses. If the infectious agent or foreign body survives, chronic inflammation ensues. And, if that defense fails, it appears that soft tissues resort to an ultimate immune defense – erecting a wall of mineral, and, eventually, bone, to wall off the noxious agent. By contrast, when skeletal bone tissue is confronted with an infectious process, such as osteomyelitis that does not give in to cellular and humoral immune defenses, bone responds by osteolysis – dissolving of the bone tissue around the noxious agent to eliminate its preferred environment. One may speculate that similar processes explain the paradox of vascular calcification in the face of osteoporosis. However, the precise mechanisms that control the relationship between chronic inflammation and ectopic calcification are still under investigation.

In the past, the paradoxical relationship between vascular calcification and osteoporosis was attributed to natural aging processes and menopause [31, 32]. However, current evidence suggests that it is independent of aging and that oxidant stress, lipids, and inflammatory cytokines may be key factors linking the two pathological processes, as described below.

Oxidant Stress, Lipids, and Inflammatory Cytokines

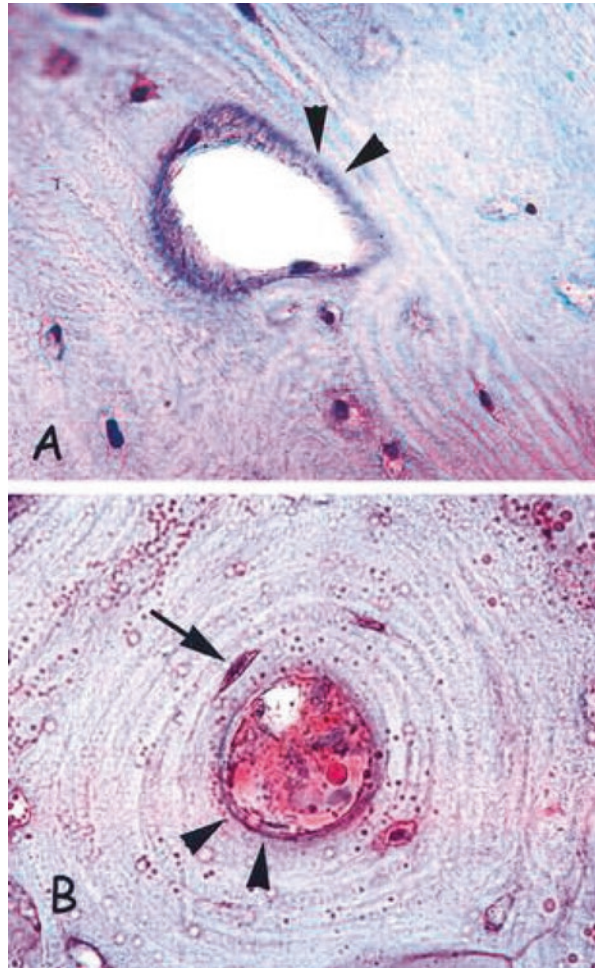
It is well established that atherogenesis is driven in large part by accumulation of LDL nanoparticles in the subendothelial space of the artery wall and oxidative modification of their phospholipid components [33]. Antibodies to these oxidized phospholipids have been shown to inhibit atherosclerosis in transgenic hyperlipidemic mice [34]. This mechanism explains many of the risk factors, including hyperlipidemia, hypertension, smoking, age, and diabetes, each of which amplifies some aspect of this process, including mechanical and chemical injury. Oxidized phospholipids trigger inflammation, causing endothelial cells to release inflammatory cytokines, which attract monocytes, which, in turn, release further cytokines. Recruitment of activated monocyte-macrophages and vascular smooth muscle cells (VSMC) to the subendothelial space forms the atherosclerotic neointima known as plaque.

VSMC may be a source of osteoblasts in the artery wall. They share embryonic mesenchymal origins with osteoblasts. In atherosclerotic plaque and in tissue culture dishes, they also have the plasticity to dedifferentiate into a “synthetic phenotype” [35]. This phenotype is associated with a substantial increase in synthesis of collagen type I, the matrix component that is key to mineralization [36], suggesting that synthetic phenotype may be a first stage of osteogenic differentiation. VSMC are also shown to redifferentiate or transdifferentiate into osteoblast-like cells [10, 37, 38]. Even endothelial cells have the plasticity to differentiate along an osteoblastic lineage, through endothelial-mesenchymal transition [39]. Several studies have shown that activated monocyte-macrophages and pro-inflammatory cytokines stimulate VSMC and valvular interstitial cells (VIC) to undergo osteoblastic differentiation and mineral deposition [14, 40–44]. Inflammatory markers colocalize with early osteogenic activity in calcific vasculopathy in mouse models [45].

The same oxidatively modified lipids and phospholipids that drive atherogenesis, known as inflammatory lipids, also affect skeletal bone. Skeletal bone is a vascularized tissue. When cut, it bleeds. The same mechanism by which LDL crosses the endothelium in arteries allows it to cross the endothelium of bone vasculature. Progenitors of bone-resorbing osteoclasts also pass through the endothelial layer of osteon vessels as monocytes. Lipids are found in the subendothelial space of osteons in human osteoporotic bone adjacent to osteoblasts, and osteoblasts have been shown to have the capacity to oxidatively modify LDL [46]. Products of that oxidative reaction are found in the bones of mice administered a high-fat diet [47] (Fig. 15.2), and bones of those mice have reduced mineral density [48, 49].

In vitro, oxidized phospholipids inhibit differentiation and mineralization of osteoblasts [50, 51] as evidenced by inhibition of alkaline phosphatase activity, type I collagen, and matrix mineralization [52] as well as enhancement of

Fig. 15.2 Staining for lipids by Oil Red O in non-osteoporotic (top) and osteoporotic (bottom) human bone. Arrow represents a typical osteocyte, and arrowhead represents perivascular space of the Haversian canal. (With permission from *Arteriosclerosis, Thrombosis and Vascular Biology* and the American Heart Association. Tintut et al. [47])



adipogenic differentiation [52]. In vivo, this results in bone loss and reduced bone strength [48, 49]. Conversely, inflammatory lipids also promote resorptive activity of bone-resorbing osteoclasts [47, 53]. Altogether, these effects are expected to promote bone loss, in a diffuse manner. One possibility is that the diffuse bone loss of osteoporosis may, in part, be caused by oxidized phospholipids and inflammation.

Statin Class of Drugs

Given the above mechanism, one would expect that reducing accumulation of LDL in the artery wall by lowering serum lipid levels would reduce vascular calcification. Lipid lowering is widely achieved in hyperlipidemic patients by statins and PCSK9 inhibitors. Yet, despite their remarkable capacity to lower circulating LDL-cholesterol levels, they do not reduce coronary artery calcification (CAC) or halt its progression. Indeed, randomized control trials show an increase in CAC progression in patients on statins even in the setting of its serum lipid-lowering effects [54–56]. This unexpected finding raises important questions about the current understanding of mechanisms linking lipids to calcification and calcification to cardiovascular events. Remarkably, current clinical recommendations are to discontinue the practice of following progression of CAC in patients on statins [57].

With respect to the skeleton, statins may promote both skeletal and ectopic bone growth. Mundy et al. reported that statins promote skeletal bone growth through bone morphogenetic protein [58], and slow-release statins have been used to treat non-healing fractures in preclinical studies. Initially, observational studies have reported dramatic reductions of fracture incidence in patients taking statins [59]; however, randomized, control trials have not confirmed this finding [60, 61].

Teriparatide

Teriparatide is an injectable recombinant human parathyroid hormone (PTH) 1-34 and an FDA-approved bone anabolic agent for osteoporosis. It is well-known that chronically and continuously elevated PTH levels, as in hyperparathyroidism, cause bone loss [62]. However, it turns out that intermittent elevations in PTH have bone anabolic effects. Thus, intermittent teriparatide injections are used to stimulate bone formation, which occurs, in part, through stimulation of insulin-like growth factor (IGF)-dependent pathways [63]. The end results include markedly enhanced bone mineral volume, micro-architecture, and overall structure. Interestingly, the efficacy of this bone anabolic agent is blunted in the presence of inflammatory lipids due to inhibited expression of bone morphogenetic protein 2 (BMP2) [64]. In vivo, PTH (1–34) anabolism is also blunted in hyperlipidemia, most likely through protein kinase A, Wnt, and insulin-like growth factor I-dependent mechanisms [65].

As for the cardiovascular system, PTH receptors are present in VSMC [66]. Chronically high levels of PTH that occur in the secondary hyperparathyroidism accompanying chronic kidney disease are associated with atherosclerosis, stiffening of arteries, hypertension, and cardiovascular events [67]. They also have a high prevalence of vascular calcification [68] and cardiovascular mortality not attributable to conventional risk factors. In contrast, intermittent activation of PTH receptors with PTH [1–34] prevented vascular calcification in diabetic low-density lipoprotein receptor-deficient mice via *Msx2* suppression [69]. Interestingly, in mice with pre-existing atherosclerotic calcification, PTH (1–34) did not affect the amount of calcification but altered micro-architecture of aortic calcium deposits, in a manner that may affect plaque stability [70]. Activation of the PTH receptors with PTHrP also inhibited matrix mineralization of vascular smooth muscle cells [71]. PTH appears to induce IL-6 and RAGE in human endothelial cells [72], but little is known about the cellular mechanisms.

Bisphosphonates

Bisphosphonates, used for treatment of osteoporosis, inhibit resorption by blocking osteoclast activity. They are now under consideration as potential therapy for vascular calcification. However, concerns about hypermineralization and low-impact fractures have led to recommendations of limits on duration of treatment. Some evidence suggests that they may reduce vascular calcification. In hemodialysis patients, etidronate was found to reduce progression of coronary and aortic calcification [73–75]. In kidney transplant patients, an 18-month treatment decreased the progression of aortic calcification [76, 77]. In the absence of chronic kidney disease, bisphosphonates do not appear to affect vascular calcification [78, 79]. In preclinical animal models, bisphosphonates inhibited warfarin or warfarin/vitamin D-induced aortic medial calcification that is similar to calcification developed in renal patients [80]. Interestingly, serum levels of calcium and phosphate did not fluctuate with the treatment, suggesting that inhibition of calcification may not be due to the transient changes in serum levels [80]. As an analogue of pyrophosphate, a potent inhibitor of vascular calcification, *in vitro* studies show that bisphosphonates inhibit vascular calcification locally through inhibiting alkaline phosphatase (ALP)-related osteogenic activity [81, 82]. Newer biologic therapy with denosumab appears to have the same effects on coronary calcification as alendronate [83].

Vitamin D and Calcium Supplementation

Vitamin D and calcium have long been recommended for osteoporosis prevention and treatment based on numerous studies that support a modest improvement in bone density. However, the vitamin D assessment (ViDA) study, a randomized,

double-blind, placebo-controlled trial of over 5000 patients, showed no benefit of vitamin D supplementation on nonvertebral fractures [84]. In addition, a recent randomized clinical trial from Canada showed no benefit and possible harm from vitamin D doses exceeding 400 IU per day; results showed a reduction in bone density at the radius with moderate and high doses of vitamin D, and a reduction in bone density in the tibia at high doses [85]. In addition, some of the publications that supported vitamin D treatment for osteoporosis have been retracted due to data fabrication, systematic authorship misconduct, text duplication, concerns about data integrity, and scientific misconduct by one particular group of authors [86]. Thus, new evidence raises some questions about the benefit of vitamin D to bone.

With respect to the vasculature, the Women's Health Initiative of the National Institutes of Health found no significant effect of calcium/vitamin D supplementation on cardiovascular disease in over 36,000 healthy postmenopausal women [87]. However, a later re-analysis of the data showed a modest increase in cardiovascular risk for women taking calcium that was masked by the widespread free use of personal calcium supplements among the subjects [88].

A source of concern is that high-dose vitamin D reliably induces vascular calcification in animals and humans [89–91], to the degree that it has been used widely as an experimental model for vascular calcification for over four decades. Although the doses in rodents are higher than those in humans, it is generally accepted that effects of high doses of agents over the short life span of a rodent are predictive of the effects of lower doses in the longer life span of humans. The mechanism by which vitamin D induces vascular calcification is not clear; however, a dose-dependent, receptor-mediated relationship has been demonstrated for 1,25-dihydroxyvitamin D₃ on vascular smooth muscle cell Ca-ATPase as well as cellular Ca²⁺ uptake [92].

In the Framingham Offspring Study, a biphasic relationship was found for vitamin D levels and cardiovascular risk, which increased at both high and low levels (<15 and > 30 ng/ml) of serum 25-hydroxy-vitamin D [93]. This study involved over 1700 asymptomatic participants without previous cardiovascular disease, with a mean follow-up of 5.4 years [93]. A similar biphasic relationship was found for vitamin D levels and vascular calcification in children on dialysis [94]. In a small study of patients on dialysis, CAC was associated with intravenous pulse dosing of active vitamin D [84].

Contrary to prior observational studies, results of the vitamin D assessment (ViDA) study showed no benefit of vitamin D supplementation on cardiovascular disease [84]. The lack of benefit to cardiovascular disease was also seen in the randomized, controlled, vitamin D and omega-3 (VITA) trial of over 25,000 subjects [84]. Another randomized controlled trial showed no effect on the risk factor profile by vitamin D supplementation [95]. Given that aortic calcification is typically more severe in patients with osteoporosis, independently of age, and that vascular calcification may come in the form ectopic bone, a key question is whether calcium and vitamin D supplements promote ectopic bone growth as much or even more than skeletal bone growth.

Acknowledgments This work was supported in part by funding from the National Institutes of Health (AG061586, HL137647).

References

1. Bostrom K, Watson KE, Horn S, Wortham C, Herman IM, Demer LL. Bone morphogenetic protein expression in human atherosclerotic lesions. *J Clin Invest.* 1993;91(4):1800–9.
2. Davaine JM, Quillard T, Chatelais M, Guilbaud F, Brion R, Guyomarch B, et al. Bone like arterial calcification in femoral atherosclerotic lesions: prevalence and role of osteoprotegerin and pericytes. *Eur J Vasc Endovasc Surg.* 2016;51(2):259–67.
3. Han KH, Hennigar RA, O'Neill WC. The association of bone and osteoclasts with vascular calcification. *Vasc Med.* 2015;20(6):527–33.
4. Ge Q, Ruan CC, Ma Y, Tang XF, Wu QH, Wang JG, et al. Osteopontin regulates macrophage activation and osteoclast formation in hypertensive patients with vascular calcification. *Sci Rep.* 2017;7:40253.
5. Qiao JH, Mertens RB, Fishbein MC, Geller SA. Cartilaginous metaplasia in calcified diabetic peripheral vascular disease: morphologic evidence of enchondral ossification. *Hum Pathol.* 2003;34(4):402–7.
6. Hunt JL, Fairman R, Mitchell ME, Carpenter JP, Golden M, Khalapyan T, et al. Bone formation in carotid plaques: a clinicopathological study. *Stroke.* 2002;33(5):1214–9.
7. Tintut Y, Abedin M, Cho J, Choe A, Lim J, Demer LL. Regulation of RANKL-induced osteoclastic differentiation by vascular cells. *J Mol Cell Cardiol.* 2005;39(2):389–93.
8. Chinetti-Gbaguidi G, Daoudi M, Rosa M, Vinod M, Louvet L, Copin C, et al. Human alternative macrophages populate calcified areas of atherosclerotic lesions and display impaired RANKL-induced osteoclastic bone resorption activity. *Circ Res.* 2017;121(1):19–30.
9. Lomashvili KA, Manning KE, Weitzmann MN, Nelea V, McKee MD, O'Neill WC. Persistence of vascular calcification after reversal of uremia. *Am J Pathol.* 2017;187(2):332–8.
10. Tintut Y, Parhami F, Bostrom K, Jackson SM, Demer LL. cAMP stimulates osteoblast-like differentiation of calcifying vascular cells. Potential signaling pathway for vascular calcification. *J Biol Chem.* 1998;273(13):7547–53.
11. Guzman RJ. Clinical, cellular, and molecular aspects of arterial calcification. *J Vasc Surg.* 2007;45 Suppl A:A57–63.
12. Guderian S, Lee S, McLane MA, Prisby RD. Progressive ossification of the bone marrow vasculature with advancing age corresponds with reduced red blood cell count and percentage of circulating lymphocytes in male Fischer-344 rats. *Microcirculation.* 2019;26:e12550.
13. Giachelli CM. Mechanisms of vascular calcification in uremia. *Semin Nephrol.* 2004;24(5):401–2.
14. Mohler ER 3rd, Gannon F, Reynolds C, Zimmerman R, Keane MG, Kaplan FS. Bone formation and inflammation in cardiac valves. *Circulation.* 2001;103(11):1522–8.
15. Steiner I, Kasparova P, Kohout A, Dominik J. Bone formation in cardiac valves: a histopathological study of 128 cases. *Virchows Arch.* 2007;450(6):653–7.
16. Hoshino T, Chow LA, Hsu JJ, Perlowski AA, Abedin M, Tobis J, et al. Mechanical stress analysis of a rigid inclusion in distensible material: a model of atherosclerotic calcification and plaque vulnerability. *Am J Physiol Heart Circ Physiol.* 2009;297(2):H802–10.
17. Guzman RJ, Brinkley DM, Schumacher PM, Donahue RM, Beavers H, Qin X. Tibial artery calcification as a marker of amputation risk in patients with peripheral arterial disease. *J Am Coll Cardiol.* 2008;51(20):1967–74.
18. Criqui MH, Denenberg JO, Ix JH, McClelland RL, Wassel CL, Rifkin DE, et al. Calcium density of coronary artery plaque and risk of incident cardiovascular events. *JAMA.* 2014;311(3):271–8.

19. Budoff MJ, Shaw LJ, Liu ST, Weinstein SR, Mosler TP, Tseng PH, et al. Long-term prognosis associated with coronary calcification: observations from a registry of 25,253 patients. *J Am Coll Cardiol.* 2007;49(18):1860–70.
20. Arnsion Y, Rozanski A, Gransar H, Friedman JD, Hayes SW, Thomson LE, et al. Comparison of the coronary artery calcium score and number of calcified coronary plaques for predicting patient mortality risk. *Am J Cardiol.* 2017;120(12):2154–9.
21. Chiu YW, Adler SG, Budoff MJ, Takasu J, Ashai J, Mehrotra R. Coronary artery calcification and mortality in diabetic patients with proteinuria. *Kidney Int.* 2010;77(12):1107–14.
22. Ehara S, Kobayashi Y, Yoshiyama M, Shimada K, Shimada Y, Fukuda D, et al. Spotty calcification typifies the culprit plaque in patients with acute myocardial infarction: an intravascular ultrasound study. *Circulation.* 2004;110(22):3424–9.
23. Yesil Y, Ulger Z, Halil M, Halacli B, Yavuz BB, Yesil NK, et al. Coexistence of osteoporosis (OP) and coronary artery disease (CAD) in the elderly: it is not just a by chance event. *Arch Gerontol Geriatr.* 2012;54(3):473–6.
24. Farhat GN, Cauley JA, Matthews KA, Newman AB, Johnston J, Mackey R, et al. Volumetric BMD and vascular calcification in middle-aged women: the study of women's health across the nation. *J Bone Miner Res.* 2006;21(12):1839–46.
25. Zhou R, Zhou H, Cui M, Chen L, Xu J. The association between aortic calcification and fracture risk in postmenopausal women in China: the prospective Chongqing osteoporosis study. *PLoS One.* 2014;9(5):e93882.
26. Dent CE, Engelbrecht HE, Godfrey RC. Osteoporosis of lumbar vertebrae and calcification of abdominal aorta in women living in Durban. *Br Med J.* 1968;4(5623):76–9.
27. Sinnott B, Syed I, Sevrakov A, Barengolts E. Coronary calcification and osteoporosis in men and postmenopausal women are independent processes associated with aging. *Calcif Tissue Int.* 2006;78(4):195–202.
28. Barengolts EI, Berman M, Kukreja SC, Kouznetsova T, Lin C, Chomka EV. Osteoporosis and coronary atherosclerosis in asymptomatic postmenopausal women. *Calcif Tissue Int.* 1998;62(3):209–13.
29. Bagger YZ, Tanko LB, Alexandersen P, Qin G, Christiansen C. Radiographic measure of aorta calcification is a site-specific predictor of bone loss and fracture risk at the hip. *J Intern Med.* 2006;259(6):598–605.
30. Kim KI, Suh JW, Choi SY, Chang HJ, Choi DJ, Kim CH, et al. Is reduced bone mineral density independently associated with coronary artery calcification in subjects older than 50 years? *J Bone Miner Metab.* 2011;29(3):369–76.
31. Manson JE, Allison MA, Rossouw JE, Carr JJ, Langer RD, Hsia J, et al. Estrogen therapy and coronary-artery calcification. *N Engl J Med.* 2007;356(25):2591–602.
32. Zittermann A, Schleithoff SS, Koerfer R. Vitamin D and vascular calcification. *Curr Opin Lipidol.* 2007;18(1):41–6.
33. Navab M, Berliner JA, Watson AD, Hama SY, Territo MC, Lusis AJ, et al. The Yin and Yang of oxidation in the development of the fatty streak. A review based on the 1994 George Lyman Duff Memorial Lecture. *Arterioscler Thromb Vasc Biol.* 1996;16(7):831–42.
34. Que X, Hung MY, Yeang C, Gonen A, Prohaska TA, Sun X, et al. Oxidized phospholipids are proinflammatory and proatherogenic in hypercholesterolaemic mice. *Nature.* 2018;558(7709):301–6.
35. Sjolund M, Madsen K, von der Mark K, Thyberg J. Phenotype modulation in primary cultures of smooth-muscle cells from rat aorta. Synthesis of collagen and elastin. *Differentiation.* 1986;32(2):173–80.
36. Okada Y, Katsuda S, Matsui Y, Watanabe H, Nakanishi I. Collagen synthesis by cultured arterial smooth muscle cells during spontaneous phenotypic modulation. *Acta Pathol Jpn.* 1990;40(3):157–64.
37. Speer MY, Yang HY, Brabb T, Leaf E, Look A, Lin WL, et al. Smooth muscle cells give rise to osteochondrogenic precursors and chondrocytes in calcifying arteries. *Circ Res.* 2009;104(6):733–41.

38. Tintut Y, Alfonso Z, Saini T, Radcliff K, Watson K, Bostrom K, et al. Multilineage potential of cells from the artery wall. *Circulation*. 2003;108(20):2505–10.
39. Bostrom KI, Yao J, Guihard PJ, Blazquez-Medela AM, Yao Y. Endothelial-mesenchymal transition in atherosclerotic lesion calcification. *Atherosclerosis*. 2016;253:124–7.
40. Towler DA. Oxidation, inflammation, and aortic valve calcification peroxide paves an osteogenic path. *J Am Coll Cardiol*. 2008;52(10):851–4.
41. Lim J, Ehsanipour A, Hsu JJ, Lu J, Pedego T, Wu A, et al. Inflammation drives retraction, stiffening, and nodule formation via cytoskeletal machinery in a three-dimensional culture model of aortic stenosis. *Am J Pathol*. 2016;186(9):2378–89.
42. Tintut Y, Patel J, Parhami F, Demer LL. Tumor necrosis factor- α promotes in vitro calcification of vascular cells via the cAMP pathway. *Circulation*. 2000;102(21):2636–42.
43. Tintut Y, Patel J, Territo M, Saini T, Parhami F, Demer LL. Monocyte/macrophage regulation of vascular calcification in vitro. *Circulation*. 2002;105(5):650–5.
44. Al-Aly Z, Shao JS, Lai CF, Huang E, Cai J, Behrmann A, et al. Aortic Msx2-Wnt calcification cascade is regulated by TNF- α -dependent signals in diabetic Ldlr $^{-/-}$ mice. *Arterioscler Thromb Vasc Biol*. 2007;27(12):2589–96.
45. Aikawa E, Nahrendorf M, Figueiredo JL, Swirski FK, Shtatland T, Kohler RH, et al. Osteogenesis associates with inflammation in early-stage atherosclerosis evaluated by molecular imaging in vivo. *Circulation*. 2007;116(24):2841–50.
46. Brodeur MR, Brissette L, Falstra L, Ouellet P, Moreau R. Influence of oxidized low-density lipoproteins (LDL) on the viability of osteoblastic cells. *Free Radic Biol Med*. 2008;44(4):506–17.
47. Tintut Y, Morony S, Demer LL. Hyperlipidemia promotes osteoclastic potential of bone marrow cells ex vivo. *Arterioscler Thromb Vasc Biol*. 2004;24(2):e6–10. <https://doi.org/10.1161/01.ATV.0000112023.62695.7f>.
48. Parhami F, Tintut Y, Beamer WG, Gharavi N, Goodman W, Demer LL. Atherogenic high-fat diet reduces bone mineralization in mice. *J Bone Miner Res*. 2001;16(1):182–8.
49. Piri F, Lu J, Ye F, Bezouglaia O, Atti E, Ascenzi MG, et al. Adverse effects of hyperlipidemia on bone regeneration and strength. *J Bone Miner Res*. 2012;27(2):309–18.
50. Tintut Y, Demer LL. Effects of bioactive lipids and lipoproteins on bone. *Trends Endocrinol Metab*. 2014;25(2):53–9.
51. Parhami F, Morrow AD, Balucan J, Leitinger N, Watson AD, Tintut Y, et al. Lipid oxidation products have opposite effects on calcifying vascular cell and bone cell differentiation. A possible explanation for the paradox of arterial calcification in osteoporotic patients. *Arterioscler Thromb Vasc Biol*. 1997;17(4):680–7.
52. Parhami F, Jackson SM, Tintut Y, Le V, Balucan JP, Territo M, et al. Atherogenic diet and minimally oxidized low density lipoprotein inhibit osteogenic and promote adipogenic differentiation of marrow stromal cells. *J Bone Miner Res*. 1999;14(12):2067–78.
53. Tintut Y, Parhami F, Tsingotjidou A, Tetradis S, Territo M, Demer LL. 8-Isoprostaglandin E2 enhances receptor-activated NF κ B ligand (RANKL)-dependent osteoclastic potential of marrow hematopoietic precursors via the cAMP pathway. *J Biol Chem*. 2002;277(16):14221–6.
54. Puri R, Nicholls SJ, Shao M, Kataoka Y, Uno K, Kapadia SR, et al. Impact of statins on serial coronary calcification during atheroma progression and regression. *J Am Coll Cardiol*. 2015;65(13):1273–82.
55. Saremi A, Bahn G, Reaven PD, Investigators V. Progression of vascular calcification is increased with statin use in the Veterans Affairs Diabetes Trial (VADT). *Diabetes Care*. 2012;35(11):2390–2.
56. Houslay ES, Cowell SJ, Prescott RJ, Reid J, Burton J, Northridge DB, et al. Progressive coronary calcification despite intensive lipid-lowering treatment: a randomised controlled trial. *Heart*. 2006;92(9):1207–12.
57. McEvoy JW, Blaha MJ, Defilippis AP, Budoff MJ, Nasir K, Blumenthal RS, et al. Coronary artery calcium progression: an important clinical measurement? A review of published reports. *J Am Coll Cardiol*. 2010;56(20):1613–22.

58. Mundy G, Garrett R, Harris S, Chan J, Chen D, Rossini G, et al. Stimulation of bone formation in vitro and in rodents by statins. *Science*. 1999;286(5446):1946–9.
59. Lin SM, Wang JH, Liang CC, Huang HK. Statin use is associated with decreased osteoporosis and fracture risks in stroke patients. *J Clin Endocrinol Metab*. 2018;103(9):3439–48.
60. Yue J, Zhang X, Dong B, Yang M. Statins and bone health in postmenopausal women: a systematic review of randomized controlled trials. *Menopause*. 2010;17(5):1071–9.
61. Pena JM, Asperg S, MacFadyen J, Glynn RJ, Solomon DH, Ridker PM. Statin therapy and risk of fracture: results from the JUPITER randomized clinical trial. *JAMA Intern Med*. 2015;175(2):171–7.
62. Cipriani C, Irani D, Bilezikian JP. Safety of osteoanabolic therapy: a decade of experience. *J Bone Miner Res*. 2012;27(12):2419–28.
63. Wang Y, Nishida S, Boudignon BM, Burghardt A, Elalieh HZ, Hamilton MM, et al. IGF-I receptor is required for the anabolic actions of parathyroid hormone on bone. *J Bone Miner Res*. 2007;22(9):1329–37.
64. Huang MS, Morony S, Lu J, Zhang Z, Bezouglia O, Tseng W, et al. Atherogenic phospholipids attenuate osteogenic signaling by BMP-2 and parathyroid hormone in osteoblasts. *J Biol Chem*. 2007;282(29):21237–43.
65. Huang MS, Lu J, Ivanov Y, Sage AP, Tseng W, Demer LL, et al. Hyperlipidemia impairs osteoanabolic effects of PTH. *J Bone Miner Res*. 2008;23(10):1672–9.
66. Okano K, Wu S, Huang X, Pirola CJ, Juppner H, Abou-Samra AB, et al. Parathyroid hormone (PTH)/PTH-related protein (PTHrP) receptor and its messenger ribonucleic acid in rat aortic vascular smooth muscle cells and UMR osteoblast-like cells: cell-specific regulation by angiotensin-II and PTHrP. *Endocrinology*. 1994;135(3):1093–9.
67. Hagstrom E, Michaelsson K, Melhus H, Hansen T, Ahlstrom H, Johansson L, et al. Plasma-parathyroid hormone is associated with subclinical and clinical atherosclerotic disease in 2 community-based cohorts. *Arterioscler Thromb Vasc Biol*. 2014;34(7):1567–73.
68. Yamada S, Giachelli CM. Vascular calcification in CKD-MBD: roles for phosphate, FGF23, and klotho. *Bone*. 2017;100:87–93.
69. Shao JS, Cheng SL, Charlton-Kachigian N, Loewy AP, Towler DA. Teriparatide (human parathyroid hormone (1-34)) inhibits osteogenic vascular calcification in diabetic low density lipoprotein receptor-deficient mice. *J Biol Chem*. 2003;278(50):50195–202.
70. Hsu JJ, Lu J, Umar S, Lee JT, Kulkarni RP, Ding Y, et al. Effects of teriparatide on morphology of aortic calcification in aged hyperlipidemic mice. *Am J Physiol Heart Circ Physiol*. 2018;314(6):H1203–H13.
71. Jono S, Nishizawa Y, Shioi A, Morii H. Parathyroid hormone-related peptide as a local regulator of vascular calcification. Its inhibitory action on in vitro calcification by bovine vascular smooth muscle cells. *Arterioscler Thromb Vasc Biol*. 1997;17(6):1135–42.
72. Rashid G, Bernheim J, Green J, Benchetrit S. Parathyroid hormone stimulates endothelial expression of atherosclerotic parameters through protein kinase pathways. *Am J Physiol Renal Physiol*. 2007;292(4):F1215–8.
73. Ariyoshi T, Eishi K, Sakamoto I, Matsukuma S, Odate T. Effect of etidronic acid on arterial calcification in dialysis patients. *Clin Drug Investig*. 2006;26(4):215–22.
74. Hashiba H, Aizawa S, Tamura K, Kogo H. Inhibition of the progression of aortic calcification by etidronate treatment in hemodialysis patients: long-term effects. *Ther Apher Dial*. 2006;10(1):59–64.
75. Nitta K, Akiba T, Suzuki K, Uchida K, Watanabe R, Majima K, et al. Effects of cyclic intermittent etidronate therapy on coronary artery calcification in patients receiving long-term hemodialysis. *Am J Kidney Dis*. 2004;44(4):680–8.
76. Torregrosa JV, Fuster D, Gentil MA, Marcen R, Guirado L, Zarraga S, et al. Open-label trial: effect of weekly risedronate immediately after transplantation in kidney recipients. *Transplantation*. 2010;89(12):1476–81.

77. Toussaint ND, Lau KK, Strauss BJ, Polkinghorne KR, Kerr PG. Effect of alendronate on vascular calcification in CKD stages 3 and 4: a pilot randomized controlled trial. *Am J Kidney Dis.* 2010;56(1):57–68.
78. Hill JA, Goldin JG, Gjertson D, Emerick AM, Greaser LD, Yoon HC, et al. Progression of coronary artery calcification in patients taking alendronate for osteoporosis. *Acad Radiol.* 2002;9(10):1148–52.
79. Tanko LB, Qin G, Alexandersen P, Bagger YZ, Christiansen C. Effective doses of ibandronate do not influence the 3-year progression of aortic calcification in elderly osteoporotic women. *Osteoporos Int.* 2005;16(2):184–90.
80. Price PA, Faus SA, Williamson MK. Bisphosphonates alendronate and ibandronate inhibit artery calcification at doses comparable to those that inhibit bone resorption. *Arterioscler Thromb Vasc Biol.* 2001;21(5):817–24.
81. Narisawa S, Harnedy D, Yadav MC, O'Neill WC, Hoylaerts MF, Millan JL. Novel inhibitors of alkaline phosphatase suppress vascular smooth muscle cell calcification. *J Bone Miner Res.* 2007;22(11):1700–10.
82. Cutini PH, Rauschemberger MB, Sandoval MJ, Massheimer VL. Vascular action of bisphosphonates: in vitro effect of alendronate on the regulation of cellular events involved in vessel pathogenesis. *J Mol Cell Cardiol.* 2016;100:83–92.
83. Iseri K, Watanabe M, Yoshikawa H, Mitsui H, Endo T, Yamamoto Y, et al. Effects of denosumab and alendronate on bone health and vascular function in hemodialysis patients: a randomized, controlled trial. *J Bone Miner Res.* 2019;34(6):1014–24.
84. Scragg RKR. Overview of results from the vitamin D assessment (ViDA) study. *J Endocrinol Investig.* 2019;42:1391.
85. Burt LA, Billington EO, Rose MS, Raymond DA, Hanley DA, Boyd SK. Effect of high-dose vitamin D supplementation on volumetric bone density and bone strength: a randomized clinical trial. *JAMA.* 2019;322(8):736–45.
86. Sato Y, Iwamoto J, Honda Y. RETRACTED: beneficial effect of etidronate therapy in chronically hospitalized, disabled patients with stroke. *J Stroke Cerebrovasc Dis.* 2010;19(3):198–203.
87. Hsia J, Heiss G, Ren H, Allison M, Dolan NC, Greenland P, et al. Calcium/vitamin D supplementation and cardiovascular events. *Circulation.* 2007;115(7):846–54.
88. Bolland MJ, Grey A, Gamble GD, Reid IR. Concordance of results from randomized and observational analyses within the same study: a re-analysis of the women's health initiative limited-access dataset. *PLoS One.* 2015;10(10):e0139975.
89. Price PA, Buckley JR, Williamson MK. The amino bisphosphonate ibandronate prevents vitamin D toxicity and inhibits vitamin D-induced calcification of arteries, cartilage, lungs and kidneys in rats. *J Nutr.* 2001;131(11):2910–5.
90. Price PA, Faus SA, Williamson MK. Warfarin-induced artery calcification is accelerated by growth and vitamin D. *Arterioscler Thromb Vasc Biol.* 2000;20(2):317–27.
91. Henley C, Colloton M, Cattle RC, Shatzen E, Towler DA, Lacey D, et al. 1,25-Dihydroxyvitamin D3 but not cinacalcet HCl (Sensipar/Mimpara) treatment mediates aortic calcification in a rat model of secondary hyperparathyroidism. *Nephrol Dial Transplant.* 2005;20(7):1370–7.
92. Inoue T, Kawashima H. 1,25-Dihydroxyvitamin D3 stimulates $^{45}\text{Ca}^{2+}$ -uptake by cultured vascular smooth muscle cells derived from rat aorta. *Biochem Biophys Res Commun.* 1988;152(3):1388–94.
93. Wang TJ, Pencina MJ, Booth SL, Jacques PF, Ingelsson E, Lanier K, et al. Vitamin D deficiency and risk of cardiovascular disease. *Circulation.* 2008;117(4):503–11.
94. Shroff R, Egerton M, Bridel M, Shah V, Donald AE, Cole TJ, et al. A bimodal association of vitamin D levels and vascular disease in children on dialysis. *J Am Soc Nephrol.* 2008;19(6):1239–46.
95. Seibert E, Lehmann U, Riedel A, Ulrich C, Hirche F, Brandsch C, et al. Vitamin D3 supplementation does not modify cardiovascular risk profile of adults with inadequate vitamin D status. *Eur J Nutr.* 2017;56(2):621–34.

Chapter 16

Cellular Contributors to Bone Homeostasis



Martina Rauner, Katharina Jähn, Haniyeh Hemmatian, Juliane Colditz,
and Claudia Goettsch

Introduction

Bone is a multi-functional organ. The skeletal system serves as connective tissue but also exhibits mechanical, metabolic, and endocrine functions [1]. It provides mechanical support to protect the brain, as well as other soft organs within the rib cage from damage. Bone is a storage site for calcium and phosphate and serves as a target organ for paracrine and endocrine factors that maintain mineral homeostasis and regulate energy outlay. Moreover, as an endocrine organ, the skeletal system contributes to body homeostasis through secreted molecules that exhibit effects on peripheral organs [2–4]. The skeleton is a complex and dynamic tissue that, in addition to its biomechanical properties, harbors stem cells and specific precursor cells of the hematopoietic and immune system [5, 6].

To maintain physiological bone mass, the skeleton undergoes constant remodeling processes. Bone remodeling is a lifelong dynamic process that guarantees efficient degradation of old bone in balance with replacement by new mineral. Bone mass is determined by the coordinated actions of four distinct bone cell types: bone-forming osteoblasts, bone-resorbing osteoclasts, bone-lining cells, and osteocytes.

M. Rauner · J. Colditz

Department of Medicine III, Medical Faculty of the Technische Universität Dresden,
Dresden, Germany

e-mail: Martina.rauner@ukdd.de; Juliane.colditz@ukdd.de

K. Jähn · H. Hemmatian

Department of Osteology and Biomechanics, University Medical Center Hamburg-
Eppendorf, Hamburg, Germany

C. Goettsch (✉)

Department of Cardiology, Medical Faculty, RWTH Aachen University, Aachen, Germany

e-mail: cgoettsch@ukaachen.de

© Springer Nature Switzerland AG 2020

E. Aikawa, J. D. Hutcheson (eds.), *Cardiovascular Calcification and Bone Mineralization*, Contemporary Cardiology,

https://doi.org/10.1007/978-3-030-46725-8_16

333

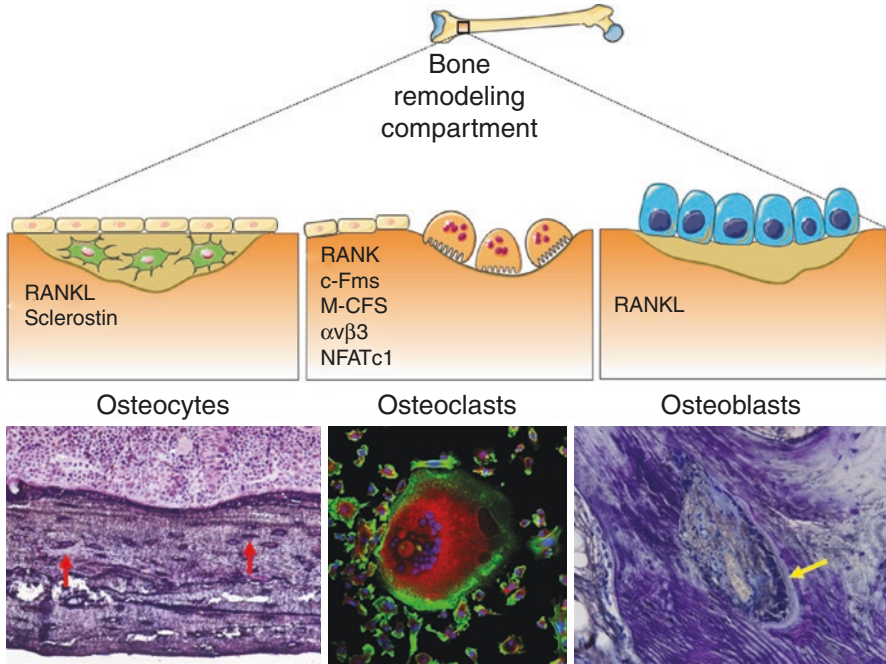


Fig. 16.1 Bone remodeling occurs in the bone remodeling compartment through the coordinated action of osteocytes, osteoblast, and osteoclasts. The molecular machinery in each cell contributes to proper cellular function. Images below: Left – osteocytes (red arrow) in murine cortical bone, silver precipitation technique: Nuclei were visualized using thionin counter stain. Middle – primary mouse osteoclast differentiated in vitro from bone marrow progenitors using M-CFS and RANKL. Immunofluorescence staining of actin rings (green), trap (red). Nuclei were visualized using DAPI (blue). Right – osteoblasts (yellow arrow) in human trabecular bone specimen embedded undecalcified in poly(methyl methacrylate), toluidine blue staining. The figure was partially created using Servier Medical Art, licensed under a Creative Commons Attribution 3.0 Unported License

Bone-lining cells build a monolayer that covers the bone surface in the quiescent state. Osteocytes, embedded within the bone matrix during skeletal maturation, are important mechanosensing cells and therefore key skeletal communicators [7]. Under physiological conditions, the equilibrium and coupling of bone resorption with bone formation is tightly fine-tuned to ensure proper bone mass and quality. Bone remodeling occurs in four steps in a highly vascularized special space called “bone remodeling compartment” (BMC, Fig. 16.1) [8]. Remodeling initiates by recruitment of osteoclasts to BMC by osteocytes. Differentiated and functional active osteoclasts cause bone resorption and concurrent recruitment of mesenchymal stem cells. Osteoblasts differentiate and form new bone. In the final step, the osteoid mineralizes [7].

In many pathophysiological conditions, the impairment of these mechanisms triggers a dysregulation of bone remodeling, causing unbalanced between bone resorption and formation. A consequential loss in bone mass and/or alteration in

bone microarchitecture can lead to skeletal destruction and increased fracture risk, in conditions like osteoporosis, rheumatoid arthritis, and skeletal metastases [9].

Osteoblasts

Osteoblasts stem from mesenchymal stem cells (MSC), similar to chondrocytes, adipocytes, myocytes, and other stromal cells. More recently, studies characterized the skeletal stem cell more precisely, showing that osteoblasts, chondrocytes, and stromal cells share a progenitor cell that does not give rise to adipocytes or myocytes, indicating that these cells are more closely related in the hierarchical tree [10]. Importantly, these observations also hold true for human skeletal stem cells [11]. Osteoblasts are specialized cells that produce the bone matrix by first laying down the organic matrix (i.e., osteoid), which mostly consists of type I collagen and other non-collagenous proteins such as osteocalcin or osteopontin, and then contributing to the mineralization of the matrix. During matrix production, osteoblasts have a cuboidal shape and are packed with endoplasmic reticulum and mitochondria. Hydroxyapatite-based microcrystals are deposited into the collagen matrix, which requires two phases: (I) the removal of acid evolved during hydroxyapatite nucleation by the osteoblast to allow for matrix deposition, and (II) mineral maturation from amorphous calcium phosphate to hydroxyapatite, which is associated with important changes in mineral orientation and organization, leading to the dense lamellar structure of mature bone. This process is critically dependent on pH and the function of tissue non-specific alkaline phosphatase (TNAP) as a supplier of phosphate, which works best at an alkaline pH [12–14].

Besides producing the bone matrix, osteoblasts have additional functions including providing a niche for hematopoietic stem cells [5, 15], as well as regulation of energy production [16, 17], male fertility [18, 19], and brain function by producing osteocalcin [20], which has been identified as a factor with hormonal actions on distant organ sites. Most importantly, however, osteoblasts are key regulators of bone resorption by osteoclasts, as they produce receptor activator of NF- κ B ligand (RANKL) and its endogenous inhibitor osteoprotegerin (OPG), to determine the rate of osteoclastogenesis and bone resorption [21–24]. Thus, bone formation and bone resorption are tightly coupled processes that underlie a strict regulation within not only the communication between osteoblasts and osteoclasts but also other cells that influence their communication, including osteocytes and immune cells.

Osteoblast Differentiation

Osteoblast differentiation is a multi-step process, beginning with maturation from stem cell into an osteoblast progenitor, then to a pre-osteoblast, and finally to a mature osteoblast. These stages are paralleled by different functional steps,

including cell proliferation, matrix production, and mineralization. Once fully matured, osteoblasts either undergo apoptosis, become quiescent bone-lining cells that can be reactivated quickly after proper stimuli (e.g., parathyroid hormone (PTH) or inhibition of sclerostin), or terminally differentiate into osteocytes. How the osteoblast fate is chosen remains largely unknown.

To differentiate, two transcription factors are absolutely necessary: Runt-related transcription factor 2 (Runx2) and osterix (Osx). Deficiency of either of these transcription factors in mice results in a non-mineralized skeleton made of only cartilage [25–27]. Both intramembranous and endochondral ossification are completely lacking in Runx2^{-/-} and Osx^{-/-} mice. These transcription factors are important not only in mice but also in humans. Mutations in the gene encoding for Runx2 are associated with cleidocranial dysplasia [28]. Several growth factor signals that are crucial for osteoblast differentiation, such as bone morphogenetic protein (BMP) signaling, fibroblast-like growth factor, or insulin-like growth factor signaling, use either Runx2 or Osx as their downstream transcriptional mediators. Besides Runx2 and Osx, Msx1 and Msx2 are critical for osteoblast differentiation in cranial bone [29]. In addition, several other transcription factors are important for osteoblastic differentiation at various sites including Dlx5, Dlx6, AP1, ATF4, NFATs, and Twist proteins [30].

Regulatory Pathways

Osteoblast differentiation is regulated by several growth factor pathways and systemic hormones (e.g., vitamin D or glucocorticoids). However, studies in mice and humans have shown that two pathways are central regulators of ossification and osteoblast differentiation. These are the BMP and Wnt signaling pathways.

BMPs belong to the transforming growth factor beta (TGF β) superfamily and have essential functions during embryogenesis, organogenesis, as well as cell proliferation and stem cell differentiation. Of the 15 identified BMPs, BMP2, 4, 6, 7, and 9 exhibit osteoinductive capabilities. They promote the commitment of mesenchymal stem cells to osteoprogenitors and further stimulate osteoblastogenesis and bone mineralization [31–33]. BMP2 and BMP4 deficiencies are embryonically lethal. Conditional knockout of BMP2 and BMP4 alone or in combination in osteoblasts results in impaired bone formation caused by dysfunctional chondrocyte and osteoblast differentiation as well as function [33, 34]. Besides the ligands, BMP receptors (e.g., ALK2, ALK3, ACVR1) in osteoblasts were also shown to play a role in ossification [35–38]. Constitutive activation and/or different ligand susceptibilities of mutated ALK2 lead to a rare genetic disease called fibrodysplasia ossificans progressiva, which is characterized by excessive heterotopic ossification [39, 40].

The BMP signal transduction is initiated upon BMP ligand binding to a receptor heterodimer complex, which consists of type I and type II BMP transmembrane serine/threonine kinase receptors (BMPR). The constitutively active BMPR type II activates BMPR type I through phosphorylation upon ligand binding. The

SMAD-dependent pathway is the classical, canonical BMP pathway and is based on the activation of R-Smads (Smad 1, 5, 8) and co-Smads (Smad 4), which, when translocated into the nucleus, can bind to BMP responsive elements and initiate the transcription of osteoblastic genes. Furthermore, BMP signaling can induce non-canonical signaling pathways, including mitogen-activated protein kinases such as extracellular signal-regulated kinases (ERK), c-Jun N-terminal kinases (JNK), and P38 mitogen-activated protein kinases (P38) to induce osteopromoting outcomes [33]. Also the phosphatidylinositol 3-kinase/protein kinase B (PI3K/AKT) pathway has been implicated to play a role in BMP-mediated signaling in osteoblasts [41, 42].

The BMP signaling pathway is regulated via numerous inhibitors including inhibitory SMADs (Smad 6, Smad 7) as well as extracellular antagonists such as gremlin, chordin, and noggin [43]. Noggin has been investigated in great detail in the context of bone. Either overexpression or conditional knockout of noggin leads to low bone mineral density and reduced bone formation [44, 45], suggesting that optimal levels of BMP signaling are required for proper bone formation.

The Wnt signaling pathway is among the most critical pathways to regulate osteoblast differentiation. Mutations in components of the Wnt signaling pathway result in drastic skeletal alterations in both mice and humans. In brief, activation of Wnt signaling leads to enhanced osteoblast differentiation and bone formation, while inhibition results in decreased osteoblastogenesis. Thus, Wnt signaling has also been a major target to develop new treatments for osteoporosis [46].

Wnt signaling exhibits a similarly complex pathway as BMP signaling, containing 19 Wnt ligands, 10 Frizzled-receptor (FZD) variants, and multiple intracellular and extracellular inhibitors [46]. Moreover, Wnt signaling is divided between canonical Wnt signaling, which uses β -catenin as transcriptional mediator, and non-canonical β -catenin-independent pathways [47]. Canonical Wnt signaling is activated when canonical Wnt ligands (e.g., Wnt1, Wnt3a, Wnt10b) bind to the FZD receptors and LDL receptor-related protein (LRP)5/6 co-receptors. This leads to the resolution of the β -catenin destruction complex, which consists of scaffold protein axin, adenomatous polyposis coli, casein kinase 1, and constitutively active glycogen synthase kinase 3. Destruction of this complex leads to phosphorylation of cytosolic β -catenin, resulting in its ubiquitination and degradation. The non-degraded β -catenin accumulates in the cytosol and eventually translocates into the nucleus where it activates the transcription of target genes by recruiting transcriptional activators to the T cell factor/lymphoid enhancer factor (TCF/LEF) transcription complex [46–48]. In contrast to the β -catenin-dependent activation of transcription factors in canonical Wnt signaling, non-canonical Wnt signaling is independent of LRPs and activates other pathways including small Rho GTPases/JNK signaling, calcium-dependent NFAT signaling, and PI3K/Akt signaling that are known to control planar cell polarity, cell differentiation, and tissue patterning. Both canonical and non-canonical signals are important regulators of trabecular and cortical bone homeostasis. Mutations in the genes encoding Wnt signaling molecules (e.g., Wnt1, Wnt5a, Wnt16) lead to altered bone phenotypes, affecting either osteoblast differentiation or osteoblast-mediated communication [49–51]. As such, human mutations in WNT1 are associated with early-onset osteoporosis, and

mutations in the WNT5A gene lead to autosomal dominant Robinow syndrome-1, which is characterized by short stature [52, 53]. In the case of LRP5, gain-of-function mutations lead to high bone mass in mice and humans, while loss-of-function mutations lead to osteopenia [54, 55].

As with all developmental pathways, Wnt signaling is tightly regulated. It can be blocked at various levels including extracellular and intracellular inhibitors. At the ligand level, secreted frizzled-related proteins and Wnt inhibitory factor 1 associate with the Wnt ligands themselves, sequestering them and thus inhibiting their binding to FZD [46, 47]. The family of Dickkopf (Dkk) proteins and sclerostin, on the other hand, bind to LRP5/6, thereby preventing their interaction with FZD. In the bone context, Dkk1 and sclerostin have been shown to be main regulators of bone mass. Deficiency of either protein leads to a high bone mass, whereas overexpression of Dkk1 or sclerostin leads to low bone mass [56–59]. Sclerostin is mainly produced by osteocytes, whereas Dkk1 is expressed in different organs including bone, skin, placenta, and the prostate. Due to the site-specific expression of sclerostin, neutralizing antibodies were developed that are now available as one of the few bone-anabolic options to treat postmenopausal osteoporosis [60]. Interestingly, however, deficiency or suppression of Dkk1 or sclerostin leads to a compensatory increase in the other Wnt inhibitor, thereby limiting the long-term efficacy of blocking sclerostin or Dkk1 [56, 61, 62]. Thus, at least experimentally, bi-specific antibodies targeting Dkk1 and sclerostin show the greatest increase in bone mass and, therefore, may be the most potent option to induce bone anabolism in the future [61].

Osteoclasts

The physiological removal of old bone by osteoclasts is necessary for growth, development, and bone remodeling to adapt the adult skeleton to function and external conditions. Loss of bone mass is the consequence of increased skeleton degradation rate relative to its formation. Pathophysiological osteoclast differentiation and activation plays a key role in osteolysis (e.g., osteoporosis). Thus, understanding the complex biology and regulatory mechanisms of osteoclasts is necessary to develop strategies to prevent pathologic bone resorption.

Osteoclasts exclusively resorb bone. They are terminally differentiated cells derived from the hematopoietic lineage and therefore phenotypically related to macrophage and dendritic cells [7]. Osteoclasts are giant multinucleated cells (Fig. 16.1) that form from maturation and fusion of mononuclear precursor cells, which differentiate from bone marrow monocytes/macrophages [7]. The origin of osteoclasts was demonstrated using a parabiosis model more than 40 years ago [63]. Recent evidence shows that osteoclasts derive from embryonic erythro-myeloid progenitors and are in fact long-lived cells that use iterative fusion of monocytic precursor cells for their maintenance throughout life [64]. Osteoclast precursor cells express cell surface receptors, like macrophage-1 (mac-1), macrophage colony-stimulating factor (M-CSF) receptor c-fms, receptor activator of NF- κ B (RANK), and receptors

for co-stimulatory molecules such as osteoclast-associated receptor (OSCAR) [65, 66]. It is suggested that the recruitment of osteoclast precursors from the bone marrow occurs by either crossing the bone-lining cells or from capillaries that penetrate into BMC [67, 68].

The generation of mature osteoclasts capable of resorbing bone is a multi-step process. It includes the presence and priming of osteoclastic precursor cells, multinucleation and maturation, and finally activation that triggers specific cytoskeletal rearrangements, cell motility, attachment to bone matrix, and resorption [7].

Osteoclast Differentiation

There are only two essential and sufficient cytokines for osteoclastogenesis in vitro: (I) macrophage colony-stimulating factor (M-CFS) that participates in promoting cell proliferation and survival of osteoclast precursors and (II) RANKL that drives osteoclast differentiation, fusion, activation, activity, and survival [24, 69, 70].

M-CFS stimulates the expression of RANK – the signaling receptor for RANKL – in osteoclast precursor cell [7]. The central role of RANKL in osteoclast differentiation led to the successful development a neutralizing antibody, denosumab, which inhibits bone resorption and reduces fracture risk [71]. Mature osteoclasts tightly adhere to bone and release hydrogen ions that acidify the interface between bone and osteoclast, leading to bone resorption.

Physiological osteoclast differentiation requires the presence of RANKL-secreting bone-resident cells, like osteoblasts, marrow stromal cells, and osteocytes [72]. Mice lacking RANK or RANKL develop osteopetrosis due to lack of osteoclasts, demonstrating the importance of the RANK/RANKL system [73, 74].

When RANKL binds to RANK expressed on osteoclast precursors, a set of transcription factors (e.g., NF- κ B, activator protein-1 (AP-1), and nuclear factor of activated T cells (NFAT)) are activated that modulate the expression of osteoclast-specific effector proteins [75].

Binding of M-CFS to its receptor c-fms activates the receptor by dimerization and promotes alteration in the cytoskeleton and expression of RANK on osteoclast precursors, increasing susceptibility to RANKL binding [7]. The transcription factor PU.1 promotes the expression c-fms. In fact, mice lacking PU.1 show a failure in macrophage differentiation [76] and inhibition of osteoclastogenesis [77].

RANK lacks intrinsic kinase activity. Therefore, the activation of RANK by RANKL causes the recruitment of intracellular adaptor protein tumor necrosis factor receptor-associated factors (TRAFs) to three different motifs of the intracellular domain of RANK [78, 79]. As a consequence, a cascade-like intracellular signaling transduction initiates osteoclast formation, function, and survival and inhibits osteoclast apoptosis via several signaling pathways. The TRAF-6 recruiting motif activates NF κ B, JNK, ERK, p38, and Akt. NF κ B signaling pathway then activates NFATc1 [80]. TRAF-6-deficient mice exhibit an osteopetrosis bone phenotype [81]. The role and function of the two other TRAF motifs are not clear yet [82].

Concurrent activation of co-stimulatory molecules/immunoreceptor tyrosine-based activation motif (ITAM) signaling (like osteoclast-associated receptor (OSCAR), DNAX-activating protein of 12 kDa (DAP12), or FC receptor common gamma subunit (FcR γ)) modulates RANK-mediated processes [83]. This causes Ca-dependent activation of calcineurin that directly activates NFATc1. Deficiency of DAP12 or FcR γ results in subtle osteoclastic defects, while deletion of both molecules causes severe osteopetrosis [84]. NFATc1 is an established master transcription factor of osteoclastogenesis. As part of a transcription factor complex with MIFT, PU1, CREB, and API1, NFATc1 participates in differentiation and fusion of osteoclasts. NFATc1-regulated genes are cathepsinK, MMP9, H⁺ ATPase, and CIC7 [85].

Osteoclast Resorptive Capacity

The bone matrix consists of inorganic (mainly crystalline hydroxyapatite) and organic components (e.g., collagen type I) [86]. Therefore, the resorption has to involve the dissolution of hydroxyapatite followed by the proteolytic cleavage of organic components.

The osteoclast activation is primarily characterized by the establishment of two essential structural and functional features for proper resorption: the ruffled border and the isolated resorption compartment [7]. The resorption compartment is isolated from the general extracellular space. It is formed by the attachment of osteoclasts to the bone matrix through a structural feature called the sealing zone. This forms a closed microenvironment between the underlying matrix and the osteoclast also called “clear zone” that is key for resorptive events. This physical interaction of bone matrix and osteoclast is mediated by integrin $\alpha\beta3$ and corresponding proteins in the extracellular matrix (e.g., osteopontin, vitronectin, or bone sialoprotein) [87]. The interaction induces cytoskeleton re-organization cooperatively with M-CFS via the c-Src-signaling complex. Osteoclasts polarize fibrillary actin to circular structures to create the typical actin ring surrounding of the ruffled border that generates the isolated resorptive compartment [88]. In vitro and in vivo studies demonstrated that integrin $\alpha\beta3$ is the main integrin mediating bone resorption [89]. Integrin $\alpha\beta3$ -deficient mice develop osteopetrosis [90].

The ruffled border is the resorptive organelle of osteoclasts and a morphological characteristic to increase the surface area [7]. The transport of protons and proteolytic enzymes into the resorption compartment is required to dissolve mineral and degrade bone matrix proteins [91]. The ruffled border is formed by migration and insertion of acidified vesicles loaded with proton pumps and cathepsin K through microtubules and actin to the plasma membrane facing the bone leading to the expression of vacuolar H⁺-adenosine triphosphate (H⁺-ATPase) and chloride channels, and release of proteolytic enzymes into the clear zone by endocytosis

[92]. Diminished function of each of the three proteins results in human disease with excess bone mass demonstrating their critical role in bone resorption [92]. H^+ -ATPase then transports protons to decrease the pH (to about 4) of the resorption compartment, while chloride ions are transported to maintain electro-neutrality. Cytoplasmic carbonic acid is the main source of protons [93]. Passive chloride-bicarbonate exchanger supplies chloride ions. Acidification mobilizes hydroxyapatite crystals from the bone and provides an optimal activity environment for proteolytic enzymes like cathepsin K [92]. Collagen type I degradation products are removed by transcytosis. Products are endocytosed and transported in vesicles to basolateral surface of the cell and discharged into surrounding intracellular fluid [94].

Fine-Tuning of Osteoclast Formation and Function

The RANKL signaling cascade is regulated at multiple levels to ensure proper controlled osteoclastogenesis. OPG is a neutral antagonist that controls the interaction between RANK and RANKL [23]. OPG has a high affinity to RANKL and acts as soluble decoy receptor. Cells of the mesenchymal origin secrete OPG basally and in response to regulatory signals like cytokines or bone-targeting steroids [95]. The OPG/RANKL system ensures physiological balance of bone resorption and formation. Genetic deletion of OPG in humans and mice causes osteoporosis, while OPG overexpression results in osteopetrosis [23, 96]. Under pro-inflammatory conditions, cytokines suppress OPG and increase RANKL, causing increased osteoclast formation and activity [95].

RANKL-independent osteoclastogenesis remains controversial. The combination of $TNF\alpha$ with $TGF\beta$ or IL6 can induce osteoclastogenesis dependent on NFATc1 and DAP12 under pathophysiological conditions [97–99]. Other studies showed that IL-1 and $TNF\alpha$ stimulate osteoclastogenesis via TRAF-6 and TRAF-2 in postmenopausal osteoporosis and rheumatoid arthritis but cannot induce it independent of RANKL [100]. IL-1 and $TNF\alpha$ seem to increase the expression of M-CFS and RANKL [101], concluding that pro-inflammatory cytokines synergize RANKL-induced osteoclastogenesis.

Interferon (IFN) γ may serve as an anti-osteoclastogenic cytokine [102]. It has been shown to be a suppressor of osteoclast formation and function via a negative feedback pathway in vitro [102], but existing data are conflicting [103]. RANKL induces IFN γ , which simultaneously suppresses RANKL and its downstream genes.

Other cytokines have also been suggested, but the data remain unclear. The lingering confusion may be related to a lack of translation of mouse observations in human physiology. For example, another c-fms ligand interleukin (IL)-34 can support osteoclastogenesis together with RANKL [104]. However, since mouse models that lack functional M-CFS reveal reduced osteoclast, IL-34 may only play a role in pathophysiological conditions like rheumatoid arthritis [105].

Osteocytes

Within the mineralized bone matrix, a cellular network of specialized bone cells directs bone homeostasis. Osteocytes are star-shaped cells that possess several long dendritic processes connecting osteocytes to one another and cells on the bone matrix surface to form a global communicative cell network in bone. Nutrient supply and waste product removal are managed by the surrounding fluid-filled interstitium. The osteocyte cell body lies within a lacuna and each process in a fluid-filled canaliculus. Through exercise and body movements, the bone matrix and thereby the fluid inside the lacuno-canalicular system are stretched and compressed and put a strain upon the osteocytes. The resultant mechanotransduction that dictates bone remodeling resulted in osteocytes being termed the “mechanosensor of bone”. Osteocytes can direct the function of both bone-producing osteoblasts and bone-resorbing osteoclasts, adapting the local bone matrix to withstand loading.

Regulatory Pathways Involved in Osteocytogenesis

Osteocytes are considered terminally differentiated osteoblasts belonging to the mesenchymal cell lineage. Once a seam of active osteoblasts “finish” their work of producing the collagen type I-rich osteoid, three potential cell fates have been discovered: I) Osteoblasts can undergo apoptosis as a final endpoint [106]. II) Some osteoblasts lose their cuboidal, active phenotype and transform into flat bone-lining cells covering inactive bone surfaces, waiting to be reactivated by signals (e.g., parathyroid hormone (PTH)) [107]. III) A selective group of osteoblasts will be embedded into the newly formed matrix. The latter process of embedding requires the osteoblast to lose most of its cytoplasm, and cell membrane extends to form dendritic processes [108]. This morphological transformation occurs stepwise to allow for an initial dendrite budding into the osteoid laid out below the cell body. During embedding the entire osteocyte forms dendrites in all directions [109]. Several proteins are sequentially expressed during osteocytogenesis and characterize the transition from an early, matrix-embedding osteocyte to a late, deeply embedded osteocyte (Table 16.1).

The molecular drivers of osteocyte differentiation are of current scientific interest, and only a few puzzle pieces have been identified so far. Factors that induce bone formation by osteoblasts (reviewed in [110]) as well as the external matrix quality can drive osteocytogenesis [111]. Some specific molecules that promote the transition of osteoblasts to osteocytes have been identified. E11/podoplanin is one driver of osteocyte transition by promoting dendrite formation [112]. Fibroblast growth factor 2 (FGF2) was identified as regulator of E11 in osteocytes. FGF2 promotes osteocytogenesis by E11 translocation to the cell membrane and increases expression of dentin matrix protein 1 (Dmp1) and phosphate-regulating gene with homologies to endopeptidases on the X chromosome (Phex) [113].

Table 16.1 Regulatory molecules and pathways involved in bone homeostasis by osteocytes

Function	Osteocytogenesis	Matrix mineralization	Phosphate homeostasis	Osteocytic osteolysis	Mechanosensation and mechanotransduction
Signaling molecule	E11/podoplanin FGF2 Dmp1 Phex miR23a TGF β Prdm16	Dmp1 Wnt3a	Dmp1 FGF23/ FGFR1 Phex MEPE/ OF45	Vacuolar ATPase MMP13/ TGF β TRAP Cathepsin K PTHrP/ PTHR1 Calcitonin Sclerostin	NO PGE2/Cx43/COX2 Wnt/ β -catenin BMPs RANKL/RANK OPG Sclerostin DKK1 IGF1 M-CSF

BMP bone morphogenetic protein, *COX2* cyclooxygenase-2, *Cx43* connexins 43, *DKK1* Dickkopf 1, *Dmp1* dentin matrix protein 1, *FGF23* fibroblast growth factor 23, *IGF1* insulin-like growth factor 1, *M-CSF* macrophage colony-stimulating factor, *MEPE* matrix extracellular phosphoglycoprotein, *NO* nitric oxide, *OPG* osteoprotegerin, *PGE2* prostaglandin E2, *Phex* X chromosome, *RANKL* receptor activator for nuclear factor κ B ligand, *TGF β* transforming growth factor-beta, *TRAP* tartrate-resistant acid phosphatase

Further, miRNAs are involved in the osteocyte differentiation. The potential contribution of miRNAs within bone became apparent through observations that the osteoblast progenitor-specific deletion of *Dicer*, a miRNA processing RNase III endonuclease, resulted in early mortality and mineralization defects in mice [114]. The miR23a cluster has been shown to regulate TGF β signaling through the repression of PR-Domain Zinc Finger Protein 16 (*Prdm16*) and thereby stimulates osteocytogenesis in mice [115].

Regulatory Pathways Involved in Mineralization

During matrix embedding and osteocyte differentiation, osteocytes are also involved in the mineralization of the newly produced matrix. Several proteins that contribute to matrix mineralization are sequentially expressed during osteocyte differentiation and can be considered differentiation markers as mentioned above.

Dmp1 is an acidic phosphoprotein and a member of the small integrin-binding ligand N-linked glycoprotein (SIBLING) family that is expressed in tooth and bone. Osteocytes produce large amounts of *Dmp1* during the mid-stage of osteocytogenesis [116]. *Dmp1* aids mineralization of the bone matrix by binding to initial calcium phosphate nanoparticles. This oligomerization stabilizes the calcium phosphate nanoparticles to direct their binding to the collagenous osteoid [117]. Initial studies also determined the mechanoresponsiveness of *Dmp1* expression in osteocytes [118]. The role of *Dmp1* in bone matrix mineralization was demonstrated by both *Dmp1*-deficient mice and the genetic analysis of patients with autosomal recessive

hypophosphatemic rickets [119, 120]. Dmp1-deficient mice showed defective mineralization of bone that coincided with impaired osteocyte differentiation. Dmp1 regulation of mineralization is based on the full-length form of the protein, which is not found in bone. Three peptide forms of Dmp1 (37kD N-terminal, 57kD C-terminal, and a chondroitin-sulfate-linked N-terminal fragment) have been identified within the mineralized matrix that all bind to hydroxyapatite and could affect mineralization [121]. Subsequently, Wnt signaling induced by Wnt3a ligand was shown to inhibit mineralization and Dmp1 expression in osteocyte cultures, resulting in altered mineral properties with larger and poorly arranged crystals negatively affecting the mechanical properties of the mineral [122]. Also, Notch signaling appears to disturb mineralization as well as osteocytogenesis in an autocrine manner, causing a disassembled deposition of hydroxyapatite and by downregulation of Wnt signaling and impaired osteocytogenesis [123, 124].

Regulatory Pathways Involved in Phosphate Homeostasis

A process inevitably linked to mineralization is the regulation of the phosphate homeostasis, and several proteins expressed by osteocytes are found to be involved in this regulation. The Dmp1 null mice exhibited decreased serum phosphate levels and elevated serum fibroblast growth factor 23 (FGF23) levels caused by excessive expression of FGF23 by osteocytes [125]. This pathological situation resembles the autosomal recessive hypophosphatemic rickets [126] characterized by inactivating mutations in Dmp1, but also the dominant form of heritable hypophosphatemic rickets due to cleavage-resistant mutations in FGF23 [127] and X-linked hypophosphatemia with mutations in the PheX protein [128]. These diseases result in high FGF23 expression by osteocytes, elevated FGF23 serum levels, and renal phosphate wasting by FGF23-induced suppression of the abundance of phosphate-transporting molecules in the proximal renal tubule leading to reduced reabsorption of phosphate from the urine. The pathologies cause similar skeletal abnormalities, including defective mineralization of the bone matrix and dysplasia pronounced as rickets during childhood and osteomalacia during adulthood. The pathological role of FGF23 is also associated with chronic kidney disease, where osteocyte expression of FGF23 serves as an endocrine regulator of the phosphaturia in the kidneys and contributes to the increased cardiovascular mortality [129].

FGF23 can be induced by several humoral factors, e.g., PTH or vitamin D (reviewed in [130]). The ratio of the mineralization-substrate phosphate to the mineralization-inhibitor pyrophosphate appears particularly important in the regulation of FGF23 secretion [131]. Mice lacking the pyrophosphate generating enzyme ectonucleotide pyrophosphatase (ENPP1) present a rickets phenotype and elevated FGF23 levels [132]. FGF23 seems to direct bone mineralization by the transcriptional suppression of TNAP. This effect was independent of the FGF23 receptor α -Klotho that is expressed at a relevant level in bone tissue [133]. While the molecular pathways regulating FGF23 production are not entirely elucidated to

date, FGF receptor 1 (FGFR1) signaling may be involved as the osteocyte-specific ablation of FGFR1 partially rescues FGF23 secretion in Hyp mice [134]. Gain-of-function mutations in FGFR1 can promote FGF23 secretion in patients [135]. The regulatory pathways to control FGF23 expression in osteocytes are tightly linked to Dmp1 and PheX expression. Double mutant PheX and Dmp1 mice (Hyp/Dmp1^{-/-}) showed non-additive elevations of serum FGF23, resulting a similar osteomalacia and rickets phenotype as seen in the single mutants [136]. Dmp1 contains the so-called ASARM motif (small protease-resistant phosphorylated acidic serine aspartate-rich MEPE-associated motif) that can be bound by PheX and prevent FGF23 transcription [137].

The intricacies of FGF23 regulation appear endless considering the revealed complexity of the posttranslational modifications of FGF23, and the protein may be protected from cleavage by O-glycosylation via polypeptide N-acetylgalactosaminyltransferase 3 (GalNT3), or phosphorylated by family with sequence similarity 20, member C (FAM20C), to favor cleavage of FGF23 [138].

Regulatory Pathways Involved in Osteocytic Osteolysis

Osteocytes control their surrounding bone matrix – the perilacunar and pericanalicular matrix – by means of osteocytic osteolysis [139]. With lactation, a calcium demanding condition due to milk production, osteocytes contribute to osteoclast-driven bone resorption and generation of free calcium from their surrounding bone matrix [140]. During this process, osteocytes demineralize their perilacunar matrix by acidifying the microenvironment involving the vacuolar ATPase as a proton pump [141]. By mechanisms unclear to date, osteocytes can resist the acidic environment produced and sustain a significantly higher viability compared to other cell types in similar conditions [141]. The process is reversible and osteocytes likely contribute to bone re-formation post-lactation [142]. During the lytic process, osteocytes not only demineralize the matrix but also utilize proteases (e.g., matrix metalloproteinase 13 (MMP13), tartrate-resistant acid phosphatase (TRAP), and cathepsin K) to digest the organic part of the perilacunar matrix [140, 143]. TGF β signaling has been shown to be involved in the process of osteocytic osteolysis involving MMP13 [144]. The osteocytic osteolysis with lactation involves the PTH related peptide (PTHrP)-induced PTHR1 signaling, which if blocked in Dmp1-expressing osteocytes prevents the enlargement of osteocyte lacunae with lactation [140].

The calcium hormone calcitonin is also implicated in osteocytic osteolysis. Lactating calcitonin receptor-deficient mice reveal larger osteocyte lacunae than littermate controls [145]. The protective role of calcitonin was indicated by calcitonin inhibition and periosteocytic demineralization in disuse osteoporosis [146].

The presence of osteocytic osteolysis remains seems a matter of controversy with immobilization or disuse (reviewed elsewhere [142]). The Wnt inhibitor sclerostin is involved in both unloading and osteocytic osteolysis. Sclerostin act in

an autocrine/paracrine fashion to induce osteocyte expression of resorptive genes and lower the pH of culture medium in vitro [147].

Regulatory Pathways Involved in Mechanosensation and Mechanotransduction

The location within a fluid-filled lacuno-canalicular system in the mineralized bone matrix makes osteocytes well-suited to sense, transduce, and translate the mechanical load that is placed upon the skeleton. Early work by Frost et al. predicted an adaptive process of bone turnover that depends on the activity level of the individual [148]. In response to mechanical loading, osteocytes release secondary messengers including prostaglandin E2 (PGE₂) and nitric oxide [149, 150], thereby regulating bone turnover. Osteocytes were shown to be highly sensitive to fluid flow in vitro that simulate forces that osteocytes could experience in vivo [151, 152]. Osteocytes also align to the load axis and possess different cytoskeletons if harboring in a non-load-bearing calvaria or a load-bearing fibula [153, 154], implying direct sensation of bone matrix deformation by osteocytes. These mechanosensation mechanisms are influenced by the morphological features of the osteocyte lacuno-canalicular network, since shape affects the applied shear stresses to osteocytes and the transmission of strain to the immediate osteocyte microenvironment [155, 156].

The mechanical forces transmitted by the fluid and matrix deformation to the osteocyte are most likely sensed by either tethering elements, connecting the dendrite to the pericanalicular matrix [157], the primary cilia of the osteocytes [158], or potentially mechanosensitive ion channels. While high-resolution imaging and experimental models support the theory that tethering elements along with strain amplification are the main osteocyte mechanosensor [159], the intracellular transmission is less clear. The primary cilium is a microtubule-based structure that extends outward from the cell. A lack of response to anabolic loading was found in osteoblast-specific kinesin-like protein 3a (Kif3a)-deficient mice [160] and osteocyte-specific polycystic kidney disease 1 (PKD1)-deficient mice [161]. Both genes regulate the function and structure of the cilium. Recently, the mechanosensitive ion channel Piezo1 was shown to play an important role in mechanosensation of osteocytes [162].

Several key molecules have been identified that are important for mechanotransduction. One of the most prominent is connexin 43 (Cx43), which functions as part of the gap junctions connecting osteocyte dendrites to one another and as part of hemichannels mediating the release of the secondary messenger PGE₂ into the fluid-filled lacuno-canalicular system [163]. The expression of Cx43 is induced in osteocytes of the alveolar bone in an in vivo model of tooth movement and in vitro induced by fluid shear stress, demonstrating the potential role of Cx43 in the regulation of bone mechanotransduction [164, 165]. Mice lacking Cx43 in osteocytes exhibit increased bone-anabolic mechanoresponsiveness in vivo and are protected

against bone loss induced by unloading [166, 167], suggesting that osteocytes restrain bone responsiveness to the mechanical stimuli through the expression of Cx43.

Immune Cells That Participate in Skeletal Homeostasis

Over the past years, the reciprocal interaction between the immune and the skeletal system gained recognition in bone research, resulting in a new interdisciplinary research field called “osteimmunology” [168–170]. The most important concepts in osteimmunology arose from the observation of increased bone loss and fracture risk in various inflammatory and autoimmune diseases such as rheumatoid arthritis and chronic viral infections [171–177]. The discovery of RANK and RANKL, two molecules that were first identified as important factors expressed on T cells and dendritic cells, and their later identification as key osteoclastogenic molecules have clearly established the link between the immune and the skeletal system. The importance of RANKL as a key regulator of osteoclastogenesis especially during inflammation was further underlined by the discovery of Kong and colleagues, who identified that activated T cells in adjuvant arthritis are capable of inducing osteoclastogenesis through the RANKL/RANK/OPG axis [172]. Since then, a number of regulatory molecules including cytokines, receptors, signaling molecules, and transcription factors have been identified in both the skeletal and the immune system [178]. Therefore, changes in one system under physiological or pathological conditions likely affect the other. Thus, understanding the mechanisms of action of osteoimmunology will help in the development of new therapeutic drugs to treat bone loss in inflammatory diseases. In the following, we will discuss the impact of different immune cell populations on bone turnover (Fig. 16.2).

For instance, macrophages promote osteoblastogenesis by the secretion of interleukin-18 [179], whereas T cells are known to influence osteoclastogenesis mainly by secretion of various cytokines such as IL-1, IL-6, IFN γ , or IL-4 [180, 181].

T Lymphocytes

Among the immune cells, T lymphocytes play a predominant role in the regulation of bone turnover. According to the subunits that form the T cell receptor (TCR), these lymphocytes can be divided into two classes expressing either $\alpha\beta$ or $\gamma\delta$ TCR on their surface [182]. The majority of T lymphocytes are $\alpha\beta$ T cells, which express either CD4 or CD8. Most of $\gamma\delta$ T cells lack CD4 and CD8 expression, and their functions remain largely unknown [183]. How T cells affect bone remodeling depends on their activation state. Under pathological conditions such as estrogen deficiency [184, 185] and inflammatory diseases such as rheumatoid arthritis and periodontitis [172, 186], activated T cells (CD4+, CD8+, and TH17) modify bone

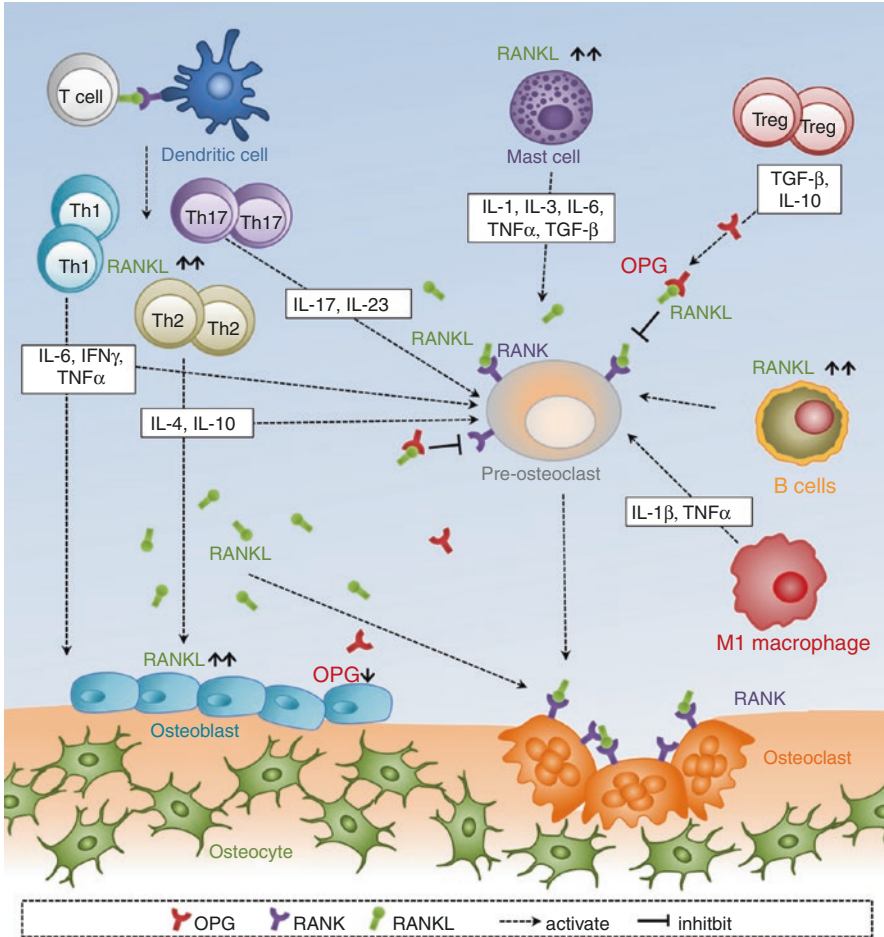


Fig. 16.2 Interaction of bone and immune cells. RANKL secreted by activated T and B cells initiates osteoclastogenesis by binding to its receptor, RANK, which is expressed on preosteoclasts. OPG secreted by osteoblasts and T_{reg} cells acts as a RANKL decoy receptor and subsequently prevents RANKL-RANK binding. Under physiologic conditions, OPG/RANKL is in equilibrium and preserves bone homeostasis. Under inflammatory conditions, RANKL is upregulated, while OPG is downregulated. T helper cells (Th1/Th2/Th17) secrete numerous pro-inflammatory cytokines, stimulating RANKL expression and thereby osteoclast formation and activity. Also pro-inflammatory M1 macrophages and mast cells are known to produce cytokines that promote bone resorption. Dendritic cells on the other hand are indirect players in inflammation-induced bone loss as they regulate T cell activity through a direct RANK-RANKL interaction

homeostasis. One of the most important findings in this context is that activated T cells express high levels of RANKL, thereby promoting osteoclastogenesis and bone loss [181]. However, little is known about the role of T cells in physiological bone homeostasis and about their crosstalk with osteoblasts. Under physiological

conditions, T cells are not considered a significant source of RANKL as T cell-deficient mice do not show diminished *Rankl* mRNA expression in their bone marrow [187]. Previous studies indicate that resting T cells blunt osteoclast formation in vitro [188] and attenuate bone resorption in vivo [187]. In line with this, T cell-deficient mice exhibit increased bone resorption, resulting in reduced bone density when compared to controls [189]. Indeed, depletion of CD4+ and CD8+ T lymphocytes in mice showed that T cells can also mediate anti-osteoclastogenic signals in vivo. The authors suggested that T cells enhance vitamin-D3-stimulated osteoclast formation in vitro by yet unknown mechanisms involving decreased OPG production [190]. CD4+ T cells can be subdivided into different subsets based on the produced cytokines (Th1 (IFN γ), Th2 (IL-4), and Th17 (IL-17)). Even though Th1 and Th2 produce cytokines that mediate osteoclast formation and function (e.g., TNF, IL-6), they might also be capable of inhibiting osteoclast differentiation by releasing IFN γ and IL-4, respectively [191]. The role of IL-17 in bone homeostasis was first demonstrated by Kotake et al. who identified IL-17 is a potent stimulator of osteoclastogenesis in the synovial fluid of rheumatoid arthritis patients [192]. Indeed, it is now validated that Th17 cells are increased in various bone diseases and that it significantly contributes to increased bone resorption [191, 193]. While the previously mentioned CD4+ T cell subsets have been shown to mainly promote osteoclastogenesis, anti-inflammatory CD4+ T_{regs} are known to inhibit osteoclast differentiation by secreting OPG [194–196]. Similar to T_{regs}, CD8+ T cells have a bone protective role, as they suppress osteoclastogenesis mainly due to soluble molecules [197].

Beside their function as regulators for osteoclastogenesis, an increasing body of evidence points toward an important role of T cells as activators of bone formation, as they are able to produce and secrete Wnt ligands (e.g., Wnt10b) that can activate Wnt signaling in osteoblastic cells [198–200]. A role of the canonical Wnt pathway in T cell biology (T cell development, CD8+ memory T cell formation, and regulatory T cell function) has been suggested in multiple experimental systems with varying results [201–204]. Chae et al. showed that Dkk1 is uniquely expressed at the cell membrane of Foxp3+ T_{reg} cells to inhibit T cell-mediated autoimmune colitis [205]. Furthermore, we previously demonstrated that T cell-specific Dkk1 deletion resulted in a high bone mass primarily due to an increased bone formation (Colditz and Rauner, unpublished data). In line with this, co-culture experiments revealed that inactive T cells promoted osteoblast differentiation. It should be noted that bone cells spontaneously or in response to specific stimuli secrete cytokines, thereby inducing the differentiation of naïve helper T cells into mature T cell populations that in turn regulate bone homeostasis [206]. Interestingly, activated T cells suppressed osteogenic differentiation and thus had opposing effects on osteoblasts than resting T cells. It was already shown that the activation of T cells increases their cytokine production, which may exert negative effects on osteoblasts [207]. Taken together, T cells can have multiple effects on bone, depending mainly on their activation status and phenotype.

B Lymphocytes

B cells not only represent an important cell population of our immune system by producing antibodies and working as antigen-presenting cells, but they are also important regulators of bone resorption as they are considered the dominant producers of bone marrow OPG [187]. B cell-deficient mice exhibit a reduced bone mass, indicating that these immune cells play an important role in the maintenance of bone homeostasis [187]. Indeed, the osteopenic phenotype of B cell knockout mice was associated with a loss of OPG mRNA and protein expression [187]. While resting B cells have not been shown to produce high amount of RANKL, they are considered an important RANKL source under inflammatory conditions [208]. B cells in multiple myeloma have been shown to increase osteoclastogenesis directly by producing RANKL [209] or indirectly by IL-7 secretion [210, 211]. Malignant B cell-derived plasma cells in multiple myeloma patients also produce an increased amount of Dkk1 and sclerostin, two important inhibitors of osteoblast differentiation [212–214]. Additionally, B lymphopoiesis is upregulated during estrogen deficiency [215], while it is downregulated by estrogen treatment [216], suggesting a role of B cells in estrogen deficiency-induced bone loss [217]. Indeed B cells that express the B220 marker have not only been shown to be able to transdifferentiate into osteoclasts in vitro [218], but they are also more abundant in ovariectomized mice [219] and have been demonstrated to secrete RANKL in estrogen-deficient postmenopausal women [220]. In line with this, mice lacking RANKL in B cells are protected from ovariectomy-induced bone loss [221]. However, peripheral blood B cells have also been shown to inhibit osteoclast formation in vitro, which is partially mediated by TGF β secretion [222], a cytokine that stimulates the apoptosis of osteoclasts [222–224]. Depletion of B cells in vivo aggravated periodontitis-induced bone loss, indicating that B cells do limit bone resorption under certain conditions [225]. Thus, the role of resting B cells in bone remodeling seems to be minimal, while activated B cells seem to play a more prominent role in many inflammatory or malignant diseases which are associated with bone changes.

Previous studies showed that T cell-deficient CD40 knockout mice are osteoporotic, suggesting that T and B cells cooperate with each other by enhancing OPG production by a CD40/CD40L mediated co-stimulation [187]. Accordingly, low bone density has been found in children with X-linked hyper-Ig syndrome, where CD40L production is impaired due to a mutation of the CD40L gene [226]. However, as T cells need to be activated to express CD40L and only a few activated T cells are found under basal conditions, the relevance of this mechanism for basal bone homeostasis remains unclear.

Mast Cells

Mast cells are found in most tissues including bone and are known to exert critical immunoregulatory roles in various immune disorders through the release of mediators such as histamine, leukotrienes, cytokines, and chemokines [227–229].

However, up until now, the exact molecular mechanisms by which mast cells contribute to the pathogenesis of arthritis, atherosclerosis, cancer, and obesity are unclear. Mast cells are known to not only produce TGF- β , TNF, IL-1, IL-3, and IL-6, cytokines known to stimulate bone resorption, but also RANKL [230, 231]. In line with this, a number of studies found an association between mastocytosis and reduced bone quality [146, 232–235]. Under physiological conditions, mast cells modulate bone homeostasis as mast cell-deficient mice exhibit enhanced osteoclastogenesis with concomitant slow formation of newly synthesized bone matrix, while mineralization rates remain normal [231]. Lack of chymase, a mast cell restricted protease, however, led to expansion of diaphyseal bone, which was associated with increased levels of a bone-anabolic serum marker and a higher periosteal bone formation rate [236]. Furthermore, mice that lack histamine decarboxylase, an enzyme required for the production of histamine, exhibited increased bone resorption [237]. An increased number of mast cells have been found in ovariectomized rat [238] as well as postmenopausal women suffering from osteoporosis [239], indicating an important role of mast cells in estrogen deficiency-induced bone loss. Overall, there is still a lack of knowledge on the role of mast cells on bone turnover under physiological and pathological conditions.

Monocytes/Macrophages

Monocytes and macrophages have crucial and distinct roles in tissue homeostasis and immunity. Macrophages are heterogeneous immune cells and are polarized into pro-inflammatory M1 and anti-inflammatory M2 macrophages depending on the environment [240]. Macrophages as well as macrophage-derived factors play an important role in the pathogenesis of inflammatory diseases. Macrophages have been shown to directly interact with bone cells and play a critical role in bone formation [241]. Under physiological conditions the majority of macrophages display an M2 phenotype, which maintain tissue homeostasis as they secrete IL-10 and TGF- β , thereby inhibiting bone resorption [242, 243]. However, under inflammatory conditions macrophages are activated and polarized to the M1 phenotype that contribute to tissue damage by the production of nitric oxide and pro-inflammatory cytokines (TNF- α , IL-1 β , and IL-12), resulting in an induction of bone resorption [244]. Bone-resident macrophages, also called “osteomacs,” have been shown to promote bone formation, as removal of osteomacs from primary calvarial osteoblast culture resulted in a significant decrease in mineralization of osteoblasts [245]. Similar to resident macrophages, inflammatory macrophages can influence bone formation. While classically M1 macrophages have been shown to produce oncostatin M [246], which promotes osteogenesis, alternatively activated M2 macrophages have been shown to induce osteoblast formation in an oncostatin M-independent manner [247, 248]. It is well established that macrophages play a crucial role in the pathogenesis of rheumatoid arthritis, as they are considered the main source of the pro-inflammatory cytokines, which in turn activate endothelial cells, induce synovial inflammation, and increase osteoclastogenesis, thus finally

leading to joint damage [249, 250]. Indeed, macrophages are able to promote T cell migration and polarization, as they secrete cytokines known to induce Th1 and Th17 polarization [251]. Furthermore the differentiation of macrophages into osteoclasts contributes to bone erosion due to induced expression of RANKL in synovial fibroblasts by pro-inflammatory cytokines [240]. Taken together, these results suggest that macrophages have crucial effects on bone remodeling during bone inflammation.

Apart from macrophages, monocytes can differentiate into dendritic cells (DC), which are the most efficient antigen-presenting cells and key players in the regulation of T cell immunity against pathogens and tumors [252]. DCs seem to not contribute to normal bone homeostasis, as DC-deficient mice have no altered bone phenotype [253]. While DCs are rarely localized in the bone under physiological conditions, active lesions in rheumatoid arthritis and periodontitis contain both mature and immature DC in different compartments of affected tissue surrounded by bone [254–259]. DCs have been described to interact through RANK-RANKL with T cells and are thereby considered active indirect players in inflammation-induced bone loss through regulation of T cell activity [254–260]. Apart from influencing T cell biology, DCs have been shown to transdifferentiate into osteoclasts in the presence M-CSF and RANKL and thereby might directly contribute to osteoclastogenesis [261]. Hence, DCs are of great importance in inflammatory conditions, while they do not seem to contribute to normal bone homeostasis.

Coupling of Bone Resorption and Formation

Bone tissue functions to withstand and enable our daily locomotion, while ensuring mineral homeostasis of the body, two intricate functions that rely on the timely and locally coupled activity of bone formation and bone resorption [262]. Osteocytes contribute to bone remodeling via osteocytic osteolysis and the regulation of mineralization; those functions will not be further elucidated here; rather the orchestration of osteoclast and osteoblast activities by osteocytes will be discussed.

The coordinated activity of bone remodeling relies on two major activities: (i) the demineralization and proteolytic degradation of the bone matrix by osteoclasts and (ii) the activity of osteoblasts to form the unmineralized type I collagen-rich osteoid. Bone remodeling may start with the formation of microcracks caused by an inappropriately high loading for the existing bone matrix quality. Thereby, RANKL is released as part of apoptotic bodies of microcrack-damaged osteocytes and is actively produced by neighboring osteocytes [263, 264]. RANKL produced by cells of the osteoblast lineage (osteoblasts and osteocytes) contributes in the activation of signaling pathways involved in osteoclast differentiation, osteoclast activity, and survival through the interaction with the surface receptor RANK to promote bone resorption [265]. With unloading, the role of osteocyte-released RANKL becomes apparent [266]. RANKL conditional knockout mice are protected from hind-limb unloading-induced bone resorption [72, 267]. RANKL is initially produced as a

membrane-bound protein that once cleaved by proteases exists also in a soluble form (sRANKL). Both forms seem to have different roles in resorption activation, with sRANKL being indispensable for estrogen deficiency-induced bone loss [268]. Further, osteocytes produce the signaling molecules M-CFS and OPG to directly drive osteoclast differentiation or oppose osteoclast formation, respectively [269, 270].

Once the resorptive activity of osteoclasts ceases and the reversal phase is initiated, bone formation proceeds. Bone formation can be both induced and inhibited by osteocyte signals depending on the loading situation. Nitric oxide, a signaling product of mechanically loaded osteocytes [149], has emerged as a stimulator for osteogenic response. Inhibition of nitric oxide in rats has been shown to inhibit bone formation [271, 272]. Accumulating evidence exists that PGE₂ secreted by mechanically loaded osteocytes through Cx43 hemichannels contribute to the bone's adaptive response to mechanical stimuli [163, 273]. Mechanical loading results in increased production of cyclooxygenase-2 (COX2), the key enzyme required for PGE₂ synthesis, as shown in bone cells of rat *in vivo* as well as in human and chicken osteocytes *in vitro* [150, 274]. On the other hand, in the absence of mechanical stimuli or with postmenopausal estrogen deficiency, the bone-anabolic Wnt signaling is inhibited in osteoblasts through the release of the Wnt inhibitors sclerostin and Dkk1 from osteocytes [56, 59]. Sclerostin inhibits the activation of Wnt/ β -catenin signaling in osteoblasts, resulting in reducing bone formation activity, but also resulting in enhanced osteoclast recruitment via increased RANKL and reduced OPG expression [275, 276]. Osteocytes respond to different stimuli (e.g., exercise, PTH, and estrogen) by secreting less sclerostin, resulting in increased activity of the Wnt signaling pathway and enhanced osteoblast-mediated bone formation [277, 278].

In addition to the regulation by osteocytes, osteoclasts couple to osteoblasts and vice versa by utilizing several factors, some of which (e.g., RANKL and OPG) have already been mentioned. However, it may not always appear straightforward to imagine that this cellular crosstalk of osteoclasts and osteoblasts exists on the same bone surface at the same time [279]. There is a true multitude of factors known to signal in between the actors of bone remodeling, and intensive reviews can be found elsewhere [280, 281]. During bone resorption some coupling factors are released from the bone matrix and could potentially act upon osteoblast precursors, signaling their replication, recruitment, and differentiation. Here, platelet-derived growth factor (PDGF), BMP2 and 4, IGF1, and TGF β 1 play a role [282–285]. In addition, osteoclasts secrete coupling factors (e.g., sphingosine-1-phosphate, cardiotrophin-1, complement factor 3a, and many more) [286–288]. Though not widely accepted, a potential cell-to-cell contact might also direct interactions between osteoclasts and osteoblasts or their progenitors. Coupling factors that are membrane-bound have been defined, and EphrinB2 [39] and Semaphorin D were proposed to be of importance in bone homeostasis [289, 290]. Future research will demonstrate the biological relevance of the individual regulatory mechanisms of bone remodeling and most likely introduce further new players into the signaling machinery.

Bone Homeostasis Contributes to the Inter-organ Crosstalk Between Bone and Peripheral Organs

For many years, bone was only considered as an endocrine target organ that responds to hormones like PTH. However, several lines of evidence suggest that the skeletal system participates in inter-organ crosstalk through secreted factors called osteokines that have effects on peripheral organs such as the muscle, liver, kidney, pancreas, and brain and the cardiovascular system. Therefore bone actively contributes to whole body homeostasis (Fig. 16.3). Mainly osteoblasts and osteocytes produce and secrete endocrine factors that are capable of altering distant tissue functions. In recent years, the function of bone-derived circulating FGF23 and osteocalcin was intensively studied.

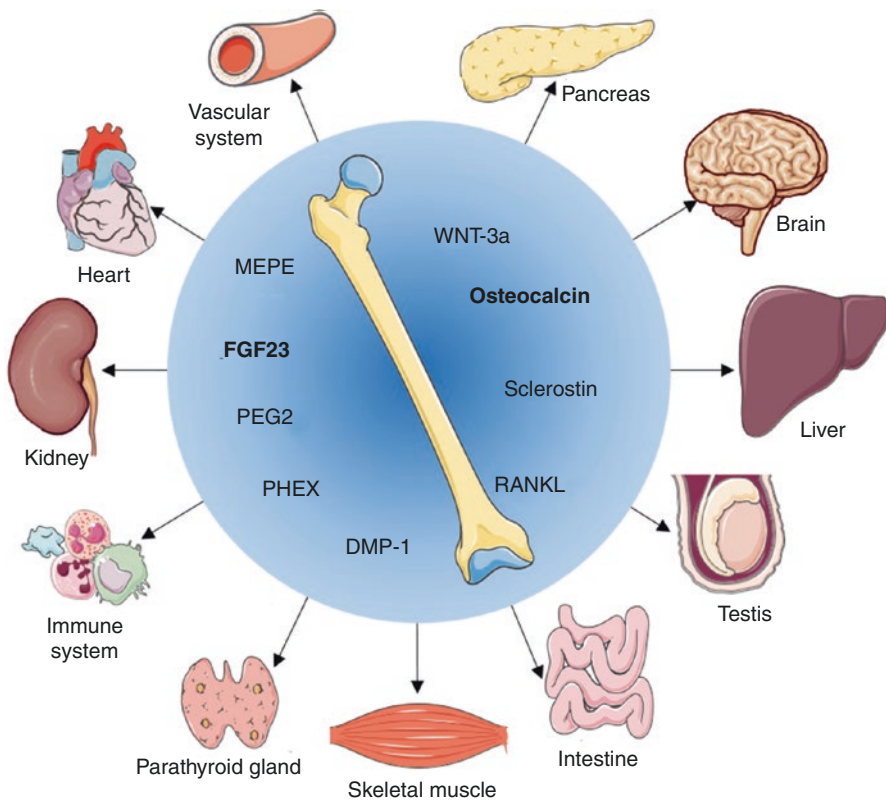


Fig. 16.3 The multifaceted inter-organ crosstalk between bone and peripheral organs through osteokines. Bone cells secrete osteokines like osteocalcin, fibroblast growth factor 23 (FGF23), dentin matrix protein-1 (DMP-1), matrix extracellular phosphoglycoprotein (MEPE), phosphateregulating gene with homologies to endopeptidases on the X chromosome (PHEX), receptor activator of nuclear factor-kappa B ligand (RANKL), prostaglandin E2 (PEG2), and WNT-3A [291]. An exemplary list of peripheral organs is shown. The figure was created using Servier Medical Art, licensed under a Creative Commons Attribution 3.0 Unported License

FGF23

FGF23 is one of the most important osteocyte-secreted molecules [292]. The binding of FGF23 to its receptor FGFR is Klotho-dependent [293]. Targets organs of FGF23 are multifaceted (e.g., kidney, parathyroid gland, and the cardiovascular system).

The FGF23 bone-kidney axis plays an important role in phosphate homeostasis that is dependent on bone-secreted FGF23. FGF23 inhibits the expression of renal sodium/phosphate co-transporters as well as 1- α hydroxylase, which are essential for renal phosphate reabsorption and vitamin D metabolism [294, 295], causing increased urinary phosphate excretion and reduced phosphate absorption.

The signaling between bone and the parathyroid gland is also bidirectional. Parathyroid gland-secreted PTH increases FGF23 expression in osteocytes, which acts on the parathyroid gland to diminish PTH secretion [292].

A major milestone in the understanding of the bone-heart/vascular axis was the observation that circulating FGF23 levels associated with altered cardiac and vascular function [296]. High serum FGF23 levels were independently associated with elevated risk for cardiac hypertrophy and mortality in patients with and without chronic kidney disease [297–300]. There are numerous explanations for the prognostic finding, including FGF23-induced endothelial dysfunction [301], arterial stiffness [301, 302], vascular calcification [303, 304], inflammation [305], stimulation of the renin-angiotensin system [306], and left ventricular hypertrophy [300, 307].

Osteocalcin

Osteocalcin (OCN) acts as a marker for osteoblast activity and bone formation and regulator of osteoclast activity. OCN is a non-collagenous, vitamin K-dependent protein that acts on multiple peripheral organs, especially in its metabolic active uncarboxylated form [308]. OCN plays an important role in brain development and cognitive function [309] and in energy metabolism [16]. Evidence from animal studies showed that OCN can have an effect on pancreas, adipose tissue, male gonads, and muscle to regulate insulin secretion, insulin sensitivity, male fertility, and muscle power through the peripheral receptor G protein-coupled receptor 6a [17, 19, 310]. Interestingly, exogenous OCN treatment preceding exercise was sufficient to enhance exercise capacity in mice [17]. OCN also affects muscle tissue in human [311]. Recent data revealed that OCN acts as a mediator for vascular calcification in vivo that is mediated by the Wnt/ β -catenin signaling pathway and mitochondrial dynamics [312].

Other Osteokines

Other osteocyte-derived osteokines (e.g., PHEX, DMP-1, sclerostin, RANKL, PGE2, and Wnt 3a) are known to have paracrine effects on peripheral tissue [292]. PGE2 and Wnt 3a, two molecules secreted in response to shear stress, support myogenesis and muscle function [313, 314]. Recently, it was shown that RANKL impairs muscles strength and insulin sensitivity in mouse and human [315].

Conclusion

The importance to maintain bone homeostasis is underlined by the tightly regulated process of bone cell communication via mechanical sensors and secreted factors. In this process each cell is highly specialized. A better understanding of bone homeostasis has led to the development of successful therapeutic strategies targeting distinct pathways (e.g., osteoclast differentiation by RANKL antibodies and osteocyte biology using sclerostin antibodies).

The knowledge that bone is not only an endocrine target organ but also signals via secreted factors to peripheral organs triggered the development of new research fields that study bidirectional inter-organ crosstalk (e.g., the bone-muscle axis (musculoskeletal research), bone-immune system axis (osteimmunology), and bone-vascular axis). Clinical findings and animal models indicate an association between osteoporosis and cardiovascular calcification [316, 317]. Various *in vitro* and *in vivo* studies suggest that cellular and molecular processes in cardiovascular calcification are similar to those seen in pathological bone remodeling. However, whether the calcification paradox is a cause of shared risk factors and common underlying mechanisms or due to unknown bone-secreted factors is currently under debate.

Placing the bone as a central organ of our body, a deeper understanding of the role of physiological and pathophysiological bone homeostasis on the secretion of molecules that affect target organs will be helpful in the identification of new targets that prevent comorbidities.

References

1. Oldknow KJ, MacRae VE, Farquharson C. Endocrine role of bone: recent and emerging perspectives beyond osteocalcin. *J Endocrinol*. 2015;225(1):R1–19.
2. Guntur AR, Rosen CJ. Bone as an endocrine organ. *Endocr Pract*. 2012;18(5):758–62.
3. DiGirolamo DJ, Clemens TL, Kousteni S. The skeleton as an endocrine organ. *Nat Rev Rheumatol*. 2012;8(11):674–83.
4. Touchberry CD, Green TM, Tchikrizov V, Mannix JE, Mao TF, Carney BW, et al. FGF23 is a novel regulator of intracellular calcium and cardiac contractility in addition to cardiac hypertrophy. *Am J Physiol Endocrinol Metab*. 2013;304(8):E863–73.

5. Calvi LM, Adams GB, Weibrecht KW, Weber JM, Olson DP, Knight MC, et al. Osteoblastic cells regulate the haematopoietic stem cell niche. *Nature*. 2003;425(6960):841–6.
6. Arai F, Suda T. Maintenance of quiescent hematopoietic stem cells in the osteoblastic niche. *Ann N Y Acad Sci*. 2007;1106:41–53.
7. Feng X, Teitelbaum SL. Osteoclasts: new insights. *Bone Res*. 2013;1
8. Hauge EM, Qvesel D, Eriksen EF, Mosekilde L, Melsen F. Cancellous bone remodeling occurs in specialized compartments lined by cells expressing osteoblastic markers. *J Bone Miner Res*. 2001;16(9):1575–82.
9. Sobacchi C, Schulz A, Coxon FP, Villa A, Helfrich MH. Osteopetrosis: genetics, treatment and new insights into osteoclast function. *Nat Rev Endocrinol*. 2013;9(9):522–36.
10. Chan CKF, Seo EY, Chen JY, Lo D, McArdle A, Sinha R, et al. Identification and specification of the mouse skeletal stem cell. *Cell*. 2015;160(1-2):285–98.
11. Chan CKF, Gulati GS, Sinha R, Tompkins JV, Lopez M, Carter AC, et al. Identification of the human skeletal stem cell. *Cell*. 2018;175(1):43–56.e21.
12. Gadaleta SJ, Paschalis EP, Betts F, Mendelsohn R, Boskey AL. Fourier transform infrared spectroscopy of the solution-mediated conversion of amorphous calcium phosphate to hydroxyapatite: new correlations between X-ray diffraction and infrared data. *Calcif Tissue Int*. 1996;58(1):9–16.
13. Reznikov N, Shahar R, Weiner S. Bone hierarchical structure in three dimensions. *Acta Biomater*. 2014;10(9):3815–26.
14. Yadav MC, Simao AMS, Narisawa S, Huesa C, McKee MD, Farquharson C, et al. Loss of skeletal mineralization by the simultaneous ablation of PHOSPHO1 and alkaline phosphatase function: a unified model of the mechanisms of initiation of skeletal calcification. *J Bone Miner Res*. 2011;26(2):286–97.
15. Zhang J, Niu C, Ye L, Huang H, He X, Tong W-G, et al. Identification of the haematopoietic stem cell niche and control of the niche size. *Nature*. 2003;425(6960):836–41.
16. Lee NK, Sowa H, Hinoi E, Ferron M, Ahn JD, Confavreux C, et al. Endocrine regulation of energy metabolism by the skeleton. *Cell*. 2007;130(3):456–69.
17. Mera P, Laue K, Ferron M, Confavreux C, Wei J, Galan-Diez M, et al. Osteocalcin signaling in myofibers is necessary and sufficient for optimum adaptation to exercise. *Cell Metab*. 2016;23(6):1078–92.
18. Oury F, Ferron M, Huizhen W, Confavreux C, Xu L, Lacombe J, et al. Osteocalcin regulates murine and human fertility through a pancreas-bone-testis axis. *J Clin Invest*. 2013;123(6):2421–33.
19. Oury F, Sumara G, Sumara O, Ferron M, Chang H, Smith CE, et al. Endocrine regulation of male fertility by the skeleton. *Cell*. 2011;144(5):796–809.
20. Oury F, Khirimian L, Denny CA, Gardin A, Chamouni A, Goeden N, et al. Maternal and offspring pools of osteocalcin influence brain development and functions. *Cell*. 2013;155(1):228–41.
21. Anderson DM, Maraskovsky E, Billingsley WL, Dougall WC, Tometsko ME, Roux ER, et al. A homologue of the TNF receptor and its ligand enhance T-cell growth and dendritic-cell function. *Nature*. 1997;390(6656):175–9.
22. Lacey DL, Timms E, Tan HL, Kelley MJ, Dunstan CR, Burgess T, et al. Osteoprotegerin ligand is a cytokine that regulates osteoclast differentiation and activation. *Cell*. 1998;93(2):165–76.
23. Simonet WS, Lacey DL, Dunstan CR, Kelley M, Chang MS, Luthy R, et al. Osteoprotegerin: a novel secreted protein involved in the regulation of bone density. *Cell*. 1997;89(2):309–19.
24. Yasuda H, Shima N, Nakagawa N, Yamaguchi K, Kinosaki M, Mochizuki S, et al. Osteoclast differentiation factor is a ligand for osteoprotegerin/osteoclastogenesis-inhibitory factor and is identical to TRANCE/RANKL. *Proc Natl Acad Sci U S A*. 1998;95(7):3597–602.
25. Ducy P, Zhang R, Geoffroy V, Ridall AL, Karsenty G. *Osf2/Cbfa1*: a transcriptional activator of osteoblast differentiation. *Cell*. 1997;89(5):747–54.
26. Nakashima K, Zhou X, Kunkel G, Zhang Z, Deng JM, Behringer RR, et al. The novel zinc finger-containing transcription factor osterix is required for osteoblast differentiation and bone formation. *Cell*. 2002;108(1):17–29.

27. Sinha KM, Zhou X. Genetic and molecular control of osterix in skeletal formation. *J Cell Biochem.* 2013;114(5):975–84.
28. Lee B, Thirunavukkarasu K, Zhou L, Pastore L, Baldini A, Hecht J, et al. Missense mutations abolishing DNA binding of the osteoblast-specific transcription factor OSF2/CBFA1 in cleidocranial dysplasia. *Nat Genet.* 1997;16(3):307–10.
29. Satokata I, Ma L, Ohshima H, Bei M, Woo I, Nishizawa K, et al. Mx2 deficiency in mice causes pleiotropic defects in bone growth and ectodermal organ formation. *Nat Genet.* 2000;24(4):391–5.
30. Komori T. Regulation of osteoblast differentiation by transcription factors. *J Cell Biochem.* 2006;99(5):1233–9.
31. Miyazono K, Kamiya Y, Morikawa M. Bone morphogenetic protein receptors and signal transduction. *J Biochem.* 2010;147(1):35–51.
32. Rahman MS, Akhtar N, Jamil HM, Banik RS, Asaduzzaman SM. TGF-beta/BMP signaling and other molecular events: regulation of osteoblastogenesis and bone formation. *Bone Res.* 2015;3:15005.
33. Wu M, Chen G, Li Y-P. TGF-beta and BMP signaling in osteoblast, skeletal development, and bone formation, homeostasis and disease. *Bone Res.* 2016;4:16009.
34. Beederman M, Lamplot JD, Nan G, Wang J, Liu X, Yin L, et al. BMP signaling in mesenchymal stem cell differentiation and bone formation. *J Biomed Sci Eng.* 2013;6(8A):32–52.
35. Kamiya N, Shuxian L, Yamaguchi R, Phipps M, Aruwajoye O, Adapala NS, et al. Targeted disruption of BMP signaling through type IA receptor (BMPRI A) in osteocyte suppresses SOST and RANKL, leading to dramatic increase in bone mass, bone mineral density and mechanical strength. *Bone.* 2016;91:53–63.
36. Kamiya N, Ye L, Kobayashi T, Lucas DJ, Mochida Y, Yamauchi M, et al. Disruption of BMP signaling in osteoblasts through type IA receptor (BMPRI A) increases bone mass. *J Bone Miner Res.* 2008;23(12):2007–17.
37. Shi C, Mandair GS, Zhang H, Vanrenterghem GG, Ridella R, Takahashi A, et al. Bone morphogenetic protein signaling through ACVR1 and BMPRI A negatively regulates bone mass along with alterations in bone composition. *J Struct Biol.* 2018;201(3):237–46.
38. Wang Y, Sun J-C, Wang H-B, Xu X-M, Kong Q-J, Wang Y-J, et al. ACVR1-knockout promotes osteogenic differentiation by activating the Wnt signaling pathway in mice. *J Cell Biochem.* 2019;120:8185–94.
39. Hatsell SJ, Idone V, Wolken DMA, Huang L, Kim HJ, Wang L, et al. ACVR1R206H receptor mutation causes fibrodysplasia ossificans progressiva by imparting responsiveness to activin A. *Sci Transl Med.* 2015;7(303):303ra137.
40. Shore EM, Xu M, Feldman GJ, Fenstermacher DA, Cho T-J, Choi IH, et al. A recurrent mutation in the BMP type I receptor ACVR1 causes inherited and sporadic fibrodysplasia ossificans progressiva. *Nat Genet.* 2006;38(5):525–7.
41. Lauzon M-A, Drevelle O, Daviau A, Faucheux N. Effects of BMP-9 and BMP-2 on the PI3K/Akt pathway in MC3T3-E1 preosteoblasts. *Tissue Eng Part A.* 2016;22(17-18):1075–85.
42. Valer JA, Sanchez-de-Diego C, Gamez B, Mishina Y, Rosa JL, Ventura F. Inhibition of phosphatidylinositol 3-kinase alpha (PI3Kalpha) prevents heterotopic ossification. *EMBO Mol Med.* 2019;11(9):e10567.
43. Lowery JW, Rosen V. The BMP pathway and its inhibitors in the skeleton. *Physiol Rev.* 2018;98(4):2431–52.
44. Canalis E, Brunet LJ, Parker K, Zanotti S. Conditional inactivation of noggin in the postnatal skeleton causes osteopenia. *Endocrinology.* 2012;153(4):1616–26.
45. Devlin RD, Du Z, Pereira RC, Kimble RB, Economides AN, Jorgetti V, et al. Skeletal overexpression of noggin results in osteopenia and reduced bone formation. *Endocrinology.* 2003;144(5):1972–8.
46. Baron R, Kneissel M. WNT signaling in bone homeostasis and disease: from human mutations to treatments. *Nat Med.* 2013;19(2):179–92.
47. Nusse R, Clevers H. Wnt/beta-catenin signaling, disease, and emerging therapeutic modalities. *Cell.* 2017;169(6):985–99.

48. Lerner UH, Ohlsson C. The WNT system: background and its role in bone. *J Intern Med.* 2015;277(6):630–49.
49. Luther J, Yorgan TA, Rolvien T, Ulsamer L, Koehne T, Liao N, et al. Wnt1 is an Lrp5-independent bone-anabolic Wnt ligand. *Sci Transl Med.* 2018;10(466):eaau7137.
50. Maeda K, Kobayashi Y, Udagawa N, Uehara S, Ishihara A, Mizoguchi T, et al. Wnt5a-Ror2 signaling between osteoblast-lineage cells and osteoclast precursors enhances osteoclastogenesis. *Nat Med.* 2012;18(3):405–12.
51. Moverare-Skrtic S, Henning P, Liu X, Nagano K, Saito H, Borjesson AE, et al. Osteoblast-derived WNT16 represses osteoclastogenesis and prevents cortical bone fragility fractures. *Nat Med.* 2014;20(11):1279–88.
52. Fahiminiya S, Majewski J, Mort J, Moffatt P, Glorieux FH, Rauch F. Mutations in WNT1 are a cause of osteogenesis imperfecta. *J Med Genet.* 2013;50(5):345–8.
53. Robinow M, Silverman FN, Smith HD. A newly recognized dwarfing syndrome. *Am J Dis Child.* 1969;117(6):645–51.
54. Boyden LM, Mao J, Belsky J, Mitzner L, Farhi A, Mitnick MA, et al. High bone density due to a mutation in LDL-receptor-related protein 5. *N Engl J Med.* 2002;346(20):1513–21.
55. Frontali M, Stomeo C, Dallapiccola B. Osteoporosis-pseudoglioma syndrome: report of three affected sibs and an overview. *Am J Med Genet.* 1985;22(1):35–47.
56. Colditz J, Thiele S, Baschant U, Niehrs C, Bonewald LF, Hofbauer LC, et al. Postnatal skeletal deletion of Dickkopf-1 increases bone formation and bone volume in male and female mice, despite increased sclerostin expression. *J Bone Miner Res.* 2018;33(9):1698–707.
57. Poole KES, van Bezooijen RL, Loveridge N, Hamersma H, Papapoulos SE, Lowik CW, et al. Sclerostin is a delayed secreted product of osteocytes that inhibits bone formation. *FASEB J.* 2005;19(13):1842–4.
58. Rauner M, Baschant U, Roetto A, Pellegrino RM, Rother S, Salbach-Hirsch J, et al. Transferrin receptor 2 controls bone mass and pathological bone formation via BMP and Wnt signaling. *Nat Metab.* 2019;1(1):111–24.
59. van Bezooijen RL, Roelen BAJ, Visser A, van der Wee-Pals L, de Wilt E, Karperien M, et al. Sclerostin is an osteocyte-expressed negative regulator of bone formation, but not a classical BMP antagonist. *J Exp Med.* 2004;199(6):805–14.
60. Cosman F, Crittenden DB, Adachi JD, Binkley N, Czerwinski E, Ferrari S, et al. Romosozumab treatment in postmenopausal women with osteoporosis. *N Engl J Med.* 2016;375(16):1532–43.
61. Florio M, Gunasekaran K, Stolina M, Li X, Liu L, Tipton B, et al. A bispecific antibody targeting sclerostin and DKK-1 promotes bone mass accrual and fracture repair. *Nat Commun.* 2016;7:11505.
62. Witcher PC, Miner SE, Horan DJ, Bullock WA, Lim K-E, Kang KS, et al. Sclerostin neutralization unleashes the osteoanabolic effects of Dkk1 inhibition. *JCI Insight.* 2018;3(11):98673.
63. Teitelbaum SL. Bone resorption by osteoclasts. *Science.* 2000;289(5484):1504–8.
64. Jacome-Galarza CE, Percin GI, Muller JT, Mass E, Lazarov T, Eitler J, et al. Developmental origin, functional maintenance and genetic rescue of osteoclasts. *Nature.* 2019;568(7753):541.
65. Arai F, Miyamoto T, Ohneda O, Inada T, Sudo T, Brasel K, et al. Commitment and differentiation of osteoclast precursor cells by the sequential expression of c-Fms and receptor activator of nuclear factor kappaB (RANK) receptors. *J Exp Med.* 1999;190(12):1741–54.
66. Lorenzo J. Osteoclast precursor cells. *Adv Exp Med Biol.* 2007;602:77–82.
67. Andersen TL, Sondergaard TE, Skorzynska KE, Dagnaes-Hansen F, Plesner TL, Hauge EM, et al. A physical mechanism for coupling bone resorption and formation in adult human bone. *Am J Pathol.* 2009;174(1):239–47.
68. Jensen PR, Andersen TL, Pennypacker BL, Duong LT, Engelholm LH, Delaisse JM. A supra-cellular model for coupling of bone resorption to formation during remodeling: lessons from two bone resorption inhibitors affecting bone formation differently. *Biochem Biophys Res Commun.* 2014;443(2):694–9.

69. Matsuzaki K, Udagawa N, Takahashi N, Yamaguchi K, Yasuda H, Shima N, et al. Osteoclast differentiation factor (ODF) induces osteoclast-like cell formation in human peripheral blood mononuclear cell cultures. *Biochem Biophys Res Commun.* 1998;246(1):199–204.
70. Itoh K, Udagawa N, Matsuzaki K, Takami M, Amano H, Shinki T, et al. Importance of membrane- or matrix-associated forms of M-CSF and RANKL/ODF in osteoclastogenesis supported by SaOS-4/3 cells expressing recombinant PTH/PTHrP receptors. *J Bone Miner Res.* 2000;15(9):1766–75.
71. McCloskey EV, Johansson H, Oden A, Austin M, Siris E, Wang A, et al. Denosumab reduces the risk of osteoporotic fractures in postmenopausal women, particularly in those with moderate to high fracture risk as assessed with FRAX. *J Bone Miner Res.* 2012;27(7):1480–6.
72. Nakashima T, Hayashi M, Fukunaga T, Kurata K, Oh-Hora M, Feng JQ, et al. Evidence for osteocyte regulation of bone homeostasis through RANKL expression. *Nat Med.* 2011;17(10):1231–4.
73. Dougall WC, Glaccum M, Charrier K, Rohrbach K, Brasel K, De Smedt T, et al. RANK is essential for osteoclast and lymph node development. *Genes Dev.* 1999;13(18):2412–24.
74. Kong YY, Yoshida H, Sarosi I, Tan HL, Timms E, Capparelli C, et al. OPGL is a key regulator of osteoclastogenesis, lymphocyte development and lymph-node organogenesis. *Nature.* 1999;397(6717):315–23.
75. Boyle WJ, Simonet WS, Lacey DL. Osteoclast differentiation and activation. *Nature.* 2003;423(6937):337–42.
76. Anderson KL, Smith KA, Conners K, McKercher SR, Maki RA, Torbett BE. Myeloid development is selectively disrupted in PU.1 null mice. *Blood.* 1998;91(10):3702–10.
77. Tondravi MM, McKercher SR, Anderson K, Erdmann JM, Quiroz M, Maki R, et al. Osteopetrosis in mice lacking haematopoietic transcription factor PU.1. *Nature.* 1997;386(6620):81–4.
78. Darnay BG, Ni J, Moore PA, Aggarwal BB. Activation of NF-kappaB by RANK requires tumor necrosis factor receptor-associated factor (TRAF) 6 and NF-kappaB-inducing kinase. Identification of a novel TRAF6 interaction motif. *J Biol Chem.* 1999;274(12):7724–31.
79. Jules J, Wang S, Shi Z, Liu J, Wei S, Feng X. The IVVY motif and tumor necrosis factor receptor-associated factor (TRAF) sites in the cytoplasmic domain of the receptor activator of nuclear factor kappaB (RANK) cooperate to induce osteoclastogenesis. *J Biol Chem.* 2015;290(39):23738–50.
80. Armstrong AP, Tometsko ME, Glaccum M, Sutherland CL, Cosman D, Dougall WC. A RANK/TRAF6-dependent signal transduction pathway is essential for osteoclast cytoskeletal organization and resorptive function. *J Biol Chem.* 2002;277(46):44347–56.
81. Lomaga MA, Yeh WC, Sarosi I, Duncan GS, Furlonger C, Ho A, et al. TRAF6 deficiency results in osteopetrosis and defective interleukin-1, CD40, and LPS signaling. *Genes Dev.* 1999;13(8):1015–24.
82. Asagiri M, Takayanagi H. The molecular understanding of osteoclast differentiation. *Bone.* 2007;40(2):251–64.
83. Zou W, Reeve JL, Liu Y, Teitelbaum SL, Ross FP. DAP12 couples c-Fms activation to the osteoclast cytoskeleton by recruitment of Syk. *Mol Cell.* 2008;31(3):422–31.
84. Mocsai A, Humphrey MB, Van Ziffle JA, Hu Y, Burghardt A, Spusta SC, et al. The immunomodulatory adapter proteins DAP12 and Fc receptor gamma-chain (FcRgamma) regulate development of functional osteoclasts through the Syk tyrosine kinase. *Proc Natl Acad Sci U S A.* 2004;101(16):6158–63.
85. Kim JH, Kim N. Regulation of NFATc1 in osteoclast differentiation. *J Bone Metab.* 2014;21(4):233–41.
86. Unal M, Creecy A, Nyman JS. The role of matrix composition in the mechanical behavior of bone. *Curr Osteoporos Rep.* 2018;16(3):205–15.
87. Nakamura I, Duong LT, Rodan SB, Rodan GA. Involvement of alpha(v)beta3 integrins in osteoclast function. *J Bone Miner Metab.* 2007;25(6):337–44.

88. Florencio-Silva R, Sasso GR, Sasso-Cerri E, Simoes MJ, Cerri PS. Biology of bone tissue: structure, function, and factors that influence bone cells. *Biomed Res Int.* 2015;2015:421746.
89. Faccio R, Takeshita S, Zallone A, Ross FP, Teitelbaum SL. c-Fms and the alphavbeta3 integrin collaborate during osteoclast differentiation. *J Clin Invest.* 2003;111(5):749–58.
90. McHugh KP, Hodivala-Dilke K, Zheng MH, Namba N, Lam J, Novack D, et al. Mice lacking beta3 integrins are osteosclerotic because of dysfunctional osteoclasts. *J Clin Invest.* 2000;105(4):433–40.
91. Mulari MT, Zhao H, Lakkakorpi PT, Vaananen HK. Osteoclast ruffled border has distinct subdomains for secretion and degraded matrix uptake. *Traffic.* 2003;4(2):113–25.
92. Ng PY, Brigitte Patricia Ribet A, Pavlos NJ. Membrane trafficking in osteoclasts and implications for osteoporosis. *Biochem Soc Trans.* 2019;47(2):639–50.
93. Nordstrom T, Rotstein OD, Romanek R, Asotra S, Heersche JN, Manolson MF, et al. Regulation of cytoplasmic pH in osteoclasts. Contribution of proton pumps and a proton-selective conductance. *J Biol Chem.* 1995;270(5):2203–12.
94. Salo J, Lehenkari P, Mulari M, Metsikko K, Vaananen HK. Removal of osteoclast bone resorption products by transcytosis. *Science.* 1997;276(5310):270–3.
95. Lacey DL, Boyle WJ, Simonet WS, Kostenuik PJ, Dougall WC, Sullivan JK, et al. Bench to bedside: elucidation of the OPG-RANK-RANKL pathway and the development of denosumab. *Nat Rev Drug Discov.* 2012;11(5):401–19.
96. Bucay N, Sarosi I, Dunstan CR, Morony S, Tarpley J, Capparelli C, et al. Osteoprotegerin-deficient mice develop early onset osteoporosis and arterial calcification. *Genes Dev.* 1998;12(9):1260–8.
97. Kim N, Kadono Y, Takami M, Lee J, Lee SH, Okada F, et al. Osteoclast differentiation independent of the TRANCE-RANK-TRAF6 axis. *J Exp Med.* 2005;202(5):589–95.
98. Yokota K, Sato K, Miyazaki T, Kitaura H, Kayama H, Miyoshi F, et al. Combination of tumor necrosis factor alpha and interleukin-6 induces mouse osteoclast-like cells with bone resorption activity both in vitro and in vivo. *Arthritis Rheumatol.* 2014;66(1):121–9.
99. O'Brien W, Fissel BM, Maeda Y, Yan J, Ge X, Gravalles EM, et al. RANK-independent osteoclast formation and bone erosion in inflammatory arthritis. *Arthritis Rheumatol.* 2016;68(12):2889–900.
100. Kwan Tat S, Padrines M, Theoleyre S, Heymann D, Fortun Y. IL-6, RANKL, TNF-alpha/IL-1: interrelations in bone resorption pathophysiology. *Cytokine Growth Factor Rev.* 2004;15(1):49–60.
101. Amarasekara DS, Yun H, Kim S, Lee N, Kim H, Rho J. Regulation of osteoclast differentiation by cytokine networks. *Immune Netw.* 2018;18(1):e8.
102. Takayanagi H, Ogasawara K, Hida S, Chiba T, Murata S, Sato K, et al. T-cell-mediated regulation of osteoclastogenesis by signalling cross-talk between RANKL and IFN-gamma. *Nature.* 2000;408(6812):600–5.
103. Gao Y, Grassi F, Ryan MR, Terauchi M, Page K, Yang X, et al. IFN-gamma stimulates osteoclast formation and bone loss in vivo via antigen-driven T cell activation. *J Clin Invest.* 2007;117(1):122–32.
104. Bostrom EA, Lundberg P. The newly discovered cytokine IL-34 is expressed in gingival fibroblasts, shows enhanced expression by pro-inflammatory cytokines, and stimulates osteoclast differentiation. *PLoS One.* 2013;8(12):e81665.
105. Adamopoulos IE, Mellins ED. Alternative pathways of osteoclastogenesis in inflammatory arthritis. *Nat Rev Rheumatol.* 2015;11(3):189–94.
106. Manolagas SC. Birth and death of bone cells: basic regulatory mechanisms and implications for the pathogenesis and treatment of osteoporosis. *Endocr Rev.* 2000;21(2):115–37.
107. Kim SW, Pajevic PD, Selig M, Barry KJ, Yang JY, Shin CS, et al. Intermittent parathyroid hormone administration converts quiescent lining cells to active osteoblasts. *J Bone Miner Res.* 2012;27(10):2075–84.
108. Holtrop ME. Light and electron microscopical structure of bone forming cells. In: Hall BK, editor. *The osteoblast and osteocyte*, vol. 1. Caldwell: The Telford Press; 1990.

109. Nijweide PJ, van der Plas A, Scherft JP. Biochemical and histological studies on various bone cell preparations. *Calcif Tissue Int.* 1981;33(5):529–40.
110. Chen X, Wang L, Zhao K, Wang H. Osteocytogenesis: roles of physicochemical factors, collagen cleavage, and exogenous molecules. *Tissue Eng Part B Rev.* 2018;24(3):215–25.
111. Mullen CA, Haugh MG, Schaffler MB, Majeska RJ, McNamara LM. Osteocyte differentiation is regulated by extracellular matrix stiffness and intercellular separation. *J Mech Behav Biomed Mater.* 2013;28:183–94.
112. Zhang K, Barragan-Adjemian C, Ye L, Kotha S, Dallas M, Lu Y, et al. E11/gp38 selective expression in osteocytes: regulation by mechanical strain and role in dendrite elongation. *Mol Cell Biol.* 2006;26(12):4539–52.
113. Ikepogu E, Basta L, Clements DN, Fleming R, Vincent TL, Buttle DJ, et al. FGF-2 promotes osteocyte differentiation through increased E11/podoplanin expression. *J Cell Physiol.* 2018;233(7):5334–47.
114. Gaur T, Hussain S, Mudhasani R, Parulkar I, Colby JL, Frederick D, et al. Dicer inactivation in osteoprogenitor cells compromises fetal survival and bone formation, while excision in differentiated osteoblasts increases bone mass in the adult mouse. *Dev Biol.* 2010;340(1):10–21.
115. Zeng HC, Bae Y, Dawson BC, Chen Y, Bertin T, Munivez E, et al. MicroRNA miR-23a cluster promotes osteocyte differentiation by regulating TGF-beta signalling in osteoblasts. *Nat Commun.* 2017;8:15000.
116. Toyosawa S, Shintani S, Fujiwara T, Ooshima T, Sato A, Ijuhin N, et al. Dentin matrix protein 1 is predominantly expressed in chicken and rat osteocytes but not in osteoblasts. *J Bone Miner Res Off J Am Soc Bone Miner Res.* 2001;16(11):2017–26.
117. He G, Gajjeraman S, Schultz D, Cookson D, Qin C, Butler WT, et al. Spatially and temporally controlled biomineralization is facilitated by interaction between self-assembled dentin matrix protein 1 and calcium phosphate nuclei in solution. *Biochemistry.* 2005;44(49):16140–8.
118. Gluhak-Heinrich J, Ye L, Bonewald LF, Feng JQ, MacDougall M, Harris SE, et al. Mechanical loading stimulates dentin matrix protein 1 (DMP1) expression in osteocytes in vivo. *J Bone Miner Res Off J Am Soc Bone Miner Res.* 2003;18(5):807–17.
119. Feng JQ, Ward LM, Liu S, Lu Y, Xie X, Yuan B, et al. Loss of DMP1 causes rickets and osteomalacia and identifies a role for osteocytes in mineral metabolism. *Nat Genet.* 2006;38(11):1310–5.
120. Ling Y, Rios HF, Myers ER, Lu Y, Feng JQ, Boskey AL. DMP1 depletion decreases bone mineralization in vivo: an FTIR imaging analysis. *J Bone Miner Res.* 2005;20(12):2169–77.
121. Gericke A, Qin C, Sun Y, Redfern R, Redfern D, Fujimoto Y, et al. Different forms of DMP1 play distinct roles in mineralization. *J Dent Res.* 2010;89(4):355–9.
122. Zhou Y, Lin J, Shao J, Zuo Q, Wang S, Wolff A, et al. Aberrant activation of Wnt signaling pathway altered osteocyte mineralization. *Bone.* 2019;127:324–33.
123. Shao J, Zhou Y, Lin J, Nguyen TD, Huang R, Gu Y, et al. Notch expressed by osteocytes plays a critical role in mineralisation. *J Mol Med.* 2018;96(3–4):333–47.
124. Shao J, Zhou Y, Xiao Y. The regulatory roles of Notch in osteocyte differentiation via the crosstalk with canonical Wnt pathways during the transition of osteoblasts to osteocytes. *Bone.* 2018;108:165–78.
125. Liu S, Zhou J, Tang W, Menard R, Feng JQ, Quarles LD. Pathogenic role of Fgf23 in Dmp1-null mice. *Am J Physiol Endocrinol Metab.* 2008;295(2):E254–E61.
126. Lorenz-Depiereux B, Bastepe M, Benet-Pages A, Amyere M, Wagenstaller J, Muller-Barth U, et al. DMP1 mutations in autosomal recessive hypophosphatemia implicate a bone matrix protein in the regulation of phosphate homeostasis. *Nat Genet.* 2006;38(11):1248–50.
127. Kenneth E. White, Wayne E. Evans, Jeffery L.H. O’Riordan, Marcy C. Speer, Michael J. Econs, Bettina Lorenz-Depiereux, et al. Autosomal dominant hypophosphataemic rickets is associated with mutations in FGF23. *Nat Genet.* 2000;26(3):345–8.
128. A gene (PEX) with homologies to endopeptidases is mutated in patients with X-linked hypophosphatemic rickets. The HYP Consortium. *Nat Genet.* 1995;11(2):130–6.
129. Silver J, Naveh-Many T. FGF-23 and secondary hyperparathyroidism in chronic kidney disease. *Nat Rev Nephrol.* 2013;9(11):641–9.

130. Erben RG. Pleiotropic actions of FGF23. *Toxicol Pathol.* 2017;45(7):904–10.
131. Murshed M, Harnay D, Millan JL, McKee MD, Karsenty G. Unique coexpression in osteoblasts of broadly expressed genes accounts for the spatial restriction of ECM mineralization to bone. *Genes Dev.* 2005;19(9):1093–104.
132. Lorenz-Depiereux B, Schnabel D, Tiosano D, Hausler G, Strom TM. Loss-of-function ENPP1 mutations cause both generalized arterial calcification of infancy and autosomal-recessive hypophosphatemic rickets. *Am J Hum Genet.* 2010;86(2):267–72.
133. Murali SK, Andrukhova O, Clinkenbeard EL, White KE, Erben RG. Excessive osteocytic Fgf23 secretion contributes to pyrophosphate accumulation and mineralization defect in Hyp mice. *PLoS Biol.* 2016;14(4):e1002427.
134. Xiao Z, Huang J, Cao L, Liang Y, Han X, Quarles LD. Osteocyte-specific deletion of Fgfr1 suppresses FGF23. *PLoS One.* 2014;9(8):e104154.
135. White KE, Cabral JM, Davis SI, Fishburn T, Evans WE, Ichikawa S, et al. Mutations that cause osteoglophonic dysplasia define novel roles for FGFR1 in bone elongation. *Am J Hum Genet.* 2005;76(2):361–7.
136. Martin A, Liu S, David V, Li H, Karydis A, Feng JQ, et al. Bone proteins PHEX and DMP1 regulate fibroblastic growth factor Fgf23 expression in osteocytes through a common pathway involving FGF receptor (FGFR) signaling. *FASEB J.* 2011;25(8):2551–62.
137. Rowe PS. Regulation of bone-renal mineral and energy metabolism: the PHEX, FGF23, DMP1, MEPE ASARM pathway. *Crit Rev Eukaryot Gene Expr.* 2012;22(1):61–86.
138. Tagliabracci VS, Engel JL, Wiley SE, Xiao J, Gonzalez DJ, Nidumanda Appaiah H, et al. Dynamic regulation of FGF23 by Fam20C phosphorylation, GalNAc-T3 glycosylation, and furin proteolysis. *Proc Natl Acad Sci U S A.* 2014;111(15):5520–5.
139. Teti A, Zallone A. Do osteocytes contribute to bone mineral homeostasis? Osteocytic osteolysis revisited. *Bone.* 2009;44(1):11–6.
140. Qing H, Ardeshirpour L, Divieti Pajevic P, Dusevich V, Jahn K, Kato S, et al. Demonstration of osteocytic perilacunar/canalicular remodeling in mice during lactation. *J Bone Miner Res.* 2012;27(5):1018–29.
141. Jahn K, Kelkar S, Zhao H, Xie Y, Tiede-Lewis LM, Dusevich V, et al. Osteocytes acidify their microenvironment in response to PTHrP in vitro and in lactating mice in vivo. *J Bone Miner Res.* 2017;32(8):1761–72.
142. Tsourdi E, Jahn K, Rauner M, Busse B, Bonewald LF. Physiological and pathological osteocytic osteolysis. *J Musculoskelet Neuronal Interact.* 2018;18(3):292–303.
143. Tang SY, Herber RP, Ho SP, Alliston T. Matrix metalloproteinase-13 is required for osteocytic perilacunar remodeling and maintains bone fracture resistance. *J Bone Miner Res.* 2012;27(9):1936–50.
144. Dole NS, Mazur CM, Acevedo C, Lopez JP, Monteiro DA, Fowler TW, et al. Osteocyte-intrinsic TGF-beta signaling regulates bone quality through perilacunar/canalicular remodeling. *Cell Rep.* 2017;21(9):2585–96.
145. Clarke MV, Russell PK, Findlay DM, Sastra S, Anderson PH, Skinner JP, et al. A role for the calcitonin receptor to limit bone loss during lactation in female mice by inhibiting osteocytic osteolysis. *Endocrinology.* 2015;156(9):3203–14.
146. Duriez R, Duriez J. Periosteocyte demineralization in disuse osteoporosis. The effect of calcitonin. *Int Orthop.* 1981;5(4):299–304.
147. Kogawa M, Wijenayaka AR, Ormsby RT, Thomas GP, Anderson PH, Bonewald LF, et al. Sclerostin regulates release of bone mineral by osteocytes by induction of carbonic anhydrase 2. *J Bone Miner Res.* 2013;28(12):2436–48.
148. Frost HM. Bone remodelling dynamics. Thomas Publishers. *Arthritis ans Theumatology.* 1964;7(5):545.
149. Klein-Nulend J, Semeins CM, Ajubi NE, Nijweide PJ, Burger EH. Pulsating fluid flow increases nitric oxide (NO) synthesis by osteocytes but not periosteal fibroblasts—correlation with prostaglandin upregulation. *Biochem Biophys Res Commun.* 1995;217(2):640–8.
150. Ajubi NE, Klein-Nulend J, Nijweide PJ, Vrijheid-Lammers T, Ablas MJ, Burger EH. Pulsating fluid flow increases prostaglandin production by cultured chicken osteocytes—a cytoskeleton-dependent process. *Biochem Biophys Res Commun.* 1996;225(1):62–8.

151. Burger EH, Klein-Nulend J, van der Plas A, Nijweide PJ. Function of osteocytes in bone – their role in mechanotransduction. *J Nutr.* 1995;125(7 Suppl):2020S–3S.
152. Klein-Nulend J, van der Plas A, Semeins CM, Ajubi NE, Frangos JA, Nijweide PJ, et al. Sensitivity of osteocytes to biomechanical stress in vitro. *FASEB.* 1995;9(5):441–5.
153. Vatsa A, Breuls RG, Semeins CM, Salmon PL, Smit TH, Klein-Nulend J. Osteocyte morphology in fibula and calvaria – is there a role for mechanosensing? *Bone.* 2008;43(3):452–8.
154. Vatsa A, Semeins CM, Smit TH, Klein-Nulend J. Paxillin localisation in osteocytes—is it determined by the direction of loading? *Biochem Biophys Res Commun.* 2008;377(4):1019–24.
155. Nicoletta DP, Moravits DE, Gale AM, Bonewald LF, Lankford J. Osteocyte lacunae tissue strain in cortical bone. *J Biomech.* 2006;39(9):1735–43.
156. Hemmatian H, Jalali R, Semeins CM, Hogervorst JMA, van Lenthe GH, Klein-Nulend J, et al. Mechanical loading differentially affects osteocytes in fibulae from lactating mice compared to osteocytes in virgin mice: possible role for lacuna size. *Calcif Tissue Int.* 2018;103(6):675–85.
157. You L-D, Weinbaum S, Cowin SC, Schaffler MB. Ultrastructure of the osteocyte process and its pericellular matrix. *Anat Rec A Discov Mol Cell Evol Biol.* 2004;278(2):505–13.
158. Nguyen AM, Jacobs CR. Emerging role of primary cilia as mechanosensors in osteocytes. *Bone.* 2013;54(2):196–204.
159. Han Y, Cowin SC, Schaffler MB, Weinbaum S. Mechanotransduction and strain amplification in osteocyte cell processes. *Proc Natl Acad Sci U S A.* 2004;101(47):16689–94.
160. Temiyasathit S, Tang WJ, Leucht P, Anderson CT, Monica SD, Castillo AB, et al. Mechanosensing by the primary cilium: deletion of Kif3A reduces bone formation due to loading. *PLoS One.* 2012;7(3):e33368.
161. Xiao Z, Dallas M, Qiu N, Nicoletta D, Cao L, Johnson M, et al. Conditional deletion of Pkd1 in osteocytes disrupts skeletal mechanosensing in mice. *FASEB J.* 2011;25(7):2418–32.
162. Li X, Han L, Nookaew I, Mannen E, Silva MJ, Almeida M, et al. Stimulation of Piezo1 by mechanical signals promotes bone anabolism. *elife.* 2019;8:e49631.
163. Cherian PP, Siller-Jackson AJ, Gu S, Wang X, Bonewald LF, Sprague E, et al. Mechanical strain opens connexin 43 hemichannels in osteocytes: a novel mechanism for the release of prostaglandin. *Mol Biol Cell.* 2005;16(7):3100–6.
164. Gluhak-Heinrich J, Gu S, Pavlin D, Jiang JX. Mechanical loading stimulates expression of connexin 43 in alveolar bone cells in the tooth movement model. *Cell Commun Adhes.* 2006;13(1–2):115–25.
165. Jiang JX, Cheng B. Mechanical stimulation of gap junctions in bone osteocytes is mediated by prostaglandin E2. *Cell Commun Adhes.* 2001;8(4–6):283–8.
166. Bivi N, Pacheco-Costa R, Brun LR, Murphy TR, Farlow NR, Robling AG, et al. Absence of Cx43 selectively from osteocytes enhances responsiveness to mechanical force in mice. *J Orthopaedic Res.* 2013;31(7):1075–81.
167. Lloyd SA, Lewis GS, Zhang Y, Paul EM, Donahue HJ. Connexin 43 deficiency attenuates loss of trabecular bone and prevents suppression of cortical bone formation during unloading. *J Bone Miner Res.* 2012;27(11):2359–72.
168. Arron JR, Choi Y. Bone versus immune system. *Nature* 2000;408(6812):535–6.
169. Greenblatt MB, Shim J-H. Osteoimmunology: a brief introduction. *Immune Network.* 2013;13:111–5.
170. Osteoimmunology: Shared mechanisms and crosstalk between the immune and bone systems. 2007;7(4):292–304.
171. Dazzi F, Ramasamy R, Glennie S, Jones SP, Roberts I. The role of mesenchymal stem cells in haemopoiesis. *Blood Rev.* 2006;20(3):161–71.
172. Kong YY, Feige U, Sarosi I, Bolon B, Tafuri A, Morony S, et al. Activated T cells regulate bone loss and joint destruction in adjuvant arthritis through osteoprotegerin ligand. *Nature.* 1999;402(6759):304–9.
173. Konishi M, Takahashi K, Yoshimoto E, Uno K, Kasahara K, Mikasa K. Association between osteopenia/osteoporosis and the serum RANKL in HIV-infected patients. *AIDS (London, England).* 2005;19:1240–1.

174. Kotake S, Udagawa N, Hakoda M, Mogi M, Yano K, Tsuda E, et al. Activated human T cells directly induce osteoclastogenesis from human monocytes: possible role of T cells in bone destruction in rheumatoid arthritis patients. *Arthritis Rheum.* 2001;44(5):1003–12.
175. Mundy GR. Metastasis to bone: causes, consequences and therapeutic opportunities. *Nat Rev Cancer.* 2002;2:584–93.
176. Shigeyama Y, Pap T, Kunzler P, Simmen BR, Gay RE, Gay S. Expression of osteoclast differentiation factor in rheumatoid arthritis. *Arthritis Rheumat.* 2000;43(11):2523–30.
177. Stellon AJ, Davies A, Compston J, Williams R. Bone loss in autoimmune chronic active hepatitis on maintenance corticosteroid therapy. *Gastroenterology.* 1985;89(5):1078–83.
178. Mori, G., D'Amelio, P., Faccio, R. & Brunetti, G. The Interplay between the Bone and the Immune System. *Clin Dev Immunol* 2013;2013:720504.
179. Cornish J, Gillespie MT, Callon KE, Horwood NJ, Moseley JM, Reid IR. Interleukin-18 is a novel mitogen of osteogenic and chondrogenic cells. *Endocrinology.* 2003;144(4):1194–201.
180. Miroslavljevic D, Quinn JMW, Elliott J, Horwood NJ, Martin TJ, Gillespie MT. T-cells mediate an inhibitory effect of Interleukin-4 on osteoclastogenesis. *J Bone Miner Res.* 2003;18(6):984–93.
181. Takayanagi H, Ogasawara K, Hida S, Chiba T, Murata S, Sato K, et al. T-cell-mediated regulation of osteoclastogenesis by signalling cross-talk between RANKL and IFN- γ . *Nature.* 2000;408(6812):600–5.
182. Mak TW, Ferrick DA. The gammadelta T-cell bridge: linking innate and acquired immunity. *Nat Med.* 1998;4:764–5.
183. Haas W, Pereira P, Tonegawa S. Gamma/Delta Cells. *Annu Rev Immunol.* 1993;11:637–85.
184. Cenci S, Toraldo G, Weitzmann MN, Roggia C, Gao Y, Qian WP, et al. Estrogen deficiency induces bone loss by increasing T cell proliferation and lifespan through IFN-induced class II transactivator. *Proc Natl Acad Sci.* 2003;100(18):10405–10.
185. Roggia C, Gao Y, Cenci S, Weitzmann MN, Toraldo G, Isaia G, et al. Up-regulation of TNF-producing T cells in the bone marrow: a key mechanism by which estrogen deficiency induces bone loss in vivo. *Proc Natl Acad Sci.* 2001;98:13960–5.
186. Kawai T, Matsuyama T, Hosokawa Y, Makihira S, Seki M, Karimbux NY, et al. B and T lymphocytes are the primary sources of RANKL in the bone resorptive lesion of periodontal disease. *Am J Pathol.* 2006;169:987–98.
187. Li Y, Toraldo G, Li A, Yang X, Zhang H, Qian WP, et al. B cells and T cells are critical for the preservation of bone homeostasis and attainment of peak bone mass in vivo. *Blood.* 2007;109:3839–48.
188. John V, Hock JM, Short LL, Glasebrook AL, Galvin RJ. A role for CD8+ T lymphocytes in osteoclast differentiation in vitro. *Endocrinology.* 1996;137(6):2457–63.
189. Toraldo G, Roggia C, Qian W-P, Pacifici R, Weitzmann MN. IL-7 induces bone loss in vivo by induction of receptor activator of nuclear factor kappa B ligand and tumor necrosis factor alpha from T cells. *Proc Natl Acad Sci U S A.* 2003;100(1):125–30.
190. Grcevic D, Lee S-K, Marusic A, Lorenzo JA. Depletion of CD4 and CD8 T lymphocytes in mice in vivo enhances 1,25-dihydroxyvitamin D3-stimulated osteoclast-like cell formation in vitro by a mechanism that is dependent on prostaglandin synthesis. *J Immunol.* 2000;165:4231–8.
191. Yuan FL, Li X, Lu WG, Zhao YQ, Li CW, Li JP, et al. Type 17 T-helper cells might be a promising therapeutic target for osteoporosis. *Mol Biol Rep.* 2012;39(1):771–4.
192. Kotake S, Udagawa N, Takahashi N, Matsuzaki K, Itoh K, Ishiyama S, et al. IL-17 in synovial fluids from patients with rheumatoid arthritis is a potent stimulator of osteoclastogenesis. *J Clin Investig.* 1999;103(9):1345–52.
193. Sato K, Suematsu A, Okamoto K, Yamaguchi A, Morishita Y, Kadono Y, et al. Th17 functions as an osteoclastogenic helper T cell subset that links T cell activation and bone destruction. *J Exp Med.* 2006;203:2673–82.
194. Kelchtermans H, Geboes L, Mitera T, Huskens D, Leclercq G, Matthys P. Activated CD4+CD25+ regulatory T cells inhibit osteoclastogenesis and collagen-induced arthritis. *Ann Rheum Dis.* 2009;68(5):744–50.

195. Zaiss MM, Axmann R, Zwerina J, Polzer K, Gückel E, Skapenko A, et al. Treg cells suppress osteoclast formation: a new link between the immune system and bone. *Arthritis Rheum.* 2007;56(12):4104–12.
196. Zaiss MM, Frey B, Hess A, Zwerina J, Luther J, Nimmerjahn F, et al. Regulatory T cells protect from local and systemic bone destruction in arthritis. *J Immunol.* 2010;184:7238–46.
197. Choi Y, Woo KM, Ko SH, Lee YJ, Park SJ, Kim HM, et al. Osteoclastogenesis is enhanced by activated B cells but suppressed by activated CD8+ T cells. *Eur J Immunol.* 2001;31(7):2179–88.
198. Hardiman G, Albright S, Tsunoda JI, McClanahan T, Lee F. The mouse Wnt-10B gene isolated from helper T cells is widely expressed and a possible oncogene in BR6 mouse mammary tumorigenesis. *Gene.* 1996;172:199–205.
199. Ouji Y, Yoshikawa M, Shiroy A, Ishizaka S. Wnt-10b secreted from lymphocytes promotes differentiation of skin epithelial cells. *Biochem Biophys Res Commun.* 2006;342:1063–9.
200. Terauchi M, Li JY, Bedi B, Baek KH, Tawfeek H, Galley S, et al. T lymphocytes amplify the anabolic activity of parathyroid hormone through Wnt10b signaling. *Cell Metab.* 2009;10:229–40.
201. Ding Y, Shen S, Lino AC, Curotto De Lafaille MA, Lafaille JJ. Beta-catenin stabilization extends regulatory T cell survival and induces anergy in nonregulatory T cells. *Nat Med.* 2008;14:162–9.
202. Guo Z, Dose M, Kovalovsky D, Chang R, O’Neil J, Look AT, et al. β -catenin stabilization stalls the transition from double-positive to single-positive stage and predisposes thymocytes to malignant transformation. *Blood.* 2007;109:5463–72.
203. van Loosdregt J, Fleskens V, Tiemessen MM, Mokry M, Van Boxtel R, Meerding J, et al. Canonical Wnt signaling negatively modulates regulatory T cell function. *Immunity.* 2013;39:298–310.
204. Xie H, Huang Z, Sadim MS, Sun Z. Stabilized beta-catenin extends thymocyte survival by up-regulating Bcl-xL. *J Immunol.* 2005;175:7981–8.
205. Chae WJ, Park JH, Henegariu O, Yilmaz S, Hao L, Bothwell ALM. Membrane-bound Dickkopf-1 in Foxp3+regulatory T cells suppresses T-cell-mediated autoimmune colitis. *Immunology.* 2017;152(2):265–75.
206. Pacifici R. Osteoimmunology and Its Implications for Transplantation. *Am J Transplant.* 2013;13(9):2245–54.
207. Pietschmann P. Principles of osteoimmunology: molecular mechanisms and clinical applications. Springer Vienna. 2011. p. 1-280.
208. Horowitz MC, Fretz JA, Lorenzo JA. How B cells influence bone biology in health and disease. *Bone* 2010;47(3):472–9.
209. Heider U, Langelotz C, Jakob C, Zavrski I, Fleissner C, Eucker J, et al. Expression of receptor activator of nuclear factor κ B ligand on bone marrow plasma cells correlates with osteolytic bone disease in patients with multiple myeloma. *Clin Cancer Res.* 2003;9(4):1436–40.
210. Giuliani N, Colla S, Morandi F, Lazzaretti M, Sala R, Bonomini S, et al. Myeloma cells block RUNX2/CBFA1 activity in human bone marrow osteoblast progenitors and inhibit osteoblast formation and differentiation. *Blood.* 2005;106(7):2472–83.
211. Giuliani N, Colla S, Sala R, Moroni M, Lazzaretti M, La Monica S, et al. Human myeloma cells stimulate the receptor activator of nuclear factor- κ B ligand (RANKL) in T lymphocytes: a potential role in multiple myeloma bone disease. *Blood.* 2002;100(13):4615–21.
212. Brunetti G, Oranger A, Mori G, Specchia G, Rinaldi E, Curci P, et al. Sclerostin is overexpressed by plasma cells from multiple myeloma patients. *Ann NY Acad Sci.* 2011;1237:19–23.
213. Colucci S, Brunetti G, Oranger A, Mori G, Sardone F, Specchia G, et al. Myeloma cells suppress osteoblasts through sclerostin secretion. *Blood Cancer J.* 2011;1(6):e27.
214. Oranger A, Carbone C, Izzo M, Grano M. Cellular mechanisms of multiple myeloma bone disease. *Clin Dev Immunol.* 2013;2013:289458.
215. Masuzawa T, Miyaura C, Onoe Y, Kusano K, Ohta H, Nozawa S, et al. Estrogen deficiency stimulates B lymphopoiesis in mouse bone marrow. *J Clin Invest.* 1994;94:1090.

216. Erlandsson MC, Jonsson CA, Islander U, Ohlsson C, Carlsten H. Oestrogen receptor specificity in oestradiol-mediated effects on B lymphopoiesis and immunoglobulin production in male mice. *Immunology*. 2003;108:346.
217. Miyaura C, Onoe Y, Inada M, Maki K, Ikuta K, Ito M, et al. Increased B-lymphopoiesis by interleukin 7 induces bone loss in mice with intact ovarian function: similarity to estrogen deficiency. *Proc Natl Acad Sci*. 2002;94:9360.
218. Sato T, Shibata T, Ikeda K, Watanabe K. Generation of bone-resorbing osteoclasts from B220+ cells: its role in accelerated osteoclastogenesis due to estrogen deficiency. *J Bone Miner Res*. 2001;16:2215.
219. Kanematsu M, Sato T, Takai H, Watanabe K, Ikeda K, Yamada Y. Prostaglandin E2 induces expression of receptor activator of nuclear factor- κ B ligand/osteoprotegerin ligand on pre-B cells: implications for accelerated osteoclastogenesis in estrogen deficiency. *J Bone Miner Res*. 2000;15:1321.
220. Eghbali-Fatourehchi G, Khosla S, Sanyal A, Boyle WJ, Lacey DL, Riggs BL. Role of RANK ligand in mediating increased bone resorption in early postmenopausal women. *J Clin Invest*. 2003;111:1221.
221. Onal M, Xiong J, Chen X, Thostenson JD, Almeida M, Manolagas SC, et al. Receptor activator of nuclear factor κ B ligand (RANKL) protein expression by B lymphocytes contributes to ovariectomy-induced bone loss. *J Biol Chem*. 2012;287:29851.
222. Weitzmann MN, Cenci S, Haug J, Brown C, DiPersio J, Pacifici R. B lymphocytes inhibit human osteoclastogenesis by secretion of TGF β . *J Cell Biochem*. 2000;78:318.
223. Chenu C, Pfeilschifter J, Mundy GR, Roodman GD. Transforming growth factor β inhibits formation of osteoclast-like cells in long-term human marrow cultures. *Proc Natl Acad Sci USA*. 1988;85:5683.
224. Hughes DE, Dai A, Tiffée JC, Li HH, Munoy GR, Boyce BF. Estrogen promotes apoptosis of murine osteoclasts mediated by TGF β . *Nat Med*. 1996;2:1132.
225. Klausen B, Hougen HP, Fiehn NEE. Increased periodontal bone loss in temporarily B lymphocyte-deficient rats. *J Periodontal Res*. 1989;24:384.
226. Lopez-Granados E, Temmerman ST, Wu L, Reynolds JC, Follmann D, Liu S, et al. Osteopenia in X-linked hyper-IgM syndrome reveals a regulatory role for CD40 ligand in osteoclastogenesis. *Proc Natl Acad Sci U S A*. 2007;104:5056–61.
227. Galli SJ, Kalesnikoff J, Grimbaldston MA, Piliponsky AM, Williams CMM, Tsai M. Mast cells as “tunable” effector and immunoregulatory cells: recent advances. *Annu Rev Immunol*. 2005;23:749.
228. Galli SJ, Tsai M, Marichal T, Tchougounova E, Reber LL, Pejler G. Approaches for analyzing the roles of mast cells and their proteases in vivo. *Adv Immunol*. 2015;126:45.
229. Voehringer D. Protective and pathological roles of mast cells and basophils. *Nat Rev Immunol*. 2013;13(5):362–75.
230. Ali AS, Lax AS, Liljestrom M, Paakkari I, Ashammakhi N, Kovanen PT, et al. Mast cells in atherosclerosis as a source of the cytokine RANKL. *Clin Chem Lab Med*. 2006;44(5):672–4.
231. Silberstein R, Melnick M, Greenberg G, Minkin C. Bone remodeling in W/W^v mast cell deficient mice. *Bone*. 1991;12:227–36.
232. Rossini M, Zanotti R, Bonadonna P, Artuso A, Caruso B, Schena D, et al. Bone mineral density, bone turnover markers and fractures in patients with indolent systemic mastocytosis. *Bone*. 2011;49:880.
233. Seitz S, Barvencik F, Koehne T, Priemel M, Pogoda P, Semler J, et al. Increased osteoblast and osteoclast indices in individuals with systemic mastocytosis. *Osteoporosis Int*. 2013;24:2325.
234. Van Der Veer E, Van Der Goot W, De Monchy JGR, Kluin-Nelemans HC, Van Doormaal JJ. High prevalence of fractures and osteoporosis in patients with indolent systemic mastocytosis. *Allergy*. 2012;67:431.
235. Guillaume N, Desoutter J, Chandesris O, Merlusca L, Henry I, Georjin-Lavialle S, et al. Bone complications of mastocytosis: a link between clinical and biological characteristics. *Am J Med*. 2013;126(1):75.e1.

236. Lind T, Gustafson AM, Calounova G, Hu L, Rasmusson A, Jonsson KB, et al. Increased bone mass in female mice lacking mast cell chymase. *PLoS One*. 2016;11:e0167964.
237. Fitzpatrick LA, Buzas E, Gagne TJ, Nagy A, Horvath C, Ferencz V, et al. Targeted deletion of histidine decarboxylase gene in mice increases bone formation and protects against ovariectomy-induced bone loss. *Proc Natl Acad Sci USA*. 2003;100:6027.
238. Lesclous P, Saffar JL. Mast cells accumulate in rat bone marrow after ovariectomy. *Cells Tissues Organs*. 1999;164:23–9.
239. Fallon MD, Whyte MP, Craig RB, Teitelbaum SL. Mast-cell proliferation in postmenopausal osteoporosis. *Calcif Tissue Int*. 1983;35:29–31.
240. Gu Q, Yang H, Shi Q. Macrophages and bone inflammation. *J Orthop Translat*. 2017;10:86–93.
241. Hume DA, Loutit JF, Gordon S. The mononuclear phagocyte system of the mouse defined by immunohistochemical localization of antigen F4/80: macrophages of bone and associated connective tissue. *J Cell Sci*. 1984;66:189–94.
242. Biswas SK, Mantovani A. Macrophage plasticity and interaction with lymphocyte subsets: cancer as a paradigm. *Nat Immunol*. 2010;11(10):889–96.
243. Dey A, Allen J, Hankey-Giblin PA. Ontogeny and polarization of macrophages in inflammation: blood monocytes versus tissue macrophages. *Front Immunol*. 2015;5:683.
244. Tan HY, Wang N, Li S, Hong M, Wang X, Feng Y. The reactive oxygen species in macrophage polarization: reflecting its dual role in progression and treatment of human diseases. *Oxidative Med Cell Longev*. 2016;2016:2795090.
245. Chang MK, Raggatt L-J, Alexander KA, Kuliwabea JS, Fazzalari NL, Schroder K, et al. Osteal tissue macrophages are intercalated throughout human and mouse bone lining tissues and regulate osteoblast function in vitro and in vivo. *J Immunol*. 2008;181:1234.
246. Guihard P, Danger Y, Brounais B, David E, Brion R, Delecrcin J, et al. Induction of osteogenesis in mesenchymal stem cells by activated monocytes/macrophages depends on oncostatin M signaling. *Stem Cells*. 2012;30:762–72.
247. Fernandes TJ, Hodge JM, Singh PP, Eeles DG, Collier FM, Holten I, et al. Cord blood-derived macrophage-lineage cells rapidly stimulate osteoblastic maturation in mesenchymal stem cells in a glycoprotein-130 dependent manner. *PLoS One*. 2013;8:e73266.
248. Horwood NJ. Macrophage Polarization and Bone Formation: A review. *Clin Rev Allergy Immunol*. 2016;51(1):79–86.
249. Dimitroulas T, Nikas SN, Trontzas P, Kitas GD. Biologic therapies and systemic bone loss in rheumatoid arthritis. *Autoimmun Rev*. 2013;12:958–66.
250. Yeo L, Adlard N, Biehl M, Juarez M, Smallie T, Snow M, et al. Expression of chemokines CXCL4 and CXCL7 by synovial macrophages defines an early stage of rheumatoid arthritis. *Ann Rheum Dis*. 2016;75:763.
251. Egan PJ, Van Nieuwenhuijze A, Campbell IK, Wicks IP. Promotion of the local differentiation of murine Th17 cells by synovial macrophages during acute inflammatory arthritis. *Arthritis Rheum*. 2008;58:3720.
252. Steinman RM, Banchereau J. Taking dendritic cells into medicine. *Nature*. 2007;449(7161):419–26.
253. McKenna HJ, Stocking KL, Miller RE, Brasel K, De Smedt T, Maraskovsky E, et al. Mice lacking flt3 ligand have deficient hematopoiesis affecting hematopoietic progenitor cells, dendritic cells, and natural killer cells. *Blood*. 2000;95(11):3489–97.
254. Cirrincione C, Pimpinelli N, Orlando L, Romagnoli P. Lamina propria dendritic cells express activation markers and contact lymphocytes in chronic periodontitis. *J Periodontol*. 2002;73:45.
255. Cutler CW, Jotwani R. Dendritic cells at the oral mucosal interface. *Journal of dental research*. 2006;85(8):678–89.
256. Highton J, Kean A, Hessian PA, Thomson J, Rietveld J, Hart DNJ. Cells expressing dendritic cell markers are present in the rheumatoid nodule. *J Rheumatol*. 2000;27:339.
257. Page G, Lebecque S, Miossec P. Anatomic localization of immature and mature dendritic cells in an ectopic lymphoid organ: correlation with selective chemokine expression in rheumatoid synovium. *J Immunol*. 2002;168(10):5333–41.

258. Page G, Miossec P. RANK and RANKL expression as markers of dendritic cell-T cell interactions in paired samples of rheumatoid synovium and lymph nodes. *Arthritis Rheum.* 2005;52:2307.
259. Thomas R, MacDonald KPA, Pettit AR, Cavanagh LL, Padmanabha J, Zehntner S. Dendritic cells and the pathogenesis of rheumatoid arthritis. *J Leukoc Biol.* 1999;66:286.
260. Santiago-Schwarz F, Anand P, Liu S, Carsons SE. Dendritic cells (DCs) in rheumatoid arthritis (RA): progenitor cells and soluble factors contained in RA synovial fluid yield a subset of myeloid DCs that preferentially activate Th1 inflammatory-type responses. *J Immunol.* 2001;167:1758–68.
261. Rivollier A, Mazzorana M, Tebib J, Piperno M, Aitsiselmi T, Rabourdin-Combe C, et al. Immature dendritic cell transdifferentiation into osteoclasts: a novel pathway sustained by the rheumatoid arthritis microenvironment. *Blood.* 2004;104(13):4029–37.
262. Seeman E. Bone modeling and remodeling. *J Bone Miner Res.* 2009;19:219–33.
263. Kennedy OD, Herman BC, Laudier DM, Majeska RJ, Sun HB, Schaffler MB. Activation of resorption in fatigue-loaded bone involves both apoptosis and active pro-osteoclastogenic signaling by distinct osteocyte populations. *Bone.* 2012;50(5):1115–22.
264. Kennedy OD, Lendhey M, Mauer P, Philip A, Basta-Pljakic J, Schaffler MB. Microdamage induced by in vivo reference point indentation in mice is repaired by osteocyte-apoptosis mediated remodeling. *Bone.* 2017;95:192–8.
265. Boyce BF. Advances in the regulation of osteoclasts and osteoclast functions. *J Dent Res.* 2013;92(10):860–7.
266. Aguirre JI, Plotkin LI, Stewart SA, Weinstein RS, Parfitt AM, Manolagas SC, et al. Osteocyte apoptosis is induced by weightlessness in mice and precedes osteoclast recruitment and bone loss. *J Bone Miner Res.* 2006;21(4):605–15.
267. Xiong J, Onal M, Jilka RL, Weinstein RS, Manolagas SC, O'Brien CA. Matrix-embedded cells control osteoclast formation. *Nat Med.* 2011;17(10):1235–41.
268. Xiong J, Cawley K, Piemontese M, Fujiwara Y, Zhao H, Goellner JJ, et al. Soluble RANKL contributes to osteoclast formation in adult mice but not ovariectomy-induced bone loss. *Nat Commun.* 2018;9(1):2909.
269. Kramer I, Halleux C, Keller H, Pegurri M, Gooi JH, Weber PB, et al. Osteocyte Wnt/beta-catenin signaling is required for normal bone homeostasis. *Mol Cell Biol.* 2010;30(12):3071–85.
270. Harris SE, MacDougall M, Horn D, Woodruff K, Zimmer SN, Rebel VI, et al. Meox2/Cre-mediated disruption of CSF-1 leads to osteopetrosis and osteocyte defects. *Bone.* 2012;50(1):42–53.
271. Fox SW, Chambers TJ, Chow JW. Nitric oxide is an early mediator of the increase in bone formation by mechanical stimulation. *Am J Phys.* 1996;270(6 Pt 1):E955–60.
272. Turner CH, Takano Y, Owan I, Murrell GA. Nitric oxide inhibitor L-NAME suppresses mechanically induced bone formation in rats. *Am J Phys.* 1996;270(4 Pt 1):E634–9.
273. Lara-Castillo N, Kim-Weroha NA, Kamel MA, Javaheri B, Ellies DL, Krumlauf RE, et al. In vivo mechanical loading rapidly activates beta-catenin signaling in osteocytes through a prostaglandin mediated mechanism. *Bone.* 2015;76:58–66.
274. Westbroek I, Ajubi NE, Alblas MJ, Semeins CM, Klein-Nulend J, Burger EH, et al. Differential stimulation of prostaglandin G/H synthase-2 in osteocytes and other osteogenic cells by pulsating fluid flow. *Biochem Biophys Res Commun.* 2000;268(2):414–9.
275. van Bezooijen RL, ten Dijke P, Papapoulos SE, Lowik CW. SOST/sclerostin, an osteocyte-derived negative regulator of bone formation. *Cytokine Growth Factor Rev.* 2005;16(3):319–27.
276. Wijenayaka AR, Kogawa M, Lim HP, Bonewald LF, Findlay DM, Atkins GJ. Sclerostin stimulates osteocyte support of osteoclast activity by a RANKL-dependent pathway. *PLoS One.* 2011;6(10):e25900.
277. Lin C, Jiang X, Dai Z, Guo X, Weng T, Wang J, et al. Sclerostin mediates bone response to mechanical unloading through antagonizing Wnt/beta-catenin signaling. *J Bone Miner Res Off J Am Soc Bone Miner Res.* 2009;24(10):1651–61.

278. Robling AG, Bellido T, Turner CH. Mechanical stimulation in vivo reduces osteocyte expression of sclerostin. *J Musculoskelet Neuronal Interact.* 2006;6(4):354.
279. Sims NA, Martin TJ. Coupling signals between the osteoclast and osteoblast: how are messages transmitted between these temporary visitors to the bone surface? *Front Endocrinol (Lausanne).* 2015;6:41.
280. Sims NA, Martin TJ. Coupling the activities of bone formation and resorption: a multitude of signals within the basic multicellular unit. *Bonekey Rep.* 2014;3:481.
281. Lerner UH, Kindstedt E, Lundberg P. The critical interplay between bone resorbing and bone forming cells. *J Clin Periodontol.* 2019;46(Suppl 21):33–51.
282. Hock JM, Canalis E. Platelet-derived growth factor enhances bone cell replication, but not differentiated function of osteoblasts. *Endocrinology.* 1994;134(3):1423–8.
283. Fiedler J, Roderer G, Gunther KP, Brenner RE. BMP-2, BMP-4, and PDGF-bb stimulate chemotactic migration of primary human mesenchymal progenitor cells. *J Cell Biochem.* 2002;87(3):305–12.
284. Xian L, Wu X, Pang L, Lou M, Rosen CJ, Qiu T, et al. Matrix IGF-1 maintains bone mass by activation of mTOR in mesenchymal stem cells. *Nat Med.* 2012;18(7):1095–101.
285. Tang Y, Wu X, Lei W, Pang L, Wan C, Shi Z, et al. TGF-beta1-induced migration of bone mesenchymal stem cells couples bone resorption with formation. *Nat Med.* 2009;15(7):757–65.
286. Pederson L, Ruan M, Westendorf JJ, Khosla S, Oursler MJ. Regulation of bone formation by osteoclasts involves Wnt/BMP signaling and the chemokine sphingosine-1-phosphate. *Proc Natl Acad Sci U S A.* 2008;105(52):20764–9.
287. Matsuoka K, Park KA, Ito M, Ikeda K, Takeshita S. Osteoclast-derived complement component 3a stimulates osteoblast differentiation. *J Bone Miner Res.* 2014;29(7):1522–30.
288. Walker EC, McGregor NE, Poulton IJ, Pompolo S, Allan EH, Quinn JM, et al. Cardiotrophin-1 is an osteoclast-derived stimulus of bone formation required for normal bone remodeling. *J Bone Miner Res.* 2008;23(12):2025–32.
289. Zhao C, Irie N, Takada Y, Shimoda K, Miyamoto T, Nishiwaki T, et al. Bidirectional ephrinB2-EphB4 signaling controls bone homeostasis. *Cell Metab.* 2006;4(2):111–21.
290. Negishi-Koga T, Shinohara M, Komatsu N, Bito H, Kodama T, Friedel RH, et al. Suppression of bone formation by osteoclastic expression of semaphorin 4D. *Nat Med.* 2011;17(11):1473–80.
291. Maurel DB, Jahn K, Lara-Castillo N. Muscle-bone crosstalk: emerging opportunities for novel therapeutic approaches to treat musculoskeletal pathologies. *Biomedicines.* 2017;5(4):E62.
292. Dallas SL, Prideaux M, Bonewald LF. The osteocyte: an endocrine cell ... and more. *Endocr Rev.* 2013;34(5):658–90.
293. Urakawa I, Yamazaki Y, Shimada T, Iijima K, Hasegawa H, Okawa K, et al. Klotho converts canonical FGF receptor into a specific receptor for FGF23. *Nature.* 2006;444(7120):770–4.
294. Gattineni J, Bates C, Twombly K, Dwarakanath V, Robinson ML, Goetz R, et al. FGF23 decreases renal NaPi-2a and NaPi-2c expression and induces hypophosphatemia in vivo predominantly via FGF receptor 1. *Am J Physiol Renal Physiol.* 2009;297(2):F282–91.
295. Shimada T, Kakitani M, Yamazaki Y, Hasegawa H, Takeuchi Y, Fujita T, et al. Targeted ablation of Fgf23 demonstrates an essential physiological role of FGF23 in phosphate and vitamin D metabolism. *J Clin Invest.* 2004;113(4):561–8.
296. Stohr R, Schuh A, Heine GH, Brandenburg V. FGF23 in cardiovascular disease: innocent bystander or active mediator? *Front Endocrinol.* 2018;9:351.
297. Souma N, Isakova T, Lipiszko D, Sacco RL, Elkind MSV, DeRosa JT, et al. Fibroblast growth factor 23 and cause-specific mortality in the general population: the northern Manhattan study. *J Clin Endocrinol Metab.* 2016;101(10):3779–86.
298. Brandenburg VM, Kleber ME, Vervloet MG, Tomaschitz A, Pilz S, Stojakovic T, et al. Fibroblast growth factor 23 (FGF23) and mortality: the Ludwigshafen risk and cardiovascular health study. *Atherosclerosis.* 2014;237(1):53–9.
299. Parker BD, Schurgers LJ, Brandenburg VM, Christenson RH, Vermeer C, Ketteler M, et al. The associations of fibroblast growth factor 23 and uncarboxylated matrix gla pro-

- tein with mortality in coronary artery disease: the Heart and Soul Study. *Ann Intern Med.* 2010;152(10):640.
300. Faul C, Amaral AP, Oskouei B, Hu MC, Sloan A, Isakova T, et al. FGF23 induces left ventricular hypertrophy. *J Clin Invest.* 2011;121(11):4393–408.
301. Silswal N, Touchberry CD, Daniel DR, McCarthy DL, Zhang SQ, Andresen J, et al. FGF23 directly impairs endothelium-dependent vasorelaxation by increasing superoxide levels and reducing nitric oxide bioavailability. *Am J Physiol Endocrinol Metab.* 2014;307(5):E426–E36.
302. Mirza MAI, Larsson A, Lind L, Larsson TE. Circulating fibroblast growth factor-23 is associated with vascular dysfunction in the community. *Atherosclerosis.* 2009;205(2):385–90.
303. Desjardins L, Liabeuf S, Renard C, Lenglet A, Lemke HD, Choukroun G, et al. FGF23 is independently associated with vascular calcification but not bone mineral density in patients at various CKD stages. *Osteoporosis Int.* 2012;23(7):2017–25.
304. Ozkok A, Kekik C, Karahan GE, Sakaci T, Ozel A, Unsal A, et al. FGF-23 associated with the progression of coronary artery calcification in hemodialysis patients. *BMC Nephrol.* 2013;14:241.
305. David V, Francis C, Babitt JL. Ironing out the cross talk between FGF23 and inflammation. *Am J Physiol-Renal.* 2017;312(1):F1–8.
306. Wohlfahrt P, Melenovsky V, Kotrc M, Benes J, Jabor A, Franekova J, et al. Association of fibroblast growth factor-23 levels and angiotensin-converting enzyme inhibition in chronic systolic heart failure. *Jacc-Heart Fail.* 2015;3(10):829–39.
307. Grabner A, Schramm K, Silswal N, Hendrix M, Yanucil C, Czaya B, et al. FGF23/FGFR4-mediated left ventricular hypertrophy is reversible. *Sci Rep.* 2017;7:1993.
308. Hauschka PV, Lian JB, Cole DE, Gundberg CM. Osteocalcin and matrix Gla protein: vitamin K-dependent proteins in bone. *Physiol Rev.* 1989;69(3):990–1047.
309. Shan C, Ghosh A, Guo XZ, Wang SM, Hou YF, Li ST, et al. Roles for osteocalcin in brain signalling: implications in cognition- and motor-related disorders. *Mol Brain.* 2019;12(1):23.
310. Ferron M, Lacombe J. Regulation of energy metabolism by the skeleton: osteocalcin and beyond. *Arch Biochem Biophys.* 2014;561:137–46.
311. Levinger I, Scott D, Nicholson GC, Stuart AL, Duque G, McCorquodale T, et al. Under carboxylated osteocalcin, muscle strength and indices of bone health in older women. *Bone.* 2014;64:8–12.
312. Rashdan NA, Sim AM, Cui L, Phadwal K, Roberts FL, Carter R, et al. Osteocalcin regulates arterial calcification via altered Wnt signaling and glucose metabolism. *J Bone Miner Res.* 2019;35(2):357–67.
313. Mo C, Romero-Suarez S, Bonewald L, Johnson M, Brotto M. Prostaglandin E2: from clinical applications to its potential role in bone- muscle crosstalk and myogenic differentiation. *Recent Pat Biotechnol.* 2012;6(3):223–9.
314. Huang J, Romero-Suarez S, Lara N, Mo C, Kaja S, Brotto L, et al. Crosstalk between MLO-Y4 osteocytes and C2C12 muscle cells is mediated by the Wnt/beta-catenin pathway. *JBMR Plus.* 2017;1(2):86–100.
315. Bonnet N, Bourgoin L, Biver E, Douni E, Ferrari S. RANKL inhibition improves muscle strength and insulin sensitivity and restores bone mass. *J Clin Invest.* 2019;129(8):3214–23.
316. Hjortnaes J, Bouten CV, Van Herwerden LA, Grundeman PF, Kluijn J. Translating autologous heart valve tissue engineering from bench to bed. *Tissue Eng Part B Rev.* 2009;15(3):307–17.
317. Rajamannan NM, Evans FJ, Aikawa E, Grande-Allen KJ, Demer LL, Heistad DD, et al. Calcific aortic valve disease: not simply a degenerative process: a review and agenda for research from the National Heart and lung and blood institute aortic stenosis working group. Executive summary: calcific aortic valve disease-2011 update. *Circulation.* 2011;124(16):1783–91.

Chapter 17

Bone Biology, Modeling, Remodeling, and Mineralization



Matthew R. Allen and Sharon M. Moe

Introduction

Arterial calcification and bone loss (osteopenia/osteoporosis) often occur in the same patient. Multiple cohort studies have described an inverse relationship: decreased bone mineral content assessed by a variety of methods is associated with increased calcification in coronary arteries, aorta, hand arteries, or heart valves. Kiel et al. [1] assessed the original population-based Framingham Heart study cohort (364 women and 190 men) and found that after more than 25 years of follow-up, the metacarpal cortical area decreased by 22% in women and 13% in men. In contrast, aorta calcification assessed semiquantitatively on lumbar spine radiographs increased over eightfold in women and sixfold in men. Importantly, after controlling for confounders, this relationship was significant in women ($p = 0.01$) but not men. A meta-analysis of four cross-sectional studies [2] found a significantly lower hip and spine bone mineral density in those with vascular calcification compared to those without calcification, and those with vascular calcification were more likely to have osteoporosis (OR = 1.72, 95% CI: 1.14–2.60).

Other studies have examined the relationship between vascular calcification and fractures. Naves et al. [3] found in 624 older individuals that the presence of severe arterial calcification by abdominal radiograph was associated with a nearly twofold increase in fractures by cross-sectional analyses. In the Perth Longitudinal Study of Aging [4], 1024 white women with moderate to severe aortic calcification assessed

M. R. Allen

Department of Anatomy, Cell Biology and Physiology, Indiana University School of Medicine and Roudebush Veterans Affairs Medical Center, Indianapolis, IN, USA

S. M. Moe (✉)

Division of Nephrology, Department of Medicine, Indiana University School of Medicine and Roudebush Veterans Affairs Medical Center, Indianapolis, IN, USA

e-mail: smoe@iu.edu

on lumbar spine films had increased risk of clinical fractures, even after adjusting for age and hip BMD (HR 1.33; 95% CI, 0.98 to 1.83, $p = 0.073$). Furthermore, the mortality of patients with a high coronary artery calcification score (>400) is nearly double when patients also have low bone mineral density [5]. Multiple other studies have found similar associations, although this does equate to causality.

One explanation for these observations is the presence of common clinical risk factors for both bone loss and arterial calcification, including advanced age, estrogen deficiency, chronic kidney disease, vitamin D deficiency, smoking, inflammation, and oxidative stress. Another hypothesis for these findings is the presence of a pool of calcium that fluxes from the bone to the artery (and presumably vice versa) [6]. However, a more likely explanation is that vascular calcification and osteopenia/osteoporosis share common mechanistic signaling pathways including mineral metabolism [7], OPG/RANKL/RANK system [8], sclerostin signaling [9], vitamin K gamma-carboxylation [10], and others described in this book. More information on skeletal vs. vascular calcification is provided in Chap. 15. A key difference between the two processes is that skeletal mineralization is a highly regulated process with developmental cues that occur in a time-dependent manner, whereas vascular calcification is a process that occurs with many of the same components as skeletal mineralization, but with aberrant environmental triggers. The purpose of the current chapter is to describe skeletal remodeling and mineralization.

Bone Biology

Components of the Bone

The bone is a composite structure comprised primarily of mineral and organic matrix [11]. By weight, the majority of the structure is mineral (typically around 65%), with organic components such as type I collagen and non-collagenous proteins accounting for roughly 25%. The bone is about 10% water [12] and contains lipids within the matrix (both cellular and extracellular) [13].

Type I collagen within bone exists in the form of fibers that, over time, become surrounded by mineral (Fig. 17.1). The collagen fibers are made of individual molecules, each containing two $\alpha 1$ and one $\alpha 2$ chains that are formed into a triple helix [14]. The chains are comprised of repeating glycine-X-Y amino acid motifs, with X and Y typically being proline and hydroxyproline. Glycine is essential for proper helical structure formation. Hydroxyproline is important for the formation of hydrogen bonds with water molecules.

The cellular production of collagen by osteoblasts is typical of any collagen-producing cell. Intracellularly, non-helical registration peptides are attached to both ends of the molecule (termed N-propeptide and C-propeptide). Once extruded from the cell into the extracellular environment, the registration portions are cleaved and the molecule is considered a mature collagen fibril – containing N- and C-telopeptide

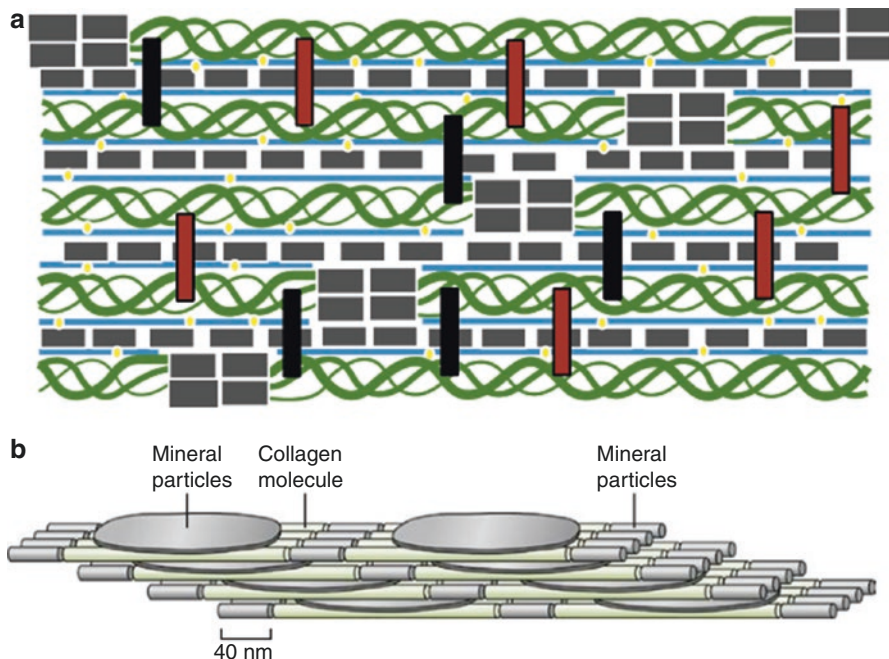


Fig. 17.1 The key components of bone matrix. **(a)** Collagen molecules (green helix) are cross-linked within the fibril by bonds that are formed through enzymatic processes and by those formed without the need for an enzymatic reaction. Enzymatically formed cross-links (black bars), such as pyridinoline or deoxypyridinoline, form near the ends of the molecules, the C- and N-termini. Nonenzymatically formed bonds (red bars), such as pentosidine, are randomly located between the molecules. Mineral (gray blocks) is deposited in the hole and pore zones between the collagen fibrils. Water (blue lines) and hydrogen bonds (yellow dots) contribute to the bonding of mineral and collagen within the fibril. **(b)** Hole and pore zones between the molecules contain plates of bone mineral (hydroxyapatite). Water is bound to collagen in these spaces, and this alters the distribution of load sharing between the collagen and bone mineral deposited in this location regions. (Images reproduced with permission from Burr and Allen [11])

end segments. The collagen fibrils aggregate and align in discrete patterns, typically forming fibers that are roughly 150 nm in diameter and 10 μm in length. The collagen molecule has various cross-links, some enzymatically mediated (such as pyridinoline and deoxypyridinoline) and others are non-enzymatically mediated (such as pentosidine, carboxymethyllysine, and vesperlysine). Cross-links serve to stabilize the collagen and impart stiffness, yet high levels are associated with tissue brittleness as they impede collagen sliding during loading [15].

Mineral within the bone is in the form of carbonated apatite. It fills gaps between collagen fibers, both at the ends of adjacent fibers and in longitudinal spaces (where it forms plate-like structures) (Fig. 17.1) [11, 16]. The initial deposition of mineral is as calcium phosphate and calcium carbonate. Over time, the mineral crystals grow such that crystal size is related to tissue age. Various cations, such as magnesium and

sodium, can substitute for calcium, while fluoride can substituted for the hydroxyl groups within the mineral. Non-collagenous proteins play a role in collagen fiber assembly and mineralization while also having functions in cell signaling [17]. Proteoglycans such as biglycan, decorin, fibromodulin, and versican bind to collagen and orchestrate aspects of bone formation and mineralization.

Water within the bone is generally classified as free or bound [12, 18]. Free water is found in the vasculature, lacunar-canalicular system, marrow, and any other spaces within the bone. This pool of water provides nourishment to the cells and likely also plays a key role in ion exchange to the blood. Bound water is attached to the collagen-mineral, either on the surface where it provides ductility during mechanical stress, within the collagen triple helix where it provides stability or within the mineral crystal lattice where it mediates mineral aggregation. Alterations in bone water have clear effects on bone mechanical properties [12, 19, 20].

Types of Bone Matrix

Bone matrix, that is, the mineral/collagen composite, is classified as either woven or lamellar. Woven bone, typical of bone formed during development, fracture healing, and some pathological conditions (such as Paget's disease), is characterized by randomly organized collagen fibers and disparate bone mineralization. It can be formed very quickly but has sub-optimal mechanical properties. Conversely, lamellar bone, produced normally in non-pathological conditions, is highly organized and mechanically optimized yet is formed relatively slowly.

Bone Formation During Development

Bone formation occurs through either intramembranous or endochondral mechanisms [11]. Intramembranous bone formation, typical of the craniofacial bones, occurs when mesenchymal cells differentiate into osteoblasts and then begin producing matrix de novo within the mesenchyme. The matrix mineralizes and entombs osteocytes, and the bone then exists and is remodeled. Endochondral bone formation, the pathway through which the majority of bones in the skeleton are formed, begins with a cartilaginous template (termed an anlage). In a series of highly coordinated, sequential steps, the cartilaginous template is replaced by the bone matrix. Most of the dynamic activity associated with endochondral bone formation occurs at the growth plate, a region within long bones that permits longitudinal growth of the mineralized organ. The process of endochondral ossification occurs with distinct regions undergoing bone modeling and remodeling, the fundamental processes that govern bone formation and renewal.

Bone Remodeling

Bone remodeling is a temporally and spatially coordinated process that functions to renew the skeleton over time. Bone remodeling is a combination of stochastic and targeted events [21, 22]. Stochastic remodeling is thought to be the primary means through which calcium homeostasis is regulated, while targeted remodeling serves to replace discrete regions of bone. Stimuli for targeting include regions with micro-damage, apoptotic osteocytes, elevated collagen cross-links, and high mineralization.

Bone remodeling occurs through a five-step process, starting with the initiating event, followed by bone resorption, reversal, formation, and then finally ending with quiescence (Fig. 17.2) [11, 23, 24]. Two key concepts of remodeling are that (1) it is spatially coordinated, where the region targeted and removed by osteoclasts is then re-formed by osteoblasts and (2) it is temporally coordinated such that osteoclasts finish resorption activity prior to osteoblasts starting formation. A bone remodeling unit is called a BMU (bone multicellular unit).

Once a bone remodeling event is initiated, osteoclast precursors are signaled to the BMU through the OPG/RANK/RANKL system where they fuse and form mature osteoclasts. These cells attach to the matrix and begin to acidify it, either on a bone surface or tunneling through the cortical bone. Resorption continues until the signal is gone – the mechanisms driving cessation of a given remodeling unit are unknown. Once resorption is finished, the reversal stage begins in which the osteoclasts leave the area and osteoblasts arrive on the scene. The process of reversal is one of emerging knowledge [25]. Historically thought of as a passive process, it is now appreciated that there is not only active communication between osteoclasts and osteoblasts but that disruption of the normal reversal compromises the whole remodeling cycle.

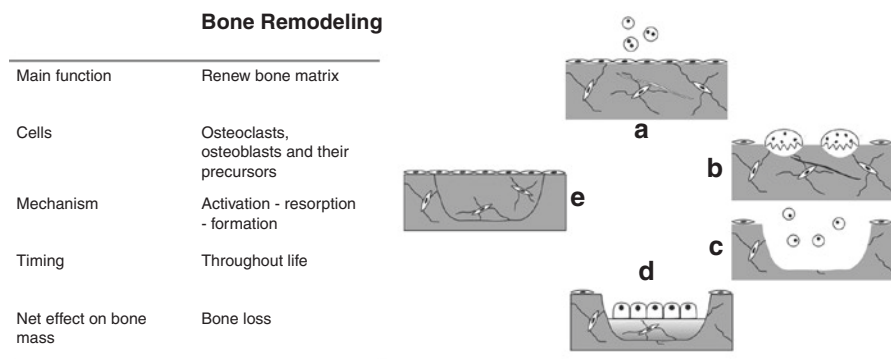


Fig. 17.2 Bone remodeling. The main characteristics are presented in the table. Right image: The remodeling cycle involves five stages: (a) activation; (b) resorption; (c) reversal; (d) formation; and (e) quiescence. At any one time, remodeling cycles throughout the body are at various stages. (Images reproduced with permission from Burr and Allen [11])

The bone formation stage of the remodeling cycle consists of osteoblastic cells producing unmineralized matrix (osteoid) which then becomes mineralized over time. Osteoblasts fill in the hemi-osteons of trabecular bone (or on the endocortical surface), or the radial cavities removed during intracortical remodeling. The amount of bone formed at any remodeling site tends to be less than the amount removed through resorption. In intracortical remodeling, this allows a central canal to remain (which contain blood vessels), the reason why slightly less bone is formed during surface-based remodeling is unknown. The smaller amount of bone formed relative to what is resorbed at a given remodeling unit is referred to as a negative bone balance. It is because of this negative bone balance at every remodeling site that bone remodeling, in general, is associated with bone loss and the higher the rate of bone remodeling the more rapid the rate of bone loss. Positive BMU balance has been shown with anabolic drug treatment [26].

Once bone formation (the production of osteoid) is complete, the newly formed bone region is covered with osteoblasts that become quiescent. These cells transform their morphology to look more like endothelial cells elongated and flat. Although they retain the phenotype of osteoblasts, they are often referred to as bone lining cells. All bone surfaces internal to the bone (trabecular, endocortical, and within central canals of osteons) are covered with bone lining cells. In response to certain stimuli, such as parathyroid hormone, bone lining cells can be activated to once again produce bone matrix [27]. This process, which is technically called bone modeling (see below), is thought to be a mechanism through which bone matrix can be quickly formed to respond to high stresses/strains.

Bone Modeling

Bone modeling is when either bone formation or bone resorption occurs without the other in a given spatial location (Fig. 17.3) [11, 23, 24]. Bone modeling is most prominent during growth but also occurs with normal aging, in periods of mechanical adaptation, and is the underlying basis of orthodontic tooth movement. Classic experiments illustrating how bone morphology changes following dramatic changes in mechanical loading (such as treatment of extreme ricketic bone) provide the clearest example of bone modeling. Driven by the altered mechanical stresses/strains on the bone, new bone formation is stimulated on periosteal surfaces of the one side of cortex. This bone formation is not preceded by bone resorption on this surface, thus bone modeling. In the same way, the cortex on the opposite periosteal surface undergoes osteoclast-based resorption, with no associated formation. These two events, occurring on different surfaces, are both bone modeling events because of the spatial uncoupling. In either resorption or formation modeling, there is typically an activating stimulus which is followed either by resorption and then quiescence or formation and quiescence. Other examples of modeling include the activity at the metaphyseal region of long bones during longitudinal bone growth, where modeling on the surfaces helps maintain the consistent shape of the bone as growth

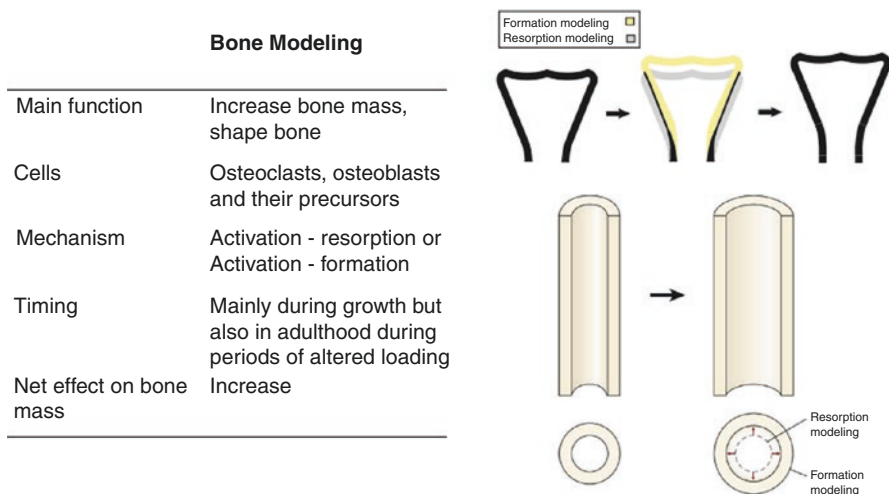


Fig. 17.3 Bone modeling. The main characteristics are presented in the table. Upper right: As the bone grows longitudinally, there is coordinated modeling activity on the metaphyseal bone surfaces that serve to preserve the bone shape. Lower right: Radial bone growth involves formation modeling on periosteal surfaces and resorption modeling on the endocortical surface. Over time, these processes preserve cortical thickness, while increasing the width of the bone. (Images reproduced with permission from Burr and Allen [11])

occurs. The majority of bone modeling is formation modeling, thus modeling is typically thought of as increasing bone mass. Although the process of bone formation during modeling or remodeling is technically complete once the local osteoblasts stop forming osteoid, an important and essential component of bone formation is the incorporation of mineral into the osteoid, described below.

Measures of Bone Modeling/Remodeling

The gold standard method for assessing bone modeling/remodeling is histomorphometry [28]. In humans, this is predominantly done using iliac crest biopsies, the lone site accessible for a tissue biopsy (technically ribs can be used but volunteers rarely line up to provide a rib biopsy) [29]. In order to make the measures of bone modeling/remodeling, fluorochrome labels (dosed orally at specific times) need to be administered prior to obtaining a biopsy (Fig. 17.4). The fluorochromes bind to the calcium that is incorporated into the mineralizing osteoid and, when viewed on a histological section under fluorescent light, provide a view of where bone formation was occurring at one or both periods of tetracycline administration. The traditional approach is to give two labels, separated by roughly 2 weeks, although some studies incorporate two sets of double labels to look at changes in the same individual over time [30, 31]. Although not often done, it is possible to differentially assess bone modeling and remodeling using histology (Fig. 17.5). This is done by

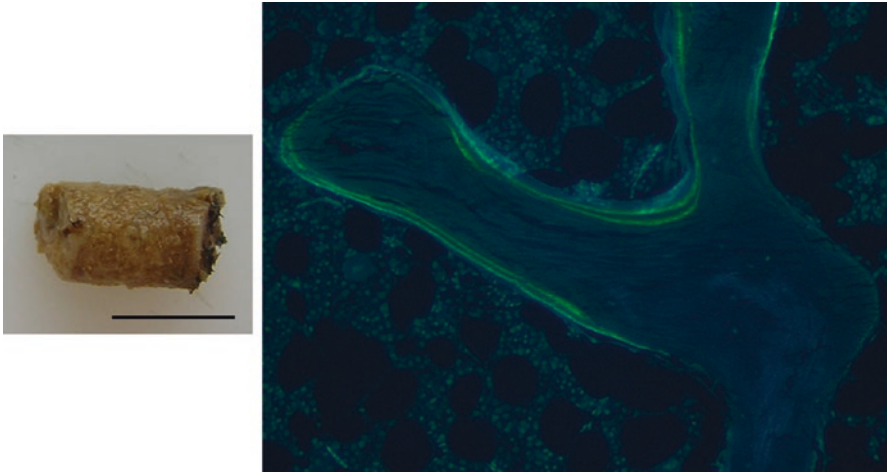


Fig. 17.4 Histological assessment of tissue-level remodeling in humans. The most common site for histological assessment in humans is on a small core of tissue from the iliac crest. If patients are administered tetracycline-based compounds prior to biopsy, tissues can be embedded, sectioned, and assessed for dynamic bone remodeling activity. Scale bar is 1 cm

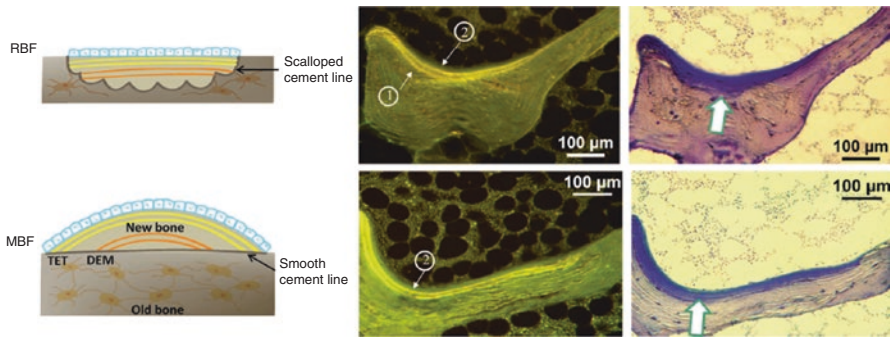


Fig. 17.5 Histological techniques exist to differentiate modeling- and remodeling-based formation. Shown are schematic illustrations of remodeling-based formation (RBF) and modeling-based formation (MBF) using two sets of double label DEM = demeclocycline (the first set of labels); TET = tetracycline (the second set of labels). Dark field images showing fluorochrome labels are in the lefthand panels with corresponding bright field images in the righthand panels. The top figures demonstrate remodeling-based bone formation on the cancellous surface. Note the first and second sets of labels (arrows with (1) and (2), lefthand panel) and the underlying scalloped reversal line (arrow, righthand panel). The bottom figures demonstrate modeling-based bone formation on the cancellous surface. Note the second set of double labels (arrow with (2), lefthand panel) and the underlying smooth cement line (arrow, righthand panel). (Images reproduced with permission from Dempster et al. [26])

assessing not just the fluorochrome labels, but then taking it one step further to assess the morphology of the remodeling unit relative to the cement line (the defined edge of the newly formed remodeling site) [26].

The main limitation of histological assessment of bone remodeling is that results are limited to iliac crest tissue. Although ample data exists to support the idea that measures at the iliac crest correlate to other sites [32–34], there remains some level of skepticism over site-to-site correlations. Clinically this limitation of site-specificity can be overcome by measuring bone formation/resorption biomarkers in the urine or serum. These biomarkers are either collagen fragments produced during collagen formation or collagen breakdown or products of osteoblast or osteoclasts. The advantage of these measures is they are easier to obtain and they provide a whole body assessment of formation/resorption. The downside of using these biomarkers is that these measures lack the specificity of a single skeletal site or between cortical and trabecular bone.

Advances in imaging are bringing forth novel approaches to assess bone modeling/remodeling. High-resolution peripheral quantitative computed tomography (HR-pQCT) has the ability to scan distal tibia and radial sites with a voxel size of $60 \mu\text{m}^3$ [35, 36]. Although this cannot resolve individual remodeling sites, parallel advances in imaging in rodents (where *in vivo* resolutions have reached $9\text{--}20 \mu\text{m}^3$) have shown what the future may hold from imaging-based assessment. For example, using repeated scans in rodents, regions where bone formation and resorption are occurring can be noted and quantified (Fig. 17.6) [37–40].

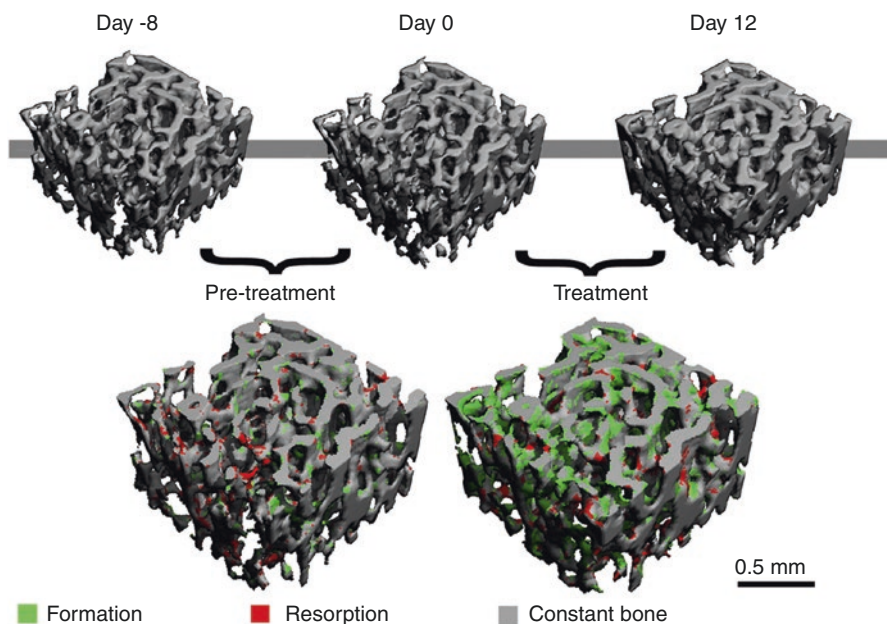


Fig. 17.6 Preclinical imaging has the ability to resolve local changes in morphology that equate to formation and resorption. In this study, rats were scanned on days 0 and 12, and the 3D *in vivo* dynamic bone histomorphometry technique was applied to identify regions of bone formation (green) and resorption (red). A subset of rats was also scanned at day 8 to allow for a pretreatment measure of bone remodeling. (Image reproduced with permission from: de Bakker et al [39])

Bone Matrix Mineralization

As is apparent from above, the process of bone modeling and remodeling is highly controlled. After the osteoblasts have laid down collagen and non-collagenous proteins, called osteoid, there is a sequence of events that result in mineralization of collagen. The cellular stimulation of mineralization, and accumulation of mineral on proteins, involves regulation by dentin matrix protein (DMP1) [41], SIBLING proteins (osteocalcin, osteopontin, and others) [42], and NOTCH signaling [43]. The process of mineralization occurs in two stages. Primary mineralization occurs rapidly, typically over 2–3 weeks, and results in nearly 70% of the total mineral accrual within the collagenous matrix. Thereafter secondary mineralization occurs, bringing the region to its physiological level of mineralization. The optimal or maximum mineralization level that a given region of bone can reach is not entirely clear. Mineral substitute 1:1 for water, such that at the level of the collagen-mineral interface, increasing the amount of mineral will lead to lower bound water. Since bound water imparts ductility to this interface, increasing mineral leads to brittleness.

While numerous studies have shown that the level of mineralization can be increased over time, this is thought to be due to more regions of a bone achieving their optimal physiological levels, rather than increasing mineral content in regions that are already close to maximally mineralized. As more regions of bone become more fully mineralized, this reduces the heterogeneity across this tissue. Heterogeneity of mineral (and likely other constituents such as collagen and water) is mechanically beneficial as it serves to arrest microdamage growth and prevent catastrophic fracture.

Similar to arterial calcification, a major driver of mineralization (calcification) are vesicles. These small vesicular structures were identified in the 1960s by electron microscopy in mouse cartilage microscopy [44, 45]. These were called matrix vesicles (MVs) because of their role in mineralizing bone matrix proteins. MVs are similar to other extracellular vesicles but have characteristics of both exosomes and microvesicles [46]. As shown in Fig. 17.7, by transmission electron microscopy, vesicles accumulate in unmineralized osteoid beneath osteoblasts. Imaging and spectroscopy techniques show the vesicles contain amorphous calcium and phosphate near the membrane which then converts into hydroxyapatite that are needle-like in shape [47]. When large enough, the crystalline structures penetrate the plasma membrane of the vesicle and form calcifying nodules (Fig. 17.7) [48].

Molecular biology studies and lessons learned from genetic mutations have allowed understanding of the sequence of events of matrix vesicle mineralization in bone [44, 46, 47, 49] and arterial calcification [50]. Inside the vesicle, calcium accumulates from abundant nearby extracellular sources or entry into the vesicle through annexin calcium channels [51]. Another, possibly additive, hypothesis is that the calcium is incorporated during the vesicle formation and may be a byproduct of the mitochondria during oxidative stress [52]. The regulation of mineral formation, however, is predominately through enzymes that control the concomitant phosphate production and entry into the vesicles (Table 17.1).

Fig. 17.7 TEM observation of matrix vesicles and calcifying nodules in osteoid. Panel (a) demonstrates many calcifying nodules (black) in the osteoid beneath mature osteoblasts (Ob). Panel (b) is a higher magnification of the osteoid; many matrix vesicles indicated by white arrowheads, calcifying nodules (CN) and collagen fibrils (Co) can be seen. Bars (a): 2 μ m, (b): 1 μ m. (From T. Hasegawa, *Histochemistry and cell biology*. 149: 289–304, 2018)

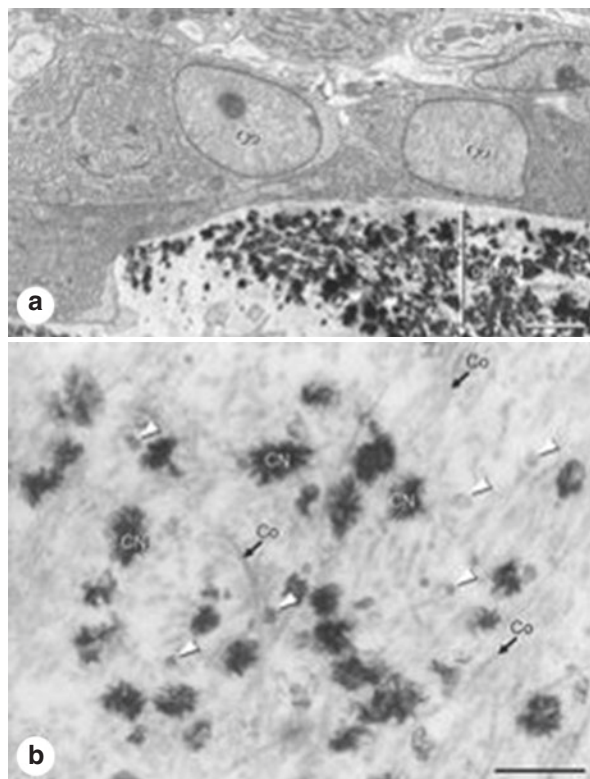


Table 17.1 Enzymes important in the regulation of matrix vesicle mineralization in the bone

	Role	Human “null” manifestation
ENPP1	Enzyme that generates pyrophosphate, inhibitor of mineralization both inside and outside of matrix vesicles	Deficiency in humans leads to spontaneous infantile arterial and periarticular mineralization [67, 68]
ANK	Transmembrane channel that allows PPi to enter and exit vesicles	Deficiency in humans leads to a decrease in extracellular PPi, mineralization in joints and other tissues [53, 69]
TNAP	Enzyme on membrane of osteoblasts and matrix vesicles that cleaves PPi to remove the mineralization inhibitory effects of PPi, thus releasing PO_4^{-3} for entry into matrix vesicles	Deficiency in humans leads to skeletal hypomineralization, seizures, and inflammation. Variety of presentations due to type of mutation and age of onset [57]
PHOSPHO1	Enzyme within matrix vesicles that degrades lipid to form free PO_4^{-3}	Unknown

ENPPI: Ecto-nucleotide pyrophosphatase/phosphodiesterase 1 is an enzyme located on the osteoblast cytoplasm and membrane and generates inorganic pyrophosphates (PPi). The PPi made intracellularly can be transported extracellular through ankyloses (Ank) channels. Conversely the ENPPI located on membrane can generate PPi through extracellular ATP. Pyrophosphate inhibits extracellular mineralization and thus regulates the amount of PO_4^{-3} free in the cytoplasm to be transported into the matrix vesicle through the plasma membrane through ankylosis (ANK), a transmembrane channel [53]. In the extracellular space, PPI help to regulate the amount of available PO_4^{-3} for mineralization.

TNAP (tissue non-specific alkaline phosphatase; also called TNSAP) is an 86 kD homodimeric protein enzyme associated with the basolateral cell membrane of osteoblasts, matrix vesicles, and calcifying nodules [54]. Approximately 95% of the total alkaline phosphatase measured routinely on blood chemistry panels in humans is TNAP; the remainder are tissue specific. TNAP hydrolyzes PPI and other phosphate esters producing inorganic PO_4^{-3} monomers that are transported into matrix vesicles [55]. The latter is believed to occur through PiT1 (type III sodium/phosphate co-transporter) [56]. By hydrolyzing PPI, the normal inhibitory effects of PPI are negated, allowing mineralization to occur. The human disease hypophosphatasia [57] is a heterogeneous group of diseases caused by a number of different loss-of-function mutations in the alkaline phosphate liver-type gene. This leads to generalized reduction of activity of TNAP. The clinical presentation can be lethal or very mild depending on the inheritance pattern, the mutation, and the age of onset, but in all patients there is a reduced level of alkaline phosphatase. In the bone, there is skeletal hypomineralization, but other systemic manifestations include seizures and inflammation. A recombinant mineral targeted TNAP is now available for treatment of these individuals [58]. Interestingly, a mouse model of *tnap*^{-/-} are born with normal bones but gradually develop skeletal deformities characterized by disorder in hydroxyapatite crystal alignment in long bones [59].

PHOSPHO1, orphan phosphatase 1 is a soluble cytosolic enzyme that catabolizes the lipids [60] but not PPI. It is located inside the MV and leads to increased intravesicle PO_4^{-3} . It is believed that PHOSPHO1 may generate the PO_4^{-3} from enzymatic action of the vesicles phospholipid membrane [61, 62], degrading phosphoethanolamine (PEA) and phosphocholine(PC) [63]. Animals deficient in PHOSPHO1 have normal bone volume but impaired mineralization [64]. The ability of PHOSPHO1 to metabolize PEA and PC, two of the most abundant lipids in the body, implies systemic effects of this enzyme and its homolog PHOSPHO2. The by-product, choline, is an important energy metabolite, and epigenomic studies have shown the importance of PHOSPHO1 in disorders of altered energy metabolism such as diabetes and obesity [65]. In addition, PHOSPHO1 is important in terminal erythropoiesis [66]. These diverse roles explain why there is no known human model of complete deficiency.

To summarize the importance of these multiple enzymes in mineralization of osteoid in bone (Fig. 17.8), the initiating step appears to be the formation of MVs from osteoblasts that contain amorphous calcium and phosphorus leading to the formation of hydroxyapatite crystals that continue to accumulate and grow inside the vesicle.

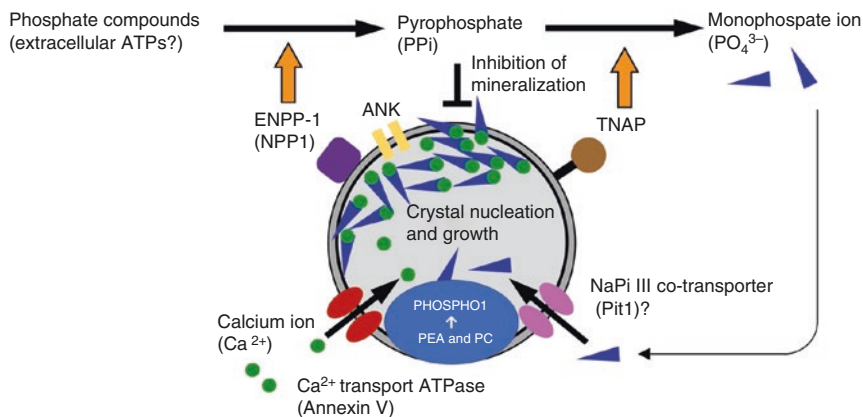


Fig. 17.8 Matrix vesicles initiate mineralization. Membrane transporters and enzymes including TNAP, ENPP1, annexins, ANK, and Pit1 on matrix vesicles play a pivotal role in Ca²⁺ (green dots) and PO₄³⁻ (blue triangles) transport into the vesicles. Inside the vesicles, PHOSPHO1 generates PO₄³⁻ from phosphoethanolamine (PEA) and phosphocholine (PC). Thereafter, amorphous calcium phosphate develops hydroxyapatite to form needle-shaped mineral crystals. Many mineral crystals penetrate the vesicles' membranes to form a globular assembly of mineralized nodules. (Adapted from T. Hasegawa et al., Japanese dental science Review. 53:34–45, 2017 [39])

The calcium is from the cell making the vesicle and/or entry into the vesicle via annexins from the extracellular space. In contrast, the phosphorus content is highly regulated and is normally in a state of inhibition through the activity of PPi and other regulatory enzymes and proteins. The activity of PPi can be inhibited by TNAP, facilitating release of PO₄³⁻ outside of the matrix vesicle with subsequent transport into the vesicle through the transporter Pit1. In addition, the presence of PHOSPHO1 inside the matrix vesicle leads to degradation of lipids, generating choline for energy and PO₄³⁻ for mineralization. The dual importance of TNAP and PHOSPHO1 is demonstrated by the finding that mice lacking either enzyme still form bone mineral, whereas the double knockout does not [64]. The result of this collective group of enzymes is highly regulated mineralization. While there are many parallels between mineralization in bone and ectopic mineralization in arteries, the difference lies in the regulation in the bone by temporal cues with redundant regulatory processes versus the induction of mineralization by aberrant environmental cues in arteries.

Funding Dr. Moe is supported by NIH P30AR072581 and R01 DK11087103 and Veterans Administration BX001471. Dr. Allen is supported by NIH R01 DK11087103 and R01 DK119266 and Veterans Affairs BX003025.

References

1. Kiel DP, Kauppila LI, Cupples LA, Hannan MT, O'Donnell CJ, Wilson PW. Bone loss and the progression of abdominal aortic calcification over a 25 year period: the Framingham Heart Study. *Calcif Tissue Int.* 2001;68(5):271–6.

2. Zhang Y, Feng B. Systematic review and meta-analysis for the association of bone mineral density and osteoporosis/osteopenia with vascular calcification in women. *Int J Rheum Dis.* 2017;20(2):154–60.
3. Naves M, Rodriguez-Garcia M, Diaz-Lopez JB, Gomez-Alonso C, Cannata-Andia JB. Progression of vascular calcifications is associated with greater bone loss and increased bone fractures. *Osteoporos Int.* 2008;19(8):1161–6.
4. Lewis JR, Eggermont CJ, Schousboe JT, Lim WH, Wong G, Khoo B, et al. Association between abdominal aortic calcification, bone mineral density, and fracture in older women. *J Bone Miner Res.* Elsevier. 2019;34(11):2052–60.
5. Ahmadi N, Mao SS, Hajsadeghi F, Arnold B, Kiramijyan S, Gao Y, et al. The relation of low levels of bone mineral density with coronary artery calcium and mortality. *Osteoporos Int.* 2018;29(7):1609–16.
6. Zeng Y, Wu J, He X, Li L, Liu X, Liu X. Mechanical microenvironment regulation of age-related diseases involving degeneration of human skeletal and cardiovascular systems. *Prog Biophys Mol Biol.* 2019;148:54–9.
7. Moe SM. Vascular calcification and renal osteodystrophy relationship in chronic kidney disease. *Eur J Clin Invest.* 2006;36(Suppl 2):51–62.
8. Rochette L, Meloux A, Rigal E, Zeller M, Malka G, Cottin Y, et al. The role of osteoprotegerin in vascular calcification and bone metabolism: the basis for developing new therapeutics. *Calcif Tissue Int.* 2019;105(3):239–51.
9. Pietrzyk B, Smertka M, Chudek J. Sclerostin: intracellular mechanisms of action and its role in the pathogenesis of skeletal and vascular disorders. *Adv Clin Exp Med.* 2017;26(8):1283–91.
10. Villa JKD, Diaz MAN, Pizzio VR, Martino HSD. Effect of vitamin K in bone metabolism and vascular calcification: a review of mechanisms of action and evidences. *Crit Rev Food Sci Nutr.* 2017;57(18):3959–70.
11. Burr DB, Allen MR. Basic and applied bone biology. 2nd ed: Academic Press; 2019.
12. Granke M, Does MD, Nyman JS. The role of water compartments in the material properties of cortical bone. *Calcif Tissue Int.* 2015;97(3):292–307.
13. During A, Penel G, Hardouin P. Understanding the local actions of lipids in bone physiology. *Prog Lipid Res.* 2015;59:126–46.
14. Garnero P. The role of collagen organization on the properties of bone. *Calcif Tissue Int.* 2015;97(3):229–40.
15. Wang X, Bank RA, TeKoppele JM, Agrawal CM. The role of collagen in determining bone mechanical properties. *J Orthop Res.* 2001;19(6):1021–6.
16. Stock SR. The mineral-collagen interface in bone. *Calcif Tissue Int.* 2015;97(3):262–80.
17. Saito M, Marumo K. Effects of collagen crosslinking on bone material properties in health and disease. *Calcif Tissue Int.* 2015;97(3):242–61.
18. Wang Y, Von Euw S, Fernandes FM, Cassaignon S, Selmane M, Laurent G, et al. Water-mediated structuring of bone apatite. *Nat Mater.* 2013;12(12):1144–53.
19. Nyman JS, Ni Q, Nicoletta DP, Wang X. Measurements of mobile and bound water by nuclear magnetic resonance correlate with mechanical properties of bone. *Bone.* 2008;42(1):193–9.
20. Maghsoudi-Ganjeh M, Wang X, Zeng X. Computational investigation of the effect of water on the nanomechanical behavior of bone. *J Mech Behav Biomed Mater.* 2020;101:103454.
21. Burr DB. Targeted and nontargeted remodeling. *Bone.* 2002;30(1):2–4.
22. Martin RB. Is all cortical bone remodeling initiated by microdamage? *Bone.* 2002;30(1):8–13.
23. Roberts WE, Epker BN, Burr DB, Hartsfield JK Jr, Roberts JA. Remodeling of mineralized tissues, part II: control and pathophysiology. *Semin Orthod.* 2006;12(4):238–53.
24. Roberts WE, Roberts JA, Epker BN, Burr DB, Hartsfield JK Jr. Remodeling of mineralized tissues, part I: the frost legacy. *Semin Orthod.* 2006;12(4):216–37.
25. Dempster DW. Tethering formation to resorption: reversal revisited. *J Bone Miner Res.* 2017;32(7):1389–90.
26. Dempster DW, Zhou H, Recker RR, Brown JP, Recknor CP, Lewiecki EM, et al. Remodeling- and modeling-based bone formation with teriparatide versus denosumab: a longitudinal analy-

- sis from baseline to 3 months in the AVA study. *J Bone Miner Res.* 2018;33(2):298–306. <https://doi.org/10.1002/jbmr.3309>.
27. Goltzman D. Physiological actions of PTH I: PTH action on the skeleton. In: *The parathyroids* 3rd ed. Academic Press; 2015. pp. 139–52.
 28. Kulak CA, Dempster DW. Bone histomorphometry: a concise review for endocrinologists and clinicians. *Arq Bras Endocrinol Metabol.* 2010;54(2):87–98.
 29. Hodgson SF, Johnson KA, Muhs JM, Lufkin EG, McCarthy JT. Outpatient percutaneous biopsy of the iliac crest: methods, morbidity, and patient acceptance. *Mayo Clin Proc.* 1986;61(1):28–33.
 30. Recker RR, Kimmel DB, Dempster D, Weinstein RS, Wronski TJ, Burr DB. Issues in modern bone histomorphometry. *Bone.* 2011;49(5):955–64.
 31. Dempster DW, Zhou H, Recker RR, Brown JP, Bolognese MA, Recknor CP, et al. Skeletal histomorphometry in subjects on teriparatide or zoledronic acid therapy (SHOTZ) study: a randomized controlled trial. *J Clin Endocrinol Metab.* 2012;97(8):2799–808.
 32. Chappard C, Marchadier A, Benhamou CL. Side-to-side and within-side variability of 3D bone microarchitecture by conventional micro-computed tomography of paired iliac crest biopsies. *Bone.* 2008;43(1):203–8.
 33. Mashiba T, Hui S, Turner CH, Mori S, Johnston CC, Burr DB. Bone remodeling at the iliac crest can predict the changes in remodeling dynamics, microdamage accumulation, and mechanical properties in the lumbar vertebrae of dogs. *Calcif Tissue Int.* 2005;77(3):180–5.
 34. Marques ID, Araujo MJ, Gracioli FG, Reis LM, Pereira RM, Custodio MR, et al. Biopsy vs. peripheral computed tomography to assess bone disease in CKD patients on dialysis: differences and similarities. *Osteoporos Int.* 2017;28(5):1675–83.
 35. Mikolajewicz N, Bishop N, Burghardt AJ, Folkestad L, Hall A, Kozloff KM, et al. HR-pQCT measures of bone microarchitecture predict fracture: systematic review and meta-analysis. *J Bone Miner Res.* 2020;35(3):446–59.
 36. Jamal SA, Nickolas TL. Bone imaging and fracture risk assessment in kidney disease. *Curr Osteoporos Rep.* 2015;13(3):166–72.
 37. Wehrle E, Tourolle Ne Betts DC, Kuhn GA, Scheuren AC, Hofmann S, Muller R. Evaluation of longitudinal time-lapsed in vivo micro-CT for monitoring fracture healing in mouse femur defect models. *Sci Rep.* 2019;9(1):17445.
 38. Altman AR, Tseng WJ, de Bakker CMJ, Chandra A, Lan S, Huh BK, et al. Quantification of skeletal growth, modeling, and remodeling by in vivo micro computed tomography. *Bone.* 2015;81:370–9.
 39. de Bakker CM, Altman AR, Tseng WJ, Tribble MB, Li C, Chandra A, et al. muCT-based, in vivo dynamic bone histomorphometry allows 3D evaluation of the early responses of bone resorption and formation to PTH and alendronate combination therapy. *Bone.* 2015;73:198–207.
 40. Brouwers JE, van Rietbergen B, Huiskes R, Ito K. Effects of PTH treatment on tibial bone of ovariectomized rats assessed by in vivo micro-CT. *Osteoporos Int.* 2009;20(11):1823–35.
 41. Ravindran S, George A. Dentin matrix proteins in bone tissue engineering. *Adv Exp Med Biol.* 2015;881:129–42.
 42. Staines KA, MacRae VE, Farquharson C. The importance of the SIBLING family of proteins on skeletal mineralisation and bone remodelling. *J Endocrinol.* 2012;214(3):241–55.
 43. Shao J, Zhou Y, Lin J, Nguyen TD, Huang R, Gu Y, et al. Notch expressed by osteocytes plays a critical role in mineralisation. *J Mol Med (Berl).* 2018;96(3–4):333–47.
 44. Anderson HC. Molecular biology of matrix vesicles. *Clin Orthop Relat Res.* 1995;314:266–80.
 45. Anderson HC, Reynolds JJ. Pyrophosphate stimulation of calcium uptake into cultured embryonic bones. Fine structure of matrix vesicles and their role in calcification. *Dev Biol.* 1973;34(2):211–27.
 46. Azoidis I, Cox SC, Davies OG. The role of extracellular vesicles in biomineralisation: current perspective and application in regenerative medicine. *J Tissue Eng.* 2018;9:2041731418810130.
 47. Hoshi K, Ozawa H. Matrix vesicle calcification in bones of adult rats. *Calcif Tissue Int.* 2000;66(6):430–4.

48. Bonucci E. The locus of initial calcification in cartilage and bone. *Clin Orthop Relat Res.* 1971;78:108–39.
49. Aszodi A, Bateman JF, Gustafsson E, Boot-Handford R, Fassler R. Mammalian skeletogenesis and extracellular matrix: what can we learn from knockout mice? *Cell Struct Funct.* 2000;25(2):73–84.
50. Goettsch C, Hutcheson JD, Aikawa M, Iwata H, Pham T, Nykjaer A, et al. Sortilin mediates vascular calcification via its recruitment into extracellular vesicles. *J Clin Invest.* 2016;126(4):1323–36.
51. Hoshi K, Ejiri S, Ozawa H. Localizational alterations of calcium, phosphorus, and calcification-related organics such as proteoglycans and alkaline phosphatase during bone calcification. *J Bone Miner Res.* 2001;16(2):289–98.
52. Shapiro IM, Golub EE, Chance B, Piddington C, Oshima O, Tuncay OC, et al. Linkage between energy status of perivascular cells and mineralization of the chick growth cartilage. *Dev Biol.* 1988;129(2):372–9.
53. Gurley KA, Reimer RJ, Kingsley DM. Biochemical and genetic analysis of ANK in arthritis and bone disease. *Am J Hum Genet.* 2006;79(6):1017–29.
54. de Bernard B, Bianco P, Bonucci E, Costantini M, Lunazzi GC, Martinuzzi P, et al. Biochemical and immunohistochemical evidence that in cartilage an alkaline phosphatase is a Ca²⁺-binding glycoprotein. *J Cell Biol.* 1986;103(4):1615–23.
55. Anderson HC, Sipe JB, Hesse L, Dhanyamraju R, Atti E, Camacho NP, et al. Impaired calcification around matrix vesicles of growth plate and bone in alkaline phosphatase-deficient mice. *Am J Pathol.* 2004;164(3):841–7.
56. Yadav MC, Bottini M, Cory E, Bhattacharya K, Kuss P, Narisawa S, et al. Skeletal mineralization deficits and impaired biogenesis and function of chondrocyte-derived matrix vesicles in phospho1(–/–) and phospho1/pi t1 double-knockout mice. *J Bone Miner Res.* 2016;31(6):1275–86.
57. Bianchi ML. Hypophosphatasia: an overview of the disease and its treatment. *Osteoporos Int.* 2015;26(12):2743–57.
58. Whyte MP, Greenberg CR, Salman NJ, Bober MB, McAlister WH, Wenkert D, et al. Enzyme-replacement therapy in life-threatening hypophosphatasia. *N Engl J Med.* 2012;366(10):904–13.
59. Tesch W, Vandenbos T, Roschgr P, Fratzl-Zelman N, Klaushofer K, Beertsen W, et al. Orientation of mineral crystallites and mineral density during skeletal development in mice deficient in tissue nonspecific alkaline phosphatase. *J Bone Miner Res.* 2003;18(1):117–25.
60. Roberts SJ, Stewart AJ, Sadler PJ, Farquharson C. Human PHOSPHO1 exhibits high specific phosphoethanolamine and phosphocholine phosphatase activities. *Biochem J.* 2004;382(Pt 1):59–65.
61. Stewart AJ, Roberts SJ, Seawright E, Davey MG, Fleming RH, Farquharson C. The presence of PHOSPHO1 in matrix vesicles and its developmental expression prior to skeletal mineralization. *Bone.* 2006;39(5):1000–7.
62. Stewart AJ, Leong DTK, Farquharson C. PLA2 and ENPP6 may act in concert to generate phosphocholine from the matrix vesicle membrane during skeletal mineralization. *FASEB J.* 2018;32(1):20–5.
63. Roberts SJ, Stewart AJ, Schmid R, Blindauer CA, Bond SR, Sadler PJ, et al. Probing the substrate specificities of human PHOSPHO1 and PHOSPHO2. *Biochim Biophys Acta.* 2005;1752(1):73–82.
64. Yadav MC, Simao AM, Narisawa S, Huesa C, McKee MD, Farquharson C, et al. Loss of skeletal mineralization by the simultaneous ablation of PHOSPHO1 and alkaline phosphatase function: a unified model of the mechanisms of initiation of skeletal calcification. *J Bone Miner Res.* 2011;26(2):286–97.
65. Willmer T, Johnson R, Louw J, Pfeiffer C. Blood-based DNA methylation biomarkers for type 2 diabetes: potential for clinical applications. *Front Endocrinol (Lausanne).* 2018;9:744.

66. Huang NJ, Lin YC, Lin CY, Pishesha N, Lewis CA, Freinkman E, et al. Enhanced phosphocholine metabolism is essential for terminal erythropoiesis. *Blood*. 2018;131(26):2955–66.
67. Rutsch F, Vaingankar S, Johnson K, Goldfine I, Maddux B, Schauerte P, et al. PC-1 nucleoside triphosphate pyrophosphohydrolase deficiency in idiopathic infantile arterial calcification. *Am J Pathol*. 2001;158(2):543–54.
68. Rutsch F, Ruf N, Vaingankar S, Toliat MR, Suk A, Hohne W, et al. Mutations in ENPP1 are associated with ‘idiopathic’ infantile arterial calcification. *Nat Genet*. 2003;34(4):379–81.
69. Gurley KA, Chen H, Guenther C, Nguyen ET, Rountree RB, Schoor M, et al. Mineral formation in joints caused by complete or joint-specific loss of ANK function. *J Bone Miner Res*. 2006;21(8):1238–47.

Chapter 18

Osteoclasts in Cardiovascular Calcification



Samantha K. Atkins, Farwah Iqbal, Johana Barrientos, Cecilia Giachelli, and Elena Aikawa

Osteoclasts Are Crucial Regulators of Bone Resorption

Calcium, the major component of bone and teeth, is abundant in the human body and can occur in three primary forms: calcium phosphate, hydroxyapatite, and magnesium whitlockite [1]. Ectopic calcification in the heart valves and vasculature is of great medical interest due to the increased risk of heart failure, atherosclerotic plaque rupture [2], thrombus [3], or stroke [4, 5]. Cardiovascular calcification, which includes calcification of the blood vessels and heart valves, is an active

Samantha K. Atkins and Farwah Iqbal contributed equally in this chapter. The other authors offered input and output feedback.

S. K. Atkins (✉) · J. Barrientos

Center for Interdisciplinary Cardiovascular Sciences, Division of Cardiovascular Medicine, Department of Medicine, Brigham and Women's Hospital, Harvard Medical School, Boston, MA, USA

e-mail: skatkins@bwh.harvard.edu; jbarrientos@bwh.harvard.edu

F. Iqbal (✉)

Center for Excellence in Vascular Biology, Division of Cardiovascular Medicine, Department of Medicine, Brigham and Women's Hospital, Harvard Medical School, Boston, MA, USA

e-mail: fiqbal1@bwh.harvard.edu

C. Giachelli

Department of Bioengineering, University of Washington, Seattle, WA, USA

e-mail: ceci@uw.edu

E. Aikawa

Center for Interdisciplinary Cardiovascular Sciences, Center for Excellence in Vascular Biology, Division of Cardiovascular Medicine, Department of Medicine, Brigham and Women's Hospital, Harvard Medical School, Boston, MA, USA

e-mail: eaikawa@bwh.harvard.edu

process regulated by numerous cell types. The mechanisms of development of ectopic calcification will not be discussed in this chapter. Instead, this chapter will focus on a particular subset of immune-derived cells known as osteoclasts, which are crucial regulators of bone remodeling due to their ability to resorb calcification. Osteoclasts are large, multinucleated bone-resorbing cells that are hematopoietic in origin [6, 7]. The potential to regress ectopic calcification may be unlocked by activation of osteoclasts in the atheroma or calcified valve, hence the need to characterize osteoclast biology outside of the bone niche. The activation of receptor activator of NF- κ B (RANK)/RANK ligand (RANKL) combined with colony-stimulating factor-receptor (c-Fms)/macrophage colony-stimulating factor (M-CSF) is required for the maturation, differentiation, fusion, and function of mature osteoclasts [8, 9]. M-CSF and RANKL direct osteoclastogenesis through activation of transcription factor nuclear factor of activated T cells 1 (NFATc1). While these canonical regulators of osteoclastogenesis are well studied, the modulatory effects of microRNAs on bone resorption and remodeling are only beginning to be understood. This chapter will summarize the signals that drive and inhibit osteoclastogenesis at the gene and protein levels. It will also discuss the bone-vascular axis in the context of atherosclerosis and calcific aortic valve disease, known as the “calcification paradox.” The mechanisms governing osteoclast differentiation and bone resorption within the bone niche may provide contextual clues of how to harness their natural potential to regress calcification in the areas such as the blood vessels and heart valves.

Osteoclastogenesis

Osteoclasts, first identified in 1873 [10], are the only bone-resorbing cell in mammals and are hematopoietic in origin. Revolutionary studies in the 1970s confirmed the hematopoietic origin of osteoclasts by transplanting osteoclast-deficient mice with either spleen or bone marrow cells from wild-type mice to restore normal bone resorption [11]. Today, it is well recognized that osteoclasts arise from hematopoietic stem cells (HSCs) from either bone marrow or peripheral blood mononuclear cells (PBMCs) [12]. Recently, and contrary to the accepted dogma regarding osteoclast formation from monocyte/macrophage precursors, murine models have demonstrated that osteoclast precursors do not express the macrophage lineage marker CD68 [13]. Mesenchymal-originating osteoblasts are primarily responsible for secreting and rebuilding bone matrix. Together with osteocytes, osteoblasts regulate mineral metabolism by producing various extracellular factors required for osteoclast proliferation, differentiation, and fusion (Fig. 18.1) [7]. Regardless of the progenitor cell, osteoclast differentiation is an orchestrated event that is composed of four main stages: (1) proliferation and differentiation; (2) osteoclast precursor cell (OCP) commitment; (3) OCP motility and fusion; and (4) mature osteoclast bone resorption.

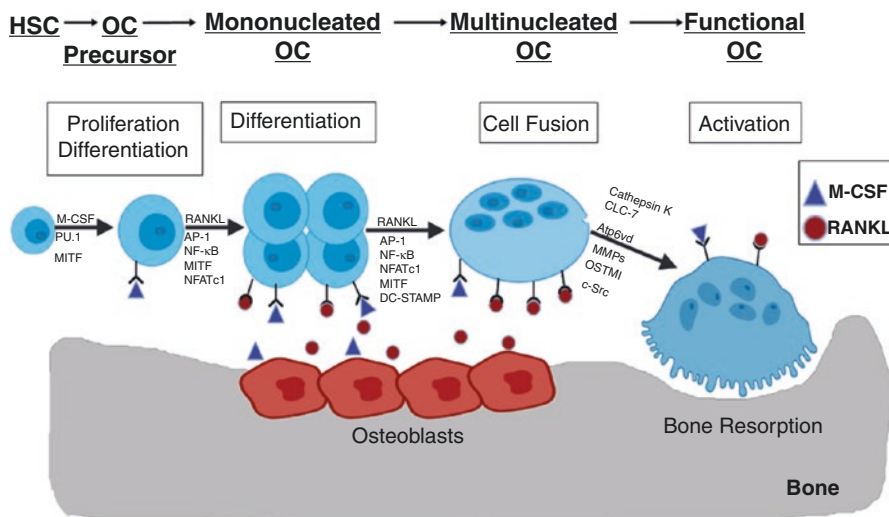


Fig. 18.1 Schematic diagram representing osteoclast differentiation and activation. (1) Proliferation and differentiation: The secretion of M-CSF activates HSCs by upregulating MITF and PU.1 transcription factors, and osteoclast precursor cells (OCPs) become mononucleated osteoclasts via RANKL and M-CSF signaling. (2) Commitment: Osteoclast differentiation: Stimulation of NF- κ B further activates NFATc1, a primary driver of osteoclast differentiation. (3) Fusion: Mononucleated osteoclasts fuse dependent on RANKL signaling and DC-STAMP. (4) Resorption: Functional osteoclasts express cathepsin K, Atp6vd, CLC-7, MMPs, OSTMI, and c-SRC for optimal bone resorption. AP-1 activator protein, Atp6v0d2 v-ATPase subunit d2, CLC-7 chloride channel 7, DC-STAMP dendritic cell-specific transmembrane protein, HSC hematopoietic stem cell, MITF microphthalmia transcription factor, MMPs matrix metalloproteinases, NF- κ B nuclear factor kappa-light-chain-enhancer of activated B cells, NFATc1 nuclear factor of activated T cell 1, OSTMI osteopetrosis-associated transmembrane protein 1, RANKL receptor activator of nuclear factor kappa-B ligand

Proliferation and Differentiation of Osteoclast Precursors

The first stage of osteoclastogenesis is proliferation and differentiation of HSCs into OCPs. The first group of genes include *M-CSF*, *Csf1r/c-Fms* (receptor for M-CSF), and transcription factor *PU.1* [14, 15]. This group of genes activate HSCs to give rise to common macrophage and osteoclast progenitors. M-CSF induces the proliferation of osteoclast precursors and upregulates RANK on the surface of osteoclasts [16]. The transcription factor PU.1 binds to the promoter of *Csf1r*, which encodes for c-Fms and further upregulates transcription [17]. Animals with deficiencies in any of these genes lack macrophages and osteoclasts, while displaying phenotypes of osteopetrosis, similar to osteopetrotic *op/op* mice [18–20]. M-CSF signaling also induces the expression of microphthalmia transcription factor (MITF), necessary for mitigating apoptosis in proliferating osteoclasts [21]. MITF binds to the *Bcl-2* promoter and upregulates the expression of Bcl-2 [22, 23]. Mutations in either *MITF* or *Bcl-2* result in an osteopetrosis phenotype [23, 24].

Both RANKL and M-CSF also activate Src signaling pathways to support osteoclast survival and differentiation. Following the activation of RANK, interactions between TRAF6 and Cbl scaffolding proteins activate the pro-survival factor PI3-kinase (PI3K)/Akt pathway [25–28]. Activated PI3K produces phosphatidylinositol (3,4,5)-trisphosphate (PIP3) at the plasma membrane and recruits Akt/PKB. Recruitment and activation of PI3K/Akt is Src-dependent, since the down-regulation of c-Src inhibits RANKL-mediated Akt activation [25]. Inhibition of PI3K reduces survival and proliferation of osteoclast precursor cells (due to attenuated NFATc1) [29]. PI3k has also been implicated in the formation of actin filament in osteoclasts [30]. Akt induces osteoclast differentiation by regulating glycogen synthase kinase-3 β (GSK3 β)/NFATc1 signaling cascade [31]. In the absence of RANKL, NFATc1 is phosphorylated by GSK3 β and remains outside of the nucleus. The leucine-rich repeat-containing G protein-coupled receptor 4 (LGR4) is a competitive receptor for RANKL. The LGR4/RANK complex activates GSK3-B. This suppresses NFATC1 and limits osteoclast differentiation [32]. Mice with LGR4 deficiency suffer from osteoporosis due to increased osteoclast activity [33–35]. RANK signaling inhibits GSK3 β by inducing phosphorylation at its inhibitory serine residue (Ser9). NFATc1 is then dephosphorylated by calcineurin, leading to its translocation into the nucleus [32]. Transgenic mice that overexpress GSK3 β develop osteopetrosis due to the lack of NFATc1 activation and absent functional osteoclasts [36]. Overexpression of Akt induces the phosphorylation and inactivation of GSK3 β , leading to NFATc1 activation and nuclear translocation [31]. M-CSF is also involved with activating Src signaling pathways [37]. M-CSF signaling recruits c-Src to activate PI3K and c-Cbl, eventually activating Akt and ERK signaling [38–41]. Similar to RANK-mediated activation of Akt, these steps promote osteoclast precursor proliferation and survival [42].

Osteoclast Precursor Commitment

The second stage is OCP commitment. In this stage, monocyte progenitors are activated through the binding of two key regulatory growth factors to their receptors: macrophage colony-stimulating factor (M-CSF) to colony-stimulating factor-1 receptor (CSF1R) and receptor activator of NF- κ B ligand (RANKL) to RANK. M-CSF and RANKL binding activates signaling cascades that queue early differentiation events and promote OCP commitment. When RANK is activated during RANKL binding, the RANK adaptor molecule TNF receptor-associated factor 6 (TRAF6) forms a complex with TGF- β -activated kinase-1 binding protein (TAB1) and TGF- β -activated kinase-1 (TAK1) to recruit SMAD3 [43]. NF- κ B translocates to the nucleus after the formation of the TRAF6-TAB1-TAK1-SMAD3 complex, which promotes the transcription of the master osteoclastogenesis transcription factor nuclear factor of activated T cells 1 (NFATc1) [44]. The roles of M-CSF, RANK/RANKL, and RANK's inhibitor osteoprotegerin (OPG) will be discussed in further detail later on in the chapter.

Osteoclast Precursor Motility and Fusion

The third stage of osteoclast differentiation is OCP motility and fusion. The main integrin involved in OCP and osteoclast motility is integrin $\alpha\text{v}\beta\text{3}$. Upon OCP $\alpha\text{v}\beta\text{3}$ substrate binding, spleen tyrosine kinase (SYK), a non-receptor tyrosine kinase, is directly phosphorylated by *c-Src* [45]. In *Syk*^{-/-} mice, OCPs have reduced adhesion and spreading and, importantly, fail to resorb bone [46]. Recently, NR4A1, an orphan member of the nuclear receptor superfamily, has been shown to be a crucial negative regulator of osteoclast precursor migration and recruitment. Myeloid-specific deletion of NR4A1 resulted in proliferation of osteoclasts with a hypermotile phenotype, while pharmacological activation of NR4A1 inhibited osteoclast migration and protected against osteoporosis in mice [47]. OCP motility is a requirement for preosteoclast fusion.

The merging of outer plasma membranes is a hallmark of OCP fusion, which eventually leads to multinucleated, functional osteoclasts. Macrophages themselves have the potential to fuse together with other macrophages to form multinucleated cells known as polykaryons, an innate immune response. However, macrophages must first become “fusion competent” to become multinucleated [48]. An essential facilitator of macrophage fusion is the signaling adaptor DNAX-activating protein 12 (DAP12). Mutations in DAP12 or TREM2 are associated with Nasu-Hakola disease, a disorder of the brain and bone, as both DAP12 and TREM2 are essential for macrophage fusion and formation of functional osteoclasts [48, 49]. When TREM2 binds to DAP12, SYK binding of TREM2 to DAP12 leads to the recruitment and activation of SYK, which results in signaling phosphoinositide 3-kinases (PI3Ks) activation in osteoclasts [48]. During inflammation, extracellular ATP and adenosine signals can be detected and transduced by purinergic P1 and P2 receptors, of which the P2RX7 receptor activated during inflammation as a “danger signal” and a common OCP fusion mediator. P2RX7 is involved in both inflammasome activation and cytokine release, and its overexpression has been shown to drive spontaneous fusion in macrophages, while antibody inhibition of P2RX7 suppresses macrophage multinucleation [50]. Because osteoclasts are involved in bone turnover, intuitively, modulation of calcium ions (Ca^{2+}) can also regulate RANKL-mediated signaling and drive OCP fusion through the potassium calcium-activated channel subfamily N member 4 (KCNN4) regulation of NFATc1.

MITF is required for the survival of osteoclast precursor cells [51–53], but also plays a role in mediating osteoclast fusion by inducing DC-STAMP expression. MITF is a unique transcription factor due to its tissue-restricted effects. The deletion of MITF affects specifically osteoclasts, melanocytes, retinal pigmented epithelium, and mast cells [54]. Osteoclasts express two major isoforms of MITF (MITF-A, MITF-E) [55, 56]. First, MITF is upregulated following M-CSF signaling. M-CSF induces the formation of MITF/PU.1 complex at the promoter regions of target genes including *Oscar*, *Acp5*, and *cathepsin K*, but not activating transcription [23, 57]. This is followed by RANK-mediated activation of MITF. RANK and TRAF6-mediated activation of MAPKs (p38) phosphorylate MITF (serine 307) and further

activate it [58–60]. This leads to the formation of NFATc1 transcriptional complex, comprised of AP-1, PU.1, and MITF. These transcription factors bind to the promoter regions of *cathepsin K*, *OCAR*, *TRAP*, and *CCL7* and promote transcription [51, 53]. MITF and NFATc1 share similar properties; both are dependent on RANKL-mediated activation, share overlapping transcription targets, and are both required for osteoclast fusion [60–63]. NFATc1 together with transcription factors, including c-Fos, MITF, and PU-1, mediate osteoclast fusion by inducing the expression of DC-STAMP, *Atp6v0d2*, and *Tks5* [62, 64, 65]. Synergistically with RANKL, tumor necrosis factor (TNF) is also involved in macrophage fusion and OCP multinucleation by activation of c-Jun N-terminal kinase (JNK) [66].

For the development of multinucleated osteoclasts, mononuclear osteoclast precursor cells are required to fuse together. Dendritic cell-specific transmembrane protein (DC-STAMP) and osteoclast stimulatory transmembrane protein (OC-STAMP) are required for osteoclast cell fusion and multinucleation [67]. Both are RANKL-induced transmembrane proteins with similar features. DC-STAMP is expressed as a dimer on the cell surface of both human and murine osteoclast precursor cells [68–70]. DC-STAMP-deficient mice exhibit moderate osteopetrosis, where TRAP-positive (tartrate-resistant acid phosphatase marker of differentiated osteoclasts) mononuclear osteoclast precursors do not fuse into functional osteoclasts [65, 71, 72]. Both DC-STAMP and OC-STAMP are required for osteoclastogenesis, since a deficiency in one cannot be compensated by the other [67]. The overexpression of DC-STAMP promotes maturation and function of multinucleated osteoclasts [42, 73, 74], but the ligand of DC-STAMP remains unknown [48]. Recently, RANKL was described to activate a tyrosine-based inhibitory motif (ITIM) on the cytoplasmic tail of DC-STAMP, mediating osteoclast differentiation via NFACTc1 [71]. Unlike DC-STAMP, OC-STAMP is only expressed by osteoclast lineage-committed cells [74, 75]. Downregulation or the inhibition of OC-STAMP significantly reduces the number of mature multinucleated osteoclasts, while overexpression significantly increases the number of mature osteoclasts [74, 75].

In addition to STAMP signaling, the Rho family of small GTPases reorganize the cytoskeleton (mainly actin) for cell fusion [59, 76]. Rho-related GTPases including Rac and Cdc41 both regulate cell shape, motility, and adherence by rearranging the actin cytoskeleton [76]. Following the formation of mature osteoclasts, the development of actin rings and resorption lacunae are regulated by Rac and Rho [77]. These GTPases also regulate cell differentiation in myoblasts and epithelium, where knockout of Rac1 leads to embryonic lethality [78]. Studies individually inhibiting Rac1 and Rac2 suggest that Rac1 is the primary regulator of osteoclastogenesis by regulating the actin cytoskeleton, cell migration, and ROS generation [79].

Osteoclast Functionality

The final stage of osteoclastogenesis is functional bone resorption. In this stage, the osteoclasts are activated and form a resorption lacuna. The group of genes responsible for functional bone resorption include *c-Src*, *CIC-7*, *Atp6i*, *cathepsin K*, and

LTBP3. These genes encode proteins that are necessary for transitioning multinucleated osteoclasts into functional, bone-resorbing osteoclasts. Mice deficient in these molecules have osteoclasts with limited bone-resorbing activity [80–85]. Following the attachment of mature osteoclasts to bone, osteoclasts become polarized multinucleated cells to accommodate the sealing zone and ruffled border [86, 87]. Osteoclasts attach and dock to bone via the sealing zones. The sealing zones are comprised of integrins and cytoskeletal and filamentous actin [42, 88]. The ruffled border secretes various hydrolytic enzymes and factors required for osteoclast resorption. The ruffled border is comprised of many folds, increasing the surface area required for bone dissolution and endocytosis of bone degraded remnants. Acidification of the lacunar compartment is necessary for bone resorption. The proton pump vacuolar ATPase (V-ATPase) couples ATP hydrolysis with proton transport across the ruffled border [89]. The V-ATPase pump works together with the chloride channel (CLC-7) to establish the acidification (~4.5) of resorptive lacunae and the extracellular space [90–93]. Decreases in pH dissolve the mineral phase to expose the organic phase for acidic proteases and phosphatases [94]. Intracellular acidification is also important for protein sorting, zymogen activation, and receptor-mediated endocytosis [95]. The V-ATPase proton pump consists of the peripheral V1 component and membrane-bound V0 component with 13 subunits [96, 97]. The V1 component is regulated by ATP hydrolysis, which drives the rotation of V0 domain and transfers protons across the membrane. In addition to ATP hydrolysis and proton transport, both the V1 and V0 components regulate V-ATPase function [98, 99]. Mutations that involve V-ATPase can lead to osteopetrosis. Deletions in the T-cell immune regulator 1 (*TCIRG1*) gene, which encodes the $\alpha 3$ subunit of V-ATPase, cause osteopetrosis [100]. Deficiencies in V-ATPase diminish extracellular acidification while maintaining intracellular lysosomal proton pump activity [100]. The *Atp6v0d2* is one of the more abundant isomers of V-ATPases active in osteoclasts and is imperative for extracellular acidification [101, 102]. The release of protons and chloride ions dissolves hydroxyapatite in resorption lacunae, while proteases including matrix metalloproteinases (MMP-9, MMP-14) and cathepsin K digest the bone matrix [103–105].

Both MMPs and cathepsins play different roles in terms of osteoclast-mediated bone resorption [106]. Cathepsin K is a cysteine protease with type I and II collagenase activity. Cathepsin K is the primary lysosomal collagenolytic proteinase in the resorbing zone. Cathepsin K-null mice and pycnodysostotic patients have osteoclasts incapable of resorbing bone, leading to the buildup of unmineralized collagen fibers [82, 107]. The unique properties of cathepsin K allow the cleavage of collagen triple helix at multiple sites [108]. Once the helix is uncoiled, proteinases with gelatinolytic properties are activated. Cathepsins are responsible for the solubilization of bone matrices, while MMPs initiate and cease the breakdown of organic matrix [81]. Studies show that cathepsin K and MMPs act serially, where MMP activity occurs before and after cathepsin K activation [109, 110]. Combination of in vivo knockout studies and clinical investigations of human disease identifies MMP-2, MMP-9, MMP-13, MMP-14, and MMP-16 necessary for normal skeletal development [111]. Both RANKL and vitamin D upregulate the production of MMP-9, which degrades only unmineralized matrix [108]. In addition to resorption,

MMP-9 is involved with osteoclast survival, chemotaxis, fusion, and activity [110, 112, 113]. Deletion of MMP-9 results in abnormalities associated with bone development and fracture repair rather than effects on bone resorption [114, 115]. MMP-2 is involved with osteoclastogenesis, since MMP-2 knockout mice had significantly reduced numbers of osteoclasts and deficits in osteoclast differentiation [116]. MMP-12 is characterized for its role in osteoclast-bone matrix interactions since it can cleave vitronectin, osteopontin, osteonectin, and bone sialoprotein [117]. Deletion of MMP-12 does not impair osteoclast function, suggesting the role of other overlapping MMPs for bone resorption [108, 117]. MMP-13 is not secreted by osteoclasts but secreted by osteoblasts or chondrocytes [118]. Nonetheless, MMP-13 is required in the subosteoclastic resorption compartment for initial osteoid solubilization by activating osteoclasts prior to bone adhesion [119]. MMP-14 is unique because it is located at the leading edge of motile osteoclasts or at the sealing zones of polarized osteoclasts [104, 120]. MMP-14 is important for regulating osteogenesis since it sheds RANKL from osteoblast membranes [121]. Lastly, tartrate-resistant acid phosphatase (TRAP), specifically TRAP5b, is an essential enzyme required for bone resorption. TRAPs are implicated directly in matrix degradation and released into the circulation following resorption [122].

The involvement of GTP-binding proteins is required to ensure appropriate targeting of transport vesicles to the ruffled border membrane [123]. Rab5c is involved with endosomal recycling, while Rab11b ensures intracellular recycling, turnover at the ruffled border, and osteoclast motility [42]. Both Rab7 and Rab9 which are identified in late endosomes of other cell types are also detected in the ruffled border. The ruffled border shares similar properties and function with late endosomal compartments [94, 124]. Many lysosomal proteins are also identified in the ruffled border, suggesting similar function or origin of transport vesicles in lysosomes.

Critical Pathways in Bone Resorption

M-CSF/RANK/RANKL/OPG

M-CSF (also known as CSF-1) plays a vital role in osteoclast proliferation and survival [125, 126]. M-CSF expressed by osteoblasts is required for progenitor cells to differentiate into osteoclasts; however, M-CSF is unable to complete the process alone [127]. M-CSF binds to its associated receptor (c-Fms), leading to the phosphorylation of tyrosine sites at its cytoplasmic tail. Phosphorylated c-Fms recruits and forms a complex with c-Src, a tyrosine kinase. This complex in turn recruits phosphatidylinositol 3-kinase (PI3K), an E3 ubiquitin ligase. The activation of these proteins triggers Akt and ERK pathways, leading to the proliferation and survival of osteoclast precursor cells [37, 39–41]. Mouse and rat models with point mutations

in the *csf1* gene and nonfunctional M-CSF lack osteoclasts and display phenotypes of osteopetrosis [20, 128]. In osteoclast precursor cells, M-CSF induces receptor activation of RANK expression to promote efficient response between the RANKL-RANK signaling [129].

RANKL (identified as OPGL, ODF, and TRANCE) binds to its associated receptor (RANK) on preosteoclasts. Transgenic mouse models with absent RANKL or RANK exhibit severe phenotypes of osteopetrosis, suggesting its indispensable role for osteoclastogenesis [130–136]. RANKL binding induces the trimerization of RANK, which then recruits adaptor molecules including TNF receptor-associated factors (TRAFs). The TRAF family of proteins is comprised of seven members (1, 2, 3, 4, 5, 6, 7) and facilitates signaling through the TNF family cytokines and pathogen-associated molecular patterns (PAMPs) [137–140]. TRAF2, TRAF5, and TRAF6 have positive effects on osteoclast differentiation, while TRAF3 demonstrates inhibitory effects [66, 141, 142]. TRAF knockout animal models identified TRAF6 as the main adaptor protein required for transducing RANK signaling for osteoclastogenesis. TRAF6 knockout mice suffer from osteopetrosis due to limited osteoclast differentiation and bone resorption [143, 144]. RANK binds to TRAF6 via three TRAF6-binding sites on its c-terminal cytoplasmic tail and induces trimerization of TRAF6 [28, 145, 146]. Hematopoietic precursor cells with mutations in RANK specifically for TRAF6-binding sites are unable to restore effective osteoclastogenesis [137, 147]. The formation of RANK/TRAF6 complex induces multiple downstream signaling pathways including the activation of transcription factors (nuclear factor kappa-light-chain-enhancer of activated B cells (NF- κ B) and activator protein-1 (AP-1)) (Fig. 18.2) [146]. Both transcription factors are activated by specific protein kinases including IKK kinases (IKK1/2) and JNK1, respectively [7]. The RANK-TRAF6 complex activates TGF- β -activated kinase 1 (TAK1), TAK-1-binding protein 1 (TAB1), and TAB2, leading to the downstream activation of the IKK complex and NF- κ B [148–150]. Activated TAK1 phosphorylates IKK which target I κ B for proteasomal degradation and releases NF- κ B from the inhibitory mechanisms of I κ B [151]. TAK1- or TAB2-deficient mice have greater bone mass and have fewer osteoclasts [152, 153].

While RANK/RANKL is known to regulate and activate the formation of osteoclasts from their precursors in bone remodeling, osteoprotegerin (OPG) protects excess resorption by binding to RANKL and preventing it from interacting with RANK [154]. The three structural domains for OPG influence biological activities including inhibition of osteoclastogenesis, interactions with other proteoglycans, and apoptosis [155]. Under inflammatory conditions, the ratio of RANKL to OPG increases resulting in increased osteoclastogenesis [156]. The RANKL/OPG ratio is a major determinant of bone mass [154, 157]. OPG-deficient mice resulted in not only osteoporosis but extensive valvular calcification. The dysfunctional equilibrium between the RANK/RANKL/OPG triad leads to pathologic conditions; therefore, novel therapeutic approaches are being researched to target these molecules [157].

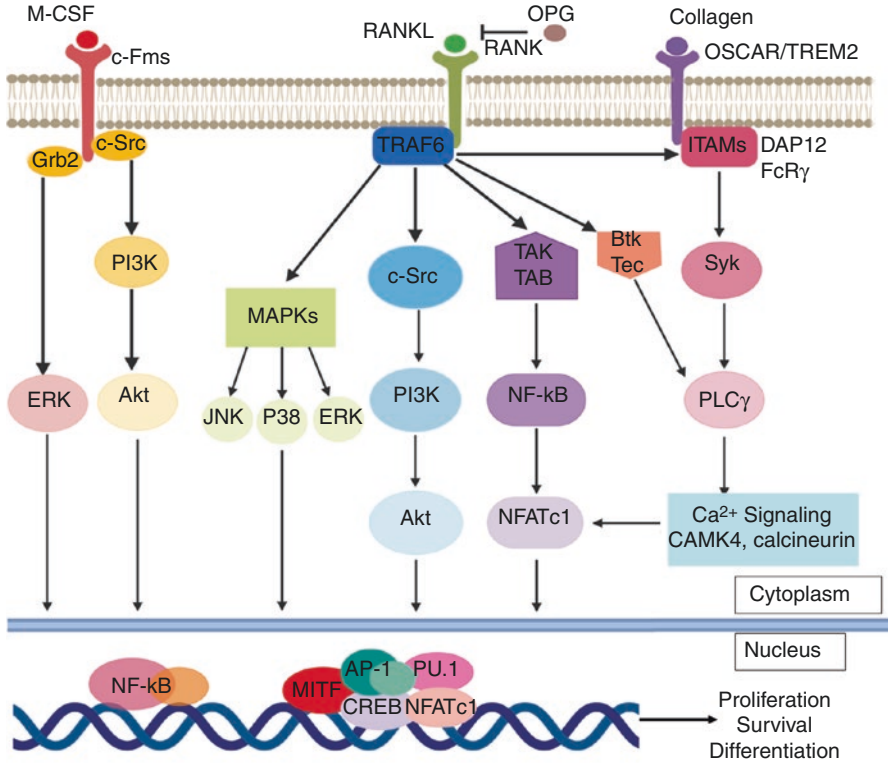


Fig. 18.2 Activated signaling pathways required for osteoclastogenesis. At the earlier stages of osteoclast differentiation, M-CSF binds to associated receptor (c-Fms) and activates Akt and ERK pathways. The transduction of these signals promotes the survival and proliferation of osteoclast precursor cells. This is followed by RANK/TRAF6-mediated activation of NF- κ B. This recruits transcription factors (MITF, CREB, AP-1, PU.1, and NFATc1) to the promoter regions of specific genes required for osteoclastogenesis. RANK also activates MAPKs and c-Src signaling pathways required for the transition of osteoclast precursor cells into mature osteoclasts. Stimulation of OSCAR and TREM2 further strengthens RANKL signaling. Induction of DAP12/FCR γ -Syk-PLC γ stimulates intracellular Ca²⁺ cycling and eventually the autoamplification of NFATc1. AP.1 activator protein, AKT Ser/Thr kinase, CREB cyclic adenosine monophosphate response element-binding protein 2, ERK extracellular signal-regulated kinases, FcR γ Fc receptor common γ subunit, MAPK, ITAM immunoreceptor tyrosine-based activation motif; mitogen-activated protein kinase, MITF microphthalmia transcription factor, PI3K, NFATc1 nuclear factor of activated T cells 1, OSCAR osteoclast-associated immunoglobulin-like receptor, OPG osteoprotegerin; phosphatidylinositol 3-kinases, PLC phospholipase C, RANKL receptor activator of nuclear factor κ B, RANKL, ligand, TAB transforming growth factor- β kinase 1 binding protein, TAK1 transforming growth factor- β kinase 1, TRAF TNF receptor-associated factors, TREM2 triggering receptor expressed on myeloid cells 1

Classical and Alternative NF- κ B Pathways in Osteogenesis

NF- κ B signaling is recognized as an earlier molecular signaling pathway induced by RANK and TRAF6 activation. NF- κ B is a family of dimeric transcription factors, which recognize the κ B DNA sequence. The NF- κ B superfamily is composed of five members, including p65 (RelA), RelB, c-Rel, NF- κ B1 (p50), and NF- κ B2 (p52 derived from p100 precursor) [23]. Both p50 and p52 heterodimerize with Rel proteins for subsequent activation [158, 159]. Mutagenesis of the p50/p52 domains of NF- κ B prevents osteoclast differentiation and results in osteopetrosis [148, 160, 161]. Typically, NF- κ B remains within the cytoplasm (inactive state) but is quickly translocated into the nucleus following RANK activation [23, 162, 163]. NF- κ B activation is dependent on two mechanisms referred to as the “classical” and “alternative” pathway. The classical method is mediated by a trimeric complex, comprised of the NF- κ B essential modulator (NEMO) and inhibitors of NF- κ B (IKK α , IKK β). This complex induces the phosphorylation and ubiquitin-mediated degradation of inhibitors of κ B (IkBs). This frees the P50/P65 dimer, which is translocated into the nucleus [151, 152, 158, 159]. The alternative (non-canonical) pathway involves NF- κ B-inducing kinase (NIK), which phosphorylates IKK α dimers. Induction of IKK α initiates cleavage of the p100/RelB complex. Following cleavage, the p52/RelB dimer translocates into the nucleus (Fig. 18.3) [23, 158, 159, 164, 165]. TRAF6 only activates the classical pathway, while both TRAF2 and TRAF5 can activate both the classical and alternative pathway [166]. The deletion of IKK α (necessary for alternative pathway) impairs *in vitro* but not *in vivo* osteoclastogenesis, while the deletion of IKK β (necessary for classical pathway) leads to osteopetrosis in both *in vitro* and *in vivo* studies [165]. Studies recognize classical pathway as a requirement for osteoclastogenesis, while the alternative pathway may not be as essential [23, 135].

c-Fos and AP-1-Associated Pathways

The activator protein 1 (AP-1) is another transcription factor complex required for osteoclastogenesis. RANK activates AP-1 through the induction of its critical component (c-Fos) [167–169]. Activated NF- κ B binds to target genes and upregulates the c-Fos component of AP-1 [7, 149]. The AP-1 transcription factor is a dimeric complex composed of Fos (c-Fos, FosB, Fra-1, Fra-2) and Jun (c-Jun, JunB, JunD) [168, 170]. Mice lacking c-Fos present with severe osteopetrosis and experience a complete block of osteoclast differentiation [149, 171, 172]. Following RANKL stimulation, *c-Fos*-deficient cells cannot activate NFATc1 required for osteoclastogenesis, while the overexpression of c-Fos binds to NFATc1 and upregulates osteoclast differentiation and function. c-Fos is recruited to the *NFATc1* promoter, 24 hours following RANKL stimulation, while induction of NFATc1 is absent in *c-Fos*-deficient cells [52, 169, 171, 173, 174]. ChIP experiments highlight the role

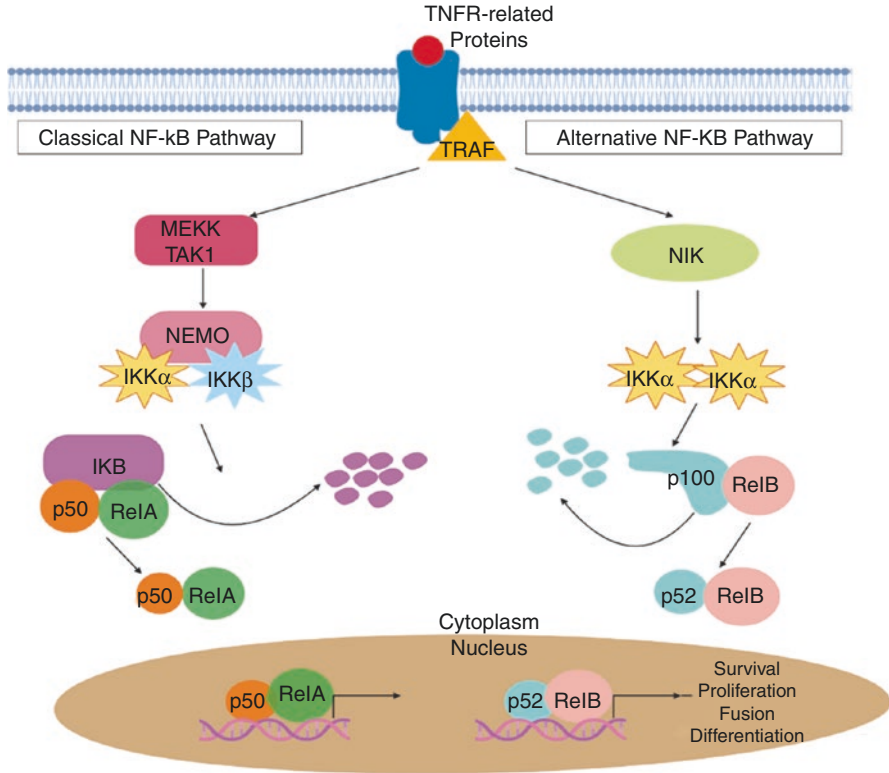


Fig. 18.3 Classical and alternative pathways of nuclear factor (NF-κB) activation in osteoclasts. Both the classical and alternative NF-κB pathways are stimulated by TNF receptor-related proteins (TNF-α, IL-1R). The classical pathway can be activated by B-cell and T-cell receptors as well. Downstream signaling forms the tri-complex, composed of NEMO, IKKα, and IKKβ. This complex phosphorylates IκB, leading to its degradation. P50 and RelA translocate into the nucleus and promote transcription of genes involved with osteoclastogenesis. The alternative pathway is activated by B-cell-activating factor receptor as well as CD40. This recruits NIK and activates IKKα. Phosphorylation of p100 results in the formation of p52 coupled with RelB. Both p52 and RelB translocate into the nucleus and activate transcription. Both pathways upregulate the expression of genes involved with osteoclast survival, proliferation, fusion, and differentiation. IKK inhibitor of NF-κB kinase, IκB inhibitors of NF-κB, MEKK mitogen-activated protein kinase kinase, NEMO NF-κB essential modulator, NIK NF-κB-inducing kinase

of AP-1 complex in the autoamplification of NFATc1 [52]. Exactly how c-Fos works with AP-1 proteins is unclear, but c-Fos in the AP-1 complex may have specific affinity to target genes required of osteoclastogenesis. Alternatively, c-Fos may facilitate AP-1 interactions with other specific transcriptional partners required for osteoclastogenesis [23]. In the context of AP-1, the Jun protein family are partners with the Fos family [175]. Mice deficient in either c-Jun or JunB are embryonically lethal, while osteoclastogenesis is not completely diminished in conditional knock-out models [168, 176].

Inflammatory Regulators of Osteoclastogenesis

Multiple studies have identified a connection between the immune and skeletal system. Multiple inflammatory stimuli affect various stages of osteoclast function. Correlation of abnormal osteoclast number and function with inflammatory diseases (rheumatoid arthritis, psoriatic arthritis, Crohn's, and celiac disease) led to the study of osteoimmunology [177, 178]. Multiple inflammatory cytokines stimulate or inhibit receptor-mediated intracellular signaling required for osteoclastogenesis. Primary osteoclastogenic cytokines include TNF- α , IL-1, IL-6, IL-7, IL-8, IL-11, IL-15, IL-17, IL-23, and IL-34 [6]. TNF- α is implicated in osteoclast differentiation, bone resorption, bone metabolism, and inflammatory bone diseases [9]. TNF- α mediates the formation of multinucleated osteoclasts in the presence of M-CSF or activates NF- κ B in the absence of RANKL [66, 179]. TNF- α can also induce RANK expression and propagate RANK signaling by activating TRAF2/5 and MAPKs to activate NF- κ B and AP-1 [66, 141, 180]. Patients with rheumatoid arthritis have increased osteoclasts and associated osteoclastogenic cytokines (IL-34), which are upregulated by TNF- α [181]. Inhibiting TNF- α with pharmacological inhibitors (infliximab) has successfully been used in patients [182].

IL-1b inflammatory cytokine is associated with osteoclast differentiation and bone resorption via RANKL signaling [183]. IL-1b indirectly stimulates TNF- α /RANK and initiates osteoclastogenesis. IL-1b stimulates p38 MAPK for osteoclast differentiation in conditions with adequate RANKL levels [184]. IL-1b also induces the expression of osteoclast proteins including TRAP, cathepsin K, MMP9, NFATc1, and MITF [185]. Inhibitors of IL-1b have successfully been used in patients with rheumatoid arthritis [186]. IL-6 stimulates the production of RANKL by osteoblasts and stromal cells [187]. IL-6 mutations inhibit osteoclast formation both in vivo and in vitro [188]. The secretion of IL-7 upregulates TNF- α , leading to increased RANKL levels and osteoclast formation [189, 190]. IL-8 is an autocrine regulator of osteoclastogenesis. RANKL signaling stimulates IL-8 secretion by osteoclasts, to further enhance RANKL-mediated osteoclastogenesis [191].

Inflammatory cytokines including IFN- α , IFN- β , and IFN- γ are characterized as anti-osteoclastogenic cytokines [9]. Both IFN- α and - β inhibit RANKL-induced osteoclastogenesis [192]. IFN- α inhibits the expression of c-Fos leading to decreased RANKL-induced osteoclastogenesis. IFN- α also activates Fas/FasL-mediated apoptosis in osteoclasts and inhibits TNF- α induced osteoclastogenesis [193]. The secretion of IFN- β negatively affects JAK1/STAT3/c-Fos signaling pathways [194]. IFN- β indirectly inhibits osteoclastogenesis by upregulating nitric oxide (NO) and NO synthase signaling [195]. IFN- γ is primarily secreted by natural killer cells, Th1 cells, and cytotoxic cells [9], which inhibits RANKL-mediated signaling [163]. In vitro studies revealed significant degradation and inactivation of TRAF6 following IFN- γ exposure [196]. Mice with deficient IFN- γ receptor have increased number of osteoclasts and bone loss (hyperactivity) [163]. Together with TLR signaling, IFN- γ downregulates RANK and c-Fms expression in osteoclast precursor cells [197]. Under some pathophysiological conditions, IFN- γ can enhance osteoclastogenesis, but the exact mechanisms are not well understood [198, 199].

MicroRNAs in Osteoclast Differentiation and Function

MicroRNA (miRNA; miR) is a short (21–27 base pairs) non-coding sequence of RNA assembled in a protein complex that posttranscriptionally regulates genes by binding to their target mRNA sequence and causing either mRNA cleavage, translation inhibition, or destabilization of the mRNA target sequence [200]. The differentiation and functionality of osteoclasts is orchestrated, in part, through miRNAs that can act as either positive or negative regulators of these processes [201]. While there are multiple miRNAs that participate in the regulation of osteoclastogenesis, a handful of positive and negative regulators will be discussed in this section.

Positive miRNA Regulators of Osteoclastogenesis

The most common models to study miRs involved in osteoclastogenesis and osteoclast function are murine. In a mouse model, the miR-29 family participates in early osteoclastogenesis, first by guiding the commitment of bone marrow precursors to osteoclast differentiation and next by facilitating in cellular motility through targeting Rho-GTPase Cdc42 and SLIT-ROBO GTPase-activating protein 2 (srgap2). Targeting srgap2 negatively regulates RAC1 and fine-tunes actin remodeling. Inhibition of miR-29 in mouse RAW264.7 cells leads to a decreased number of osteoclasts that lack motility [202]. Also during the early stages of osteoclastogenesis, three miRs from the same family, miR-99b/let-7e/125a, are significantly upregulated. They participate in OCP fusion, by fine-tuning thrombospondin transcription to facilitate the interaction with DC-STAMP, CD-47, and thrombospondin. In addition, miR-let-7e participates in osteoclast differentiation by targeting integrin $\alpha 4\beta 1$ [203]. While some miRNAs participate in osteoclast differentiation, motility, and fusion, others can prevent apoptosis. Upregulation of miR-21 promotes cellular survival through directly targeting the cell-surface death-receptor FAS-ligand (FASLG) present on OCPs, preosteoclasts, and mature osteoclasts in a murine model [204]. Other miRNAs influence the activity of mature osteoclasts through actin ring organization. Once osteoclasts are mature and adherent to the resorption area, miR-31 upregulation is thought to play a role in forming the sealing zone by organizing the actin ring formation through degradation of RhoA [205].

Some miRNAs have been discovered in osteoporosis models where increased osteoclastogenesis leads to decreased bone mineral density (BMD). miR-34c is involved in Notch signaling of osteoblasts, and in vivo, the upregulation of miR-34c has been associated with increased formation of osteoclasts leading to age-dependent osteoporosis [206]. While the role of osteoblasts in osteoclastogenesis has been well characterized in terms of the RANKL/OPG axis, the modulation that osteoclasts have on osteoblasts is less understood. Recently, elevated serum levels of exosomal-derived miR-214-3p have been shown to be linked with a reduction in bone formation in postmenopausal women and ovariectomized mice. This miRNA enhanced osteoclast formation and activity while inhibited osteoblast activity, suggesting that

osteoclasts can transfer miRNAs to osteoblasts through exosomes to inhibit bone formation [207]. Researchers have begun to postulate the miRNAs can be used as biomarkers for bone diseases. Additional miRNAs involved in bone metabolism that may serve as potential biomarkers or therapeutic targets are elegantly reviewed by Foessel et al. [208].

Negative miRNA Regulators of Osteoclastogenesis

In the early stages of osteoclast differentiation, expression of miR-124 in mouse bone marrow macrophages suppresses NFATc1, RhoA, and Rac1 expression to decrease OCP proliferation and motility [209]. Ectopic expression of three miRs, miR-133a, miR-141, and miR-219, also inhibits early stages of osteoclast differentiation by directly targeting *Mitf* [210]. During OCP motility and fusion stages, miR-7b upregulation leads to downregulation in DC-STAMP through NFATc1 and c-Fos signaling [211]. Alternatively, miR-26a can inhibit the osteoclast fusion protein DC-STAMP by targeting connective tissue growth factor (Ctgf). The degradation of Ctgf by miR-26a prevents DC-STAMP signaling [212]. Although miRs have been shown to modulate NFATc1 and other osteoclast-related gene expression patterns, the opposite is also possible in that osteoclast-associated genes like NFATc1 and NF- κ B can bind directly to the promoter regions of certain miRs to counterbalance osteoclastogenesis. For example, during early OCP commitment and differentiation, the binding of RANKL to RANK causes the recruitment of the adaptor protein TRAF6 as previously described. NFATc1 directly binds to the promoter region of miR-125a whose expression in human PBMCs downregulates TRAF6. Likewise, NF- κ B directly binds to the promoter of miR-146a [213]. In human PBMCs, miR-146a has been demonstrated to directly inhibit osteoclast formation, and in vivo overexpression in an osteoarthritic mouse model was shown to attenuate bone loss [214]. This data suggests there may be an underlying mechanism involved in both regular bone resorption and inflammatory disorders for osteoclasts to act as self-regulatory and may lead to potential therapeutic targets for osteoporosis. Finally, miRs can also negatively regulate osteoclast function through downregulation of proteases. miR-186 and miR-365 negatively regulate MMP-9 and cathepsin K, respectively, in murine models [215, 216].

The Calcification Paradox

Ectopic calcification found in the major blood vessels and cardiac valves was once considered a passive process, but is now regarded as a highly active, cell-mediated process [217]. Clinical studies have associated cardiovascular calcification with decreased bone mineral density (BMD). This conflicting association has been termed the “calcification paradox” [218]. Both osteoporosis and atherosclerosis

significantly increase morbidity and mortality [219–221]. Negative associations between BMD and cardiovascular calcification have been clinically demonstrated in the general population [219, 222], postmenopausal women [223–225], CKD patients [226], and those with progressive bone loss associated with Paget's disease, with the highest incidences occurring in CKD and osteoporosis [218]. These associations between decreased BMD and ectopic calcification have been found in the arteries as well as the heart valves [227]. The underlying mechanism driving the association between increased ectopic calcification and decreased BMD remains to be clarified and will be explored in this section.

There are two main types of calcification that can affect the blood vessels. The first type is intimal calcification, which is characterized by focal calcification within the atherosclerotic plaque milieu. The second type is media calcification and is characterized by arterial stiffening from diffuse calcification of the medial layer named Mönckeberg's sclerosis or arteriosclerosis which is associated with aging, type 2 diabetes, CKD, and osteoporosis [218]. While the mechanisms between vascular and valvular calcification may differ, it is worth noting that valvular calcification predominantly affects the leaflet fibrosa. Despite potential mechanistic differences, a similar negative correlation between BMD and calcific aortic valve disease (CAVD) has been observed [228].

Some studies have postulated that the negative correlation between BMD and ectopic calcification is a direct result of osteoporosis; i.e., that calcium lost in the bones is reallocated to the vessel walls and cardiac valves [227]. However, more recent studies have shed light on the disrupted signaling pathways in plaque-resident macrophages. While cardiovascular calcification follows a similar process to bone formation, inflammatory processes typically proceed or coincide with calcification [229]. These inflammatory processes cause an influx of monocyte-derived macrophages in the cardiac valves and atherosclerotic plaque. Why then do these macrophages fail to differentiate into functional bone-resorbing osteoclasts? And how can osteoclastogenesis be upregulated in the long bones in osteoporosis, but downregulated in the areas of ectopic calcification? While TRAP-positive, multinucleated osteoclast-like cells have been reported in human atheromata [230], these cells fail to resorb adjacent calcification. Simultaneously, these macrophages, along with SMCs, release calcifying extracellular vesicles that promote ossification. In fact, up to 13% of calcified lesions show true ectopic bone formation, even containing marrow elements, while the remainder is more similar to dystrophic calcification [231]. Perhaps, the unorganized nature of ectopic ossification leads to a decreased propensity for macrophages to become bone-resorbing osteoclasts; or, conversely, perhaps dystrophic calcification in general would have more favorable resorption kinetics, but the surrounding tissue milieu prevents osteoclastogenesis. It could be that the structure of ectopic mineralization impacts the potential for resorption; in fact, finite element analysis studies have suggested that while microcalcifications destabilize plaques, macrocalcification can help prevent plaque rupture [232]. Physiologically, it may be more advantageous to drive the formation of macrocalcification in the vasculature. Plaque rupture is deadly, and we must consider the potential compromise to the mechanical integrity of the vessel or valve during mineral resorption.

Understanding the kinetics around mineral resorption in the cardiovascular system is paramount before trying to resolve mineralization in humans. Key questions we must consider are as follows: Could the mineralization structure affect resorption potential? What happens to the remaining extracellular matrix components during resorption? And, importantly, could resorption compromise the biomechanical integrity of cardiovascular tissues?

In terms of the cardiovascular milieu, one potential mechanism preventing mineral resorption involves inflammatory signals within the sites of ectopic calcification acting as inhibitory signals to macrophage osteoclastogenesis. As described above interleukins (ILs) involved in inflammatory diseases have been shown to enhance osteoclastogenesis. However, in a recent study by Chinetti-Gbaguidi et al., researches have demonstrated increases in anti-inflammatory IL-4 near areas of calcification in atherosclerotic plaques. IL-4 leads to a reduction in NFATc1 transcription and results in osteoclast-like cells that have low calcification resorption potential due to impaired cathepsin K expression [233]. The results of that study indicate that plaque-resident macrophages surrounding areas of calcification are phenotypically defective from becoming functional osteoclasts. While pro-inflammatory signals enhance osteoclast differentiation and function, anti-inflammatory signals may have an opposing effect; therefore, macrophage heterogeneity may be an underpinning mechanism for the calcification paradox [234]. Alternatively, inorganic phosphate in ectopic calcification can prevent osteoclastogenesis and has been hypothesized to result in nonfunctional osteoclast-like cells [235]. Additionally, some clinical studies have demonstrated a link between aortic valve stenosis and circulating levels of osteoclastic inhibitor molecule OPG [236, 237]. The heterogeneity of macrophages and their response to pro- and anti-inflammatory stimuli may impact cardiovascular calcification via defective differentiation into osteoclast-like cells that are incapable of mineral resorption. Identifying disrupted signaling pathways in macrophages near areas of calcification may aid in the development of anti-calcification therapies and help solve the calcification paradox [234].

References

1. Wasilewski GB, Vervloet MG, Schurgers LJ. The bone—vasculature axis: calcium supplementation and the role of vitamin K. *Front Cardiovasc Med.* 2019;6(February):1–16. <https://doi.org/10.3389/fcvm.2019.00006>.
2. Hutcheson JD, Maldonado N, Aikawa E. Small entities with large impact: Microcalcifications and atherosclerotic plaque vulnerability. *Curr Opin Lipidol.* 2014;25(5):327–32. <https://doi.org/10.1097/MOL.000000000000105>.
3. Ahmed AKA, Finocchi V, Al-Agib S. Inferior vena cava calcification, a possible link with recurrent deep venous thrombosis and pulmonary embolism: a case study and review of literature. *BJR Case Reports.* 2018;4:20180018. <https://doi.org/10.1259/bjrcr.20180018>.
4. Benjamin E, Virani S, Callaway C, et al. American heart association 2018 statistics at glance. 2018. <https://healthmetrics.heart.org/wp-content/uploads/2018/02/At-A-Glance-Heart-Disease-and-Stroke-Statistics-2018.pdf>.

5. Sobiczewski W, Wirtwein M, Trybala E, Gruchala M. Severity of coronary atherosclerosis and stroke incidence in 7-year follow-up. *J Neurol*. 2013;260(7):1855–8. <https://doi.org/10.1007/s00415-013-6892-4>.
6. Amarasekara DS, Yun H, Kim S, Lee N, Kim H, Rho J. Regulation of Osteoclast Differentiation by Cytokine Networks. *Immune Netw*. 2018;18(1):e8. <https://doi.org/10.4110/in.2018.18.e8>.
7. Boyle WJ, Simonet WS, Lacey DL. Osteoclast differentiation and activation. *Nature*. 2003;423(6937):337–42. <https://doi.org/10.1038/nature01658>.
8. Takayanagi H. Osteoimmunology: shared mechanisms and crosstalk between the immune and bone systems. *Nat Rev Immunol*. 2007;7:292–304. <https://doi.org/10.1038/nri2062>.
9. Walsh MC, Kim N, Kadono Y, et al. OSTEOIMMUNOLOGY: Interplay Between the Immune System and Bone Metabolism. *Annu Rev Immunol*. 2006:33–63. <https://doi.org/10.1146/annurev.immunol.24.021605.090646>.
10. Kolliker A. Die Normale Resorption Des Knochengewebes Und Ihre Bedeutung Fur Die Entstehung Der Typischen Knochenformen. 1873.
11. Walker DG. Bone resorption restored in osteopetrotic mice by transplants of normal bone marrow and spleen cells. *Science*. 1975;190(4216):784–5. <https://doi.org/10.1126/science.1105786>.
12. Udagawa N, Takahashi N, Akatsu T, et al. Origin of osteoclasts: mature monocytes and macrophages are capable of differentiating into osteoclasts under a suitable microenvironment prepared by bone marrow-derived stromal cells. *Proc Natl Acad Sci*. 1990;87(18):7260–4. <https://doi.org/10.1073/pnas.87.18.7260>.
13. Jackson MF, Scatena M, Giachelli CM. Osteoclast precursors do not express CD68: results from CD68 promoter-driven RANK transgenic mice. *FEBS Lett*. 2017;591(5):728–36. <https://doi.org/10.1002/1873-3468.12588>.
14. McKercher SR, Torbett BE, Anderson KL, et al. Targeted disruption of the PU.1 gene results in multiple hematopoietic abnormalities. *EMBO J*. 1996;15:5647–58. <https://doi.org/10.1002/j.1460-2075.1996.tb00949.x>.
15. Dai XM, Ryan GR, Hapel AJ, et al. Targeted disruption of the mouse colony-stimulating factor 1 receptor gene results in osteopetrosis, mononuclear phagocyte deficiency, increased primitive progenitor cell frequencies, and reproductive defects. *Blood*. 2002;99:111–20. <https://doi.org/10.1182/blood.V99.1.111>.
16. Ross FP, Teitelbaum SL. $\alpha\text{v}\beta\text{3}$ and macrophage colony-stimulating factor: Partners in osteoclast biology. *Immunol Rev*. 2005. <https://doi.org/10.1111/j.0105-2896.2005.00331.x>.
17. Zhang DE, Hetherington CJ, Chen HM, Tenen DG. The macrophage transcription factor PU.1 directs tissue-specific expression of the macrophage colony-stimulating factor receptor. *Mol Cell Biol*. 1994. <https://doi.org/10.1128/mcb.14.1.373>.
18. Tondravi MM, McKercher SR, Anderson K, et al. Osteopetrosis in mice lacking haematopoietic transcription factor PU.1. *Nature*. 1997. <https://doi.org/10.1038/386081a0>.
19. Kimura K, Kitaura H, Fujii T, Ishida M, Hakami Z, Takano-Yamamoto T. An anti-c-Fms antibody inhibits osteoclastogenesis in a mouse periodontitis model. *Oral Dis*. 2014. <https://doi.org/10.1111/odi.12117>.
20. Felix R, Cecchini MG, Fleisch H. Macrophage colony stimulating factor restores in vivo bone resorption in the OP/OP osteopetrotic mouse. *Endocrinology*. 1990. <https://doi.org/10.1210/endo-127-5-2592>.
21. Weilbaecher KN, Motyckova G, Huber WE, et al. Linkage of M-CSF signaling to Mitf, TFE3, and the osteoclast defect in Mitfmi/mi mice. *Mol Cell*. 2001. [https://doi.org/10.1016/S1097-2765\(01\)00360-4](https://doi.org/10.1016/S1097-2765(01)00360-4).
22. McGill GG, Horstmann M, Widlund HR, et al. Bcl2 regulation by the melanocyte master regulator Mitf modulates lineage survival and melanoma cell viability. *Cell*. 2002. [https://doi.org/10.1016/S0092-8674\(02\)00762-6](https://doi.org/10.1016/S0092-8674(02)00762-6).
23. Asagiri M, Takayanagi H. The molecular understanding of osteoclast differentiation. *Bone*. 2007. <https://doi.org/10.1016/j.bone.2006.09.023>.

24. Hodgkinson CA, Moore KJ, Nakayama A, et al. Mutations at the mouse microphthalmia locus are associated with defects in a gene encoding a novel basic-helix-loop-helix-zipper protein. *Cell*. 1993. [https://doi.org/10.1016/0092-8674\(93\)90429-T](https://doi.org/10.1016/0092-8674(93)90429-T).
25. Wong BR, Besser D, Kim N, et al. TRANCE, a TNF family member, activates Akt/PKB through a signaling complex involving TRAF6 and c-Src. *Mol Cell*. 1999. [https://doi.org/10.1016/S1097-2765\(00\)80232-4](https://doi.org/10.1016/S1097-2765(00)80232-4).
26. Arron JR, Vologodskaja M, Wong BR, et al. A positive regulatory role for Cbl family proteins in tumor necrosis factor-related activation-induced cytokine (TRANCE) and CD40L-mediated Akt activation. *J Biol Chem*. 2001. <https://doi.org/10.1074/jbc.M100414200>.
27. Vanhaesebroeck B, Alessi DR. The PI3K-PKB1 connection: More than just a road to PKB. *Biochem J*. 2000. <https://doi.org/10.1042/0264-6021:3460561>.
28. Ye H, Arron JR, Lamothe B, et al. Distinct molecular mechanism for initiating TRAF6 signalling. *Nature*. 2002. <https://doi.org/10.1038/nature00888>.
29. Lee SE, Woo KM, Kim SY, et al. The phosphatidylinositol 3-Kinase, p38, and extracellular signal-regulated kinase pathways are involved in osteoclast differentiation. *Bone*. 2002. [https://doi.org/10.1016/S8756-3282\(01\)00657-3](https://doi.org/10.1016/S8756-3282(01)00657-3)
30. Chellaiah M, Fitzgerald C, Alvarez U, Hruska K. c-Src is required for stimulation of gelsolin-associated phosphatidylinositol 3-kinase. *J Biol Chem*. 1998. <https://doi.org/10.1074/jbc.273.19.11908>.
31. Moon JB, Kim JH, Kim K, et al. Akt Induces Osteoclast Differentiation through Regulating the GSK3 β /NFATc1 Signaling Cascade. *J Immunol*. 2012. <https://doi.org/10.4049/jimmunol.1101254>.
32. Park JH, Lee NK, Lee SY. Current understanding of RANK signaling in osteoclast differentiation and maturation. *Mol Cells*. 2017. <https://doi.org/10.14348/molcells.2017.0225>.
33. Jin Y, Yang Y. LGR4: A new receptor for a stronger bone. *Sci China Life Sci*. 2016. <https://doi.org/10.1007/s11427-016-5068-8>.
34. Luo J, Yang Z, Ma Y, et al. LGR4 is a receptor for RANKL and negatively regulates osteoclast differentiation and bone resorption. *Nat Med*. 2016. <https://doi.org/10.1038/nm.4076>.
35. Styrkarsdottir U, Thorleifsson G, Sulem P, et al. Nonsense mutation in the LGR4 gene is associated with several human diseases and other traits. *Nature*. 2013. <https://doi.org/10.1038/nature12124>.
36. Jang HD, Shin JH, Park DR, et al. Inactivation of glycogen synthase kinase-3 β is required for osteoclast differentiation. *J Biol Chem*. 2011. <https://doi.org/10.1074/jbc.M111.256768>.
37. Xiong Y, Song D, Cai Y, Yu W, Yeung YG, Stanley ER. A CSF-1 receptor phosphotyrosine 559 signaling pathway regulates receptor ubiquitination and tyrosine phosphorylation. *J Biol Chem*. 2011. <https://doi.org/10.1074/jbc.M110.166702>.
38. Lee AW-M, States DJ. Both Src-dependent and -independent mechanisms mediate phosphatidylinositol 3-kinase regulation of colony-stimulating factor 1-activated mitogen-activated protein kinases in myeloid progenitors. *Mol Cell Biol*. 2000;20(18):6779 LP-6798. <https://doi.org/10.1128/MCB.20.18.6779-6798.2000>.
39. Horne WC, Sanjay A, Bruzzaniti A, Baron R. The role(s) of Src kinase and Cbl proteins in the regulation of osteoclast differentiation and function. *Immunol Rev*. 2005. <https://doi.org/10.1111/j.0105-2896.2005.00335.x>.
40. Sanjay A, Houghton A, Neff L, et al. Cbl associates with Pyk2 and Src to regulate Src kinase activity, $\alpha\beta$ 3 integrin-mediated signaling, cell adhesion, and osteoclast motility. *J Cell Biol*. 2001. <https://doi.org/10.1083/jcb.152.1.181>
41. Yokouchi M, Kondo T, Sanjay A, et al. Src-catalyzed phosphorylation of c-Cbl Leads to the interdependent ubiquitination of both proteins. *J Biol Chem*. 2001. <https://doi.org/10.1074/jbc.M102219200>.
42. Plotkin LI, Bruzzaniti A. Chapter 6: Molecular signaling in bone cells: Regulation of cell differentiation and survival. In: Donev RBT-A in PC and SB, editor. *Intracellular signalling proteins*, vol. 116. Cambridge, MA: Academic Press; 2019. p. 237–81. <https://doi.org/10.1016/bs.apcsb.2019.01.002>.

43. Yasui T, Kadono Y, Nakamura M, et al. Regulation of RANKL-induced osteoclastogenesis by TGF- β through molecular interaction between Smad3 and Traf6. *J Bone Miner Res.* 2011;26(7):1447–56. <https://doi.org/10.1002/jbmr.357>.
44. Chen ZJ. Ubiquitin signalling in the NF- κ B pathway. *Nat Cell Biol.* 2005;7(8):1–9. <https://www.ncbi.nlm.nih.gov/pubmed/16056267>.
45. Novack DV, Faccio R. Osteoclast motility: Putting the brakes on bone resorption. *Ageing Res Rev.* 2011;10(1):54–61. <https://doi.org/10.1016/j.arr.2009.09.005>.
46. Faccio R, Novack DV, Zallone A, Ross FP, Teitelbaum SL. Dynamic changes in the osteoclast cytoskeleton in response to growth factors and cell attachment are controlled by β 3 integrin. *J Cell Biol.* 2003;162(3):499–509. <https://doi.org/10.1083/jcb.200212082>.
47. Scholtyssek C, Ipseiz N, Böhm C, et al. NR4A1 Regulates Motility of Osteoclast Precursors and Serves as Target for the Modulation of Systemic Bone Turnover. *J Bone Miner Res.* 2018;33(11):2035–47. <https://doi.org/10.1002/jbmr.3533>.
48. Pereira M, Petretto E, Gordon S, Bassett JHD, Williams GR, Behmoaras J. Common signaling pathways in macrophage and osteoclast multinucleation. *J Cell Sci.* 2018;131(11):1–11. <https://doi.org/10.1242/jcs.216267>.
49. Humphrey MB, Daws MR, Spusta SC, et al. TREM2, a DAP12-associated receptor, regulates osteoclast differentiation and function. *J Bone Miner Res.* 2006;21(2):237–45. <https://doi.org/10.1359/JBMR.051016>.
50. Di Virgilio F, Vuerich M. Purinergic signaling in the immune system. *Auton Neurosci Basic Clin.* 2015;191:117–23. <https://doi.org/10.1016/j.autneu.2015.04.011>.
51. Kim Y, Sato K, Asagiri M, Morita I, Soma K, Takayanagi H. Contribution of nuclear factor of activated T cells c1 to the transcriptional control of immunoreceptor osteoclast-associated receptor but not triggering receptor expressed by myeloid cells-2 during osteoclastogenesis. *J Biol Chem.* 2005. <https://doi.org/10.1074/jbc.M505820200>.
52. Asagiri M, Sato K, Usami T, et al. Autoamplification of NFATc1 expression determines its essential role in bone homeostasis. *J Exp Med.* 2005. <https://doi.org/10.1084/jem.20051150>.
53. Matsumoto M, Sudo T, Saito T, Osada H, Tsujimoto M. Involvement of p38 mitogen-activated protein kinase signaling pathway in osteoclastogenesis mediated by receptor activator of NF- κ B ligand (RANKL). *J Biol Chem.* 2000. <https://doi.org/10.1074/jbc.M001229200>.
54. Steingrímsson E, Moore KJ, Lamoreux ML, et al. Molecular basis of mouse microphthalmia (mi) mutations helps explain their developmental and phenotypic consequences. *Nat Genet.* 1994. <https://doi.org/10.1038/ng1194-256>.
55. Lu SY, Li M, Lin YL. Mitf regulates osteoclastogenesis by modulating NFATc1 activity. *Exp Cell Res.* 2014. <https://doi.org/10.1016/j.yexcr.2014.08.018>.
56. Lu SY, Li M, Lin YL. Mitf induction by RANKL is critical for osteoclastogenesis. *Mol Biol Cell.* 2010. <https://doi.org/10.1091/mbc.E09-07-0584>.
57. Feng HT, Cheng T, Steer JH, et al. Myocyte enhancer factor 2 and microphthalmia-associated transcription factor cooperate with NFATc1 to transactivate the V-ATPase d2 promoter during RANKL-induced osteoclastogenesis. *J Biol Chem.* 2009. <https://doi.org/10.1074/jbc.M901670200>.
58. Mansky KC, Sankar U, Han J, Ostrowski MC. Microphthalmia transcription factor is a target of the p38 MAPK pathway in response to receptor activator of NF- κ B ligand signaling. *J Biol Chem.* 2002. <https://doi.org/10.1074/jbc.M111696200>.
59. Vives V. Modulation of osteoclast differentiation and bone resorption by Rho GTPases. *Small GTPases.* 2014. <https://doi.org/10.4161/sgtp.28119>.
60. Sharma SM, Bronisz A, Hu R, et al. MITF and PU.1 recruit p38 MAPK and NFATc1 to target genes during osteoclast differentiation. *J Biol Chem.* 2007. <https://doi.org/10.1074/jbc.M609723200>.
61. So H, Rho J, Jeong D, et al. Microphthalmia transcription factor and PU.1 Synergistically induce the leukocyte receptor osteoclast-associated receptor gene expression. *J Biol Chem.* 2003. <https://doi.org/10.1074/jbc.M302940200>.

62. Kim K, Lee SH, Jung HK, Choi Y, Kim N. NFATc1 induces osteoclast fusion via up-regulation of Atp6v0d2 and the Dendritic Cell-Specific Transmembrane Protein (DC-STAMP). *Mol Endocrinol*. 2008. <https://doi.org/10.1210/me.2007-0237>.
63. Thesingh CW, Scherft JP. Fusion disability of embryonic osteoclast precursor cells and macrophages in the micropthalmic osteopetrotic mouse. *Bone*. 1985. [https://doi.org/10.1016/8756-3282\(85\)90406-5](https://doi.org/10.1016/8756-3282(85)90406-5).
64. Oikawa T, Oyama M, Kozuka-Hata H, et al. Tks5-dependent formation of circumferential podosomes/invadopodia mediates cell-cell fusion. *J Cell Biol*. 2012. <https://doi.org/10.1083/jcb.201111116>.
65. Yagi M, Ninomiya K, Fujita N, et al. Induction of DC-STAMP by alternative activation and downstream signaling mechanisms. *J Bone Miner Res*. 2007. <https://doi.org/10.1359/jbmr.070401>.
66. Kanazawa K, Kudo A. TRAF2 is essential for TNF- α -induced osteoclastogenesis. *J Bone Miner Res*. 2005. <https://doi.org/10.1359/JBMR.041225>.
67. Chiu YH, Ritchlin CT. DC-STAMP: a key regulator in osteoclast differentiation. *J Cell Physiol*. 2016. <https://doi.org/10.1002/jcp.25389>.
68. Kukita T, Wada N, Kukita A, et al. RANKL-induced DC-STAMP is essential for osteoclastogenesis. *J Exp Med*. 2004. <https://doi.org/10.1084/jem.20040518>.
69. Mensah KA, Grace Chiu Y, Xing L, Ritchlin C, Schwarz EM. The surface expression level of DC-STAMP defines the fusogenic potential of osteoclast precursors (OCP): RANKL-induced DC-STAMP^{lo} OCP are the master-fusogens. *Arthritis Rheum*. 2009. <https://acr.confex.com/acr/2009/webprogram/Paper10994.html>.
70. Miyamoto T. The dendritic cell-specific transmembrane protein DC-STAMP is essential for osteoclast fusion and osteoclast bone-resorbing activity. *Mod Rheumatol*. 2006; <https://doi.org/10.1007/s10165-006-0524-0>.
71. Chiu YH, Schwarz E, Li D, et al. Dendritic cell-specific transmembrane protein (DC-STAMP) regulates osteoclast differentiation via the Ca²⁺/NFATc1 Axis. *J Cell Physiol*. 2017. <https://doi.org/10.1002/jcp.25638>.
72. Yagi M, Miyamoto T, Sawatani Y, et al. DC-STAMP is essential for cell-cell fusion in osteoclasts and foreign body giant cells. *J Exp Med*. 2005. <https://doi.org/10.1084/jem.20050645>.
73. Vignery A. Macrophage fusion: The making of osteoclasts and giant cells. *J Exp Med*. 2005. <https://doi.org/10.1084/jem.20051123>.
74. Yang M, Birnbaum MJ, Mackay CA, Mason-Savas A, Thompson B, Odgren PR. Osteoclast stimulatory transmembrane protein (OC-STAMP), a novel protein induced by RANKL that promotes osteoclast differentiation. *J Cell Physiol*. 2008. <https://doi.org/10.1002/jcp.21331>.
75. Kim MH, Park M, Baek SH, Kim HJ, Kim SH. Molecules and signaling pathways involved in the expression of OC-STAMP during osteoclastogenesis. *Amino Acids*. 2011. <https://doi.org/10.1007/s00726-010-0755-4>.
76. Fenteany G, Glogauer M. Cytoskeletal remodeling in leukocyte function. *Curr Opin Hematol*. 2004. <https://doi.org/10.1097/00062752-200401000-00004>.
77. Razzouk S, Lieberherr M, Cournot G. Rac-GTPase, osteoclast cytoskeleton and bone resorption. *Eur J Cell Biol*. 1999. [https://doi.org/10.1016/S0171-9335\(99\)80058-2](https://doi.org/10.1016/S0171-9335(99)80058-2).
78. Lee KH, Lee SH, Kim D, et al. Promotion of skeletal muscle differentiation by K252a with tyrosine phosphorylation of focal adhesion: A possible involvement of small GTPase Rho. *Exp Cell Res*. 1999. <https://doi.org/10.1006/excr.1999.4648>.
79. Wang Y, Lebowitz D, Sun C, Thang H, Grynblas MD, Glogauer M. Identifying the relative contributions of Rac1 and Rac2 to osteoclastogenesis. *J Bone Miner Res*. 2008. <https://doi.org/10.1359/jbmr.071013>.
80. Lowe C, Yoneda T, Boyce BF, Chen H, Mundy GR, Soriano P. Osteopetrosis in Src-deficient mice is due to an autonomous defect of osteoclasts. *Proc Natl Acad Sci U S A*. 1993. <https://doi.org/10.1073/pnas.90.10.4485>.
81. Kiviranta R, Morko J, Alatalo SL, et al. Impaired bone resorption in cathepsin K-deficient mice is partially compensated for by enhanced osteoclastogenesis and increased expression

- of other proteases via an increased RANKL/OPG ratio. *Bone*. 2005. <https://doi.org/10.1016/j.bone.2004.09.020>.
82. Gowen M, Lazner F, Dodds R, et al. Cathepsin K knockout mice develop osteopetrosis due to a deficit in matrix degradation but not demineralization. *J Bone Miner Res*. 1999. <https://doi.org/10.1359/jbmr.1999.14.10.1654>.
 83. Frattini A, Orchard PJ, Sobacchi C, et al. Defects in TCIRG1 subunit of the vacuolar proton pump are responsible for a subset of human autosomal recessive osteopetrosis. *Nat Genet*. 2000; <https://doi.org/10.1038/77131>.
 84. Kornak U, Kasper D, Bösl MR, et al. Loss of the CIC-7 chloride channel leads to osteopetrosis in mice and man. *Cell*. 2001. [https://doi.org/10.1016/S0092-8674\(01\)00206-9](https://doi.org/10.1016/S0092-8674(01)00206-9).
 85. Dabovic B, Levasseur R, Zambuto L, Chen Y, Karsenty G, Rifkin DB. Osteopetrosis-like phenotype in latent TGF- β binding protein 3 deficient mice. *Bone*. 2005. <https://doi.org/10.1016/j.bone.2005.02.021>.
 86. Baron R, Neff L, Louvard D, Courtoy PJ. Cell-mediated extracellular acidification and bone resorption: Evidence for a low pH in resorbing lacunae and localization of a 100-kD lysosomal membrane protein at the osteoclast ruffled border. *J Cell Biol*. 1985. <https://doi.org/10.1083/jcb.101.6.2210>
 87. Väänänen HK, Zhao H, Mulari M, Halleen JM. The cell biology of osteoclast function. *J Cell Sci*. 2000;113:377–81.
 88. Helfrich MH, Nesbitt SA, Dorey EL, Horton MA. Rat osteoclasts adhere to a wide range of rgd (arg-gly-asp) peptide-containing proteins, including the bone sialoproteins and fibronectin, via a $\beta 3$ integrin. *J Bone Miner Res*. 1992. <https://doi.org/10.1002/jbmr.5650070314>.
 89. Väänänen HK, Karhukorpi EK, Sundquist K, et al. Evidence for the presence of a proton pump of the vacuolar H⁺-ATPase type in the ruffled borders of osteoclasts. *J Cell Biol*. 1990. <https://doi.org/10.1083/jcb.111.3.1305>.
 90. Feng S, Deng L, Chen W, Shao J, Xu G, Li YP. Atp6v1c1 is an essential component of the osteoclast proton pump and in F-actin ring formation in osteoclasts. *Biochem J*. 2009. <https://doi.org/10.1042/BJ20081073>.
 91. Lee SH, Rho J, Jeong D, et al. V-ATPase V0 subunit d2-deficient mice exhibit impaired osteoclast fusion and increased bone formation. *Nat Med*. 2006. <https://doi.org/10.1038/nm1514>.
 92. Scimeca JC, Franchi A, Trojani C, et al. The gene encoding the mouse homologue of the human osteoclast-specific 116-kDa V-ATPase subunit bears a deletion in osteosclerotic (oc/oc) mutants. *Bone*. 2000. [https://doi.org/10.1016/S8756-3282\(99\)00278-1](https://doi.org/10.1016/S8756-3282(99)00278-1).
 93. Kasper D, Planells-Cases R, Fuhrmann JC, et al. Loss of the chloride channel CIC-7 leads to lysosomal storage disease and neurodegeneration. *EMBO J*. 2005. <https://doi.org/10.1038/sj.emboj.7600576>.
 94. Lacombe J, Karsenty G, Ferron M. Regulation of lysosome biogenesis and functions in osteoclasts. *Cell Cycle*. 2013. <https://doi.org/10.4161/cc.25825>.
 95. Forgac M. Vacuolar ATPases: rotary proton pumps in physiology and pathophysiology. *Nat Rev Mol Cell Biol*. 2007. <https://doi.org/10.1038/nrm2272>.
 96. Duan X, Yang S, Zhang L, Yang T. V-ATPases and osteoclasts: ambiguous future of V-ATPases inhibitors in osteoporosis. *Theranostics*. 2018. <https://doi.org/10.7150/thno.28391>.
 97. Mazhab-Jafari MT, Rohou A, Schmidt C, et al. Atomic model for the membrane-embedded VO motor of a eukaryotic V-ATPase. *Nature*. 2016. <https://doi.org/10.1038/nature19828>.
 98. Nishi T, Forgac M. The vacuolar (H⁺)-ATPases — nature's most versatile proton pumps. *Nat Rev Mol Cell Biol*. 2002;3(2):94–103. <https://doi.org/10.1038/nrm729>.
 99. Jefferies KC, Cipriano DJ, Forgac M. Function, structure and regulation of the vacuolar (H⁺)-ATPases. *Arch Biochem Biophys*. 2008;476(1):33–42. <https://doi.org/10.1016/j.abb.2008.03.025>.
 100. Makaryan V, Rosenthal EA, Bolyard AA, et al. TCIRG1-Associated Congenital Neutropenia. *Hum Mutat*. 2014. <https://doi.org/10.1002/humu.22563>.
 101. Wu H, Xu G, Li YP. Atp6v0d2 is an essential component of the osteoclast-specific proton pump that mediates extracellular acidification in bone resorption. *J Bone Miner Res*. 2009. <https://doi.org/10.1359/jbmr.081239>.

102. Ayodele BA, Mirams M, Pagel CN, Mackie EJ. The vacuolar H⁺-ATPase V0subunit d2is associated with chondrocyte hypertrophy and supports chondrocyte differentiation. *Bone Reports*. 2017. <https://doi.org/10.1016/j.bonr.2017.08.002>
103. Kim K, Punj V, Kim JM, et al. MMP-9 facilitates selective proteolysis of the histone H3 tail at genes necessary for proficient osteoclastogenesis. *Genes Dev*. 2016. <https://doi.org/10.1101/gad.268714.115>.
104. Sato T, Ovejero MDC, Hou P, et al. Identification of the membrane-type matrix metalloproteinase MT1-MMP in osteoclasts. *J Cell Sci*. 1997.
105. Gelb BD, Shi G-P, Chapman HA, Desnick RJ. Pycnodysostosis, a Lysosomal disease caused by Cathepsin K deficiency. *Science*. 1996. <https://doi.org/10.1126/science.273.5279.1236>.
106. Delaissé JM, Andersen TL, Engsig MT, Henriksen K, Troen T, Blavier L. Matrix metalloproteinases (MMP) and cathepsin K contribute differently to osteoclastic activities. *Microsc Res Tech*. 2003. <https://doi.org/10.1002/jemt.10374>.
107. Saftig P, Hunziker E, Wehmeyer O, et al. Impaired osteoclastic bone resorption leads to osteopetrosis in cathepsin-K-deficient mice. *Proc Natl Acad Sci U S A*. 1998. <https://doi.org/10.1073/pnas.95.23.13453>.
108. Paiva KBS, Granjeiro JM. Matrix metalloproteinases in bone resorption, remodeling, and repair. In: *Progress in molecular biology and translational science*. 2017. <https://doi.org/10.1016/bs.pmbts.2017.05.001>.
109. Everts V, Delaissé J-M, Korper W, Niehof A, Vaes G, Beertsen W. Degradation of collagen in the bone-resorbing compartment underlying the osteoclast involves both cysteine-proteinases and matrix metalloproteinases. *J Cell Physiol*. 1992. <https://doi.org/10.1002/jcp.1041500202>.
110. Everts V, Delaissé JM, Korper W, Beertsen W. Cysteine proteinases and matrix metalloproteinases play distinct roles in the subosteoclastic resorption zone. *J Bone Miner Res*. 1998. <https://doi.org/10.1359/jbmr.1998.13.9.1420>.
111. Liang HPH, Xu J, Xue M, Jackson C. Matrix metalloproteinases in bone development and pathology: current knowledge and potential clinical utility. *Met Med*. 2016. <https://doi.org/10.2147/mmm.s92187>.
112. Kusano K, Miyaura C, Inada M, et al. Regulation of matrix metalloproteinases (MMP-2,-3,-9, and -13) by interleukin-1 and interleukin-6 in mouse calvaria: Association of MMP induction with bone resorption. *Endocrinology*. 1998. <https://doi.org/10.1210/endo.139.3.5818>.
113. Blavier L, Delaissé JM. Matrix metalloproteinases are obligatory for the migration of preosteoclasts to the developing marrow cavity of primitive long bones. *J Cell Sci*. 1995;108(Pt 12): 3649–59.
114. Colnot C, Thompson Z, Miclau T, Werb Z, Helms JA. Altered fracture repair in the absence of MMP9. *Development*. 2003. <https://doi.org/10.1242/dev.00559>.
115. Hill PA, Murphy G, Docherty AJP, et al. The effects of selective inhibitors of matrix metalloproteinases (MMPs) on bone resorption and the identification of MMPs and TIMP-1 in isolated osteoclasts. *J Cell Sci*. 1994;107(Pt 11):3055–64.
116. Mosig RA, Dowling O, DiFeo A, et al. Loss of MMP-2 disrupts skeletal and craniofacial development and results in decreased bone mineralization, joint erosion and defects in osteoblast and osteoclast growth. *Hum Mol Genet*. 2007. <https://doi.org/10.1093/hmg/ddm060>.
117. Hou P, Troen T, Ovejero MC, et al. Matrix metalloproteinase-12 (MMP-12) in osteoclasts: New lesson on the involvement of MMPs in bone resorption. *Bone*. 2004. <https://doi.org/10.1016/j.bone.2003.08.011>.
118. Johansson N, Saarialho-Kere U, Airola K, et al. Collagenase-3 (MMP-13) is expressed by hypertrophic chondrocytes, periosteal cells, and osteoblasts during human fetal bone development. *Dev Dyn*. 1997. [https://doi.org/10.1002/\(SICI\)1097-0177\(199703\)208:3<387::AID-AJA9>3.0.CO;2-E](https://doi.org/10.1002/(SICI)1097-0177(199703)208:3<387::AID-AJA9>3.0.CO;2-E).
119. Yamagiwa H, Tokunaga K, Hayami T, et al. Expression of metalloproteinase-13 (collagenase-3) is induced during fracture healing in mice. *Bone*. 1999. [https://doi.org/10.1016/S8756-3282\(99\)00157-X](https://doi.org/10.1016/S8756-3282(99)00157-X).
120. Irie K, Tsuruga E, Sakakura Y, Muto T, Yajima T. Immunohistochemical localization of membrane type 1-matrix metalloproteinase (MT1-MMP) in osteoclasts in vivo. *Tissue Cell*. 2001; <https://doi.org/10.1054/tice.2001.0201>.

121. Hikita A, Yana I, Wakeyama H, et al. Negative regulation of osteoclastogenesis by ectodomain shedding of receptor activator of NF- κ B ligand. *J Biol Chem*. 2006; <https://doi.org/10.1074/jbc.M606656200>.
122. Shaw N, Högl W. Biochemical markers of bone metabolism. In: *Pediatric Bone*. 2012. <https://doi.org/10.1016/B978-0-12-382040-2.10015-2>.
123. Itzstein C, Coxon FP, Rogers MJ. The regulation of osteoclast function and bone resorption by small GTPases. *Small GTPases*. 2011;2:117–30.
124. Ferron M, Settembre C, Shimazu J, et al. A RANKL-PKC β -TFEB signaling cascade is necessary for lysosomal biogenesis in osteoclasts. *Genes Dev*. 2013. <https://doi.org/10.1101/gad.213827.113>.
125. Wiktor-Jedrzejczak W, Bartocci A, Ferrante AW, et al. Total absence of colony-stimulating factor 1 in the macrophage-deficient osteopetrotic (op/op) mouse. *Proc Natl Acad Sci U S A*. 1990. <https://doi.org/10.1073/pnas.87.12.4828>.
126. Yoshida H, Hayashi SI, Kunisada T, et al. The murine mutation osteopetrosis is in the coding region of the macrophage colony stimulating factor gene. *Nature*. 1990. <https://doi.org/10.1038/345442a0>
127. Boyce BF, Xing L. Biology of RANK, RANKL, and osteoprotegerin. *Arthritis Res Ther*. 2007;9(SUPPL.1):1–7. <https://doi.org/10.1186/ar2165>.
128. Marks SC, Wojtowicz A, Szperl M, et al. Administration of colony stimulating factor-1 corrects some macrophage, dental, and skeletal defects in an osteopetrotic mutation (toothless, tl) in the rat. *Bone*. 1992. [https://doi.org/10.1016/8756-3282\(92\)90365-4](https://doi.org/10.1016/8756-3282(92)90365-4).
129. Kim JH, Kim N. Regulation of NFATc1 in osteoclast differentiation. *J Bone Metab*. 2014;21(4):233. <https://doi.org/10.11005/jbm.2014.21.4.233>.
130. Hanada R, Hanada T, Sigl V, Schramek D, Penninger JM. RANKL/RANK-beyond bones. *J Mol Med*. 2011. <https://doi.org/10.1007/s00109-011-0749-z>.
131. Jones DH, Kong YY, Penninger JM. Role of RANKL and RANK in bone loss and arthritis. *Ann Rheum Dis*. 2002;61:ii32–9.
132. Sobacchi C, Schulz A, Coxon FP, Villa A, Helfrich MH. Osteopetrosis: Genetics, treatment and new insights into osteoclast function. *Nat Rev Endocrinol*. 2013. <https://doi.org/10.1038/nrendo.2013.137>.
133. Odgren PR, Kim N, MacKay CA, Mason-Savas A, Choi Y, Marks SC. The role of RANKL (TRANCE/TNFSF11), a tumor necrosis factor family member, in skeletal development: Effects of gene knockout and transgenic rescue. *Connect Tissue Res*. 2003;44(Suppl 1): 264–71.
134. Walsh MC, Choi Y. Biology of the TRANCE axis. *Cytokine Growth Factor Rev*. 2003. [https://doi.org/10.1016/S1359-6101\(03\)00027-3](https://doi.org/10.1016/S1359-6101(03)00027-3).
135. Kong YY, Yoshida H, Sarosi I, et al. OPGL is a key regulator of osteoclastogenesis, lymphocyte development and lymph-node organogenesis. *Nature*. 1999. <https://doi.org/10.1038/16852>
136. Theill LE, Boyle WJ, Penninger JM. RANK-L AND RANK: T cells, bone loss, and mammalian evolution. *Annu Rev Immunol*. 2002. <https://doi.org/10.1146/annurev.immunol.20.100301.064753>.
137. Armstrong AP, Tometsko ME, Glaccum M, Sutherland CL, Cosman D, Dougall WC. A RANK/TRAF6-dependent signal transduction pathway is essential for osteoclast cytoskeletal organization and resorptive function. *J Biol Chem*. 2002. <https://doi.org/10.1074/jbc.M202009200>.
138. Bouwmeester T, Bauch A, Ruffner H, et al. A physical and functional map of the human TNF- α /NF- κ B signal transduction pathway. *Nat Cell Biol*. 2004. <https://doi.org/10.1038/ncb1086>
139. Bradley JR, Pober JS. Tumor necrosis factor receptor-associated factors (TRAFs). *Oncogene*. 2001. <https://doi.org/10.1038/sj.onc.1204788>.
140. Inoue J Ichiro, Ishida T, Tsukamoto N, et al. Tumor necrosis factor receptor-associated factor (TRAF) family: Adapter proteins that mediate cytokine signaling. *Exp Cell Res*. 2000. <https://doi.org/10.1006/excr.1999.4733>.

141. Kanazawa K, Azuma Y, Nakano H, Kudo A. TRAF5 functions in both RANKL- and TNF α -induced osteoclastogenesis. *J Bone Miner Res.* 2003. <https://doi.org/10.1359/jbmr.2003.18.3.443>.
142. Hauer J, Püschner S, Ramakrishnan P, et al. TNF receptor (TNFR)-associated factor (TRAF) 3 serves as an inhibitor of TRAF2/5-mediated activation of the noncanonical NF- κ B pathway by TRAF-binding TNFRs. *Proc Natl Acad Sci U S A.* 2005. <https://doi.org/10.1073/pnas.0500187102>.
143. Lomaga MA, Yeh WC, Sarosi I, et al. TRAF6 deficiency results in osteopetrosis and defective interleukin-1, CD40, and LPS signaling. *Genes Dev.* 1999. <https://doi.org/10.1101/gad.13.8.1015>.
144. Naito A, Azuma S, Tanaka S, et al. Severe osteopetrosis, defective interleukin-1 signalling and lymph node organogenesis in TRAF6-deficient mice. *Genes to Cells.* 1999. <https://doi.org/10.1046/j.1365-2443.1999.00265.x>.
145. Kadono Y, Okada F, Perchonock C, et al. Strength of TRAF6 signalling determines osteoclastogenesis. *EMBO Rep.* 2005. <https://doi.org/10.1038/sj.embor.7400345>.
146. Wong BR, Josien R, Lee SY, Vologodskaia M, Steinman RM, Choi Y. The TRAF family of signal transducers mediates NF- κ B activation by the TRANCE receptor. *J Biol Chem.* 1998. <https://doi.org/10.1074/jbc.273.43.28355>.
147. Kobayashi N, Kadono Y, Naito A, et al. Segregation of TRAF6-mediated signaling pathways clarifies its role in osteoclastogenesis. *EMBO J.* 2001. <https://doi.org/10.1093/emboj/20.6.1271>.
148. Xing L, Bushnell TP, Carlson L, et al. NF- κ B p50 and p52 Expression Is Not Required for RANK-Expressing Osteoclast Progenitor Formation but Is Essential for RANK- and Cytokine-Mediated Osteoclastogenesis. *J Bone Miner Res.* 2002. <https://doi.org/10.1359/jbmr.2002.17.7.1200>.
149. Grigoriadis AE, Wang ZQ, Cecchini MG, et al. c-Fos: A key regulator of osteoclast-macrophage lineage determination and bone remodeling. *Science.* 1994. <https://doi.org/10.1126/science.7939685>.
150. Mizukami J, Takaesu G, Akatsuka H, et al. Receptor Activator of NF- B Ligand (RANKL) Activates TAK1 Mitogen-Activated Protein Kinase Kinase through a Signaling Complex Containing RANK, TAB2, and TRAF6. *Mol Cell Biol.* 2002. <https://doi.org/10.1128/mcb.22.4.992-1000.2002>.
151. Wang C, Deng L, Hong M, Akkaraju GR, Inoue JI, Chen ZJ. TAK1 is a ubiquitin-dependent kinase of MKK and IKK. *Nature.* 2001. <https://doi.org/10.1038/35085597>.
152. Lamothe B, Lai Y, Xie M, Schneider MD, Darnay BG. TAK1 Is essential for osteoclast differentiation and is an important modulator of cell death by apoptosis and necroptosis. *Mol Cell Biol.* 2013. <https://doi.org/10.1128/mcb.01225-12>.
153. Yamamoto A, Miyazaki T, Kadono Y, et al. Possible involvement of I κ B kinase 2 and MKK7 in osteoclastogenesis induced by receptor activator of nuclear factor κ B ligand. *J Bone Miner Res.* 2002. <https://doi.org/10.1359/jbmr.2002.17.4.612>.
154. Boyce BF, Xing L. The RANKL/RANK/OPG Pathway. *Curr Osteoporos Rep.* 2007;5:98–104. <https://doi.org/10.1007/s11914-007-0024-y>.
155. Yamaguchi K, Kinoshita M, Goto M, et al. Characterization of structural domains of human osteoclastogenesis inhibitory factor. *J Biol Chem.* 1998;273(9):5117–23. <https://doi.org/10.1074/jbc.273.9.5117>.
156. Roodman GD. Osteoclast differentiation. *Crit Rev Oral Biol Med.* 1991;2(3):389–409. <https://doi.org/10.1177/10454411910020030601>.
157. Theoleyre S, Wittrant Y, Kwan Tat S, Fortun Y, Redini F, Heymann D. The molecular triad OPG/RANK/RANKL: involvement in the orchestration of pathophysiological bone remodeling. <https://doi.org/10.1016/j.cytogfr.2004.06.004>.
158. Ghosh S, Karin M. Missing pieces in the NF- κ B puzzle. *Cell.* 2002. [https://doi.org/10.1016/S0092-8674\(02\)00703-1](https://doi.org/10.1016/S0092-8674(02)00703-1).
159. Hayden MS, Ghosh S. Shared Principles in NF- κ B Signaling. *Cell.* 2008. <https://doi.org/10.1016/j.cell.2008.01.020>.

160. Iotsova V, Caamaño J, Loy J, Yang Y, Lewin A, Bravo R. Osteopetrosis in mice lacking NF- κ B1 and NF- κ B2. *Nat Med*. 1997. <https://doi.org/10.1038/nm1197-1285>.
161. Franzoso G, Carlson L, Xing L, et al. Requirement for NF- κ B in osteoclast and B-cell development. *Genes Dev*. 1997. <https://doi.org/10.1101/gad.11.24.3482>.
162. Anderson DM, Maraskovsky E, Billingsley WL, et al. A homologue of the TNF receptor and its ligand enhance T-cell growth and dendritic-cell function. *Nature*. 1997. <https://doi.org/10.1038/36593>.
163. Takayanagi H, Ogasawara K, Hida S, et al. T-cell-mediated regulation of osteoclastogenesis by signalling cross-talk between RANKL and IFN- γ . *Nature*. 2000. <https://doi.org/10.1038/1038/35046102>.
164. Novack DV, Yin L, Hagen-Stapleton A, et al. The I κ B function of NF- κ B2 p100 controls stimulated osteoclastogenesis. *J Exp Med*. 2003. <https://doi.org/10.1084/jem.20030116>.
165. Ruocco MG, Maeda S, Park JM, et al. I κ B kinase (IKK) β , but not IKK α , is a critical mediator of osteoclast survival and is required for inflammation-induced bone loss. *J Exp Med*. 2005. <https://doi.org/10.1084/jem.20042081>.
166. Boyce BF, Xiu Y, Li J, Xing L, Yao Z. NF- κ B-mediated regulation of osteoclastogenesis. *Endocrinol Metab*. 2015. <https://doi.org/10.3803/EnM.2015.30.1.35>.
167. Wagner EF. Functions of AP1 (Fos/Jun) in bone development. In: *Annals of the Rheumatic Diseases*. 2002.
168. Wagner EF, Eferl R. Fos/AP-1 proteins in bone and the immune system. *Immunol Rev*. 2005. <https://doi.org/10.1111/j.0105-2896.2005.00332.x>.
169. Takayanagi H, Kim S, Koga T, et al. Induction and activation of the transcription factor NFATc1 (NFAT2) integrate RANKL signaling in terminal differentiation of osteoclasts. *Dev Cell*. 2002. [https://doi.org/10.1016/S1534-5807\(02\)00369-6](https://doi.org/10.1016/S1534-5807(02)00369-6).
170. Eferl R, Wagner EF. AP-1: A double-edged sword in tumorigenesis. *Nat Rev Cancer*. 2003. <https://doi.org/10.1038/nrc1209>.
171. Wang ZQ, Ovitt C, Grigoriadis AE, Möhle-Steinlein U, Rütther U, Wagner EF. Bone and haematopoietic defects in mice lacking c-fos. *Nature*. 1992; <https://doi.org/10.1038/360741a0>.
172. Johnson RS, Spiegelman BM, Papaioannou V. Pleiotropic effects of a null mutation in the c-fos proto-oncogene. *Cell*. 1992. [https://doi.org/10.1016/0092-8674\(92\)90592-Z](https://doi.org/10.1016/0092-8674(92)90592-Z).
173. Ikeda F, Nishimura R, Matsubara T, et al. Critical roles of c-Jun signaling in regulation of NFAT family and RANKL-regulated osteoclast differentiation. *J Clin Invest*. 2004. <https://doi.org/10.1172/JCI200419657>.
174. Matsuo K, Galson DL, Zhao C, et al. Nuclear factor of activated T-cells (NFAT) rescues osteoclastogenesis in precursors lacking c-Fos. *J Biol Chem*. 2004. <https://doi.org/10.1074/jbc.M313973200>.
175. David JP, Sabapathy K, Hoffman O, Idarraga MH, Wagner EF. JNK1 modulates osteoclastogenesis through both c-Jun phosphorylation-dependent and -independent mechanisms. *J Cell Sci*. 2002. <https://doi.org/10.1242/jcs.00082>.
176. Kenner L, Hoebertz A, Beil T, et al. Mice lacking JunB are osteopenic due to cell-autonomous osteoblast and osteoclast defects. *J Cell Biol*. 2004. <https://doi.org/10.1083/jcb.200308155>.
177. Arron JR, Choi Y. Bone versus immune system. *Nature*. 2000; <https://doi.org/10.1038/35046196>.
178. Danks L, Takayanagi H. Immunology and bone. *J Biochem*. 2013. <https://doi.org/10.1093/jb/mvt049>.
179. Komine M, Kukita A, Kukita T, Ogata Y, Hotokebuchi T, Kohashi O. Tumor necrosis factor- α cooperates with receptor activator of nuclear factor κ B ligand in generation of osteoclasts in stromal cell-depleted rat bone marrow cell culture. *Bone*. 2001. [https://doi.org/10.1016/S8756-3282\(01\)00420-3](https://doi.org/10.1016/S8756-3282(01)00420-3).
180. Zhang YH, Heulsmann A, Tondravi MM, Mukherjee A, Abu-Amer Y. Tumor necrosis factor- α (TNF) stimulates RANKL-induced osteoclastogenesis via coupling of TNF type 1 receptor and RANK signaling pathways. *J Biol Chem*. 2001. <https://doi.org/10.1074/jbc.M008198200>.

181. Hwang SJ, Choi B, Kang SS, et al. Interleukin-34 produced by human fibroblast-like synovial cells in rheumatoid arthritis supports osteoclastogenesis. *Arthritis Res Ther*. 2012. <https://doi.org/10.1186/ar3693>.
182. Corrado A, Neve A, Maruotti N, Cantatore FP. Bone effects of biologic drugs in rheumatoid arthritis. *Clin Dev Immunol*. 2013. <https://doi.org/10.1155/2013/945945>.
183. Ruscitti P, Cipriani P, Carubbi F, et al. The role of IL-1 β in the bone loss during rheumatic diseases. *Mediators Inflamm*. 2015. <https://doi.org/10.1155/2015/782382>.
184. Wei S, Kitaura H, Zhou P, Patrick Ross F, Teitelbaum SL. IL-1 mediates TNF-induced osteoclastogenesis. *J Clin Invest*. 2005. <https://doi.org/10.1172/JCI200523394>.
185. Jules J, Zhang P, Ashley JW, et al. Molecular basis of requirement of receptor activator of nuclear factor κ B signaling for interleukin 1-mediated osteoclastogenesis. *J Biol Chem*. 2012. <https://doi.org/10.1074/jbc.M111.296228>.
186. Dinarello CA, Simon A, Van Der Meer JWM. Treating inflammation by blocking interleukin-1 in a broad spectrum of diseases. *Nat Rev Drug Discov*. 2012. <https://doi.org/10.1038/nrd3800>.
187. Yoshitake F, Itoh S, Narita H, Ishihara K, Ebisu S. Interleukin-6 directly inhibits osteoclast differentiation by suppressing receptor activator of NF- κ B signaling pathways. *J Biol Chem*. 2008. <https://doi.org/10.1074/jbc.M607999200>.
188. Axmann R, Böhm C, Krönke G, Zwerina J, Smolen J, Schett G. Inhibition of interleukin-6 receptor directly blocks osteoclast formation in vitro and in vivo. *Arthritis Rheum*. 2009. <https://doi.org/10.1002/art.24781>.
189. Roato I, Brunetti G, Gorassini E, et al. IL-7 up-regulates TNF- α -dependent osteoclastogenesis in patients affected by solid tumor. *PLoS One*. 2006. <https://doi.org/10.1371/journal.pone.0000124>.
190. Weitzmann MN, Cenci S, Rifas L, Brown C, Pacifici R. Interleukin-7 stimulates osteoclast formation by up-regulating the T-cell production of soluble osteoclastogenic cytokines. *Blood*. 2000;96(5):1873–8.
191. Kopesky P, Tiedemann K, Alkhekhia D, et al. Autocrine signaling is a key regulatory element during osteoclastogenesis. *Biol Open*. 2014. <https://doi.org/10.1242/bio.20148128>.
192. Xiong Q, Zhang L, Ge W, Tang P. The roles of interferons in osteoclasts and osteoclastogenesis. *Jt Bone Spine*. 2016. <https://doi.org/10.1016/j.jbspin.2015.07.010>.
193. Avnet S, Cenni E, Perut F, et al. Interferon- α inhibits in vitro osteoclast differentiation and renal cell carcinoma-induced angiogenesis. *Int J Oncol*. 2007;30(2):469–76.
194. Lee Y, Hyung SW, Hee JJ, et al. The ubiquitin-mediated degradation of Jak1 modulates osteoclastogenesis by limiting interferon- β -induced inhibitory signaling. *Blood*. 2008. <https://doi.org/10.1182/blood-2007-03-082941>.
195. Zheng H, Yu X, Collin-Osdoby P, Osdoby P. RANKL stimulates inducible nitric-oxide synthase expression and nitric oxide production in developing osteoclasts: An autocrine negative feedback mechanism triggered by RANKL-induced interferon- β via NF- κ B that restrains osteoclastogenesis and bone resorp. *J Biol Chem*. 2006. <https://doi.org/10.1074/jbc.M513225200>.
196. Böhm C, Hayer S, Kilian A, et al. The α -Isoform of p38 MAPK Specifically Regulates Arthritic Bone Loss. *J Immunol*. 2009. <https://doi.org/10.4049/jimmunol.0901026>.
197. Ji J-D, Park-Min K-H, Shen Z, et al. Inhibition of RANK Expression and Osteoclastogenesis by TLRs and IFN- γ in Human Osteoclast Precursors. *J Immunol*. 2009. <https://doi.org/10.4049/jimmunol.0900072>.
198. Baker PJ, Dixon M, Evans RT, Dufour L, Johnson E, Roopenian DC. CD4+ T cells and the proinflammatory cytokines gamma interferon and interleukin-6 contribute to alveolar bone loss in mice. *Infect Immun*. 1999.
199. Gao Y, Grassi F, Ryan MR, et al. IFN- γ stimulates osteoclast formation and bone loss in vivo via antigen-driven T cell activation. *J Clin Invest*. 2007. <https://doi.org/10.1172/JCI30074>.
200. Bartel DP. MicroRNAs: Target Recognition and Regulatory Functions. *Cell*. 2009;136(2):215–33. <https://doi.org/10.1016/j.cell.2009.01.002>.

201. Hrdlicka HC, Lee S-K, Delany AM. MicroRNAs Are Critical Regulators of Osteoclast Differentiation. *Curr Mol Biol Reports*. 2019;5(1):65–74. <https://doi.org/10.1007/s40610-019-0116-3>.
202. Franceschetti T, Kessler CB, Lee SK, Delany AM. MiR-29 promotes murine osteoclastogenesis by regulating osteoclast commitment and migration. *J Biol Chem*. 2013;288(46):33347–60. <https://doi.org/10.1074/jbc.M113.484568>.
203. de la Rica L, García-Gómez A, Comet NR, et al. NF- κ B-direct activation of microRNAs with repressive effects on monocyte-specific genes is critical for osteoclast differentiation. *Genome Biol*. 2015;16(1):1–17. <https://doi.org/10.1186/s13059-014-0561-5>.
204. Sugatani T, Hruska KA. Down-regulation of miR-21 biogenesis by estrogen action contributes to osteoclastic apoptosis. *J Cell Biochem*. 2013;114(6):1217–22. <https://doi.org/10.1002/jcb.24471>.
205. Mizoguchi F, Murakami Y, Saito T, Miyasaka N, Kohsaka H. MiR-31 controls osteoclast formation and bone resorption by targeting RhoA. *Arthritis Res Ther*. 2013;15(5):R102. <https://doi.org/10.1186/ar4282>.
206. Bae Y, Yang T, Zeng HC, et al. miRNA-34c regulates Notch signaling during bone development. *Hum Mol Genet*. 2012;21(13):2991–3000. <https://doi.org/10.1093/hmg/dds129>.
207. Li D, Liu J, Guo B, et al. Osteoclast-derived exosomal miR-214-3p inhibits osteoblastic bone formation. *Nat Commun*. 2016;7:1–16. <https://doi.org/10.1038/ncomms10872>.
208. Foessel I, Kotzbeck P, Obermayer-Pietsch B. miRNAs as novel biomarkers for bone related diseases. *J Lab Precis Med*. 2019;4:2. <https://doi.org/10.21037/jlpm.2018.12.06>.
209. Lee Y, Kim HJ, Park CK, et al. MicroRNA-124 regulates osteoclast differentiation. *Bone*. 2013;56(2):383–9. <https://doi.org/10.1016/j.bone.2013.07.007>.
210. Ell B, Mercatali L, Ibrahim T, et al. Tumor-Induced Osteoclast miRNA Changes as Regulators and Biomarkers of Osteolytic Bone Metastasis. *Cancer Cell*. 2013;24(4):542–56. <https://doi.org/10.1016/j.ccr.2013.09.008>.
211. Dou C, Zhang C, Kang F, et al. MiR-7b directly targets DC-STAMP causing suppression of NFATc1 and c-Fos signaling during osteoclast fusion and differentiation. *Biochim Biophys Acta Gene Regul Mech*. 2014;1839(11):1084–96. <https://doi.org/10.1016/j.bbarm.2014.08.002>.
212. Kim K, Kim JH, Kim I, et al. MicroRNA-26a regulates RANKL-induced osteoclast formation. *Mol Cells*. 2014;38(1):75–80. <https://doi.org/10.14348/molcells.2015.2241>.
213. Taganov KD, Boldin MP, Chang KJ, Baltimore D. NF- κ B-dependent induction of microRNA miR-146, an inhibitor targeted to signaling proteins of innate immune responses. *Proc Natl Acad Sci U S A*. 2006;103(33):12481–6. <https://doi.org/10.1073/pnas.0605298103>.
214. Nakasa T, Shibuya H, Nagata Y, Niimoto T, Ochi M. The inhibitory effect of microRNA-146a expression on bone destruction in collagen-induced arthritis. *Arthritis Rheum*. 2011;63(6):1582–90. <https://doi.org/10.1002/art.30321>.
215. Ma Y, Yang H, Huang J. Icarin ameliorates dexamethasone-induced bone deterioration in an experimental mouse model via activation of microRNA-186 inhibition of cathepsin K. *Mol Med Rep*. 2018;17(1):1633–41.
216. Li G, Bu J, Zhu Y, Xiao X, Liang Z, Zhang R. Curcumin improves bone microarchitecture in glucocorticoid-induced secondary osteoporosis mice through the activation of microRNA-365 via regulating MMP-9. *Int J Clin Exp Pathol*. 2015;8(12):15684–95.
217. Rajamannan NM, Evans FJ, Aikawa E, et al. Calcific aortic valve disease: not simply a degenerative process: A review and agenda for research from the National Heart and Lung and Blood Institute Aortic Stenosis Working Group. Executive summary: Calcific aortic valve disease-2011 update. *Circulation*. 2011;124(16):1783–91. <https://doi.org/10.1161/CIRCULATIONAHA.110.006767>.
218. Persy V, D’Haese P. Vascular calcification and bone disease: the calcification paradox. *Trends Mol Med*. 2009;15(9):405–16. <https://doi.org/10.1016/j.molmed.2009.07.001>.
219. Hyder JA, Allison MA, Criqui MH, Wright CM. Association between systemic calcified atherosclerosis and bone density. *Calcif Tissue Int*. 2007;80(5):301–6. <https://doi.org/10.1007/s00223-007-9004-6>.

220. Budoff MJ, Shaw LJ, Liu ST, et al. Long-Term Prognosis Associated With Coronary Calcification. Observations From a Registry of 25,253 Patients. *J Am Coll Cardiol.* 2007;49(18):1860–70. <https://doi.org/10.1016/j.jacc.2006.10.079>.
221. Bliuc D, Nguyen ND, Milch VE, Nguyen TV, Eisman JA, Center JR. Mortality risk associated with low-trauma osteoporotic fracture and subsequent fracture in men and women. *JAMA - J Am Med Assoc.* 2009;301(5):513–21. <https://doi.org/10.1001/jama.2009.50>.
222. Mussolino ME, Madans JH, Gillum RF. Bone mineral density and stroke. *Stroke.* 2003;34(5):5–7. <https://doi.org/10.1161/01.str.0000065826.23815.a5>.
223. Hak AE, Pols HAP, Van Hemert AM, Hofman A, Witteman JCM. Progression of aortic calcification is associated with metacarpal bone loss during menopause. *Atherosclerosis.* 2000;20:1926–31.
224. Bauer DC, Palermo L, Black D, Cauley JA. Quantitative ultrasound and mortality: A prospective study. *Osteoporos Int.* 2002;13(8):606–12. <https://doi.org/10.1007/s001980200081>.
225. Otto CM, Lind BK, Kitzman DW. Association of aortic-valve sclerosis with cardiovascular mortality and morbidity in the elderly. *N Engl J Med.* 1999;341(3):142–7.
226. Byon CH, Chen Y. Molecular Mechanisms of Vascular Calcification in Chronic Kidney Disease: The Link between Bone and the Vasculature. *Curr Osteoporos Rep.* 2015;13(4):206–15. <https://doi.org/10.1007/s11914-015-0270-3>.
227. Aksoy Y, Yagmur C, Tekin GO, et al. Aortic valve calcification: Association with bone mineral density and cardiovascular risk factors. *Coron Artery Dis.* 2005;16(6):379–83. <https://doi.org/10.1097/00019501-200509000-00007>.
228. Yuksel A, Cengiz Y, Gulacan T, et al. Aortic valve calcification: association with bone mineral density and cardiovascular risk factors. *Coron Artery Dis.* 2005;16(6):379–83.
229. Aikawa E, Nahrendorf M, Figueiredo J, et al. Osteogenesis Associates With Inflammation in Early-Stage Atherosclerosis Evaluated by Molecular Imaging In Vivo. *Circulation.* 2007;116:2841–50. <https://doi.org/10.1161/CIRCULATIONAHA.107.732867>.
230. Qiao JH, Mishra V, Fishbein MC, Sinha SK, Rajavashisth TB. Multinucleated giant cells in atherosclerotic plaques of human carotid arteries: Identification of osteoclast-like cells and their specific proteins in artery wall. *Exp Mol Pathol.* 2015;99(3):654–62. <https://doi.org/10.1016/j.yexmp.2015.11.010>.
231. Mohler E III, Gannon F, Reynolds C, Zimmerman R, Keane MG, Kaplan FS. Bone Formation and Inflammation in Cardiac Valves. *Circulation.* 2001;103:1522–8. <https://doi.org/10.1161/01.CIR.103.11.1522>.
232. Maldonado N, Kelly-Arnold A, Vengrenyuk Y, et al. A mechanistic analysis of the role of microcalcifications in atherosclerotic plaque stability: Potential implications for plaque rupture. *Am J Physiol - Hear Circ Physiol.* 2012;303(5):619–28. <https://doi.org/10.1152/ajpheart.00036.2012>.
233. Chinetti-Gbaguidi G, Daoudi M, Rosa M, et al. Human Alternative Macrophages Populate Calcified Areas of Atherosclerotic Lesions and Display Impaired RANKL-Induced Osteoclastic Bone Resorption Activity. *Circ Res.* 2017;121(1):19–30. <https://doi.org/10.1161/CIRCRESAHA.116.310262>.
234. Rogers MA, Aikawa M, Aikawa E. Macrophage heterogeneity complicates reversal of calcification in cardiovascular tissues. *Circ Res.* 2017;121(1):5–7. <https://doi.org/10.1161/CIRCRESAHA.117.311219.Macrophage>.
235. Massy ZA, Mentaverri R, Mozar A, Brazier M, Kamel S. The pathophysiology of vascular calcification: are osteoclast-like cells the missing link? *Diabetes Metab.* 2008;34(SUPPL. 1):16–20. [https://doi.org/10.1016/S1262-3636\(08\)70098-3](https://doi.org/10.1016/S1262-3636(08)70098-3).
236. Helske S, Kovanen PT, Lindstedt KA, et al. Increased circulating concentrations and augmented myocardial extraction of osteoprotegerin in heart failure due to left ventricular pressure overload. *Eur J Heart Fail.* 2007;9(4):357–63. <https://doi.org/10.1016/j.ejheart.2006.10.015>.
237. Ueland T, Aukrust P, Dahl CP, et al. Osteoprotegerin levels predict mortality in patients with symptomatic aortic stenosis. *J Intern Med.* 2011;270(5):452–60. <https://doi.org/10.1111/j.1365-2796.2011.02393.x>.

Part IV
Imaging, Treatment, and Target Discovery

Chapter 19

Imaging Cardiovascular Calcification Activity with ^{18}F -Fluoride PET



Evangelos Tzolos and Marc R. Dweck

Introduction

Calcification is a common response to vascular injury and a key pathological process in atherosclerosis, heart valve disease, and peripheral vascular disease. Imaging of vascular calcification has previously been limited to computed tomography (CT), which detects large macroscopic deposits of calcium. However, by the time such deposits can be detected, the disease process leading to their formation is often resolved. There is, therefore, great interest in detecting the earlier stages of calcium formation, microcalcification, when the disease process remains active and calcification activity ongoing.

^{18}F -Fluoride PET has recently emerged as an imaging modality capable of detecting such calcification activity, and over the past 10 years, this approach has been applied to multiple different cardiovascular disease states. This has provided important insight in the underlying pathophysiology of these conditions and unique information that may prove of clinical utility in the future. In this review we will first discuss how ^{18}F -fluoride PET works and then explore how this approach has been used to study calcification activity in aortic stenosis, mitral annular calcification, bioprosthetic valve degeneration, abdominal aortic aneurysm disease, erectile dysfunction, cardiac amyloidosis, and both carotid and coronary atherosclerosis. We will discuss studies that have employed both PET/CT and MR/PET imaging techniques.

E. Tzolos · M. R. Dweck (✉)
British Heart Foundation Centre for Cardiovascular Sciences, University of Edinburgh,
Edinburgh, UK
e-mail: marc.dweck@ed.ac.uk

How Does ^{18}F -Fluoride PET Work?

Positron Emission Tomography

Advanced hybrid PET/CT and MR/PET scanners now provide detailed molecular information about the activity of specific disease processes occurring in the body. In principle, the activity of any biological process can be a subject to study the availability of a targeted PET radiotracer. After manufacture, these radiotracers are injected in to the body and accumulate in areas where that disease process is active, emitting radiation that can be detected by the PET scanner to create an image. Since the PET images lack spatial resolution, they are fused with an anatomical dataset provided by either CT or MR acquired simultaneously with the patient remaining in the same position on a single gantry. These anatomical scans also provide attenuation correction allowing precise quantification of tracer accumulation in different tissues. Indeed modern hybrid PET/CT and MR/PET now effectively combine functional information from PET with fine anatomical detail from CT or MR, such that the activity of a range of pathological processes can be visualized within very small structures in the body [1]. Current clinical computed tomography (CT) and magnetic resonance systems are only able to accurately identify macrocalcification with a diameter between 200 and 500 μm [2, 3]. Fusion PET/CT and PET/MR can visualize microcalcification (<50 μm) not visible on the computed tomography or magnetic resonance systems.

PET/CT has been extensively used in the clinical assessment of patients with cancer for many years, resulting in the widespread accessibility of scanners [4]. Recent technological innovations including motion correction, improved PET resolution, and fusion with detailed CT angiographic images have allowed the use of this technology to image the heart and cardiovascular system. To date most studies have made use of established tracer already widely available for oncology imaging. These include ^{18}F -fluorodeoxyglucose (^{18}F -FDG) as a marker of vascular inflammation but more recently ^{18}F -fluoride to investigate calcification activity.

^{18}F -Fluoride is a PET tracer with favorable pharmacokinetic properties and an excellent safety profile that has been used since the 1960 as a bone tracer [5, 6]. After intravenous injection, approximately 70% of ^{18}F -fluoride is plasma-based with the remaining 30% found in erythrocytes. Because of its small size and negligible protein binding, ^{18}F -fluoride demonstrates almost complete clearance from the blood stream on first pass [7, 8], resulting in low blood pool activity. One hour after administration of ^{18}F -labeled NaF, only about 10% of the injected dose remains in the blood. Moreover, ^{18}F -fluoride uptake in the myocardium is even lower than in the blood pool, allowing relatively low levels of uptake in adjacent structures such as the aortic valve and coronary arteries readily apparent with excellent signal to noise.

The mechanism of ^{18}F -fluoride uptake in bone is well-established. First it diffuses via the capillary network into the bone extracellular fluid. Then it exchanges with hydroxyl groups on exposed regions of hydroxyapatite crystals on the bone

surface, to form fluoroapatite. The intensity of the signal depends both on the bone blood flow and also upon the surface area of exposed hydroxyapatite, which is increased in regions of new bone formation and remodeling [5, 6, 9]. As a result, ¹⁸F-fluoride has been widely utilized as a marker of bone turnover and used to study various bone-related clinical conditions such as Paget's disease [10, 11], osteoporosis [11], and fracture healing [12].

Like bone, hydroxyapatite is also the key structural component of vascular calcium and perhaps similar mechanisms of binding appear to underlie ¹⁸F-fluoride uptake in the vasculature. Indeed, Beanlands et al. [13] recently established the association between ¹⁸F-fluoride activity and histological staining for hydroxyapatite in excised atherosclerotic plaque. More recently, Creager et al. [14], showed that ¹⁸F-fluoride preferentially binds to the surface of hydroxyapatite in regions remote to established macrocalcification. Moreover, they confirmed that near-infrared fluorescence calcium tracer OsteoSense (OsteoSense680, Perkin Elmer, NEV10020EX) also binds preferentially to hydroxyapatite similarly to ¹⁸F-fluoride. These findings were supported by histology in coronary artery and carotid endarterectomy samples. There was a linear correlation between the OsteoSense and ¹⁸F-fluoride autoradiography signal. More importantly, the investigators using PET/CT demonstrated ¹⁸F-fluoride activity in noncalcified regions (PET-positive/CT-negative) suggesting that ¹⁸F-fluoride binding cannot be explained by the presence of macrocalcification alone.

The surface area of exposed hydroxyapatite also appears to govern the vascular ¹⁸F-fluoride signal. Electron microscopy studies have demonstrated that during the early stages of calcification, hydroxyapatite crystals are nanosized, very thin, and long [15]. This results in a much larger surface area of hydroxyapatite for ¹⁸F-fluoride binding in the early stages of microcalcification compared to macroscopic calcification in which much of the hydroxyapatite is internalized and not accessible to the tracer.

Irkle et al. [16] showed that binding of ¹⁸F-fluoride to calcium appears to be critically dependent upon the surface area of calcium orthophosphate available for incorporation. ¹⁸F-Fluoride, therefore, preferentially binds regions of newly developing microcalcification (beyond the resolution of CT), which have a nanocrystalline structure and very high surface area, rather than to large macroscopic deposits, where much of the calcium is internalized and, therefore, not available for binding. Aikawa's studies also confirmed that ¹⁸F-fluoride binds predominantly to hydroxyapatite, similar to the near-infrared imaging calcium tracer, OsteoSense, previously shown and now broadly used to visualize microcalcifications in small animal models of atherosclerosis and aortic valve calcification [17]. This phenomenon first demonstrated in mice has been confirmed in human patients and now is active area of investigation.

¹⁸F-Fluoride binds to developing microcalcification beyond the resolution of CT. It, therefore, provides a marker of early calcification and possibly calcification activity, demonstrating a close association with histological markers of osteogenic activity including alkaline phosphatase staining ($r = 0.65$; $p = 0.04$) [18]. Moreover, it provides different information to the established macrocalcification detected on CT: an observation recreated in each disease state ¹⁸F-fluoride has been investigated but first described by Derlin et al. in a study of 75 patients undergoing whole-body ¹⁸F-fluoride PET/CT [19]. Increased ¹⁸F-fluoride uptake in large vessels (aorta,

carotids, and femoral arteries) was observed in about three quarters of the patients. Yet uptake was detected remotely for calcium on CT, and, remarkably, only 12% of all calcified plaques on CT demonstrated increased ^{18}F -fluoride uptake.

Aortic Stenosis

Aortic stenosis is the most common form of valve disease in the Western world, and its burden is set to increase over the coming decades [20]. Despite this, there are no medical therapies to delay disease progression, and the only current available treatment options are aortic valve replacement and valvuloplasty, to which not all patients are suited. The development of effective medical therapies will be accelerated by an improved understanding of the underlying pathology and the development of biomarkers of disease activity that might be used as endpoints to test the efficacy of potential interventions.

Ring of Fire was the first prospective cardiovascular ^{18}F -fluoride PET study. It recruited 121 patients with calcific aortic valve disease (20 controls, 20 aortic sclerosis, 25 mild, 33 moderate, and 23 severe aortic stenosis) underwent both ^{18}F -FDG and ^{18}F -fluoride PET/CT imaging and repeat echocardiography and CT calcium scoring to track disease progression. Increased ^{18}F -fluoride uptake was clearly observed in patients with aortic valve disease compared to controls (2.87 ± 0.82 vs. 1.55 ± 0.17 ; $p < 0.001$), and activity increased progressively with more advanced stages of aortic stenosis. Increased ^{18}F -FDG activity was also detected; however, uptake values were lower than ^{18}F -fluoride and only increased gradually with disease severity. Valvular ^{18}F -fluoride activity, therefore, far exceeded ^{18}F -FDG uptake in the later stages of moderate and severe stenosis (the opposite pattern to that observed in regions of atherosclerosis) confirming that calcification but not inflammation is the predominant process in the late stages of aortic stenosis and perhaps explaining the disappointing results of statin therapy in aortic stenosis [21–23].

When patients returned for repeat CT calcium scoring of the valve in 1 and 2 years, new calcium could be spotted in the areas of increased ^{18}F -fluoride activity seen on the baseline scan. As a consequence, a close correlation was observed between the baseline valvular ^{18}F -fluoride uptake and the progression of the aortic valve CT calcium score ($r = 0.80$; 95% CI: 0.69 to 0.87; $p < 0.001$), with PET appearing to offer some additional predictive information over and above the baseline calcium score (Fig. 19.1). Moreover, this translated into an ability to predict hemodynamic progression on echocardiography, with moderate correlations also observed between ^{18}F -fluoride activity and the mean ($r = 0.32$; 95% CI: 0.13 to 0.50; $p = 0.001$) and peak ($r = 0.32$; 95% CI: 0.12 to 0.49; $p = 0.002$) aortic valve gradients. Finally, after a median of 1526 days of follow-up, ^{18}F -fluoride emerged as a prognostic marker serving as an independent predictor of the combined endpoint of aortic valve replacement and cardiovascular mortality (hazard ratio, 1.55; 95% CI, 1.33 to 1.81, after adjusting for age and sex; $p < 0.001$).

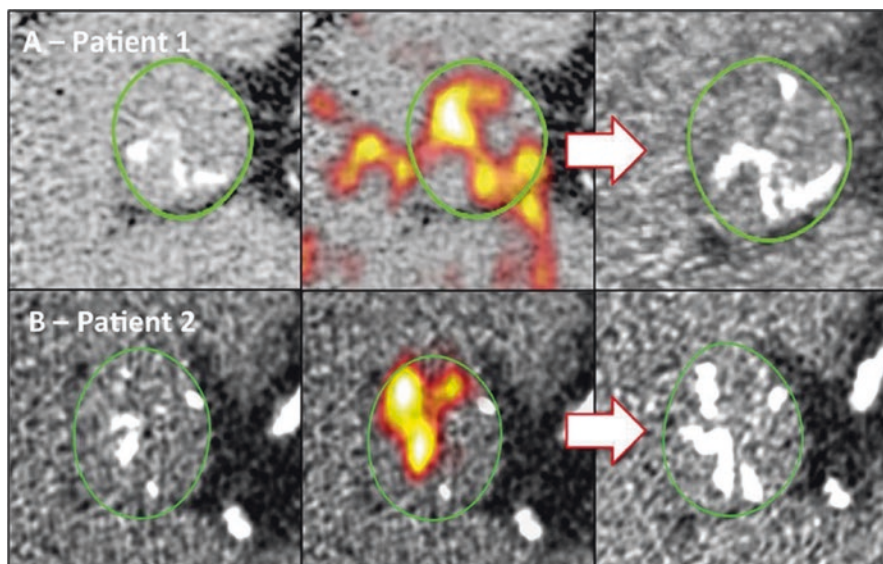


Fig. 19.1 Change in aortic valve CT calcium score and ^{18}F -fluoride PET activity after 1 year. Baseline CT calcium scores (left) for patients 1 and 2 (top and bottom). Fused coaxial ^{18}F -fluoride PET/CT scans (middle) show fluoride uptake (red yellow areas) in a different distribution to the calcium observed in CT. On the repeat CT calcium scores scans performed after 1-year follow-up (right), new areas of macroscopic calcium can be observed in much the same distribution as the ^{18}F -fluoride PET activity observed at baseline. (Jenkins et al. [23])

Mitral Annular Calcification

Mitral annular calcification (MAC) is associated with aortic, coronary artery, and aortic valve calcification and with both mitral valve dysfunction and cardiovascular events; however, its pathophysiology and mechanism remain incompletely understood [24, 25]. In a recent study Massera et al. [26] employed a multimodality imaging approach including ^{18}F -fluoride and ^{18}F -FDG positron emission tomography. Patients who had MAC (34% of patients) had increased inflammatory and calcification activity by positron emission tomography imaging in the mitral annulus, with PET uptake again observed in a different distribution to calcium on CT. A strong correlation was observed between mitral annular ^{18}F -fluoride activity and baseline CT-MAC score ($r = 0.79$, $P < 0.001$), while a moderate correlation was observed with ^{18}F -FDG uptake ($r = 0.32$, $P = 0.001$). MAC progression on repeat computed tomography scans after 2 years appeared to occur at sites of increased baseline ^{18}F -fluoride activity with a close association observed between baseline ^{18}F -fluoride and the change in CT calcium score ($r = 0.75$, $P < 0.001$) (Fig. 19.2). By contrast, traditional cardiovascular risk factors and calcification activity in bone or remote atherosclerotic areas were not associated with disease activity or progression. Similar to aortic stenosis, these data suggest that MAC is characterized by a vicious

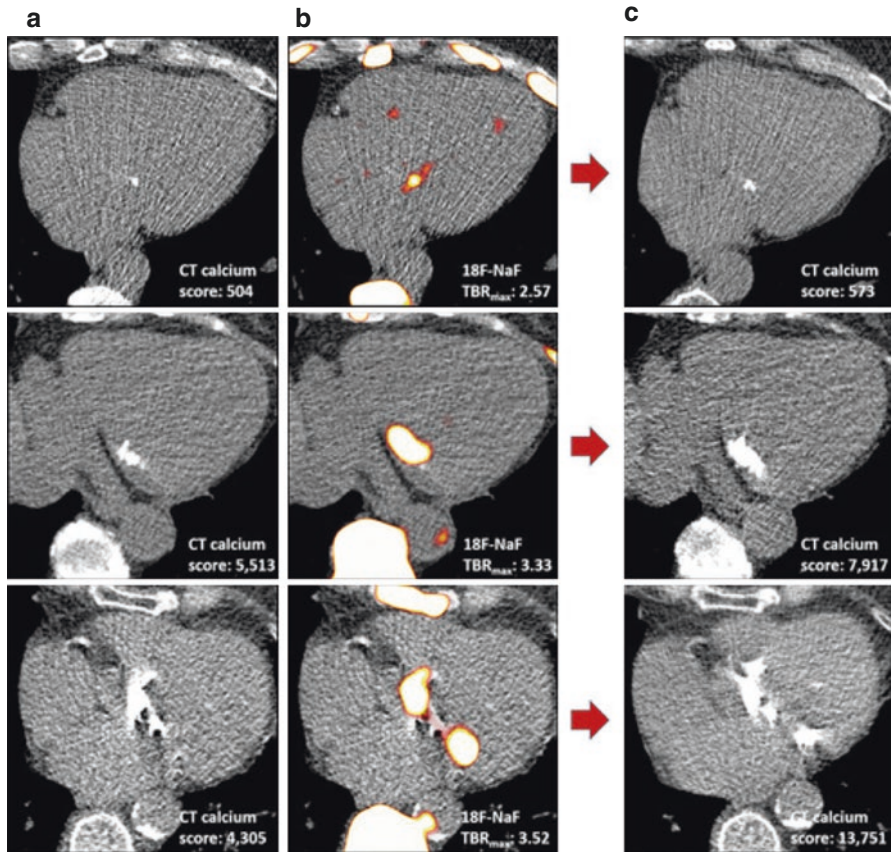


Fig. 19.2 Baseline computed tomography mitral annular calcification (CT-MAC), ^{18}F -fluoride positron emission tomography (PET) activity, and 2-year progression in three patients. First row, mild MAC at baseline (a), associated with mild mitral annular ^{18}F -fluoride uptake (b) and modest progression after 2 years (change in CT-MAC 69 AU (c)). Second row, moderate MAC at baseline (a), moderate ^{18}F -fluoride uptake (b), and intermediate progression after 2 years (change in CT-MAC 2404 AU (c)). Third row, severe MAC at baseline (a), bifocal high-intensity ^{18}F -fluoride uptake (b), and rapid progression (change in CT-MAC 9446 AU (c)). Note de novo areas of MAC that developed at the site of intense ^{18}F -fluoride uptake in the lateral annulus. (Massera et al. [26])

cycle of established calcium causing increased mechanical stress and injury that prompts further calcification activity and that successful therapies will need to focus on breaking this vicious cycle of calcification.

Bioprosthetic Valve Degeneration

The only available treatment for the patients that progress to symptomatic severe aortic stenosis remains the surgical implantation of a new valve or a transcatheter aortic valve replacement. In the United States alone, more than 90,000 surgical

aortic valve replacements are performed annually, with over 75% featuring bioprosthetic valves [27]. Furthermore, over 80,000 transcatheter aortic valve implantation procedures have been performed since 2011 [13]. Recently Carlidge et al. showed that ¹⁸F-fluoride could play a significant role in predicting bioprosthetic valve degeneration [28].

The pathophysiology of bioprosthetic valve degeneration is still to be understood, but calcification appears to be the final common pathway of degeneration and the major pathological contributor to both progressive valve narrowing and leaflet tears [29]. The current standard of care relies on serial clinical assessment and echocardiography aimed at detecting the valve dysfunction that occurs only toward the end stages of the degeneration process. Unfortunately, despite close monitoring many patients present acutely with valve failure complications due to rapid onset of valvular obstruction or regurgitation. Repeat operation carries a high risk with emergency repeat aortic valve replacement surgery associated with a mortality of 22.6% compared with 1.4% for elective repeat surgery [30]. Allowing valve degeneration to be identified early would allow close tailored monitoring and better timing of repeat elective intervention, thereby reducing morbidity and mortality.

Given that calcification is one of the key pathological processes underlying bioprosthetic valve degeneration, Carlidge et al. hypothesized that increased ¹⁸F-fluoride uptake would identify prosthetic valve degeneration and predict subsequent deterioration in bioprosthetic valve function. They recruited patients over 40 years of age who had undergone previous surgical aortic valve replacement using a bioprosthetic valve. Fifteen failed explanted bioprosthetic aortic valves were obtained for ex vivo investigation. All 15 valves demonstrated ¹⁸F-fluoride leaflet uptake that correlated with a range of histological markers of bioprosthetic tissue degeneration. In particular, ¹⁸F-fluoride activity detected both micro- and macrocalcific deposits within the valve leaflets that colocalized predominantly with regions of pannus (fibrous thickening) and thrombus formation on histology. However, ¹⁸F-fluoride uptake was additionally observed in the absence of calcification on histology at sites of leaflet thickening and disrupted collagen architecture (Fig. 19.3).

Seven participants were recruited to the cohort with suspected bioprosthetic valve failure. Increased ¹⁸F-fluoride PET leaflet uptake was observed in the bioprosthetic valves of all these patients, and target to background ratios (TBR) values were nearly three times higher than in patients without known valvular dysfunction (TBR 2.91 [interquartile range (IQR), 1.75 to 4.09] vs. 1.12 [IQR, 1.04 to 1.51]; $p < 0.001$). Seventy-one patients without known bioprosthetic valve dysfunction were also studied. Increased ¹⁸F-fluoride uptake was more common than abnormalities on CT and was seen in 24 patients (34%) (TBR 1.55 [IQR: 1.44 to 1.88]). Similar to the ex vivo findings, increased ¹⁸F-fluoride uptake colocalized with areas of spotty calcification, noncalcific leaflet thickening (suggestive of thrombus), and pannus observed on the CT, but was also observed remote from CT abnormalities. Sixty-seven of the patients without established valve degeneration at baseline underwent repeat echocardiography at 2 years and demonstrated increased peak velocities compared with baseline (2.87 [IQR, 2.52 to 3.13] m/s vs. 2.73 [IQR, 2.38 to 3.07] m/s; $p = 0.002$). The 24 patients with increased ¹⁸F-fluoride uptake at baseline demonstrated clear evidence of deteriorating bioprosthetic function after 2 years, whereas patients without uptake displayed no change in valve function (change in peak velocity, 0.30 [IQR, 0.13 to

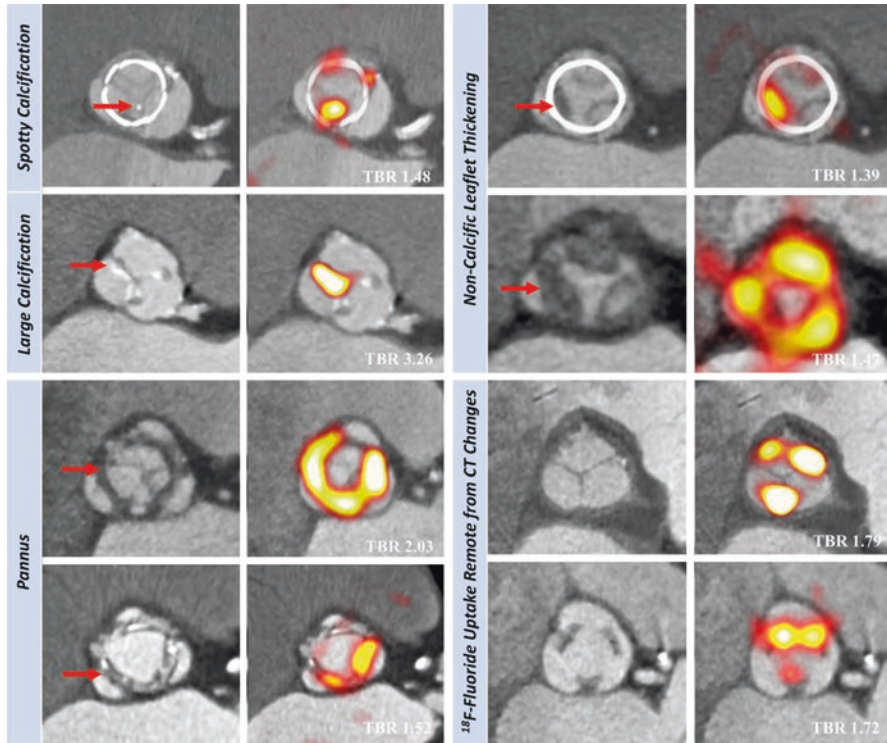


Fig. 19.3 In vivo ^{18}F -fluoride PET and CT imaging of patients with bioprosthetic aortic valves. Baseline CT (left) and ^{18}F -fluoride PET (right) images from patients with bioprosthetic aortic valves. En face CT images of aortic bioprosthetic valves showing spotty calcification and large calcification (top left), circumferential pannus (bottom left), and noncalcific leaflet thickening suggestive of thrombus (top right) (all abnormalities identified by red arrows). Hybrid en face PET/CT images in the same patients: increased bioprosthetic ^{18}F -fluoride activity (red/yellow areas) is observed in each patient colocalizing with the CT abnormalities. ^{18}F -Fluoride activity was also commonly observed remote from leaflet changes on CT (bottom right). Target-to-background (TBR) values are annotated on the hybrid PET/CT images in white text. (Cartlidge et al. [28])

0.61] vs. 0.01 [IQR, -0.05 to 0.16] m/s/year; $p < 0.001$). Similarly, valves demonstrated progressive hemodynamic deterioration during follow-up on moving across tertiles of ^{18}F -fluoride uptake, while baseline ^{18}F -fluoride uptake correlated strongly with all echocardiographic measures of hemodynamic progression regardless of the method used to quantify ^{18}F -fluoride uptake. Ten patients developed new bioprosthetic valve dysfunction during follow-up: two with valve regurgitation, six with valve stenosis, and two with mixed dysfunction. Of these patients, 5 had an abnormal baseline CT, whereas all ten patients had increased ^{18}F -fluoride uptake (TBR 1.89 [IQR: 1.46 to 2.59]), and this included the seven patients with the highest TBR values in the cohort. This study suggests that ^{18}F -fluoride uptake has a role as an early maker of bioprosthetic valve degeneration and an independent predictor of deteriorating bioprosthetic valve performance, outperforming all other variables, with potential to identify patients at pending risk of valve failure.

Coronary Atherosclerosis

James Muller introduced the concept of the vulnerable plaque in 1989 when he described “hemodynamically insignificant, albeit dangerous lesions” [31], at high risk of rupturing and causing myocardial infarction. Subsequently multiple observational studies have confirmed that most of the plaques causing myocardial infarction are non-flow limiting at the time of antecedent angiography. Cardiovascular research of the last two decades has now established that ruptured plaques exhibit common key histopathological features including a thin fibrous cap (<65 μm), large necrotic core, a positively remodeled vessel, macrophage infiltration resulting in plaque inflammation, hypoxia leading to neovascularization, and finally early stage microcalcification [32–36]. Histopathological features of rupture-prone plaques are also reviewed in Chap. 2.

^{18}F -FDG is an excellent tracer for identifying inflammation in large arteries such as the aorta and carotids [37–40]. However, due to its limited specificity and its strong uptake in the left ventricular myocardium, imaging of the coronary arteries is impaired. By contrast, ^{18}F -fluoride demonstrates an excellent signal to noise ratio in the coronary arteries with very low uptake in the adjacent myocardium. Moreover, as a marker of developing microcalcification, this tracer appears capable of providing important clinical information with respect to disease activity and as a marker of potentially unstable coronary plaque [41, 42] (Fig. 19.4).

Dweck et al. first described ^{18}F -fluoride uptake in the coronary arteries as a novel marker of plaque biology in subjects with and without aortic valve disease [43], with excellent reproducibility and feasibility. Furthermore, increased uptake of this

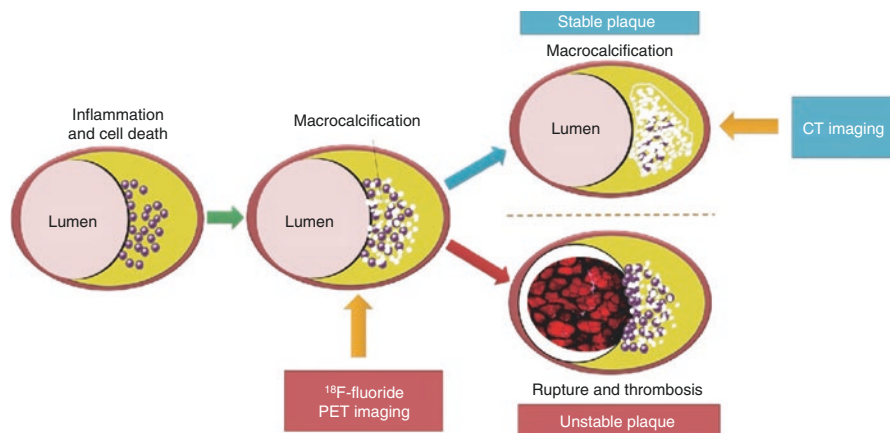


Fig. 19.4 ^{18}F -Fluoride binds to regions of microcalcification prior to the presence of CT determined macrocalcification. ^{18}F -Fluoride binds in relation to the exposed surface area of hydroxyapatite. This explains why uptake is proportionally greatest in the early, active stage of microcalcification while the plaque remains vulnerable to rupture. This stage precedes the potential development of stable, macroscopic calcification that is detected by traditional CT imaging. PET, positron emission tomography; CT, computed tomography. (Adamson et al. [42])

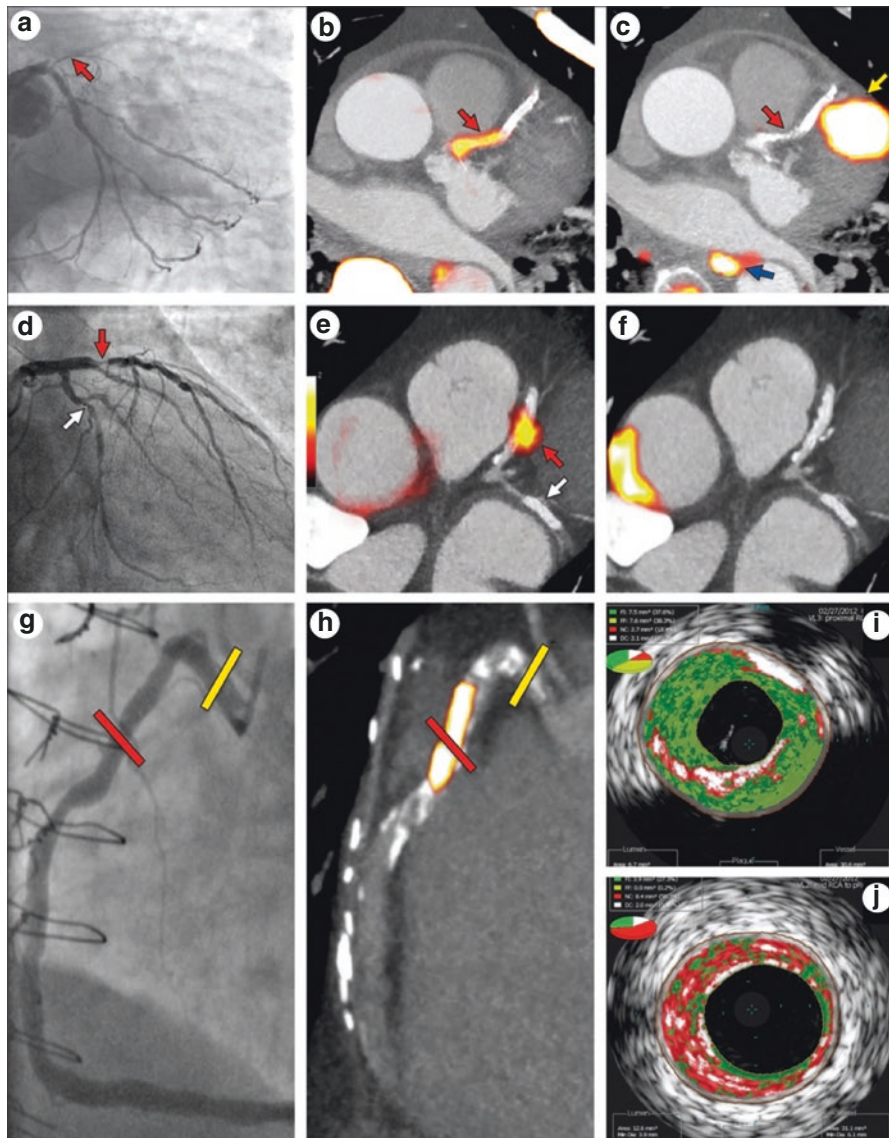
tracer localized to individual coronary plaques and importantly identified patients with increased Framingham risk scores and a history of prior MACE. This study again confirmed that ^{18}F -fluoride provides different information to the presence of coronary calcium on CT. Indeed, >40% of patients with coronary artery calcium scores >1000 Agatston Units did not demonstrate increased ^{18}F -fluoride uptake, suggesting that ^{18}F -fluoride might be able to differentiate between dormant and active atherosclerotic disease states in patients with advanced plaque burden.

In a subsequent study, Joshi et al. [44] recruited 40 patients with stable angina referred for invasive angiography, who all underwent ^{18}F -NaF PET/CT imaging alongside CT coronary angiography, invasive coronary angiography, and intravascular ultrasound. Increased tracer activity localized to individual coronary plaques in approximately 40% of patients. Using intravascular ultrasound (IVUS) and CT, they have demonstrated that these plaques had multiple high-risk features, including microcalcification, positive remodeling, and a large necrotic core. It was impossible, however, to undertake histological analysis of the ^{18}F -fluoride signal in these patients. Instead, the authors confirmed that increased ^{18}F -fluoride activity colocalizes to carotid plaques (removed at the time of endarterectomy) with histological evidence of increased macrophage accumulation, cell death, and calcification.

In a similar study, Li et al. [45] demonstrated that increased ^{18}F -fluoride uptake in the coronary arteries was observed in patients at increased cardiovascular risk. Finally, Oliveira-Santos M. et al. showed that patients with ≥ 5 risk factors (60%) had increased overall ^{18}F -NaF uptake (1.1 ± 0.3 vs. 0.7 ± 0.3 , $p < 0.01$) and that a positive correlation was observed between ^{18}F -fluoride uptake and the predicted fatal cardiovascular risk score ($r = 0.49$, $p = 0.01$) [46].

For the first time, Joshi et al. examined ^{18}F -fluoride PET uptake fused with contrast-enhanced CT coronary angiography using ECG gating to correct for cardiac motion [44]. In 37 out of 40 patients following a recent type 1 myocardial infarction, the authors observed increased ^{18}F -fluoride uptake at the exact site of the culprit coronary plaque (that had ruptured and caused the event) independent of the effects of coronary stenting (Fig. 19.5).

Fig. 19.5 Focal ^{18}F -fluoride and ^{18}F -fluorodeoxyglucose uptake in patients with myocardial infarction and stable angina. Patient with acute ST-segment elevation myocardial infarction with (a) proximal occlusion (red arrow) of the left anterior descending artery on invasive coronary angiography and (b) intense focal ^{18}F -fluoride (uptake at the site of the culprit plaque (red arrow) on PET/CT. ^{18}F -fluorodeoxyglucose PET/CT image (c) showing no uptake at the site of the culprit plaque patient with anterior non-ST-segment elevation myocardial infarction with (d) culprit (red arrow; left anterior descending artery) and bystander non-culprit (white arrow; circumflex artery) lesions on invasive coronary angiography that were both stented during the index admission. Only the culprit lesion had increased ^{18}F -NaF uptake on PET/CT (e, f) ^{18}F -fluorodeoxyglucose PET/CT showing no uptake either at the culprit or the bystander stented lesion. In a patient with stable angina, invasive coronary angiography (g) showed non-obstructive disease in the right coronary artery. Corresponding PET/CT scan (h) showed a region of increased ^{18}F -NaF activity (positive lesion, red line) in the mid-right coronary artery and a region without increased uptake in the proximal vessel (negative lesion, yellow line). Radiofrequency intravascular ultrasound shows that the ^{18}F -NaF negative plaque (i) is principally composed of fibrous and fibrofatty tissue (green) with confluent calcium (white with acoustic shadow) but little evidence of necrosis. On the contrary, the ^{18}F -NaF positive plaque (j) shows high-risk features such as a large necrotic core (red) and microcalcification (white). (Joshi et al. [44])



Encouraging the retrospective identification of culprit plaque is not of major clinical value. The real challenge is to assess prospectively whether ^{18}F -fluoride can identify patients at increased risk of subsequent MI. This question is being addressed in the Prediction of Recurrent Events with ^{18}F -Fluoride to Identify Ruptured and High-Risk Coronary Artery Plaques in Patients with Myocardial Infarction (PRE ^{18}F FIR) Study (NCT02278211). PRE ^{18}F FIR is a multicenter observational study that will follow about 700 high-risk patients with coronary artery disease to determine whether baseline ^{18}F -fluoride PET imaging can identify patients at increased risk of subsequent myocardial infarction and whether it can predict coronary arterial disease progression. Meanwhile, the Dual Antiplatelet Therapy to Inhibit Coronary Atherosclerosis and Myocardial Injury in Patients with Necrotic High-risk Coronary Plaque Disease (DIAMOND) Study (NCT02110303) will be the first randomized controlled trial to examine the relationship between ^{18}F -fluoride uptake and high-sensitivity troponin concentrations and whether the latter can be modified through the use of potent antiplatelet agents.

Carotid Atherosclerosis

Atherosclerosis affects arteries and structures outside the heart in the same way described in the coronary arteries. Indeed, carotid atherosclerotic plaque rupture is a major cause of stroke and most commonly associated with vulnerable plaques characterized by increased inflammation, cell death, and microcalcification. The rationale for carotid ^{18}F -fluoride PET imaging is, therefore, similar to the coronary arteries.

Vesey et al. [47] reported a case-control study examining the use of NaF and FDG PET/CT after transient ischemic attack or minor stroke. They evaluated 26 patients following a recent cerebrovascular event. Eighteen patients were found to have a culprit carotid stenosis awaiting carotid endarterectomy and 8 patients lacked an identifiable carotid atheromatous culprit (controls). All individuals underwent PET/CT scanning using FDG and NaF. In the subset of patients who underwent carotid endarterectomy, histological analysis was performed on the excised plaques. The authors observed increased NaF uptake within culprit lesions in comparison to the contralateral artery and arteries from controls. Uptake was focal, readily identifiable, and discriminated between culprit and non-culprit. ^{18}F -Fluoride uptake was associated with high-risk plaque phenotype and predicted cardiovascular risk (Fig. 19.6).

In contrast, while ^{18}F -FDG uptake was present in plaque and correlated with cardiovascular risk, it was more diffuse and prone to spillover and therefore less discriminatory. ^{18}F -FDG also failed to correlate with established high-risk plaque morphological features. In a smaller study of nine patients, Quirce et al. [48] explored ^{18}F -fluoride and ^{18}F -FDG uptake in symptomatic patients. They showed that ^{18}F -fluoride uptake appeared to be higher in the symptomatic carotid and that ^{18}F -FDG uptake was non-discriminatory. ^{18}F -Fluoride uptake correlated with plaque burden, positive remodeling, and luminal stenosis: all established markers of plaque risk. Similarly, in a smaller study by Cocker et al. [49], 11 patients (69 ± 5 years old, 3 women) with high-risk cerebrovascular disease who were scheduled for endarterectomy were recruited.

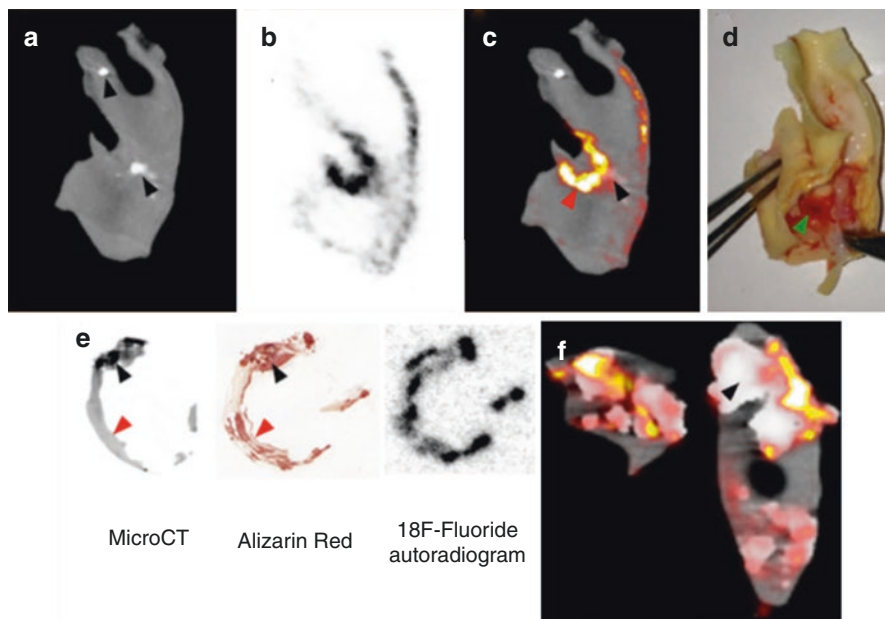


Fig. 19.6 ^{18}F -Fluoride micro-positron emission tomography (PET)/computed tomography (CT), autoradiography, and alizarin red staining. Two examples of ex vivo ^{18}F -fluoride micro-PET/CT are shown (a–d, f). (a) Coronal micro CT slice; (b) corresponding micro PET; (c) fused image; (d) the plaque. Green arrow, adherent thrombus over plaque rupture. Red arrow, associated area of ^{18}F -fluoride uptake (microcalcification). Black arrows, Areas of macrocalcification showing comparatively little uptake (a, c, f). These examples show that ^{18}F -fluoride provides information of the presence of microcalcification and does not simply highlight all calcification. (e) An example of micro-CT slice registered to an alizarin red-stained section and the corresponding autoradiogram from a specimen that had been incubated whole in ^{18}F -fluoride. It can be seen that the tracer is unable to penetrate the deeper layers of macrocalcification (black arrow) but is able to highlight microcalcification beyond the resolution of even micro-CT (red arrow), thus explaining the findings in the micro-PET/CT images (Vesey et al. [47])

^{18}F -NaF PET/CT imaging of the carotid arteries was acquired within 2 weeks before surgery. Plaque associated with symptoms had evidence for greater ^{18}F -NaF uptake than plaque not associated with symptoms. ^{18}F -NaF uptake was related to active microcalcification (hydroxyapatite stained with Goldner's trichrome) rather than the overall extent of calcification (Alizarin Red S), consistent with ^{18}F -NaF acting as a marker of calcification and developing microcalcification.

Abdominal Aortic Aneurysms

^{18}F -Fluoride has recently been investigated in abdominal aortic aneurysm disease (AAA). In the SOFIA³ study, Forsythe et al. [50] first performed micro-PET/CT and histological analysis of excised aneurysm tissue ($n = 72$), establishing once more

that ^{18}F -fluoride acts as a marker of calcification activity. Then in prospective case-control ($n = 20$ per group) and longitudinal cohort ($n = 72$) studies, patients with AAA (aortic diameter > 40 mm) and control subjects (aortic diameter < 30 mm) underwent abdominal ultrasound, ^{18}F -NaF PET/CT, CT angiography, and calcium scoring. Clinical endpoints were aneurysm expansion and the composite of AAA repair or rupture. Aneurysms in the highest tertile of ^{18}F -NaF uptake expanded 2.5 \times more rapidly than those in the lowest tertile (3.10 [interquartile range (IQR): 2.34 to 5.92 mm/year] vs. 1.24 [IQR: 0.52 to 2.92 mm/year]; $p = 0.008$) and were nearly three times as likely to experience AAA repair or rupture (15.3% vs. 5.6%; log-rank $p = 0.043$). This predictive effect was independent of the size of the aneurysm (the current gold standard for aneurysm assessment). The authors also showed that CT calcium scoring was not associated with expansion or AAA events, again highlighting the different information on calcification provided by PET and CT. This interesting finding requires confirmation in a larger trial, while ongoing studies are investigating the utility of ^{18}F -fluoride PET in thoracic aortic aneurysms and dissection (FAASt study, NCT03647566).

Penile Uptake

Finally, in a recent study Nakahara et al. [51] investigated ^{18}F -fluoride uptake in the penile arteries of prostate cancer patients as a potential marker of erectile dysfunction (ED). The authors demonstrated that NaF uptake in the cavernous and dorsal penile arteries (remote from the urethra) was associated with the both the presence of existing erectile dysfunction and the likelihood of its development in the future. Indeed, penile ^{18}F -fluoride activity in prevalent ED (SUVmax 1.88; IQR: 1.67 to 2.16) and incident ED (SUVmax 1.86; IQR: 1.72 to 2.08) was 30% higher than in no ED (SUVmax 1.42; IQR: 1.25 to 1.54) patients ($p < 0.001$). Using an SUV max cutoff value of 1.56, NaF uptake showed a sensitivity of 85% and a specificity of 80% on ROC curve analysis for prevalent or incident erectile dysfunction. The authors concluded that due to the limited spatial resolution (3 to 5 mm) of PET imaging, it is not certain if the penile NaF uptake is localized to cavernous arteries. Since there was no significant correlation between iliac calcification and penile fluoride uptake, they assume that is also possible that calcification could be associated with the venous compartment or smooth muscle cell damage leading to possible venous insufficiency and ED. Further studies are keenly anticipated.

Limitations

Both positron emission tomography/computed tomography and positron emission tomography/magnetic resonance imaging of the heart have evolved significantly over the last decade. Despite that they still face significant challenges. These include

radiation exposure, the high costs of imaging, and relatively limited access to scanners particularly in the developing world.

In addition, PET imaging of the heart is made more complicated by the impact of cardiac, respiratory, and gross patient movement on positron emission tomography image quality. In order to overcome these obstacles, several image optimization studies have been undertaken leading to novel imaging reconstructions and the development of novel software that can accurately read fused images. In the beginning the fused images were not corrected for cardiac motion. Originally in order to overcome this obstacle, Pawade et al. [52] used only the PET counts from the end-diastolic phase ignoring more than 3/4 of the total PET signal leading to reduction of noise and better image registration. Doris et al. [53] used an alternative technique to preserve all PET data and at the same time reduce the background noise using an anatomy-guided registration algorithm. Lassen et al. [54], using joint corrections for cardiac, respiratory, and gross patient motion in combination with background blood pool corrections markedly improved test-retest reproducibility of coronary ^{18}F -NaF PET. The excellent ^{18}F -fluoride PET coronary plaque imaging reproducibly has been established in several other studies [55–58]. Recently Andrews et al. [59] showed that PET/MR demonstrates good visual and quantitative agreement with PET/CT. These well-established techniques allow for accurate image co-registration, precise localization of ^{18}F -fluoride activity, and highly reproducible tracer localization.

Conclusion

^{18}F -Fluoride PET has now been investigated across the cardiovascular system and consistently provides complementary information to CT regarding calcification activity and vascular injury. This technique has already provided some key pathophysiological insights with further work now required to investigate whether it can advance patient diagnosis and risk prediction.

Acknowledgments and Funding ET was supported by a grant from Dr. Miriam and Sheldon G. Adelson Medical research Foundation. DEN (CH/09/002, RE/13/3/30183, RG/16/10/32375) and MRD (FS/14/78/31020) are supported by the British Heart Foundation. DEN is the recipient of a Wellcome Trust Senior Investigator Award (WT103782AIA) and MRD of Sir Jules Thorn Award for Biomedical Research Award (2015).

References

1. Bockisch A, Beyer T, Antoch G, Freudenberg LS, Kuhl H, Debatin JF, et al. Positron emission tomography/computed tomography–imaging protocols, artifacts, and pitfalls. *Mol Imaging Biol.* 2004;6(4):188–99.
2. Ritman EL. Small-animal CT – Its difference from, and impact on, clinical CT. *Nucl Instrum Methods Phys Res A.* 2007;580(2):968–70.

3. Baheza RA, Welch EB, Gochberg DF, Sanders M, Harvey S, Gore JC, et al. Detection of microcalcifications by characteristic magnetic susceptibility effects using MR phase image cross-correlation analysis. *Med Phys*. 2015;42(3):1436–52.
4. Lubbers M, Dedic A, Coenen A, Galema T, Akkerhuis J, Bruning T, et al. Calcium imaging and selective computed tomography angiography in comparison to functional testing for suspected coronary artery disease: the multicentre, randomized CRESCENT trial. *Eur Heart J*. 2016;37(15):1232–43.
5. Blau M, Ganatra R, Bender MA. 18 F-fluoride for bone imaging. *Semin Nucl Med*. 1972;2(1):31–7.
6. Hawkins RA, Choi Y, Huang SC, Hoh CK, Dahlbom M, Schiepers C, et al. Evaluation of the skeletal kinetics of fluorine-18-fluoride ion with PET. *J Nucl Med*. 1992;33(5):633–42.
7. Hoh CK, Hawkins RA, Dahlbom M, Glaspy JA, Seeger LL, Choi Y, et al. Whole body skeletal imaging with [18F]fluoride ion and PET. *J Comput Assist Tomogr*. 1993;17(1):34–41.
8. Blake GM, Park-Holohan SJ, Cook GJ, Fogelman I. Quantitative studies of bone with the use of 18F-fluoride and 99mTc-methylene diphosphonate. *Semin Nucl Med*. 2001;31(1):28–49.
9. Blau M, Nagler W, Bender MA. Fluorine-18: a new isotope for bone scanning. *J Nucl Med*. 1962;3:332–4.
10. Cook GJ, Blake GM, Marsden PK, Cronin B, Fogelman I. Quantification of skeletal kinetic indices in Paget's disease using dynamic 18F-fluoride positron emission tomography. *J Bone Miner Res*. 2002;17(5):854–9.
11. Messa C, Goodman WG, Hoh CK, Choi Y, Nissenson AR, Salusky IB, et al. Bone metabolic activity measured with positron emission tomography and [18F]fluoride ion in renal osteodys-trophy: correlation with bone histomorphometry. *J Clin Endocrinol Metab*. 1993;77(4):949–55.
12. Hsu WK, Feeley BT, Krenek L, Stout DB, Chatziioannou AF, Lieberman JR. The use of 18F-fluoride and 18F-FDG PET scans to assess fracture healing in a rat femur model. *Eur J Nucl Med Mol Imaging*. 2007;34(8):1291–301.
13. Brennan JM, Thomas L, Cohen DJ, Shahian D, Wang A, Mack MJ, et al. Transcatheter versus surgical aortic valve replacement: propensity-matched comparison. *J Am Coll Cardiol*. 2017;70(4):439–50.
14. Creager MD, Hohl T, Hutcheson JD, Moss AJ, Schlotter F, Blaser MC, et al. (18)F-Fluoride Signal Amplification Identifies Microcalcifications Associated With Atherosclerotic Plaque Instability in Positron Emission Tomography/Computed Tomography Images. *Circ Cardiovasc Imaging*. 2019;12(1):e007835.
15. Rey C, Combes C, Drouet C, Glimcher MJ. Bone mineral: update on chemical composition and structure. *Osteoporos Int*. 2009;20(6):1013–21.
16. Irkle A, Vesey AT, Lewis DY, Skepper JN, Bird JL, Dweck MR, et al. Identifying active vascular microcalcification by (18)F-sodium fluoride positron emission tomography. *Nat Commun*. 2015;6:7495.
17. Aikawa E, Nahrendorf M, Sosnovik D, Lok VM, Jaffer FA, Aikawa M, et al. Multimodality molecular imaging identifies proteolytic and osteogenic activities in early aortic valve disease. *Circulation*. 2007;115(3):377–86.
18. Dweck MR, Jenkins WS, Vesey AT, Pringle MA, Chin CW, Malley TS, et al. 18F-sodium fluoride uptake is a marker of active calcification and disease progression in patients with aortic stenosis. *Circ Cardiovasc Imaging*. 2014;7(2):371–8.
19. Derlin T, Richter U, Bannas P, Begemann P, Buchert R, Mester J, et al. Feasibility of 18F-sodium fluoride PET/CT for imaging of atherosclerotic plaque. *J Nucl Med*. 2010;51(6):862–5.
20. Nkomo VT, Gardin JM, Skelton TN, Gottdiener JS, Scott CG, Enriquez-Sarano M. Burden of valvular heart diseases: a population-based study. *Lancet (London, England)*. 2006;368(9540):1005–11.
21. Dweck MR, Jones C, Joshi NV, Fletcher AM, Richardson H, White A, et al. Assessment of valvular calcification and inflammation by positron emission tomography in patients with aortic stenosis. *Circulation*. 2012;125(1):76–86.

22. Dweck MR, Khaw HJ, Sng GK, Luo EL, Baird A, Williams MC, et al. Aortic stenosis, atherosclerosis, and skeletal bone: is there a common link with calcification and inflammation? *Eur Heart J*. 2013;34(21):1567–74.
23. Jenkins WS, Vesey AT, Shah AS, Pawade TA, Chin CW, White AC, et al. Valvular (18)F-fluoride and (18)F-Fluorodeoxyglucose uptake predict disease progression and clinical outcome in patients with aortic stenosis. *J Am Coll Cardiol*. 2015;66(10):1200–1.
24. Barasch E, Gottdiener JS, Larsen EK, Chaves PH, Newman AB, Manolio TA. Clinical significance of calcification of the fibrous skeleton of the heart and aortosclerosis in community dwelling elderly. The Cardiovascular Health Study (CHS). *Am Heart J*. 2006;151(1):39–47.
25. Fox CS, Vasan RS, Parise H, Levy D, O'Donnell CJ, D'Agostino RB, et al. Mitral annular calcification predicts cardiovascular morbidity and mortality: the Framingham Heart Study. *Circulation*. 2003;107(11):1492–6.
26. Massera D, Trivieri MG, Andrews JPM, Sartori S, Abgral R, Chapman AR, et al. Disease activity in mitral annular calcification. *Circ Cardiovasc Imaging*. 2019;12(2):e008513.
27. Brown JM, O'Brien SM, Wu C, Sikora JA, Griffith BP, Gammie JS. Isolated aortic valve replacement in North America comprising 108,687 patients in 10 years: changes in risks, valve types, and outcomes in the Society of Thoracic Surgeons National Database. *J Thorac Cardiovasc Surg*. 2009;137(1):82–90.
28. Cartledge TRG, Doris MK, Sellers SL, Pawade TA, White AC, Pessotto R, et al. Detection and prediction of bioprosthetic aortic valve degeneration. *J Am Coll Cardiol*. 2019;73(10):1107–19.
29. Rodriguez-Gabella T, Voisine P, Puri R, Pibarot P, Rodes-Cabau J. Aortic bioprosthetic valve durability: incidence, mechanisms, predictors, and management of surgical and transcatheter valve degeneration. *J Am Coll Cardiol*. 2017;70(8):1013–28.
30. Vogt PR, Brunner-LaRocca H, Sidler P, Zund G, Truniger K, Lachat M, et al. Reoperative surgery for degenerated aortic bioprostheses: predictors for emergency surgery and reoperative mortality. *Eur J Cardiothorac Surg*. 2000;17(2):134–9.
31. Muller JE, Tofler GH, Stone PH. Circadian variation and triggers of onset of acute cardiovascular disease. *Circulation*. 1989;79(4):733–43.
32. Burke AP, Farb A, Malcom GT, Liang YH, Smialek J, Virmani R. Coronary risk factors and plaque morphology in men with coronary disease who died suddenly. *N Engl J Med*. 1997;336(18):1276–82.
33. Burke AP, Kolodgie FD, Farb A, Weber DK, Malcom GT, Smialek J, et al. Healed plaque ruptures and sudden coronary death: evidence that subclinical rupture has a role in plaque progression. *Circulation*. 2001;103(7):934–40.
34. Falk E, Nakano M, Bentzon JF, Finn AV, Virmani R. Update on acute coronary syndromes: the pathologists' view. *Eur Heart J*. 2013;34(10):719–28.
35. Finn AV, Nakano M, Narula J, Kolodgie FD, Virmani R. Concept of vulnerable/unstable plaque. *Arterioscler Thromb Vasc Biol*. 2010;30(7):1282–92.
36. Virmani R, Burke AP, Farb A, Kolodgie FD. Pathology of the vulnerable plaque. *J Am Coll Cardiol*. 2006;47(8 Suppl):C13–8.
37. Yun M, Yeh D, Araujo LI, Jang S, Newberg A, Alavi A. F-18 FDG uptake in the large arteries: a new observation. *Clin Nucl Med*. 2001;26(4):314–9.
38. Yun M, Jang S, Cucchiara A, Newberg AB, Alavi A. 18F FDG uptake in the large arteries: a correlation study with the atherogenic risk factors. *Semin Nucl Med*. 2002;32(1):70–6.
39. Tatsumi M, Cohade C, Nakamoto Y, Wahl RL. Fluorodeoxyglucose uptake in the aortic wall at PET/CT: possible finding for active atherosclerosis. *Radiology*. 2003;229(3):831–7.
40. Tahara N, Kai H, Yamagishi S, Mizoguchi M, Nakaura H, Ishibashi M, et al. Vascular inflammation evaluated by [18F]-fluorodeoxyglucose positron emission tomography is associated with the metabolic syndrome. *J Am Coll Cardiol*. 2007;49(14):1533–9.
41. Joshi NV, Vesey A, Newby DE, Dweck MR. Will 18F-sodium fluoride PET-CT imaging be the magic bullet for identifying vulnerable coronary atherosclerotic plaques? *Curr Cardiol Rep*. 2014;16(9):521.

42. Adamson PD, Vesey AT, Joshi NV, Newby DE, Dweck MR. Salt in the wound: (18)F-fluoride positron emission tomography for identification of vulnerable coronary plaques. *Cardiovasc Diagn Ther.* 2015;5(2):150–5.
43. Dweck MR, Chow MW, Joshi NV, Williams MC, Jones C, Fletcher AM, et al. Coronary arterial 18F-sodium fluoride uptake: a novel marker of plaque biology. *J Am Coll Cardiol.* 2012;59(17):1539–48.
44. Joshi NV, Vesey AT, Williams MC, Shah AS, Calvert PA, Craighead FH, et al. 18F-fluoride positron emission tomography for identification of ruptured and high-risk coronary atherosclerotic plaques: a prospective clinical trial. *Lancet.* 2014;383(9918):705–13.
45. Li Y, Berenji GR, Shaba WF, Tafti B, Yevdayev E, Dadparvar S. Association of vascular fluoride uptake with vascular calcification and coronary artery disease. *Nucl Med Commun.* 2012;33(1):14–20.
46. Oliveira-Santos M, Castelo-Branco M, Silva R, Gomes A, Chichorro N, Abrunhosa A, et al. Atherosclerotic plaque metabolism in high cardiovascular risk subjects - a subclinical atherosclerosis imaging study with (18)F-NaF PET-CT. *Atherosclerosis.* 2017;260:41–6.
47. Vesey AT, Jenkins WS, Irkle A, Moss A, Sng G, Forsythe RO, et al. (18)F-Fluoride and (18) F-Fluorodeoxyglucose Positron Emission Tomography After Transient Ischemic Attack or Minor Ischemic Stroke: Case-Control Study. *Circ Cardiovasc Imaging.* 2017;10(3):e004976.
48. Quirce R, Martinez-Rodriguez I, Banzo I, Jimenez-Bonilla J, Martinez-Amador N, Ibanez-Bravo S, et al. New insight of functional molecular imaging into the atheroma biology: 18F-NaF and 18F-FDG in symptomatic and asymptomatic carotid plaques after recent CVA. Preliminary results. *Clin Physiol Funct Imaging.* 2016;36(6):499–503.
49. Cocker MS, Spence JD, Hammond R, Wells G, deKemp RA, Lum C, et al. [(18)F]-NaF PET/CT identifies active calcification in carotid plaque. *JACC Cardiovasc Imaging.* 2017;10(4):486–8.
50. Forsythe RO, Dweck MR, McBride OMB, Vesey AT, Semple SI, Shah ASV, et al. (18) F-sodium fluoride uptake in abdominal aortic aneurysms: The SoFIA(3) Study. *J Am Coll Cardiol.* 2018;71(5):513–23.
51. Nakahara T, Narula J, Tijssen JGP, Agarwal S, Chowdhury MM, Coughlin PA, et al. (18) F-fluoride positron emission tomographic imaging of penile arteries and erectile dysfunction. *J Am Coll Cardiol.* 2019;73(12):1386–94.
52. Pawade TA, Cartlidge TR, Jenkins WS, Adamson PD, Robson P, Lucatelli C, et al. Optimization and Reproducibility of Aortic Valve 18F-Fluoride Positron Emission Tomography in Patients With Aortic Stenosis. *Circ Cardiovasc Imaging.* 2016;9(10):e005131.
53. Doris MK, Otaki Y, Krishnan SK, Kwiecinski J, Rubeaux M, Alessio A, et al. Optimization of reconstruction and quantification of motion-corrected coronary PET-CT. *J Nucl Cardiol.* 2018;27:494–504 (2020).
54. Lassen ML, Kwiecinski J, Dey D, Cadet S, Germano G, Berman DS, et al. Triple-gated motion and blood pool clearance corrections improve reproducibility of coronary (18)F-NaF PET. *Eur J Nucl Med Mol Imaging.* 2019;46(12):2610–20.
55. Moss AJ, Doris MK, Andrews JPM, Bing R, Daghm M, van Beek EJR, et al. Molecular coronary plaque imaging using (18)F-fluoride. *Circ Cardiovasc Imaging.* 2019;12(8):e008574.
56. Doris MK, Rubeaux M, Pawade T, Otaki Y, Xie Y, Li D, et al. Motion-corrected imaging of the aortic valve with (18)F-NaF PET/CT and PET/MRI: a feasibility study. *J Nucl Med.* 2017;58(11):1811–4.
57. Doris MK, Rubeaux M, Pawade T, Otaki Y, Xie Y, Li D, et al. Motion-corrected imaging of the aortic valve with. *J Nucl Med.* 2017;58(11):1811–4.
58. Kwiecinski J, Adamson PD, Lassen ML, Doris MK, Moss AJ, Cadet S, et al. Feasibility of coronary (18)F-sodium fluoride positron-emission tomography assessment with the utilization of previously acquired computed tomography angiography. *Circ Cardiovasc Imaging.* 2018;11(12):e008325.
59. Andrews J, Moss A, Doris M, Pawade T, Adamson P, MacNaught G, et al. 18 F-fluoride pet MR in valvular and coronary heart disease; a pilot investigational study. *Heart.* 2018;104(Suppl 5):A12.

Chapter 20

The Role of Elastin Degradation in Vascular Calcification: Possibilities to Repair Elastin and Reverse Calcification



Fatema-Tuj Zohora, Nasim Nosoudi, Saketh Ram Karamched,
and Naren Vyavahare

Abbreviations

ACA	Aortic calcification area
ACEi	Angiotensin-converting enzyme inhibitors
AGE	Advanced glycation end products
ALP	Alkaline phosphatase
ARBs	Angiotensin receptor blockers
B-GP or β -GP	Beta-glycerophosphate
Ca	Calcium
CAC	Coronary artery calcium
CAD	Coronary artery disease
CaSRs	Calcium-sensing receptors
CCBs	Calcium channel blockers
CKD	Chronic kidney disease
DTPA	Diethylenetriaminepentaacetic acid
ECM	Extracellular matrix
EDPs	Elastin-derived peptides
EDTA	Ethylenediaminetetraacetic acid
ERC	Elastin receptor complex
ESRD	End-stage renal disease
FGF2	Fibroblast growth factor 2

F.-T. Zohora · S. R. Karamched · N. Vyavahare (✉)
Bioengineering, Clemson University, Clemson, SC, USA
e-mail: narenv@clemson.edu

N. Nosoudi
College of Information Technology and Engineering, Marshall University,
Huntington, WV, USA

HA	Hydroxyapatite
HAECs	Human aortic endothelial cells
HASMCs	Human aortic smooth muscle cells
huRANKL-KI	Human RANKL knock in
IFN γ	Interferon gamma
IL-1 β	Interleukin-1 beta
LAP	Latency-associated peptides
LLC	Large latent complex
LOX	Lysyl oxidase
LRP6	Low-density lipoprotein receptor-related protein 6
LTBP	Latent TGF- β binding protein
LVH	Left ventricular hypertrophy
MAC	Medial arterial calcification
MAGP	Microfibril-associated glycoprotein
MCRAs	Mineralocorticoid receptor antagonists
MGP	Matrix Gla protein
MMP	Matrix metalloproteinase
MS	Marfan's syndrome
OPG	Osteoprotegerin
P	Phosphate
PGG	Pentagalloyl glucose
Pi	Inorganic phosphate
PLGA	Poly(lactic-co-glycolic acid)
PPi	Pyrophosphate
PTH	Parathyroid hormone
PWV	Pulse wave velocity
RAAS	Renin-angiotensin-aldosterone system
RAGE	Receptor for advanced glycation end products
sHPT	Secondary hyperparathyroidism
SMCs	Smooth muscle cells
SM α A	Smooth muscle alpha actin
STS	Sodium thiosulfate
TGF-b	Transforming growth factor-beta
TIMP	Tissue inhibitor of matrix metalloproteinases
TNF α	Tumor necrosis factor alpha
VC	Vascular calcification
VDRAs	Vitamin D receptor activators
VEGF	Vascular endothelial growth factor
Vit D3	Vitamin D3
Vit K	Vitamin K
Vit K2	Vitamin K2
VSMCs	Vascular smooth muscle cells

Definitions

Due to diversity in uses in the literature of the term “elastin” and its derivatives, a Glossary is included here for reference.

Elastic fiber	Also referred to as elastin fiber. Insoluble cross-linked fiber found in connective tissue and consisting of elastin and associated microfibrillar proteins.
Degraded elastic fiber	The changes in the structure of elastic fiber due to mechanical loading, oxidative stress, inflammation, proteolysis, and calcium deposition, that results in fragmentation of elastic fiber. The damage in elastic fiber causes release of elastin peptides that initiate inflammatory cascades.
Elastin	Insoluble protein formed from tropoelastin and a component of elastic fiber. Elastin itself as a component of elastic fiber is also damaged by factors described under degraded elastin fiber.
Elastin gene (ELN)	The gene that provides instructions for cells to manufacture the soluble protein tropoelastin.
Tropoelastin (TE)	Water-soluble protein and precursor to the insoluble structural protein elastin.

Introduction

Vascular Calcification in Intima and Media

As described in previous chapters in this book, two types of calcification are observed in the vasculature, calcification of intimal plaque (*also known as* calcific atherosclerosis) [1–4] and medial arterial calcification (MAC, *also known as* calcific arteriosclerosis or Monckeberg’s sclerosis) [5] that is associated with the elastic lamina. Intimal calcification is typically considered the last step in classical atherosclerosis and is a multifactorial process involving inflammation, macrophage infiltration, and transformation to foam cells, dyslipidemia, and presence of advanced glycation end products (AGEs). On the contrary, medial calcification is characterized by diffuse mineral deposition circumferentially along or within elastic lamellae of the medial layer of the arterial wall. It can occur independently or in conjunction with intimal calcification and is more common in chronic kidney disease (CKD) or diabetic patients [6, 7]. Morphologically, at the macroscopic scale,

atherosclerotic calcification occurs as dispersed, spotty, and patchy deposits of calcium in a matured plaque, whereas MAC gives a “tram-line”- or “railroad track”-like appearance as more and more lengths of the arterial tree calcify. At micro- and nanoscopic scale, each type begins at an early stage often undetectable in standard clinical tests [8] and by currently available imaging modalities. Intimal calcification results in vessel narrowing and dysfunction, possibly causing a thrombotic event eventually [9]. MAC, on the other hand, contributes to loss in vessel elasticity, increased arterial stiffness resulting in increased pulse pressures, increased systolic blood pressure, and left ventricular hypertrophy (LVH) ultimately causing arrhythmias and heart failure [10].

To understand how elastic lamina degradation in the artery plays a significant role in both types of calcification, we first need to review the structure of arteries.

Elastin Is an Integral Part of the Arterial Structure to Maintain Homeostasis of Cells

Arterial walls comprise of three basic layers: intima, media, and adventitia. The architectural components determine the function of each layer (Fig. 20.1) [11]. The innermost layer of the wall, intima, is directly adjacent to the lumen and consisted of a single layer of endothelial cells anchored to a basal lamina composed of laminin, collagen type IV, and proteoglycans [12]. The media is the largest among all three layers in the arterial wall structure. A series of “lamellar units” forms the basis

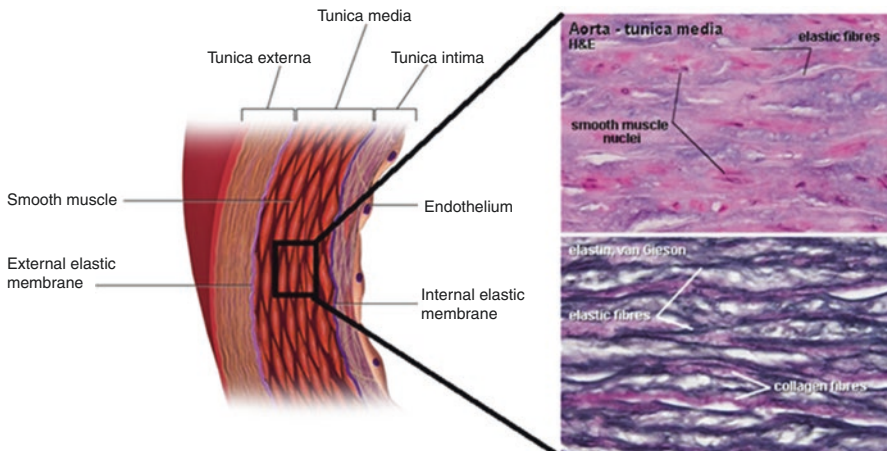


Fig. 20.1 Arteries have three distinct regions – tunica intima, tunica media, and tunica adventitia (**left**). They are separated by internal elastic lamina (IEL) and external elastic lamina (EEL). Elastic laminae are the prominent feature of tunica media of arteries and are essential to maintain the three-layered structure and cellular homeostasis (**top right** – H&E, and **bottom right** – VVG stain for elastin of the tunica media) [11]

of this layer and described as concentric fenestrated elastic lamellae separated by the interlamellar spaces composed of vascular smooth muscle cells (VSMCs), collagens type I, III, and IV, and proteoglycans [13]. In terms of their anatomical location in the aortic tree, these lamellar units differ in numbers, thickness, endogenous molecular composition, as well as biological functions [14]. In the adult human, the thoracic aorta consists of 56 elastic lamellae, whereas the abdominal aorta comprises only 28 units with strikingly higher thickness than thoracic lamellar units [15]. The tension per lamellar unit is markedly constant between abdominal vs. thoracic aorta across all species, although marked differences have been found in adult human, which contains significantly elevated tension/lamellar unit in the abdominal aorta [15].

The internal elastic lamina supports the basement membrane, which is attached with the endothelial layers in the intima. Moreover, in large arteries, the external elastic lamina separates media from the outermost layer of adventitia [14]. The ability of fibroblasts and endothelial cells to synthesize elastin indicates that they might participate in the construction of external and internal elastic lamina, respectively, probably in responding to medial cell signals [16]. The adventitia is the relatively thin outermost layer composed mainly of a collagen-rich matrix. Because of the abundance of collagenous matrix, the adventitia is the strongest among all three layers [17]. The primary function of adventitia is to protect the vessel from extensive distensibility during elastic recoil [17]. Fibroblasts are the predominant cell types in this layer but may also contain immune cells and lipids. The microenvironment of adventitia is complex and dynamic that operates as a “processing center” for integrating, storing, retrieval, and release of molecular components associated with vessel wall function. Adventitia also provides a niche for resident or circulating stem/progenitor cells that take part in vascular repair in response to various stimuli through vasa vasorum [17]. It also assists in inflammatory cell trafficking. Additionally, vasa vasorum may serve as a conduit for progenitor cells to travel to the intima, where they differentiate into VSMCs [17].

It is thus clear that in healthy artery, intima, media, and adventitia are separated by elastic lamellar structures. Any migration of inflammatory cells and progenitor cells or smooth muscle cell (SMC) proliferation in pathological vascular calcification process would need elastic lamina compromised. The role of elastic lamina degradation is greatly under-recognized in most mechanistic descriptions of atherosclerotic plaque formation.

Elastin Is Essential for Regulating Arterial Mechanical Properties

In the arterial wall, the structural proteins are responsible for the material or intrinsic stiffness of the aorta [18]. The two major extracellular matrix (ECM) proteins in the large elastic arteries are elastin and collagen. The proportion and unique assembly of elastin and collagen in the vascular wall impart passive mechanical behavior

of large arteries [19]. VSMCs in the medial layer are responsible for actomyosin contraction and cell-ECM signaling for mechanical homeostasis in muscular arteries (composed mainly of VSMCs and less elastin in the media in contrast to large arteries, where elastin is more abundant), however, contributes only minimally to the mechanical properties of large elastic arteries [20].

Elastin is profound in the major blood vessels of nearly all vertebrates formed of a pulsatile, high-pressure closed circulatory system [21]. Elastic fiber imparts reversible distensibility to the large arteries, allowing the aorta to deform during cyclic hemodynamic loading, with no permanent deformation or energy dissipation upon load retrieval [12]. Collagen, on the other hand, supports tensile strength and prevents excessive vessel distension at high pressure [22]. Arterial distension during systole and elastic recoil during diastole provide the dampening function of large arteries, known as Windkessel effect, which converts the pulsatile flow into a constant flow, thereby ensuring steady-state perfusion from the left ventricle to the distal arterioles and capillaries [20]. Perturbation in Windkessel effect either by genetic or acquired elastinopathies jeopardizes the microcirculation of downstream organs, such as the brain and kidney [12].

Unlike other ECM components that show continual remodeling over the lifespan of organisms, mature elastin formation and elastic fiber assembly occur in a defined and limited period primarily during early development with little remodeling later in life, which makes the elastin unique among all ECM molecules [23]. Of note however is that tropoelastin continues to be manufactured by cells later in life but is not completely converted into cross-linked elastin protein or elastic fiber. This incomplete elastogenesis explains why high levels of tropoelastin are found in atherosclerotic plaque and blood, for example, in older adults [24, 25].

Further, elastic fiber fragmentation due to age or disease results in altered ECM biochemical compositions [22]. Since elastic fiber cannot be regenerated in adult tissues, the degraded elastin is replaced by more collagen, which increases the collagen to elastic fiber ratio, allowing the mechanical shifts toward the stiffer scale of collagen fibers, which are approximately 100–1000-folds stiffer than elastic fibers [26]. The stiffness is further increased by calcification that is mediated by elastin degradation as described later in this chapter. The pulse wave velocity (PWV), which is a measure of a pressure wave that propagates through the vascular tree as a function of time, is dependent on intrinsic stiffness of the arterial wall [18]. PWV increases with the increased arterial stiffness and it is inversely proportional to the arterial wall distensibility [27]. PWV is considered as a reliable approach to measure intrinsic stiffness of large arteries [27]. However, this approach requires careful consideration as the concept of PWV relies on Moens-Korteweg equation, which assumes that, the aorta is perfectly cylindrical with no branching or tapering, and consisting of a linear elastic, isotropic material that undergoes small distortions during cardiac cycle, neither of which is specifically accurate [12]. Increased PWV can be a predictor of future cardiovascular events.

Lastly, the large elastic arteries, in addition to their nonlinear mechanical properties, also show viscoelastic behavior marked by energy loss (limited and minimal, 15–20%) during cyclic loading and unloading, that participates in the dampening of traveling pressure waves [19]. It is accepted that energy losses or viscous losses are due to VSMCs or collagen and proteoglycans [19]. Enhanced viscous contribution

to the aortic wall is an important and independent predictor of coronary artery disease [19]. Using mice lacking elastin ($Eln^{-/-}$), lysyl oxidase ($Lox^{-/-}$), and fibulin-4 ($Fbln4^{-/-}$), Kim et al. showed that not just presence of elastin but cross-linking and proper assembly of elastic fiber is essential for low energy loss in the large elastic arteries [19]. Thus, elastin in arteries plays a significant role in arterial biomechanics and fluid dynamics of blood. Any degradation of elastic lamella can affect both and cause cells to respond to these altered conditions.

Proper Elastic Fiber Assembly During Development Is Required to Resist Vascular Calcification

Elastic fiber assembly is a complex process and comprises tightly coordinated spatiotemporal regulation of approximately 30 different proteins [12, 28]. Amorphous elastin is the core component of elastic fiber. The other major component of elastic fiber is the scaffolds of fibrillin-rich microfibrils, comprised largely of fibrillin-1 and fibrillin-2 [28] (Fig. 20.2). Few other known elastic fiber-associated molecules are fibulin family of ECM proteins. The cells secrete microfibrils to the extracellular space before the expression of tropoelastin. Fibulin-1, an essential assembly protein found to be coregulated with early markers of VSMCs α SMA and 1E12 antigen during aortic vessel wall development and prior to the presence of elastin precursors, suggests that formation of microfibrils is independent of tropoelastin formation since some flexible tissues lacking elastin also contain abundant microfibrils [28, 29]. Fibulin-2 binds elastin to fibrillin-rich microfibrils, whereas fibulin-5 provides cell anchorage to elastic fibers via interacting with cell-surface integrins [30]. Moreover, fibulin-4 and fibulin-5 regulate size and conformation of growing elastin aggregates [12]. All these accessory proteins form a complex with elastin or microfibrils resulting in formation of mature elastic fibers. Indeed, the structure of mature elastic fiber differs as required by tissues, which implies tissue-specific functionalities of elastic fibers [28].

After microfibrillar scaffolds are present in the ECM, tropoelastin is shuttled to the specific location on the cell surface via secretory vesicles [31]. Aggregates of tropoelastin then deposit onto the preformed microfibrillar structure, and through

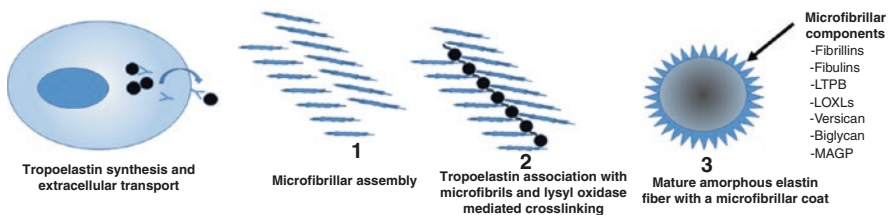


Fig. 20.2 Microfibril and elastic fiber formation. (1) Fibrillin is assembled into microfibrillar arrays. Mature microfibrils form parallel bundles that may be stabilized at inter-microfibrillar cross-linked regions. (2) In elastic tissues, tropoelastin is deposited on microfibril bundles, and lysyl oxidase-derived cross-links (Desmosine and isodesmosine) then stabilize the elastin core

the catalysis of lysyl oxidase (LOX), the oxidative deamination converts peptidyl lysine residues of tropoelastin into allysine. Following oxidation reaction, a sequence of condensation reaction takes place between unconverted lysine residues and the newly formed allysine group to produce covalent cross-links, desmosine, and isodesmosine [12]. These cross-links between tropoelastin units covalently bind tropoelastin molecules with one another to form elastin matrix [26]. Thus, desmosine links serve to anchor the entire elastin matrix, and the deformability of its cross-links imparts the elasticity to elastic fiber [26, 27]. Besides, desmosine concentration in the whole tissue hydrolysates strongly associates with the total elastin in that tissue, providing the basis for elastin quantification [32].

The importance of elastin cross-linking and proper assembly of elastic fiber has been demonstrated in a substantial number of research studies. These studies found the decisive role of structural malfunction of elastin to either acquired or genetic diseases. Examples include Marfan syndrome (MS), a genetic connective tissue disorder caused by mutations in fibrillin-1 microfibrils. Since microfibrils guide the assembly of developing elastic fiber via regulating tropoelastin deposition during embryogenesis or early development, it was presumed that MS-associated vascular disease results in when mutations in fibrillin-1 gene lead to the disruption of microfibrillar assembly of elastic fiber and inhibit their maturation. However, by developing a fibrillin-1 targeting mice model, Pereira et al. [33] reported that fibrillin-1 predominantly regulates tissue homeostasis probably by assisting the proper organization of collagenous tissue in the adventitia, which supports the majority of hemodynamic stress. Therefore, aortic dilatation in MS is primarily due to the malfunction of the microfibrillar array in the adventitia and consequent loss of tensile strength to sustain hemodynamic stress. This mechanical failure in adventitia is followed by overstretching and breakdown of medial elastic laminae, a process that results as part of the dysfunction of fibrillin-1 microfibrils to create a wavy structure of elastic lamellae and to anchor the basal lamina in the intima [33]. A separate study showed that fibrillin-1 expresses in late embryonic development and its synthesis parallels with the appearance of developed organ structures.

Conversely, fibrillin-2 turns up in early stages and predominately governs the elastic fiber assembly [34]. These findings suggest that, directly or indirectly, both forms of fibrillin microfibrils contribute to the elastin structure and function. Moreover, to get an insight on how fibrillin-1 associates with the MS pathogenesis, the researchers developed mice model with targeted mutations in fibrillin-1 gene that triggered severe elastic lamellae fragmentation and calcification in the aortic media, as well as adventitial dilatation and fibroblasts hyperplasia overserved at 6 weeks of age, followed by intimal hyperplasia at 9 weeks [35].

Another essential component of elastic fiber-associated microfibrils is the latent TGF- β binding protein (LTBP) that sequesters pleiotropic cytokine transforming growth factor-beta (TGF- β) in the elastic lamina. TGF- β is multifunctional, and its bioactivity is necessary for numerous cellular processes. Through TGF- β sequestration, fibrillin microfibrils regulate elastic fiber formation, various cell signaling, tissue development, and homeostasis [36]. In vivo, cells secrete TGF- β either as a small latent complex consisting of TGF- β including its latency-associated

propeptide (LAP) or as a large latent complex (LLC), which contains LTBP, TGF- β , and LAP [37]. LTBP1 and LTBP3 can efficiently form a complex with all three isoforms of TGF- β [38]. Small glycoproteins or matrix-associated Gla proteins MAGPs (MAGP1 and MAGP2) are also localized to the microfibrils. Besides fibrillins, MAGPs are thought to be essential constituents of microfibrils that take part in elastin synthesis. MAGP due to γ -carboxylation are inhibitors of vascular calcification. Thus, improper elastic lamina assembly can cause loss of TGF- β anchoring to elastin fibers and loss of MAGPs that protect elastin from calcifying. As discussed below, an activated TGF- β can cause vascular calcification.

Elastin Degradation and Vascular Calcification

Elastin is one of the most stable proteins in our body with a half-life of 70 years or more. Because of its almost nonexistent turnover rate, elastin is prone to accumulation of age-related changes [26]. In addition to the age-associated decrease in elastin fiber content, changes occur to the structure of elastin fiber due to repeated mechanical loading, oxidative stress, proteolysis during inflammatory conditions with evident fragmentation and rupture, and calcification (Fig. 20.3).

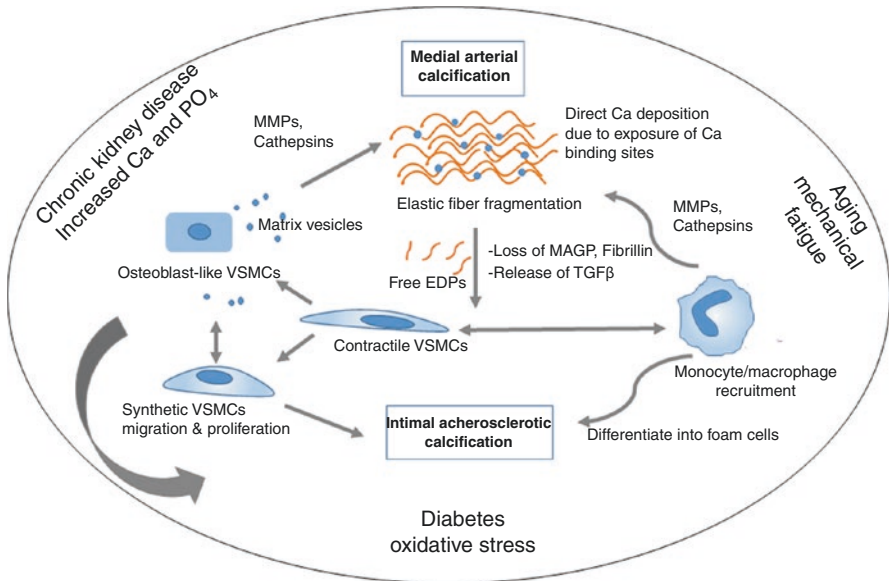


Fig. 20.3 Elastic lamina degradation is the central process in intimal and medial calcification. During aging and diseases processes, inflammatory cells can degrade elastin, releasing elastin-derived peptides (EDPs) and other elastin-associated proteins than can lead to further inflammatory cell recruitment, the proliferation of vascular smooth muscle cells (SMCs), and transformation in osteoblast-like cells. Degraded elastin can become a nidus for calcium binding, and osteoblast-like cells can further aggravate intimal and medial calcification

As shown above, amorphous elastin protein is surrounded by glycoproteins such as fibrillins and fibulins and thus protected. These negatively charged microfibrils prevent elastin calcification. It has been shown that fibrillin knockout mice show the disintegration of elastic fiber and severe calcification in aortic media [35]. Moreover, loss of MAGP has been associated with severe elastin fragmentation and calcification. As reported by Luo et al., mice lacking MAGP died within 2 months after birth due to acute calcification in arterial elastic lamina resulting in rupture of the abdominal or thoracic aorta [39].

Loss of microfibrillar protein coat of elastin can expose amorphous elastin to calcium binding. Elastin contains uncharged or neutral binding sites that have a strong affinity for positive calcium ions. The extensive glycine content along with the bulky side-chain residues provides specific conformational changes in elastin with a strong affinity for cations [40]. Elastin, being positively charged due to the bound calcium ions, attracts charge-neutralizing carbonate and phosphate ions, allowing further binding of calcium ions – an iterative process that ensues until the initiation of crystallization. Binding calcium ions to a single peptide chain and, particularly, sharing calcium ions between two peptide chains rigidify the elastin structures and causes the loss of its elasticity. Further, charge repulsion between the adjacent calcium ions might extend the elastin structure; as such calcification is expected in extended areas of elastin. Thus, charge neutralization theory indicates that there must be a physiological mechanism in elastin-rich tissues that protects elastin from calcification [40].

Role of Elastolytic Enzymes in Calcification

There is a large amount of literature suggesting how VSMC transformation to osteoblast-like phenotype causes vascular calcification [41]. However, we hypothesize that elastic lamina fragmentation occurs before this transformation to take place. Elastic fiber is susceptible to proteolytic degradation during physiological or pathological processes, such as aging, inflammation, or atherosclerosis. Elastases or elastolytic enzymes are peptidases that cleave soluble and insoluble elastin fiber. These include serine, cysteine, and metalloproteinases. Matrix metalloproteinases (MMP-2, -7, -9, and -12) and cysteine cathepsins (Cat L, K, S, and V) have been particularly implicated in elastic fiber degradation. Pathology-associated matrix metalloproteinase overexpression, such as MMP-2 (gelatinase A), MMP-7 (matrilysin), MMP-9 (gelatinase B), and MMP-12 (macrophage metalloproteinase), can substantially degrade elastin framework [42]. Enhanced enzymatic activity leads to the deposition of lipids and calcium, which is undeniably a cause of elastic fragmentation [43]. An imbalance between elastin-degrading MMPs and endogenous tissue inhibitors of MMPs (TIMPs) causes excessive MMP activity and pathologic degradation of elastin, linking elastic fiber degeneration and inflammation. Several studies have reported a key association between MMP upregulation, especially MMP-2 and MMP-9, and vascular calcification [44–46]. Vyavahare et al. identified

overexpression of MMP-2 and MMP-9 near calcifying elastin fragments in purified elastin implants [47]. Aluminum chloride pretreatment of these purified elastin implants imparted resistance to calcification due to irreversible Al^{3+} ion binding and subsequent structural alterations [47]. Further, they demonstrated that periadventitial treatment with calcium chloride-induced MMP-2 and MMP-9 mediated chronic aortic degradation and aneurysms and elastin calcification in rat abdominal aortas. This was supported by the complete absence of elastin calcification in both MMP-2 and MMP-9 knockout mice which underwent the same $CaCl_2$ treatment [48]. Moreover, a substantial research study evidenced the overexpression of MMPs in atherosclerotic lesions that are highly linked to arterial medial degradation [49]. Arterial medial elastic degradation and consequent dilatation of the aortic wall are characteristic features of aortic aneurysm development. Plaque rupture and development of aneurysms are two complications associated with atherosclerosis. MMPs and MMP inhibitors TIMP-1, -2, and -3 are overexpressed in atherosclerotic plaque. Evidence suggests the overexpression of TIMP-1 during aneurysmal medial degradation, where it colocalized with the VSMCs [49]. Additionally, the atherosclerotic lesions of TIMP deficient mice possessed substantial elastic lamellae degradation, medial ruptures, macrophage infiltration, and pseudo-microaneurysms formation, due to the decreased inhibition of MMP activity [49].

Cysteine cathepsins (CatL, CatS, CatK, and CatV) are also among the most potent elastases. Inflammatory cells secrete cytokines and growth factors such as $TNF\alpha$, $INF\gamma$, $IL-1\beta$, $FGF2$, and $VEGF$ typically found in human atherosclerotic plaques. These pro-inflammatory factors stimulate medial VSMCs or intimal endothelial cells to secrete cysteine proteases that degrade elastin and collagens [50]. It has been demonstrated that they are major contributors to the progression of atherosclerosis, medial calcification, calcific aortic valve disease, and plaque rupture [51–53]. In contrast to healthy vessels, high serum content of lysosomal cysteine proteases and concurrently decreased endogenous inhibitor cystatin C levels are observed in human atheroma [50]. The study suggests a reciprocal relationship between cathepsins and their most abundant inhibitor cystatin C in diseased arterial tissues of human [50]. Decreased cystatin C content has been found in both aneurysmal and atherosclerotic lesions in humans. Under inflammatory conditions, cystatin C regulates cysteine protease activity by VSMCs. Cystatin C-deficient apolipoprotein E-null mice developed fragmented elastic lamina in the arterial media and aortic expansion, although no effect has been observed in atheroma plaque sizes, lipid core sizes, and macrophage accumulation in the intima [50]. However, this is in contrast with other research where cathepsin S-deficient apolipoprotein E-null mice reduced atherosclerotic lesion size, lipid content, and macrophage accumulation. Thus, it is possible that cystatin C deficiency affects several other cysteine proteases, such as cathepsin B and L whose proteolytic activity in the pathology of atherogenesis is still not determined [50].

Moreover, Aikawa et al. found conclusive *in vivo* evidence that CatS-driven elastolysis accelerates arterial and aortic valve calcification in CKD while inhibition of elastolysis with a selective CatS inhibitor restores elastin and reduces atherosclerotic inflammation and calcification [53]. These results were further supported by

recent work of Andraut et al., who showed the degradation of vascular elastin by CatK, S, and V directly stimulates the mineralization of elastin. Elastin peptides released by cathepsin-mediated degradation can cause SMC-osteoblast phenotypic changes and cellular calcification [54]. In support of this study, Sinha and Vyavahare confirmed that elastin peptides promote VSMCs osteogenesis via overexpressing elastin-laminin receptor I [41]. Thus, elastin degradation might precede VSMC calcification.

Role of Elastin-Derived Peptides

Not only degradation of elastin can cause elastic lamina calcification as shown above, but the degradation of elastin can release elastin degradation products, also called elastin-derived peptides (EDPs) typically made of hexapeptide VGVAPG, a peptide sequence repeated six times in human tropoelastin [43]. The VGVAPG carries a motif GXXPG (X stands for any amino acid) in its primary structure, which stabilizes a type-VIII beta-turn conformation, allowing conjugation with its analogous cell-surface receptor, elastin receptor complex (ERC) [43]. Hence, VGVAPG is bioactive and actively associates with vascular disease progression. The increased serum concentration of free EDPs has been observed in patients with diabetes, hypertension, age-related macular degeneration, atherosclerosis, ischemic heart disease, hyperlipidemia, and breast cancer. Indeed, elastin fragments are the consequence of physiological or pathological processes, but the free EDPs can further exacerbate the disease by acting as chemo-attractant for inflammatory cells. An *in vitro* VSMCs cultures in high glucose conditions with exogenously added EDPs along with TGF β -1 (can be released due to loss of TGF β binding protein on elastin) significantly enhanced osteogenic differentiation of VSMCs. Subsequent pathway analysis revealed that EDPs in high glucose concentration induced the overexpression of cell-surface receptors: elastin-laminin receptor I (ELRI) and activin receptor-like kinase 5 (ALK5), resulting in activation of osteogenic markers, RUNX2, ALP, and OCN. Blocking of these receptors strongly inhibited osteogenic protein expression [41]. Moreover, EDPs shows chemotactic activity and is a potent chemoattractant for inflammatory cells, such as monocytes or macrophages. Macrophages could then degrade elastin by secreting pro-inflammatory cytokines. Macrophages and VSMCs also release calcifying extracellular vesicles that contribute to formation of microcalcifications and ultimately develop advance intimal atherosclerotic calcification [55, 56]. More information of extracellular vesicles can be found in Chap. 5. Additionally, research evidence suggests that EDPs cause an imbalance between pro-inflammatory and anti-inflammatory macrophage (M1/M2) ratio, which is a critical factor for aneurysm formation. By stimulating M1 polarization, EDPs fostered pro-inflammatory conditions in aortic tissues. When EDPs are neutralized with antibody treatment, C57Bl/6 mice showed reduced MMP activity, aortic dilatation, and pro-inflammatory cytokine expression at both early and late periods of aneurysm induction [57].

Elastin-Associated Components That Activate Osteogenesis Through Degradation of Elastic Fibers

A recent study demonstrated the essential role of microfibrils on TGF- β bioavailability [37]. Deposition of a large latent complex containing LTBP1 is mostly dependent on the pericellular assembly of microfibrils, and it is a tightly regulated process that governs the interaction between LTBP1, fibrillin-1, integrin $\alpha 5\beta 1$, heparan sulfate, and microfibril-associated molecules such as fibulin-4 and MAGP1 [37]. Disruption of microfibrillar assembly impedes deposition of LTBP1 in the fibrillin microfibrils and activates TGF- β [37]. Altered TGF- β signaling may also result from improper elastic fiber assembly or proteolytic degradation of elastic fibers [12]. Increased TGF- β activity, as well as its high concentration in circulation, has been demonstrated in Marfan syndrome [58]. Mice deficient of fibulin-4 showed defective elastic laminae in the aortic wall, resulting in the formation of aortic aneurysms, wall stiffening, and subsequently aortic dissection and active TGF- β signaling, suggesting that microfibrillar regulation of TGF- β bioavailability and dysregulation of TGF- β are highly linked to vascular pathologies [59]. Also, TGF- β is known as a potent inducer of key osteogenic transcription factor RUNX2. Activation of MMP9 and subsequent TGF- β signaling has been observed in warfarin-induced elastocalcinosis model, in both ex vivo and in vivo experiments [60]. These findings indicate the role of TGF- β in arterial elastin calcification.

Role of Elastin Degradation in Atherosclerotic Calcification

Calcification is a hallmark of advanced atherosclerosis. Lansing et al. identified that elastic tissue calcification occurs without intimal plaque formation, but the converse is not true [61]. Elastin fiber degeneration and its primary role in plaque formation in human atherosclerosis have been reported as early as 1950. Bobryshev et al. showed that calcification occurring within the intima also requires preexisting structural changes, such as unesterified cholesterol or altered elastin fibers [62]. More recently, Gayral et al. provide evidence that elastin-derived peptides (EDPs) have a role in atherosclerosis development in mouse models, and this relies on PI3K γ activity within leukocyte during atherogenesis [63]. In humans, the serum concentration of elastin-derived peptides increases during atherosclerosis and correlates with the degree and progression of vascular disease.

Further, degradation of extracellular matrix including elastin by MMPs not only induces alterations in the preexisting structural conformation but also influences plaque development at various stages, for example, promoting the migration and proliferation of VSMCs [64]. Elastin degrading CatK and S were also found to be expressed in human atherosclerotic lesions. In advanced atherosclerotic lesions, both CatK and S are found localized in VSMCs of the fibrous cap and surrounding macrophages and in the areas of fragmented elastin [65, 66]. Besides CatK, S, and

L were also reported in VSMCs and macrophages of advanced atheromas and abdominal aortic aneurysms.

Arterial wall remodeling in atherosclerosis along with elastolysis includes the initial recruitment of inflammatory cells through the basement membrane and migration of VSMCs from the media into the intimal layer through the broken elastic lamellae. It is viewed that an intact extracellular matrix prevents phenotypic switching and keeps VSMC in their contractile state. Breakdown of ECM, especially of elastin fiber, by MMPs and cathepsins released from any of the inflammatory cells, would promote the phenotypic switch in VSMCs, cell proliferation, and migration [67, 68]. Elastin breakdown is thus a critical step in the advancement of atherosclerosis and represents an important therapeutic target to prevent plaque development. Current therapeutic strategies for atherosclerotic disease are not geared toward stabilization of elastin fiber network. Targeting and stabilizing elastin fiber in early atherosclerotic lesions could result in a novel therapeutic effect by preventing migration, proliferation, and phenotype switching of VSMCs in atherosclerotic plaque formation.

In summary, elastic lamina degradation plays a significant role in all types of the vascular calcification process. It maintains VSMCs in the contractile phenotype and prevents cellular migration. Inflammatory conditions can lead to fragmentation of elastic lamina that can exacerbate calcification process by either directly depositing hydroxyapatite crystals on elastin to cause medial calcification or releasing elastin-associated proteins such as TGF- β and MAGPs that can indirectly promote calcification. Moreover, EDPs can signal inflammatory cells recruitment as well as the transformation of cells into osteoblast-like phenotypes causing further vascular calcification. Fragmentation of elastic lamina can cause VSMCs to become synthetic type and can cause neointimal hyperplasia and further atherosclerotic calcification [69].

Potential Treatment Strategies to Prevent Vascular Calcification

As shown in Fig. 20.3, vascular calcification is orchestrated by a variety of factors in aging and disease conditions. Researchers have tried to target one or more of these factors to inhibit the progression of vascular calcification. Table 20.1 describes various past methods attempted in animal models or clinical settings with some success.

Prevention of Vascular Calcification in Chronic Kidney Disease (CKD)

Therapeutic approaches and inventions that may stabilize and potentially reverse vascular calcification (VC) may be of immense value to patients with CKD also covered in Chap. 8. Most of the treatment methods in use have been limited to

Table 20.1 Treatment strategies for vascular calcification

Treatments	Experimental/disease-associated VC	Administration route	Mechanisms/targeted pathways	Genotypic/phenotypic outcomes
NaHS (H ₂ S donor) [94]	High glucose-treated HASMCs	–	↓Stat3/cathepsin signaling	↓Runx2, ALP activity, calcium deposition ↑Elastin protein
Ginsenoside Rb1 [111]	In vitro, β-GP treated VSMCs; In vivo, CKD-related VC rat	Intraperitoneal injection	↓Wnt/β-Cat pathway	↓Osteogenic transdifferentiation ↓Calcium deposition
Knockdown of macrophage TRPC3 [97]	MacTpc3 ^{-/-} Ldlr ^{-/-} mice (advanced atherosclerosis)	–	↓BMP-2 signaling	↓Plaque calcification ↓BMP2, Runx2, phospho-SMAD1/5
Sevelamer carbonate [112]	Ldlr ^{-/-} mice (CKD)	Diet	↓PTH levels	↓Aortic calcium content ↑Bone volume
Dual-targeted therapy: EDTA followed by PGG nanoparticles [108]	Rats (abdominal aortic aneurysms)	Tail vein injection	EDTA removes Ca by chelating action; PGG binds elastin and possibly blocks calcium nucleation sites on elastin	↓Elastin breakdown and calcification ↻Elastin lamina and vascular function
Dorsomorphin homologue 1 [113]	In vitro, Pi-treated HASMCs; Ex vivo, aorta culture	–	↓BMP/Smad1/5/8 signaling	↓Pi-induced Ca deposition ↓Medial artery calcification
Pyridoxamine and alagebrium [93]	Rats (Diabetic)	Chow-fed/diet	↓AGE-RAGE or downstream signaling	↓Medial calcification
Apocynin [93]	Rats (diabetic)	Chow-fed	↓RAGE activation ↓Reactive oxygen species	↓Femoral artery calcification
Perindopril [98]	Patients with coronary atherosclerosis, n = 118	Oral	↓Angiotensin-converting enzyme	↻Regressed plaques with little (<25%) or no calcium

(continued)

Table 20.1 (continued)

Treatments	Experimental/disease-associated VC	Administration route	Mechanisms/targeted pathways	Genotypic/phenotypic outcomes
Perindopril, valsartan [72]	Patients with type I diabetes with albuminuria, $n = 478$	Oral	↓ Angiotensin-converting enzyme/angiotensin II receptor	↓CAC progression
α -Lipoic acid [114]	Calcifying VSMCs treated with Pi	–	↑Mitochondrial function ↑Gas6/Axl/Akt pathway	↓VSMCs apoptosis ↓Aortic calcification
Magnesium [115]	High P-treated VSMCs	–	↓Wnt/ β -cat pathway	↓osteogenic transcripts-Runx2, osterix ↑Calcification inhibitors-MGP, OPG
Magnesium [115]	High P-treated rat aorta	–	↑TRPM7 ↑Pit-1	↓Aortic calcium content
EDTA-tetracycline [99]	Patients, $n = 100$ (CAD)	Chemotherapy	Blood nanobacteria	↓Calcified plaque volume ↗Reversed CAC score
Calcitriol, paricalcitol [116]	Ldlr ^{-/-} mice (CKD)	–	↓PTH levels (via vitamin D receptor activation)	↓Osteogenic genes (at optimal doses)
Biphosphonates (etidronate or pamidronate) [117]	Rats (adenine-induced renal failure)	Subcutaneous injection	↓Hydroxyapatite formation	↓Aortic calcification ↓Bone formation ≈Bone resorption (Pamidronate, 100-fold more potent)
EDTA, STS, DTPA [102]	HA powder Calcified porcine elastin Calcified human aorta	–	Direct Ca removal by chelating action	↗Reversed calcification (Only EDTA and DTPA were effective)
EDTA-loaded PLGA [102]	In vivo, rat abdominal aorta	Local delivery	Direct Ca removal	↗Calcified elastin
BMP-7 [118]	Ldlr ^{-/-} mice (uremic)	Intraperitoneal delivery	–	↓Aortic calcium content ↓Osteogenic marker-osteocalcin
GM6001 [119]	Rats (periadventitial CaCl ₂)	Catheter	↓MMP activity	↓Aortic calcium content

Doxycycline [119]	Rats (Subcutaneous vit D3)	Subcutaneous injection	↓MMP activity	↓Aortic calcium content
Pyrophosphate [120]	Rats (uremic)	Intraperitoneal injection	↓Release of Ca ²⁺ ↓Hydroxyapatite growth	↓Aortic calcium content ≈Bone formation
Sodium thiosulfate [121]	A female patient with calcific uremic arteriolopathy	Intraperitoneal injection	Binds with vascular Ca salts and form highly soluble calcium thiosulfate salt	↻Calcium deposits
Osteoclasts [88]	Ex vivo, calcified aortic elastin	–	–	↻Mineral content
Sevelamer [88]	In vivo, coimplantation of pure elastin with allogenic osteoclasts	Subdermal	–	↓Elastin mineralization ↓Elastin degradation
Sevelamer [88]	Rats (Uremic)	Dietary restriction	↓Circulatory phosphate imbalance ↓Hyperphosphatemia	↓Vascular calcification
Calcitriol withdrawal [122]	Rats (calcitriol-induced VC via intraperitoneal injection)	–	↓PTH levels ↑Calcium reabsorption by macrophages	↻Calcium deposits
Peptide intermedin [123]	Rats (vit D3 + nicotine)	Subcutaneous injection	↑cMGP levels	↓Aortic calcium content ↓ALP activity
Valproic acid [124]	In vitro, β-GP or phosphate-treated; in vivo, rats (chronic renal failure)	–	↑Phosphate-induced autophagy	↓Vascular calcification
Metformin [125]	In vitro, β-GP-treated female rat VSMCs	–	↑AMPK-eNOS-NO pathway	↓Osteoblast specific genes ↑SMCs markers
Teriparatide [92]	Ldlr ^{-/-} mice (diabetic)	Subcutaneous injection	Managing secondary hyperparathyroidism	↓Aortic osteopontin and Msx2 expression

(continued)

Table 20.1 (continued)

Treatments	Experimental/disease-associated VC	Administration route	Mechanisms/targeted pathways	Genotypic/phenotypic outcomes
Quercetin [126]	In vitro, Pi-treated VSMCs; in vivo, rats (adenine-induced VC)	Oral gavage	↓Expression of Drp1 ↓Mitochondrial fission ↓Oxidative stress ↓Pi-induced apoptosis	↓Vascular calcification
NaPi2a inactivation [127]	<i>Klotho</i> ^{-/-} <i>NaPi2a</i> ^{-/-} mice	–	↓Serum phosphate levels	↓Vascular calcification
NaHS [128]	Rat (vit D3 and nicotine treated)	Intraperitoneal injection	↑H ₂ S/CSE pathway	↓Aortic calcium content, ALP activity, and OPG
EDTA-loaded albumin nanoparticles [107]	CaCl ₂ -induced local abdominal aortic calcification	Intravenous injection	Direct Ca removal by chelating action	↔Medial elastic calcification
NH ₄ NO ₃ [129]	Klotho-hypomorphic (<i>Kl/Kl</i>) mice	Drinking water	↓Osteogenic signaling	↓Vessel and other tissue calcification
Fetuin-A [130]	In vitro, VSMCs	–	↓Apoptosis and caspase cleavage	↓Vesicle-mediated VSMCs calcification
Statins [131]	Pi-treated VSMCs	–	↑Gas6/Axl-PI3K/Akt pathway	↓VSMCs apoptosis and calcification
Fetuin-A inactivation [132]	Fetuin-A/ApoE-deficient mice	–	–	↑Atherosclerotic calcification in CKD
Paclitaxel [133]	In vitro, Pi-treated VSMCs; Ex vivo, mouse aorta	–	↑Microtubule stabilization	↓Osteogenic signal ↓Matrix vesicle
FGF21 [134]	Rat VSMCs treated with calcifying medium	–	↑PI3K/Akt pathway ↓P38 ↑OPG/RANKL pathway	↓Mineral deposition ↓Apoptosis
Omentin [135]	Calcifying VSMCs	–	↑PI3K/Akt pathway	↓Osteocalcin, ALP activity, matrix mineralization
Eicosapentaenoic acid [136]	Rats (warfarin/vit K-induced arterial medial calcification)	–	↓Macrophage infiltration ↓MMP-9, and MCP-1	↓Aortic osteogenic markers

3,5,3'-triodothyronine (T3) [137]	Rat VSMCs treated with calcifying medium	-	↑PI3K/Akt pathway	↓Phenotypic transformation of calcified VSMCs
Vit K2 [138]	Rats (Warfarin treated)	Diet	↑Gas6/Axl pathway	↓Aortic calcification and apoptosis
Cinacalcet [139]	Rats (Uremic)	Oral	Managing secondary hyperparathyroidism	↓Runx2, osteocalcin, osteopontin
Atorvastatin [140]	In vitro, TGF-β1-stimulated VSMCs calcification	-	↑β-catenin pathway	↑TGF-β-stimulated calcification
Denosumab [85]	huRANKL-KI mice	Subcutaneous injection	↑Autophagy ↓Receptor activator of NF-κB ligand (RANKL)	↓Vascular calcium deposition
Estrogen [141]	In vitro, HAECs & HASMCs; In vivo, ApoE ^{-/-} mice (ovariectomized)	Osmotic mini pump	↓RANKL signaling ↓BMP pathway	↓Atherosclerotic plaque and calcification ↓Vascular MGP expression
Amlodipine [142]	Rat (warfarin+vit K)	Chow-fed	↓Endothelin signaling	↓Medial elastocalcinosis ↔Medial elastocalcinosis ↔Pulse pressure
Resveratrol [143]	In vitro, Pi-stimulated SMCs; in vivo, Rats (renal failure)	-	↑SIRT1 activation	↓Osteoblastic transdifferentiation
Fibulin-3 [144]	Phosphate-treated HASMCs	-	↓Vascular oxidative stress	↓Calcium deposition ↓Osteochondrogenic markers
Lanthanum carbonate [145]	Rats (renal failure)	Diet	↓Circulatory phosphate imbalance	↓Development of arterial calcification
Tanshinone IIA [146]	Rats (atherosclerosis)	Oral	↓Oxidized low-density lipoprotein	↓Plaque lipid and calcification

(continued)

Table 20.1 (continued)

Treatments	Experimental/disease-associated VC	Administration route	Mechanisms/targeted pathways	Genotypic/phenotypic outcomes
N3 Fatty acids [101]	Bovine calcifying vascular cells	–	↑P38-MAPK and PPAR- γ signaling ↓IL-6	↓Osteoblastic differentiation
Targeted deletion of Msx1 and Msx2 gene [96]	Ldlr ^{-/-} mice (diabetic atherosclerosis)	–	↓Shh and Wnt signaling	↓Aortic calcium ↓Pulse wave velocity or aortic stiffness
Bafilomycin A1, methylamine [147]	Primary HASMCs treated with high phosphate	–	Alkalinization of acidic intracellular compartments	↓ALP activity and calcium content
PHOSPHO1 gene suppression [148]	Pi-treated murine VSMCs	–	↓Phosphatase activity that participate in the matrix vesicle-mediated mineralization	↓VSMCs calcification
LRP6 [95]	Ldlr ^{-/-} mice (diabetic atherosclerosis)	–	↓Noncanonical Wnt signaling	↓Atherosclerotic calcification
AlCl ₃ pretreatment [47]	Rats	Subdermal purified elastin implant	Irreversible binding of Al ions to elastin, resulting in conformational changes	↓Elastin calcification
BB-1101(MMP inhibitor) [45]	Rats	Subdermal purified elastin implant	↓Tenascin C	↓Elastin calcification

Symbol: ↓ decreased or downregulated, ↑ increased or activated, ≈ no change, ↻ reversed

optimizing and managing the dysregulated mineral metabolism and bone turnover diseases, both of which are characteristic to CKD. It should be noted here that the strong relationship between progressing renal dysfunction and increased presence and severity of VC means that primary prevention may potentially have a positive impact on VC. A good number of clinical trials in patients with hypertension and normal renal function have shown that antihypertensive treatments reduce aortic stiffness [70, 71]. Different classes of antihypertensive drugs may have different effects on arterial stiffness. Calcium channel blockers (CCBs), angiotensin-converting enzyme inhibitors (ACEi), and mineralocorticoid receptor antagonists (MCRAs) have a beneficial effect in reducing arterial stiffness and central blood pressure. ACEi, angiotensin receptor blockers (ARBs), and aldosterone antagonists interfere with the renin-angiotensin-aldosterone system (RAAS) and confer benefits on vasculature beyond merely controlling the blood pressure. In a prospective randomized trial with 31 patients having essential hypertension and left ventricular hypertrophy (LVH), the effects of combined therapy of an ARB (Valsartan) and ACEi (Perindopril) were studied and compared with those of respective monotherapies. The findings suggested that compared to respective monotherapies, perindopril and valsartan together exerted more significant favorable effects [72].

Beyond primary prevention using antihypertensives, secondary prevention of VC by correcting hyperphosphatemia and secondary hyperparathyroidism (sHPT), which are universal consequences of renal failure, embodies a central clinical approach. This is accomplished by oral phosphate binders, active vitamin D compounds, calcimimetics, adjusting calcium concentration in the dialysate, and surgical correction of sHPT.

Oral phosphate binders are the mainstay in the management of serum phosphate levels in patients undergoing dialysis. These medications bind to phosphate in the gut, either by forming an insoluble complex or by binding it into a resin and are usually classified as calcium-containing (calcium acetate, calcium carbonate, calcium ketoglutarate, etc.) and calcium-free (magnesium carbonate, lanthanum carbonate, sevelamer hydrochloride, and sevelamer carbonate, etc.). A total of 119 hemodialysis patients with no sign of coronary calcification showed little evidence of disease development over the next 18 months, either on calcium-containing phosphate binders or sevelamer (calcium-free). However, subjects with a history of at least mild coronary calcification had significant progression at 6, 12, and 18 months following treatment with those on calcium-containing phosphate binders showing rapid progression [73].

Ameliorating the effects of sHPT is a vital approach to treat disordered bone and mineral metabolism. Although high parathyroid hormone itself does not correlate positively with and may not cause vascular calcification, its management may help in minimizing hypocalcemia. Management of sHPT is achieved by active vitamin D compounds and calcimimetics. Vitamin D plays an important role in multiple metabolic pathways, including regulation of mineral metabolism. Active vitamin D formulations or vitamin D receptor activators (VDRAs) including calcitriol, alfacalcidol, doxercalciferol, and paricalcitol have been prescribed in the treatment of sHPT in CKD. Hemodialysis and peritoneal dialysis patients who received

VDRA experience better survival outcomes than those who do not, regardless of their PTH levels [74]. Calcitriol, alfacalcidol, and doxercalciferol can effectively lower PTH but have the side effect of heightening gastrointestinal absorption of Ca and P causing an undesirable load [75]. Paricalcitol may preferentially target the parathyroid gland while avoiding the gastrointestinal effect and thus is less associated with VC [76].

Calcimimetics are compounds that mimic the effects of Ca *in vivo*. They can work as a treatment for hyperparathyroidism by binding to calcium-sensing receptors (CaSRs) in the parathyroid glands. By binding to CaSRs, calcimimetics allosterically modulate them to become more sensitive to existing levels of circulating Ca, and they, in turn, suppress the excess secretion of PTH. The only significant randomized study to assess the effects of calcimimetics is the ADVANCE study with cinacalcet which showed that along with the use of VDRA therapy, cinacalcet slowed the progression of VC over VDRA therapy alone in hemodialysis patients [77]. However, a more recent EVOLVE study reported that cinacalcet failed to significantly reduce the risk of death or major cardiovascular events in patients with moderate-to-severe sHPT who were undergoing dialysis [78]. For progressive, biochemically severe, and often symptomatic sHPT, surgical removal of a part of the parathyroid gland, known as parathyroidectomy, may be the treatment of choice. Subtotal parathyroidectomy has been shown to arrest the progression of CAC in dialysis patients [79]. However, total parathyroidectomy was associated with better survival, probably due to decreased cardiovascular mortality [80].

In addition to these preventative treatment strategies, there have been several potential therapies that tried to target the calcification process directly. Pyrophosphate (PPi) is a potent inhibitor of calcium crystallization that circulates at sufficient concentrations to prevent hydroxyapatite formation, thus serves as an endogenous inhibitor of calcification. Besides dialysis patients, humans lacking ectonucleotide pyrophosphorylase (Enpp1), the enzyme that synthesizes extracellular PPi, are also known to develop MAC at an early age. However, rapid hydrolysis of PPi *in vivo* limits this therapy and in turn prompted the development and use of nonhydrolyzable analogs, known as bisphosphonates. They interfere with osteoclasts activity, induce apoptosis, and prevent hydroxyapatite nucleation and growth. Because osteoporosis is highly linked to vascular calcification (VC), bisphosphonates seems a promising therapy to treat VC [81]. However, preventing vascular calcification with systemically delivered bisphosphonates without affecting bone mineralization is a problem due to its strong association with the bone [82]. It may be possible that local therapy would prevent calcification as others have shown that binding bisphosphonates to the bioprosthetic aortic valve tissue prevents its calcification [83].

In patients with different stages of CKD, serum phosphorus is strongly associated with increased vascular calcification and decreased bone strength. Akin to bisphosphonates, osteoprotegerin (OPG) inhibits bone resorption. OPG is a soluble decoy receptor for RANKL. RANKL ligation with RANK receptor (expressed on osteoclasts precursor) is essential for osteoclasts differentiation. OPG-deficient adult and adolescent mice have been found to developed medial calcification in the

aorta and renal arteries along with the decreased overall bone density, suggesting an active role of OPG in vascular calcification [84]. RANKL suppression by denosumab showed reduced accumulation of aortic calcium in glucocorticoid-induced osteoporotic mice [85].

Studies, although small, with etidronate show a beneficial effect in CKD and ESRD patients. In a study with a mean patient age of 63.2 ± 8.2 and mean duration of dialysis of 7.4 ± 5.5 , 35 patients were administered etidronate for 14 days over three cycles. CAC progression in these patients was significantly less pronounced during treatment than compared to the period before treatment was initiated [86]. However, there is still a debate over the efficiency of bisphosphonate therapy, and results differ by the agent in question; different studies suggest a beneficial role of etidronate, pamidronate to a limited extent but not alendronate or ibandronate [87]. Owing to their potential effects on bone formation and accumulation in renal failure because of their clearance by kidneys, bisphosphonates are not recommended as a therapy for the treatment of uremic vascular calcification. Since bone regulation and arterial calcification shares some similarities, studies have been utilized site-specific delivery of autologous or allogenic osteoclasts with a hypothesis that osteoclasts will demineralize calcified elastin without compromising the structural integrity of elastic fibers. The study revealed that osteoclasts can prevent or decalcify elastin, both in vitro and in vivo, while preserving the structural integrity of elastin [88]. However, successful delivery and activation of osteoclasts to the site of calcification remains a challenge. Wu et al. developed a local cell-based therapy to treat ectopic calcification by engineering monocytic precursors that in response to a small molecule turns into osteoclasts. The osteoclastic differentiation is RANKL and M-CSF independent as well as unresponsive to its decoy receptor, osteoprotegerin [89].

Sodium thiosulfate (STS) is a small molecule acting as a vasodilator, antioxidant, and a calcium chelator in vivo. In two preliminary studies with hemodialysis patients, STS was able to delay the progression of CAC after 4–5 months of intravenous administration but with a flipside of decline in bone mineral density of the hip in one study [90, 91]. Additional clinical trials are underway, and at this time, STS is not recommended for use elsewhere.

Finally, teriparatide is a recombinant protein, consisting of a fraction of human parathyroid hormone, particularly the first 34 amino acids from N terminus. It stimulates new bone formation and restores structural defects caused by osteoporosis. Currently, teriparatide is the only FDA-approved medicine to treat osteoporosis. Owing to its regulatory effects of serum phosphate and calcium levels, teriparatide studies have been conducted to uncover its therapeutic role in treating vascular calcification. Shao et al. revealed that teriparatide regulates bone and vascular mineralization process synchronously. In low-density lipoprotein receptor-deficient (*Ldlr^{-/-}*) diabetic mice, subcutaneous injection of teriparatide (5 days/week for 4 weeks) markedly enhanced skeletal osteopontin (OPN) expression and bone mineral content, however suppressed aortic OPN and *Mx2* expression as well as mineral accumulation; suggesting that teriparatide reciprocally regulates bone and vascular calcification in responding to diabetes and dyslipidemia [92].

Prevention of Vascular Calcification in Diabetics

Arterial diseases, such as atherosclerosis, calcium deposition, and elastin loss in the tunica media, are frequent and primary causes of disability and mortality in diabetic patients. The study mentioned in the earlier section by Shao et al. evidenced that teriparatide exerts beneficial effects in regulating early stages of macrovascular complications associated with diabetes and dyslipidemia. In a clinical study with 478 young type I diabetic patients having albuminuria, ACEi/ARB treatment significantly lowered CAC progression over ~2.5 years compared to those without any treatment [72]. Signaling pathways have also been investigated as a way of treating VC in diabetes mellitus. One of the most significant is AGE-RAGE signaling. Activation of advanced glycation end products (AGE) signaling is mediated by its receptor RAGE that has been established to strongly correlate with diabetes-induced femoral artery calcification. An *in vivo* experiment showed that RAGE inhibitors – pyridoxamine and alagebrium – blocked time-dependent AGE deposition in femoral arteries of diabetic rats. Additionally, *ex vivo* study emphasized that inhibiting AGE-RAGE pathways or their downstream signaling molecules reduced diabetes-induced medial arterial calcification [93]. Moreover, NAHS (a hydrogen sulfide donor) treatment mitigated calcification and elastin loss in high glucose-induced calcified human aortic SMCs via inhibiting Stat3/CatS pathway [94].

In diabetic *Ldlr*^{-/-} mice, atherosclerotic calcification was prevented by treating with LRP6 (low-density lipoprotein receptor-related protein 6) that suppressed non-canonical Wnt signaling pathway known for their positive role in promoting osteochondrogenic differentiation [95]. The same diabetic atherosclerotic *Ldlr*^{-/-} mice model was used for targeted deletion of vascular *Msx1*, and *Msx2* (promotes osteogenesis) gene leads to the reduction of atherosclerotic calcification and aortic stiffness coupled with the suppression of multiple Wnt genes [96].

Prevention of Vascular Calcification in Atherosclerosis

Atherosclerotic plaque calcification can be either metastatic (calcification with active osteogenic remodeling or extracellular vesicle release) or dystrophic (necrotic tissue calcification). It is not differentiated very well in the literature, and there are no therapies to just reversing calcification in atherosclerosis.

Most of the studies are looking at modulation of osteogenesis in arteries comprising cartilage/bone formation. Recent research demonstrated that macrophage-specific loss of calcium-permeable ion channel TRPC3 in *Ldlr*^{-/-} mice significantly decreased plaque size, lipid contents, macrophages, as well as a marked reduction of BMP2, Runx2, and phospho-SMAD1/5 in macrophage-rich areas [97]. The effects of ACE inhibition on coronary plaque progression in humans in relation to its calcium content have been investigated in a study named PERSPECTIVE. A substudy of the EUROPA trial, PERSPECTIVE tested the effect of perindopril on

the coronary plaque. Only plaques with a calcium score of 0–25% regressed with perindopril in comparison to a placebo, but plaques with moderate (25–50%) and high (50–100%) calcification progressed equally as in placebo group [98].

Further research has been implemented with EDTA-tetracycline (combined ET) chemotherapy in patients ($n = 100$) with stable coronary artery disease (CAD) and definite coronary artery calcification (CAC) scores. This combined ET therapy lasted for 4 months, and 77 patients completed the entire treatment. As hypothesized, all of the patients were positive for nanobacteria (blood pathogens that are able to trigger inflammation, atherogenesis, thrombus formation, and calcification and participate in CAD progression) serology and/or antigen. In most patients (responders, $n = 44$), CAC scores significantly decreased during combined ET therapy, indicating regression of calcified plaque volume in the coronary artery. Additionally, the patients showed improved angina and lipid profiles with no negative physiological responses [99]. However, the study lacked a control group, and a long-term follow-up study is necessary to see if the disease relapsed in the responders after the completion of chemotherapy.

Dietary intake of N-3 fatty acids (part of fish oil) has been shown to reduce CAC scores in populations that use more fish in their diet [100]. Others have shown that N-3 fatty acids can reduce alkaline phosphatase activity and mineralization of VSMCs [101]. More research and better controlled prospective clinical studies are needed to test if plaque calcification can be prevented. It has been recently hypothesized that any microcalcification either metastatic or dystrophic can cause drastic changes in local mechanical properties of soft arterial tissues and can trigger plaque rupture propagation and intraplaque hemorrhages. Therefore, preventing formation of microcalcification is an important step for preventing plaque rupture. We also hypothesize that elastic lamina breaking is a prerequisite for plaque development, and thus stabilizing or repairing elastic lamina would prevent further plaque development.

Regression of Preexisting Vascular Calcification: Calcium Sequestration

Nearly all studies on calcification mentioned above either act as limiting or preventive measures for further increase in vascular calcification. The remaining calcification in the artery may still create vascular complications. The question remains as to whether patients can be put on medication when they have little to no calcification to prevent its formation. Therefore, it necessitates the new treatment strategies that will efficiently stop and regress existing calcification with fully restoring elastin and arterial function and reverse the disease process. One such process of calcium sequestration by calcium chelators would be a possible option. Chelating agents – ethylenediaminetetraacetic acid (EDTA), diethylenetriaminepentaacetic acid (DTPA), and sodium thiosulfate (STS) – have been tested for their ability to remove

calcium from hydroxyapatite (HA) powder, calcified porcine, and human aorta in ex vivo. Both EDTA and DTPA efficiently removed calcium from HA and calcified aortas while leaving intact elastin architecture during chelation [102]. In vivo animal study further support that EDTA-loaded PLGA (poly(lactic-co-glycolic acid)) nanoparticles delivered via local periaortic regressed elastin-specific aortic calcification [102].

Chelation therapy often involves the injection of the disodium EDTA chemical to chelate or bind calcium, trace elements, and other divalent cations. EDTA binds divalent and some trivalent cations (including calcium, magnesium, lead, cadmium, zinc, iron, aluminum, and copper), to assist cations urinary elimination. The Trial to Assess Chelation Therapy (TACT) was funded by the National Center for Complementary and Alternative Medicine starting in 2003 to determine the safety and effectiveness of EDTA chelation therapy in individuals with coronary artery disease and has been finished since 2013 [103]. Primary published results showed that intravenous chelation therapy with EDTA decreased the risk of adverse cardiovascular outcomes, especially in diabetic patients. However, the study did not test the effect of therapy on vascular calcification. Based on encouraging results, TACT II study is now underway only in the diabetic patients [104]. Unfortunately, this clinical trial is only testing heart function and removal of toxic metals in the urine and not studying coronary calcification score. Moreover, routine chelation therapies have shown many side effects like renal toxicity, hypocalcemia, and bone loss [105]. Chelation therapy is still a controversial topic as no systemic scientific studies have proven its ability to reverse cardiovascular calcification. The treatment of lead toxicity with chelation was first reported with EDTA in the early 1950s [102]. In 1956, the apparent success of EDTA in reducing metastatic calcium deposits led to its treatment for various forms of atherosclerotic disease in angina patients. Over the next decades, EDTA chelation therapy use was added for coronary and peripheral artery diseases [103]. The 2007 National Health Statistics Report showed chelation use had increased by 68% (from 66,000 to 111,000 adults using chelation therapy) since 2002. However, the indications for therapy were not clearly defined.

Targeted Drug Delivery to Degraded Elastin to Reverse Vascular Calcification and Repair Elastin Causing a Return of Homeostasis in Arteries

Bone mineralization and VC have many similarities, and one cannot expect to reduce vascular calcification without affecting bone resorption by systemic therapies. As EDTA systemic therapy shows some promise on reduction of vascular calcification, but still can affect bone density, one intriguing option is to target EDTA directly to the vascular calcification site. From the previous discussion in this chapter, one can think to target vascular calcification by targeting local MMPs or inflammatory cells like macrophages. However, inflammatory cells and enzymes are present in a multitude of conditions and not inherent to the vasculature. Moreover,

inflammation is a dynamic process, and matrix-degrading enzymes are transient and can change with progressive disease conditions. Cellular targeting would deliver drugs to the cytoplasm and not to the extracellular matrix. However, as shown above, elastic lamina is present in all vasculature, and its degradation is a prerequisite in most of the vascular calcifications (intimal atherosclerotic calcification or medial arteriosclerotic calcification); thus it is imperative that if one can find ways to target drugs to this degraded elastic lamina, it is possible to deliver drug locally or site-specifically. Such targeting would require a significantly lower dose of the drug and thus cause lower systemic toxicity and bone resorption. Our group tested this innovative idea. We showed that amorphous elastin core protein is exposed during degradation and provides a suitable target for nanoparticles (NPs) if NPs are decorated on the surface with an antibody that recognizes only this amorphous elastin. This targeting system also offers the advantage of increasing particle retention in the ECM in comparison to cell marker systems [106] that can deliver drugs to cells. Elastin antibody was conjugated to NPs with PEG spacers to improve the circulation time of the nanoparticles (Fig. 20.4).

Site-specific nanoparticle-based targeted EDTA delivery to the calcified aorta could lower the required EDTA dosage compared to systemic EDTA chelation therapy as a result of improved bioavailability and sustained release at the site. Our group has initially developed a targeted delivery of NPs for reversal of elastin-specific medial artery calcification (MAC) that would avoid side effects associated with systemic EDTA chelation therapy like bone loss. We have shown that the NPs coated with elastin antibody that recognizes only degraded elastin and spares healthy nondegraded elastin can be targeted to VC sites in a rat model of calcium chloride-induced vascular calcification (Fig. 20.4) [106]. We developed NPs from the synthetic polymer as poly-lactic acid or biopolymers such as albumin.

Calcium chloride (CaCl_2) injury model was used to create local arterial calcification (located in the abdominal aortic region) in rats. Calcification was allowed to develop for 1 week, and elastin antibody-conjugated EDTA (EL-NP-EDTA)-loaded NPs or IgG antibody-conjugated EDTA (IgG-NP-EDTA)-loaded NPs were injected through the tail vein (10 mg of NPs/kg body weight in 0.1 ml saline). Rats were euthanized 2 weeks after the injection. Within 2 weeks of injections, we observed a complete reversal of calcification from four out of five arteries in EL-NP-EDTA group as confirmed by alizarin red staining, microCT, and quantitative calcium scores. On the other hand, IgG-NP-EDTA-loaded NPs did not deliver EDTA to the site and did not remove any calcium (Fig. 20.5) [107]. Such targeted therapy did not cause any changes in bone morphology or biomechanics.

As we could remove earlier deposits (1 week after injury), we wanted to test if we can remove mineral deposits that is at moderate to late stage. Thus, in the next study, the calcification was allowed to develop for 4 weeks instead of 1 week. Treatment started after 4 weeks and lasted for another 4 weeks [108]. We showed that targeted EDTA therapy removed advanced VC. We also wanted to find out further if, after removal of mineral from fragmented elastin, we could reverse elastin damage. Calcium deposits were successfully removed from the elastin, but the elastin fibers damage was irreversible and EDTA therapy alone was not effective to repair fragmented elastin,

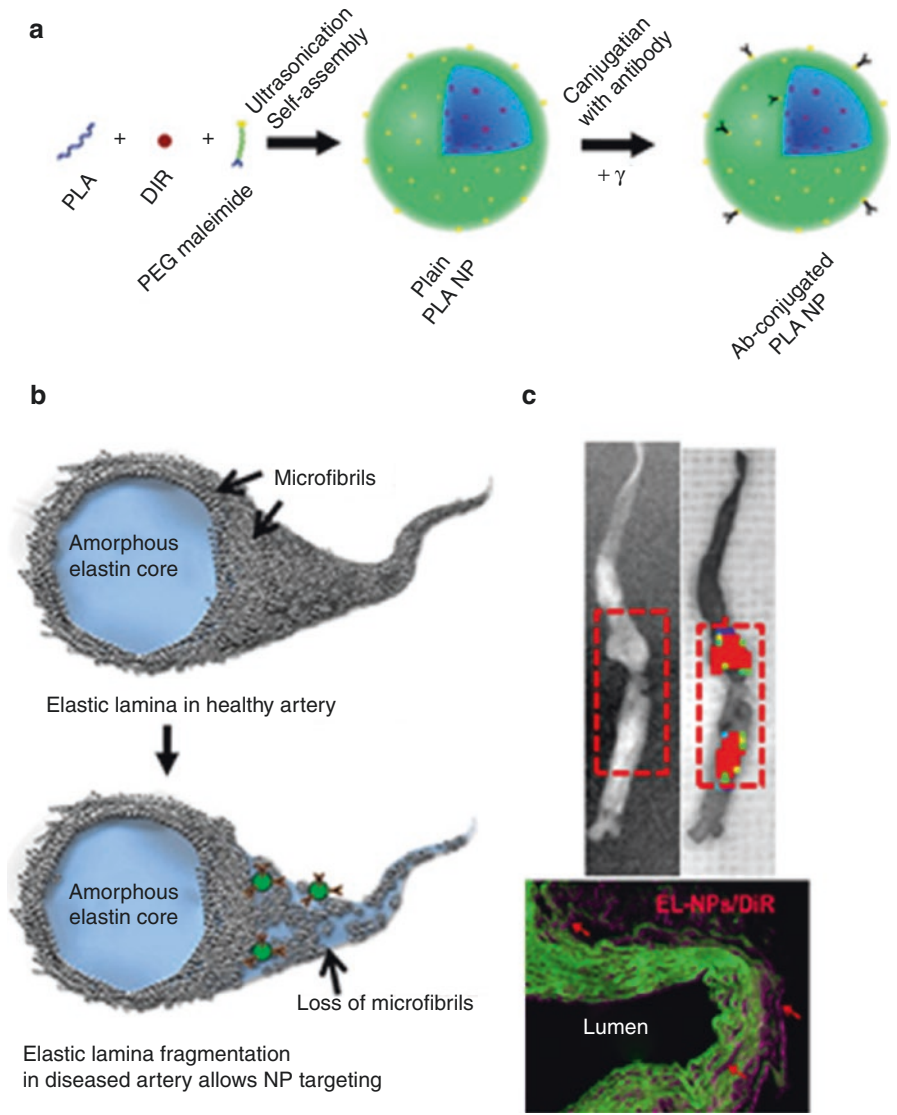


Fig. 20.4 (a) Nanoparticle schematic. Nanoprecipitation method was used to create PLA nanoparticles (NPs). DiR fluorescent dye (red) was incorporated to track particles. Particle surfaces were coated with PEG maleimide groups (PEG as green, maleimide as yellow) where antibodies were bound with thiol chemistry. (b) Elastic lamina fibers schematic. In healthy elastic lamina, core amorphous elastin is coated on the surface with microfibrils such as fibrillins and fibulins. In the diseased state, the microfibrillar proteins degrade along with amorphous elastin, thus exposing core amorphous elastin. NPs coated with antibodies that are specific to core elastin are used to target degraded elastic lamina in the diseased artery while sparing healthy vessel with native elastic lamina [106], (c) NPs can be targeted to the calcification site in CaCl_2 injury rat model. Image on the left is X-ray showing calcification of the aorta, and the image on the right shows DiR dye-loaded NPs target the calcified area. Histology shows NPs (Purple DiR stain) enter aorta from the adventitial side, green autofluorescence of elastin in the aorta. (Reprinted with permission)

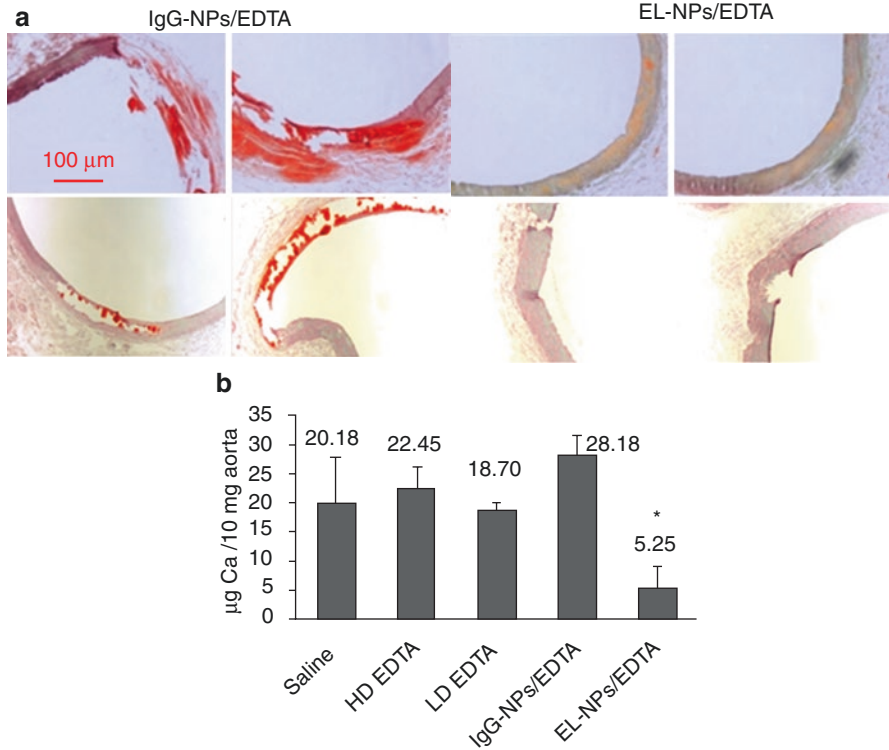


Fig. 20.5 Evaluation of aortic calcification for both systemic EDTA chelation therapy and targeted EDTA chelation therapy. (a) Aortic calcification evaluated by Alizarin red stain for control IgG antibody-coated and EDTA-loaded NPs (IgG-NPs-EDTA) does not remove calcium deposits, and elastin antibody-coated and EDTA-loaded NPs (EL-NPs-EDTA) group shows removal of calcium deposits ($n = 5$) [107], the quantitative data corroborates histology results, and HD EDTA and LD EDTA are systemic EDTA alone delivery. (Reprinted with permission)

suggesting that elastin degradation at the site of injury was persistent even after removal of mineral and needs another therapy to regenerate elastic lamina. To repair elastic lamina after removal of calcification, we tested the dual therapy of EL-NP-EDTA + EL-NP-PGG. Pentagalloyl glucose (PGG) has been previously shown to regenerate lost elastin [109] and could serve as an effective treatment option for early-to middle-stage aneurysms in order to prevent disease progression [108]. We could first deliver EDTA-loaded NPs and then follow them with PGG-loaded NPs. This dual therapy not only removed vascular calcification but also restored elastic lamina and improved vascular function (Fig. 20.6) [108]. When PGG was delivered, we observed an increase in desmosine content in the dual therapy of EL-NP-EDTA + EL-NP-PGG group compared to EL-NP-EDTA group alone. Histological staining (Verhoeff-Van Gieson) demonstrated complete restoration of the elastic lamina in a dual therapy group (Fig. 20.7). The dual therapy group also showed suppression of local inflammation, reduction of MMPs, and restoration of VSMC phenotype and improved

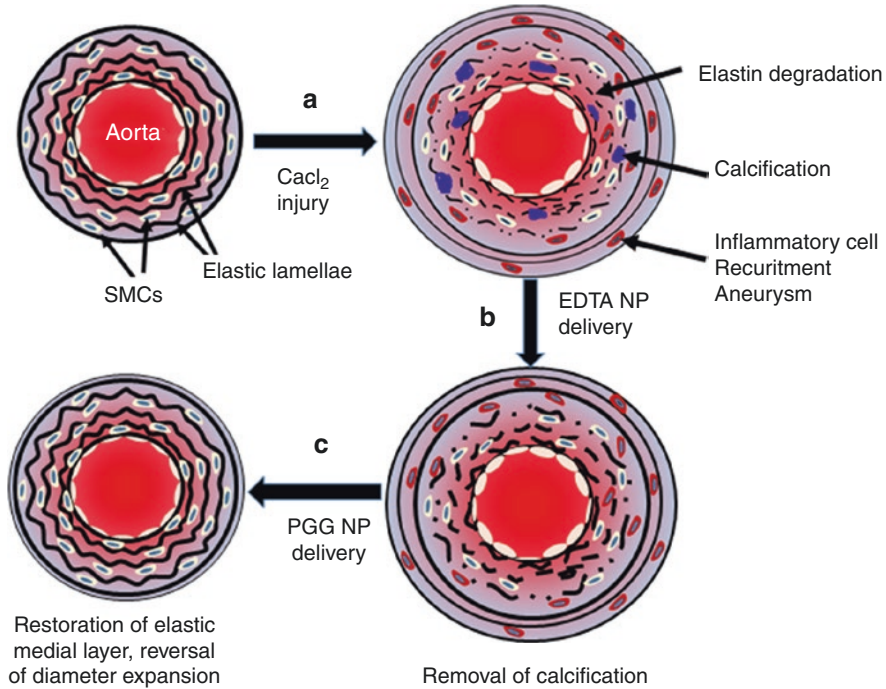


Fig. 20.6 Dual nanoparticle therapy reverses calcification and aneurysms: (A) Rat abdominal aorta 30 days after CaCl_2 injury shows degradation of elastic lamina, loss of SMCs, calcification (purple), adventitial inflammation (red cells), and diameter expansion and aneurysm development; (B) Systemic EDTA-loaded nanoparticle therapy that is targeted to aneurysmal site by tagging with elastin antibody that recognizes degraded elastin removed calcification (purple) from the aorta; (C) further systemic PGG-loaded nanoparticles delivered PGG to the aneurysm site and reversed aneurysmal expansion and inflammation and restored elastic lamina and SMCs [108]

mechanical property of the artery. Systemic inflammation was also reduced most probably due to further inhibition of elastin degradation and generation of EDPs [108]. These results clearly demonstrated that our therapeutic approach could not only remove calcium but could also repair the vascular damage.

Although proof of concept studies were exciting to show that we can now deliver drugs to the site of elastic lamina damage, the calcium chloride-induced VC model was not considered clinically relevant to CKD as blood chemistry of these animals was normal. To show such therapies can work for CKD patients, we wanted to study this therapy in animal models of CKD. Several research groups have used the adenine diet rat model for studying mechanisms of MAC in the context of CKD. Feeding rats with adenine causes kidney failure. Renal pathology of this model mimics the clinical situation with the development of hyperphosphatemia, hypocalcemia, severe secondary hyperparathyroidism, and other biochemical changes such as elevated serum creatinine and elevated blood urea nitrogen that lead to vascular calcification similar to what is observed in CKD patients. In this adenine rat model, we

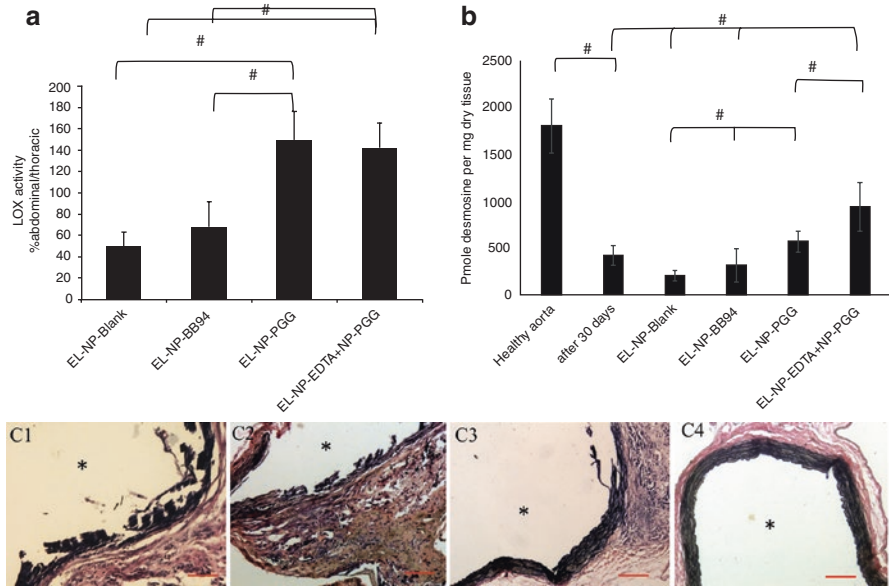


Fig. 20.7 (a) LOX activity in the abdominal part (CaCl₂ injured) over the thoracic aorta (non-injured, healthy), showing that LOX activity was reduced in the EL-NP-Blank and EL-NP-BB94 groups. The EL-NP-PGG and EL-NP-EDTA+EL-NP-PGG groups showed increased LOX; both are significantly higher than the EL-NP-Blank and EL-NP-BB94 groups. (b) Desmosine content of aorta 30 days post-injury and in the four NP groups was compared to the healthy non-injured abdominal aorta. CaCl₂ injury caused a substantial decrease in desmosine. Desmosine content was not improved after delivery of blank or BB-94-loaded NPs (EL-NP-Blank or EL-NP-BB94). The EL-NP-EDTA+EL-NP-PGG group showed the highest desmosine content among the four groups [108]. (Reprinted with permission)

demonstrated that NPs loaded with EDTA and targeted to calcified aorta effectively removed calcification as confirmed by in vivo ultrasound, whole-mount aorta alizarin red stain, histology with von Kossa stain, and quantitative calcium levels [110]. Surprisingly, when rats were allowed to survive after stopping the NP therapy (EDTA-NPs-LT), calcification continued to decrease and did not reoccur (Fig. 20.8). We are currently testing if we can repair arteries and prevent further vascular disease despite the presence of CKD in these animals.

Summary

Elastic laminae are an essential component of healthy arteries. Elastin biosynthesis is a complex process with many proteins involved in the elastic fiber formation. Once formed, elastic fibers have a long half-life and low remodeling potential. During aging and vascular diseases, loss and fragmentation of elastic fibers and degradation of elastin are hallmarks of disease progression. Imbalance of MMPs

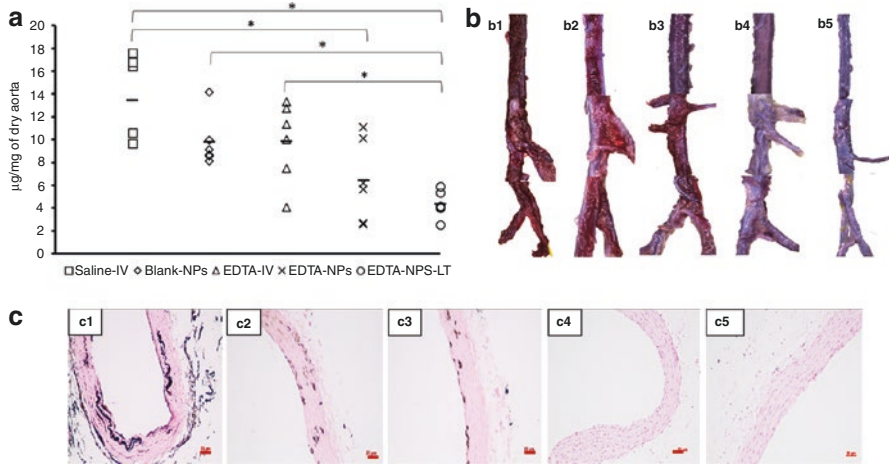


Fig. 20.8 Reversal of calcification in CKD model by EDTA nanoparticle therapy; **(a)** calcium quantification in the aortas of all the treatment groups. Saline-IV group showed the maximum amount of calcium per aortic dry weight. Blank-NPs and EDTA-IV groups did not show significantly reduced calcium levels. Both EDTA-NPs and EDTA-NPs-LT groups show a significant reduction in calcium compared to saline-IV group. **(b)** Whole-mount aortas stained with Alizarin red S to visualize calcium indicated that saline-IV **(b1)** and blank NPs **(b2)** group have bright red staining for Ca while slightly reduced red staining in the EDTA-IV group **(b3)**. Alizarin red stain is completely absent in EDTA-NPs **(b4)** and EDTA-NPs-LT groups **(b5)**. **(c)** Paraffin-embedded sections of the aortas stained with von Kossa stain (black) revealed Ca deposits in saline-IV **(c1)** and blank NPs groups **(c2)** along the degraded elastic lamina, and these calcium deposits were slightly reduced in EDTA-IV group **(c3)**. EDTA-NPs **(c4)** and EDTA-NPs-LT groups **(c5)** showed no calcium deposits. Scale bar 50 µm [110]. (Reprinted with permission)

and TIMPs and cathepsins can tilt the scales to elastic fiber degradation. The fragmentation of elastic lamina can lead to loss of cellular homeostasis. Contractile VSMCs differentiate into synthetic phenotypes and can proliferate causing intimal hyperplasia. Elastin-derived peptides are chemotactic to the inflammatory cells and can exacerbate the inflammation process. Elastin-derived peptides and TGF- β released due to loss of elastin-associated LTPB trigger VSMC differentiation into osteoblast-like cells that can secrete extracellular vesicles and cause vascular calcification. Loss of inhibitory molecules in the elastin matrix such as fibrillins and MAGPs can allow calcium deposition on elastic fibers. This process is hastened in diabetic condition due to oxidative damage and advanced glycation end products (AGEs) and in CKD that causes hyperphosphatemia, hypocalcemia, and severe secondary hyperparathyroidism. Many researchers have investigated methods to halt the calcification process by a variety of agents given systemically. Since these agents are not targeted to the vascular calcification sites, side effects do exist for such treatments. Because elastic lamina fragmentation and exposure of amorphous elastin is found in every vascular condition, we developed a nanoparticle-based delivery approach that only targets these drug-loaded nanoparticles to the site of elastin degradation while sparing healthy elastic lamina. By virtue of the close

proximity of collagen and elastin fibers, there is a potentially significant side benefit of removing calcification from collagen fibers as well. Such therapy has allowed us to target calcium-sequestering molecules such as EDTA to the medial calcification sites in two different animal models. We showed that such treatment can reverse already developed vascular calcification. We further show that after removal of calcium deposits, we were able to target polyphenol PGG to the site of elastin damage, and it can repair elastic lamina, decrease local and systemic inflammation, and allow VSMCs to return to their normal phenotype. Such targeted therapies are attractive for clinical translation.

Acknowledgments This work was funded in part by the National Institutes of Health (NIH) grants (R01HL145064, R01HL133662, P30GM131959, P20GM103444) and Hunter Endowment at Clemson University to NRV. Authors also acknowledge constructive discussion with Douglas Mulhall for preparation of this manuscript.

References

1. Ketteler M, Schlieper G, Floege J. Calcification and cardiovascular health – new insights into an old phenomenon. *Hypertension*. 2006;47(6):1027–34.
2. Schlieper G, Schurgers L, Brandenburg V, Reutelingsperger C, Floege J. Vascular calcification in chronic kidney disease: an update. *Nephrol Dial Transplant*. 2015;31:31.
3. Schlieper G, Hess K, Floege J, Marx N. The vulnerable patient with chronic kidney disease. *Nephrol Dial Transplant*. 2015;31:382.
4. Moe SM, Chen NX. Mechanisms of vascular calcification in chronic kidney disease. *J Am Soc Nephrol*. 2008;19(2):213–6.
5. Lehto S, Niskanen L, Suhonen M, Rönnemaa T, Laakso M. Medial artery calcification: a neglected harbinger of cardiovascular complications in non–insulin-dependent diabetes mellitus. *Arterioscler Thromb Vasc Biol*. 1996;16(8):978–83.
6. Lanzer P, Boehm M, Sorribas V, Thiriet M, Janzen J, Zeller T, et al. Medial vascular calcification revisited: review and perspectives. *Eur Heart J*. 2014;35(23):1515–U24.
7. Mizobuchi M, Towler D, Slatopolsky E. vascular calcification: the killer of patients with chronic kidney disease. *J Am Soc Nephrol*. 2009;20(7):1453–64.
8. Rogers M, Goettsch C, Aikawa E. Medial and intimal calcification in chronic kidney disease: stressing the contributions. *Am Heart Assoc*. 2013;2:e000481.
9. Savage T, Clarke AL, Giles M, Tomson CR, Raine AE. Calcified plaque is common in the carotid and femoral arteries of dialysis patients without clinical vascular disease. *Nephrol Dial Transplant*. 1998;13(8):2004–12.
10. London GM, Guerin AP, Marchais SJ, Metivier F, Pannier B, Adda H. Arterial media calcification in end-stage renal disease: impact on all-cause and cardiovascular mortality. *Nephrol Dial Transplant*. 2003;18(9):1731–40.
11. Blausen S.com staff. Medical gallery of Blausen Medical 2014. *WikiJ Med*. 2014;1(2):10.
12. Cociolone AJ, Hawes JZ, Staiculescu MC, Johnson EO, Murshed M, Wagenseil JE. Elastin, arterial mechanics, and cardiovascular disease. *Am J Physiol Heart Circ Physiol*. 2018;315(2):H189–205.
13. Dingemans KP, Teeling P, Lagendijk JH, Becker AE. Extracellular matrix of the human aortic media: an ultrastructural histochemical and immunohistochemical study of the adult aortic media. *Anat Rec*. 2000;258(1):1–14.
14. El-Hamamsy I, Yacoub MH. Cellular and molecular mechanisms of thoracic aortic aneurysms. *Nat Rev Cardiol*. 2009;6(12):771.

15. Wolinsky H. Comparison of medial growth of human thoracic and abdominal aortas. *Circ Res.* 1970;27(4):531–8.
16. Karnik SK, Wythe JD, Sorensen L, Brooke BS, Urness LD, Li DY. Elastin induces myofibrillogenesis via a specific domain, VGVAPG. *Matrix Biol.* 2003;22(5):409–25.
17. Maleszewski J, Lai C, Veinot J. Anatomic considerations and examination of cardiovascular specimens (excluding devices). In: *Cardiovascular pathology*. New York: Elsevier; 2016. p. 1–56.
18. Cecelja M, Chowiecnyk P. Role of arterial stiffness in cardiovascular disease. *JRSM Cardiovasc Dis.* 2012;1(4):1–10.
19. Kim J, Staiculescu MC, Cociolone AJ, Yanagisawa H, Mecham RP, Wagenseil JE. Crosslinked elastic fibers are necessary for low energy loss in the ascending aorta. *J Biomech.* 2017;61:199–207.
20. Lacolley P, Regnault V, Segers P, Laurent S. Vascular smooth muscle cells and arterial stiffening: relevance in development, aging, and disease. *Physiol Rev.* 2017;97(4):1555–617.
21. Sage H, Gray W. Studies on the evolution of elastin – I. Phylogenetic distribution. *Comp Biochem Physiol B.* 1979;64(4):313–27.
22. Wagenseil JE, Mecham RP. Elastin in large artery stiffness and hypertension. *J Cardiovasc Transl Res.* 2012;5(3):264–73.
23. Parks WC, Secrist H, Wu LC, Mecham R. Developmental regulation of tropoelastin isoforms. *J Biol Chem.* 1988;263(9):4416–23.
24. Phinikaridou A, Lacerda S, Lavin B, Andia ME, Smith A, Saha P, et al. Tropoelastin: a novel marker for plaque progression and instability. *Circ Cardiovasc Imaging.* 2018;11(8):e007303.
25. Krettek A, Sukhova GK, Libby P. Elastogenesis in human arterial disease: a role for macrophages in disordered elastin synthesis. *Arterioscler Thromb Vasc Biol.* 2003;23(4):582–7.
26. Greenwald S. Ageing of the conduit arteries. *J Pathol.* 2007;211(2):157–72.
27. Asmar R, Benetos A, Topouchian J, Laurent P, Pannier B, Brisac A-M, et al. Assessment of arterial distensibility by automatic pulse wave velocity measurement: validation and clinical application studies. *Hypertension.* 1995;26(3):485–90.
28. Kielty CM, Sherratt MJ, Shuttleworth CA. Elastic fibres. *J Cell Sci.* 2002;115(14):2817–28.
29. Hungerford JE, Owens GK, Argraves WS, Little CD. Development of the aortic vessel wall as defined by vascular smooth muscle and extracellular matrix markers. *Dev Biol.* 1996;178(2):375–92.
30. Argraves WS, Greene LM, Cooley MA, Gallagher WM. Fibulins: physiological and disease perspectives. *EMBO Rep.* 2003;4(12):1127–31.
31. Vrhovski B, Weiss AS. Biochemistry of tropoelastin. *Eur J Biochem.* 1998;258(1):1–18.
32. Starcher BC. Determination of the elastin content of tissues by measuring desmosine and isodesmosine. *Anal Biochem.* 1977;79(1–2):11–5.
33. Pereira L, Andrikopoulos K, Tian J, Lee SY, Keene DR, Ono R, et al. Targetting of the gene encoding fibrillin–1 recapitulates the vascular aspect of Marfan syndrome. *Nat Genet.* 1997;17(2):218.
34. Zhang H, Hu W, Ramirez F. Developmental expression of fibrillin genes suggests heterogeneity of extracellular microfibrils. *J Cell Biol.* 1995;129(4):1165–76.
35. Pereira L, Lee SY, Gayraud B, Andrikopoulos K, Shapiro SD, Bunton T, et al. Pathogenetic sequence for aneurysm revealed in mice underexpressing fibrillin-1. *Proc Natl Acad Sci.* 1999;96(7):3819–23.
36. Sherratt MJ. Tissue elasticity and the ageing elastic fibre. *Age (Dordr).* 2009;31(4):305–25.
37. Massam-Wu T, Chiu M, Choudhury R, Chaudhry SS, Baldwin AK, McGovern A, et al. Assembly of fibrillin microfibrils governs extracellular deposition of latent TGF β . *J Cell Sci.* 2010;123(17):3006–18.
38. Robertson IB, Rifkin DB. Regulation of the bioavailability of TGF- β and TGF- β -related proteins. *Cold Spring Harb Perspect Biol.* 2016;8(6):a021907.
39. Luo G, Ducy P, McKee MD, Pinero GJ, Loyer E, Behringer RR, et al. Spontaneous calcification of arteries and cartilage in mice lacking matrix GLA protein. *Nature.* 1997;386(6620):78.

40. Urry D. Neutral sites for calcium ion binding to elastin and collagen: a charge neutralization theory for calcification and its relationship to atherosclerosis. *Proc Natl Acad Sci.* 1971;68(4):810–4.
41. Sinha A, Vyavahare NR. High-glucose levels and elastin degradation products accelerate osteogenesis in vascular smooth muscle cells. *Diab Vasc Dis Res.* 2013;10(5):410–9.
42. Duca L, Floquet N, Alix AJ, Haye B, Debelle L. Elastin as a matrikine. *Crit Rev Oncol Hematol.* 2004;49(3):235–44.
43. Blaise S, Romier B, Kawecki C, Ghirardi M, Rabenoelina F, Baud S, et al. Elastin-derived peptides are new regulators of insulin resistance development in mice. *Diabetes.* 2013;62(11):3807–16.
44. Simionescu D, Simionescu A, Deac R. Detection of remnant proteolytic activities in unimplanted glutaraldehyde-treated bovine pericardium and explanted cardiac bioprostheses. *J Biomed Mater Res.* 1993;27(6):821–9.
45. Vyavahare N, Jones PL, Tallapragada S, Levy RJ. Inhibition of matrix metalloproteinase activity attenuates tenascin-C production and calcification of implanted purified elastin in rats. *Am J Pathol.* 2000;157(3):885–93.
46. Wang M, Kim SH, Monticone RE, Lakatta EG. Matrix metalloproteinases promote arterial remodeling in aging, hypertension, and atherosclerosis. *Hypertension.* 2015;65(4):698–703.
47. Vyavahare N, Ogle M, Schoen FJ, Levy RJ. Elastin calcification and its prevention with aluminum chloride pretreatment. *Am J Pathol.* 1999;155(3):973–82.
48. Basalyga DM, Simionescu DT, Xiong W, Baxter BT, Starcher BC, Vyavahare NR. Elastin degradation and calcification in an abdominal aorta injury model: role of matrix metalloproteinases. *Circulation.* 2004;110(22):3480–7.
49. Lemaître V, Soloway PD, D'Armiento J. Increased medial degradation with pseudo-aneurysm formation in apolipoprotein E–knockout mice deficient in tissue inhibitor of metalloproteinases-1. *Circulation.* 2003;107(2):333–8.
50. Sukhova GK, Wang B, Libby P, Pan J-H, Zhang Y, Grubb A, et al. Cystatin C deficiency increases elastic lamina degradation and aortic dilatation in apolipoprotein E–null mice. *Circ Res.* 2005;96(3):368–75.
51. Cheng XW, Huang Z, Kuzuya M, Okumura K, Murohara T. Cysteine protease cathepsins in atherosclerosis-based vascular disease and its complications. *Hypertension.* 2011;58(6):978–86.
52. Fonovic M, Turk B. Cysteine cathepsins and extracellular matrix degradation. *Biochim Biophys Acta.* 2014;1840(8):2560–70.
53. Aikawa E, Aikawa M, Libby P, Figueiredo JL, Rusanescu G, Iwamoto Y, et al. Arterial and aortic valve calcification abolished by elastolytic cathepsin S deficiency in chronic renal disease. *Circulation.* 2009;119(13):1785–94.
54. Andrault P-M, Panwar P, Mackenzie NC, Brömme D. Elastolytic activity of cysteine cathepsins K, S, and V promotes vascular calcification. *Sci Rep.* 2019;9(1):9682.
55. New SE, Goettsch C, Aikawa M, Marchini JF, Shibasaki M, Yabusaki K, et al. Macrophage-derived matrix vesicles: an alternative novel mechanism for microcalcification in atherosclerotic plaques. *Circ Res.* 2013;113(1):72–7.
56. Hutcheson JD, Goettsch C, Bertazzo S, Maldonado N, Ruiz JL, Goh W, et al. Genesis and growth of extracellular-vesicle-derived microcalcification in atherosclerotic plaques. *Nat Mater.* 2016;15(3):335.
57. Dale MA, Xiong W, Carson JS, Suh MK, Karpisek AD, Meisinger TM, et al. Elastin-derived peptides promote abdominal aortic aneurysm formation by modulating M1/M2 macrophage polarization. *J Immunol.* 2016;196(11):4536–43.
58. Matt P, Schoenhoff F, Habashi J, Holm T, Van Erp C, Loch D, et al. Circulating TGF β in Marfan's syndrome. *Circulation.* 2009;120(6):526.
59. Hanada K, Vermeij M, Garinis GA, De Waard MC, Kunen MG, Myers L, et al. Perturbations of vascular homeostasis and aortic valve abnormalities in fibulin-4 deficient mice. *Circ Res.* 2007;100(5):738–46.

60. Bouvet C, Moreau S, Blanchette J, de Blois D, Moreau P. Sequential activation of matrix metalloproteinase 9 and transforming growth factor β in arterial elastocalcinos. *Arterioscler Thromb Vasc Biol.* 2008;28(5):856–62.
61. Lansing AI, Alex M, Rosenthal TB. Calcium and elastin in human arteriosclerosis. *J Gerontol.* 1950;5(2):112–9.
62. Bobryshev YV. Calcification of elastic fibers in human atherosclerotic plaque. *Atherosclerosis.* 2005;180(2):293–303.
63. Gayral S, Garnotel R, Castaing-Berthou A, Blaise S, Fougerat A, Berge E, et al. Elastin-derived peptides potentiate atherosclerosis through the immune Neu1–PI3K γ pathway. *Cardiovasc Res.* 2013;102(1):118–27.
64. Galis ZS, Khatri JJ. Matrix metalloproteinases in vascular remodeling and atherogenesis: the good, the bad, and the ugly. *Circ Res.* 2002;90(3):251–62.
65. Sukhova GK, Shi G-P, Simon DI, Chapman HA, Libby P. Expression of the elastolytic cathepsins S and K in human atheroma and regulation of their production in smooth muscle cells. *J Clin Invest.* 1998;102(3):576–83.
66. Rodgers KJ, Watkins DJ, Miller AL, Chan PY, Karanam S, Brissette WH, et al. Destabilizing role of cathepsin S in murine atherosclerotic plaques. *Arterioscler Thromb Vasc Biol.* 2006;26(4):851–6.
67. Li DY, Brooke B, Davis EC, Mecham RP, Sorensen LK, Boak BB, et al. Elastin is an essential determinant of arterial morphogenesis. *Nature.* 1998;393(6682):276.
68. Bennett MR, Sinha S, Owens GK. Vascular smooth muscle cells in atherosclerosis. *Circ Res.* 2016;118(4):692–702.
69. Pai AS, Giachelli CM. Matrix remodeling in vascular calcification associated with chronic kidney disease. *J Am Soc Nephrol.* 2010;21(10):1637–40.
70. Dudenbostel T, Glasser SP. Effects of antihypertensive drugs on arterial stiffness. *Cardiol Rev.* 2012;20(5):259.
71. Rattazzi M, Bertacco E, Puato M, Faggini E, Pualetto P. Hypertension and vascular calcification: a vicious cycle? *J Hypertens.* 2012;30(10):1885–93.
72. Maahs DM, Snell-Bergeon JK, Kinney GL, Wadwa RP, Garg S, Ogden LG, et al. ACE-I/ARB treatment in type 1 diabetes patients with albuminuria is associated with lower odds of progression of coronary artery calcification. *J Diabetes Complicat.* 2007;21(5):273–9.
73. Block GA, Spiegel DM, Ehrlich J, Mehta R, Lindbergh J, Dreisbach A, et al. Effects of sevelamer and calcium on coronary artery calcification in patients new to hemodialysis. *Kidney Int.* 2005;68(4):1815–24.
74. Teng M, Wolf M, Lowrie E, Ofsthun N, Lazarus JM, Thadhani R. Survival of patients undergoing hemodialysis with paricalcitol or calcitriol therapy. *N Engl J Med.* 2003;349(5):446–56.
75. Tentori F, Hunt W, Stidley C, Rohrscheib M, Bedrick E, Meyer K, et al. Mortality risk among hemodialysis patients receiving different vitamin D analogs. *Kidney Int.* 2006;70(10):1858–65.
76. Sprague SM, Llach F, Amdahl M, Taccetta C, Batlle D. Paricalcitol versus calcitriol in the treatment of secondary hyperparathyroidism. *Kidney Int.* 2003;63(4):1483–90.
77. Raggi P, Chertow GM, Torres PU, Csiky B, Naso A, Nossuli K, et al. The ADVANCE study: a randomized study to evaluate the effects of cinacalcet plus low-dose vitamin D on vascular calcification in patients on hemodialysis. *Nephrol Dial Transplant.* 2010;26(4):1327–39.
78. Investigators ET. Effect of cinacalcet on cardiovascular disease in patients undergoing dialysis. *N Engl J Med.* 2012;367(26):2482–94.
79. Bleyer AJ, Burkart J, Piazza M, Russell G, Rohr M, Carr JJ. Changes in cardiovascular calcification after parathyroidectomy in patients with ESRD. *Am J Kidney Dis.* 2005;46(3):464–9.
80. Iwamoto N, Sato N, Nishida M, Hashimoto T, Kobayashi H, Yamasaki S, et al. Total parathyroidectomy improves survival of hemodialysis patients with secondary hyperparathyroidism. *J Nephrol.* 2012;25(5):755–63.
81. Price PA, Faus SA, Williamson MK. Bisphosphonates alendronate and ibandronate inhibit artery calcification at doses comparable to those that inhibit bone resorption. *Arterioscler Thromb Vasc Biol.* 2001;21(5):817–24.

82. Neven EG, De Broe ME, d'Haese PC. Prevention of vascular calcification with bisphosphonates without affecting bone mineralization: a new challenge? *Kidney Int.* 2009;75(6):580–2.
83. Rapoport HS, Connolly JM, Fulmer J, Dai N, Murti BH, Gorman RC, et al. Mechanisms of the in vivo inhibition of calcification of bioprosthetic porcine aortic valve cusps and aortic wall with triglycidylamine/mercapto bisphosphonate. *Biomaterials.* 2007;28(4):690–9.
84. Bucay N, Sarosi I, Dunstan CR, Morony S, Tarpley J, Capparelli C, et al. Osteoprotegerin-deficient mice develop early onset osteoporosis and arterial calcification. *Genes Dev.* 1998;12(9):1260–8.
85. Helas S, Goetsch C, Schoppet M, Zeitz U, Hempel U, Morawietz H, et al. Inhibition of receptor activator of NF- κ B ligand by denosumab attenuates vascular calcium deposition in mice. *Am J Pathol.* 2009;175(2):473–8.
86. Nitta K, Akiba T, Suzuki K, Uchida K, Watanabe R-I, Majima K, et al. Effects of cyclic intermittent etidronate therapy on coronary artery calcification in patients receiving long-term hemodialysis. *Am J Kidney Dis.* 2004;44(4):680–8.
87. Toussaint ND, Lau KK, Strauss BJ, Polkinghorne KR, Kerr PG. Effect of alendronate on vascular calcification in CKD stages 3 and 4: a pilot randomized controlled trial. *Am J Kidney Dis.* 2010;56(1):57–68.
88. Simpson CL, Lindley S, Eisenberg C, Basalyga DM, Starcher BC, Simionescu DT, et al. Toward cell therapy for vascular calcification: osteoclast-mediated demineralization of calcified elastin. *Cardiovasc Pathol.* 2007;16(1):29–37.
89. Wu M, Rementer C, Giachelli CM. Vascular calcification: an update on mechanisms and challenges in treatment. *Calcif Tissue Int.* 2013;93(4):365–73.
90. Adirekkit S, Sumethkul V, Ingsathit A, Domrongkitchaiporn S, Phakdeekitcharoen B, Kantachavesiri S, et al. Sodium thiosulfate delays the progression of coronary artery calcification in haemodialysis patients. *Nephrol Dial Transplant.* 2010;25(6):1923–9.
91. Mathews SJ, De Las FL, Podaralla P, Cabellon A, Zheng S, Bierhals A, et al. Effects of sodium thiosulfate on vascular calcification in end-stage renal disease: a pilot study of feasibility, safety and efficacy. *Am J Nephrol.* 2011;33(2):131–8.
92. Shao J-S, Cheng S-L, Charlton-Kachigian N, Loewy AP, Towler DA. Teriparatide (human parathyroid hormone (1–34)) inhibits osteogenic vascular calcification in diabetic low density lipoprotein receptor-deficient mice. *J Biol Chem.* 2003;278(50):50195–202.
93. Brodeur MR, Bouvet C, Bouchard S, Moreau S, Leblond J, deBlois D, et al. Reduction of advanced-glycation end products levels and inhibition of RAGE signaling decreases rat vascular calcification induced by diabetes. *PLoS ONE.* 2014;9(1):e85922.
94. Zhou Y-B, Zhou H, Li L, Kang Y, Cao X, Wu Z-Y, et al. Hydrogen sulfide prevents elastin loss and attenuates calcification induced by high glucose in smooth muscle cells through suppression of Stat3/Cathepsin S signaling pathway. *Int J Mol Sci.* 2019;20(17):4202.
95. Cheng S-L, Ramachandran B, Behrmann A, Shao J-S, Mead M, Smith C, et al. Vascular smooth muscle LRP6 limits arteriosclerotic calcification in diabetic LDLR $^{-/-}$ mice by restraining noncanonical Wnt signals. *Circ Res.* 2015;117(2):142–56.
96. Cheng S-L, Behrmann A, Shao J-S, Ramachandran B, Krcma K, Arredondo YB, et al. Targeted reduction of vascular Msx1 and Msx2 mitigates arteriosclerotic calcification and aortic stiffness in LDLR-deficient mice fed diabetogenic diets. *Diabetes.* 2014;63(12):4326–37.
97. Dube PR, Chikkamenahalli LL, Birnbaumer L, Vazquez G. Reduced calcification and osteogenic features in advanced atherosclerotic plaques of mice with macrophage-specific loss of TRPC3. *Atherosclerosis.* 2018;270:199–204.
98. Bruining N, de Winter S, Roelandt JR, Rodriguez-Granillo GA, Heller I, van Domburg RT, et al. Coronary calcium significantly affects quantitative analysis of coronary ultrasound: importance for atherosclerosis progression/regression studies. *Coron Artery Dis.* 2009;20(6):409–14.
99. Maniscalco BS, Taylor KA. Calcification in coronary artery disease can be reversed by EDTA-tetracycline long-term chemotherapy. *Pathophysiology.* 2004;11(2):95–101.
100. Otto CM. Heartbeat: highlights from this issue. *BMJ: Publishing Group Ltd./British Cardiovascular Society;* 2015.

101. Abedin M, Lim J, Tang T, Park D, Demer L, Tintut Y. N-3 fatty acids inhibit vascular calcification via the p38-mitogen-activated protein kinase and peroxisome proliferator-activated receptor- γ pathways. *Circ Res*. 2006;98(6):727–9.
102. Lei Y, Grover A, Sinha A, Vyavahare N. Efficacy of reversal of aortic calcification by chelating agents. *Calcif Tissue Int*. 2013;93(5):426–35.
103. Lamas GA, Goertz C, Boineau R, Mark DB, Rozema T, Nahin RL, et al. Effect of disodium EDTA chelation regimen on cardiovascular events in patients with previous myocardial infarction: the TACT randomized trial. *JAMA*. 2013;309(12):1241–50.
104. Escolar E, Lamas GA, Mark DB, Boineau R, Goertz C, Rosenberg Y, et al. The effect of an EDTA-based chelation regimen on patients with diabetes mellitus and prior myocardial infarction in the trial to assess chelation therapy (TACT). *Circulation*. 2014;7(1):15–24.
105. Atwood KC IV, Woeckner E, Baratz RS, Sampson WI. Why the NIH trial to assess chelation therapy (TACT) should be abandoned. *Medscape J Med*. 2008;10(5):115.
106. Sinha A, Shaporev A, Nosoudi N, Lei Y, Vertegel A, Lessner S, et al. Nanoparticle targeting to diseased vasculature for imaging and therapy. *Nanomedicine*. 2014;10(5):e1003–e12.
107. Lei Y, Nosoudi N, Vyavahare N. Targeted chelation therapy with EDTA-loaded albumin nanoparticles regresses arterial calcification without causing systemic side effects. *J Control Release*. 2014;196:79–86.
108. Nosoudi N, Chowdhury A, Siclari S, Karamched S, Parasaram V, Parrish J, et al. Reversal of vascular calcification and aneurysms in a rat model using dual targeted therapy with EDTA- and PGG-loaded nanoparticles. *Theranostics*. 2016;6(11):1975.
109. Sinha A, Nosoudi N, Vyavahare N. Elasto-regenerative properties of polyphenols. *Biochem Biophys Res Commun*. 2014;444(2):205–11.
110. Karamched SR, Nosoudi N, Moreland HE, Chowdhury A, Vyavahare NR. Site-specific chelation therapy with EDTA-loaded albumin nanoparticles reverses arterial calcification in a rat model of chronic kidney disease. *Sci Rep*. 2019;9(1):2629.
111. Zhou P, Zhang X, Guo M, Guo R, Wang L, Zhang Z, et al. Ginsenoside Rb1 ameliorates CKD-associated vascular calcification by inhibiting the Wnt/ β -catenin pathway. *J Cell Mol Med*. 2019;23:7088.
112. Mathew S, Lund RJ, Strebeck F, Tustison KS, Geurs T, Hruska KA. Reversal of the adynamic bone disorder and decreased vascular calcification in chronic kidney disease by sevelamer carbonate therapy. *J Am Soc Nephrol*. 2007;18(1):122–30.
113. Lin T, Wang X-L, Zettervall SL, Cai Y, Guzman RJ. Dorsomorphin homologue 1, a highly selective small-molecule bone morphogenetic protein inhibitor, suppresses medial artery calcification. *J Vasc Surg*. 2017;66(2):586–93.
114. Kim H, Kim HJ, Lee K, Kim JM, Kim HS, Kim JR, et al. α -Lipoic acid attenuates vascular calcification via reversal of mitochondrial function and restoration of Gas6/Axl/Akt survival pathway. *J Cell Mol Med*. 2012;16(2):273–86.
115. de Oca AM, Guerrero F, Martinez-Moreno JM, Madueno JA, Herencia C, Peralta A, et al. Magnesium inhibits Wnt/ β -catenin activity and reverses the osteogenic transformation of vascular smooth muscle cells. *PLoS ONE*. 2014;9(2):e89525.
116. Mathew S, Lund RJ, Chaudhary LR, Geurs T, Hruska KA. Vitamin D receptor activators can protect against vascular calcification. *J Am Soc Nephrol*. 2008;19(8):1509–19.
117. Lomashvili KA, Monier-Faugere M-C, Wang X, Malluche HH, O'Neill WC. Effect of bisphosphonates on vascular calcification and bone metabolism in experimental renal failure. *Kidney Int*. 2009;75(6):617–25.
118. Davies MR, Lund RJ, Hruska KA. BMP-7 is an efficacious treatment of vascular calcification in a murine model of atherosclerosis and chronic renal failure. *J Am Soc Nephrol*. 2003;14(6):1559–67.
119. Qin X, Corriere MA, Matrisian LM, Guzman RJ. Matrix metalloproteinase inhibition attenuates aortic calcification. *Arterioscler Thromb Vasc Biol*. 2006;26(7):1510–6.
120. O'Neill WC, Lomashvili KA, Malluche HH, Faugere M-C, Riser BL. Treatment with pyrophosphate inhibits uremic vascular calcification. *Kidney Int*. 2011;79(5):512–7.

121. Mataic D, Bastani B. Intraperitoneal sodium thiosulfate for the treatment of calciphylaxis. *Ren Fail.* 2006;28(4):361–3.
122. Bas A, Lopez I, Perez J, Rodriguez M, Aguilera-Tejero E. Reversibility of calcitriol-induced medial artery calcification in rats with intact renal function. *J Bone Miner Res.* 2006;21(3):484–90.
123. Cai Y, Xu M-J, Teng X, Zhou YB, Chen L, Zhu Y, et al. Intermedin inhibits vascular calcification by increasing the level of matrix γ -carboxyglutamic acid protein. *Cardiovasc Res.* 2009;85(4):864–73.
124. Dai X-Y, Zhao M-M, Cai Y, Guan Q-C, Zhao Y, Guan Y, et al. Phosphate-induced autophagy counteracts vascular calcification by reducing matrix vesicle release. *Kidney Int.* 2013;83(6):1042–51.
125. Cao X, Li H, Tao H, Wu N, Yu L, Zhang D, et al. Metformin inhibits vascular calcification in female rat aortic smooth muscle cells via the AMPK-eNOS-NO pathway. *Endocrinology.* 2013;154(10):3680–9.
126. Cui L, Li Z, Chang X, Cong G, Hao L. Quercetin attenuates vascular calcification by inhibiting oxidative stress and mitochondrial fission. *Vasc Pharmacol.* 2017;88:21–9.
127. Ohnishi M, Nakatani T, Lanske B, Razzaque MS. In vivo genetic evidence for suppressing vascular and soft-tissue calcification through the reduction of serum phosphate levels, even in the presence of high serum calcium and 1, 25-dihydroxyvitamin d levels. *Circ Cardiovasc Genet.* 2009;2(6):583–90.
128. Wu SY, Pan CS, Geng B, Zhao J, Yu F, YZ PANG, et al. Hydrogen sulfide ameliorates vascular calcification induced by vitamin D3 plus nicotine in rats I. *Acta Pharmacol Sin.* 2006;27(3):299–306.
129. Leibrock CB, Feger M, Voelkl J, Kohlhofer U, Quintanilla-Martinez L, Kuro-o M, et al. Partial reversal of tissue calcification and extension of life span following ammonium nitrate treatment of klothe-deficient mice. *Kidney Blood Press Res.* 2016;41(1):99–107.
130. Reynolds JL, Skepper JN, McNair R, Kasama T, Gupta K, Weissberg PL, et al. Multifunctional roles for serum protein fetuin-a in inhibition of human vascular smooth muscle cell calcification. *J Am Soc Nephrol.* 2005;16(10):2920–30.
131. Son B-K, Kozaki K, Iijima K, Eto M, Nakano T, Akishita M, et al. Gas6/Axl-PI3K/Akt pathway plays a central role in the effect of statins on inorganic phosphate-induced calcification of vascular smooth muscle cells. *Eur J Pharmacol.* 2007;556(1–3):1–8.
132. Westenfeld R, Schäfer C, Krüger T, Haarmann C, Schurgers LJ, Reutelingsperger C, et al. Fetuin-A protects against atherosclerotic calcification in CKD. *J Am Soc Nephrol.* 2009;20(6):1264–74.
133. Lee K, Kim H, Jeong D. Microtubule stabilization attenuates vascular calcification through the inhibition of osteogenic signaling and matrix vesicle release. *Biochem Biophys Res Commun.* 2014;451(3):436–41.
134. Cao F, Liu X, Cao X, Wang S, Fu K, Zhao Y, et al. Fibroblast growth factor 21 plays an inhibitory role in vascular calcification in vitro through OPG/RANKL system. *Biochem Biophys Res Commun.* 2017;491(3):578–86.
135. Duan X-Y, Xie P-L, Ma Y-L, Tang S-Y. Omentin inhibits osteoblastic differentiation of calcifying vascular smooth muscle cells through the PI3K/Akt pathway. *Amino Acids.* 2011;41(5):1223–31.
136. Kanai S, Uto K, Honda K, Hagiwara N, Oda H. Eicosapentaenoic acid reduces warfarin-induced arterial calcification in rats. *Atherosclerosis.* 2011;215(1):43–51.
137. Chang X, Zhang B, Lihua L, Feng Z. T3 inhibits the calcification of vascular smooth muscle cells and the potential mechanism. *Am J Transl Res.* 2016;8(11):4694.
138. Jiang X, Tao H, Qiu C, Ma X, Li S, Guo X, et al. Vitamin K2 regression aortic calcification induced by warfarin via Gas6/Axl survival pathway in rats. *Eur J Pharmacol.* 2016;786:10–8.
139. Kawata T, Nagano N, Obi M, Miyata S, Koyama C, Kobayashi N, et al. Cinacalcet suppresses calcification of the aorta and heart in uremic rats. *Kidney Int.* 2008;74(10):1270–7.

140. Liu D, Cui W, Liu B, Hu H, Liu J, Xie R, et al. Atorvastatin protects vascular smooth muscle cells from TGF- β 1-stimulated calcification by inducing autophagy via suppression of the β -catenin pathway. *Cell Physiol Biochem*. 2014;33(1):129–41.
141. Osako MK, Nakagami H, Koibuchi N, Shimizu H, Nakagami F, Koriyama H, et al. Estrogen inhibits vascular calcification via vascular RANKL system: common mechanism of osteoporosis and vascular calcification. *Circ Res*. 2010;107(4):466–75.
142. Essalihi R, Zandvliet ML, Moreau S, Gilbert L-A, Bouvet C, Lenoël C, et al. Distinct effects of amlodipine treatment on vascular elastocalcinosis and stiffness in a rat model of isolated systolic hypertension. *J Hypertens*. 2007;25(9):1879–86.
143. Takemura A, Iijima K, Ota H, Son B-K, Ito Y, Ogawa S, et al. Sirtuin 1 retards hyperphosphatemia-induced calcification of vascular smooth muscle cells. *Arterioscler Thromb Vasc Biol*. 2011;31(9):2054–62.
144. Luong TT, Schelski N, Boehme B, Makridakis M, Vlahou A, Lang F, et al. Fibulin-3 attenuates phosphate-induced vascular smooth muscle cell calcification by inhibition of oxidative stress. *Cell Physiol Biochem*. 2018;46(4):1305–16.
145. Neven E, Dams G, Postnov A, Chen B, De Clerck N, De Broe ME, et al. Adequate phosphate binding with lanthanum carbonate attenuates arterial calcification in chronic renal failure rats. *Nephrol Dial Transplant*. 2009;24(6):1790–9.
146. Tang F, Wu X, Wang T, Wang P, Li R, Zhang H, et al. Tanshinone II A attenuates atherosclerotic calcification in rat model by inhibition of oxidative stress. *Vasc Pharmacol*. 2007;46(6):427–38.
147. Alesutan I, Musculus K, Castor T, Alzoubi K, Voelkl J, Lang F. Inhibition of phosphate-induced vascular smooth muscle cell osteo-/chondrogenic signaling and calcification by bafilomycin A1 and methylamine. *Kidney Blood Press Res*. 2015;40(5):490–9.
148. Kiffer-Moreira T, Yadav MC, Zhu D, Narisawa S, Sheen C, Stec B, et al. Pharmacological inhibition of PHOSPHO1 suppresses vascular smooth muscle cell calcification. *J Bone Miner Res*. 2013;28(1):81–91.

Chapter 21

Clinical Trials and Calcification-Based Treatment Decisions



Jane A. Leopold

Cardiovascular calcification is a highly prevalent pathophenotype associated with risk factors for atherosclerotic disease, including normal aging, chronic kidney disease, and diabetes mellitus. In fact, in the Multi-Ethnic Study of Atherosclerosis (MESA) study, there was concordance between Framingham risk score and coronary artery calcium scores [1]. The prevalence of calcification in the coronary vessels increases with age and is present in more than 90% of men and 67% of women over age 70 years [2]. Calcium burden was similar between men and women but lower in African Americans compared to Caucasians. Coronary artery calcification was observed in 70.4%, 52.0%, 56.6%, and 59.2% of men of Caucasian, African American, Hispanic, and Chinese ethnicity, respectively [1].

The association between cardiovascular calcification and major adverse cardiac events are well documented. In the MESA study, individuals with a coronary calcium score of >300 had a 6.84 (95% CI: 2.93–15.99) increased risk of myocardial infarction: the risk was 3.89 (95% CI: 1.72–8.79) when the calcium score was 1–100 [3, 4]. Interestingly, approximately 18% of participants who did not have coronary calcification at the index study went on to develop coronary calcification during a 3-year follow-up period [5]. When examined in a meta-analysis of 30 studies that included 218,080 patients, the risk of cardiovascular mortality was markedly increased in patients with chronic kidney disease (OR = 6.22; 95% CI: 2.73, 14.14) or diabetes mellitus (OR = 2.27; 95% CI: 1.07–3.04) (Fig. 21.1) [6]. Taken together, the presence of a high burden of coronary artery calcification combined with the high prevalence in patients with diabetes mellitus or chronic kidney disease likely explains the high risk for cardiovascular events in these populations.

J. A. Leopold (✉)
Division of Cardiovascular Medicine, Brigham and Women's Hospital,
Harvard Medical School, Boston, MA, USA
e-mail: jleopold@bwh.harvard.edu

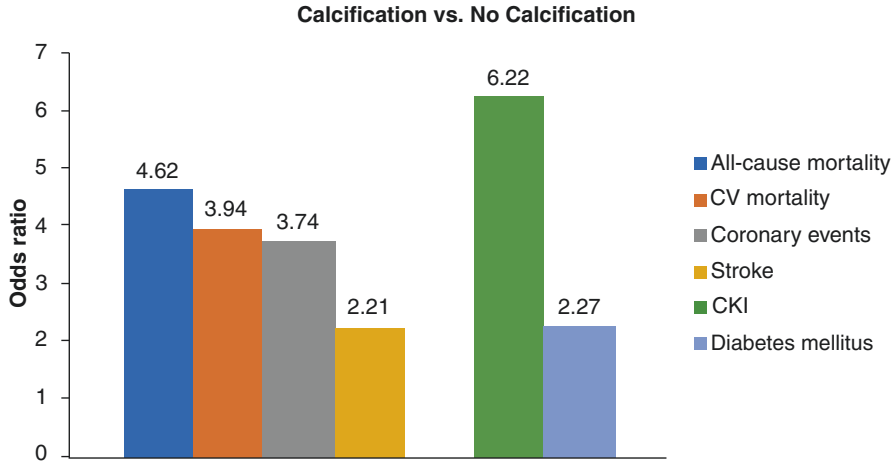


Fig. 21.1 Vascular calcification, risk of adverse events, and risk associated with chronic kidney disease and diabetes mellitus. When present, vascular calcification is associated with an increased risk of adverse events, including all-cause mortality, cardiovascular (CV) mortality, coronary heart disease events, and stroke. Patients with chronic kidney disease (CKD) or diabetes mellitus are at increased risk of developing vascular calcification. (Adapted from Ref. [6])

Cardiovascular disease remains the leading cause of death throughout the world with ~15 million deaths in 2016 [7]. This has been associated with an ~\$320 billion annual expenditure for healthcare related to cardiovascular disease in 2015, which is estimated to grow to \$820 billion by 2030 [8]. Owing to the high risk of major adverse cardiovascular events associated with vascular calcification, efforts to reduce the burden of calcium in the hope of improving outcomes are underway. These efforts have focused mainly on two areas: drug development and repurposing, as there are currently no effective therapies that target cardiovascular calcification and selection of devices utilized during percutaneous coronary or peripheral interventions for symptomatic atherosclerotic disease. This chapter will focus on clinical trials that inform decision-making with respect to currently available and future methods to assess cardiovascular calcification, pharmacologic interventions, and the invasive diagnosis and treatment of symptomatic vascular disease in calcified vessels.

Clinical Studies of Methods to Assess Cardiovascular Calcification

Following large-scale population-based studies that revealed a relationship between coronary artery calcification and major adverse cardiovascular outcomes in asymptomatic individuals, noninvasive evaluation of coronary artery calcification,

primarily via multidetector CT scanning, has emerged as a valuable tool for assessing cardiovascular risk [9–13]. Early clinical studies from single centers demonstrated that coronary artery calcification had predictive value and improved risk stratification of patients with intermediate Framingham risk scores [14]. This has been shown in both young and elderly individuals, diabetes mellitus, and smokers [15–18]. Population-based cohort studies, such as the MESA study, have confirmed the benefits of coronary CT assessments for risk prediction [4]. The Heinz Nixdorf Recall (Risk Factors, Evaluation of Coronary Calcium and Lifestyle) study included 4487 participants in its initial study and scheduled follow-up studies after 5 years. Here the prevalence of coronary artery calcification was found to be 82% in men ($n = 1918$) and 55% in women ($n = 2148$) [13]. The Rotterdam Study, which included 7893 individuals who were age 55 years or older, reported a median coronary artery calcium score of 98, which was similar to MESA and the Heinz Nixdorf Recall study [19]. The Framingham Heart Study added coronary artery calcium studies to the Offspring and Third Generation cohorts. After 7 years of follow-up, the investigators found that both the presence of calcium in the proximal dominant vessel and the number of vessels with calcium were associated with major adverse cardiovascular events [20].

Coronary artery calcium has also been measured in young adults aged 32–46 years in the Coronary Artery Risk Development in Young Adults (CARDIA) study. This prospective study demonstrated that coronary artery calcium scores >0 were not uncommon and that this predicted cardiovascular risk, beyond the traditional coronary heart disease risk factors [21]. The Jackson Heart Study reported similar findings in an African American population. In this group, coronary artery calcium scores also predicted risk beyond traditional risk factors and identified individuals for primary prevention [22, 23]. The Women’s Health Initiative reported the same in postmenopausal women [24].

Coronary artery plaque characteristics that are associated with adverse cardiovascular events were evaluated in the Scottish Computed Tomography of the HEART Trial (SCOT-HEART). In a post hoc analysis of this study, which evaluated patients with stable chest pain using coronary CT angiography, the investigators aimed to determine the association between clinical outcomes and adverse coronary plaque characteristics seen on the coronary CT angiogram. Of the 4146 patients enrolled in the study, 1778 underwent a coronary CT angiogram. As part of the analysis, 15 coronary segments per patient were examined for focal calcifications, which may be linked to plaque destabilization and rupture leading to adverse clinical events. Patients who had a higher calcium score were also found to have a higher cardiovascular risk score. In fact, compared to patients with nonobstructive disease, those patients with obstructive coronary artery disease had an eightfold higher calcium score (435 vs. 54 Agatston units, $p < 0.001$). Moreover, those patients with a coronary artery calcium score ≥ 1000 Agatston units were found to have a 13-fold increase in nonfatal myocardial infarction or death attributable to coronary heart disease. Thus, a higher burden of coronary plaque calcification portends increased risk of adverse cardiovascular events [25].

To date, the only risk score that incorporates coronary artery calcification in the model was derived from the MESA study. This model includes age, gender, race/ethnicity, diabetes, current smoking, family history, cholesterol, systolic blood pressure, the use of lipid lowering and hypertension medications, and coronary artery calcification and was created to predict the 10-year coronary heart disease risk [26]. Unsupervised machine learning has been applied to define characteristics associated with adverse events. Algorithms using chest and abdominal CT scans from 2924 asymptomatic participants in the Framingham Heart Study revealed that global calcification, defined as aortic, thoracic, coronary, and valvular calcification, was one of the components that conferred increased cardiovascular risk [23].

Despite the evidence that coronary artery calcification improves clinical risk assessment beyond traditional cardiovascular risk factors, clinical practice guidelines have not universally included coronary artery calcium score. The 2019 American College of Cardiology/American Heart Association guidelines for the primary prevention of cardiovascular disease now recognize that in adults at intermediate risk for coronary heart disease events, coronary artery calcium scores can be effective for reclassifying risk that would ultimately determine treatment. The guidelines now recommend that initiation of statin therapy is reasonable in patients with a coronary artery calcium score of ≥ 100 Agatston units. Individuals with a calcium score of 0 were considered low risk and didn't warrant pharmacological intervention, unless they had diabetes mellitus, active tobacco use, a family history, or chronic inflammatory conditions. By contrast, for individuals with a score of 1–99 Agatston units, where risk reclassification was only modest, the consensus opinion was to discuss risk and repeat the scan in 5 years [27].

Blood Calcification Propensity and Cardiovascular Events

A novel methodology to assess blood calcification propensity has now been described. This method involves a blood test that examines an individual's potential for ectopic calcification by measuring the time to form primary calciprotein particles in serum (Fig. 21.2). The timing of spontaneous formation of secondary calciprotein particles is, in part, dependent upon serum concentrations of calcification inhibitors, such as fetuin-A and pyrophosphate among others [28, 29]. If the transformation time (T_{50}) is short, this indicates that there is rapid formation of calciprotein particles and a higher blood calcification propensity. This finding has been associated with an increased risk of adverse clinical outcomes. In patients with stage 3 or 4 chronic kidney disease, or following renal transplantation, the test was inversely correlated with all-cause mortality [29, 30].

The relationship between calcification propensity evaluated by serum T_{50} and cardiovascular events was tested in the Evaluation of Cinacalcet Therapy to Lower Cardiovascular Events (EVOLVE) trial. In this study, baseline serum samples from 2785 eligible patients with chronic kidney disease on dialysis were evaluated for calcification propensity. Approximately 30% of the patients had diabetes mellitus,

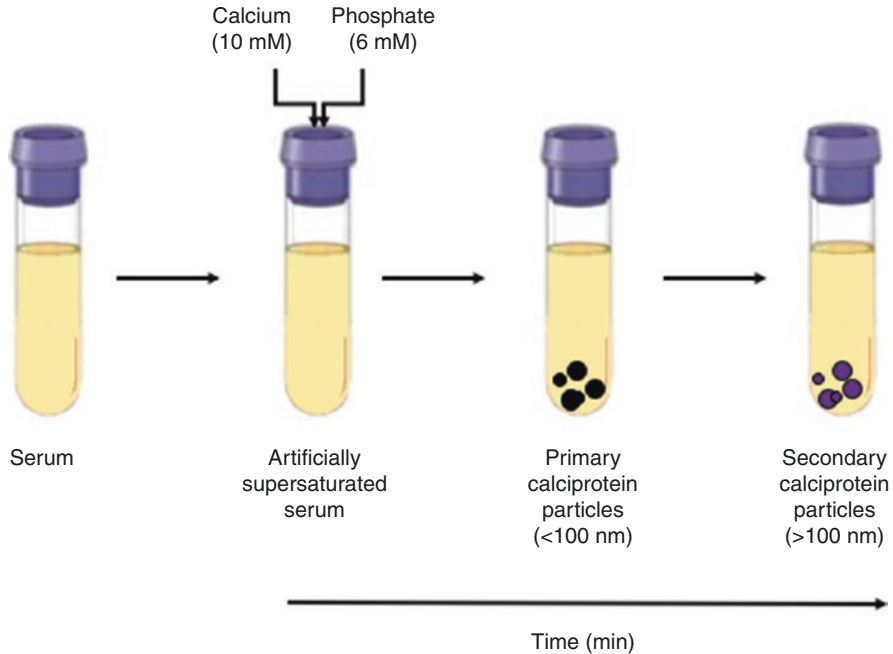


Fig. 21.2 Principle of blood calcification propensity measurement. A new serum assay is able to determine the propensity for blood calcification. In this test, a laser is used to determine light scatter in serum that is artificially supersaturated with calcium and phosphate. The addition of calcium and phosphate to serum results in the formation of primary calciprotein particles. These particles undergo spontaneous transformation to secondary particles that contain calcium phosphate in crystalline form and serum proteins. The time for 50% transformation from primary to secondary particles is indicative of an individual's ability to inhibit calcification [28]

and 23% had established coronary artery disease. The primary composite endpoint included all-cause mortality, myocardial infarction, heart failure, unstable angina requiring hospitalization, or a peripheral vascular event. After a median follow-up period of 619 days, the primary composite endpoint was reached in 1350 patients. A lower T_{50} time was associated with increased risk of cardiovascular events with a HR = 1.38 (95% CI: 1.19, 1.60, $p < 0.001$) for myocardial infarction, HR = 1.22 (95% CI: 1.05, 1.42, $p = 0.01$) for peripheral vascular events, and HR = 1.10 (95% CI: 1.00, 1.20, $p = 0.05$) for cardiovascular death. Interestingly, the T_{50} time was not associated with unstable angina or heart failure [31]. While this study had several limitations, including use of only baseline samples and a retrospective study design, the findings are not surprising as it has long been recognized that hemodialysis patients have excess morbidity and mortality, mostly attributable to cardiovascular events [32].

More recently, calcification propensity was evaluated in 3404 patients enrolled in the longitudinal Chronic Renal Insufficiency Cohort Study. Mean follow-up time for participants was an average of 7.1 years. In this prospective cohort, a lower T_{50}

time was associated with an increased risk of atherosclerotic cardiovascular disease (HR = 1.14; 95% CI: 1.09–1.24), which was not independent of renal function [33]. In a subgroup of 1274 patients who had coronary artery calcification measured by CT scan, approximately 65% had prevalent coronary calcification. In these patients, the T₅₀ time was found to be associated with the severity of coronary calcification. At 3-year follow-up, 20% of patients who did not have coronary artery calcification at baseline developed incident coronary calcification, while 19% with calcification present at baseline demonstrated calcification progression. Here, a lower T₅₀ time and hence a higher serum calcification propensity were associated with coronary artery calcification progression and severity [34]. Worsening calcification propensity over 24 months was associated with an increased hazard for cardiovascular mortality (HR = 2.15; 95% CI: 1.15–3.97, $p = 0.02$) [35]. To date, tests of calcification propensity have only been applied to patients with some degree of chronic kidney disease or on hemodialysis. Whether or not this test has applicability in broader community-based populations or in select patients at risk for or with established atherosclerotic cardiovascular disease remains to be determined.

Clinical Trials of Pharmacological Therapeutics

At present, there is no known pharmacologic therapy that has definitively been shown to prevent or regress established cardiovascular calcification in a double-blind randomized clinical trial and been incorporated into mainstream guidelines and practice. However, several therapies have shown promise in smaller studies or clinical trials. In many instances, early studies have been done in select patient subsets, such as chronic kidney disease that have a high propensity for cardiovascular calcification. Whether or not results from these studies have utility in other patient populations is unknown.

Vitamin K

Vitamin K is a fat-soluble vitamin that mediates blood coagulation as well as cardiovascular calcification through its regulation of the calcification inhibitor matrix Gla protein (MGP). Vitamin K is necessary for the carboxylation of glutamic acid in activation of MGP. Vitamin K levels are maintained through the diet by intake of leafy green vegetables or ingestion of fermented foods, which are then processed by commensal bacteria; however, many patients are vitamin K deficient. This is well documented in patients with chronic kidney disease and may be a larger problem in the population as a whole [36–38]. A recent survey found that only 58–63% of diabetic women and 61–68% of women without diabetes mellitus reported daily intake of vegetables [39]. Furthermore, clinical studies of patients taking warfarin, a vitamin K antagonist, have demonstrated increased vascular calcification compared to

patients who do not take this drug. A post hoc analysis of eight randomized trials that included serial intravascular ultrasound evaluated the effect of warfarin on calcification in patients with coronary artery disease. Of the 171 patients who were treated with warfarin, there was a significant annualized increase in calcification as compared to 4129 individuals who were not taking warfarin. Warfarin was found to be independently associated with increased calcification (OR, 1.2; 95% CI, 1.1–1.3, $p = 0.003$), and the annual increase in calcification occurred independent of changes in atheroma volume [40]. This has also been observed in the peripheral vasculature. A cohort analysis of 430 patients matched by age, sex, and diabetes status revealed that the prevalence of peripheral vascular calcification was significantly higher in warfarin-treated patients (30.2% vs 20.9%, $p = 0.0023$) [41]. To demonstrate that warfarin likely had a causal effect, a randomized trial of 66 patients with nonvalvular atrial fibrillation was conducted. Patients were randomized to warfarin or apixaban for 1 year, and coronary CT angiography was performed to evaluate calcium burden. Here, CT scans demonstrated lower levels of calcified plaque volume in apixaban-treated patients as compared to those randomized to warfarin [42].

The association between vitamin K deficiency and cardiovascular calcification has led to the strategy of vitamin K supplementation as a method to limit calcification and subsequent adverse events. A meta-analysis that included 12,888 patients enrolled in 13 controlled trials and 14 longitudinal studies found that vitamin K supplementation was associated with a reduction in decarboxylated MGP and a significant 9.1% decrease in vascular calcification [43]. Clinical trials are underway that will evaluate the efficacy of vitamin K supplementation on the progression of coronary artery calcification. Results from these trials will be critical to understand whether or not this will be a viable therapeutic option for patients. In a recently reported double-blind, placebo-controlled, randomized trial of vitamin K supplementation in patients with type 2 diabetes mellitus and established cardiovascular disease, calcification was measured after 6 months using ^{18}F -NaF positron emission tomography. After 6 months, vitamin K supplementation was associated with an increase, and not a decrease, in femoral artery calcification [44]. Since this finding is in contradistinction to results from prior studies, additional data will be required prior to issuing recommendations pertaining to vitamin K supplementation to reduce cardiovascular calcification.

Sodium Thiosulfate

Sodium thiosulfate is an inorganic sodium salt with reducing properties and has clinical application in the treatment of cyanide poisoning [45]. Sodium thiosulfate to limit cardiovascular calcification has been trialed in hemodialysis patients. In one study of 87 patients with coronary calcium scores >300 , patients received intravenous infusions twice weekly. After 4 months, vascular calcification increased in 63% of patients in the control group, but only 25% of patients received sodium thiosulfate ($p = 0.03$). This benefit, however, occurred at the expense of a decrease

in bone mineral density, and patients who were treated with sodium thiosulfate experienced metabolic acidosis and persistent anorexia [46]. In a second pilot study, 22 hemodialysis patients were treated with sodium thiosulfate 3 times weekly. After 5 months, there was no difference in the mean annualized rate of calcification; however, 14 out of 22 patients did demonstrate progression of coronary artery calcification [47]. While these results appear promising, the side effects of this agent, namely, metabolic acidosis and bone toxicity, suggest that it is unlikely to have the acceptable long-term safety profile required to treat cardiovascular calcification.

Bisphosphonates

The bisphosphonates are used widely to prevent and treat osteoporosis. These drugs are analogs of pyrophosphate, which inhibits calcification by chelating calcium ions in hydroxyapatite. Early clinical studies with these agents reported conflicting results. One study evaluated alendronate in 56 patients with osteoporosis compared to matched controls and a referent cohort. After 2 years, there was no observable difference in coronary artery calcification between groups [48]. Another study performed in women age 55–80 years who were treated for 3 years with either oral or intravenous ibandronate found that there was no difference in the rate of aortic calcification at the end of the study between groups [49]. Similarly, a pilot randomized controlled trial of alendronate in 51 patients with stage 3–4 chronic kidney disease revealed that compared to placebo, at 18 months there was no difference in the progression of ectopic calcification in the aorta in alendronate-treated patients [50]. This is in contrast to several small studies in hemodialysis patients that reported a positive effect of bisphosphonates on cardiovascular calcification. In these studies, which each enrolled fewer than 25 patients, treatment with bisphosphonates was associated with either halting or reversing the progression of aortic calcification [51, 52].

A recent randomized trial of etidronate in patients with pseudoxanthoma elasticum was performed to test the hypothesis that a bisphosphonate could limit arterial calcification in this patient population with low pyrophosphate levels. A cohort of 74 patients was randomized to etidronate (20 mg/kg for 2 weeks every 12 weeks) or placebo. After 12 months of follow-up, arterial calcification assessed by CT scan was decreased by 4% in etidronate-treated patients but increased by 8% in control subjects. However, when quantified by ¹⁸F-sodium positron emission tomography activity, there was no difference observed between the active treatment and placebo group. Importantly, while patients assigned to etidronate were more likely to experience hyperphosphatemia, this was reversible, and there were no safety issues noted [53].

There have been some issues raised with respect to the long-term durability of these drugs to prevent or limit cardiovascular calcification owing to concerns related to bone density and cardiac arrhythmias. There has been a long-standing debate

regarding the effect of bisphosphonates on skeletal toxicity. This has been attributed to the bisphosphonate drug selected, oral versus intravenous administration, dosage regimen with continuous dosing versus cyclical dosing, and the patient's comorbidity profile [54]. Another issue was raised by the finding that patients treated with parenteral zoledronic acid annually for osteoporosis management had a higher signal of atrial fibrillation [55]. This has not been explored further, so it is unknown if bisphosphonate drugs played a causal role in arrhythmia generation. These agents continue to be investigated and these issues remain to be resolved.

Magnesium

Magnesium is suggested to prevent cardiovascular calcification by regulating calcium influx, mediating pro-calcific enzyme activity, and stimulating activity of calcification inhibitory enzymes [56]. Magnesium also prevents the transformation of calcium phosphate nanocrystals to apatite [56]. In patients with chronic kidney disease, in dialysis patients, and in patients with prevalent cardiovascular calcification, increased cardiovascular mortality has been associated with low serum magnesium levels [57–60]. Small observational clinical studies have suggested that there may be some benefit to magnesium supplementation. A pilot study in seven hemodialysis patients found that after 18 months of supplementation with magnesium carbonate, there was no progression of coronary artery calcification by CT scan [61]. These findings were confirmed in a similarly small study that compared magnesium supplementation with magnesium carbonate and calcium acetate as a phosphate binder with calcium acetate alone. After 1 year, calcification assessed by X-ray was improved in 15% of the magnesium group compared to 0% in the calcium acetate group [62]. Another small study that included 34 patients with chronic kidney disease (stage 3, 4) and trialed short-term magnesium hydroxide for 8 weeks was shown to decrease calcification propensity measured in the serum [63]. Currently, there is a randomized clinical trial of 250 patients with chronic kidney disease that is underway that will test magnesium hydroxide versus placebo on coronary artery calcium score after 1 year of treatment [64].

SNF472

The investigational agent, SNF472, a myo-inositol hexaphosphate, is a hexasodium salt of phytate and is under development for the treatment of cardiovascular calcification. This agent may have utility in patients on hemodialysis as phytate is a low molecular mass and highly soluble crystallization inhibitor [65]. The safety and tolerability of SNF472 were demonstrated in healthy volunteers and dialysis patients. In a Phase I study, there were no clinically significant effects, and pharmacodynamic analyses showed that SNF472 decreased hydroxyapatite crystallization

potential in dialysis patients [66]. A phase 2b double-blind, placebo-controlled study of SNF472 in hemodialysis patients randomized patients to one of two doses of SNF472 delivered three times per week with dialysis or placebo and evaluated calcification by CT scan after 1 year. After 1 year, the coronary artery calcium volume score was significantly lower in patients treated with SNF472 as compared to placebo (11% vs 20%, $p = 0.016$). There was also a decrease in the progression of calcification in the aortic valve (14% vs. 98%, $p < 0.001$). There was no difference between active treatment and placebo groups with respect to treatment-emergent adverse events. Thus, while SNF472 attenuated progression of coronary artery and aortic valve calcification in this patient population, it remains to be determined if this translates to an effect on cardiovascular outcomes and is translatable to other patient populations at high risk for cardiovascular calcification [67].

Denosumab

Denosumab is an FDA-approved human monoclonal antibody against the receptor activator of NF- κ B ligand (RANKL) and is used primarily to treat bone tumors and osteoporosis. Theoretically, denosumab may limit cardiovascular calcification by preventing RANKL interaction with its receptor and preventing deposition of calcified minerals. A post hoc analysis of postmenopausal women at high risk for cardiovascular events examined lateral spine X-rays to evaluate for progression of aortic calcification. The frequency of aortic calcification progression and adverse cardiovascular events over 3 years was not different between the denosumab and placebo groups [68]. The phase 2 SALTIRE II trial is currently evaluating the effect of denosumab and alendronate as interventions for calcific aortic stenosis. Patients with calcific aortic stenosis assessed by echocardiography will be treated with denosumab, alendronate, or both, or placebo and calcification will be examined using standard CT calcium scoring and with ^{18}F -fluoride positron emission tomography activity.

While many of the aforementioned agents have shown promise in the treatment of cardiovascular calcification, evidence to support routine use in broader patient populations remains limited. This is not surprising that the mechanism for cardiovascular calcification and, therefore, the appropriate pharmacological intervention, likely differs between patient subsets. Moreover, safety and efficacy profiles will need to be evaluated on a longer-term basis to understand optimal dosing regimens. Forthcoming results from randomized trials to resolve these questions are eagerly awaited.

Clinical Studies of the Invasive Diagnosis and Treatment of Cardiovascular Calcification

It has been recognized that conventional coronary angiography does not always demonstrate coronary calcification adequately leading to an underappreciation of the

severity of calcification. In a series of 1155 target lesions in native coronary arteries, angiography detected calcification in 38% of the stenoses, and 26% were classified as moderately calcified, while 12% were severely calcified. These same stenoses were then evaluated with intravascular ultrasound. This imaging modality detected calcium deposits in 73% of lesions, indicating that coronary calcification is both common and frequently underestimated [69]. Optical coherence tomography, which has a higher resolution than intravascular ultrasound, can assess calcium arc and length in a coronary artery but has limited depth penetration and, therefore, is likely to miss deep intramural calcium [70]. This imaging modality can also provide an assessment of the degree of the calcific arch in the vessel cross section; calcium area, thickness, and length; and, calcium three-dimensional volume [71]. A head-to-head comparison of the two imaging modalities with angiography revealed that angiography detected calcium in only 40% of lesions, while intravascular ultrasound and optical coherence tomography detected calcium in 83% and 77% of stenoses, respectively [72].

In contemporary percutaneous coronary intervention (PCI), significant coronary calcification is present in approximately 20% of patients, and these patients are characterized by a demographic, clinical, and angiographic pathophenotype that differs from that observed in individuals with less severe calcification [73]. The introduction of next-generation DES hasn't reduced the hazard associated with calcification, and calcified lesions are associated with a threefold increase in adverse events [74]. A large registry analysis of 16,001 patients from a single academic medical center revealed that patients with moderate or severe target lesion calcification tended to be older, Caucasian, have a higher body mass index, less likely to be a current smoker, and more likely to have renal dysfunction, anemia, and peripheral arterial disease. They had more complex target lesions (classified B2/C) with a higher SYNTAX score and had a higher rate of procedural complications. Within this group, moderate to severe calcification was associated with an increased risk of death, myocardial infarction, and/or target vessel revascularization [75]. These patients also have higher 30-day rates of major bleeding (11.2% vs. 7.2% vs. 5.9%, $p = 0.0003$) compared to patients with moderate or mild or no target lesion calcium [76]. Coronary lesion calcification also impacts chronic total occlusion procedures. In 1476 procedures performed across 11 centers in the United States between 2012 and 2016, moderate to severe calcification was identified in 58% of target lesions. Percutaneous revascularization of calcified chronic total occlusion lesions often required a change in procedural strategy with increased use of the retrograde approach, more contrast use, and increased radiation exposure as well as lower success rates and increased incidence of adverse cardiovascular events (3.7% vs. 1.8%, $p = 0.033$) compared to patients without calcified stenoses [77].

Percutaneous Coronary Intervention for Calcified Plaques and Coronary Arteries

Given the high prevalence of coronary calcification, patients who require PCI present a unique challenge. The optimal treatment for calcified plaque modification in

complex coronary anatomies remains a decision point for coronary interventions that has been the subject of clinical trials. The standard method of using a balloon inflated to high pressure to release the coronary plaque can result in vessel dissection and perforation when calcified stenoses are present. The risk of not achieving adequate enlargement of a coronary lumen due to inability to release or “crack” a calcified stenosis is incomplete expansion or malapposition of a coronary stent, which predisposes to stent failure and adverse clinical outcomes [78]. At present, clinical trials to treat calcified coronary stenoses in the cardiac catheterization laboratory have focused on rotational atherectomy (Fig. 21.3), orbital atherectomy, excimer laser coronary atherectomy, or shockwave lithotripsy.

Rotational atherectomy relies on a diamond-encrusted elliptical burr that rotates at high speeds (140,000–180,000 rpm) and pulverizes calcified or inelastic tissue, while the relatively normal elastic arterial wall remains uninjured. The device

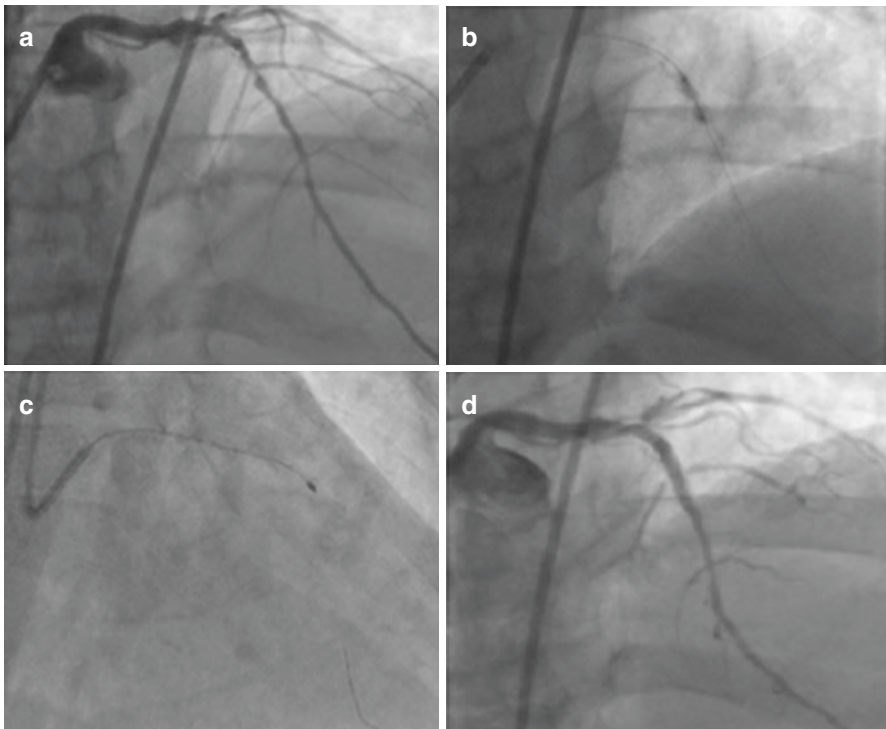


Fig. 21.3 Atherectomy in a calcified coronary stenosis. (a) A left anterior descending artery has a significant calcified stenosis in the midsection of the vessel. (b) Attempts to dilate the stenosis with balloon angioplasty were unsuccessful as the balloon would not expand fully (dogbone shape) owing to the calcified stenosis. (c) Rotational atherectomy was used to debulk calcium from the vessel. The burr can be seen on the angioplasty wire. (d) After rotational atherectomy, the lesion was dilated with a scored angioplasty balloon and stented. The final result shows an enlarged and patent vessel

ablates the calcified tissue to particles smaller than a red blood cell, which allows them to mix with blood and is ultimately taken up by macrophages [79–82]. Early clinical trials that compared rotational atherectomy with balloon angioplasty for de novo calcified coronary stenoses or for in-stent restenosis demonstrated equivocal results with respect to rotational atherectomy. In these studies, rotational atherectomy adequately increased the lumen diameter but was associated with high rates of restenosis. A meta-analysis that included 9222 patients enrolled in 16 early trials (1993–2002) revealed that the rate of periprocedural myocardial infarction was increased with rotational atherectomy compared to balloon angioplasty (OR = 1.83; 95% CI: 1.43–2.34) despite similar angiographic outcomes [83]. Similarly, a more recent review that included 3474 patients enrolled in 12 clinical trials (2002–2012) found that there was no difference between rotational atherectomy with adjunctive balloon angioplasty as compared to balloon angioplasty alone with respect to restenosis rates at 6 months or 1 year. There was also no difference in the risk of in-hospital major adverse cardiac events (RR; 1.27; 95% CI: 0.86–1.90) [84].

Our current clinical evidence supporting the use of rotational atherectomy comes from the Rotational Atherectomy Prior to Taxus Stent Treatment for Complex Native Coronary Artery Disease (ROTAXUS) and the Comparison of Strategies to PREPARE Severely CALCified Coronary Lesions (PREPARE-CALC) trials. The ROTAXUS trial enrolled 240 patients with calcified coronary stenoses and randomized them to rotational atherectomy and stent implantation versus stent implantation alone (standard treatment). There was a higher rate of procedural success in the rotational atherectomy arm (92.5% vs. 83.3%) as well as a high crossover rate from the standard treatment group. At follow-up, there was no difference between the groups with respect to restenosis, target lesion revascularization, or adverse events. The trial, however, was criticized for missing follow-up angiography in 20% of patients, which likely affected the power of the study, as well as the use of a first-generation drug-eluting stent [85]. The PREPARE-CALC study, in contrast, randomized 200 patients to rotational atherectomy versus a cutting or scoring balloon prior to implantation of a third-generation drug-eluting stent. This trial also demonstrated a higher rate of procedural success for rotational atherectomy (98% vs. 81%). At 9-month follow-up, there were no differences between groups with respect to late lumen loss, target lesion revascularization, or adverse events. Taken together, these trials form the basis for the modern approach of selecting rotational atherectomy as a primary strategy for stenosis modification prior to stenting when severely calcified coronary lesions are present [86].

Orbital atherectomy, which is similar to rotational atherectomy, utilizes an eccentrically rotating 1.25 mm crown coated with diamonds on the front and back ends. The device has a low (80,000 rpm) and high (120,000 rpm) rotational speed, and the technique to ablate heavily calcified plaque is dependent upon contact time between the crown and the plaque. Safety and efficacy of this device was trialed in the ORBIT II trial, which enrolled 443 patients across the United States from 49 centers [87]. In this study, the primary safety endpoint, freedom from 30-day adverse cardiac events, and the primary efficacy endpoint (residual stenosis <50% after stenting and absence of in-hospital events) were met in 90% and 89% of

participants, respectively. A real-world registry of 458 patients with complex comorbidities found that no reflow, dissection, or perforation associated with using this device occurred in <1% of cases with a 12.6% rate of major adverse cardiovascular and cerebrovascular events at 1 year [88].

Excimer laser has also shown utility for modification of calcified coronary plaques. The technique relies on photoablation of calcified plaque by photochemical, photothermal, and photomechanical methodologies. The laser can break molecular bonds, heat the plaque, or heat liquid near the plaque to create exploding bubbles that modify the plaque. This device is typically selected for coronary stenoses that can't be dilated with procedural success rates of 93% reported [89]. However, more calcification in the plaque appears to decrease the laser efficacy, and intravascular imaging has shown that while laser increased the vessel cross-sectional area, this occurred without significant modification of the calcified areas [90, 91]. Evidence does support the use of laser to crack calcium behind stent struts in undilatable in-stent restenosis, especially when this occurred as a result of an underexpanded stent [92, 93].

A lithotripsy balloon has been developed as a device to treat deep intravascular calcium. The balloon emits pulsatile mechanical energy at a frequency of 1 Hz that cracks and fractures calcified plaques and calcium present in deeper layers of the vessel wall. In 43% of cases, this device was shown to fracture an arc of calcium in the vessel lumen and create multiple fractures in more than a quarter of the cases. Importantly, there was a higher rate of fracture when there was a greater burden of calcium [94]. The Disrupt Coronary Artery Disease II study evaluated safety and efficacy of lithotripsy in 120 patients with severe coronary artery calcification enrolled between 2018 and 2019 in 9 countries. There was 100% success in device delivery and use. In this study, myocardial infarction occurred in 5.8% of patients. A subset of patients underwent optical coherence tomography imaging, which demonstrated calcium fractures in 78.7% of lesions [95]. Other limited studies have similarly reported no safety concerns, and larger-scale trials are currently underway.

The presence of calcified coronary stenoses as well as calcified coronary arteries is well recognized to increase the technical complexity of PCI. Calcification that limits plaque or lesion expansion predisposes to less than optimal stent expansion, which is associated with stent failure and major adverse cardiovascular events. Rotational atherectomy has been a mainstay as a therapeutic modality to treat calcified coronary stenoses, and other devices with adequate safety and efficacy profiles are emerging, some with niche indications. Intravascular imaging, which facilitates stenting procedures in the absence of coronary calcification, remains critical to define the calcium burden within a vessel and guide device selection for lesion modification. Device selection can be operator-dependent, but considerations include eccentricity versus concentricity of calcification, length of calcium, depth of calcium, and ability to deliver devices. Nonetheless, clinical trials have established that successful treatment of calcified stenoses for stent delivery and expansion is critical to limit procedural complications and adverse outcomes.

Coronary Artery Bypass Grafting Surgery in Patients with Calcified Coronary Arteries

In those instances where surgical coronary artery bypass grafting (CABG) is the preferred revascularization strategy, calcified coronary arteries represent a significant challenge for the surgeon. In high-risk patients, calcified coronary arteries and calcified stenoses have been associated with incomplete revascularization, atheroembolic complications, and worse clinical outcomes [96, 97]. Patients with calcified coronary arteries are also more likely to develop calcifications in saphenous vein bypass grafts, which predict both early and late graft failure [98]. It has been hypothesized that severe calcification impacts outcomes owing to loss of pulsatility in the vessels and an increase in ischemic events owing to endothelial dysfunction and atheroembolic events from calcified plaques despite bypassing significant stenoses [99]. Calcified vessels are also likely to increase the difficulty of creating vascular anastomoses and may affect the ability to achieve complete revascularization [100, 101]. Patients with significant aortic calcification also have restrictions on aortic cross-clamping during surgery owing to the high risk for cerebral embolization and stroke [102].

Patients with chronic kidney disease on hemodialysis have a high prevalence of vascular calcification and represent a high-risk patient population that frequently requires CABG for symptomatic coronary artery disease. Observational studies, including one that followed 1300 patients on hemodialysis, have shown that patients with chronic kidney disease on hemodialysis have higher operative mortality (7.8% vs. 2.1%) and 30-day mortality rates (4.8% vs 1.4%) [103]. These patients were also more likely to develop perioperative complications, such as mediastinitis and stroke [104]. A cohort of 21,981 hemodialysis patients from the US Renal Data System that underwent surgical or percutaneous revascularization revealed that CABG was associated with a lower composite of death or myocardial infarction (HR = 0.88; 95% CI: 0.86–0.91) and mortality (HR = 0.87; 95% CI: 0.84–0.90) compared to PCI at 5 years suggesting that, when appropriate, surgical revascularization may be preferred over PCI. Overall, it's been reported that long-term outcomes are improved following CABG compared to optimal medical therapy [105, 106].

In patients without chronic kidney disease, post hoc analyses of randomized trials have shown that coronary calcification is associated with an increase in adverse events for patients that undergo CABG. In the Acute Catheterization and Urgent Intervention Triage Strategy (ACUITY) trial which examined heparin versus bivalirudin in patients with acute coronary syndromes, patients with severe coronary artery calcification that underwent CABG were older and more likely to have hypertension, chronic kidney disease, and a higher thrombolysis in myocardial infarction (TIMI) risk score than patients with mild or no calcification. The presence of severe calcification was associated with higher rates of myocardial infarction (22.5% vs. 13.8%, $p = 0.03$) and death (11.8% vs. 4.5%, $p = 0.007$) at 1 year following CABG [99, 107, 108]. In the Synergy between Percutaneous Coronary Intervention and Cardiac Surgery (SYNTAX) study, severe lesion calcification was present in 588

patients that underwent surgical revascularization. This cohort had a higher mortality rate (17.1% vs 9.9%, $p < 0.001$) at 5-year follow-up compared to patients without severe calcification. Furthermore, they had a higher rate of the composite endpoint of death and myocardial infarction (19.4% vs. 13.2%, $p = 0.003$) [109]. These 1-year mortality rates in patients with severe coronary calcification are substantially higher than those reported in other contemporary studies of CABG (3.5–4.2%), although patients with heavy calcification were more likely to be included in the registry arm of surgical trials, so the absolute mortality rate following CABG for this patient population may be higher.

Peripheral Arterial Disease and the Role of Calcification in Treatment Decision-Making

Vascular calcification is also prevalent in the peripheral vasculature although exact estimates vary (Fig. 21.4). In an unselected group of 650 patients that were asymptomatic and being evaluated for preventative care, 61% had evidence of atherosclerotic calcification in their coronary, carotid, aorta, or iliac vessels [110]. Calcification was associated with increased age, and in those patients that were ≥ 70 years,

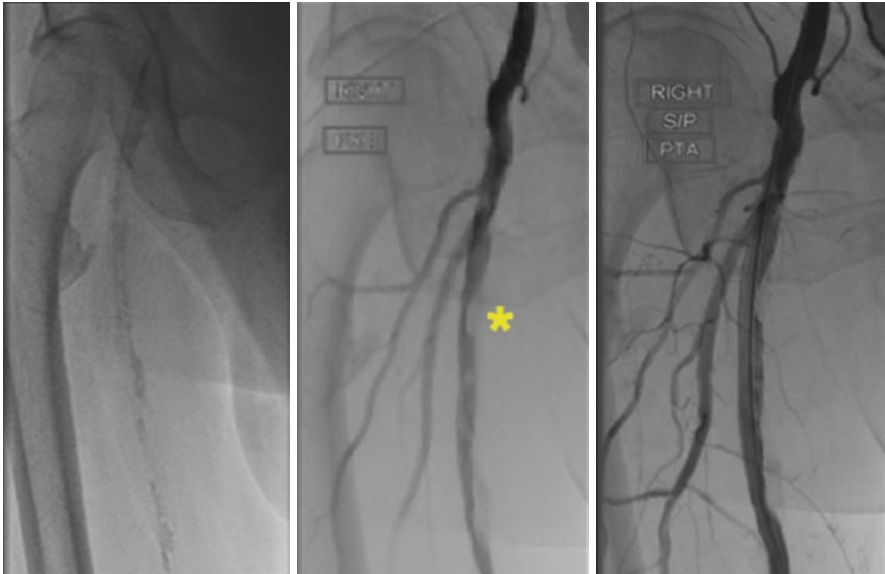


Fig. 21.4 Peripheral arterial calcification. Vascular calcification is highly prevalent in the peripheral arteries. Calcification can be seen with fluoroscopy (left panel). Following the injection of contrast, a significant calcified stenosis in the superficial femoral artery is seen (asterisk) (middle panel). After atherectomy, angioplasty, and stent placement, the vessel lumen is increased

vascular calcification was present in all vascular beds. In a large cohort study that included 4291 individuals who were followed for a mean of 7.8 years, prevalence of calcification in the coronary, carotid, aorta, and iliac arteries ranged from 31% to 55%. Interestingly, while coronary artery calcification was associated with cardiovascular mortality, the presence of calcium in other major vascular beds, namely, the carotid, aorta, and iliac vessels, was associated with all-cause mortality [111].

Clinical decision-making for therapeutic interventions in patients with peripheral arterial is limited by the fact that many patients with severe calcification were excluded from clinical trials. Balloon angioplasty of calcified lesions doesn't provide adequate lumen expansion with significant early elastic recoil, which contributes to observed poor outcomes [112]. There have been similar issues with nitinol stents in femoropopliteal vessels owing to high compressive forces exerted by rigid calcified plaques that prevent in full stent expansion [113]. However, newer nitinol stents with closed cell designs that allow for greater resistance to calcified plaque compression have been shown to have greater lumen preservation in severely calcified stenoses compared to traditional stents [114].

Atherectomy has been trialed in the peripheral vasculature with studies performed with varying degrees of procedural and early success [114–119]. The DEFINITIVE Ca++ registry evaluated the safety and efficacy of directional atherectomy to treat moderate to severely calcified femoropopliteal vessels. This trial enrolled 133 patients and found that directional atherectomy was safe and resulted in adequate debulking (<50% residual diameter) in 92% of the lesions treated with a 33% mean residual diameter stenosis. There was a 52.3% increase in the number of patients who were asymptomatic at the 30-day follow-up visit with 88.5% of patients showed clinical improvement [120].

Significant peripheral vascular calcification has also been implicated as a barrier to the efficacy of drug-coated balloons. In 60 patients with severe claudication or rest pain, the presence of circumferential calcium in the vessels was associated with a 50% increase in loss of patency. Although the mechanism for reduced efficacy wasn't clear, it was hypothesized that this occurred as a result of the calcium, which acted as a barrier to the drug reaching or penetrating the vessel wall [121]. To improve patency rates, other investigators trialed debulking of severe vascular calcification using atherectomy prior to drug-coated balloon intervention. In a small 30-patient trial with severe claudication or threatened limbs where severe calcification was identified, debulking was associated with a 90% patency rate at 1 year [122]. The more recent Directional Atherectomy Followed by a Paclitaxel-Coated Balloon to Inhibit Restenosis and Maintain Vessel Patency – A Pilot Study of Anti-Restenosis Treatment (DEFINITIVE-AR) trial randomized patients to directional atherectomy and drug-coated balloon or drug-coated balloon alone. In this study, technical success was higher for the arm with directional atherectomy (89.6% vs 64.2%, $p = 0.004$). There was no difference, however, in 1-year percent diameter stenosis assessed by angiography or target lesion revascularization between the groups [117].

The thoracic and abdominal aortas are prone to aneurysm formation with abdominal aortic aneurysms affecting 4.8% of individuals with a preponderance in men

[123]. Among 356 patients that underwent infrarenal abdominal aortic aneurysm repair, aortoiliac calcification was associated with mortality with patients who had high calcium scores had lower probability of 5-year survival [124]. Thoracic aneurysms tend to be more heterogeneous with both genetic and atherosclerotic etiologies. Endovascular interventions have decreased the short-term risks related to the intervention; however, they have not mitigated longer-term risk of cardiovascular events [125]. In a study that included 196 patients with abdominal aortic aneurysms where 85 patients had an endovascular repair and 18 had a surgical repair, aortic calcium score was related significantly to all-cause mortality (OR = 2.25; 95% CI: 1.59–9.47, $p < 0.001$) and predictive of cardiac mortality (OR = 1.32; 95% CI: 1.08–2.76, $p = 0.003$). With respect to thoracic aneurysms, 123 patients were studied with 75 patients undergoing endovascular repair. Here calcium score was also related to all-cause mortality (OR = 6.44; 95% CI: 2.57–6.14, $p < 0.001$) and cardiac mortality (OR = 3.46; 95% CI: 1.97–4.34, $p = 0.002$) [126]. Given the relationship between calcification and stent failure, it is not surprising that calcification is a noted risk factor for graft-related complications after endovascular aneurysm repair. Studies of patients who underwent endovascular repair revealed that calcification in the neck of the aneurysm and common iliac vessels was associated with increased risk for graft-related failure [127].

Calcification of the Mitral Valve

Calcification of the mitral annulus is reported in 8–15% of individuals without known coronary artery disease but increases with age and risk factors, such as chronic kidney disease (Fig. 21.5) [128–132]. When present, mitral annular

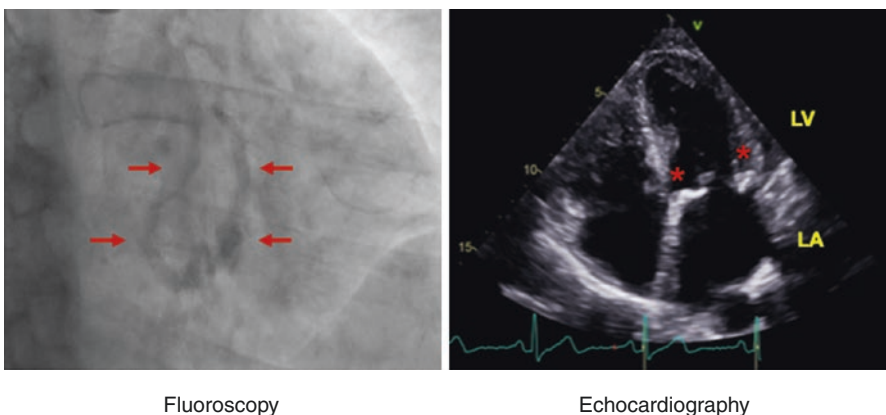


Fig. 21.5 Mitral annular calcification. Calcification of the mitral annulus occurs frequently and is often seen by fluoroscopy at the time of routine cardiac catheterization (red arrows, left). Mitral annular calcification is also seen on echocardiography. Calcification appears as bright white areas at the edges of the mitral valve leaflets (below red asterisks). LA left atrium, LV left ventricle

calcification is associated with an increased risk of cardiovascular disease and mortality [133]. The Framingham Heart Study reported that there was an increased risk of incident cardiovascular disease (HR = 1.5; 95%CI: 1.1, 2.0) and death attributable to cardiovascular disease (HR = 1.6; 95% CI: 1.1, 2.3) in patients with mitral annular calcification [133]. Mitral annular calcification has also been linked to an increased risk for stroke, possibly due to atrial fibrillation or other conduction system abnormalities, which were found to be prevalent in only 34% of control subjects but 70% of patients with mitral annular calcification [30, 134]. Patients with mitral annular calcification were also shown to have a higher rate of intraventricular conduction delays, bundle branch block, and atrioventricular block [135, 136]. Atrial fibrillation is prevalent in patients with mitral annular calcification, and the Framingham Heart Study and MESA reported a hazard ratio of 1.5–1.9 for atrial fibrillation in their respective community-based populations [137, 138].

Mitral annular calcification has implications for percutaneous and surgical interventions that involve the mitral valve. Among patients referred for mitral valve surgeries, mitral annular calcification is associated with injury to the left circumflex coronary artery and cardiac rupture when the valve requires debridement [139, 140]. Surgical approaches that have tried to avoid disrupting the calcium ring have led to perivalvular leakage or high gradients [140, 141]. Owing to this, the current approach is to decalcify the annulus via dissection [139]. Although mitral annular calcification was initially considered a contraindication to the percutaneous MitraClip procedure, case series have demonstrated that it is feasible and was not associated with a decrease in procedural success or durability of repair [142, 143].

In patients with mitral valve stenosis, valve calcification is recognized as a predictor of poor immediate and long-term clinical outcomes [144–147]. In fact, the Abascal-Wilkins echocardiography score, which predicts the success of percutaneous balloon mitral valvuloplasty for patients with mitral stenosis, includes valvular calcification in the scoring system with a score = 1 indicating a single area of calcification while a score = 4 indicating calcification is present throughout most of the valve leaflets. For overall scores >8, based on assessment of leaflet mobility, valve thickness, subvalvular thickening, and valvular calcification, surgery is preferred [148]. Nonetheless, a contemporary analysis of 1024 patients who underwent percutaneous balloon mitral valvuloplasty for mitral stenosis compared outcomes in patients with and without calcified valves. Immediate result post-procedure was classified as good for 80% of 314 patients with calcification as compared to 93% of 710 patients without calcified valves. Patients with calcified valves were also less likely to achieve good functional results, defined as New York Heart Association Class I or II and survival without reintervention or cardiovascular death. Thus, percutaneous balloon mitral valvuloplasty remains a frontline therapy for patients with calcific mitral stenosis [149]. More recently, investigators have moved forward with transcatheter mitral valve implantation for inoperable severely calcified mitral valves. In a small report of 11 patients, the procedural success rate was 73% and without paravalvular leaks [150]. Therefore, it is likely that in well-selected patients, this procedure may have benefit, but larger series, clinical trial, and outcome data is needed.

Clinical studies and decision-making regarding aortic valve calcification is reviewed in Chap. 22.

Conclusion

Calcification in the cardiovascular system is highly prevalent and associated with worse clinical outcomes. Advances in imaging technologies have allowed for more precise detection of calcified vessels, and CT scans are increasingly employed as a diagnostic modality to assess patient risk. In addition, novel blood assays to assess calcification potential are proving useful in high-risk patient populations, such as patients with chronic kidney disease, but the broad applicability of the test to other patient populations remains to be determined. Pharmacological therapeutics to prevent and/or regress calcification are under development or moving forward in early phase clinical trials, suggesting that it is likely that these agents will soon have a role in the management of patients with calcified vessels. For patients with symptomatic vascular disease that require percutaneous or surgical revascularization, it is clear that the presence of calcification is associated with higher risk and higher rates of major adverse cardiovascular events despite the introduction of newer devices and techniques. Thus, it remains imperative that promising new therapies and interventions continue to be trialed in more patients with cardiovascular calcification in randomized clinical trials to aid clinical decision-making.

References

1. Okwuosa TM, Greenland P, Burke GL, Eng J, Cushman M, Michos ED, et al. Prediction of coronary artery calcium progression in individuals with low Framingham Risk Score: the Multi-Ethnic Study of Atherosclerosis. *JACC Cardiovasc Imaging*. 2012;5(2):144–53.
2. Wong ND, Kouwabunpat D, Vo AN, Detrano RC, Eisenberg H, Goel M, et al. Coronary calcium and atherosclerosis by ultrafast computed tomography in asymptomatic men and women: relation to age and risk factors. *Am Heart J*. 1994;127(2):422–30.
3. Detrano R, Guerci AD, Carr JJ, Bild DE, Burke G, Folsom AR, et al. Coronary calcium as a predictor of coronary events in four racial or ethnic groups. *N Engl J Med*. 2008;358(13):1336–45.
4. Bild DE, Detrano R, Peterson D, Guerci A, Liu K, Shahar E, et al. Ethnic differences in coronary calcification: the Multi-Ethnic Study of Atherosclerosis (MESA). *Circulation*. 2005;111(10):1313–20.
5. DeFilippis AP, Blaha MJ, Ndumele CE, Budoff MJ, Lloyd-Jones DM, McClelland RL, et al. The association of Framingham and Reynolds risk scores with incidence and progression of coronary artery calcification in MESA (Multi-Ethnic Study of Atherosclerosis). *J Am Coll Cardiol*. 2011;58(20):2076–83.
6. Rennenberg RJ, Kessels AG, Schurgers LJ, van Engelshoven JM, de Leeuw PW, Kroon AA. Vascular calcifications as a marker of increased cardiovascular risk: a meta-analysis. *Vasc Health Risk Manag*. 2009;5(1):185–97.
7. World Health Organization. Fact sheets cardiovascular diseases. who.int. 2020.
8. CDC Foundation. Heart disease and stroke cost America nearly \$1 billion a day in medical costs, lost productivity. cdcfoundation.org. 2015.
9. Bild DE, Bluemke DA, Burke GL, Detrano R, Diez Roux AV, Folsom AR, et al. Multi-Ethnic Study of Atherosclerosis: objectives and design. *Am J Epidemiol*. 2002;156(9):871–81.
10. Hoffmann U, Massaro JM, Fox CS, Manders E, O'Donnell CJ. Defining normal distributions of coronary artery calcium in women and men (from the Framingham Heart Study). *Am J Cardiol*. 2008;102(9):1136–41, 41.e1.

11. Oei HH, Vliedenthart R, Hak AE, Iglesias del Sol A, Hofman A, Oudkerk M, et al. The association between coronary calcification assessed by electron beam computed tomography and measures of extracoronary atherosclerosis: the Rotterdam Coronary Calcification Study. *J Am Coll Cardiol.* 2002;39(11):1745–51.
12. Greenland P, Blaha MJ, Budoff MJ, Erbel R, Watson KE. Coronary calcium score and cardiovascular risk. *J Am Coll Cardiol.* 2018;72(4):434–47.
13. Schmermund A, Mohlenkamp S, Stang A, Gronemeyer D, Seibel R, Hirche H, et al. Assessment of clinically silent atherosclerotic disease and established and novel risk factors for predicting myocardial infarction and cardiac death in healthy middle-aged subjects: rationale and design of the Heinz Nixdorf RECALL Study. Risk Factors, Evaluation of Coronary Calcium and Lifestyle. *Am Heart J.* 2002;144(2):212–8.
14. Greenland P, LaBree L, Azen SP, Doherty TM, Detrano RC. Coronary artery calcium score combined with Framingham score for risk prediction in asymptomatic individuals. *JAMA.* 2004;291(2):210–5.
15. Raggi P, Gongora MC, Gopal A, Callister TQ, Budoff M, Shaw LJ. Coronary artery calcium to predict all-cause mortality in elderly men and women. *J Am Coll Cardiol.* 2008;52(1):17–23.
16. Raggi P, Shaw LJ, Berman DS, Callister TQ. Prognostic value of coronary artery calcium screening in subjects with and without diabetes. *J Am Coll Cardiol.* 2004;43(9):1663–9.
17. Shaw LJ, Raggi P, Berman DS, Callister TQ. Coronary artery calcium as a measure of biologic age. *Atherosclerosis.* 2006;188(1):112–9.
18. McEvoy JW, Blaha MJ, Nasir K, Blumenthal RS, Jones SR. Potential use of coronary artery calcium progression to guide the management of patients at risk for coronary artery disease events. *Curr Treat Options Cardiovasc Med.* 2012;14(1):69–80.
19. Yano Y, O'Donnell CJ, Kuller L, Kavousi M, Erbel R, Ning H, et al. Association of coronary artery calcium score vs age with cardiovascular risk in older adults: an analysis of pooled population-based studies. *JAMA Cardiol.* 2017;2(9):986–94.
20. Ferencik M, Pencina KM, Liu T, Ghemigian K, Baltrusaitis K, Massaro JM, et al. Coronary artery calcium distribution is an independent predictor of incident major coronary heart disease events: results from the Framingham Heart Study. *Circ Cardiovasc Imaging.* 2017;10(10):e006592.
21. Carr JJ, Jacobs DR Jr, Terry JG, Shay CM, Sidney S, Liu K, et al. Association of coronary artery calcium in adults aged 32 to 46 years with incident coronary heart disease and death. *JAMA Cardiol.* 2017;2(4):391–9.
22. Sung JH, Yeboah J, Lee JE, Smith CL, Terry JG, Sims M, et al. Diagnostic value of coronary artery calcium score for cardiovascular disease in African Americans: the Jackson Heart Study. *Br J Med Med Res.* 2016;11(2). pii: BJMMR/2016/21449. Epub 2015 Sep 21.
23. Shah RV, Yeri AS, Murthy VL, Massaro JM, D'Agostino R Sr, Freedman JE, et al. Association of multiorgan computed tomographic phenomap with adverse cardiovascular health outcomes: the Framingham Heart Study. *JAMA Cardiol.* 2017;2(11):1236–46.
24. Manson JE, Allison MA, Carr JJ, Langer RD, Cochrane BB, Hendrix SL, et al. Calcium/vitamin D supplementation and coronary artery calcification in the Women's Health Initiative. *Menopause.* 2010;17(4):683–91.
25. Williams MC, Moss AJ, Dweck M, Adamson PD, Alam S, Hunter A, et al. Coronary artery plaque characteristics associated with adverse outcomes in the SCOT-HEART study. *J Am Coll Cardiol.* 2019;73(3):291–301.
26. McClelland RL, Jorgensen NW, Budoff M, Blaha MJ, Post WS, Kronmal RA, et al. 10-year coronary heart disease risk prediction using coronary artery calcium and traditional risk factors: derivation in the MESA (Multi-Ethnic Study of Atherosclerosis) with validation in the HNR (Heinz Nixdorf Recall) study and the DHS (Dallas Heart Study). *J Am Coll Cardiol.* 2015;66(15):1643–53.
27. Arnett DK, Blumenthal RS, Albert MA, Buroker AB, Goldberger ZD, Hahn EJ, et al. 2019 ACC/AHA guideline on the primary prevention of cardiovascular disease: executive summary: a report of the American College of Cardiology/American Heart Association task force on clinical practice guidelines. *Circulation.* 2019;140(11):e563–e95.

28. Pasch A, Farese S, Graber S, Wald J, Richtering W, Floege J, et al. Nanoparticle-based test measures overall propensity for calcification in serum. *J Am Soc Nephrol.* 2012;23(10):1744–52.
29. Smith ER, Ford ML, Tomlinson LA, Bodenham E, McMahon LP, Farese S, et al. Serum calcification propensity predicts all-cause mortality in predialysis CKD. *J Am Soc Nephrol.* 2014;25(2):339–48.
30. Keyzer CA, de Borst MH, van den Berg E, Jahnhen-Dechent W, Arampatzis S, Farese S, et al. Calcification propensity and survival among renal transplant recipients. *J Am Soc Nephrol.* 2016;27(1):239–48.
31. Pasch A, Block GA, Bachtler M, Smith ER, Jahnhen-Dechent W, Arampatzis S, et al. Blood calcification propensity, cardiovascular events, and survival in patients receiving hemodialysis in the EVOLVE trial. *Clin J Am Soc Nephrol.* 2017;12(2):315–22.
32. Thompson S, James M, Wiebe N, Hemmelgarn B, Manns B, Klarenbach S, et al. Cause of death in patients with reduced kidney function. *J Am Soc Nephrol.* 2015;26(10):2504–11.
33. Bundy JD, Cai X, Mehta RC, Scialla JJ, de Boer IH, Hsu CY, et al. Serum calcification propensity and clinical events in CKD. *Clin J Am Soc Nephrol.* 2019;14(11):1562–71.
34. Bundy JD, Cai X, Scialla JJ, Dobre MA, Chen J, Hsu CY, et al. Serum calcification propensity and coronary artery calcification among patients with CKD: the CRIC (chronic renal insufficiency cohort) study. *Am J Kidney Dis.* 2019;73(6):806–14.
35. Lorenz G, Steubl D, Kemmer S, Pasch A, Koch-Sembdner W, Pham D, et al. Worsening calcification propensity precedes all-cause and cardiovascular mortality in haemodialyzed patients. *Sci Rep.* 2017;7(1):13368.
36. Schurgers LJ, Barreto DV, Barreto FC, Liabeuf S, Renard C, Magdeleyns EJ, et al. The circulating inactive form of matrix gla protein is a surrogate marker for vascular calcification in chronic kidney disease: a preliminary report. *Clin J Am Soc Nephrol.* 2010;5(4):568–75.
37. Holden RM, Morton AR, Garland JS, Pavlov A, Day AG, Booth SL. Vitamins K and D status in stages 3–5 chronic kidney disease. *Clin J Am Soc Nephrol.* 2010;5(4):590–7.
38. Nigwekar SU, Bloch DB, Nazarian RM, Vermeer C, Booth SL, Xu D, et al. Vitamin K-dependent carboxylation of matrix Gla protein influences the risk of calciphylaxis. *J Am Soc Nephrol.* 2017;28(6):1717–22.
39. Julius JK, Fernandez CK, Grafa AC, Rosa PM, Hartos JL. Daily fruit and vegetable consumption and diabetes status in middle-aged females in the general US population. *SAGE Open Med.* 2019;7:2050312119865116.
40. Andrews J, Psaltis PJ, Bayturan O, Shao M, Stegman B, Elshazly M, et al. Warfarin use is associated with progressive coronary arterial calcification: insights from serial intravascular ultrasound. *JACC Cardiovasc Imaging.* 2018;11(9):1315–23.
41. Han KH, O'Neill WC. Increased peripheral arterial calcification in patients receiving warfarin. *J Am Heart Assoc.* 2016;5(1). pii: e002665. <https://doi.org/10.1161/JAHA.115.002665>.
42. Win TT, Nakanishi R, Osawa K, Li D, Susaria SS, Jayawardena E, et al. Apixaban versus warfarin in evaluation of progression of atherosclerotic and calcified plaques (prospective randomized trial). *Am Heart J.* 2019;212:129–33.
43. Lees JS, Chapman FA, Witham MD, Jardine AG, Mark PB. Vitamin K status, supplementation and vascular disease: a systematic review and meta-analysis. *Heart.* 2019;105(12):938–45.
44. Zwakenberg SR, de Jong PA, Bartstra JW, van Asperen R, Westerink J, de Valk H, et al. The effect of menaquinone-7 supplementation on vascular calcification in patients with diabetes: a randomized, double-blind, placebo-controlled trial. *Am J Clin Nutr.* 2019;110(4):883–90.
45. Baskin SI, Horowitz AM, Nealley EW. The antidotal action of sodium nitrite and sodium thiosulfate against cyanide poisoning. *J Clin Pharmacol.* 1992;32(4):368–75.
46. Adirekkiat S, Sumethkul V, Ingsathit A, Domrongkitchaiporn S, Phakdeekitcharoen B, Kantachuesiri S, et al. Sodium thiosulfate delays the progression of coronary artery calcification in haemodialysis patients. *Nephrol Dial Transplant.* 2010;25(6):1923–9.
47. Mathews SJ, de Las Fuentes L, Podaralla P, Cabellon A, Zheng S, Bierhals A, et al. Effects of sodium thiosulfate on vascular calcification in end-stage renal disease: a pilot study of feasibility, safety and efficacy. *Am J Nephrol.* 2011;33(2):131–8.

48. Hill JA, Goldin JG, Gjertson D, Emerick AM, Greaser LD, Yoon HC, et al. Progression of coronary artery calcification in patients taking alendronate for osteoporosis. *Acad Radiol.* 2002;9(10):1148–52.
49. Tanko LB, Qin G, Alexandersen P, Bagger YZ, Christiansen C. Effective doses of ibandronate do not influence the 3-year progression of aortic calcification in elderly osteoporotic women. *Osteoporos Int.* 2005;16(2):184–90.
50. Toussaint ND, Elder GJ, Kerr PG. Bisphosphonates in chronic kidney disease; balancing potential benefits and adverse effects on bone and soft tissue. *Clin J Am Soc Nephrol.* 2009;4(1):221–33.
51. Hashiba H, Aizawa S, Tamura K, Kogo H. Inhibition of the progression of aortic calcification by etidronate treatment in hemodialysis patients: long-term effects. *Ther Apher Dial.* 2006;10(1):59–64.
52. Ariyoshi T, Eishi K, Sakamoto I, Matsukuma S, Odate T. Effect of etidronic acid on arterial calcification in dialysis patients. *Clin Drug Investig.* 2006;26(4):215–22.
53. Kranenburg G, de Jong PA, Bartstra JW, Lagerweij SJ, Lam MG, Ossewaarde-van Norel J, et al. Etidronate for prevention of ectopic mineralization in patients with pseudoxanthoma elasticum. *J Am Coll Cardiol.* 2018;71(10):1117–26.
54. Schantl AE, Ivarsson ME, Leroux J-C. Investigational pharmacological treatments for vascular calcification. *Adv Ther.* 2019;2:1800094.
55. Black DM, Delmas PD, Eastell R, Reid IR, Boonen S, Cauley JA, et al. Once-yearly zoledronic acid for treatment of postmenopausal osteoporosis. *N Engl J Med.* 2007;356(18):1809–22.
56. Massy ZA, Druke TB. Magnesium and cardiovascular complications of chronic kidney disease. *Nat Rev Nephrol.* 2015;11(7):432–42.
57. Kanbay M, Yilmaz MI, Apetrii M, Saglam M, Yaman H, Unal HU, et al. Relationship between serum magnesium levels and cardiovascular events in chronic kidney disease patients. *Am J Nephrol.* 2012;36(3):228–37.
58. Sakaguchi Y, Fujii N, Shoji T, Hayashi T, Rakugi H, Isaka Y. Hypomagnesemia is a significant predictor of cardiovascular and non-cardiovascular mortality in patients undergoing hemodialysis. *Kidney Int.* 2014;85(1):174–81.
59. Molnar AO, Biyani M, Hammond I, Harmon JP, Lavoie S, McCormick B, et al. Lower serum magnesium is associated with vascular calcification in peritoneal dialysis patients: a cross sectional study. *BMC Nephrol.* 2017;18(1):129.
60. Ishimura E, Okuno S, Yamakawa T, Inaba M, Nishizawa Y. Serum magnesium concentration is a significant predictor of mortality in maintenance hemodialysis patients. *Magnes Res.* 2007;20(4):237–44.
61. Spiegel DM, Farmer B. Long-term effects of magnesium carbonate on coronary artery calcification and bone mineral density in hemodialysis patients: a pilot study. *Hemodial Int.* 2009;13(4):453–9.
62. Tzanakis IP, Stamataki EE, Papadaki AN, Giannakis N, Damianakis NE, Oreopoulos DG. Magnesium retards the progress of the arterial calcifications in hemodialysis patients: a pilot study. *Int Urol Nephrol.* 2014;46(11):2199–205.
63. Bressendorff I, Hansen D, Schou M, Silver B, Pasch A, Bouchelouche P, et al. Oral magnesium supplementation in chronic kidney disease stages 3 and 4: efficacy, safety, and effect on serum calcification propensity—a prospective randomized double-blinded placebo-controlled clinical trial. *Kidney Int Rep.* 2017;2(3):380–9.
64. Bressendorff I, Hansen D, Schou M, Kragelund C, Brandi L. The effect of magnesium supplementation on vascular calcification in chronic kidney disease—a randomised clinical trial (MAGiCAL-CKD): essential study design and rationale. *BMJ Open.* 2017;7(6):e016795.
65. Perello J, Gomez M, Ferrer MD, Rodriguez NY, Salcedo C, Buades JM, et al. SNF472, a novel inhibitor of vascular calcification, could be administered during hemodialysis to attain potentially therapeutic phytate levels. *J Nephrol.* 2018;31(2):287–96.

66. Perello J, Joubert PH, Ferrer MD, Canals AZ, Sinha S, Salcedo C. First-time-in-human randomized clinical trial in healthy volunteers and haemodialysis patients with SNF472, a novel inhibitor of vascular calcification. *Br J Clin Pharmacol*. 2018;84(12):2867–76.
67. Raggi P, Bellasi A, Bushinsky D, Bover J, Rodriguez M, Ketteler M, et al. Slowing progression of cardiovascular calcification with SNF472 in patients on hemodialysis: results of a randomized, phase 2b study. *Circulation*. 2020;141:728–39.
68. Samelson EJ, Miller PD, Christiansen C, Daizadeh NS, Grazette L, Anthony MS, et al. RANKL inhibition with denosumab does not influence 3-year progression of aortic calcification or incidence of adverse cardiovascular events in postmenopausal women with osteoporosis and high cardiovascular risk. *J Bone Miner Res*. 2014;29(2):450–7.
69. Mintz GS, Popma JJ, Pichard AD, Kent KM, Satler LF, Chuang YC, et al. Patterns of calcification in coronary artery disease. A statistical analysis of intravascular ultrasound and coronary angiography in 1155 lesions. *Circulation*. 1995;91(7):1959–65.
70. Mehanna E, Bezerra HG, Prabhu D, Brandt E, Chamie D, Yamamoto H, et al. Volumetric characterization of human coronary calcification by frequency-domain optical coherence tomography. *Circ J*. 2013;77(9):2334–40.
71. De Maria GL, Scarsini R, Banning AP. Management of calcific coronary artery lesions: is it time to change our interventional therapeutic approach? *JACC Cardiovasc Interv*. 2019;12(15):1465–78.
72. Wang X, Matsumura M, Mintz GS, Lee T, Zhang W, Cao Y, et al. In vivo calcium detection by comparing optical coherence tomography, intravascular ultrasound, and angiography. *JACC Cardiovasc Imaging*. 2017;10(8):869–79.
73. Bourantas CV, Zhang YJ, Garg S, Iqbal J, Valgimigli M, Windecker S, et al. Prognostic implications of coronary calcification in patients with obstructive coronary artery disease treated by percutaneous coronary intervention: a patient-level pooled analysis of 7 contemporary stent trials. *Heart*. 2014;100(15):1158–64.
74. Onuma Y, Tanimoto S, Ruygrok P, Neuzner J, Piek JJ, Seth A, et al. Efficacy of everolimus eluting stent implantation in patients with calcified coronary culprit lesions: two-year angiographic and three-year clinical results from the SPIRIT II study. *Catheter Cardiovasc Interv*. 2010;76(5):634–42.
75. Copeland-Halperin RS, Baber U, Aquino M, Rajamanickam A, Roy S, Hasan C, et al. Prevalence, correlates, and impact of coronary calcification on adverse events following PCI with newer-generation DES: findings from a large multiethnic registry. *Catheter Cardiovasc Interv*. 2018;91(5):859–66.
76. Genereux P, Madhavan MV, Mintz GS, Maehara A, Kirtane AJ, Palmerini T, et al. Relation between coronary calcium and major bleeding after percutaneous coronary intervention in acute coronary syndromes (from the Acute Catheterization and Urgent Intervention Triage Strategy and Harmonizing Outcomes with Revascularization and Stents in Acute Myocardial Infarction Trials). *Am J Cardiol*. 2014;113(6):930–5.
77. Karacsonyi J, Karpaliotis D, Alaswad K, Jaffer FA, Yeh RW, Patel M, et al. Impact of calcium on chronic total occlusion percutaneous coronary interventions. *Am J Cardiol*. 2017;120(1):40–6.
78. Genereux P, Redfors B, Witzenbichler B, Arsenaault MP, Weisz G, Stuckey TD, et al. Two-year outcomes after percutaneous coronary intervention of calcified lesions with drug-eluting stents. *Int J Cardiol*. 2017;231:61–7.
79. Shavadia JS, Vo MN, Bainey KR. Challenges with severe coronary artery calcification in percutaneous coronary intervention: a narrative review of therapeutic options. *Can J Cardiol*. 2018;34(12):1564–72.
80. Mintz GS, Potkin BN, Keren G, Satler LF, Pichard AD, Kent KM, et al. Intravascular ultrasound evaluation of the effect of rotational atherectomy in obstructive atherosclerotic coronary artery disease. *Circulation*. 1992;86(5):1383–93.
81. Gupta T, Weinreich M, Greenberg M, Colombo A, Latib A. Rotational atherectomy: a contemporary appraisal. *Interv Cardiol*. 2019;14(3):182–9.

82. Farb A, Roberts DK, Pichard AD, Kent KM, Virmani R. Coronary artery morphologic features after coronary rotational atherectomy: insights into mechanisms of lumen enlargement and embolization. *Am Heart J*. 1995;129(6):1058–67.
83. Bittl JA, Chew DP, Topol EJ, Kong DF, Califf RM. Meta-analysis of randomized trials of percutaneous transluminal coronary angioplasty versus atherectomy, cutting balloon atherotomy, or laser angioplasty. *J Am Coll Cardiol*. 2004;43(6):936–42.
84. Wasiak J, Law J, Watson P, Spinks A. Percutaneous transluminal rotational atherectomy for coronary artery disease. *Cochrane Database Syst Rev*. 2012;12:CD003334.
85. Abdel-Wahab M, Baev R, Dieker P, Kassner G, Khattab AA, Toelg R, et al. Long-term clinical outcome of rotational atherectomy followed by drug-eluting stent implantation in complex calcified coronary lesions. *Catheter Cardiovasc Interv*. 2013;81(2):285–91.
86. Abdel-Wahab M, Toelg R, Byrne RA, Geist V, El-Mawardy M, Allali A, et al. High-speed rotational atherectomy versus modified balloons prior to drug-eluting stent implantation in severely calcified coronary lesions. *Circ Cardiovasc Interv*. 2018;11(10):e007415.
87. Chambers JW, Feldman RL, Himmelstein SI, Bhatheja R, Villa AE, Strickman NE, et al. Pivotal trial to evaluate the safety and efficacy of the orbital atherectomy system in treating de novo, severely calcified coronary lesions (ORBIT II). *JACC Cardiovasc Interv*. 2014;7(5):510–8.
88. Lee MS, Shlofmitz E, Park KW, Goldberg A, Jeremias A, Shlofmitz R. Orbital atherectomy of severely calcified unprotected left main coronary artery disease: one-year outcomes. *J Invasive Cardiol*. 2018;30(7):270–4.
89. Bilodeau L, Fretz EB, Taeymans Y, Koolen J, Taylor K, Hilton DJ. Novel use of a high-energy excimer laser catheter for calcified and complex coronary artery lesions. *Catheter Cardiovasc Interv*. 2004;62(2):155–61.
90. Bittl JA. Excimer laser angioplasty: focus on total occlusions. *Am J Cardiol*. 1996;78(7):823–4.
91. Mintz GS, Kovach JA, Javier SP, Pichard AD, Kent KM, Popma JJ, et al. Mechanisms of lumen enlargement after excimer laser coronary angioplasty. An intravascular ultrasound study. *Circulation*. 1995;92(12):3408–14.
92. Latib A, Takagi K, Chizzola G, Tobis J, Ambrosini V, Niccoli G, et al. Excimer Laser LEsion modification to expand non-dilatable stents: the ELLEMENT registry. *Cardiovasc Revasc Med*. 2014;15(1):8–12.
93. Lee T, Shlofmitz RA, Song L, Tsiamtsiouris T, Pappas T, Madrid A, et al. The effectiveness of excimer laser angioplasty to treat coronary in-stent stenosis with peri-stent calcium as assessed by optical coherence tomography. *EuroIntervention*. 2019;15(3):e279–e88.
94. Ali ZA, Brinton TJ, Hill JM, Maehara A, Matsumura M, Karimi Galougahi K, et al. Optical coherence tomography characterization of coronary lithoplasty for treatment of calcified lesions: first description. *JACC Cardiovasc Imaging*. 2017;10(8):897–906.
95. Ali ZA, Nef H, Escaned J, Werner N, Banning AP, Hill JM, et al. Safety and effectiveness of coronary intravascular lithotripsy for treatment of severely calcified coronary stenoses: the disrupt CAD II study. *Circ Cardiovasc Interv*. 2019;12(10):e008434.
96. Osswald BR, Blackstone EH, Tochtermann U, Schweiger P, Thomas G, Vahl CF, et al. Does the completeness of revascularization affect early survival after coronary artery bypass grafting in elderly patients? *Eur J Cardiothorac Surg*. 2001;20(1):120–5; discussion 5–6.
97. Nakayama Y, Sakata R, Ura M, Miyamoto TA. Coronary artery bypass grafting in dialysis patients. *Ann Thorac Surg*. 1999;68(4):1257–61.
98. Castagna MT, Mintz GS, Ohlmann P, Kotani J, Maehara A, Gevorkian N, et al. Incidence, location, magnitude, and clinical correlates of saphenous vein graft calcification: an intravascular ultrasound and angiographic study. *Circulation*. 2005;111(9):1148–52.
99. Ertelt K, Genreux P, Mintz GS, Reiss GR, Kirtane AJ, Madhavan MV, et al. Impact of the severity of coronary artery calcification on clinical events in patients undergoing coronary artery bypass grafting (from the Acute Catheterization and Urgent Intervention Triage Strategy Trial). *Am J Cardiol*. 2013;112(11):1730–7.
100. Genreux P, Palmerini T, Caixeta A, Rosner G, Green P, Dressler O, et al. Quantification and impact of untreated coronary artery disease after percutaneous coronary intervention: the

- residual SYNTAX (Synergy Between PCI with Taxus and Cardiac Surgery) score. *J Am Coll Cardiol*. 2012;59(24):2165–74.
101. Rosner GF, Kirtane AJ, Genereux P, Lansky AJ, Cristea E, Gersh BJ, et al. Impact of the presence and extent of incomplete angiographic revascularization after percutaneous coronary intervention in acute coronary syndromes: the Acute Catheterization and Urgent Intervention Triage Strategy (ACUITY) trial. *Circulation*. 2012;125(21):2613–20.
 102. Yamaguchi A, Adachi H, Tanaka M, Ino T. Efficacy of intraoperative epi-aortic ultrasound scanning for preventing stroke after coronary artery bypass surgery. *Ann Thorac Cardiovasc Surg*. 2009;15(2):98–104.
 103. Yamauchi T, Miyata H, Sakaguchi T, Miyagawa S, Yoshikawa Y, Takeda K, et al. Coronary artery bypass grafting in hemodialysis-dependent patients: analysis of Japan Adult Cardiovascular Surgery Database. *Circ J*. 2012;76(5):1115–20.
 104. Liu JY, Birkmeyer NJ, Sanders JH, Morton JR, Henriques HF, Lahey SJ, et al. Risks of morbidity and mortality in dialysis patients undergoing coronary artery bypass surgery. Northern New England Cardiovascular Disease Study Group. *Circulation*. 2000;102(24):2973–7.
 105. Chang TI, Shilane D, Kazi DS, Montez-Rath ME, Hlatky MA, Winkelmayer WC. Multivessel coronary artery bypass grafting versus percutaneous coronary intervention in ESRD. *J Am Soc Nephrol*. 2012;23(12):2042–9.
 106. Afsar B, Turkmen K, Covic A, Kanbay M. An update on coronary artery disease and chronic kidney disease. *Int J Nephrol*. 2014;2014:767424.
 107. Serruys PW, Morice MC, Kappetein AP, Colombo A, Holmes DR, Mack MJ, et al. Percutaneous coronary intervention versus coronary-artery bypass grafting for severe coronary artery disease. *N Engl J Med*. 2009;360(10):961–72.
 108. Farkouh ME, Domanski M, Sleeper LA, Siami FS, Dangas G, Mack M, et al. Strategies for multivessel revascularization in patients with diabetes. *N Engl J Med*. 2012;367(25):2375–84.
 109. Bourantas CV, Zhang YJ, Garg S, Mack M, Dawkins KD, Kappetein AP, et al. Prognostic implications of severe coronary calcification in patients undergoing coronary artery bypass surgery: an analysis of the SYNTAX study. *Catheter Cardiovasc Interv*. 2015;85(2):199–206.
 110. Hirsch AT, Haskal ZJ, Hertzner NR, Bakal CW, Creager MA, Halperin JL, et al. ACC/AHA 2005 Practice Guidelines for the management of patients with peripheral arterial disease (lower extremity, renal, mesenteric, and abdominal aortic): a collaborative report from the American Association for Vascular Surgery/Society for Vascular Surgery, Society for Cardiovascular Angiography and Interventions, Society for Vascular Medicine and Biology, Society of Interventional Radiology, and the ACC/AHA Task Force on Practice Guidelines (Writing Committee to Develop Guidelines for the Management of Patients with Peripheral Arterial Disease): endorsed by the American Association of Cardiovascular and Pulmonary Rehabilitation; National Heart, Lung, and Blood Institute; Society for Vascular Nursing; TransAtlantic Inter-Society Consensus; and Vascular Disease Foundation. *Circulation*. 2006;113(11):e463–654.
 111. Rifkin DE, Ix JH, Wassel CL, Criqui MH, Allison MA. Renal artery calcification and mortality among clinically asymptomatic adults. *J Am Coll Cardiol*. 2012;60(12):1079–85.
 112. Capek P, McLean GK, Berkowitz HD. Femoropopliteal angioplasty. Factors influencing long-term success. *Circulation*. 1991;83(2 Suppl):I70–80.
 113. Bausback Y, Botsios S, Flux J, Werner M, Schuster J, Aithal J, et al. Outback catheter for femoropopliteal occlusions: immediate and long-term results. *J Endovasc Ther*. 2011;18(1):13–21.
 114. Scheinert D, Grummt L, Piorowski M, Sax J, Scheinert S, Ulrich M, et al. A novel self-expanding interwoven nitinol stent for complex femoropopliteal lesions: 24-month results of the SUPERA SFA registry. *J Endovasc Ther*. 2011;18(6):745–52.
 115. Das T, Mustapha J, Indes J, Vorhies R, Beasley R, Doshi N, et al. Technique optimization of orbital atherectomy in calcified peripheral lesions of the lower extremities: the CONFIRM series, a prospective multicenter registry. *Catheter Cardiovasc Interv*. 2014;83(1):115–22.
 116. Kim JH, Ahanchi SS, Panneton JM. Identifying the target lesions for 245 laser angioplasty cases and a review of the literature. *Vasc Endovasc Surg*. 2012;46(8):640–7.

117. Zeller T, Langhoff R, Rocha-Singh KJ, Jaff MR, Blessing E, Amann-Vesti B, et al. Directional atherectomy followed by a paclitaxel-coated balloon to inhibit restenosis and maintain vessel patency: twelve-month results of the DEFINITIVE AR study. *Circ Cardiovasc Interv.* 2017;10(9):e004848.
118. Shrikhande GV, McKinsey JF. Use and abuse of atherectomy: where should it be used? *Semin Vasc Surg.* 2008;21(4):204–9.
119. Todd KE Jr, Ahanchi SS, Maurer CA, Kim JH, Chipman CR, Panneton JM. Atherectomy offers no benefits over balloon angioplasty in tibial interventions for critical limb ischemia. *J Vasc Surg.* 2013;58(4):941–8.
120. Roberts D, Niazi K, Miller W, Krishnan P, Gammon R, Schreiber T, et al. Effective endovascular treatment of calcified femoropopliteal disease with directional atherectomy and distal embolic protection: final results of the DEFINITIVE Ca(+)(+) trial. *Catheter Cardiovasc Interv.* 2014;84(2):236–44.
121. Rocha-Singh KJ, Zeller T, Jaff MR. Peripheral arterial calcification: prevalence, mechanism, detection, and clinical implications. *Catheter Cardiovasc Interv.* 2014;83(6):E212–20.
122. Cioppa A, Stabile E, Popusoi G, Salemme L, Cota L, Pucciarelli A, et al. Combined treatment of heavy calcified femoro-popliteal lesions using directional atherectomy and a paclitaxel coated balloon: one-year single centre clinical results. *Cardiovasc Revasc Med.* 2012;13(4):219–23.
123. Li X, Zhao G, Zhang J, Duan Z, Xin S. Prevalence and trends of the abdominal aortic aneurysms epidemic in general population—a meta-analysis. *PLoS One.* 2013;8(12):e81260.
124. TerBush MJ, Rasheed K, Young ZZ, Ellis JL, Glocker RJ, Doyle AJ, et al. Aortoiliac calcification correlates with 5-year survival after abdominal aortic aneurysm repair. *J Vasc Surg.* 2019;69(3):774–82.
125. Lederle FA, Freischlag JA, Kyriakides TC, Padberg FT Jr, Matsumura JS, Kohler TR, et al. Outcomes following endovascular vs open repair of abdominal aortic aneurysm: a randomized trial. *JAMA.* 2009;302(14):1535–42.
126. Chowdhury MM, Zielinski LP, Sun JJ, Lambracos S, Boyle JR, Harrison SC, et al. Editor’s choice – calcification of thoracic and abdominal aneurysms is associated with mortality and morbidity. *Eur J Vasc Endovasc Surg.* 2018;55(1):101–8.
127. Wyss TR, Dick F, Brown LC, Greenhalgh RM. The influence of thrombus, calcification, angulation, and tortuosity of attachment sites on the time to the first graft-related complication after endovascular aneurysm repair. *J Vasc Surg.* 2011;54(4):965–71.
128. Fertman MH, Wolff L. Calcification of the mitral valve. *Am Heart J.* 1946;31:580–9.
129. Allison MA, Cheung P, Criqui MH, Langer RD, Wright CM. Mitral and aortic annular calcification are highly associated with systemic calcified atherosclerosis. *Circulation.* 2006;113(6):861–6.
130. Kanjanathai S, Nasir K, Katz R, Rivera JJ, Takasu J, Blumenthal RS, et al. Relationships of mitral annular calcification to cardiovascular risk factors: the Multi-Ethnic Study of Atherosclerosis (MESA). *Atherosclerosis.* 2010;213(2):558–62.
131. Asselbergs FW, Mozaffarian D, Katz R, Kestenbaum B, Fried LF, Gottdiener JS, et al. Association of renal function with cardiac calcifications in older adults: the cardiovascular health study. *Nephrol Dial Transplant.* 2009;24(3):834–40.
132. Foley PW, Hamaad A, El-Gendi H, Leyva F. Incidental cardiac findings on computed tomography imaging of the thorax. *BMC Res Notes.* 2010;3:326.
133. Fox CS, Vasan RS, Parise H, Levy D, O’Donnell CJ, D’Agostino RB, et al. Mitral annular calcification predicts cardiovascular morbidity and mortality: the Framingham Heart Study. *Circulation.* 2003;107(11):1492–6.
134. Nair CK, Runco V, Everson GT, Boghairi A, Mooss AN, Mohiuddin SM, et al. Conduction defects and mitral annulus calcification. *Br Heart J.* 1980;44(2):162–7.
135. Nestico PF, Depace NL, Morganroth J, Kotler MN, Ross J. Mitral annular calcification: clinical, pathophysiology, and echocardiographic review. *Am Heart J.* 1984;107(5 Pt 1):989–96.

136. Fulkerson PK, Beaver BM, Auseon JC, Graber HL. Calcification of the mitral annulus: etiology, clinical associations, complications and therapy. *Am J Med.* 1979;66(6):967–77.
137. O’Neal WT, Efirid JT, Nazarian S, Alonso A, Heckbert SR, Soliman EZ. Mitral annular calcification and incident atrial fibrillation in the Multi-Ethnic Study of Atherosclerosis. *Europace.* 2015;17(3):358–63.
138. Fox CS, Parise H, Vasan RS, Levy D, O’Donnell CJ, D’Agostino RB, et al. Mitral annular calcification is a predictor for incident atrial fibrillation. *Atherosclerosis.* 2004;173(2):291–4.
139. Carpentier AF, Pellerin M, Fuzellier JF, Relland JY. Extensive calcification of the mitral valve annulus: pathology and surgical management. *J Thorac Cardiovasc Surg.* 1996;111(4):718–29; discussion 29–30.
140. Okada Y. Surgical management of mitral annular calcification. *Gen Thorac Cardiovasc Surg.* 2013;61(11):619–25.
141. Maisano F, Caldarola A, Blasio A, De Bonis M, La Canna G, Alfieri O. Midterm results of edge-to-edge mitral valve repair without annuloplasty. *J Thorac Cardiovasc Surg.* 2003;126(6):1987–97.
142. Bilge M, Ali S, Alsancak Y, Yasar AS. Percutaneous mitral valve repair with the MitraClip system in mitral regurgitation due to mitral annular calcification. *J Heart Valve Dis.* 2015;24(3):316–9.
143. Cheng R, Tat E, Siegel RJ, Arsanjani R, Hussaini A, Makar M, et al. Mitral annular calcification is not associated with decreased procedural success, durability of repair, or left ventricular remodelling in percutaneous edge-to-edge repair of mitral regurgitation. *EuroIntervention.* 2016;12(9):1176–84.
144. Palacios IF, Block PC, Wilkins GT, Weyman AE. Follow-up of patients undergoing percutaneous mitral balloon valvotomy. Analysis of factors determining restenosis. *Circulation.* 1989;79(3):573–9.
145. Iung B, Cormier B, Ducimetiere P, Porte JM, Nallet O, Michel PL, et al. Immediate results of percutaneous mitral commissurotomy. A predictive model on a series of 1514 patients. *Circulation.* 1996;94(9):2124–30.
146. Meneveau N, Schiele F, Seronde MF, Breton V, Gupta S, Bernard Y, et al. Predictors of event-free survival after percutaneous mitral commissurotomy. *Heart.* 1998;80(4):359–64.
147. Bouleti C, Iung B, Laouenan C, Himbert D, Brochet E, Messika-Zeitoun D, et al. Late results of percutaneous mitral commissurotomy up to 20 years: development and validation of a risk score predicting late functional results from a series of 912 patients. *Circulation.* 2012;125(17):2119–27.
148. Abascal VM, Wilkins GT, O’Shea JP, Choong CY, Palacios IF, Thomas JD, et al. Prediction of successful outcome in 130 patients undergoing percutaneous balloon mitral valvotomy. *Circulation.* 1990;82(2):448–56.
149. Bouleti C, Iung B, Himbert D, Messika-Zeitoun D, Brochet E, Garbarz E, et al. Relationship between valve calcification and long-term results of percutaneous mitral commissurotomy for rheumatic mitral stenosis. *Circ Cardiovasc Interv.* 2014;7(3):381–9.
150. Puri R, Abdul-Jawad Altisent O, del Trigo M, Campelo-Parada F, Regueiro A, Barbosa Ribeiro H, et al. Transcatheter mitral valve implantation for inoperable severely calcified native mitral valve disease: a systematic review. *Catheter Cardiovasc Interv.* 2016;87(3):540–8.

Chapter 22

Surgical Versus Transcatheter Aortic Valve Replacement



Farhang Yazdchi and Prem Shekar

Epidemiology and Mechanism of Calcific Aortic Stenosis

Senile progressive degenerative calcification leads to thickening of aortic valve (AV) cusps, resulting in aortic valve stenosis (AS). In developed countries, AS is the most prevalent of all valvular heart diseases. The prevalence of severe AS is 1.3% in patients aged 65–75, 2.4% in those aged 75–85, and 4% in those older than 85 years [1]. Risk factors are similar to those of coronary artery disease including age, male sex, hyperlipidemia, and evidence of active inflammation [2]. There is high coincidence of coronary artery disease and AS. Taylor et al., on a large population study of African-American patients, reported that those with AV sclerosis were 4.26 times more likely to have events related to coronary heart disease than those without AV sclerosis [3]. However, the mechanism of the two disease seems to be different. Detailed mechanisms of calcific aortic valve disease are provided in Chap. 4.

Symptoms and Severity of Aortic Stenosis

Patients with AS have a long latent period before symptoms appear. When patients become symptomatic from severe AS, usually after the sixth decade of life, there is a rapid decline in mean survival (Fig. 22.1). Classic symptoms include angina, syncope, and dyspnea [4]. The onsets of dyspnea and heart failure are predictors for worse prognosis in the natural history of AS with 50% mortality in 2 years if left untreated (Fig. 22.2) [4]. Normal aortic valve area (AVA) is 3–4 cm². When valve

F. Yazdchi (✉) · P. Shekar
Division of Cardiac Surgery, Brigham and Women's Hospital, Harvard Medical School,
Boston, MA, USA
e-mail: fyazdchi@bwh.harvard.edu

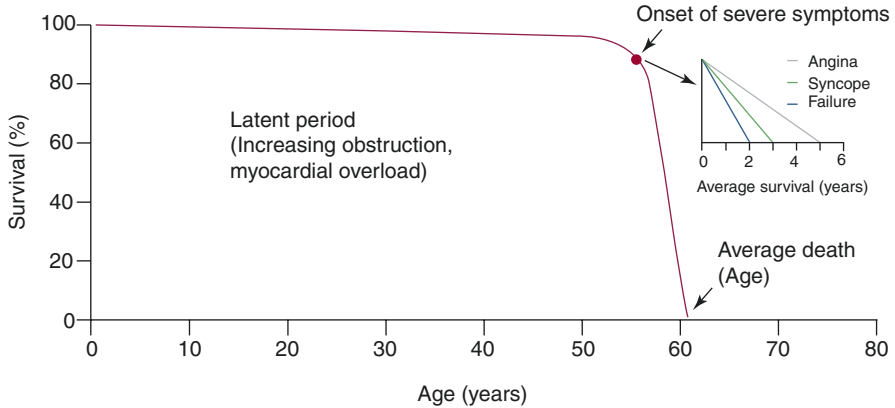


Fig. 22.1 Survival of patients with aortic stenosis over time. A long latent asymptomatic period with normal survival, followed by rapid decline in survival once symptoms develop. (Modified figure) [4]

area becomes $\leq 0.8 \text{ cm}^2$, the mean gradient across the AV exceeds 40 mmHg, or the velocity across the AV exceeds 4 m/sec, it is considered severe AS. AVA of $< 0.5 \text{ cm}^2$ is considered critical stenosis [5]. Symptomatic severe AS is due to an obstruction to cardiac output. Therefore, effective mechanical relief in the form of surgical or transcatheter aortic valve replacement (TAVR) is indicated according to American Heart Association/American College of Cardiology (AHA/ACC) guidelines [5].

Surgical Aortic Valve Replacement

Over the last several decades, surgical aortic valve replacement (SAVR) has been the gold standard for treatment of AS. Two major types of prosthetic AV are available: mechanical and bioprosthetic valves. There are advantages and disadvantages to each. An ideal heart valve prosthesis with the durability of a mechanical prosthesis and low thrombogenicity of a bioprosthetic valves has not yet been manufactured. The technique of SAVR is described in detail elsewhere [6].

Mechanical Valves

Historical background and improvements in hemodynamic design: Dr. Charles Hufnagel, who had worked at Dr. Dwight Harken's laboratory at the Peter Bent Brigham Hospital, implanted the first in the world aortic "assist" valve in a 30-year-old woman with rheumatic disease in 1952. The Hufnagel valve consisted of a pea-size ball inside a chambered tube placed in descending aorta. More than 200

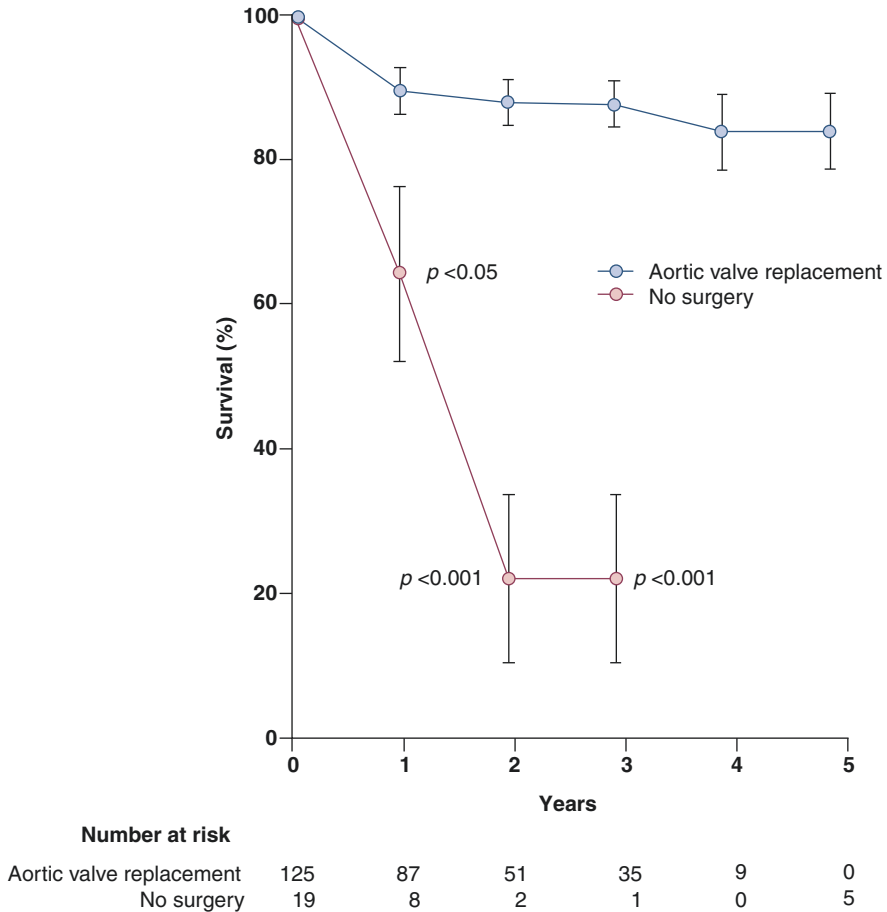


Fig. 22.2 Mean survival of patients with symptoms of aortic stenosis. (Modified figure) [58]

Hufnagel valves were implanted in patients with aortic insufficiency [7]. Dr. Harken later developed the Harken-Soroff ball valve, a ball valve with a fabricated stainless steel double cage. Several brands and models of ball valves were introduced in the 1960s, namely, the Starr-Edwards (SE) caged-ball valve (Fig. 22.3), Magovern-Cromie valve, Smeloff-Cutter valve, Debakey-Surgitool, and Braunwald-Cutter valve (a silicon rubber ball cage with titanium housing and a ring covered with Dacron fabric).

Disc valves were introduced in the late 1960s. They allowed blood to flow in a more natural way while reducing damage to red blood cells from destructive, mechanical forces. They had superior hemodynamics compared to ball valves. Three landmark, non-tilting disc valves were the Kay-Shiley, Beall-Surgitool, and Cooley-Cutter biconical disc valves. Five landmark tilting disc valves were the Bjork-Shiley flat, Bjork-Shiley convexo-concave, Lillehei-Kaster, Omniscience,

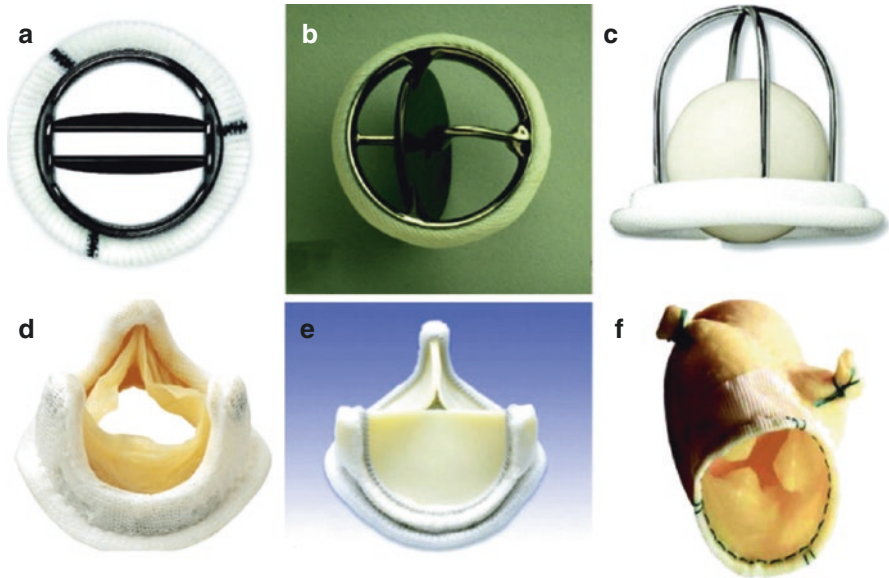


Fig. 22.3 Prosthetic heart valves. (a) Bileaflet mechanical valve (St Jude); (b) monoleaflet mechanical valve (Medtronic Hall); (c) caged-ball valve (Starr-Edwards); (d) stented porcine bioprosthesis (Medtronic Mosaic); (e) stented pericardial bioprosthesis (Carpentier-Edwards Magna); (f) stentless porcine bioprosthesis (Medtronic Freestyle) [59]

Omnicarbon, and Medtronic Hall tilting disc valves [8]. Unfortunately, the struts of these valves tended to fracture over time due to fatigue and design flaw. Later, silicon was replaced by pyrolytic carbon which helped to reduce wear and tear.

The two major bileaflet mechanical heart valves, the St. Jude Medical (SJM) bileaflet valve (Fig. 22.3) and CarboMedics bileaflet valve, were produced in the late 1970s and are still in use today without major change in design. The hinge mechanism located near the central axis of the housing mimics human physiology and makes these valves superior to previous designs. Discs are made of pyrolytic carbon, and the sewing ring is made of either PTFE or Dacron. SJM mechanical valves have been used with excellent results [9]. The CarboMedics (CM) mechanical valve has similar design to the SJM valve. It has a solid pyrolite carbon housing and flat leaflets made of pyrolite carbon-coated graphite that is impregnated with tungsten. The pyrolite carbon housing is reinforced by an outer ring composed of titanium that eliminates the risk of leaflet escape. Bileaflet valves have been used in both the aortic and mitral position with excellent long-term durability and freedom from reoperation [10]. The standard aortic valve prosthesis has the sewing cuff located at the outflow level of the valve cylinder. Both SJM and CM valves have supra-annular models where the sewing cuff has been transferred to the inflow level of the valve cylinder, allowing the valve to be upsized by one to two sizes. This is very important for optimizing hemodynamics and preventing patient-prosthesis mismatch [11]. The On-X valve is a newer-generation mechanical bileaflet valve

[12]. Use of pure pyrolytic carbon (devoid of silicon), and design modifications such as more natural length-to-diameter ratio and leaflet opening angle, has translated into increased strength, improved valve hemodynamics, and reduced hemolysis and thrombogenicity. The 2014 AHA/ACC guidelines for the management of patients with valvular heart disease recommend an international normalized ratio (INR) of 2.5 (range, 2–3) in patients with a mechanical valve in the aortic position. However, based on the results of the Prospective Randomized On-X Anticoagulation Clinical Trial (PROACT) [13], the Food and Drug Administration (FDA) approved use of this valve in April 2015 with a lower INR goal of 1.5–2.0 in the aortic position. This reduction in INR goal led to a statistically significant reduction in the combined endpoint of clots, bleeding events, and stroke rates with 9/patient-years for the lower INR group compared with 12/patient-years in the standard INR group.

Bioprosthetic Valves

Durability and hemodynamic performance are of utmost importance when selecting a bioprosthetic aortic valve for patients. The earlier-generation stented bioprosthetic valves included the Medtronic Hancock II Ultra (Medtronic Minneapolis, MN), which is a porcine bioprosthesis, and the Carpentier-Edwards Perimount (Edwards Lifesciences LLC, Irvine, CA), which is a pericardial bioprosthesis. These two valves have shown very good long-term durability in multiple studies [14–18]. Design of some of these earlier-generation valves intentionally allowed them to be implanted in the supra-annular position, allowing upsizing to achieve maximal hemodynamics and decrease the incidence of patient-prosthesis mismatch. The newer-generation prostheses are processed in a zero- or low-pressure fixation with anti-mineralization. This reduces material fatigue and calcification over time. Stents are thinner, allowing a lower profile to minimize protrusion into the aortic wall and facilitating coronary clearance. The third-generation bovine bioprostheses include the Carpentier-Edwards Magna Ease (Edwards Lifesciences, LLC) (Fig. 22.3) and the Trifecta (Abbott Vascular, Santa Clara, California). The Magna Ease has a narrow sewing cuff and was designed for supra-annular placement. It has demonstrated excellent durability and hydrodynamic performance [19]. The Trifecta is a pericardial valve that utilizes pericardium around the exterior of the stent, allowing a larger opening diameter to maximize flow. These characteristics make it an attractive option for the small aortic annulus. That said, Wendt et al. [20] compared the hemodynamic performance of the Trifecta versus the Perimount Magna and Magna Ease valve prostheses, in a nonrandomized, observational, single-center study, concluding no influence of prosthesis type on mean pressure gradient or aortic valve area.

More recently, Edwards Lifesciences has manufactured a new bioprosthetic valve, the INSPIRIS RESILIA, with the goal to improve durability by reducing prosthesis calcification. This valve was built based on the design of the Carpentier-Edwards Perimount Magna Ease valve. RESILIA tissue is bovine pericardial tissue

transformed by novel integrity preservation technology which permanently blocks residual aldehyde groups known to bind to calcium. As a result, the valve may have a longer shelf life and improved durability when implanted. The Inspiris valve has an expandable frame designed to allow for the possibility of valve-in-valve transcatheter aortic valve re-replacement if indicated in the future. This valve has been studied in the COMMENCE trial [21] with reported 2-year outcomes demonstrating early safety and effectiveness and has received FDA approval.

Stentless AV and root replacement using homografts or porcine xenograft (Fig. 22.3) has fallen out of favor in recent years mainly due to the complexity of the technique, limited durability despite excellent hemodynamics, and difficult reoperations. Use of homografts is limited to the treatment of active aortic valve endocarditis, particularly in patients with root abscesses [22].

Choice of Valve Type

Mechanical valves affect quality of life with the need for lifelong anticoagulation. According to AHA/ACC guidelines, the class 1 indications for prosthetic valve choice include the valve type being a shared decision between the patient and physician and bioprosthetic valves being recommended in patients of any age for whom anticoagulant therapy is contraindicated, cannot be managed appropriately, or is not desired. In other cases, the choice of valve is debatable, with no strong preference for one type over the other based on the guidelines. For elderly patients over age 70, the decision is easy, and most physicians and patients agree on biological valves, either via a surgical or transcatheter approach. For patients between the ages of 60 and 70, the decision is more debatable. Patients younger than age 60 tend to favor mechanical valves in order to avoid reoperation in future. However, this trend has changed in favor of bioprosthetic valves in recent years [23]. The primary motive for this is to avoid anticoagulation and subsequent lifestyle change with the added benefit of allowing for transcatheter valve-in-valve options should the bioprosthetic device fail. It is important to implant the largest bioprosthetic valve possible during the initial surgery to optimize the frame to accommodate a large valve in the future should valve-in-valve procedure become necessary.

Life Expectancy with Prosthetic Valves

Bouhout et al. [24], in a study of young, low-risk adults (<65 years) undergoing elective isolated mechanical AVR, demonstrated that survival is lower than expected in the age- and gender-matched general population in Quebec, Canada (actuarial survival at 1, 5, and 10 years was $98\% \pm 1\%$, $95\% \pm 1\%$, and $87\% \pm 1\%$, respectively). Expected survival in the age- and gender-matched general population was 99.6%, 97.6%, and 94.2% at 1, 5, and 10 years, respectively. The risk of a major

valve-related event such as endocarditis, major bleeding, valve thrombosis, prosthesis dysfunction such as paravalvular leak, and thromboembolism was 27% within 10 years in these young patients. Zellner et al. [25] looked at competing risks after mechanical valve replacement in both the aortic and mitral positions. Freedom from all complications (death, reoperation, endocarditis, major bleeding, stroke) in 15 years was only 41.5% for the AVR group. The decreased life expectancy compared to the general population after AVR is not inclusive to mechanical valves but also to bioprosthetic valves. A Canadian study of a younger patient population showed reduced life expectancy with bioprosthetic aortic valves compared with an age- and gender-matched Quebec population and was comparable to mechanical valves [26]. A randomized clinical trial from Italy showed no difference in survival between biologic and mechanical valves in the aortic position at 13 years [27]. In addition, a large database study of the STS registry including more than 30,000 patients aged between 65 and 80 years old showed no survival difference between biologic and mechanical valves [28]. This study showed significantly higher probability of reoperation in those with biologic valves due to structural valve deterioration.

Chikwe et al. [29], using the state of New York database, showed no difference in survival with biologic or mechanical valves implanted either in the aortic or mitral position in patients between 50 and 69 years old. In the same study, incidence of thromboembolism and incidence of major bleeding requiring transfusion were significantly higher in patients with mechanical valves, whereas risk of reoperation for structural valve problems was higher in patients with biologic valves. More recently however, in a large observational study of California State patients, a survival advantage of 4 percent at 15 years was shown in younger patients (45–54 years old) in favor of those who received mechanical aortic valves compared to those who received biologic valves [30]. Patients older than 54 years had similar survival with either valve type in that study.

Anticoagulation

Implantation of a mechanical heart valve mandates lifelong anticoagulation with warfarin. Unfortunately, this may dictate lifestyle change for some patients. A limitation with use of warfarin is difficulty controlling the international normalized ratio (INR) within the therapeutic level, described by using the term “time within therapeutic range” (TTR). One study showed that in the first 6 months of initiating warfarin, TTR was only 32% [31]. Patients who are not in TTR are exposed to bleeding risk if the INR is higher or thromboembolism if the INR is lower. A randomized control trial showed weekly self-testing of INR has no superiority over monthly clinic testing in reducing the risk of stroke, major bleeding episodes, and death among patients who are taking warfarin because of mechanical heart valves or atrial fibrillation [32]. Unlike warfarin, novel oral anticoagulants (NOACs), including direct thrombin and factor Xa inhibitors, do not need to be monitored with regular

labs, but these new anticoagulants are not approved for prosthetic heart valves. A randomized clinical trial comparing dabigatran, an oral direct thrombin inhibitor, with warfarin was terminated prematurely because of an excess of thromboembolic and bleeding events among patients in the dabigatran group [33].

Prosthetic valve thrombosis (PVT) is a rare but devastating complication affecting primarily mechanical valves. The occurrence of PVT depends to some extent on valve model, as well as patient compliance with oral anticoagulation, and is more common in the mitral position than the aortic. Two early RCTs [34, 35] showed statistically significant increase in bleeding with mechanical valves. However, Stassano et al. [27] in a RCT showed, at mean follow-up of 106 ± 28 months, there were no differences in linearized rate of thromboembolism, bleeding, endocarditis, and valve thrombosis between those who received mechanical and bioprosthetic aortic valves (1.47%/patient-year vs. 0.72%/patient-year). A statistical trend ($p = 0.08$) for increased bleeding in the mechanical group was noted however. Of note, 21% of patients in the bioprosthetic group in that study was receiving warfarin at the time of follow-up for other reasons. The bleeding rate in patients with bioprosthetic valves who were not receiving warfarin was less than those with mechanical valves on warfarin. Emergent reoperation for thrombectomy and valve replacement is necessary once PVT is diagnosed. A study from Montreal Heart Institute [36] showed high hospital and operative mortality in addition to poor long-term survival after redo valve replacement for thrombosis with 10-year actuarial survival rate of $46\% \pm 10\%$.

Trends in Choice of Prosthetic Aortic Valves

Despite excellent long-term results with implantation of mechanical valves, the recent trend in their use has declined compared to bioprosthetic valves, even in younger patients, particularly those who pursue an active lifestyle without anticoagulation. Brown et al. [23] reported on 108,687 isolated AVRs over a 10-year period from the Society of Thoracic Surgeons (STS) database showing increase in bioprosthetic use from 43.6% in 1997 to 78.4% in 2006. Similar trends were seen at our institution with an increased use of bioprosthetic valves from 20% to more than 60% in patients aged less than 60 years during past several years. Nowadays, younger patients are leaning more toward tissue valves in order to participate in an active lifestyle by avoiding anticoagulation. Awareness of the advantages and disadvantages of the two valve types has increased in the online information era. As such, patients have usually already made up their mind prior to pre-operative clinic visits with their surgeon. The operative mortality of repeat AVR is acceptable but higher than first-time AVR at 4.6% according to the STS database [37]. On the other hand, the advent of transcatheter aortic valve-in-valve replacement option has changed the landscape in the patient decision-making process despite uncertainty with regard to valve durability and valve thrombosis after valve-in-valve replacement. Candidacy for transcatheter options at time of need for reintervention is not guaranteed [37].

Patients in need of concomitant procedures such as coronary artery revascularization or concomitant aortic surgery for aneurysm replacement may not be candidates for transcatheter valve-in-valve intervention when their bioprosthetic valves fail over time. Patients must be informed of these potential situations prior to deciding on their valve type.

Transcatheter Aortic Valve Replacement

Transcatheter aortic valve replacement (TAVR) is a minimally invasive percutaneous approach to treat patients with symptomatic AS without sternotomy or cardiopulmonary bypass. In less than 8 years since FDA approval of this technology for extreme- and high-risk patients for surgery, TAVR has progressed from a procedure of last resort to a viable alternative to surgery in most patients with native (non-bicuspid) AS as well as those with bioprosthetic aortic valve failure.

Evolution of TAVR Indications

The rationale for the invention of TAVR was to offer a treatment for patients with symptomatic severe AS who presented with prohibitive risk for SAVR. Two clinical trials, including the PARTNER IB [38] (completed, FDA approval 11/2011) with the Edwards Sapien valve and the CoreValve US Pivotal Trial [39] (completed, FDA approval 1/2014), showed significant improvement in mortality with TAVR for patients with extreme surgical risk or those deemed inoperable (STS risk score of >15–50) when compared to medical therapy or balloon valvuloplasty alone. For high-risk patients, the PARTNER IA trial [40] (completed, FDA approval 5/2012) demonstrated non-inferiority of TAVR compared to surgery, and the CoreValve US Pivotal Trial (completed, FDA approval 6/2014) showed that all-cause mortality and major adverse cardiovascular and cerebrovascular event (MACCE) rates after TAVR were significantly better compared to SAVR, including better valve hemodynamics for high-risk patients. These satisfactory results led to the expansion of TAVR studies to include intermediate risk patients ($4\% < \text{STS score} < 8\%$) with severe AS. The PARTNER 2A (with Edwards Sapien valve) [41] (completed, FDA approval 8/2016) and SURTAVI trials (with CoreValve) [41] showed that TAVR was non-inferior to surgery in terms of mortality, with lower mean gradients and larger aortic-valve areas compared to surgery. Patterns of adverse events in this intermediate risk cohort were different with each procedure. Surgery was associated with higher rates of acute kidney injury, atrial fibrillation, and blood transfusions, whereas TAVR had higher rates of permanent pacemaker implantation and residual aortic regurgitation [42] (Table 22.1).

Following the favorable results of these trials, a clinical trial was conducted for low-risk patients with STS mortality risk $<4\%$ to compare transfemoral TAVR using

Table 22.1 Summary of 30-day outcomes in trials of TAVR versus SAVR in patients at intermediate or low surgical risk [42]

Outcome	PARTNER 2A		PARTNER 2A (transfemoral access cohort)		PARTNER S3		SURTAVI		NOTION	
	Intermediate		Intermediate		Intermediate		Intermediate		Low	
Intervention	TAVR	SAVR	TAVR	SAVR	TAVR	SAVR	TAVR	SAVR	TAVR	SAVR
Patients (n)	1011	1021	775	775	1077	944	864	796	145	135
All-cause death (%)	3.9	4.1	3.0	4.1	1.1	4.0	2.2	1.7	2.1	3.7
Stroke (%)	3.2	4.3	4.2	6.3	2.7	6.1	3.4	5.6	1.4	3.0
Major or life-threatening bleeding (%)	10.4	43.4	6.7	41.4	4.6	46.7	12.2	9.3	11.3	20.9
Major vascular complications (%)	7.9	5.0	8.5	3.9	6.1	5.4	6.0	1.1	5.6	1.5
Acute kidney injury (%)	1.3	3.1	0.5	3.0	0.5	3.3	1.7	4.4	0.7	6.7
New-onset atrial fibrillation (%)	9.1	26.4	4.9	26.7	5.0	28.3	12.9	43.4	16.9	57.8
New permanent pacemaker (%)	8.5	6.9	8.1	7.1	10.2	7.3	25.9	6.6	34.1	1.6

a balloon-expandable valve with SAVR. This trial, published in May 2019, showed the rate of composite of death, stroke, and rehospitalization at 1 year was significantly lower with TAVR compared to surgery [43]. This result led to FDA approval for TAVR for low-risk patients. These studies have shown that TAVR reduces composite endpoint of all-cause mortality, cardiovascular mortality, and repeat hospitalization with improvement in mean aortic valve gradient, valve area, NYHA functional class, 6-minute walk test, and quality of life.

Use of TAVR has rapidly increased over the past several years. According to STS/ACC/TVT registry public reporting, more than 600 institutions perform TAVR in the United States as of March 2019. In other words, 1 TAVR site exists for every 80,000 people over the age of 65 with a steady growth in number each year. The number of TAVR procedures surpassed the number of isolated SAVR in 2016 and continues to rise, with more than 51,000 commercial TAVR procedures performed in the year 2018. The proportion of patients with intermediate STS risk of mortality who are receiving TAVR has steeply increased from 5% of all TAVRs in 2014 to more than 43% in 2018. With FDA approval of the procedure for low-risk patients, it is predictable that this technology will be applied to low-risk, and perhaps younger, patients, more frequently in coming years. However, adoption of TAVR to this extent must be taken with caution until several concerns regarding this procedure resolve.

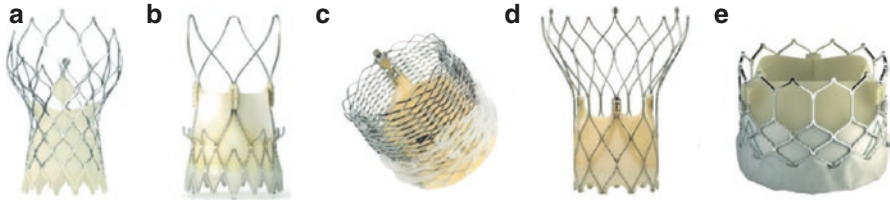


Fig. 22.4 Latest-generation transcatheter heart valves. (a) Self-expanding valve, CoreValve Evolut PRO (Medtronic, USA); (b) self-expanding valve, ACURATE neo TF (Boston Scientific, USA); (c) mechanically expandable valve, LOTUS Edge (Boston Scientific, USA); (d) self-expanding valve, Portico (Abbott, USA); (e) balloon-expanding valve, SAPIEN 3 (Edwards Lifesciences, USA) [42]

Conduction system abnormalities and high-rate of 30-day new permanent pacemaker (PPM) implantation after TAVR remain an ongoing concern without improvement over the last several years, despite the development of new generations of valves (Fig. 22.4). According to a TVT registry study, the rate of 30-day PPM implantation is 6.7% and varies among those receiving self-expanding valves (25.1%) versus balloon-expanding valves (4.3%) [44]. The study showed early PPM implantation is associated with a higher mortality and a composite of mortality and heart failure at 1 year, adverse outcomes that are not acceptable for a lower-risk, younger patient population.

Stroke remains a potentially devastating complication after TAVR as well, ranging from 3.5% to 5.5% in different studies [41, 45]. Few embolic protection devices are under further investigation with the goal to decrease stroke rates with TAVR [46–48]. Another concern is the high rate of unplanned 30-day hospital readmission after TAVR with no improvement over the past few years according to a report from the National Cardiovascular Data Registry (NCDR). The 30-day readmission rate was 9.2% in a TVT registry study with the rate being higher for high-risk patients compared to low-risk patients [49].

Long-term durability of TAVR valves remains an unanswered question as most clinical trials in the field are only few years old compared with the excellent benchmark for long-term durability of surgical valves shown in multiple studies as mentioned earlier in this chapter. Daubert et al., in a longitudinal assessment of the PARTNER I trial, demonstrated that valve performance and cardiac hemodynamics are stable in both TAVR and SAVR patients alive at 5 years [50]. A 5-year report of the PARTNER I trial did show higher rates of moderate to severe aortic insufficiency in TAVR patients (14% versus 1%, $p < 0.0001$), which was associated with increased 5-year risk of mortality in that study [51]. When counseling younger patients, it is critical to inform them about the uncertainty in long-term durability at this time as well as the higher rate of paravalvular leak, especially with the earlier generation of TAVR valves. The lifelong treatment strategy of aortic valve stenosis in younger low-risk patients is yet to be defined. Whether surgical aortic valve replacement with biological valves (to avoid anticoagulation) should be the first treatment step followed by subsequent transcatheter valve-in-valve implantation for

failed bioprosthesis or TAVR as the first-line therapy followed by SAVR and subsequent TAVR for failed bioprosthesis is still being debated. Leaving calcium and/or degenerated bioprosthetic valves behind in TAVR and valve-in-valve procedures may add to the complexity of future reoperations or expose patients to patient-prosthesis mismatch if an appropriate-size valve cannot fit.

Pre-procedural Evaluation

Patients who are considered for TAVR procedure undergo extensive pre-procedural evaluation by the “heart team” that includes an interventional cardiologist and a cardiac surgeon. A full Heart Team assessment is mandatory before any decision can be made to determine whether TAVR or SAVR is the best choice for that individual patient. The work-up includes echocardiograms; computed tomography angiography of the chest, abdomen, and pelvis; cardiac catheterization; pulmonary function testing; and carotid Doppler studies. Despite the development of a risk model specifically for TAVR [52], the Society of Thoracic Surgeons (STS) risk model is still used by most centers to calculate the predicted risk of mortality and morbidity for TAVR, categorizing patients into low, intermediate, and high risk. Aside from the STS risk score, other factors play an important role in decision-making. For example, porcelain aortas and prior mediastinal radiation are both associated with worse outcomes in SAVR but are not included in the STS risk model. These factors may deem a patient technically inoperable, qualifying them for TAVR instead [53]. In contrary, patients who in addition to severe AS have other cardiac diseases such as coronary artery disease, other valvular disease, atrial fibrillation, or ascending aortic aneurysm that can be addressed with concomitant surgery may benefit more from a surgical approach instead of TAVR.

Procedure and Recovery

As experience with transcatheter aortic valve replacement (TAVR) has increased, some centers have performed transfemoral (TF) TAVR in a standard cardiac catheterization laboratory without general anesthesia or transesophageal echocardiography (TEE), the so-called minimalist approach as opposed to a standard approach (SA) performed in a hybrid operating room [54]. In the minimalist approach to TAVR, the patient is sedated with midazolam and fentanyl. Femoral access is obtained with micro-puncture technique under fluoroscopic guidance. Two pre-closure sutures are placed with Perclose devices (Abbott Vascular, Abbott Park, Illinois) after entry into the femoral artery and will be tied down to close the artery once sheaths were removed at the conclusion of the procedure. For patients with severely calcified, limited size, or tortuous iliofemoral arteries, alternative peripheral access options are subclavian and carotid artery. Alternative central access

options are trans-aortic and trans-apical approaches. However, trends in using central access have significantly decreased in favor of femoral and peripheral alternative approaches [55]. Caval-aortic access is another alternative approach used in some centers [56]. Once access is obtained, the operator delivers the TAVR valve to the stenotic aortic valve through a series of wire and catheter techniques and the designed delivery system for deployment under rapid ventricular pacing. Valve position and hemodynamics are confirmed using echocardiography and angiography, with special care taken to ensure the absence of significant paravalvular leak. Post-procedurally, patients are monitored in the perioperative recovery unit for a few hours with special attention paid to vascular access sites and vital signs. Then, most patients are transferred to the floor and discharged on post-operative day one. Dual antiplatelet therapy (DAPT) with aspirin and clopidogrel is common practice after TAVR. If patients are on an anticoagulation regimen for other reasons, a single antiplatelet therapy (SAPT) regimen with aspirin or no antiplatelet therapy at all is chosen by most physicians. The best antithrombotic therapy after TAVR is yet to be determined despite ongoing clinical trials [57].

Conflict of Interest Statement and Acknowledgments Authors have nothing to disclose regarding commercial support. We acknowledge Dr. Morgan Harloff's contribution in editing of this chapter.

References

1. Supino PG, Borer JS, Preibisz J, Bornstein A. The epidemiology of valvular heart disease: a growing public health problem. *Heart Fail Clin.* 2006;2(4):379–93.
2. Aronow WS, Ahn C, Kronzon I, Goldman ME. Association of coronary risk factors and use of statins with progression of mild valvular aortic stenosis in older persons. *Am J Cardiol.* 2001;88(6):693–5.
3. Taylor HA Jr, Clark BL, Garrison RJ, Andrew ME, Han H, Fox ER, et al. Relation of aortic valve sclerosis to risk of coronary heart disease in African-Americans. *Am J Cardiol.* 2005;95(3):401–4.
4. Ross J Jr, Braunwald E. Aortic stenosis. *Circulation.* 1968;38(1 Suppl):61–7.
5. American College of Cardiology/American Heart Association Task Force on Practice G, Society of Cardiovascular A, Society for Cardiovascular A, Interventions, Society of Thoracic S, Bonow RO, et al. ACC/AHA 2006 guidelines for the management of patients with valvular heart disease: a report of the American College of Cardiology/American Heart Association Task Force on Practice Guidelines (writing committee to revise the 1998 Guidelines for the Management of Patients With Valvular Heart Disease): developed in collaboration with the Society of Cardiovascular Anesthesiologists: endorsed by the Society for Cardiovascular Angiography and Interventions and the Society of Thoracic Surgeons. *Circulation.* 2006;114(5):e84–231.
6. Cohn L, Adams DH. Cardiac surgery in the adult. In: Cohn L, editor. 5th ed. New York: McGraw-Hill; 2016. p. 649–695.
7. Gott VL, Alejo DE, Cameron DE. Mechanical heart valves: 50 years of evolution. *Ann Thorac Surg.* 2003;76(6):S2230–9.
8. Milano AD, Bortolotti U, Mazzucco A, Guerra F, Magni A, Gallucci V. Aortic valve replacement with the Hancock standard, Bjork-Shiley, and Lillehei-Kaster prostheses. A comparison based on follow-up from 1 to 15 years. *J Thorac Cardiovasc Surg.* 1989;98(1):37–47.

9. Remadi JP, Baron O, Roussel C, Bizouarn P, Habasch A, Despins P, et al. Isolated mitral valve replacement with St. Jude medical prosthesis: long-term results: a follow-up of 19 years. *Circulation*. 2001;103(11):1542–5.
10. Nishida T, Sonoda H, Oishi Y, Tanoue Y, Nakashima A, Shiokawa Y, et al. Single-institution, 22-year follow-up of 786 CarboMedics mechanical valves used for both primary surgery and reoperation. *J Thorac Cardiovasc Surg*. 2014;147(5):1493–8.
11. Gillinov AM, Blackstone EH, Alster JM, Craver JM, Baumgartner WA, Brewster SA, et al. The Carbomedics top hat supraannular aortic valve: a multicenter study. *Ann Thorac Surg*. 2003;75(4):1175–80.
12. Chaudhary R, Garg J, Krishnamoorthy P, Shah N, Feldman BA, Martinez MW, et al. On-X valve: the next generation aortic valve. *Cardiol Rev*. 2017;25(2):77–83.
13. Puskas J, Gerdisch M, Nichols D, Quinn R, Anderson C, Rhenman B, et al. Reduced anticoagulation after mechanical aortic valve replacement: interim results from the prospective randomized on-X valve anticoagulation clinical trial randomized Food and Drug Administration investigational device exemption trial. *J Thorac Cardiovasc Surg*. 2014;147(4):1202–10; discussion 10–1
14. Chan V, Kulik A, Tran A, Hendry P, Masters R, Mesana TG, et al. Long-term clinical and hemodynamic performance of the Hancock II versus the Perimount aortic bioprostheses. *Circulation*. 2010;122(11 Suppl):S10–6.
15. Rizzoli G, Mirone S, Ius P, Polesel E, Bottio T, Salvador L, et al. Fifteen-year results with the Hancock II valve: a multicenter experience. *J Thorac Cardiovasc Surg*. 2006;132(3):602–9, 9 e1–4.
16. Jamieson WR, Germann E, Aupart MR, Neville PH, Marchand MA, Fradet GJ. 15-year comparison of supra-annular porcine and PERIMOUNT aortic bioprostheses. *Asian Cardiovasc Thorac Ann*. 2006;14(3):200–5.
17. Valfre C, Ius P, Minniti G, Salvador L, Bottio T, Cesari F, et al. The fate of Hancock II porcine valve recipients 25 years after implant. *Eur J Cardiothorac Surg*. 2010;38(2):141–6.
18. Une D, Ruel M, David TE. Twenty-year durability of the aortic Hancock II bioprosthesis in young patients: is it durable enough? *Eur J Cardiothorac Surg*. 2014;46(5):825–30.
19. Raghav V, Okafor I, Quach M, Dang L, Marquez S, Yoganathan AP. Long-term durability of Carpentier-Edwards magna ease valve: a one billion cycle in vitro study. *Ann Thorac Surg*. 2016;101(5):1759–65.
20. Wendt D, Thielmann M, Plicht B, Assmann J, Price V, Neuhauser M, et al. The new St Jude trileaflet versus Carpentier-Edwards Perimount magna and magna ease aortic bioprosthesis: is there a hemodynamic superiority? *J Thorac Cardiovasc Surg*. 2014;147(5):1553–60.
21. Puskas JD, Bavaria JE, Svensson LG, Blackstone EH, Griffith B, Gammie JS, et al. The COMMENCE trial: 2-year outcomes with an aortic bioprosthesis with RESILIA tissue. *Eur J Cardiothorac Surg*. 2017;52(3):432–9.
22. Foghsgaard S, Bruun N, Kjaergard H. Outcome of aortic homograft implantation in 24 cases of severe infective endocarditis. *Scand J Infect Dis*. 2008;40(3):216–20.
23. Brown JM, O'Brien SM, Wu C, Sikora JA, Griffith BP, Gammie JS. Isolated aortic valve replacement in North America comprising 108,687 patients in 10 years: changes in risks, valve types, and outcomes in the Society of Thoracic Surgeons National Database. *J Thorac Cardiovasc Surg*. 2009;137(1):82–90.
24. Bouhout I, Stevens LM, Mazine A, Poirier N, Cartier R, Demers P, et al. Long-term outcomes after elective isolated mechanical aortic valve replacement in young adults. *J Thorac Cardiovasc Surg*. 2014;148(4):1341–6.e1.
25. Zellner JL, Kratz JM, Crumbley AJ 3rd, Stroud MR, Bradley SM, Sade RM, et al. Long-term experience with the St. Jude Medical valve prosthesis. *Ann Thorac Surg*. 1999;68(4):1210–8.
26. Forcillo J, El Hamasy I, Stevens LM, Badrudin D, Pellerin M, Perrault LP, et al. The perimount valve in the aortic position: twenty-year experience with patients under 60 years old. *Ann Thorac Surg*. 2014;97(5):1526–32.

27. Stassano P, Di Tommaso L, Monaco M, Iorio F, Pepino P, Spampinato N, et al. Aortic valve replacement: a prospective randomized evaluation of mechanical versus biological valves in patients ages 55 to 70 years. *J Am Coll Cardiol*. 2009;54(20):1862–8.
28. Brennan JM, Edwards FH, Zhao Y, O'Brien S, Booth ME, Dokholyan RS, et al. Long-term safety and effectiveness of mechanical versus biologic aortic valve prostheses in older patients: results from the Society of Thoracic Surgeons Adult Cardiac Surgery National Database. *Circulation*. 2013;127(16):1647–55.
29. Chikwe J, Chiang YP, Egorova NN, Itagaki S, Adams DH. Survival and outcomes following bioprosthetic vs mechanical mitral valve replacement in patients aged 50 to 69 years. *JAMA*. 2015;313(14):1435–42.
30. Goldstone AB, Chiu P, Baiocchi M, Lingala B, Patrick WL, Fischbein MP, et al. Mechanical or biologic prostheses for aortic-valve and mitral-valve replacement. *N Engl J Med*. 2017;377(19):1847–57.
31. Beyth RJ, Quinn L, Landefeld CS. A multicomponent intervention to prevent major bleeding complications in older patients receiving warfarin. A randomized, controlled trial. *Ann Intern Med*. 2000;133(9):687–95.
32. Matchar DB, Jacobson A, Dolor R, Edson R, Uyeda L, Phibbs CS, et al. Effect of home testing of international normalized ratio on clinical events. *N Engl J Med*. 2010;363(17):1608–20.
33. Eikelboom JW, Connolly SJ, Brueckmann M, Granger CB, Kappetein AP, Mack MJ, et al. Dabigatran versus warfarin in patients with mechanical heart valves. *N Engl J Med*. 2013;369(13):1206–14.
34. Hammermeister K, Sethi GK, Henderson WG, Grover FL, Oprian C, Rahimtoola SH. Outcomes 15 years after valve replacement with a mechanical versus a bioprosthetic valve: final report of the veterans affairs randomized trial. *J Am Coll Cardiol*. 2000;36(4):1152–8.
35. Oxenham H, Bloomfield P, Wheatley DJ, Lee RJ, Cunningham J, Prescott RJ, et al. Twenty year comparison of a Bjork-Shiley mechanical heart valve with porcine bioprostheses. *Heart*. 2003;89(7):715–21.
36. Durrleman N, Pellerin M, Bouchard D, Hebert Y, Cartier R, Perrault LP, et al. Prosthetic valve thrombosis: twenty-year experience at the Montreal Heart Institute. *J Thorac Cardiovasc Surg*. 2004;127(5):1388–92.
37. Kaneko T, Vassileva CM, Englum B, Kim S, Yammine M, Brennan M, et al. Contemporary outcomes of repeat aortic valve replacement: a benchmark for transcatheter valve-in-valve procedures. *Ann Thorac Surg*. 2015;100(4):1298–304; discussion 304
38. Leon MB, Smith CR, Mack M, Miller DC, Moses JW, Svensson LG, et al. Transcatheter aortic-valve implantation for aortic stenosis in patients who cannot undergo surgery. *N Engl J Med*. 2010;363(17):1597–607.
39. Arnold SV, Reynolds MR, Wang K, Magnuson EA, Baron SJ, Chinnakondepalli KM, et al. Health status after transcatheter or surgical aortic valve replacement in patients with severe aortic stenosis at increased surgical risk: results from the CoreValve US pivotal trial. *JACC Cardiovasc Interv*. 2015;8(9):1207–17.
40. Smith CR, Leon MB, Mack MJ, Miller DC, Moses JW, Svensson LG, et al. Transcatheter versus surgical aortic-valve replacement in high-risk patients. *N Engl J Med*. 2011;364(23):2187–98.
41. Leon MB, Smith CR, Mack MJ, Makkar RR, Svensson LG, Kodali SK, et al. Transcatheter or surgical aortic-valve replacement in intermediate-risk patients. *N Engl J Med*. 2016;374(17):1609–20.
42. Puri R, Chamandi C, Rodriguez-Gabella T, Rodes-Cabau J. Future of transcatheter aortic valve implantation – evolving clinical indications. *Nat Rev Cardiol*. 2018;15(1):57–65.
43. Mack MJ, Leon MB, Thourani VH, Makkar R, Kodali SK, Russo M, et al. Transcatheter aortic-valve replacement with a balloon-expandable valve in low-risk patients. *N Engl J Med*. 2019;380(18):1695–705.
44. Fadahunsi OO, Olowoyeye A, Ukaigwe A, Li Z, Vora AN, Vemulapalli S, et al. Incidence, predictors, and outcomes of permanent pacemaker implantation following transcatheter aortic

- valve replacement: analysis from the U.S. Society of Thoracic Surgeons/American College of Cardiology TVT registry. *JACC Cardiovasc Interv.* 2016;9(21):2189–99.
45. Reardon MJ, Van Mieghem NM, Popma JJ, Kleiman NS, Sondergaard L, Mumtaz M, et al. Surgical or transcatheter aortic-valve replacement in intermediate-risk patients. *N Engl J Med.* 2017;376(14):1321–31.
 46. Kapadia SR, Kodali S, Makkar R, Mehran R, Lazar RM, Zivadinov R, et al. Protection against cerebral embolism during transcatheter aortic valve replacement. *J Am Coll Cardiol.* 2017;69(4):367–77.
 47. Abdul-Jawad Altisent O, Puri R, Rodes-Cabau J. Embolic protection devices during TAVI: current evidence and uncertainties. *Rev Esp Cardiol (Engl Ed).* 2016;69(10):962–72.
 48. Ndunda PM, Vindhya MR, Muutu TM, Fanari Z. Clinical outcomes of sentinel cerebral protection system use during transcatheter aortic valve replacement: a systematic review and meta-analysis. *Cardiovasc Revasc Med.* 2019. pii: S1553–8389(19)30257-X. <https://doi.org/10.1016/j.carrev.2019.04.023>.
 49. Sanchez CE, Hermiller JB Jr, Pinto DS, Chetcuti SJ, Arshi A, Forrest JK, et al. Predictors and risk calculator of early unplanned hospital readmission following contemporary self-expanding transcatheter aortic valve replacement from the STS/ACC TVT-registry. *Cardiovasc Revasc Med.* 2020;21(3):263–70. <https://doi.org/10.1016/j.carrev.2019.05.032>.
 50. Daubert MA, Weissman NJ, Hahn RT, Pibarot P, Parvataneni R, Mack MJ, et al. Long-term valve performance of TAVR and SAVR: a report from the PARTNER I trial. *JACC Cardiovasc Imaging.* 2016. pii: S1936–878X(16)30895-6. <https://doi.org/10.1016/j.jcmg.2016.11.004>. (Epub ahead of print)
 51. Mack MJ, Leon MB, Smith CR, Miller DC, Moses JW, Tuzcu EM, et al. 5-year outcomes of transcatheter aortic valve replacement or surgical aortic valve replacement for high surgical risk patients with aortic stenosis (PARTNER 1): a randomised controlled trial. *Lancet.* 2015;385(9986):2477–84.
 52. Edwards FH, Cohen DJ, O'Brien SM, Peterson ED, Mack MJ, Shahian DM, et al. Development and validation of a risk prediction model for in-hospital mortality after transcatheter aortic valve replacement. *JAMA Cardiol.* 2016;1(1):46–52.
 53. Makkar RR, Jilaihawi H, Mack M, Chakravarty T, Cohen DJ, Cheng W, et al. Stratification of outcomes after transcatheter aortic valve replacement according to surgical inoperability for technical versus clinical reasons. *J Am Coll Cardiol.* 2014;63(9):901–11.
 54. Babaliaros V, Devireddy C, Lerakis S, Leonardi R, Iturra SA, Mavromatis K, et al. Comparison of transfemoral transcatheter aortic valve replacement performed in the catheterization laboratory (minimalist approach) versus hybrid operating room (standard approach): outcomes and cost analysis. *JACC Cardiovasc Interv.* 2014;7(8):898–904.
 55. Patel JS, Krishnaswamy A, Svensson LG, Tuzcu EM, Mick S, Kapadia SR. Access options for transcatheter aortic valve replacement in patients with unfavorable aortoiliac anatomy. *Curr Cardiol Rep.* 2016;18(11):110.
 56. Rodes-Cabau J, Puri R, Chamandi C. The caval-aortic access for performing TAVR: pushing the limits of alternative access for nontransfemoral candidates. *J Am Coll Cardiol.* 2017;69(5):522–5.
 57. Raheja H, Garg A, Goel S, Banerjee K, Hollander G, Shani J, et al. Comparison of single versus dual antiplatelet therapy after TAVR: a systematic review and meta-analysis. *Catheter Cardiovasc Interv.* 2018;92(4):783–91.
 58. Schwarz F, Baumann P, Manthey J, Hoffmann M, Schuler G, Mehmel HC, et al. The effect of aortic valve replacement on survival. *Circulation.* 1982;66(5):1105–10.
 59. Huang G, Rahimtoola SH. Prosthetic heart valve. *Circulation.* 2011;123(22):2602–5.

Chapter 23

Target Discovery in Calcification Through Omics and Systems Approaches



Mark C. Blaser, Arda Halu, Louis A. Soddic, Masanori Aikawa, and Elena Aikawa

Mark C. Blaser, Arda Halu and Louis A. Soddic contributed equally.

M. C. Blaser (✉)

Center for Interdisciplinary Cardiovascular Sciences, Division of Cardiovascular Medicine, Department of Medicine, Brigham and Women's Hospital, Harvard Medical School, Boston, MA, USA

e-mail: mblaser@bwh.harvard.edu

A. Halu

Center for Interdisciplinary Cardiovascular Sciences, Division of Cardiovascular Medicine, Department of Medicine, Brigham and Women's Hospital, Harvard Medical School, Boston, MA, USA

Channing Division of Network Medicine, Department of Medicine, Brigham and Women's Hospital, Harvard Medical School, Boston, MA, USA

e-mail: ahalu@bwh.harvard.edu

L. A. Soddic

Center for Interdisciplinary Cardiovascular Sciences, Division of Cardiovascular Medicine, Department of Medicine, Brigham and Women's Hospital, Harvard Medical School, Boston, MA, USA

Department of Anesthesiology, Perioperative and Pain Medicine, Brigham and Women's Hospital, Harvard Medical School, Boston, MA, USA

e-mail: lsoddic@partners.org

M. Aikawa

Center for Interdisciplinary Cardiovascular Sciences, Division of Cardiovascular Medicine, Department of Medicine, Brigham and Women's Hospital, Harvard Medical School, Boston, MA, USA

Channing Division of Network Medicine, Department of Medicine, Brigham and Women's Hospital, Harvard Medical School, Boston, MA, USA

Center for Excellence in Vascular Biology, Division of Cardiovascular Medicine, Department of Medicine, Brigham and Women's Hospital, Harvard Medical School, Boston, MA, USA

e-mail: maikawa@bwh.harvard.edu

© Springer Nature Switzerland AG 2020

E. Aikawa, J. D. Hutcheson (eds.), *Cardiovascular Calcification and Bone Mineralization*, Contemporary Cardiology,

https://doi.org/10.1007/978-3-030-46725-8_23

E. Aikawa

Center for Interdisciplinary Cardiovascular Sciences,
Center for Excellence in Vascular Biology, Division of Cardiovascular Medicine,
Department of Medicine, Brigham and Women's Hospital, Harvard Medical School,
Boston, MA, USA
e-mail: eaikawa@bwh.harvard.edu

Omics-Informed Pathobiology and Drug Discovery

Cardiovascular disease is the leading cause of mortality worldwide [1], and ectopic calcification is a key contributor to and predictor of cardiovascular morbidity and mortality [2, 3]. Indeed, from calcification of the cardiovascular system's vessels and valves (typically the result of hyperlipidemic atherosclerosis [Chap. 4], renal failure-induced hyperphosphatemia [Chap. 7], or genetic disorders such as progeria [Chap. 11]) to autoimmune-associated connective tissue mineralization (e.g., scleroderma; see Chap. 12), or defects in favorable calcification (osteoporosis vs. bone regeneration, Chaps. 15, 16, 17, and 18), the effects of anomalous mineral formation can impact nearly all of the body's tissues and organ systems. While these calcific disorders share similarities in end-stage phenotype, where ectopic or dystrophic calcification (or lack thereof) impacts function, their causation and driving mechanisms appear to be inherently context- and tissue-dependent (reviewed in [4]).

Once the onset of pathological calcification begins, clinicians have a sparse toolbox with which to tackle this ailment. While lipid-lowering therapeutics (e.g., statins) have revolutionized vascular medicine, these drugs target precursors to the calcific process and do not have anti-calcific action in and of themselves – paradoxically, statins even appear to promote coronary artery calcification through mechanisms yet to be understood [5]. Treatment of calcification in the context of chronic kidney disease tends to focus on traditional, modifiable risk factors such as hypertension or on abnormal mineral metabolism [6] – again, neither the calcification process itself nor regression of calcification is currently treatable. This failure to bring pharmacological therapies to the clinic is due in large part to poor understanding of the mechanisms responsible for initiating and driving progression of these disparate calcific disorders; this has resulted in an inability to carefully target calcification in a focused manner.

One promising means of rapidly tackling this currently intractable problem is the growing use of omics strategies to study the holistic totality of complex biological systems. Technological advances in next-generation sequencing and mass spectrometry enable order-of-magnitude increases in throughput and resolution and promise to allow a deeper understanding of pathobiology when coupled with pioneering advances in data integration, analysis, and visualization [7]. In this chapter, we examine the latest efforts to apply omics techniques to better understand the causes, initiating events, pathogenesis, driving mechanisms, and potential therapeutic

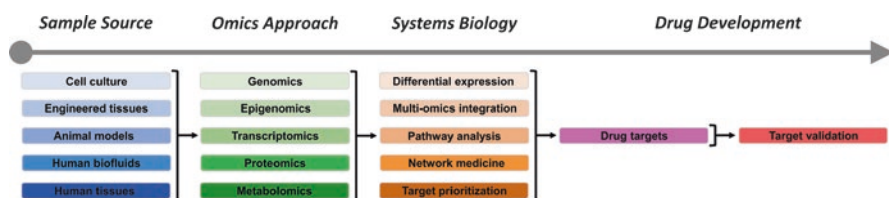


Fig. 23.1 Leveraging omics for target discovery and drug development. Holistic applications of next-generation sequencing and mass spectrometry enable a newfound ability to infer biological mechanisms and prioritize drug targets. Samples can be obtained from a wide variety of in vivo, ex vivo, and in vitro sources derived from both animals and humans. Multiple omics approaches have been well-established and allow sequencing of DNA and RNA, examination of histone modifications or DNA methylation, quantification of protein expression and post-translational modifications, and study of metabolites. Systems biology techniques are then leveraged to integrate these data, extract biological insight, and select promising candidates for further validation

reversal of calcification. We will trace our way from studies of the genome to the phenome, followed by an in-depth discussion of how systems biology is revolutionizing both the integration of these omics layers and the extraction of biologically meaningful insights from these complex datasets (Fig. 23.1). Indeed, the field's nascent ability to infer biological mechanisms and prioritize drug targets in silico is enabling a radical change in the economics and pace of drug development [8].

Interrogation of Nucleic Acids: Genomics and Transcriptomics

Genome-Wide Studies on Cardiovascular Calcification

Calcification is an active, complex, pathological thread that precedes many forms of cardiovascular disease including aortic stenosis (AS), myocardial infarction (MI), cerebral vascular accidents (CVA), and abdominal aortic aneurysms. Like many of these diseases, calcification is incredibly common and tends to run in families with documented heritability as high as 50% [9]. Unlike devastating end-stage cardiovascular events, calcification can be monitored and diagnosed. As a result, significant pursuits to uncover common genetic variants associated with calcification have been conducted through genome-wide association studies (GWAS).

Using high-resolution computed tomography, a meta-analysis from five independent community-based cohorts with replication in three additional cohorts identified one SNP on chromosome 9p21 (rs1333049) and one SNP on chromosome 6p24 (rs9349379) associated with coronary calcification (CAC) at genome-wide significance. Both loci were previously uncovered in GWAS in patients with MI, but still the exact functional mechanism driving these associations remains unclear. Many of the associated SNPs on chromosome 9p21 reside far from known annotated genes, the closest being the cell cycle regulators *CDKN2A* and *CDKN2B*. There is,

however, variant proximity to a recently discovered antisense long noncoding RNA called *ANRIL* (antisense noncoding RNA in the *INK3* locus). Variant-mediated MI risk may therefore be due to the alteration of gene expression orchestrated by *ANRIL* dysregulation. Chromosome 6p24 contains the gene *PHACTR1* which is an inhibitor of protein phosphatase 1 [10]. The functional link between these variants and MI/CAC risk is however still unclear. Additional GWAS of vascular calcification have been conducted in other vessels most notably the aorta and the intracranial carotid artery. Once again, associations were noted at chromosome 9p21 [11, 12].

GWAS conducted on patients with valvular calcification have also uncovered novel risk-associated alleles. Most notably, one SNP on chromosome 6 in the *LPA* gene was found to be associated with aortic valve calcification in patients of European descent and subsequently replicated in cohorts from multiple ethnic groups. *LPA* encodes apolipoprotein(a) which is a component of lipoprotein(a), a particle well-known to be associated with coronary artery disease. Interestingly, levels of lipoprotein(a) were also associated with aortic valve calcification, and *LPA* genotype was linked to aortic stenosis providing evidence of causation between this variant and valvular calcification. Two additional SNPs on chromosome 2 near the *IL1F9* gene were associated with mitral annular calcification but could not be replicated in additional cohorts [13].

Despite over a decade of GWAS on calcification and other cardiovascular cohorts, a disappointingly low number of variants have been replicated and validated. Some limitations to these approaches include the large cohorts required to conduct these studies on phenotypes that are complex and likely contain heterogeneous subclasses. Calcification alone can be intimal or medial, can occur in different arteries and locations of the heart, and is strongly influenced by racial background. These findings also call into question the degree to which common variants contribute to genetic diversity of common diseases. GWA studies, for example, typically rely on minor allele frequencies greater than 1%. Rare alleles may have a significant impact on diseases like calcification. Such variants will require higher levels of genetic surveillance such as whole genome and whole exome sequencing. These techniques will also augment the discovery of larger changes in genetic information such as copy number variants and nucleotide insertions and deletions [14].

Transcriptomics Bridges the Gap Between Genetic and Environmental Regulation of Calcification

While DNA sequences certainly provide a framework for heritability, alterations in gene expression can arise due to additional genetic factors such as epigenetics, environmental regulation, and how genes interact with one another. Gene expression signatures provide unique identities to complex diseases like calcification and allow us to uncover pathways integral to the development and evolution of pathology over time. These pathways then serve as potential targets to reverse or slow down the course of disease.

Transcriptomics developed during a transition from candidate gene expression studies to entire gene expression surveillance using microarrays. With advances in next-generation sequencing technology and reduction of sequencing costs, hybridization-based chip arrays gave way to RNA-seq. RNA-seq has many advantages over microarrays, including the detection of low-expressed transcripts and the identification of novel transcripts, but does require handling and processing of large data [14, 15]. Both techniques, however, are still used today depending on the interests of the investigator, and both techniques require functional studies to validate candidate dysregulated genes. These platforms can also be combined with GWA studies in expression quantitative trait loci studies. With regard to calcification, for example, the genotype of certain SNPs in the *RUNX2* (runt-related transcription factor 2) locus was shown to be correlated with *RUNX2* expression and calcified aortic valves [16].

Our knowledge of vascular calcification has advanced tremendously through the use of transcriptomics in many biological systems including calcifying cells in tissue culture, peripheral blood cells in patients with vascular calcification, human biopsy samples, animal models, and more recently cargo-containing extracellular vesicles such as exosomes [15, 17]. Most notably, gene expression profiles have demonstrated that while calcification involves shared biological processes, it also has unique signaling components that vary with anatomical location, environmental stressors, and pre-existing comorbidities [18, 19]. Several studies have surveyed intimal atherosclerosis and demonstrated an upregulation of processes expected of this disease including proliferation, calcification, oxidative stress, and immune response [19, 20]. Others have examined medial calcification through chronic uremia models and cell cultures of calcifying vascular smooth muscle cells (SMCs). While certain ontologies linked to mineralization and extracellular matrix were dysregulated, including well-known inhibitors of calcification such as osteopontin (Spp1) and matrix γ -carboxyglutamate protein (Mgp) [21], many smooth muscle-specific genes remained active suggesting a detectable yet limited trans-differentiation of vascular SMCs into an osteoblast-like phenotype [22, 23]. Anatomical location also has unique calcification signatures. Human carotid plaques have transcriptomes enriched in immune processes, while those from the femoral aorta have substantial osteogenic signatures [24]. Even within carotid plaques, those from symptomatic patients have even less osteogenic gene expression profiles than asymptomatic patients, suggesting an active role of calcification in preventing plaque rupture [25]. Transcriptome analysis on calcified and noncalcified aortic valves, on the other hand, has highlighted the importance of an intermediate fibrotic signature as sclerosis progresses [26–28]. Other investigators have also used transcriptome profiles of peripheral blood cells in patients with diseased and healthy vessels to more precisely study the circulating immune contributions to calcification [29, 30].

Transcriptomics have also advanced our understanding of noncoding RNA expression in cardiovascular disease, most notably microRNAs (miRNAs) and long noncoding RNAs (lncRNAs). miRNAs are small noncoding RNAs that regulate the stability of protein-coding mRNAs. Several miRNAs have demonstrated a role in the pathogenesis of calcification. To name a few, mir-133a, mir-204, and mir-30b-c have been shown to lower calcification by suppressing *RUNX2*, while mir-32 and

mir-221/222 increase calcification by altering PTEN (phosphatase and tensin homolog) and Enpp1/Pit-1 (ectonucleotide phosphodiesterase 1/Pi cotransporter-1), respectively [31]. lncRNAs are longer transcripts that do not encode proteins. The extent of their function in cells is still unknown, but many have been shown to bind and regulate mRNAs, miRNAs, and proteins. Similar to many pathological states, lncRNAs have also been shown to play a role in calcification [32]. In fact, many of these lncRNAs have undergone functional validation to demonstrate a bonafide role in the calcification phenotype. For instance, the long noncoding RNA HOTAIR has lower expression in bicuspid compared to tricuspid aortic valves, and siRNA knock-down of this transcript in valvular interstitial cells (VICs) leads to an increase in genes linked to calcification including bone morphogenic protein 2 (BMP-2) [33].

More recently, RNA-seq has advanced to enable the description of global gene expression landscapes on the cellular level through single-cell RNA-seq (scRNA-seq). There are several different forms of this technology although the most common forms involve separation of cells into droplets prior to library formation and sequencing. Needless to say, the amount of data and complexity of normalization, transformation, and statistical analysis is increasingly more complex than RNA-seq. An adaptation to scRNA-seq is single nuclear RNA-seq (snRNA-seq). In most instances, nuclei are significantly smaller than cells which simplifies the fluidic components of cell separation. Nuclei can capture similar representative pulls of cellular RNA and also permit freezing of tissue prior to processing. Single-cell technology can be superior to whole-tissue RNA-seq in that it can be used to identify differentially expressed genes in small cell populations which would otherwise be masked by more abundant cell types. Furthermore, single-cell transcriptomics has the ability to identify novel subtypes of cells and cells transitioning between phenotypes [34]. A recent application of these techniques surveyed the aortic macrophage population in normal chow-fed and high-fat diet low-density lipoprotein receptor-deficient mice. Unique subpopulations of macrophages were identified in healthy and diseased aorta including one population of macrophages unique to atherosclerotic aortas with high expression of *Trem2* (triggered receptor expressed on myeloid cells 2) and a gene signature similar to osteoclasts [35].

Epigenetics and the Genetic Structure of Calcification

Epigenetics is a new and exciting field of gene regulation. Like our DNA sequence, these marks can be inherited, but they can also be altered by the environment. DNA methylation is one of the most well-studied modifications in this field and represents a form of gene silencing. DNA methylation involves methylation of CpG dinucleotides which tend to cluster in promoter regions upstream of protein-coding genes. There are many different methods that can be used to assay genome-wide differential patterns of DNA methylation. These include commercial microarrays and bisulfate sequencing, which relies on the principle that methylated cytosines are resistant to deamination to uracil by bisulfate treatment [14]. We are just beginning to elucidate the role of DNA methylation in vascular and valvular calcification. In

calcified aortic valves, genome-wide studies have demonstrated the existence of thousands of differentially methylated DNA sites compared to normal valves [36]. Functional validation of many of these methylated genes has also been performed. The promoter of the long noncoding RNA *H19*, for example, is hypo-methylated in calcified human aortic valves compared to normal valves. Overexpression of *H19* is thought to drive the osteogenic phenotype through NOTCH1 regulated expression of *RUNX2* and *BMP2* [37]. Conversely, DNA methylation of phospholipid phosphatase 3 (PLPP3) was increased in calcified aortic valves compared to normal valves. Phosphatases degrade lipid mediators, which have been shown to have strong osteogenic potential, and thus gene silencing of these enzymes may contribute to the calcification of aortic valves [38]. There is also evidence of DNA methylation contributing to vascular calcification. Stroke patients with methylation of the *CDKN2B* gene have higher amounts of carotid artery calcification [39]. In addition, methylation of miR-34b may promote vascular SMC calcification through NOTCH signaling [40]. As sequencing costs continue to decline and big data computation becomes faster and more accurate, we will begin to see more genome-wide studies of DNA methylation aimed at uncovering the pathogenesis of calcification.

Epigenetics also encompasses the complex world of DNA structure. Chromatin is composed of more than just DNA. We now know that chromosomes are complex three-dimensional structures whereby DNA is coiled around histone proteins to form functional units known as nucleosomes. These histone proteins undergo chemical modifications, which in turn regulates the degree to which chromatin is tightly condensed and thus less transcriptionally active, or loosely packed and more open to gene expression. The most common forms of histone modification include lysine methylation and acetylation. These residues are modified by large families of enzymes that can either add or subtract these chemical marks. Histone-DNA interactions can also be destabilized directly in an ATP-dependent manner through large chromatin remodeling complexes such as SWI/SNF. Currently there are several methods available to the scientific community for evaluating two-dimensional chromatin structure. This includes antibody-based techniques for histones and transcription factors such as chromatin immunoprecipitation (ChIP), nuclease-based assays with agents such as micrococcal nuclease (MNase), and most recently techniques that probe transposase-sensitive areas of open chromatin using a method known as assay for transposase-accessible chromatin (ATAC). These methods can be scaled to a genome-wide level through sequencing [41]. Three-dimensional chromatin structure that allows distant parts of chromatin to interact with each other can also be surveyed through techniques such as Hi-C [42]. One of the most notable and well-studied regulators of vascular calcification is the histone deacetylase sirtuin 1 (SIRT1). SIRT1 opposes osteogenic programming and can block hyperphosphatemia-induced calcification of vascular SMCs, at least in part through inhibition of *RUNX2* and senescent pathways [43]. SIRT1 levels have also been shown to be reduced in calcified aortic valves [44]. Furthermore, endothelial cell-mediated epigenetic drivers of valvular calcification have been investigated. Using human-induced pluripotent stem cell-derived endothelial cells, one group demonstrated that NOTCH1 haploinsufficiency altered the activation of anti-osteogenic and anti-inflammatory pathways normally provoked by shear stress. Mechanistically, they argue that transcription factor dosage preferentially affects

certain gene targets through altered H3K27 acetylation at NOTCH1-bound enhancers leading to specific pathogenic states [45]. These are just a few examples of how epigenetics has uncovered novel components in vascular osteogenesis and has demonstrated that we have just begun to scratch the surface of the complex genetic process of calcification. With the creation of more sophisticated methods of epigenetics, such as surveying chromatin on a single-cell level, we will begin to dive deeper into the mysteries of calcification and perhaps discover novel methods to eradicate this disease.

Evaluating Roles for Functional Biomolecules in Calcification Via Proteomics and Metabolomics

Mass Spectrometry as a Tool to Investigate Protein-Mediated Regulation of Calcification

As the key functional biomolecules, proteins are intimately associated with disease progression and development. Importantly, it is now well-appreciated that levels of transcription and translation are often poorly correlated [46], thereby further motivating the study of protein levels in addition to those techniques we have already discussed. Protein abundance has traditionally been quantified by antibody-based approaches (e.g., Western blots, ELISAs), but these techniques are challenged by low protein abundance and have a limited throughput and linear range. The application of mass spectrometry to protein profiling is dramatically changing this landscape. In a typical proteomics experiment, protein samples are isolated from cultured cells or cell culture supernatant, animal/human biofluids (e.g., plasma, serum, urine, cerebrospinal fluid, etc.), or engineered, animal, or human tissues and organs. Peptides are then typically generated by proteolytic enzymatic digestion (most commonly, trypsin and/or Lys-C are employed). These resultant peptides are then separated by liquid or gas chromatography and fed into an ion source where the peptides are ionized and sent to the mass spectrometer. There, they may fragment further into predictable pieces; the masses of the intact peptides or fragments are then measured by the spectrometer. Subsequently, bioinformatics software is used to match peptide fragment mass spectra against known protein databases. There are two primary quantitative methods: stable isotope labeled or label-free [47]. Under label-free conditions, samples are simply injected into the mass spectrometer, and relative changes in peptide abundance between samples are measured directly from the resultant spectra. This approach is simpler and can be more easily expanded into larger sample sizes but requires greater technical uniformity and high sample-to-sample consistency due to the absence of internal standards. Alternatively, peptides can be labeled with sample-specific isotope-labeled chemical tags (e.g., tandem mass tags [TMT] or isobaric tags [iTRAQ]) that enable sample multiplexing: during fragmentation, these tags are sample-specific, and their relative intensities are directly proportional to relative abundance of that particular peptide between samples.

To date, the application of proteomics to the study of calcific aortic valve disease or aortic stenosis has remained limited, due primarily to the high capital expense and technical complexity of this approach. Initial work to define the proteome of valvular calcification that contributes to CAVD and AS began in 2012, when the Barderas group identified 35 protein species enriched in stenotic aortic valves vs. non-diseased controls using 2D differential electrophoresis and mass spectrometry [48]. Follow-up studies by the same group employed TMT and identified statistically significant alterations in 56 proteins, of which 13 were derived from the extracellular matrix [49]. Protein-protein interaction networks subsequently identified a tight cluster of biglycan, periostin, decorin, lumican, and prolargin. The dominance of proteoglycans in this cluster is notable, as altered proteoglycan synthesis, breakdown, and accumulation are also well-documented in atherosclerotic calcification [50]. In a seminal study, Schlotter et al. employed both global unlabeled and label-based tandem mass tag proteomics to quantify 1872 proteins in excised diseased human aortic valves [51]. Stenotic aortic valves were manually segmented into stages of disease, and global unlabeled proteomics revealed significant enrichment of homeostatic collagens in the non-diseased stage, myofibrogenesis and oxidative stress in the fibrotic stage, and pro-calcifying proteins such as fetuin A and tissue non-specific alkaline phosphatase (TNAP or ALPL) in the calcified end-stage of disease (Fig. 23.2). Subsequently, the three individual layers of stenotic human aortic valves were then each isolated by laser capture microdissection and underwent comparative TMT proteomics. Overall, 117, 83, and 131 proteins were found to be overrepresented by abundance in the fibrosa, spongiosa, and ventricularis, respectively. Notably, glial fibrillary acidic protein (GFAP) was discovered to be almost exclusively expressed in the spongiosa. Though fibrosis is generally believed to precede and directly potentiate the onset of valvular calcification, it was the calcification-protected ventricularis that was enriched in markers of myofibroblastic activation (e.g., MYH11, TAGLN2, CNN1, MYLK, etc.). The calcification-prone fibrosa was instead enriched in proteoglycans, apolipoproteins, and ANGPTL2, a circulating glycoprotein known to modulate endothelial dysfunction, drive osteochondrogenic differentiation, and associate with an increased risk of cardiovascular events [52, 53]. This group followed up with further *in vitro* proteomics of side-specific VIC outgrowth cultures and showed that unlike in human tissue, phosphate-containing media drove calcification of VIC cultures in the absence of contributors from the plasma proteome (e.g., APO(a) or Lp(a), APOC3, FETUB, etc.). These findings suggest that plasma proteins which otherwise contributed to human CAVD pathogenesis are not induced in established culture models of VIC calcification. The whole-tissue valvular secretome was first assessed in 2013, when intact stenotic aortic valve leaflets were cultured for up to 5 days and underwent mass spectrometry [54]. Sixty-one secreted proteins were identified by the addition of labeled amino acids in the culture media, of which only one, the actin-binding protein gelsolin, was also found in an independent cohort of plasma samples. Gelsolin was enriched in the CAVD secretome when compared with that of controls – this was notably opposite to the trend of downregulated gelsolin in the secretome from atherosclerotic coronary arteries and points to a novel differentiator between vascular

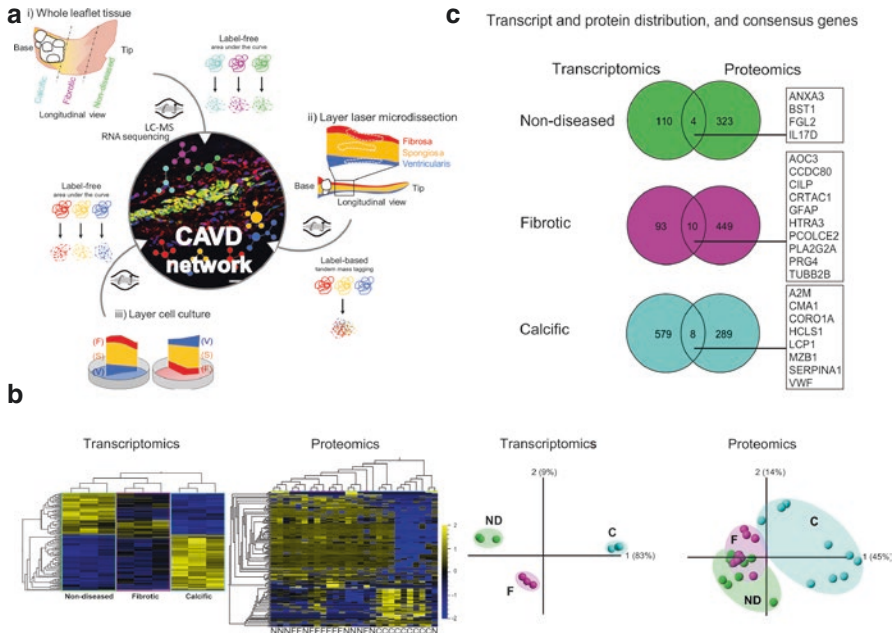


Fig. 23.2 Multi-omics study of cardiovascular calcification. **(a)** Schematic example of a proteomics-based study of valvular calcification that incorporates an examination of stages of disease and anatomical tissue variability *ex vivo*, along with *in vitro* side-specific calcification assays and concomitant omics. **(b)** Transcriptomics and proteomics heat maps and principal component analyses of transcript and protein expression by disease stage (N = non-diseased, F = fibrotic, C = calcified) provide mechanistic insight into the progression of calcification. **(c)** Over-represented transcript and protein lists often have limited overlap and poor correlation, despite isolation from the same donors. This is due to a number of factors, including differential turnover kinetics and regulatory mechanisms. The limited cell density in some fibrous cardiovascular tissues exacerbates this effect, and more sophisticated approaches to integrate multi-omics data are often necessary. (Adapted from Ref. [51])

and valvular calcification. Unfortunately, traditional bulk mass spectrometry sample preparation does not allow the assessment of specific protein localization within a tissue sample of interest. In matrix-assisted laser desorption ionization imaging mass spectrometry (MALDI-IMS), tissue sections bound to a sacrificial matrix are ionized point by point using a laser, a mass spectrum is recorded for each point, and a spatial proteome is then reconstructed *in silico* at a current lateral resolution of approximately 50 μm [55]. MALDI-based analysis of the spatial distribution of proteins and peptides across serial histological sections of stenotic aortic valve tissues found that NDRG-2 and collagen VI were strongly segregated to regions immediately surrounding calcific nodules and may modulate VIC apoptosis and fibrocalcific disease progression [55]. Recently, Goto and colleagues also utilized proteomics to carefully characterize the *in vitro* calcification behavior of human aortic VICs. Using primary VICs derived from a number of human donors with

CAVD, they probed the passage dependency of VIC responses to several classical calcification media. Notably, they performed whole-cell, cytoplasmic, and nuclear fraction proteomics and found, in an unbiased manner, that abundance of TNAP correlated with passage-dependent calcification in media that contained an inorganic source of phosphate [56]. Calcification potential dropped over four passages in these VICs, as did TNAP protein abundance and activity. In contrast, VICs maintained robust calcification potential over many passages when cultured in media containing inorganic phosphate, and there was no passage dependency of TNAP abundance or activity in this media type. Others have performed similar studies in calcifying bovine-derived aortic VICs, where abundance of 44 proteins was significantly altered by pro-inflammatory lipopolysaccharide (LPS) stimulation [57]. Among the many functions of these proteins was control of cell redox/nitric oxide homeostasis and nitric oxide synthase bioactivity, furthering the notion that oxidative stress is a central driver of LPS-induced VIC calcification *in vitro*.

Vascular calcification has also been the focus of a number of proteomics-based studies. In one clinical study of 196 patients with suspected coronary artery disease, targeted plasma proteomics of 358 proteins was fed into machine learning models in order to develop risk predictions for the presence of high-risk plaques or absence of coronary atherosclerosis [58]. Thirty-five protein biomarkers were identified which were predictive of the presence of high-risk plaques at an area under the curve (AUC) of 0.79 (a statistically significant improvement vs. prediction based only on clinical characteristics, AUC = 0.64). A different set of 34 proteins predicted the absence of coronary artery disease (CAD) with AUC = 0.85 (significant vs. clinical characteristics alone, AUC = 0.70). Other efforts have involved the concurrent analysis of transcriptomics and global proteomics from both carotid endarterectomies and paired plasma samples [59], which found biliverdin reductase B (BLVRB) to be a novel biomarker of intraplaque hemorrhage and unstable CAD. Schlotter et al.'s staged approach to investigating the pathogenesis of calcification mentioned above was previously employed to examine liver calcification, through the examination of noncalcified, precalcified, and calcified regions of human liver [60]. Prior work had demonstrated the involvement of myofibroblasts in mineralization of the liver, and so actin cytoskeleton remodeling proteins were targeted by mass spectrometry, which revealed abundant expression of the RAS GTPase-activating proteins IQGAP1 and IQGAP2, the myofibroblasts present at the periphery of calcific nodules. These investigators went on to identify an IQGAP1- β -catenin complex involved in the regulation of liver myofibroblast cytoskeletal dynamics in response to livery injury. Others have utilized targeted mass spectrometry panels to identify a host of serum biomarkers that were predictive of the onset of chronic kidney disease, including mediators of inflammation (IL-6, TNF- α) and modulators of mineralization and osteoblastic/clastic differentiation (OPG, OPN, OCN, FGF-23, and fetuin-A) [61]. Wang et al. identified Smarca4 as a novel mediator of hyperphosphatemic vascular calcification using rat aortic SMCs cultured in media containing β -glycerophosphate and LC-MS/MS: 113 proteins with altered enrichment vs. control media held functions associated with cell adhesion molecule binding and blood vessel development. Smarca4, a chromatin

remodeling ATPase, had a particularly high fold change between media conditions, and its gene expression was subsequently confirmed to be significantly elevated in a rat model of hyperphosphatemic vascular calcification and likely modulates mineralization through miR-133b and miR-155 [62]. Novel and highly sensitive mass spectrometric approaches to examine the matrisome's (extracellular matrix and ECM-binding proteins) involvement in vascular calcification have included the development of quantitative detergent solubility profiling (QDSP), which has been validated in animal models: four protein fractions were isolated using a steadily increasing proportion of detergent from the atherosclerotic aortas of high-fat, high-cholesterol-fed *ApoE*^{-/-} mice [63] and underwent label-free proteomics. This method of selectively and controllably freeing ECM-bound proteins yielded a number of novel targets that were enriched in atherosclerotic lesions, including the bone matrix protein Tnfrsf11b. Furthermore, they detected osteoclast-specific ATPases in both plaques and macrophages, which may be indicative of roles for macrophages in mineral clearance from plaques.

Nanometer-scale extracellular vesicles (EVs) have recently been implicated as active contributors to cardiovascular calcification [64, 65]. EVs are membrane-bound particles that are actively released by all eukaryotic cell types and are found throughout the body's tissues, organs, and biofluids. EVs carry bioactive cargos (e.g., RNA, proteins, metabolites) and actively mediate intercellular communication. Mass spectrometry has become a favored tool to interrogate EV protein cargoes, due in no small part to requirement for sensitive analysis of limited protein yields from these tiny structures. When employed to profile EVs obtained from the culture of vascular SMCs in control and calcifying media, mass spectrometry identified over 400 proteins, of which 48 were found exclusively in calcifying vascular SMC-derived EVs [66]. These proteins included TNAP and multiple isoforms of annexins – membrane proteins known to potentiate vesicle calcification in vitro [67]. In the context of hyperphosphatemia, matrix vesicles elaborated by cultured VICs were demonstrated by proteomics to be strongly enriched in exosomal markers (CD9, CD63, LAMP-1) and contained dramatic upregulation of eight annexin isoforms when compared with those excreted by VICs cultured in control media [68]. Others have shown significant overlap in the EV cargo proteomes of vesicles produced by vascular SMCs cultured in hyperphosphatemic conditions and those derived from mineralizing chondrocytes [69] or osteoblasts [70]. Along with unbiased approaches, proteomics has also been exploited to examine specific, difficult-to-assay biochemical mechanisms. For example, the multiligand sorting receptor sortilin (SORT1) regulates the loading of TNAP into vascular SMC-derived EVs, thereby promoting EV-driven calcification [71]. This loading functionality of sortilin was likely regulated by posttranslational modification, and while sortilin contains a number of candidate phosphorylation sites, an absence of phospho-specific sortilin antibodies leads Goettsch and colleagues to develop a targeted mass spectrometry-based strategy to monitor sortilin phosphorylation at serine 825. In this manner, these investigators determined that levels of pSer825 in human SMCs were dramatically elevated in calcifying culture conditions, as well as in calcified mouse arteries and human carotid endarterectomies [66].

Much like with scRNA-seq, there has also been a recent push to expand proteomics into the single-cell realm, primarily through the application of mass cytometry (CyTOF). Here, heavy metal-conjugated antibodies are used to label cells, which are then nebulized into single-cell droplets [72]. Plasma is utilized to ionize the metal-conjugated antibodies; the resultant ions are analyzed per single-cell droplet in a time-of-flight mass spectrometer, where an ion's velocity is determined by its mass-to-charge ratio. Unlike traditional fluorescent-based flow cytometry which tops out at no more than 20 color channels, CyTOF is currently capable of quantitative measurements of protein abundance across up to 135 channels – ion signals on the time-of-flight mass spectrometer suffer nowhere near the same degree of spectral overlap as the fluorophores typically used in cytometry [72]. This technique therefore lends itself to an unbiased, detailed, and complete examination of, for example, an entire signaling network of interest or immunophenotyping the cellular components of complex tissues such as are present in calcified blood vessels, valves, or soft tissues. CyTOF approaches are now being combined with scRNA-seq to perform multi-omics on diseased cardiovascular tissues at a single-cell resolution: one such study examined the immune cell repertoire of atherosclerosis in *ApoE*^{-/-} and *Ldlr*^{-/-} mice [73]. Another has identified alterations in specific CD4⁺ T cell subsets between asymptomatic vs. symptomatic human carotid artery plaques and found evidence of macrophage subsets that modulate plaque vulnerability and were associated with recent ischemic cerebrovascular events [74]. Moving forward, the expansion of single-cell proteomics beyond the limited segment of the proteome accessible to CyTOF will enable order-of-magnitude improvements in the biological complexity which can be captured. Novel techniques such as Single-Cell ProtEomics by Mass Spectrometry (SCoPE-MS), where single cells are picked, TMT-labeled, and undergo mass spectrometry along with a larger population of differently TMT-labeled carrier cells that potentiate peptide sequence identification by providing additional ions [75], or perhaps those based on a revival of Edman protein sequencing [76] hold promise in this regard.

Metabolomics: Assessing the Final Link Between Genotype and Phenotype

Metabolites are small molecules produced as the substrates, intermediates, and products of metabolism. Metabolites may be endogenous (breakdown products of compounds produced by the organism of interest; e.g., amino acids, fatty acids, nucleic acids, sugars, etc.) or exogenous (drugs, environmental contaminants, xenobiotics). Importantly, metabolites represent the biomolecules that are closest to phenotype and directly represent biochemical activity [77]. Modern metabolomics leverage mass spectrometry in much the same ways as do proteomics – metabolites are extracted and purified from samples of interest, and the molecular masses and

fragmentation patterns of the isolated metabolites are determined. These masses and fragments are then compared against databases of known and predicted metabolites to assign compound identifications [78]. Mass spectrometry-based metabolomics remain in their infancy, and applications of this technique to the study of calcification have focused almost exclusively on blood metabolites.

One large multicenter study examined the plasma metabolome of 2324 patients who underwent coronary angiography for expected CAD [79]. Five resultant clinical phenotypes were described (normal, nonobstructive CAD, stable angina, unstable angina, acute myocardial infarction), and 89 differential metabolites were identified. These metabolites implicated phospholipid catabolism, amino acid metabolism, and bile acid biosynthesis. Twelve panels of metabolomics-based biomarkers provided strong predictive values of 89.2–96.0% for differential diagnosis between the clinical phenotypes. In another blood-based study of 1111 participants, the circulating metabolome was compared with extra- and intracranial carotid artery calcification as measured by computed tomography [80]. Upon examination of associations between calcium scores and metabolites, the authors found that the ketone body 3-hydroxybutyrate was significantly associated with intracranial carotid artery calcification, and glycoprotein acetyls were associated with calcification in both regions. In the context of chronic kidney disease-associated calcification, targeted assessment of arginine metabolites from the blood of *Ldlr*^{-/-} mice with 5/6 nephrectomy and fed a high-fat diet revealed that levels of asymmetric dimethyl arginine were elevated in mice with CKD [81]. Deranged nitric oxide synthesis may therefore be implicated in hyperphosphatemic vascular calcification. Others have utilized rats with adenine-induced CKD to examine the impact of removing gut-derived uremic toxins through pharmacotherapy [82]. Pharmacologic intervention significantly reduced over half of all metabolites that were increased in plasma, liver, and heart in response to adenine and determined that eight gut-derived uremic toxins defined the onset of CKD. As metabolomic sample preparation techniques mature, an expansion is occurring beyond biofluids in an effort to examine tissue metabolomes. An example of such a study is that of Vorkas and colleagues, who extracted metabolites from 126 aortic aneurysms, carotid endarterectomies, or femoral endarterectomies [83]. They performed consecutive aqueous and organic extractions from mechanically homogenized tissue samples and employed hydrophilic interaction liquid chromatography and reversed-phase chromatography in tandem with mass spectrometry to define 226 unique tissue-derived metabolites. When the metabolome of mature plaques was compared with that of tissues undergoing early intimal thickening, compounds from the cholesterol, purine, pyrimidine, and ceramide pathways were significantly enriched [84]. Importantly, β -oxidation intermediates indicative of impaired and dysregulated fatty acid metabolism and overall mitochondrial dysfunction were detected. The future widespread use of tissue metabolomics promises to further clarify the mechanistic contributions of altered metabolism to the initiation and progression of calcification.

Systems-Based Computational Approaches in Cardiovascular Calcification

Bioinformatics to Extract Biological Insights

Cardiovascular calcification is a multi-factorial pathological process that involves dynamic interactions between a large number of biological elements. This molecular complexity makes it highly conducive to holistic, data-driven approaches, which have recently emerged in medicine as indispensable counterparts to the traditional reductionist, hypothesis-driven standpoint. Equipped with an ever-growing collection of computational tools that take into account the interdependencies between molecular entities, the field of systems biology, powered by high-resolution molecular profiling (“omics”) techniques and large-scale biomedical knowledge bases, has started making a crucial impact on the study of vascular and valvular calcification. In this section, we will overview some examples of recent such efforts.

The first stage of a typical bioinformatics workflow in clinical research involves next-generation sequencing or omics profiling on case and control samples to quantify the differences in their expression levels. This step is invariably followed by normalization and standardization of the data, which is usually done using well-established protocols that are omics-specific. The second stage involves the statistical treatment of the data to determine the strongest signals and to cluster samples into biologically coherent groups, usually through various forms of differential expression analysis and multivariate statistical analyses such as principal component analysis (PCA) or hierarchical clustering. The third and final stage generally involves some combination of pathway and network analyses to extract the most refined and pertinent information related to the biology in question and is perhaps the stage with the most room for creative use of state-of-the-art methods. Pathway analysis serves to mitigate the complexity and improve the interpretability of the data by summarizing long lists of molecules in terms of familiar biological processes. Networks provide a natural means to represent large-scale complex interactions and are therefore the cornerstone of systems-based approaches in medicine [85]. Molecular networks are typically built and analyzed in this stage to infer key pathways and biomarkers, as well as to predict novel disease-related molecules and therapeutic candidates.

Transcriptome profiling, especially whole-genome techniques such as RNA sequencing (RNA-seq), has been the technology of choice and often the starting point of many studies that use systems-driven approaches to investigate cardiovascular diseases [86], including cardiovascular calcification. Sen et al. [29] used RNA-seq to compare lymphoblastoid cell lines from coronary artery calcification (CAC) cases and controls to identify 186 differentially expressed transcripts, which showed significant enrichment with literature-curated CAD-associated genes. Analyzing the identified transcripts by a dedicated integrated systems biology analysis software revealed networks associated with cardiovascular system development, lipid metabolism, and cyclic AMP metabolism, suggesting possible

mechanisms through which CAC may be related to CAD etiology. The effect of shear stress and NOTCH1 signaling on the human aortic valve endothelium was studied by White et al. [87] by jointly analyzing RNA-seq and ChIP-seq data on primary human aortic valve endothelial cells (HAVECs). The authors integrated differential expression analysis with ChIP-seq peak scores to determine the direct transcriptional targets of NOTCH1 in HAVECs and used the resulting gene sets with pathway and Gene Ontology (GO) over-representation analysis. The potential targets activated by both NOTCH1 and shear stress were associated with maintaining noncalcified bone growth plates, repressing osteogenesis, and preventing atherosclerosis, vascular calcification, and angiogenesis and included matrix gla protein (MGP). Perisic et al. [88] analyzed the gene expression in carotid endarterectomies and peripheral blood from patients with symptomatic and asymptomatic carotid stenosis. Gene set enrichment analysis (GSEA) was performed to determine the significant biological processes, and prediction modeling was used to classify plaques from symptomatic versus asymptomatic patients. The authors built functional networks, which were associated with atherosclerosis mapped to hypoxia, chemokines, calcification, actin cytoskeleton, and extracellular matrix (ECM). Rukov et al. [21] studied vascular calcification in the context of chronic uremia and chronic kidney disease (CKD), where they performed RNA sequencing on rat aortas with and without uremia. A bioinformatics pipeline consisting of differential expression analysis, GO cluster analysis, and pathway enrichment analysis revealed pathways and ontologies related to ECM, ossification, and Jak/STAT and MAPK signal transduction, demonstrating the shift in the transcriptional program of the calcified aorta from vascular tissue toward an osteochondrocytic profile. To elucidate the mechanisms distinguishing pathological vascular calcification from physiological bone calcification, Alves et al. [22] carried out a comparative transcriptomic profiling of calcifying vascular SMCs and osteoblasts, followed by bioinformatics analyses. PCA on the time-course gene expression data revealed distinct global expression patterns between the two cell types. K-means clustering was performed on the temporal expression profiles of the differentially expressed genes during calcifying vascular SMC development and osteoblast differentiation to identify six distinct clusters representing groups of genes with similar regulation patterns over time. Correlation analyses revealed shared biological axes between calcifying vascular SMCs and osteoblasts. Strong positive correlations were found between calcifying vascular SMCs and osteoblasts for biomineral tissue development, while bone-related processes such as regulation of osteoblast differentiation showed strong negative correlations, suggesting the uniqueness of calcifying vascular SMCs.

Noncoding RNAs, particularly microRNAs (miRNAs) and long noncoding RNAs (lncRNAs), are increasingly being implicated in cardiovascular diseases as potential biomarkers and therapeutics [89, 90]. Chaturvedi et al. [91] studied the transcriptional control of miRNAs in vascular calcification in a CKD rat model through miRNA microarray expression profiling. The authors obtained post-transcriptional regulatory networks of miRNAs dysregulated between vascular SMCs and extracellular vesicles (EVs) following a multi-step bioinformatics pipeline. Differentially expressed miRNAs were fed into two parallel computational

miRNA target prediction methods. The target mRNAs identified by the consensus of these two methods and regulated by multiple differentially expressed miRNAs were considered for further regulatory network construction. The functional and pathway enrichment of the genes controlled by multiple miRNAs recapitulated pathways previously implicated in vascular calcification. This approach also revealed several novel miRNAs whose targets were enriched in pathways that were not previously associated with vascular calcification or EV formation. Coffey et al. [92] examined the valve miRNA profiles of human aortic valve samples with and without aortic stenosis (AS) following a systems biology approach that involved the integration of mRNA and miRNA information. Network clustering based on co-expression of differentially expressed miRNAs revealed clusters of miRNAs that were enriched in distinct biological processes such as glycosaminoglycan biosynthesis for upregulated miRNAs and regulation of actin cytoskeleton for downregulated miRNAs. Differentially expressed miRNAs and mRNAs between control and AS samples were integrated on a per-sample basis for the *in silico* reconstruction of post-transcriptional regulatory networks where mRNA targets were predicted using a computational miRNA-mRNA interaction prediction tool. Finally, building an integrated network of miRNAs, mRNAs, transcription factors, and drugs helped the identification of drugs targeting upregulated and highly connected mRNAs, highlighting potential novel therapies for AS. The mechanistic involvement of lncRNAs in vascular calcification was recently studied by Jeong et al. [93]. The authors performed RNA sequencing on rat vascular SMCs and employed a three-step analysis pipeline which searched for lncRNAs that were (i) differentially expressed during vascular calcification, (ii) conserved across species, and (iii) had literature evidence of their genomic neighborhood in the context of calcification, calcium regulation, or related processes. They studied the regulatory network of *Lrrc75a-as1*, one of the four candidate lncRNAs identified by this bioinformatic approach, by using a miRNA target prediction tool and identified 47 putative target miRNAs interacting with *Lrrc75a-as1* in a sequence-specific manner, suggesting that *Lrrc75a-as1* may regulate vascular calcification through interaction with these miRNAs.

Mass spectrometry-based techniques such as proteomics have been gaining prominence in cardiovascular research [94], since the measurement of protein levels represents a direct proxy of biological function [95]. Proteomic data has been successfully combined with bioinformatics methods in cardiovascular calcification research. Langley et al. [96] studied the proteomics of carotid endarterectomy samples from symptomatic and asymptomatic patients, where they focused on the ECM proteome seeking to identify the molecular predictors of symptomatic atherosclerotic plaques. They constructed co-expression networks from proteins differentially expressed between carotid plaques from symptomatic and asymptomatic patients. Proteins of similar functions such as matricellular proteins and glycoproteins were co-clustered in these networks. Furthermore, the connectivity patterns between the constituent proteins of the four-biomarker signature that improved clinical risk prediction (matrix metalloproteinase 9, S100A8/S100A9, cathepsin D, and galectin-3-binding protein) were captured in these co-expression networks. Wierer et al. [63] studied the changes in the proteome of the mouse aorta following atherosclerotic

plaque development using high-resolution mass spectrometry. Unsupervised hierarchical clustering of the significantly regulated proteins resulted in four major clusters, which were subsequently analyzed for functional annotation enrichment. Clusters wherein proteins were specifically regulated during atherogenesis contained a large number of known factors related to atherosclerotic plaque development. In one of these clusters, proteins associated with bone-related GO terms were also enriched, hinting at vascular calcification, a hallmark of atherogenesis. Additionally, proteins known to promote and inhibit calcification were both increased at later time points of atherogenesis, suggesting the complex interplay of positive and negative regulators of vascular calcification. Schanstra et al. [97] studied the proteomes of peripheral arteries from early-stage and advanced-stage CVD patients with the aim of discovering novel therapeutic candidates for CVD, taking a computational drug repurposing route. The CVD proteomic signature, consisting of differentially expressed proteins, was tested for pathway enrichment and then queried against the Connectivity Map database [98] for small molecules that could potentially reverse this signature. Twelve molecules were predicted to significantly reverse the CVD signature, and among these, arachidonic acid trifluoromethyl ketone (AACOCF3), an inhibitor of cytosolic phospholipase A2 (cPLA2), showed the highest negative enrichment score. Treatment with AACOCF3 significantly reduced vascular calcification and inhibited osteogenic signaling in vivo in a cholecalciferol-overload mouse model and in vitro in human aortic SMCs, providing a proof of concept of the utility of computational repositioning in vascular calcification drug discovery.

Multi-omics Data Integration

Network-based and other data integration methods are increasingly being used in biomedical research under the umbrella of “integrative omics” to simultaneously analyze different omics types [99]. This approach is especially promising because often the molecular sources of variability are not known beforehand, and therefore the biological complexity of human disease might not be fully captured by considering a single data modality. Guauque-Olarte et al. [16] used an integrative genomics workflow to describe the first genome-wide association study (GWAS) in aortic stenosis (AS). Two GWAS on AS patients were combined in a meta-analysis, and expression of susceptibility genes from both studies was analyzed through RNA-seq in human valves with and without AS. Pathway analysis was conducted at the level of SNPs, enabling the detection of subtle effects of multiple SNPs in the same gene set. In parallel to RNA-seq, genome-wide genotyping and gene expression profiling were performed on an independent set of human aortic valves for expression quantitative trait loci (eQTL) profiling. The authors devised an integration scheme where differentially expressed genes from RNA-seq were filtered for (i) being 1 Mb up- or downstream of SNPs with $P < 1 \times 10^{-4}$ in the GWAS

meta-analysis, (ii) participating in molecular pathways known to be altered in the development and progression of AS, and (iii) belonging to the set of identified significant eQTLs. This analytical workflow resulted in the identification of *RUNX2* as a potential driver of AS and *CACNA1C* as a new AS susceptibility gene. Mourino-Alvarez et al. [100] used an integrative omics approach combining plasma proteomics and metabolomics to characterize the molecular determinants differentiating between AS and aortic regurgitation (AR), using the latter as control. Multivariate analyses consisting of PCA and hierarchical clustering were used on proteomics and metabolomics data for an unsupervised separation of AS and AR samples. Significantly altered proteins and metabolites in AS were classified by their annotated functions into four molecular panels related to coagulation, inflammation and immune response, response to ischemia, and lipid metabolism. Receiver operating characteristic (ROC) curves confirmed the predictive power of these panels, suggesting their use as potential diagnostic and prognostic markers in AS. Schlotter et al. [51] investigated calcific aortic valve disease (CAVD) in both the spatial and temporal dimensions combining multi-omics with network medicine approaches (Fig. 23.3). Transcriptomics and proteomics were performed on stenotic human aortic valves segmented to reflect the stages of disease progression as well as anatomical tissue layers. A fold change-based over-representation approach determined mutually exclusive sets of genes and proteins that characterize each stage/layer. The enriched pathways of each stage and layer were represented in pathway networks whereby tightly connected clusters of pathways provided salient groups of biological processes. Stage/layer-specific proteins were mapped onto the global human protein-protein interaction (PPI) network to determine the key molecular drivers of CAVD progression. Subsequent betweenness centrality analysis revealed fibronectin-1 as one of the most central proteins in both the calcific stage network and the fibrosa layer network. Finally, network proximity analysis implicated the molecular association of CAVD with inflammatory and fibrotic diseases, pointing to possible shared mechanisms with these diseases.

Systems-based computational approaches have so far proven to be instrumental in shedding light on the potential mechanisms underlying cardiovascular calcification. Nevertheless, dissecting the molecular markers of phenotypic heterogeneity, reliably subtyping patients based on the identified biomarkers, and designing personalized therapies remain major challenges. As the analysis tools of systems medicine, data collection methods of omics technologies, and annotation capabilities of large-scale biomolecular and pharmacogenomic databases continue to improve in constant feedback with each other, we will witness major leaps in addressing these challenges. Advances in cloud computing will further aid systems-based approaches by improving the scalability and reproducibility of computationally intensive analytical workflows [101]. Finally, the integrated analysis of multi-omics will become a ubiquitous practice with the further development of methods that can efficiently and simultaneously analyze all omics types from genomics to metabolomics, empowering the precision medicine of calcific disease.

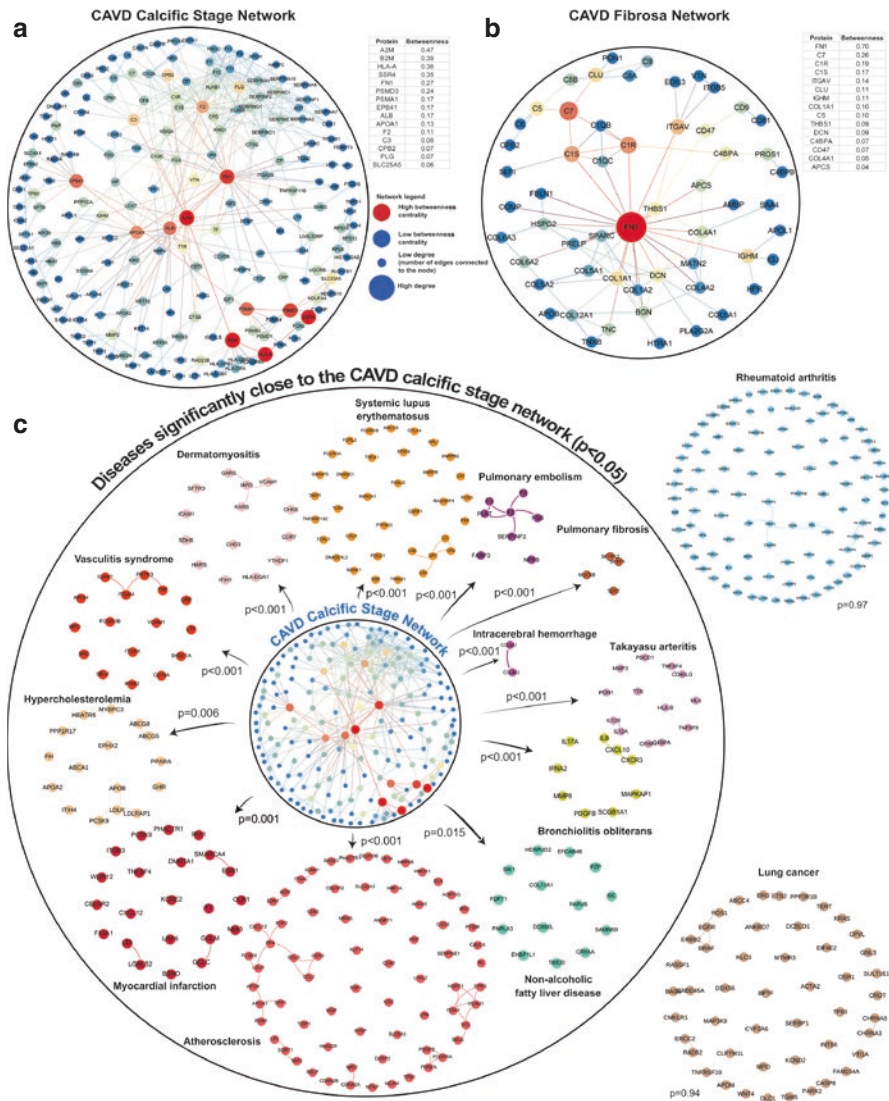


Fig. 23.3 Network medicine-based analyses of aortic valve calcification. **(a)** A protein-protein interaction (PPI) subnetwork generated from proteomics of calcified human aortic valve tissue identifies a number of key proteins (red) implicated in calcification. **(b)** PPI network generated from region-specific proteomics of the disease-prone fibrosa valve layer identifies a specific fibronectin isoform as a putative mediator of disease progression. **(c)** Disease association networks demonstrate significant associations (based on average network distance) between the CAVD protein-protein interaction network and those of other cardiovascular, malignant, metabolic, and autoimmune diseases. Diseases inside the circle (e.g., atherosclerosis, systemic lupus erythematosus) were significantly associated with aortic stenosis, while those outside (e.g., rheumatoid arthritis) were not. (Adapted from Ref. [51])

The Promise of Omics-Driven Target Discovery

The ongoing confluence of personalized medicine and omics approaches is poised to revolutionize our understanding of and approaches to the treatment of calcific disorders. Several lingering challenges remain, particularly in the context of causal (driving) or correlative (reactive) changes in omics datasets. Differentiating causal vs. correlative changes through omics analyses remains difficult, though multi-omics integration holds some promise in this regard. Determination of causal drivers is likely to consistently require follow-up testing in *in vitro*/*in vivo* models of disease, in combination with temporal studies to investigate whether a causal variation precedes or is caused by the phenotype of interest (reviewed in [102]). In the future, we can also expect to see the further democratization of these omics techniques as access to sequencing, mass spectrometry, and high-powered computation becomes progressively more economical. Usage of omics is likely to expand far beyond a precious few clinical samples, toward a standard role in the biomedical scientist's toolkit for routine studies of calcific diseases in animal and cell culture models. Intelligent synthesis of extensive, multi-species, and multi-omics datasets across *ex vivo*, *in vivo*, and *in vitro* experimental conditions will be essential in order to derive accurate and validatable mechanistic insights [103]. It is also important to consider that there is a growing movement away from the use of animals in research – indeed, the EPA recently announced plans to eliminate testing in mammals by the year 2035, and other governmental, academic, and commercial research and pharmaceutical initiatives are likely to closely follow suit. Preclinical work that is currently performed in animal models of calcific diseases will undoubtedly shift toward tissue-engineered models that recapitulate key aspects of the disease micro-environment, and target discovery will increasingly rely on *in silico* modeling based on prior datasets [104, 105]. In contrast to efforts to reduce the usage of animals, omics-based studies in humans are poised to dramatically increase in scale: as we plumb the depths of increasingly smaller effect sizes or work to composite polygenic effects, we will undoubtedly come to rely heavily on databases that combine multi-omics datasets with rich, high-quality clinical phenotyping in hundreds of thousands of individuals such as the UK Biobank, the National Institutes of Health's All of Us, or Veterans Affairs Million Veteran Program [106]. As this exciting field develops, fundamental questions arise: Are we prepared to navigate the ethical, legal, and social ramifications of widespread genomic testing? Do large human cohorts contain participants of sufficient racial and ethnic diversity to ensure that variant associations are relevant to at-risk populations? What additional training do front-line clinicians require in order to most effectively leverage omics-derived calcification therapeutics? Most importantly, how do we undertake targeted delivery of therapeutics or prioritize non-promiscuous targets in order to safely regress pathological calcification without impacts on skeletal integrity? Finding answers to these concerns is essential. In the end, unbiased omics may hold the most promise as a means to kick-start efforts to bridge the fundamental knowledge gap present in our understanding and treatment of aberrant calcification.

Acknowledgments This work is supported by the National Institutes of Health (NIH) grants R01HL136431, R01HL141917, and R01HL147095. We are grateful to Dr. Sasha A. Singh for her expertise in and assistance regarding proteomics and mass spectrometry.

References

1. Benjamin EJ, Muntner P, Alonso A, Bittencourt MS, Callaway CW, Carson AP, et al. Heart disease and stroke statistics-2019 update: a report from the American Heart Association. *Circulation*. 2019;139(10):e56–e528.
2. Rennenberg RJ, Kessels AG, Schurgers LJ, van Engelshoven JM, de Leeuw PW, Kroon AA. Vascular calcifications as a marker of increased cardiovascular risk: a meta-analysis. *Vasc Health Risk Manag*. 2009;5(1):185–97.
3. Hutcheson JD, Blaser MC, Aikawa E. Giving calcification its due: recognition of a diverse disease: a first attempt to standardize the field. *Circ Res*. 2017;120(2):270–3.
4. Karwowski W, Naumnik B, Szczepanski M, Mysliwiec M. The mechanism of vascular calcification – a systematic review. *Med Sci Monit*. 2012;18(1):Ra1–11.
5. Puri R, Nicholls SJ, Shao M, Kataoka Y, Uno K, Kapadia SR, et al. Impact of statins on serial coronary calcification during atheroma progression and regression. *J Am Coll Cardiol*. 2015;65(13):1273–82.
6. Palit S, Kendrick J. Vascular calcification in chronic kidney disease: role of disordered mineral metabolism. *Curr Pharm Des*. 2014;20(37):5829–33.
7. Alekseyev YO, Faz al. A next-generation sequencing primer-how does it work and what can it do? *Acad Pathol*. 2018;5:2374289518766521.
8. Matthews H, Hanison J, Nirmalan N. “Omics”-informed drug and biomarker discovery: opportunities, challenges and future perspectives. *Proteomes*. 2016;4(3):28.
9. Pérez-Hernández N, Aptilon-Duque G, Blachman-Braun R, Vargas-Alarcón G, Rodríguez-Cortés AA, Azrad-Daniel S, et al. Vascular calcification: current genetics underlying this complex phenomenon. *Chin Med J*. 2017;130(9):1113–21.
10. O’Donnell CJ, Kavousi M, Smith AV, Kardina SLR, Feitosa MF, Hwang S-J, et al. Genome-wide association study for coronary artery calcification with follow-up in myocardial infarction. *Circulation*. 2011;124(25):2855–64.
11. van Setten J, Isgum I, Smolonska J, Ripke S, de Jong PA, Oudkerk M, et al. Genome-wide association study of coronary and aortic calcification implicates risk loci for coronary artery disease and myocardial infarction. *Atherosclerosis*. 2013;228(2):400–5.
12. Adams HH, Ikram MA, Vernooij MW, van Dijk AC, Hofman A, Uitterlinden AG, et al. Heritability and genome-wide association analyses of intracranial carotid artery calcification: the Rotterdam study. *Stroke*. 2016;47(4):912–7.
13. Thanassoulis G, Campbell CY, Owens DS, Smith JG, Smith AV, Peloso GM, et al. Genetic associations with valvular calcification and aortic stenosis. *N Engl J Med*. 2013;368(6):503–12.
14. Schnabel RB, Baccarelli A, Lin H, Ellinor PT, Benjamin EJ. Next steps in cardiovascular disease genomic research—sequencing, epigenetics, and transcriptomics. *Clin Chem*. 2012;58(1):113–26.
15. Xu S. Transcriptome profiling in systems vascular medicine. *Front Pharmacol*. 2017;8:563.
16. Guauque-Olarte S, Messika-Zeitoun D, Droit A, Lamontagne M, Tremblay-Marchand J, Lavoie-Charland E, et al. Calcium signaling pathway genes RUNX2 and CACNA1C are associated with calcific aortic valve disease. *Circ Cardiovasc Genet*. 2015;8(6):812–22.
17. Krohn JB, Hutcheson JD, Martínez-Martínez E, Aikawa E. Extracellular vesicles in cardiovascular calcification: expanding current paradigms. *J Physiol*. 2016;594(11):2895–903.
18. Rutsch F, Nitschke Y, Terkeltaub R. Genetics in arterial calcification: pieces of a puzzle and cogs in a wheel. *Circ Res*. 2011;109(5):578–92.

19. Seo D, Wang T, Dressman H, Herderick Edward E, Iversen Edwin S, Dong C, et al. Gene expression phenotypes of atherosclerosis. *Arterioscler Thromb Vasc Biol.* 2004;24(10):1922–7.
20. Deshpande V, Sharma A, Mukhopadhyay R, Thota LNR, Ghatge M, Vangala RK, et al. Understanding the progression of atherosclerosis through gene profiling and co-expression network analysis in Apobtm2SgyLdlrtm1Her double knockout mice. *Genomics.* 2016;107(6):239–47.
21. Rukov JL, Gravesen E, Mace ML, Hofman-Bang J, Vinther J, Andersen CB, et al. Effect of chronic uremia on the transcriptional profile of the calcified aorta analyzed by RNA sequencing. *Am J Physiol Renal Physiol.* 2016;310:F477–91.
22. Alves RD, Eijken M, van de Peppel J, van Leeuwen JP. Calcifying vascular smooth muscle cells and osteoblasts: independent cell types exhibiting extracellular matrix and biomineralization-related mimics. *BMC Genomics.* 2014;15:965.
23. Alloza I, Goikuria H, Idro JL, Trivino JC, Fernandez Velasco JM, Elizagaray E, et al. RNAseq based transcriptomics study of SMCs from carotid atherosclerotic plaque: BMP2 and IDs proteins are crucial regulators of plaque stability. *Sci Rep.* 2017;7(1):3470.
24. Steenman M, Espitia O, Maurel B, Guyomarch B, Heymann M-F, Pistorius M-A, et al. Identification of genomic differences among peripheral arterial beds in atherosclerotic and healthy arteries. *Sci Rep.* 2018;8(1):3940.
25. Karlöf E, Seime T, Dias N, Lengquist M, Witasp A, Almqvist H, et al. Correlation of computed tomography with carotid plaque transcriptomes associates calcification with lesion-stabilization. *Atherosclerosis.* 2019;288:175–85.
26. Gomes AV. Spatiotemporal multi-omics-derived atlas of calcific aortic valve disease. *Circulation.* 2018;138(4):394–6.
27. Guauque-Olarte S, Droit A, Tremblay-Marchand J, Gaudreault N, Kalavrouziotis D, Dagenais F, et al. RNA expression profile of calcified bicuspid, tricuspid, and normal human aortic valves by RNA sequencing. *Physiol Genomics.* 2016;48(10):749–61.
28. Theriault S, Gaudreault N, Lamontagne M, Rosa M, Boulanger MC, Messika-Zeitoun D, et al. A transcriptome-wide association study identifies PALMD as a susceptibility gene for calcific aortic valve stenosis. *Nat Commun.* 2018;9(1):988.
29. Sen SK, Barb JJ, Cherukuri PF, Accame DS, Elkahloun AG, Singh LN, et al. Identification of candidate genes involved in coronary artery calcification by transcriptome sequencing of cell lines. *BMC Genomics.* 2014;15:198.
30. Sen Shurjo K, Boelte Kimberly C, Barb Jennifer J, Joehanes R, Zhao X, Cheng Q, et al. Integrative DNA, RNA, and protein evidence connects TREML4 to coronary artery calcification. *Am J Hum Genet.* 2014;95(1):66–76.
31. Nanoudis S, Pikilidou M, Yavropoulou M, Zebekakis P. The role of MicroRNAs in arterial stiffness and arterial calcification. An update and review of the literature. *Front Genet.* 2017;8:209.
32. Kim YK, Kook H. Diverse roles of noncoding RNAs in vascular calcification. *Arch Pharm Res.* 2019;42(3):244–51.
33. Carrion K, Dyo J, Patel V, Sasik R, Mohamed SA, Hardiman G, et al. The long non-coding HOTAIR is modulated by cyclic stretch and WNT/beta-CATENIN in human aortic valve cells and is a novel repressor of calcification genes. *PLoS One.* 2014;9(5):e96577.
34. Nguyen QH, Pervolarakis N, Nee K, Kessenbrock K. Experimental considerations for single-cell RNA sequencing approaches. *Front Cell Dev Biol.* 2018;6:108.
35. Cochain C, Vafadarnejad E, Arampatzi P, Pelisek J, Winkels H, Ley K, et al. Single-cell RNA-Seq reveals the transcriptional landscape and heterogeneity of aortic macrophages in murine atherosclerosis. *Circ Res.* 2018;122(12):1661–74.
36. Gošev I, Zeljko M, Đurić Ž, Nikolić I, Gošev M, Ivčević S, et al. Epigenome alterations in aortic valve stenosis and its related left ventricular hypertrophy. *Clin Epigenetics.* 2017;9(1):106.
37. Hadji F, Boulanger MC, Guay SP, Gaudreault N, Amellah S, Mkannez G, et al. Altered DNA methylation of long noncoding RNA H19 in calcific aortic valve disease promotes mineralization by silencing NOTCH1. *Circulation.* 2016;134(23):1848–62.

38. Mkannez G, Gagné-Ouellet V, Jalloul Nsaibia M, Boulanger M-C, Rosa M, Argaud D, et al. DNA methylation of a PLPP3 MIR transposon-based enhancer promotes an osteogenic programme in calcific aortic valve disease. *Cardiovasc Res.* 2018;114(11):1525–35.
39. Zhou S, Zhang Y, Wang L, Zhang Z, Cai B, Liu K, et al. CDKN2B methylation is associated with carotid artery calcification in ischemic stroke patients. *J Transl Med.* 2016;14(1):333.
40. Lin X, Li F, Xu F, Cui R-R, Xiong D, Zhong J-Y, et al. Aberration methylation of miR-34b was involved in regulating vascular calcification by targeting Notch1. *Aging (Albany NY).* 2019;11(10):3182–97.
41. Klemm SL, Shipony Z, Greenleaf WJ. Chromatin accessibility and the regulatory epigenome. *Nat Rev Genet.* 2019;20(4):207–20.
42. Lieberman-Aiden E, van Berkum NL, Williams L, Imakaev M, Ragoczy T, Telling A, et al. Comprehensive mapping of long-range interactions reveals folding principles of the human genome. *Science.* 2009;326(5950):289.
43. Bartoli-Leonard F, Wilkinson FL, Langford-Smith AWW, Alexander MY, Weston R. The interplay of SIRT1 and Wnt signaling in vascular calcification. *Front Cardiovasc Med.* 2018;5:183.
44. Carter S, Miard S, Roy-Bellavance C, Boivin L, Li Z, Pibarot P, et al. Sirt1 inhibits resistin expression in aortic stenosis. *PLoS One.* 2012;7(4):e35110-e.
45. Theodoris CV, Li M, White MP, Liu L, He D, Pollard KS, et al. Human disease modeling reveals integrated transcriptional and epigenetic mechanisms of NOTCH1 haploinsufficiency. *Cell.* 2015;160(6):1072–86.
46. Eraslan B, Wang D, Gusic M, Prokisch H, Hallström BM, Uhlén M, et al. Quantification and discovery of sequence determinants of protein-per-mRNA amount in 29 human tissues. *Mol Syst Biol.* 2019;15(2):e8513.
47. Singh SA, Aikawa E, Aikawa M. Current trends and future perspectives of state-of-the-art proteomics technologies applied to cardiovascular disease research. *Circ J.* 2016;80(8):1674–83.
48. Martín-Rojas T, Gil-Dones F, Lopez-Almodovar LF, Padial LR, Vivanco F, Barderas MG. Proteomic profile of human aortic stenosis: insights into the degenerative process. *J Proteome Res.* 2012;11(3):1537–50.
49. Martín-Rojas T, Mourino-Alvarez L, Alonso-Orgaz S, Rosello-Lleti E, Calvo E, Lopez-Almodovar LF, et al. iTRAQ proteomic analysis of extracellular matrix remodeling in aortic valve disease. *Sci Rep.* 2015;5:17290.
50. Gutierrez P, O'Brien KD, Ferguson M, Nikkari ST, Alpers CE, Wight TN. Differences in the distribution of versican, decorin, and biglycan in atherosclerotic human coronary arteries. *Cardiovasc Pathol.* 1997;6(5):271–8.
51. Schlotter F, Halu A, Goto S, Blaser MC, Body SC, Lee LH, et al. Spatiotemporal multi-omics mapping generates a molecular atlas of the aortic valve and reveals networks driving disease. *Circulation.* 2018;138:377–93.
52. Tanoue H, Morinaga J, Yoshizawa T, Yugami M, Itoh H, Nakamura T, et al. Angiotensin-like protein 2 promotes chondrogenic differentiation during bone growth as a cartilage matrix factor. *Osteoarthr Cartil.* 2018;26(1):108–17.
53. Gellen B, Thorin-Trescases N, Sosner P, Gand E, Saulnier PJ, Ragot S, et al. ANGPTL2 is associated with an increased risk of cardiovascular events and death in diabetic patients. *Diabetologia.* 2016;59(11):2321–30.
54. Alvarez-Llamas G, Martín-Rojas T, de la Cuesta F, Calvo E, Gil-Dones F, Dardé VM, et al. Modification of the secretion pattern of proteases, inflammatory mediators, and extracellular matrix proteins by human aortic valve is key in severe aortic stenosis. *Mol Cell Proteomics.* 2013;12(9):2426–39.
55. Mourino-Alvarez L, Iloro I, de la Cuesta F, Azkargorta M, Sastre-Oliva T, Escobes I, et al. MALDI-imaging mass spectrometry: a step forward in the anatomopathological characterization of stenotic aortic valve tissue. *Sci Rep.* 2016;6:27106.
56. Goto S, Rogers MA, Blaser MC, Higashi H, Lee LH, Schlotter F, et al. Standardization of human calcific aortic valve disease in vitro modeling reveals passage-dependent calcification. *Front Cardiovasc Med.* 2019;6:49.

57. Bertacco E, Million R, Arrigoni G, Faggin E, Iop L, Puato M, et al. Proteomic analysis of clonal interstitial aortic valve cells acquiring a pro-calcific profile. *J Proteome Res.* 2010;9(11):5913–21.
58. Bom MJ, Levin E, Driessen RS, Danad I, Van Kuijk CC, van Rossum AC, et al. Predictive value of targeted proteomics for coronary plaque morphology in patients with suspected coronary artery disease. *EBioMedicine.* 2019;39:109–17.
59. Matic LP, Jesus Iglesias M, Vesterlund M, Lengquist M, Hong M-G, Saieed S, et al. Novel multiomics profiling of human carotid atherosclerotic plaques and plasma reveals biliverdin reductase B as a marker of intraplaque hemorrhage. *JACC: Basic Transl Sci.* 2018;3(4):464–80.
60. Kalantari F, Auguste P, Ziafazeli T, Tzimas G, Malmström L, Bioulac-Sage P, et al. Proteomics analysis of liver pathological calcification suggests a role for the IQ motif containing GTPase activating protein 1 in myofibroblast function. *Proteomics Clin Appl.* 2009;3(3):307–21.
61. Mihai S, Codrici E, Popescu ID, Enciu A-M, Rusu E, Zilisteanu D, et al. Proteomic biomarkers panel: new insights in chronic kidney disease. *Dis Markers.* 2016;2016:11.
62. Wang C, Tang Y, Wang Y, Li G, Wang L, Li Y. Label-free quantitative proteomics identifies Smarca4 is involved in vascular calcification. *Ren Fail.* 2019;41(1):220–8.
63. Wierer M, Prestel M, Schiller HB, Yan G, Schaab C, Azghandi S, et al. Compartment-resolved proteomic analysis of mouse aorta during atherosclerotic plaque formation reveals osteoclast-specific protein expression. *Mol Cell Proteomics: MCP.* 2018;17:321.
64. Hutcheson JD, Goettsch C, Bertazzo S, Maldonado N, Ruiz JL, Goh W, et al. Genesis and growth of extracellular-vesicle-derived microcalcification in atherosclerotic plaques. *Nat Mater.* 2016;15(3):335–43.
65. Blaser MC, Aikawa E. Roles and regulation of extracellular vesicles in cardiovascular mineral metabolism. *Front Cardiovasc Med.* 2018;5:187.
66. Hutcheson JD, Goettsch C, Pham T, Iwashita M, Aikawa M, Singh SA, et al. Enrichment of calcifying extracellular vesicles using density-based ultracentrifugation protocol. *J Extracell Vesicles.* 2014;3:25129.
67. Chen NX, O'Neill KD, Chen X, Moe SM. Annexin-mediated matrix vesicle calcification in vascular smooth muscle cells. *J Bone Miner Res.* 2008;23(11):1798–805.
68. Cui L, Rashdan NA, Zhu D, Milne EM, Ajuh P, Milne G, et al. End stage renal disease-induced hypercalcemia may promote aortic valve calcification via Annexin VI enrichment of valve interstitial cell derived-matrix vesicles. *J Cell Physiol.* 2017;232(11):2985–95.
69. Kapustin AN, Davies JD, Reynolds JL, McNair R, Jones GT, Sidibe A, et al. Calcium regulates key components of vascular smooth muscle cell-derived matrix vesicles to enhance mineralization. *Circ Res.* 2011;109(1):e1–12.
70. Kapustin AN, Chatrou ML, Drozdov I, Zheng Y, Davidson SM, Soong D, et al. Vascular smooth muscle cell calcification is mediated by regulated exosome secretion. *Circ Res.* 2015;116(8):1312–23.
71. Goettsch C, Hutcheson JD, Aikawa M, Iwata H, Pham T, Nykjaer A, et al. Sortilin mediates vascular calcification via its recruitment into extracellular vesicles. *J Clin Invest.* 2016;26(4):1323–36.
72. Matos TR, Liu H, Ritz J. Research techniques made simple: experimental methodology for single-cell mass cytometry. *J Invest Dermatol.* 2017;137(4):e31–e8.
73. Winkels H, Ehinger E, Vassallo M, Buscher K, Dinh HQ, Kobiyama K, et al. Atlas of the immune cell repertoire in mouse atherosclerosis defined by single-cell RNA-sequencing and mass cytometry. *Circ Res.* 2018;122(12):1675–88.
74. Fernandez DM, Rahman AH, Fernandez NF, Chudnovskiy A, Amir EAD, Amadori L, et al. Single-cell immune landscape of human atherosclerotic plaques. *Nat Med.* 2019;25(10):1576–88.
75. Budnik B, Levy E, Harmange G, Slavov N. SCoPE-MS: mass spectrometry of single mammalian cells quantifies proteome heterogeneity during cell differentiation. *Genome Biol.* 2018;19(1):161.

76. Swaminathan J, Boulgakov AA, Hernandez ET, Bardo AM, Bachman JL, Marotta J, et al. Highly parallel single-molecule identification of proteins in zeptomole-scale mixtures. *Nat Biotechnol.* 2018;36:1076.
77. Guijas C, Montenegro-Burke JR, Warth B, Spilker ME, Siuzdak G. Metabolomics activity screening for identifying metabolites that modulate phenotype. *Nat Biotechnol.* 2018;36(4):316–20.
78. Wang JH, Byun J, Pennathur S. Analytical approaches to metabolomics and applications to systems biology. *Semin Nephrol.* 2010;30(5):500–11.
79. Fan Y, Li Y, Chen Y, Zhao Y-J, Liu L-W, Li J, et al. Comprehensive metabolomic characterization of coronary artery diseases. *J Am Coll Cardiol.* 2016;68(12):1281–93.
80. Vojinovic D, van der Lee SJ, van Duijn CM, Vernooij MW, Kavousi M, Amin N, et al. Metabolic profiling of intra- and extracranial carotid artery atherosclerosis. *Atherosclerosis.* 2018;272:60–5.
81. Mathew AV, Zeng L, Byun J, Pennathur S. Metabolomic profiling of arginine metabolome links altered methylation to chronic kidney disease accelerated atherosclerosis. *J Proteomics Bioinform.* 2015;Suppl 14. <https://doi.org/10.4172/0974-276X.S14-001>.
82. Velenosi TJ, Hennop A, Feere DA, Tieu A, Kucey AS, Kyriacou P, et al. Untargeted plasma and tissue metabolomics in rats with chronic kidney disease given AST-120. *Sci Rep.* 2016;6:22526.
83. Vorkas PA, Isaac G, Anwar MA, Davies AH, Want EJ, Nicholson JK, et al. Untargeted UPLC-MS profiling pipeline to expand tissue metabolome coverage: application to cardiovascular disease. *Anal Chem.* 2015;87(8):4184–93.
84. Vorkas PA, Shalhoub J, Isaac G, Want EJ, Nicholson JK, Holmes E, et al. Metabolic phenotyping of atherosclerotic plaques reveals latent associations between free cholesterol and ceramide metabolism in atherogenesis. *J Proteome Res.* 2015;14(3):1389–99.
85. Barabási A-L, Gulbahce N, Loscalzo J. Network medicine: a network-based approach to human disease. *Nat Rev Genet.* 2011;12:56.
86. Wirka RC, Pjanic M, Quertermous T. Advances in transcriptomics. *Circ Res.* 2018;122:1200–20.
87. White MP, Theodoris CV, Liu L, Collins WJ, Blue KW, Lee JH, et al. NOTCH1 regulates matrix gla protein and calcification gene networks in human valve endothelium. *J Mol Cell Cardiol.* 2015;84:13–23.
88. Perisic L, Aldi S, Sun Y, Folkersen L, Razuvaev A, Roy J, et al. Gene expression signatures, pathways and networks in carotid atherosclerosis. *J Intern Med.* 2016;279:293–308.
89. Poller W, Dimmeler S, Heymans S, Zeller T, Haas J, Karakas M, et al. Non-coding RNAs in cardiovascular diseases: diagnostic and therapeutic perspectives. *Eur Heart J.* 2018;39:2704–16.
90. Romaine SPR, Tomaszewski M, Condorelli G, Samani NJ. MicroRNAs in cardiovascular disease: an introduction for clinicians. *Heart.* 2015;101:921–8.
91. Chaturvedi P, Chen NX, O'Neill K, McClintick JN, Moe SM, Janga SC. Differential miRNA expression in cells and matrix vesicles in vascular smooth muscle cells from rats with kidney disease. *PLoS One.* 2015;10:e0131589.
92. Coffey S, Williams MJA, Phillips LV, Galvin IF, Bunton RW, Jones GT. Integrated microRNA and messenger RNA analysis in aortic stenosis. *Sci Rep.* 2016;6:36904.
93. Jeong G, Kwon D-H, Shin S, Choe N, Ryu J, Lim Y-H, et al. Long noncoding RNAs in vascular smooth muscle cells regulate vascular calcification. *Sci Rep.* 2019;9:5848.
94. Lindsey ML, Mayr M, Gomes AV, Delles C, Arrell DK, Murphy AM, et al. Transformative impact of proteomics on cardiovascular health and disease. *Circulation.* 2015;132:852–72.
95. Cox J, Mann M. Is proteomics the new genomics? *Cell.* 2007;130:395–8.
96. Langley SR, Willeit K, Didangelos A, Matic LP, Skrobilin P, Barallobre-Barreiro J, et al. Extracellular matrix proteomics identifies molecular signature of symptomatic carotid plaques. *J Clin Investig.* 2017;127:1546–60.
97. Schanstra JP, Luong TT, Makridakis M, Van Linthout S, Lygirou V, Latosinska A, et al. Systems biology identifies cytosolic PLA2 as a target in vascular calcification treatment. *JCI Insight.* 2019;4:e125638.

98. Lamb J, Crawford ED, Peck D, Modell JW, Blat IC, Wrobel MJ, et al. The connectivity map: using gene-expression signatures to connect small molecules, genes, and disease. *Science*. 2006;313:1929–35.
99. Karczewski KJ, Snyder MP. Integrative omics for health and disease. *Nat Rev Genet*. 2018;19:299–310.
100. Mourino-Alvarez L, Baldan-Martin M, Gonzalez-Calero L, Martinez-Laborde C, Sastre-Oliva T, Moreno-Luna R, et al. Patients with calcific aortic stenosis exhibit systemic molecular evidence of ischemia, enhanced coagulation, oxidative stress and impaired cholesterol transport. *Int J Cardiol*. 2016;225:99–106.
101. Navale V, Bourne PE. Cloud computing applications for biomedical science: a perspective. *PLoS Comput Biol*. 2018;14:e1006144.
102. Hasin Y, Seldin M, Lusis A. Multi-omics approaches to disease. *Genome Biol*. 2017;18(1):83.
103. Rogers MA, Aikawa E. Cardiovascular calcification: artificial intelligence and big data accelerate mechanistic discovery. *Nat Rev Cardiol*. 2019;16:261–74.
104. van der Valk D, van der Ven C, Blaser M, Grolman J, Wu P-J, Fenton O, et al. Engineering a 3D-bioprinted model of human heart valve disease using nanoindentation-based biomechanics. *Nano*. 2018;8(5):296.
105. Fernandes M, Patel A, Husi H. C/VDdb: a multi-omics expression profiling database for a knowledge-driven approach in cardiovascular disease (CVD). *PLoS One*. 2018;13(11):e0207371.
106. Bahcall OG. UK Biobank — a new era in genomic medicine. *Nat Rev Genet*. 2018;19(12):737.

Index

A

- Abascal-Wilkins echocardiography score, 499
- Abdominal aorta, 497
- Abdominal aortic aneurysms (AAA), 18F-fluoride PET, 435, 436
- Abnormal ankle-brachial index (ABI), 169
- Activated valve interstitial cells (aVIC), 49
- Activator protein 1 (AP-1), 401, 402
- Activin receptor-like kinase-2 (ALK2), 307
- Acute coronary syndrome (ACS), 17
- Advanced glycation end products (AGE) signaling, 443, 464
- Adventitia, 445
- Agatston Units, 484
- Ageing, 150
- Albright hereditary osteodystrophy (AHO), 300
- Aldosterone antagonists, 461
- Aluminum chloride, 451
- Amorphous elastin protein, 447, 450
- Angiotensin receptor blockers (ARBs), 461
- Angiotensin-converting enzyme inhibitors (ACEi), 461
- Anti-calcific proteins, 281
- Anti-calcific transmembrane proteins, 281
- Anticoagulation, aortic valve replacement, 515, 516
- Aortic calcification, 469
- Aortic stenosis, 510
 - 18F-fluoride PET, 426
 - mean survival of patients with symptoms of, 511
 - symptoms and severity of, 509, 510
- Aortic valves (AVs)
 - development, 50–54
 - extracellular matrix, 51
 - embryonic origins of, 51–52
 - signaling pathways involved in, 53
 - transcription factors involved in, 52, 53
 - structure, 48
 - valvular interstitial cells, 49, 50
- Aortic valve (AV) calcification, 32, 118
 - bicuspid and unicuspid, 33, 34
 - network medicine-based analyses of, 544
 - semicircular cusps, 30
 - tricuspid, 31–33
- Aortic valve CT calcium score, 427
- Aortic valve replacement (AVR), 47
 - anticoagulation, 515, 516
 - aortic stenosis, symptoms and severity of, 509, 510
 - bioprosthetic valves, 513, 514
 - calcific aortic stenosis, epidemiology and mechanism of, 509
 - life expectancy with prosthetic valves, 514, 515
 - mechanical valves, 510–513
 - prosthetic aortic valves, choice of, 516, 517
 - surgical aortic valve replacement, 510
 - transcatheter aortic valve replacement, 517
 - evolution, 517–520
 - pre-procedural evaluation, 520
 - procedure and recovery, 520, 521
 - valve type, choice of, 514
- Apabetalone, 155

- Arterial and valvular calcification
 Hutchinson-Gilford progeria syndrome, 74
 microenvironments and cells
 B cells, 80
 calcification morphology, 74, 75
 dendritic cells, 80
 endothelial cells, 77, 78
 macrophages/monocytes, 79, 80
 mast cells, 80
 progenitor cells, 77
 smooth muscle cells, 76
 T lymphocytes, 78, 79
 tissue microenvironment, 74–76
 vascular dendritic cells, 76, 80
 molecular mechanisms
 endogenous calcification
 inhibitors, 82, 83
 genetic drivers of calcification, 84
 inflammation, lipids, and oxidative stress, 83, 84
 mineral metabolism, 81–82
 valvular calcification, 85
 vascular calcification, 74, 85
 Arterial calcification, 373
 Arterial distension, 446
 Arterial wall calcification, 14
 Ataxia telangiectasia, 150
 Atherectomy, 492, 497
 Atherosclerosis, 242, 464, 465
 Atherosclerotic calcification, 5, 453, 454
 Atherosclerotic intimal calcification, 14
 Atherosclerotic medial calcification, 14
Atp6v0d2, 397
 Atrial fibrillation, 499
- B**
 Backscattered electrons, 221
 Baseline computed tomography mitral annular calcification (CT-MAC), 428
 Basic Helix-Loop-Helix (bHLH)
 transcription, 52
 Bicuspid aortic valve (BAV), 33, 35, 48, 120, 187
 Bileaflet mechanical heart valves, 512
 Bioinformatics, cardiovascular calcification, 539–542
 Biologic agents, 257
 Bioprostheses
 prevention, 207
 valvular heart disease, 187
 Bioprosthetic aortic valves, 516, 517
 Bioprosthetic heart valve calcification
 animal models, 197
 biological factors, 201
 biomechanical factors, 202
 heart valve replacement, 187–189, 191, 192
 immunologic factors, 202, 203
 native heart valve function, 184, 185
 non-calcific mechanisms, 203, 204
 prevention, 204, 205, 207–209
 structural valve degeneration, 192, 195, 196
 substrate factors, 201, 202
 valvular heart disease, 186, 187
 Bioprosthetic valves, aortic valve replacement, 513, 514
 Biprosthetic valve degeneration, 18F-fluoride PET, 428–430
 Bisphosphonates, 256, 326, 488, 489
 Bixalomer, 154
 Blast injury, 298
 Blood calcification
 cardiovascular events, 484–486
 propensity, 484–486
 Blood-nerve barrier (BNB), 302
 Bloom syndrome, 150
 B lymphocytes, 350
 Bone
 bone matrix
 mineralization, 382, 384, 385
 types of, 376
 components of, 374–376
 formation during development, 376
 measurement, bone modeling/remodeling, 379, 381
 modeling, 378, 379
 remodeling, 377, 378
 Bone gamma-carboxyglutamate protein (Bglap), 278
 Bone homeostasis
 B lymphocytes, 350
 bone resorption and formation, 352, 353
 inter-organ crosstalk, 354–356
 mast cells, 350, 351
 monocytes and macrophages, 348, 351, 352
 osteoblasts
 BMP receptors, 336, 337
 BMPR, 336
 definition, 335
 Dkk1 deficiency or suppression, 338
 Frizzled-receptor (FZD) variants, 337
 functions, 335
 gain-of-function mutations, 338
 hydroxyapatite-based microcrystals, 335
 osteoblast differentiation, 335
 SMAD-dependent pathway, 337

- T-cell factor/lymphoid enhancer factor (TCF/LEF) transcription complex, 337
- TGF β , 336
- tissue non-specific alkaline phosphatase, 335
- transcription factors, 336
- Wnt signaling, 337, 338
- osteoclasts
 - formation and function, 341
 - ITAM signaling, 340
 - macrophage colony stimulating factor (M-CFS), 339
 - NF κ B signaling pathway, 339
 - origin, 338
 - pathophysiological osteoclast differentiation and activation, 338
 - RANKL, 339
 - resorptive capacity, 340, 341
- osteocytes
 - definition, 342
 - mechanosensation and mechanotransduction, 346, 347
 - mineralization, 343, 344
 - osteocytic osteolysis, 345, 346
 - osteocytogenesis, 342
 - phosphate homeostasis, 344, 345
- osteimmunology, 347
- T lymphocytes, 347, 349
- Bone loss, 373
- Bone matrix
 - components of, 375
 - mineralization, 382, 384, 385
 - types of, 376
- Bone mechanics, 376
- Bone mineral density, 404
- Bone mineral disorder (BMD), 137
- Bone mineralisation, 466
- Bone morphogenetic protein (BMP), 23
 - bone morphogenetic protein 2 (BMP2), 325
 - bone morphogenetic protein 4 (BMP4), 31
 - bone morphogenetic protein 7 (BMP-7), 148
- Bone remodeling, 333, 334
- Bone resorption, regulators of, 391, 392
- Bromodomain and extra-terminal (BET) proteins, 155
- Brownian motion, 102
- C**
- Calcific aortic stenosis, epidemiology and mechanism of, 509
- Calcific aortic valve disease (CAVD), 5, 543
- anti-miRs and antagomiRs, 129
- aortic valve
 - development, 50–54
 - structure, 48
 - valve cell diversity, 49–50
- aortic valve replacement, 47
- biomechanical forces, 118–120
- development of, 118
- endothelial dysfunction, 118
- mechanosensing, 121–123
- mechanosensors in, 121
- miRNAs, 123–127
 - shear-dependent, 127–128
 - stretch-dependent, 128–129
 - undefined mechanosensitivity, 124–127
- miRNA-mimics, 129
- osteogenic differentiation, 118
- pathogenesis of, 48
- reactivation of developmental pathways
 - bone-like process of
 - calcification, 59–61
 - calcifying aortic VICs, 59
 - developmental transcription factors, 61
 - intersecting signaling pathways, 62
 - Notch signaling pathway, 58
 - Wnt/ β -catenin, 58
- skeletal development
 - cartilage and bone tissue, characteristics of, 55
 - endochondral bone formation, 54
 - signaling pathways involved in, 57
 - transcriptional regulation of, 56
 - valve and, 58
 - structure and biomechanical forces, 119
- Calcific atherosclerosis, 320, 443
- Calcific vasculopathy, 319
- Calcification
 - functional biomolecules, evaluating
 - roles for
 - mass spectrometry, 532, 533, 535–537
 - metabolites, 537, 538
 - nucleic acids, interrogation of
 - epigenetics and genetic structure, 530–532
 - genetic and environmental regulation, transcriptomics bridges, 528–530
 - genome-wide studies, cardiovascular calcification, 527, 528
 - mitral valve, 498, 499
 - omics-driven target discovery, promise of, 545
 - paradox, 7, 405
 - systems-based computational approaches
 - bioinformatics, 539–542
 - multi-omics data integration, 542, 543

- Calcified coronary arteries, coronary artery bypass grafting surgery with, 495, 496
- Calcified coronary stenosis, 494
 - atherectomy in, 492
- Calcified nodule, 18
- Calcified plaques, 491–494
- Calcified stenotic aortic valve, 34
- Calcified vessels, 495
- Calcifying extracellular vesicles, 98, 99
- Calcimimetics, 462
- Calcinosis
 - biologic agents, 257
 - bisphosphonates, 255
 - calcium channel blockers, 255
 - clinical presentation, 250, 251
 - crystal composition, 248
 - diagnostic approach, 253, 254
 - ENPP1, 249
 - human leukocyte antigen, 249
 - in juvenile dermatomyositis, 248
 - intravenous immunoglobulin, 256
 - nonmedical therapies, 257
 - subcutaneous tissues, 247
 - systemic sclerosis disease subsets, 252
 - therapies for inflammation, 254, 255
 - warfarin, 256
- Calcinosis, calcium into the skin, 247
- Calcitonin gene related peptide (CGRP), 302
- Calcium, 382, 391, 467
- Calcium channel blockers (CCBs), 255, 461
- Calcium chloride (CaCl₂) injury model, 467
- Calcium diffusion inhibitor, 207
- Calcium sensing receptors (CaSRs), 462
- Calcium sequestration, vascular calcification, 465–467, 469–471
- Camurati-Engelmann disease (CED), 57
- CarboMedics (CM) mechanical valve, 512
- Carboxylated MGP (cMGP), 146
- Cardiovascular calcification, 241, 481
 - atherosclerotic calcification, 5
 - calcium-based mineral, 3
 - clinical studies, methods to assess, 482–484
 - ectopic calcification, 3, 4
 - electron microscopes, 219, 220
 - marker and maker of cardiovascular morbidity, 4, 5
 - multi-omics study of, 534
 - osteoclasts in
 - bone resorption, regulators of, 391, 392
 - osteoclastogenesis, 392–398
 - c-Fos and AP-1-associated pathways, 401, 402
 - inflammatory regulators, 403
 - M-CSF/RANK/RANKL/OPG, 398–400
 - microRNA, 404, 405
 - osteogenesis, NF- κ B pathways in, 401, 402
 - paradox, 405–407
 - physiological and pathological calcification, 6, 7
 - scanning electron microscopy
 - biological material, 223–226
 - imaging, 221–223
 - transmission electron microscopy
 - biological material, 228–232
 - imaging, 227, 228
- Cardiovascular disease, 482, 526
- Cardiovascular events, 484–486
- Cardiovascular mineralization, 6
- Carotid atherosclerosis, 18F-fluoride PET, 434, 435
- Carotid plaque, 30
- Cathepsins, 397, 451
- Celecoxib, 305
- Cell fragments, 200
- c-Fos, 401, 402
- Chelation therapy, 466
- Chronic kidney disease, on hemodialysis, 495
- Chronic kidney disease (CKD), 472
 - definition, 137
 - dysregulated mineral metabolism, 141
 - ectopic calcification, 143
 - effect of, 147
 - on hemodialysis, 495
 - mechanisms of calcification, 144
 - ageing-related DNA-damage, 150, 151
 - apoptosis of VSMCs, 145
 - extracellular vesicle release, 145
 - inflammation, 152, 153
 - oseto/chondrocytic differentiation, 149
 - physiological calcification inhibitors, 146, 148, 149
 - senescence, 150, 151
 - risk factors of
 - ectopic calcification and cardiovascular disease, 140, 141
 - hypercalcemia and hyperphosphatemia, 139, 140
 - ineffective FGF23, 138
 - Klotho deficiency, 138
 - reduced Ca intake, 139
 - uremic milieu, 142

- Vitamin D deficiency, 139
 - treatment strategies, 154
 - directly target calcification, 155, 156
 - reduce risk factors of
 - calcification, 153–155
 - vascular calcification, 454, 461–463
 - Chronic total occlusion (CTO), 27
 - Cinacalcet, 155
 - Clinical decision-making, for therapeutic interventions, 497
 - Clinical trials
 - blood calcification propensity and cardiovascular events, 484–486
 - calcified plaques and coronary arteries, percutaneous coronary intervention for, 491–494
 - clinical studies of methods, 482–484
 - coronary artery bypass grafting surgery, calcified coronary arteries, 495, 496
 - invasive diagnosis and cardiovascular calcification treatment, 490, 491
 - mitral valve, calcification of, 498, 499
 - peripheral arterial disease and calcification, treatment decision-making, 496–498
 - pharmacological therapeutics
 - bisphosphonates, 488, 489
 - denosumab, 490
 - magnesium, 489
 - SNF472, 489, 490
 - sodium thiosulfate, 487, 488
 - vitamin K, 486, 487
 - Cockayne syndrome, 150
 - Collagen, 446
 - Common disease-associated pathological calcification, 14
 - Conduction system abnormalities, 519
 - Congenital bicuspid valves, 34
 - Coronary arteries, percutaneous coronary intervention, calcified plaques and, 491–494
 - Coronary artery bypass grafting (CABG) surgery, calcified coronary arteries, 495, 496
 - Coronary artery calcification (CAC), 325, 484
 - atherosclerosis progression, natural history of, 15, 17–19
 - atherosclerotic intimal calcification and progression, 19, 21, 23
 - Coronary atherosclerosis, 18F-fluoride PET, 431, 432, 434
 - Coronary autopsy, 143
 - Coronary calcification, 22–23
 - Coronary and aortic calcification, 326
 - Cryo-electron microscopy (cryo-EM), 107
 - CSF-1, 398
 - Csflr*, 393
 - C-type natriuretic peptide (CNP), 31
 - Cystatin C, 451
 - Cysteine cathepsins, 451
- D**
- Decellularization, 208
 - Dendritic cells, 80
 - Dendritic-cell specific transmembrane protein (DC-STAMP), 396
 - Denosumab, clinical trials, 490
 - Dentin matrix protein (DMP1), 382
 - Diabetics, vascular calcification, 464
 - Diffuse cutaneous systemic sclerosis (dcSSc), 252
 - Drug discovery, omics-informed pathobiology and, 526
 - Dual antiplatelet therapy (DAPT), 521
 - Dual nanoparticle therapy, 470
 - Dynamic light scattering (DLS), 101–103
- E**
- Ecto-nucleotide pyrophosphatase/phosphodiesterase 1, 384, 462
 - Ectopic calcification, 143, 526
 - Elastic fiber formation, 447
 - Elastic fiber fragmentation, 446
 - Elastic fiber-associated microfibrils, 448
 - Elastic lamina degradation, 449
 - Elastin
 - degradation, and vascular calcification, 449, 450
 - atherosclerotic calcification and, 453, 454
 - elastin-associated components, 453
 - elastin-derived peptides, role of, 452
 - elastolytic enzymes, role of, 450–452
 - vascular calcification
 - arterial mechanical properties, regulation, 445–447
 - arterial structure, integral part of, 444, 445
 - assembly during development, 447–449
 - degradation and, 450
 - Elastin-derived peptides (EDPs), 452
 - Elastolytic enzymes, in calcification, 450–452

Electron microscopy, 219, 220
 Endochondral bone formation, 376
 Endothelial cells, 77, 78
 Endothelial-to-mesenchymal transition (EndMT), 50, 51, 78
 Endovascular interventions, 173, 174
 Epigenetics, 530–532
 Erectile dysfunction (ED), 436
 Ethylenediamine tetra-acetic acid-tetracycline, 465
 Etidronate, 488
 Excimer laser, 494
 Extracellular matrix (ECM) proteins, 49, 445
 dysregulation, 58
 Extracellular vesicles (EVs), 144
 biomolecular analysis of, 108, 109
 diagnostic/prognostic biomarkers, 111
 EV-based diagnostics/therapeutics, 112
 physical analysis of
 DLS, 101–103
 particle-by-particle analysis, 103–106
 physiological and pathological calcification, 97–99
 pro-calcific conditions, 111
 structural analysis of, 106–108
 in vascular calcification, 100, 101
 visualize and analyze mineral properties, 109–111

F

Fetuin-A, 146
 FGF23, 355
 Fibrillin, 447
 Fibrillin 2, 448
 Fibrillin-rich microfibrils, 447
 Fibroblast growth factor 23 (FGF23), 138
 Fibroblasts, 445
 Fibrocalcific plaques, 18
 Flow cytometry (FCM) techniques, 104
 18F-Fluoride PET, imaging cardiovascular calcification activity with, 423
 abdominal aortic aneurysms, 435, 436
 aortic stenosis, 426
 biprosthetic valve degeneration, 428–430
 carotid atherosclerosis, 434, 435
 coronary atherosclerosis, 431, 432, 434
 limitations, 436, 437
 medial artery calcification, 427
 penile uptake, 436
 positron emission tomography, 424–426
 18F-Fluorodeoxyglucose, 432
 Focused Ion Beam, 232
 Free water, 376

G

G protein-coupled receptors (GPCR), 122
 Gene set enrichment analysis (GSEA), 540
 Genome-wide association study (GWAS), 542
 Glial fibrillary acidic protein (GFAP), 533
 Glomerular filtration rate (GFR), 137
 Glutaraldehyde, 189, 208
 Glutaraldehyde neutralization, 208
 Glycerin, 374
 Glycoproteins, 450
 G-protein couple receptor 4 (LGR4), 394
 Gray-level co-occurrence matrix, 284
 GTP-binding proteins, 398

H

Healed plaque ruptures (HPR), 18
 Hematopoietic stem cells (HSCs), 392
 Hemodialysis, 495
 Henry's Equation, 102
 Heterotopic ossification (HO)
 aetiology and epidemiology, 299, 300
 biology
 cells, 302, 303
 environment/inflammation, 300, 301
 blast injury, 298
 blast-injured population, 308
 diagnosis, 304
 multidisciplinary approach, 308
 preventions, 304–306
 therapies, 307, 308
 treatment, 306
 Hierarchical clustering, 539
 Histomorphometry, 379
 Histone-DNA interactions, 531
 Hufnagel valve, 510
 Human aortic valve endothelial cells (HAVECs), 127, 540
 Human atherosclerosis progression, 16
 Hutchinson-Gilford progeria syndrome, 74
 atherosclerosis, 242
 cardiovascular calcification, 241, 242
 endothelial pathology, 240
 mechanisms of calcification, 236, 237, 239
 normal aging, 243
 vascular smooth muscle cell pathology, 240
 Hutchinson-Gilford progeria syndrome (HGPS), 151, 235
 Hydroxyapatite (HA), 143, 425

I

Il-1b inflammatory cytokine, 403
 Imaging cardiovascular calcification activity

- with 18F-fluoride PET, 423
 - abdominal aortic aneurysms, 435, 436
 - aortic stenosis, 426
 - biprosthetic valve
 - degeneration, 428–430
 - carotid atherosclerosis, 434, 435
 - coronary atherosclerosis, 431, 432, 434
 - limitations, 436, 437
 - medial artery calcification, 427
 - penile uptake, 436
 - positron emission
 - tomography, 424–426
- In Vivo¹⁸F-fluoride PET, 430
- Inflammation, 301
- Inflammatory cytokines, 403
- Inflammatory lipids, 324
- Inorganic pyrophosphates (PPi), 384
- Interleukins (ILs), 407
- Internal elastic lamina, 445
- Intimal calcium progression, 26
- Intramembranous bone formation, 376
- Intravascular ultrasound (IVUS), 432
- Intravenous immunoglobulin, 256

- K**
- Klotho, 83
- Klotho deficiency, 138
- Klotho mutation, 150
- Krüppel-like factor 2, 240

- L**
- Lamellar bone, 376
- Latency-associated propeptide (LAP), 448–449
- Latent TGF- β binding protein (LTBP), 448
- Leaflet dysplasia, 33
- Limited cutaneous systemic sclerosis (lcSSc), 247, 252
- Lipid pool, 15
- Lithotripsy balloon, 494
- Long-noncoding RNAs (lncRNAs), 529, 540
- Lysyl oxidase (LOX), 448

- M**
- Macrocalcification, 435
- Macrophages, 79, 80, 452
- Macrophage colony-stimulating factor (M-CSF), 394, 398
- Magna Ease, 513
- Magnesium, clinical trials, 489
- Marfan Syndrome (MS), 448, 453
- Mass spectroscopy (MS), 108, 532, 533, 535–537
- Matrix Gla protein (MGP), 486, 540
- Matrix vesicle, 383
 - initiate mineralization, 385
 - mineralization, regulation of, 383
- Matrix-assisted laser desorption/ionization imaging mass spectrometry (MALDI-IMS), 534
- Matrix-assisted laser desorption/ionization (MALDI) approaches, 112
- Mechanical stress, 184, 186, 187, 202
- Mechanical valves, aortic valve
 - replacement, 510–513
- Medial arterial calcification (MAC), 169–171, 443, 467
- Medial calcification, 443
- Medial calcium progression, 25
- Mesenchymal stem cell (MSC), 302
- Mesenchymal stem cell-like cells, 77
- Mesenchymal-originating osteoblasts, 392
- Metabolomics, 537, 538
- Micro CT, 24
- Micro RNAs (miRNAs), 540
- Microcalcification, 20–21, 431
- Microfibril, 447
- Microfibril-associated glycoprotein (MAGPs), 449
- Microphthalmia transcription factor (MITF), 393, 395
- MicroRNA (miRNA, miR), 404, 529
 - miR-26a, 405
 - miR-29b, 124
 - miR-30b, 127
 - miR-34a, 124
 - miR-92a, 124
 - miR-138, 124
 - miR-141, 127
 - miR-148-3p, 128
 - miR-181b, 128
 - miR-195, 127
 - miR-214, 128
 - miR-449c-5p, 127
 - miR-483-3p, 128
 - miR-486-5p, 128
 - miR-638, 127
 - negative miRNA regulators,
 - osteoclastogenesis, 405
 - positive miRNA regulators,
 - osteoclastogenesis, 404, 405
- Mineralocorticoid receptor antagonists (MCRAs), 461
- miRNA-mimics, 129
- Mitral annular calcification (MAC), 427, 428, 498, 499

- Mitral valve calcification, 498, 499
 mitral annular calcification, 38
 pathology of, 36, 39
 structure of, 35, 36
- MMP-13, 398
- Modeling-based formation (MBF), 380
- Monckeberg's sclerosis, 5, 24, 143, 443
- Monoleaflet mechanical valve, 512
- Multi-Ethnic Study of Atherosclerosis (MESA), 32
- Multi-omics data integration, calcification, 542, 543
- Multi-omics study, of cardiovascular calcification, 534
- Myocardial infarction, 432
- Myofibrogenesis, 533
- N**
- N-3 fatty acids, 465
- Nanometer-scale extracellular vesicles (EVs), 536
- Nanoparticles (NPs), 467
- Nanoparticle tracking analysis (NTA), 103
- Nanoparticle-based targeted EDTA delivery, 467
- Nano-precipitation method, 468
- Nasu-Hakola disease, 395
- Negative miRNA, of osteoclastogenesis, 405
- Network medicine, 543
- Network medicine-based analyses, of aortic valve calcification, 544
- NF- κ B pathways, in osteogenesis, 401, 402
- Nijmegen breakage syndrome, 150
- Nodular calcification, 19
- Non-coding RNAs, 540
- Novel Oral Anticoagulants (NOACs), 515
- NR4A1, 395
- Nucleic acids, interrogation of
 epigenetics and genetic structure, 530–532
 genetic and environmental regulation, transcriptomics bridges, 528–530
 genome-wide studies, cardiovascular calcification, 527, 528
- O**
- Omics, leveraging, target discovery and drug development, 527
- Omics-driven target discovery, promise of, 545
- Omics-informed pathobiology, and drug discovery, 526
- On-X valve, 512
- Orbital atherectomy, 493
- Orphan phosphatase 1, 384
- Oseto/chondrocytic differentiation, 149
- Osteoblasts, 334, 374
 bone morphogenetic protein receptors, 336, 337
- BMPR, 336
 definition, 335
 Dkk1 deficiency or suppression, 338
 Frizzled-receptor (FZD) variants, 337
 functions, 335
 gain-of-function mutations, 338
 hydroxyapatite-based microcrystals, 335
 osteoblast differentiation, 335
 SMAD-dependent pathway, 337
 T-cell factor/lymphoid enhancer factor (TCF/LEF) transcription complex, 337
- TGF β , 336
 tissue non-specific alkaline phosphatase, 335
 transcription factors, 336
 Wnt signaling pathway, 337, 338
- Osteocalcin (OCN), 355
- Osteoclast functionality, 396–398
- Osteoclast precursors
 commitment, 394
 motility and fusion, 395, 396
 proliferation and differentiation of, 393, 394
- Osteoclast stimulatory transmembrane protein (OC-STAMP), 396
- Osteoclastogenesis, 392
 activated signaling pathways required for, 399
 osteoclast differentiation and activation, 393
 osteoclast functionality, 396–398
 osteoclast precursors
 commitment, 394
 motility and fusion, 395, 396
 proliferation and differentiation of, 393, 394
- Osteoclasts
 cardiovascular calcification
 bone resorption, regulators of, 391, 392
 osteoclastogenesis, 392–398
 c-Fos and AP-1-associated pathways, 401, 402
 inflammatory regulators, 403
 M-CSF/RANK/RANKL/OPG, 398–400
 microRNA, 404, 405

- osteogenesis, NF- κ B pathways in, 401, 402
- paradox, 405–407
- formation and function, 341
- ITAM signaling, 340
- macrophage colony stimulating factor (M-CFS), 339
- NF κ B signaling pathway, 339
- RANK, 339
- RANKL, 339
- resorptive capacity, 340, 341
- Osteocytes
 - definition, 342
 - mechanosensation and mechanotransduction, 346, 347
 - mineralization, 343, 344
 - osteocytic osteolysis, 345
 - osteocytogenesis, 342
 - phosphate homeostasis, 344, 345
- Osteogenesis, NF- κ B pathways in, 401, 402
- Osteoid, 383
- Osteopontin, 148
- Osteoprotegerin (OPG), 31, 148, 462
- OsteoSense, 425

- P**
- Palovarotene, 307
- Parathyroid hormone (PTH), 325
- PECAM-1, 122
- Penile uptake, 18F-fluoride PET, 436
- Percent stenosis, 28
- Perclose devices, 520
- Peripheral arterial disease
- Peripheral artery calcification, 167, 170–175, 496
 - carotid artery calcification, 29
 - large vessels, 23
 - lower extremity calcification, 27
 - medial calcification, 24–26
 - medium sized arteries, 23
 - small arteries, 23, 24
- Peripheral artery disease
 - arterial stiffness, 174
 - clinical trials, 496–498
 - calcification, 171, 496–498
 - diabetes, 168, 169
 - end-stage renal disease, 168, 169
 - histology, 171
 - outcomes of patients, 171, 172
 - treatment, 173, 174
 - treatment decision-making, 496–498
- Peripheral artery disease (PAD), 24
- Permanent pacemaker (PPM), 519
- PHOSPHO1, 384
- PIEZO1, 123
- Placenta
 - animal model development studies, 271, 272
 - anti-calcific transcription factors, 282
 - anti-calcific transmembrane proteins, 281
 - calcification, 264, 265, 267
 - calcium and phosphate homeostasis, 269–271
 - computer vision, 283, 284
 - fetal development, 263
 - mineral deposits, 268
 - pregnancy, 263
 - pro-calcific transcription factors, 280
 - pro-calcific transmembrane proteins, 277
 - secreted anti-calcific factors, 281
 - secreted pro-calcific factors, 277–279
- Placental dysfunction, 264, 267, 268, 270
- Plaque erosion (PE), 18
- Plaque rupture (PR), 17
- Plasma, 537
- Poly ADP ribose polymerases (PARP), 151
- Polykaryons, 395
- Polyphenol, 473
- Porcine aortic valves (PAV), 127
- Positive miRNA, of osteoclastogenesis, 404, 405
- Positron emission tomography (PET), 18F-fluoride PET, 424–426
- Prediction of Recurrent Events, 434
- Principal component analysis (PCA), 539
- Pro-calcific transcription factors, 280
- Progressive osseous heteroplasia (POH), 299
- Prophylaxes, 308
- Prosthetic aortic valves, choice of, 516, 517
- Prosthetic heart valves, 512
- Prosthetic valve(s), 514, 515
- Prosthetic valve thrombosis (PVT), 516
- Protein-protein interaction (PPI)
 - subnetwork, 544
 - networks, 533
- Proton pump vacuolar ATPase, 397
- Pulse wave velocity (PWV), 446
- Punctate calcification, 19
- Pyrophosphate (PPi), 147, 462

- R**
- RANK, 399
- RANKL, 394, 399
- Raphe, 33

Reactive oxygen species (ROS), 237
 Receiver-operating-characteristic (ROC) curves, 543
 Remodeling-based formation (RBF), 380
 Renin-Angiotensin-Aldosterone System (RAAS), 461
 Rotational atherectomy, 492

S

Scanning electron microscopy (SEM), 106, 221–224, 226
 scRNA-seq, 530
 Secondary hyperparathyroidism (SHPT), 137
 Secreted pro-calcific factors, 277
 Self-expanding valve, 519
 Selected area electron diffraction (SAED), 227
 Senescence-associated secretory phenotype (SASP), 151
 Senolytics, 156
 Sevelamer, 154
 Sheet calcification, 19, 23
 Single antiplatelet therapy (SAPT), 521
 Single Cell ProtEomics, 537
 Single-cell RNA-seq (scRNA-seq), 530
 SJM mechanical valves, 512
 Skeletal and cardiovascular mineralization
 clinical significance, 321–322
 collagen-based crystal propagation, 320
 ectopic bone, 320
 electron microprobe analysis, 320
 extracellular vesicle release, 320
 gene expression cascades, 320
 inflammatory cytokines, 323–325
 lipids, 323–325
 location of, 320–321
 mechanism of, 319
 mineralizing matrix, 320
 osteoporosis, 322, 323
 oxidant stress, 323–325
 statin class of drugs, 325
 structure of arterial and bone tissues, 321
 teriparatide, bisphosphonates, 326
 vitamin D and calcium supplementation, 326–327
 Skeletal muscle cells, 76, 302
 proliferation, 445
 SNF472, clinical trials, 489, 490
 Sodium thiosulfate (STS), 463
 clinical trials, 487, 488
 Spinal cord injury (SCI), 300
 Spleen tyrosine kinase (SYK), 395
 Stable angina, 432

Stokes-Einstein relationship, 102
 Structural valve degeneration (SVD), 192, 196
 Surgical aortic valve replacement (SAVR), 510, 518
 Systemic sclerosis disease subsets, 252
 Systemic sclerosis sine scleroderma, 252

T

T cell immune regulator 1 (*TCIRG1*) gene, 397
 T lymphocytes, 78, 79, 347, 349
 Target discovery, leveraging omics for, 527
 Targeted drug delivery, vascular calcification, 466, 467, 469, 470
 Teriparatide, 463
 That contains acellular debris, 15
 Thin cap fibroatheroma (TCFA), 16
 Thin fibrous cap fibroatheroma (TCFA), 17
 Tissue non-specific alkaline phosphatase (TNAP), 98, 237, 335, 384
 Tissue-level remodeling, 380
 Transcatheter aortic valve implantation (TAVI), 47, 190
 Transcatheter aortic valve replacement (TAVR), 517, 518
 evolution, 517–520
 pre-procedural evaluation, 520
 procedure and recovery, 520, 521
 Transcatheter heart valves, 519
 Transcriptome profiling, 539
 Transcriptomics, 528–530
 Transforming growth factor beta (TGF β), 302
 Transmission electron microscopy (TEM) analyzes, 106, 226, 228, 230, 231
 Traumatic brain injury (TBI), 300
 Trichothiodystrophy, 150
 Tricuspid aortic valve (TAV), 120
 Tunable resistive pulse sensing (TRPS), 104
 Tunica adventitia, 444
 Tunica intima, 444
 Tunica media, 444
 Type I collagen, 374

U

Unicuspid aortic valves, 33

V

Valve interstitial cells (VIC), 48
 Valve type, choice of, 514
 Valvular calcification, 13

- Valvular endothelial cells (VECs), 31, 118
 - Valvular interstitial cells (VICs), 76, 118
 - Vascular ageing, 151
 - Vascular calcification, 143, 482, 535
 - calcium sequestration, 465, 466
 - targeted drug delivery and repair
 - elastin, 466, 467, 469–471
 - elastin
 - arterial mechanical properties, regulation, 445–447
 - arterial structure, integral part of, 444, 445
 - assembly during development, 447–449
 - degradation and, 450
 - elastin degradation and, 449, 450
 - atherosclerotic calcification and, 453, 454
 - elastin-associated components, 453
 - elastin-derived peptides, role of, 452
 - elastolytic enzymes, role of, 450–452
 - in intima and media, 443, 444
 - potential treatment strategies
 - in atherosclerosis, 464, 465
 - chronic kidney disease, 454, 461–463
 - in diabetics, 464
 - treatment strategies for, 455–460
 - Vascular dendritic cells, 80
 - Vascular smooth muscle cells (VSMCs), 145, 175, 323, 445, 452
 - Vitamin D assessment study (ViDA), 327
 - Vitamin D deficiency, 155
 - Vitamin D receptor(s) (VDRs), 140
 - Vitamin D receptor activators (VDRA), 153
 - Vitamin K, clinical trials, 486, 487
 - Vulnerable plaque, 17, 431
- W**
- Warfarin, 256, 515
 - Werner syndrome, 150
 - Whole-tissue valvular secretome, 533
 - Windkessel effect, 321, 446
 - Woven bone, 376